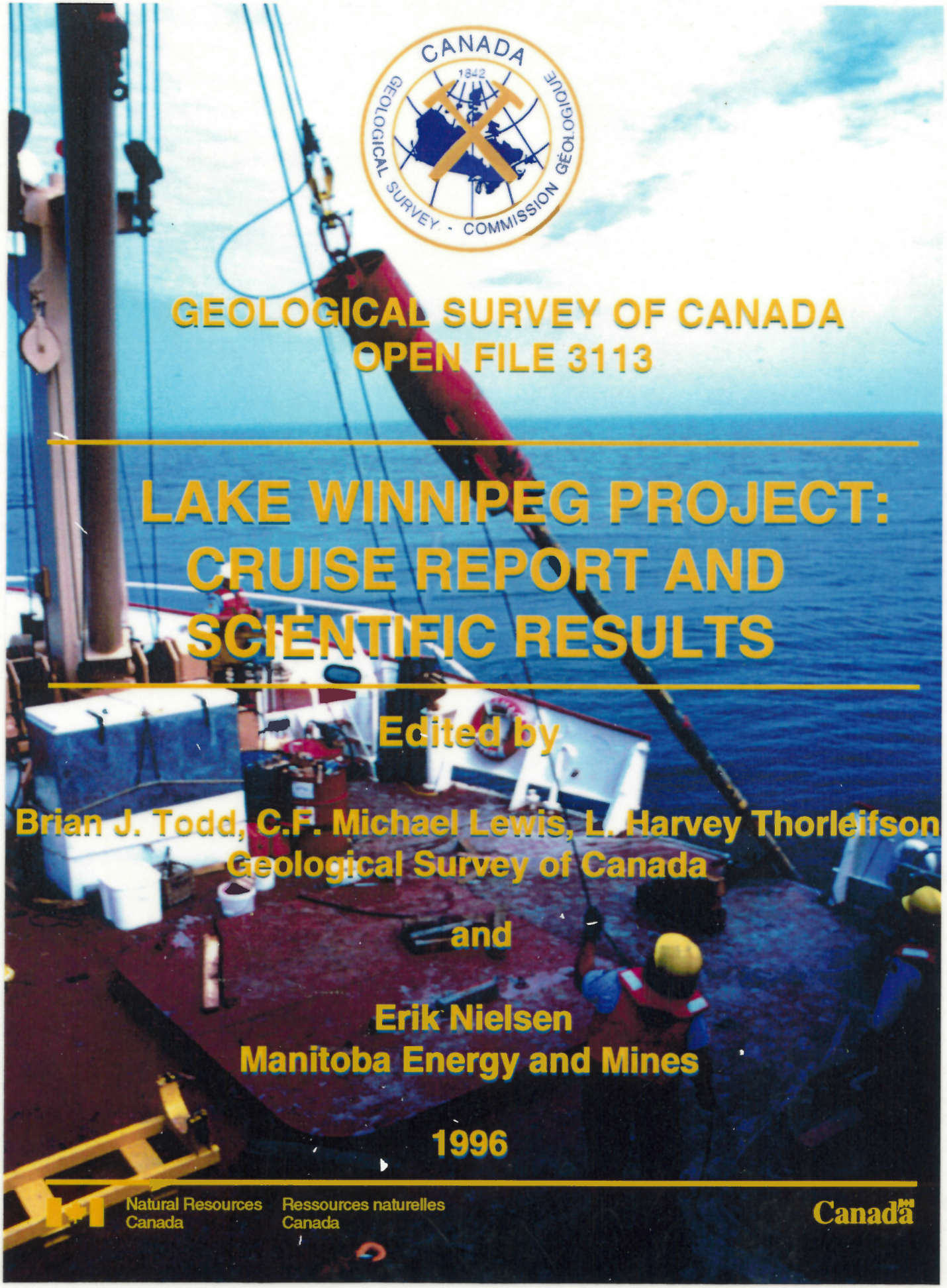

GEOLOGICAL SURVEY OF CANADA
OPEN FILE 3113

LAKE WINNIPEG PROJECT: CRUISE REPORT AND SCIENTIFIC RESULTS

Edited by

Brian J. Todd, C.F. Michael Lewis, L. Harvey Thorleifson
Geological Survey of Canada

and

Erik Nielsen
Manitoba Energy and Mines

1996

Natural Resources Canada
Ressources naturelles Canada
Canada

This document was produced by scanning the original publication.
Ce document est le produit d'une numérisation par balayage de la publication originale.

This document was produced by scanning the original publication.

Ce document est le produit d'une numérisation par balayage de la publication originale.

GEOLOGICAL SURVEY OF CANADA
OPEN FILE 3113

LAKE WINNIPEG PROJECT: CRUISE REPORT AND SCIENTIFIC RESULTS

Edited by

Brian J. Todd, C.F. Michael Lewis, L. Harvey Thorleifson
Geological Survey of Canada

and

Erik Nielsen
Manitoba Energy and Mines

1996

Natural Resources Canada | Ressources naturelles Canada

Canada

Frontispiece

GSC Photo Archives No. 1348, J.B. Tyrrell

Geological Survey of Canada field party in 1890, north shore of Lake Winnipeg.

"...behind the beach is an almost vertical cliff, rising in places to a height of forty feet, composed at the bottom of a stiff blue alluvial clay, and at the top of a mossy peat."

J.B. Tyrrell in D.B. Dowling, Geological Survey of Canada Annual Report, 1898

TABLE OF CONTENTS

1. Preface ...3

2. Cruise report of the 1994 Lake Winnipeg Project: *Namao* 94-900 - *B.J. Todd* **...7**

2.1 Introduction ...9
2.2 Narrative account of cruise ...9
2.3 Navigation and positioning ...13
2.4 Geophysical survey ...14
2.4.1 Multi-channel seismic reflection system ...15
2.4.2 High resolution seismic reflection system ...15
2.4.3 Sidescan sonar ...16
2.4.4 Marine radar ...16
2.4.5 Marine magnetometer ...16
2.4.6 Magnetic tape recording ...16
2.5 Coring and large grab samples ...17
2.5.1 Long cores ...17
2.5.2 Box cores ...18
2.5.3 Large bottom grabs ...18
2.6 Limnological Sampling ...18
2.6.1 Bottom sediment sampling ...18
2.6.2 Water column analyses ...18
2.6.3 Biological sampling ...18
2.6.4 Water sampling ...19
2.6.5 Air sampling ...19
Appendix 1: Marine magnetometer survey data ...59
Appendix 2: Temperature, conductivity, and turbidity profiles ...69

3. Geophysical survey results ... 77

3.1 Seismostratigraphy of Lake Winnipeg sediments- *B.J. Todd and C.F.M. Lewis* ...79
3.2 Precambrian geology of the Lake Winnipeg area - *W. Weber* ...119
3.3 Paleozoic geology of the Lake Winnipeg area and repositioning of the Precambrian-Paleozoic boundary - *R.K. Bezys* ...127
3.4 Quaternary geology of the Lake Winnipeg area - *E. Nielsen and L.H. Thorleifson* ... 141

4. Coring results ...159

4.1 Lithology and seismostratigraphy of long cores, and a reconstruction of Lake Winnipeg water level history - *C.F.M. Lewis and B.J. Todd* ...161
4.2 Physical properties and stratigraphic correlation of Lake Winnipeg sediments - *K. Moran and C.A. Jarrett* ...193
4.3 Paleomagnetic analysis of Lake Winnipeg core 122a - *J.W. King and C. Gibson* ...203
4.4 Bulk composition, texture, and mineralogy of Lake Winnipeg core and surface grab samples - *W.M. Last ...209*

4.5 Geochemistry of Lake Winnipeg sediments - *P.J. Henderson* ...221
4.6 Recent sedimentation rates and toxic metal concentrations in Lake Winnipeg sediments - *W.L. Lockhart* ...237
4.7 Pore-water chemistry of Lake Winnipeg sediments - *R.N. Betcher and W.M. Buhay* ...241
4.8 Stable isotopic composition of pore water and organic matter from Lake Winnipeg sediments - *W.M. Buhay* ...253
4.9 Ostracode stratigraphy of Lake Winnipeg sediments - *C.G. Rodrigues* ...261
4.10 Thecamoebian stratigraphy of Lake Winnipeg sediments - *S.M. Burbidge and C.J. Schröder-Adams* ...267
4.11 Fossil and modern phytoplankton from Lake Winnipeg - *H.J. Kling* ...283
4.12 Paleobotany of Lake Winnipeg sediments - *R.E. Vance* ...311

5. Sampling survey results ...313

5.1 Sampling polychlorinated biphenyls in Lake Winnipeg - *G. Fisher-Smith and K. Friesen* ...315
5.2 The crustacean plankton community of Lake Winnipeg in 1929, 1969 and 1994 - *A.G. Salki* ...319
5.3 Benthic invertebrates of Lake Winnipeg - *D.G. Cobb* ...345
5.4 The fish and fisheries of Lake Winnipeg - *W.G. Franzin, K.W. Stewart, L. Heuring and G. Hanke* ...349

6. Shoreline survey results ...353

6.1 Shore-zone morphology and processes of Lake Winnipeg - *D.L. Forbes and D. Frobel* ...355
6.2 Lake Winnipeg coastal submergence over the last three centuries - *E. Nielsen* ...393
6.3 Lake Agassiz beaches and reconstruction of lower lake levels in the Shield Margin area, northwest of Lake Winnipeg - *I. McMartin* ...403
6.4 Paleoshoreline and lake gauge evidence for post-Lake Agassiz regional tilting in Manitoba - *G. Tackman and D. Currey* ...421
6.5 Estimating postglacial rebound tilt in Manitoba: present status and future prospects - *A. Lambert* ...435

7. Appendices ...443

7.1 Summary core logs and corresponding seismostratigraphic sequences - *C.F.M. Lewis and B.J. Todd* ...443
7.2 Downcore plots of Lake Winnipeg sediment physical properties - *K. Moran and C.A. Jarrett* ...471
7.3 Bulk composition, texture, and mineralogy of Lake Winnipeg sediments - *W.M. Last* ...485
7.4 Geochemistry of Lake Winnipeg sediments - *P.J. Henderson* ...585
Appendix 1: Bulk sediment geochemistry - Lake Winnipeg long cores ...586
Appendix 2: Multi-parameter correlations -Lake Winnipeg long cores ...629
Appendix 3: Bulk sediment geochemistry - Bottom sediment samples ...651

1. Preface

1. Preface

Lake Winnipeg is the eleventh largest lake in the world. With an area 25% larger than Lake Ontario, it stands as a major feature on the Canadian landscape. Not only is the lake used for the purpose of fisheries and recreation, it is vital to the Manitoba economy due to its role in hydroelectric generation.

Despite its significance, Lake Winnipeg has been the subject of little study. Hydrographic charting has shown the offshore lakebed to be quite flat and shallow; water depths are about 9 m in the South Basin and 16 m in the North Basin. Aside from various surveys on land, the only major previous scientific effort was a limnological survey led by the Freshwater Institute of Fisheries and Oceans Canada in 1969. This survey included the collection of bottom sediment samples at fifty sites and the collection of several short sediment cores.

Knowledge of the geology of Lake Winnipeg, and hence the structure of the basin and its long-term evolution, has been limited to predictions from studies on land. An offshore survey of Lake Winnipeg therefore was proposed by the staff of the Geological Survey of Canada (GSC) and Manitoba Energy and Mines in 1993, on the basis of a need for an enhanced understanding of regional geological history.

The survey was carried out as a result of endorsements and financial support provided by Manitoba Hydro and the Manitoba Sustainable Development Innovations Fund, whose interest in the lake was bolstered by concerns regarding the cause of Lake Winnipeg shoreline erosion. Each of these agencies committed funds equivalent to 20% of the operating total of what became the Lake Winnipeg Project. Links were established with ongoing research at the Freshwater Institute, as well as with several university-based research programs. After the remaining funds were made available by GSC and the availability of the Canadian Coast Guard Ship (CCGS) *Namao* was confirmed, an organizational meeting was held in Winnipeg in May, 1994, and plans were made to conduct a scientific cruise in August, 1994 and a shoreline survey in September, 1994.

The GSC cruise, designated *Namao* 94-900, began with a northbound geophysical survey, followed by a southbound coring phase. Air and water sampling were undertaken concurrently with the northbound geophysical phase. A grid of geological bottom sediment samples, coupled with biological and water sampling, was carried out from the ship's launch during the southbound coring phase. A few weeks later, a comprehensive survey of the Lake Winnipeg mainland shoreline was carried out.

Geophysical data were processed at GSC Ottawa during the winter of 1994/95. Lake Winnipeg sediment cores were thoroughly processed at GSC Dartmouth in October, 1994. Subsamples of the sediments were distributed for analyses at several laboratories across North America. Preliminary results were presented at a workshop in Winnipeg hosted by Manitoba Energy and Mines in March, 1995.

The present volume provides technical data from the cruise, a report summarizing the shoreline survey, progress reports on the various initiatives arising from the cruise, and reports from other studies which were closely affiliated with those of the Lake Winnipeg project.

Two major questions are being addressed by the Lake Winnipeg Project:

1. What is the structure of the Lake Winnipeg basin?

The results of the Project summarized in this volume indicate that the actual structure of sediment and rock below the lake dramatically differs from expectations. Prior to the cruise, it was thought that carbonate and clastic rocks, such as limestone and sandstone, extend to the eastern shore, and that these rocks were buried by at most 15 m of sediment. In fact, sedimentary rocks, which show numerous probable karst features, only extend 10 km east from the end of Long Point in the North Basin, and terminate at an impressive buried escarpment in the middle of the South Basin. Beyond these Paleozoic rocks, sediments consisting almost entirely of Lake Agassiz clay reach unexpected thicknesses of over 50 m in the South Basin and over 100 m in the North Basin. Till is not extensive, but is present as two formerly unrecognized major moraines. Sediments deposited in Lake Winnipeg, which rarely exceed 10 m in thickness, rest on a regionally pervasive angular unconformity and are ornamented in places by a complex array of furrows formed by the action of pressure ridges in lake ice. Vigourous currents have stripped sediments from The Narrows and east of Black Island, producing the greatest water depths in the lake, over 60 m.

2. Are present-day sedimentary processes on Lake Winnipeg superimposed on long-term evolutionary trends?

Without knowledge of the history of a lake recorded in its sediments, it is difficult to determine whether a lake was in a state of equilibrium prior to human intervention, or whether recent perturbation is only an addendum to profound natural changes. A crucial factor is lake level, which, over geological time measured in centuries and millennia, can change dramatically in response to gradual uplift and tilting of the basin as well as to climatic change.

The Lake Winnipeg Project has produced data which indicates that Lake Winnipeg has, for centuries, been undergoing a gradual southward migration. Sediment cores from the centre of the South Basin revealed that

Lake Winnipeg offshore sediments have buried richly fossiliferous organic material which could only have been deposited at a previously existing shoreline. Radiocarbon and paleomagnetic analysis of this material indicate that most of the South Basin was dry land 4000 years ago. A survey of shoreline features, which form over centuries, indicates a lack of features attributable to lake-level decline, and an abundance of features characteristic of gradual transgression. The dominant control which has caused southward transgression appears to be tilting, as a result of the uplift of the Hudson Bay region caused by the melting and breakup of the continental ice sheet about 10,000 years ago. Superimposed on this control are the likely influences of climate change and increased inflow due to a mid-Holocene diversion of the Saskatchewan River to Lake Winnipeg.

These observations are a brief glimpse of the comprehensive scientific material which has been assembled by the Lake Winnipeg Project team and is presented in this GSC Open File Report. Project participants will again meet at the Annual Meeting of the Geological Association of Canada to be held in Winnipeg in May of 1996. At that time, data will have undergone further analysis, and plans for follow-up study and publication will be finalized.

From its inception to the publication of this report, the Lake Winnipeg Project has been a cooperative effort. At this point, the editors wish to express their sincere gratitude to the many individuals and agencies who made the Lake Winnipeg Project a success.

The support and guidance of management teams at the Terrain Sciences Division, Geological Survey of Canada, and the Geological Survey of Canada (Atlantic) is acknowledged. The enthusiastic interest and leadership provided by Dr. W. D. McRitchie (Director, Manitoba Energy and Mines, Geological Services) was crucial to the initiation of the project.

Manitoba Hydro can be credited with making the Project happen and for keeping progress on track. Their early endorsement of a broad program of basic science set the tone for the activity and its support. Interest and guidance provided by Mr. R.R. Raban and Ms. H. S. Zbigniewicz of the Hydraulic Operations Department of Manitoba Hydro has been very much appreciated.

A major contribution was made by the Canadian Coast Guard, facilitated by Captain Manu Unni-Nayar, Coast Guard Central Region Headquarters, Sarnia, Ontario. The interest and unfailing assistance provided by Captain Vic Isidoro and the officers and crew of the CCGS *Namao* greatly aided field activity. We are especially grateful for their efforts in striving toward our sometimes unrealistic objectives, and for the interest they demonstrated in the science. Ray Settee and the staff of the Canadian Coast Guard Base in Selkirk are also acknowledged for their role in handling the complicated logistics of an ambitious survey.

Barbara McKay of Public Works Canada is acknowledged for her role in the design of the marine radar catamaran, as are Neil Carlson and the staff of Carlson Structural Glass

for the fabrication, testing and post-cruise repair and storage of the *Atik-a-meg*.

Paula Nygaard of Natural Resources Canada is thanked for her provision of practical assistance in Winnipeg.

Keith Manchester and the staff of the Program Support Subdivision, GSC Atlantic, are acknowledged for their role in arranging for equipment used offshore.

Long hours were contributed by Mike Gorveatt, Tony Atkinson, Larry Johnson, Robbie Burns, Kevin Wagner, and Jean Pilon during setup of the ship. While offshore, often in challenging circumstances, outstanding efforts to acquire high quality data were made by Tony Atkinson, Robbie Burns, Kevin Wagner, Jean Pilon and Fred Jodrey.

The breadth of the research was greatly enhanced by the participation of the Freshwater Institute. Lyle Lockhart played a major role in the sediment coring work offshore, and participation of Institute members in analyses resulting from the cruise was organized by Bill Franzin. Everett Fee kindly assisted with CTD profiling.

Kate Moran, Catherine Jarrett, Gordon Cameron, and Bob Archer generously worked with the editors at GSC Atlantic to coordinate two weeks of intensive activity related to processing of the cores.

The major role played by Robbie Burns and Sue Pullan in the processing of seismic data and the sterling editorial efforts contributed by Jim Fergusson and Sharon Parnham are acknowledged with appreciation.

The comprehensive scope of the Lake Winnipeg Project is simply the sum of effort being made by a large number of scientists at laboratories across North America. Their willingness to show an interest in the Project at short notice is very much appreciated, and it is hoped that their investment of precious resources will be fruitful.

The contributions to this progress report were thoroughly reviewed and improved by the effort of GSC reviewers. The efforts of Dan Boyle, Scott Dallimore, Clément Prévost, Roger McNeely, Rod Klassen, Thane Anderson, Art Dyke, Penny Henderson, Isabelle McMartin, Dan Kerr, Andrée Blais, and Tony Lambert are acknowledged with appreciation.

Brian J. Todd
Geological Survey of Canada,
601 Booth Street,
Ottawa, Ontario K1A 0E8

C. F. Michael Lewis
Geological Survey of Canada (Atlantic),
P.O. Box 1006,
Dartmouth, Nova Scotia B2Y 4A2

L. Harvey Thorleifson
Geological Survey of Canada,
601 Booth Street,
Ottawa, Ontario K1A 0E8

Erik Nielsen
Manitoba Energy and Mines,
1395 Ellice Avenue,
Winnipeg, Manitoba R3G 3P2

2. Cruise report - *Namao* 94-900

2. Cruise report of the 1994 Lake Winnipeg Project: *Namao* 94-900

B.J. Todd[1]

Geological Survey of Canada
601 Booth Street, Ottawa, Ontario K1A 0E8

2.1 INTRODUCTION

An offshore survey of Lake Winnipeg was proposed by the staff of the Geological Survey of Canada (GSC) and Manitoba Energy and Mines (MEM) in 1993 on the basis of a need for an enhanced understanding of regional geological history. Previous knowledge of the geology of Lake Winnipeg was limited to study of land adjacent to the lake, and the results of a limnological survey carried out in 1969 by the Freshwater Institute of Fisheries and Oceans Canada in Winnipeg, under the direction of G. Brunskill. The latter survey included the collection of bottom sediment samples at 50 sites and the collection of several short cores.

Subsequent to the initial proposal, Manitoba Hydro and the Manitoba Sustainable Development Innovations Fund endorsed the project, largely due to concerns regarding the cause of Lake Winnipeg shoreline erosion. Each agency committed funds equivalent to 20% of the operating total of what became the Lake Winnipeg Project. Links were established with ongoing research at the Freshwater Institute, as well as with several university-based research programs. After GSC funds and the availability of the Canadian Coast Guard Ship (CCGS) *Namao* were confirmed, an organizational meeting was held in Winnipeg in May, 1994, and plans were made to conduct a scientific cruise in August, 1994, and a shoreline survey in September, 1994.

The GSC cruise *Namao* 94-900 on board the CCGS *Namao* (Fig. 1) began with the geophysical survey phase from August 4 to August 19, 1994 (corresponding to Julian days 216 to 231). Following the geophysical survey phase, the geological coring phase took place from August 21 (Day 233) to August 30 (Day 242). Air and water sampling were undertaken concurrently during the northbound geophysical phase. During the southbound coring phase, limnological samples consisting of geological bottom sediment samples, as well as biological and water samples, were obtained on a grid using the ship's launch.

The CCGS *Namao* was operated under the direction of Captain V. Isidoro; the officers and crew of the vessel ably assisted in the survey and sampling (Table 1). The vessel was built in 1975 at Riverton Boat Works, Riverton, Manitoba as a navigational aids tender. The ship is 33.5 m in length, 8.5 m in width and has a draft of 2.1 m. On-board berths permitted a scientific staff of six (Table 2). Todd and Lewis remained on board for the duration of the cruise to provide continuity between the geophysical survey and the geological coring. Todd directed the geophysical survey and Lewis directed the coring survey. Pilon, Burns, Atkinson and Wagner were on board for the geophysical survey phase; Jodrey, Thorleifson, Nielsen, and Lockhart were on board for the coring phase. Thorleifson directed the sampling survey with assistance from Nielsen. While sleeping quarters could be accessed daily on land, Fisher-Smith organized air and water sampling during the South Basin portion of the cruise and Lewis assumed these duties thereafter. Several guests joined the cruise during days when road access permitted (Table 3).

This report is intended to provide a description of day-to-day activities on board ship, to provide an overview of technical aspects of the equipment used, and to present a summary of geophysical and geological data obtained during *Namao* 94-900. In the following narrative account of the day-to-day activities (Section 2.2), reference is made to instrumentation and data which are fully described in later sections of the cruise report.

Hereafter in the cruise report, monthly days are accompanied by their corresponding Julian days. In the narrative account of the cruise (Section 2.2), time of day is given as local ship time, i.e. Central Daylight Time (CDT). Elsewhere, logged times are given as UTC (Universal Time Coordinated) which, for Lake Winnipeg, is five hours later than CDT. Thus 1200 hours ship time (CDT) is 1700 hours UTC.

2.2 NARRATIVE ACCOUNT OF CRUISE

The CCGS *Namao* was inspected by M. Gorveatt and B. Chapman (Atlantic Geoscience Centre; now GSCA or Geological Survey of Canada Atlantic) in May, 1994, and plans were made with the cooperation of the ship's crew for modifications and outfitting of the ship.

---

1. with contributions from C.F.M. Lewis, L.H. Thorleifson, R.A. Burns, M. Gorveatt, A. Atkinson, L. Johnson, F. Jodrey (Geological Survey of Canada), D.M. Lombardi (Seaforth Engineering Group), K. Friesen and G. Fisher-Smith (University of Winnipeg), and L. Lockhart (Freshwater Institute, Fisheries and Oceans Canada). An exhaustive review by Harvey Thorleifson prevented omissions of fact and improved the report.

Cruise activity began under the direction of M. Gorveatt, who supervised assembly of the scientific equipment for the cruise at GSCA in Dartmouth. The equipment was transported by truck to the Terrain Sciences Division (TSD) of the Geological Survey of Canada (Ottawa) by tractor trailer from **July 25-27 (Days 206-208)**. Scientific equipment from TSD was then added to the load and the full complement of gear was transported to the Canadian Coast Guard Base at Selkirk, Manitoba from **July 27-30 (Days 208-211)**. Scientific and technical staff arrived in Winnipeg on **July 28 and 29 (Days 209 and 210)**. On **July 29 (Day 210)**, the marine radar vessel, christened the *Atik-a-meg* (meaning "whitefish" in the Cree language) was inspected at Carlson Structural Glass in Winnipeg and trucked by Carlson personnel to the Selkirk Coast Guard Base. The *Atik-a-meg* was then assembled and underwent sea trials on the Red River.

Because the layout and size of the CCGS *Namao* did not allow for a scientific laboratory on the main deck of the ship, materials were purchased to construct a lab in the main hold (Fig. 2). Construction and outfitting of the lab began on **July 30 (Day 211)** and continued until **August 3 (Day 215)** under the direction of M. Gorveatt (GSCA). During this time, all geophysical survey equipment was loaded onto the CCGS *Namao* from the dock, navigational gear was mounted in the bridge and on the upper deck under the direction of L. Johnson (GSCA), all data recording and logging gear was secured in the lab, and all the gear to be towed was secured on the deck. GSC staff were lodged at hotels in Winnipeg during this period.

An ATCO trailer, placed on the aft upper deck, was outfitted by GSC staff to provide sleeping accommodation for four scientific staff during the survey. Space was made available in a ship's cabin for two members of the scientific staff.

Geological coring equipment was placed in storage at the Selkirk Coast Guard Base until completion of the initial geophysical survey phase.

H. Zbigniewicz of Manitoba Hydro, and several staff members of the Freshwater Institute, visited the ship during the outfitting period at the Selkirk Coast Guard Base.

On **August 4 (Day 216)**, the CCGS *Namao* left the Selkirk Coast Guard Base at 0915 and steamed downstream through Netley Marsh to the mouth of the Red River. At 1100, scientific staff and ship's crew were mustered on the boat deck for fire and emergency procedure drill. The DGPS (Differential Global Positioning System) navigation system malfunctioned until the ship reached the South Basin at approximately 1200. Lake conditions were calm. During the afternoon, **line SB1** was surveyed from south to north in the South Basin. The purpose of this initial line was to familiarize scientific staff and ship's crew with gear deployment and retrieval, and to test the geophysical equipment in an unfamiliar geological environment. Gear deployment began at 1352 and continued until 1510. Seistec data were recorded and the seismic and radar systems underwent checks. The scientific crew with accommodation on board consisted of Todd, Lewis, Pilon, Atkinson, Burns, and Wagner. The cruise was joined for the day by Fisher-Smith and Friesen, who installed air and water sampling gear, and by Thorleifson. By 1730, all gear was retrieved and the ship reached Gimli pier at 1815.

On **August 5 (Day 217)**, the CCGS *Namao* departed Gimli pier at 0830 and steamed to the eastern shore of the South Basin in calm conditions. **Line SB2** was run from south to north offshore from Grand Marais Point in order to detect any evidence for an offshore extension of the point. Discussions on board had suggested that Grand Marais Point and Willow Point (on the western shore of the South Basin) may be remnants of a previous southern shore of the South Basin. After the short south-north section, the ship headed west and steamed for Gimli to obtain information across the South Basin. The cruise was again joined for the day by Fisher-Smith, Friesen and Thorleifson, who had found accommodation on land the previous night. All survey gear was retrieved and secured on board by 1518 and the CCGS *Namao* was at the Gimli pier at 1535. Arrangements on land regarding logistics and liaison were managed by Nielsen.

The weekend of **August 6 and 7 (Days 218 and 219)** was spent tied up in Gimli harbour. Cruise planning, survey line layout and navigational computer data entry took place on the bridge during both days. At the same time, further hardware alterations and additions were performed in the lab and with the equipment at the stern. The marine magnetometer was tested and a magnetics base station was set up at the golf course adjacent to the Gimli airport. The base station magnetometer was supplied by the GSC Geomagnetics Laboratory in Ottawa.

On **August 8 (Day 220)** the CCGS *Namao* departed Gimli pier at 0900 and steamed south to the mouth of the Red River. The geophysical gear was deployed in calm conditions at 1045. **Line SB3** was then run from south to north to the latitude of Drunken Point. The sidescan sonar was made operational, revealing evidence of furrowing of the lake bottom by ice keels. The marine magnetometer was also deployed, thus completing the first simultaneous streaming of all the geophysical survey instruments. The cruise was joined for the day by Fisher-Smith and guests Buhay and Betcher. The survey gear was retrieved by 1832 and the ship was secured at Gimli pier at 2012.

On **August 9 (Day 221)**, the CCGS *Namao* departed Gimli harbour at 0830 and steamed north to Drunken Point on the western shore of the South Basin. On board for the day were Thorleifson, Nielsen and Fisher-Smith. Weather conditions were fair with a light breeze. All survey gear was deployed at 0935 and **line SB4** was surveyed from west to east. At 1500, the ship's heading was altered to the southeast and the line was continued past Elk Island into Traverse Bay. The air compressor (that powered the sleeve gun) first malfunctioned

at 1250 and was finally shut down due to low air pressure and mechanical problems at 1534. GSC staff and ship's engineers worked on rebuilding the compressor and succeeded at 2030. Unfortunately, no seismic data were obtained in Traverse Bay. At 1730, all geophysical gear was retrieved and the ship steamed around Elk Island and put into Victoria Beach at 1836.

August 10 (Day 222) dawned with wind and showers, but conditions then cleared for excellent surveying weather. Guests Weber and Bezys, as well as Fisher-Smith, came on board for a two-day stay. The CCGS *Namao* departed Victoria Beach at 0831 and steamed northwest to begin **line SB5** from a known position along **line SB4**. Geophysical gear were deployed by 0935 and the line was run to the northeast towards the southern shore of Black Island. The DGPS navigation system, which had suffered numerous failures in the previous two days, behaved more dependably. Also, the rebuilt compressor functioned faultlessly. Unlike the previous survey lines farther south in the South Basin, **line SB5** showed relatively little masking of reflectors by gas trapped in the sediments. In order to obtain a paper record of the 24-channel seismic system, channel 4 was tapped, filtered, and displayed on a spare EPC graphic recorder. The geophysical gear was retrieved at 1732 and the CCGS *Namao* steamed north between Hecla Island and Black Island, reaching Gull Harbour wharf on northern Hecla Island at 1836. Guests found accommodation in Gull Harbour for the night.

August 11 (Day 223) was sunny and warm with light winds. The CCGS *Namao* departed Gull Harbour at 0843 and steamed to the northeast end position of **line SB5** south of Black Island. Deployment of geophysical gear was completed at 0935 and the ship surveyed **line SB6** around the eastern end of Black Island, the first time that the CCGS *Namao* had ever taken that route. Seistec data through this deepest area of Lake Winnipeg showed a suite of dramatic features related to complex sedimentation and erosion patterns. In contrast, results of surveying into Washow Bay northwest of Black Island were disappointing because of extensive gas masking. By 1746, the geophysical gear was retrieved and the CCGS *Namao* steamed northward to Pine Dock which was reached at 1906. The ship was met by Nielsen and Thorleifson, who provided transportation to Winnipeg for Weber, Bezys and Fisher-Smith, as well as for a number of large-volume water samples which were taken directly to cold storage.

August 12 (Day 224) started fair and calm but ended with stormy conditions. The CCGS *Namao* departed Pine Dock at 0832 and began deploying survey equipment. All gear was in the water by 0910 and **line SB7** was surveyed in a zigzag pattern to the northwest through The Narrows. Sand waves on the lakefloor imaged by both the Seistec and sidescan sonar systems suggest that high velocity bottom currents flow between the North Basin and the South Basin through The Narrows. The weather quickly deteriorated after 1600. At 1730, gear retrieval commenced and proved to be very challenging: damage was inflicted on the *Atik-a-meg* as the craft was pulled alongside the hull of the CCGS *Namao*. By 1800, all gear was secured on board and the ship came about, ran south with the waves and put into Matheson Island at 1948.

Rough conditions on **August 13 (Day 225)** precluded geophysical surveying. The CCGS *Namao* departed Matheson Island at 0935 and steamed north to Berens River on the eastern shore of the North Basin, arriving at 1418. The passage was quite rough with a lot of water taken over the bridge. An incomplete seal on a cable access pipe above the chart storage rack resulted in wet charts. GSC staff remedied this oversight. The DGPS navigation system was reaching the northern limit of the small antenna and it was decided to switch to the larger, satellite-tracking antenna. However, this antenna had been damaged during shipment from Dartmouth. Ship's engineers fabricated a steel mounting pole for the antenna shell and also repaired the internal mechanism. Telephone discussions with the lessor of the navigation equipment in Nova Scotia resulted in the correct wiring of the new antenna and gyro compass to the GPS receiving unit.

Strong winds and rough water prevailed on **August 14 (Day 226)**. The CCGS *Namao* departed Berens River at 0600 and made a rough passage northwest to George Island, arriving at 1048. The weather steadily improved once the ship had tied up at the fish plant dock but geophysical surveys were limited to a test of the radar equipment across the dunes from the north beach to the anchorage basin.

August 15 (Day 227) began with wind and moderate waves, but conditions improved throughout the day. The CCGS *Namao* departed George Island at 0700 and steamed northeast to Poplar River on the eastern shore of the North Basin where gear was deployed at 0915. **Line NB8** was surveyed to the southwest passing just north of Little George Island. A large ridge, probably a moraine, was imaged as the chain of islands was crossed. Southwest of the ridge, the ship's course was altered to westward. Unfortunately, the Seistec power supply malfunctioned between 1340 and 1553. The final portion of **line NB8** was run northwest towards Long Point on the western shore of the North Basin. Once the Seistec system was repaired, the records revealed a disturbed, or disrupted, character to the Lake Agassiz sediments. The transition from undisturbed to disturbed was not imaged due to the Seistec malfunction. The geophysical gear was retrieved by 2004 and the CCGS *Namao* returned to George Island at 2230.

Frustratingly, **August 16 (Day 228)** dawned very windy. The CCGS *Namao* departed George Island at 0600 to head back to the western end of **line NB8** to continue the survey northeast to Warren Landing. However, the lake was quite rough. The ship hove to in the lee of Little Sandy Island, waiting for the weather to improve. Eventually, the ship returned to George Island and tied up at 1012. By that time, wind speed was decreasing, so a decision was made to steam to Warren Landing at the northeast end of the North Basin in order to position the ship for a survey to Grand Rapids on the

following day. At 1250, the CCGS *Namao* left George Island and arrived at Warren Landing at 1818.

On **August 17 (Day 229)**, the CCGS *Namao* departed Warren Landing at 0530. All geophysical gear was deployed by 0648 and **line NB9** was surveyed southwest to Grand Rapids in calm and sunny conditions. Much of the central portion of the Seistec profile suffered record degradation due to gas. By 1904, all gear was retrieved and the ship proceeded to the Grand Rapids Coast Guard dock where she was secured at 1954. Atkinson left the ship for Winnipeg and Jodrey arrived.

On **August 18 (Day 230)**, Pilon and coxswain F. Gnitzinger surveyed around Selkirk Island with the *Atik-a-meg* towed by the CCGS *Namao*'s launch, an twin-outboard-powered open aluminum boat. The CCGS *Namao* departed Grand Rapids at 0700 and joined the west end of **line NB8** at 1125 and surveyed **line NB10** north to intersect **line NB9**. Nielsen and Thorleifson came on board for the day. The geophysical survey gear was retrieved at 1828 and the ship returned to Grand Rapids, stopping briefly to service a weather buoy. The CCGS *Namao* was secured at the dock at 2224.

The final geophysical survey day was **August 19 (Day 231)**. Once again the lake was perfectly flat. Burns and Pilon departed from Grand Rapids for Winnipeg, stopping at the Gimli golf club to demobilize the magnetic base station. The CCGS *Namao* departed Grand Rapids at 0700 and began **line NB11** at 0920, surveying north toward Limestone Point from a position along **line NB9**. Limnological sampling crew Thorleifson and Nielsen, with coxswain F. Gnitzinger, departed in the launch at 1000 and completed three sites. At 1600, the geophysical survey gear was retrieved and the launch was secured at 1655. At 1750, the sampling crew again departed, with coxswain Babisky, completed another three sites and returned to Grand Rapids. The ship arrived at Grand Rapids at 2122.

August 20 (Day 232) was spent preparing the ship for the change from geophysical surveying to coring. Wagner departed for Winnipeg and Lockhart arrived. Fisher-Smith transported water samples to Winnipeg. The CCGS *Namao*'s launch was deployed from 0854 to 1135 with a Coast Guard crew to service a light on Selkirk Island. Thorleifson and Nielsen accompanied the launch crew. During the course of the day on board the ship, geophysical records were reviewed to select coring sites, the geophysical lab in the hold was partially demobilized, and all empty boxes in the hold were removed and loaded onto the Coast Guard truck for storage at the Selkirk base. A large volume of geological sampling gear was loaded onto the ship, but a cable and core head were still in transit from Dartmouth. The scientific crew on board ship now consisted of Todd, Lewis, Jodrey, Thorleifson, Nielsen and Lockhart.

The morning of **August 21 (Day 233)** was spent testing the box corer. The CCGS *Namao* departed Grand Rapids at 0930 and steamed to **box core site 101** along **line NB9** just off the Saskatchewan River mouth east of Grand Rapids. At 1047 the first box core was taken and judged to be unacceptable because the device sank into the very soft lakefloor mud. Wide, wooden planks were then attached to the feet of the box corer and it was redeployed to obtain a successful sample at 1146. By 1306, the ship was once again secured at the Grand Rapids Coast Guard dock. At 1440, the truck arrived carrying the cable and core head. The crew put the new cable on the crane and transferred the head weight from the truck to the foredeck. In the evening, Coast Guard crew worked with GSC personnel in running through procedures for a piston core setup and deployment in anticipation of the following day's work.

On **August 22 (Day 234)** the CCGS *Namao* departed Grand Rapids for the last time during the cruise at 0630 and steamed northeast toward Warren Landing along **line NB9**. At 1030, **box core site 102** was successfully recovered and nearby **piston core site 103** was completed at 1130. Two gravity cores at **site 103** were unsuccessful because material escaped from the bottom of the core barrel. The waves began to build and the CCGS *Namao* headed for Warren Landing in rough conditions, arriving at 1600. Core processing was undertaken on the dock while Nielsen and Thorleifson examined and sampled outcropping stratigraphy along the shore west of Warren Landing.

The wind dropped overnight and the morning of **August 23 (Day 235)** was calm and perfect for sampling. The CCGS *Namao* departed Warren Landing at 0830 and steamed southwest to the start of **line NB9**. **Gravity core site 104** was collected at 1006, followed by **piston core site 104a** at the same location. Just to the northeast, **piston core site 105** was successful at 1348, followed by **piston core site 106** (southwest of **site 104**) at 1530. The ship's position relative to the selected piston core site coordinates improved from 130 feet to 30 feet to only 6 feet, thus indicating that the bridge crew quickly grasped the manipulation of the piston corer and the DGPS core site positioning display. The ship returned to Warren Landing at 1705. During the day, limnological sampling crew Thorleifson, Nielsen and coxswain Magnusson completed four sites and returned to Warren Landing.

The wind increased overnight and the CCGS *Namao* departed Warren Landing at 0700 on **August 24 (Day 236)** in swells. The ship steamed south to intersect **line NB8** where **piston core site 107** was collected at 1240. A gravity core at the same site failed at 1319. At 1355, limnological sampling crew Thorleifson, Fontaine and coxswain Magnusson left the ship, but wind conditions prevented any sampling and they proceeded to George Island. The ship proceeded southwest along **line NB8** where the piston corer was lost at **site 108**. Apparently, the cable parted at the spool, the strain enhanced by the simultaneous upward movement of the ship's bow on the crest of an oncoming wave and the downward free-fall of the corer. A box core was obtained and a gravity core was

attempted at **site 108** at 1550 and 1608, respectively. The CCGS *Namao* steamed east to George Island, arriving at 1750. Core processing proceeded on board while Nielsen, Thorleifson and Babisky inspected the geology of the island, noting the prevalence of Precambrian- and absence of Paleozoic-type lithologies in boulders at the shoreline as well as the presence of shipwreck debris.

On **August 25 (Day 237)**, the CCGS *Namao* departed from George Island at 0700 in a northwest swell. At 0852, limnological sampling crew Thorleifson, Nielsen and coxswain Babisky departed from the ship. At 0950, blind (i.e. no geophysical data) **gravity core site 109** was attempted north of Berens Island but little sediment was recovered. Further to the south near Little Tamarack Island, another blind **gravity core (site 110a)** was taken at 1306, accompanied by **box core site 110b** at the same location. DGPS navigation malfunctioned for most of the day. The equipment lessor in Dartmouth telephoned and advised that the satellite operators had altered their system without prior notification. Some manipulation of electronic components fully restored the DGPS system. **Grab sample sites 111 and 112** were collected at 1508 and 1524 in The Narrows along **line SB7** at the location of the sand waves. Because the weather was by now so calm, the ship proceeded south into Washow Bay to intersect **line SB6** where **gravity core site 113a** and **box core site 113b** were collected at 1744 and 1752, respectively. The CCGS *Namao* continued steaming south, arriving at Gull Harbour at 1910. The limnological sampling crew joined the ship as she arrived at Gull Harbour, having completed eight sites. Jodrey and Nielsen drove to the Winnipeg airport to pick up a corer trip arm sent from the Pacific Geoscience Centre.

On **August 26 (Day 238)**, the CCGS *Namao* departed Gull Harbour at 0830 and steamed south into the South Basin. P. Henderson was on board for the day. A fire and emergency drill was held from 0856 to 0911. Limnological sampling crew Thorleifson, Nielsen and coxswain Magnusson completed six sites and proceeded to Gimli. **Box core site 114** was obtained at 1015 along **line SB5**. **Gravity core site 115** followed at 1051 near Pearson Reef, also along **line SB5**. The ship steamed south to intersect **line SB3** and **box core site 116** was retrieved northeast of Gimli at 1240. By 1342, the ship had made its way through the world windsurfing races to tie up at Gimli pier. The core cooler was once again repaired by a local refrigeration repairman. Cores were processed and two GSC personnel drove to Selkirk Coast Guard Base to retrieve shipping cases. R. Fulton visited the ship in the evening and discussed results with Lewis and Todd.

August 27 (Day 239) was spent tied up at Gimli pier. More equipment in the lab was demobilized and stored in shipping cases. Geophysical records were reviewed to select sample sites. Thorleifson tended to a dental emergency in Winnipeg.

The lake conditions on **August 28 (Day 240)** were rough. The Hon. Jon Gerrard, Secretary of State (Science, Research and Development), visited the ship for the day accompanied by his family. The CCGS *Namao* departed Gimli pier at 0817 and made a rough passage northeast to **line SB4** where **box core site 117** was obtained at 1004, even though the device tripped slightly prematurely. The ship returned to Gimli harbour at 1124. Discussions with Jon Gerrard were held during the day, and he and his family departed at 1500. Geophysical records were reviewed for site selection.

August 29 (Day 241) was calm and the CCGS *Namao* departed Gimli harbour at 0830 and steamed east to **line SB4** in Traverse Bay. Limnological sampling crew Thorleifson, Henderson and coxswain Magnusson departed the ship at 0924, completed seven sites, and returned to Gimli. **Box core site 118** was obtained at 1043 followed by **gravity core site 119** just north of Elk Island. The bottom core barrel was bent at site 119, probably upon impacting hard Lake Agassiz clay. Farther north from Elk Island, **piston core site 120** succeeded in retrieving Lake Agassiz clay at 1325. **Gravity core site 121** was obtained at 1506 along **line SB4** off Drunken Point. The CCGS *Namao* then steamed south to intersect **line SB3** off Gimli where **gravity core site 122a** was retrieved at 1644. Guests Buhay and Pashadal were on board for the day. The ship returned to Gimli harbour at 1736 and cores were processed late into the evening.

The final survey day was **August 30 (Day 242)**. Guests McRitchie, Teller and Betcher came on board for the passage from Gimli to Selkirk. The CCGS *Namao* departed Gimli harbour at 0830 and steamed northeast to reoccupy the last site of the previous day. At **piston core site 122b**, the corer was lost overboard due to failure of the fiege fitting connecting the cable to the piston. The ship proceeded south along **line SB3** to **box core site 123** which was successful on the second attempt at 1127. Limnological sampling crew Thorleifson, Nielsen and coxswain Magnusson completed two sites and proceeded to the dock at the mouth of the Red River. The CCGS *Namao* rendezvoused with the launch crew and steamed up river to dock at the Selkirk Coast Guard Base at 1442. Demobilization of equipment proceeded for the rest of the day.

August 31 (Day 243) and **September 1 (Day 244)** were spent removing equipment from the CCGS *Namao*, breaking down the lab in the hold, packing shipping cases, and storing the cases in the Coast Guard warehouse to await transport to Ottawa and Dartmouth. Seismic equipment was shipped to St. John's to join another cruise. Water and biological samples were delivered to the Freshwater Institute in Winnipeg.

2.3 NAVIGATION AND POSITIONING

Equipment description - The satellite-referenced Global Positioning System (GPS) in differential mode was used on board the CCGS *Namao* to obtain the ship's position. Most of the equipment was leased for the duration of the survey from

Seaforth Engineering Group in Dartmouth, Nova Scotia. The GPS navigation hardware and software consisted of the following:

Magnavox 4200D six channel GPS receiver
STARFIX II differential correction data (single reference station - Duluth, Minnesota)
STARFIX II 5600 receiver
STARFIX II omni-directional antenna (for use in the South Basin)
STARFIX II single horn receiving antenna and LNA/downconverter (for use in the North Basin)
Azimuth controller model 5250
Sperry SR-50 portable gyro compass (for use with the single horn antenna)
12 volt DC and 24 volt DC power supplies
IBM-compatible 386 computer
GPSLOG Geological Survey of Canada GPS data logging software
Magnavox 4200CDU software for GPS receiver control
AGCNAV Geological Survey of Canada navigation display/logging software

Procedures and methods - To assist ship's officers in conning the ship for line running and positioning for samples, the Magnavox 4200D GPS receiver and STARFIX II 5600 were installed on the bridge. The whip antenna to receive signals from a suite of GPS satellites was mounted on the rail above the bridge. As well, the omni-directional GPS antenna was mounted on the forward rail on top of the bridge and the gyro-stabilized single horn antenna was mounted on a steel pole on the aft rail above the bridge (Fig. 3). These two antennae received signals from a geosynchronous satellite relaying the Duluth, Minnesota reference signal. The omni-directional antenna and the single horn antenna were 17.1 m and 14.1 m from the stern, respectively (Fig. 3). The omni-directional antenna was used when surveying in the South Basin and the single horn antenna was used in the North Basin.

Differential mode GPS (DGPS) was acquired on the Lake Winnipeg survey using the Duluth reference station. In any survey, three (and preferably four) satellites are required to calculate a differential position. Differential mode improved positional accuracy from 50-70 m (non-differential mode) to 10 m or better. The outputs from the STARFIX system were individual corrections for each satellite observed at Duluth. These data were combined with the satellites observed from the ship using the Magnavox 4200D receiver. The corrected output provided time (UTC), latitude, longitude, course over the ground and speed over the ground. These data were recorded at a 15 s interval on the hard disk of the 386 computer.

Geophysical survey lines were drawn on Canadian Hydrographic Service Charts 6241, 6251 and 6248. Way points were calculated from these charts and entered into the computer using AGCNAV. The desired survey line was then displayed on the computer monitor along with actual ship's position obtained from the DGPS receiver. Other information, such as course, speed and range, were also displayed on screen. This combined display enabled the ship's crew to accurately steer along planned geophysical survey lines. A second computer was mounted in the geophysical lab in the hold and the navigation screen on the bridge was duplicated to enable accurate watch keeping.

Geological sampling positions were determined by first inspecting high-resolution seismic records. For a selected feature on the record, a corresponding day and time were noted. Stored navigation files were then interrogated to find the latitude and longitude corresponding to the selected day and time. The computer display on the bridge was then altered from line-running mode to point mode. Thus the ship could accurately reoccupy a position to deploy the sampling devices.

Operational performance - Several technical difficulties were encountered in setting up both the hardware and software for the DGPS system due to lack of familiarity with the equipment coupled with inadequate documentation. Although the system did not function for intermittent periods of time, inspection of the track charts demonstrates that no significant portions of the navigation data are missing. Spikes along the track lines represent momentary aberrations in the logged ship locations that have not been edited from the navigation files. The DGPS system often malfunctioned when the ship was manoeuvring to occupy a sampling station. This led to delays in sampling in order to wait for the navigation system to function properly. In general, more system down time was experienced in the North Basin than in the South Basin. Seaforth Engineering Group did advise the GSC that this was likely to happen because in the North Basin the ship is far from the ground reference station at Duluth.

2.4 GEOPHYSICAL SURVEY

Lakebed morphology was imaged with sidescan sonar and its subbottom profiled with a high-resolution seismic reflection profiler (Seistec) and a sleeve gun multichannel seismic system along transects through major basins of the lake. An experimental deployment of a ground penetrating radar was housed in a twin-hulled craft (the *Atik-a-meg*) built expressly for that purpose. A marine magnetometer was operated as well. This array of geophysical instruments was towed from the CCGS *Namao* (Fig. 4).

The geophysical survey data, though limited in coverage compared to the large area of the lake, were generally of high quality. East-west transects, with south-north tie lines, were run in both the South and North Basins, as well as in the connecting narrows and islands area. No data were acquired in the southern part of the North Basin owing to high wind and wave conditions. Nonetheless, over 500 km of geophysical track lines were obtained. Several significant observations were made on board, including 1) evidence for substantial westward relocation of the estimated position of the Precambrian-

Palaeozoic contact, 2) basins of substantial depth beneath this shallow, flat-bottomed lake containing over 100 m of sediment, 3) previously undocumented features such as furrows in lakefloor sediment attributed to scouring by ice keels and sand waves indicating high current flow. Sediments attributed to glacial Lake Agassiz and a number of moraines were clearly imaged. These sediments are truncated by a regional unconformity and are overlain by sediments of Lake Winnipeg; the latter commonly reach thicknesses of 9 m or more in the offshore basins. Lack of seismic penetration over broad areas was thought to be due to gas disseminated within the sediments.

2.4.1 Multi-channel seismic reflection system

Equipment description - The multi-channel seismic reflection profiling system was composed of an EG&G R24 Strataview seismograph recording signals received from a seismic eel. Power was supplied to the seismograph by a Lambda EWS 300-12 switching regulator DC power supply fed by ship's power. The seismograph contains instantaneous floating point amplifiers with a 32 bit floating point digital signal processor. Preamplifier gain was set at 36 dB with a maximum input signal of 300 mV peak-to-peak. When operating in its marine mode, the seismograph operates with a replace function and an autosave function. These features allow recording and storage of records in less than 5 seconds. Each seismic record consists of 24 channels with 1024 samples per channel at a 0.25 millisecond (ms) sample rate. The record length is 256 ms and the file size is 106 kilobytes. Using a 0.25 ms sample rate provides a recorded bandwidth of 2-1200 Hz with a dynamic range of 104 dB. To avoid clipping the recorded seismic signal, the seismograph used a trigger lockout time of 4.8 seconds that prevented the seismograph from triggering on the Seistec pulse. The Seistec was disabled as the sleevegun shot was received by the seismograph, and the Seistec was then enabled. The Seistec firing rate was 0.25 seconds.

Within the seismograph is an IBM-compatible computer using an 80486 processor with a data storage capacity of 340 megabytes and 8 megabytes of RAM. A SCSI interface allowed external data storage on a 1.2 gigabyte drive, thereby allowing storage of a large number of records without leaving the "record" mode on the seismograph. In the evening, seismic data were downloaded from the 1.2 gigabyte drive to 150 megabyte Bernoulli disks in an external twin Bernoulli drive. Approximately 1400 records were stored on each Bernoulli disk.

The seismic eel consists of 24 receivers spaced at a 5 metre interval (115 m live section) (Fig. 5). Each receiver consists of 2 AQ-16 hydrophones wired in parallel with a 0.5 metre separation. Each hydrophone has a frequency response of ± 0.5 dB from 0.5 Hz to 3 kHz, a sensitivity of -97 dB referenced to 1 V per microbar, a capacitance of 3500 picofarads, and a depth rating of 1828 metres. The output signal from each pair of hydrophones passes into an AQ-300 differential input/output preamplifier. The preamplifier has an input impedance of 30 Mohm, a gain of 20.8 dB with a 20 Kohm resistor installed, a bandwidth of 3 dB points 0.3 Hz to 14 KHz, a current of 750 microamps, a voltage of 8-30 V and a common mode rejection ratio of greater than 80 dB.

The seismic energy source used was a 10 cubic inch sleeve gun operated at an air pressure of 1900 psi (Fig. 6). The fore-and-aft offset from the source to the first hydrophone was 10 m; the streamer was towed 3 m to port from the source (Figs. 3, 4). Approximately a 5 ms sleevegun delay was removed by a trigger. This trigger also masked the Seistec boomer when the sleevegun was fired at a 5-second interval.

Operational performance - Almost 54000 records were recorded in ten surveying days (Table 4). As well as these reflection records, many refraction records were recorded. These latter records will assist in velocity determinations of different materials. The breakdown of the AGC compressor on August 9 (Day 221) resulted in the loss of seismic data in Traverse Bay along line SB4. As well, digital data collected along line NB9 have been lost. These data were logged on Bernoulli disks and the disk numbers were entered in the observer's written log. However, no trace has been found of these missing disks to date. Thus, a total of 458 line-km of multichannel seismic data exists (Table 4).

2.4.2 High resolution seismic reflection system

Equipment description - The high resolution seismic reflection system (Seistec) consisted of the following components:

ORE Geopulse power supply (175 joules)
Huntec model 4425 boomer mounted under a surface-towed surfboard (seismic energy source)
IKB-Seistec line-in-core hydrophone array (seismic energy receiver)
AGC firing computer
Raytheon TDU1200 graphic recorder
Analogue magnetic tape on Hewlett-Packard 3968 tape recorder
Digital magnetic tape on SE880 tape recorder

Procedures and methods - The Seistec receiver (Fig. 7) was towed from the upper deck crane to starboard from the stern (Figs. 3, 4). The cone houses a seven-element, acceleration-cancelling stick hydrophone array. In spite of the height of the upper deck from the surface of the water, the crane's articulation allowed the tow point of the Seistec to be lowered a few metres to provide smooth towing. The boomer surfboard (Fig. 8) was towed from the starboard aft main deck (Figs. 3, 4). Under most survey weather conditions and ship's survey speed (about 4 knots, or 7.41 km/hr), the surfboard planed down to 1-2 m below water surface, thereby obtaining good 'coupling' of the seismic energy with the water.

The system was fired at a 1/4 second firing rate controlled

by the AGC firing computer. Every twentieth shot was suppressed to allow the sleeve gun system to fire. This permitted the two seismic systems to operate without their energy source signals being detected on the other system's receiver. The ORE power supply was mounted under a protective plywood box on the stern protected by the upper deck overhang. The data were displayed on-line using a dual-channel EPC 9800 graphic recorder at two sweep speeds providing, on the same paper output, a record 125 ms in length (upper record) and 62.5 ms in length (lower record). Having two vertical scales of data recorded simultaneously greatly enhances the interpreter's ability to identify features and discriminate real reflectors from noise and system artefacts. The Seistec data were also output on a Raytheon TDU1200 48.25 cm thermal paper plotter.

Operational performance - The Seistec high-resolution profiler system worked flawlessly except for a malfunction of the ORE power supply for two hours along line NB8 on August 15 (Day 227). Electronic components had overheated and failed. The problem was repaired and no further malfunctions occurred. Rough weather and variable towing speeds sometimes degraded the record. Overall, however, the records obtained from this system produced the most detailed, highest-resolution images of the sedimentary sequences from the lake bottom to bedrock. Consequently, coverage by this system on the widely-spaced lines around the lake were given highest priority resulting in the collection of 547 line-kilometres of Seistec profiles (Table 4).

2.4.3 Sidescan sonar

Equipment description - The sidescan sonar system consisted of the following:

Klein 100 kHz towfish
Klein digitizer and signal processor box
Klein 531T 3-channel recorder

Procedures and methods - The sidescan sonar towfish (Fig. 9) was towed off the port bow by a block attached to the crane (Fig. 3). The towfish was lowered by hand to a depth of about 2 m below the water surface. The shallow draft of the CCGS *Namao* offered no interference to the system at this depth. The port and starboard side-looking channels were used on the 100 m slant range during the survey.

Operational performance - The sidescan sonar system was made operational on line SB3 (August 8, Day 220) and 509 km of high quality records were obtained throughout the duration of the survey (Table 4).

2.4.4 Marine radar

Equipment description - A ground probing radar (GPR) was experimentally deployed during the course of the Lake Winnipeg survey. In order to operate offshore, a non-metallic, non-conductive housing was designed and built. The craft took the form of a fibreglass catamaran designed to house self-contained electronics and two GPR antennae, a transmitter in one hull and a receiver in the other hull. The craft was designed by staff of the GSC and the Winnipeg office of Public Works Canada, and was built by Carlson Structural Glass of Winnipeg (Fig. 10). Digital pulseEKKO IV GPR equipment (Sensors and Software Ltd., Toronto) was used, incorporating signal stacking and digital data processing. Both 25 MHZ antennae, for deeper and less detailed records, and 50 MHZ antennae, for shallower and more detailed records, were used.

Procedures and methods - The GPR equipment was operated without any umbilical connection to the ship. The catamaran was towed 20 m astern of the port side of the ship (Figs. 3, 4). Power was supplied by rechargeable batteries capable of a full day's operation. Data were transferred from the catamaran to the ship by UHF 900 MHZ data transmission. The receiver, mounted at the port stern, supplied data to an RS-232 port of a portable IBM-compatible computer. Profiles were plotted on-screen on a real-time basis and stored on the computer hard disk for later printing on a dot-matrix printer and transfer to Bernoulli disks.

Operational performance - Radar profiling met with limited success offshore due to the depth of water and the widespread extent of clay on the lakefloor. Profiles were obtained offshore, but differentiation of interference from towed cables, the lakefloor, and subbottom reflectors could not be made with confidence. Better results were obtained onshore and in shallow water. The system has potential for profiling in the coastal zone and in lakes having less clay-rich sediment.

2.4.5 Marine magnetometer

A GSM-19MD marine magnetometer manufactured by GEM Systems Inc. (Richmond Hill, Ontario) was deployed on all the geophysical survey lines except for SB1 and SB2. The sealed fish (Fig. 11) contained an Overhauser sensor; signals generated in the sensor were processed in a fish-mounted microprocessor and transferred digitally through the tow cable (which also served as the power cable). The value of the magnetic field was logged each second and magnetometer profiles were plotted (Appendix 1). Although the background values of magnetic field strength (59 000 to 60 000 nT) are typical for this area, there are inexplicable, regular gaps in the data, shown by the smooth, straight-line intervals. All marine magnetic data recorded on the Lake Winnipeg survey contains data gaps of the same duration. This may be related to a memory or software problem in the microprocessor.

2.4.6 Magnetic tape recording

Analogue magnetic tapes were recorded with a Hewlett Packard Model 3968 8-channel tape recorder. Recording was done at a tape speed of 3 3/4 inches per second (9.5 cm/s). Recording channels are given in Table 5. Digital recordings

were made using an SE880 recorder. Analogue and digital tape start and stop times are given in Tables 6 and 7, respectively.

2.5 CORING AND LARGE GRAB SAMPLES

2.5.1 Long cores

Eighteen widely-spaced sites were occupied and thirteen long gravity and piston cores, ranging in length from 2 m to 8 m, were obtained to sample the sediment in order to verify stratigraphy or features identified on the geophysical records (Table 8). Samples of the Lake Winnipeg and Lake Agassiz sediment sequences were recovered in both the North and South Basins (Fig. 12).

Coring system - The CCGS *Namao*, being designed as a navigational aids tender, is well suited for handling large equipment on the foredeck and for deployment over the side. The vessel is equipped with a 9 m cable boom having a 5 ton primary runner. The foredeck is approximately 8.5 m by 8.5 m in size with a raised hatch cover in the centre of the deck.

The AGC wide-diameter and Benthos medium-diameter piston coring systems were the primary tools used on the cruise. These systems and all other equipment were designed and built to be used on designated research vessels as well as ships of opportunity. This simplified the preparation, installation and handling of the corer on the CCGS *Namao*.

The coring systems consisted of the following components:

Core head - modified Benthos core head (907 kg, 2000 lb)
Core head - Benthos core head (907 kg, 2000 lb)
Murphy gravity corer (100 kg, 220 lb)
Core barrel - 4.25 inch (10.8 cm) inside diameter (ID) with 0.375 inch (0.95 cm) wall thickness for use with the first core head
Core barrel - 3 inch (6 cm) ID with 0.25 inch (0.64 cm) wall thickness for use with the second core head
Couplings - straight for wide-diameter core barrels, threaded for Benthos core barrels
Core barrel liner - cellulose acetate butyrate of 4.14 inch (10.52 cm) outer diameter (OD) and 3.904 inch (9.92 cm) ID or 2.875 inch (7.3 cm) OD and 2.625 inch (6.67 cm) ID
Trip arm
Trigger weight

Deployment and recovery of piston corer - The core head was rigged diagonally across the foredeck (Fig. 13). Each barrel was installed from the core head downward. As the core head and protruding barrels were set up, they were kept stable by wooden blocking. A maximum barrel length of 9 m was rigged due to space and handling limitations and the depth of the water in Lake Winnipeg. A rope was passed through the core head and each barrel and liner as they were inserted. The rope was then used to pull the wire cable through, attached to the piston. At the core site, the trigger weight cable was put through a snatch block on the boom's second runner and shackled to the side of the ship. The boom was lifted up until the trigger weight cleared the deck, then the weight was lowered over the side. It was left hanging from the side of the ship for later attachment of the trigger arm.

To deploy the piston corer, a harness was attached from the boom's second runner to the core barrels. The boom was used to lift and direct the barrels through an opening in the starboard rail (Figs. 14, 15). The whole system was boomed up and allowed to slide over the edge until vertical (Fig. 16). The trip arm and trigger weight were attached and the corer was positioned so its safety pin could be removed and the corer lowered to the lake bottom until it triggered. The triggering was automatic and was signalled by a recoil in the cable as the heavy corer "fell" freely into the sediment. On recovery, the reverse order of operations was used to place the core-filled corer on the foredeck. The core liner was then extruded from the core barrels (Fig. 17), cut in 5 foot-long (1.5 m) sections, sealed at the ends, labelled and stored upright in a core cooler on the foredeck (Fig. 3). At the conclusion of the cruise, this core cooler was transported to the GSCA core storage facility at the Bedford Institute of Oceanography in Dartmouth, Nova Scotia.

Two sets of piston coring gear were lost during the cruise, a highly unusual rate of loss. These losses were attributed to the remarkable ease of penetration of the corer into the soft lakefloor mud. The result of this condition was an excess velocity of the corehead weight when the piston encountered the stop; breakage of the cable and fiege fitting resulted. The degree to which these coring conditions were unanticipated is highlighted by the concern raised at the beginning of the cruise that the corehead weight on board might be insufficient to penetrate into the subbottom. The heavier corehead, which had originally been slated for use in Lake Winnipeg, had been lost in Lake Ontario in July, 1994, prior to its planned shipment to Selkirk.

It should be noted that the core cooler required repairs at Gimli twice during the cruise; waves breaking over the ship in rough weather had soaked the exposed control mechanism at the base of the cooler and caused it to malfunction. It was inadvisable to place the core cooler in such an exposed area on the foredeck, but the limited space on board the CCGS *Namao* precluded any other solution. In the future, however, the core cooler should be first placed in the hold of the ship before the geophysical lab is constructed.

As a result of the problems with the cooler and the unreliable behaviour of its internal fan system, some stored cores suffered freezing along their mid-sections, thus eliminating the possibility of meaningful studies of the physical properties of these zones.

Coring sites - In all, 18 deployments of coring devices were

undertaken on the cruise (Fig. 12). As listed in Table 8, there was one deployment of the AGC wide diameter long gravity corer (site 104a), six deployments of the AGC wide diameter piston core (sites 103, 104b, 105, 106, 107a, 108a), two deployments of the Murphy wide diameter gravity core (sites 107b, 108c), seven deployments of the Benthos long gravity core (sites 109, 110a, 113a, 115, 119, 121, 122a), and two deployments of the Benthos piston core (sites 120, 122b). In all cases except sites 109 and 110a, the ship was positioned at coring targets selected from Seistec profiles (Table 9). The AGC wide diameter piston corer was lost at site 108c and the Benthos piston corer was lost at site 122b.

2.5.2 Box cores

A series of 10 box cores were obtained from widely-spaced sites around Lake Winnipeg (Table 10, Fig. 18). The objective for all these samples was to obtain a high-resolution core of recent sedimentation for the study of pollution history and environmental change. The box corer obtains a cubic sample from the floor of the lake measuring about a half metre in each dimension. The device was retrieved over the side (Fig. 19), placed on the foredeck for cleaning and opening (Fig. 20) and then carefully subsampled using 10 cm diameter tubes and a vacuum pump to force the tubes into the sediment without disturbance (Fig. 21). Four tubes were obtained from each box core: two were used by the Freshwater Institute, one by the University of Manitoba, and one was sent to the GSCA core storage facility as an archive sample.

2.5.3 Large bottom grabs

Two Van Veen grab samples verified the presence of a thin veneer of mud over coarse sand in inferred large sand waves at The Narrows (Table 11).

2.6 LIMNOLOGICAL SAMPLING

2.6.1. Bottom sediment sampling

In order to map the texture and composition of bottom sediments, in particular the analysis of several variables not addressed by the 1969 Freshwater Institute survey, a systematic set of geological bottom sediment samples was collected. Prior to the cruise, 50 evenly spaced target sites were designated, with a more dense sampling grid in the South Basin. Figure 22 shows the actual stations occupied during the cruise. All samples were taken from the ship's launch. Positioning was determined using a portable GPS unit which displayed navigation instructions. An intact bottom sediment sample was recovered using a Ponar dredge or, in a few cases, an Eckman dredge (Table 12). Opening of the dredge permitted the intact sample to be placed in a plastic pan in the boat. A one litre sample was recovered from sediments within 5 cm of the sediment-water interface. This activity was assigned the lowest priority of the geological objectives. No samples were obtained at times when wave conditions prevented safe use of the launch. No sampling was done from the ship, in order to avoid interference with coring operations. Although 33 sampling stations were occupied (Fig. 22, Table 12), only 31 bottom sediment samples were obtained. At stations 9 and 38, a hard lake bottom was encountered, and no sediment was recovered.

2.6.2 Water column analyses

Air temperature, surface water temperature, and a Secchi disk measurement were recorded at all 33 sampling sites. Conductivity-temperature-depth (CTD) profiles were only taken at 24 of the sites, due to the necessity that the equipment be transferred to another Freshwater Institute project prior to the last two days of sampling.

Air and surface water temperature were recorded at each site using a digital thermometer. Secchi disk measurements, a measure of light transmission and hence turbidity, were made by lowering a standard black and white Secchi disk until it was not visible, and by recording the depth at which it was again visible while being raised.

CTD profiles (Appendix 2) were measured using an automated, self contained instrument supplied by the Freshwater Institute. After being turned on, the instrument was lowered by hand to the bottom at an approximate rate of 1 m per second, raised, and switched off. Temperature, conductivity, transmissivity and depth, as indicated by a pressure transducer, were recorded by the instrument at 1/3 second intervals. Date and time were automatically recorded by the instrument at power on. At the end of the cruise, the instrument was dismantled and data were down loaded to the RS-232 port of a portable IBM-compatible computer. Data obtained in air and during raising of the instrument were discarded. Profiles include data from below the sediment-water interface, due to the pointed, elongate geometry of the instrument.

Guidance and processing of the CTD data were generously contributed by Dr. Everett Fee of the Freshwater Institute.

2.6.3 Biological sampling

During the northbound leg of the cruise, phytoplankton samples consisting of 0.25 litres of surface water treated with a preservative were collected at 12 stations. These samples were obtained by pumping from approximately 1 m depth near the bow. During the southbound leg, a phytoplankton sample was taken at each sampling station. These samples were obtained from between the surface and about 0.5 m depth by dipping a rinsed plastic pail.

A zooplankton net haul was obtained by lowering a net until contact of the lower extremity of the net was made with the bottom. After a five second pause, the net was raised at a rate of about 0.75 to 1 m per second. Contents of the net were drained into a jar and the net was rinsed twice. Recovered

plankton were preserved in formaldehyde.

Excess dredged sediment remaining after the bottom sediment sample was taken was screened in order to recover benthic organisms, which were preserved in formaldehyde. Time constraints prevented quantitative recovery.

A few trawls to net pelagic fish along offshore transects were attempted, but were unsuccessful.

2.6.4 Water sampling

Two sets of water samples were taken during the cruise. Large volume water samples (20 L) were taken for the investigation of trace organic contaminants by the University of Winnipeg. A total of twelve samples were pumped into precleaned stainless steel transfer tanks using a submersible pump. The tanks were stored in a cooler on board to maintain a temperature of 2-8° C to preserve sample integrity. Smaller water samples, also acquired with the submersible pump, were taken at 21 sites during the northbound cruise and 33 sites on the southbound cruise for a complete analysis of water quality by the Freshwater Institute in Winnipeg. Subsamples, collected for dissolved silicon and dissolved organic carbon analyses, were placed in 100 mL jars containing a preservative. Further subsamples were filtered on board for the determination of chlorophyll, and particulate silicon, carbon, nitrogen, and phosphorus.

2.6.5 Air sampling

A total of ten air sample transects for the University of Winnipeg were taken over the duration of the cruise using a Grasby G.M.W. high-volume air sampler mounted at the bow of the ship (Fig. 3). The air sampler was fitted with a glass sampling head consisting of two filters in series, a glass fibre filter with a pore size of 1 μm followed by a three inch long plug of polyurethane foam. The glass fibre filter was used to trap persistent organic contaminants which are sorbed to particulate matter with a diameter of 1 μm. The polyurethane foam provided a trap for volatile and semi-volatile organic contaminants that exist in the vapour phase. Due to the low concentrations of the target organic contaminants in the air and water, it was necessary to sample large volumes of both matrices to ensure sufficient material for detection. The high-volume air sampler was, therefore, in use for as long as possible during each day of the cruise. Sampling was restricted to slow cruising speed and to times when prevailing winds carried the ship's exhaust away from the air sampler. During air sampling, wind speed and direction, air temperature, and atmospheric pressure were recorded at regular intervals. At the end of a sampling period, the filter and foam plug were placed in cleaned glass containers and frozen.

LIST OF TABLES

Table 1: List of Canadian Coast Guard personnel.

Table 2: List of scientific personnel.

Table 3: List of guests.

Table 4: Geophysical records.

Table 5. Analogue recording channels.

Table 6: Analogue tapes start and stop times.

Table 7: Digital tapes start and stop times.

Table 8: *Namao* 94-900 coring and large grab sample inventory.

Table 9: *Namao* 94-900 long core data.

Table 10: *Namao* 94-900 box core data.

Table 11: *Namao* 94-900 large grab sample description.

Table 12: Sampling survey data.

Table 1: List of Canadian Coast Guard personnel.

Title	Name
Commanding Officer	V. Isidoro
First Officer	S. Babisky
Chief Engineer	D. Richmond
First Engineer	D. Gnitzinger
Boatswain	F. Gnitzinger
Deckhand	W. Magnusson
Deckhand	J. Bartley
Deckhand	K. Cooke, Jr.
Deckhand/Steward	B. Sparks
Oiler	D. Fontaine
Cook	W. Peristy

Table 2: List of scientific personnel.

Title and duties	Name	Affiliation	Dates on board
Chief Scientist (Geophysical and coring surveys)	B.J. Todd	GSC, TSD	July 29-August 31
Scientist (Geophysical and coring surveys)	C.F.M. Lewis	GSCA	August 3-30
Scientist (Limnological sampling survey)	L.H. Thorleifson	GSC, TSD	August 4,5,9,18-30
Scientist (Liaison and logistics)	E. Nielsen	MEM	August 9,18-30
Scientist (Marine radar)	J. Pilon	GSC, TSD	July 29-August 18
Scientist (Air and water sampling)	G. Fisher-Smith	U of W	August 4-11,19
Scientist (Box core sampling)	L. Lockhart	FOC	August 20-30
Technologist (Multichannel seismic, watch keeping)	R.A. Burns	GSC, TSD	August 3-18
Technologist (Electronics, watch keeping)	A. Atkinson	GSCA	July 29-August 17
Technologist (Coring)	F.D. Jodrey	GSCA	August 18-September 1
Technologist (Mechanical, watch keeping)	K. Wagner	GSCA	July 29-August 19
Technologist (Navigation)	L. Johnson	GSCA	July 29-August 1
Logistics Manager	M. Gorveatt	GSCA	July 31-August 4

GSC: Geological Survey of Canada
TSD: Terrain Sciences Division
GSCA: Geological Survey of Canada (Atlantic)
MEM: Manitoba Energy and Mines
U of W: University of Winnipeg
FOC: Fisheries and Oceans Canada (Freshwater Institute)

Table 3: List of guests.

Name	Affiliation	Dates on board
K. Friesen	U of Winnipeg	August 4, 5
W.M. Buhay	U of Waterloo	August 8, 29
R. N. Betcher	MWRB	August 8, 30
W. Weber	MEM	August 10, 11
R.K. Bezys	MEM	August 10, 11
P.J. Henderson	GSC, TSD	August 26, 29
Hon. J. Gerrard and family (5)	Government of Canada	August 28
C. Pashadal	U of Manitoba	August 29
W.D. McRitchie	MEM	August 30
J.T. Teller	U of Manitoba	August 30

MWRB: Manitoba Water Resources Branch

Table 4: Geophysical records.

Date (August)	Julian day	Line No.	Line length (km)	Start / End times (UTC)			
				Seistec	Multi-channel seismic	Sidescan sonar	Marine Magnetometer
4	216	SB 1	14.2	1600-2000	tests	—	—
5	217	SB 2	23.4	1518-2000	1543-2004	—	—
8	220	SB 3	45.4	1410-2302	1558-2300	1623-2359	1741-2313
9	221	SB 4	43.3	1503-2220	1530-1830	1517-2220	1510-2236
10	222	SB 5	41.8	1440-2215	1610-2204	1443-2206	1545-2207
11	223	SB 6	58.8	1440-2231	1500-2230	1434-2230	1431-2233
12	224	SB 7	60	1405-2230	1430-2230	1408-2230	1407-2230
15	227	NB 8	62.6	1340-228/0045	1450-228/0045	1405-228/0044	1411-2400
17	229	NB 9	95.6	1145-2346	1200-2316	1148-2345	1151-2347
18	230	NB 10	53.3	1621-2310	1630-2310	1611-2311	1626-2319
19	231	NB 11	48.1	1413-2115	1420-2100	1425-2100	1419-2107

Table 5. Analogue recording channels.

Channel No.	Parameter	Type of recording
1	Port sidescan signal	FM (frequency modulation)
2	Sidescan reference trigger	DR (direct recording)
3	Starboard sidescan signal	FM
4	Seistec signal	DR
8	Voice annotation	FM

Table 6: Analogue tapes start and stop times.

Tape number	Start time	Stop time	Line Number
1	220 / 1705	220 /1901	SB3
2	220 / 1902	220 / 2143	SB3
3	220 / 2145	220 / 2259	SB3
4	221 / 1519	221 / 1700	SB4
5	221 / 1658	221 / 1836	SB4
6	221 / 1836	221 / 2030	SB4
7	221 / 2040	221 / 2220	SB4
8	222 / 1527	222 / 1707	SB5
9	222 / 1708	222 / 1843	SB5
10	222 / 1845	222 / 2135	SB5
11	222 / 2133	222 / 1710	SB5 & SB6
12	223 / 1711	223 / 1847	SB6
13	223 / 1848	223 / 2030	SB6
14	223 / 2032	223 / 2216	SB6
15	223 / 2218	224 / 1556	SB6 & SB7
16	224 / 1600	224 / 1736	SB7
17	224 / 1736	224 / 1915	SB7
18	224 / 1915	224 / 2054	SB7
19	224 / 2054	224 / 2230	SB7
20	227 / 1415	227 / 1552	NB8
21	227 / 1554	227 / 1730	NB8
22	227 / 1730	227 / 1928	NB8
23	227 / 1728	227 / 2107	NB8
24	227 / 2108	228 / 0008	NB8
25	228 / 0008	229 / 1254	NB8 & NB9
26	229 / 1256	229 / 1435	NB9
27	229 / 1435	229 / 1614	NB9
28	229 / 1614	229 / 1750	NB9
29	229 / 1750	229 / 1928	NB9
30	229 / 1928	229 / 2106	NB9
31	229 / 2106	229 / 2246	NB9
32	229 / 2247	229 / 2345	NB9
33	230 / 1614	230 / 1751	NB10
34	230 / 1752	230 / 1927	NB10
35	230 / 1928	230 / 2106	NB10
36	230 / 2106	230 /2240	NB10
37	230 / 2141	230 / 2311	NB10
38	231 / 1430	231 / 1629	NB11
39	231 / 1629	231 / 1709	NB11
40	231 / 1709	231 / 1945	NB11
41	231 / 1945	231 / 2100	NB11

Table 7: Digital tapes start and stop times.

Tape number	Start time	Stop time	Line Number
1	217 / 1605	217 / 2004	SB2
2	220 / 1545	220 / 2259	SB3
3	221 / 1505	221 / 2220	SB4
4	222 / 1612	222 / 2204	SB5
5	223 / 1435	223 / 2230	SB6
6	224 / 1430	224 / 2230	SB7
7	227 / 1425	228 / 0030	NB8
8	229 / 1155	229 / 2345	NB9
9	230 / 1630	230 / 2311	NB10
10	231 / 1413	231 / 2120	NB11

Table 8: *Namao* 94-900 coring and large grab sample inventory.

Sample Number	Sample Type	Geographic Location	Julian Day / UTC Time	Latitude Longitude	Water Depth (m)	Seistec Line Time
101	box core	western North Basin	233 / 1646	53 12.02 99 06.99	12.2	NB9 229 / 2345
102	box core	central North Basin	234 / 1526	53 28.10 98 20.20	15.9	NB9 229 / 1539
103	AGC wide diameter piston core	central North Basin	234 / 1642	53 27.29 98 21.95	15.9	NB9 229 / 1558
104a	AGC wide diameter long gravity core	northeast North Basin	235 / 1506	53 35.05 98 05.11	16.1	NB9 229 / 1257
104b	AGC wide diameter piston core	northeast North Basin	235 / 1627	53 35.04 98 05.07	15.8	NB9 229 / 1257
105	AGC wide diameter piston core	northeast North Basin	235 / 1848	53 35.64 98 03.80	15.9	NB9 229 / 1243
106	AGC wide diameter piston core	northeast North Basin	235 / 2031	53 34.70 98 05.83	17.1	NB9 229 / 1305
107a	AGC wide diameter piston core	north of George Is.	236 / 1740	52 55.85 97 47.31	17.1	NB8 227 / 1717
107b	Murphy wide diameter gravity core	north of George Is.	236 / 1815	52 55.83 97 47.31	17.1	NB8 227 / 1718
108a	AGC wide diameter piston core	west of George Is.	236 / 2014	52 50.41 98 02.30	18.3	NB8 227 / 2057
108b	box core	west of George Is.	236 / 2050	52 50.41 98 02.29	17.1	NB8 227 / 2057
108c	Murphy wide diameter gravity core	west of George Is.	236 / 2108	52 50.39 98 02.27	23.5	NB8 227 / 2057
109	Benthos long gravity core	north of Berens Is.	237 / 1447	52 31.60 97 22.25	15.2	—
110a	Benthos long gravity core	southern North Basin	237 / 1806	52 00.15 97 01.45	11.3	—

Sample Number	Sample Type	Geographic Location	Julian Day / UTC Time	Latitude Longitude	Water Depth (m)	Seistec Line Time
110b	box core	southern North Basin	237 / 1806	52 00.15 97 01.45	11.3	—
111	Van Veen grab	The Narrows	237 / 2008	51 45.65 96 51.65	25	SB7 224 / 1941
112	Van Veen grab	The Narrows	237 / 2025	51 45.71 96 51.76	25.6	SB7 224 / 1942
113a	Benthos long gravity core	Washow Bay	237 / 2244	51 24.09 96 37.53	9.8	SB6 223 / 2138
113b	box core	Washow Bay	237 / 2252	51 24.08 96 37.52	9.8	SB6 223 / 2138
114	box core	South Basin	238 / 1515	50 58.74 96 39.39	10.7	SB5 222 / 1814
115	Benthos long gravity core	South Basin (Pearson Reef)	238 / 1551	50 56.76 96 40.90	10.7	SB5 222 / 1733
116	box core	South Basin	238 / 1741	50 39.86 96 47.98	10.1	SB3 220 / 1946
117	box core	South Basin	240 / 1504	50 50.00 96 49.20	10.4	SB4 221 / 1619
118	box core	Traverse Bay South Basin	241 / 1543	50 45.32 96 29.15	7.9	SB4 221 / 2105
119	Benthos long gravity core	Traverse Bay South Basin	241 / 1622	50 48.19 96 31.81	9.8	SB4 221 / 2008
120	Benthos piston core	Traverse Bay South Basin	241 / 1825	50 48.91 96 32.70	10.1	SB4 221 / 1952
121	Benthos long gravity core	South Basin	241 / 2006	50 50.00 96 49.20	10.4	SB4 221 / 1619
122a	Benthos long gravity core	South Basin	241 / 2144	50 39.39 96 48.28	9.8	SB3 220 / 1937
122b	Benthos piston core	South Basin	242 / 1503	50 39.40 96 48.28	10.1	SB3 220 / 1937
123	box core	South Basin	242 / 1627	50 32.49 96 49.99	9.1	SB3 220 / 1723

Note: 1. Wide diameter cores are 10 cm in diameter; other cores are 6 cm in diameter.
2. The head weight for piston and gravity cores was 907 kg (2000 lb).

Table 9: *Namao* 94-900 long core data.

Sample Number	Sample Type	Geographic Location	Corer Length (cm)	Apparent Penetration (cm)	No. of Sections	Core Length (cm)	Notes
103	AGC wide diameter piston core	central North Basin	900	950	3	816	Objective: Winnipeg Sequence and contact over middle reflection package of Agassiz Sequence 1. Clean trip; core head came down hard on piston and cable. Sea state about 0.5-1.0 m; ship probably heaving 2. Board attached to base of trip weights to ensure triggering occurred at sediment-water interface
104a	AGC wide diameter long gravity core	northeast North Basin	900	940	3	375	Objective: sample thin Winnipeg Sequence unconformably overlying upper Agassiz Sequence 1. Lowered into bottom under power; no free fall 2. Two interpretations of limited core recovery - 1) corer penetrated but sediment was bypassed (F. Jodrey) or 2) corer penetrated 3.75 m, then fell over into soft surface mud (M. Lewis) 3. Live animals seen moving at top of core, so no sediment was lost from Winnipeg Sequence. Base was firm grey clay, sticky, slippery and grit-free
104b	AGC wide diameter piston core	northeast North Basin	900	not clear	5	670	Objective: same as 104a 1. 2 foot free fall. Clean triggering, no "bang" on piston core 2. Corer triggered while ship maneuvering to get on exact station coordinates. Corer weights were thought to be dragging so winchman reeled in cable. Triggering occurred while this was happening so corer may have penetrated off vertical
105	AGC wide diameter piston core	northeast North Basin	900	570	6	612	Objective: Sample thin Winnipeg Sequence unconformably overlying lower part of Agassiz Sequence 1. Good triggering, no bang on piston 2. Bottomed on gravel layer (in AB section) over hard dense clay (in AB and cutter)
106	AGC wide diameter piston core	northeast North Basin	900	800	6	800	Objective: Sample thin Winnipeg Sequence and the unconformably underlying middle Agassiz Sequence 1. Good triggering; corehead did not come down hard on piston 2. Grey silt at top over grey clay with no trace of silt
107a	AGC wide diameter piston core	north of George Is.	900	870	5	715	Objective: Sample thin (2-3 m) Winnipeg Sequence over unconformity truncating underlying Agassiz Sequence 1. Easy trigger; core weight did not come down hard on piston 2. Ship was heaving 60 cm in waves, determined by change of water depth registered on ship's echo sounder (Raytheon RTT 1000)
107b	Murphy wide diameter gravity core	north of George Is.	—	—	—	3	Objective: Sample upper 1-2 m of Winnipeg Sequence 1. Cutoff sock was fitted over retaining fingers to enhance retention of core - with little effect 2. Bag saved of 3 cm remaining on fingers 3. Very soft mud

Sample Number	Sample Type	Geographic Location	Corer Length (cm)	Apparent Penetration (cm)	No. of Sections	Core Length (cm)	Notes
108a	AGC wide diameter piston core	west of George Is.	900	—	—	—	Objective: Sample Winnipeg Sequence (about 5 m) and underlying unconformity into undisturbed, then disturbed Agassiz Sequence 1. Corer lost. Upon triggering, corer head came down hard on piston at same time as ship was heaving upward; cable parted at drum. Ship was heaving at least 60 cm in waves, as for 107a.
108c	Murphy wide diameter gravity core	west of George Is.	?	—	—	—	1. Drop site was 195 feet SE of planned site 2. No recovery
109	Benthos long gravity core	north of Berens Is.	600	—	—	—	Objective: "blind" sample of southern North Basin sediment; no seismic profile available 1. Corer lowered under power; no free fall 2. Cutter sample only 3. Recovered hard friable clay; no mud
110a	Benthos long gravity core	southern North Basin	600	—	2	237	Objective: "Blind" sample of sediments in southern North Basin; no seismic profiles available 1. Corer lowered into bottom under power; no free fall 2. Hard clay under soft, olive-grey mud
113a	Benthos long gravity core	Washow Bay	600	700	2	216	Objective: Sample of Winnipeg Sequence in Washow Bay (about 9 m thick on Seistec record) 1. Recovery only on second attempt 2. Mud at base
115	Benthos long gravity core	South Basin (Pearson Reef)	600	380	2	283	Objective: Sample paleoshoreface (?) sand deposits beneath about 4 m of Winnipeg Sequence 1. Cutter empty and damaged 2. Cutter edge is curled up in a few places, implying corer struck stones in gravel 3. Base of core is sand under mud
119	Benthos long gravity core	Traverse Bay South Basin	900	270	3 and cutter	329	Objective: Sample thin Winnipeg Sequence, unconformity and underlying Agassiz Sequence 1. 1.5 m drop 2. Bent lowest barrel 3. Hard grey clay in cutter; laminations seen through liner of AB section
120	Benthos piston core	Traverse Bay South Basin	600	—	3 and cutter	359	Objective: Winnipeg Sequence, unconformity and underlying Agassiz Sequence 1. 7 foot free fall 2. Hard orange brown clay in cutter and catcher and on shoulder of first coupling 3. Piston did not detach (as it was supposed to) and was located 5 feet below core head. As only about 5 feet of hard clay was recovered, yet it penetrated >10 feet of clay, the core and piston must have been pulled down 5 feet during pullout

Sample Number	Sample Type	Geographic Location	Corer Length (cm)	Apparent Penetration (cm)	No. of Sections	Core Length (cm)	Notes
121	Benthos long gravity core	South Basin	900	930	6 and cutter	558	Objective: Sample thick Winnipeg Sequence over Agassiz sequence, basal disturbed part 1. 5 foot free fall 2. Liner probably not aligned between barrels 3. Fell OK without tightening cable. Cable had wound around pipe/corehead which fell free with mild thump during up haul 4. Firm grey clay with white silt partings in base of core
122a	Benthos long gravity core	South Basin	900	960	5 and cutter	488	Objective: Thick Winnipeg Sequence over Agassiz Sequence with 'offset' reflections 1. 5 foot free fall 2. Straight drop; tough pullout as ship listed slightly
122b	Benthos piston core	South Basin	900	—	—	—	Objective: Recover high quality thick Winnipeg Sequence over Agassiz clay at site of previous gravity core (site 122a) 1. No free fall; set to trigger at sediment surface 2. Perfect triggering; ship paused during 0.5 m heavings; occurred above water. Trigger arm rose about 2 feet before releasing core head 3. Lost corer; fiege fitting broke at hole around pin connecting it to the piston

Table 10: *Namao* 94-900 box core data.

Core Sample Number	Geographic Location	Corer Length (cm)	Total Length (cm)	Notes
101	western North Basin	60	47	Objective: High-resolution core of recent sedimentation for study of pollution history and recent environmental change 1. High quality box core obtained on second attempt when two 2" by 6" planks were attached to the base of the box core frame to prevent excessive penetration into the very soft surface mud. 2. Core location is immediately offshore mouth of the Saskatchewan River. Sample should be characteristic of Saskatchewan River sediment input. 3. Four sample tubes were recovered: I) L. Lockhart (FWI); sample sliced at 1 cm interval ii) L. Lockhart (FWI); all bottled for biota iii) L. Lockhart (FWI) for W. Last (U. of Manitoba); sliced at 1 cm interval iv) GSC (AGC) whole core tube
102	central North Basin	60	52	Objective: as for 101 1. Rough lake, ship was heaving about 0.6 m. Surface oxidized sediment was slightly pushed to one side, probably by box movement during penetration 2. Four sample tubes as in 101
108b	west of George Is.	60	47	Objective: High resolution sample of recent Lake Winnipeg sedimentation in central-western North Basin 1. Good quality core, nearly full 2. Bagged 0-2 cm for screening for coarse fraction and ostracodes 3. Four sample tubes as for 101
110b	southern North Basin	60	47	Objective: High resolution sample of recent sediment accumulation in southern North Basin 1. Good quality core, nearly full 2. Bagged 0-2 cm 3. Four sample tubes as for 101
113b	Washow Bay	70	50	Objective: High resolution sample of recent sediment accumulation in Washow Bay 1. Good quality core, nearly full 2. Bagged 0-2 cm 3. Four sample tubes as for 101
114	South Basin	70	58	Objective: High resolution sample of recent sediment accumulation in northern South Basin 1. Good quality core, full. Brown surface on soft grey mud. 2. Four sample tubes as for 101
116	South Basin	70	50	Objective: High resolution sample of recent sediment accumulation in southern South Basin 1. Good quality core, full. 2. Bagged 0-2 cm 3. Four sample tubes as for 101

Core Sample Number	Geographic Location	Corer Length (cm)	Total Length (cm)	Notes
117	South Basin	—	—	Objective: High resolution sample of recent sediment accumulation in South Basin 1. Good quality core despite rough weather. 2. Bagged 0-2 cm 3. Four sample tubes as for 101
118	Traverse Bay South Basin	60	38	Objective: High resolution sample of recent sediment accumulation in Traverse Bay 1. Good quality core, about 3/4 full 2. Bagged 0-2 cm 3. Four sample tubes as for 101
123	South Basin	60	—	Objective: Sample undisturbed sediments, based on Seistec profile evidence, for study of recent sediment accumulation at southern end of South Basin 1. Two attempts; first attempt rejected because of some disturbance; sampler was dragged on bottom 2. Some grey mud lumps dropped onto sediment surface from interior of upper framework, probably emplaced during first try. Sample tube positions selected to minimize their presence but some may be present. 3. Bagged 0-2 cm. 4. Four sample tubes as for 101.

Note: 10 cm diameter core tubes used to subsample box cores.

Table 11: *Namao* 94-900 large grab sample description.

Sample Number	Sample Type	Geographic Location	Notes
111	Van Veen grab	The Narrows	Objective: Sample from 5-m high sand wave observed on Seistec record 1. Photographed and bagged 2. 0-1 cm soft oxidized brown mud 1-2 cm clean coarse sand 2-3 cm hard grey clay
112	Van Veen grab	The Narrows	Objective: Sample from area adjacent to 5-m high sand wave observed on Seistec record 1. Photographed and bagged 2. Brown soft mud over hard grey clay with scattered patches of m-c sand plus large water-worn clam shell fragment on interface (with sand)

Table 12: Sampling survey data.

Count	Site	Latitude (deg, min)	Longitude (deg, min)	Date (August)	Time (CDT)	Weather	Sounder depth (ft)	CTD line (m)	Corrected depth (m)	Secchi depth (m)	Air temp. (C)	Water temp. (C)	Benthos sample method	Bottom sediment
1	1	53 13.300	98 50.940	19	2020	sunny, calm	44	14.5	13.9	2.5	18.8	19.1	3/4 Ponar minus 1 litre	clay
2	2	53 25.706	98 49.224	19	1830	sunny, calm	45	15.0	14.3	3.3	19.8	19.0	2/3 Ponar - 1 litre	clay
3	3	53 38.274	98 47.271	19	1600	sunny, calm	42	13.0	12.4	3.0	19.8	18.9	Full Eckman	clay
4	4	53 44.190	98 27.919	19	1435	sunny, calm	42	13.4	12.8	4.0	19.7	18.4	Full Eckman	clay
5	5	53 36.512	98 11.055	23	1000	overcast, swell		15.5	14.8	2.4	17.9	17.2	Ponar - 1 litre	clay
6	6	53 31.239	98 30.061	19	1240	sunny, calm	49	15.3	14.6	3.5	17.8	20.2	Full Eckman	clay
7	7	53 18.967	98 32.018	19	1035	sunny, calm	51	15.7	15.0	2.9	18.4	18.5	Full Eckman	clay
8	8	53 24.024	98 13.103	23	1310	overcast, swell		16.0	15.3	2.5	20.3	17.5	Ponar - 1 litre	clay
9	9	53 29.300	97 53.861	23	1130	overcast, swell		14.8	14.1	1.7	18.0	17.2	none	none
10	10	53 16.711	97 56.121	23	1430	overcast, swell		17.0	16.3	2.2	19.1	17.8	Ponar - 1 litre	sandy silt
11	25	52 18.121	97 12.594	25	0945	sunny, breeze		9.8	9.3	1.0	18.8	18.8	Ponar - 1 litre	silty clay
12	28	52 06.703	97 07.820	25	1120	sunny, breeze		10.0	9.6	1.0	19.3	19.0	Ponar - 1 litre	clay
13	29	51 57.373	97 01.207	25	1230	sunny, breeze		11.3	10.8	0.8	20.8	20.1	Ponar - 1 litre	silty clay
14	30	51 48.211	96 54.496	25	1345	sunny, breeze		13.0	12.4	0.8	18.4	20.8	Ponar - 1 litre	silty clay
15	31	51 39.262	96 44.596	25	1450	sunny, breeze		15.0	14.3	0.8	19.8	20.0	3/4 Ponar - 1 litre	sandy silty clay
16	32	51 28.969	96 40.737	25	1620	sunny, breeze		9.3	8.8	0.6	23.8	20.8	Ponar - 1 litre	silty clay
17	33	51 19.138	96 35.290	25	1740	sunny, breeze		12.8	12.2	0.6	21.9	21.9	3/4 Ponar - 1 litre	sandy silty clay
18	34	51 12.028	96 34.802	25	1830	sunny, breeze		12.4	11.9	0.6	19.2	20.2	Ponar - 1 litre	gravelly clay
19	35	51 06.645	96 29.857	26	0930	sunny, breeze		10.4	9.9	0.8	18.3	19.5	Ponar - 1 litre	clay

Count	Site	Latitude (deg, min)	Longitude (deg, min)	Date (August)	Time (CDT)	Weather	Sounder depth (ft)	CTD line (m)	Corrected depth (m)	Secchi depth (m)	Air temp. (C)	Water temp. (C)	Benthos sample method	Bottom sediment
20	36	51 01.311	96 35.414	26	1025	sunny, breeze		10.5	10.0	1.1	16.8	19.4	Ponar - 1 litre	silty clay
21	37	50 55.909	96 30.504	29	1410	overcast, windy	34		10.4	1.0	18.3	18.6	Ponar - 1 litre	clay
22	38	50 50.468	96 25.701	29	1330	overcast, windy	26		7.9	0.7	17.0	18.5	none	none
23	39	50 44.993	96 25.962	29	1115	overcast, windy	26		7.9	0.7	15.2	18.0	½ Ponar - 1 litre	soft over hard clay
24	40	50 39.645	96 24.620	29	1230	overcast, windy	15		4.6	0.6	16.7	18.1	3/4 Ponar - 1 litre	sand
25	41	50 50.573	96 36.018	29	1500	sunny, breeze	35		10.7	0.6	16.0	19.2	Ponar - 1 litre	clay
26	42	50 56.942	96 40.796	26	1110	sunny, breeze		10.1	9.7	1.0	17.1	19.6	Ponar - 1 litre	clay
27	43	50 56.339	96 51.179	26	1150	sunny, breeze		8.8	8.4	0.8	17.1	19.7	Ponar - 1 litre	silty clay
28	44	50 50.782	96 46.148	26	1250	sunny, breeze		10.2	9.8	1.3	18.1	19.7	Ponar - 1 litre	clay
29	45	50 45.311	96 41.381	29	1000	overcast, windy	33		10.1	0.8	15.4	18.0	Ponar - 1 litre	clay
30	46	50 45.456	96 51.561	26	1345	overcast, calm		10.0	9.6	1.1	19.0	19.8	Ponar - 1 litre	clay
31	47	50 39.981	96 46.846	29	1600	cloud, windy	39		11.9	1.0	16.1	18.6	Ponar - 1 litre	clay
32	49	50 34.718	96 52.046	30	0900	cloud, windy	28		8.5	0.4	13.5	16.9	Ponar - 1 litre	clay
33	50	50 29.275	96 47.308	30	1100	cloud, windy	23		7.0	0.3	12.6	17.1	Ponar - 1 litre	clay

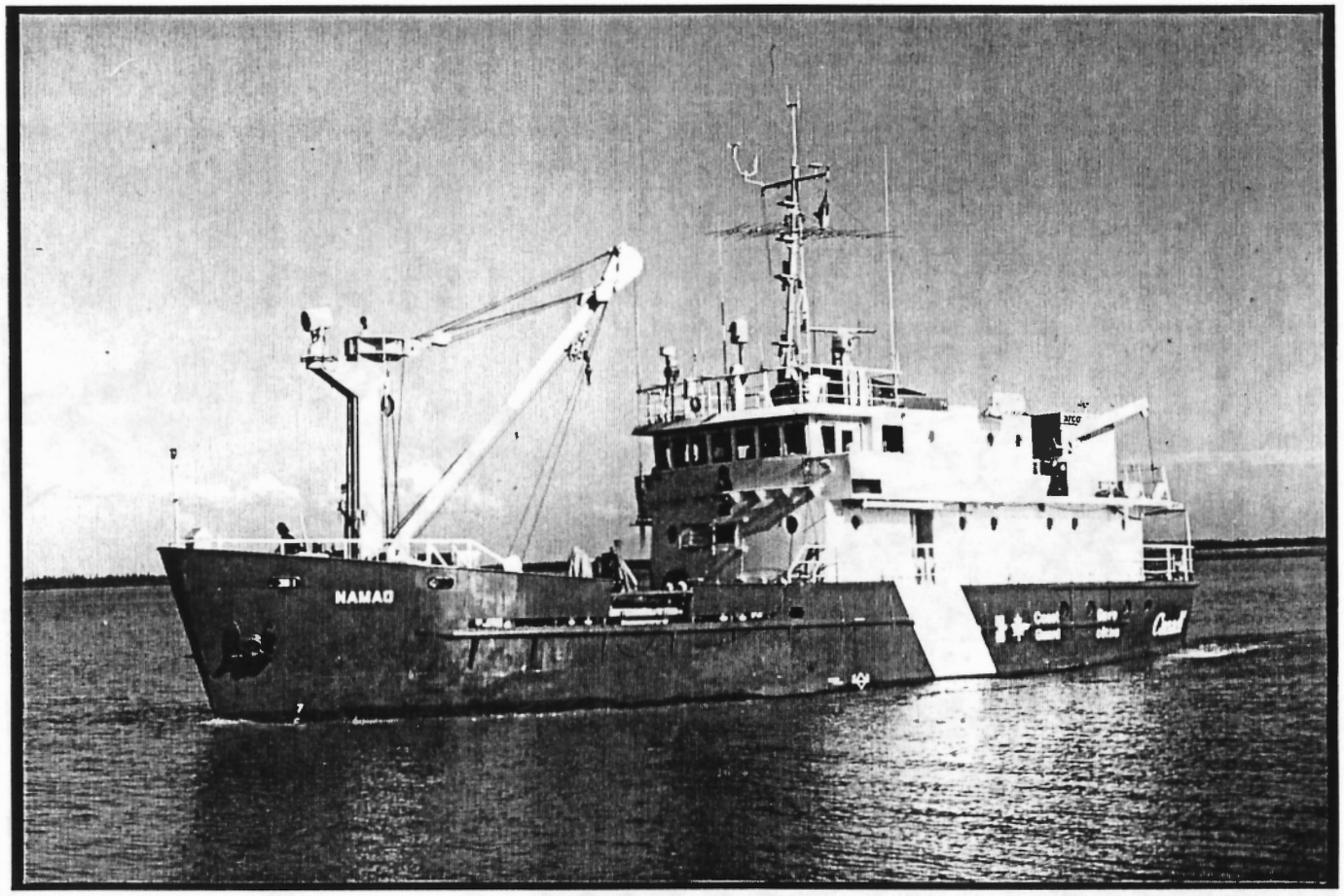

GSC photo 1995-174C, L.H. Thorleifson

Figure 1. CCGS *Namao*.

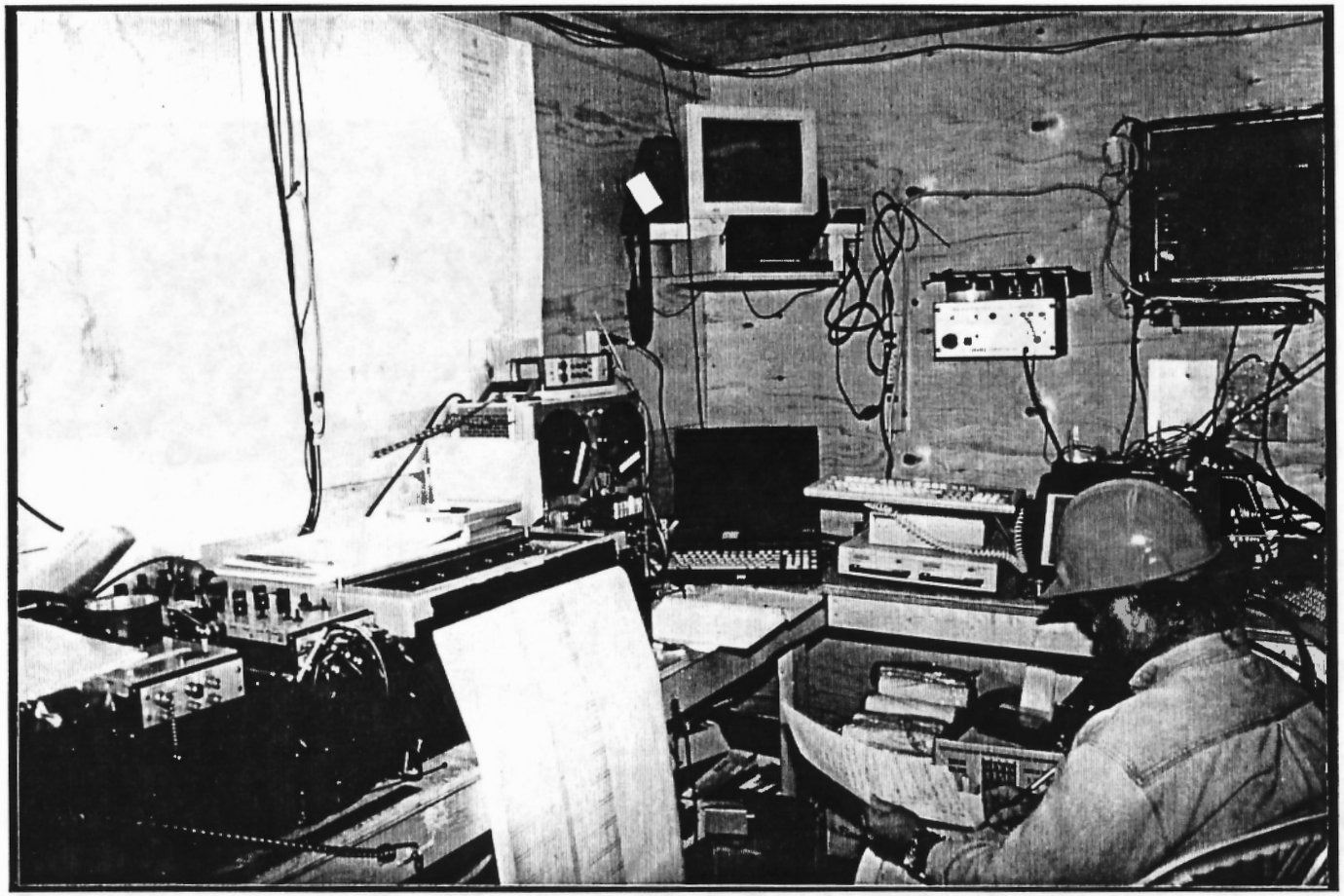

GSC photo 1995-174G, B.J. Todd

Figure 2. Interior of the geophysical laboratory in the hold of the CCGS *Namao.*

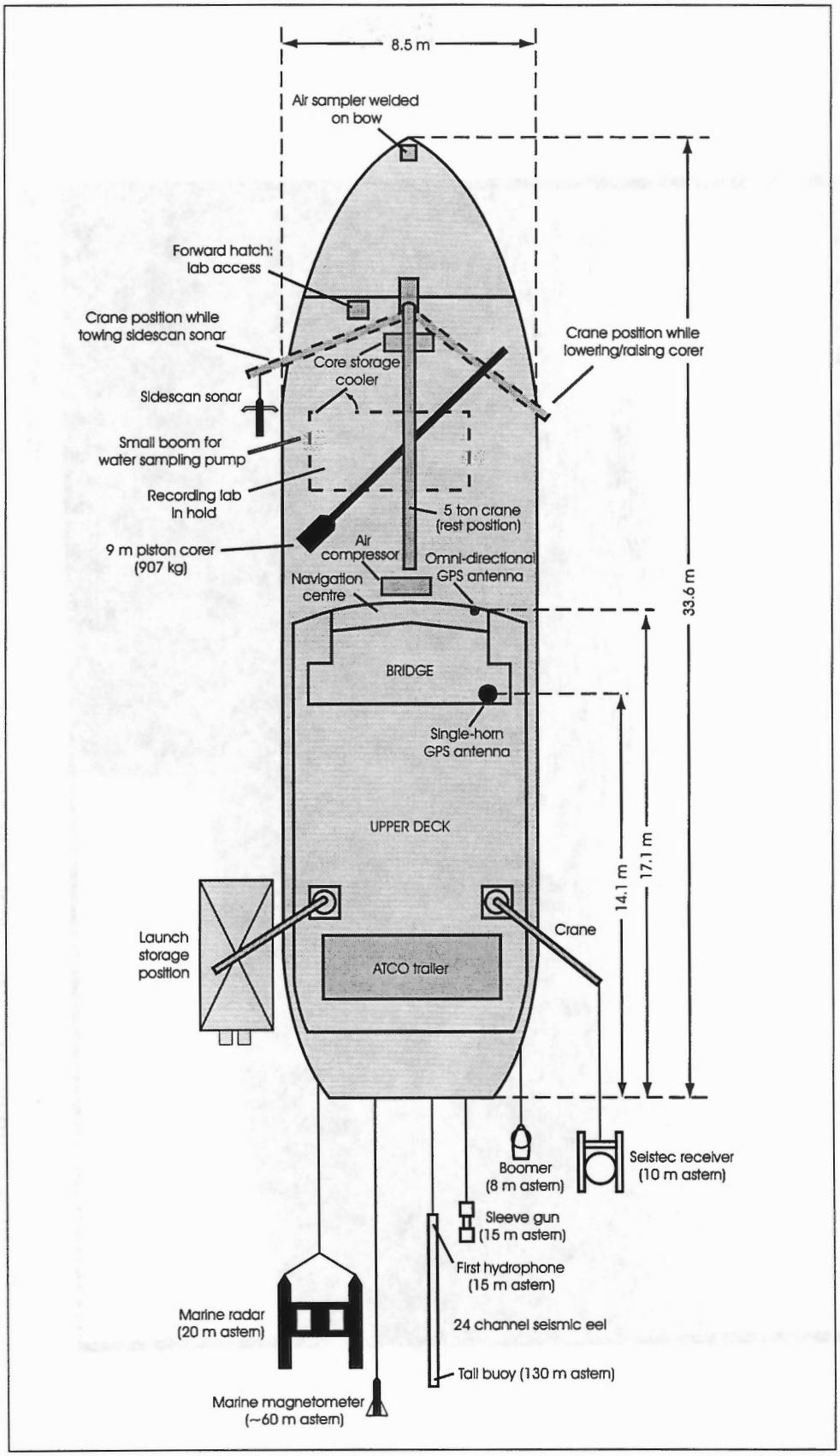

Figure 3. Layout of scientific equipment on CCGS *Namao*.

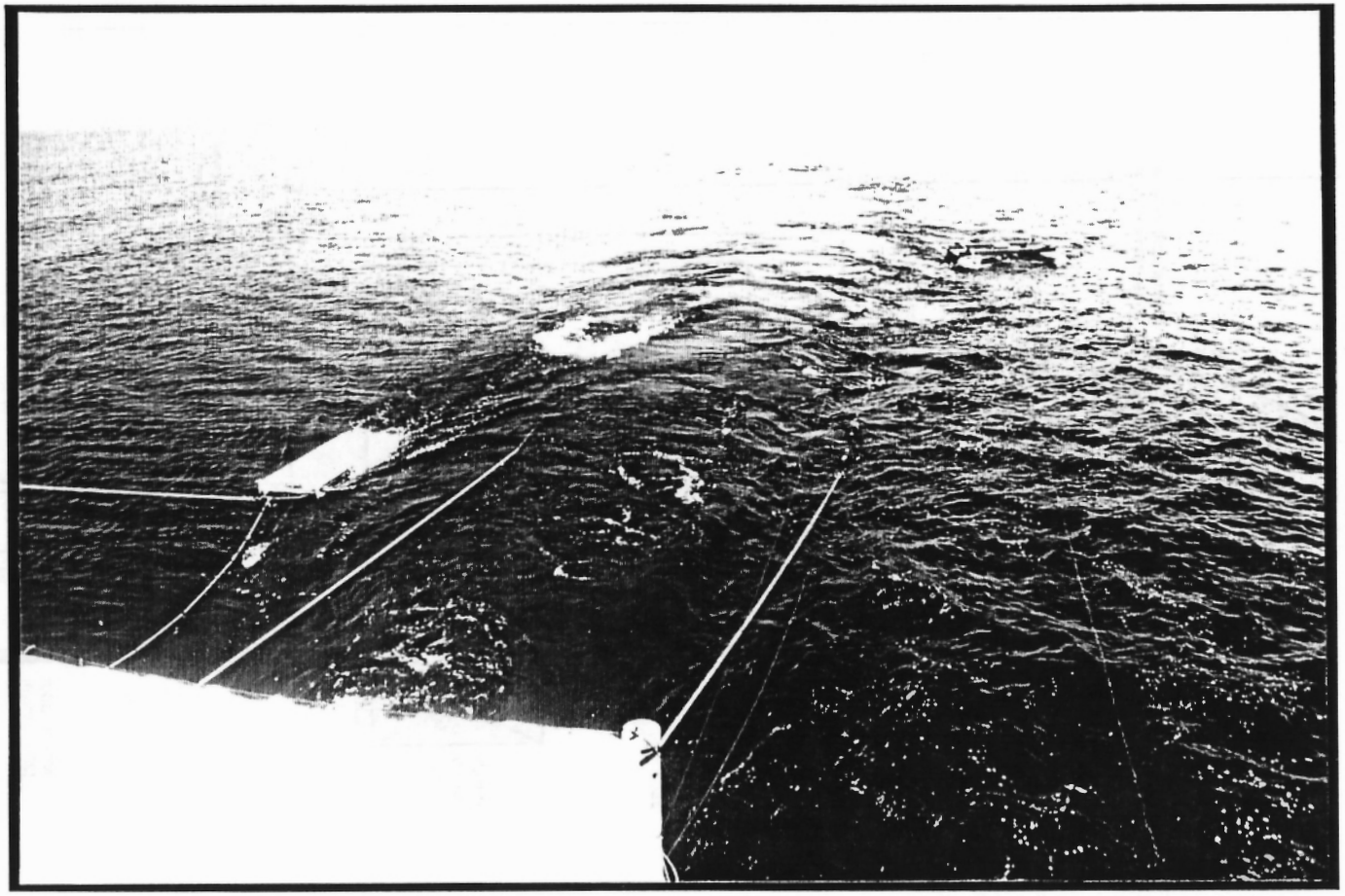

GSC photo 1995-174B, B.J. Todd

Figure 4. Streaming geophysical gear astern of the CCGS *Namao*. From left to right are the Seistec receiver and boomer, the sleeve gun, the seismic eel, the magnetometer, and the marine radar catamaran.

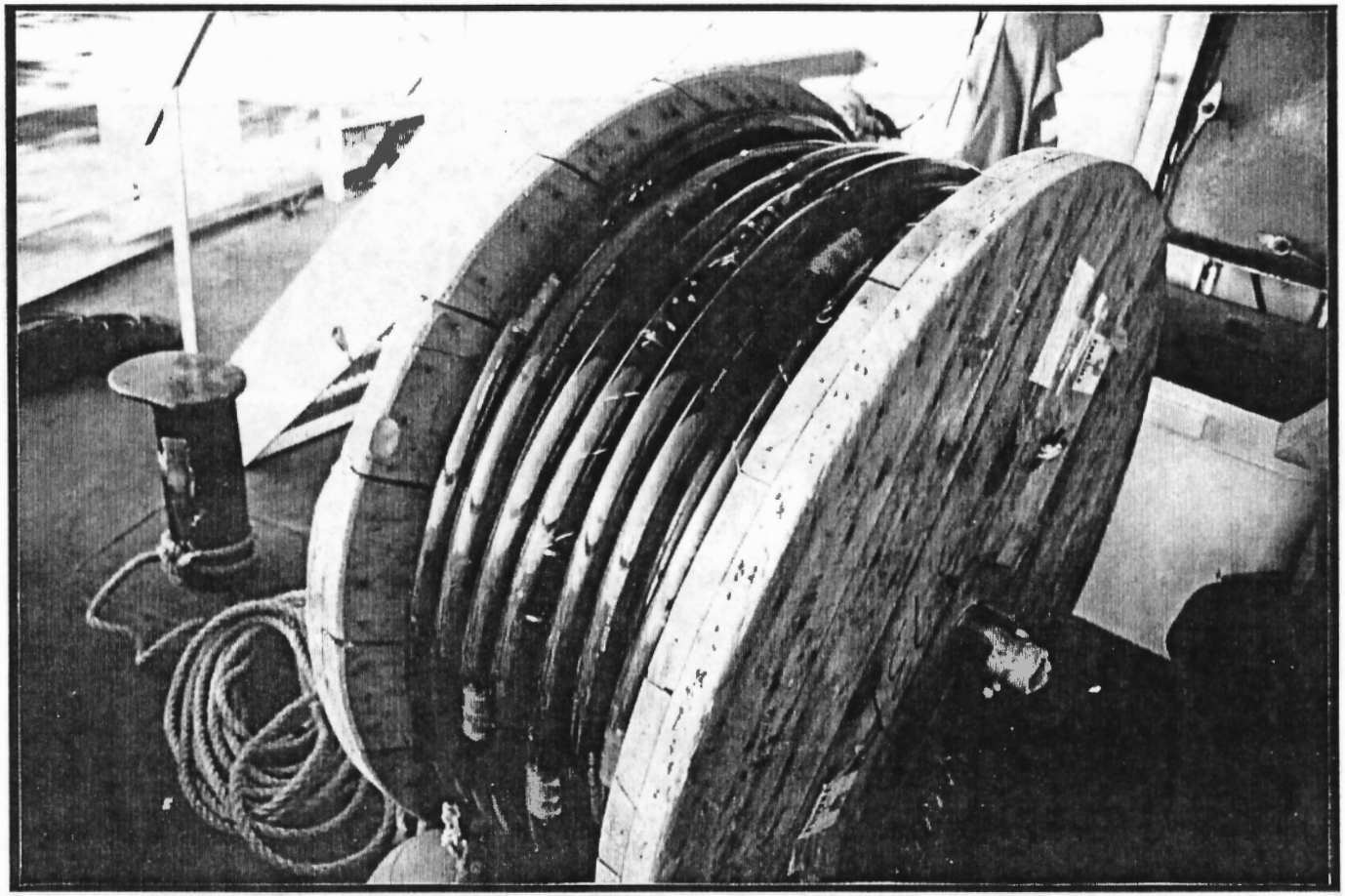

GSC photo 1995-174H, B.J. Todd

Figure 5. Seismic eel.

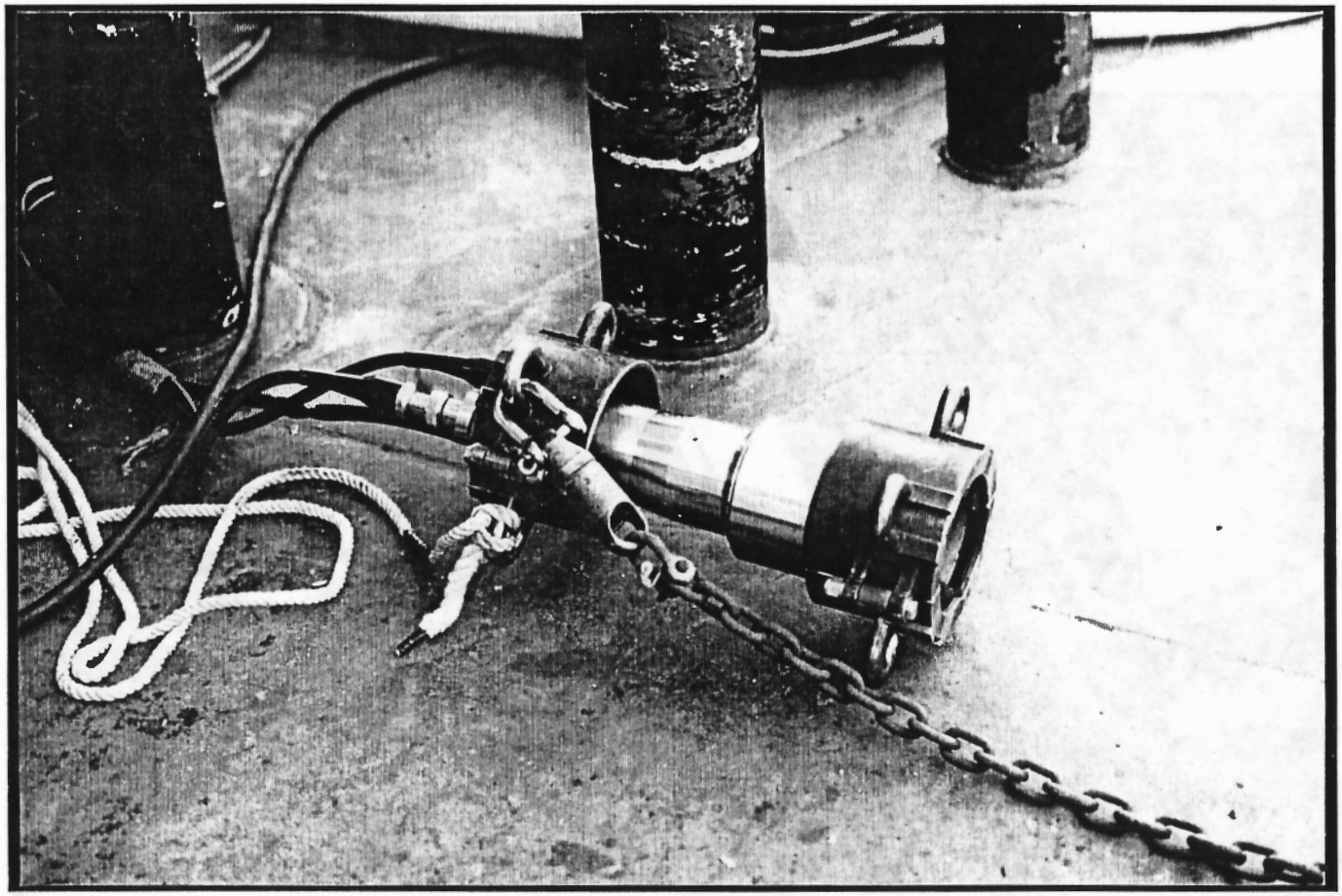

GSC photo 1995-174J, L.H. Thorleifson

Figure 6. Sleeve gun.

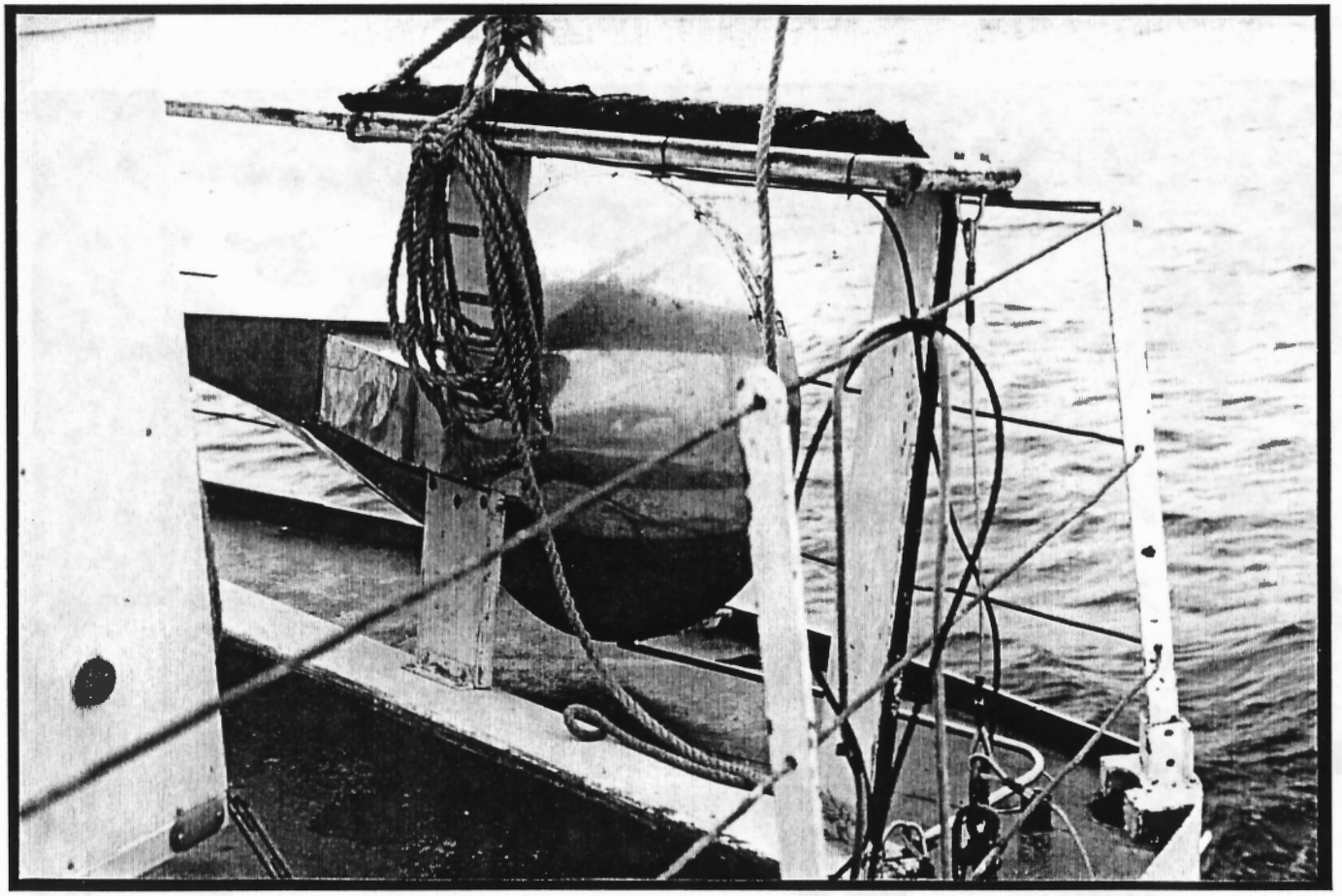

GSC photo 1995-174M, L.H. Thorleifson

Figure 7. Top side of the Seistec receiver, here resting on its side.

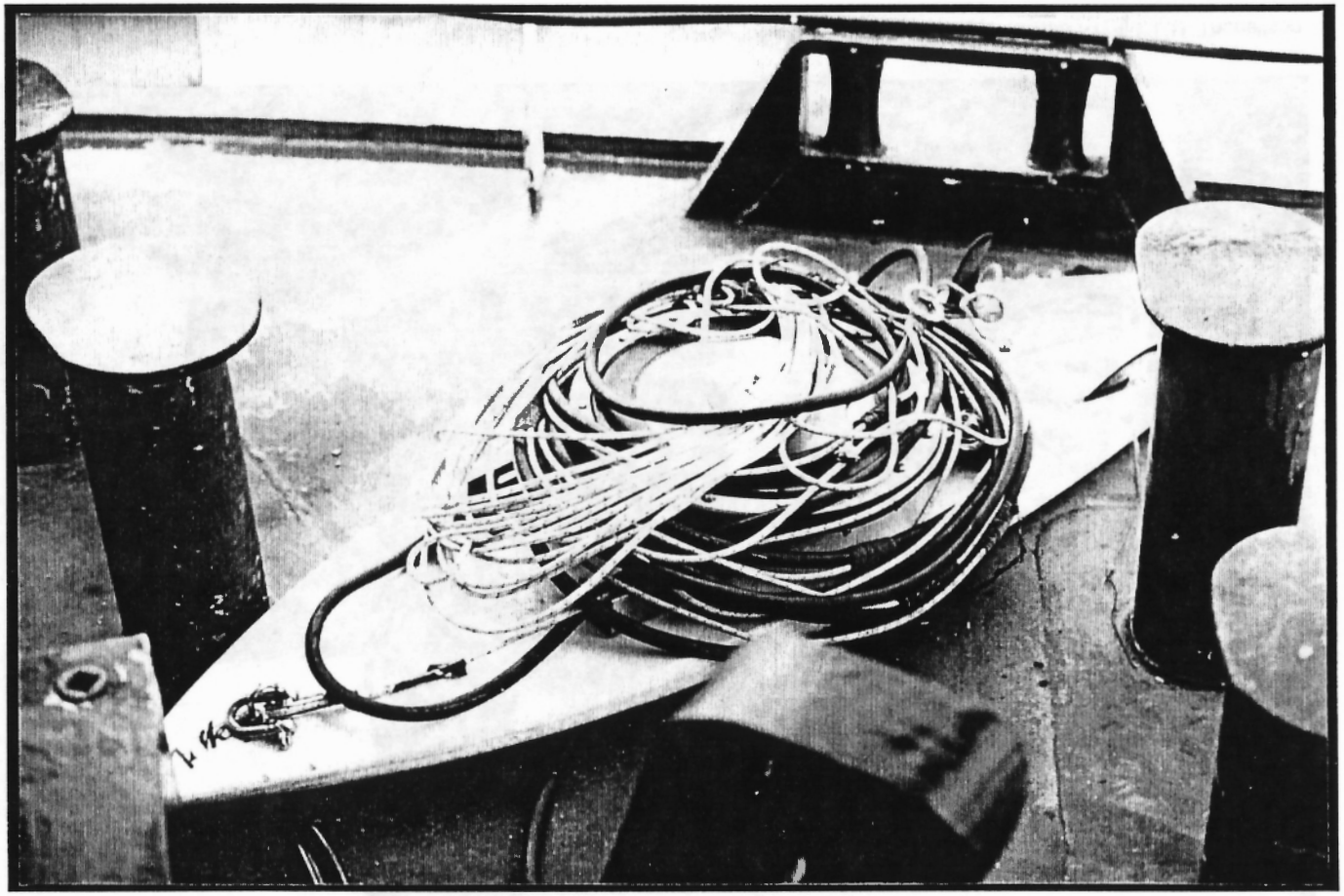

GSC photo 1995-174K, L.H. Thorleifson

Figure 8. Boomer mounted under surfboard.

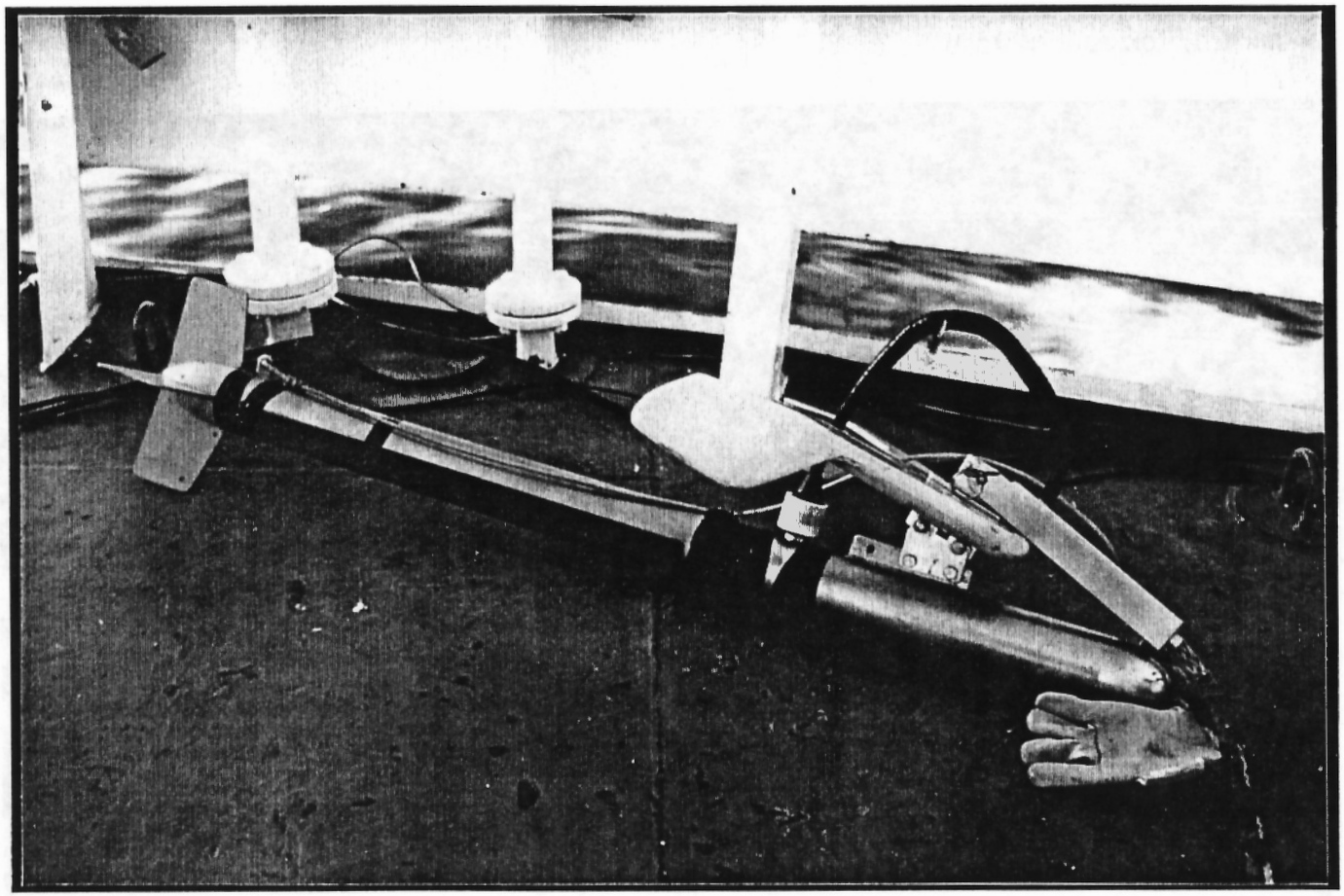

GSC photo 1995-174I, B.J. Todd

Figure 9. Sidescan sonar towfish.

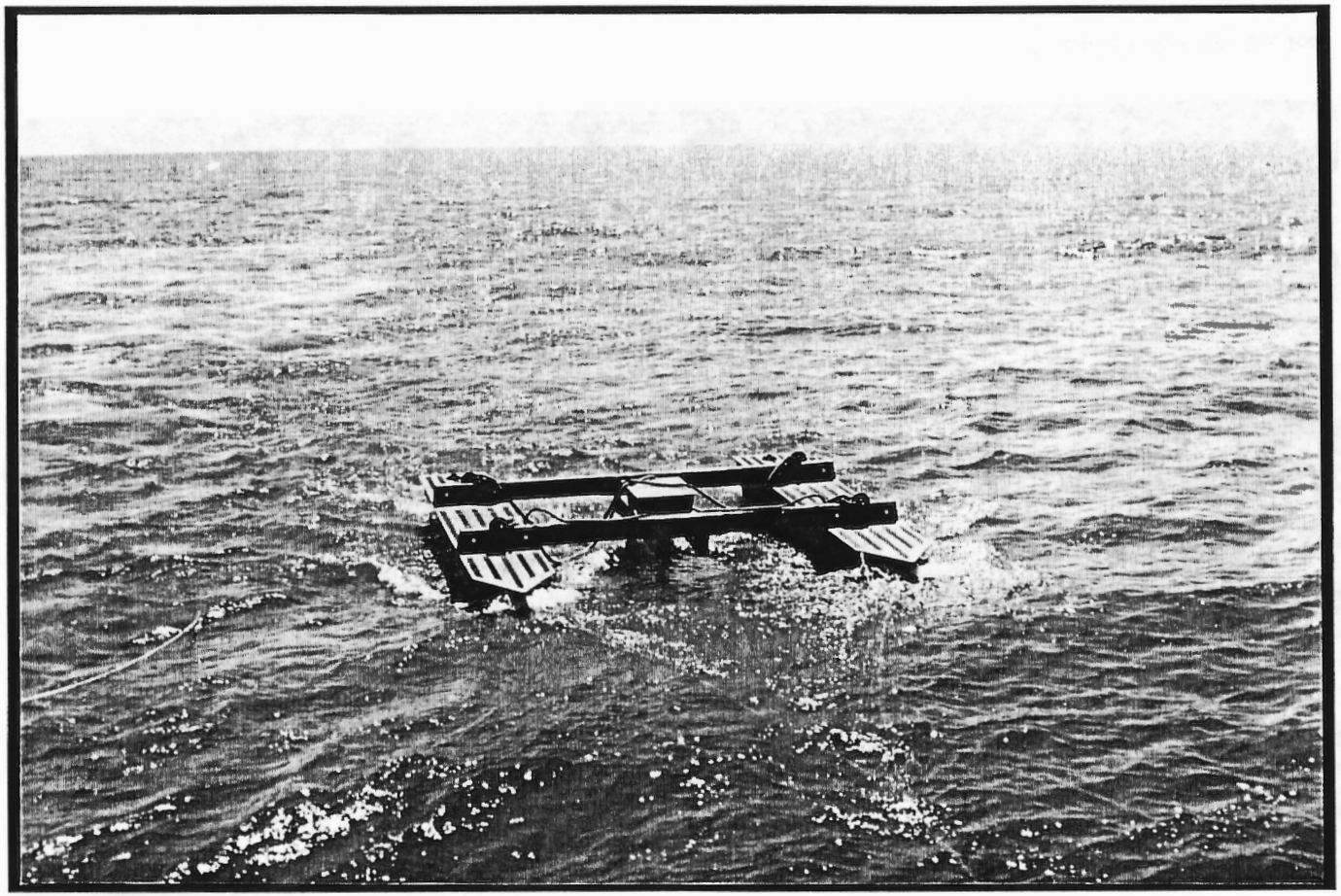

GSC photo 1995-174D, L.H. Thorleifson

Figure 10. Marine radar catamaran.

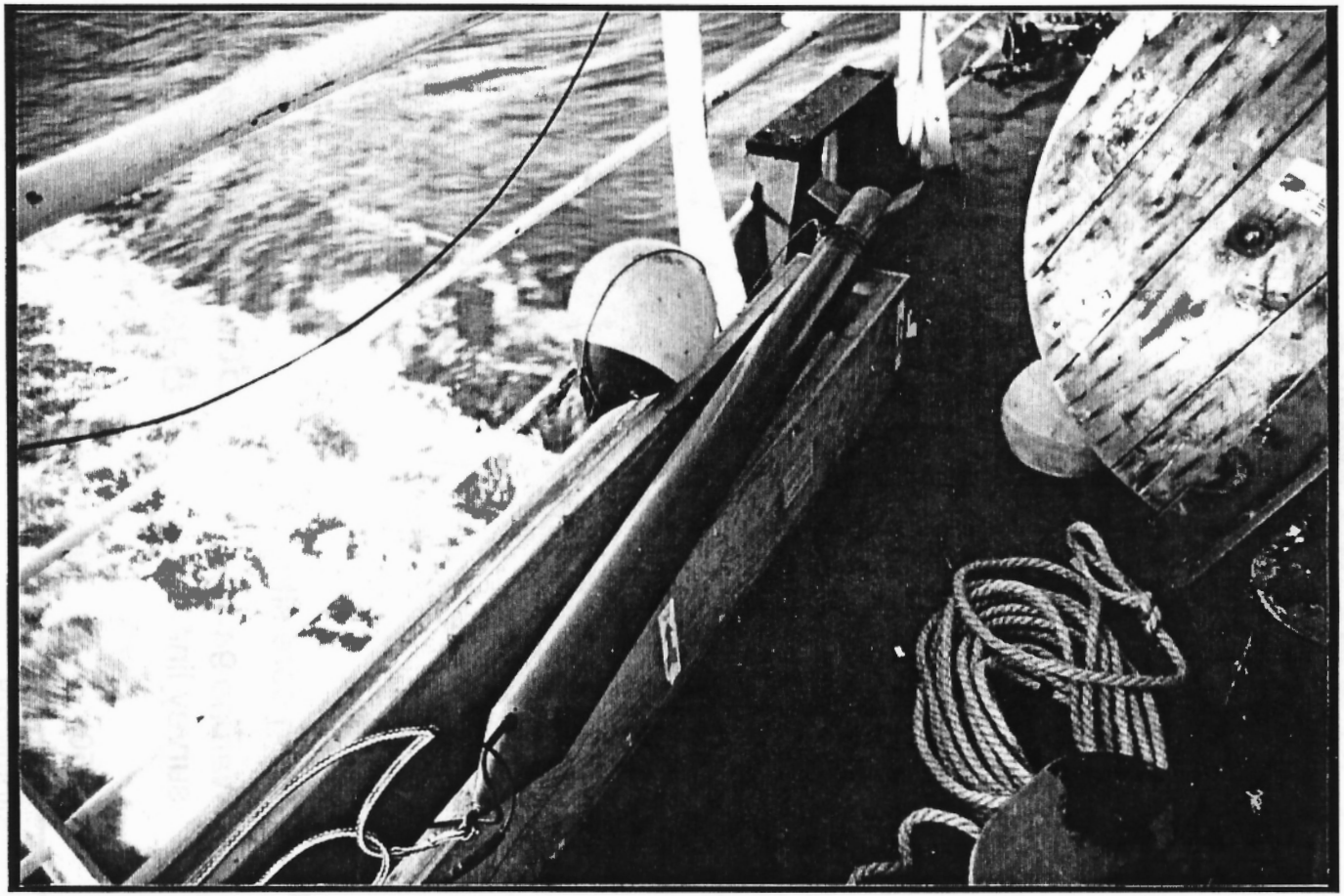

GSC photo 1995-174N, B.J. Todd

Figure 11. Marine magnetometer.

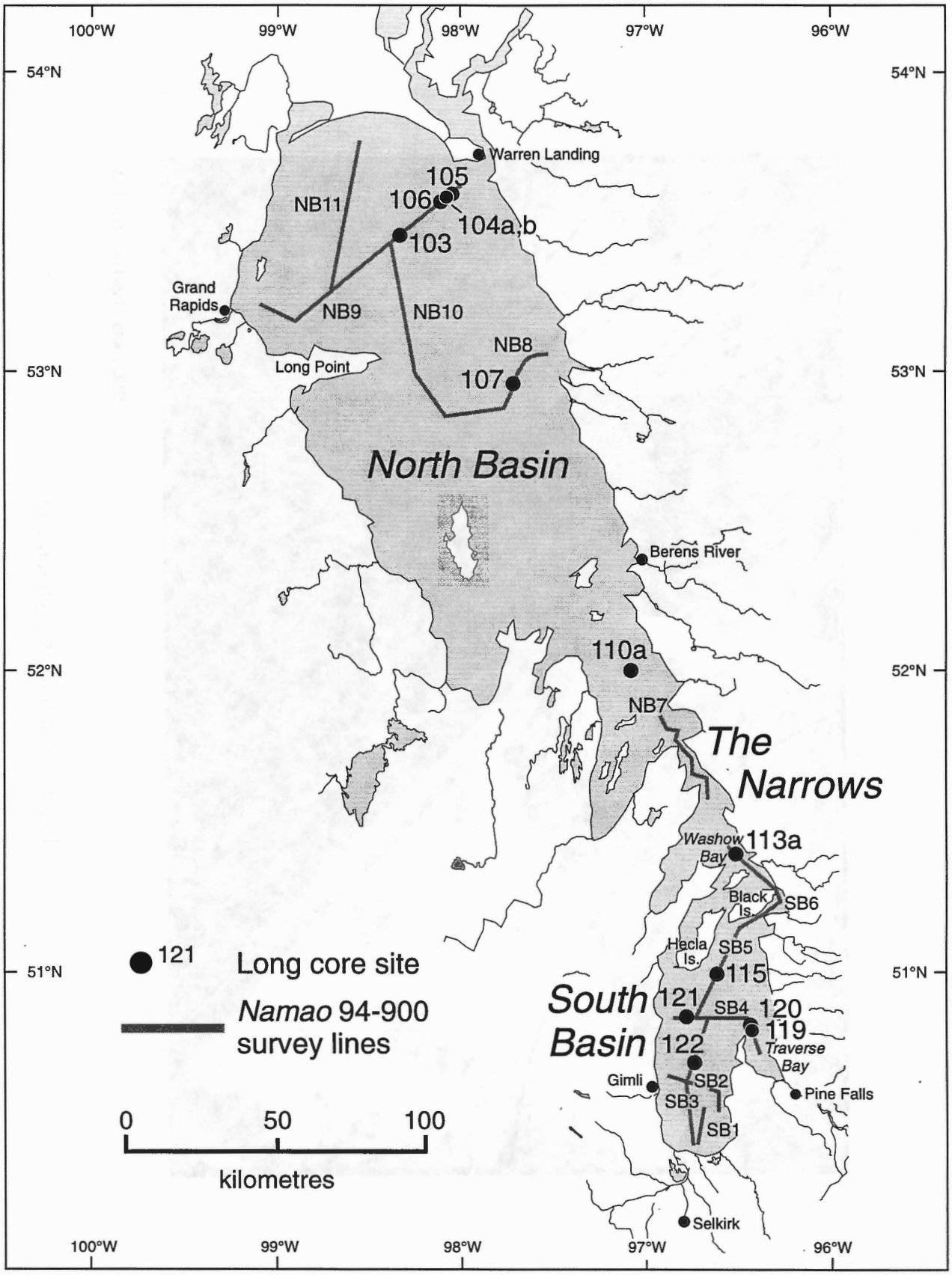

Figure 12. Location of long core sites.

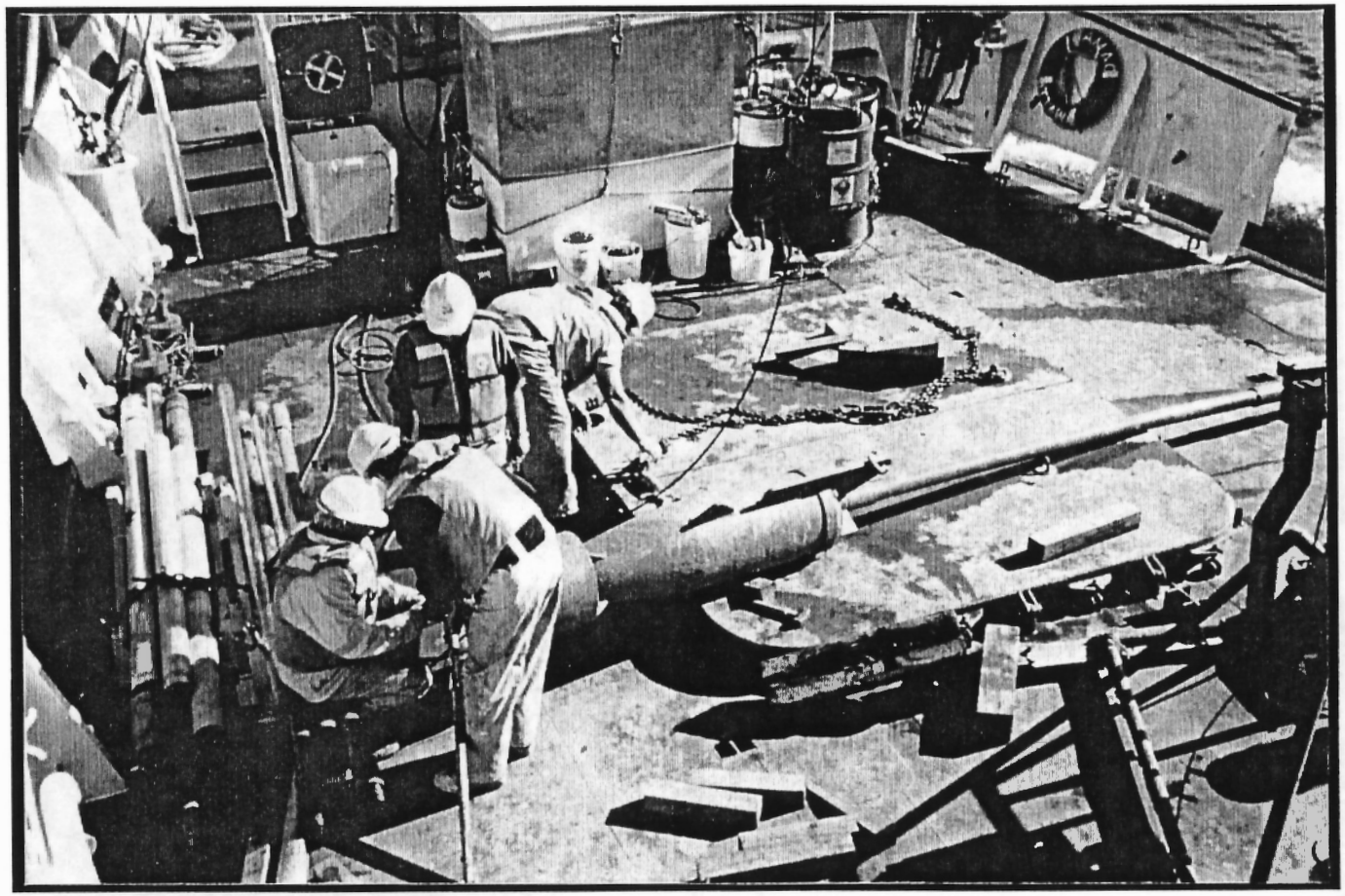

GSC photo 1995-174F, E. Nielsen

Figure 13. Assembling piston corer on foredeck.

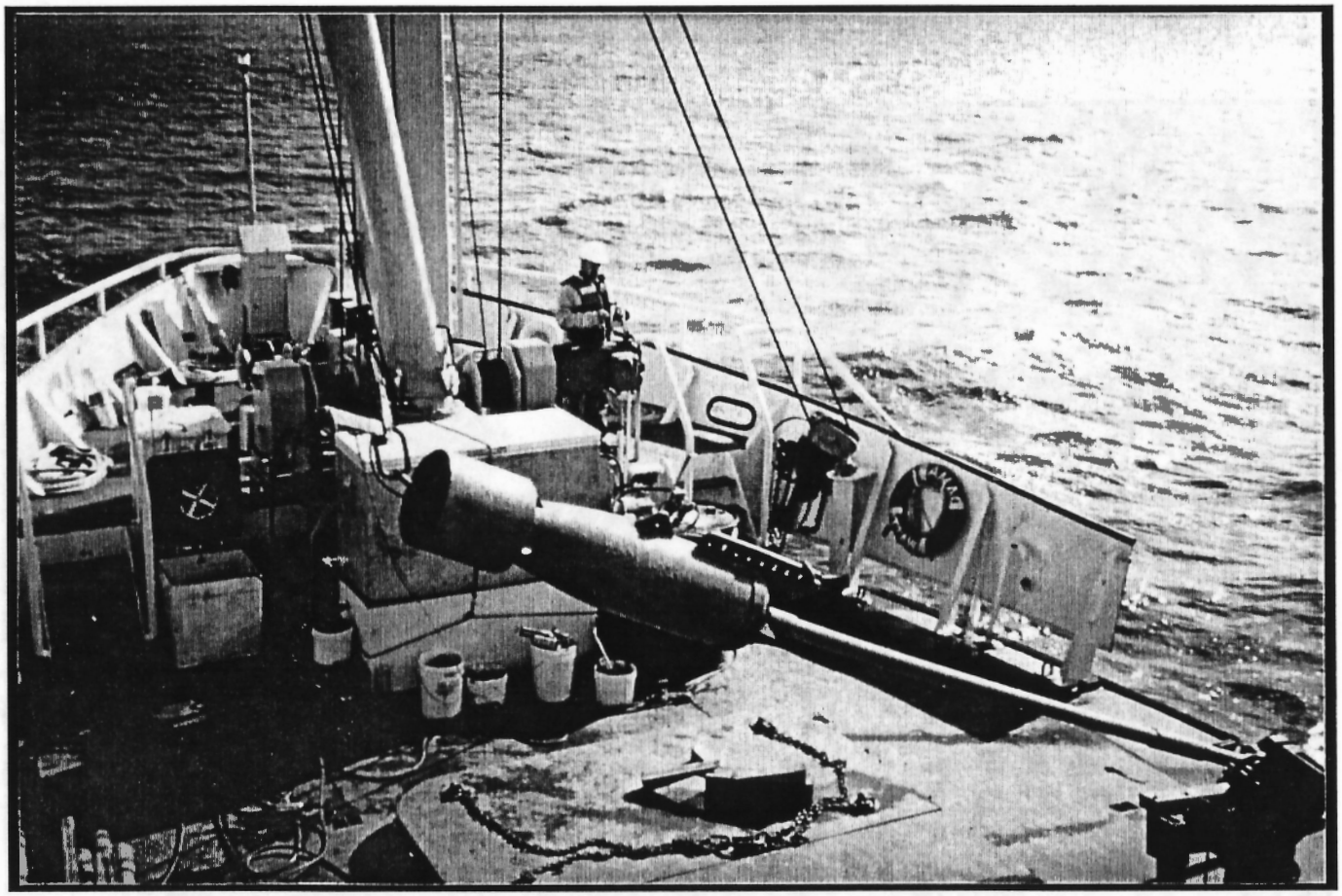

GSC photo 1995-174E, E. Nielsen

Figure 14. Piston corer being raised off foredeck by crane.

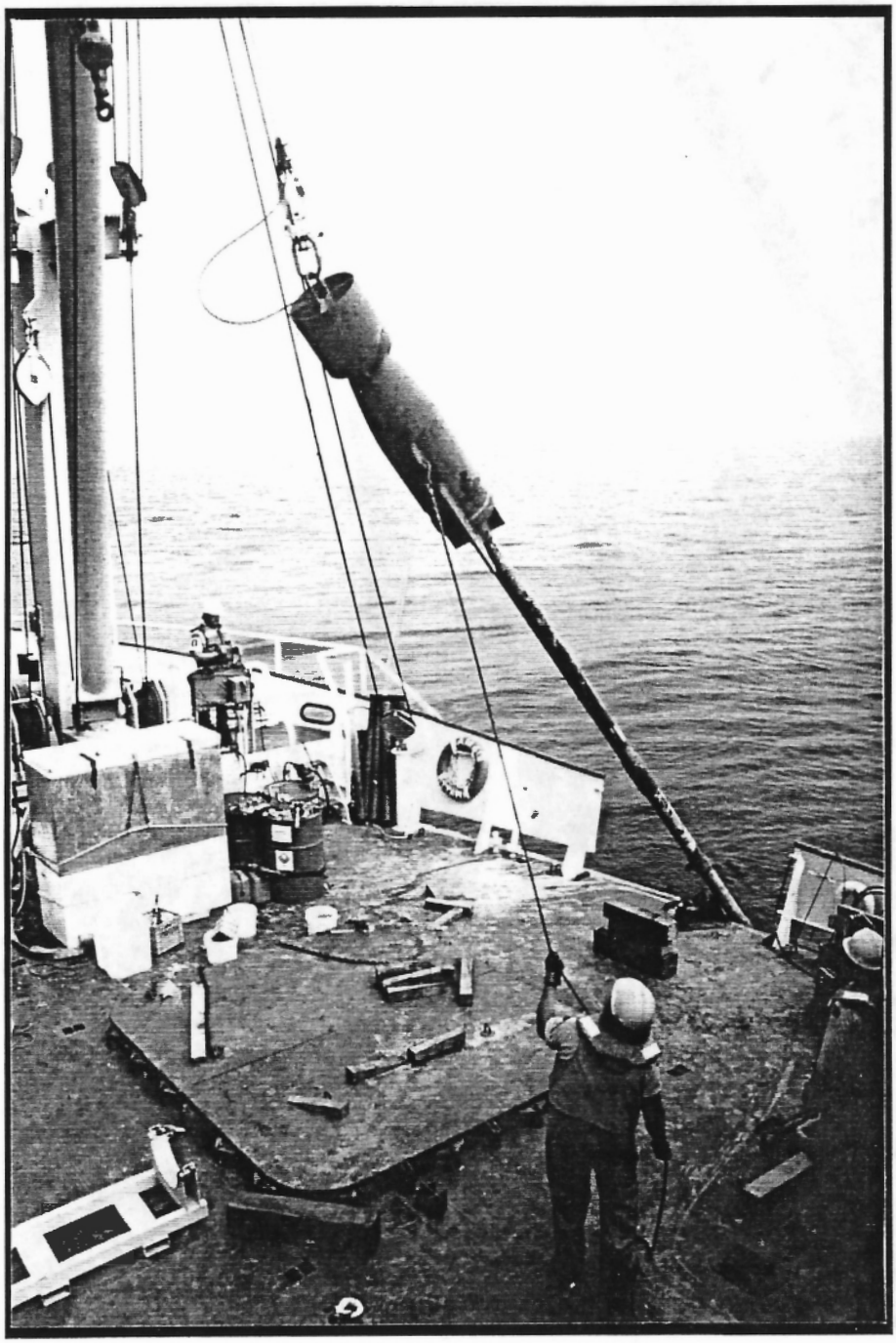

GSC photo 1995-174Q, B.J. Todd

Figure 15. Deploying corer by sliding barrels through gap in starboard rail.

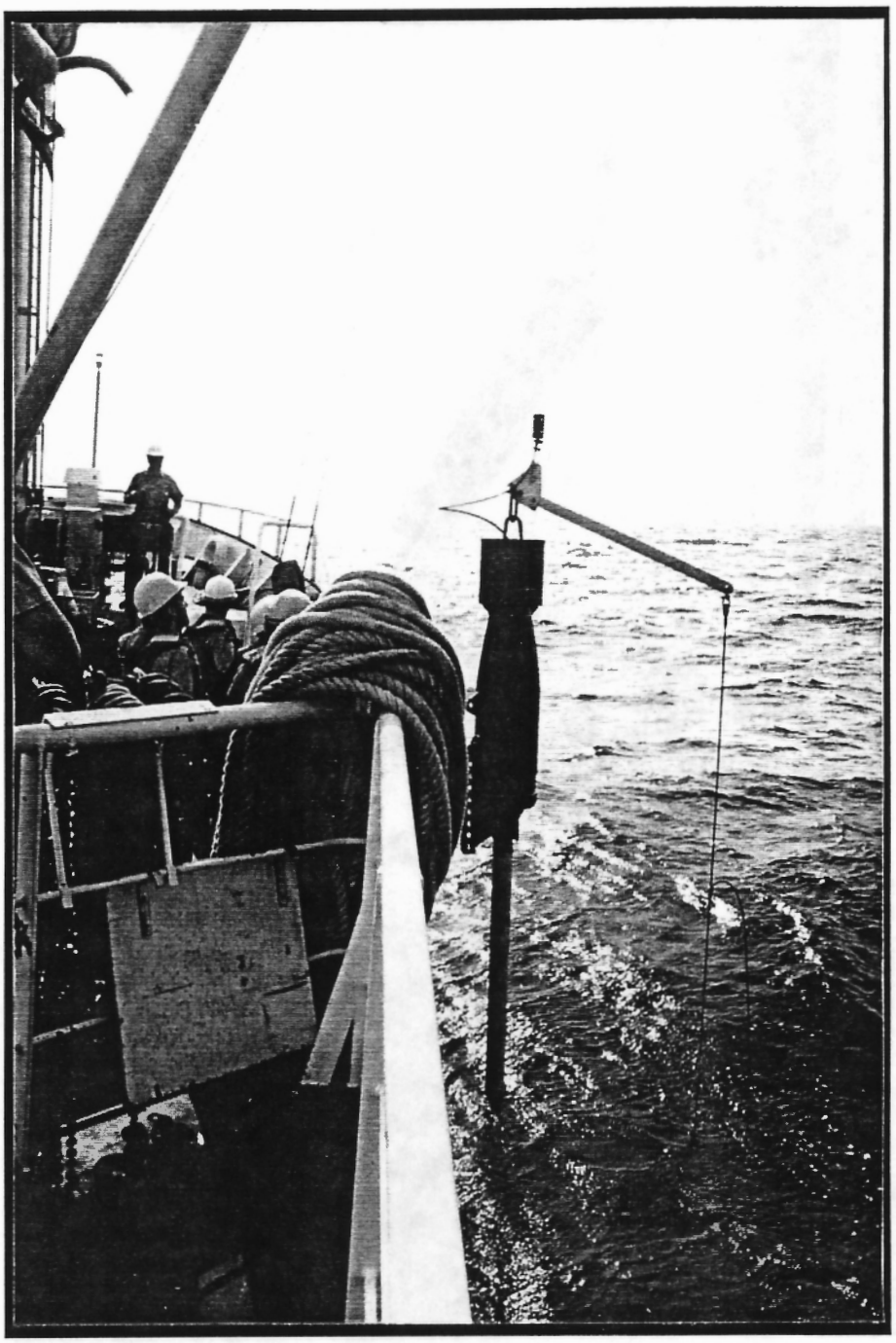

GSC photo 1995-174P, E. Nielsen

Figure 16. Piston corer hanging on starboard side prior to lowering to lakefloor.

GSC photo 1995-174R, B.J. Todd

Figure 17. Core liner being extruded from piston corer barrels.

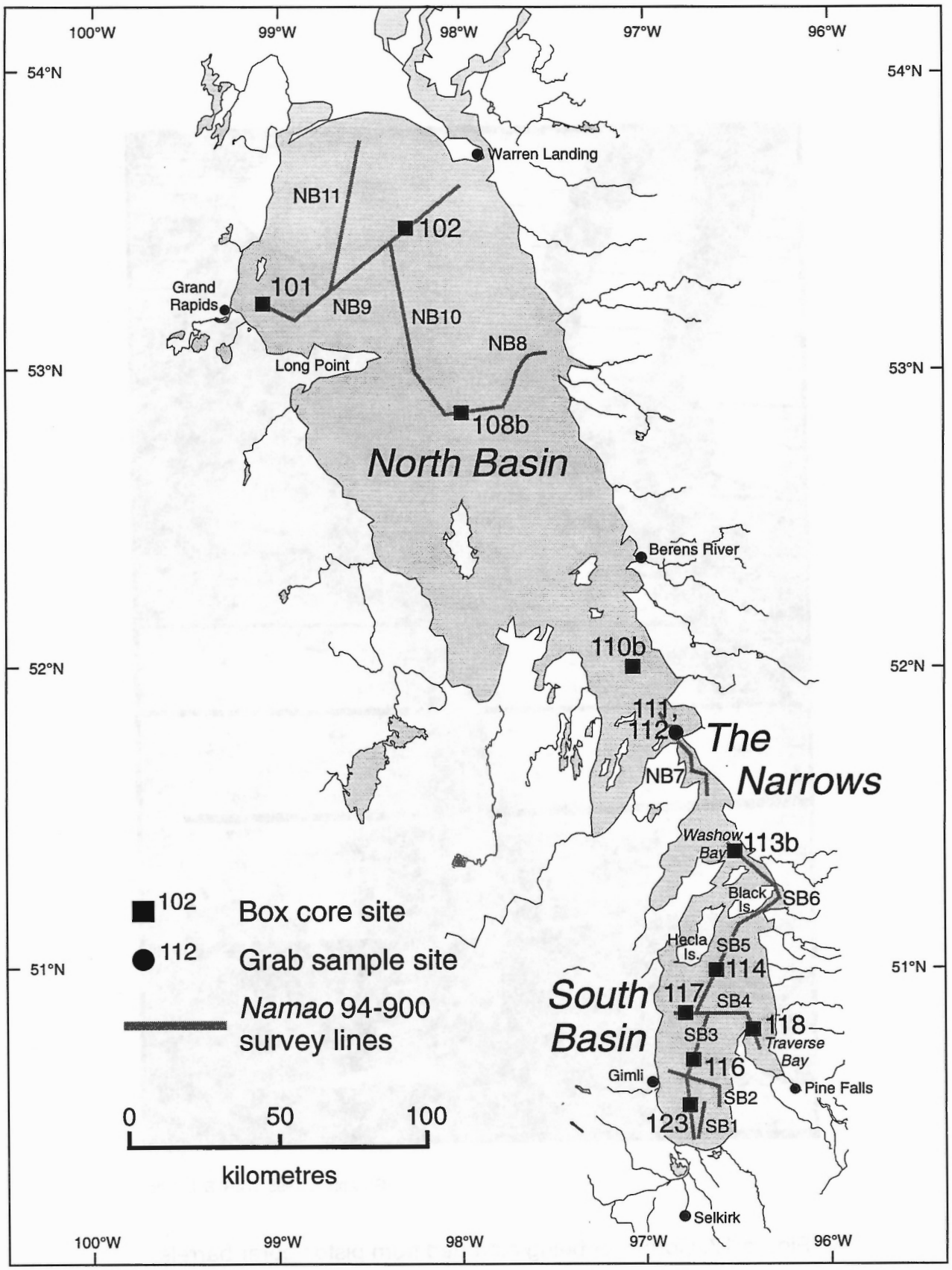

Figure 18. Location of box core sites and large grab samples.

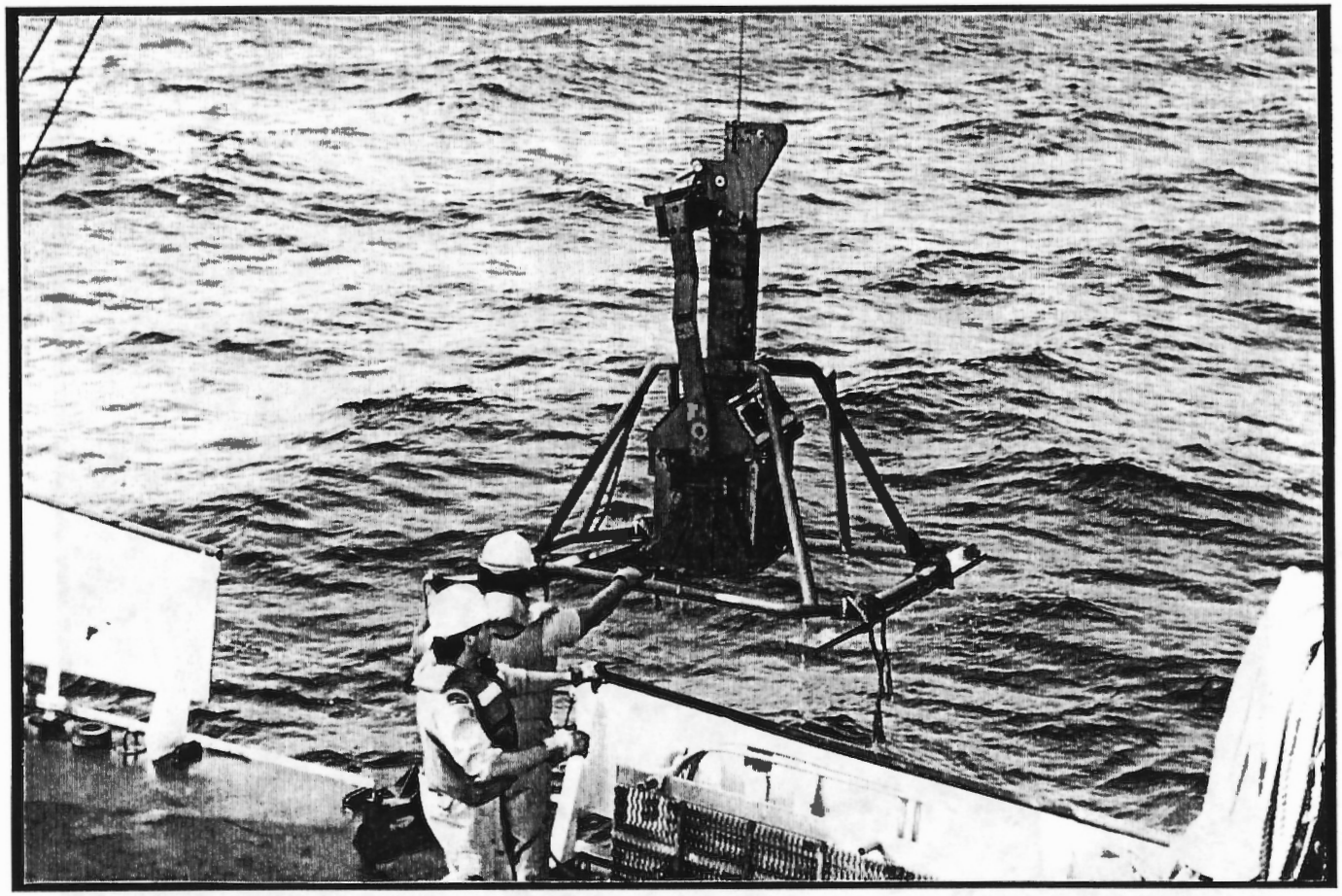

GSC photo 1995-174O, L.H. Thorleifson

Figure 19. Retrieving box corer.

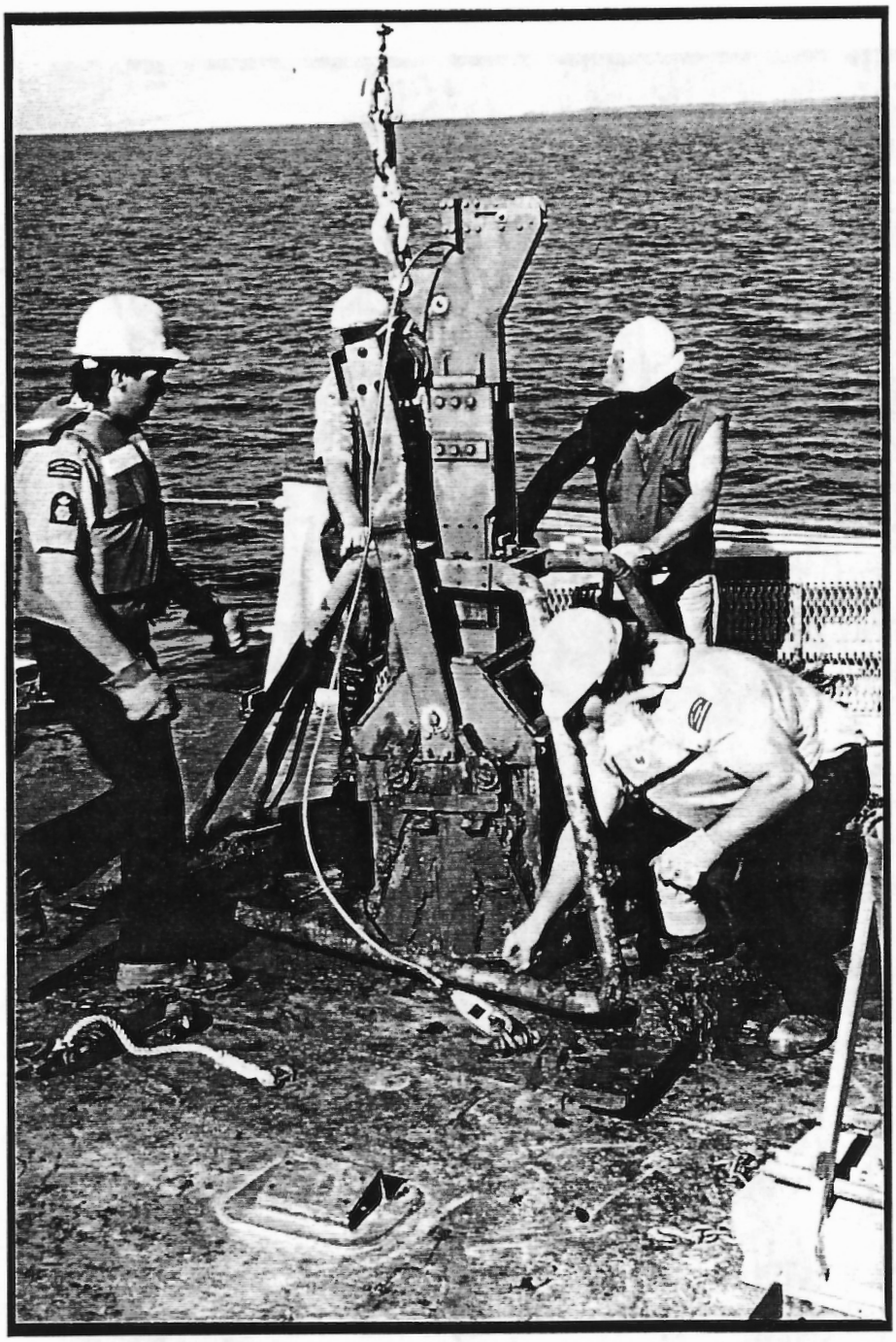

GSC photo 1995-174L, B.J. Todd

Figure 20. Box corer on foredeck.

GSC photo 1995-174A, E. Nielsen

Figure 21. Insertion of wide diameter sampling tubes into box corer sediment aided by vacuum pump.

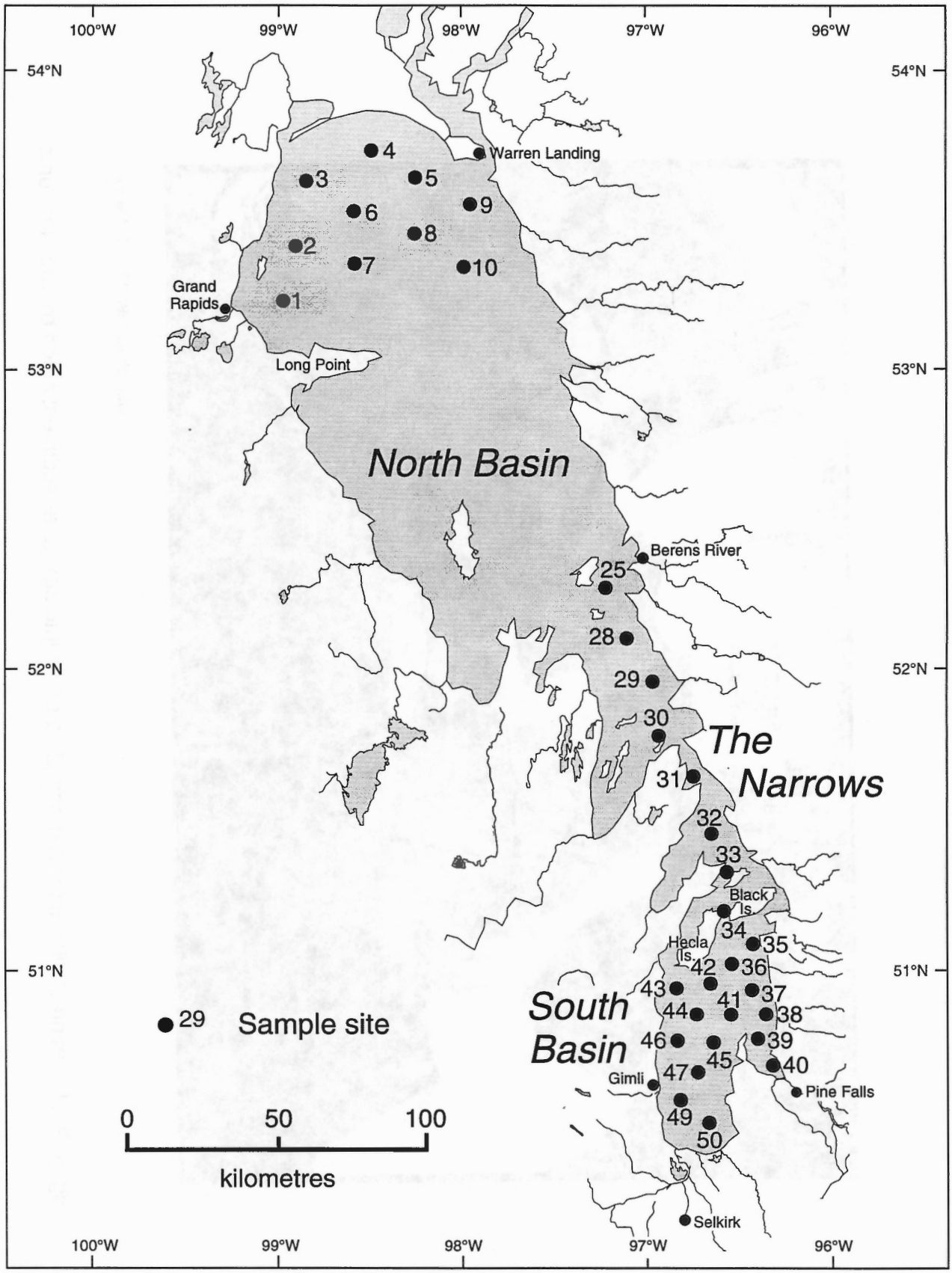

Figure 22. Location of sampling survey stations.

Appendix 1:

Marine magnetometer survey data

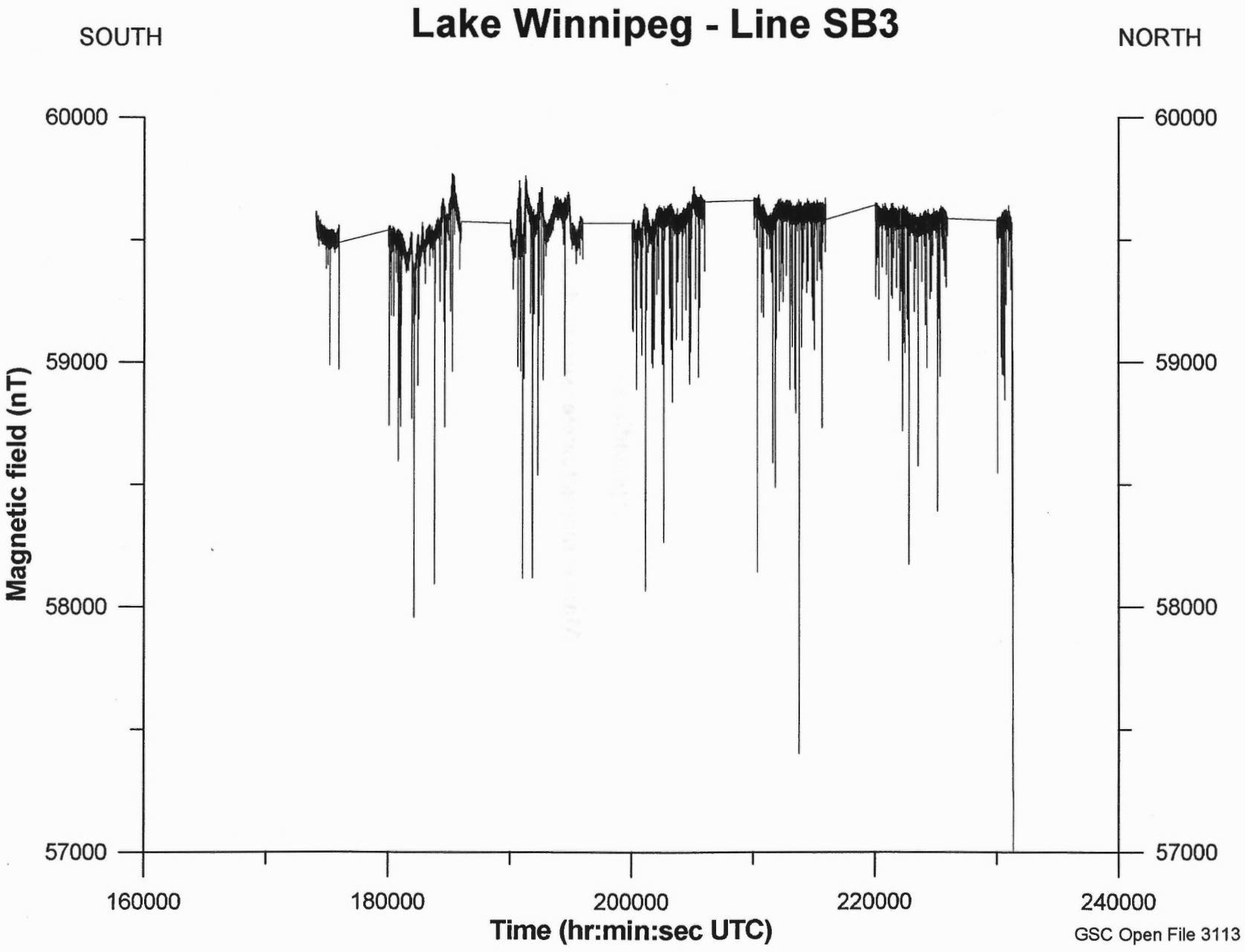
Lake Winnipeg - Line SB3
SOUTH
NORTH
60000
59000
58000
57000
Magnetic field (nT)
160000
180000
200000
220000
240000
Time (hr:min:sec UTC)
GSC Open File 3113

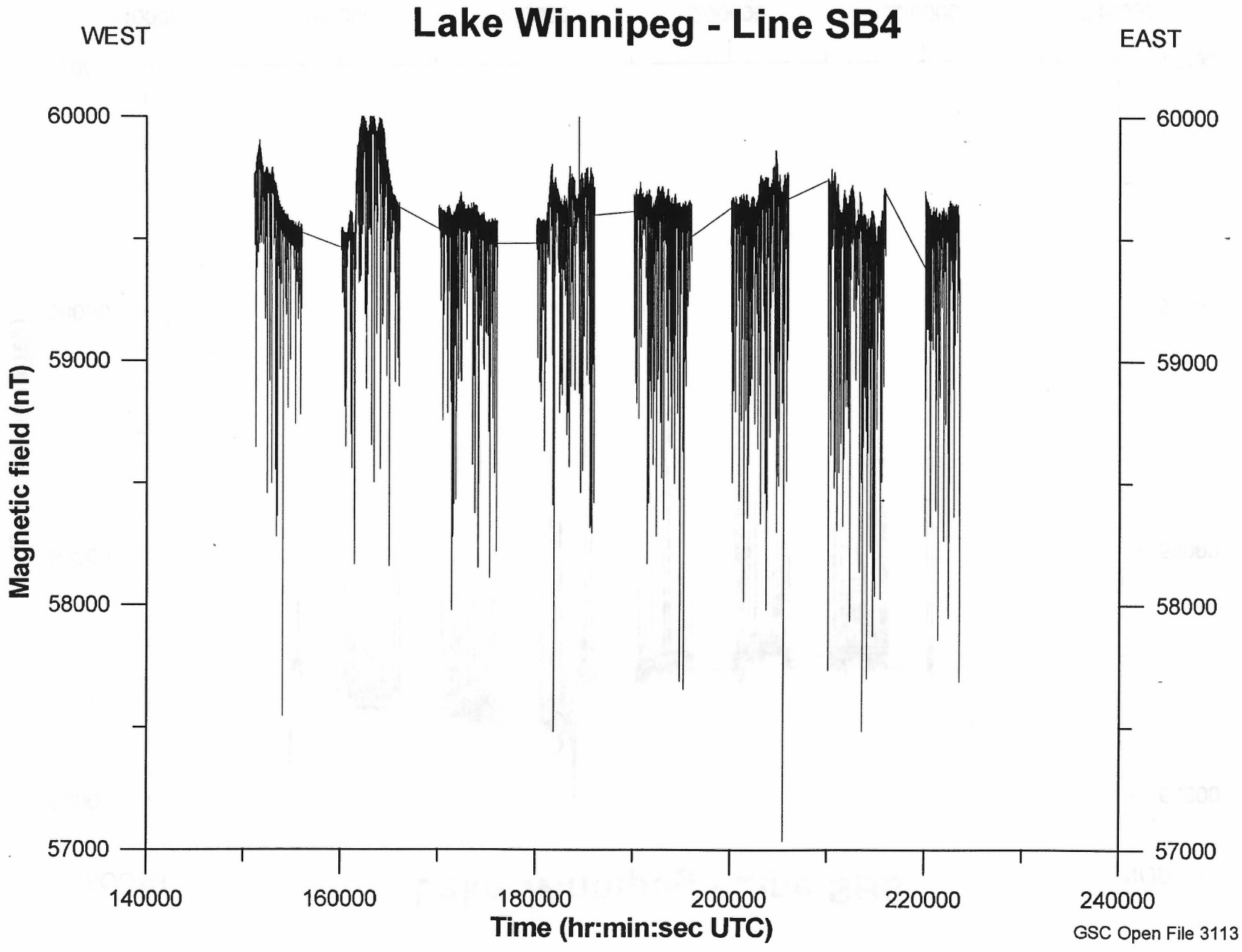
Lake Winnipeg - Line SB4
WEST
EAST
60000
59000
58000
57000
Magnetic field (nT)
140000
160000
180000
200000
220000
240000
Time (hr:min:sec UTC)
GSC Open File 3113

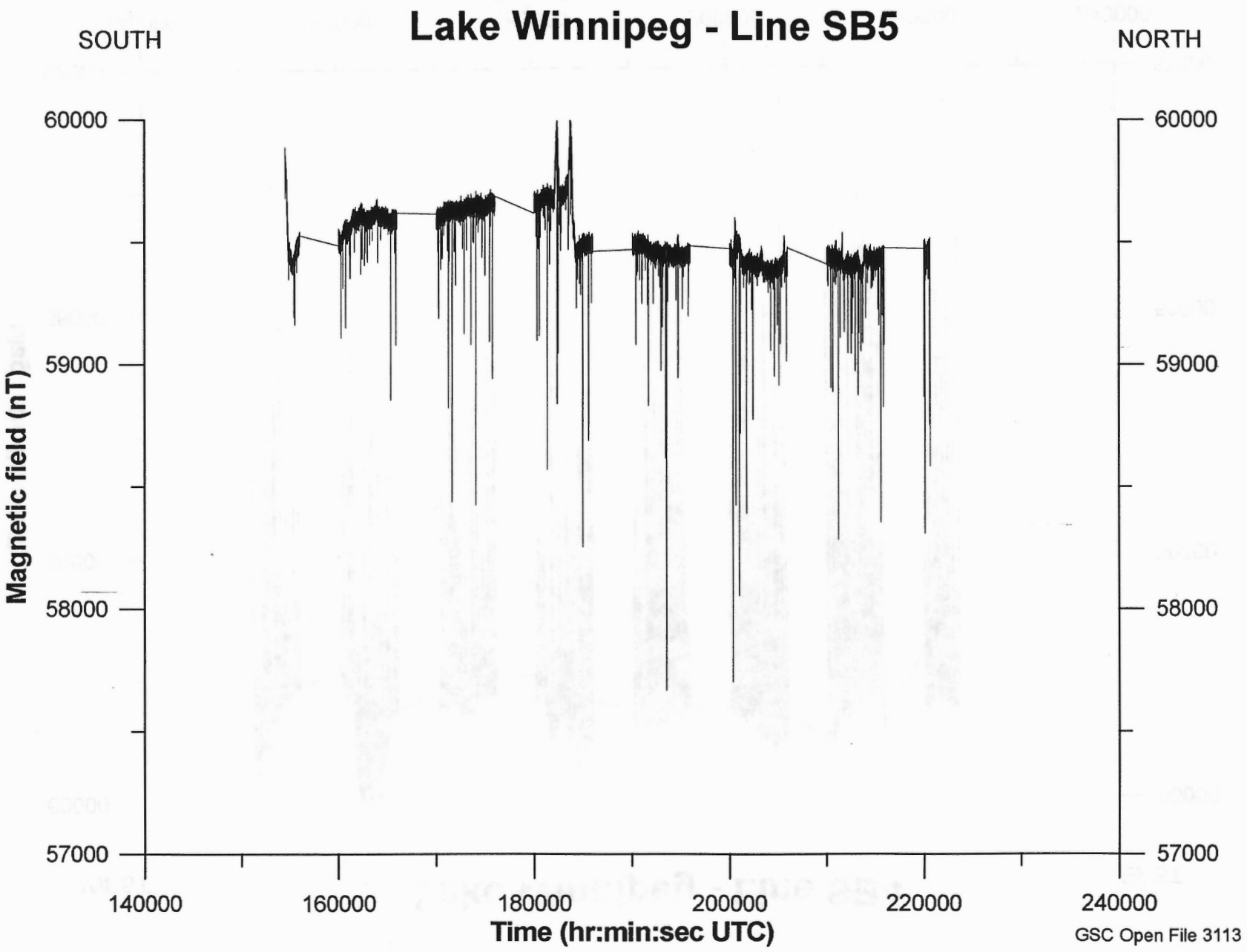
Lake Winnipeg - Line SB5
SOUTH
NORTH
60000
59000
58000
57000
Magnetic field (nT)
140000
160000
180000
200000
220000
240000
Time (hr:min:sec UTC)
GSC Open File 3113

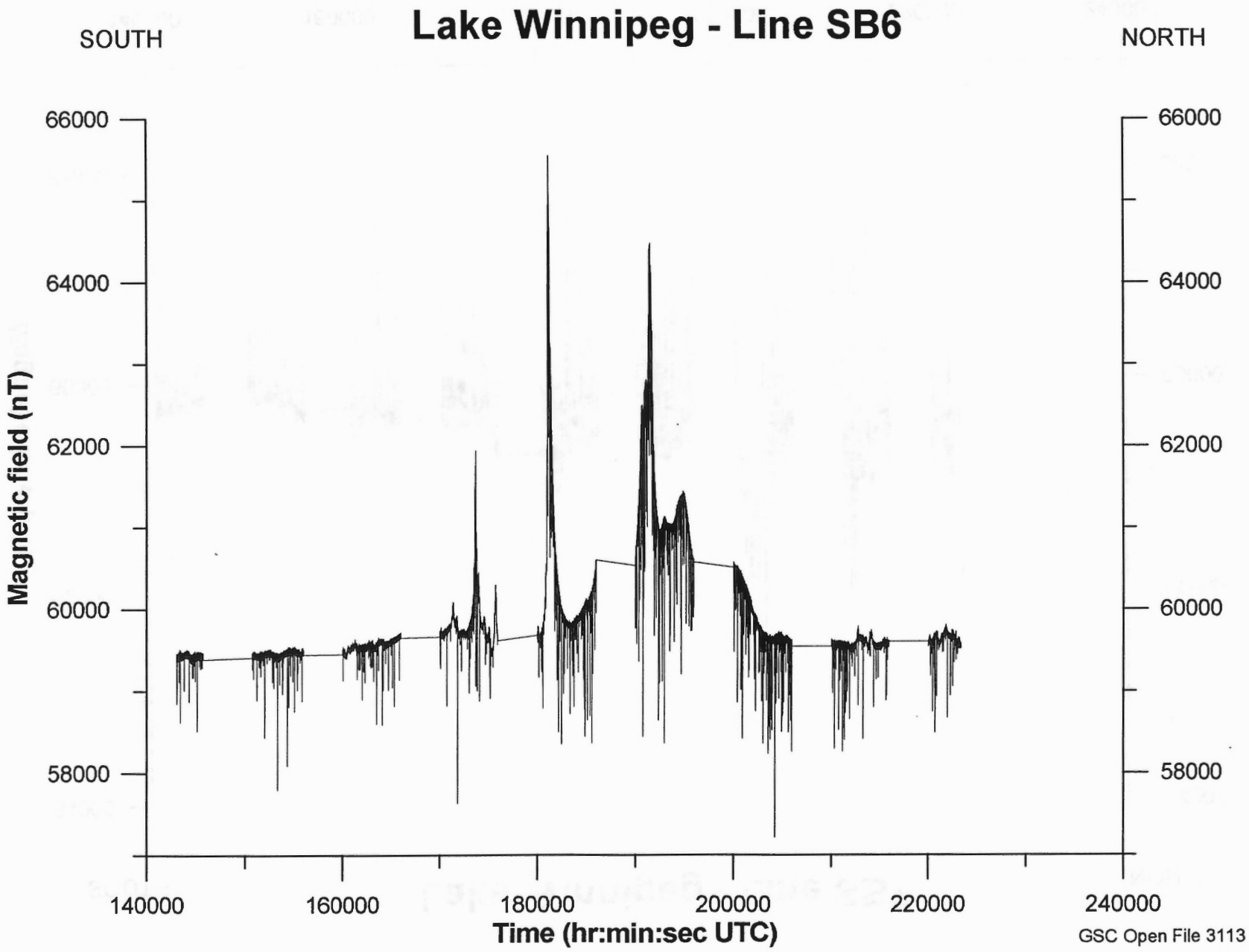
Lake Winnipeg - Line SB6
SOUTH
NORTH
66000
64000
62000
60000
58000
Magnetic field (nT)
140000
160000
180000
200000
220000
240000
Time (hr:min:sec UTC)
GSC Open File 3113

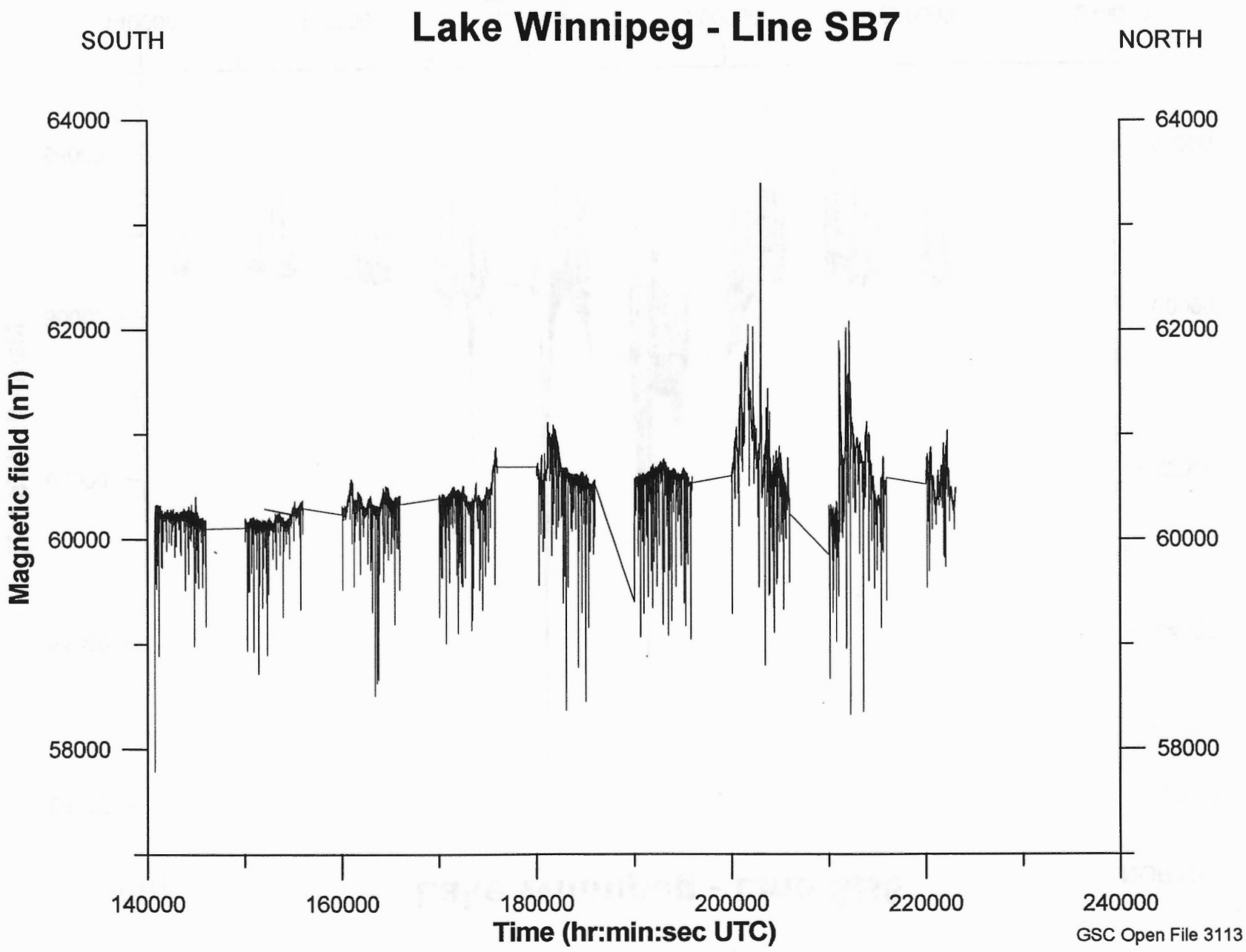
Lake Winnipeg - Line SB7
SOUTH
NORTH
64000
62000
60000
58000
Magnetic field (nT)
140000
160000
180000
200000
220000
240000
Time (hr:min:sec UTC)
GSC Open File 3113

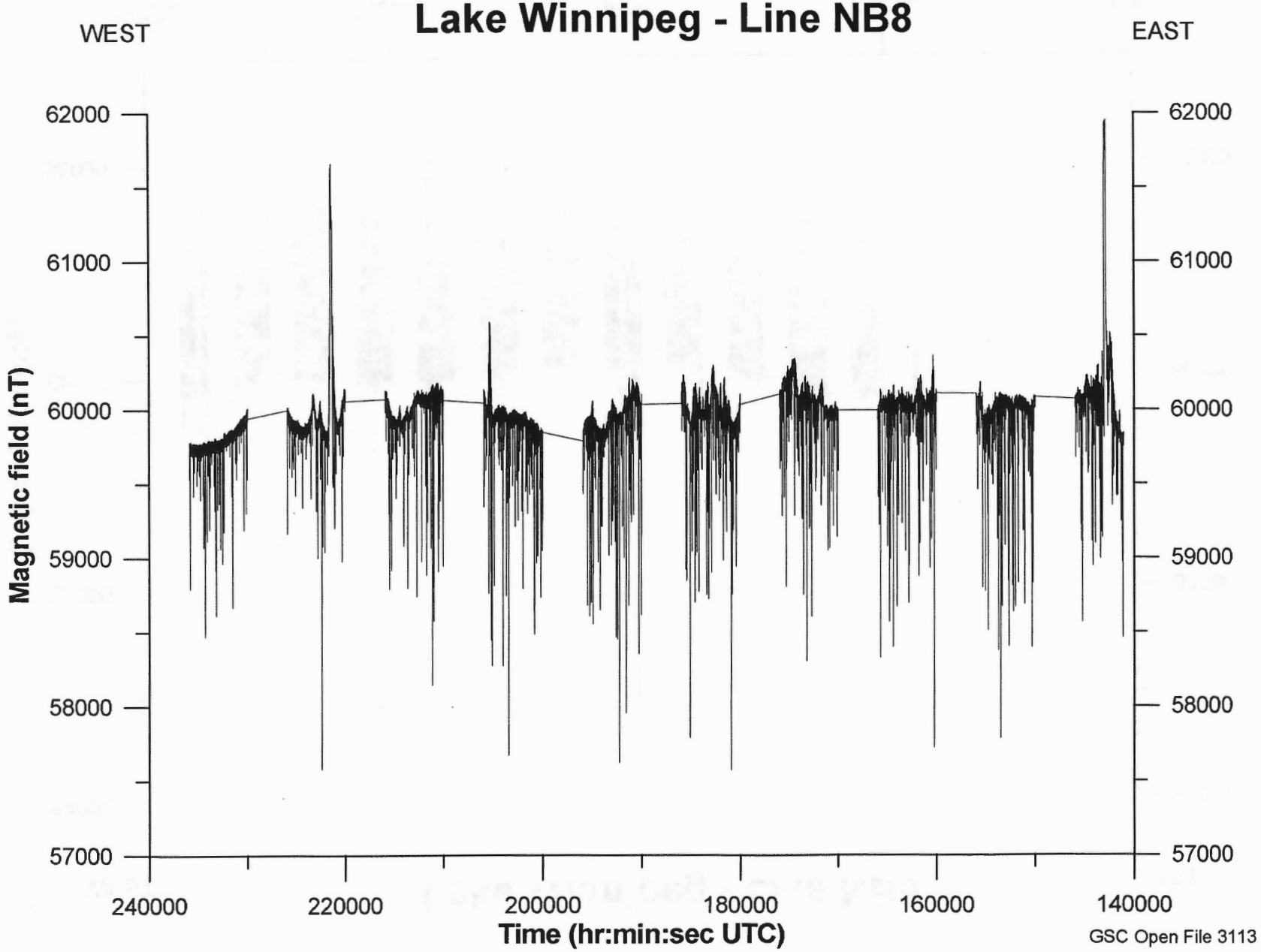
Lake Winnipeg - Line NB8
WEST
EAST
62000
61000
60000
59000
58000
57000
Magnetic field (nT)
240000
220000
200000
180000
160000
140000
Time (hr:min:sec UTC)
GSC Open File 3113

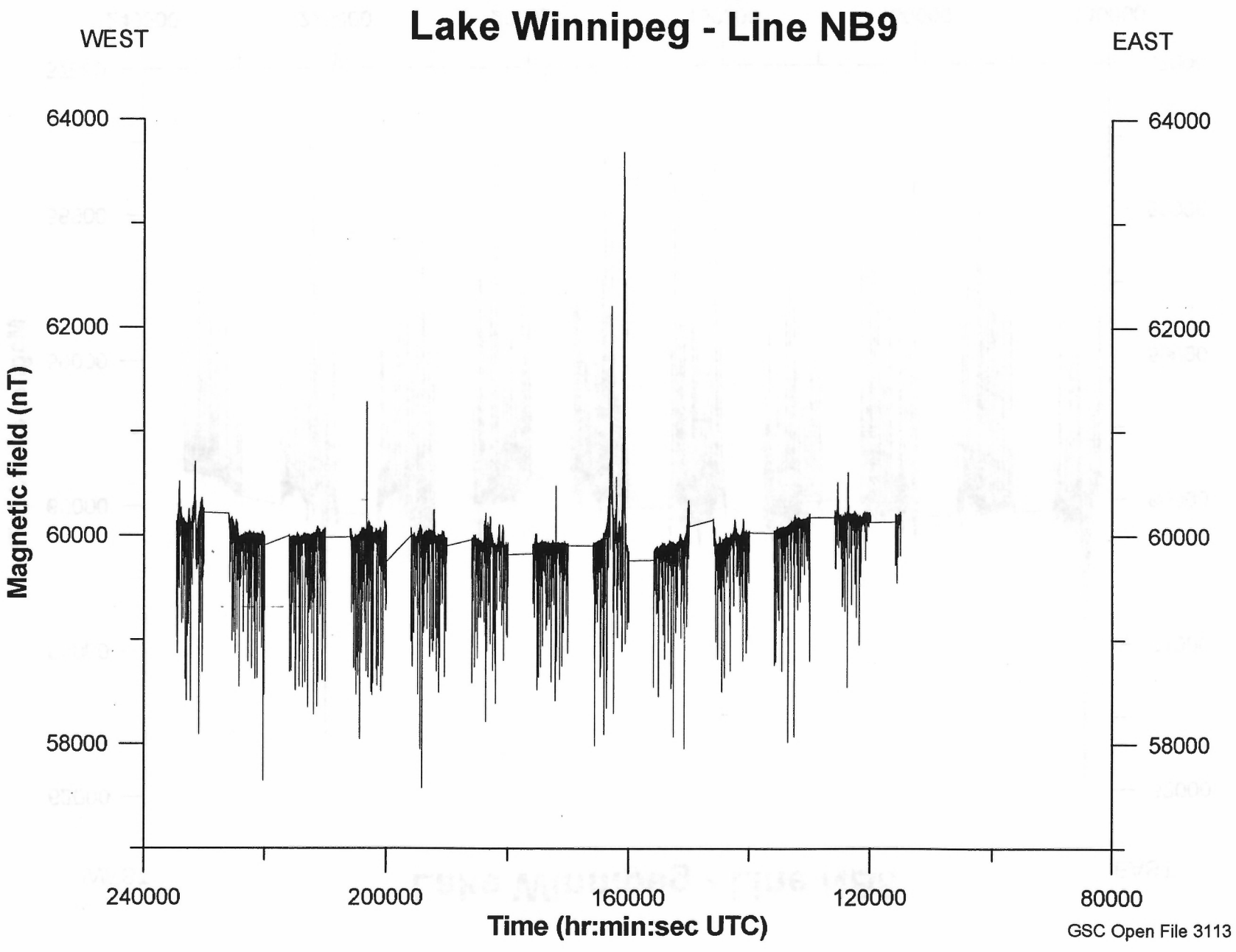
Lake Winnipeg - Line NB9
WEST
EAST
64000
62000
60000
58000
Magnetic field (nT)
240000
200000
160000
120000
80000
Time (hr:min:sec UTC)
GSC Open File 3113

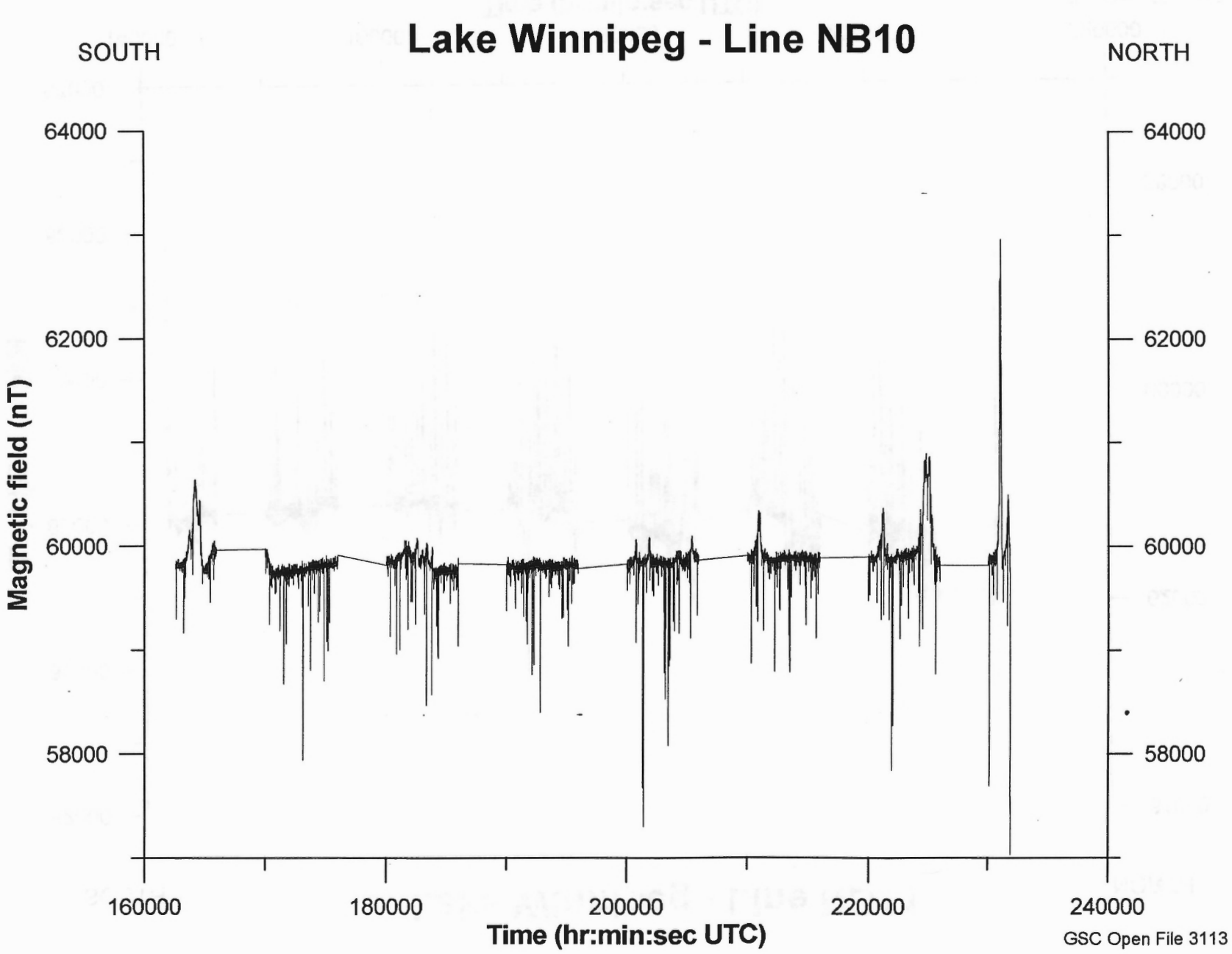
Lake Winnipeg - Line NB10
SOUTH
NORTH
64000
62000
60000
58000
Magnetic field (nT)
160000
180000
200000
220000
240000
Time (hr:min:sec UTC)
GSC Open File 3113

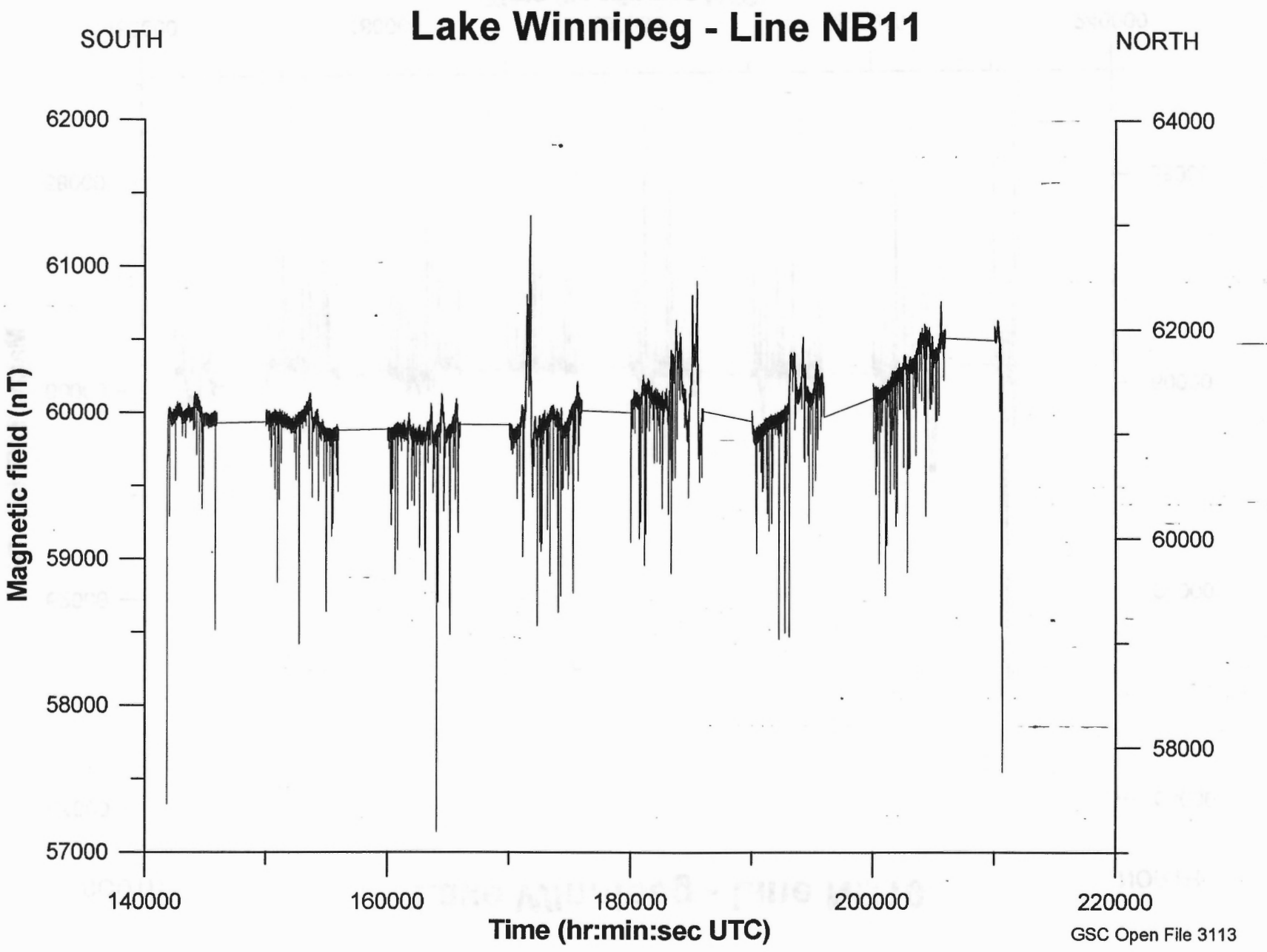
Lake Winnipeg - Line NB11
SOUTH
NORTH
62000
61000
60000
59000
58000
57000
64000
62000
60000
58000
Magnetic field (nT)
140000
160000
180000
200000
220000
Time (hr:min:sec UTC)
GSC Open File 3113

Appendix 2:

Temperature, conductivity and turbidity profiles

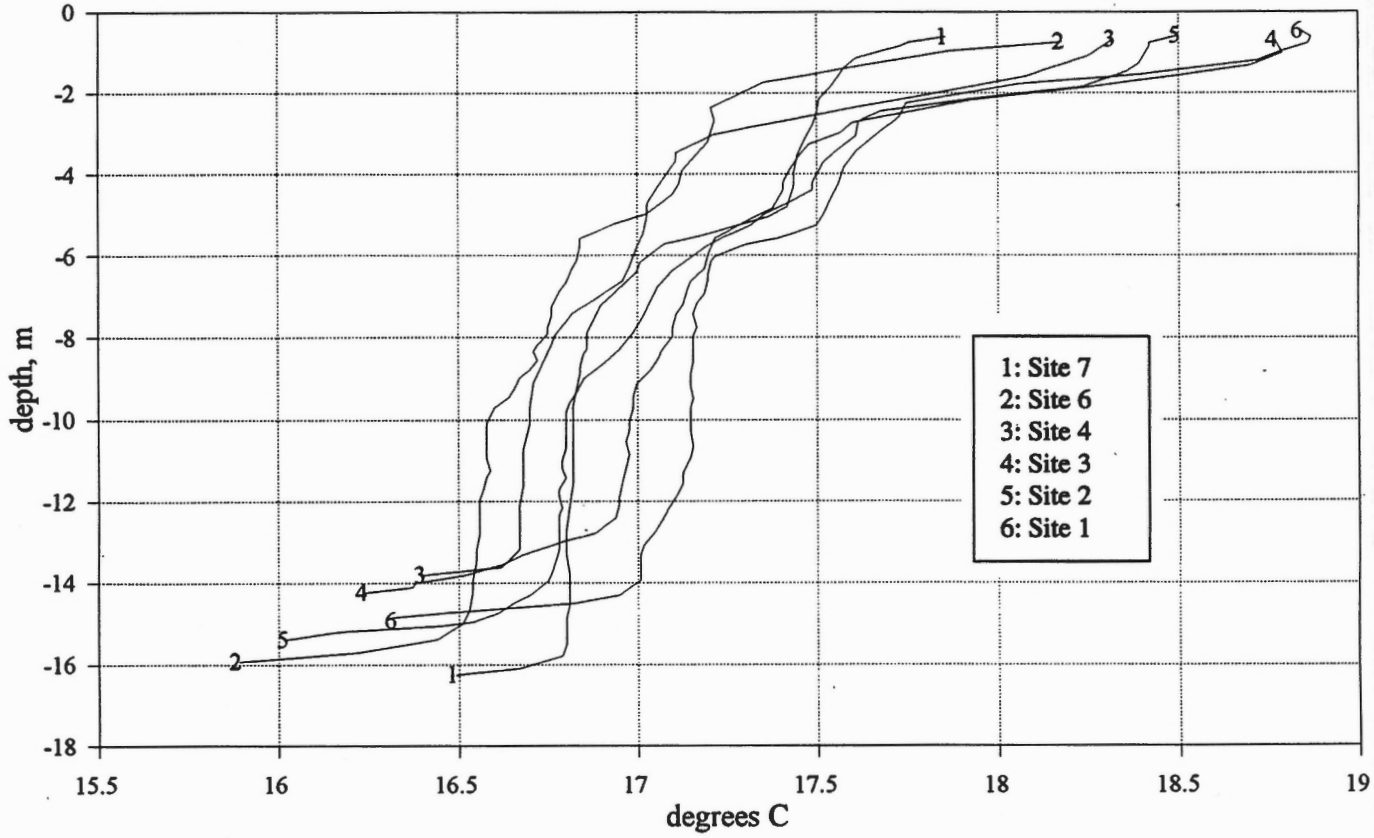
depth, m
degrees C
1: Site 7
2: Site 6
3: Site 4
4: Site 3
5: Site 2
6: Site 1

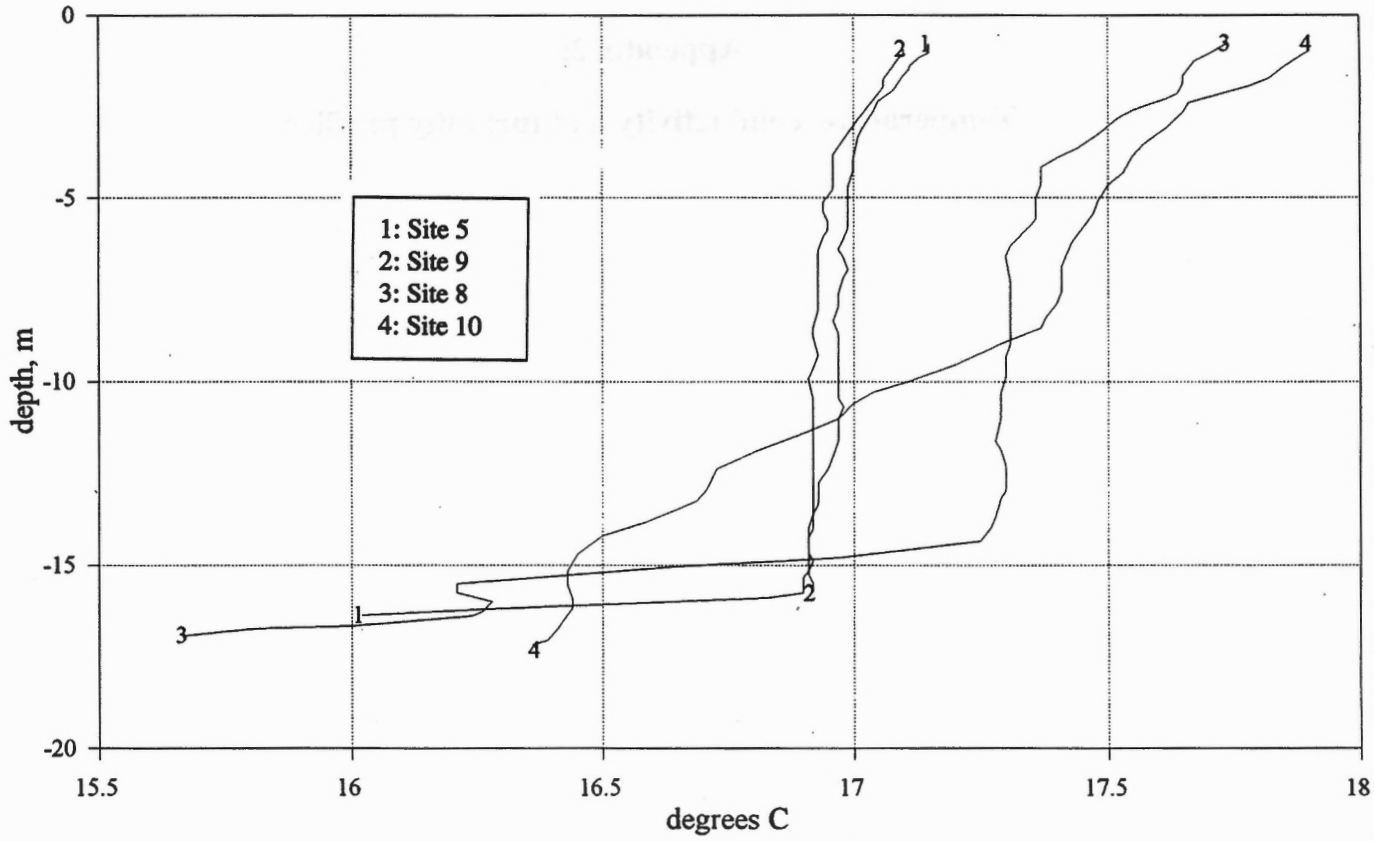
depth, m
degrees C
1: Site 5
2: Site 9
3: Site 8
4: Site 10

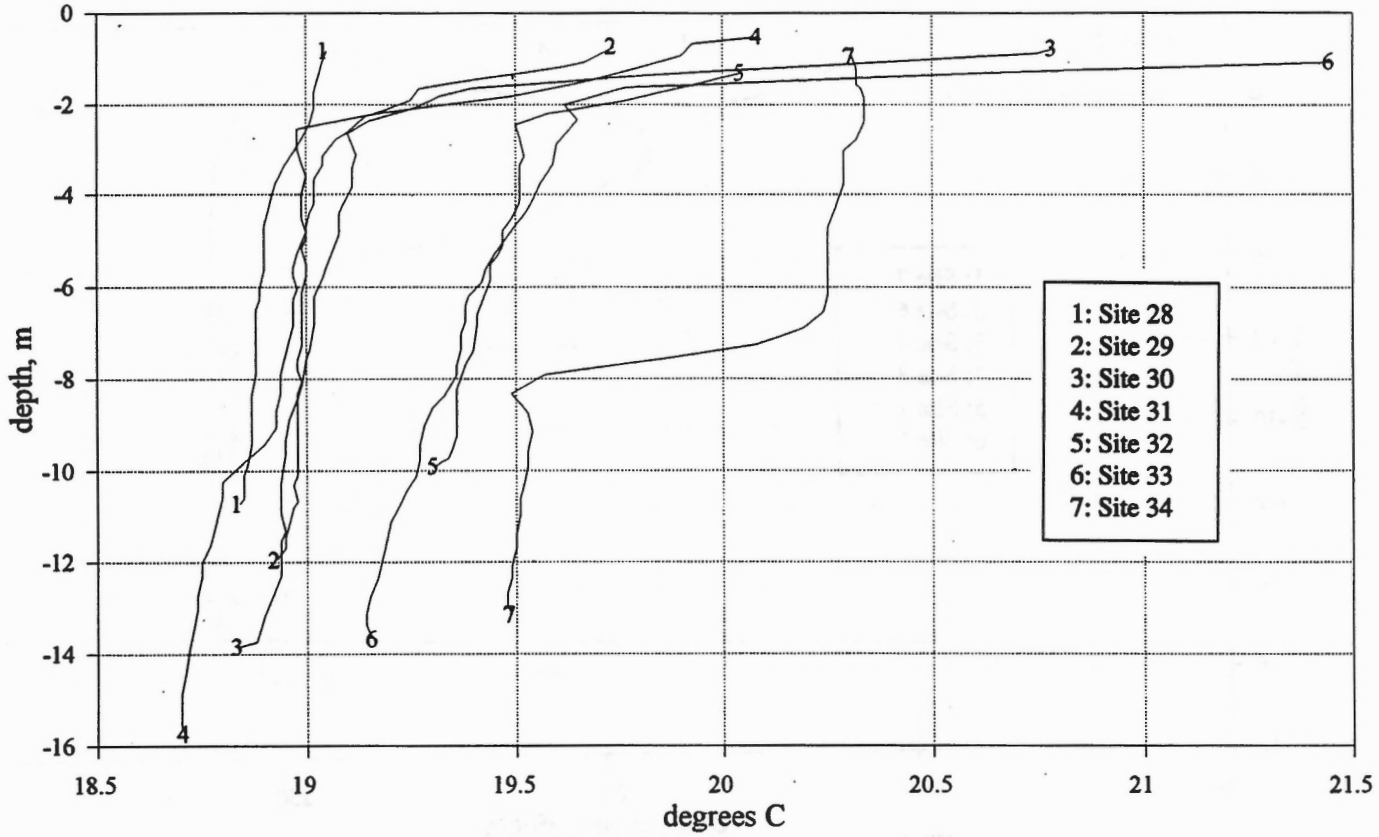
depth, m
degrees C
1: Site 28
2: Site 29
3: Site 30
4: Site 31
5: Site 32
6: Site 33
7: Site 34

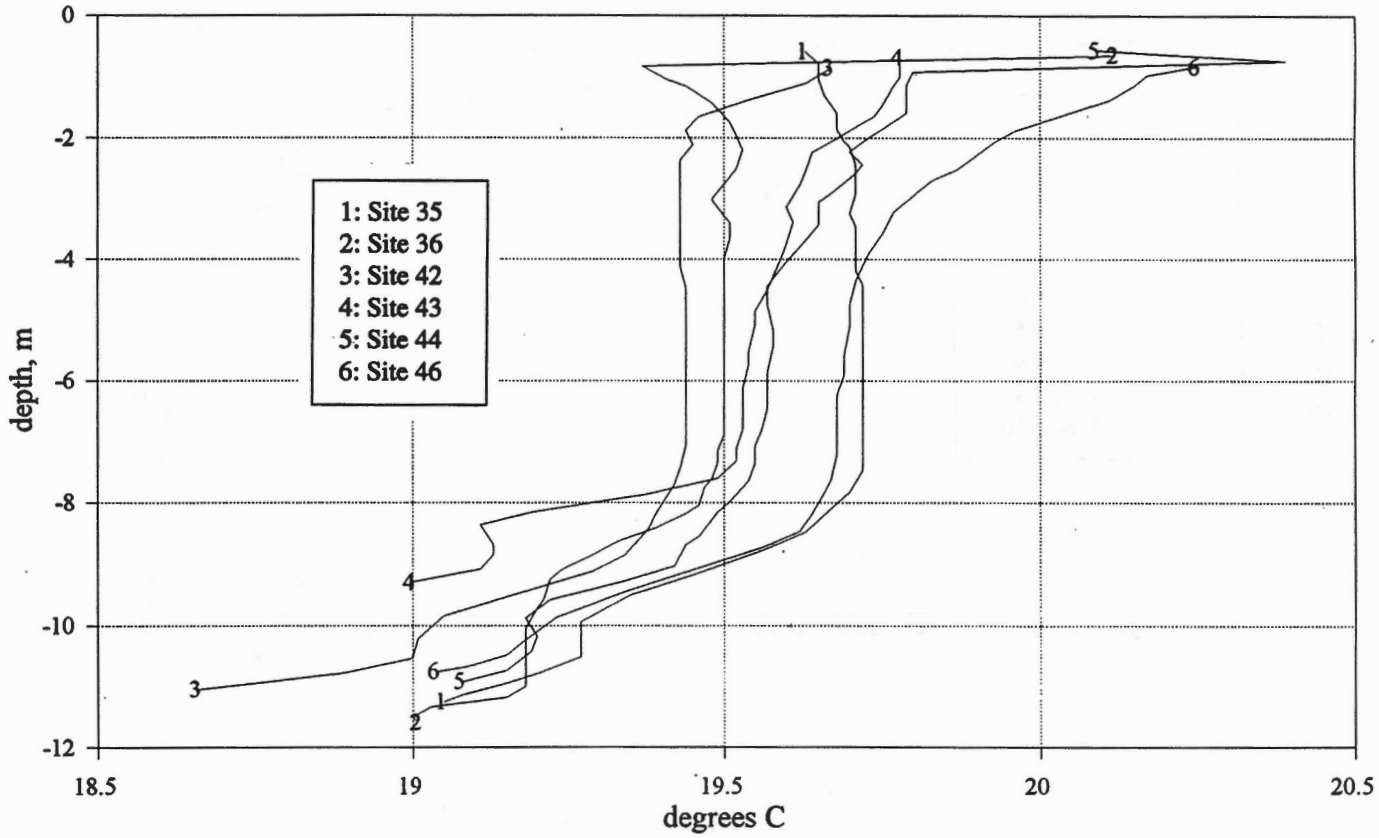
depth, m
degrees C
1: Site 35
2: Site 36
3: Site 42
4: Site 43
5: Site 44
6: Site 46

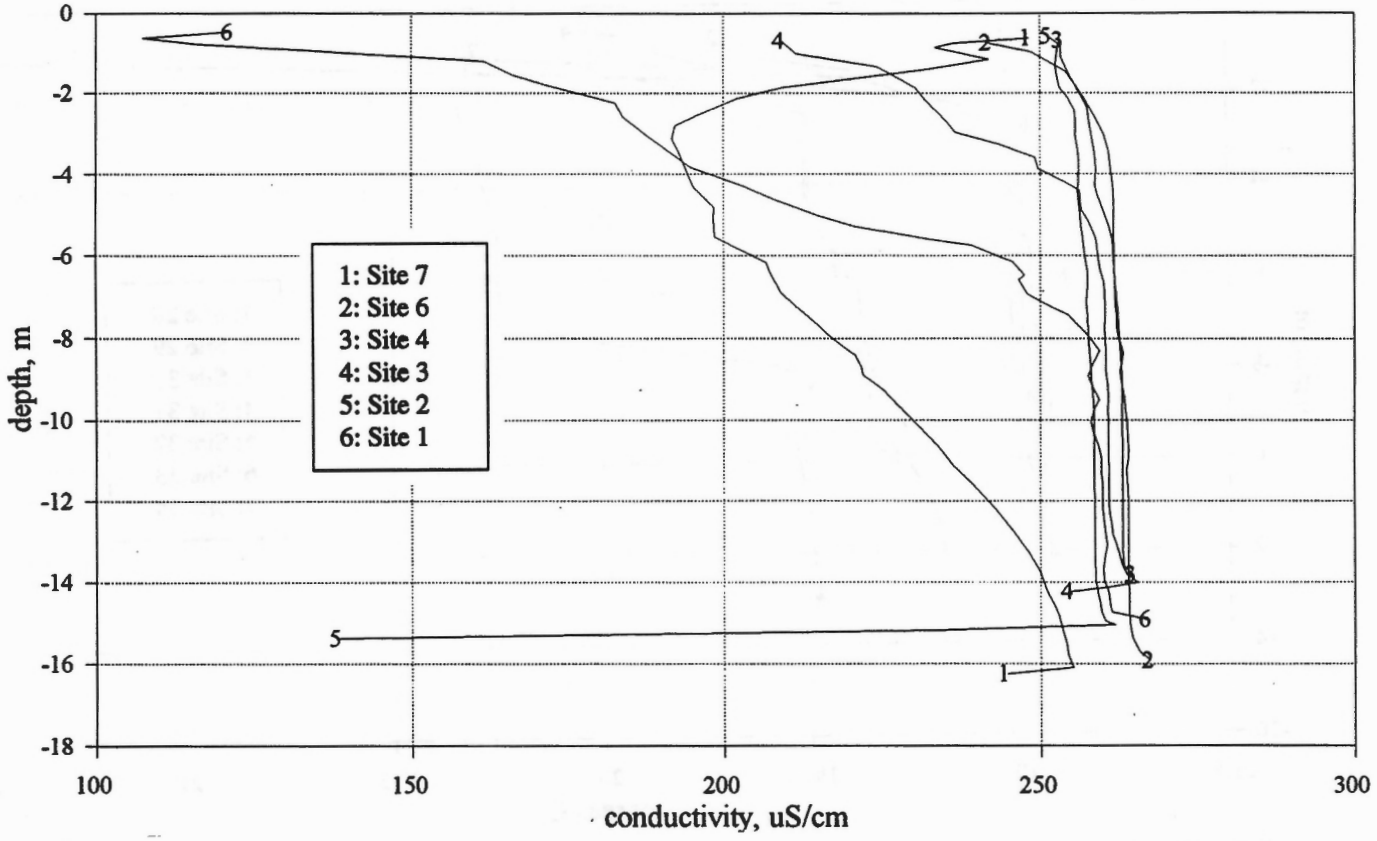
1: Site 7
2: Site 6
3: Site 4
4: Site 3
5: Site 2
6: Site 1
depth, m
conductivity, uS/cm

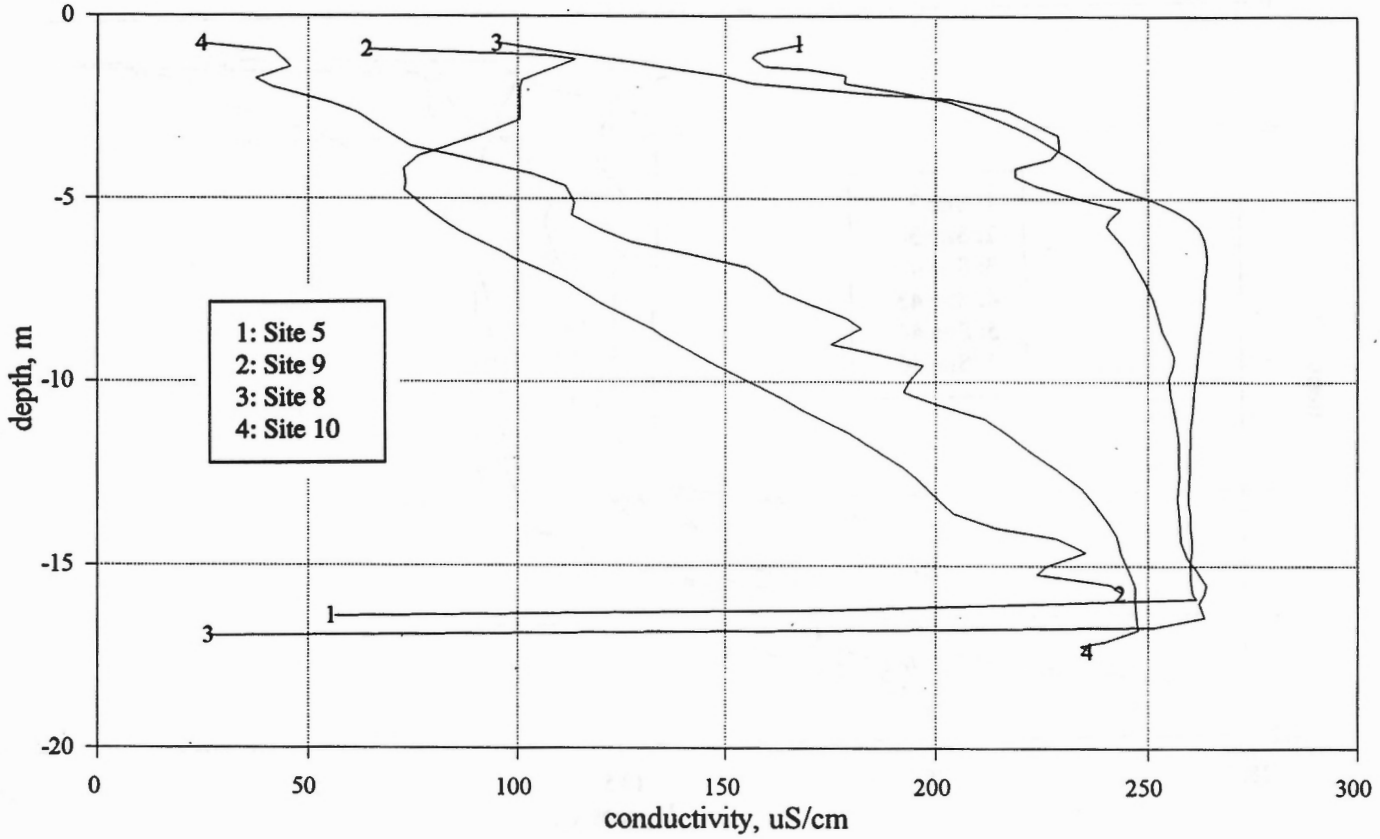
1: Site 5
2: Site 9
3: Site 8
4: Site 10
depth, m
conductivity, uS/cm

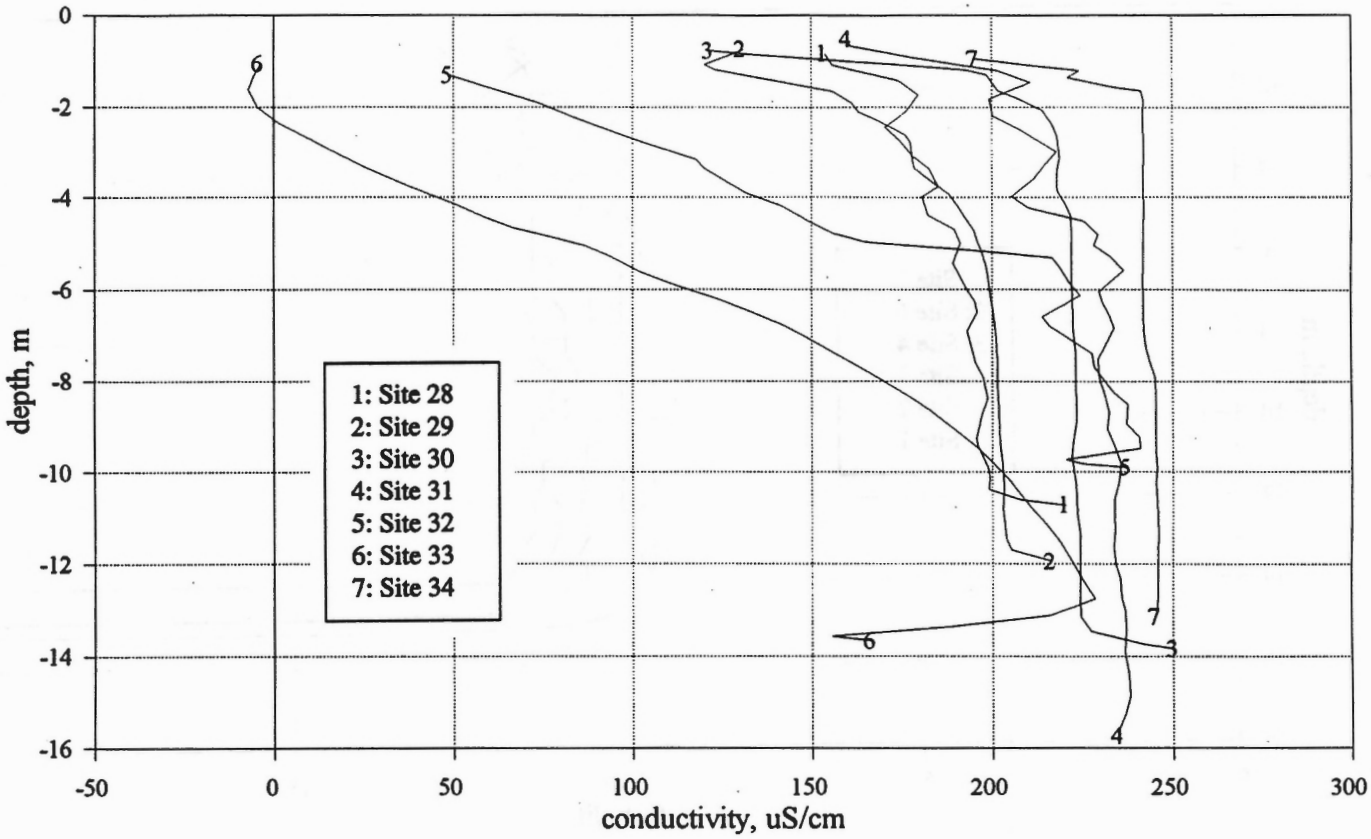
depth, m
0
-2
-4
-6
-8
-10
-12
-14
-16
-50
0
50
100
150
200
250
300
conductivity, uS/cm
1: Site 28
2: Site 29
3: Site 30
4: Site 31
5: Site 32
6: Site 33
7: Site 34

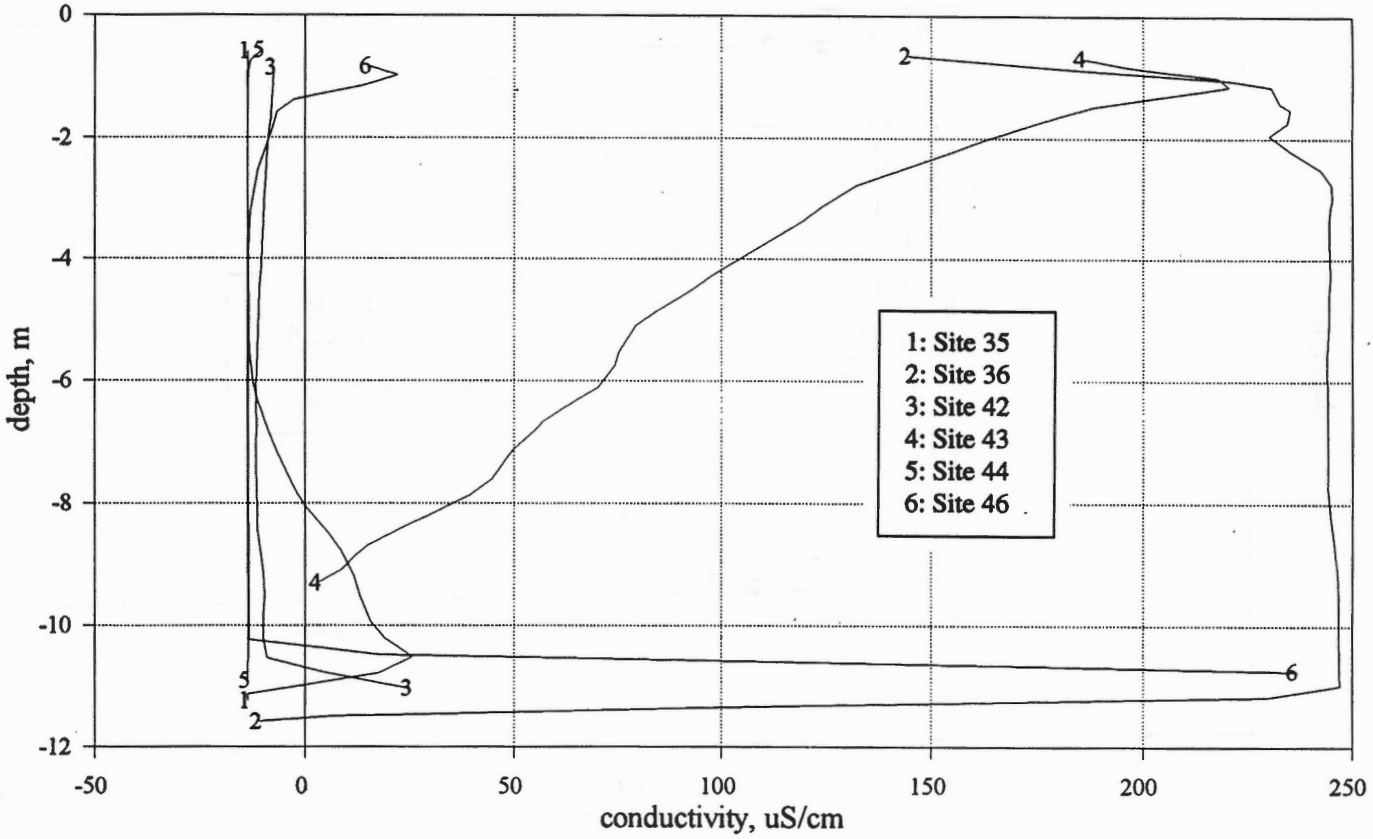
depth, m
0
-2
-4
-6
-8
-10
-12
-50
0
50
100
150
200
250
conductivity, uS/cm
1: Site 35
2: Site 36
3: Site 42
4: Site 43
5: Site 44
6: Site 46

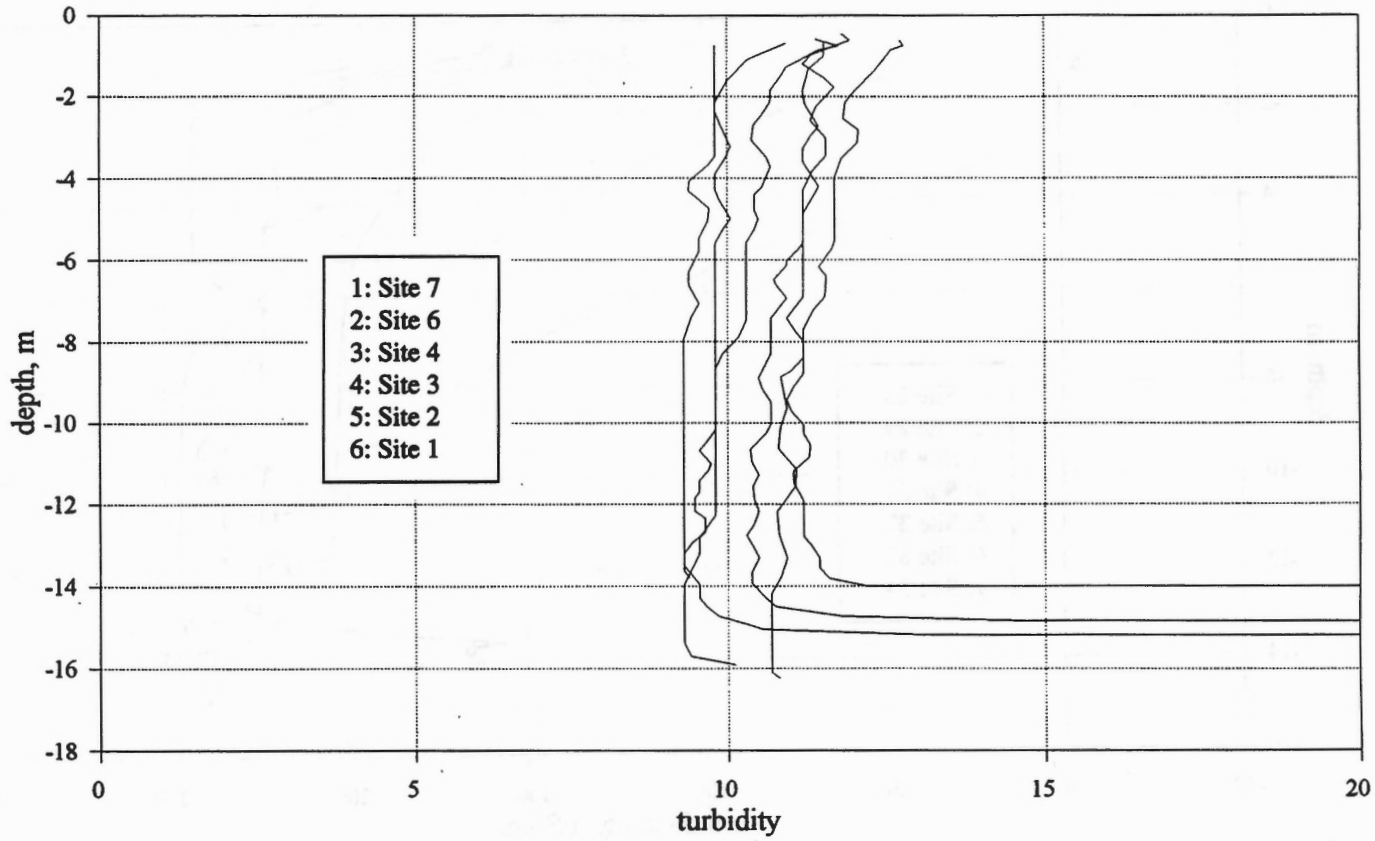
0
-2
-4
-6
-8
-10
-12
-14
-16
-18
depth, m
0
5
10
15
20
turbidity
1: Site 7
2: Site 6
3: Site 4
4: Site 3
5: Site 2
6: Site 1

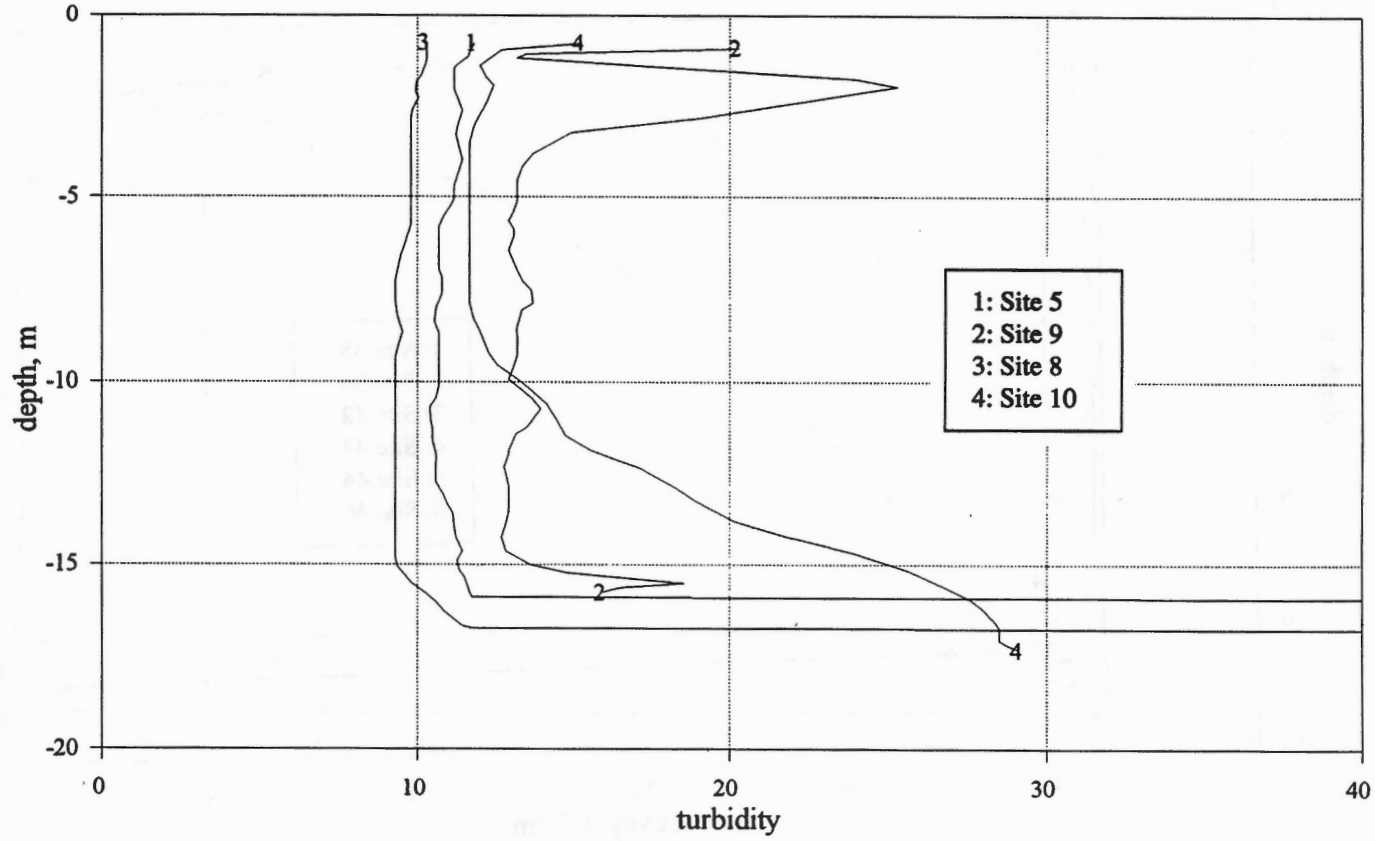
0
-5
-10
-15
-20
depth, m
0
10
20
30
40
turbidity
1: Site 5
2: Site 9
3: Site 8
4: Site 10

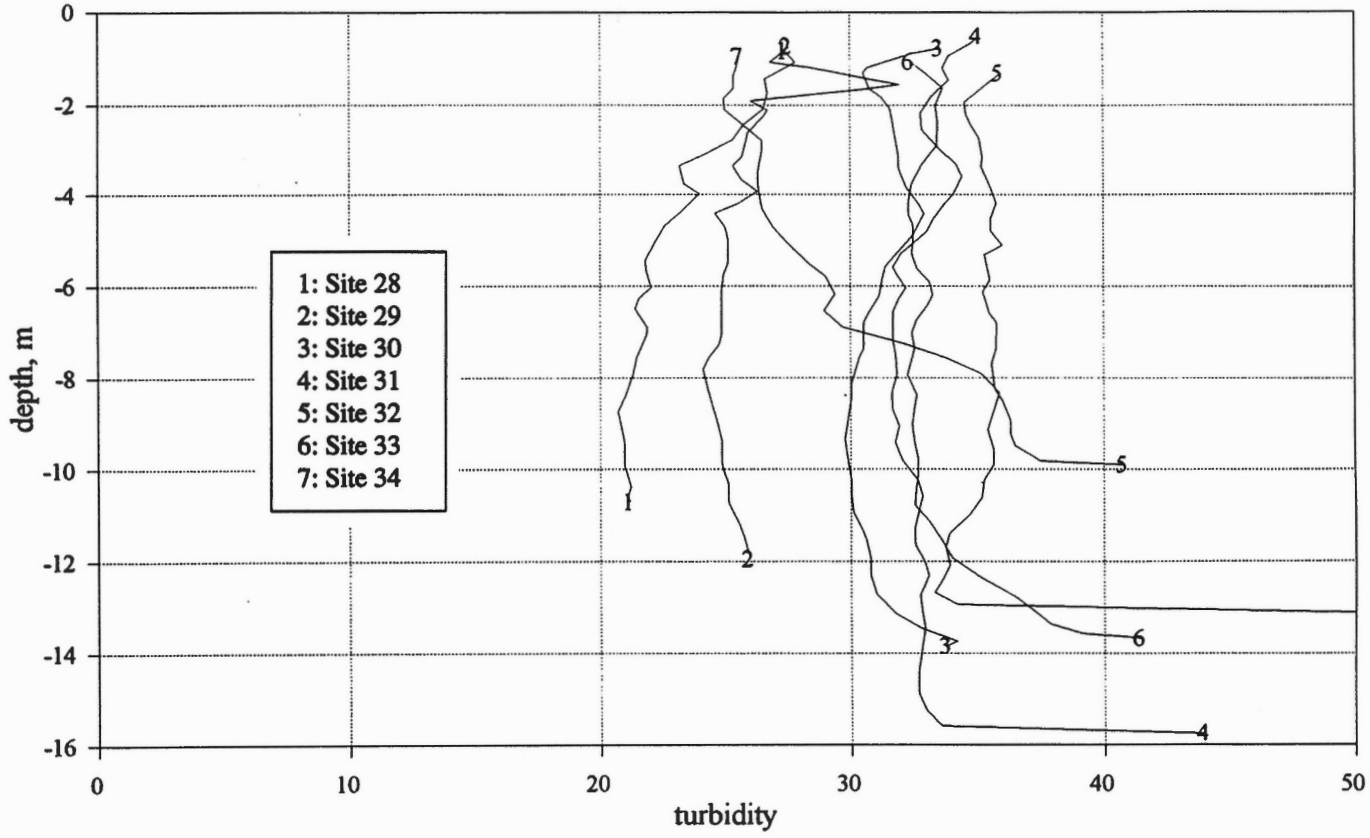
1: Site 28
2: Site 29
3: Site 30
4: Site 31
5: Site 32
6: Site 33
7: Site 34
depth, m
turbidity
0
-2
-4
-6
-8
-10
-12
-14
-16
0
10
20
30
40
50

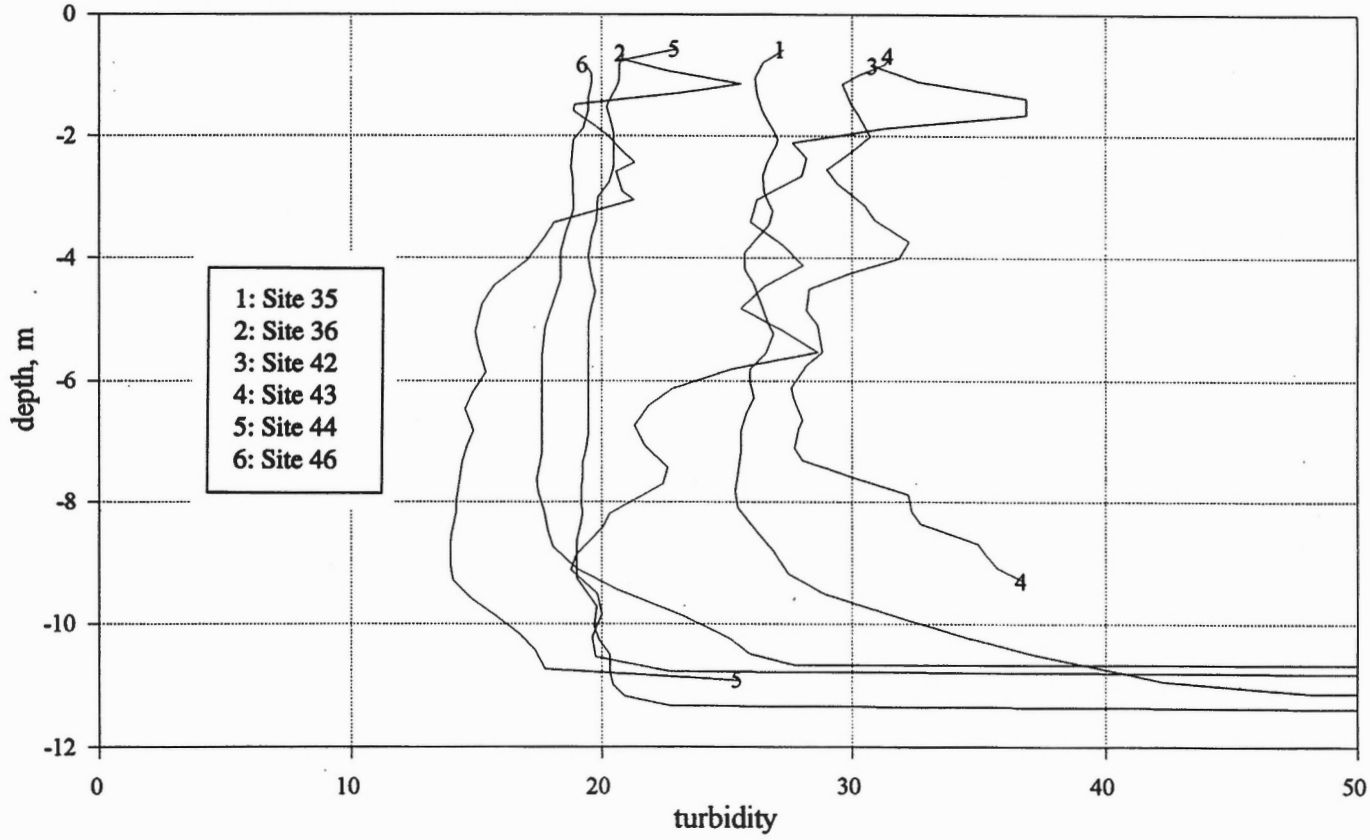
1: Site 35
2: Site 36
3: Site 42
4: Site 43
5: Site 44
6: Site 46
depth, m
turbidity
0
-2
-4
-6
-8
-10
-12
0
10
20
30
40
50

3. Geophysical survey results

3.1 Seismostratigraphy of Lake Winnipeg sediments

B.J. Todd

Geological Survey of Canada
601 Booth Street, Ottawa, Ontario K1A 0E8

C.F.M. Lewis

Geological Survey of Canada (Atlantic)
P.O. Box 1006, Dartmouth, Nova Scotia B2Y 4A2

ABSTRACT

In August, 1994, high-resolution single- and multi-channel seismic profiles, as well as sidescan sonar profiles, were obtained in Lake Winnipeg to investigate the seismostratigraphy of the sediments and the morphology and seismic velocity of underlying bedrock. The data, though limited in coverage compared to the large area of the lake, are generally of high quality. East-west transects, with south-north tie lines, were run in both the South and North Basins, as well as in the connecting Narrows and islands area. Over 500 km of geophysical track lines were obtained, revealing evidence for substantial westward relocation of the previously estimated position of the boundary between rock of Precambrian and Palaeozoic age, unanticipated basins of substantial depth containing as much as 100 m of what appears to be postglacial clay, and bedrock ridges. The glacial Lake Agassiz sediment sequence and some ice marginal morainic deposits are clearly imaged. The Lake Agassiz sediments are truncated and overlain by sediments of post-glacial Lake Winnipeg; the latter commonly reach thicknesses of 9 m or more in the offshore basins. The Lake Winnipeg sediments are gas-charged in many places, obliterating the seismic profiles. A mud-buried paleobeach and shoreface were profiled in the northern part of the South Basin about 15 m below present lake level. Sand waves in The Narrows are evidence of high-velocity bottom currents. Furrows in lakefloor sediment imaged in both the South and North Basins are ascribed to scouring by ice keels.

INTRODUCTION

Seismostratigraphy involves the determination of the nature and geological history of sediments from seismic evidence. Separate depositional sequences are defined by locating their boundaries, usually unconformities. For the Lake Winnipeg Project, a single-channel high-resolution seismic reflection profiling system was employed to profile the structure of sediments below the lakefloor. This system provided vertical resolution of reflecting horizons of 15-30 cm and penetration of up to 60 m. Also employed was a multi-channel seismic reflection system that provided deeper penetration into the subbottom to image the bedrock surface beneath the sediments.

Physiography

Lake Winnipeg lies at the boundary between the low-relief Interior Plains and the southwestern Canadian Shield. At 24,400 km^2, Lake Winnipeg is 25% larger in surface area than Lake Ontario and almost as large as Lake Erie.

Lake Winnipeg is divided into the South and North Basins, separated by a region of islands and constricted passages only a few kilometres wide called The Narrows (Fig. 1). The lake is 218.6 m above sea level (mean lake level 1901) and is oriented southeast-northwest in central southern Manitoba between 50° and 54° North latitude (Fig. 1). Lake Winnipeg is 430 km in length and reaches 100 km in width in the North Basin. The South Basin measures 90 km north-south and 40 km east-west and has a flat lakefloor with water depths averaging 12 m (Canadian Hydrographic Service, 1986). From Black Island to The Narrows, the lake is a complex of islands and passages with an irregular lakefloor bathymetry reaching charted depths of 61 m (Canadian Hydrographic Service, 1981). The North Basin extends almost 240 km south-north and reaches a width of 100 km. The most prominent shoreline feature is Long Point which extends 40 km into the lake from the western shore. The lakefloor in the North Basin is generally flat with an average water depth of 16-17 m. In contrast, the lakefloor adjacent to the eastern shore of the basin has a rugged bathymetry (Canadian Hydrographic Service, 1982).

The current bathymetric chart of the North Basin (Canadian Hydrographic Service, 1982) is based on a number of cross-lake bathymetric traverses conducted by the Geological Survey of Canada between 1901 and 1904, with additional work offshore Berens River from 1932 to 1934. Knowledge of the bathymetry of the South Basin dates from the same early Geological Survey of Canada surveys, with additional Canadian Hydrographic Service surveys in 1974.

Previous work

Lake Winnipeg is bounded by Precambrian rock of the Superior Province (>2.5 Ga) on its eastern shore (Weber, this volume) while its western shore is composed of Paleozoic carbonate rock and sandstone of the Williston Basin. The eastern shore of the lake can be viewed as a number of straight segments trending roughly north-northwest (Fig. 1). This trend is subparallel to the regional structure of lower Palaeozoic strata which is interpreted as the result of late Palaeozoic to early Mesozoic uplift of the Precambrian basement in eastern Manitoba (Bezys, this volume). The segmented nature of the eastern shore suggests that at least part of the this shore may be fault-controlled.

Until this survey, the Precambrian-Paleozoic contact was

thought to lie near the eastern shore of Lake Winnipeg. The poorly-exposed contact, where data are available, seems to consist of an escarpment of Ordovician Red River Formation carbonates overlying poorly-consolidated sandstones of the Winnipeg Formation (Betcher, 1986). Paleozoic strata dip to the southwest and the sequence increases in thickness to about 100 m at the western shore of Lake Winnipeg. Fault control of the Precambrian-Paleozoic contact (and possibly the north-trending eastern shore of the South Basin) is supported by data on the structural relief of the contact south of the lake which suggests that east side-up faulting or flexing (of unknown age), and not erosion, may be responsible for the present shield edge (Bezys, this volume).

Fractures that are subparallel to the eastern shore of Lake Winnipeg occur in the Superior Province and have been interpreted (in the Kirkland Lake area) as part of a late-tectonic, rift-related fracture system that appears to form one of the controlling factors for the distribution of kimberlites. Thus, a better understanding of the control for the eastern shore of Lake Winnipeg may contribute towards a better assessment of mineral deposits or may assist in mineral exploration.

The subaerial mapping of the extent of Lake Agassiz encompasses just over a century, from the 1870s to the 1980s (Elson, 1983). The Red, Winnipeg, Dauphin, Saskatchewan and numerous smaller rivers have drained much of Manitoba, Saskatchewan and the adjacent parts of the United States since late glacial and early Holocene times. Water draining this huge watershed has deposited sediments in Lake Winnipeg that have recorded and continue to record geomorphic and climate changes, isostatic tilting and anthropogenic modifications to the surrounding landscape. In Lake Winnipeg, the deposition and resuspension of the Red River sediment load was first described by Upham (1890). During the century since Upham's work, investigations in Lake Winnipeg have focussed on chemical, mineralogical and grain size studies (e.g. Ward, 1926; Bajkov, 1930; Kushnir, 1971; Brunskill and Graham, 1979). To date, there have been no published sonar or seismic profiles of the subbottom sediments of Lake Winnipeg, although Brunskill and Graham (1979) made a few comments regarding sediment thickness on the basis of unpublished sonar profiles. Because portions of the lake are a vestige of Lake Agassiz, the nature and depositional framework of sediments beneath those areas provide an opportunity for insight into the paleolimnology of Lake Agassiz.

SURVEY METHODS

The geophysical survey methods used aboard the CCGS *Namao* were described in detail in the cruise report (Todd, this volume). Given the large area of Lake Winnipeg and the limited survey time available, a strategic data set was collected (Fig. 1) covering the major depocentres defined by Brunskill and Graham (1979). Lines SB3 and SB5 transect the South Basin from south to north. Lines SB2 and SB4 transect the South Basin for west to east, with the latter line extending into Traverse Bay. Line SB6 transects the narrow channel to the east of Black Island, the area of Lake Winnipeg having the greatest charted water depths. Line SB7 was run in a zigzag pattern through The Narrows. Although poor weather precluded geophysical surveys in the southern portion of the North Basin, the northern portion of the basin was well-covered. Line NB8 runs roughly west-east across the Little Sandy Island-George Island chain. Line NB9 crosses the entire North Basin from Grand Rapids in the west to Warren Landing in the east, while lines NB10 and NB11 provide a south-north transect of the basin, crossing line NB9.

Survey speeds were generally about 4 knots (7.4 km/hr) to obtain geophysical records of high spatial resolution. All data were logged in Universal Time Coordinated (UTC) which is 5 hours ahead of Central Daylight Time (CDT), the local time used aboard the ship. All data were recorded both on paper and on magnetic tape. The marine survey was controlled by precise navigation in order to accurately run geophysical survey lines. Differential Global Positioning System (DGPS) with a base station at Duluth, Minnesota, was employed, providing positional accuracy of less than 10 m. In the North Basin, the DGPS ship's positions were consistently about 1 nautical mile (1852 m) southeast of the ship's positions marked on the Canadian Hydrographic Service Chart 6241 by the ship's navigator.

Single-channel seismic system

The IKB-Seistec™ (hereafter, the Seistec) single-channel seismic reflection profiling system was the primary tool used to image the lateral and vertical geometries of unlithified sediment in Lake Winnipeg. The system consists of a Huntec 4425 boomer (seismic energy source) mounted under a surface-towed surfboard and a 'line-in-cone' hydrophone array receiver. The boomer generates a continuous series of acoustic pulses or pressure waves in the water by implosion through the rapid movement of a spring-loaded plate. The seismic energy in each pulse travels down to, and reflects from, interfaces at the lakefloor and subsurface. Reflected energy (pulses) travels back to the lake surface and is detected by pressure-sensitive hydrophones in the receiver. For each 'shot' from the boomer, a 'trace' of reflected energy was recorded graphically and digitally on board ship. These traces were collected side-by-side on a graphic recorder as the ship steamed along each survey line, thereby producing a cross-sectional view, in reflection two-way-time (TWT), of the subsurface reflecting horizons.

The records obtained with this system were of excellent quality and provided the highest resolution of the lakefloor sediments above acoustic basement. (Acoustic basement is an informal designation used in high-resolution seismostratigraphy denoting material which resists penetration by seismic energy; such material can be hard sediments or bedrock). Consequently, line coverage by this system was given highest priority in completing the planned survey lines. The Seistec

system operates at frequencies between 2 and 8 kHz. It has the ability to vertically resolve strata with thicknesses of approximately 0.25 m in water depths of 2-100 m accompanied by depth penetration of up to 80 m in soft sediments (Simpkin and Davis, 1993). The system was fired at a 0.25 s interval with an average survey speed of 4 knots (7.41 km/hr) thereby sampling the subsurface every 0.5 m horizontally.

The Seistec records total 85.7 hours of recorded data, which translated to 198 m of paper records.

Multi-channel seismic system

The multi-channel seismic system, consisting of a seismic energy source and a 24-channel receiving eel, operates with the same physical principles as the single-channel seismic system described above. The seismic energy source is compressed air which is released rapidly in bursts beneath the water surface from a sleeve gun. The input signal (tens to hundreds of hertz) does not attenuate as quickly in the subsurface as does energy from higher frequency sound sources. Consequently, the depth of penetration of the sound energy into the subsurface is greater, but the vertical resolution of the reflecting horizons is less than higher-frequency systems. Thus the multi-channel seismic system can provide information about the deeper structure beneath the lakefloor, specifically the surface morphology of, and seismic velocities within, harder sediments and bedrock. These records were consulted to determine thickness of soft sediments where the Seistec system was unable to penetrate to acoustic basement.

The 10 cu. in. (164 cm^3) sleeve gun was towed 15 m astern of the ship at a depth of about 1 m and was fired at an interval of 5 s. The vertical resolution of this system is estimated to be 3-5 m with a horizontal resolution of 20 m at 4 knots. Reflecting signals received on the 24-channel eel were digitally recorded for post-cruise processing. Simultaneously, one channel from the eel was amplified, filtered and displayed on a graphic recorder on board ship. These shipboard records were for quality control only; because of the graphic recorder setup, the records were compressed horizontally and, consequently, are not of sufficient quality to reproduce in this report.

Accompanying this report are fourteen sheets of seismic profiles recorded with the multichannel seismic system. It is important to note that these sheets display only one channel (channel 4) of the 24 channels recorded digitally. Processing costs did not allow multichannel processing of the entire suite of data; nonetheless the fourteen seismic profile sheets harbour an abundance of geological information. Three separate sheets are included in the report which demonstrate, using data from line NB10, the improvement in resolution of reflectors that can be obtained after full multichannel processing.

Characteristics of seismic reflection profiles

Seismic reflection systems are characterized by a frequency range and related vertical and horizontal resolution and depth penetration. The higher the frequency of the seismic source, the thinner the bed that can be resolved, but energy penetration into the earth decreases with increasing frequency (Sheriff and Geldart, 1982).

The interpretation of seismic reflection data involves the expression of the seismic information in geological terms. Records from seismic profiling systems *appear* to be geological cross-sections and are often (and sometimes erroneously) interpreted as such, to a first approximation. In seismic profiles the vertical axis is expressed in two-way-travel time (i.e. the time elapsed while the seismic energy travels from the source at the surface, down to a reflector and returns upward to the detector) although the reflector may not be vertically below the source. Seismic reflection profiles then, are not *directly* comparable to traditional geological cross-sections in which both the horizontal and vertical scales are units of distance, and features in vertical alignment are correctly represented (Sheriff and Geldart, 1982). Successful interpretation of seismic profiles in Lake Winnipeg depended mainly on a proper consideration of 1) the reflection process and horizontal resolution, 2) reflector geometry and 3) vertical exaggeration. Seismic reflections are generated by surfaces of strata having differing acoustical properties.

Horizontal resolution

The first Fresnel zone is the portion of a plane reflector mainly effective in generating a reflection (Fig. 2a). When the wavefront encounters the reflector, the reflected signal is generated by the interaction of the wavefront over the first Fresnel zone, defined by the intersection area of the seismic wave as it advances 1/4 of a wavelength (the wavelength is equivalent to the velocity of a seismic wave divided by its frequency). Thus, information is obtained *not* about the reflector at point P (the reflection point of the geometrical ray), but rather an average over the whole Fresnel zone. This effect limits the horizontal resolution that can be expected from the seismic reflection method, even though the Fresnel zones of successive reflections in this survey overlapped 8-10-fold. Generally, only the average structure over an area the size of the first Fresnel zone can be perceived. For example, at a water depth of 100 m, a reflected 3000 Hz signal represents an area with a radius of 4.0 m (horizontal resolution 50 m^2) while at a water depth of 20 m, the radius horizontal resolution is improved to about 2.3 m. Thus, horizontal changes in structure smaller than these radii may not be resolved. Fresnel zones are considerably greater for sleevegun seismic profiles. For example, at a water depth of 100 m, a 100 Hz sleevegun seismic wave would be reflected from an area with a radius of 27.6 m.

Reflector geometry

The simplest geometry of seismic reflection is shown in Figure 2b,i. A plane horizontal reflector is overlain by a medium of constant velocity. In this case, the time (i.e. seismic) section is similar in appearance to the depth (i.e. geological) section. However, if the geological structure is more complex, the time section may look very different from the geological section. The problem arises because the reflected ray path is perpendicular to the *reflector*, but the reflection record is plotted vertically below the *receiver*. For example, in Figure 2b,ii, a point reflector in the depth section (e.g. a boulder or rock edge) gives rise to a hyperbola in the time section. Anticlines (Fig. 2b,iii) appear broadened and synclines can show a suite of effects (Fig. 2b,iv). If the syncline curvature is greater than that of the incoming wavefront, synclines appear inverted and resemble anticlines (Sheriff and Geldart, 1982). In summary, regions of complex geological structure can produce confused seismic sections from which it is difficult to deduce the geometry of the corresponding geological section, thus rendering definitive interpretation unlikely. These problems were kept in mind during the interpretation of the seismic profiles. In general, the interpretation of the seismic profiles from Lake Winnipeg as geological cross sections was straightforward as in Figure 2b,i, though influenced by considerations of geometry, horizontal resolution and vertical exaggeration.

Vertical exaggeration

Vertical exaggeration occurs when the vertical scale of the recorded seismic profile is larger than the horizontal scale. Vertical exaggeration makes subtle effects more evident. Consequently, the recording scales on the Lake Winnipeg survey were set at high vertical exaggeration so that discontinuities and displacements would be plainly visible. Seismic time sections involve some variable vertical exaggeration because the velocity of sound in sediments varies naturally (usually increasing) with depth. However, identification and interpretation of features on seismic reflection sections are greatly affected by the rather large vertical exaggerations produced during recording. The paper records of seismic data from the Lake Winnipeg survey were produced on board ship with an inherent vertical exaggeration of 8.7, 11.6 and 17.4 times.

Sidescan sonar

Sidescan sonar is a high-resolution, very high frequency swath acoustic system used in offshore surveys to obtain images of lakefloor morphology (Fig. 3). The system used in this survey was a Klein 531T sidescan sonar with a graphic recorder on board ship and, in the water column, a towfish which operated at 100 kHz. At this frequency, reflections could be generated from surfaces with radii as small as 1.75 m at a range of 100 m or 0.35 m at 20 m range. The sidescan insonified the lakefloor to ranges up to 100 m on both sides of the towed fish. Acoustic returns from each of the sidescan channels and the profiler were displayed on a graphic recorder. The reflected signals received by the fish provided a map view of the lakefloor. The output from this instrument provides information on the morphology of the lakefloor as well as textural information. For example, rock gives a much stronger (darker) reflected signal than does silt, and individual topographic features cast recognizable acoustic shadows.

The major difference between sidescan and seismic reflection systems is that the purpose of the sidescan is to obtain very high-resolution images of acoustic energy reflected and backscattered off the lakefloor, as opposed to changes within the sediments beneath the surface of the lakefloor. Backscatter is a microscale process of multiple reflection of acoustic energy by facets of individual grains of sediment on the lakefloor (Fig. 3). Some of the micro-reflected energy is directed back towards the source (towfish) where it is received as backscatter. In comparison, reflection of acoustic energy is a single event at a larger scale involving the surface of the lakefloor or large targets such as boulders but not individual grains of sand or mud (Kleinrock, 1992; Hobbs and Dame, 1992).

Sidescan sonar records are displayed as gray-scale images that appear similar to aerial photographs in that they show features on the lakefloor in plan view. The view is commonly exaggerated in the cross-track direction, depending on the speed of the survey vessel and the range selected for recording. The records display the character of lakefloor roughness and details of lakefloor structure and allow determination of the shape, orientation and dimensions of structures (morphology) as well as the fine-scale acoustic character of sediments (texture) on the lakefloor. Data from the system portrays strong received energy as dark features on a light background; returns from positive (bumps) and negative (depressions) topographic features show characteristic patterns (Fig. 3). Areas of acoustic roughness (e.g. rock or gravel) will appear darker than areas which are more acoustically smooth (e.g. sand or mud).

The sidescan sonar records total 74.5 hours of recorded data and were plotted on 285 m of paper records.

SEISMOSTRATIGRAPHY: REFLECTORS AND SEQUENCES

The Seistec single-channel seismic reflection profiles were the principal data used in the study of Quaternary sediments in Lake Winnipeg. Sleeve gun multi-channel reflection profiles were used to determine the depth to, and morphology of, acoustic basement. The seismic reflections were interpreted according to the principles of reflector identification discussed by Mitchum, Vail and Sangree (1977) and Mitchum, Vail and Thompson (1977). Reflections are assumed to be conformable with sedimentary bedding and that they are chronostratigraphic horizons which can be traced from place to place and utilized

for correlation between sites within depositional basins. Reflections which are regional in extent and which truncate underlying reflections define the boundaries of packages or sequences of sediment. Three such regional reflectors were colour-coded on copies of the seismic reflection profiles. These comprise, in order of increasing depth and age, the lakefloor and two unconformities (Fig. 4, Table 1).

Commonly, the sediment sequences between reflectors are named for their upper bounding reflector colour code. In this paper, however, we use the informal interpretive designations Winnipeg Sequence for the lakefloor sediments and Agassiz Sequence for the underlying sediments (Fig. 4, Table 1), based on convincing regional geological relationships. The informal designation Acoustic Basement Sequence is used for deposits below the deepest unconformity (Fig. 4, Table 1), so named because little or no seismic energy is able to penetrate this sequence. The structural configuration and extent of the Winnipeg, Agassiz, and Acoustic Basement Sequences are described below.

The Winnipeg Sequence and various stratigraphic levels of the Agassiz Sequence were penetrated by piston and gravity cores. The preliminary correlations of the lithologies in the cores and the sequence boundaries in the seismic profiles are illustrated and discussed by Lewis and Todd (this volume). The principal purpose of the cores is to provide information on the physical nature of the seismostratigraphic sequences.

Facies variations and areas of complex stratigraphy are evident within the sequences, especially the thick Agassiz Sequence. These details were not mapped in this preliminary study. However, the attributes of these stratigraphic subdivisions are identified in terms of their acoustic signature, geometry, distribution and bounding units as summarized in Table 1 and in the subsequent discussion. The units are discussed in order from oldest to youngest.

Acoustic Basement Sequence

The seismic reflection profile sheets (included with this volume) show the morphology of the surface of the Acoustic Basement Sequence along the survey lines. It is important to recognize that these data are a display of *one channel only* of the 24 channels of data recorded using the multi-channel seismic reflection system. The cost of full multi-channel processing for all the data collected is prohibitive.

The Seistec system was rarely effective in profiling acoustic basement because it employs a higher frequency seismic energy source than the sleeve gun used in the multi-channel system. In the following discussions, depths in metres were estimated by multiplying two-way travel time (ms) by 0.75, hence a seismic velocity of 1500 m/s is assumed for both water and sediments. The South Basin is described first, followed by the islands and The Narrows region, and finally the North Basin. In general, the Acoustic Basement Sequence shows two reflection configurations: a chaotic reflection configuration with some penetration of seismic energy is interpreted as till whereas a high-amplitude reflector with no penetration is interpreted as bedrock (Fig. 4, Table 1). Areas where the latter reflector shows low relief is usually interpreted as being Paleozoic carbonate, a clastic rock, whereas high relief is characteristic of Precambrian crystalline rock. Areas of moderate relief may be either Paleozoic or Precambrian.

South Basin

Line SB2 runs from west to east across the South Basin (Fig. 1). At the west end of the line from 217/2004 to 217/1845, the reflector from the upper surface of acoustic basement is at about 50 ms (TWT), implying a depth of about 35 m below lake level. (Reflectors below this depth are multiples of the real reflectors and hence do not represent additional reflecting horizons). This profile of the western South Basin is in agreement with that presented for adjacent land by Betcher (1986), who reported a sediment thickness of about 30 m at Gimli (Fig. 1). At 217/1845 is an escarpment, referred to here as the South Basin Escarpment, at which the upper surface of acoustic basement dips to the east and reaches a depth of about 60 m (80 ms TWT). The surface maintains this depth east to 217/1700 where reflectors are obscured, presumably by gas. The implied depth to the base of sediments in the eastern South Basin, 60 m below lake level, strongly contradicts predictions based on observations on land (e.g. Betcher, 1986). The position of the reflector at 80 ms is comparable to drill hole intersections of Precambrian rock at Grand Beach (Fig. 1). Hence it appears that all or most of the Paleozoic section may be absent in the eastern South Basin. This would imply that Paleozoic rock which outcrops and has been drilled along the eastern shore of the South Basin is an outlier. Stoney Point, at the southeast shore of the South Basin (Fig. 1), is a Paleozoic outcrop at the eastern extent of an area of thin sediments (Betcher, 1986) and may represent the crest of the South Basin Escarpment. It is conceivable that the escarpment, running north from Stoney Point, through the South Basin, to Hecla Island and The Narrows, represents a slope capped by the Dog Head Member of the Red River Formation (Bezys, this volume).

Approximately 25 km to the north, line SB4 lies roughly parallel to line SB2 (Fig. 1). At the west end of line SB4, the upper surface of acoustic basement is again at a depth of about 35 m (40-50 ms TWT). The South Basin Escarpment observed on line SB2 is present on this line at 221/1555. Here the top of acoustic basement dips to the east and reaches a depth of about 60 m (70-80 ms TWT). East toward Traverse Bay, the acoustic basement surface maintains a position of 60-80 ms (TWT) but shows shorter wavelength irregularities on its surface.

Line SB3 runs from south to north and intersects both lines SB2 and SB4 (Fig. 1). Reflectors at the southern end of line SB3 at the mouth of the Red River are obscured by gas. Near 220/1710, the surface of acoustic basement lies between 20 and

40 ms (TWT); it is a generally smooth surface with broad undulations. The upper surface of acoustic basement deepens gradually to the north reaching about 90 ms (TWT). At 220/1835 the surface shows a distinct step down to the north of about 15 ms (TWT) amplitude. This feature is correlated with the South Basin Escarpment interpreted on lines SB2 and SB4; its gradual slope represents an oblique section down the face of the escarpment. At 220/1940 is a "peak" of acoustic basement 20 ms (TWT) in amplitude. This feature is about 120 m wide and 15 m high and is interpreted to be an esker or a small moraine. Other similar peaks of acoustic basement are clearly imaged on the Seistec record of line SB3 but are not discernable on the seismic sheets.

Line SB5 runs south to north from an intersection with line SB4 (Fig. 1). At the south end of line SB5, the upper surface of acoustic basement is at a depth of about 60 m (70-80 ms TWT). North toward Hecla Island (Fig. 1), the upper surface of acoustic basement becomes increasingly shallow and eventually outcrops above the lakefloor at 222/1725-1729. At this location, sidescan sonar records show gravel and boulders, suggesting that the feature charted as Pearson Reef (Fig. 1; Canadian Hydrographic Service, 1986) is an outcropping moraine, named here the Pearson Reef Moraine. The moraine is correlated with the acoustic basement high seen on line SB4 at 221/1614-1628. North of the Pearson Reef Moraine on line SB5, the acoustic basement surface drops to 60-80 ms (TWT). Line SB5 is entirely located below the South Basin Escarpment. Away from the Pearson Reef Moraine, the surface is characterized by ambiguous moderate relief. Correlation to drill holes at Grand Beach suggests the surface is Precambrian rock. Conversely, as line SB5 approaches Black Island, the acoustic basement surface takes on a "blocky" appearance (222/1900), which could be regarded as characteristic of carbonate bedrock terrain (Todd and Lewis, 1993).

In summary, the Acoustic Basement Sequence in the South Basin is interpreted as a discontinuous till mantle over bedrock. The generally smooth nature of the upper surface of acoustic basement in the western South Basin suggests that bedrock in this area is Paleozoic carbonate. The moderate relief acoustic basement of the eastern South Basin is ambiguous and could be Paleozoic or Precambrian bedrock, although correlation to drilling on land favours interpretation as Precambrian. These two zones are separated by the prominent South Basin Escarpment (Fig. 5). Very limited seismic energy penetration into till, such as Pearson Reef Moraine, suggests that it is a hard reflecting surface and is therefore well-compacted. Peaks in the surface of acoustic basement seen on both seismic and Seistec records may represent small moraines or eskers. Pearson Reef is, in comparison, a much larger moraine.

Islands and The Narrows

Line SB6 traverses the narrow, deep water channel around the east side of Black Island and north into Washow Bay (Fig. 1). On the western portion of the line, the surface of acoustic basement is smooth, suggesting that this portion of the line is underlain by Paleozoic rock. A transition to an irregular acoustic basement surface of steep peaks occurs near 223/1540; this irregular surface outcrops on the lakefloor between 223/1700-1800 where overlying sediments have been removed by erosion. An irregular acoustic basement morphology is typical of seismic images in Precambrian terrain (Todd and Lewis, 1993). From the transition at 223/1540 to the north end of line SB6 at 223/2231, acoustic basement, where it is detected, undoubtedly is Precambrian rock. At 223/1800, the area of the deepest charted point in Lake Winnipeg was crossed and the lakefloor is at 60 ms (TWT), or about 45 m.

Line SB7 traverses, in a zigzag pattern, The Narrows and then north into Washow Bay at the south end of the North Basin (Fig. 1). The irregular surface of acoustic basement along all of line SB7 is typical of Precambrian terrain. Sidescan sonar records of acoustic basement outcrop show a rough lakefloor morphology with high reflectivity, also typical of Precambrian rock.

High relief lakefloor observed on the bathymetric recorder of the CCGS *Namao* between Hecla and Black Islands suggests the presence of Precambrian rock in the channel.

North Basin

Line NB8 runs west-east in the central North Basin (Fig. 1). In the east, the line is situated offshore Poplar River where spires of Precambrian rock project above the water level forming many small islands. The moderate to high relief acoustic basement surface from the east end of the line at 227/1340 westward to 227/1854 suggests that basement in this area is Precambrian rock. The Precambrian-Paleozoic contact is ambiguous, but is located within a few kilometres of 227/1854; from here west to the end of the line at 228/0045, the acoustic basement surface is comparatively smooth and lies at a depth of 60-80 ms (TWT). Two features are distinct on this seismic profile. Firstly, a clearly-imaged moraine outcrops at 227/1800-1813, where sidescan sonar records (not shown here) imaged boulders and gravel on the otherwise smooth and featureless lakefloor. Orientation of the stoss and lee sides of the moraine, named here the George Island Moraine, suggest the glacial ice flow which built the moraine was from the northeast. The other feature imaged on this seismic record are notches in Paleozoic bedrock at 227/1907 and 1910 near the Precambrian-Paleozoic contact and at 227/2045. A possible mechanism for notch formation in the Paleozoic bedrock is karstification. Furthermore, it is possible that Paleozoic carbonate extends slightly farther east than suggested here and that the surface shows high relief due to the presence of karst features. The apparent absence of Paleozoic rock around the Sandy and George Islands is compatible with the lack of Paleozoic erratics on these islands as observed by Dowling (1900).

Line NB10 intersects the west end of line NB8 (Fig.1) and

extends to the north. Whereas 70% of the high-resolution Seistec record collected along line NB10 was rendered uninterpretable by gas masking, the seismic record obtained using the sleeve gun is of high quality and clearly images acoustic basement. The southern portion of line NB10 has a smooth acoustic basement surface, interpreted as Paleozoic rock, at 50-70 ms (TWT) extending from the south end of the line at 230/1621 to the unambiguous Precambrian-Paleozoic contact at 230/1814. At this location, the surface of acoustic basement drops sharply to the north to 100 ms (TWT) and greater. The irregular Precambrian acoustic basement surface extends north to the end of line NB10 at 230/2310. The greatest depth to acoustic basement surface during the Lake Winnipeg Project was imaged on this line; at 230/2014 the surface reaches 160 ms (TWT) which is equivalent to a depth of at least 120 m.

Long Point, which projects into the North Basin from the western shore of the lake (Fig. 1), is part of the extensive The Pas Moraine (Klassen, 1967). The offshore extension of the moraine is clearly imaged on line NB10 between 230/1730-1810. Here, a lens of material, situated directly east of Long Point, reaches a thickness of about 30 m (40 ms TWT) and is perched on Paleozoic basement. Sediments of the Agassiz and Winnipeg Sequences completely bury the sediment lens.

Multi-channel seismic processing was applied to this portion of line NB10 (230/1747-1927) where it intersects the Precambrian-Paleozoic contact. These data are shown on three sheets included with this report. At the top of each sheet is a single-channel display with the corresponding stacked and migrated section below. Details of the processing parameters are given in Table 2. Sheet 1 is the southern sheet and contains the northern flank of The Pas Moraine. The Precambrian-Paleozoic contact is clearly imaged at 230/1814, having a small lens of till mantling the contact zone. To the north (sheets 2, 3) is Precambrian bedrock lying between 80 and 130 ms (TWT) (60-100 m). A thin till lens 10-30 ms thick mantles bedrock from 230/1858-1909; reflections from the bedrock surface below the till are clear.

Line NB11 is oriented south-north in the northern part of the North Basin (Fig. 1). At the south end of this line, smooth acoustic basement surface lies at a depth of 80-100 ms (TWT). Several irregular depressions on basement are interpreted as karst features. The surface rises gradually, with minor steps, to the north just reaches the lakefloor to outcrop at 231/1618. Dark backscatter on the sidescan sonar record from the outcrop is difficult to interpret. Based on the strong reflection amplitude of the surface, and its stepped morphology, the feature is interpreted as a bedrock ridge. Correlation to line NB9 indicates a strike of roughly NNW-SSE; the ship's track on line NB11 intersected the strike of the moraine at a small angle making it appear broad on the seismic record. An extremely abrupt change in the smooth acoustic basement morphology is interpreted as the Precambrian-Paleozoic contact at 231/1854. North of this location and extending to the northern end of the line at 231/2115, the acoustic basement surface is rough, similar in appearance to acoustic basement mapped on lines NB10 and NB8.

Line NB9 transects the North Basin from Grand Rapids in the west to Warren Landing in the east (Fig. 1). Although only a portion of the multi-channel seismic data is available, the profile was interpreted in conjunction with the full Seistec profile of this line (not shown here). The Precambrian-Paleozoic contact was not imaged. However, its location can be constrained. On the eastern portion of line NB9, from the start of the line to 229/1630, Seistec data clearly show the irregular acoustic basement surface of Precambrian rock. Paleozoic rock is interpreted, despite extensive zones of gas-masking, from 229/1850 to the west. This latter interpretation, based on Seistec data, is corroborated by the seismic profile on which acoustic basement exhibits the smooth surface characteristic of Paleozoic rock. At the east end of the seismic profile between 229/1939-1941 is the west flank of the bedrock ridge also imaged on line NB11. The surface of acoustic basement reaches 90 ms (TWT) at 229/2005 and rises gently to the west. At 229/2233, a pronounced notch in the blocky bedrock reflector may be evidence of karst features. Paleozoic bedrock outcrops at the lakefloor between 229/2155-2203 (Fig. 6).

In summary, the Acoustic Basement Sequence in the North Basin is composed of Precambrian rock, Paleozoic rock, and till. Precambrian rock underlies the eastern portion and Paleozoic rock underlies the western portion of the North Basin (Fig. 5). The George Island Moraine is expressed above the lake surface as the chain of islands from George Island in the southeast to Little Sandy Island in the northwest. The offshore extension of The Pas Moraine is apparent on line NB10, buried by Agassiz and Winnipeg Sequence sediments. Lines NB11 and NB9 intersected a bedrock ridge in the northern portion of the North Basin. Interpretation of the basement contact, moraines and bedrock ridge is shown in Figure 5.

Agassiz Sequence

The seismic character of the Agassiz Sequence is well displayed in a Seistec record from line NB11 in the North Basin (Fig. 8). Reflectors in the sequence are medium- to high-amplitude, parallel, wavy and laterally continuous. Commonly, as in this example, the Agassiz Sequence can be divided into lower, middle and upper units, in which the middle unit reflectors exhibit a reduced reflection amplitude. The sediments have the form of a sheet drape; sediments evenly drape underlying acoustic basement, mimicking its topography. The bedrock contact occurs in the middle of this record: to the left is Paleozoic bedrock with a flat upper surface, and to the right is the irregular surface of Precambrian bedrock.

The upper bounding surface of the Agassiz Sequence is truncated by a sharply-defined angular unconformity, named here the Agassiz Unconformity (Fig. 8). This unconformity can be traced on all seismic profiles obtained in Lake Winnipeg. In

some of the deepest water areas in the North Basin where sediment accumulation is thickest, the unconformity becomes parallel to bedding and is difficult to define. We suggest that in these areas, there may be no hiatus between the Agassiz Sequence and overlying Winnipeg Sequence. Unfortunately, these depths can not be easily cored but could be sampled by drilling.

A number of enigmatic features occur within the Agassiz Sequence. In the South Basin, prominent "broken" reflectors, which can be traced horizontally over a substantial distance (Fig. 9), are composed of short reflector segments whose ends appear to be vertically offset. The "broken" reflector horizons conformably drape acoustic basement highs (Fig. 10). These horizons are interpreted as evidence that Agassiz Sequence sediments have undergone syn- or post-depositional faulting. The age of the faulting is pre-Winnipeg Sequence because the Agassiz Unconformity and the Winnipeg Sequence are not offset (Figs. 9, 10). Alternatively, the reflector segments could be different sedimentary strata with local zones of increased permeability which host gas and cause high amplitude reflections.

In some areas in both the South and North Basins, the lower Agassiz Sequence exhibits an incoherent, homogeneous reflection pattern in which the horizontally continuous, parallel reflections, typical of the Agassiz Sequence elsewhere, are rare to absent (Figs. 11, 12). The original geometry of these disturbed zones probably consisted of horizontally continuous, parallel beds but this geometry has been disrupted, and in some areas eradicated, by a syn- or post-depositional event. Loading and shear, for example by a glacial re-advance, could provide a mechanism to disrupt the original sediment geometry. However, there is no evidence of an unconformity associated with such an event. It may be more likely that the original bedding was disrupted by dewatering during compaction.

Agassiz Sequence sediments commonly outcrop in Lake Winnipeg from Black Island to The Narrows (Fig. 1) where the action of strong currents has cut into the Agassiz Sequence (Figs. 13, 14). These areas offer the opportunity to sample the Agassiz Sequence at a range of stratigraphic levels.

Winnipeg Sequence

Sediments of the Winnipeg Sequence unconformably overlie the Agassiz Sequence. Reflectors within the Winnipeg Sequence generally exhibit a lower reflection amplitude and are less laterally continuous than reflectors in the Agassiz Sequence. Where visible, Winnipeg Sequence reflectors are smooth, parallel to sub-parallel and even. The overall aspect of this sequence is that it is more acoustically transparent than the underlying Agassiz Sequence (Figs. 6, 8-12).

The Winnipeg Sequence is thickest in the centres of the South and North Basins where it reaches a thickness of up to 11 m (15 ms TWT). The distribution of this sequence is sporadic to absent in areas of Precambrian outcrop at the eastern margin of the North Basin, in areas of Paleozoic outcrop in the western North Basin (Fig. 6), and in regions of high current flow like the Black Island-The Narrows region (Figs. 13, 14).

In some areas, the Winnipeg Sequence directly overlies acoustic basement where the Agassiz Sequence is absent. The upper surface of the sequence is normally smooth lakefloor which is disrupted in places by furrows.

Disseminated gas, possibly both biogenic and petrogenic (derived from bedrock) in origin, is a common occurrence in the Winnipeg and Agassiz Sequences (Fig. 15). Gas percolates upward through the sediment column until it encounters a horizon of favourable permeability (Hovland and Judd, 1988). The gas then tends to travel horizontally along these preferred horizons, producing reflections of enhanced amplitude (Fig. 15). Penetration of the high-frequency Seistec reflection system was often limited by gas. In the North Basin, 40% of the profiles were masked by gas, providing little more information than the lakefloor reflection. In the South Basin, gas masking was more prevalent, with 60% of the profiles affected. Fortunately, the response of the low frequency sleeve gun seismic system was less influenced by the presence of disseminated gas and this system achieved penetration along a much greater proportion of the profiles.

A number of constructional and erosional features were identified in the Winnipeg Sequence. A paleobeach on the north flank of Pearson Reef Moraine is situated immediately above the Agassiz Unconformity and is buried by typical Winnipeg Sequence sediments. A wave-cut platform, beach ridge deposits and foreset beds are clearly imaged (Fig. 16). At this site, gravity core 115 sampled sand at the base of the core beneath 268 cm of grey silty clay (Lewis and Todd, this volume). In the deep water channel around Black Island (Fig. 1), multiple cycles of erosion and sedimentation can be recognized (Figs. 17, 18). An example of possible groundwater discharge was observed near Black Island (Fig. 19). Here the lakefloor and near-lakefloor reflectors are not detected by the Seistec reflection system. Upwelling fluids, possibly water from the Winnipeg Sandstone, may have charged the sediments at this location to the degree that their density is not significantly different from that of the lakewater.

SIDESCAN SONAR FEATURES

The majority of the lakefloor is featureless. However, several types of lakefloor morphological features were imaged by the sidescan sonar system.

Bedrock outcrop

Bedrock outcrop was only documented in a few locations along the geophysical survey lines because most of the bedrock beneath Lake Winnipeg is mantled with a thick accumulation

of sediment. The bedrock outcrop shown in Figure 20 is located north of The Narrows along strike with its straight eastern shoreline (Fig. 1). This sidescan sonar image demonstrates the highly-reflective bedrock surfaces and boulders with fine-grained sediment ponded between bedrock highs. Irregular bedrock topography evident on the corresponding Seistec record suggests this outcrop is Precambrian bedrock.

Furrows

Recent lakefloor sediments in parts of the South and North Basins exhibit linear to curvilinear furrows (Figs. 21, 22). These furrows are about 1 m deep, tens of meters wide and up to kilometres in length, and berms of sediment deposited on both sides of the furrow rise about 0.5 m above the lakefloor. These linear features include abrupt terminations, changes in orientation and cross-cutting patterns.

This disruption of recent lakefloor sediments is attributed to scouring by ice. The scouring process is envisioned as initially requiring the accumulation, or stacking, of slabs of lake ice into pressure ridges. The combined weight of the stacked ice slabs depresses the entire mass; the base, or keel, of this mass is pressed into the soft lakefloor sediments. Wind and currents drive icebergs in the ocean (Todd et al., 1988) and presumably these agents drive ice islands in Lake Winnipeg in the same way. Wide ice islands would have wide, multiple-ridged keels which produce wide furrows in the lakefloor as shown in plan view in Figure 21. In this example, a younger, narrower furrow cross-cuts an older, wider furrow. Sediment scoured by a multiple-ridged keel is shown in cross-section in Figure 22 in which a number of closely-spaced furrows are present.

Ice scouring is not ubiquitous in Lake Winnipeg. Furrows are common in the southern South Basin (south of 50°35' N) and in northwestern North Basin. It is likely that, in these regions, ice-accumulation conditions, meteorological patterns and water depth combine to encourage scouring of the lakefloor.

Scouring of lakefloor sediments by lake ice has been documented in Lake Erie (Grass, 1984) where a 10 m-high ice island was observed to be grounded in 18 m of water, similar to Lake Winnipeg water depths. A subsequent geophysical survey in Lake Erie revealed that this grounded island produced a furrow in the lakefloor 2.5 km long, 30 m wide and 1.5 m deep, once again, comparable to furrows observed in Lake Winnipeg.

Bedforms

Bedforms, presumably indicating vigourous, sand-transporting bottom currents, are present in Lake Winnipeg.

Flow-parallel bedforms

A linear pattern of lakefloor features is present in The Narrows (Fig. 23). These may represent sand transported by high-velocity bottom currents and deposited as sand ribbons not associated with obstacles, or the features may occur downstream of boulders which act as obstructions to current flow. Alternatively, the features may be erosional remnants.

Flow-transverse bedforms

A sand wave field was observed at the north entrance to The Narrows on both the Seistec and sidescan sonar systems (Figs. 24, 25). The largest sand wave in the field is approximately 6 m in height (8 ms TWT) and 74 m wide. The south-facing sides of all the sand waves are more steeply-dipping than the north-facing sides. Current speed and direction in The Narrows are bimodal with reversals in direction occurring at intervals of several days (Kenney, 1979). Current speeds are greatest in the centre of The Narrows channel, with a maximum recorded speed of 90.2 cm/s to the south during a period of light winds (Kenney, 1979).

Grab samples in the vicinity of the large sand wave contained a centimetre-thick layer of soft oxidized mud overlying clean, coarse sand and fragments of hard grey clay (Todd, this volume). The presence of surface mud suggests that high current velocities here are episodic and that current velocities in The Narrows diminish to permit clay-sized particles to settle out of suspension.

Linear Acoustic Backscattering Anomalies (LABA)

Linear Acoustic Backscattering Anomaly (LABA) is a descriptive term used to describe linear areas of dark return on sidescan sonar records (Cameron and Lewis, 1994; Lewis et al., 1995). LABAs commonly occur on the Lake Winnipeg lakefloor and measure up to hundreds of metres long and tens of metres wide. LABAs show no relief on the lakefloor and no sign of subsurface disturbance or correlation with other subsurface features recognized on Seistec or seismic profiles.

LABAs have been described in Lake Ontario and are thought to be associated with fluid sand expulsion, faulting, and ship debris (Thomas et al., 1989; Wallach, 1990; Cameron and Lewis, 1994; Lewis et al., 1995). LABAs in Lake Winnipeg may be degraded remnants of ice furrows, but further detailed study of LABA sediments is needed to solve their origin and significance.

SUMMARY

Seismic and sidescan sonar profiles were obtained in Lake Winnipeg during August, 1994 from the Canadian Coast Guard Ship *Namao*. Seismic profiles indicate the morphology of the bedrock surface. In most cases, a clear distinction between low

relief Paleozoic carbonate rock, punctuated by probable karst features, and high relief Precambrian rock can be made. In the North Basin, the eastern limit of Paleozoic rock is clearly demarcated 10 km east of the tip of Long Point, well to the west of previous estimates of its position. In the South Basin, all or most of the Paleozoic sequence terminates at a prominent buried escarpment in the centre of the basin, indicating that Paleozoic rock known from drilling and outcrops on the eastern shore is an outlier.

Major moraines are apparent as abrupt, large ridges which vary in acoustic appearance. These include the Pearson Reef Moraine in the South Basin, and, in the North Basin, The George Island Moraine and the offshore extension of The Pas Moraine. Little evidence for extensive or thick till was observed. Instead, fine-grained sediments of Lake Agassiz rest directly on bedrock over most of the South and North Basins. Hence an episode of erosion to bedrock was associated with glaciation and/or deglaciation.

Well-stratified Agassiz Sequence sediments, exceeding thicknesses of 100 m and commonly divisible into three units, conformably drape underlying relief. Southeast of Long Point, stratification in these sediments is severely disrupted, perhaps by dewatering. Elsewhere, minor faulting can be observed.

The contact between the Agassiz Sequence and Winnipeg Sequence sediments is a marked angular unconformity which indicates several metres of erosion. The low-relief character of this unconformity precludes subaerial erosion and the lack of till, moraines, or extensive deformation precludes glacial erosion. Waves appear to be the most likely erosional agent, either in early Lake Winnipeg or waning Lake Agassiz.

Winnipeg Sequence sediments are faintly stratified to massive and reach about 10 m in thickness. Furrows on the surface of these sediments are on the order of 1 m deep, tens of metres wide and several kilometres long. The furrows are interpreted as recent ice keel scours associated with wind-driven ice pressure ridges.

Winnipeg Sequence sediments, in places very thin, mantle most of the lakefloor. Outcrops of Paleozoic rock, Precambrian rock, and till were observed. Deep erosion of Agassiz Sequence sediments by recent currents was observed east and north of Black Island. Multiple cycles of erosion and sedimentation were recognized south of Black Island. In The Narrows, vigorous currents are thought to be the cause of flow-parallel ridges tens of metres long and flow-transverse sand waves as much as 6 m high and tens of metres long.

ACKNOWLEDGMENTS

We would like to thank the Lake Winnipeg Project team for making the seismic survey possible. Captain Vic Isidoro and the officers and crew of the CCGS *Namao* provided enthusiastic support for the work, both in the planning stage and on board ship. During the cruise, Robert Burns supervised the multi-channel seismic data acquisition, Anthony Atkinson was responsible for both the Seistec and sidescan sonar systems, and Kevin Wagner nursed the air compressor and kept the sleeve gun working. The seismic data were processed by Robert Burns, Susan Pullan, and David Schieck; we thank them for their timely efforts. The concepts put forward in this paper are derived from many hours of discussions the authors enjoyed with Harvey Thorleifson, Erik Nielsen, Werner Weber and Ruth Bezys on the CCGS *Namao*. Harvey Thorleifson provided a particularly thorough and insightful review of our understanding of Lake Winnipeg seismostratigraphy, and of the geological proposals put forward in this paper. Figures 2 and 3 were prepared under the direction of Gary Grant of the GSC (Atlantic) Publications and Illustrations Group.

REFERENCES

Bajkov, A.
1930. Biological conditions of Manitoban lakes; Contributions to Canadian Biology and Fisheries, v. 5, p. 383-422.

Betcher, R.N.
1986. Groundwater availability map series, Selkirk area (62I); Manitoba Water Resources Branch.

Brunskill, G.J. and Graham, B.W.
1979. The offshore sediments of Lake Winnipeg; Canadian Fisheries and Marine Service Manuscript Report No. 1540, 75 p.

Cameron, G.D.M. and Lewis, C.F.M.
1994. Linear acoustic backscattering anomalies in Lake Ontario: their anthropogenic origins; in Program with abstracts, Geological Association of Canada-Mineralogical Association of Canada joint annual meeting, Waterloo, Ontario, 1994, v. 19, p. A17.

Canadian Hydrographic Service
1981. Observation Point to Grindstone Point, Chart 6258; scale 1:480 000.

Canadian Hydrographic Service
1982. Berens River to Nelson River; scale 1:255 723.

Canadian Hydrographic Service
1986. Red River to Gull Harbour, Chart 6251; scale 1:100 000.

Dowling, D.B.
1900. Report on the geology of the west shore and islands of Lake Winnipeg; Geological Survey of Canada Annual Report for 1898, Part F, 98 p.

Elson, J.A.
1983. Glacial Lake Agassiz - discovery and a century of research; in eds. J.T. Teller and L. Clayton, Glacial Lake Agassiz, Geological Association of Canada Special Paper 26, p. 21-41.

Grass, J.D.
1984. Ice scour and ice ridging studies in Lake Erie; in Proceedings of the 7th International Symposium on Ice, International Association for Hydraulic Research, Hamburg, Germany, v. III, p. 471-476.

Hobbs, C.H. III and Dame, J.K. II.
1992. Very-high resolution, seismic reflection profiling and other acoustic techniques with examples from Virginia; in ed. R.A. Geyer, CRC handbook of geophysical exploration at sea, 2nd edition, hard minerals, CRC Press, p. 193-211.

Hovland, M. and Judd, A.G.
1988. Seabed pockmarks and seepages; Graham and Trotman Inc., Sterling House, London, 293 p.

Kenney, B.C.
1979. Lake surface fluctuations and the mass flow through The Narrows of Lake Winnipeg; Journal of Geophysical Research, v. 84, p. 1225-1235.

Klassen, R.W.
1967. Surficial geology of the Waterhen-Grand Rapids area, Manitoba; Geological Survey of Canada Paper 66-36, 6 p.

Kleinrock, M.C.
1992. Capabilities of some systems used to survey the deep-sea floor; in ed. Richard A. Geyer, CRC handbook of geophysical exploration at sea, 2nd edition, hard minerals, CRC Press, p. 35-86.

Kushnir, D.W.
1971. Sediments in the South Basin of Lake Winnipeg; Unpublished M.Sc. thesis, University of Manitoba, Winnipeg, 92 p.

Lewis, C.F.M., Cameron, G.D.M., King, E.L., Todd, B.J. and Blasco, S.M.
1995. Structural contour, isopach and feature maps of Quaternary sediments in western Lake Ontario; Atomic Energy Control Board Report INFO-0555, 117 p.

McQuillin, R., Bacon, M. and Barclay, W.
1984. An introduction to seismic interpretation; Gulf Publishing Company, 287 p.

Mitchum, R.M. Jr., Vail, P.R. and Sangree, J.B.
1977. Seismic stratigraphy and global changes of sea level, part 6: stratigraphic interpretation of seismic reflection patterns in depositional sequences; in ed. C.E. Payton, Seismic stratigraphy - applications to hydrocarbon exploration, American Association of Petroleum Geologists, Memoir 26, Tulsa, p. 117-133.

Mitchum, R.M. Jr., Vail, P.R. and Thompson, S., III.
1977. Seismic stratigraphy and global changes of sea level, part 2: the depositional sequence as a basic unit for stratigraphic analysis; in ed. C.E. Payton, Seismic stratigraphy - applications to hydrocarbon exploration, American Association of Petroleum Geologists, Memoir 26, Tulsa, p. 53-62.

Simpkin, P.G. and Davis, A.
1993. For seismic profiling in very shallow water, a novel receiver; Sea Technology, v. 34, p. 22-28.

Sheriff, R.E. and Geldart, L.P.
1982. Exploration seismology, Vol. 1, History, theory, and data acquisition; Cambridge University Press, 253 p.

Thomas, R.L., McMillan, R.K., Keyes, D.L. and Mohajer, A.A.
1989. Surface sedimentary signatures of neotectonism as determined by sidescan sonar in western Lake Ontario; in Program with abstracts, Geological Association of Canada - Mineralogical Association of Canada, Joint Annual Meeting, Montréal, Québec, v. 14, p. A128.

Todd, B.J. and Lewis, C.F.M.
1993. A reconnaissance geophysical survey of the Kawartha Lakes and Lake Simcoe, Ontario; Géographie physique et Quaternaire, v. 7, p. 313-323.

Todd, B.J., Lewis, C.F.M. and Ryall, P.J.C.
1988. Comparison of trends of iceberg scour marks to iceberg trajectories and evidence of paleocurrent trends on Saglek Bank, northern Labrador Shelf; Canadian Journal of Earth Sciences, v. 25, p. 1374-1383.

Upham, W.
1890. Report on exploration of the Glacial Lake Agassiz in Manitoba; Geological Survey of Canada Annual Report for 1888-1889, v. 5, Section E, 156 p.

Wallach, J.L.
1990. Newly discovered geological features and their potential impact on Darlington and Pickering; Atomic Energy Control Board Report INFO-0342, 20 p.

Ward, G.
1926. Seasonal variation in the composition of the Red River; Unpublished M.Sc. thesis, University of Manitoba, Winnipeg, 24 p.

Table 1: Seismostratigraphy of Lake Winnipeg sediments

SEQUENCE DESIGNATION	REFLECTION CONFIGURATION	GEOMETRY/ DISTRIBUTION	BOUNDING UNITS & SEDIMENT TYPE
WINNIPEG SEQUENCE	Weak, smooth, parallel to subparallel, even, coherent reflections; otherwise transparent. Acoustically more transparent than underlying Agassiz Sequence. Obscured by disseminated gas in many places.	Continuous, usually ponded blanket from zero to several metres thickness. Thickest (up to 11 m or 15 ms TWT) in central South and North Basins.	Smooth upper surface (lakefloor). Usually overlies Agassiz Sequence; locally overlies acoustic basement or bedrock. Soft dark gray mud with black FeS streaks, non-calcareous.
AGASSIZ SEQUENCE	Medium to high amplitude, closely-spaced, parallel, wavy (sometimes contorted), continuous, coherent reflections imparting a bedded/laminated aspect. Conformable mimicking of relief on underlying acoustic basement/bedrock usually imparts an overall wave-like undulation to the reflections. Commonly can be sub-divided into a lower, middle and upper units; middle unit reflections are lower amplitude. Obscured by disseminated gas in many places.	Generally several to tens of metres thick; draped, suspension settling, basin-fill depositional style. Thickest (>75 m or 100 ms TWT) in central North Basin.	Upper surface delineated by a regional high-amplitude continuous reflector. Usually overlain by Winnipeg Sequence but often outcrops at lakefloor. Dark gray mud, compact, massive to banded, calcareous.
ACOUSTIC BASEMENT SEQUENCE	Incoherent or chaotic reflections impart a homogeneous aspect. Other areas are reflection free, with no seismic energy penetration.	Often a constructional geometry (i.e. as opposed to a ponded basin fill)	Well defined upper surface. Divisible into areas of low, medium and high relief. Thought to consist of till and bedrock.

Table 2. Seismic processing parameters.

1. Single-channel - common offset gathers

Trace number = 3
Offset from source = 20 m
Automatic gain control with 80 ms window
Digital bandpass filter 100-600 Hz

2. Multi-channel

Reformat to SEGY
Trace edits
Spherical divergence correction
5 component surface-consistent deconvolution
Surface-consistent mean trace equalization
Common depth point gather
Semblance velocity analysis
First break mute
6-fold stack
Kirchoff-summation migration
Bandpass filter 10/60 - 300/370 Hz
Mean trace equalization

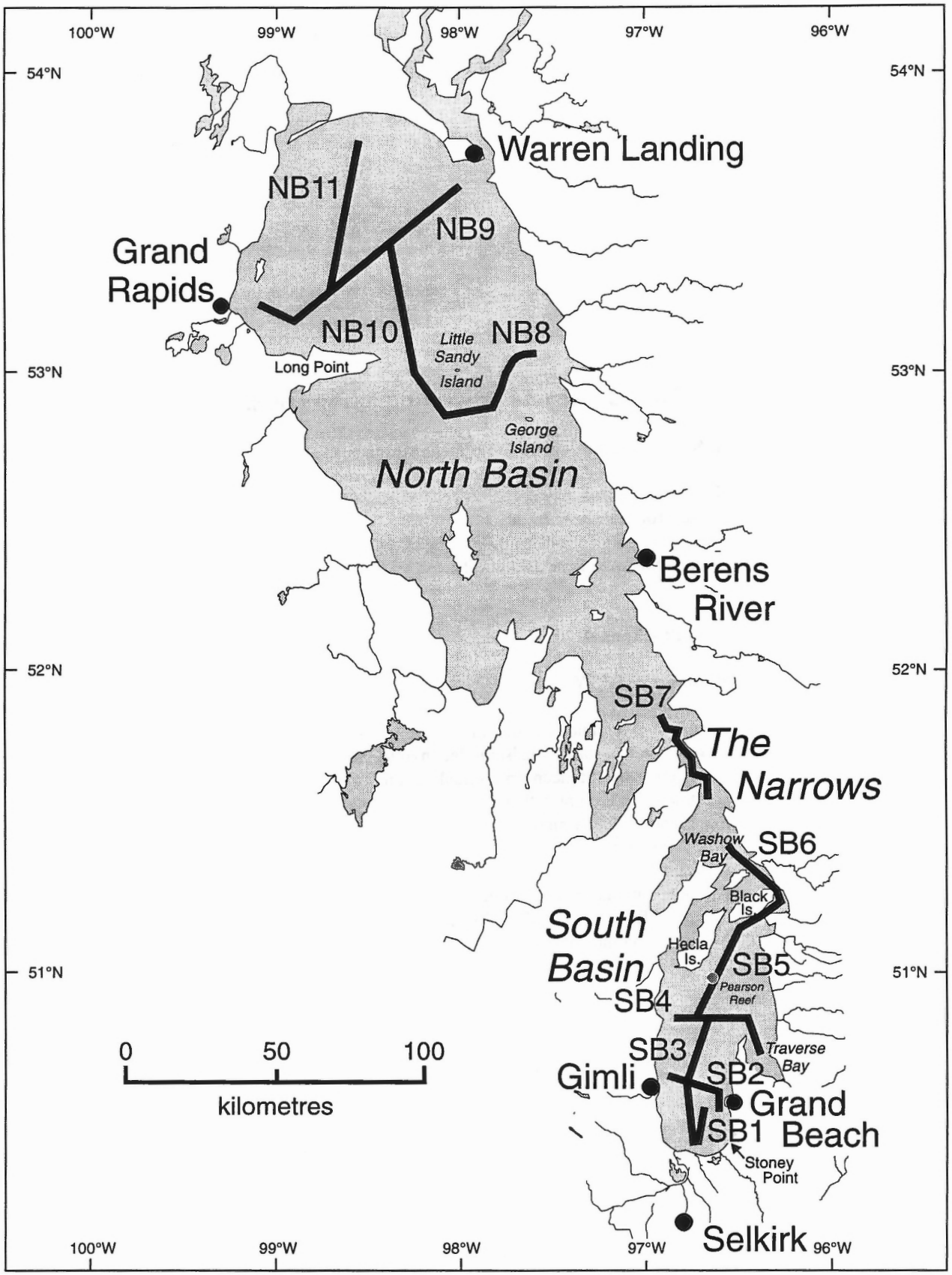

Figure 1. Geophysical survey lines in Lake Winnipeg.

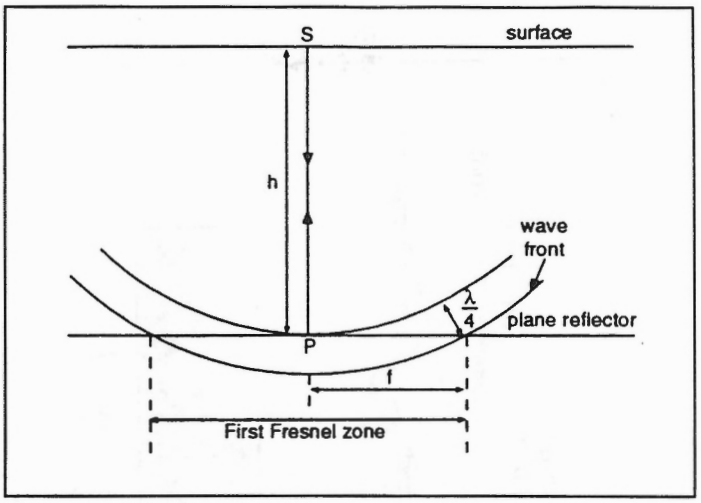

Figure 2a. Sketch of first Fresnel zone (after Sheriff and Geldart, 1982 in Lewis et al., 1995).

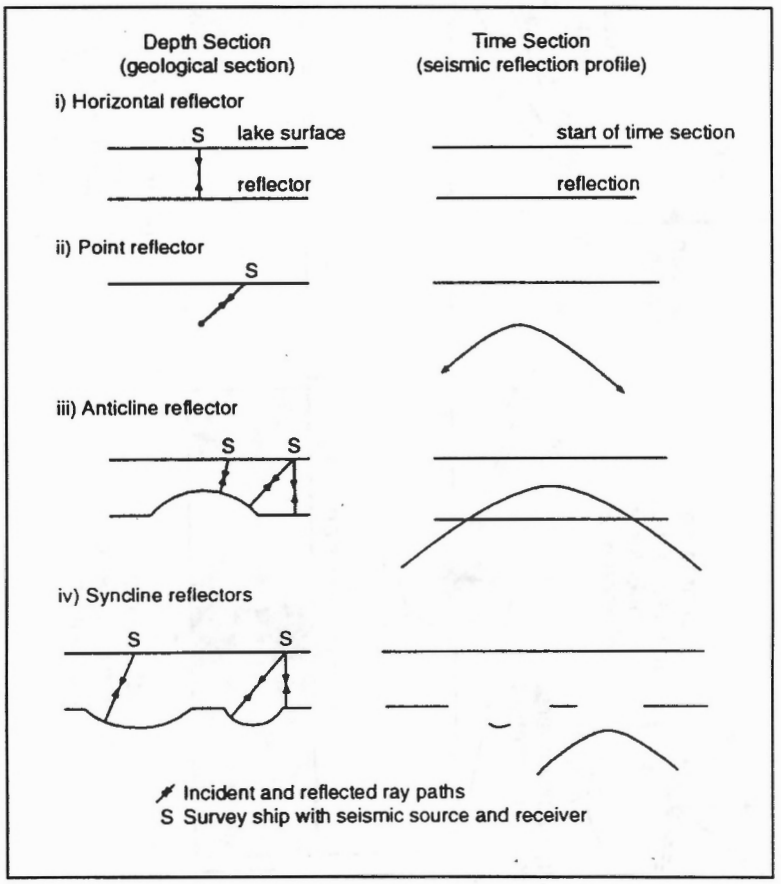

Figure 2b. The configuration of reflections in seismic profiles (right column) may not represent actual structure of the geological section (left column), as shown for the simplified point reflector, anticline and syncline examples above. The seismic reflection profile and geological section are geometrically equivalent only for horizontal reflectors (after McQuillin et al., 1984, Figures 2-17, 2-19 in Lewis et al., 1995).

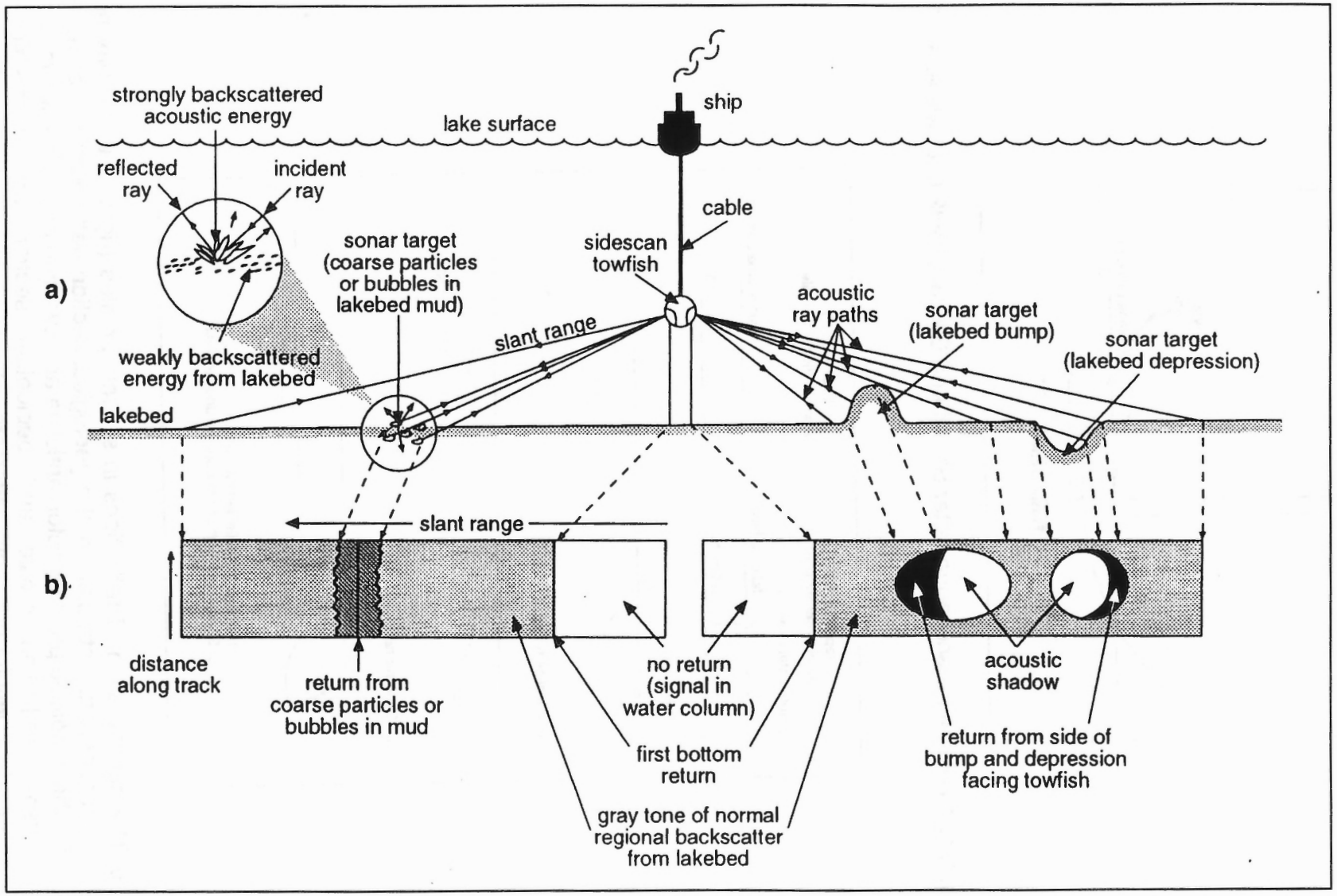

Figure 3. Schematic diagram of sidescan sonar survey system showing a) vertical profile with ship and towfish moving into page and sonar beams directed athwartship showing selected acoustic ray paths, and b) the recorded sidescan record, a "planview" image of lakefloor features (after Kleinrock, 1992, and Hobbs and Dame, 1992 in Lewis et al., 1995).

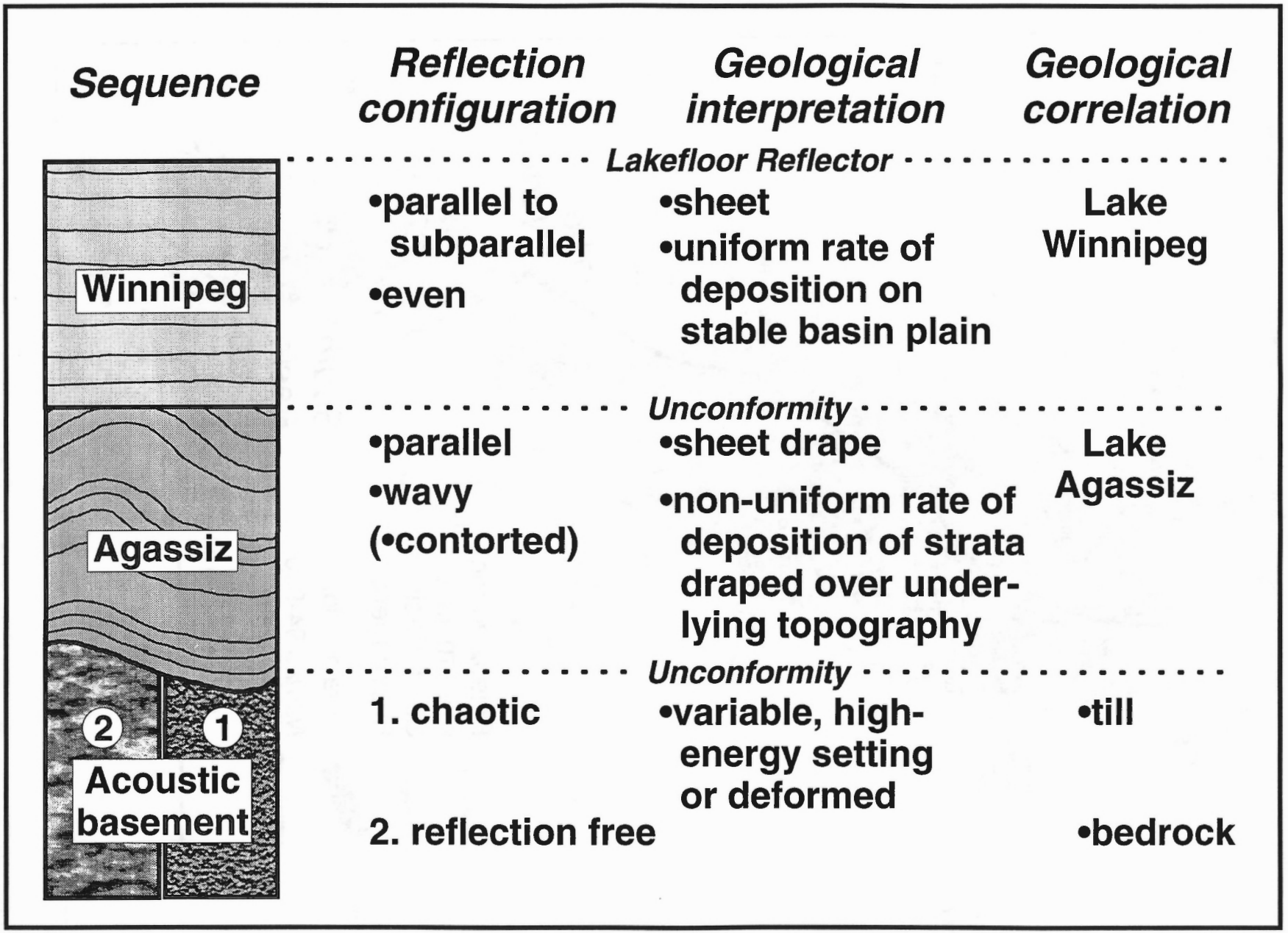

Figure 4. Summary of Lake Winnipeg seismostratigraphy.

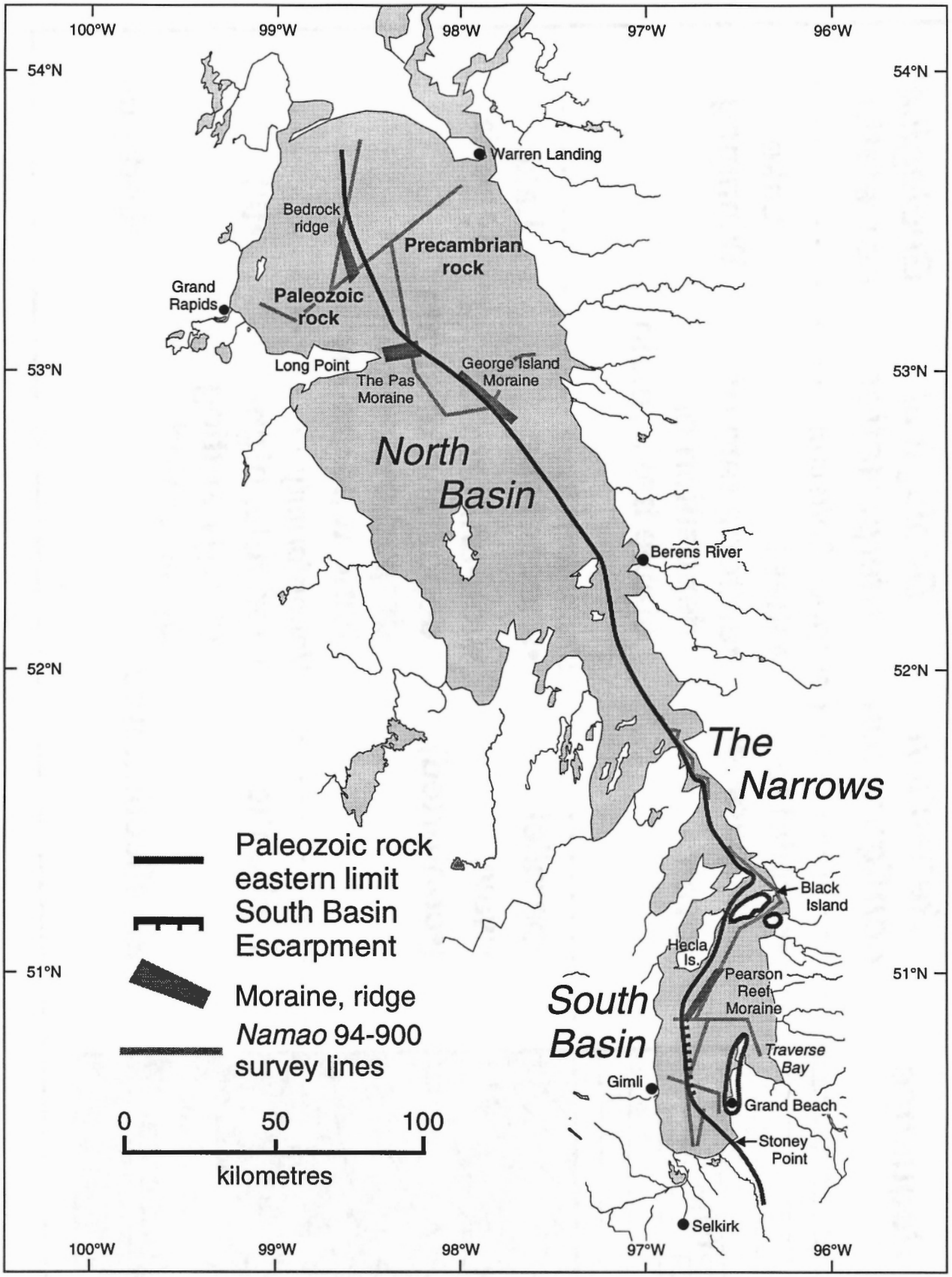

Figure 5. Acoustic Basement Sequence and features interpreted from seismic profiles.

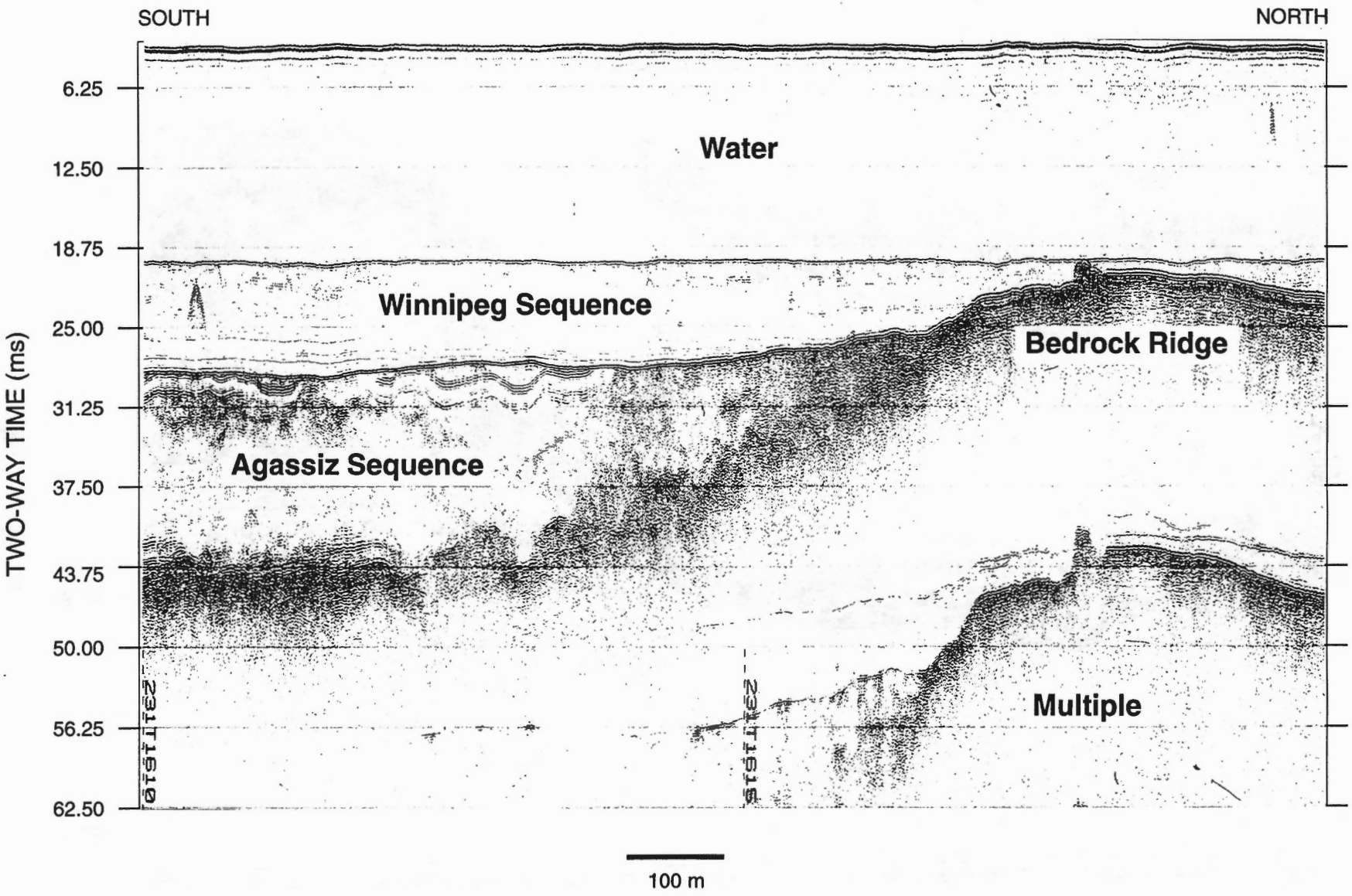

Figure 6. Bedrock ridge, North Basin (Seistec record, line NB11, Day 231, 1610 UTC). Estimated vertical distance between horizontal scale lines is 4.7 m.

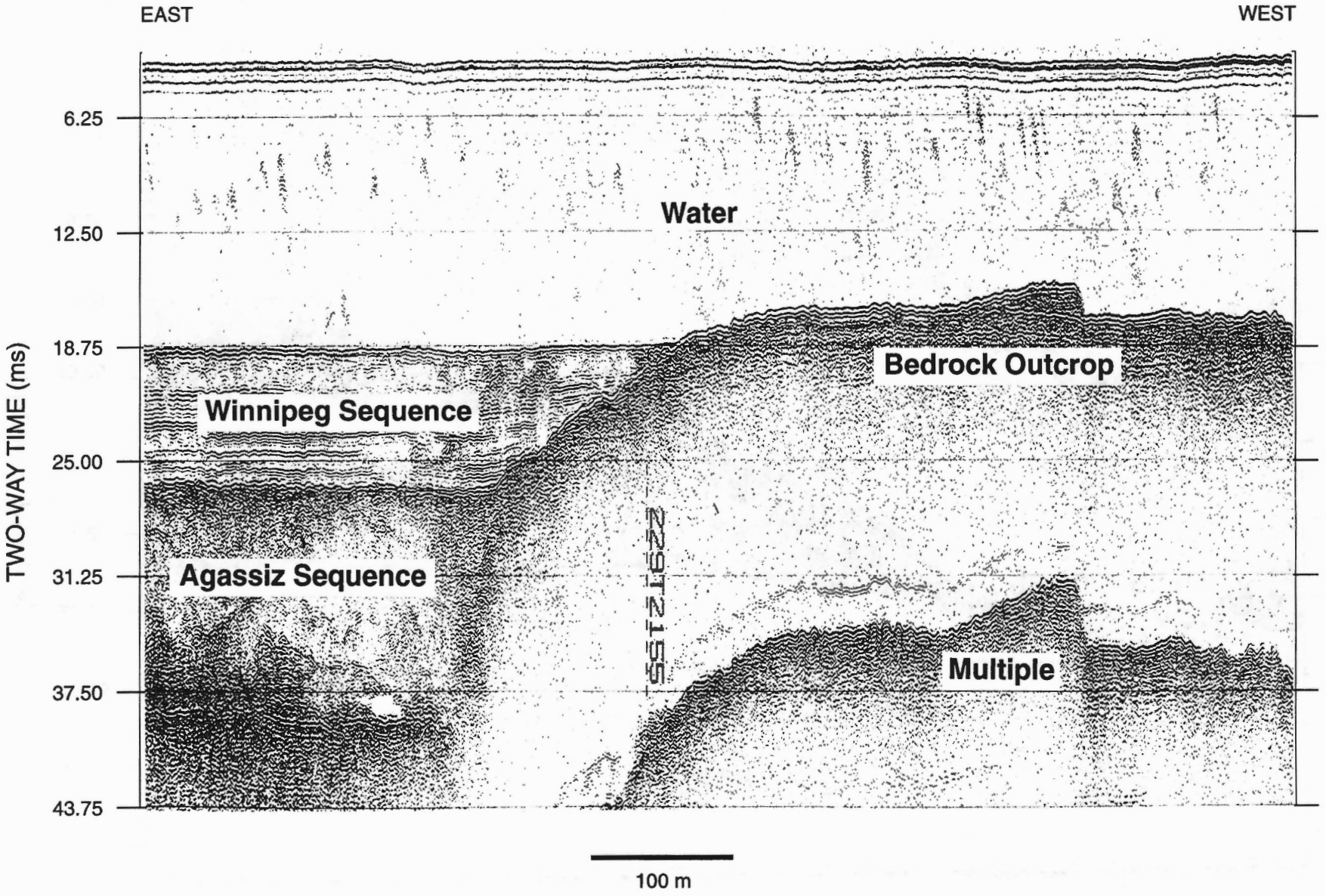

Figure 7. Paleozoic bedrock outcrop above lakefloor, North Basin (Seistec record, line NB9, Day 229, 2152 UTC). Estimated vertical distance between horizontal scale lines is 4.7 m.

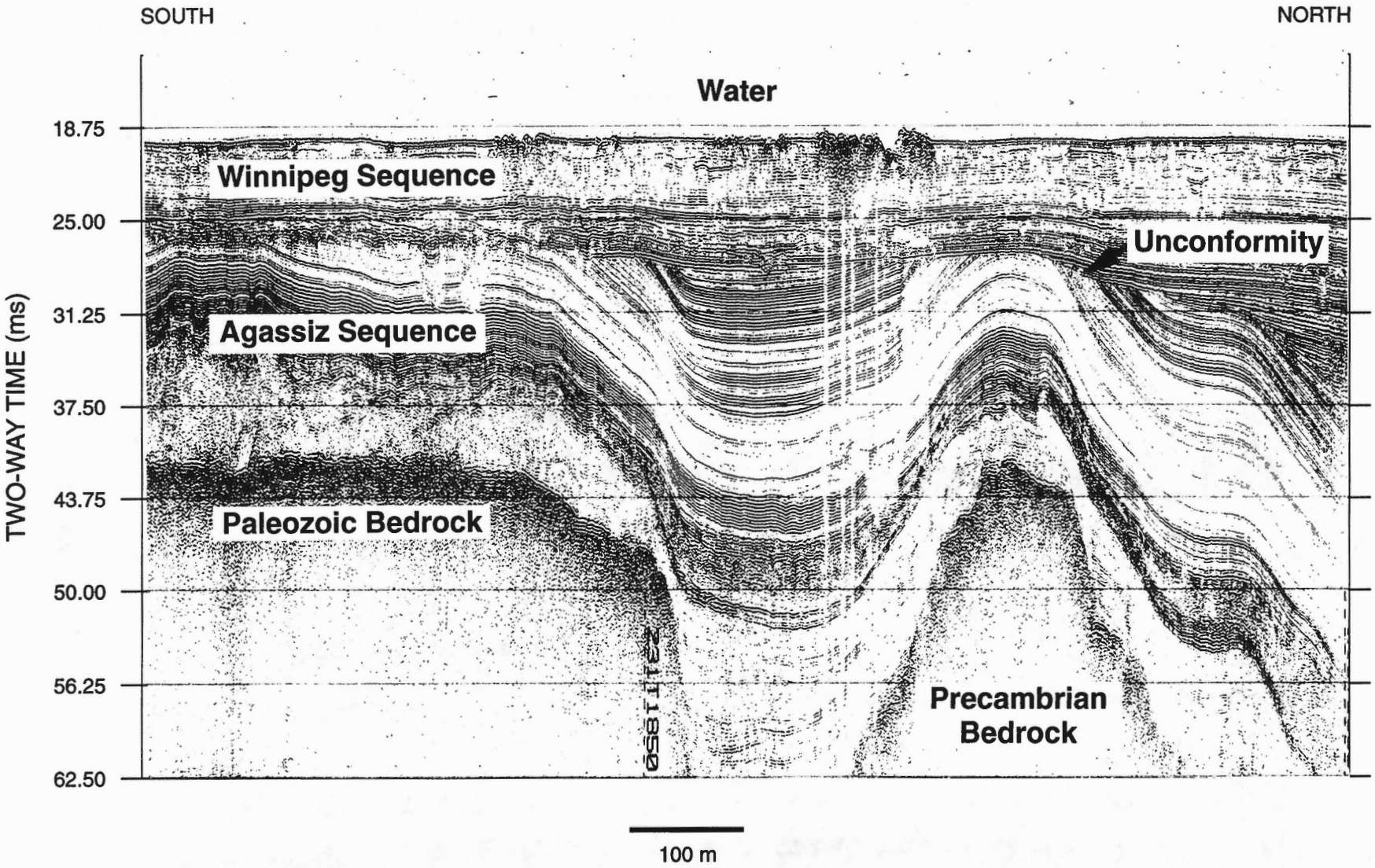

Figure 8. Agassiz and Winnipeg Sequence sediments conformably overlying Precambrian-Paleozoic bedrock, North Basin. Paleozoic bedrock on left, contact at 231/1851, Precambrian bedrock at right. The Agassiz Sequence consists of a succession of three reflective zones, each comprising high amplitude, parallel reflectors over a transparent section; in the "valley" at 231/1851, tops of the upper, middle, and lower reflective zones occur at 28.5 ms, 43.8 ms, and 58.5 ms, respectively. Note ice-scoured surface sediment (Seistec record, line NB11, Day 231, 1847 UTC). Estimated vertical distance between horizontal scale lines is 4.7 m.

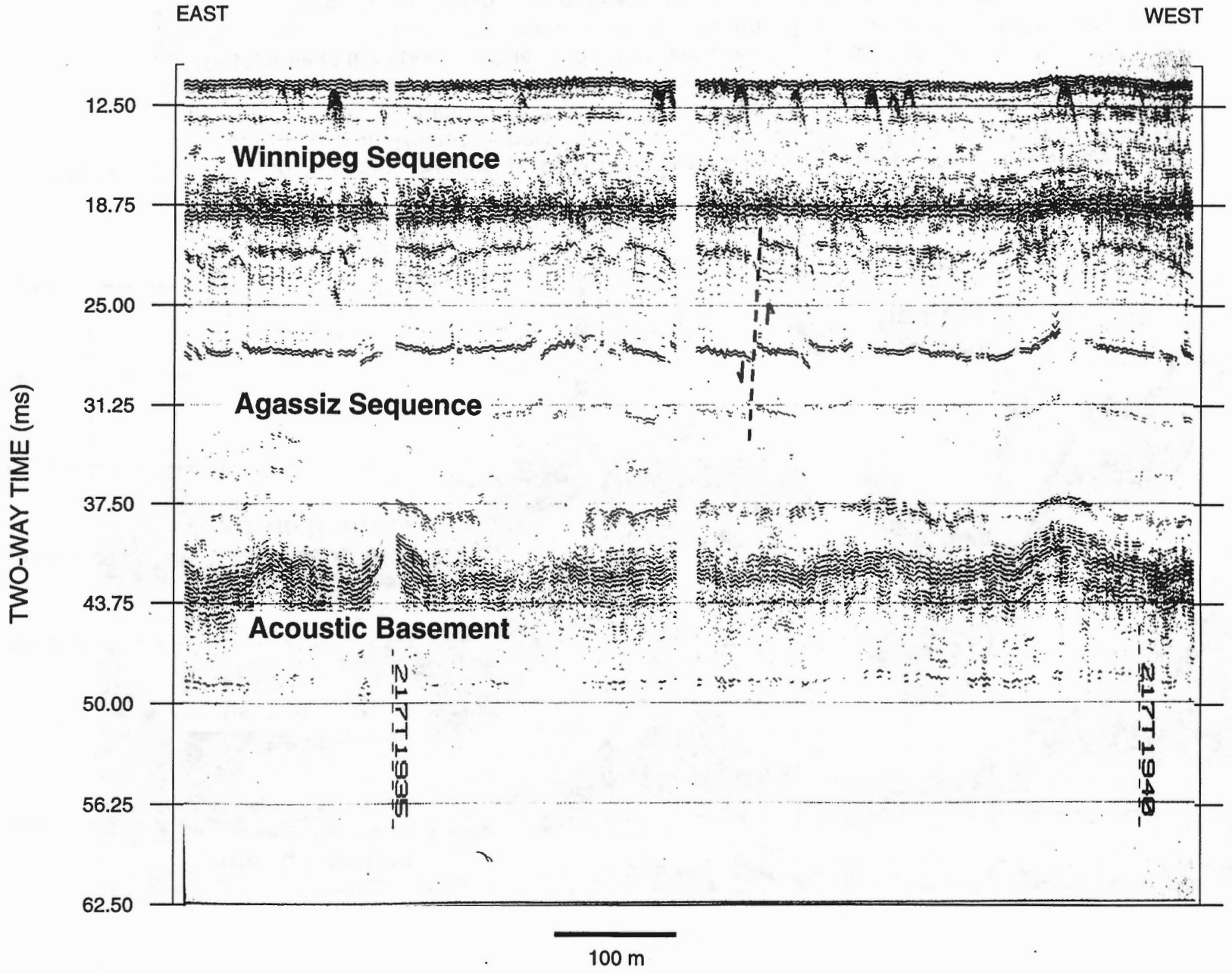

Figure 9. "Broken" or segmented reflectors in Agassiz Sequence, South Basin (Seistec record, line SB2, Day 217, 1935 UTC). Estimated vertical distance between horizontal scale lines is 4.7 m.

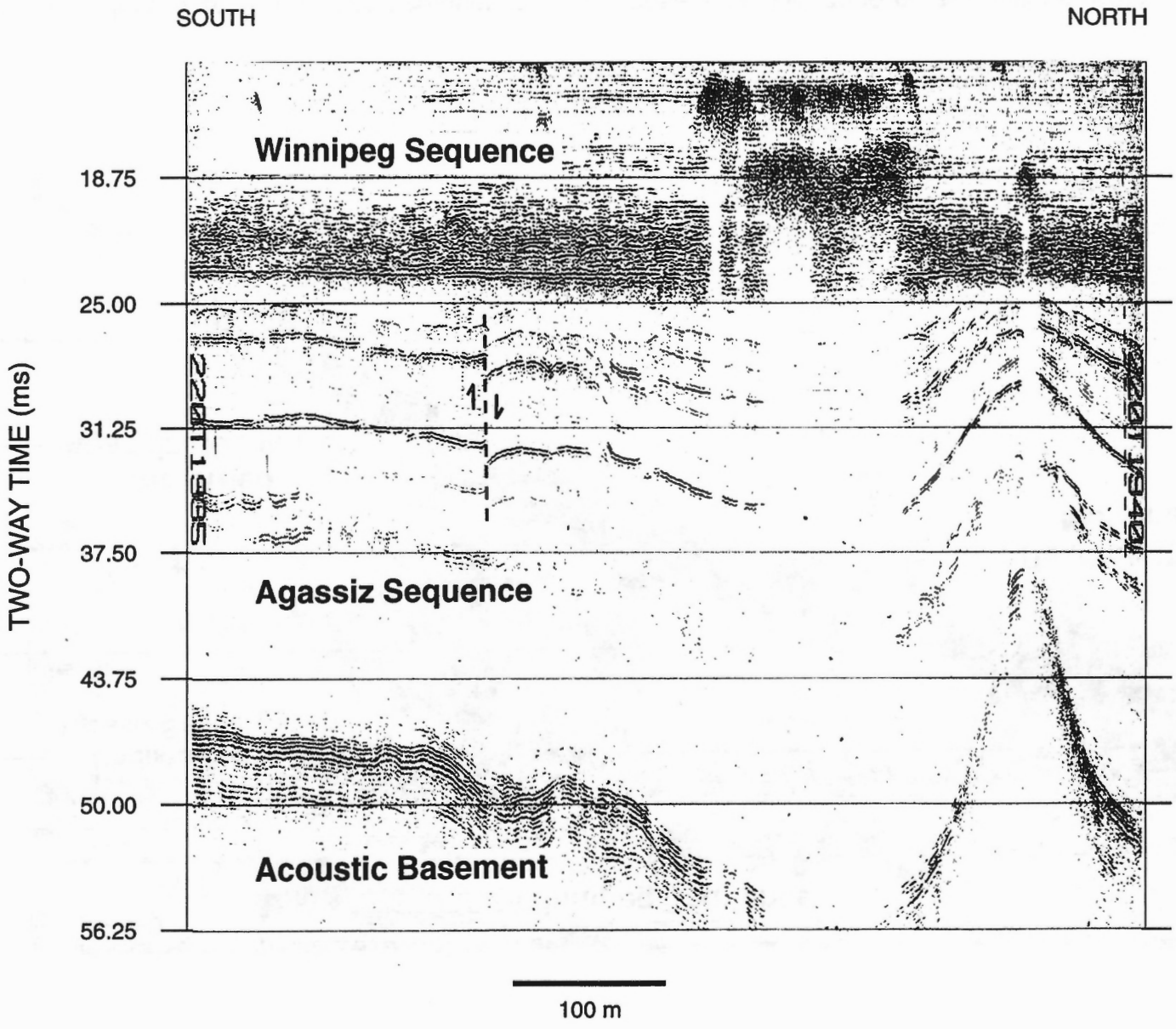

Figure 10. "Broken" or segmented reflectors in Agassiz Sequence and sediments conformably draped over acoustic basement high, South Basin (Seistec record, line SB3, Day 220, 1935 UTC). Estimated vertical distance between horizontal scale lines is 4.7 m.

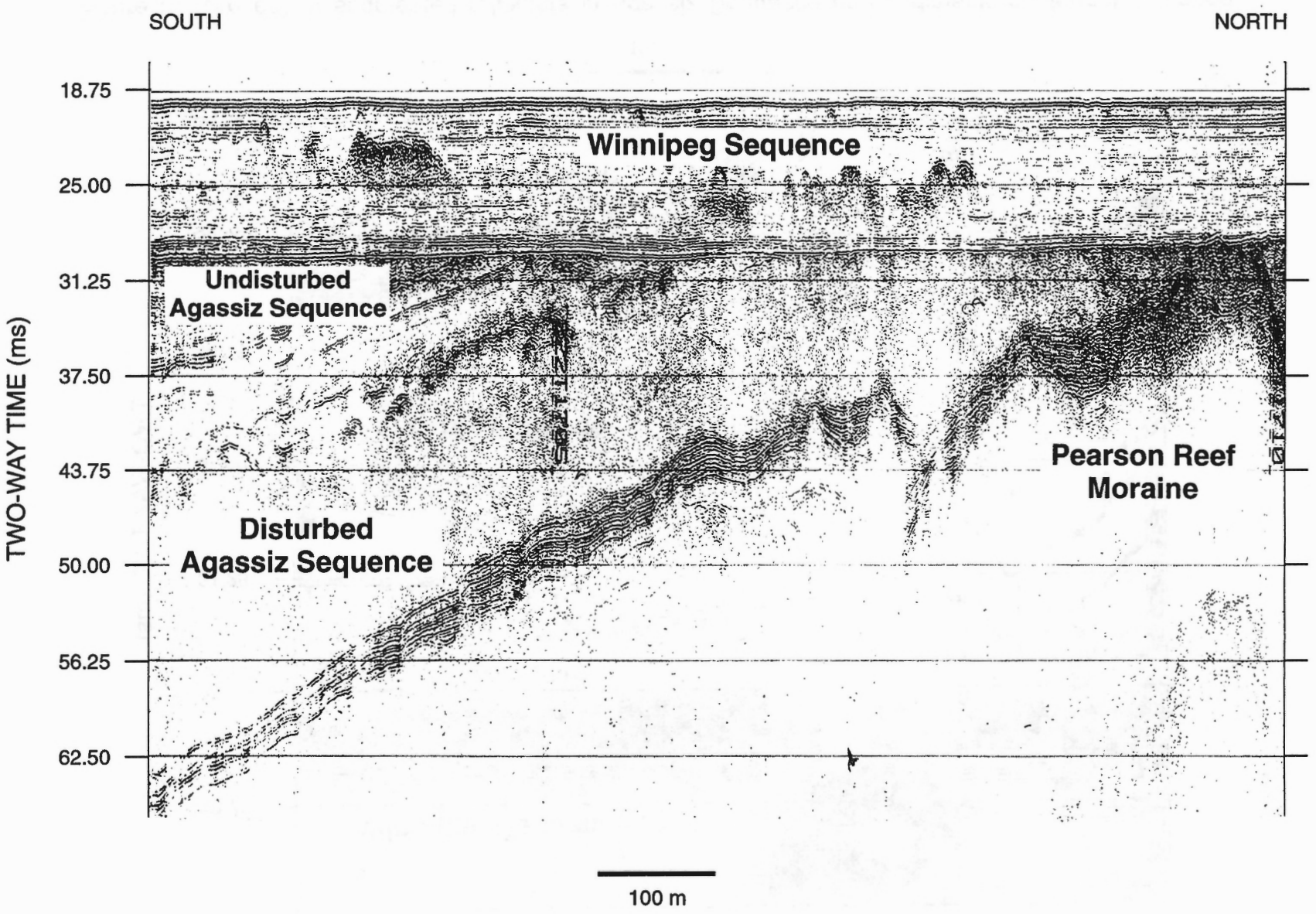

Figure 11. Disturbed zone in Agassiz Sequence over a basal reflective zone on south flank of Pearson Reef Moraine, South Basin (Seistec record, line SB5, Day 222, 1702 UTC). Estimated vertical distance between horizontal scale lines is 4.7 m.

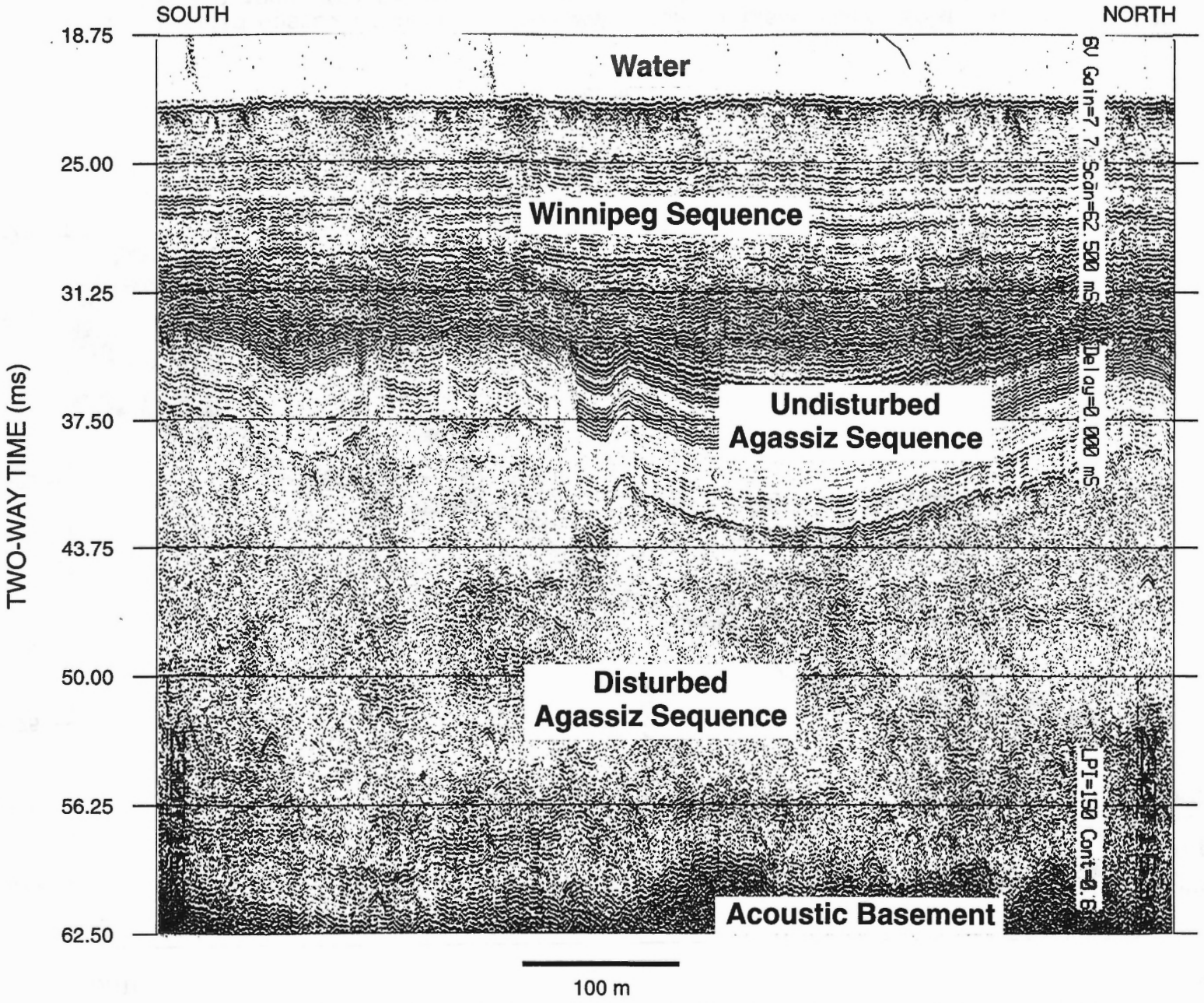

Figure 12. Disturbed zone in lower Agassiz Sequence, North Basin (Seistec record, line NB10, Day 230, 1625 UTC). Estimated vertical distance between horizontal scale lines is 4.7 m.

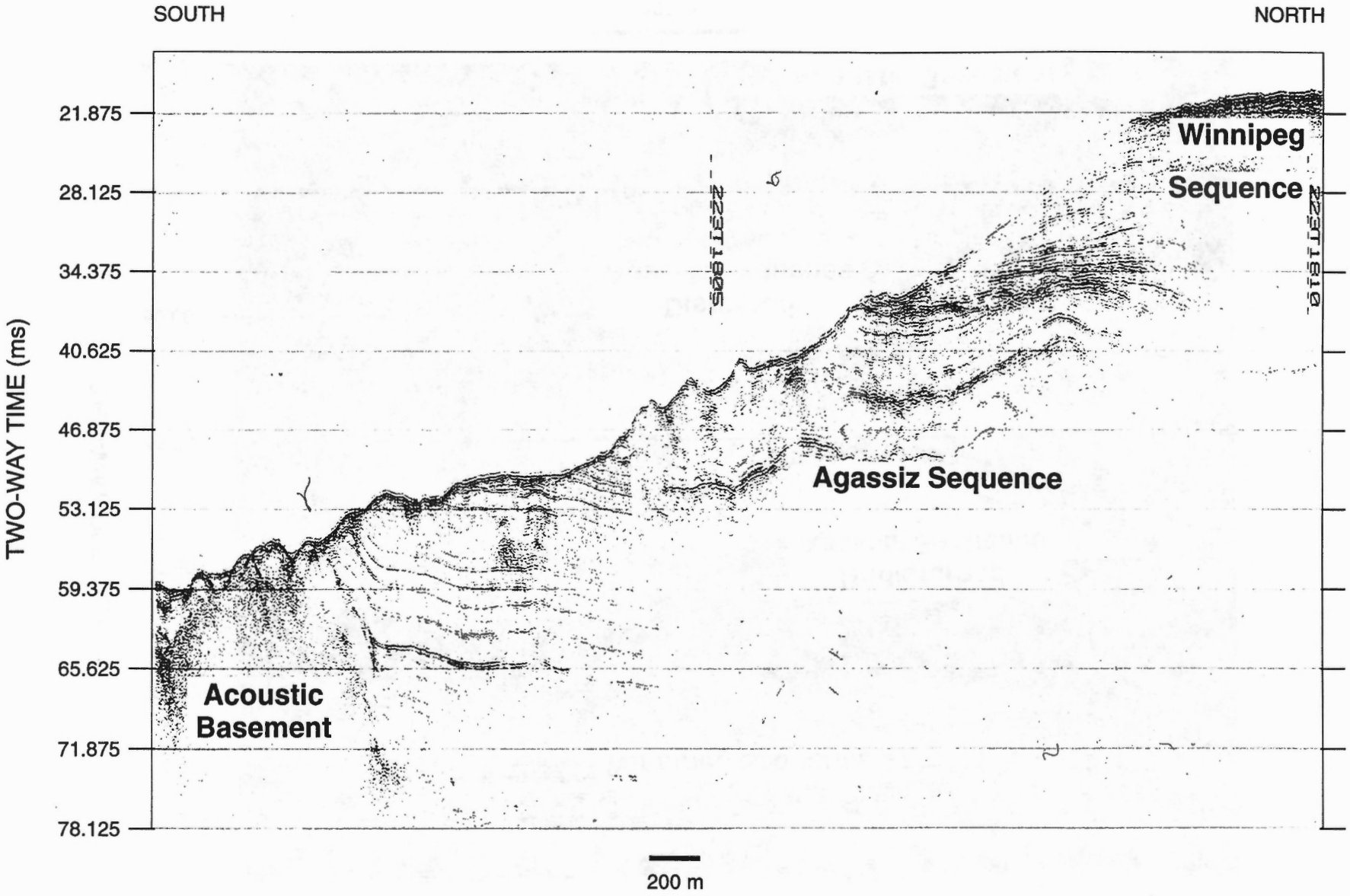

Figure 13. Truncated Agassiz Sequence in deep water, north of Black Island (Seistec record, line SB6, Day 223, 1803 UTC). Estimated vertical distance between horizontal scale lines is 4.7 m.

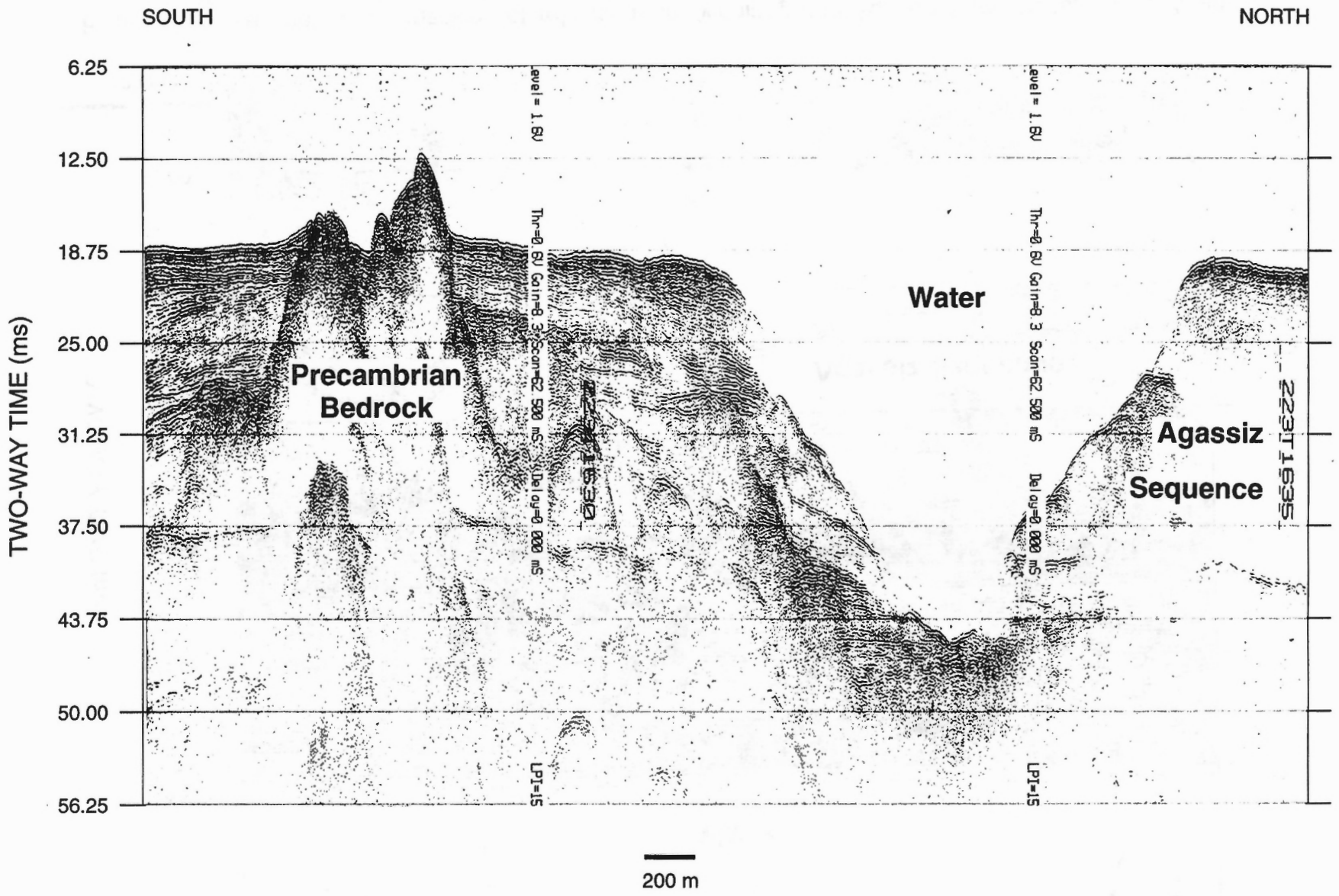

Figure 14. Precambrian basement outcrop (left) and deep erosional notch in Agassiz Sequence (right), south of Black Island (Seistec record, line SB6, Day 223, 1627 UTC). Estimated vertical distance between horizontal scale lines is 4.7 m.

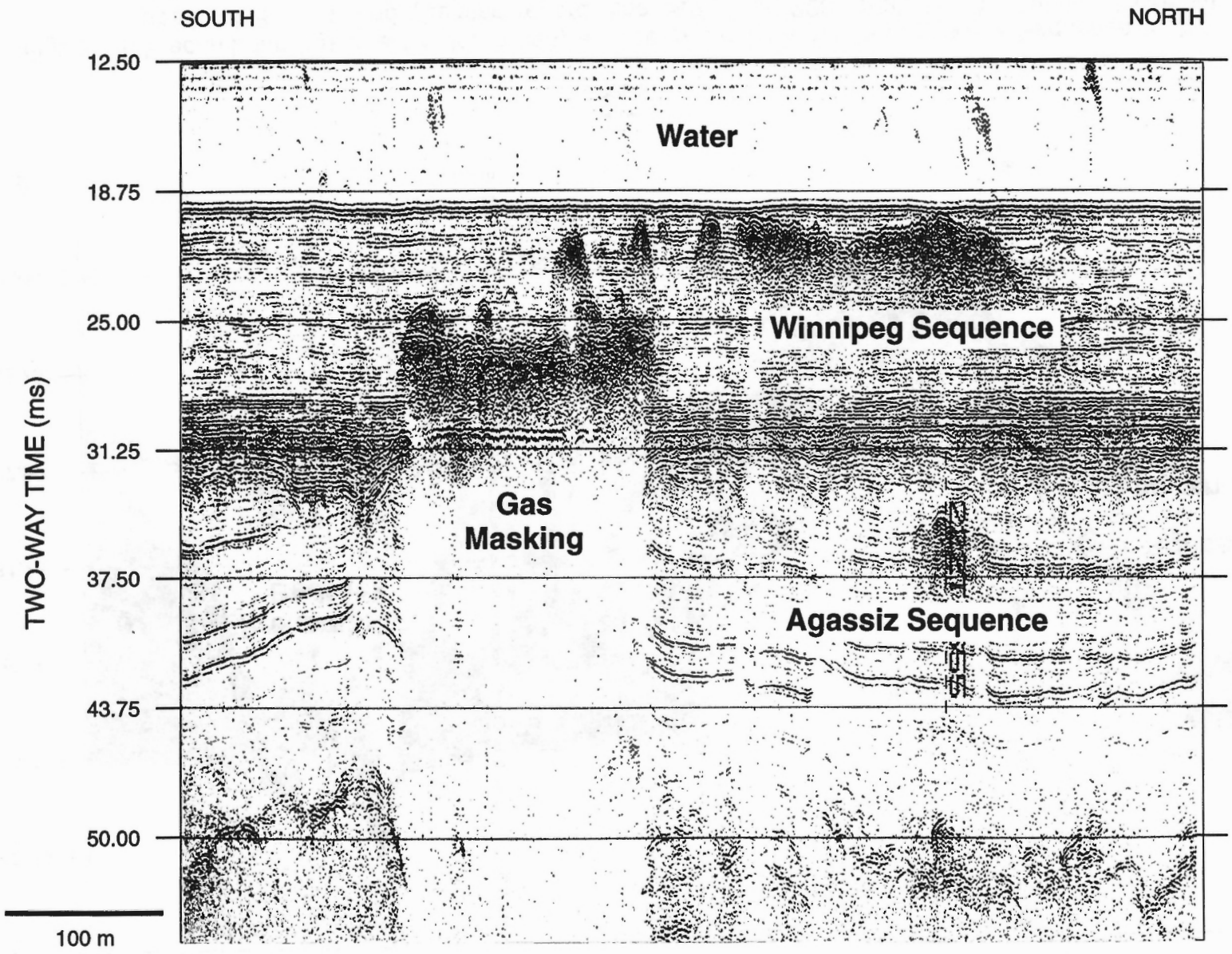

Figure 15. Disseminated gas masking of reflections in Winnipeg and Agassiz Sequences, South Basin (Seistec record, line SB5, Day 222, 1651 UTC). Note the strong reflection, probably caused by gas concentration along the Agassiz Unconformity, about 30-31 ms depth just above the gas masking. Estimated vertical distance between horizontal scale lines is 4.7 m.

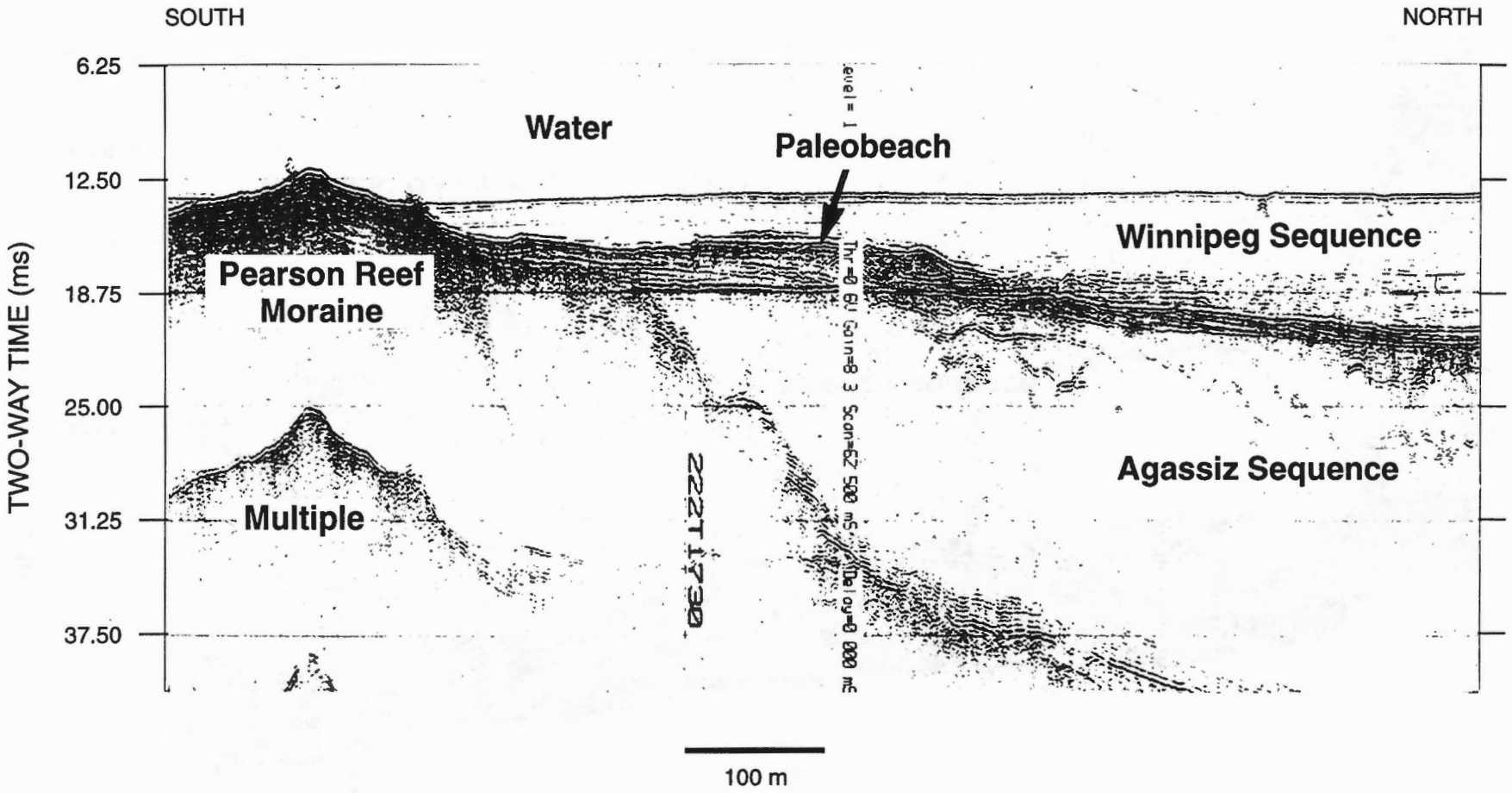

Figure 16. Paleobeach on north flank of Pearson Reef Moraine, South Basin (Seistec record, line SB5, Day 222, 1727 UTC). Estimated vertical distance between horizontal scale lines is 4.7 m.

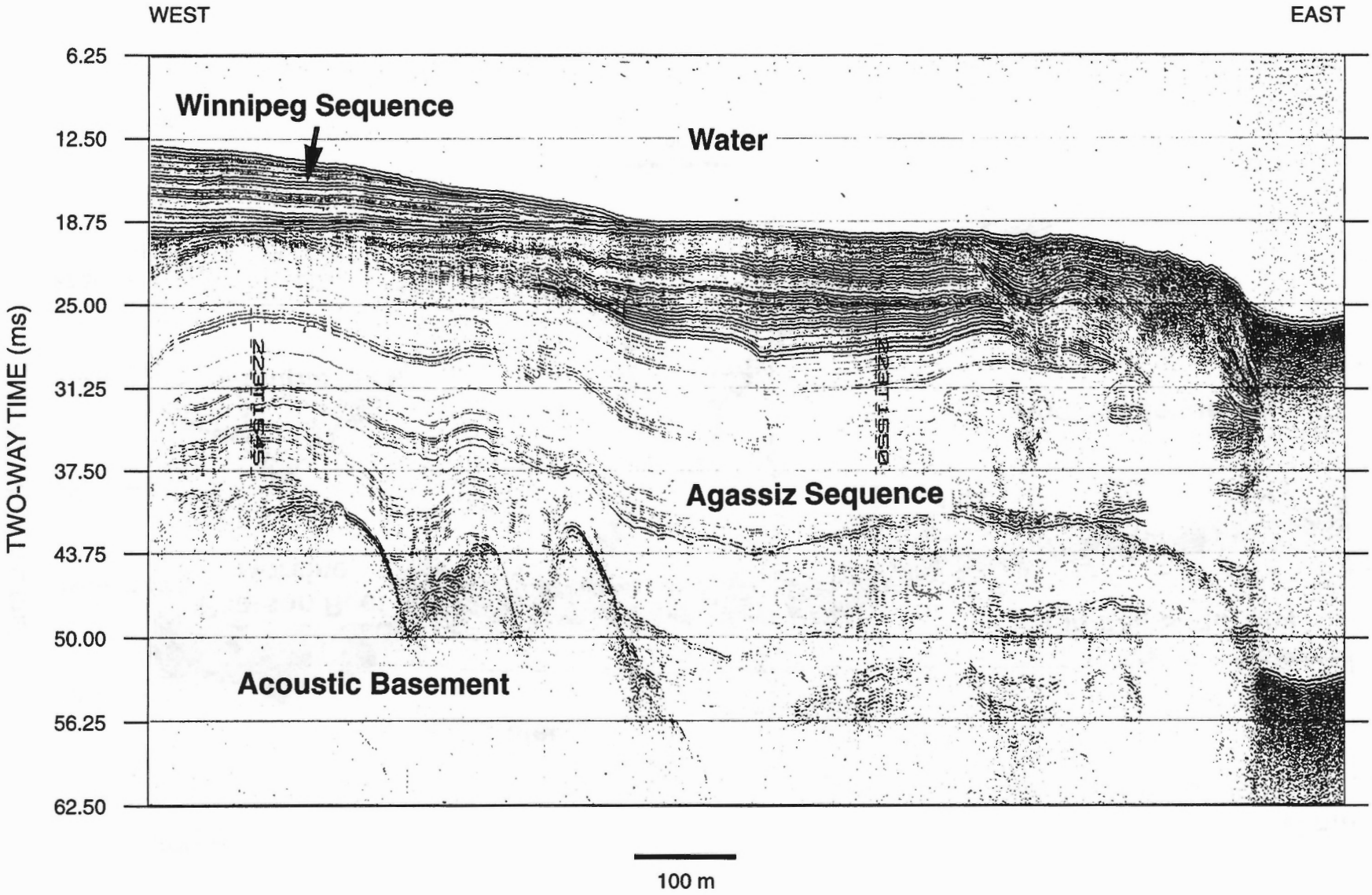

Figure 17. Complex sedimentation pattern, south of Black Island (Seistec record, line SB6, Day 223, 1544 UTC). Estimated vertical distance between horizontal scale lines is 4.7 m.

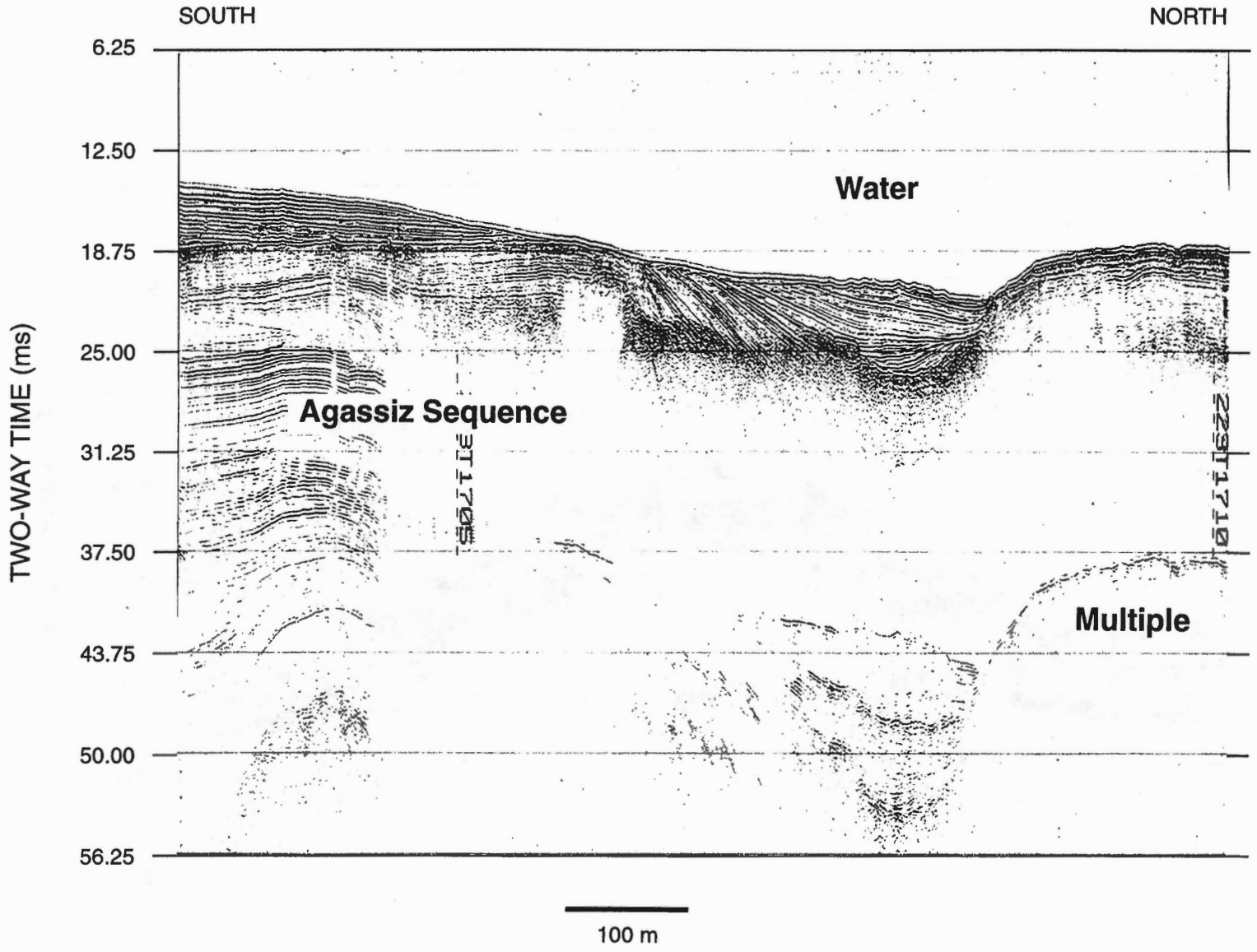

Figure 18. Foreset beds and complex sedimentation pattern in channel east of Black Island (Seistec record, line SB6, Day 223, 1703 UTC). Estimated vertical distance between horizontal scale lines is 4.7 m.

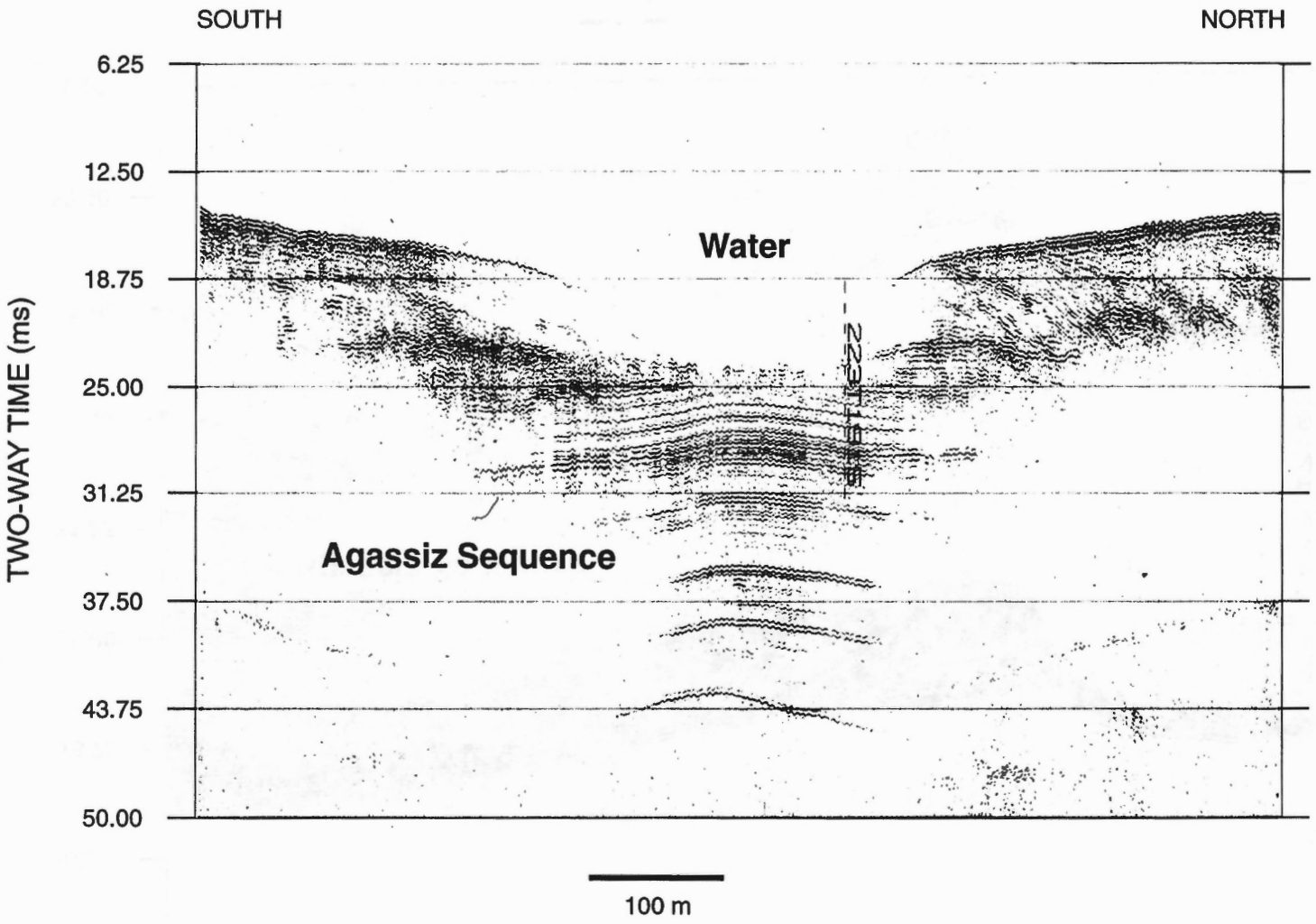

Figure 19. Disappearing reflectors in sediment, north of Black Island (Seistec record, line SB6, Day 223, 1911 UTC). Estimated vertical distance between horizontal scale lines is 4.7 m.

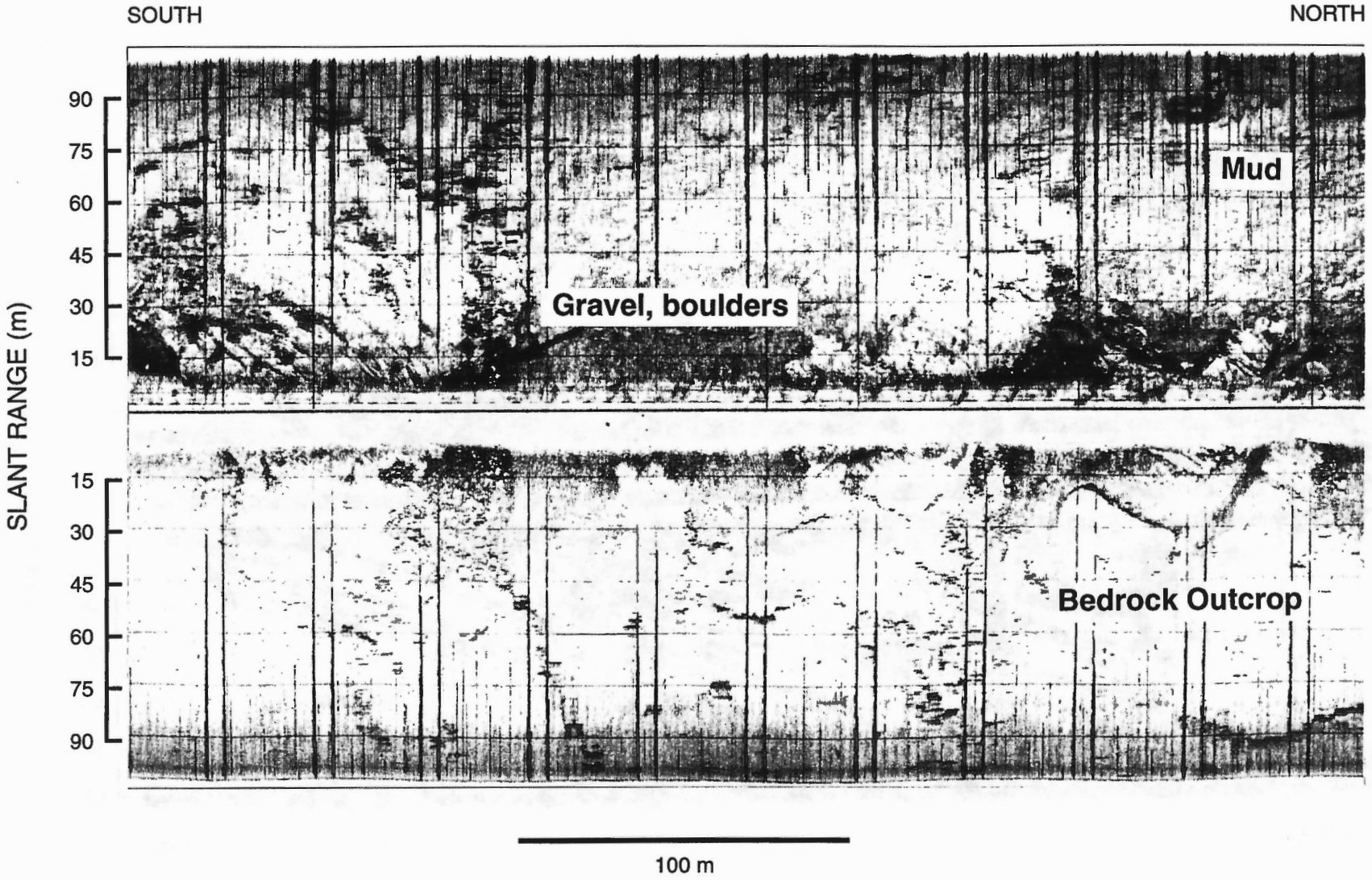

Figure 20. Coarse-grained sediments and bedrock outcrop, The Narrows. Water depth approximately 7.3 m. (Sidescan sonar record, line SB7, Day 224, 2036.9 to 2039.9 UTC).

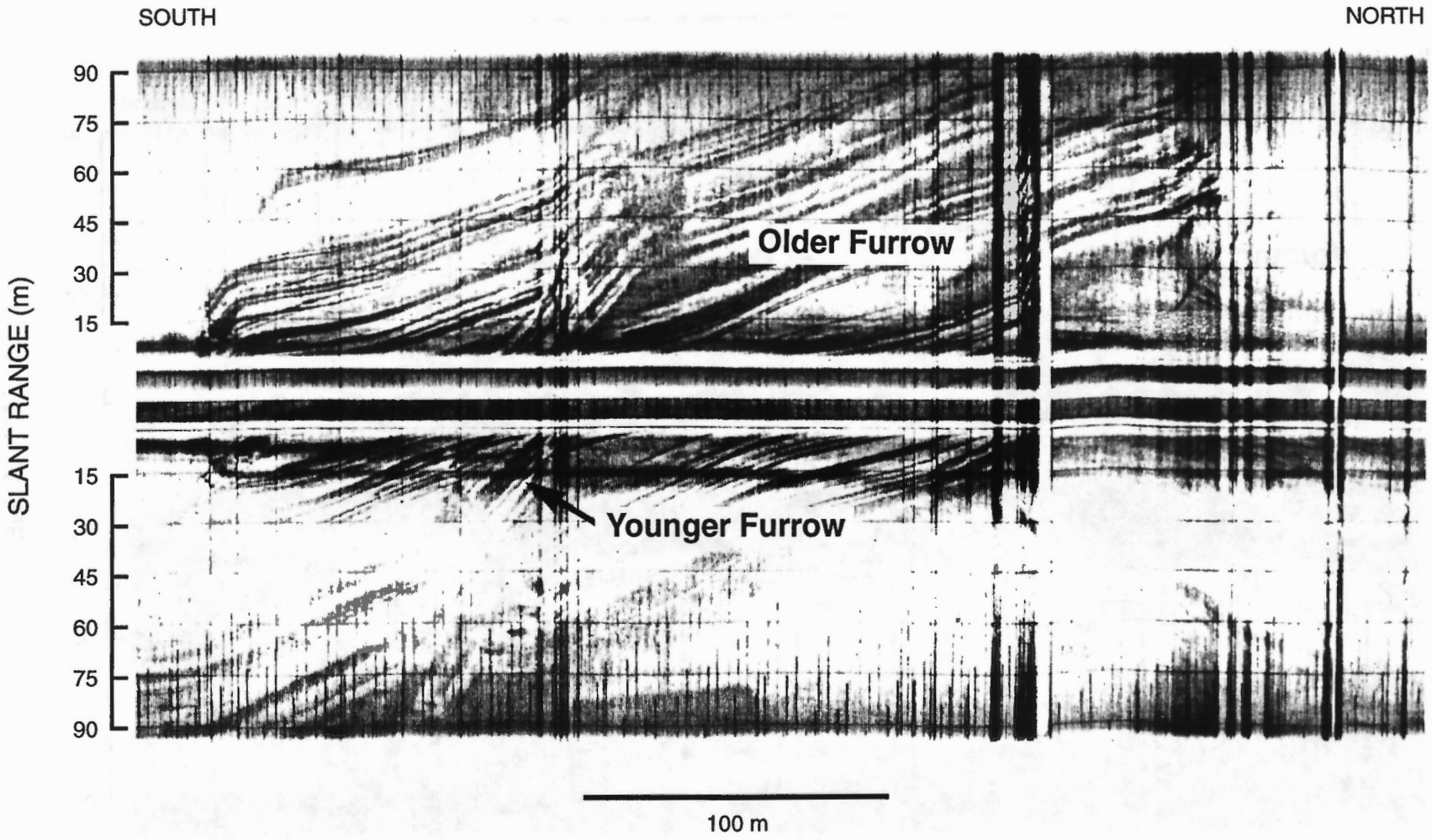

Figure 21. Ice-scoured lakefloor, South Basin. Water depth approximately 9.5 m. (Sidescan sonar record, line SB3, Day 220, 1642 to 1647 UTC).

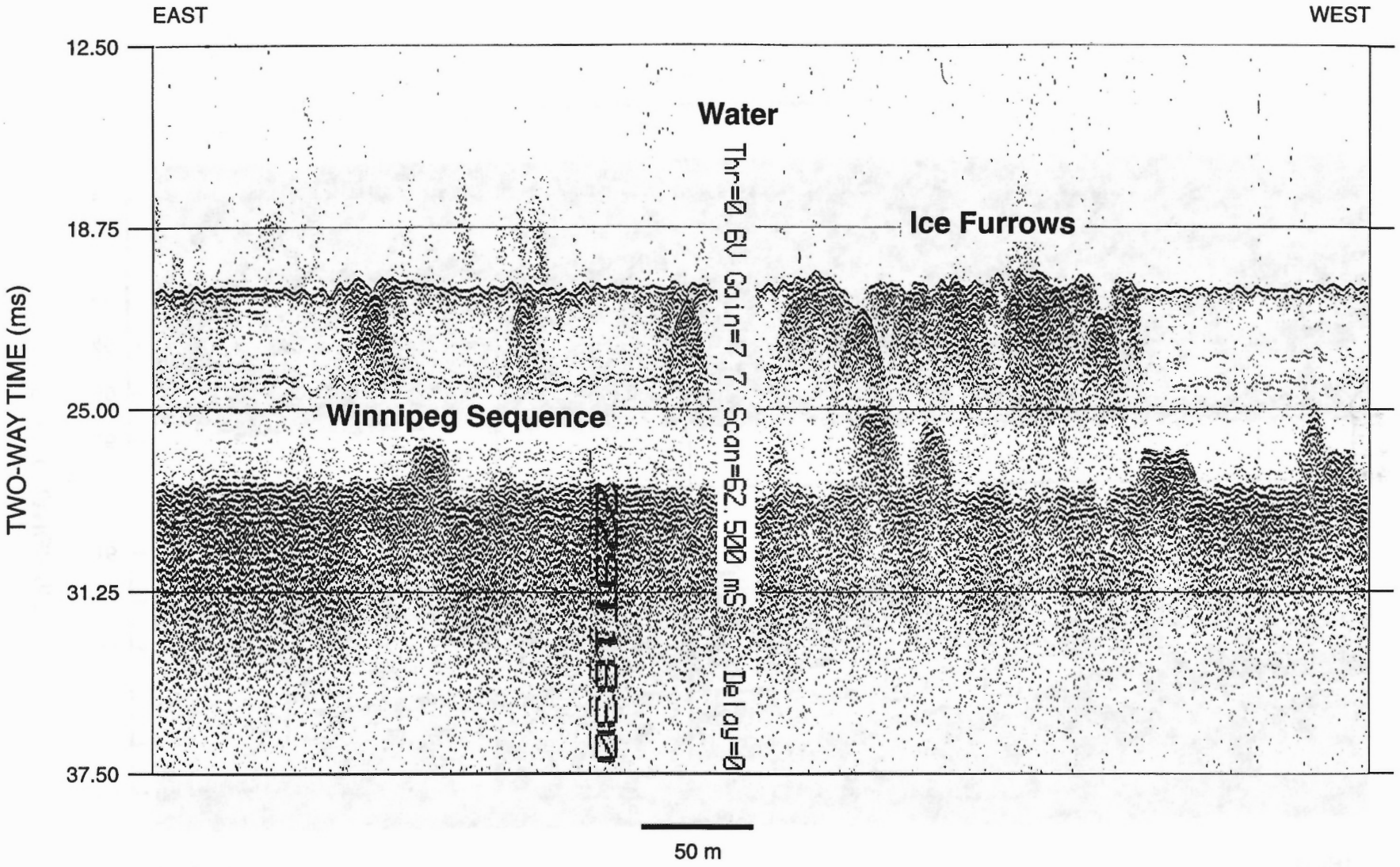

Figure 22. Ice-scoured lakefloor, North Basin (Seistec record, line NB9, Day 229, 1829 UTC). Estimated vertical distance between horizontal scale lines is 4.7 m.

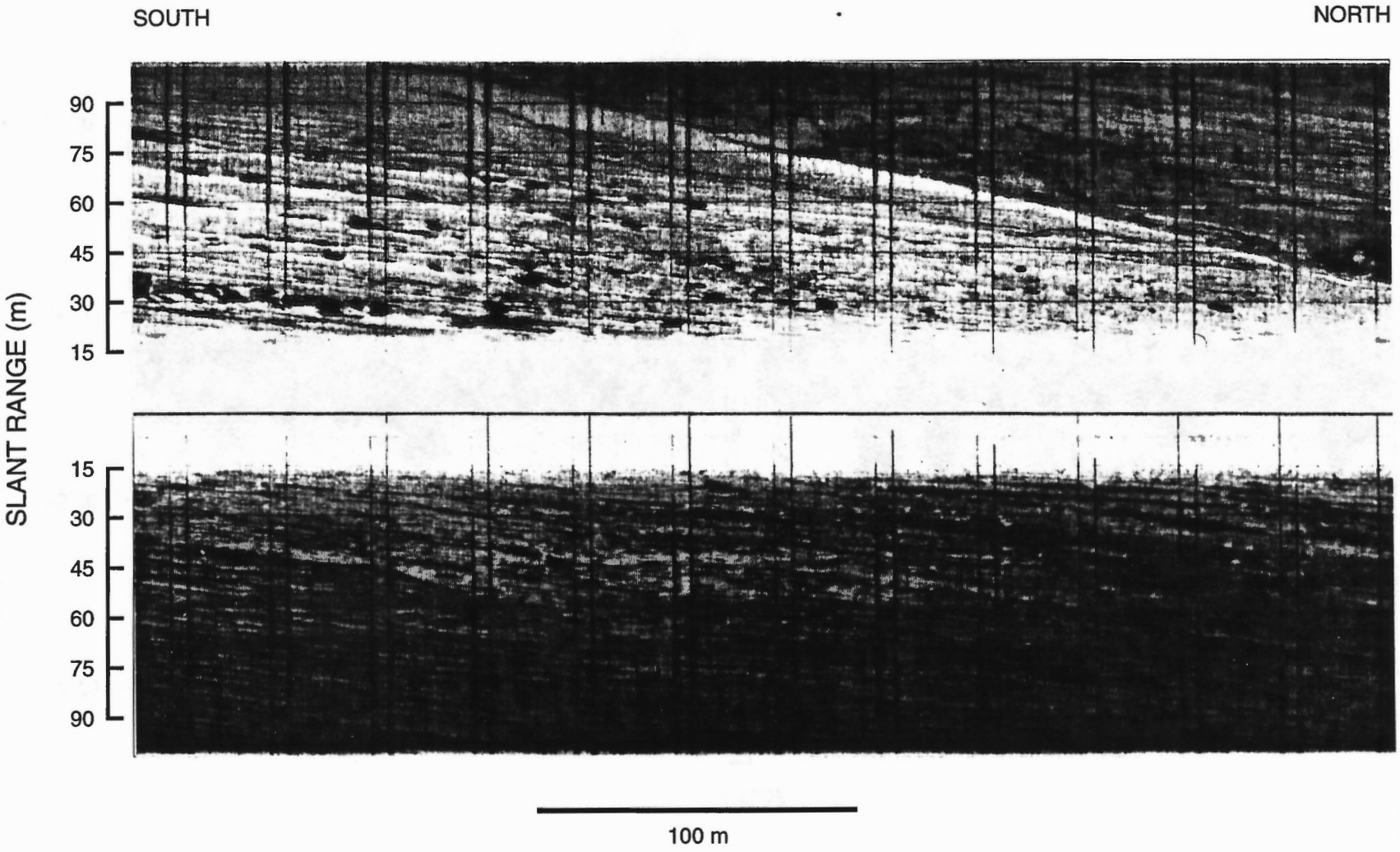

Figure 23. Flow-parallel lakefloor features, The Narrows. Water depth approximately 20.1 m. (Sidescan sonar record, line SB7, Day 224, 1925.9 to 1929.1 UTC).

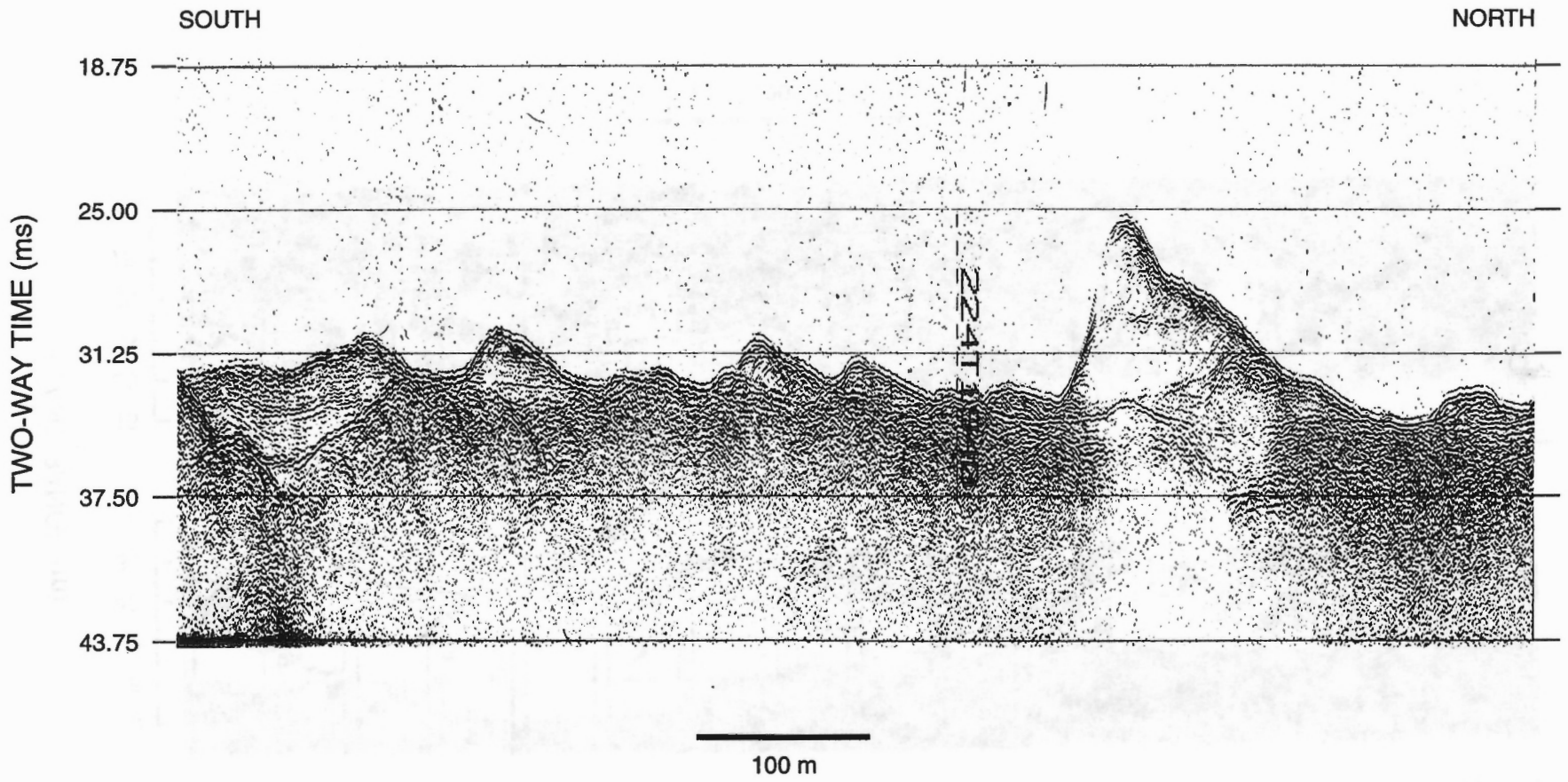

Figure 24. Sand wave field in deep water at north entrance to The Narrows (Seistec record, line SB7, Day 224, 1936 UTC). Estimated vertical distance between horizontal scale lines is 4.7 m.

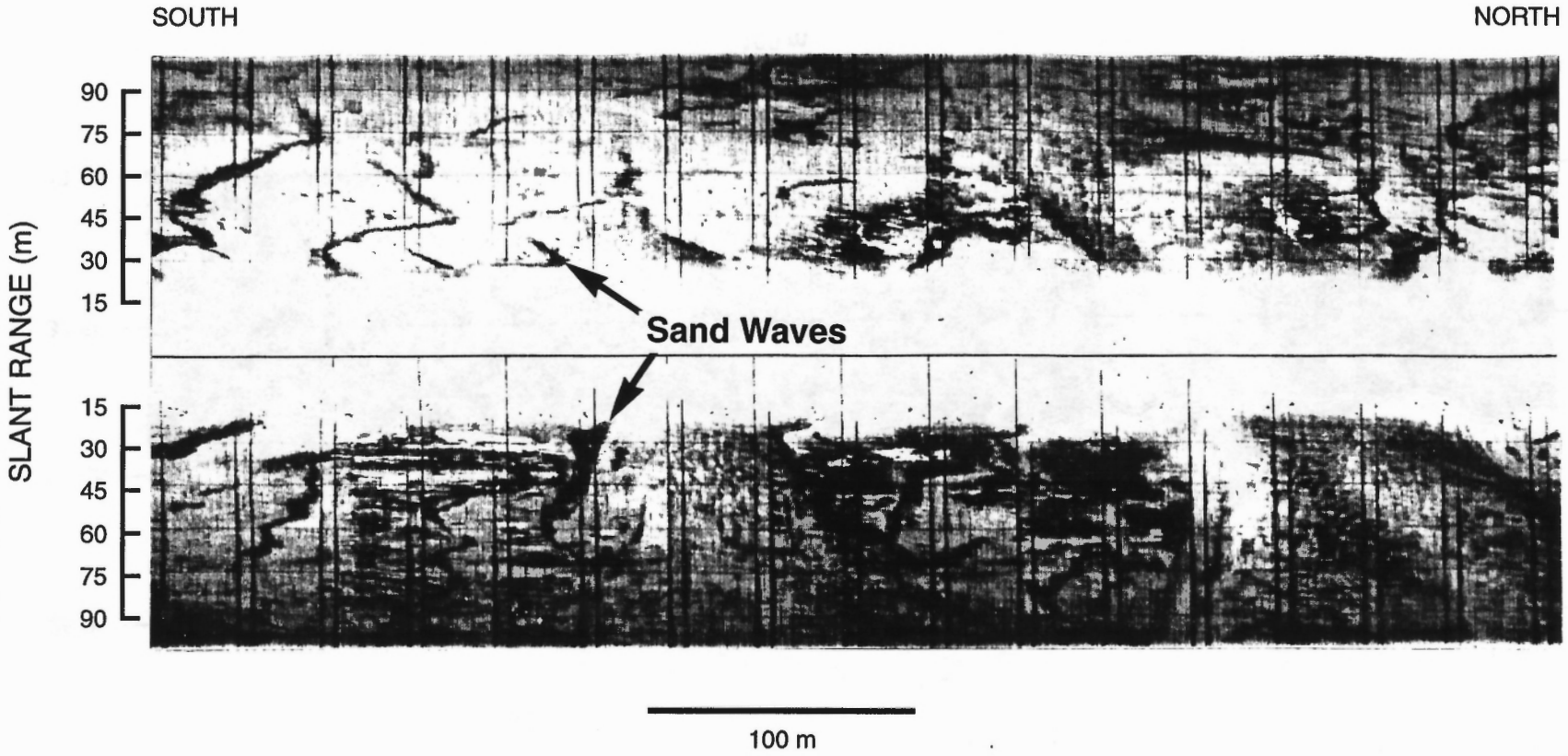

Figure 25. Sand wave field at north entrance to The Narrows. Area of figure corresponds to Seistec record in Figure 24. Water depth approximately 19.2 m. (Sidescan sonar record, line SB7, Day 224, 1937.2 to 1941.4 UTC).

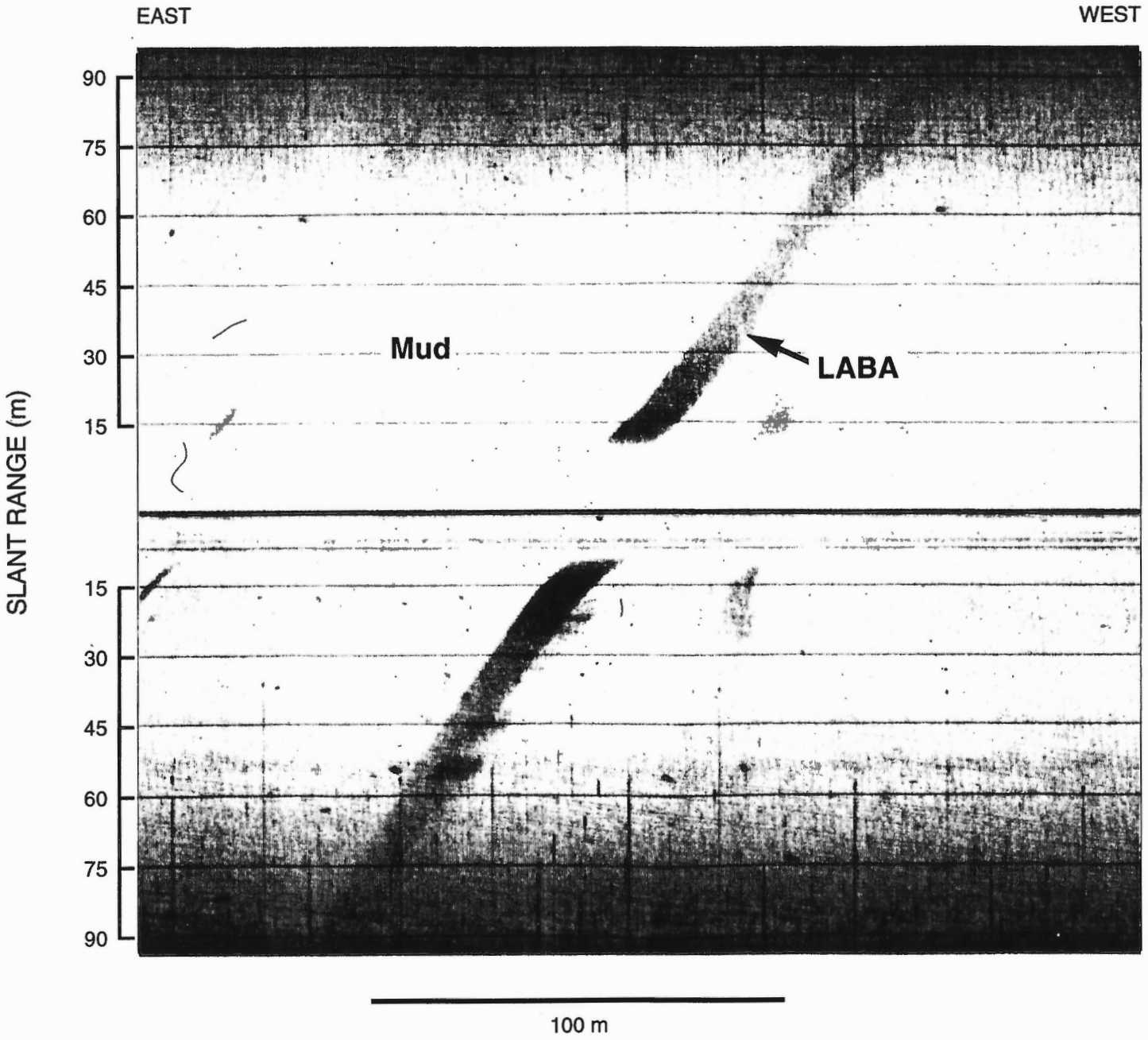

Figure 26. Linear Acoustic Backscatter Anomaly (LABA), North Basin. Water depth approximately 14.6 m. (Sidescan sonar record, line NB9, Day 229, 2243.1 to 2245.1 UTC).

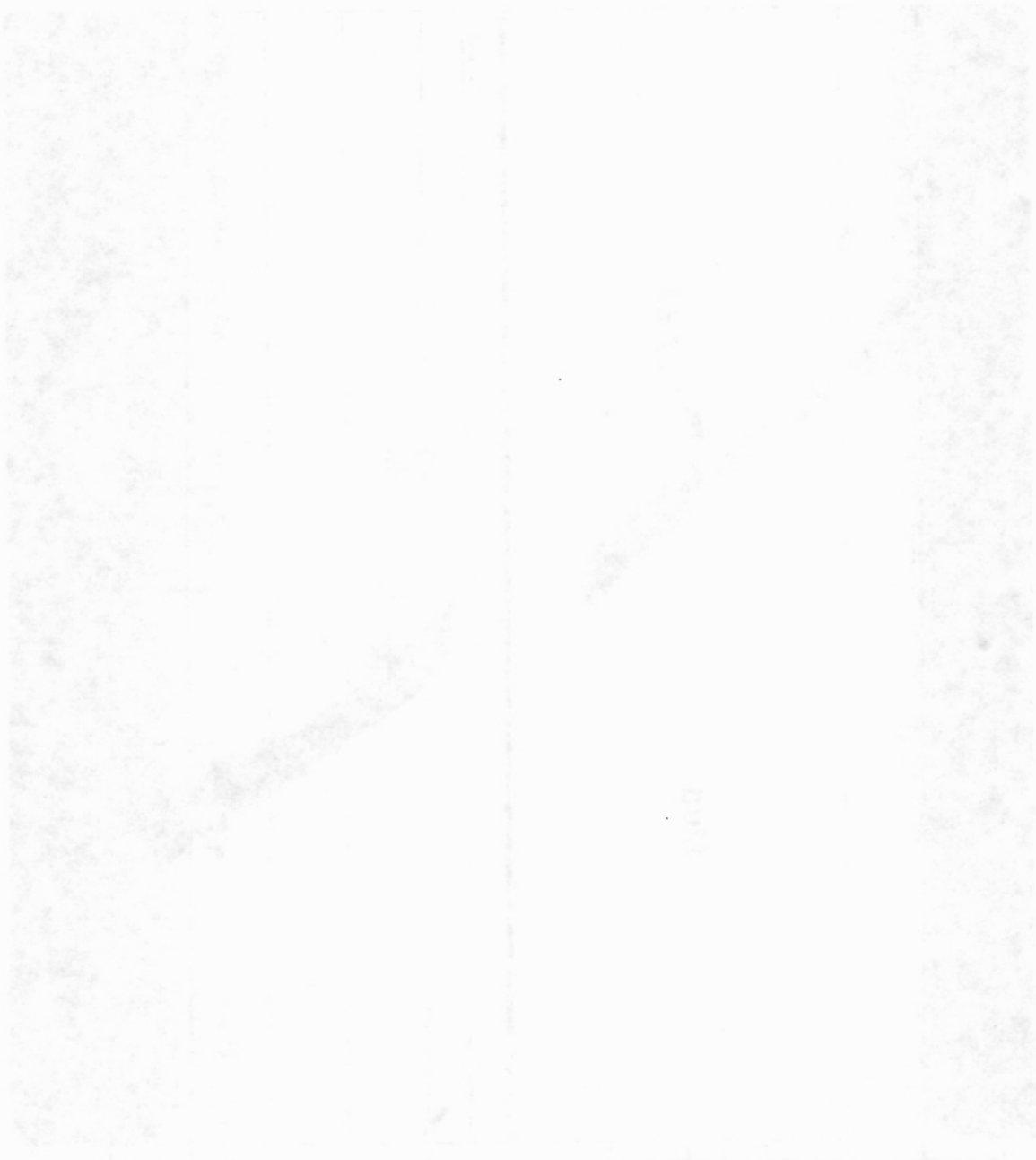

3.2 Precambrian geology of the Lake Winnipeg area

W. Weber

Manitoba Energy and Mines
1395 Ellice Avenue, Winnipeg, Manitoba R3G 3P2

BACKGROUND

Lake Winnipeg extends along the contact between Precambrian and Paleozoic rocks (Manitoba Mineral Resources Division, 1979). The eastern shore is underlain by Precambrian rocks. The western shore of the lake is underlain by Paleozoic rocks which overlie the westerly-dipping Precambrian basement. Until the present study, the exact position of the Paleozoic/Precambrian contact under Lake Winnipeg has been unknown. For the Geological Map of Manitoba (Manitoba Mineral Resources Division, 1979) the contact between the Paleozoic and Precambrian rocks in the North Basin had been extrapolated from drill core information using the intersection of the dip of this basement surface with the earth's surface. In The Narrows and the South Basin, bedrock exposures allow for the approximate positioning (within 1-3 km) of the Precambrian/Paleozoic contact assuming "straight" extensions of known contacts. Faulting in the Black Island area resulted in an irregularity of this contact (Bezys, this volume).

The geology of Precambrian rocks east of Lake Winnipeg is known from exposures (Fig. 1). The structure and lithologies of Precambrian rocks underneath the Paleozoic cover (west of Lake Winnipeg) has been interpreted from aeromagnetic signatures (Geological Survey of Canada, 1993; Fig. 1), since Paleozoic rocks are non-magnetic and therefore transparent to the magnetic characteristics of the underlying Precambrian basement. In some locations west of Lake Winnipeg diamond drilling into the Precambrian has provided ground truthing of aeromagnetic signatures, as in the Thompson Belt (see Fig.1).

PRECAMBRIAN GEOLOGY OF THE LAKE WINNIPEG AREA

Based on known and interpreted Precambrian geology (Fig. 1) the Lake Winnipeg area is underlain by easterly trending Archean greenstone/granitoid belts, and metasedimentary/gneissic and plutonic belts of the western Superior Province. Northwest of the lake these belts are truncated by the NE trending Thompson Belt, which is part of the Churchill-Superior Boundary zone that formed as a result of collision between the Superior Province and the Trans-Hudson Orogen (of the Churchill Province) 1.8 Ga ago (Weber, 1990).

The belt structure of the western Superior Province is the result of convergence of >2.7 Ga island arcs, accreted basins and older granitoid basement, and Late Archean (>2.7 Ga) transpressional tectonics that formed easterly dextral shear zones and parallel and oblique thrusts (Williams et al., 1992). Based on lithotectonic entities and major transpressional shear/fault zones, the western Superior Province in Manitoba is generally divided into the following subprovinces, from south to north (Fig. 1):

Wabigoon
Winnipeg River
Bird River
English River
Uchi
Berens
Island Lake
Molson Lake
Cross Lake (or Gods Lake)

In Manitoba, the boundary between Uchi and Berens subprovinces is an easterly trending thrust fault. Mapping and aeromagnetic signatures indicate that near the east shore of Lake Winnipeg this fault swings to the northwest, parallel to the lake shore (Brown, 1981). Aeromagnetic signatures indicate a parallel structure along the east shore of the Narrows.

Proterozoic structures are indicated by NW striking mafic dykes of the Kenora swarms that are exposed in NW Ontario.

RESULTS FROM THE SEISMIC SURVEYS

A preliminary evaluation of the Seistec data and a single channel output of the unprocessed multi-channel seismic data obtained during the 1994 Lake Winnipeg survey has yielded the following results.

1. The location of the Precambrian/Paleozoic contact has been determined on line NB11 (Figs. 2, 3; Bezys, this volume), and, with some uncertainty, on lines SB6, NB7 - NB10). The contact is indicated where a strong, flat reflector, with steps possibly indicating faults (Fig. 3), meets a poor reflector with irregular relief. It revises the contact presently shown on geological maps of the North Basin (Fig. 1).

2. The extension of the Uchi/Berens Subprovince boundary fault near Black Island was confirmed. Reflectors with a highly irregular relief are interpreted to be associated with the Precambrian surface because they are basement to a seismically-layered package likely representing sediments. Based on comparison with exposed Precambrian rocks the high

relief of the basement is interpreted to be the surface expression of a fault, in this case of a fault between Black Island and the east shore of Lake Winnipeg related to the Uchi/Berens Subprovince boundary fault (Figs. 1, 3, 4).

3. A probable Paleozoic fault north of The Narrows, may possibly be a reactivated Archean structure. A distinct relief difference in the seismic reflections (believed to originate from the Precambrian surface) just north of The Narrows (line SB7, Fig. 5) is interpreted as a post-Precambrian fault. Drill hole data discussed by Bezys (this volume) support this interpretation. This structure is coincident with a strong aeromagnetic lineament parallel to the Uchi/Berens Subprovince boundary fault. The northern extension of this fault can be identified and traced on line NB7 for ca. 10 km and can possibly be correlated with faults on line NB8 which would extend this fault for ca. 150 km.

Future processing of the multi channel seismic data should provide more information on major structures within the Precambrian.

REFERENCES

Brown, A.
1981. Geology of the Manigotogan-Black Island-Rice River area, Manitoba; Geological Survey of Canada, Open File 812, 201p.

Geological Survey of Canada
1993. Manitoba Magnetic Anomaly Map, Geophysics Division, Geological Survey of Canada, Energy, Mines and Resources, Canada, scale 1: 1 000 000.

Manitoba Mineral Resources Division
1979. Geological Map of Manitoba, scale 1:1 000 000, Map 79-2.

Weber, W.
1990. The Churchill-Superior Boundary zone, southeast margin of the Trans-Hudson Orogen: a review; in eds. J.F. Lewry and M.R. Stauffer, The Early Proterozoic Trans-Hudson Orogen of North America, Geological Association of Canada Special Paper 37, p. 41-57.

Williams, H.R., Stott, G.M., Thurston, P.C., Sutcliffe, R.H., Bennett, G., Easton, R.M. and Armstrong, D.K.
1992. Tectonic evolution of Ontario: summary and synthesis; in eds. P.C. Thurston, H.R. Williams, R.H. Sutcliffe and G.M. Stott, Geology of Ontario, Special Volume 4, Part 2, p. 1255-1332.

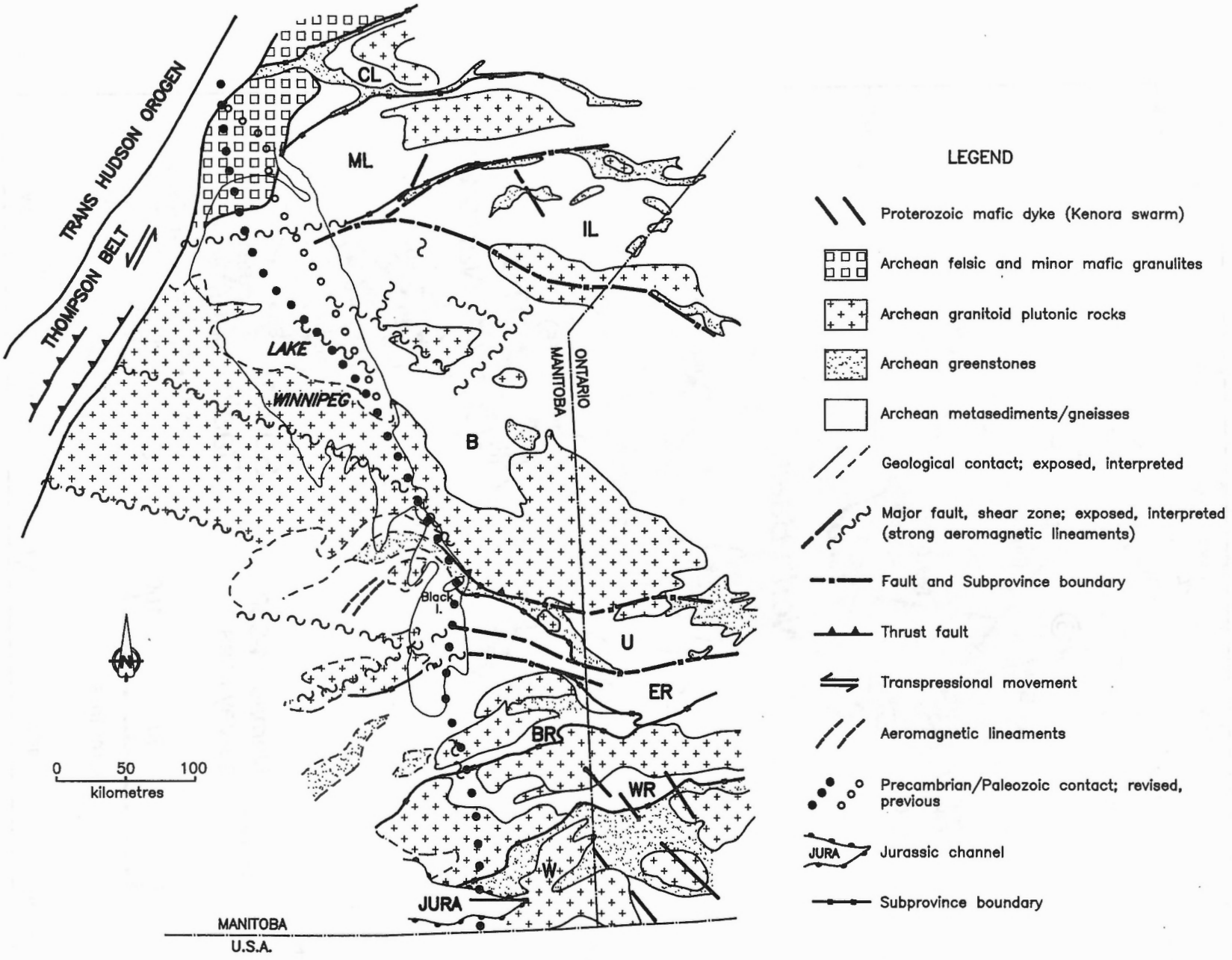

Figure 1. Geological map of the Precambrian rocks in the Lake Winnipeg area. Subprovinces: W-Wabigoon, WR-Winnipeg River, BR-Bird River, ER-English River, B-Berens, IL-Island Lake, ML-Molson Lake, CL-Cross Lake.

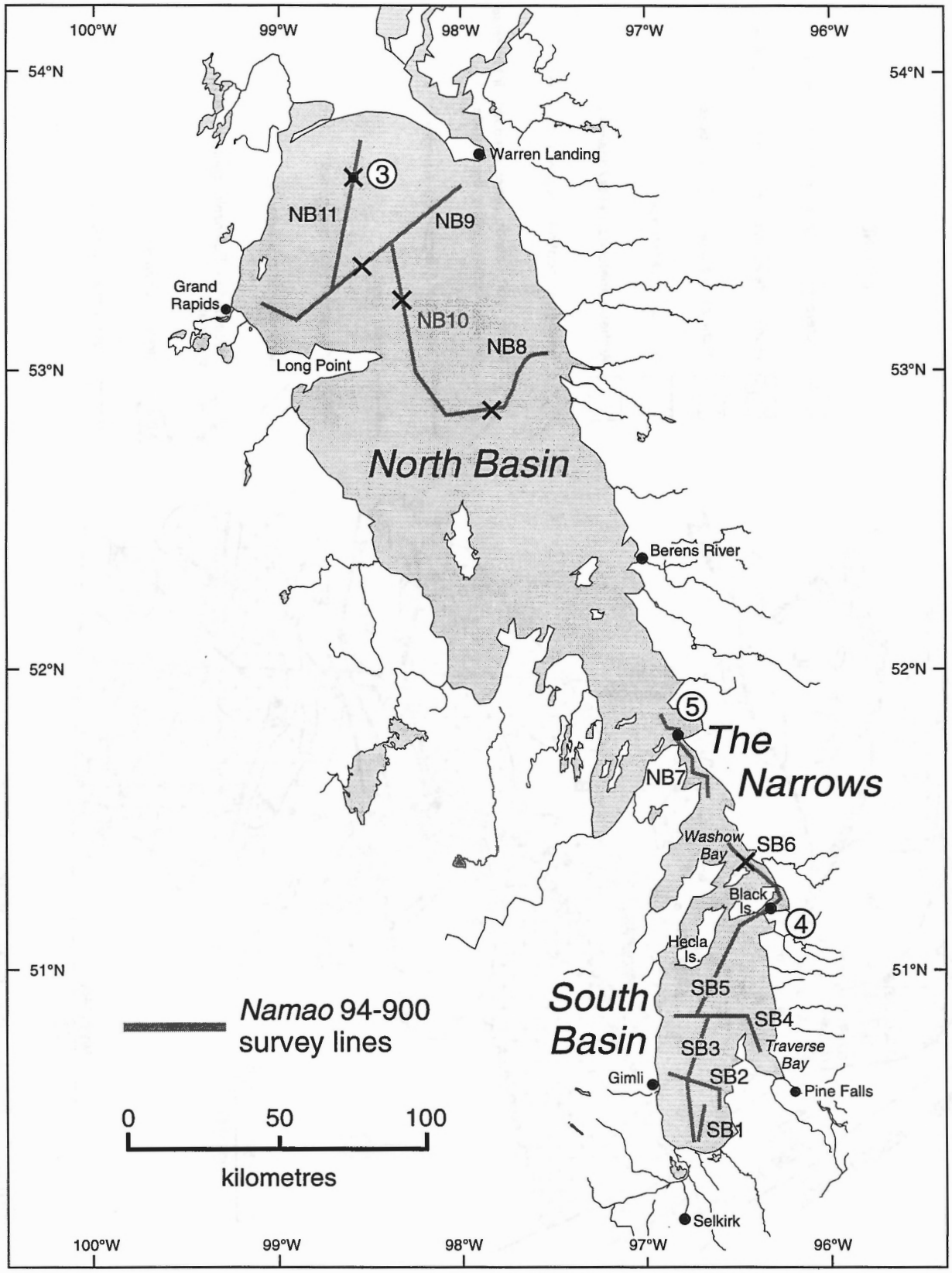

Figure 2. Geophysical survey lines in Lake Winnipeg. Crosses mark the location of Precambrian-Paleozoic contact determined from this study. Numbers 3 to 5 identify figure locations.

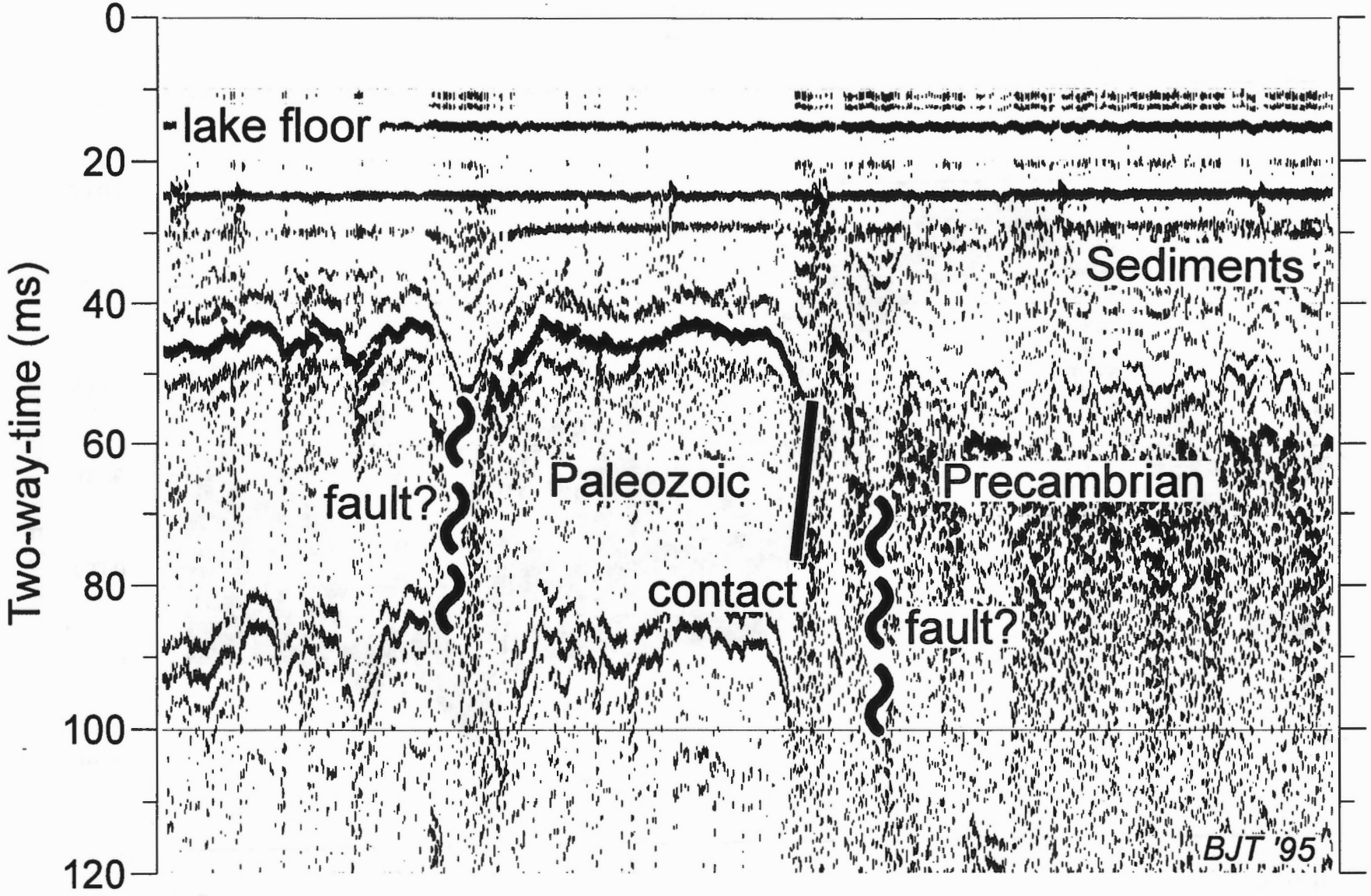

Figure 3. Seismic profile showing the interpreted contact between Paleozoic on the left and Precambrian to the right (line NB11, 231/1850, see Fig. 2 for location).

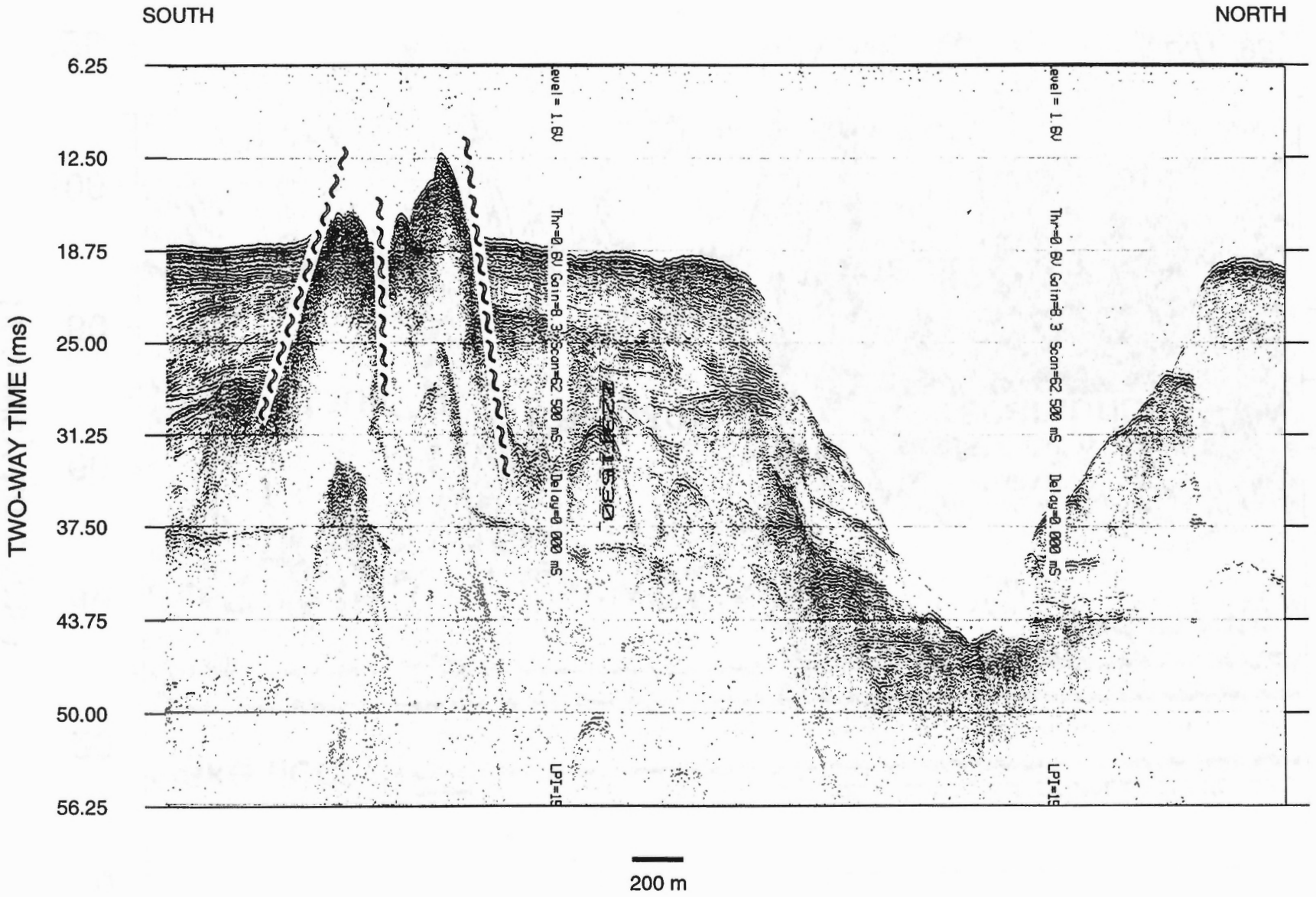

Figure 4. Seistec record (line SB6, 223/1630) showing seismically-layered package (Quaternary sediments) overlying, and in places ponded between, Precambrian bedrock with high relief.

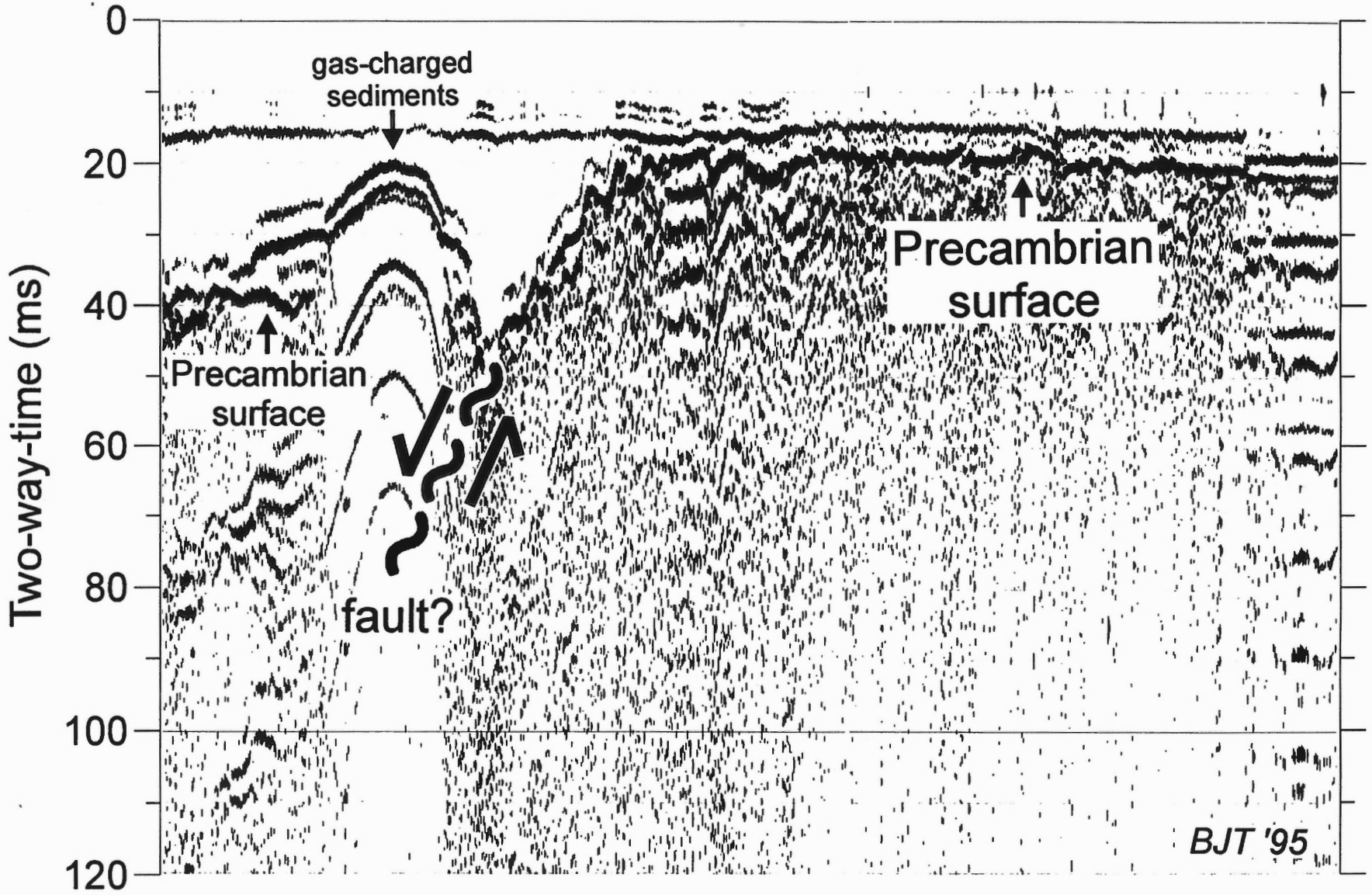

Figure 5. Seismic record (line SB7, 224/2000) showing an abrupt change in relief of the main reflector (identified as Precambrian surface), interpreted to have resulted from Paleozoic faulting, possibly along a reactivated Archean structure (see Figure 2).

3.3 Paleozoic geology of the Lake Winnipeg area and repositioning of the Precambrian - Paleozoic boundary

R. K. Bezys

Manitoba Energy and Mines
1395 Ellice Avenue, Winnipeg Manitoba R3G 3P2

ABSTRACT

Lake Winnipeg is bounded by Precambrian rocks on its eastern shore and Paleozoic carbonate rocks to the west. The boundary between the Precambrian and Paleozoic rocks was previously estimated to lie toward the eastern edge of the lake. The sequence representing the boundary consists of Ordovician Red River and Winnipeg Formations overlying Precambrian rocks. The Paleozoic sequence ranges in thickness from zero at the Precambrian-Paleozoic boundary to approximately 100 m at the western shoreline. The sequence consists of clastic sediments (Winnipeg Formation) overlain by carbonates (Red River Formation).

New seismic reflection data from the Lake Winnipeg Project indicate that the actual position of the Precambrian-Paleozoic boundary in the North Basin is approximately 60 km west of the previously inferred position. Indirect evidence of faulting along the Precambrian-Paleozoic boundary is demonstrated at The Narrows, Green Oak and in the North Basin.

INTRODUCTION

The subcrop-outcrop map of the Paleozoic erosional surface depicts the geology of the area in the vicinity of Lake Winnipeg (Fig. 1). Figure 2 outlines some of the Paleozoic tectonic elements that have been modified by tectonic features emanating from the Precambrian basement. The most dominant feature is the northeast trending Churchill-Superior Boundary Zone (CSBZ) situated northwest of Lake Winnipeg's North Basin. This zone marks the collision zone of two major Precambrian terranes, the Archean Superior and Proterozoic/Archean Churchill provinces along the eastern margin of the Trans-Hudson Orogen (not indicated on Fig. 2).

East-west trending orogenic belts (possibly Greenstone Belts) within the Archean Superior block may have affected Paleozoic deposition (McCabe and Barchyn, 1982). As well, the Superior Province may have evoked a slightly different response to tectonic forces, giving rise to both basin subsidence to the west and uplift to the east relative to the Churchill Province Block (McCabe, 1967). The structural uplift to the east may be attributed to the Severn Arch. Due to these variable episodes of uplift and subsidence, the depositional and erosional patterns for most Paleozoic Formations in southwestern Manitoba are somewhat anomalous relative to the regional Williston Basin framework.

REGIONAL PALEOZOIC GEOLOGY

The Precambrian, in the extreme southwestern corner of Manitoba, is overlain by approximately 1300 m of Paleozoic strata which dip gently, approximately 2 to 2.5 m per km, to the southwest (Fig. 3) and outcrop at the eastern shore of Lake Winnipeg (Fig. 1). The stratigraphic package corresponds to the Tippecanoe Sequence of Sloss (1963). This wedge of Paleozoic strata was partially uplifted and truncated by post-Silurian to pre-Jurassic erosion so that Paleozoic formations now outcrop or subcrop in a series of north to northwest-trending belts in the Interlake area west of Lake Winnipeg (Fig. 1).

Lake Winnipeg is flanked by Precambrian (Superior Province) rocks on its eastern shore and Paleozoic carbonate rocks (Williston Basin) to the west. The thickness of the Paleozoic ranges from zero at the Precambrian-Paleozoic boundary, to approximately 100 metres on the lake's western shoreline. The Paleozoic sequence consists of Ordovician age strata, with Devonian strata outcropping in the western Interlake region (Figs. 1, 4). The Winnipeg Formation consists of arenaceous mudstone and siltstone overlying sandstone ranging in thickness from 45 m in the South Basin to approximately 7 m within the North Basin (Fig. 5). Likewise, the Red River Formation ranges from a thickness of 130 m in the South Basin to approximately 50 m in the North Basin. In the South Basin, the formation consists of dolomite and limestone (Dog Head, Cat Head and Selkirk members = lower Red River) overlain by argillaceous dolomite and intraformational breccia beds (Fort Garry Member = Upper Red River). The lower Red River is entirely dolomite in the North Basin. Along the North Basin's western shoreline, the Stony Mountain Formation (massive dolomite) overlies the recessive Fort Garry Member. This sequence is depicted as spectacular 6 to 12 m high cliffs along the shoreline.

It is important to note that the Lower Paleozoic sequence in the Williston Basin extended much further east than is depicted today (McCabe and Barchyn, 1982). Stratigraphic isopachs of the formations within this sequence decrease from south to north, trend east-west, and are thickest in the City of Winnipeg area. These trends imply uplift and truncation of the eastern boundary of the Williston Basin in the Lake Winnipeg area (Norford et al., 1994). What is present today is only half

of what originally existed of the Lower Paleozoic Williston Basin sequence.

STRUCTURE

The entire post-Silurian period was a time of differential uplift and erosion. This series of events is evidenced by the distribution of Jurassic red beds and evaporites which, at least locally, over-step deeply eroded Paleozoic strata to rest directly on Precambrian basement in the area southeast of the City of Winnipeg (see extent of Jurassic sediments in Fig. 1). Also, this is probably the time of emergence of the Precambrian Shield in eastern Manitoba as a paleo-geographic feature, of which the Severn Arch is a part (Fig. 2).

The post-Paleozoic tectonic framework is markedly different with the result that the outcrop-subcrop belts are seen to be discordant to the present depositional trends on the Paleozoic erosion surface. Figure 5 depicts the Lower Paleozoic Winnipeg Formation structure contour and isopach map. It is evident on the map that the isopach trends are perpendicular to the basin's eastern edge, not circular as it is around a typical basin edge. McCabe (1967) suggested that the anomalous east-west depositional trend of the Ordovician strata might be related to the effect of a major discontinuity in the underlying Precambrian basement. McCabe suggested that the Churchill Province, relative to the Superior Province, has undergone greater subsidence during depositional episodes compensated for by relatively greater uplift during erosional episodes. The CSBZ marks the collision zone between these two provinces. The east-west depositional trend of the Ordovician strata is also parallel to the east-west trend of the magnetic anomalies and Greenstone Belts in the Precambrian basement in the Superior Province.

The author believes that the discordancy seen in the Ordovician depositional patterns is a result of post-Silurian uplift and truncation, resulting in the emergence of the Severn Arch. If this is the case, the original Ordovician depositional sequence extended much further east than presently depicted. This is based on the structure contour and isopach maps for the Lower Paleozoic formations, as well as the similarities in these formations between the Williston and Hudson Bay basins until Devonian time. After Silurian time there was a barrier between these basins (McCabe and Barchyn, 1982; Sanford et al., 1985). Evidence of uplift and truncation along the eastern boundary of the Williston Basin in Manitoba can also be seen in basin margin structural cross sections.

PALEOZOIC GEOLOGY OF THE LAKE WINNIPEG AREA

Figure 6 depicts the location of two cross sections in the Lake Winnipeg area. Cross section A-A', located at The Narrows, shows the correlation of two stratigraphic core holes, Pascar #2 and WRB #1 (unpublished core hole data), to the Precambrian outcrop on the eastern shoreline (Fig. 7). Based on stratigraphic regional dips to the southwest, it can be concluded that the Precambrian of the eastern shoreline has been uplifted relative to its regional structural trends. A similar cross section, B-B', was constructed across the Precambrian-Paleozoic boundary at Green Oak, Manitoba, south of Lake Winnipeg (Fig. 8) (McCabe, 1983). Based on the same principles as depicted in cross section A-A', it is implied that the Precambrian basement has been uplifted relative to its regional trends. These cross sections may depict faulting near and along the Precambrian-Paleozoic boundary. Precambrian northwest-trending lineaments are present along the eastern shore at The Narrows. These lineaments may represent reactivated basement faults (Weber, this volume).

Other research indicates tectonic movements may have been active during Paleozoic time in the William Lake area, northwest of Lake Winnipeg along the CSBZ (Bezys, in prep.). The driving forces are the reactivation of basement faults or lineaments. Relief differences on top of the Precambrian are as much as 29 m between drillholes spaced half a kilometre apart.

POSITION OF THE PRECAMBRIAN - PALEOZOIC BOUNDARY

Figure 6 depicts the location of the transect lines surveyed during the 1994 Lake Winnipeg Study. Figure 9 is a map of the interpreted location of the pre-1994 Precambrian-Paleozoic boundary and the new interpretation of its location. The location of the pre-1994 boundary was primarily determined by extending the regional, estimated thicknesses of the Stony Mountain and Red River formations in an easterly direction towards the east side of the lake. The location of the pre-1994 Precambrian-Paleozoic boundary, on land to the north of Lake Winnipeg, was determined in a similar manner, as there are no outcrops or drillholes available in the area to substantiate this location.

Interpretation of the seismic reflection data from the Lake Winnipeg survey places the Precambrian-Paleozoic boundary, in the North Basin, approximately 60 km to the west of the old boundary (Fig. 9). The seismic profile along NB11 in Figure 10, represents the Precambrian-Paleozoic boundary and possible evidence of faulting at this contact. In conjunction with the indirect evidence of uplift associated with the Precambrian-Paleozoic boundary at The Narrows and at Green Oak, this is an indication of faulting, based on the elevation of the Precambrian being higher than the top of the Paleozoic. This is probably a function of Precambrian tectonic action.

In the South Basin, the Precambrian-Paleozoic boundary is shifted to the west by approximately 15km. East-west seismic transects SB2 (at 1960) and SB3 (at 1980) reveal the presence of a Paleozoic escarpment, approximately 30 m high. This correlates with the known thickness of Paleozoic sediments intersected in water wells at Grand Beach, located

on the east side of the lake (Betcher, 1986). Based on regional structural and isopach trends for the South Basin area of Lake Winnipeg, this escarpment probably represents the Dog Head Member of the Red River Formation. Paleozoic strata present at Grand Beach, Elk Island, Seymourville and Black Island are now considered to be outliers.

CONCLUSIONS

With regards to the structural evolution of the Paleozoic strata in the Lake Winnipeg area, much has been gained from the new geophysical data gathered from the Lake Winnipeg Project. This paper presents evidence of uplift and truncation along the eastern boundary of the Williston Basin in Manitoba, which probably resulted in the establishment of the Severn Arch. Is it just coincidence that the lake straddles this erosional boundary between two geologic rock terranes, the Precambrian and the Paleozoic? Or, has Precambrian tectonic activity, such as basement faulting, resulted in the initial Lake Winnipeg basin to form where it is today? Indirect evidence of faulting along the Precambrian-Paleozoic boundary is demonstrated at Green Oak, The Narrows, and in the North Basin, but further seismic work in the Lake Winnipeg area and drilling may help identify faults.

ACKNOWLEDGEMENTS

Thanks are extended to H. Thorleifson, B. Todd, M. Lewis and E. Nielsen for allowing me to participate in this project. As well, I thank W. Weber, G. Conley and S.R. Dallimore for critically reviewing this paper and their helpful insights.

REFERENCES

Betcher, R.N.
1986. Groundwater availability Map Series, Selkirk (62I). Manitoba Water Resources Branch.

Bezys, R.K.
In prep. Sub-Paleozoic structure in Manitoba's northern Interlake along the Churchill Superior Boundary Zone: A detailed investigation of the Falconbridge William Lake study area; Manitoba Energy and Mines, Minerals Division, Open File Report OF94-3.

Gerhard, L.E., Anderson, S.B. and Fisher, D.W.
1990. Petroleum geology of the Williston Basin; in eds. M.W. Leighton, D.R. Kolata, D.F. Oltz and J.J. Eidel, Interior Cratonic Basin, American Association of Petroleum Geologists, Memoir 51, p. 507-559.

McCabe, H.R.
1967. Tectonic framework of Paleozoic formations in Manitoba; Transaction of the Canadian Institute of Mining and Metallurgy, v. 70, p. 180-189.

McCabe, H.R.
1983. GS-22 stratigraphic mapping and stratigraphic and industrial minerals corehole program; Manitoba Energy and Mines, Mineral Resources Division, Report of field activities, 1983, p. 122-130.

McCabe, H.R. and Barchyn, D.
1982. Paleozoic stratigraphy of southwestern Manitoba; Geological Association of Canada Field Trip Guidebook, 1982, no. 10, 48 p.

Manitoba Mineral Resources Division
1979. Geological map of Manitoba; Scale 1:1 000 000, Map 79-2.

Norford, B.S., Haidl, F.M., Bezys, R.K., Cecile, M.P., McCabe, H.R. and Paterson, D.F.
1994. Middle Ordovician to Lower Devonian strata of the Western Canada Sedimentary Basin; in Geological atlas of the Western Canada Sedimentary Basin, G.D. Mossop and I. Shetsen (compilers), Calgary, Canadian Society of Petroleum Geologists and Alberta Research Council, p. 109-127.

Sanford, B.V., Thompson, F.J. and McFall, G.H.
1985. Plate tectonics - a possible controlling mechanism in the development of hydrocarbon traps in southwestern Ontario; Bulletin of Canadian Petroleum Geology, v. 33, p. 52-71.

Sloss, L.L.
1963. Sequences in the cratonic interior of North America; Geological Society of America Bulletin, v. 74, p. 93-114.

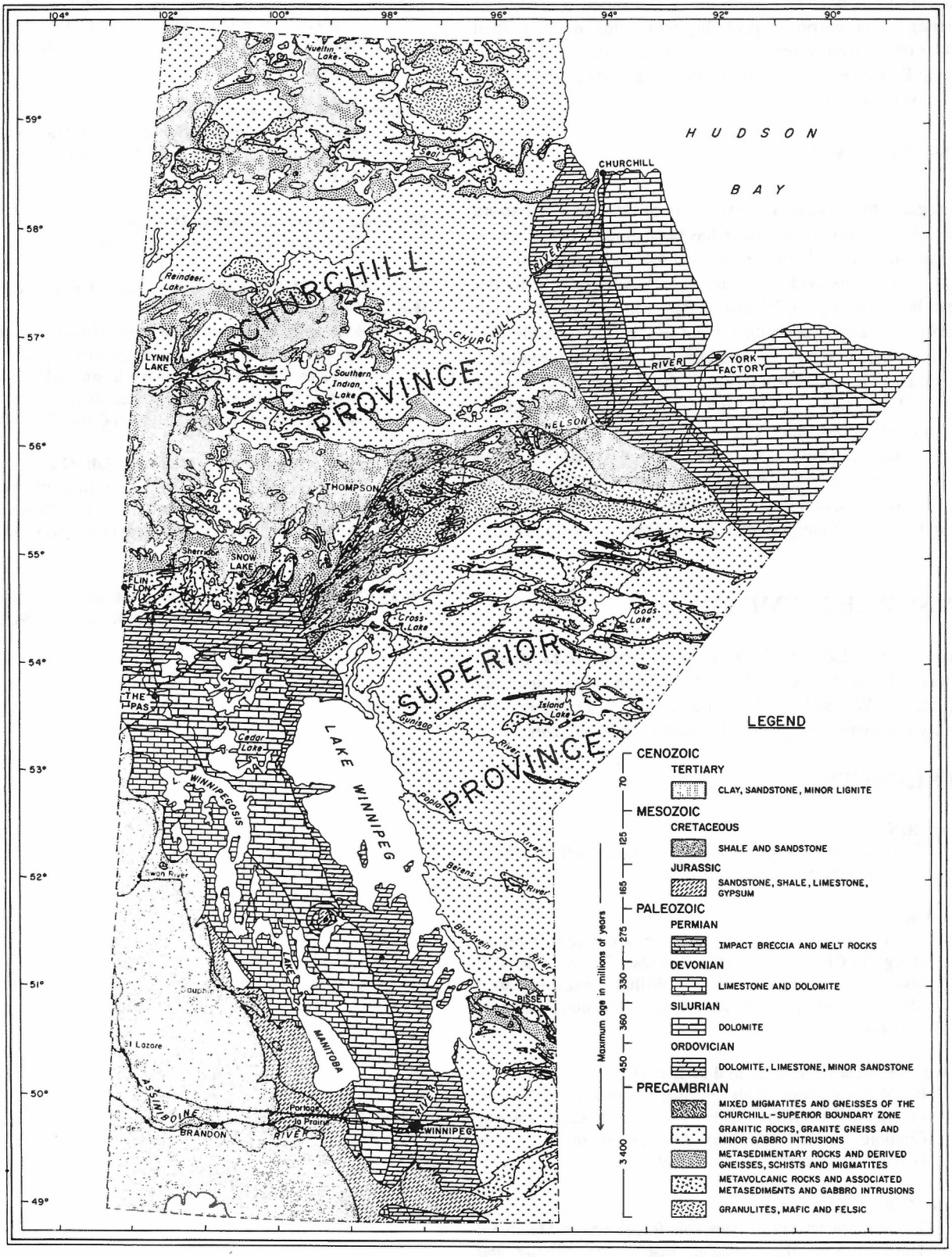

Figure 1. Geological map of Manitoba.

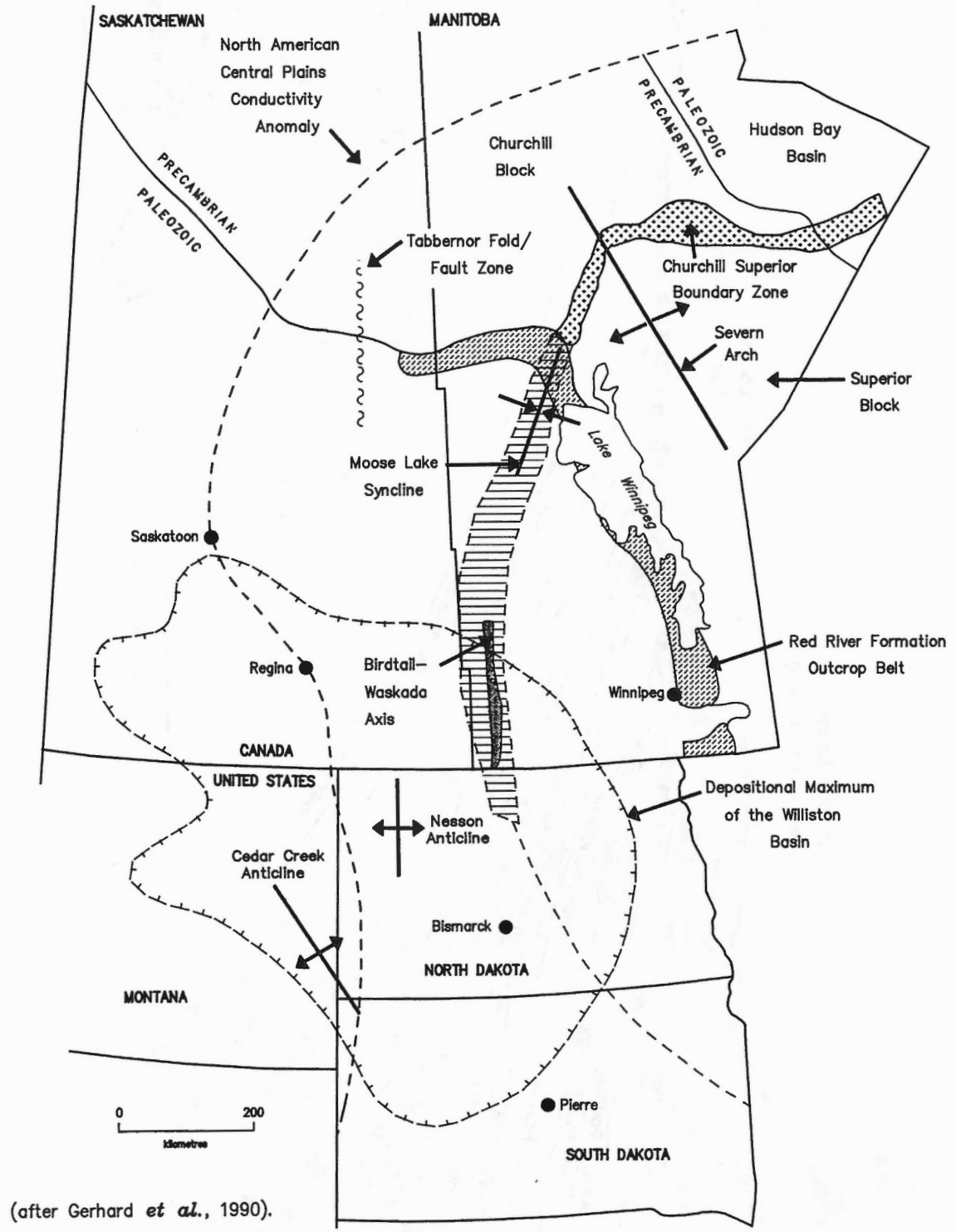

(after Gerhard *et al.*, 1990).

Figure 2. Major structural features within the Williston Basin.

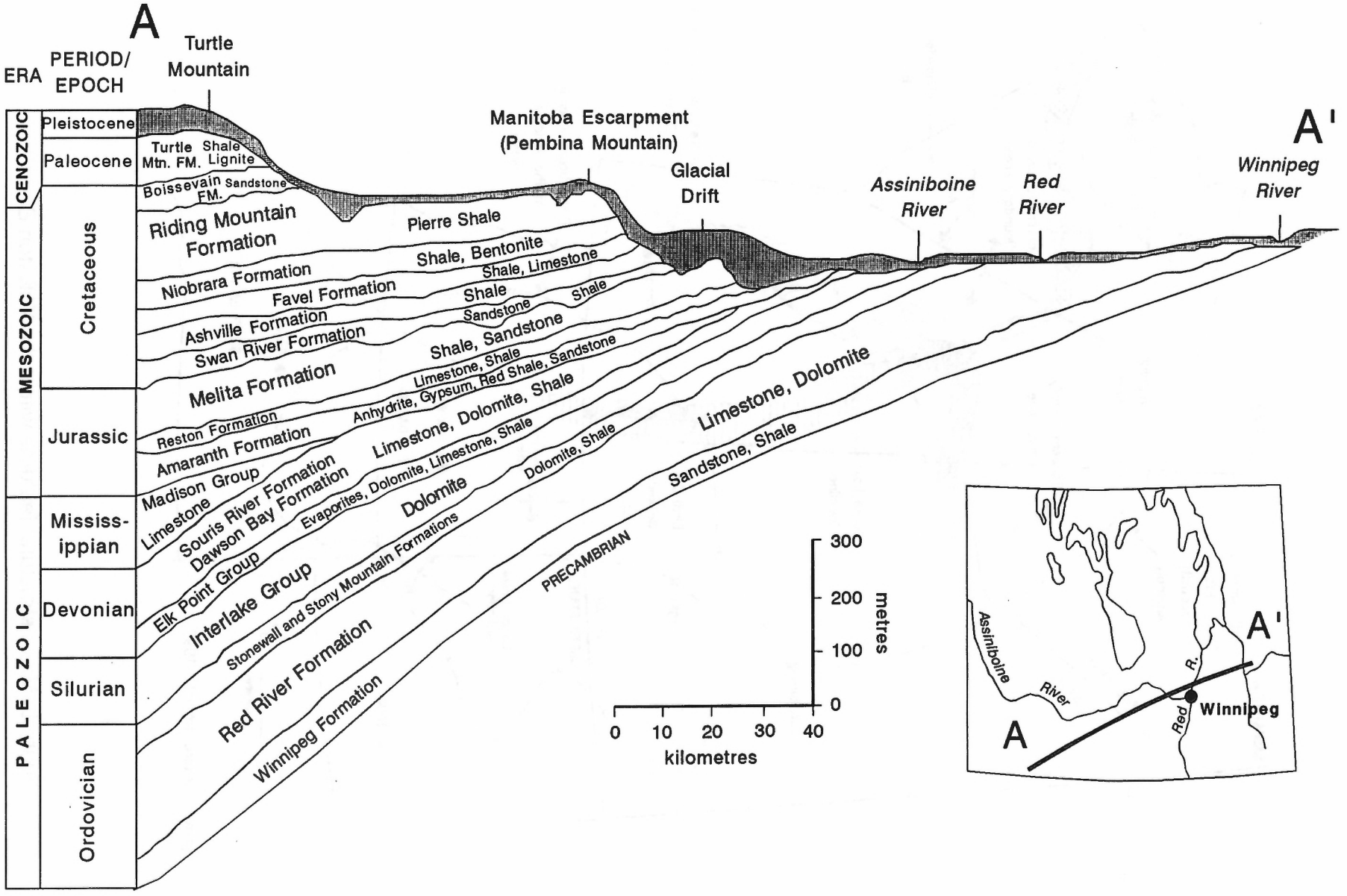

Figure 3. Regional structural cross section showing Paleozoic to Cenozoic formations in southern Manitoba.

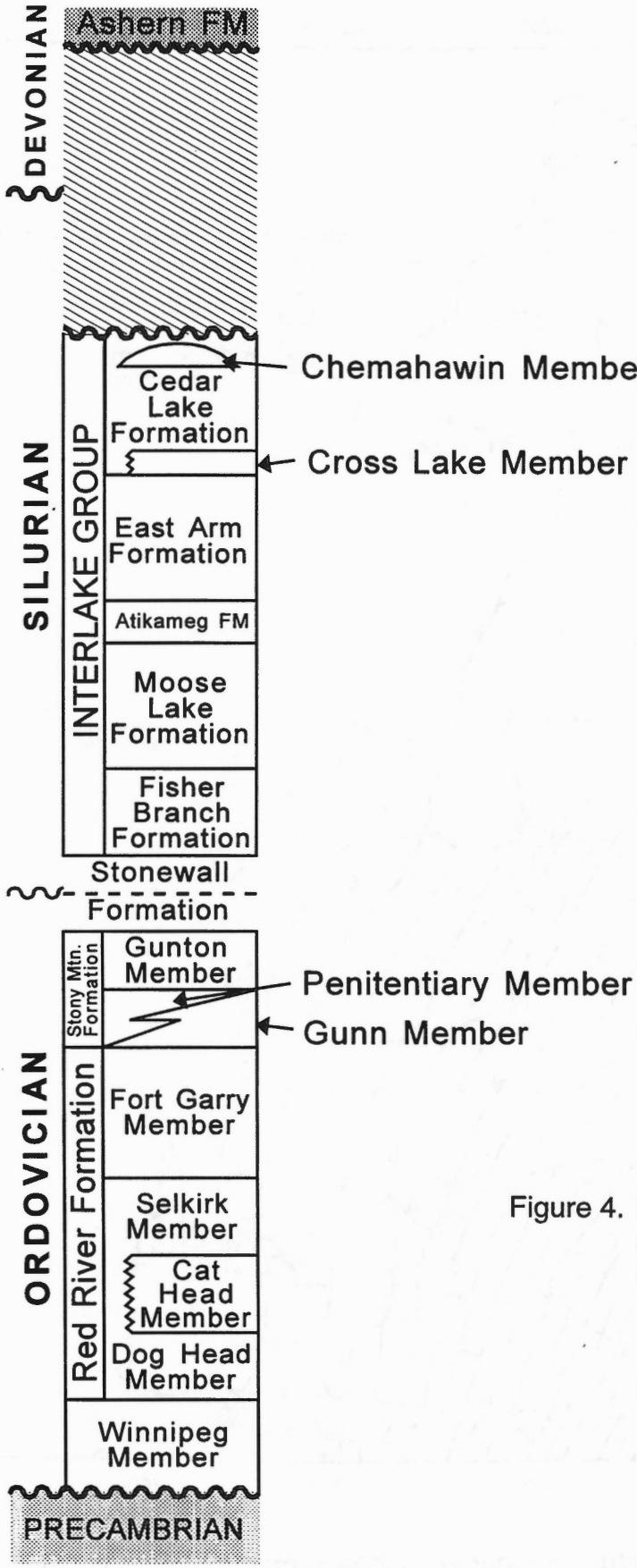

Figure 4. Lower Paleozoic stratigraphic section in the Lake Winnipeg area.

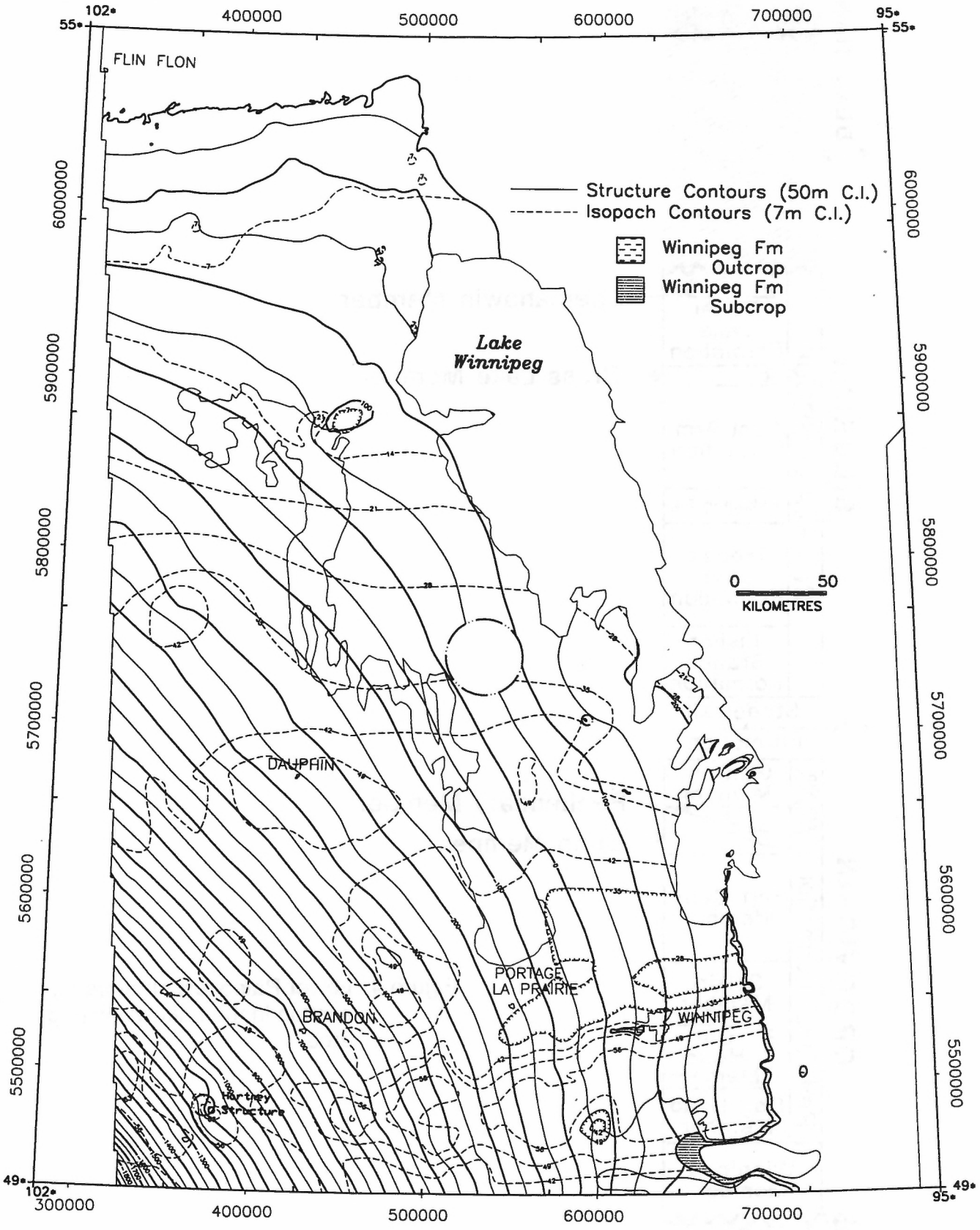

Figure 5. Winnipeg Formation structure contour and isopach map for southwestern Manitoba.

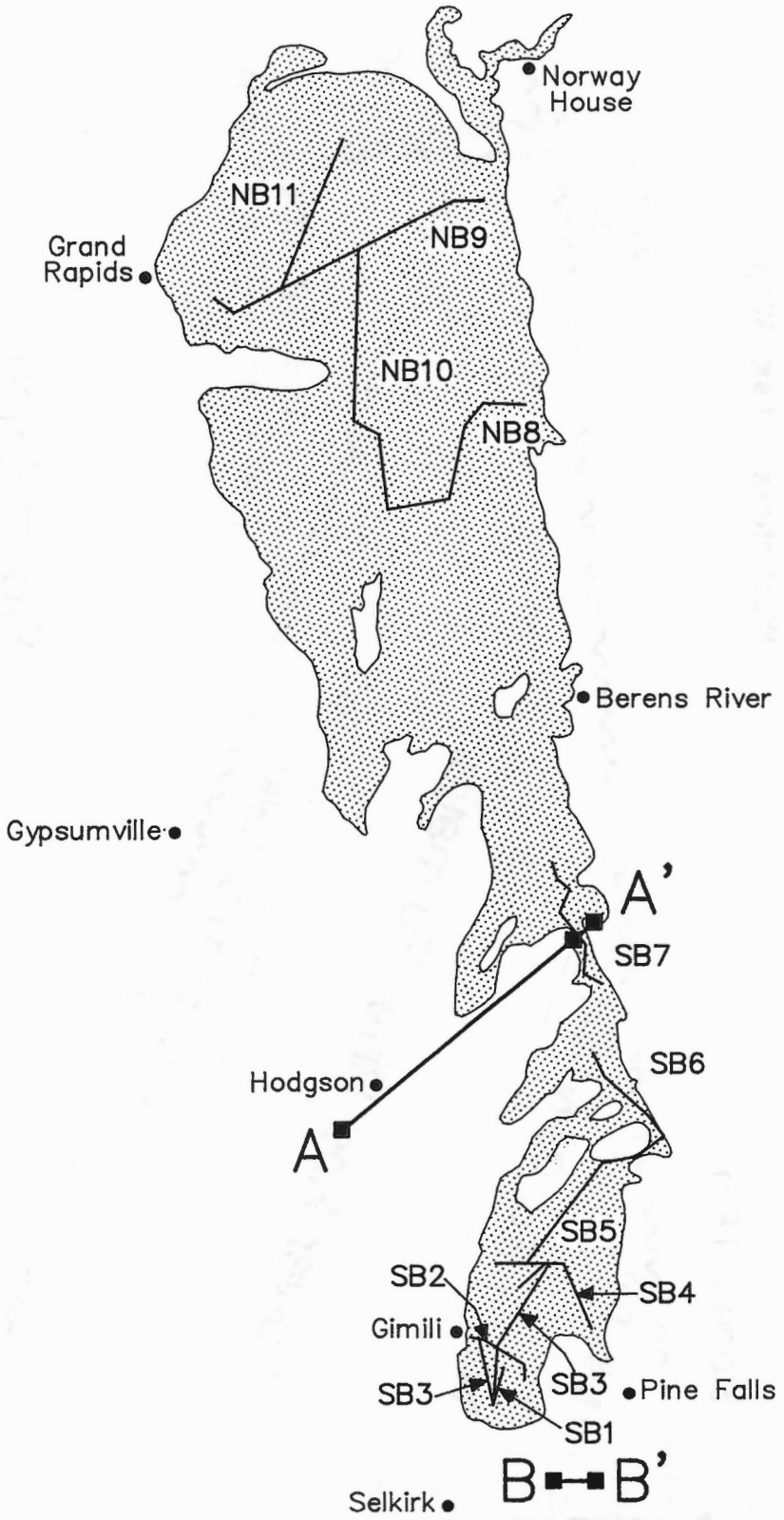

Figure 6. Location of cross sections A-A' and B-B', and location of Lake Winnipeg survey lines.

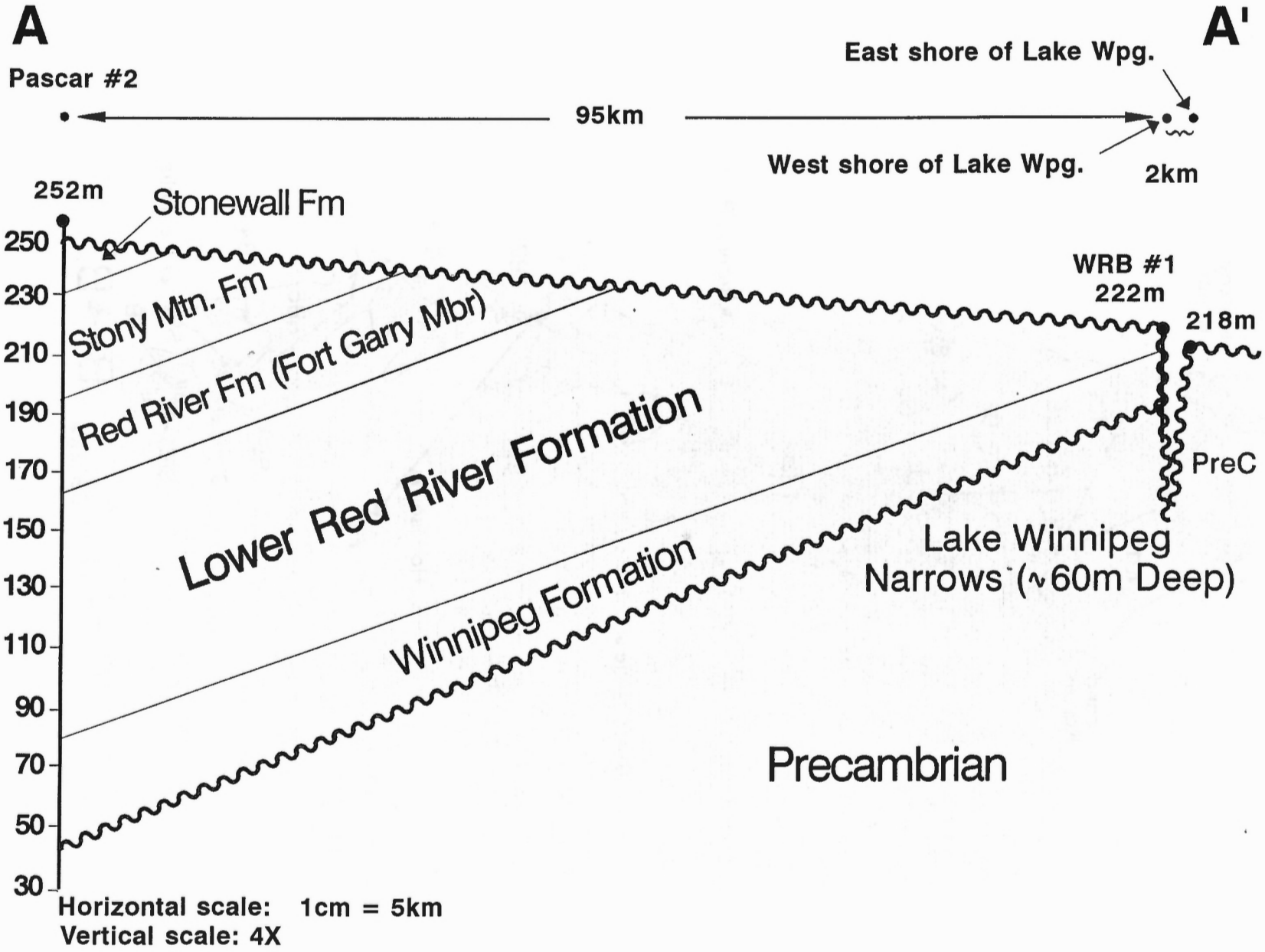

Figure 7. Structural cross section A-A' at The Narrows.

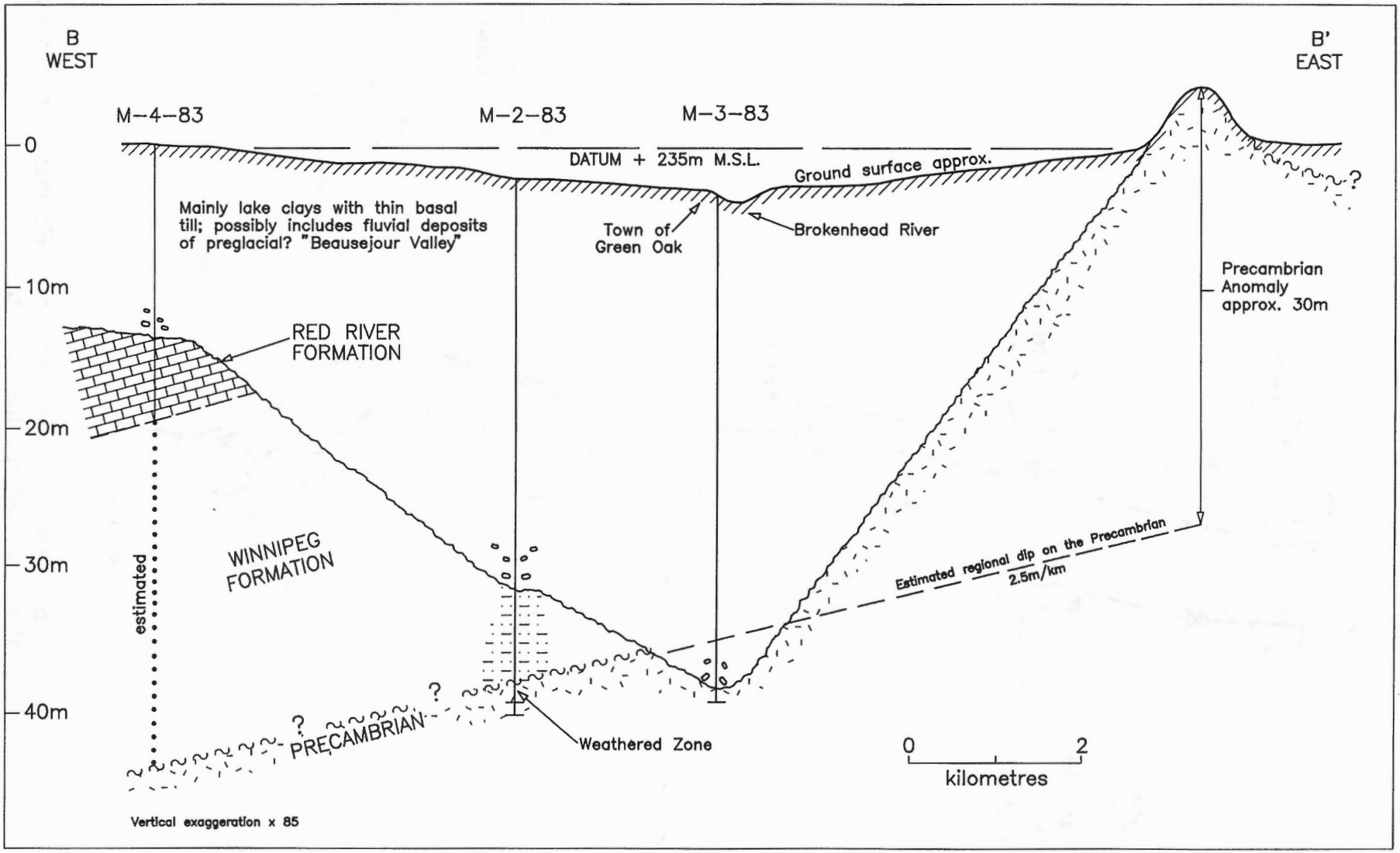

Figure 8. Structural cross section B-B' at Green Oak.

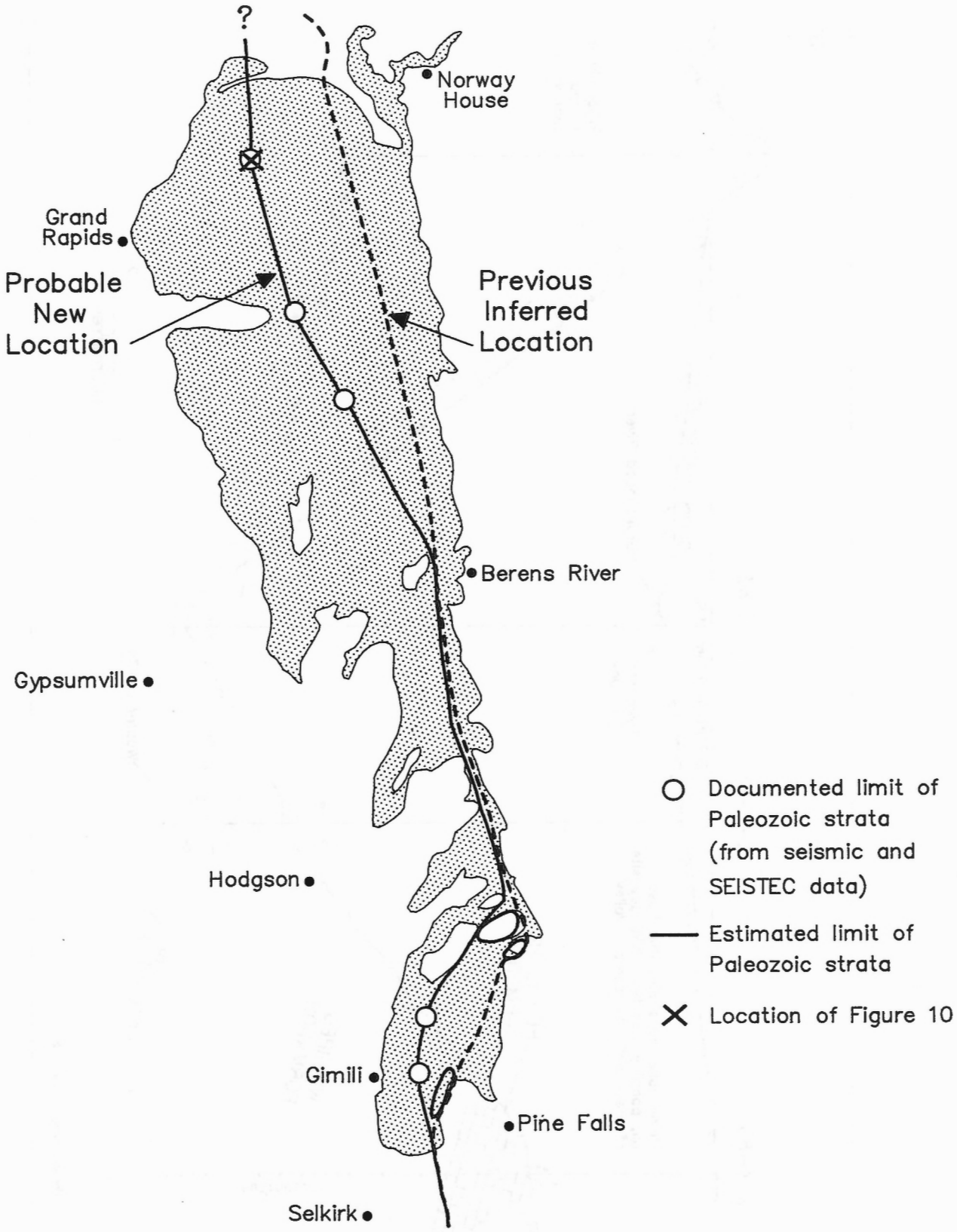

Figure 9. The pre-1994 location of the Precambrian-Paleozoic boundary and the probable new location of the boundary.

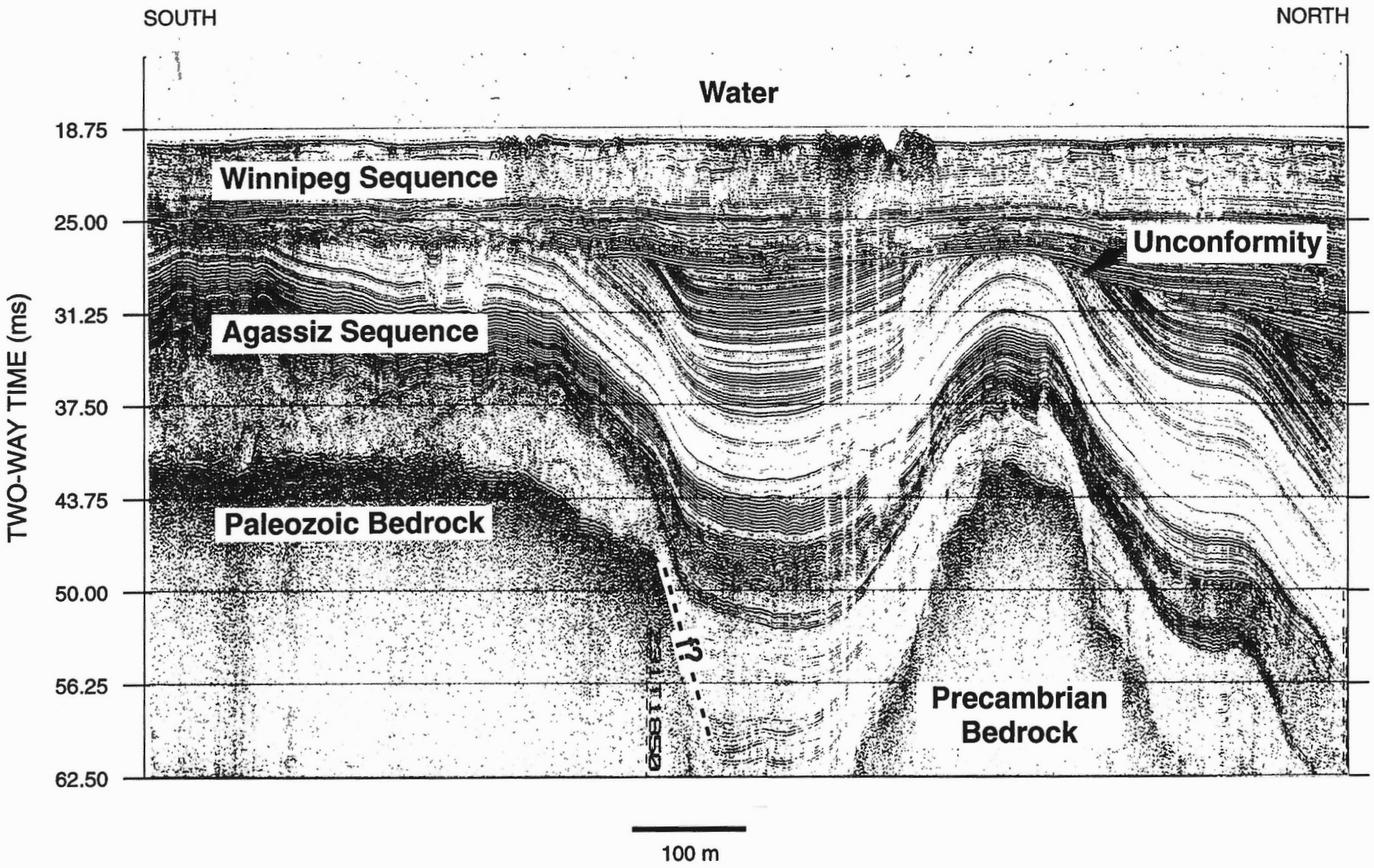

Figure 10. Seismic reflection profile of Precambrian-Paleozoic boundary, line NB11, North Basin (f=fault).

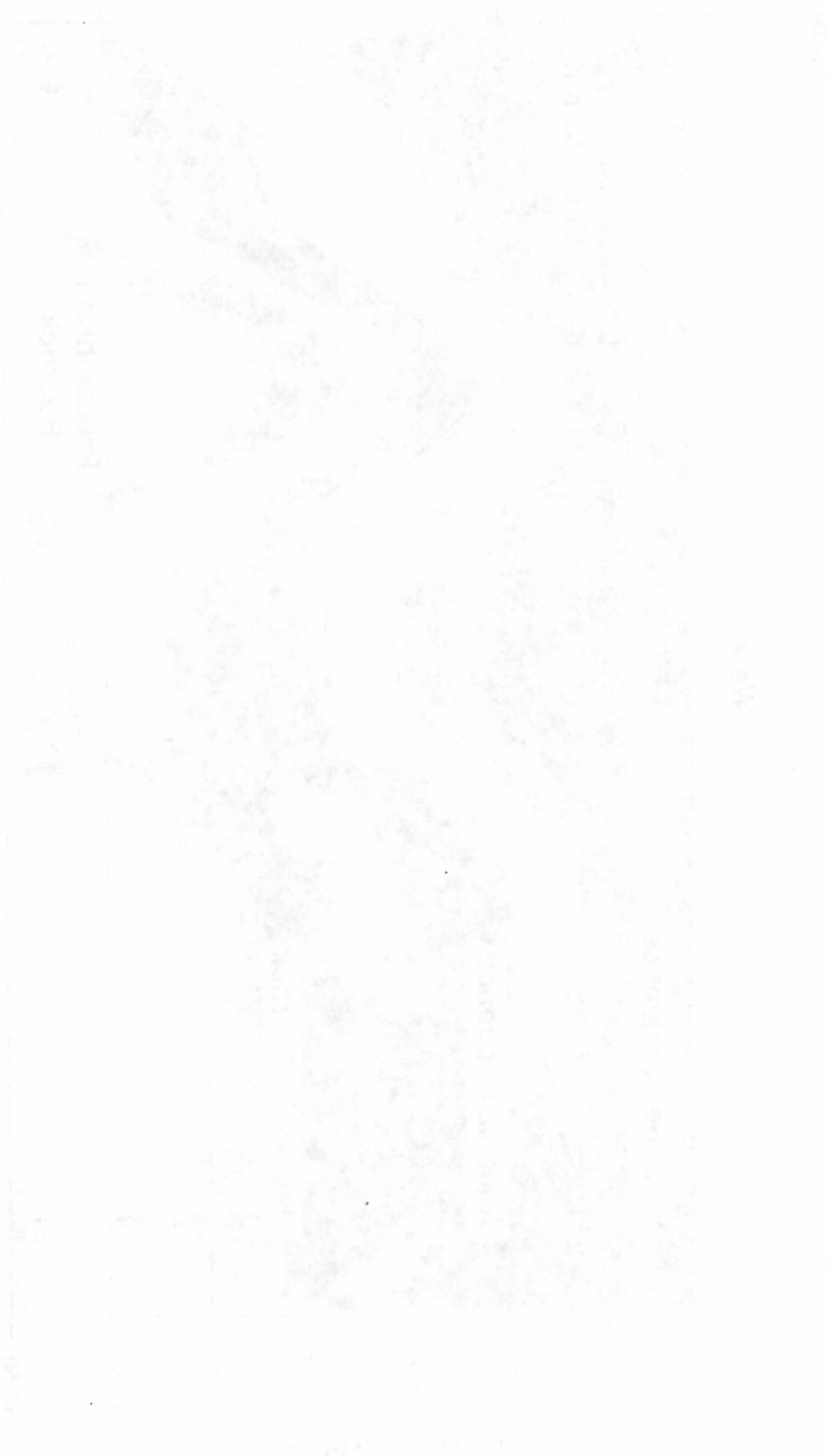

3.4 Quaternary geology of the Lake Winnipeg area

Erik Nielsen

Manitoba Energy and Mines
1395 Ellice Avenue, Winnipeg, Manitoba R3G 3P2

L. Harvey Thorleifson

Geological Survey of Canada
601 Booth Street, Ottawa, Ontario K1A 0E8

INTRODUCTION

Lake Winnipeg lies at the boundary between thin, sandy glacial sediments of the Canadian Shield to the east and thicker, silty drift which overlies lower Paleozoic sedimentary rocks on the western shore. Quaternary sediments make up several major features of the shoreline, as well as blanketing much of the lake bottom with glacial, glaciolacustrine, and lacustrine sediments. An understanding of onshore Quaternary geology therefore will significantly aid interpretation of observations offshore.

The eastern shore of Lake Winnipeg is underlain by Precambrian rocks of Archean age. These rocks comprise gneisses and granitoid rocks interrupted in the Manigotagan area by metavolcanic and associated metasedimentary rocks of the Rice Lake greenstone belt (Manitoba Mineral Resources Division, 1979; Weber, this volume). Sandstone and dolomite of Ordovician and lower Silurian ages occur on most of the islands and along the western shore of the lake (Bezys, this volume). The 400-km-long axis of Lake Winnipeg follows the contact between the Precambrian and Paleozoic rocks.

The area was glaciated by generally southwestward ice flow of the continental ice sheet. Carbonate rocks of the western shore have generated areas of thick drift which include large glacial geomorphological features. Shield rocks to the east have generated little sediment, so bedrock outcrop is extensive. The shield to the north of the lake is more extensively drift covered due to the presence of sediment supplied to the ice sheet by Paleozoic rocks and reworked Quaternary sediments derived from the Hudson Bay Lowland. Fine grained sediments deposited in Lake Agassiz are extensive to the south and north of the lake. Pioneering studies of Lake Winnipeg geology were carried out a century ago by Dowling (1900) and by Tyrrell and Dowling (1900). These authors mapped striation patterns and described geomorphology, glacial history and modern Lake Winnipeg beaches. Quaternary geological investigations which have been completed more recently in the region have focussed on areas inland (Fig. 1). It is the purpose of this paper to synthesize the results of these studies and to correlate the onshore Quaternary geology with the results of the 1994 Lake Winnipeg geophysical survey.

THICKNESS OF SEDIMENTS

Sediment thicknesses are not well known to the east and northwest of Lake Winnipeg due to low relief and scarcity of drill hole information. Widespread bedrock outcrop on the east side of the lake suggests that the overburden is generally less than 10 metres deep (Fig. 2). Sediments are more continuous and hence thicker over the Paleozoic rocks to the west, but thicknesses in excess of 20 metres would be considered rare. The thickest sediment is recorded along the western shore of the South Basin, where rock is intersected at a depth of 40 to 50 m, but this is not typical of the Interlake region (Betcher, 1986). Sediment in major moraines southeast and northwest of Lake Winnipeg is in places more than 60 m thick (Lebedin, 1978; Klassen 1967). South of Lake Winnipeg, in the Red River valley, the drift is in places over 40 m thick but the average is about 20 m (Render, 1970). North of Lake Winnipeg, Bell (1978) reported overburden thickness comparable to that of the Red River valley.

GLACIAL SEDIMENTS OF THE SHIELD

Till outcrops sporadically on the east side of Lake Winnipeg, but where it occurs it is a thin, loose, sandy diamicton derived almost exclusively by the erosion of local Precambrian rocks. Carbonate erratics from the Hudson Bay Lowland are common in the till near Jenpeg, 100 km north of the northern shore of Lake Winnipeg, but have not been observed farther south. Carbonate erratics occur in the till south of Black River, on the east side of South Basin, and are attributed to southeasterly glacial transport from the Manitoba Interlake and Lake Winnipeg basin (Tyrrell and Dowling, 1900). Observations by the first author in the Manigotagan, Island Lake and Norway House areas indicate that till forms a single, thin and discontinuous veneer, draped over the bedrock. Thicker accumulations occur in depressions or as lee-side till, down-ice from bedrock obstructions. The till surface, on topographically high areas, is commonly capped by a boulder lag formed by wave action during the regression of Lake Agassiz (Henderson, 1994). Till in low lying areas is generally capped by fine textured glaciolacustrine sediments and recent organic deposits.

Tyrrell (1890) indicated that the shore from Limestone Bay to Mossy Point, at the north end of Lake Winnipeg, consists of a narrow beach backed by an almost vertical cliff, in places 12 m high, composed of 'stiff blue alluvial clay' overlain by peat. The clay was reported to extend along the east side of Lake Winnipeg. Dowling (1900) recorded discontinuous stratified silt and clay in this region, extending inland to an elevation of approximately 45 m above the level of Lake Winnipeg. Varved silt and clay, typical of the Lake

Agassiz sediments on the east side of Lake Winnipeg, have been observed by the first author to be overlain by Holocene fluvial overbank sediments near the mouth of the Winnipeg River (Fig. 3).

GLACIAL SEDIMENTS OF THE INTERLAKE

In marked contrast to the eastern side of Lake Winnipeg, compact, fissile, silty till overlying carbonate bedrock to the west of the lake forms an almost continuous sheet. Drumlinoid ridges, clustered in fields and variously trending south-southwest, south and southeast are a common feature of the Interlake, south of The Pas Moraine (Fig. 4). These streamlined forms are parallel in the north but fan out towards the south and southeast. The drumlinoid ridges are up to 10 km long and 400 m wide but vary considerably throughout the region (Fig. 5). They are generally only 1 to 2 m high, but reach heights in excess of 10 m in, for example, the Fisher Branch area (Fig. 1; Groom, 1985). Nielsen (1989) postulated that the drumlinoid ridges in the southern Interlake were due to late glacial surging of the ice front into Lake Agassiz. North of The Pas Moraine, till is scarce and the area is dominated by nearly flat-lying dolomitic bedrock (Klassen, 1967).

Till of the Interlake is silty, very calcareous, and contains an abundant gravel fraction consisting mostly of carbonate pebbles. Precambrian rock types in the 4-16 mm size fraction comprise 16-18% of the till in the southern Interlake (Nielsen, 1989) but only 11% in the Fisher Branch area (Groom, 1985). In the area south of The Narrows, 5-10 km down ice from the shield, Groom found these rocks constitute 37% of the pebble fraction.

In the Fisher Branch area, glaciolacustrine sediments composed of silt and clay rhythmites range from 1 to 10 m in thickness. The thicker deposits occur at lower elevations closer to Lake Winnipeg (Groom, 1985). Klassen (1967) reported 6 m of massive clay near Grand Rapids and along creeks south of The Pas Moraine. In the Red River basin south of Lake Winnipeg, glaciolacustrine sediments reach thicknesses of 20 m (Render, 1970).

Clay thicknesses reported in the Grass River Basin, north of Lake Winnipeg, average 18 m and reach maximum values up to 45 m (Bell, 1978). Seismic profiles from the North Basin of Lake Winnipeg (Todd and Lewis, this volume) indicate that glaciolacustrine sediments reach thicknesses of 100 m. Hence the low lying area along the Paleozoic-Precambrian contact beneath Lake Winnipeg, and the low region along the Nelson River extending north from Lake Winnipeg, acted as a major axis of fine textured glaciolacustrine sediment accumulation.

Most of the southern Interlake is covered with 0.5 to 3 m of drift-ice turbate formed by the action of wind-driven icebergs and shore ice which impinged on till and glaciolacustrine sediments at the bottom of Lake Agassiz (Nielsen, 1989). The resulting sediment consists of complex mixtures of buff coloured till and olive grey glaciolacustrine silt and clay (Fig. 6). Iceberg plough marks occur extensively in the southern Interlake (Fig. 7). These features typically are about 30 m wide and from 0.5 to 6 km long with berms less than a metre high on both sides (Fig. 8). The plough marks curve and intersect, forming a network of low depressions.

Furrows formed by drifting icebergs are common in both offshore Lake Agassiz sediments and in till up to an elevation of about 300 m (Fig. 7). Their absence above this elevation presumably resulted from water being too shallow to allow bergs to enter the area. Iceberg plough marks do not occur to the east of the Mantagao Moraine, a glaciofluvial deposit extending north-south in the centre of the Interlake area (Fig. 7), possibly as a result of this area being glaciated while scouring was occurring in the lake adjacent to the moraine. By the time the area to the east of the moraine was deglaciated, the level of Lake Agassiz may have dropped so bergs could not enter, or the icebergs had decreased in size and lacked a draft sufficient to scour the lake bottom in this newly deglaciated area.

Furrows made up of numerous short, straight, parallel depressions are interpreted as having been formed by multiple-keeled shore ice. They have been observed by the first author at a few west-sloping areas in the southern Interlake, between elevations of approximately 260 and 270 m.

TILL STRATIGRAPHY

Klassen (1967) described two tills units in the Grand Rapids area. The upper unit, a 0.6 m thick pale brown till, was reported to be separated from the underlying 5 m thick light grey till by a striated boulder pavement. The striae on the boulder pavement suggest the upper till was deposited by southerly flowing ice.

Multiple tills were described in the southern Interlake, between Lake Winnipeg and Lake Manitoba, by Nielsen (1989). The lowest of these tills, the Inwood till, is over-consolidated, pinkish grey in colour, and associated with striae on the underlying bedrock trending 170°. Drumlinoid ridges in the area consist of >0.5 m of relatively soft diamicton in places mixed with glaciolacustrine clay. This diamicton, termed Komarno till, resembles the underlying Inwood till in texture but may be differentiated from it by the presence of olive grey glaciolacustrine clay inclusions, a slightly darker colour and, more importantly, a lower consolidation. The presence of horizontal fissility, a discontinuous boulder pavement at the contact with the underlying Inwood till, the fluted surface, the southeasterly fabric and associated striae trending southeast (105-140°) indicate the Komarno till was deposited subglacially. The clay inclusions are widespread, indicating Komarno till formed as result of a glacier advance into Lake Agassiz. Iceberg turbate is differentiated from

Komarno till by the presence of iceberg plough marks.

Sections at Hillside Beach on the northwestern side of the Belair Moraine expose two tills (Nielsen and Matile, 1982). The 2 m thick lower till is light grey in colour, contains 31% Precambrian clasts in the fine pebble fraction and has a southwesterly pebble fabric. It is overlain by 3 m of yellowish grey till with 38% Precambrian clasts and a south-southwesterly pebble fabric. The contact between the two tills is marked by a boulder pavement and thin discontinuous sand beds. The section is capped by a thin sand and gravel lag.

MORAINES

The Belair, Mantagao, The Pas and Hargrave Moraines (Fig. 9) have been identified by previous onshore surveys in the Lake Winnipeg region (Matile and Groom, 1987; Groom, 1985; Klassen, 1967; Tarnocai, 1970). The Pearson Reef and George Island Moraines were identified during the 1994 geophysical survey of Lake Winnipeg (Todd and Lewis, this volume). A northwest trending ridge, southeast of Eagle Island at the northern end of the lake may also be a moraine, or a till-mantled bedrock ridge.

The Belair and Mantagao Moraines are known to be composed of interbedded glaciofluvial sand and gravel. The George Island Moraine, where it outcrops as a series of islands, also consists of sand and gravel (Dowling, 1900). The Pas moraine is composed of till. The Hargrave moraine is a complex of clay with minor till (Tarnocai, 1970; unpublished Manitoba Hydro reports). Little can be determined from seismic profiles regarding the internal composition of the Pearson Reef Moraine.

Matile and Groom (1987) described the south-trending, 70 km long Belair Moraine, as a series of off-lapping subaqueous outwash fans, in places more than 60 m thick. The moraine formed at the confluence of two converging ice lobes; one from the Interlake flowing towards the southeast and the other from northwestern Ontario flowing towards the southwest. Paleocurrent directions in the fans are southerly, parallel to the long axis of the ridge. Stratigraphy and evidence for glacial overriding indicates a complex late glacial history for the formation of the moraine (Fig. 10; Lebedin, 1978).

The Pearson Reef Moraine likely correlates to the southern limit of outcropping till in the southern Interlake, as well as to a buried moraine located between Portage la Prairie and Lake Manitoba (Fenton and Anderson, 1971). This margin may be the limit of the ice flow responsible for the fluted terrain of the Interlake.

The Mantagao Moraine extends discontinuously over a 95 km distance south and southeast from Sturgeon Bay, on Lake Winnipeg, to Fisher Branch. This glaciofluvial deposit is arcuate in plan, averages 12 m in height and is composed of sand and gravel in the north, grading to sand in the south (Groom, 1985) . Paleocurrent directions are parallel to the long axis of the ridge, indicating an interlobate origin. This conclusion is supported by striations converging on the moraine from both sides. The general ice flow during the formation of the moraine was towards the southeast.

The Pas Moraine, of which Long Point is the eastern extension, is a high ridge composed of up to 30 m of till flanked by Lake Agassiz beaches. The moraine is arcuate in plan and asymmetrical in profile, with the crest near the southern edge. Seismic profiles from 15 km east of Long Point indicate that the moraine extends at least this far into Lake Winnipeg (Todd and Lewis, this volume). The Pas Moraine was formed during a major stillstand or readvance of ice flowing towards the southwest. Klassen (1967) interpreted the flutes on the northern slope of the moraine as evidence of glacial overriding, although deposition of the proximal slope in contact with flowing ice may have formed these features.

The George Island Moraine (Todd and Lewis, this volume) extends above lake level to form a chain of islands more than 30 km long in the North Basin southeast of Long Point. These islands include Little Sandy, Big Sandy, Cannibal, Little George and George Islands. George Island, the largest of the chain, rises more than 20 m above the lake and is composed of cross-bedded glaciofluvial sand and gravel with paleocurrent directions towards the southwest. Dowling (1900) noted that the boulders on the southern shore of the island (Fig. 11), many of which are in excess of one metre in diameter, are composed exclusively of 'Archaean gneiss, schist and granite'. Sand dunes up to 15 m high are found at the western end of the island. Seismic profiling across the ridge (Fig. 12) indicates it is asymmetrical in profile, the crest being near the edge of a south-facing escarpment. Between Cannibal Island and Little George Island, the moraine rises approximately 15 m above the underlying Precambrian bedrock surface. The moraine likely formed during a stillstand in the general recession of ice flowing towards the southwest, and correlation to The Pas Moraine seems likely.

The land separating Lake Winnipeg from Playgreen Lake, and discontinuous, poorly-defined extensions to the west and east, was named the Hargrave Moraine by Tarnocai (1970; Figure 9). This arcuate, low ridge is 140 km long and 3 to 5 km wide. Sections along the north shore of Lake Winnipeg, between Warren Landing and Limestone Bay, expose only fine-grained sediments capped by peat. Landsat images suggest the moraine continues east from Montreal Point, on the east side of Lake Winnipeg, towards the Hudwin Moraine near the Ontario border (Klassen, 1983). Excavations across the moraine at Two Mile Channel, 14 km west of Warren Landing, intersected 20 m of fine grained sediments over Precambrian bedrock (Manitoba Hydro, unpublished report). The upper 10 m of the moraine is above the level of Lake Winnipeg. One topographic profile indicates that this feature is asymmetrical in profile (Figure 13), the highest part of the ridge being near the southern steeper slope. To the west, this possible moraine

merges with a bedrock escarpment, northwest of Lake Winnipeg. As a whole, the structure and texture of this feature do not conclusively indicate that it is, indeed, a moraine. More convincing is the fact that a radiating array of eskers terminates at this position. If it is a moraine, the texture of the material could conceivably have resulted from an ice advance into Lake Agassiz which overrode and moulded silt and clay. Fine grained sediments winnowed from the glaciofluvial deposits which terminate at this feature presumably contributed to the filling of the North Basin by thick Lake Agassiz silt and clay deposits.

ICE FLOW HISTORY

The Lake Winnipeg basin owes its origin to repeated glaciation and the exhumation of relatively soft lower Paleozoic bedrock along the shield margin. Stratigraphic evidence for all but the last glacial episode in the area is, however, absent.

Sparse data from the east side of the lake indicate ice flow to the southwest. Tyrrell and Dowling (1900), as well as Henderson (1994), also recorded younger striations trending more southerly.

In the Interlake, ice flow recorded by striations and the orientation of drumlinoid ridges indicates a more complex sequence. Older striations indicate southwesterly and southerly flow, but the final, major flow to the southeast, along the axis of the valley, is the most pervasive event. Southeasterly flow apparently converged with southwesterly ice flow from the shield and along the Belair Moraine and further north in the Black Island - Manigotogan area (Henderson, 1994). The Mantagao Moraine marks a later zone of convergence, which probably formed as the ice front was at the Pearson Reef Moraine.

Topography influenced southeasterly ice flow in the Interlake. South of The Pas Moraine, south-southeasterly to south-southwesterly trending striations and drumlinoid ridges (Klassen, 1967) form a radiating pattern in part controlled by the topography. At the same time, ice in the central Interlake was diverted around the almost 100 m high topographic rise north of Lake St. Martin.

Striations which predate the final southeast Interlake ice flow and preceding shield-derived southwest flow also are present. In the Manigotagan area and on Black Island, older striations trend south-southwest, southeast and south (Henderson, 1994). Striations trending southeast and predating southwest striations were mapped at Gypsumville by Wardlaw et al. (1969) and in the northern Interlake by Klassen (1969).

LAKE AGASSIZ SHORELINES

Lake Agassiz shorelines in the region were first examined by Tyrrell (1891), who observed shorelines between Lake Winnipegosis and Cedar Lake, at 855 and 891' (261 and 272 m), and at Grand Rapids, at elevations of 790, 800, 805, and 850' (241, 244, 245, and 259 m).

Upham (1895; p. 472-473), who did not conduct field work north of Riding Mountain, correlated the three lower shorelines at Grand Rapids to shorelines near Winnipeg. Upham indicated his belief that the late shorelines of Lake Agassiz are nearly horizontal, that no tilting has occurred in post-Lake Agassiz time, and that Lake Winnipeg has receded 20' (6 m) due to outlet erosion.

Tyrrell (1917) observed several shorelines along the railway at, and northeast from, The Pas. Two beaches near The Pas were reported to have elevations of 880 and 924' (268 and 282 m). At a site described as mile 31 of the railway, a gravel ridge at 904' (276 m) was observed. A strong beach with an elevation of 848' (258 m) was reported for mile 109, at the railway siding now known as Ponton. An engineer reported to Tyrrell that a gravel ridge at 805' (245 m) occurred near the railway at mile 127.

Johnston (1919) examined the same railway transect in more detail. The beach at The Pas was reported to be continuous for nearly 15 miles (24 km) from Westray, south of The Pas, to within 3 miles of The Pas. Elevations reported for this beach were 898 and 906' (274 and 276 m). The elevation of the shoreline near Ponton at mile 109, which had been observed by Tyrrell, was reported to be 845' (258 m), and another shoreline at 828' (252 m) was recognized at Mile 110. No additional shorelines were seen to the northeast.

Johnston (1946) plotted the first shoreline diagram for Lake Agassiz. To the named sequence identified by Upham (1895), Johnston added The Pas, Lower Pas, Gimli, and Grand Rapids levels. Shorelines on the portage between Reed and File Lakes at 955, 973, and 986' (291, 297, and 300 m) were correlated to The Pas and higher levels. The Gimli shoreline, mapped west of the south basin of Lake Winnipeg, was correlated to the high shoreline at Grand Rapids. A complex water plane geometry was suggested by correlation of the lower shoreline at Grand Rapids with the shorelines at Ponton.

Elson (1967) discarded Johnston's correlation of shorelines at Grand Rapids to those at Ponton, but schematically added a low, nearly horizontal level named the Pipun. Perhaps this was based on the Mile 127 shoreline occurrence reported by Tyrrell (1917), which would have been near a railway siding named Pipun.

Grice (1970) mapped earlier recognized shorelines at Grand Rapids at 250 and 262 m. Additional shorelines at 225 and 230 m were reported and correlated to the Pipun level proposed by Elson (1967). Possible abandoned courses of the Saskatchewan River between Cross Lake and Lake Winnipeg were identified. A role for regional tilting in post-Lake Agassiz time was doubted.

Ringrose (1975) traced what she referred to as the Minago beach north and south from Ponton. A radiocarbon age of 8310 ± 180 (GSC-1679) was obtained from mollusc shells in sediments of this shoreline. Ringrose proposed that the southern shore of this phase of Lake Agassiz was near the Narrows of Lake Winnipeg. Isostatic rebound was cited as the cause for the later filling of the south basin.

Bell (1978) proposed the name 'Ponton Beaches' for the Mile 109/110 shorelines. Information obtained from a highway survey by Bell implied that the upper shoreline at Ponton has an elevation of 833' (254 m), slightly lower than earlier reports. Bell concluded that the mechanisms responsible for the diversion of the Saskatchewan River were the breaching of Lake Agassiz beaches near Grand Rapids as well as isostatic uplift, with a dominant or equal role for the former.

Klassen (1983) reported shorelines between 266 and 274 m, 50 km north of Grand Rapids. A level lower than Ponton, the Fidler, was indicated on the basis of shorelines at 250 to 265 m.

Matile and Groom (1987) recognized the Burnside, Stonewall, The Pas and the Gimli beaches around the Belair Moraine and Groom (1985) recognized the Stonewall, The Pas, Gimli and the Grand Rapids beaches in the Fisher Branch area.

The observation that the Minago River occupies a channel formerly associated with a much larger river was first made by Tyrrell (1902), Dowling (1903), and Klassen (1983). More detailed examination of this feature, which supports the suggestion that this channel is the former course of the Saskatchewan River, has been conducted by McMartin (this volume).

In summary, early exploration by Tyrrell in the Lake Winnipeg area included recognition of shorelines later named The Pas, Gimli, Grand Rapids, and Ponton levels of late Lake Agassiz, and the promotion by Warren Upham of the concept that the Lake Winnipeg region has not undergone differential uplift in post-Lake Agassiz time. Johnston vastly improved the resolution with which the levels could be traced, although his correlation of the type Grand Rapids shoreline to the type Ponton was a gross error. Very significantly, Johnston's shoreline diagram showed a substantial gradient for The Pas, Gimli, and Grand Rapids shorelines, thus refuting Upham's claim of a lack of post-Lake Agassiz tilting. The implication that Lake Winnipeg has been tilted in post-Lake Agassiz time was not mentioned. Elson corrected Johnston's error with respect to correlation from Grand Rapids to Ponton, but his addition of a near-horizontal Pipun level was an unexplained enigma which returned to Upham's model for a lack of post-Lake Agassiz tilting. In contrast with the bewildered treatment of the Ponton by Johnston and Elson, later mapping of this shoreline, by the apparently independent efforts of Ringrose and Bell, with an extra point added by Grice, better established the existence of this level. Recent mapping by McMartin has greatly improved the resolution with which this and other shorelines have been mapped. Ringrose was first to propose transgression of Lake Winnipeg in published literature. Klassen added the Fidler level, documented at two sites, as the final, very late, very low recorded level of Lake Agassiz. The consensus of opinions offered by Ringrose, Bell, and Klassen, was that differential uplift caused the diversion of the Saskatchewan River.

ACKNOWLEDGMENTS

Isabelle McMartin of the Geological Survey of Canada supplied unpublished striation directions from the Grand Rapids area. Constructive reviews of the manuscript by Glenn Conley and Gaywood Matile of Manitoba Energy and Mines and by Isabelle McMartin of the Geological Survey of Canada are acknowledged with appreciation.

REFERENCES

Antevs, E.
1931. Late-glacial correlations and ice recession in Manitoba; Geological Survey of Canada, Memoir 168, 76 p.

Bell, C.K.
1978. Geology, Wekusko Lake map area; Geological Survey of Canada, Memoir 384, 84 p.

Betcher, R.N.
1986. Groundwater availability map series, Selkirk area (62I); Manitoba Natural Resources, Water Resources.

Dowling, D.B.
1900. Report on the geology of the west shore of Lake Winnipeg; Geological Survey of Canada, Annual Report, v. 11, Part F, 100 p.

1903. Report on geological explorations in Athabaska, Saskatchewan, and Keewatin districts; Geological Survey of Canada, Annual Report, v. 13, Part F, 44 p.

Elson, J.A.
1967. Geology of Glacial Lake Agassiz; in ed. W.J. Mayer-Oakes, Life, land and water, University of Manitoba Press, Winnipeg, p. 36-95.

Fenton, M.M. and Anderson, D.
1971. Pleistocene stratigraphy of the Portage la Prairie area, Manitoba; in ed. A.C. Turnock, Geoscience studies in Manitoba, Geological Association of Canada Special Paper 9, p. 271-276.

Grice, R.H.
1970. Quaternary geology of the Grand Rapids area; Canadian Journal of Earth Sciences, v. 7, p. 853-857.

Groom, H.D.
1985. Surficial geology and aggregate resources of the Fisher Branch area: Local Government District of Fisher and Rural Municipality of Bifrost; Manitoba Energy and Mines, Mineral Resources Division, Aggregate Report 84-2, 33 p.

Henderson, P.H.
1994. Surficial geology and drift composition of the Bissett - English Brook area, Rice Lake Greenstone Belt, southeastern Manitoba; Geological Survey of Canada, Open File 2910, 190 p.

Johnston, W.A.
1919. Reconnaissance soil survey of the area along Hudson Bay Railway; Geological Survey of Canada, Summary Report for 1917, Part D, p. 25-36.

1946. Glacial Lake Agassiz with special reference to the mode of deformation of the beaches; Geological Survey of Canada, Bulletin 7, 20 p.

Klassen, R.W.
1967. Surficial geology of the Waterhen-Grand Rapids area, Manitoba; Geological Survey of Canada, Paper 66-36, 6 p.

1983. Lake Agassiz and the late glacial history of northern Manitoba; in eds. J.T. Teller and L. Clayton, Glacial Lake Agassiz, Geological Association of Canada Special Paper 25, p. 97-115.

Lebedin, J.
1978. Groundwater resources of the Beausejour area; Canada Department of Regional Economic Expansion, Prairie Farm Rehabilitation Administration, Engineering Services, Regina.

Manitoba Mineral Resources Division.
1979. Geological map of Manitoba, Scale 1: 1,000,000, Map 79-2

Matile, G.L.D. and Groom, H.D.
1987. Late Wisconsinan stratigraphy and sand and gravel resources in the Rural Municipality of Lac du Bonnet and Local Government District of Alexander; Manitoba Energy and Mines, Mines Branch, Aggregate Report AR 85-2, 44 p.

Nielsen, E.
1989. Quaternary stratigraphy and overburden geochemistry in the Phanerozoic terrane of southern Manitoba; Manitoba Energy and Mines, Geological Paper GP 87-1, 78 p.

Nielsen, E. and Conley, G.
1994. Sedimentology and geomorphic evolution of the south shore of Lake Winnipeg; Manitoba Energy and Mines, Geological Report GR 94-1, 58 p.

Nielsen, E. and Matile, G.L.D.
1982. Till stratigraphy and proglacial lacustrine deposits in the Winnipeg area; Geological Association of Canada, Field Trip Guidebook, No. 1, 22 p.

Render, F.W.
1970. Geohydrology of the metropolitan Winnipeg area as related to groundwater supply construction; Canadian Geotechnical Journal, v. 7, p. 243-274.

Ringrose, S.
1975. A re-evaluation of the Lake Agassiz shoreline data from north central Manitoba; The Albertan Geographer, no. 11, p. 33-41.

Tarnocai, C.
1970. Glacial history, surface deposits, soils and vegetation of Wekusko and portions of Cross Lake, Norway House and Grand Rapids map area, Manitoba; 14th Annual Manitoba Soil Science Meeting, p. 22-25.

Tyrrell, J.B.
1890. Operations of the Geological Survey For the Year 1890; Annual Report, v. 5, p. 32A.

1891. Pleistocene of the Winnipeg basin; American Geologist. v. 8. p. 19-28.

1902. Report on explorations in the north-eastern portion of the District of Saskatchewan and the adjacent parts of the District of Keewatin; Geological Survey of Canada, Annual Report, v. 13, Part F, p. 1-48.

1917. Records of Lake Agassiz in southeastern Manitoba and adjacent parts of Ontario, Canada; Discussion; Geological Society of America Bulletin, v. 28, p. 146-148.

Tyrrell, J.B. and Dowling, D.B.
1900. Report on the east shore of Lake Winnipeg and adjacent parts of Manitoba and Keewatin; Geological Survey of Canada, Annual Report, v. 11, Part G, 98 p.

Upham, W.
1895. The Glacial Lake Agassiz; United States Geological Survey, Monograph 25, 658 p.

Wardlaw, N.C., Stauffer, M.R. and Hoque, M.
1969. Striations, giant grooves and superposed drag folds, Interlake area, Manitoba; Canadian Journal of Earth Sciences, v. 6, p. 577-593.

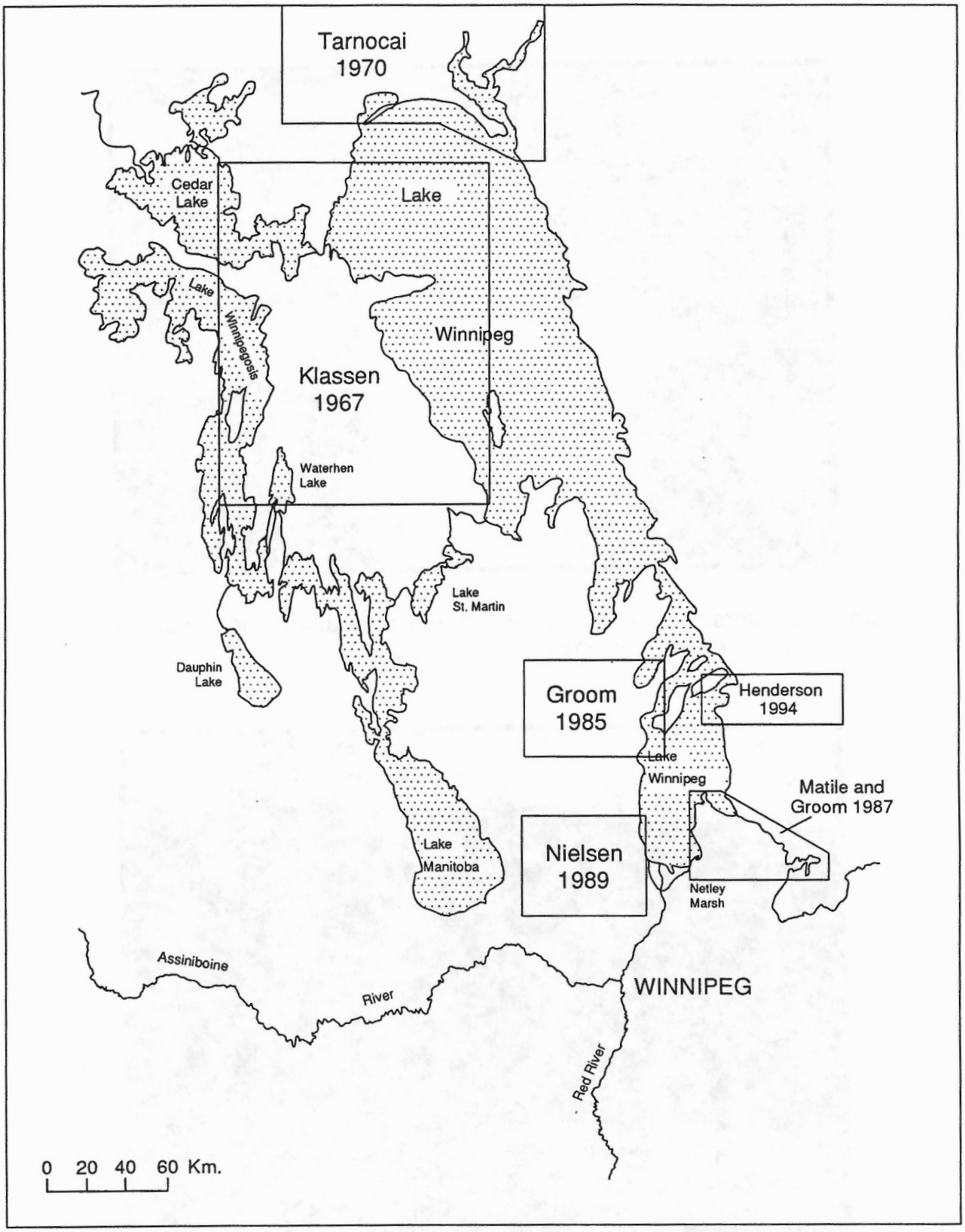

Figure 1. Location of Quaternary geological surveys in the Lake Winnipeg area.

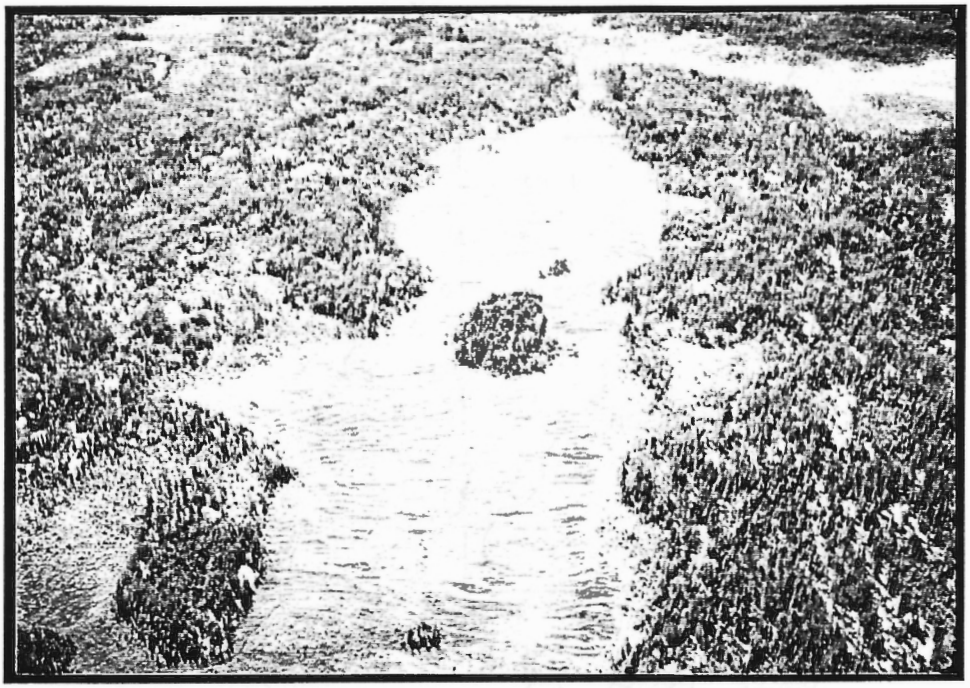

Figure 2. Scattered Precambrian bedrock outcrops and string bogs, northeast shore of Lake Winnipeg.

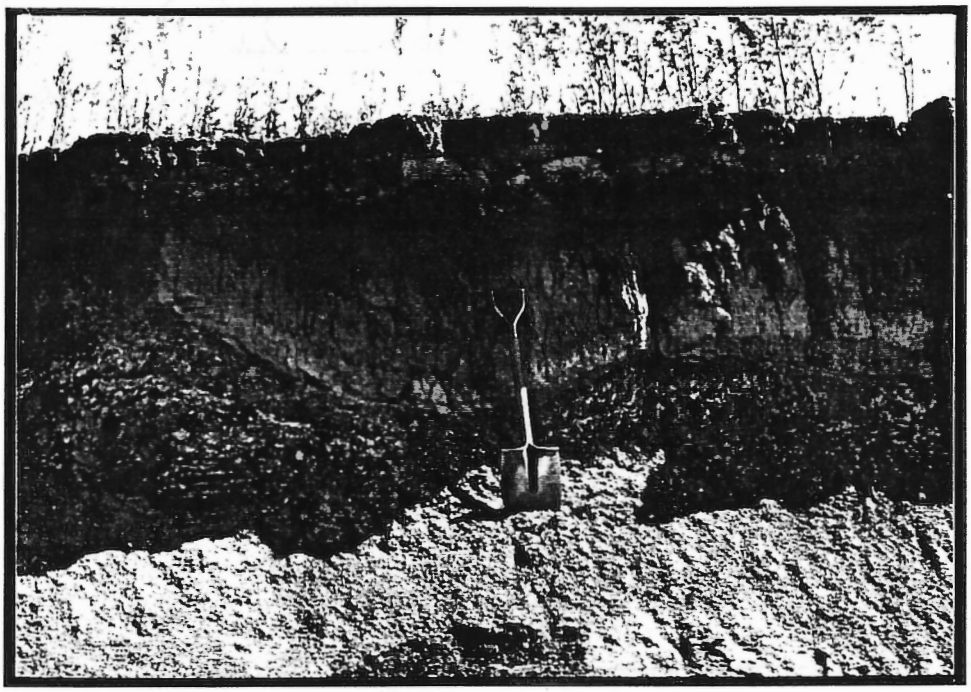

Figure 3. Varved silt and clay overlain by alluvium near the mouth of the Winnipeg River.

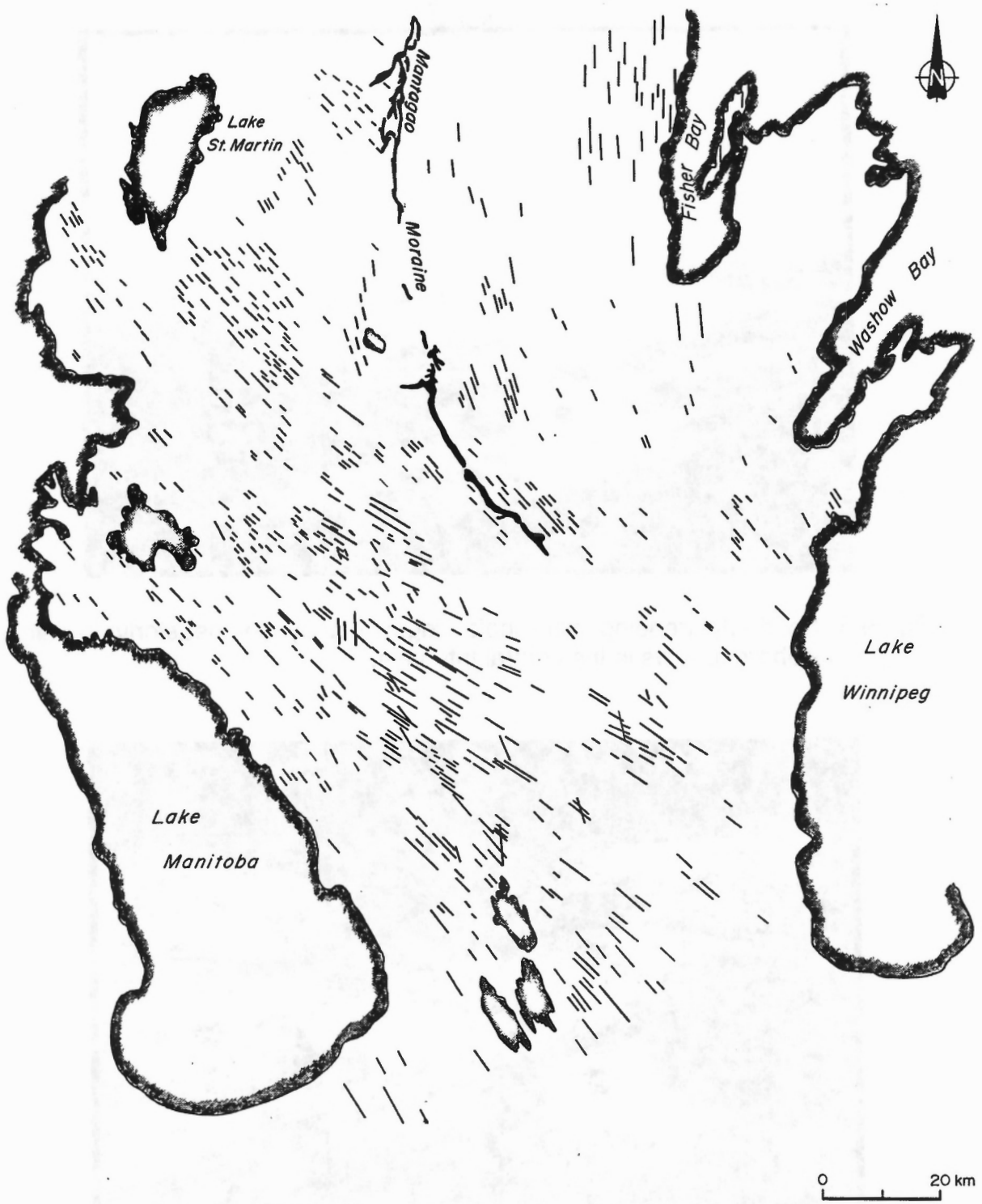

Figure 4. Distribution of drumlinoid ridges in the southern Interlake.

Figure 5. Southerly trending drumlinoid ridges cut by southeasterly trending iceberg furrows in the central Interlake.

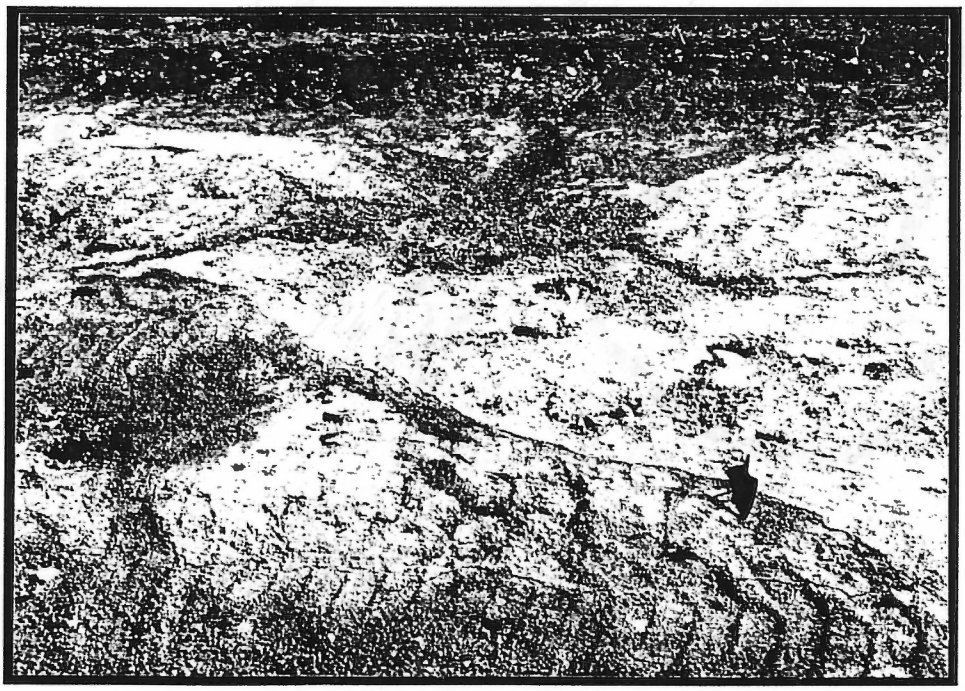

Figure 6. Iceberg turbate.

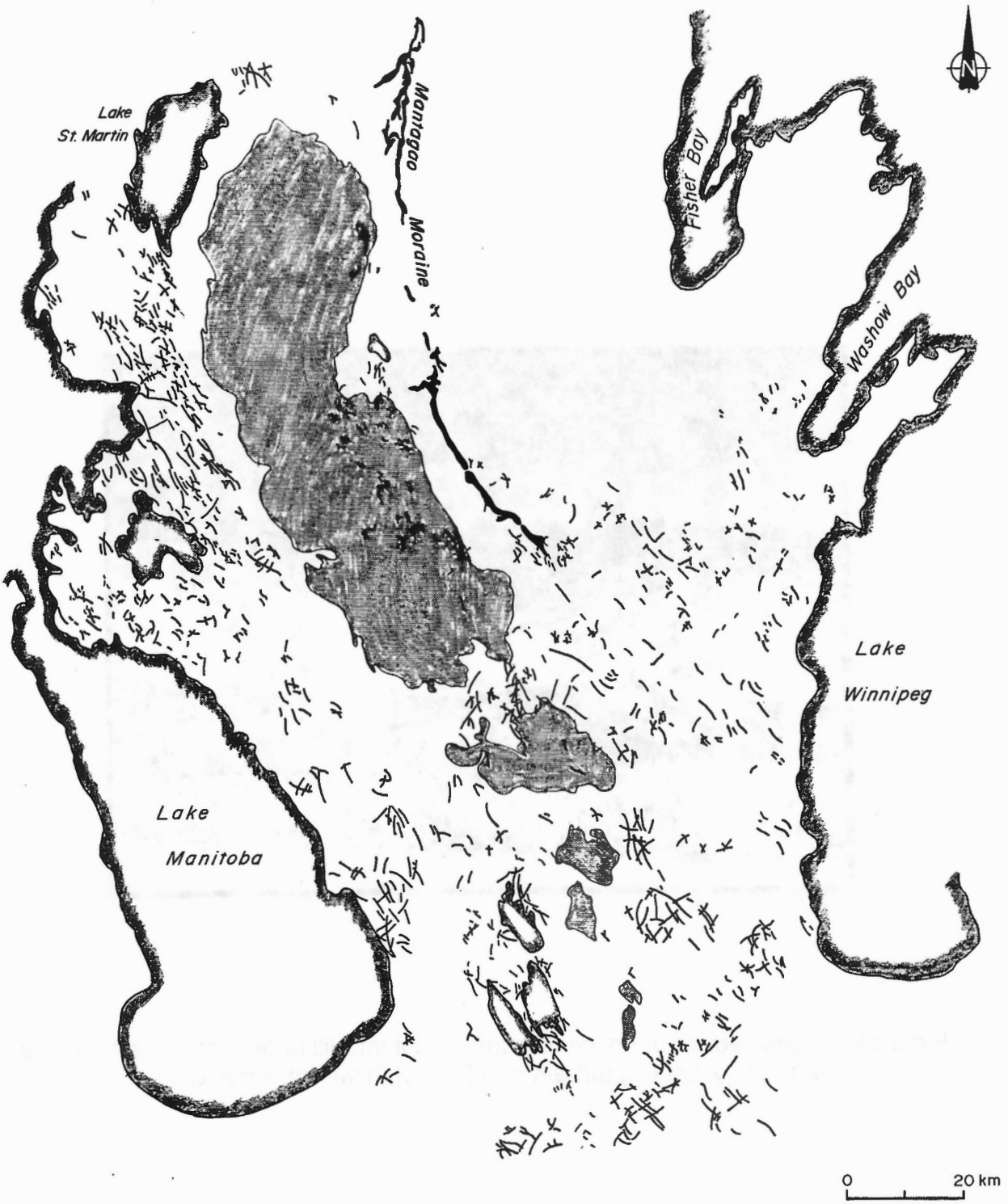

Figure 7. Distribution of iceberg furrows in the southern Interlake. Area above 300 m elevation is shaded.

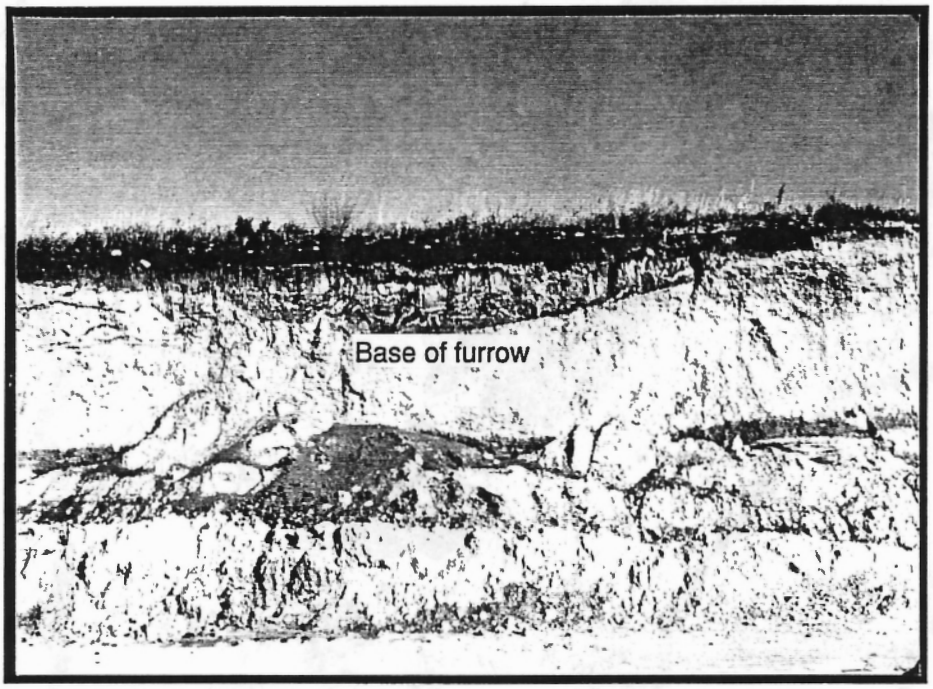

Figure 8. Cross section of an iceberg furrow cut into till near Gimli. The furrow is flanked by iceberg turbate and filled with varved silt and clay.

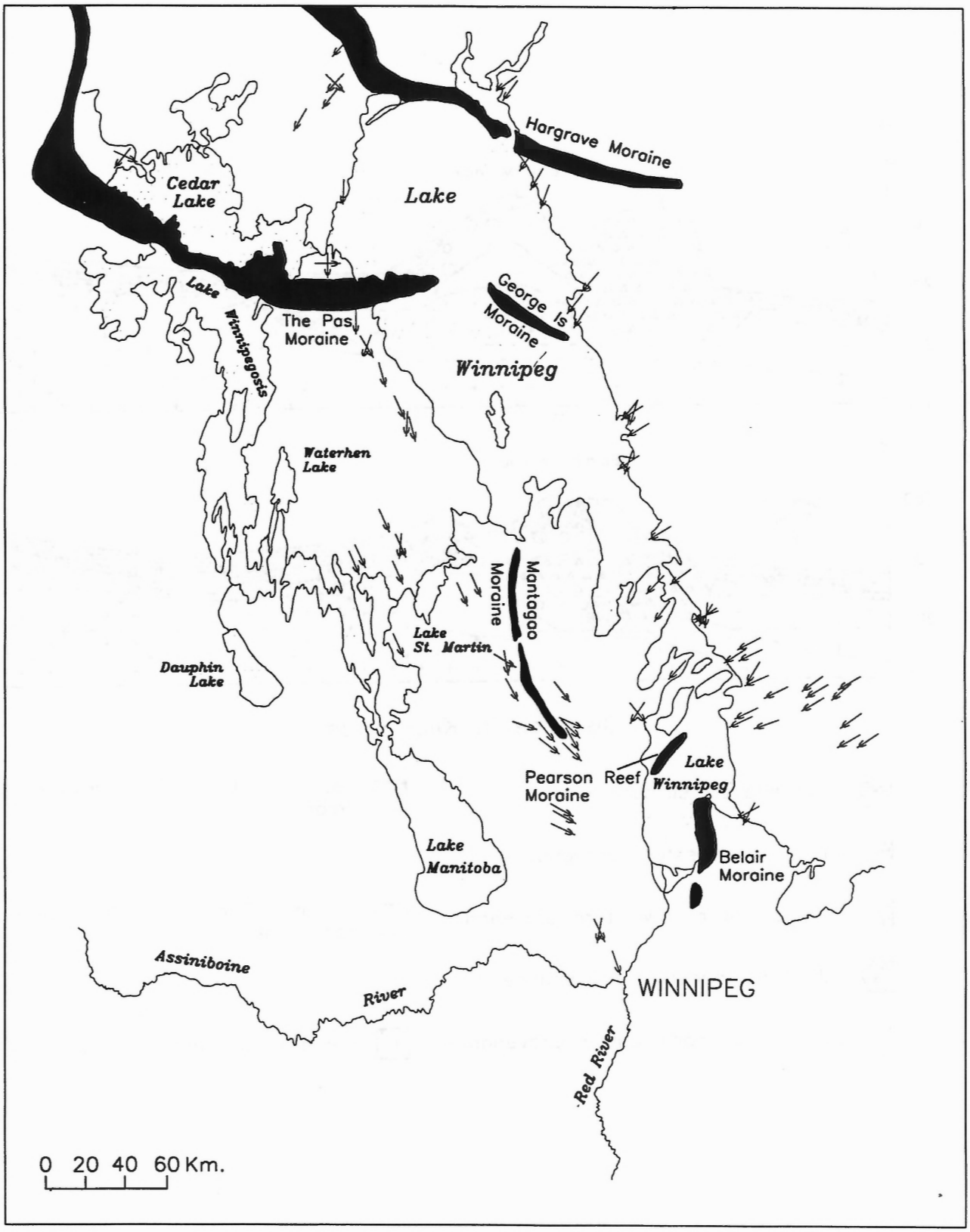

Figure 9. Location of moraines and main striation directions in the Lake Winnipeg area.

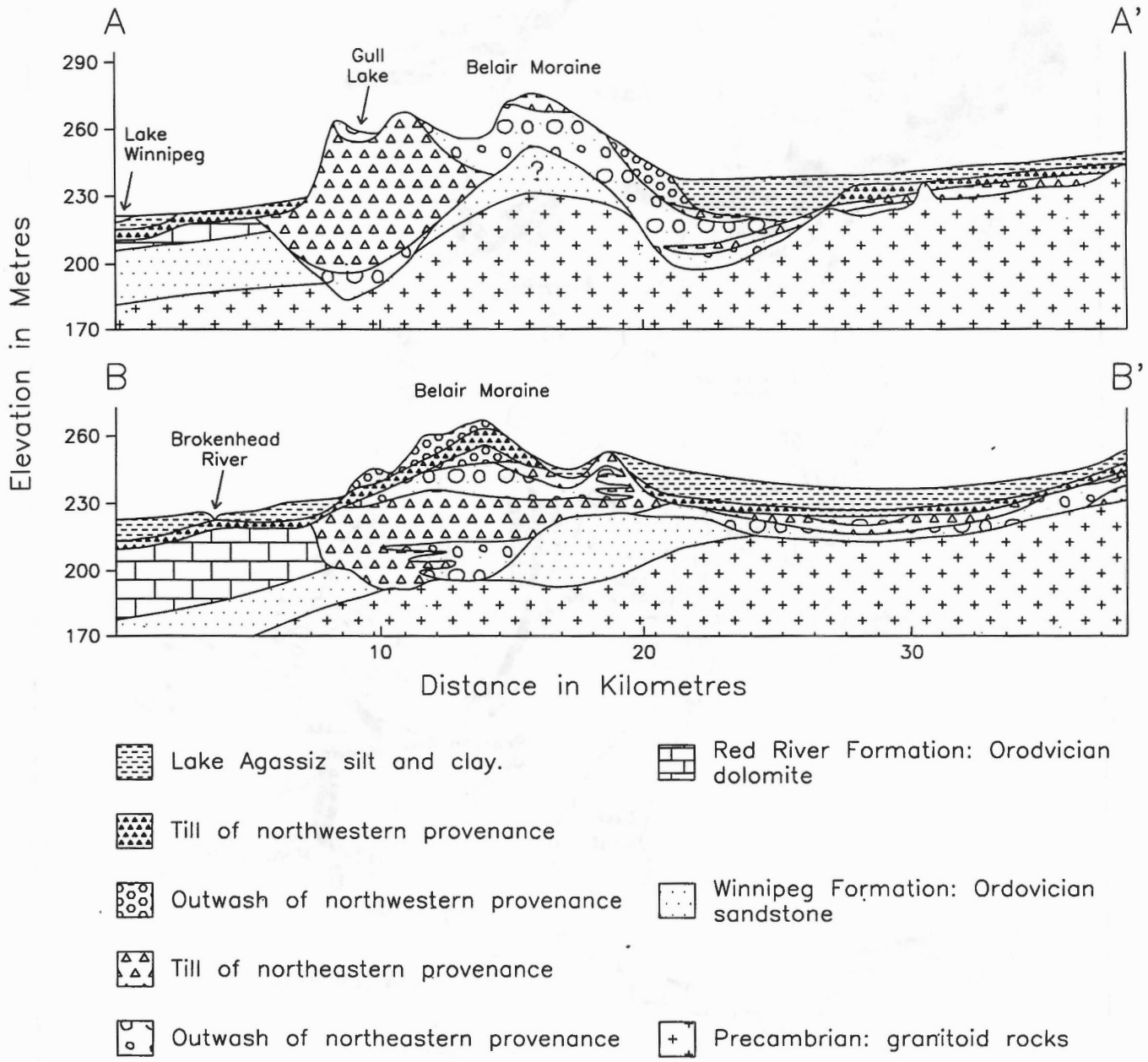

Figure 10. Cross sections of the Belair Moraine (after Lebedin, 1978). Section A-A' extends east from the south end of Lake Winnipeg. Section B-B' also extends east, just south of the lake.

Figure 11. Boulder beach and moraine on the south shore of George Island (reproduced from Dowling, 1900).

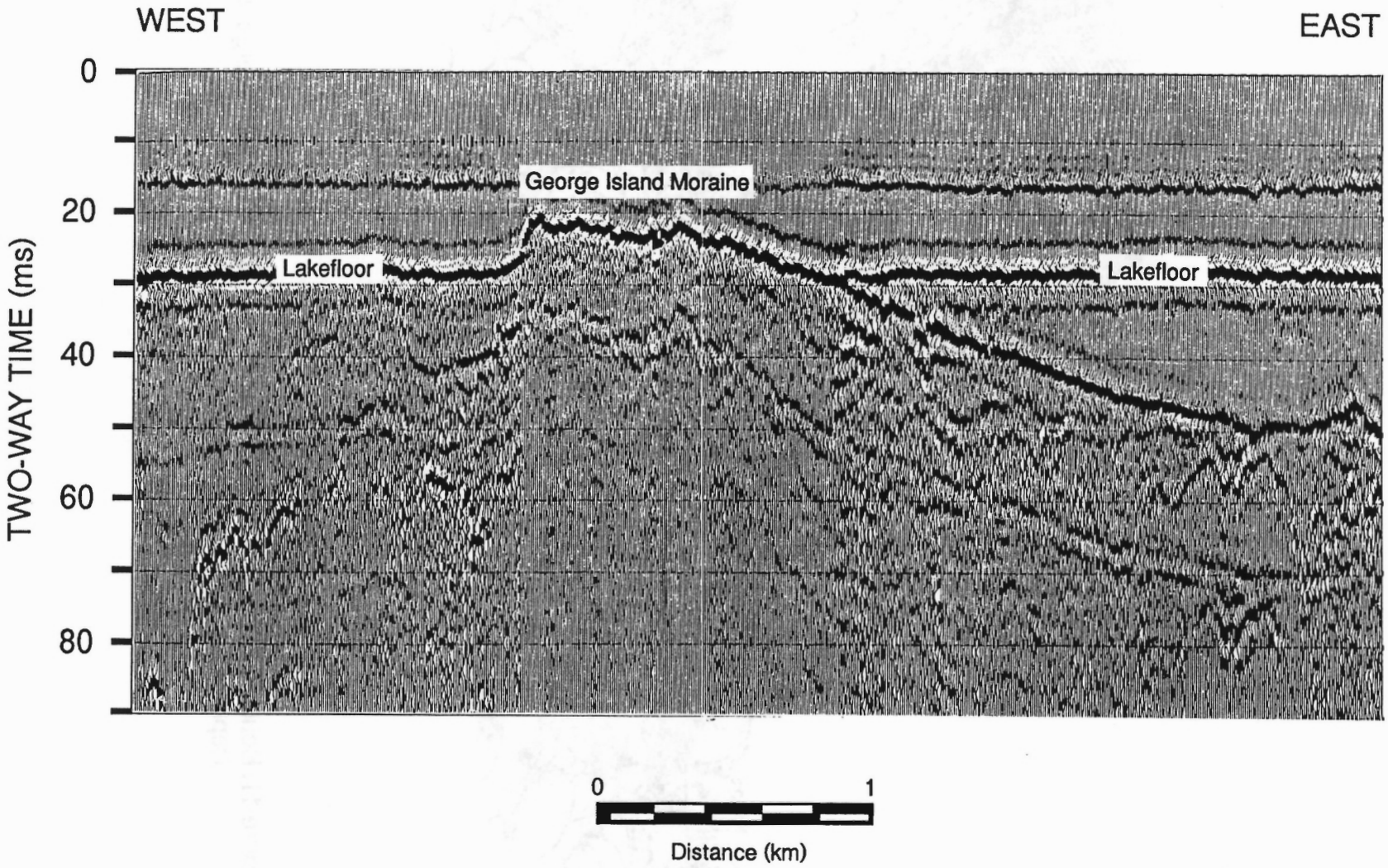

Figure 12. Seismic profile across the George Island Moraine (Todd and Lewis, this volume).

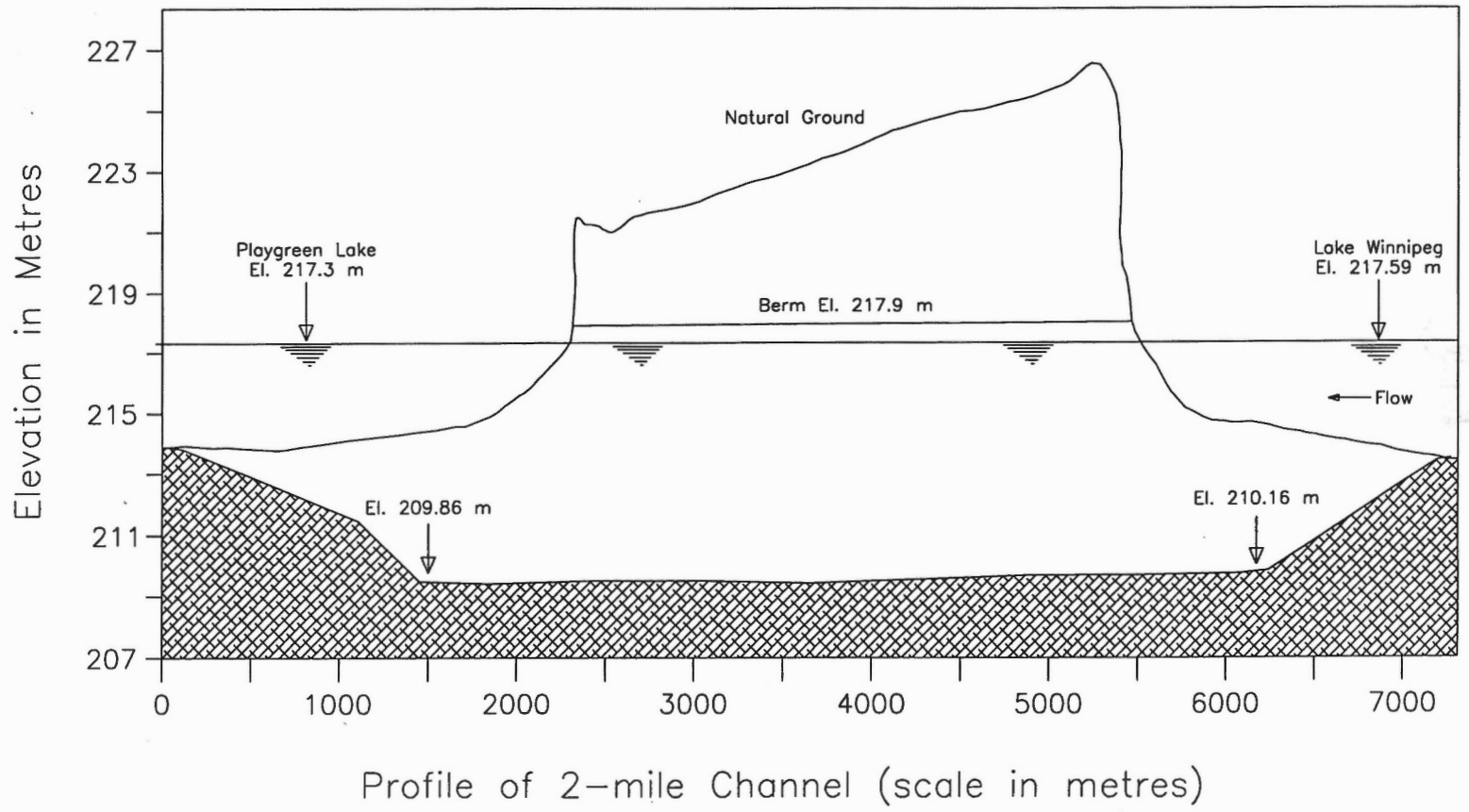

Figure 13. Topographic profile across the Hargrave Moraine, from an unpublished Manitoba Hydro report.

4. Coring results

4.1 Lithology and seismostratigraphy of long cores, and a reconstruction of Lake Winnipeg water level history

C.F. Michael Lewis

Geological Survey of Canada (Atlantic)
P.O. Box 1006, Dartmouth, Nova Scotia B2Y 4A2

Brian J. Todd

Geological Survey of Canada
601 Booth Street, Ottawa, Ontario K1A 0E8

ABSTRACT

The lithology of twelve long cores recovered from Lake Winnipeg in 1994 is presented in summary core logs with corresponding seismic reflection profiles illustrating the seismostratigraphy. A seismically prominent regional reflector, the Agassiz Unconformity, marks the boundary between the underlying Agassiz Sequence (interpreted as deposits of glacial lake Agassiz) and the overlying Winnipeg Sequence (interpreted as deposits of Lake Winnipeg). Subdivisions of the Agassiz Sequence are recognized in high-resolution seismic profiles in the South and North Basins.

A reconstruction of relative water levels in the Lake Winnipeg basin is based on an estimate of the regional post-glacial tilt rate; the relative water level changes stem from uplift of the lake outlet at a rate exceeding that of the rest of the basin. From 7.5 ka (thousands of radiocarbon years before present) to 2.5 ka, the lake level was controlled by the outlet at Warren Landing at the north end of the North Basin; about 2.5 ka, control passed northward to Whiskey Jack Narrows as Playgreen Lake upstream of this constriction rose and merged with Lake Winnipeg. A simplified profile of the Agassiz Unconformity is used to illustrate water-level change along the axis of Lake Winnipeg from 9.5 ka to 2000 years into the future. For most of the Lake Winnipeg basin the changes in lake level have been tens of metres ranging up to 50 m in the south with associated subaerial exposure. An independent southern and central Lake Winnipeg were impounded behind sills above the Warren Landing level. These lakes drained northward over the sills into northern Lake Winnipeg. At 2.5 ka northern and southern Lake Winnipeg coalesced to a common water level. Regional tilting and the concomitant submergence of the South Basin are expected to continue. The model predictions are consistent with radiocarbon-dated peat zones in the South Basin.

INTRODUCTION

Background

The Lake Winnipeg Project was designed (*i*) to elucidate the architecture of sedimentary deposits within the Lake Winnipeg basin, and (ii) to enhance our understanding of the geological history, especially the water-level history, of the lake and its predecessor, glacial Lake Agassiz. Important aspects of the latter objective include the role of glacio-isostatic tilting in controlling long term water-level change, and other influences such as paleoriver diversion into, or away from, the basin. Climate change undoubtedly plays a role in the geological evolution of Lake Winnipeg, but this topic is not addressed in this paper. This report describes and correlates the lithology of long cores and high-resolution seismostratigraphy for the sedimentary deposits within the Lake Winnipeg basin. It also develops a simplified model for reconstructing the water level history of Lake Winnipeg based on regional tilting of the Earth's crust.

Methods

As described by Todd and Lewis (this volume), a series of high-resolution seismic reflection profiles was first obtained in Lake Winnipeg (Fig. 1). Preliminary interpretation done onboard ship identified the distribution and truncation of seismic reflections and sequence boundaries within the sediments, and characterized the morphology of the underlying bedrock. Based on this interpretation, a number of geologically strategic core sites were identified to determine the relationship of seismic reflections to sediments.

Twelve long cores (up to 9 m in length) were recovered from Lake Winnipeg from the CCGS *Namao* in August, 1994 (Fig. 1). The coring procedure consisted of dropping a 9 m-long steel barrel with cellulose-acetate-butyrate plastic liner into the lakebed under a 900 kg head weight in either a piston corer or a gravity corer configuration. The inside diameters of the core liners were either 10 cm or 6 cm (Todd, this volume). The cores in their liners were segmented into 1.5 m sections, sealed and stored vertically onboard ship in a refrigerated chest at 4° C. The cores were transported by truck to the Geological Survey of Canada (GSC) core storage facility in Dartmouth, Nova Scotia.

The long cores were analyzed for their physical properties (Moran and Jarrett, this volume), described and subsampled at the GSC Marine Core Processing Laboratory in Dartmouth, Nova Scotia in October, 1994. Following whole-core X-ray imaging and non-destructive measurement of gamma ray attenuation, *P*-wave velocity and magnetic susceptibility, each core section was split longitudinally into archive and working halves. The fresh surface of the archive half was immediately

photographed and visually examined while strength testing and subsampling for further analyses were carried out on the working half. Both core halves were subsequently wrapped in impermeable plastic and returned to cold storage.

Colour measurements, in an 8-mm aperture, were obtained at 5-cm intervals with a spectral colour photometer (Moran and Jarrett, this volume). Selected values from this data set, expressed in Munsell Soil Colour terminology, are used in this report.

Sediment texture was first estimated visually, then adjusted where needed to conform with measurements of sediment grain size determined at 10-cm intervals (Last, this volume). Carbonate content was estimated from the degree of effervescence observed in sediment samples upon application of 10% HCl acid; slower-reacting carbonates, such as dolomite, may be underestimated or not detected through the use of this method.

The sediment lithology presented in the core logs of this report (Appendix 7.1) is based on the foregoing observations and a review of the core photographs and X-ray imagery. In this preliminary interpretation, the lithologic units are correlated with the seismostratigraphic sequence boundaries and facies at each coring site.

SEISMOSTRATIGRAPHY AND LONG CORES

Seismostratigraphy

In this report, the terms "reflection" and "reflector" are applied in the following way: "reflections" are acoustic phenomena recorded in seismic reflection profiles, and "reflectors" are the physical property changes (acoustic impedance contrasts) within the sediment column which cause the reflections. Reflectors are physical boundaries within the sediments, which are thought to be geologically meaningful; they are inferred or interpreted from the acoustic reflections. It is anticipated that synthetic seismograms will be completed from the measured physical properties and compared with the field results to verify the reflections interpreted in this report.

Another seismostratigraphic term commonly used in the description of reflections is "amplitude". High amplitude reflections appear as intensely dark events on seismic records; conversely, low amplitude reflections are weaker, lighter events. An absence of reflections on a seismic record is referred to as transparent.

In the following paragraphs, the description of the seismic sequences and their subdivisions are based on variations in the properties of acoustic reflections as recorded with a specific broadband boomer sound source and a IKB-Seistec™ line-in-cone receiving array, tuned to receive reflections in the 2-8 kHz frequency range (Todd, this volume). Surveys with other reflection equipment operating at different frequencies will produce records of somewhat different character. As an extreme example, the subdivisions of the Agassiz Sequence are not recognized at all in the much lower frequency (10s to 100s Hz) seismic profiles accompanying the report by Todd and Lewis (this volume).

Typical seismostratigraphy of the sediments of the Lake Winnipeg basin is shown in the several panels of Figure 2. An Acoustic Basement Sequence, interpreted as till or bedrock, is conformably overlain by the Agassiz Sequence, interpreted as deposits of glacial Lake Agassiz. The Agassiz Sequence is separated from the overlying Winnipeg Sequence, interpreted as deposits of Lake Winnipeg, by the prominent Agassiz Unconformity (AU). The basis of the interpretation of these first-order seismostratigraphic components are discussed in Todd and Lewis (this volume).

In the South Basin, the Basal Reflective Interval at the base of the Agassiz Sequence immediately overlies the Acoustic Basement Sequence (Fig. 2, left panel). This interval has high amplitude, closely-spaced, parallel, continuous, coherent reflections. In contrast, the overlying Disturbed Interval exhibits rare, disseminated, incoherent reflections such that this interval appears almost transparent. Overlying this interval is the Segmented Reflective Interval. Within this interval, medium to high amplitude, widely-spaced, parallel, coherent reflections are laterally segmented (i.e. discontinuous). Significantly, reflections can be traced laterally from segment to segment across vertical offsets as shown in Todd and Lewis (this volume). Immediately underlying the Agassiz Unconformity, and comprising the topmost interval of the Agassiz Sequence, is the Higher Reflective Interval (Fig. 2, centre bottom panel). In this interval, reflections are low to medium amplitude, closely-spaced, parallel, continuous and coherent. Above the Agassiz Unconformity, the Winnipeg Sequence is characterized near its base, in places, by low amplitude, parallel, coherent reflections; otherwise this sequence appears transparent.

The upper central panel in Figure 2 (line SB5) illustrates South Basin seismostratigraphy on the flank of Pearson Reef Moraine (see Todd and Lewis, this volume, Figs. 1, 16). At this particular site, the Higher Reflective Interval appears to be missing (eroded?), and the uppermost interval in the Agassiz Sequence is designated the Lower Clinoform Interval. The Agassiz Unconformity (AU) separates this interval from an overlying Upper Clinoform Interval in the Winnipeg Sequence. Clinoforms are sets of sub-parallel sloped reflections which at their ends, tend to curve and merge with the lower and upper boundaries of the set. They commonly represent progradational sand deposits (Todd and Lewis, this volume). Here, they are interpreted as two sets of beaches, an earlier beach below the AU and a later beach above. The earlier beach may be a shore deposit of a late phase of glacial Lake Agassiz. As will be shown later, the younger beach is probably a deposit of an

early phase of southern Lake Winnipeg. Typical Winnipeg Sequence reflections onlap the Upper Clinoform Interval.

The seismostratigraphy of the North Basin of Lake Winnipeg is illustrated in the right panel (line NB9) of Figure 2. Again, the Acoustic Basement Sequence is conformably overlain by the Agassiz Sequence, which in turn is overlain by the Winnipeg Sequence. The prominent Agassiz Unconformity separates the Agassiz Sequence from the Winnipeg Sequence. In the North Basin, the Agassiz Sequence is divided into three distinct intervals: the Lower, Middle and Upper Reflective Intervals. The Lower Reflective Interval is a band of high amplitude, parallel reflections which conformably overlies the Acoustic Basement Sequence. The Middle Reflective Interval is characterized by a package of high amplitude, parallel reflections above a transparent zone that overlies the Lower Reflective Interval. The Upper Reflective Interval also comprises a band of parallel reflections over a transparent zone. Parallel reflections within the topmost Upper Reflective Interval are mostly of high amplitude, making their truncation by the Agassiz Unconformity all the more striking.

Lithologic Units and seismic sequences

The strategy for siting long cores to determine the relationship of sediments to seismic reflections resulted in the recovery of 11 cores at targets selected from the seismic profiles. One additional core was collected without seismic control. All 11 cores with seismic control penetrated the Winnipeg Sequence. Eight of these cores penetrated to different stratigraphic levels in the underlying Agassiz Sequence, four cores each in the North and South Basins (Fig. 3).

Simplified descriptions of lithologic units in the North and South Basins, based on the summary descriptions of all the long cores (Appendix 7.1), are diagrammatically illustrated in Figure 4 with key characteristics of the seismic sequences where available. In the following paragraphs, the lithology and sediment facies and the character of the corresponding seismic sequences are described from the lakefloor downward.

Winnipeg Sequence

Throughout the lake, the uppermost metre to few metres of sediment typically comprise soft, dark olive gray, silt-clay mud (Fig. 4). This mud is reduced (i.e. low Eh or low oxidation-reduction potential) as black FeS streaks are evident in some upper sections and the mud colour becomes lighter and browner upon exposure to air. Also, a strong odour of hydrogen sulphide is emitted when dilute hydrochloric acid (HCl) is applied to the mud. Lower sections show faint, diffuse, discontinuous bands of slightly lighter gray colour. Sand grains commonly occur in the mud at its lower erosional contact with firmer silty clay; in places, silt and sand layers with shells mark the basal erosional contact. These muds correlate to the Winnipeg Sequence, and are interpreted as the cumulated deposition of Lake Winnipeg. The basal erosional contact correlates to the prominent regional reflector which truncates underlying reflections and is recognized as the Agassiz Unconformity (Todd and Lewis, this volume).

Agassiz Sequence - North Basin

In the northeastern and eastern part of the North Basin, the underlying Agassiz Sequence has been partially sampled in cores 103 to 107 inclusive (Fig. 1). These cores, described in Appendix 7.1, indicate a thick succession of firm silty clay rhythmites topped by a unit of firm banded silty clay (Fig. 4). This succession is interpreted to have originated as deposition in glacial Lake Agassiz, the rhythmites (varves) representing seasonal variation in deposition. The lowest rhythmites are couplets, <1 cm thick, of lighter and darker olive gray silty clay; some dropstones and grit are present in the basal section. These sediments correlate to the Lower Reflective Interval. A central section of the Lake Agassiz succession consists of thicker brownish gray and olive gray silty clay rhythmites (1-5 cm), commonly interbedded with highly calcareous white silt microlaminations; the rhythmites thin to <1 cm up- and down-core within the section. This central section of rhythmite deposition correlates to the Middle Reflective Interval in seismic profiles. The uppermost sediments of the Lake Agassiz succession are sampled only in core 107 and consist of gray banded silty clay. This banded clay is interpreted as deposition during late stages of Lake Agassiz when the ice margin had receded a large distance north of the site. The banded clay possibly correlates to the Upper Reflective Interval. However, this core site is 60 km south of the other cores in North Basin and it is possible that the banded silty clay is a facies equivalent of the rhythmite deposition sampled farther north, perhaps that in the Middle Reflective Interval.

A hard, gray stony diamict was sampled at one location (core 105) beneath the succession of silty clay rhythmites in the North Basin. The diamict is interpreted as a glacial deposit and it correlates to the surface of the Acoustic Basement Sequence at this site.

Agassiz Sequence - South Basin

The stratigraphy of the complex Agassiz Sequence in the South Basin (Fig. 4) was only sporadically sampled at the base of cores 119, 120, 121 and 122 (Fig. 1, Appendix 7.1). The Agassiz Unconformity at the base of the Winnipeg Sequence is seismically prominent as a high amplitude reflection and this erosion surface is confirmed in the cores. Beneath the Agassiz Unconformity, the Agassiz Sequence sediments that were penetrated by the long corer are divided into the Higher Reflective Interval, the Segmented Reflective Interval, and the Disturbed Interval. Banded silty clay and silty clay rhythmites, correlated to the Higher Reflective Interval, were sampled in Traverse Bay (Fig. 1)(core 119, Appendix 7.1). The sediment is stiff to hard and some silty clay bands were orange-brown in colour. Short sections of the Segmented Reflective Interval in cores 120 and 122 show diffusely banded silty clay and

complex brownish gray, silty clay rhythmites. These sections just below the AU are stiff and hard, and show a dry texture in Traverse. A short section of stiff gray silty clay containing silt clasts and a dolomite dropstone in core 121 is the only sample recovered from the Disturbed Interval. This facies may represent a deposit of glacial Lake Agassiz sediment and ice-rafted debris, mixed, possibly, by iceberg scour or glacial overriding, for example. The Basal Reflective Interval just above the Acoustic Basement in the South Basin possibly represents an early period of rhythmite deposition in Lake Agassiz, based on the similarity of its acoustic character to that of the reflective intervals in the North Basin where rhythmites were consistently sampled.

CHRONOLOGY

Age determinations are available for core 122 in the South Basin (Table 1, Fig. 5). A single well-preserved *Scirpus* achene was recovered from peat beneath typical Winnipeg Sequence sediments and radiocarbon-dated to 4040±70 BP by accelerator mass spectrometry (AMS)(Vance, this volume). The dated sample was from a 9 cm-long section containing two beds of fine-grained peat and clayey silt grading down to stiff clayey silt of the Agassiz Sequence (Appendix 7.1). The bedded and graded character of this section suggests that the peat particles were eroded and redeposited at this site. The well-preserved macrofossil assemblage from the section indicates the site was close to a shoreline at that time (Vance, this volume). A strong contrast in the consistency of the dated marsh sediments (firm) to that in the underlying clayey silt of glacial Lake Agassiz (stiff) suggests these sediments are of different age. The Lake Agassiz sediment may have undergone a period of subaerial exposure and drainage before the formation of a marsh on its surface. The overlying soft olive gray mud with shells at its base (Winnipeg Sequence) indicates the site was subsequently transgressed by Lake Winnipeg. This age determination is considered quite reliable on the basis of excellent preservation of the dated seed and lack of mixing with older organic material; it is interpreted to indicate the age of onset of flooding of a pre-Lake Winnipeg marshy land surface.

King and Gibson (this volume) were able to correlate the geomagnetic secular variation recorded in core 122 to calibrated sites in Minnesota and the northeastern United States. Their age picks were expressed in radiocarbon years and plotted in Figure 5. The varve (calendar) ages from the Minnesota record of King and Gibson (this volume) were converted to thousands of radiocarbon years before present for this plot using the calibrations of Stuiver and Pearson (1986) and Pearson and Stuiver (1986). The geomagnetic age information and the achene AMS date are in complete agreement, and the trend through these data constitute a preliminary age model for sediments of the Winnipeg Sequence in the South Basin. Much more chronologic control is needed to verify the geomagnetic age estimates. The uppermost part of the model in core 122 and the apparent change in accumulation rate indicated by the inflection at 230 cm are uncontrolled. The lower inflection at about 300 cm depth or 2-2.3 ka (thousands of radiocarbon years before present) age is more reliable, and may indicate a significant increase in the linear rate of sedimentation in the South Basin during the last two millennia, increasing from 80 to 250 cm/1000 years.

Radiometric and AMS dating were also attempted on a series of mud samples, but the resulting ages are rejected due to their large offsets ranging from 4 to 7 kiloyears relative to the achene date and the assumption that lake bottom sediments should have a zero age. These offsets are possibly due to the presence of pre-Quaternary carbon derived from Cretaceous and other rocks.

REGIONAL TILT AND THE WATER LEVEL HISTORY OF LAKE WINNIPEG

Introduction

As discussed by Nielsen and Thorleifson (this volume), prevailing opinions on whether the Lake Winnipeg region has been uplifted in post-Lake Agassiz time have evolved, although most early writing suggested that no tilting had occurred. Recent confirmation, however, that the Hudson Bay coast of Manitoba continues to rise, that the Great Lakes continue to be tilted, and that late Lake Agassiz shorelines northwest of Lake Winnipeg have been tilted (McMartin, this volume), indicates that the Lake Winnipeg basin almost certainly has been tilted in post-Lake Agassiz time. It therefore can be inferred that Lake Winnipeg initially formed as a much smaller water body which transgressed southward as its outlet rose more rapidly than other parts of the basin. The rebound was a progressive and long lasting regional tilt upward to the north-northeast which clearly deformed the shorelines of glacial Lake Agassiz. Isobases or lines joining points of equal uplift, indicated by the Agassiz shorelines, have been drawn at 100 km intervals by Teller and Thorleifson (1983) and are shown in Figure 1 for the Lake Winnipeg region; the direction of uptilting is perpendicular to these trends at 34°. The southward expansion of Lake Winnipeg occurs because it drains northward, and its control sill at the head of Nelson River is rising faster than all other parts of its basin. Thus a reconstruction of water levels relative to the basin should be achievable by calculating former configurations of the basin using an appropriate estimate of the regional tilt rate. Penner and Swedlo (1974) developed a set of conjectural water planes for Lake Winnipeg based on isostatic rebound at Churchill, Manitoba. We develop a new reconstruction of water level change based on recent estimates of crustal tilt within the Lake Winnipeg basin. Other components of water level change such as water supply variations or changes in outlet control will be superimposed on the regional tilt effect. Components of water level change due to climatic change would also be superimposed on the regional tilt effect but are not available for this reconstruction.

Regional Tilt

Estimates of crustal tilt rates in Manitoba affecting the Lake Winnipeg region are listed in Table 2. These estimates are based on the gradients of upwarped shorelines of glacial Lake Agassiz (Teller and Thorleifson, 1983, McMartin, this volume), the tilt of post-Lake Agassiz lake shores in the Lake Winnipegosis and Lake Dauphin basins (Fig. 1)(Nielsen, 1987; Tackman and Currey, this volume), the occurrence of *in situ* tree stumps beneath southern Lake Winnipeg (Nielsen, this volume), the historical trends in water-level gauge records in lakes Winnipeg and Manitoba (Tackman and Currey, this volume), and the predictions of numerical models of glacio-isostatic recovery in Manitoba (Lambert, this volume).

Two questions arise in modelling the regional tilt of the Lake Winnipeg basin. First, did the tilt rate vary with time during the evolution of Lake Winnipeg since 8 ka? Secondly, did the tilt rate vary within the region, or can a single estimate be used to satisfactorily model tilt over the whole region? The first question is clearly applicable to the older shorelines. Gradients of successively younger Lake Agassiz shorelines diminish rapidly with time (11-8 ka) as displayed in strandline diagrams (Johnston, 1946; Elson, 1967; Walcott, 1972; Teller and Thorleifson, 1983). These observations suggest that the rate of crustal tilting decayed quickly during the glacial retreat (crustal unloading). The question remains whether the uplift rate continued to decay at the same rate or at a lesser rate during the subsequent 8000 years.

The second question is also important for the older shorelines as the strandline diagrams mentioned above show that gradients on individual beaches steepen to the north. This indicates more rapid uplift (higher tilt rate) in the northern than in the southern part of the region. There is some indication that the north-south differences decrease with time, so the question becomes: do the north-south differences become insignificant within the Lake Winnipeg basin for the post-Lake Agassiz period?

The graph in Figure 6 explores these questions. It shows the results of applying two models, linear and exponential, to the decay of uplift in post-Lake Agassiz time. The Lower Campbell shore of glacial Lake Agassiz was chosen because its presence encompasses the Lake Winnipeg basin, and its widely observed shore gradient defines the cumulated effect of regional tilting. In the southern part of the region the tilt amounts to 37 m/100 km, between Isobases 5 and 6, and in the northern part of the region, 55 m/100 km, between Isobases 7 and 8. These gradients have been decayed linearly (open symbols at 500-year intervals, Fig. 6) and exponentially (solid symbols at 500-year intervals, Fig. 6) over 9500 radiocarbon years, the approximate age of the Lower Campbell beach (Teller, 1989; L.H. Thorleifson, personal communication, 1995).

Eleven gradients younger than the Lower Campbell shore which have been observed or inferred within the region (Table 2) are plotted on Figure 6 for comparison with the exploratory tilt decay models. Although there is wide scatter in the data points, they most closely follow the exponential trends of predicted gradients. This suggests that an exponential model of decreasing tilt with decreasing age would best represent the variation in tilt throughout the region for most of the Holocene; a linear fit would likely be suitable for shorter periods of time or within a limited area. The regional differences in tilt rate between northern and southern areas are indicated by the separation between the two exponential curves. The differences are less than the scatter among the data points. The differences also decrease with time, and become negligible in the post-8 ka period. We conclude that, for this initial reconstruction, an average tilting function with broad error limits can be applied to the whole Lake Winnipeg region for most of the Holocene by fitting an exponential curve to the available indicators of tilt rate listed in Table 2 including the tilt rate of the Lower Campbell shoreline based on its average gradient between Isobases 5 and 8 (Fig. 1).

The function describing rate of tilt versus age for the Lake Winnipeg region is shown in Figure 7. A linear regression on the relationship between the natural logarithms of observed or inferred tilt rate and their radiocarbon age (Table 2) yielded the expression:

$$\log_e(\text{tilt rate}) \pm 0.408 = 0.0949(\text{age ka}) + 0.3$$

where 0.408 is the standard error of estimate for the logarithm of the tilt rate. The exponential expression of this regression as displayed in Figure 7 is:

$$\text{tilt rate} = \exp^{((0.0949(\text{age ka})+0.3)\pm 0.408)}.$$

The mean estimate for tilt rate versus age (solid symbols, Fig. 7) is used throughout this reconstruction of former and future configurations of the Lake Winnipeg basin. The direction of maximum tilt is assumed to be 34°, perpendicular to the regional isobases (Fig. 1).

Paleohydrology

Here, we investigate two indirect effects of regional tilting on Lake Winnipeg: 1) the diversion of the Saskatchewan River into the lake (McMartin, this volume), and 2) the progressive transfer of lake-level control from the head of Nelson River at Warren Landing to Whiskey Jack Narrows downstream.

Lake Winnipeg is a central component of the large Nelson River drainage basin which extends across the middle North American continent from the Rocky Mountains in Alberta to Hudson Bay. The Lake Winnipeg water budget is mostly supported by inflows of the Winnipeg River draining northwestern Ontario and adjacent United States (mean monthly flow of 771 m^3s^{-1}), Saskatchewan River draining southern Alberta and central Saskatchewan (mean monthly

flow of 677 m^3s^{-1}), Red River draining southern Manitoba and adjacent United States (mean monthly flow of 159 m^3s^{-1}), Dauphin River draining central Manitoba (mean monthly flow of 57 m^3s^{-1}), and other smaller streams. Variations in discharge and historically recorded lake levels are shown in Figure 8 (Lakes Winnipeg and Manitoba Board, 1958); the mean lake level is 217.4 m above sea level (asl) and this implies a mean discharge of about 2500 m^3s^{-1}. This figure shows that if the Saskatchewan River were diverted from Lake Winnipeg today, the lake level would decline about 0.6 m. Most of the Lake Winnipeg outflow passes through Playgreen Lake and Whiskey Jack Narrows (Fig. 1). A small part (18%) passes down the eastern branch of the Nelson River (Lakes Winnipeg and Manitoba Board, 1958); this fraction is ignored in the present analysis.

Does Warren Landing sill control Lake Winnipeg water level?

The shallowest section of lakebed over which water must flow to enter the Nelson River outlet at Warren Landing is presumed to be the control section (Fig. 9). The section is relatively wide, flat and shallow. It is further assumed that it can be represented by a rectangular section of equal area; such an approximation (1370 m wide x 3.8 m deep) is shown by the rectangle in Figure 9a. The outlet can then be modelled as a broad-crested weir (Tinkler et al., 1992; Tinkler and Pengelly, 1995) as is done for outflow over wide sills between the Great Lakes (Horton, 1927). Under conditions of free flow (i.e. no backwater effects at the weir) the lake level behind the sill can be calculated as the height of flow **h** over the base of the weir according to the weir equation (Henderson, 1970; Tinkler et al., 1992; Tinkler and Pengelly, 1995):

$$\text{Discharge} = 1.71 \times (\text{width of weir}) \times h^{1.5}$$

For a mean flow of 2500 m^3s^{-1}, a flow height of 1.0-1.1 m is indicated, and for a reduced flow representing the diversion of the Saskatchewan River, the equivalent height is 0.8-0.9 m (stippled area, Fig. 9a). As the base of the weir model is at a present depth of 3.8 m, it is apparent that, if the lake were controlled by the Warren Landing section, the lake level would be about 3.0 m lower than at present when the Saskatchewan River bypassed Lake Winnipeg, and 2.7 m lower when the inflow passed through the lake. Variations in modelling the outlet (Fig. 9) using compound weirs or assuming the deepest part of the sill was only scoured recently all suggest the lake must be 2.8-3.1 m lower than present if it were controlled by the Warren Landing Sill. Thus, the present mean lake level is not consistent with a weir model of flow over the lake bottom near Warren Landing; it is concluded that the Warren Landing outlet does not control Lake Winnipeg.

Whiskey Jack Narrows control

The 2-3-m discrepancy between the modelled and present lake level indicates that some assumption underlying the application of the weir equation is not fulfilled. The most likely failed assumption is the requirement for free flow, as the downstream gradient of the Nelson River through Playgreen Lake is extremely low, about 1 m over 100 km, before the River descends 9-10 m through Whiskey Jack Narrows and Whiskey Jack Channel (Lakes Winnipeg and Manitoba Board, 1958)(Fig. 1). A sill in lower Playgreen Lake just 8 km upstream of Whiskey Jack Narrows appears to be drowned by about 2 m according to the same analysis as applied to the Warren Landing sill. It appears that flow resistance in Whiskey Jack Narrows is contributing to the control of upstream lake levels.

When did Whiskey Jack Narrows begin exerting its control on upstream lakes? In the early stages of Nelson River drainage, about 7.5 ka, regional tilt would have positioned the (present) water surface in Whiskey Jack Narrows only 1.7 m lower, relative to the lower Playgreen Lake sill. This is sufficient to account for the 2-m drowning observed under modern discharge conditions. Hence it is likely that water level in the lower part of Playgreen Lake has always been controlled by Whiskey Jack Narrows.

However, the same conclusion does not hold for Lake Winnipeg and the Warren Landing sill. Because of the greater distance of separation (62 km in the direction of maximum tilt), regional tilting would have initially placed the water surface in Whiskey Jack Narrows 10-11 m lower than the Warren Landing sill. We assume this drop would have been sufficient to allow discharge from early Lake Winnipeg to flow freely over the sill at Warren Landing, with relative lake level stabilized about 3 m below present as predicted by the weir outlet models shown in Figure 9. This condition would apply when the Saskatchewan River bypassed Lake Winnipeg. An early period of free flow below Warren Landing is also indicated by an inspection of the hydrographic charts for upper Playgreen Lake (Canadian Hydrographic Service, 1989, 1990). Submerged channels and slackwater in the mouths of tributary creeks are suggestive of a once lower base level, since drowned by a rising lake. With time, differential uplift between the sites would have reduced this gradient. We assume the Whiskey Jack Narrows backwater effect began to influence the Warren Landing sill when the water surface at Whiskey Jack Narrows rose to within 1 m of the early Lake Winnipeg level, as indicated by the gradient of the outlet river under conditions of modern discharge (Lakes Winnipeg and Manitoba Board, 1958). Using the mean regional tilt rate derived earlier, calculations suggest that the uplift of Whiskey Jack Narrows began to influence Lake Winnipeg water level about 2.5 ka.

Saskatchewan River diversion

The age of the diversion of the Saskatchewan River from its former route to Nelson River via Minago River (Fig. 1) is only generally known. Radiocarbon ages of shells (5.5 ka) and basal peat (2.5 ka) in the abandoned channel led McMartin (this volume) to suggest the switch occurred in mid-Holocene time.

For this reconstruction, we assume the transfer occurred gradually (linearly) between 5.5 and 2.5 ka; ultimately increasing the lake level by 0.6 m (Fig. 8) at 2.5 ka as Lake Winnipeg came under the control of Whiskey Jack Narrows.

Water-level change along the axis of Lake Winnipeg

Present profile of Lake Winnipeg

A simplified profile showing the configuration of the lakebed and the Agassiz Unconformity (AU) (Fig. 10) is projected onto the line of maximum tilt which is orthogonal to the isobases of equal uplift (Fig. 1). The profile generally follows the long axis of the lake using information from the long cores (Appendix 7.1), and data selected from the seismic records and bathymetric charts. Some sampled areas are not traversed, such as Traverse Bay and the area northeast of George and Little Sandy Islands (Fig.1). The character of the early Lake Winnipeg basin is traced by the Agassiz Unconformity. A sub-basin in the south is open-ended towards the mouth of the Red River and its deposits, but rises to high parts of the lakebed joining Hecla and Black Islands and the mainland, here called the Hecla-Black Sill (Fig. 1). North of this sill, the AU descends to depths of 36 m in The Narrows and rises again to the lakebed at a shallow high between Berens Island and Pigeon Point on the mainland; this high is here called Pigeon Sill (Fig. 1). From Pigeon Sill the AU descends into a northern sub-basin which is terminated by a low-amplitude rise opposite Long Point. From Long Point the AU drops abruptly to its deepest point in North Basin on this profile, and rises slowly under the most northerly sub-basin toward the Warren Landing outlet sill. The extension of the profile to the north connects to the present water surface at Whiskey Jack Narrows only, and does not represent the AU configuration.

Sedimentation in Lake Winnipeg has filled the southern sub-basin and the southern part of the North Basin to about 10 m present water depth. Deep water in The Narrows is a focus for fast-flowing currents (Todd and Lewis, this volume) so it is possible that its depth has increased due to erosional downcutting during Lake Winnipeg's lifespan. Sedimentation has filled much of the northern sub-basin to a present water depth of 16 m.

Past and future profiles of Lake Winnipeg

Over the 7500- to 8000-year lifespan of Lake Winnipeg, the lakebed profile has been dynamic, starting with the AU as an initial profile in most places. This profile has built up to the present lakebed by sedimentary infilling of the lows, and by erosion of the highs, the shore zone and constrictions such as The Narrows. Because the AU has been more or less stable, we will show the change in its configuration with time relative to the paleo-lake level(s) as an indicator of the transition from glacial Lake Agassiz and the evolution of Lake Winnipeg. This has been accomplished by calculating the change in elevation relative to lake level at Warren Landing of each of the reference points on the AU in the Lake Winnipeg long-axis profile (Fig. 10).

For each reference point in the basin, the elevation of the AU relative to the mean lake level at Warren Landing for age A ka, AU_A, (the relative elevation in Figures 11 to 15) is calculated by the following expressions:

$$AU_A = AU_o + \Delta E_A - \Delta W_A$$

where AU_A = AU relative elevation for radiocarbon age A ka,

AU_o = depth (m) of the Agassiz Unconformity at the reference point below present lake level. AU_o is negative where the AU is presently below the mean level of Lake Winnipeg,

ΔW_A = relative lake level (m) at Warren Landing for age A ka (Table 3),

ΔE_A = change in elevation (m) due to tilt between Warren Landing and the reference point over the period A kiloyears, calculated as:

$$\Delta E_A = T * A * D/100$$

where T = tilt rate (m/1000 years/100 km) for age A ka (Fig. 7),

A = age in ka,

D = distance of the reference point from Warren Landing (km) measured perpendicular to the isobases along azimuth 34° (Fig. 1).

For an AU elevation relative to the level of an independent lake, such as central or southern Lake Winnipeg, the AU relative elevation for the reference site, AU_A as calculated above, is diminished by the corresponding AU relative elevation of the lake's impounding sill.

The results (Fig. 11a) show the deep waters of successive phases of glacial Lake Agassiz (at 9.5, 9.0 and 8.5 ka) through the transition to Lake Winnipeg at 8.0 and 7.5 ka. Figure 11b shows four previous AU configurations of Lake Winnipeg at 7.5, 6, 4 and 2 ka, the present configuration (0 ka) and a projected configuration 2000 years into the future (-2 ka; thin line). The zero line on the AU relative elevation scale (Fig. 11) is the lake level for each of the AU profile representations; it is the then current lake level at Warren Landing. Those parts of the AU profiles shown above this line were above the Warren Landing lake level; the scale at left indicates the height in metres of former AU positions above Lake Winnipeg. Conversely, profile segments below the reference line indicate when and to what depth the AU has been submerged in Lake Winnipeg. For most of the Lake Winnipeg basin, more than 50 km south of Warren Landing, the changes in relative lake level

have been in the order of tens of metres ranging up to almost 50 m at the southern end of South Basin.

The paleohydrological changes in lake level described in a previous section are relatively small, ranging from a position about -3 m in the earliest lake phases (7.5-5 ka) before progressing up to the present level (Table 3). Climatic changes owing to variation in the long term ratio of precipitation to evaporation and the resultant influence on the water budget of Lake Winnipeg are not yet known or evaluated but may be significant. The water level in Dauphin Lake, 150 km to the west (Fig. 1), for example, has fluctuated through a range of 2.5 m over the past 8000 years, with its highest level occurring about 4.5 ka and its lowest about 2.3 ka (Tackman and Currey, this volume).

Predicted history of Lake Winnipeg

The relative changes of basin configuration and water level implied by Figure 11 can be described speculatively. These changes are also shown at 500-year intervals at key sites, specifically, the sills (Fig. 12) and the core sites (Figs. 13, 14, 15). The earliest stages show (Fig. 11a) that most change in water depth (AU relative elevation) resulted from the declining levels of glacial Lake Agassiz. The erosional Agassiz Unconformity is the probable result of wave and drift-ice abrasion of the lakebed during the declining phases of Lake Agassiz and the early low-water phases of Lake Winnipeg. By 8 ka, during the last-shown phase of Lake Agassiz, an independent southern Lake Winnipeg had formed behind the Hecla-Black Sill leaving many areas of present Lake Winnipeg exposed for several thousand years above lake level (e.g. core sites 119, 120, 121, 122, Fig. 15). By 7.5 ka (Fig. 11b), only the northern part of the lake was submerged under a lake (northern Lake Winnipeg) controlled by the Warren Landing Sill. In most areas south of the 225 km position on the distance scale (Fig. 11b), the AU was now above this level and impounded small independent lakes behind both the Hecla-Black and Pigeon Sills. These water bodies drained northward over the sills to the northern Lake Winnipeg (Fig. 12). This northern Lake Winnipeg drained over the Warren Landing Sill at about 3 m below present level into the Nelson River. The southern shore of southern Lake Winnipeg in the South Basin lay at about the site of core 115, shown by the predicted AU subaerial exposure at site 115 (Fig. 14). Waves at this southern shore may have constructed the upper paleobeach at Pearson Reef interpreted by Todd and Lewis (this volume), and recognized as the Upper Clinoform seismic facies in the site 115 seismic profile in Appendix 7.1. Lake Agassiz may have constructed the lower paleobeach, recognized as the Lower Clinoform facies, during its regression across this area between 8.5 and 8 ka (Fig. 11a).

By 6 ka, the situation was similar in that the southern independent lakes were still in existence. They had deepened and transgressed their southern boundaries. The southern shore of northern Lake Winnipeg in the North Basin had also migrated southward towards the Pigeon Sill.

By 4 ka, northern Lake Winnipeg had backflooded and transgressed southward across Pigeon Sill (Fig. 12), The Narrows and Washow Bay (site 113) to Hecla and Black Islands. Southern Lake Winnipeg behind the Hecla-Black Sill appears to have flooded much of the South Basin (Fig. 11b). This lake was ~6 m higher than northern Lake Winnipeg at 4 ka (Hecla-Black Sill, Fig. 12).

The Hecla-Black Sill was inundated about 2.5 ka and the northern and southern parts of Lake Winnipeg coalesced to a common water level controlled by the Warren Landing outlet and then Whiskey Jack Narrows in rapid succession (Fig. 12). By 2 ka the Hecla-Black Sill was submerged about 2 m. Water continued to deepen at the southern shore with a strong tendency to migrate farther southward. These conditions of deepening water continued to the present (0 ka)(Fig. 11b). The Hecla-Black and Pigeon Sills reached their present depths of submergence of 9.5 m and 10 m respectively. In the remainder of the lake the AU achieved its modern configuration as shown earlier in Figure 10.

A slight swell in the lakefloor between southern Hecla Island and the eastern shore south of Elk Island is evident on bathymetric charts. Unfortunately, no seismic survey data are available in this area. A possible buried ridge of glacial deposits across the South Basin is hypothesized. Assuming it acted as a sill during the development of southern Lake Winnipeg and taking its present relative elevation as -13 m (0.9 m below the present lakefloor), this hypothetical ridge could have maintained separate water bodies in the South Basin until about 6 ka (sites 121, 122, Fig. 15) with some intriguing but speculative implications. Initially, the lake behind this sill might have been 2 m higher than the lake behind the Hecla-Black Sill. Until 6 ka, mixing of Red River and Winnipeg River inflows could have occurred only in the northern part of the South Basin (sites 115, 119, 120). Only after this hypothetical sill was submerged (about 6 ka) could Winnipeg River and Red River waters mix in the southern part of the South Basin (sites 121, 122) as they do today.

Some comparisons between relative elevation of observed Lake Agassiz shorelines and model relative elevations can be made. Differences in relative elevation between the model results for Isobases 8 and 6 and the Agassiz shorelines shown by Teller and Thorleifson (1983) for 9.5 ka and 9.0 ka are in the order of 38 m and 23 m, respectively. These values are similar to the equivalent error estimates of the model, +39 and -24 m, and +35 and -22 m, respectively. The errors (differences) diminish rapidly with decreasing age as the model is designed for the post-Lake Agassiz period (<8 ka). For example, differences in relative elevation between the model results for Isobases 8 and 7 and Agassiz shorelines at 8.5 ka and 8.0 ka shown by McMartin (this volume) are in the order of 4 m each, well within the model error estimates of +15 and -9 m, and +13 and -8 m, respectively.

In future, regional tilting is expected to continue and its general effect on the configuration of the basin is easily computed. A projection of the position of the AU 2000 years hence is shown (Fig. 11b). Although the rate of regional tilting is decreasing, the increased submergence of the southern shore of the South Basin is predicted to amount to about 6.5 m. The rise in relative lake level in the South Basin is greatly amplified because of the large distance (to the lake level control at Whiskey Jack Narrows) over which regional tilting operates.

Validation and discussion of the reconstruction model

Some testing of the reconstruction model can be accomplished by comparing its water level predictions at two sites where radiocarbon-dated peat zones have been found in the South Basin of Lake Winnipeg. These data were not used in constructing the regional tilt rate function, and so are independent of the model results. As described earlier, two thin layers of peat in clayey silt in core 122 appear to represent the onset of inundation of a vegetated shoreline environment. A well-preserved bulrush achene from peat on the Agassiz Unconformity was dated at 4040±70 years BP (Table 1). This dated peat is plotted on three scenarios of the history of AU relative elevation at site 122 (Fig. 16). At 4 ka, the mean AU estimate predicts the lake to be about 1 m above the peat at site 122. This is exactly the environment of initial inundation that is implied by the clay and peat beds in the sediment column at site 122.

A 40-cm thick section of *in situ* peat over clay was recovered in a borehole through the sand deposits north of Victoria Beach and south of Elk Island on the east side of the South Basin (Penner and Swedlo, 1974; Teller, 1980)(Table 1). The surface of the underlying clay is assumed to be the Agassiz Unconformity. The upper part of the peat layer has a radiocarbon age of 1060±210 years and the lower part 1660±60 years. The position and duration of this peat accumulation is plotted on Figure 16 for three scenarios of the history of AU relative elevation at Elk Island. The relationship of lake level change to peat here is more complex than at site 122. It is possible that onset of peat accumulation was encouraged by the storage of increased moisture at the site driven by the rapidly rising lake level. At the time of onset of peat accumulation the mean AU estimate predicts the actual lake surface to be about 3.5 m lower. The mean AU relative elevation curve indicates that most of Traverse Bay had been flooded by this time (e.g. water depths of 3 to 5 m are predicted for sites 119 and 120, Fig. 15). This flooding would have reduced groundwater drainage from the site (a local high) and enhanced conditions for peat accumulation. The lake is predicted to be about 2 m lower than the peat surface (assuming it was not eroded) at the time of cessation of peat deposition. This is an area of coastal sand accumulation (Penner and Swedlo, 1974; Forbes and Frobel, this volume), and it is possible the site was covered at this time by sand deposited from storm waves washing over or near the site.

Both the Elk Island and site 122 curves of mean AU relative elevation in Figure 16 show a significant increase in the rate of water level rise (increased rate of decline in AU relative elevation) at 2.5 ka as a result of the transfer of lake level control within a few hundred years from Hecla-Black Sill to Warren Landing outlet, then to the more rapidly rising Whiskey Jack Narrows (e.g. inflections in the trend of AU relative elevation at sites 121 and 122, Fig. 15). This modelled transfer correlates with an apparent increase in the rate of sedimentation in the South Basin (see earlier section on Chronology and Fig. 5). It is not an improbable connection, as increases in lake level rise often enhance shoreline erosion and sediment supply. This connection favours the mean estimate of AU relative elevation (Fig. 16) as inflections in the AU curves for the highest and lowest estimates call for the onset of Whiskey Jack Narrows control at substantially different times, 3.5 ka (lowest estimate) and 2-1.5 ka (highest estimate). Since control of level switched to Whiskey Jack Narrows about 2.5 ka, water levels have risen throughout the Lake Winnipeg basin and this rise may explain the evidence of transgressive shore processes noted by Forbes and Frobel (this volume).

This comparison (Fig. 16) of predicted water depth changes (change in AU relative elevation) with independent geologic evidence of former shore environments shows how the geological record can define rates of crustal tilting or constrain rates estimated from other evidence. In essence Lake Winnipeg is a large-scale tiltmeter. Once the inferred outlet history is confirmed, and climate and other non-tilting effects are resolved, a geological record of paleo-coastal change within the basin can potentially be interpreted as a long-term tilt record for the region.

A similar history to that predicted here can be interpreted from the conjectural water planes of Penner and Swedlo (1974) which imply the former existence of independent lakes in southern and central areas of the Lake Winnipeg basin. In their analysis, central lake Winnipeg would coalesce with northern Lake Winnipeg about 4.8 ka and this lake would, in turn, coalesce with southern Lake Winnipeg after 4 ka. The ages of these events are similar to predictions by our model using the lowest standard error estimates of tilt rate (Fig. 16) which are similar to the uplift rates derived by Penner and Swedlo (1974).

The model predictions developed here are consistent with the available independent data on changes in lake level and basin sedimentation. This is remarkable, given the scatter in the estimates of regional tilting used to formulate the model. Further validation is needed, including an assessment of the effects of post-glacial climate change. Nonetheless, the model appears to offer considerable potential for reconstructing, predicting and understanding the history of bathymetric and shoreline change in Lake Winnipeg.

SUMMARY

The data and ideas presented in this paper have their origin in the seismic reflection profiles and the suite of twelve cores collected in Lake Winnipeg by the CCGS *Namao* in 1994. The sediment lithology was summarized in core logs and correlated with seismostratigraphic sequence boundaries and facies (Appendix 7.1). A lithologic and seismostratigraphic model was developed for Lake Winnipeg. An Acoustic Basement Sequence, interpreted as till or bedrock, is conformably overlain by the Agassiz Sequence, interpreted as deposits of glacial Lake Agassiz. The Agassiz Sequence is separated from the overlying Winnipeg Sequence, interpreted as deposits of Lake Winnipeg, by the prominent Agassiz Unconformity. Lithologically, the Acoustic Basement Sequence was found to be hard, gray stony glacial diamict at one site. The Agassiz Sequence is characterized by banded silty clay and rhythmites. The Winnipeg Sequence consists of soft, silt-clay mud. This general lithologic and seismostratigraphic scheme is refined by recognizing, in the Agassiz Sequence, three intervals in the North Basin and four in the South Basin.

In this paper, the water level history in the Lake Winnipeg basin was developed as a function of the regional glacio-isostatic tilt. Analysis of the pertinent information published by other workers indicates that an exponential tilting function can be applied to the entire Lake Winnipeg region for the late- and post-Lake Agassiz period.

Our paleohydrological analysis of the outlets of Lake Winnipeg indicates that a progressive transfer of lake-level control took place from the head of the Nelson River at Warren Landing (7.5-2.5 ka) to the more rapidly rising Whiskey Jack Narrows downstream (2.5 ka to the present and continuing). We assume that the transfer of the Saskatchewan River flow from the Minago River channel to Lake Winnipeg occurred between 5.5 and 2.5 ka, ultimately increasing the lake level by 0.6 m at 2.5 ka. The effects of climate change on the level of the lake are not known or addressed in this paper.

Water-level change in Lake Winnipeg was modelled by first projecting a profile of the Agassiz Unconformity along the line of maximum tilt in the Lake Winnipeg region. The tilt function was applied to determine the configuration of the AU profile at 500 year intervals from 9.5 ka to the present and 2000 years into the future. In the late stages of glacial Lake Agassiz, deep water depths were becoming more shallow. By about 8 ka, southern Lake Winnipeg emerged as an independent basin controlled by Hecla-Black Sill. By 7.5 ka, northern Lake Winnipeg was controlled by Warren Landing Sill. Continuing tilt caused northern Lake Winnipeg to backflood across Pigeon Sill and coalesce with central Lake Winnipeg about 4 ka. By 2.5 ka, the northern and southern lakes coalesced across Hecla-Black Sill and water level control for the entire lake switched from Warren Landing to Whiskey Jack Narrows. The model predicts a future 6.5 m water level increase in 2000 years at the southern shore of the South Basin. Model predictions are validated by two dated peat occurrences in the South Basin, one in the offshore (4040±70 BP) and one on the eastern shore (1660±60 BP and 1060±210 BP).

ACKNOWLEDGEMENTS

We thank all partners in the Lake Winnipeg Project for their enthusiastic participation. Erik Nielsen and Harvey Thorleifson provided key information, encouragement and crucial discussions leading to the completion of this manuscript. John Bateman provided advice on computer software. Gary Tackman and Donald Currey kindly provided the basemap for our Figure 1.

REFERENCES

Canadian Hydrographic Service.
1988. Montreal Point to Kettle Island, Chart 6258; Canada Department of Fisheries and Oceans, Ottawa, scale 1: 25 000.

Canadian Hydrographic Service.
1989. Martin Point to Wightman Point, Chart 6260; Canada Department of Fisheries and Oceans, Ottawa, scale 1: 25 000.

Canadian Hydrographic Service.
1990. Kettle Island to Martin Point, Chart 6259; Canada Department of Fisheries and Oceans, Ottawa, scale 1: 25 000.

Elson, J.A.
1967. Geology of glacial Lake Agassiz, in ed. W. Mayer-Oakes, Life, land and water; Manitoba University Press, Winnipeg, Manitoba, p. 37-96.

Henderson, F.M.
1970. Open channel flow; MacMillan, New York, 522 p.

Horton, R.E.
1927. Hydrology of the Great Lakes; report of the engineering board of review of the Sanitary District of Chicago on the lake lowering controversy and a program of remedial measures, Part III, Appendix II, 432 p.

Johnston, W.A.
1946. Glacial Lake Agassiz with special reference to the mode of deformation of the beaches; Geological Survey of Canada, Bulletin 7, 20 p.

Lakes Winnipeg and Manitoba Board.
1958. Report on measures for the control of the waters of Lakes Winnipeg and Manitoba, Province of Manitoba; Report to the Governments of Manitoba and Canada, Winnipeg and Ottawa, 58 p. and 8 appendices.

Nielsen, E.
1987. Origin and paleoecology of post-Lake Agassiz raised beaches in Manitoba; Canadian Journal of Earth Sciences, v. 24, p. 1478-1485.

Pearson, G.W. and Stuiver, M.
1986. High precision calibration of the radiocarbon time scale, 500-2500 BC; Radiocarbon, v. 28, no. 2B, p. 839-862.

Penner, F. and Swedlo, A.
1974. Lake Winnipeg shoreline erosion, sand movement, and ice effects study; Water Resources Branch, Manitoba Department of Mines, Resources and Environmental Management, Report to Lake Winnipeg, Churchill and Nelson Rivers Study Board, Winnipeg, Manitoba, 110 p.

Stuiver, M. and Pearson, G.W.
1986. High precision calibration of the radiocarbon time scale, AD 1950-500 BC; Radiocarbon, v. 28, no. 2B, p. 805-838.

Teller, J.T.
1980. Radiocarbon dates in Manitoba; Manitoba Mineral Resources Division, Manitoba Department of Energy and Mines, Geological Report GR80-4, 61 p.

Teller, J.T.
1989. Importance of the Rossendale site in establishing a deglacial chronology along the southwestern margin of the Laurentide Ice Sheet; Quaternary Research, v. 32, p. 12-23.

Teller, J.T. and Thorleifson, L.H.
1983. The Lake Agassiz-Lake Superior connection; in eds. J.T. Teller and L. Clayton, Glacial Lake Agassiz, Geological Association of Canada, Special Paper 25, p. 261-290.

Tinkler, K.J., Pengelly, J.W., Parkins, W.G. and Terasmae, J.
1992. Evidence for high water levels in the Erie basin during Younger Dryas Chronozone; Journal of Paleolimnology, v. 7, p. 215-234.

Tinkler, K.J. and Pengelly, J.W.
1995. Great Lakes response to catastrophic inflows from Lake Agassiz: some simulations of a hydraulic geometry for chained lake systems; Journal of Paleolimnology, v. 13, p. 251-266.

Walcott, R.I.
1972. Late Quaternary vertical movements in eastern North America: quantitative evidence of glacio-isostatic rebound; Reviews of Geophysics and Space Physics, v. 10, p. 849-884.

LIST OF TABLES

Table 1. Radiocarbon dates.
Table 2. Estimates of crustal tilt in the Lake Winnipeg region.
Table 3.Warren Landing lake level relative to present mean lake level.

Table 1. Radiocarbon dates.

Site and sample data	Sample depth interval (cm)	Material dated	$^{13}C/^{12}C$ ratio	Method& Conventional ^{14}C age (yBP)[1]
Core 122 Beta-81330 (CAMS-19445) Elevation: 207.4 m asl	17-23	bulk sediment (mud)	-27.7 ‰	AMS: 3990±50
Core 122 Beta-81331 (CAMS-19446) Elevation: 206.4 m asl	118-123	bulk sediment (mud)	-27.9 ‰	AMS: 5820±50
Core 122 Beta-81332 (CAMS-19447) Elevation: 205.7 m asl	188-192	bulk sediment (mud)	-27.7 ‰	AMS: 6900±60
Core 122 Beta-81333 (CAMS-19448) Elevation: 204.9 m asl	268.5-272	bulk sediment (mud)	-27.5 ‰	AMS: 7570±50
Core 122 Beta-81334 (CAMS-19449) Elevation: 204.4 m asl	318.5-322	bulk sediment (mud)	-28.4 ‰	AMS: 7560±70
Core 122 Beta-81335 Elevation: 203.7 m asl	388.5-392	bulk sediment (mud)	-16.1 ‰	Radiometric: 11 050±270
Core 122 CAMS-17434 Elevation: 203.3 m asl	425-433	Bulrush achene (*Scirpus*)	not reported	AMS: 4040±70[2]
50°44′ N, 96°33′ W (Elk Island-Victoria Beach) GSC 1980 Elevation: 214.6 m asl	top of 40-cm peat layer	*In situ* peat under sand and over clay	not reported	Radiometric: 1060±210[3]
50°44′ N, 96°33′ W (Elk Island-Victoria Beach) GSC 1977 Elevation: 214.3 m asl	base of 40-cm peat layer	*In situ* peat under sand and over clay	not reported	Radiometric: 1660±60[3]

1. Radiocarbon years before present normalized to -25 per mil where $^{13}C/^{12}C$ data available; error is one standard deviation
2. From Vance (this volume)
3. From Penner and Swedlo, 1974; Teller, 1980

Table 2. Estimates of crustal tilt in the Lake Winnipeg region.

Age (ka BP)	Gradient (m/km)	Tilt Rate m/kyr/100 km	Tilt Direction Azimuth (degrees)	Basis	Reference
1×10^{-3}	1.01×10^{-5}	1.0 ±0.2	033	Average of ICE3G and ICE4G numerical model outputs of glacio-isostatic uplift	Lambert, this volume
2×10^{-2}	2.3×10^{-5}	2.3 ±0.8	051	Lake Manitoba water level trend	Tackman and Currey, this volume
4×10^{-2}	2.1×10^{-5}	2.1 ±0.3	042	Lake Winnipeg water level trend	Tackman and Currey, this volume
3×10^{-1}	2.03×10^{-3}	0.68	034	*In situ* tree stumps submerged by rising Whiskey Jack Narrows	Nielsen, this volume
4.05	0.1	2.3 ±0.4	048	Dauphin I shore, Dauphin Lake basin	Tackman and Currey, this volume
4.55	0.097	2.1	041	Dawson shore, L. Winnipegosis basin	Nielsen et al., 1987
7.5	0.185	2.4 ±0.5	044	Dauphin IV shore, Dauphin Lake basin	Tackman and Currey, this volume
8	0.28	3.5	039	Phase 4/5 shore, L. Agassiz	McMartin, this volume
8.4	0.16	1.8	038	Phase 3 shore, L. Agassiz, lower estimate of tilt	McMartin, this volume

Age (ka BP)	Gradient (m/km)	Tilt Rate m/kyr/100 km	Tilt Direction Azimuth (degrees)	Basis	Reference
8.4	0.28	3.5	038	Phase 3 shore, L. Agassiz, higher estimate of tilt	McMartin, this volume
8.5	0.2	2.4	032	Phase 1 shore, L. Agassiz	McMartin, this volume
9.5	0.473	5.04	034	Lower Campbell shore, L. Agassiz, average gradient Isobases 5-8	Teller and Thorleifson, 1983

Table 3. Warren Landing lake level relative to present mean lake level.

Age (ka)	ΔW_A, Relative Lake Level (m)	Source
-2	1.4	2.5 ka to -2 ka: Calculated as the differential uplift of Whiskey Jack Narrows relative to Warren Landing using mean tilt rates in Figure 7.
-1.5	1.1	
-1	0.8	
-0.5	0.4	
0	0.0	
0.5	-0.4	
1	-0.9	
1.5	-1.5	
2	-2.0	
2.5	-2.4	
3	-2.5	5 ka to 2.5 ka: Warren Landing control level (Fig. 9) + 0.1 m for each 0.5 ka after 5.5 ka (total 0.6 m) for Saskatchewan River diversion.
3.5	-2.6	
4	-2.7	
4.5	-2.8	
5	-2.9	
5.5	-3	7.5 ka to 5.5 ka: Lake level controlled by the Warren Landing Sill (Fig. 9).
6	-3	
6.5	-3	
7	-3	
7.5	-3	
8	18	Phase 5 (Lake Agassiz) water depth on Isobase 8 (McMartin, this volume)
8.5	88	Phase 1 (Lake Agassiz) water depth on Isobase 8 (McMartin, this volume)
9	220	Hillsboro phase (Lake Agassiz) water depth on Isobase 8 (Teller and Thorleifson, 1983)
9.5	263	Lower Campbell phase (Lake Agassiz) water depth on Isobase 8 (Teller and Thorleifson, 1983)

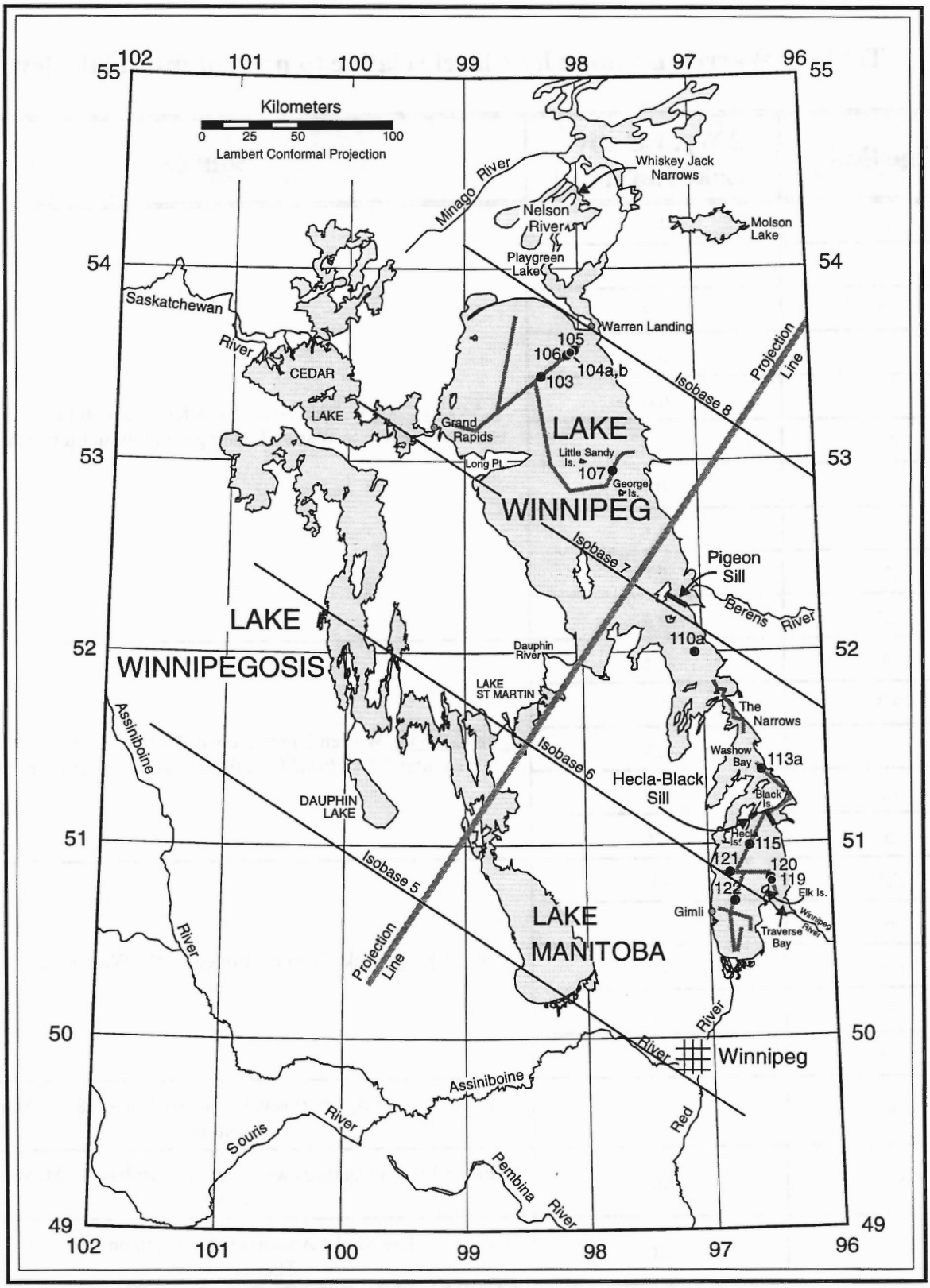

Figure 1. Location map of Lake Winnipeg in southern Manitoba. Long core sites are indicated by numbered dots on geophysical survey lines. Sills are labelled. Isobases are from Teller and Thorleifson (1983). Basemap modified from Tackman and Currey (this volume).

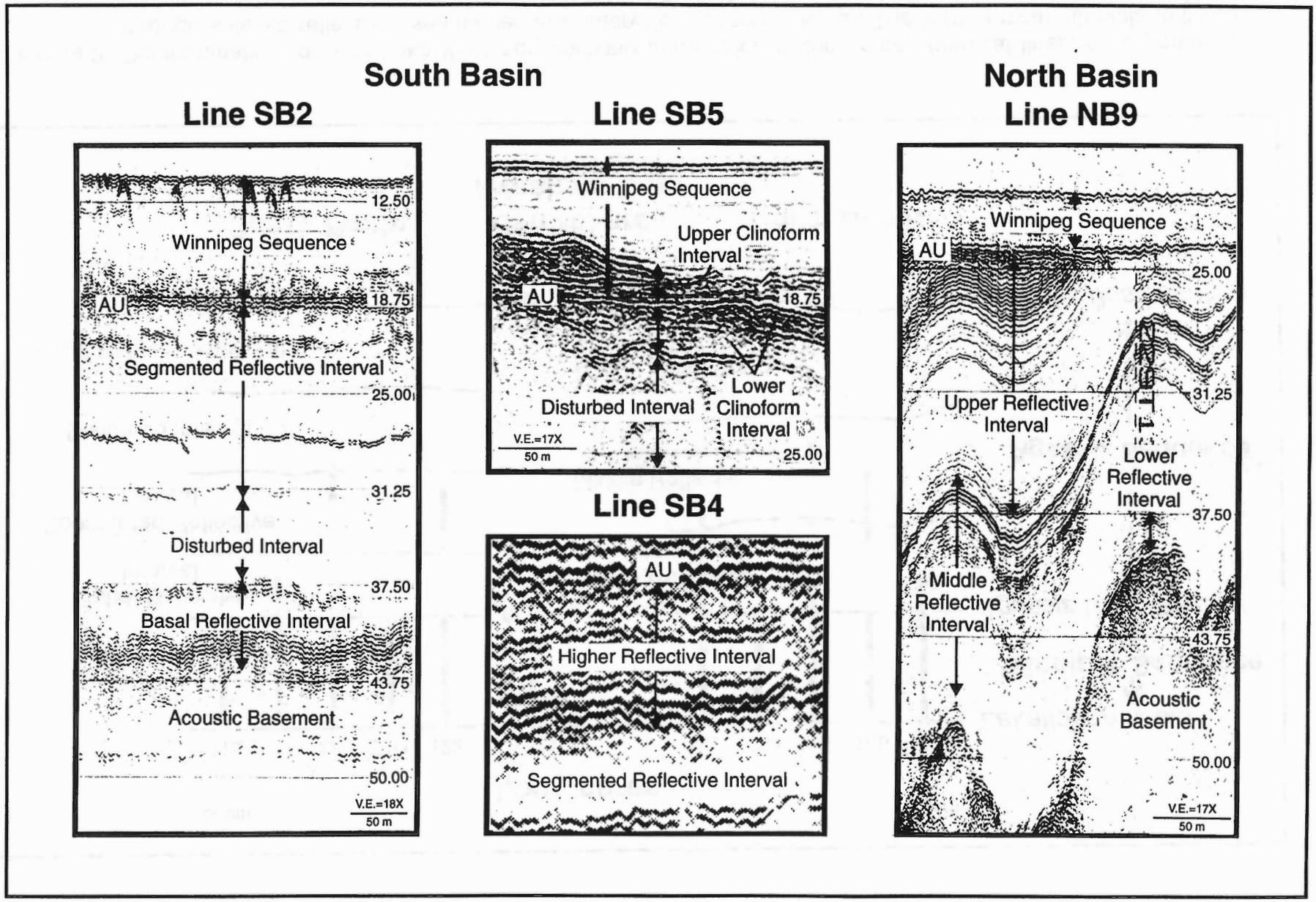

Figure 2. Seismostratigraphic subdivisions in the South and North Basins of Lake Winnipeg. Horizontal scale lines are two-way time in milliseconds. AU represents Agassiz Unconformity.

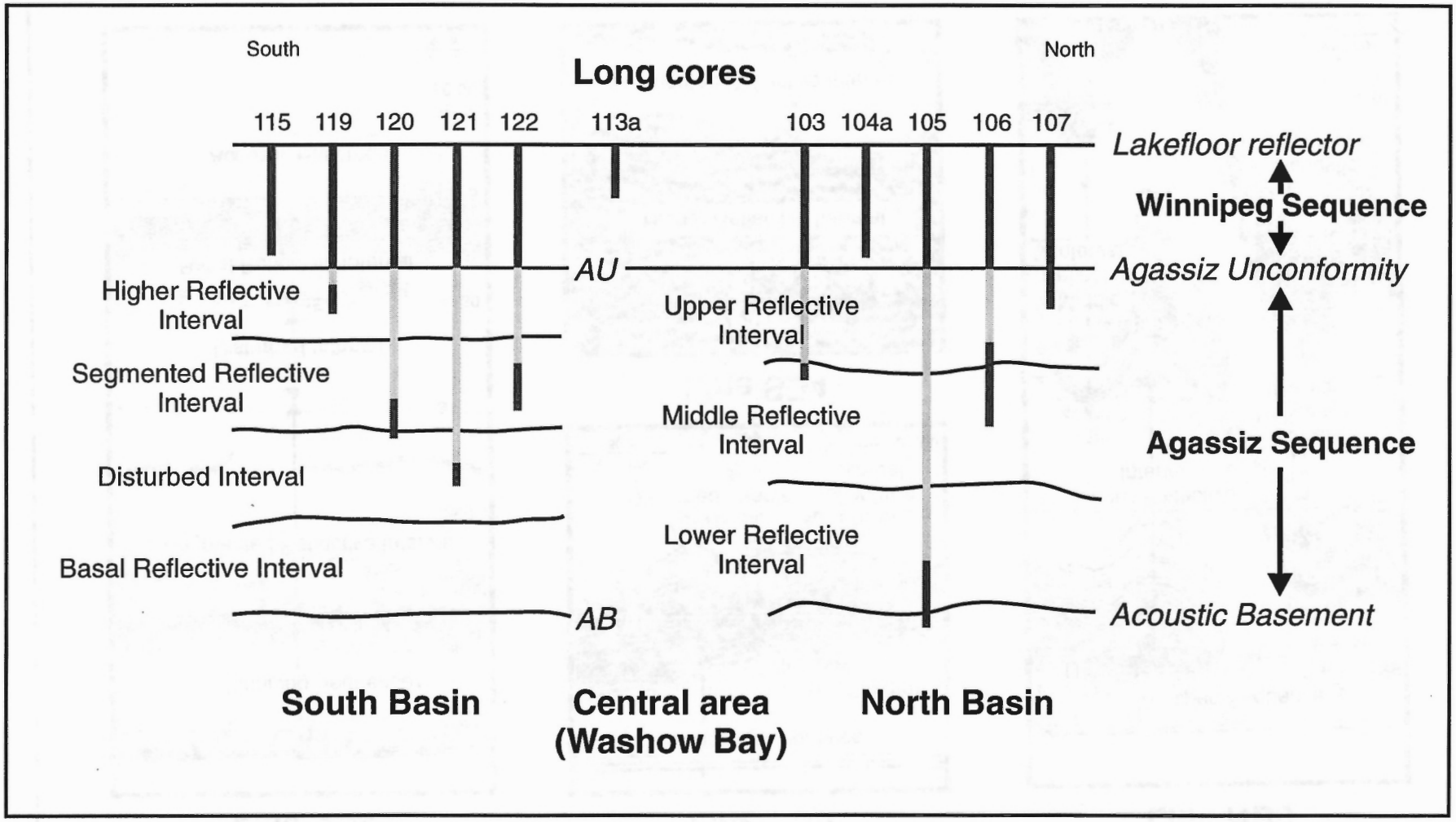

Figure 3. Diagrammatic profile of Lake Winnipeg showing penetration of long cores (vertical lines, solid portions) through seismic reflectors, sequences and intervals (horizontal lines). The light vertical intervals indicate missing (eroded) section at the Agassiz Unconformity (AU). AB represents Acoustic Basement.

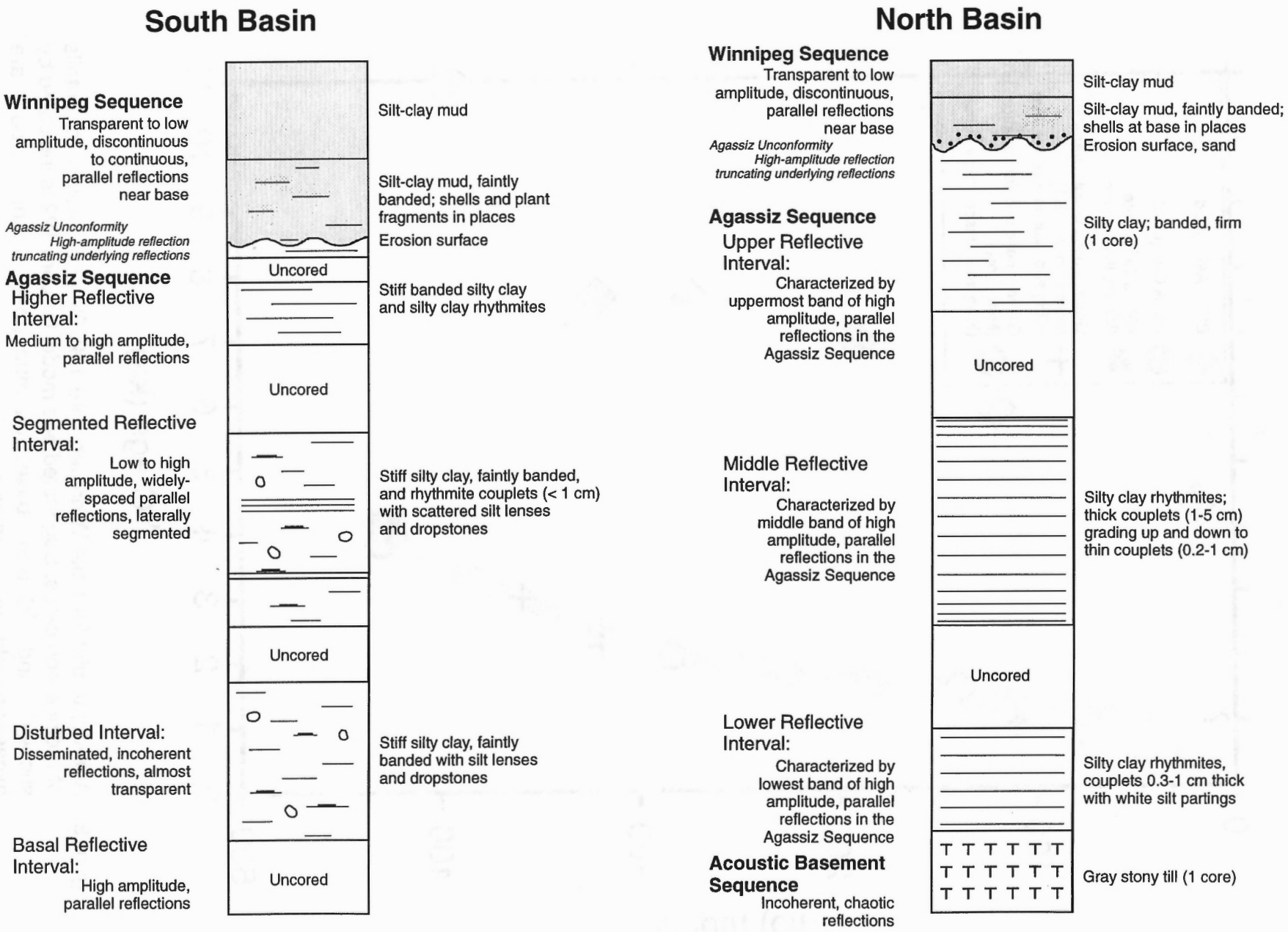

Figure 4. Generalized lithology and seismic stratigraphy in the South and North Basins of Lake Winnipeg.

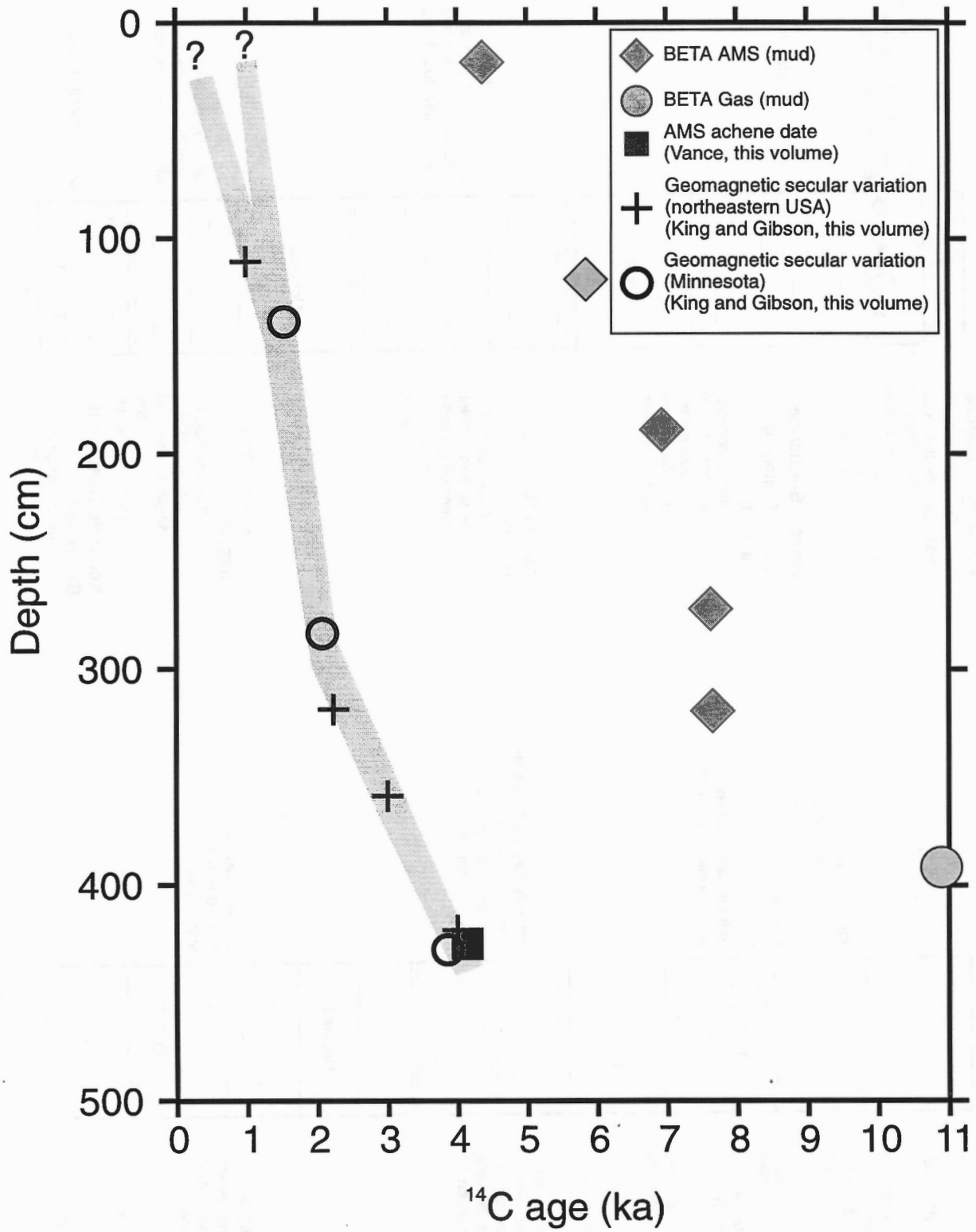

Figure 5. Age-depth plot for Lake Winnipeg core 122. Refer to Table 1 for details of radiocarbon dates. Suggested age model for core 122 is indicated by stippled band. ^{14}C ages based on mud (total organic carbon) are excessively old and are rejected.

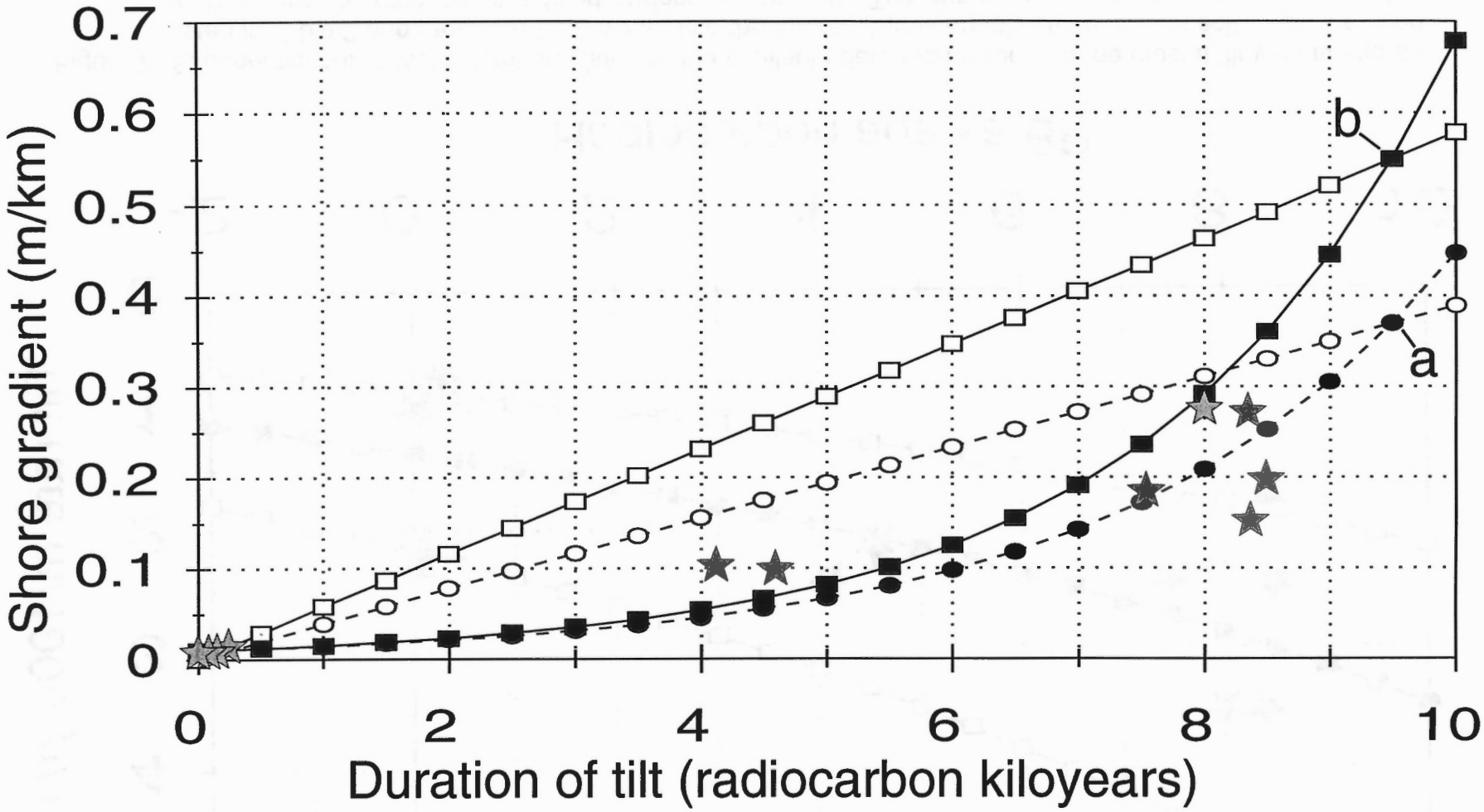

Figure 6. Exploratory models of shore gradient versus duration of tilt in radiocarbon kiloyears for the Lake Winnipeg region. The observed gradients between Isobases 5 and 6 (a) and between Isobases 7 and 8 (b) of the Lower Campbell shore of glacial Lake Agassiz which formed about 9.5 ka are decayed linearly (open symbols) and exponentially (solid symbols) to simulate possible trends in tilting during the Holocene. See Figure 1 for location of isobases. Curves with elliptical symbols are based on the southern gradient (a); those with rectangular symbols on the northern gradient (b). The stars which represent other observed gradients (exclusive of the Lower Campbell shore) listed in Table 2 plot around the solid-symbol curves, suggesting that the tilt rate in the Lake Winnipeg region has decayed exponentially with time since the early Holocene.

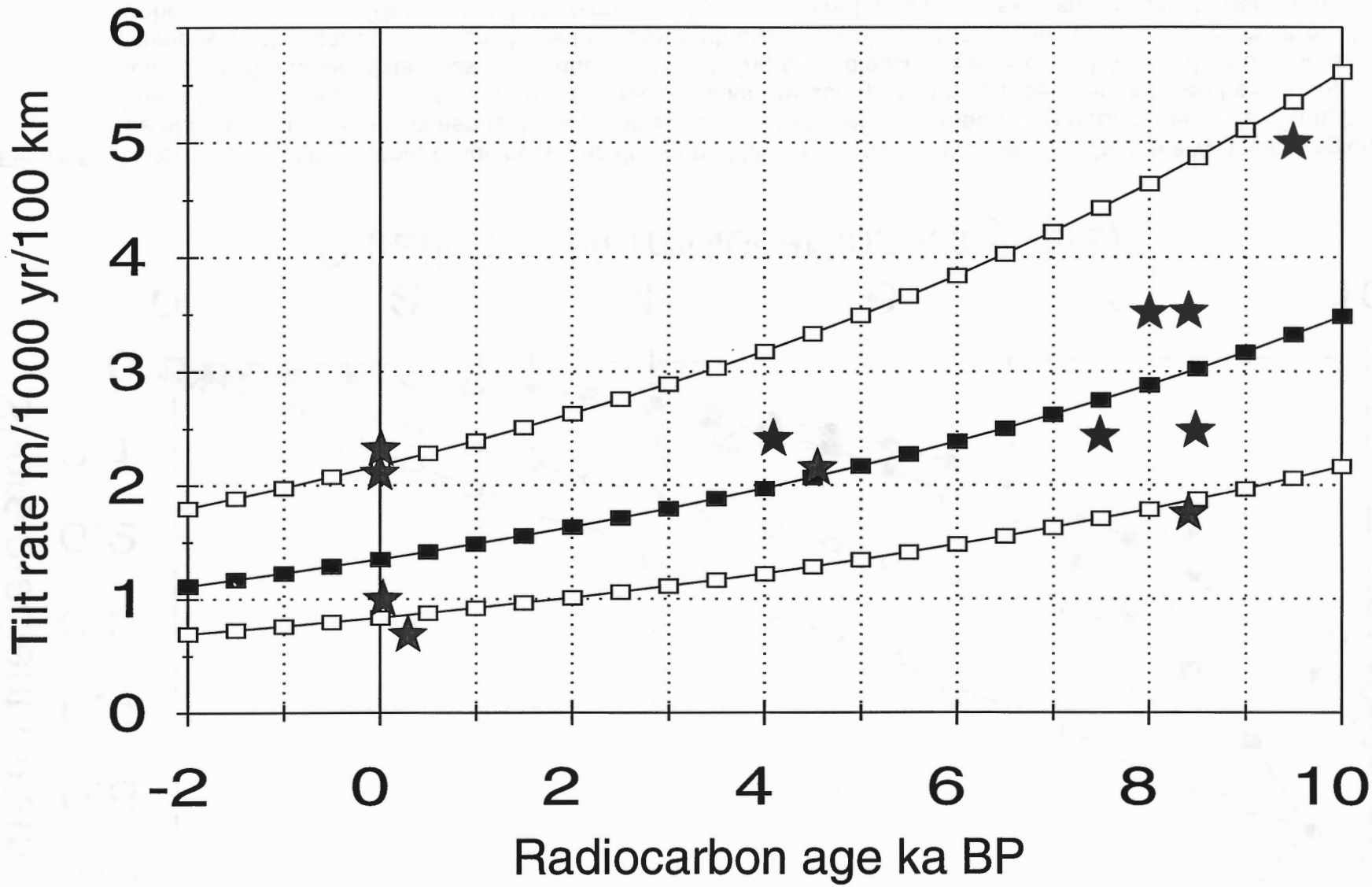

Figure 7. Exponential curve (solid symbols) fitted to the available data (stars) for average crustal tilt versus age as listed in Table 2 and projected 2000 years into the future. Values on this curve for a specific age are used in this paper to reconstruct a tilted surface of that age. The curves with open symbols represent the standard errors on the estimates of tilt rate based on the regression of $\log_e$ (tilt rate) and age.

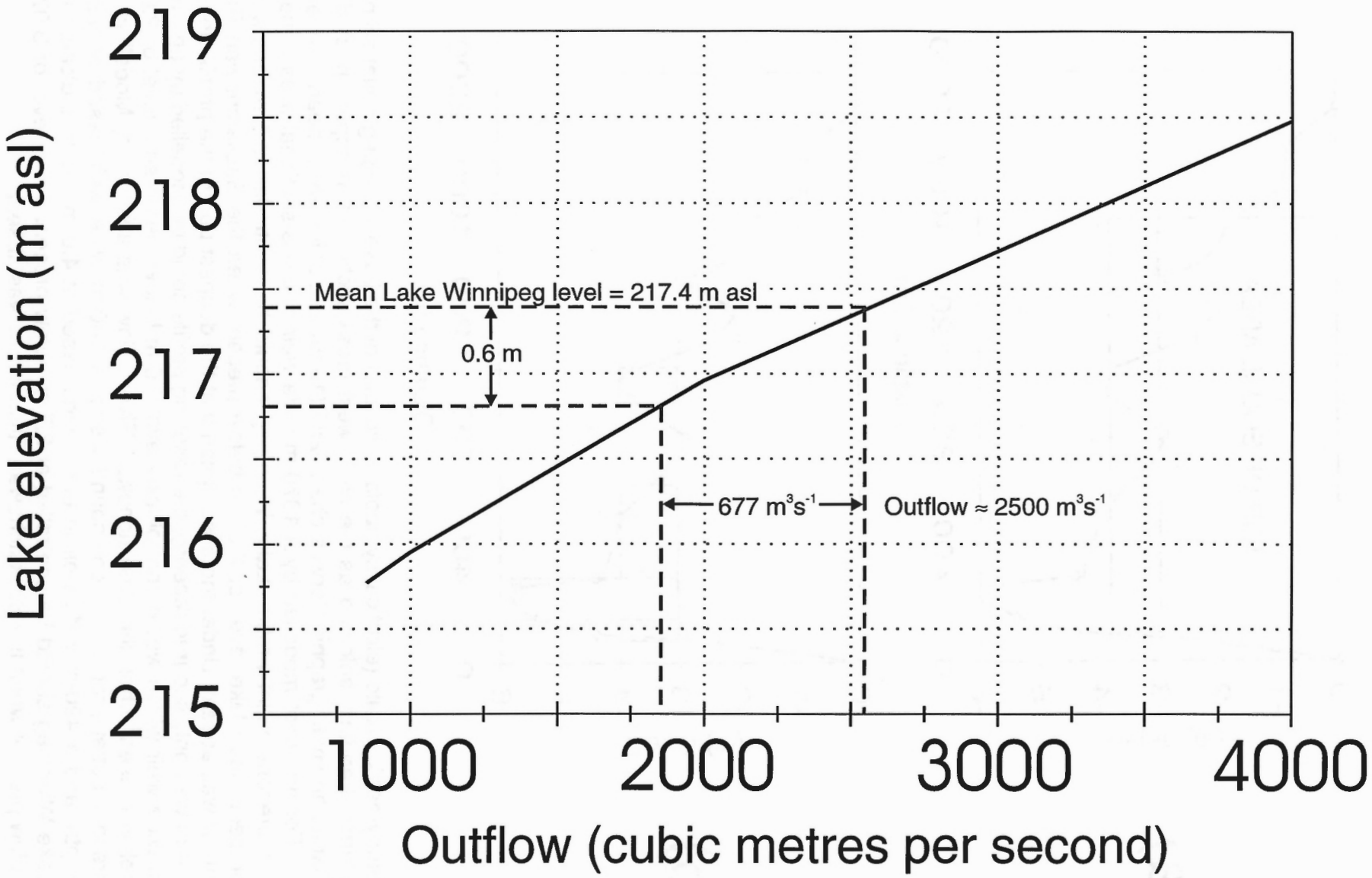

Figure 8. Lake elevation versus discharge of Lake Winnipeg for its natural outlet (from Lakes Winnipeg and Manitoba Board, 1958). The present mean level and a reduced level are shown; the reduced level shows the effect of removing the mean inflow of the Saskatchewan River.

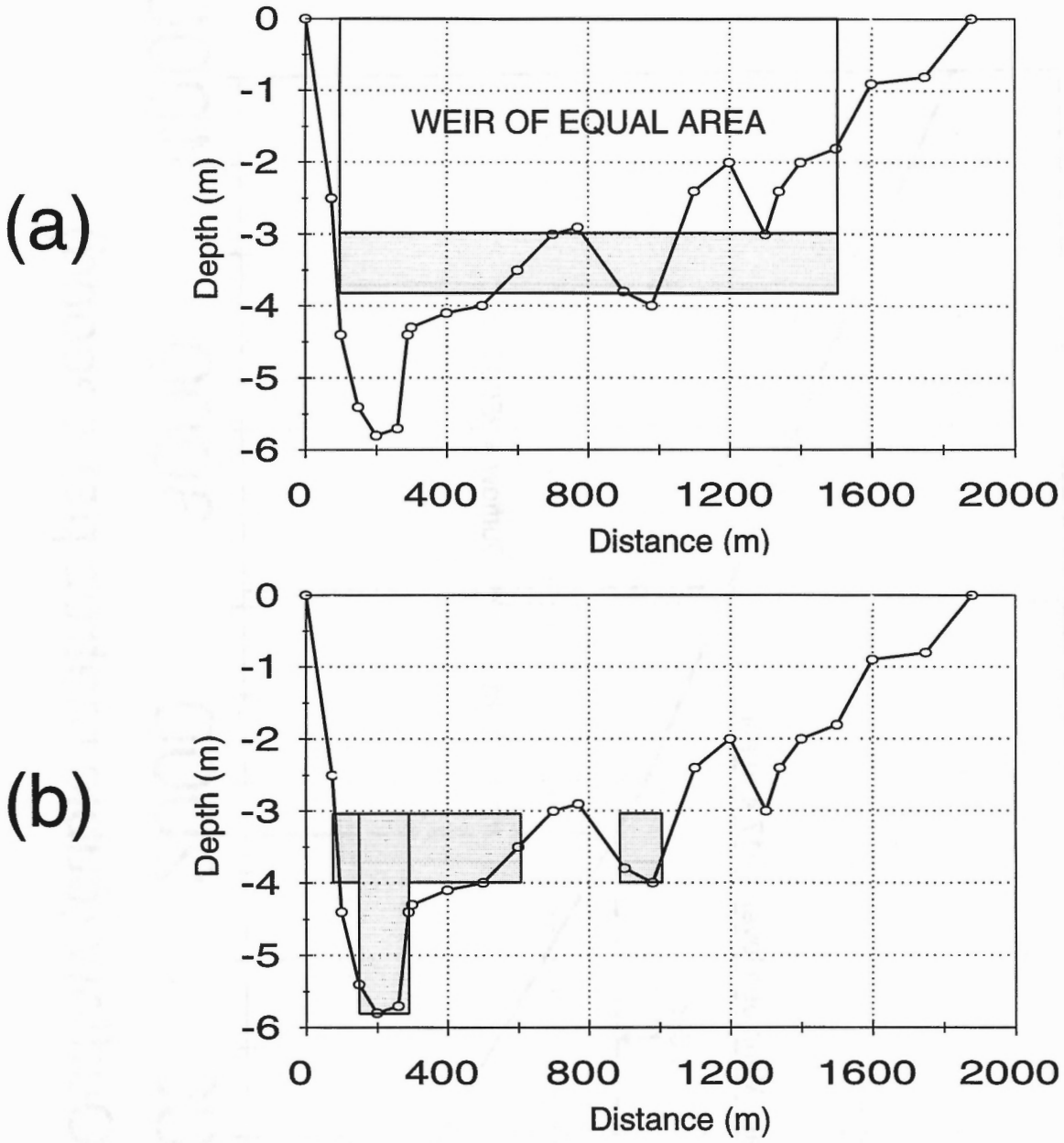

Figure 9. Bathymetric profile (elliptical symbols, solid line) of the Lake Winnipeg outlet sill near Warren Landing, selected as the shallowest cross-section from depths posted on Canadian Hydrographic Service chart 6258 (1988) and adjusted to mean lake level. (a) For an outlet modelled by a 1370-m wide weir of cross-sectional area equal to the present outlet profile, Lake Winnipeg should be controlled 2.7 m below the present mean lake level, or 2.95 m below present when the Saskatchewan River inflow was absent. Under the assumption that the deepest part of the profile under -4.4 m was only scoured recently, the resulting profile could be modelled by an 1100-m wide weir which would control lake level 2.6 m below the present level or 2.8 m below present when the Saskatchewan River inflow was absent. (b) Modelling the present outlet profile with compound weirs (a 140-m wide weir based at 5.8 m depth, and a 490-m wide weir in three parts based at 4.0 m depth) indicates that Lake Winnipeg should be controlled at 2.7 m below present mean level or 3.07 m below present when the Saskatchewan River inflow was absent.

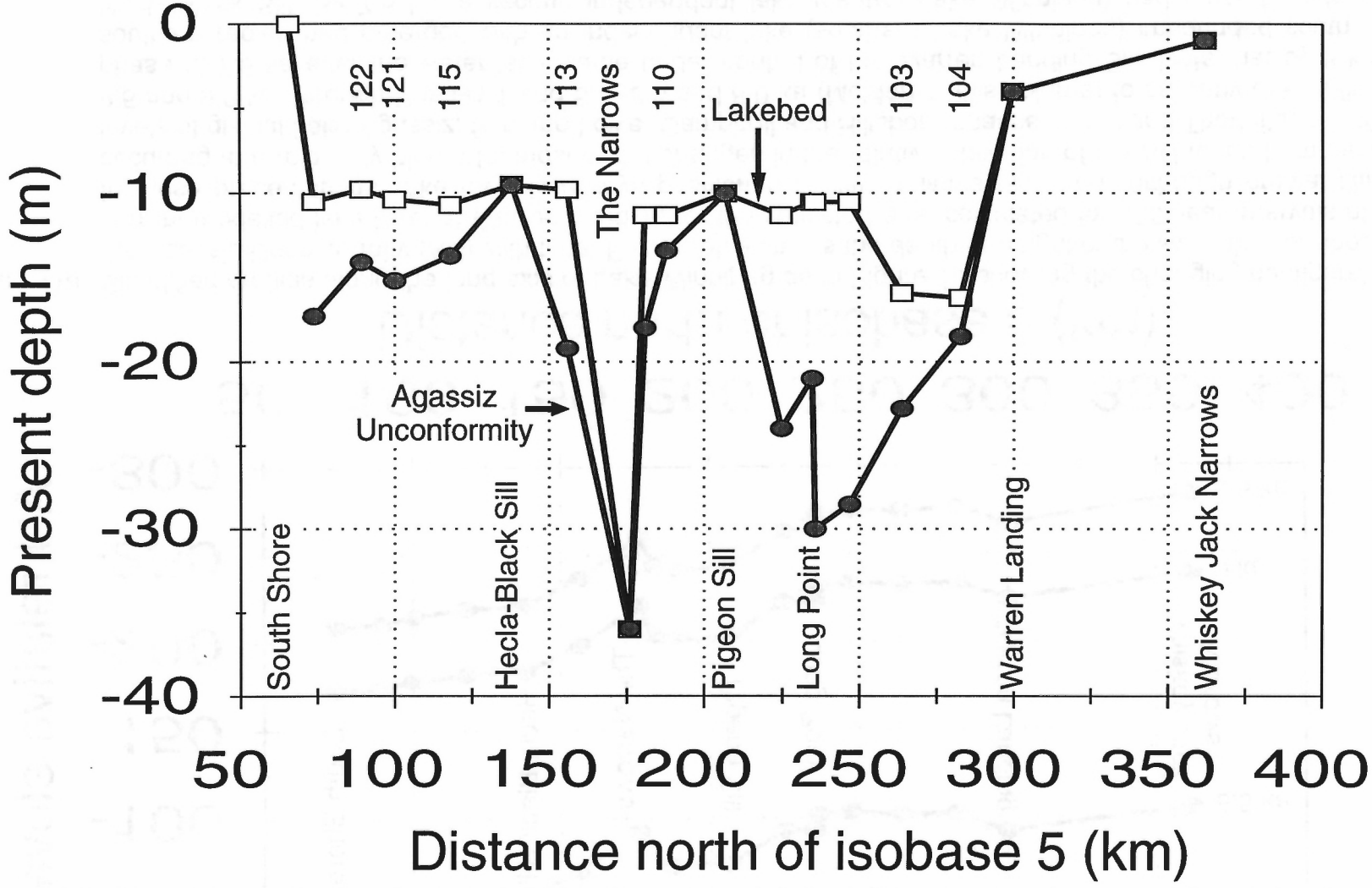

Figure 10. Simplified profile showing the depth to the present lakebed (open rectangular symbols) and the Agassiz Unconformity (solid elliptical symbols) along the long axis of Lake Winnipeg through core sites and geophysical lines of the present survey. The data are projected onto a line perpendicular to the isobases of the region (Fig. 1); isobases 6, 7 and 8 correspond to 100, 200 and 300 km on the distance scale, respectively. Numbered sites are cores (Appendix 7.1); other sites are from seismic profiles or bathymetric charts. The extension at right to Whiskey Jack Narrows is on the water surface, not the riverbed profile. The profile of the Agassiz Unconformity is used in Figure 11 to portray the changing configuration of the Lake Winnipeg basin at previous and future times.

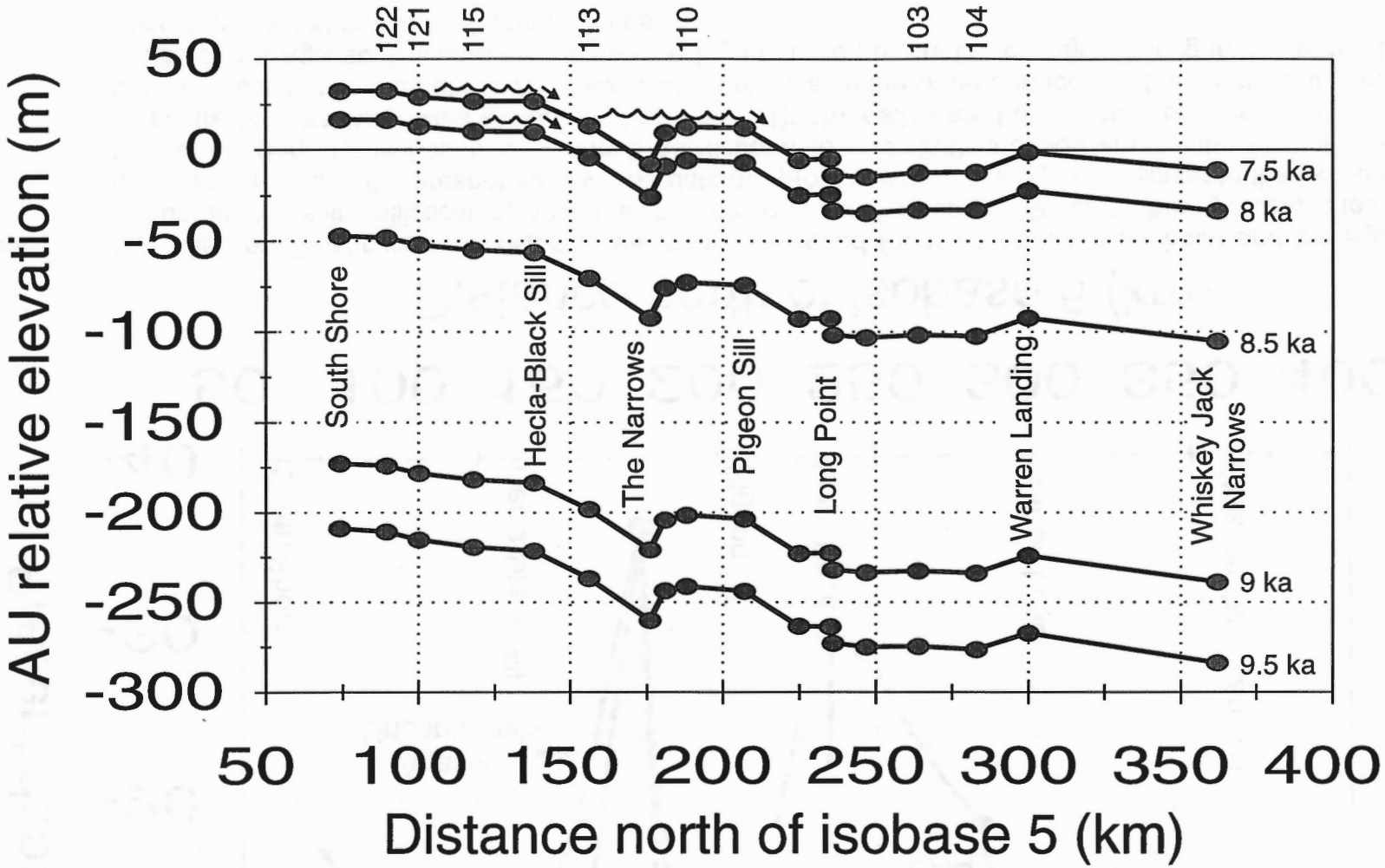

Figure 11a. Simplified profiles along the long axis of Lake Winnipeg as in Figure 10 showing the changing configuration of the Agassiz Unconformity (AU) with time. Each profile shows the depth or height of the AU below or above the current modelled lake level at Warren Landing for the indicated age, calculated for 500-year intervals of time. In these presentations, lake level is always positioned at zero relative elevation. Although crustal tilting is occurring at a relatively high rate, most of the changes in the relative elevation of the AU result from declining levels of glacial Lake Agassiz, from the Lower Campbell and Hillsboro phases (Teller and Thorleifson, 1983) at 9.5 and 9.0 ka, through Phases 1 and 5 at 8.5 and 8.0 ka (McMartin, this volume) to an early Lake Winnipeg phase at 7.5 ka after the water level came under control of the Warren Landing Sill. Note that by 8 ka, the southern region had emerged with an independent lake (southern Lake Winnipeg) impounded south of the Hecla-Black Sill. By 7.5 ka, a second independent lake (central Lake Winnipeg) had formed south of the Pigeon Sill.

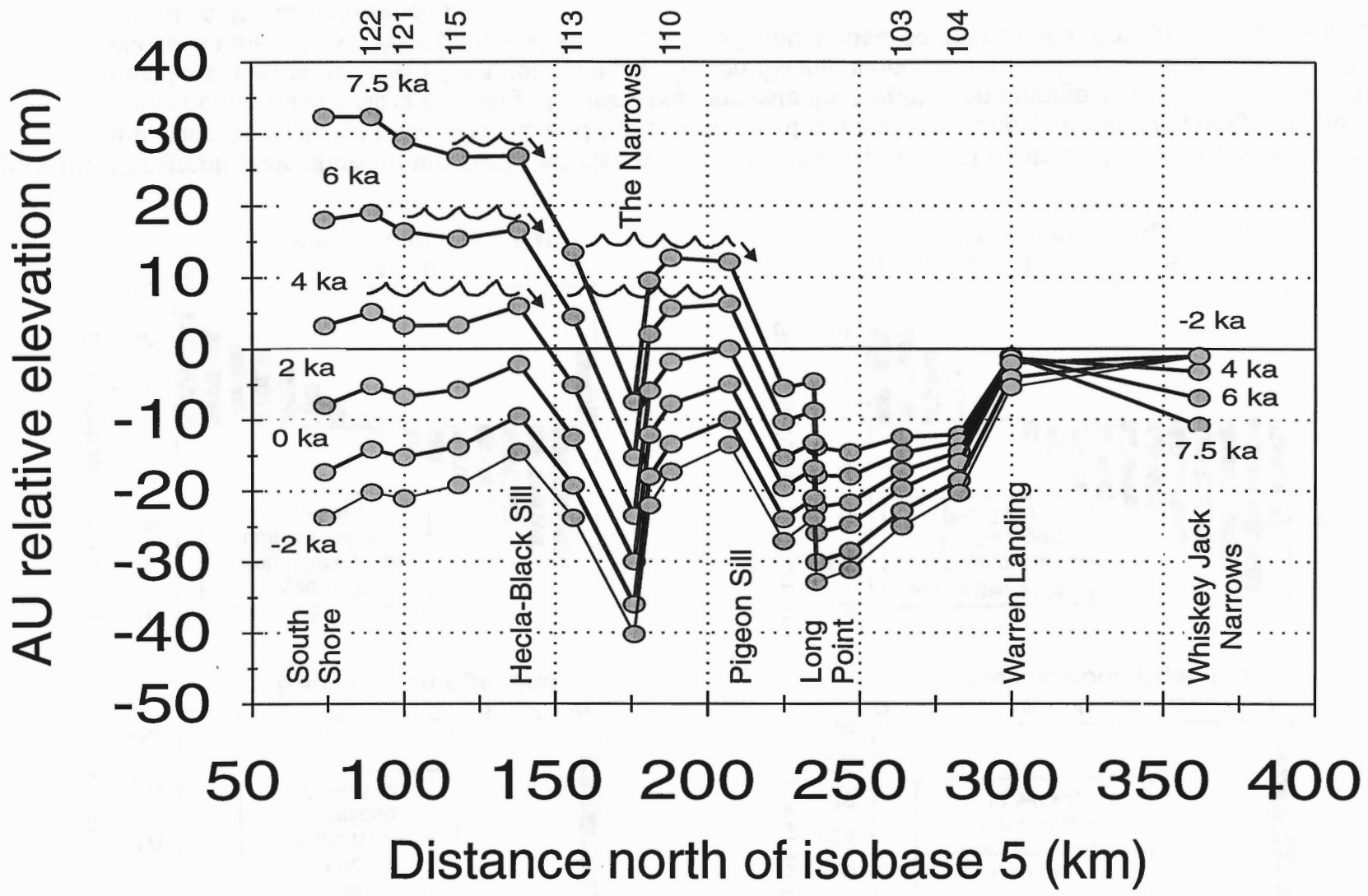

Figure 11b. In this illustration, continued crustal tilting accounts for most changes in AU relative elevation. The AU profile at 7.5 ka is repeated from Figure 11a. The independent central Lake Winnipeg is maintained behind the Pigeon Sill until 4 ka. The independent southern Lake Winnipeg continues behind the Hecla-Black Sill until 2.5 ka. Whiskey Jack Narrows takes control of Lake Winnipeg from the Hecla-Black and Warren Landing Sills shortly after 2.5 ka. The relatively rapid uplift of this most northern lake-level control causes relatively rapid submergence throughout Lake Winnipeg, but especially in its distant southern basin. A prediction of the future AU profile in 2000 years (-2 ka) is indicated by the thin line.

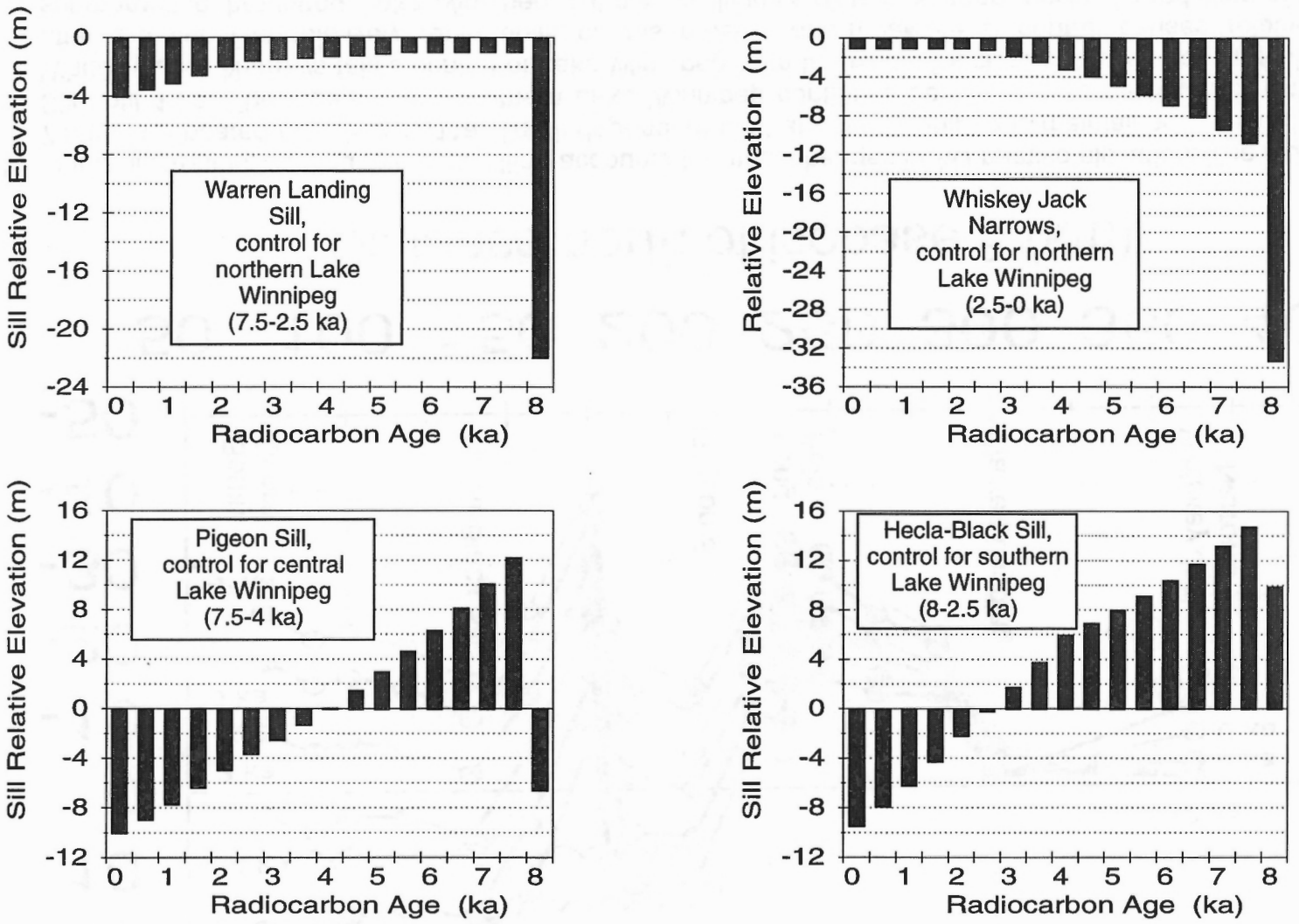

Figure 12. Bar graph plots showing the predicted history of the relative elevation of control sills and narrows during the transition from glacial Lake Agassiz and the development of Lake Winnipeg (8-0 ka). Dropping bars indicate the depth to which a sill is submerged. Rising bars indicate the height of an emergent sill above the level of the next lake downstream. At 7.5 ka, for example, Pigeon Sill impounded central Lake Winnipeg about 12-12.5 m above northern Lake Winnipeg, and Hecla-Black Sill impounded southern Lake Winnipeg about 14.5-15 m above central Lake Winnipeg.

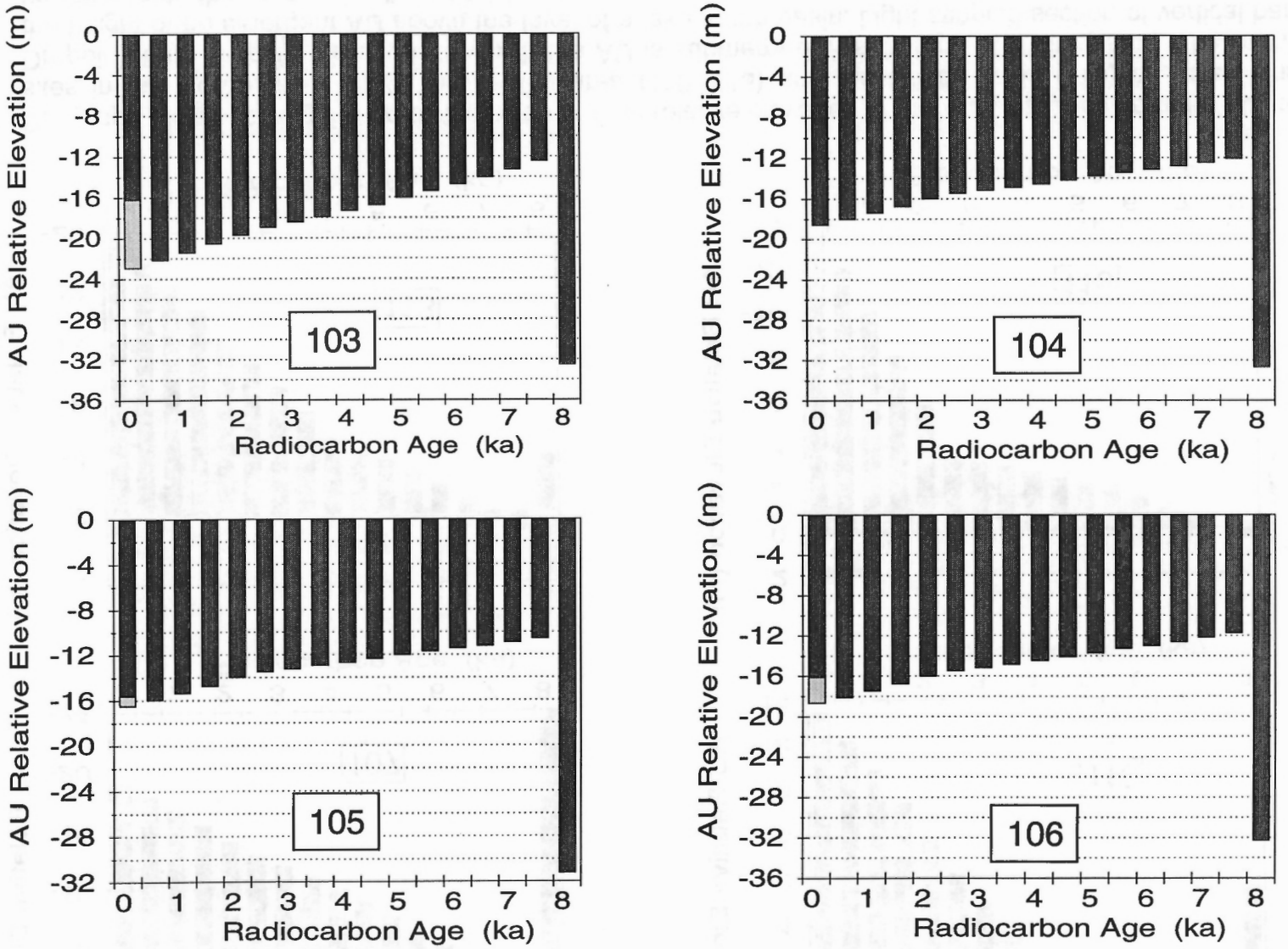

Figure 13. Bar graph plots showing the predicted history of the relative elevation of the Agassiz Unconformity (AU) at four core sites in the North Basin of Lake Winnipeg. Dropping bars indicate the depth to which the AU is submerged. Light stippled section of vertical bars at 0 ka represents the present sediment thickness, where known, above the AU (Appendix 7.1), i.e. the thickness of the Winnipeg Sequence.

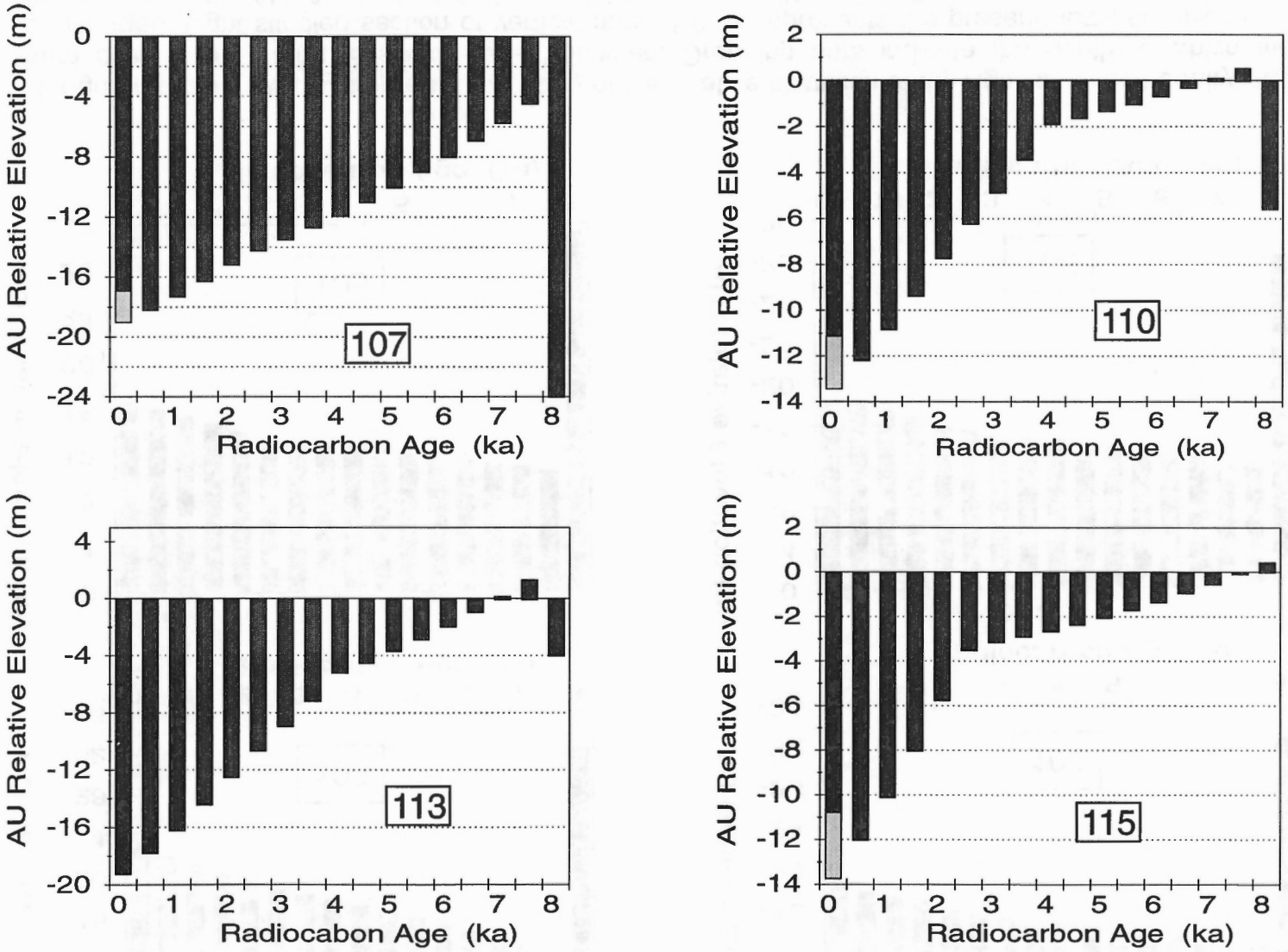

Figure 14. Bar graph plots showing the predicted history of the relative elevation of the Agassiz Unconformity (AU) at core sites in the North Basin (107), the central area (110, 113) and the South Basin (115) of Lake Winnipeg. Dropping bars indicate the depth to which the AU is submerged. Rising bars at a site within a basin indicate the height of an emergent AU above the level of a lake in the basin. Light stippled section of vertical bars at 0 ka represents the present sediment thickness, where known, above the AU (Appendix 7.1), i.e. the thickness of the Winnipeg Sequence.

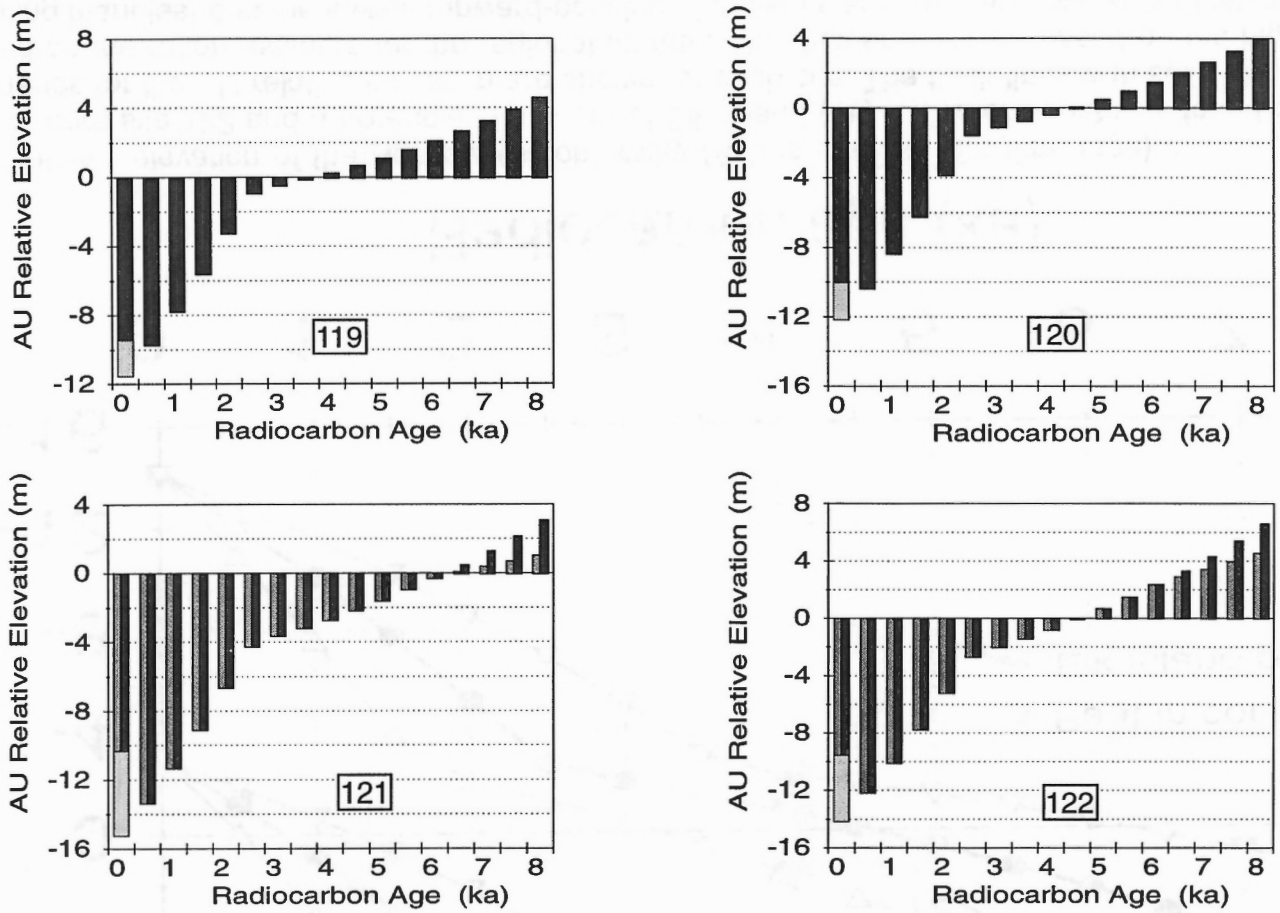

Figure 15. Bar graph plots showing the predicted history of the relative elevation of the Agassiz Unconformity (AU) at two core sites in Traverse Bay (119, 120) and two other core sites in the South Basin (121, 122) of Lake Winnipeg. Rising bars indicate the height of an emergent AU above a lake in the basin. Dropping bars indicate the depth to which the AU is submerged. The double bars for sites 121 and 122 portray the trends of AU relative elevation under two scenarios for southern Lake Winnipeg. The first scenario (right side of bars, darker tone) assumes southern Lake Winnipeg was entirely controlled by the Hecla-Black Sill. In the second scenario (left side of bars, lighter tone), the southern part of southern Lake Winnipeg was controlled for a time (8-6.5 ka) by a speculative sill between southern Hecla Island and the eastern shore south of Elk Island. Light stippled section of vertical bars at 0 ka represents the present sediment thickness, where known, above the AU (Appendix 7.1), i.e. the thickness of the Winnipeg Sequence.

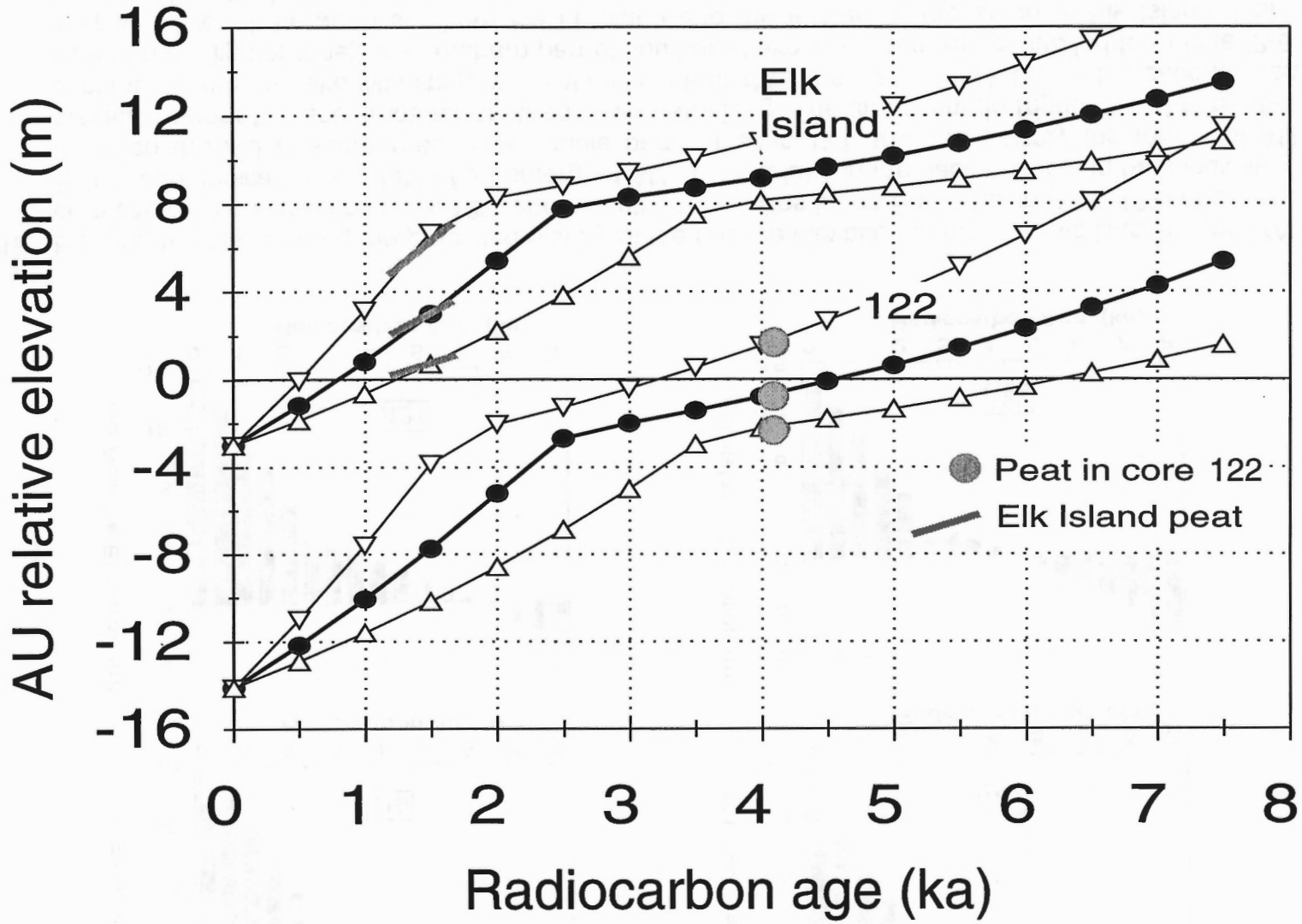

Figure 16. The relative elevation of the Agassiz Unconformity (AU) is tracked with time (age) at two sites in the South Basin, core site 122 and a borehole site south of Elk Island (Fig. 1), where peat was found on the AU. Three scenarios for the AU relative elevation are shown for each site. The thick lines with solid elliptical symbols are based on the mean estimate for the regional tilt rate. The thinner lines are based on the highest (downward-pointing triangles) and the lowest (upward-pointing triangles) standard error estimates of tilt rate. The peats are plotted on the various AU scenarios at their radiocarbon-determined ages. See text for discussion.

4.2 Physical properties and stratigraphic correlation of Lake Winnipeg sediments

K. Moran

Geological Survey of Canada (Atlantic)
P.O. Box 1006, Dartmouth, Nova Scotia B2Y 4A2

C.A. Jarrett

K&K Geoservices
17 Hawthorne Street, Dartmouth, Nova Scotia B2Y 2Y4

INTRODUCTION

Lake Winnipeg sediment cores were collected during the cruise *Namao* 94-900 in both the Lake Winnipeg North Basin and the South Basin. Both piston (PC) and gravity core (GC) methods were used (Todd, this volume). Sediment physical properties were measured post-cruise at the Bedford Institute of Oceanography. The properties measured were whole core magnetic susceptibility, bulk density, acoustic compressional wave velocity, undrained shear strength and digital colour reflectance. The methods used followed those described by the Shipboard Scientific Party (1995).

The measurements of bulk density, magnetic susceptibility, and acoustic velocity were made using a whole core multi-sensor track (MST) at a vertical resolution of 1 cm. Undrained shear strength was measured, where possible, at a nominal resolution of 10 cm, and colour was measured at a 5 cm resolution. The MST and colour data were used to construct complete stratigraphic sections from selected cores in the North and South Basins. These constructs represent the most complete stratigraphy and are recommended for interpretation of age, sedimentation and mass accumulation rates in both basins. Shear strength was measured to estimate thickness of eroded sediments and for ice load estimates within the basal tills. In addition, the bulk density and acoustic velocity data can be used to construct synthetic seismograms for direct correlation of core data and seismic reflection data (Todd and Lewis, this volume).

COMPOSITE STRATIGRAPHY

The physical property results from all cores are plotted as a function of depth below core top (Appendix 7.2). PC103, PC106, and PC105 were selected from northern Lake Winnipeg to construct a complete stratigraphic section, referred to here as a composite. PC103 sampled the thickest section of upper Lake Winnipeg sediments. PC106 sampled both Lake Winnipeg and Lake Agassiz sediments, and PC105 sampled primarily Lake Agassiz sediment and till. The colour reflectance, plotted using the international colour standards (L*, a*, b*), was the primary data set used to construct the composite by correlation of the downcore signals (Fig. 1). L* is the ratio of black to white wavelength bands, a* is the ratio of red to green, and b* is the ratio of blue to yellow. The correlation was made by shifting one data set (in depth) against another until the best correlation was found among all three parameters. Although not always peak for peak, the correlation was very good. There are a few small offsets in absolute values (e.g. between a* from PC105 and a* from PC106) which are likely associated with a small variation in composition due to the natural lateral variations in sedimentation over the same time period. The offsets in depth for PC106 and PC105 used to construct the composite are 520 cm and 980 cm, respectively.

The composite for northern Lake Winnipeg was used to plot the MST data as a check on the composite construction and to interpret the general properties of the sediment units within the North Basin. When plotted as a composite (Fig. 2), the data show good agreement. Based on both the sediment physical properties, the visual core description, and the seismic reflection data, the northern Lake Winnipeg composite is divided into three lithostratigraphic units: Lake Winnipeg, Lake Agassiz, and till. Lake Winnipeg sediment is generally low bulk density that increases with depth, typical of normal consolidation. Lake Agassiz sediment has a higher bulk density which increases with depth. This higher density may represent either a compositional difference from Lake Winnipeg sediment and/or the unit has undergone basin-wide erosion. A till unit is at the base of the composite. This unit has very high bulk density, which is likely due to overconsolidation from ice loading. The undrained shear strength (S_u) of the till (see PC105, Appendix 7.2) is approximately 85 kPa. A normally consolidated saturated fine-grained sediment has a S_u/P_o' ratio of 0.2, where P_o' is the effective overburden stress as calculated from the buoyant bulk density. Consequently, the normally consolidated S_o at the stratigraphic level of the till is 11 kPa. Thus, the difference between the measured shear strength and the normally consolidated shear strength is the strength-gain associated with loading by the ice sheet. The estimated minimum thickness of the ice sheet to produce this load is 50 m. Both the magnetic susceptibility and the acoustic velocity mimic the downcore variation in bulk density in all of the lithostratigraphic units. This suggests that the composition of these units does not vary significantly with depth.

Gravity cores 120, 121 and 122 were selected to construct a composite in southern Lake Winnipeg following the same method as the northern cores. The composite, constructed using colour data, includes GC121 at the top, GC122 in the middle, and GC120 at the base (Fig. 3). There is very good agreement among the shifted data signals. The composite depth of GC121

is the same as its core depth; GC122 is shifted by 98 cm, and GC120 is shifted by 285 cm. As with the northern composite, there are small offsets in the absolute values of a* among the cores, again suggesting lateral variation in sediment composition.

The physical property data was plotted in composite depth, showing good agreement (Fig. 4). The acoustic velocity data was of very poor quality because of cracks in the core and is not included in the interpreted composite. The only exception to the generally good correlation is the low bulk density values at the top of GC120 at a composite depth interval of 280-320 cm. These low values may either represent core disturbance or an interval of stratigraphically younger sediment. The composite section is interpreted to include two units: Lake Winnipeg and Lake Agassiz. Similar to the northern composite, the Lake Winnipeg bulk density is low, but increases with depth. The Lake Agassiz sediment has higher bulk density values. The magnetic susceptibility mimics the down-core trend in bulk density in the upper 550 cm of composite depth, again suggesting minimal variation of sediment composition within the sediment units.

NORTH AND SOUTH COMPARISON

The composites from the North and South Basins have similar absolute values in physical properties, suggesting similar stress histories between the basins. However, the thickness of the Lake Winnipeg sediment is less in the South Basin (ca. 4.5 m) than in the North Basin (ca. 6.5 m), suggesting different sedimentation rates or an age difference between the onset of deposition of Lake Winnipeg sedimentation between the basins. If we assume that the difference is due to a sedimentation rate difference and that the rate in the South Basin is 100 cm/ka for Lake Winnipeg sediment, then the rate for the same sediment in the North Basin is ca. 150 cm/ka. On the other hand, if we assume a constant sedimentation rate across both basins, then the time difference between the onset of Lake Winnipeg sedimentation is 2 ka. The base of the Lake Agassiz sediment was not sampled in the South Basin, mainly because the piston corer was not available for sampling. Consequently, differences in this unit are not easily determined.

SUMMARY

Sediment physical properties were measured on the gravity and piston cores collected during *Namao* 94-900. The properties were used here to construct stratigraphic composite sections for the purpose of evaluating basin-wide depositional histories and to assist in the interpretation (and sample selection) for biostratigraphy, and paleomagnetic and rock magnetic stratigraphy. The data (density and shear strength) can also be used to estimate stress history of each of the lithostratigraphic units and their variations across the basin. In addition, a quantitative link of the core data with the high resolution seismic reflection data can be performed through the construction of synthetic seismograms at each core site using the core-measured bulk density and acoustic velocity data. These data are included here in graph form in Appendix 7.2.

REFERENCES

Shipboard Scientific Party
1995. Explanatory notes; in eds. Curry, Shackleton, Ricater, et al., Initial reports of the ocean drilling program, College Station, Texas, v. 154.

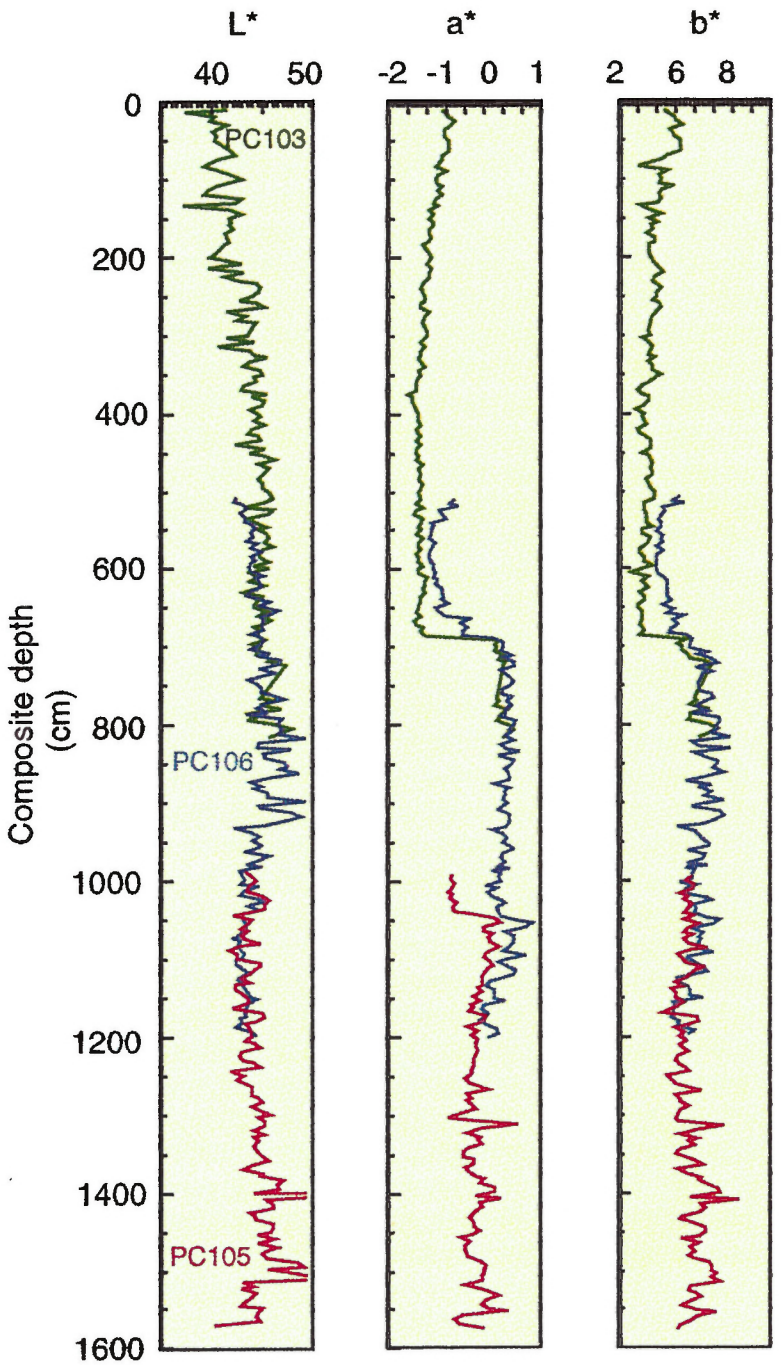

Figure 1. Composite stratigraphy of sediment from the North Basin of Lake Winnipeg. The composite was constructed using digital colour reflectance data (shown here) and physical property data (Fig. 2). PC103 represents the upper Lake Winnipeg sediments. PC106 overlaps with PC103 at 500 cm depth on PC103. PC105 overlaps with PC106 at 480 cm depth on PC106. The composite stratigraphic section is comprised of an upper 660 cm of Lake Winnipeg sediment that overlies almost 4 m of Lake Agassiz sediment and till at its base.

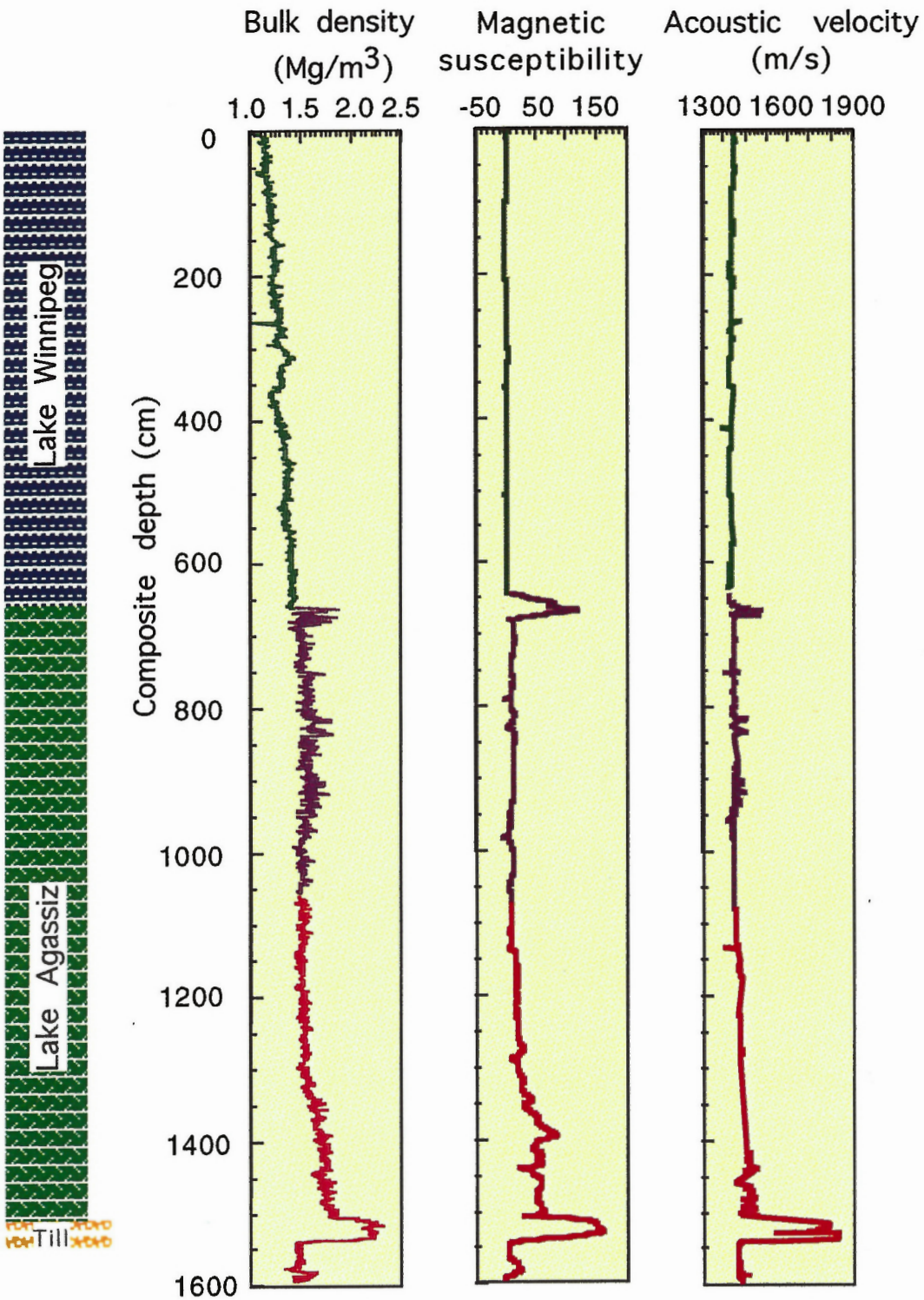

Figure 2. Composite depth of sediment from the North Basin of Lake Winnipeg plotted with physical properties from piston cores 103, 105 and 106. Note the higher values of bulk density of the Lake Agassiz sediment and till at the base of the composite.

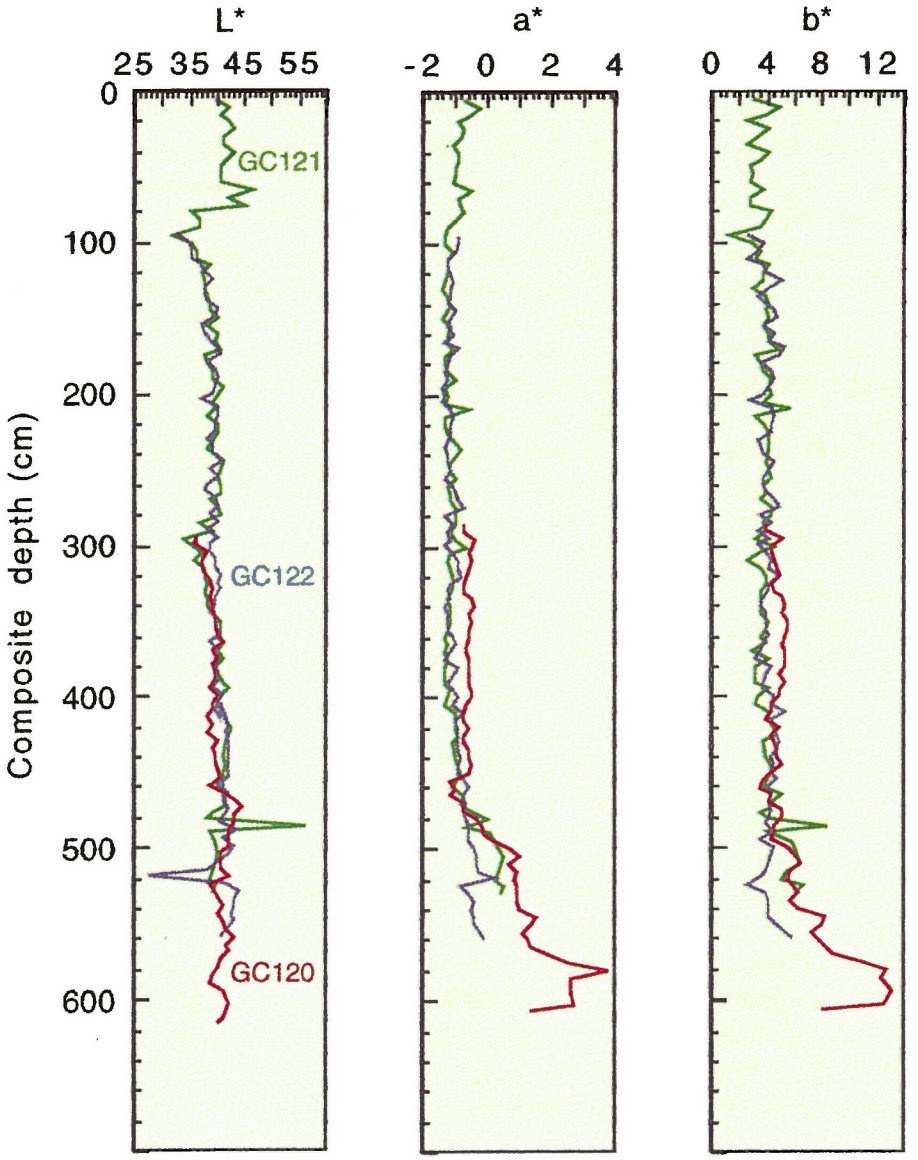

Figure 3. Composite stratigraphy of sediment from the South Basin of Lake Winnipeg. The composite was constructed using digital colour reflectance data (shown here) and physical property data (Fig. 4). GC122 overlaps with GC121 at 95 cm depth on GC121. GC120 overlaps with GC122 at 200 cm depth on GC122. The composite stratigraphic section is comprised of an upper 470 cm of Lake Winnipeg sediment that overlies Lake Agassiz sediment.

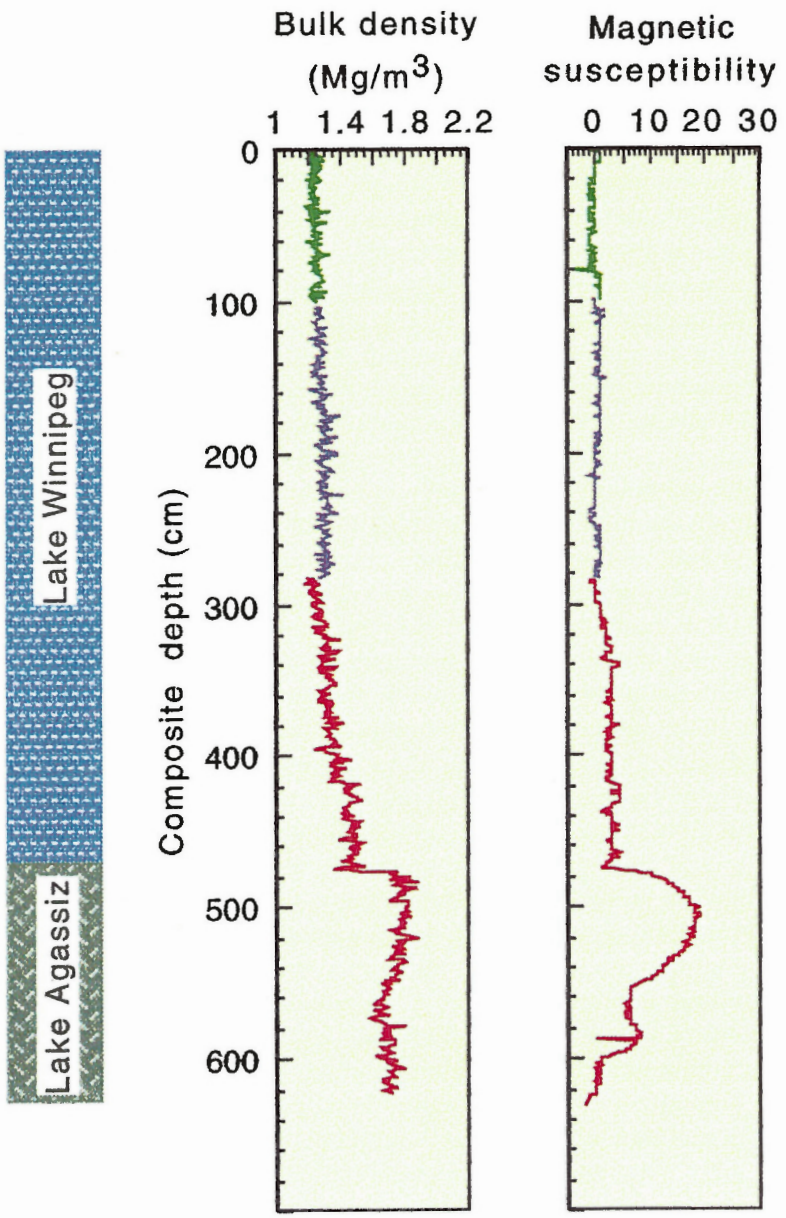

Figure 4. Composite depth of sediment from the South Basin of Lake Winnipeg plotted with physical properties from cores 120, 121 and 122. Note the higher values of bulk density of the Lake Agassiz sediment.

4.3 Paleomagnetic analysis of Lake Winnipeg core 122a

John W. King and Carol Gibson

Graduate School of Oceanography
University of Rhode Island, Narragansett, Rhode Island 02882

The Earth's magnetic field is a vector and can be completely characterized by three components at any point in space and time. The first component is the angle of deviation between geographic north and magnetic north in the horizontal plane or declination. The second component is the dip angle of the magnetic vector below the horizontal plane or inclination. The final component is the magnitude of the field or geomagnetic intensity. Geomagnetic secular variation (SV) is the "typical" temporal variation of the three components of the Earths' magnetic field in between polarity transitions. The peak-to-trough amplitudes of North American secular variation features for the last 12,500 yr are ≤ 40° for inclination, ≤ 50° for declination, and ≤ a factor of 3 for intensity (King et al., 1983a). Studies in North America indicate that secular variation patterns are reproducible on a regional scale of 3000-5000 km (King et al., 1983a; 1983b) and are very useful for stratigraphic correlation and dating.

The most powerful approach to obtaining accurate age determinations from lake sediments is the multidisciplinary use of SV, radiocarbon dating, and biostratigraphic (i.e. pollen) studies. A preliminary SV study of Core 122a from southern Lake Winnipeg used a modification of this approach. One AMS radiocarbon date of 4040±70 yr BP. (Vance, this volume) from a well-preserved seed located between 425-433 cm was available from this core. A paleomagnetic study was undertaken of Core 122a using the archive half and doing measurements of the whole core using a pass-through cryogenic magnetometer. The results of this study were compared and correlated to geomagnetic secular variation curves from Elk Lake, Minnesota (Sprowl, 1985) and the Northeastern United States (King, unpublished data) and age estimates were obtained.

The geomagnetic SV curves for inclination (Fig. 1) and declination (Fig. 2) from Elk Lake are dated by varve counts. On the other hand, the SV curves for inclination (Fig. 3) and declination (Fig. 4) for the Northeastern U.S. represent a composite of 12 cores from three lakes that are dated by 40 conventional radiocarbon dates.

The results obtained from Lake Winnipeg Core 122a are shown in Figure 5. The age estimate in varve years of the correlations with the Elk Lake record and the age estimates in radiocarbon years of the correlations with the Northeastern U.S. are also shown in Figure 5. A fairly consistent age model emerges from these SV age estimates and in addition the SV age model is consistent with the radiocarbon date. The large peak in the magnetization curve (J) shown in Figure 5 at ~ 4.2 m is at the unconformity between Lake Winnipeg and Lake Agassiz sediments. The age estimate for this unconformity in the southern basin of Lake Winnipeg is ~ 4000 years. The time averaged linear sedimentation rate in Core 122a from southern Lake Winnipeg is 0.105 cm/year. Future multidisciplinary studies using SV curves and radiocarbon dating should be able to determine ages of stratigraphic units and sedimentation rates at other sites within the lake.

REFERENCES

King, J. W., Banerjee, S.K., Marvin, J. and Lund, S.
1983a. Use of small-amplitude paleomagnetic fluctuations for correlation and dating of continental climatic changes; Palaeogeography, Palaeoclimatology, Palaeoecology, v. 42, p. 167-183.

King, J. W., Banerjee, S.K. and Marvin, J.
1983b. A new rock-magnetic approach to selecting sediments for geomagnetic paleointensity studies: application to paleointensity for the last 4000 years; Journal of Geophysical Research, v. 88, p. 5911-5921.

Sprowl, D. R.
1985. The paleomagnetic record from Elk Lake, Minnesota, and its implications; Unpublished Ph.D. thesis, University of Minnesota, Minneapolis, 145 p.

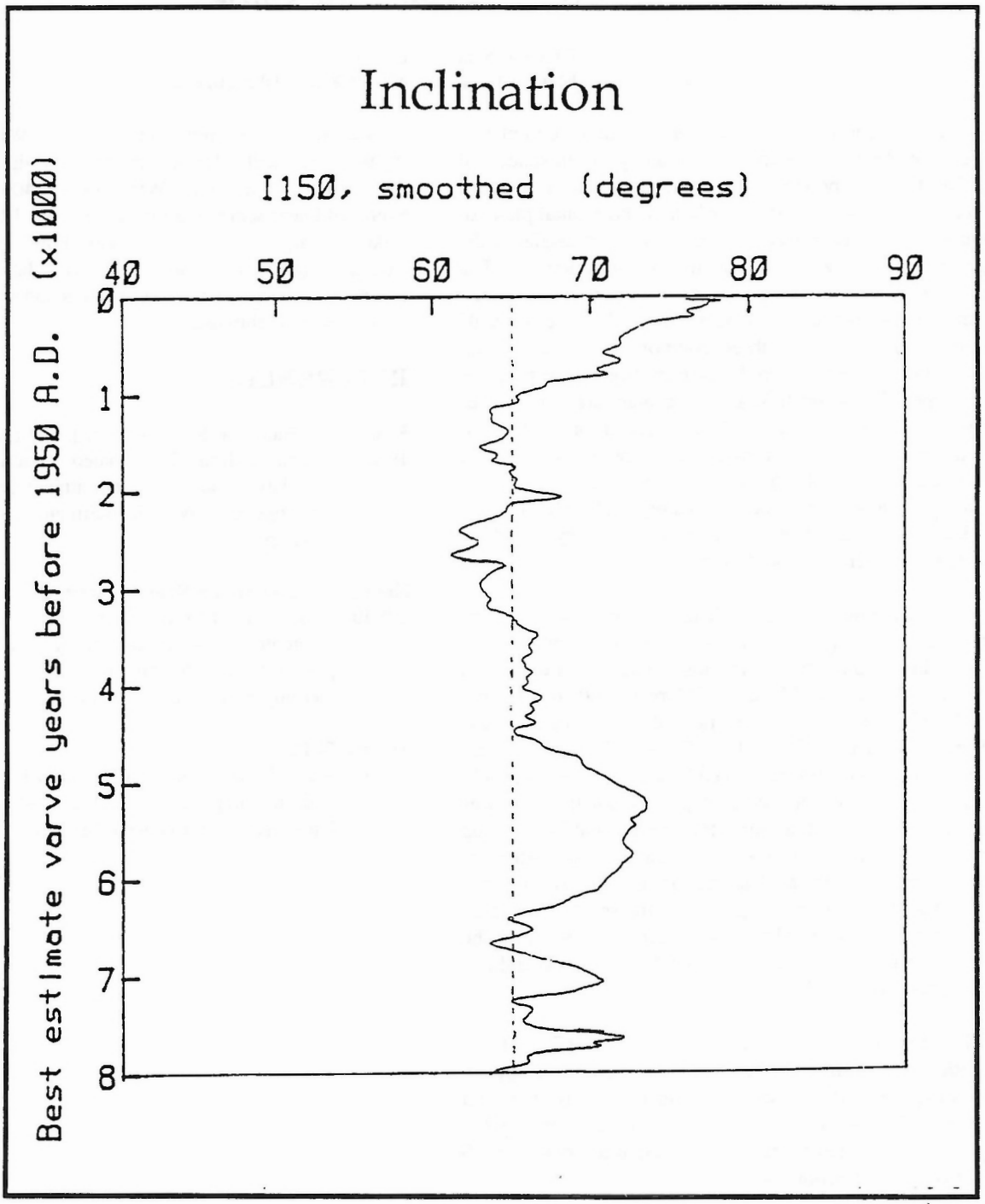

Figure 1. Elk Lake smoothed inclination vs. best estimate varve years. The dashed line is the expected axial geocentric dipole inclination of 65.1° for the site latitude (Sprowl, 1985).

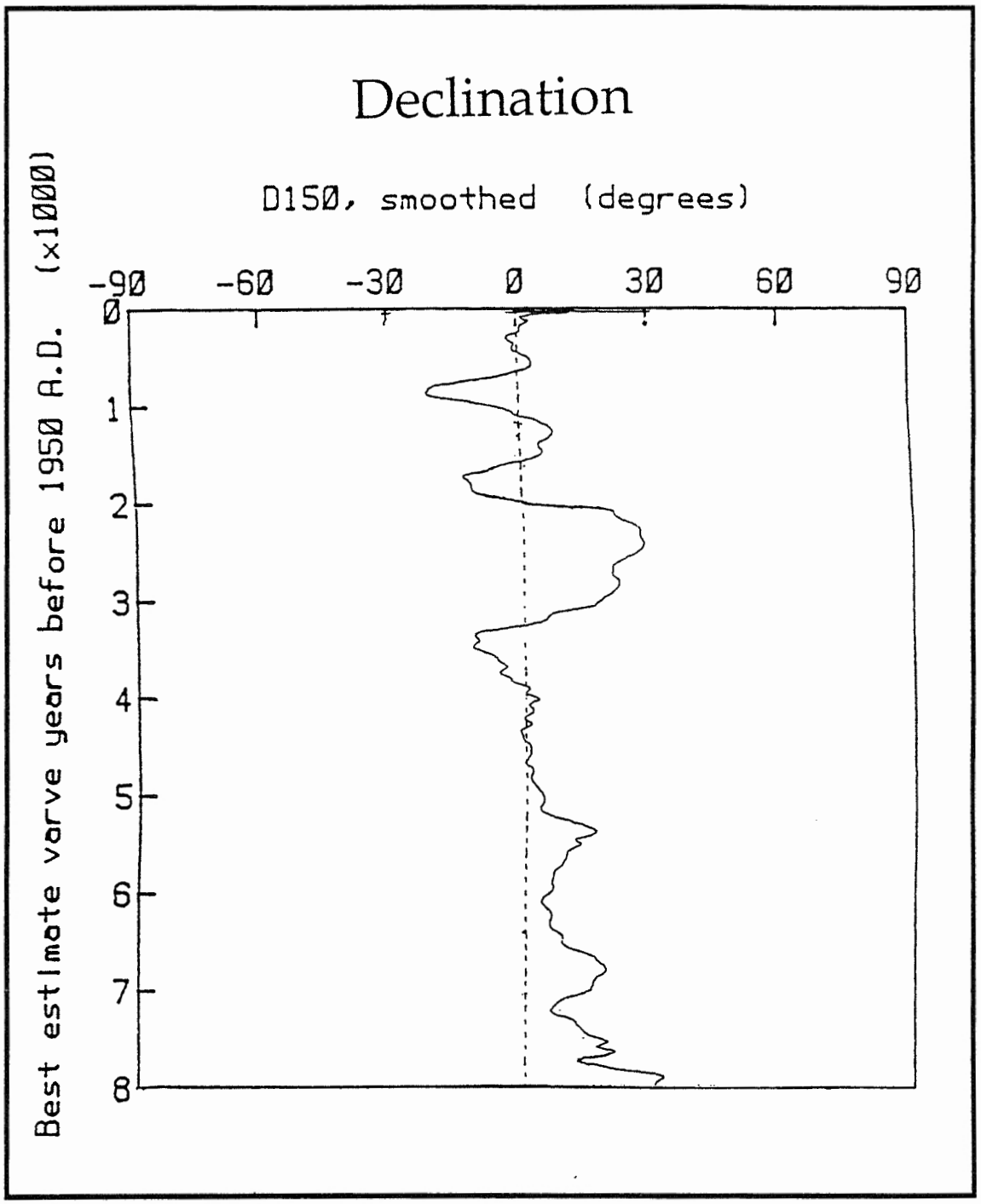

Figure 2. Elk Lake smoothed declination vs. best estimate varve years. The dashed line is the expected axial geocentric dipole inclination of 0° (Sprowl, 1985).

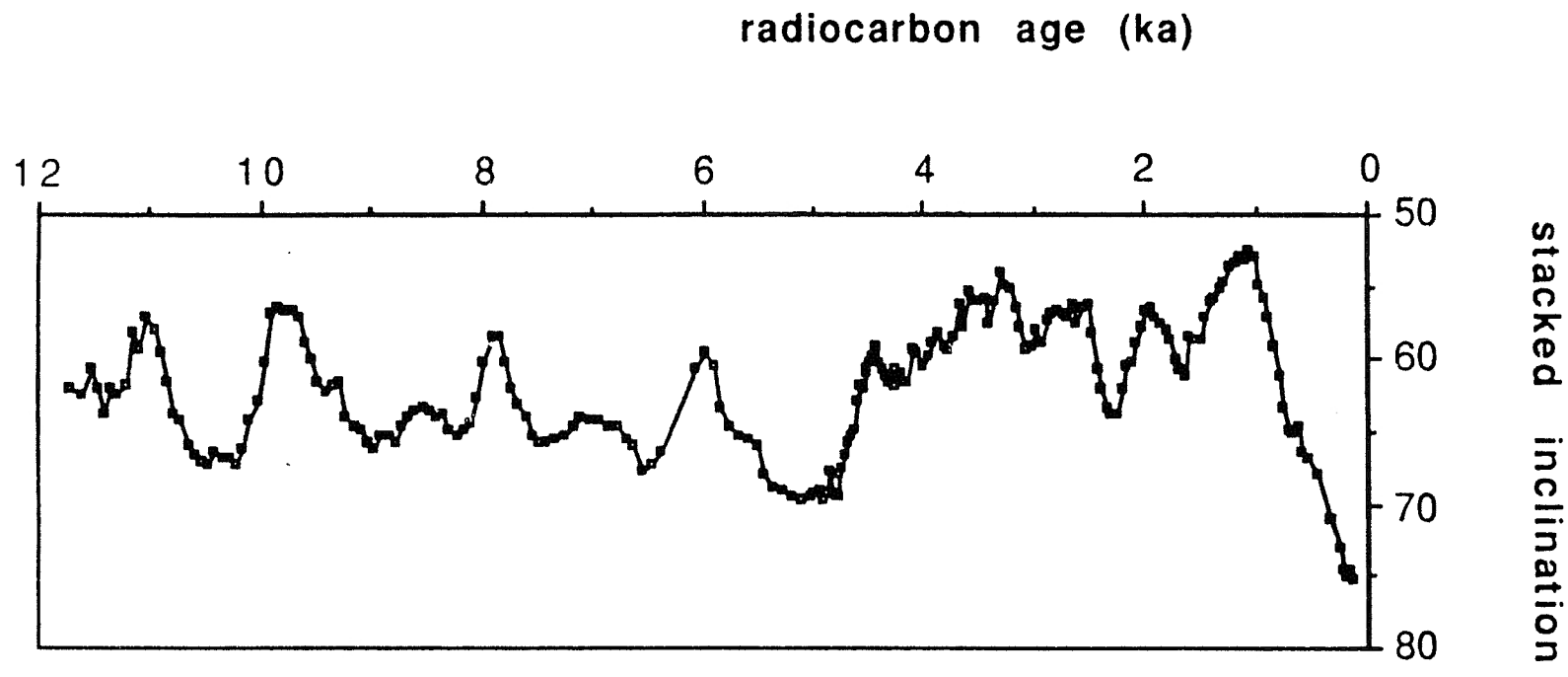

Figure 3. Stacked inclination record from Seneca Lake, N.Y., LeBoeuf, Pa., and Sandy Lake, Pa. vs. radiocarbon age.

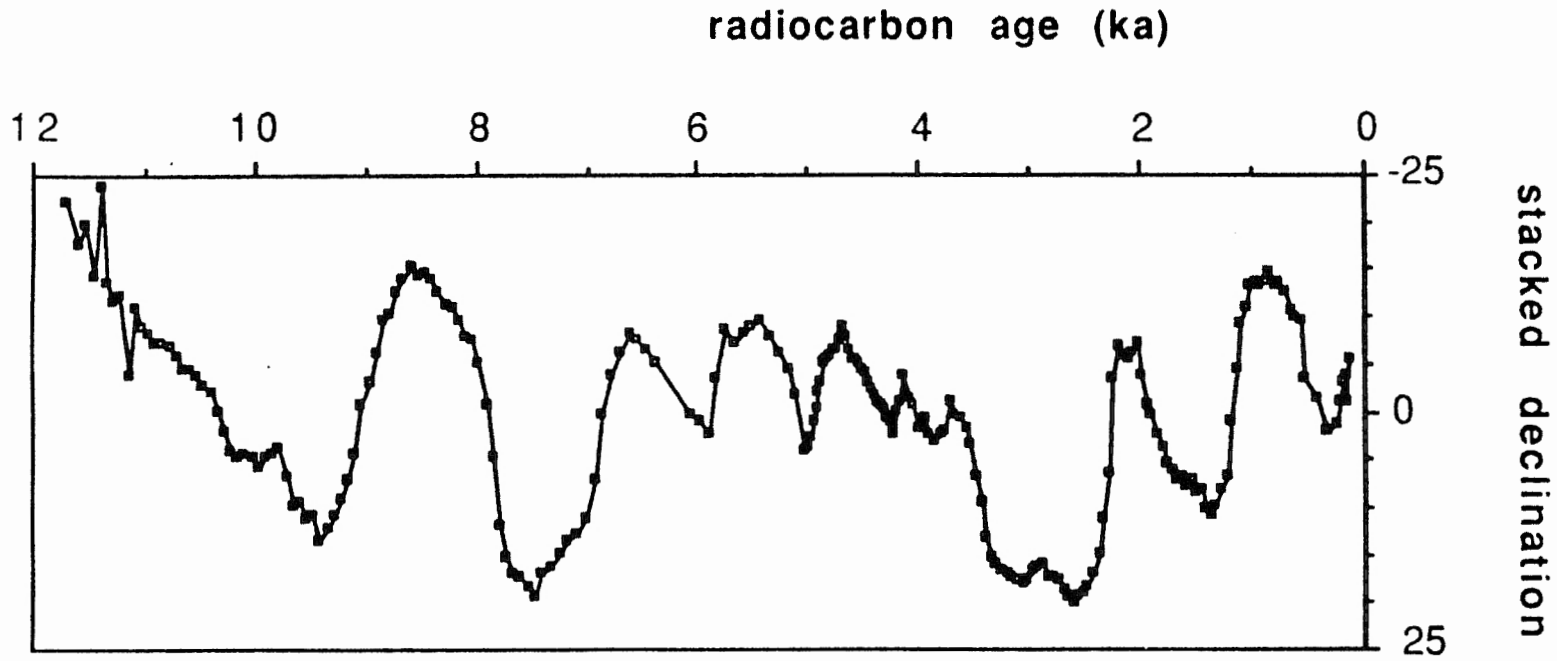

Figure 4. Stacked declination record from Seneca Lake, N.Y., LeBoeuf, Pa., and Sandy Lake, Pa. vs. radiocarbon age.

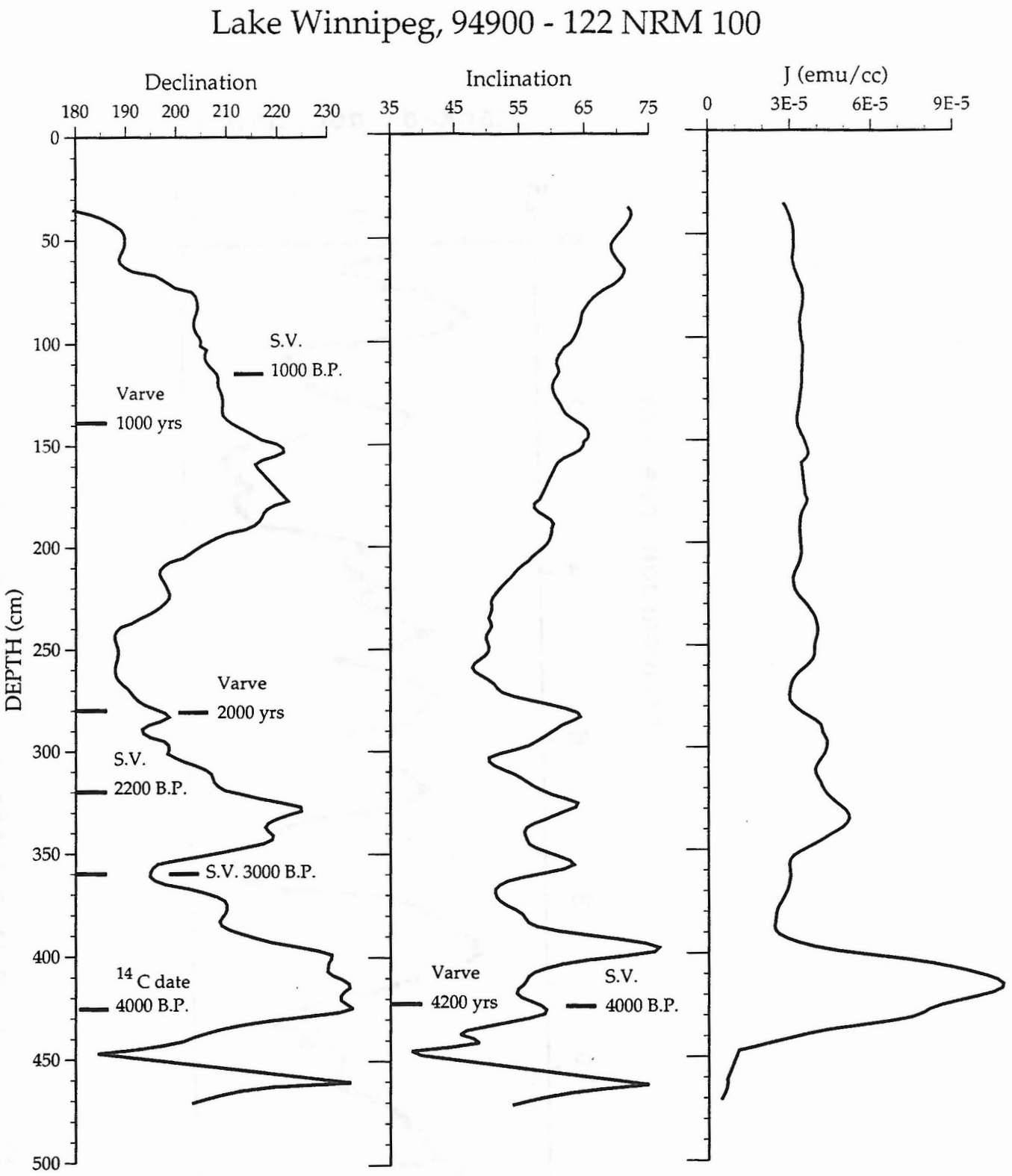

Figure 5. Declination, inclination, and magnetization curves for Lake Winnipeg Core 122 vs. depth. Age estimates are shown on the figure.

4.4 Bulk composition, texture, and mineralogy of Lake Winnipeg core and surface grab samples

W.M. Last

Department of Geological Sciences
University of Manitoba, Winnipeg, Manitoba R3T 2N2

INTRODUCTION

Western Canada contains millions of lakes ranging in size from small, ephemeral, prairie potholes and sloughs to several of the largest bodies of water in the world. These lakes play a pivotal role in controlling present land use characteristics of the region and are instrumental in helping to dictate the extent and speed at which future development will proceed. However, the lakes are extremely sensitive to natural changes brought about by both extrinsic factors, such as climate and vegetation change, and intrinsic factors, including basin filling and water chemistry changes. The lakes are also subject to human modification through increased agricultural, industrial and recreational activities. Although in the past decade a considerable effort has been made to assess chemical stress and the resultant impact on the lakes of western Canada, such determinations are generally complicated by the absence of information regarding the natural state and natural long-term fluctuations of the lacustrine environment. Consequently, the water resources manager must often make decisions based on incomplete, or in some cases erroneous, assumptions about natural conditions and variability. Distinguishing between natural changes and those perturbations caused by cultural stress is difficult but extremely important in order to correctly interpret any variation in critical environmental factors such as salinity, chemistry, sedimentation rates or biota in these lakes.

The sediment in a lake basin can provide a permanent historical record of changes that occur in the lake and catchment area because the basin is a sink for both dissolved and suspended material, including chemical and detrital contaminants. This sediment reflects both natural environmental changes, which can be related to climate, geology, hydrology, and vegetation, as well as those changes which are brought about by humans. In the past century, human activities such as ploughing, cropping, construction, paving, and drainage diversion have influenced erosion and sediment yield in nearly all of the watersheds of western Canada. Elevated levels of aqueous contaminants and pollutants have also resulted as a direct consequence of these and other human activities. By establishing a lake basin's sediment response both to long-term geological and climate-related phenomena and to more recent anthropogenic physical and chemical impacts, the environmental influence of humans can be discriminated from natural and perhaps longer cycles of climatically-induced conditions. The postglacial sediments contained in Lake Winnipeg, one of the largest lakes in western Canada, offer an excellent opportunity to examine the climatic/hydrological history of a large portion of western Canada as well as to assess the direct and indirect impact of human activities in the drainage basin and region.

PREVIOUS WORK AND OBJECTIVES OF THIS STUDY

Despite its obvious scientific and economic importance, very little is known about the sediments, sedimentary processes, and sedimentary history of Lake Winnipeg. Indeed, there are no formally published works describing or discussing the offshore sediments of this large lacustrine basin. What little is known about the sedimentary environment of the lake to date comes mainly from unpublished M.Sc. theses (Ward, 1926; Kushnir, 1971) and an unpublished government manuscript report (Brunskill and Graham, 1979). The latter provides data on grain size, mineralogy, and chemical composition of the surficial sediments from 50 offshore sites in the lake and descriptive-geochemical stratigraphic data from 13 short (1 m length) cores.

It is clear from these previous unpublished research efforts that the sediment record preserved in the Lake Winnipeg basin contains an abundance of paleolimnological, paleohydrological, and paleoclimatic data. The overall objective of this part of the project is to investigate, on a reconnaissance basis and in a relatively short period of time, a selected number of sediment parameters which are: (a) useful in characterizing and describing the lacustrine deposits and contemporary sedimentary and environmental conditions of the basin and watershed, and (b) potentially important in helping to reconstruct the developmental history of the lake and its watershed.

LABORATORY METHODS

General Comments

As part of a multi-disciplinary study of Lake Winnipeg, a total of 922 sediment samples were analyzed at the Lake Sedimentology Research Laboratory, Department of Geological Sciences, University of Manitoba, during the period November, 1994 to February, 1995 (Table 1). These samples include 548 samples from long cores (core lengths greater than 1 m), 341 samples from short cores (core lengths less than 1

m), and 33 samples of surface grab sediment, all acquired during August, 1994.

Short core samples were received from Dr. L. Lockhart (Freshwater Institute, Winnipeg) during the period October to December, 1994, whereas the surface sediment samples and all samples from the long cores arrived at the Sedimentology Laboratory between November 14 and December 6, 1994. All surface samples and long core samples were subsampled and any remaining material was sent to Dr. P. Henderson (GSC, Ottawa) for further processing.

The samples provided were analyzed for the following physical, mineralogical, and geochemical parameters: moisture content, organic matter content, total carbonate mineral content, detailed particle size spectrum, bulk mineralogy, detailed carbonate and evaporite mineralogy, detailed clay mineralogy, organic matter geochemistry, stable carbon isotopic ratio of organic matter, and detailed petrography (Table 2). All physical, mineralogical, and petrographic analyses were performed at University of Manitoba. Organic matter geochemistry and isotopic composition were determined by outside laboratories. The choice of analytical methods used to evaluate these sediment parameters was dictated by a combination of factors including: availability of equipment and technical expertise within the departmental laboratories, previous use of particular methods in other local or regional sediment studies, and the specific objective of the analysis.

Sampling Interval

One of the most important considerations in any sediment core subsampling scheme is the question of sampling interval. Ideally, the analytical subsampling should only be done after a chronostratigraphic framework has been established for the sequence (Engstrom and Wright, 1984; Dearing and Foster, 1986), however in practice this is not usually feasible. The number and density of a particular analysis per unit length of core controls the researcher's ability to identify temporal changes of the parameter in the sedimentary record. In general, the temporal resolution increases with a decrease in subsample interval. However, as shown by Bortleson (1970), a point is reached at which a further decrease in subsample interval will not yield meaningful results because of such interference factors as bioturbation, ion mobility, and turbulent mixing of the sediment.

The subsampling interval used in other lake sediment investigations is by no means standard. For example, Thomas and Soltero (1977) examined several chemical parameters of cores from Long Lake, Washington, using subsamples at every 5 mm. Because of very low sedimentation rates, Maher (1977) used a sampling interval as small as 2 mm in Lake Superior. Last and Schweyen (1985) used a 1 cm interval in the finely laminated late Holocene sequence of Waldsea Lake, Saskatchewan. Bortleson (1970) and Bortleson and Lee (1972) used analyses at every 3 to 5 cm for a one metre core and every 50 cm for a 10 metre core from Lake Mendota, Wisconsin. Previous Great Lakes sediment profile work (e.g. Kemp and Thomas, 1976) commonly used a 1 to 2 cm interval for the first 10 cm, a 5 cm interval for the next 20 cm and a 10 cm interval for the remainder of the core. Much of the grain size, mineralogical, and geochemical work on the well-studied Elk Lake sequence in Minnesota used a sample spacing of approximately 15 cm (Bradbury and Dean, 1993). In Lake Manitoba, immediately adjacent to Lake Winnipeg, a 1-2 cm interval was used for the upper 4 m of section and a 5 cm interval applied to the remaining part of the sequence.

Because of the large amount of core acquired as part of this project and the general lack of obvious visual stratigraphic variation, a rather coarse and uniform sampling interval of 10 cm was used for the long cores. The short cores were subsampled at either 1 cm or 2 cm intervals.

Bulk Composition

Moisture Content

The moisture content of the sediment was determined by heating a known weight of wet sediment at 75° C to 85° C for 24 to 36 hours and computing the weight loss. This weight loss was assumed to be due to evaporation of free pore water rather than to any loss of structural (lattice-bound) hydroxyl groups or to volatilization, oxidation, or other breakdown of organic matter. The weight loss was calculated and expressed as percent of water in the wet sediment. Replicate analyses were run every 25 samples.

Organic matter

An indication of the amount of organic matter present in the sediment was obtained by heating a portion of the oven-dried sediment to 450° C to 500° C for one hour (modified after Dean, 1974). The resulting weight loss, expressed as a percentage of the oven-dry weight, was taken to represent the loss due to ignition of organic material. Replicate analyses were run every 25 samples. From this loss on ignition value (L.O.I.), an estimate of the organic carbon content (O.C.) can be determined by applying the appropriate conversion factor (O.C./L.O.I. = 1/2.54; Last, 1980; Dean, 1981).

Total Carbonate Mineral Content

An approximation of the total amount of carbonate minerals present in the sediment was obtained by heating a portion of the oven-dried, organic-free sediment to 1000° C for one hour (modified after Dean, 1974). The resulting weight loss, expressed as a percentage of the oven-dry weight, was taken to represent the loss due to thermal decomposition of carbonate minerals. Although it is well accepted that the decomposition of various reduced sulfide minerals in the sediment can also contribute to this weight loss (Kovac, 1985; Kovac and Last, 1991), the general lack of pyrite and other sulfides in the X-ray

diffraction analyses suggests that this contribution from sulfides is negligible. The relationship between this loss on combustion value (L.O.C.) and the sum of all carbonate minerals from X-ray diffraction (Carbxrd) is: L.O.C. = 2.64 + 0.29 Carbxrd. Replicate analyses were run every 25 samples.

Textural Analysis

Particle size and textural data for the Lake Winnipeg sediment samples were acquired using a Galai 2010 PSA automated particle size analyzer. This equipment is based on the time of transition principle of laser analysis and should not be confused with light scattering or laser diffraction techniques used by other particle size instruments such as those manufactured by Malvern, Coulter, and Elzone (Agrawal et al., 1991; Jonasz, 1991). In the Galai PSA unit, a one micron laser beam is scanned in a circle at a fixed frequency through an aqueous solution containing the particles. The interaction pulses between the beam and the particles are detected by a photodiode detector. The time of interaction as the beam is obscured by each particle is used to produce particle size (diameter) information (Aharonson et al., 1986). In a comprehensive comparison study of many different particle size analytical techniques, Syvitski et al. (1991) shows that the Galai equipment provides a considerably more accurate and precise estimate of both grain size mean and mode for silt and clay-rich samples relative to other automated equipment.

The samples were pretreated with 3% hydrogen peroxide, disaggregated and subjected to ultrasonic vibration for three minutes. Because of the presence of gypsum in the samples, a 1% solution of Triton X100, rather than disodium hexametaphosphate (Calgon), was used as the dispersion agent. All samples were analyzed using a S.N.F. (signal normalization factor) of between 0.2 and 0.5, and a S.D.U. (solution density unit) value of between 1500 and 3000. Acrylic cuvettes (10x10x48mm) were used throughout and changed every 50 samples. A magnetic stirrer was used to assure uniform distribution of the grains during measurement.

Data were obtained for each 0.2 micron interval from grain diameters of 0.5 micron to 62.5 microns where possible or, if the sample contained sandy material, for each 0.5 micron interval from 0.5 micron to 300 microns. In this report the following grain size subdivisions are used: Clay: material finer than 3.9 microns in diameter; Silt: material having a diameter in the range of 3.9 to 62.5 microns; Sand: material having a diameter in the range of 62.5 to 2000 microns (Shepard, 1954). Replicate analyses were run every 25 samples and standards run every 100 samples. Laser alignment was checked every four hours. The length of runs (i.e. number of individual grains evaluated) was controlled by obtaining a 99% confidence level in the accumulated data.

From these raw data, various tabular, graphical, and statistical summaries for each sample were prepared, including: mean diameter (calculated by method of moments; Allen, 1981) and standard deviation; median diameter, mode, percent distribution table, range distribution table, and various cumulative and histogram graphs.

Mineralogical Parameters

General Comments

All mineralogical analyses were conducted using a Philips Automated Powder Diffraction System PW1710. Monochromated CuKα radiation with Ni filtering generated at 40 kilowatts and 20 milliamperes was used throughout unless otherwise noted. In all cases, the sediment samples were first pre-treated with 10% hydrogen peroxide, washed with distilled water, dispersed ultrasonically, and dried at room temperature prior to analyses.

Bulk Mineralogy

X-ray diffractometry (XRD) was used to qualitatively and quantitatively examine the mineralogy of the non-size-fractionated sediment of Lake Winnipeg. Randomly oriented XRD samples were prepared by mounting a finely-powdered sediment subsample on a standard frosted glass slide (further details on slide preparation can be found in Klug and Alexander, 1974, and Müller, 1967). One slide per sample was prepared and irradiated in one direction from 3° 2Θto 70° 2Θ. Replicate analyses were run every 25 samples. Scanning speed was generally at 2° 2Θ per minute and range C.P.S. was set at 200 counts per second. Other instrument settings were: 10° beam slit, 0.01 cm detector slit, 1 second measurement constant, and 0.01 step size.

Bulk-sediment mineral identification was done on the basis of d-spacing values using standard indices (A.S.T.M. X-ray Power Diffraction File; Chen, 1977). Mineral identification was aided by the use of an automated peak-match computer program (Marquart, 1986).

The abundance of the various minerals were interpreted from the diffractograms using the intensity of the strongest peak for each mineral as outlined by Schultz (1964) and Last (1980). Basically this technique involves comparing the mineral's peak intensity in the naturally occurring mixture to the intensity of a pattern run on a sample of the pure mineral. That is, in effect an "intensity factor" is applied to the mineral peak height. These intensity factors were derived from duplicate diffractometer traces of slides of the pure minerals and various mixtures of known quantity. Where possible, the minerals in the prepared slides were obtained from local or regional bedrock sources (Kovac, 1985). The intensity factors used in this study agree very well with those used by Schultz (1964), Last (1980), Howe et al. (1976), and Callender (1968).

Using this method, the sums of all the mineral constituents in all of the samples analyzed varied between 80 and 126% (mean = 109%). The sums were normalized to 100%. Replicate

analyses suggest that the precision of any individual mineral determination is ±8%.

It is important to note that this procedure is designed to derive relative percentage estimates of each mineral independently. That is, none of the individual mineral components were derived by taking the difference between the sum of the constituents and 100%. This, of course, is not the case with the semi-quantitative estimates for the individual clay mineral components. Nevertheless, the fact that the bulk mineral component data do constitute a closed data set (that is, the sum of all parameter values is equal to 100%), places some restraint on the interpretation of individual component trends and statistical analysis. However, because of the greater number of components in this data set compared to, for example, the clay mineralogy or textural (percent sand, silt, clay) parameters, the severity of these restraints is lessened.

Detailed Carbonate and Evaporite Mineralogy

X-ray diffractometry was used to examine the detailed carbonate and evaporite mineralogy and geochemistry of Lake Winnipeg samples. Randomly-oriented powdered mounts of the samples were irradiated from 7° 2Θ to 14° 2Θ, and 25° 2Θ to 38° 2Θ at a scanning speed of 0.125° 2Θ per minute. All other instrument settings and speeds were as described above.

This detailed X-ray diffraction analysis greatly enhanced the ability to decipher the presence of various evaporite minerals, and disordered calcite, nonstoichiometric dolomite, and other carbonate minerals in the sediment of Lake Winnipeg. The disordered species of calcite is recognized by a shift in the mineral's X-ray reflections toward higher diffraction angles (corresponding to smaller lattice spacing). The disordered and nonstoichiometric dolomite reflections were similarly displaced: toward lower diffraction angles if Ca-rich; toward higher angles if Mg-rich. The ordering reflections of the nonstoichiometric dolomite were also greatly reduced, however, this was not quantified in this study. Finally, the reflections for magnesite were almost always shifted toward lower angles. This is most probably due to slight hydration of this magnesium carbonate mineral (Last and De Deckker, 1990; Last, 1993).

An estimate of the amount of magnesium (or calcium) incorporation into the calcite or dolomite lattice was made on the basis of the amount of this shift in the X-ray diffraction peak of the strongest calcite reflection (104) using the curves presented by Goldsmith and Graf (1958) and the empirical relationship described by Hardy and Tucker (1988). The 3.34 Å (101) quartz reflection was used as an internal standard. Because both "normal" (3.03 Å) calcite and high-Mg calcite were sometimes present in the bulk samples, an approximation of the relative abundance of the two varieties was made according to Berner (1966). This technique basically is a comparison of areas under the two peaks (i.e. area under 3.03 Å peak + area under the higher angle peak = unity). This ratio was then applied to the percent total calcite derived from the fast scan to approximate the percentage "normal" calcite and the percentage high-Mg calcite in the bulk sample.

Although, as pointed out by Berner (1966) and Milliman and Bornhold (1973), the above techniques for evaluation of mole composition of MgCO3 in calcite or dolomite are not strictly reliable because of differences in diffraction efficiency, crystallinity, preferred orientation, and absorption characteristics, they are, nonetheless, the most commonly used non-chemical procedures for approximating percentages of the various species of disordered calcite and nonstoichiometic dolomite (Callender, 1968; Chen, 1977; Müller and Wagner, 1978; Magaritz and Kafri, 1981; Last, 1982). Hein et al. (1979) indicate that this technique has an accuracy of about one mole percent.

Clay Mineralogy

All samples to be examined for detailed clay mineralogy were size fractionated using standard laboratory wet sieve and centrifuging techniques as outlined by Folk (1968) and Tanner and Jackson (1947). Qualitative and semi-quantitative clay mineral analyses were conducted on the finer than 4 μm size fraction of the sediment using X-ray diffraction techniques. Initial quantitative experiments suggested that there is very little difference between the finer than 4 μm, finer than 2 μm, and finer than 1 μm size fractions. The finer than 4 μm fraction was chosen for routine evaluation because of the relative speed with which it was separated from the coarser, non-clay size fraction, and the convenience of this separation in the general scheme of textural/mineralogical analyses.

Diffractograms of the clay slides were irradiated on a Philips powder diffractometer using nickel-filtered CuK alpha radiation generated at forty kilowatts and twenty milliamperes. Further pertinent equipment settings included: 1° beam slit, 0.006 inch detector slit, 400 range counts per second, and two seconds times constant with the zero suppressor at zero. Traces were initially obtained (i.e. prior to treatment) from 2° 2Θ to 30°2Θ. The slides were scanned in one direction only at a rate of 0.60° 2Θ per minute. Oriented clay mineral mounts were prepared by allowing an aliquot of the aqueous clay-sized slurry to dry on a petrographic slide using the membrane filter-peel technique of Drever (1973). Frosted petrographic slides were used throughout this project to prevent the clay film from curling and cracking. This technique has been shown to reduce much of the error introduced by inherent particle size segregation (and, hence, mineral segregation) of the clay film.

Two additional slides for each sample were prepared from the clay-sized solution. One of the slides was placed in an ethylene glycol environment for at least 48 hours (Brunton, 1955). The other was heated to 550° C for one hour (Carroll, 1970). Both the heated and glycolated slides were irradiated in one direction from 3° 2Θ to 15° 2Θ; the heated slide was also run from 24° 2Θ to 27° 2Θ.

These X-ray diffraction patterns were used to qualitatively identify the main clay mineral components and to make semi-quantitative estimates of the relative amounts of the major clay mineral groups present: illite, expandable-lattice clay minerals (which include minerals of the montmorillonite group, vermiculite, expanding chlorites, and various mixed-layer species), kaolinite, and chlorite. Illite was defined on the diffractograms by a sharp peak at 10 Å (8.8° 2Θ) which was not affected by glycolation or heating. The expandable clay group was identified on the basis of its expanding lattice. After glycolation the material exhibits a peak at about 17 Å (5.19° 2Θ; variable peak depending on the exact composition of the expandable lattice material). However, heating at over 300° C will cause a shift in the peak position from 17 Å to 10 Å (Carroll, 1970). Furthermore, the glycolated and heated traces can be used to qualitatively determine the presence and type of mixed-layered clays in the overall expandable group (Thorez, 1975). The kaolinite and chlorite groups were identified by their combined, overlapping reflection at 7 Å (12.4° 2Θ) from the glycolated slide. These two components were separated on the basis of the relative difference in peak height of the 7 Å peak after glycolation and heating as outlined by Biscaye (1965) and Thorez (1975). The presence or absence of chlorite was also confirmed by the 14 Å (6.3° 2Θ) and 3.5 Å (25.2° 2Θ) peaks.

Semi-quantitative calculation of the main clay mineral groups was made using a method similar to that described by Biscaye (1965) using the weighting factors of: difference in intensities of the 10 Å glycolated versus heated peaks for the expandable layer clays; four times (4X) the intensity of the 10 Å (glycolated) peak for the illite group; and twice (2X) the 7 Å glycolated peak for kaolinite and chlorite. Qualitative evaluations of the mixed layer components were supplied according to the techniques outlined by Thorez (1975). The weighted peak intensities were summed with the weighted intensity of each group times 100 and divided by this sum giving the "percentage" of each component.

Although this technique is a very commonly used method for semi-quantitative evaluation of clay minerals and is also used by the Institute of Sedimentary and Petroleum Geology, North Dakota Geological Survey, Manitoba Department of Energy and Mines, and the Alberta Geological Survey, it must be emphasized that truly quantitative evaluations are not possible in complex clay mineral assemblages without use of very detailed and "non-routine" methods.

Geochemical Parameters

Stable Carbon Isotope Ratios

Stable carbon isotope ratios were determined using standard techniques as summarized by Pratt and Threlkeld (1984). A subsample of oven-dried bulk sample was powdered and treated with HCl to dissolve any carbonate mineral matter. The residue was washed, dried, and combusted at 1000°C. The δ13C of the resulting CO_2 gas was determined using a Finnigan MAT 251 isotope ratio mass spectrometer.

Organic Geochemistry

Standard Rock-Eval techniques (Espitalie et al., 1977; Kovac, 1985) were used to evaluate the geochemical characteristics of the organic matter of Lake Winnipeg sediment. Approximately 1 g of oven-dried bulk sample was powdered and dry-sieved to remove material coarser than 62 microns. A subsample of this material was then heated in a helium flushed system from 200° to 550° C at a uniform rate. The volatilized products were split and directed on one line to a flame ionization detector and on the other to a thermal conductivity detector. In addition, the total organic carbon (TOC) for an acid treated subsample of the material was determined using a coupled Hewlett-Packard C-H-N analyzer. The Hydrogen Index (HI) was calculated from the ratio of hydrocarbon gases generated at temperatures from 300° to 500°C/TOC; the Oxygen Index (OI) was determined from the ratio of CO_2/TOC. The organic matter type was approximated by plotting the HI versus OI on a modified van Krevelen diagram (Espitalie et al., 1977)

Petrography

A Cambridge Stereoscan 120 Scanning Electron Microscope (SEM) and a Kevex energy dispersive system (EDS) were used to investigate the micromorphology, composition, and detailed petrography of selected samples. Bulk sediment samples of 5 to 10 mm in diameter were prepared as outlined in Goldstein et al. (1984) and Trewin (1988), and were glued to standard SEM mounts with conductive silver paint. The mounts were coated with gold and palladium by sputtering. The normal operating conditions of the SEM/EDS equipment were 20 kV acceleration voltage at 20 mm working distance under less than 10^{-6} torr vacuum.

Results and Discussion

The Appendix provides a summary of the quantitative data obtained from Lake Winnipeg sediment up to the end of March, 1995. Indicated on the first table are a sequence number, site identifier, sampling midpoint depth in cm below the top of the core, moisture content, organic matter, total carbonate mineral content, and textural analysis. The second table includes normalized percentages for quartz, K-feldspar, plagioclase, amphibole, clay minerals, calcite, high-Mg calcite, protodolomite, dolomite, monohydrocalcite, aragonite, magnesite, thenardite, gypsum, and pyrite. The third table includes percent magnesium in calcite, magnesium in high-Mg calcite, calcium in protodolomite, calcium in dolomite, organic geochemistry reported as pyrolysis yields, and normalized clay mineralogy values as percent expandable lattice clay minerals, illite, as well as kaolinite plus chlorite. Much of this numerical stratigraphic information is also shown in graphical form in the attached Appendix.

Not included in these summary tables and graphs are the following data: (I) detailed particle size results for each sample (i.e., amount of sample per 0.2μm or 0.5μm size interval); (ii) graphical summaries (i.e., histogram and cumulative curves) for particle size results for each sample; (iii) raw X-ray diffraction data for each sample; (iv) list of minerals present in each sample; (v) Tmax for each sample analyzed for organic geochemistry; and (vi) results of SEM petrographic investigations. The data in items (I) through (v) consist of approximately 10,700 hardcopy pages (about 4.5 Mb on disk) and therefore cannot be provided with this report. However, these data are available on computer disks or hardcopy to any interested researcher. The data from item (vi) above (SEM/EDS petrographic results) are largely graphical in nature and will be presented in association with formal scientific publications. Finally, some of the geochemical isotopic analyses from the organic matter have not yet been received from the outside laboratory. These data will be made available to interested researchers as soon as they become available.

The data gathering phase of this part of the Lake Winnipeg project is nearly complete. With the exception of a relatively small number of isotopic analyses which are presently being undertaken, all analyses and data that were originally proposed to be collected, have been collected. Clearly, there is a large amount of physical, mineralogical, geochemical, and lithostratigraphic information now available for the Lake Winnipeg stratigraphic sequence. The interpretation phase of this part of the project is underway. As soon as the various long cores are correlated and a composite stratigraphic section compiled by Dr. K. Moran (GSC), interpretation of long-term fluctuations in the physical, mineralogical, and geochemical parameters detailed in this report can proceed. Similarly, as soon as the results of ^{210}Pb and ^{137}Cs chronostratigraphic studies being conducted by Dr. L. Lockhart are made available, interpretation of the fluctuations in the short cores can be undertaken.

ACKNOWLEDGMENTS

This work on Lake Winnipeg was made possible by grants from the Faculty of Science, University of Manitoba, the President's NSERC GRG Program, Challenge '94, and Career Start. The Lake Sedimentology Laboratory at University of Manitoba and my continuing work on lake sediments of western Canada is supported by operating grants from the Natural Sciences and Engineering Research Council of Canada, the Palliser Triangle Global Change Program, and the University of Manitoba. I wish to express a most sincere thank you to my three technicians, G. Carelse, R. Belsham, and A. Ross, who worked so hard during the four month period November-February to complete the preparation, processing, and analyses of these 1186 samples on schedule. The contents of this report and all the data collected as part of this work remain the property of WML who retains all copyright; no data included in this report nor any portion of this report may be copied without the permission of the author.

REFERENCES

Agrawal, Y.C., McCave, I.N. and Riley, J.B.
1991. Laser diffraction size analysis; in ed. J.P.M. Syvitski, Principles, methods, and application of particle size analysis, Cambridge University Press, Cambridge, p. 119-128.

Aharonson, E.F., Karasikov, N., Roitberg, M. and Shamir, J.
1986. GALAI-CIS-1 - A novel approach to aerosol particle size analysis; Journal of Aerosol Science v. 17, p. 530-536.

Allen, T.
1981. Particle size measurement (3rd Edition); Chapman & Hall, 423 p.

Berner, R. A.
1966. Chemical diagenesis of some modern carbonate sediments; American Journal of Science, v. 264, p. 1-36.

Biscaye, P.E.
1965. Mineralogy and sedimentation of recent deep-sea clay in the Atlantic Ocean; Geological Society of America Bulletin v. 76, p. 803-832.

Bortleson, G.C.
1970. The chemical investigation of recent lake sediments from Wisconsin lakes; Unpublished Ph.D. thesis, University of Wisconsin, Madison, 278 p.

Bortleson, G.C. and Lee, G.F.
1972. Recent sedimentary history of Lake Mendota, Wisconsin; Environmental Science and Technology, v. 6, p. 799-808.

Bradbury, J.P. and Dean, W.E.
1993. Elk Lake, Minnesota: evidence for rapid climate change in the north-central United States; Geological Society of America Special Paper 276, 336 p.

Brunskill, G.J. and Graham, B.W.
1979. The offshore sediments of Lake Winnipeg; Canadian Fisheries and Marine Service Manuscript Report No. 1540, 75 p.

Brunton, G.
1955. Vapor presssure glycolation of oriented clay minerals; American Mineralogist, v. 40, p. 124-126.

Callender, E.
1968. The postglacial sedimentology of Devil's Lake, North Dakota; Unpublished Ph.D. thesis, University of North Dakota, Grand Forks, 245 p.

Carroll, D.
1970. Clay minerals: a guide to their X-ray identification; Geological Society of America Special Paper 126, 80 p.

Chen, P.Y.
1977. Table of key lines in X-ray powder diffraction patterns of minerals in clays and associated rocks; Indiana Geological Survey Occasional Paper 21, 67 p.

Dean, W.E.
1974. Determination of carbonate and organic matter in calcareous sediments and sedimentary rocks by loss on ignition: comparison with other methods; Journal of Sedimentary Petrology, v. 44, p. 242-248.

1981. Carbonate minerals and organic matter in sediments of modern north temperate hard-water lakes; in eds. F.G. Ethridge and R.M. Flores, Recent and ancient nonmarine depositional environments: models for exploration, Society of Economic Paleontologists and Mineralogists Special Publication No. 31 p. 213-231.

Dearing, J.A. and Foster, I.D.L.
1986. Lake sediments and palaeohydrological studies; in ed. B.E. Berglund, Handbook of Holocene palaeoecology and palaeohydrology, John Wiley & Sons, New York, p. 67-90.

Drever, J.I.
1973. The preparation of oriented clay mineral specimens for X-ray diffraction analysis by a filter-membrane peel technique; American Mineralogist, v. 58, p. 553-554.

Engstrom, D.R. and Wright, H.E.
1984. Chemical stratigraphy of lake sediments as a record of environmental change; in eds. E.Y. Haworth and J.W.G. Lund, Lake sediments and environmental history, University of Minnesota Press, Minneapolis, p. 11-68.

Espitalie, J., Laporte, J.L., Madec, M., Marquis, F., Leplat, P., Poulet, J. and Boutefeu, A.
1977. Rapid method of characterizing source rocks and their petroleum potential and degree of maturity; Revue de l'Institut Francais du Petrole, v. 32, p. 23-42.

Folk, R.L.
1968. Petrology of sedimentary rocks; Hemphill, Austin, Texas, 170 p.

Goldsmith, J.R. and Graf, D.L.
1958. Relations between lattice constraints and composition of the Ca-Mg carbonates; American Mineralogist, v. 43, p. 84-101.

Goldstein, J.I., Newbury, D.E., Echlin, P., Joy, D.C., Fiori, C. and Lifshin, E.
1984. Scanning electron microscopy and X-ray microanalysis; Plenum Press, New York, 673 p.

Hardy, R. and Tucker, M.
1988. X-ray powder diffraction of sediments; in ed. M. Tucker, Techniques in sedimentology, Blackwell, Oxford, p. 191-228.

Hein, J., O'Neil, J. and Jones, M.
1979. Origin of authigenic carbonates in sediment from the deep Bering Sea; Sedimentology, v. 26, p. 681-705.

Hower, J., Eslinger, E.V., Hower, M.E. and Perry, E.D.
1976. Mechanism of burial metamorphism of argillaceous sediment, mineralogical and chemical evidence; Geological Society of America Bulletin, v. 87, p. 725-737.

Jonasz, M.
1991. Size, shape, composition, and structure of microparticles from light scattering; in ed. J.P.M. Syvitski, Principles, methods, and application of particle size analysis, Cambridge University Press, Cambridge, p. 143-162.

Kemp, A.L. and Thomas, R.L.
1976. Cultural impact on the geochemistry of the sediments of Lakes Ontario, Erie, and Huron; Geoscience Canada, v. 3, p. 191-207.

Klug, H.P. and Alexander, L.E.
1974. X-ray diffraction procedures for polycrystalline and amorphous materials; Wiley, New York, 966 p.

Kovac, L.J.
1985. Upper Cretaceous oil shales of Manitoba and Saskatchewan; Unpublished M.Sc. thesis, University of Manitoba, Winnipeg, 181 p.

Kovac, L.J. and Last, W.M.
1991. Mineralogy and geochemistry of Cretaceous oil shales in Manitoba; in eds. J.E. Christopher and F.M. Haidl, Sixth international Williston Basin symposium, Saskatchewan Geological Society Special Publication Number 11, p. 275-282.

Kushnir, D.W.
1971. Sediments in the South Basin of Lake Winnipeg; Unpublished M.Sc. thesis, University of Manitoba, Winnipeg, 183 p.

Last, W. M.
1993. Geolimnology of Freefight Lake: an unusual hypersaline lake in the northern Great Plains of western Canada; Sedimentology, v. 40, p. 431-448.

1982. Holocene carbonate sedimentation in Lake Manitoba, Canada; Sedimentology, v. 29, p. 691-704.

1980. Sedimentology and post-glacial history of Lake Manitoba; Unpublished Ph.D. thesis, University of Manitoba, Winnipeg, 688 p.

Last, W.M. and De Deckker, P.
1990. Modern and Holocene carbonate sedimentology of two saline volcanic maar lakes, southern Victoria; Sedimentology, v. 37, p. 967-981.

Last, W.M. and Schweyen, T.H.
1985. Late Holocene history of Waldsea Lake, Saskatchewan, Canada; Quaternary Research, v. 24, p. 219-234.

Magaritz, M. and Kafri, U.
1981. Stable isotope and Sr/Ca evidence of diagenetic dedolomitization in a schizohaline environment: Cenomanian of northern Israel; Sedimentary Geology, v. 28, p. 29-41.

Maher, L. J.
1977. Palynological studies in the western arm of Lake Superior; Quaternary Research, v. 7, p. 14-44.

Marquart, R.G.
1986. μPDSM: Mainframe search/match on an IBM PC; Powder Diffraction, v. 1, p. 34-36.

Milliman, J. D. and Bornhold, B. D.
1973. Peak height versus peak intensity analysis of X-ray diffraction data; Sedimentology, v. 20, p. 445-448.

Müller, G.
1967. Methods in sedimentary petrology; Hafner Press, New York, 283 p.

Müller, G. and Wagner, F.
1978. Holocene carbonate evolution in Lake Balaton (Hungary), a response to climate and impact of man; in eds. A. Matter and M.E. Tucker, Modern and Ancient Lake Sediments, International Association of Sedimentology Special Publication, v. 2, p. 55-80.

Pratt, L.M. and Threlkeld, C.N.
1984. Stratigraphic significance of 13C/12C ratios in mid-Cretaceous rock of the western interior, U.S.A.; in eds. D.F. Stott and D.J. Glass, The Mesozoic of middle North America, Canadian Society of Petroleum Geologists Memoir 9, p. 305 - 312.

Schultz, L.G.
1964. Quantitative interpretation of mineralogical composition from X-ray and chemical data for the Pierre Shale; United States Geological Survey Professional Paper 391-C, 31 p.

Shepard, F.P.
1954. Nomenclature based on sand-silt-clay ratios; Journal of Sedimentary Petrology, v. 24, p. 151-158.

Syvitski, J.P.M., LeBlanc, K.W.G. and Asprey, K.W.
1991. Interlaboratory, interinstrument calibration experiment; in ed. J.P.M. Syvitski, Principles, methods, and application of particle size analysis, Cambridge University Press, Cambridge, p. 174-193.

Tanner, C.B. and Jackson, M.L.
1947. Soil Analysis; Soil Science Society of America Proceedings, v. 12, p. 60-65.

Thorez, J.
1975. Phyllosilicates and clay minerals: a laboratory handbook for their X-ray diffraction analysis; Editions G. Lelotte, Dison, Belgium, 579 p.

Thomas, S.R. and Soltero, R.A.
1977. Recent sedimentary history of a eutrophic reservoir, Long Lake, Washington; Journal of the Fisheries Research Board of Canada, v. 34, p. 669-676.

Trewin, N.
1988. Use of the scanning electron microscope in sedimentology; in ed. M. Tucker, Techniques in sedimentology, Blackwell, Oxford, p. 229-273.

Ward, G.
1926. Seasonal variation in the composition of the Red River; Unpublished M.Sc. thesis, University of Manitoba, Winnipeg, 24 p.

Table 1. Total number of samples analyzed and depth range of samples

SAMPLE	DEPTH RANGE (cm)	TOTAL SAMPLES ANALYZED	TOTAL REPLICATES ANALYZED	TOTAL ANALYSES
Long Cores				
103	5-815	82	3	85
104a	5-365	37	1	38
104b	5-75	8	1	9
105	5-505	51	2	53
106	5-695	70	3	73
107	5-695	70	3	73
110a	5-225	23	1	24
113a	5-205	21	1	22
115	5-265	27	1	28
120	5-345	35	1	36
121	5-545	55	2	57
122	5-475	48	2	50
Subtotal - Long Cores		**527**	**21**	**548**
Short Cores				
1a (101)	1-42	42	2	44
2a (102)	1-42	41	1	42
3a (108)	1-45	45	2	47
4a (110)	1-43	43	1	44
5a (113)	1-40	40	1	41
6a (114)	1-41	41	2	43
7a (116)	1-38	38	1	39
8a (117)	1-40	40	1	41
Subtotal - Short Cores		**330**	**11**	**341**
Surface Sediment		**31**	**2**	**33**
Total		**888**	**34**	**922**

Table 2: Sediment parameters evaluated.

PHYSICAL PARAMETERS

- Moisture Content
- Organic Matter Content
- Total Carbonate Mineral Content
- Detailed Particle Size Spectrum (0.5μm to 60μm at 0.2μm resolution when possible or 0.5μm to 150μm at 0.5μm resolution)
- Sand, Silt, Clay Content
- Mean Grain Size and Standard Deviation
- Median Grain Size
- Modal Size

MINERALOGICAL PARAMETERS

- Qualitative Bulk Mineralogy
- Quantitative Bulk Mineralogy
- Qualitative Clay Mineralogy on Size-fractionated Samples
- Quantitative Clay Mineralogy on Size-fractionated Samples
- Detailed Carbonate Mineralogy and Geochemistry High-Mg Calcite, Low-Mg Calcite, Stoichiometric and well ordered Dolomite, Nonstoichiometric and poorly ordered Dolomite, Mg composition of Dolomite, Mg composition of Calcite
- Detailed Evaporite Mineralogy

CHEMICAL PARAMETERS

- Carbon stable isotope ratios of organic matter
- Organic matter Hydrogen Index
- Organic matter Oxygen Index
- Total Organic Carbon
- Peak yield temperature

Table 3. Number of samples analyzed according to analytical parameter.

SAMPLE	PHYSICAL PARAMETERS				MINERALOGICAL PARAMETERS				GEOCHEMISTRY		
	Moisture Content	Organic Matter Content	Total CO_3 Mineral Content	Detailed Particle Size	Qualitative Bulk Mineralogy	Quantitative Bulk Mineralogy	Detailed CO_3 Evaporite Mineralogy	Detailed Clay Mineralogy	Organic Matter Geochem	$\delta^{13}C$ of Organic Matter	SEM Petrog.
103	85	85	85	85	85	82	82	5	35	35	40
104a	38	38	38	38	38	37	37	8	0	0	0
104b	9	9	9	9	9	8	8	0	0	0	0
105	53	53	53	53	53	51	51	0	0	0	0
106	73	73	73	73	73	70	70	0	0	0	0
107	129	129	129	129	129	126	126	27	0	0	0
110a	24	24	24	24	24	23	23	23	0	0	0
113a	22	22	22	22	22	21	21	0	0	0	0
115	28	28	28	28	28	27	27	0	0	0	0
120	36	36	36	36	36	35	35	0	0	0	0
121	57	57	57	57	57	55	55	20	0	0	0
122a	50	50	50	50	50	48	48	0	35	35	0
1a (101)	44	44	0	44	44	42	42	0	0	0	0
2a (102)	42	42	0	42	42	41	41	0	0	0	0
3a (108)	47	47	0	47	47	45	45	0	0	0	0
4a (110)	44	44	0	44	44	43	43	0	0	0	0
5a (113)	41	41	0	41	41	40	40	0	0	0	0
6a (114)	43	43	0	43	43	41	41	0	0	0	0
7a (116)	39	39	39	39	39	38	38	0	0	0	0
8a (117)	41	41	41	41	41	40	40	0	0	0	0
Surface Sediment	53	53	53	53	53	51	51	0	0	0	0
Totals	998	998	737	998	998	964	964	60	70	70	40

4.5 Geochemistry of Lake Winnipeg sediments

P. J. Henderson

Geological Survey of Canada
601 Booth Street, Ottawa, Ontario K1A 0E8

INTRODUCTION

Thirteen long cores and thirty-one bottom sediment samples were collected in Lake Winnipeg as part of the cruise 94-900 of the CCGS *Namao* (Fig. 1). Core sites were selected in order to ground-truth seismostratigraphic facies and to provide a complete section of the sediments underlying the lake. These deposits have been interpreted as glacial, glaciolacustrine and post-glacial lacustrine sediments based on their seismic character (Todd and Lewis, this volume; Lewis and Todd, this volume). This sampling strategy ensured that the sediment collected in the cores will provide a record of the sedimentation history of the basin. Sediment composition reflects sediment input sources modified to varying degrees by post-depositional chemical and biochemical processes and is essential to understanding the history of the basin. The geochemistry, in conjunction with mineralogical, textural and organic data (Last, this volume), will provide detailed information on variations in the source area (provenance) of sediment associated with the various phases of lake history, as well as providing clues to environmental change in the basin and catchment areas, and post-depositional changes (diagenesis) within the basin.

The bottom sediment samples were collected in order to provide an even coverage of lakebed composition and biota. The composition of these samples reflects modern sedimentation in Lake Winnipeg and provides an opportunity to test for contamination from anthropogenic sources.

Lake sediments are composed of an organic and inorganic component. Organic matter may be either transported into (allochthonous), or produced within, the basin (autochthonous) and can complex or adsorb high concentrations of metallic ions. Other authigenic components, i.e. formed within the sediments or the water column, include biochemically precipitated carbonate minerals, amorphous and cryptocrystalline iron and manganese oxyhydroxides, sulphides and sulphates, phosphates and biogenic silica. The allogenic inorganic component consists predominantly of clays, feldspars, quartz and carbonate derived from erosion in the catchment area and deposited through glacial, glaciofluvial or lacustrine processes, or from air-borne particulate matter (dust). Metals may be bound to these clastic particles, particularly clays, and transported into the basin. The challenge in interpreting geochemical variations involves isolating effects resulting from physical factors and/or secondary reactions from those imposed by provenance. This paper will outline trends in sediment geochemistry within and between long cores collected in Lake Winnipeg, focusing on the distinctive characteristics of the post-glacial (Lake Winnipeg) and glacially derived (Lake Agassiz) deposits in the North Basin and South Basin of the lake. The geochemistry of the bottom sediment samples will also be presented and discussed briefly.

GEOLOGICAL SETTING AND PROVENANCE

The geological setting of the Lake Winnipeg area is described by Weber (this volume) and Bezys (this volume). The northern and eastern parts of the basin are dominated by Precambrian terrane consisting predominantly of granitoid rocks, greenstone belts and gneisses. Paleozoic carbonate rocks, primarily dolomites of the Williston Basin, underlie the western and southern parts of the basin. Carbonate rocks of similar composition also outcrop in the Hudson Bay basin to the north and northeast. Southwest of Lake Winnipeg and Lake Manitoba, Mesozoic sedimentary rocks, predominantly shales, overlie the Paleozoic sequence and form the Manitoba Escarpment.

Sediments on land adjacent to Lake Winnipeg include clay to the south, silty till to the west, and sandy till to the east (Manitoba Mineral Resources Division, 1981). During glaciation, the Lake Winnipeg area was covered by ice flowing from the north and northeast. Sediment transported by the glacier was deposited as till throughout the area with the composition varying depending on bedrock composition and glacial transport distance. As a consequence of ice flow from the northeast, carbonate rocks outcropping in the Hudson Bay Basin were transported across the Precambrian terrane of northern Manitoba (Nielsen and Thorleifson, this volume). During ice retreat, the entire area was inundated by proglacial Lake Agassiz, resulting in the deposition of thick sequences of glaciolacustrine sediments in depressions. The lake history is complex due to fluctuations in the ice margin, isostatic uplift and the resulting changes in outlets over time (McMartin, this volume).

Glacial sediments provided the main sediment source for former glaciofluvial and modern systems carrying sediment into the basin. Based on compositional studies from tills exposed onshore (Henderson, 1994; 1995), some generalities can be made on the chemical and mineralogical characteristics of glacial sediments derived from the various geological terranes in the area. Tills characteristic of Precambrian terrane on the west side of Lake Winnipeg are non-calcareous and

generally have higher concentrations of trace elements than those derived from Paleozoic carbonate rocks. Paleozoic derived tills are highly calcareous. Tills overlying the Paleozoic terrane in The Interlake region are all silty and calcareous with depressed trace element values except for localized anomalous areas (Nielsen, 1989). Tills derived from Mesozoic shales outcropping west of the lake are characterized by relatively high concentrations of zinc and vanadium (Schreiner, 1990).

LITHOSTRATIGRAPHY

Sediments cored in Lake Winnipeg are divisible into two major units, Lake Winnipeg and Lake Agassiz sediments (Lewis and Todd, this volume; Fig. 2). In the North Basin, the lower unit consists of a hard, compact, rhythmically bedded to banded, generally calcareous sequence. Rhythmites consist of fining upward silt/clay beds which range in colour from light grey brown to dark grey or grey brown and vary in thickness from millimetres to several centimetres. In general, rhythmites thin upcore. In South Basin cores, fining upward sequences are not developed. The sediments consist of light to dark brown laminated to faintly or distinctly banded hard clay. Red brown clay to silty clay beds up to 1 cm thick interrupt or dominate the laminated sequence. Occasional pebbles, interpreted as dropstones, are also present. This sequence is interpreted as the deposits of Glacial Lake Agassiz. Rhythmites are regarded as the products of density underflows derived directly or indirectly from the glacier. As a consequence, the composition of the coarser portion of the rhythmite should provide an indication of the composition of sediment transported by the ice. The finer fraction may also represent sediment suspended in the water column as well as material derived from more diverse sources. At present, the cause of laminated sediment in the South Basin is unclear.

The upper sequence consists of a massive to diffusely-banded grey to grey brown mud. It is soft and generally non-calcareous. Occasional thin sand beds are present. The contact between this unit and the underlying sediments is an unconformity (Todd and Lewis, this volume) on which coarser material and shells occur in some cases. This unit represents post glacial deposition in Lake Winnipeg. The sediment is thought to be derived from rivers flowing into the lake, shoreline erosion, the atmosphere, biogenic sources and anthropogenic sources. The presence of ice scours on the lakebed (Todd and Lewis, this volume) suggests the sediment may be highly reworked locally.

SAMPLING AND ANALYTICAL METHODS

All cores were sampled at 10 cm intervals. A total of 556 sediment samples were collected from approximately 1/4 of the core over a 2-3 cm interval. In sampling, no attention was paid to grain size variations in rhythmite sequences in the Lake Agassiz sediments or diffuse banding and colour variations in the Lake Winnipeg sequence, although well-defined erosional contacts were respected.

Subsamples of both the long cores and bottom sediment samples were analyzed by Chemex, Inc., of Mississauga, Ont. Approximately 1 g of the material was analyzed after a total (nitric-perchloric-hydrofluoric acid) leach. Al, Ba, Be, Bi, Ca, Co, Cu, Cr, Cd, Fe, K, Mg, Mn, Mo, Na, Ni, P, Sr, Ti, V, W, and Zn concentrations were determined using ICP-AES (inductively coupled plasma-atomic emission spectrometry). Ag and Pb concentrations were determined by AAS (atomic absorption spectrophotometry). In addition, As was analyzed by AAS following nitric-aqua regia partial digestion. Analytical precision and accuracy was monitored by analyzing laboratory standards with each submitted batch of samples. The analytical results for the long cores are presented in Appendix 1. Results from the analyses of bottom sediment samples are given in Appendix 3.

OVERVIEW OF LONG CORE DATA

Lake Winnipeg consists of two main basins separated by The Narrows. Cores 103 to 107 and 110 were collected in the North Basin, Core 113 in The Narrows, and Cores 115 and 119 to 122a in the South Basin (Fig. 1). Geochemical analyses of sediment collected from cores show subtle and, in some cases, dramatic differences in values within both the Lake Winnipeg and Lake Agassiz sequences. These differences may correspond to interpreted seismic and sedimentological facies. This discussion will concentrate, initially, on the gross geochemical character of the sediments, outline the geochemical variation in cores collected throughout the entire Lake Winnipeg basin and, finally, focus on a more detailed examination of the distribution of specific elements in the Lake Winnipeg and Lake Agassiz sediments.

Correlations

Multi-parameter correlations of analytical results from both Lake Winnipeg and Lake Agassiz sediments for each core vary in strength and character. Two basic associations have been recognized, regardless of sediment origin (Appendix 2).

The first association is defined by the strong positive correlation of Al with most elements, particularly Ba, Co, Cr, Cu, Fe, K, Ni, P, Ti, V and Zn, and a weak to negative correlation with Ca, Mg, and, in some cases, Sr. Strong internal correlations are commonly present within this major group of elements and fair to good correlations may be present with organic content. There is no apparent relationship to a particular size fraction in most cases. The positive association of elements is interpreted as primarily representative of the silicate minerals, particularly clays and feldspars, but may also include secondary minerals and associated trace elements. Using the total leach, sample digestion is complete for most elements. Bulk analyses of this type are best for elements ascribed to a single sedimentary component, e.g. Na and K,

which occur predominantly in lattices of silicate minerals and can be associated with detrital mineral particles derived primarily from the Precambrian terrane. Analyses are less reliable for elements derived from several different components, e.g. Fe and Mn, which may occur as absorbed metals associated with oxyhydroxides, carbonates and clay minerals as well as in the lattices of silicate minerals (Engstrom and Wright, 1984).

The second association is defined by the positive correlation of Ca with Mg and, commonly, Sr and Na, and the negative to poor correlation of Ca with most other elements (Appendix 2). This elemental association is interpreted as largely representative of the carbonate component of the sediment. Correlations between Ca concentrations and carbonate content as determined by Last (this volume) are strong and support this interpretation. In this study, however, no distinction has been made between clastic, authigenic or biogenic carbonate.

Gross Geochemical Trends

Regional trends are apparent on plots which display data from all cores collected in Lake Winnipeg with the exception of core 119 (Fig. 3). For the purposes of illustration, the cores are organized systematically from north to south (north at top); for each core, the geochemical variation is shown from top to bottom; breaks between cores are emphasized with blank rows, although cores 122a and 115 have internal blanks caused by insufficient sample material for analysis. It is important to note that the relative proportion of sediment representing the Lake Winnipeg and Lake Agassiz sequences varies between cores (Fig. 2).

Calcium

The most extreme variation in sediment geochemistry is shown by the distribution of Ca (Fig. 3a) and Mg. The Ca concentration has been shown to be associated with the carbonate content of the sediment and, therefore, may be biogenic, authigenic, or derived from a Paleozoic source. For all cores, Ca content decreases upcore. This gradational change is associated with the transition from Lake Agassiz (higher Ca values) to Lake Winnipeg sedimentation. On a basin wide scale, Ca values are consistently higher in the northern cores (104-106) in both sedimentary facies. In the South Basin, the Ca content at the base of core 122a and, to a lesser extent, core 121 is comparable to that observed at the base of the northern cores.

Potassium

The distribution of K within the cores is shown in Fig. 3b. As mentioned earlier, K occurs predominantly in lattices of silicate minerals and will provide an indication of the relative change in the allogenic component of the sediment associated with these detrital minerals which are derived primarily from the Precambrian terrane. There is a slight tendency for K values to increase upcore although no consistent pattern is present. The most striking feature of K distribution is the consistently higher values present in cores collected in the North Basin, and at the base of core 120 (Lake Agassiz sequence) in the South Basin. This general pattern of K distribution is similar to that observed in Na, and suggests that sediments in the North Basin have a higher detrital component than those of the South Basin.

Manganese

The variation in Mn content is shown in Fig. 3c. Mn in known to occur as oxides or hydroxides and, under normal oxidizing conditions, is concentrated at the sediment-water interface in the lacustrine environment (Rose et al., 1979). Surface sediments, however, may not be recovered by a piston core. In most Lake Winnipeg cores (with the possible exception of cores 103, 107, 115 and 121), Mn concentrations are elevated at the top of the core which suggests complete to near complete recovery of the section. The presence of excess Pb_{210} in the upper samples of core 103 (Lockhart, pers. comm., 1995) supports this suggestion. The Mn content within most cores is also elevated at the interpreted top of the Lake Agassiz sequence and tends to decrease down-core. This suggests a redox front may be or have been present at the top of the Lake Agassiz sequence. In general, the Mn content of sediments in the South Basin is higher than the North Basin in both sedimentary facies.

Vanadium

The V distribution within the cores is shown in Fig. 3d. In most cores, the V content is elevated in the Lake Winnipeg sequence and increases upward (Fig. 3d). On a basin-wide scale, however, V concentrations are generally higher in the South Basin in all (or parts of all) sedimentary facies. This may be a function of the organic content which has a similar regional distribution pattern in the lake sediments (Last, this volume), or may be due to provenance. High V concentrations are associated with Cretaceous shales outcropping in the Manitoba Escarpment west of Lake Winnipeg (Schreiner, 1990); however, the element is also associated with Fe, Mn oxides and hydroxides and organic matter (Rose et al., 1979).

LAKE WINNIPEG SEQUENCE

General Geochemistry

The geochemistry of Lake Winnipeg sediments follows the geochemical trends discussed above and reveals more specific aspects of the chemical stratigraphy. Based on the analytical results (Appendix 1), concentrations of Ca, Mg, K, Na, Cu, Ni, and Sr in the Lake Winnipeg sequence are elevated in some or all cores collected in the North Basin; Mn and V concentrations are elevated in those collected in the South Basin (Fig. 4).

Although Ca and Mg concentrations increase upward in the Lake Winnipeg sequence in all cores, the values of these elements are markedly elevated throughout the northernmost cores (cores 104-106) (Fig. 4). Ca values range from approximately 2-5% and are only exceeded in samples collected near the base of the Lake Winnipeg sediments in cores collected further south. The general distribution pattern of Mg and Sr is similar. The Ca source is linked primarily to the carbonate content of the sediments as indicated by the strong positive correlation between Ca and carbonate concentrations (Appendix 2); however, this carbonate may be biogenic or derived from a Paleozoic source. Shells have been observed near the base of the Lake Winnipeg sequence in these cores and, overall, there is a poor correlation of Ca with Mg, which suggests the biogenic component may be significant. A source of Paleozoic carbonate debris transported from the Hudson Bay Lowlands is also present in deposits north and northwest of Lake Winnipeg. A major source of Lake Winnipeg sediments may be reworking of these glacigenic and glaciolacustrine sediments. Consequently, the unusually high concentrations of Ca, Mg and Sr throughout the northernmost cores may be a function of the accessibility of Paleozoic-derived debris.

The decrease in Ca content upcore through the Lake Winnipeg sequence has been observed throughout the basin. This depletion occurs in conjunction with a decrease in total carbonate, calcite and dolomite (Last, this volume) and ostracodes (Rodrigues, this volume). Whether this Ca depletion is primary, due to non-deposition, or secondary, due to dissolution, is unknown. If secondary, it suggests that the sediment/water interface has become undersaturated with respect to carbonate in most of the lake.

With the exception of core 110a, K, Na, Cu, and Ni (and to a lesser extent Ba and Cr) values are all higher in cores from the North Basin. This group of elements is generally associated with a Precambrian source terrane; high K and Na with feldspars and high trace metals with clay and other primary minerals. This indicates a higher allogenic component in sediments of the North Basin compared to those of the South Basin. This conclusion would also suggest that Lake Winnipeg sediments in the North Basin are siltier, although this is not obvious from textural data (Last, this volume). Enrichment of Precambrian-derived elements in the North Basin is not unreasonable since the basin lies south of or on the Paleozoic/Precambrian contact and is surrounded by surficial sediments derived from ice flow across this terrane.

Both Mn and V concentrations are elevated within the Lake Winnipeg sediments of the South Basin. The geochemistry of both these elements is complex. Mn can be associated with Mg and Fe in mafic and ultramafic igneous rocks derived from Precambrian terrane, siderite ($FeCO_3$) from Paleozoic terrane, or may form secondary (Fe, Mn) oxides or hydroxides which tend to adsorb trace metals. Although Mn correlations vary in the cores collected in the South Basin (Appendix 2), there is no indication of a positive association with the carbonate component; associations are primarily with Fe and trace metals and, in the case of core 115 and 122a, with Al and Ba as well. This suggests Mn occurs predominantly as oxides or associated with clay minerals and that the authigenic component of the Lake Winnipeg sediments in the South Basin is higher than the North Basin.

A similar conclusion may be derived from the V distribution in the cores. V is associated with Fe, Mn-oxides and organic matter, as well as Cretaceous shales outcropping on the Manitoba Escarpment west of the lake. Because the Assiniboine River drains the Cretaceous terrane and flows ultimately into Lake Winnipeg, a source of V is present in the South Basin. The available V and other trace elements may be coprecipitated with or adsorbed on Mn-oxide minerals or organic matter. Lake Winnipeg sediments in the South Basin do have a higher organic content than those of the North Basin (Last, this volume). However, a strong positive correlation is not evident between V and organic matter in all of these cores. Correlations are primarily with Al, Fe, K, Ti and trace metals which suggests an association of V with Fe/Mn oxides and clay minerals as indicated by the Mn distribution.

North Basin

Where thick sequences of the Lake Winnipeg sequence are preserved in the North Basin, two sedimentary (and seismic) facies have been recognized (Todd and Lewis, this volume; Lewis and Todd, this volume) (e.g. cores 103, 106, 107). The lowermost facies consists of soft, banded, dark grey to grey brown silty clay with diffuse millimeter to centimeter-scale layers of lighter grey clay or, as in the case of core 106, silt and fine sand. This unit is non- to weakly calcareous. Small shells or shell fragments have been observed within this sediment (see core 106) and associated with the erosional contact at the base of the Lake Winnipeg sequence. The lower unit grades upward to massive, soft, brown grey silty clay. The upper facies is generally non-calcareous near the sediment/water interface, becoming slightly calcareous with depth.

The most complete Lake Winnipeg section is preserved in core 103 (Fig. 5). Within this core, the most pronounced geochemical variations are present between Lake Agassiz and Lake Winnipeg sediments. More subtle differences are recognized between facies within the Lake Winnipeg sequence. In the lower banded unit, Ti, V and Zn concentrations, in addition to those of other trace metals, are somewhat depressed. This subtle geochemical depletion, coupled with the obvious sedimentological difference, indicates a separate depositional regime which may be linked to an early stage in the development of the lake. In the early Holocene, drainage from the west via the Saskatchewan River was routed north through the Minago River Channel (McMartin, this volume) and bypassed Lake Winnipeg. During this phase, those elements associated with Cretaceous sediments to the west were not transported to the North Basin and, consequently,

concentrations would be lower than the later phase when the river drained into the North Basin via Cedar Lake.

South Basin

Only one sedimentary facies has been recognized in Lake Winnipeg sediments in the South Basin. The unit is composed of soft dark brown to grey brown silty clay which becomes firmer at depth. It appears somewhat mottled with discontinuous lenses and/or laminations defined primarily by colour variations. Isolated silty or fine sand laminations or lenses are present throughout but more common in the lower part of the section. The upper part of the unit is non-calcareous; the lower part weakly to moderately calcareous.

The longest section of Lake Winnipeg sediment is preserved in core 121 (Fig. 6). The geochemical variation for some elements is shown in conjunction with the variation in organic content (Last, this volume). As with the previous core, the most pronounced difference is between sediments of the Lake Agassiz and Lake Winnipeg sequence. Within the Lake Winnipeg section, the organic content and concentration of Ti, Mn, Zn and V (as well as other elements not shown) is seen to increase upcore; Ca values decrease upcore. Correlations between organic content and elements exhibiting a similar distribution pattern are fair to weak, however (Appendix 3), which suggests that concentrations of these elements are not solely a function of organic content and may, in part, be related to other factors, e.g. provenance or texture.

LAKE AGASSIZ SEQUENCE

North Basin

Three seismic sequences have been recognized in the Lake Agassiz sediments in the North Basin (Todd and Lewis, this volume). Core sites were chosen in order to sample sediments representative of each package and develop a complete section. Table 1 summarizes the general stratigraphic position of each core as defined by Todd and Lewis (this volume), sediment description (Lewis and Todd, this volume) and geochemical composition. Because the character of the Lake Agassiz rhythmite sequences varies, the average geochemical composition has also been calculated for each unit. No systematic pattern was recognized. Rhythmites vary in thickness from millimeters at the base of the section, to several centimeters in the central part of the section, and one centimeter or less in the upper part of the section. Compositional variation appears related predominantly to differences in the relative proportion of silt and clay within the rhythmite sequences and is best seen in the Ca distribution (Fig. 7). The recognized variation in sedimentation style throughout the sequence suggests some fluctuations in the ice margin during deglaciation.

South Basin

The Lake Agassiz sequence in the South Basin differs from the north in several respects. The sediment is composed of thin beds or laminations with no evident textural variation. These laminations tend to be thin (<1mm) and vary in colour from light and dark brown grey to orange. They may be interspersed with calcareous silty laminations and/or thick orange brown clay bands. Erosional surfaces and minor faulting is evident within the sequence. With the exception of the silty layers, the sediment is non- to weakly calcareous. The proposed section through the Lake Agassiz sequence is shown in Table 2, although the stratigraphic position of the Lake Agassiz sequence in core 122a is undefined. Sedimentological and geochemical variations similar to those seen in the North Basin are present.

BOTTOM SEDIMENT SAMPLES

The results for the geochemical analyses of Lake Winnipeg bottom sediment samples collected by Ponar dredge are shown in Appendix 3. Results are generally similar to those observed in the upper Lake Winnipeg sequence of the cores. Two sites in the South Basin (33 and 40) have anomalously low trace element concentrations which are believed to be related to the sandy texture of these samples. In general, Ca, Mg, Sr and Na and K concentrations are higher in bottom sediment samples collected in the North Basin; As, Mn, Pb, V and Zn concentrations are higher in samples from the South Basin. Higher concentrations in the South Basin may relate to contamination entering Lake Winnipeg via the Red and Winnipeg Rivers.

SUMMARY

Two distinct sediment sequences have been identified in Lake Winnipeg. The lower sequence was deposited in Glacial Lake Agassiz; the upper in Lake Winnipeg. These units are distinguishable by seismic, sedimentological and compositional criteria. The geochemistry of the sediments also reflects this two-part stratigraphy, as well as showing variation between the North and South Basins of Lake Winnipeg.

The Lake Winnipeg sequence is characterized, in general, by a decrease in Ca and associated elements upcore. Lake Winnipeg sediments in the North Basin exhibit: (a) a relatively high Ca, Mg and Sr content, particularly in the northern cores, which is believed to be related to Paleozoic debris transported from the Hudson Bay basin; (b) a relatively high K and Mg content suggesting a higher allogenic component than sediments in the South Basin; © a depletion in V at the base of the Lake Winnipeg section which may be related to divergence of sediment inflow from the west when the Saskatchewan River bypassed Lake Winnipeg and flowed north through the Minago River channel.

Lake Winnipeg sediments in the South Basin are characterized by high concentrations of V, Mn and other trace elements. This suggests the geochemistry is influenced more by secondary processes than sediments in the North Basin. High V values may be related to erosion and fluvial transport of sediment derived from the V-enriched Cretaceous rocks in the Manitoba Escarpment through the Assiniboine River which drains ultimately into the South Basin of Lake Winnipeg.

The geochemistry and sedimentology of Lake Agassiz sediments shows no systematic pattern upcore. The geochemistry of the Lake Agassiz sequence in the South Basin suggests the deposits are derived primarily from a Precambrian terrane or have been leached of carbonate. The sedimentation style is different than that observed in the north and the implications of this are not understood.

ACKNOWLEDGMENTS

This study is completely dependent on the co-operation of all members of the Lake Winnipeg project. I would particularly like to thank Harvey Thorleifson and Erik Nielsen for involving me in the project; Bill Last for sharing data on sediment composition and texture; Mike Lewis and Brian Todd for planning and conducting the coring; and Kate Moran for heading the core sampling team. Thanks also to Patti Lindsay for co-ordinating sample analyses.

REFERENCES

Engstrom, D.R. and Wright, Jr., H.E.
1984. Chemical stratigraphy of lake sediments as a record of environmental change; in eds. E.Y. Haworth and J.W.G. Lund, Lake sediments and environmental history: studies in palaeolimnology and palaeoecology in honour of Winifred Tutin, University of Minnesota Press, Minneapolis, Minnesota, p. 11-67.

Henderson, P.J.
1994. Surficial geology and drift composition of the Bissett-English Brook area, Rice Lake Greenstone Belt, southeastern Manitoba; Geological Survey of Canada, Open File 2910.

1995. Surficial geology and drift composition of the Annabel Lake-Amisk Lake area, Saskatchewan (NTS 63L/9, L/16, and part of 63K/12 and K/13); Geological Survey of Canada, Open File 3026.

Manitoba Mineral Resources Division
1981. Surficial Geological map of Manitoba. Map 81-1, scale 1:1 000 000.

Nielsen, E.
1989. Quaternary stratigraphy and overburden geochemistry in the Phanerozoic terrane of southern Manitoba; Manitoba Energy and Mines, Geological Paper GP87-1, 78 p.

Rose, A.W., Hawkes, H.E. and Webb, J.S.
1979. Geochemistry in mineral exploration (2nd ed.); Academic Press Inc. (London) Ltd., London, England, 657 p.

Schreiner, B.
1990. Lithostratigraphic correlation of Saskatchewan tills; a mirror image of Cretaceous bedrock; Saskatchewan Research Council, Publication R-1210-3-E-90, 114 p.

TABLE 1: NORTH BASIN - Lake Agassiz sequence

Core	Interval	Description	Mean Concentration															
			Al	*Ca*	*Co*	*Cr*	*Cu*	*Fe*	*K*	*Mg*	*Mn*	*Na*	*Ni*	*P*	*Pb*	*Sr*	*Ti*	*V*	*Zn*
Upper Reflection Package																			
107	194-696	Firm, banded grey clay; moderately calcareous; diffuse rhythmic bedding; silt lenses and laminations.	*Total Population (194-696 cm)*																
			8.3	3.3	17.9	105.8	38.7	4.0	2.4	2.4	691.4	1.4	49.5	658.2	19.1	203.1	0.4	117.9	105.3
Middle Reflection Package																			
103	686-816	Firm laminated clay, couplets 1 cm thick; increase in thickness downcore; calcareous	Total Population (686-816 cm)																
			8.0	4.1	17.9	115.2	45.6	4.5	2.7	2.6	723.8	1.2	54.0	682.5	25.5	185.5	0.4	106.1	110.8
106	182-789	182-260; Rhythmites 0.5-1cm thick; silt laminations; calcareous	Total Population (182-695 cm)																
			7.5	5.8	18.6	105.7	37.6	4.1	2.4	2.5	612.9	1.2	49.8	670.0	15.6	185.4	0.3	104.2	105.2
		260-415; Rhythmites 3-5cm thick; silt layer laminated; contains silty partings; calcareous	Lake Agassiz (185-245 cm)																
			7.8	5.0	19.4	107.6	38.9	4.3	2.7	2.7	630.7	1.3	51.7	704.3	14.6	185.0	0.3	103.1	108.9
		420-695; Rhythmites 2-4cm thick; silt partings absent below 535 cm; calcareous	Lake Agassiz (255-415 cm)																
			6.5	8.6	15.5	89.4	30.6	3.3	2.3	2.6	586.8	1.2	39.4	644.7	14.0	196.4	0.3	86.2	84.1
			Lake Agassiz (425-695 cm)																
			8.1	4.2	20.3	115.3	41.6	4.6	2.5	2.3	624.3	1.2	55.6	676.8	16.8	178.9	0.4	115.3	117.0
Lower Reflection Package																			
105	64.5-596	65-300 cm; Firm, thinly banded, couplets; 0.5-1cm thick; calcareous	Total Population (65-596cm)																
			7.8	4.7	16.7	110.2	40.2	4.0	2.4	2.4	649.2	1.5	50.7	642.0	17.5	213.1	0.3	103.1	98.4
		300-440 cm; Thickly banded red brown clay; 1 cm thick; silt partings below 350 cm; calcareous.	Lake Agassiz (65 - 295cm)																
			8.3	3.8	19.0	122.0	45.4	4.5	2.6	2.4	720.8	1.3	57.3	669.2	19.3	196.6	0.4	116.4	113.4
		440-510; Rhythmites, thin, gritty, drop-stone; calcareous.	Lake Agassiz (305 - 435 cm)																
			7.5	5.2	15.4	103.4	37.0	3.6	2.3	2.3	597.9	1.6	46.9	636.4	16.1	228.7	0.3	94.7	88.4
		510-539; till	Lake Agassiz (445 - 505 cm)																
			6.6	7.0	11.6	83.3	28.4	2.8	2.1	2.3	506.4	1.6	35.6	560.0	13.7	238.4	0.3	74.3	66.9

TABLE 2: SOUTH BASIN - Lake Agassiz Sequence

Core	Interval	Description	Mean Concentration															
			Al	*Ca*	*Co*	*Cr*	*Cu*	*Fe*	*K*	*Mg*	*Mn*	*Na*	*Ni*	*P*	*Pb*	*Sr*	*Ti*	*V*	*Zn*
Upper Reflection Package																			
119	171-321	Stiff to hard, banded light and dark brn. grey clay. Bands 0.25-0.5 cm thick; below 220cm may be orange brn.. Thin mm-scale calcareous silt laminations throughout at 2-20cm intervals. Laminations eroded in places.	Total Population (171-321 cm)															
			7.61	4.09	16.29	95.93	37.79	3.76	2.27	3.26	640.00	1.22	44.86	627.86	13.71	165.36	0.34	123.00	95.86
Middle Reflection Package																			
120	196-354	196-245 Stiff, hard dk. gry brn. silty clay; cumbly; banded gry and brn clay below 201cm.; weakly to non-calcareous.	Total Population (195-345 cm)															
			8.84	1.50	19.63	110.44	43.00	4.33	2.25	1.74	696.56	1.24	55.06	744.38	20.13	216.38	0.37	150.88	118.63
			Lale Agassiz (195-245 cm)																
			8.77	1.50	20.83	112.67	44.50	4.43	2.49	1.87	829.17	1.72	58.17	796.67	20.00	262.83	0.38	123.33	120.00
		245-318 Laminated dark brn gry clay with 1-5cm thick orange bands; thickness and frequency increases downward. Non-calcareous with exception of silty lenses and laminations. Granitic dropstones.	Lake Agassiz (255-315 cm)															
			9.20	1.28	20.00	116.57	45.29	4.36	2.27	1.70	592.14	1.13	59.43	754.29	20.86	212.57	0.38	168.29	120.86
		318-349 Orange clay with diffuse banding; calcareous; fractured.	Lake Agassiz (325-345 cm)															
			8.12	2.00	16.33	91.67	34.67	4.08	1.72	1.53	675.00	0.52	38.67	616.67	18.67	132.33	0.33	165.33	110.67
		349-354 Thinly laminated light and dk. brn clay; laminations irregular thickness (<1-1mm); non-calcareous,																	
Lower Reflection Package																			
121	475-547 (cm)	Stiff, thinly laminated dark brn. clay; weakly to moderately calcareous; lt. grey buff clasts and layers of calcareous silt common from 480-495 cm; dolomitic dropstone.	Total Population (485-545 cm)															
			8.35	3.13	15.14	93.71	33.00	3.86	1.84	1.89	562.86	0.58	42.14	565.71	22.00	135.29	0.31	168.43	105.71

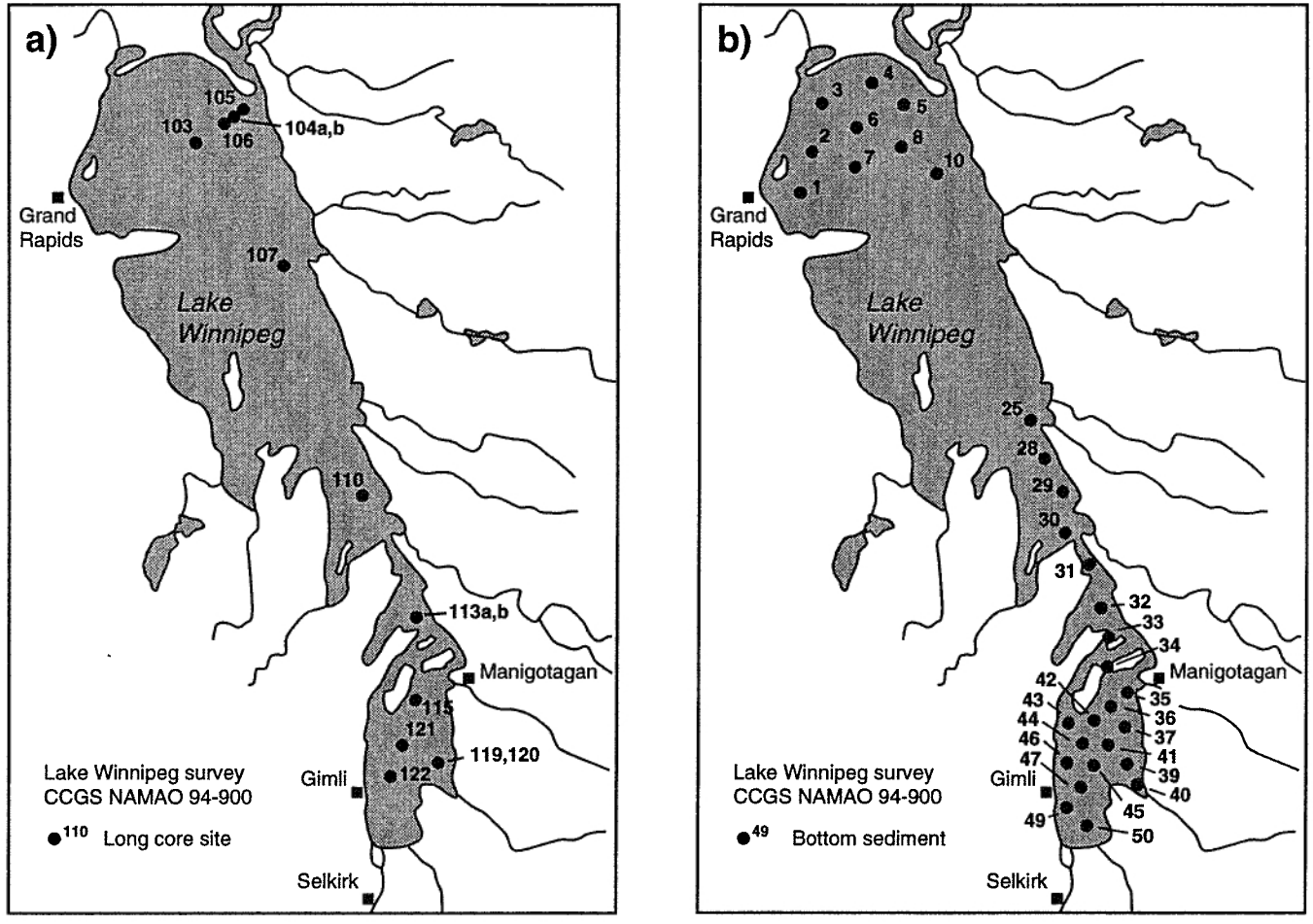

Figure 1: Location of long core sites and bottom sediment samples collected in Lake Winnipeg, ***Namao*** cruise 94-900. **a)** long core sites, **b)** bottom sediment sample locations

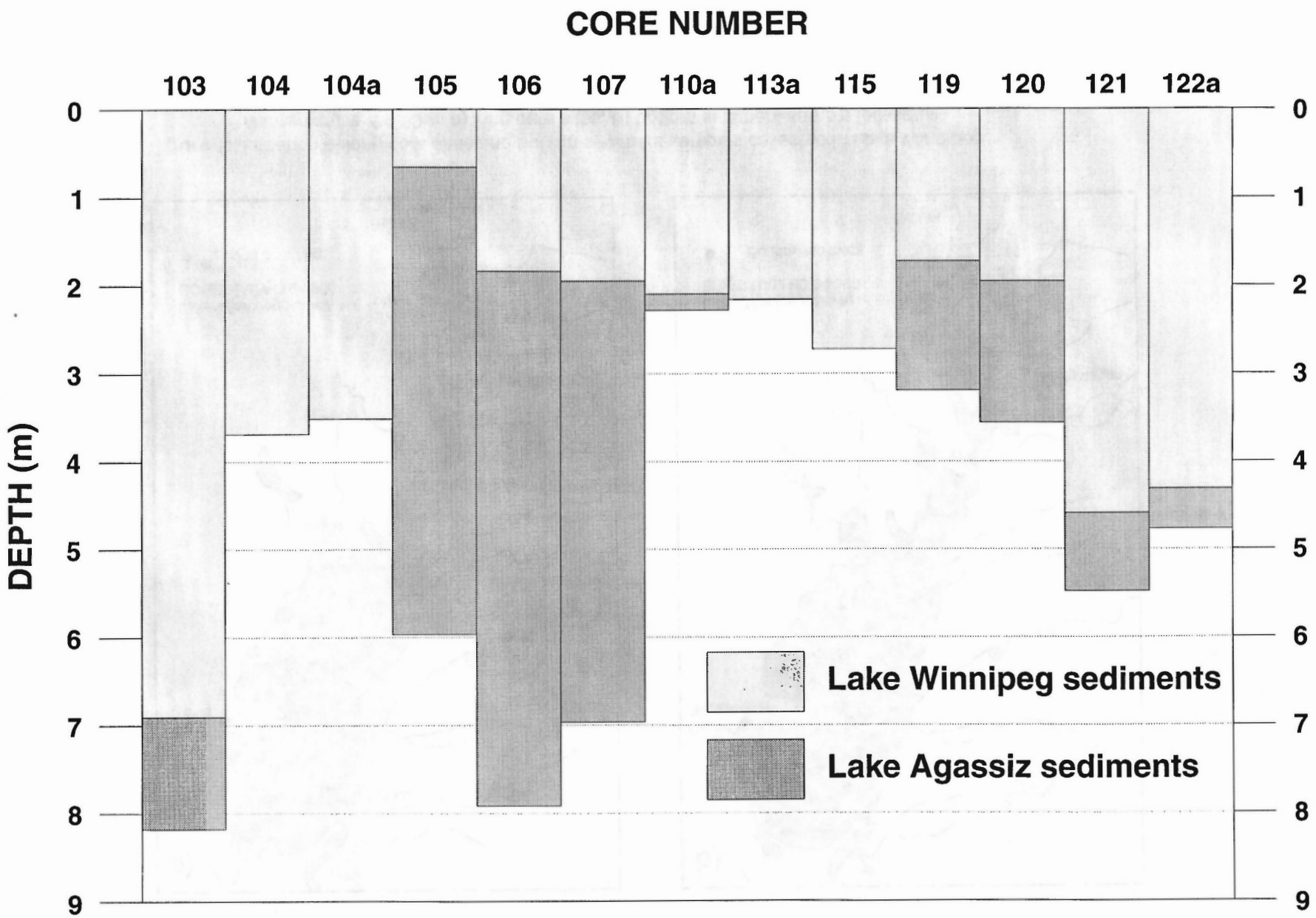

Figure 2. Summary of core sedimentology based on visual observations (Lewis and Todd, this volume).

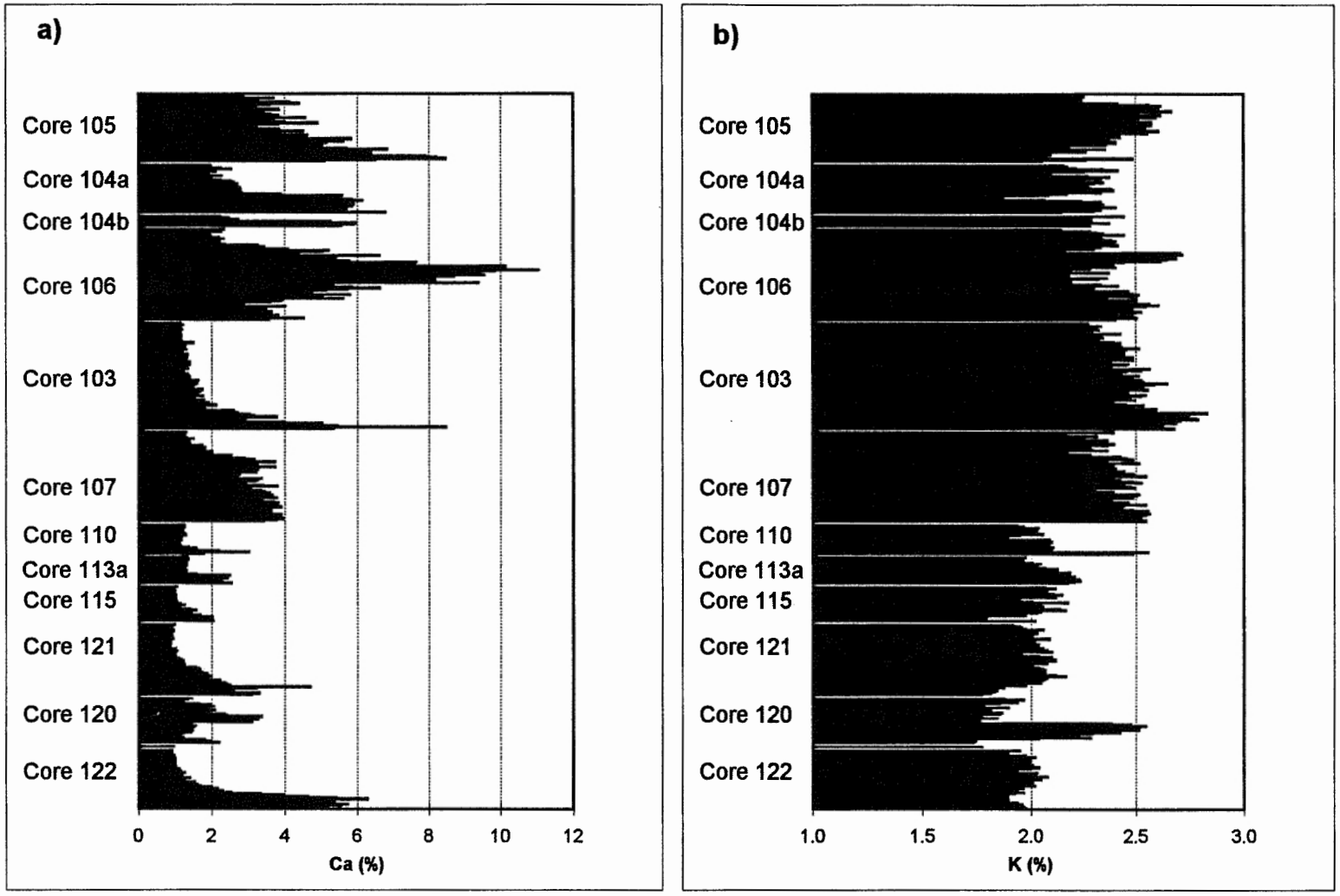

Figure 3: Geochemical variation in cores collected in Lake Winnipeg: a) Ca, b) K.

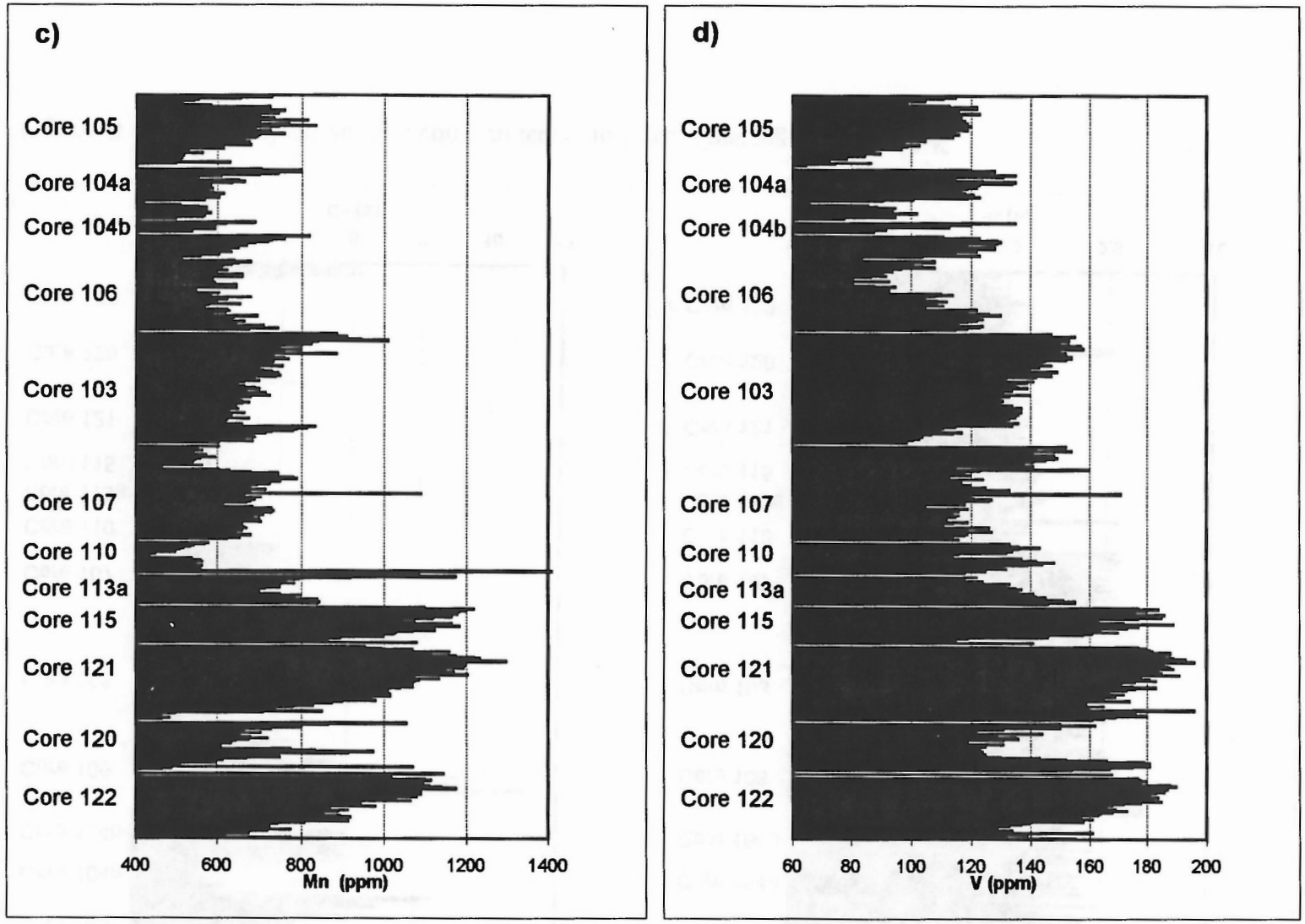

Figure 3: Geochemical variation in cores collected in Lake Winnipeg: c) Mn, d) V.

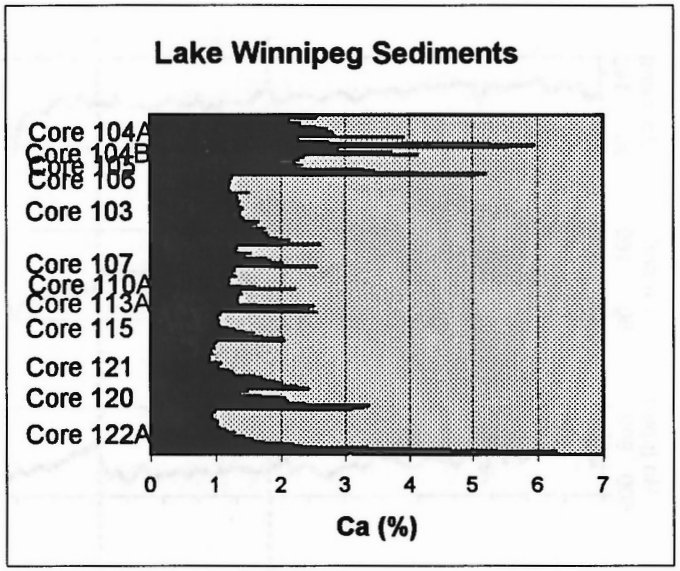

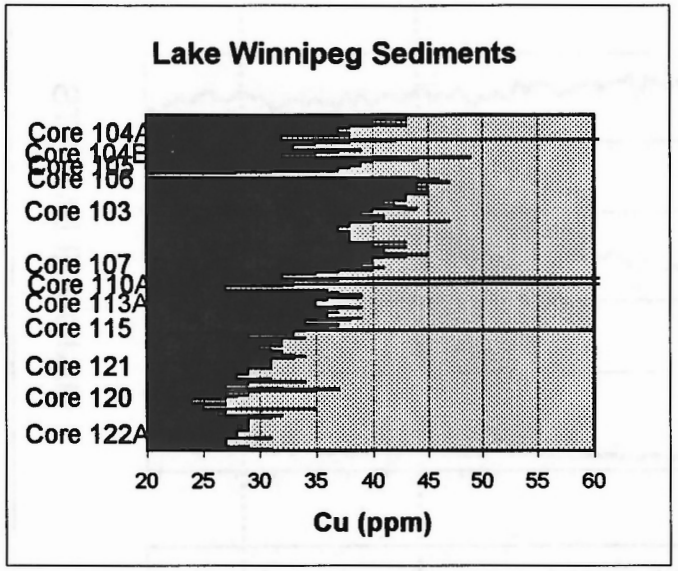

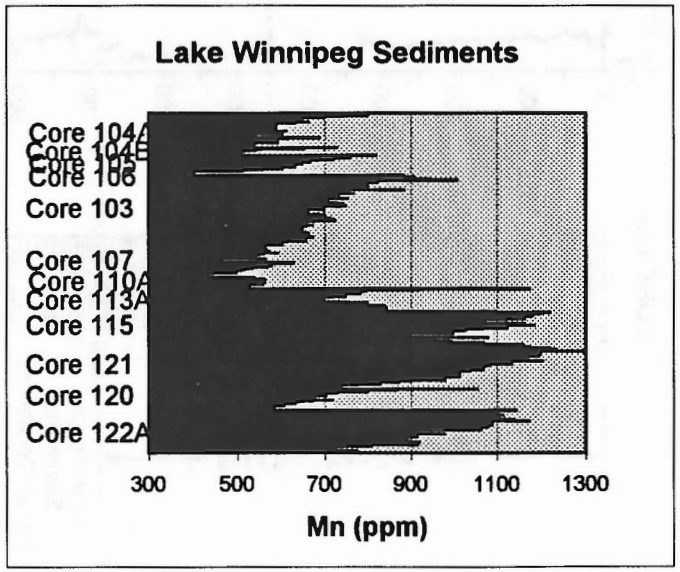

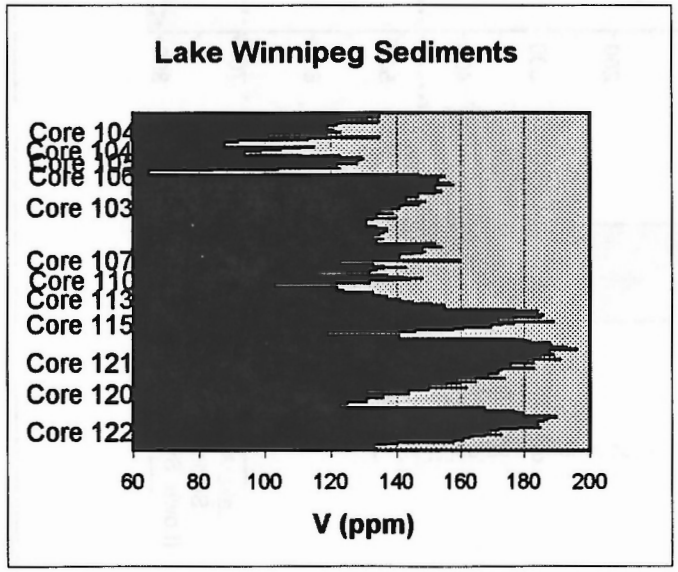

Figure 4: Distribution of Ca, Cu, Mn and V in the Lake Winnipeg sequence of the cores.

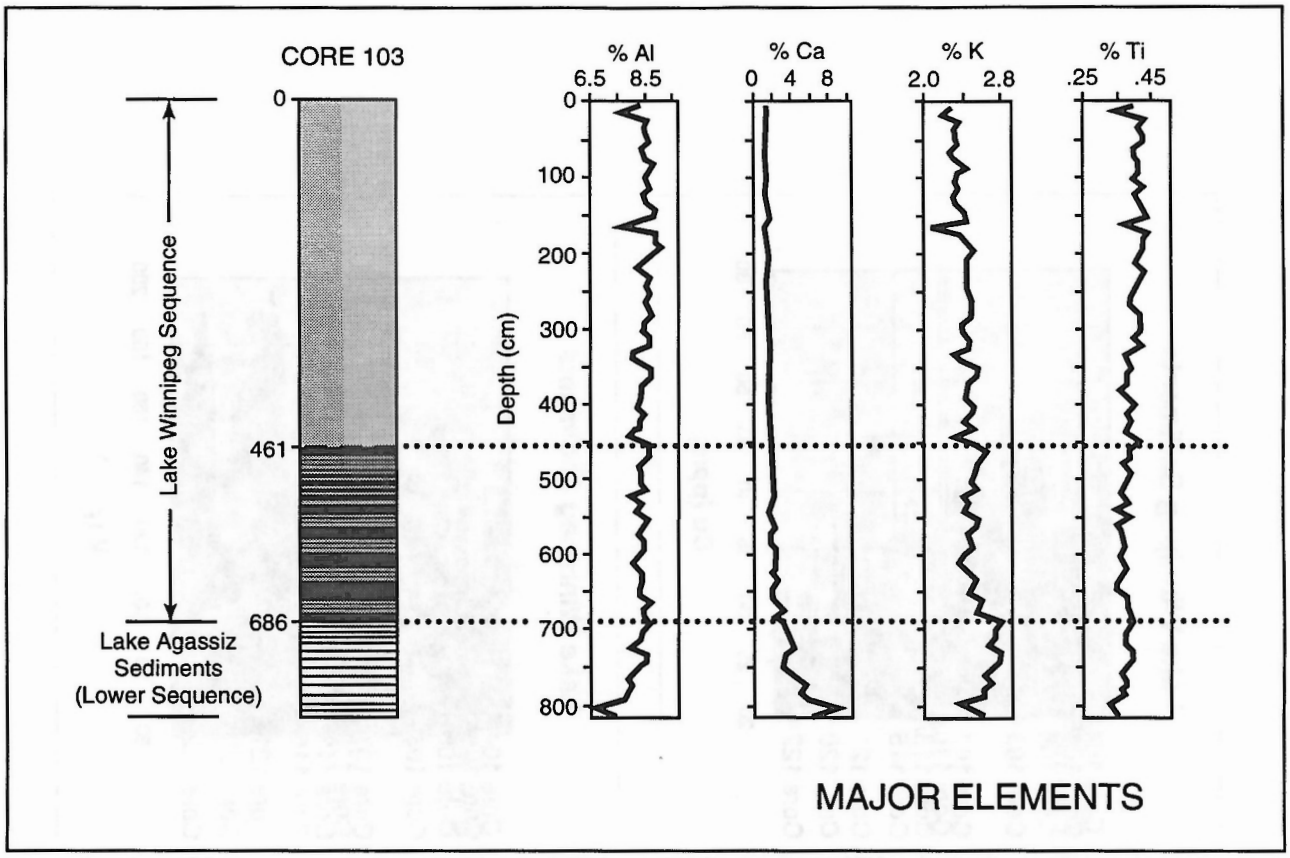

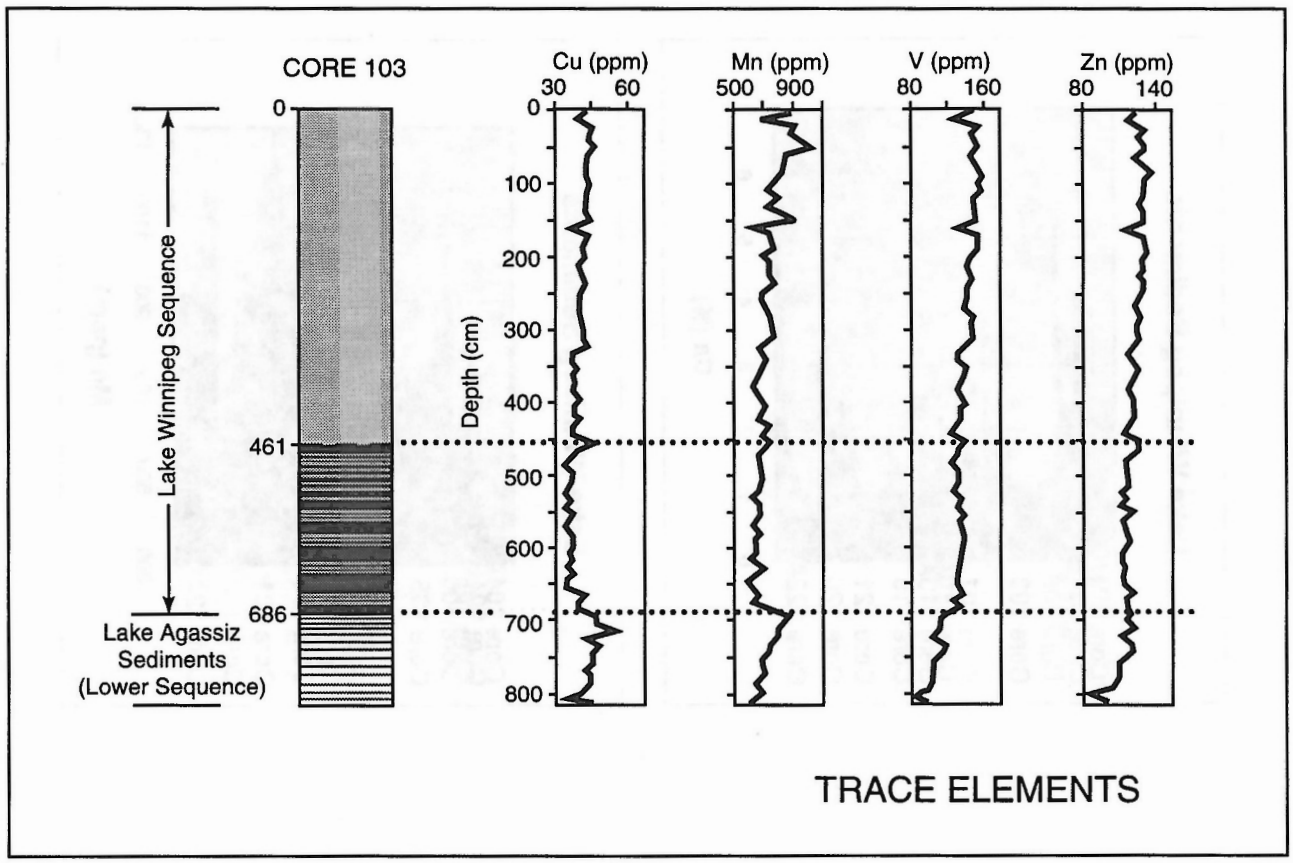

Figure 5: Geochemical stratigraphy of Lake Winnipeg sequence in core 103, North Basin

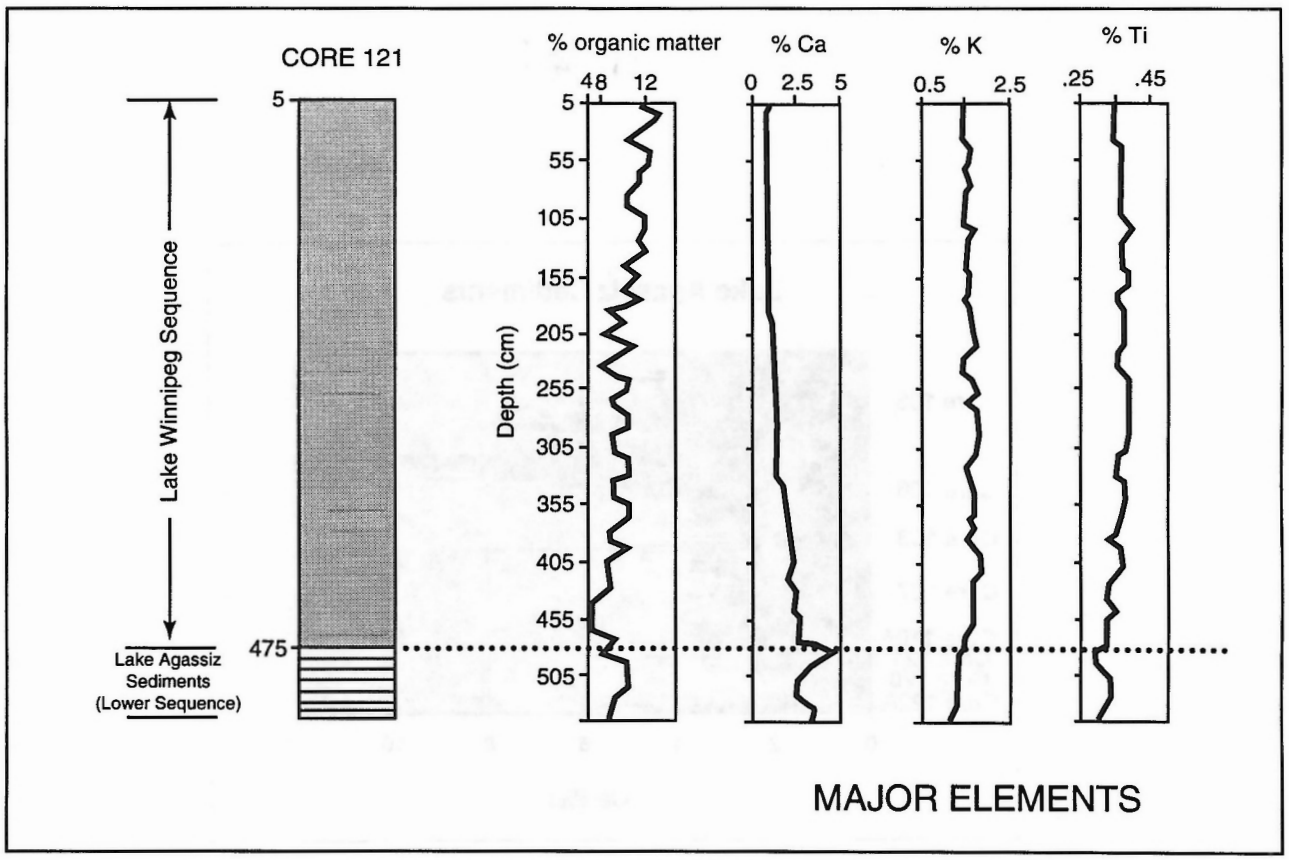

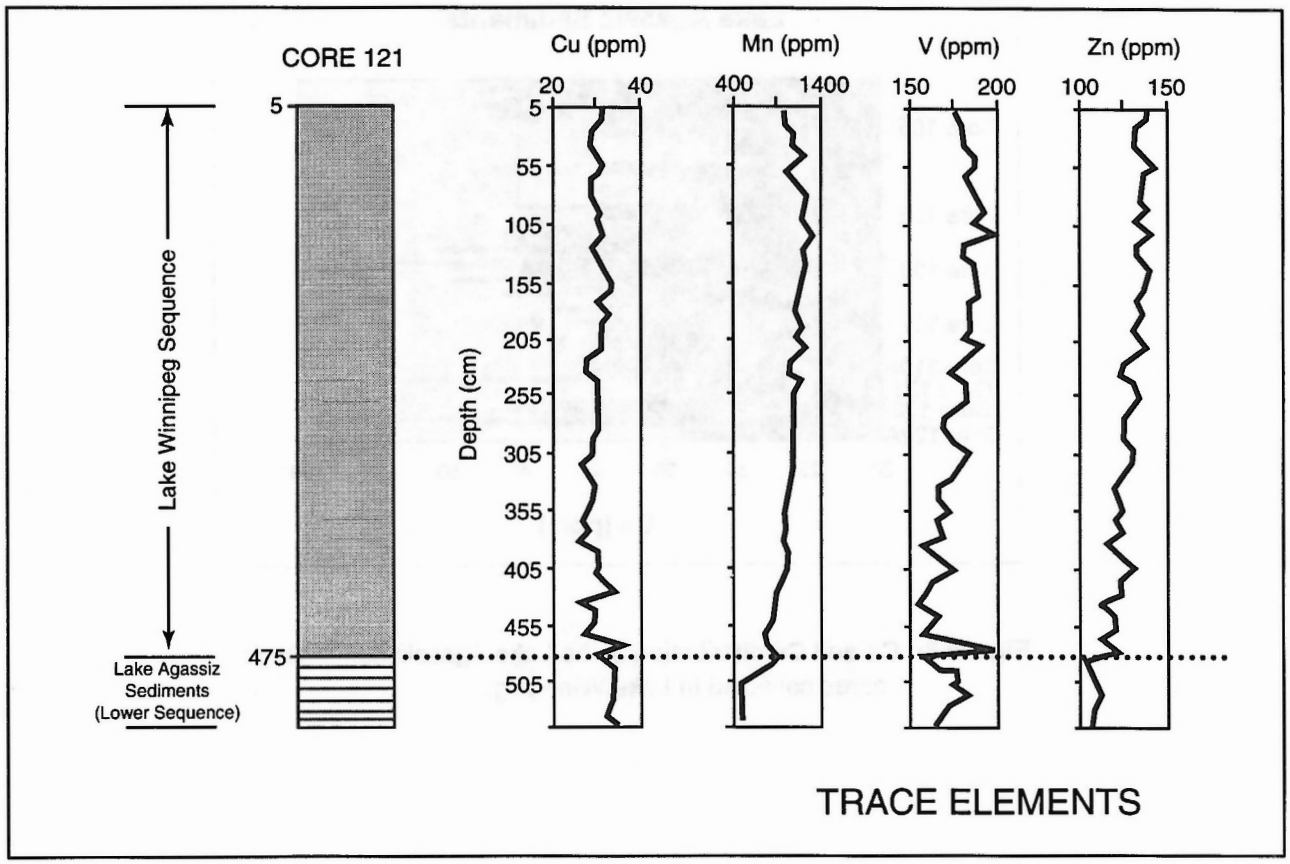

Figure 6: Geochemical stratigraphy of Lake Winnipeg sequence in core 121, South Basin

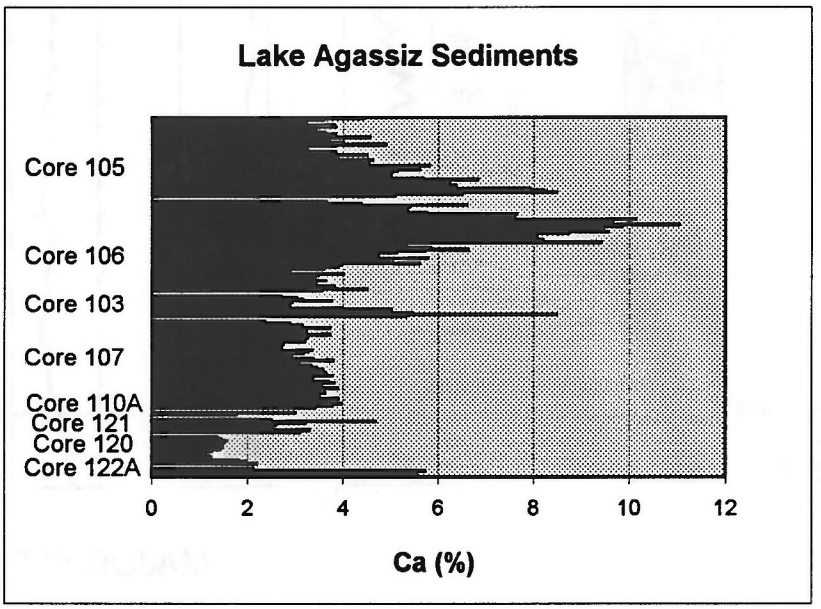

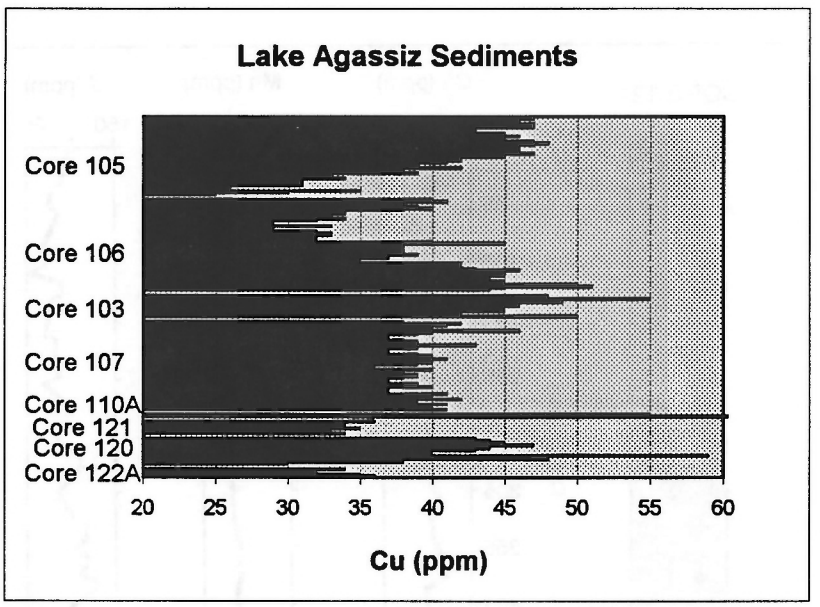

Figure 7: Ca and Cu distribution in the Lake Agassiz sequence in cores collected in Lake Winnipeg.

4.6 Recent sedimentation rates and toxic metal concentrations in Lake Winnipeg sediments

W. Lyle Lockhart

Department of Fisheries and Oceans
Freshwater Institute, 501 University Crescent, Winnipeg, Manitoba R3T 2N6

INTRODUCTION

Analyses of bottom sediment samples, box cores, and long cores collected from the CCGS *Namao* during the 1994 Lake Winnipeg Project are underway at the Freshwater Institute. The principal topics being coordinated by the author are radiochemical dating of recent sedimentation rates and the concentrations of toxic metals in the sediments.

BOTTOM SEDIMENT SAMPLES

Bottom sediment samples (Todd, this volume) were freeze dried, subsampled, and digested with nitric, perchloric, hydrofluoric and sulfuric acids in Teflon beakers. Final volumes were adjusted to 25 mL. All of the metals reported (Table 1), except mercury and cadmium, were analysed by flame atomic absorption spectroscopy. Cadmium was analysed by graphite furnace atomic absorption and mercury by cold vapour atomic absorption. Samples analysed for mercury required a separate digestion with aqua regia. National Research Council of Canada standard reference sediments were analysed concurrently as a measure of analytical quality.

The distribution of metals in the sediments showed higher levels of mercury, cadmium and lead in the South Basin than in the North Basin. The reasons for this geographic variation are speculative, but two hypotheses are the different geological settings of the two basins and anthropogenic input to the South Basin from the Red River and Assiniboine River.

BOX CORES

Locations and other data pertaining to the ten box cores collected in Lake Winnipeg during August, 1994 are given by Todd (this volume). The sites were numbered by the author as follows: box core 101: 1; 102: 2; 108: 3; 110: 4; 113: 5; 114: 6; 116: 7; 117: 8; 118: 9; 123: 10.

When a filled box corer was returned to the deck of the ship, the top of the corer apparatus was removed to expose the surface of the sediment (Todd, this volume; Figs. 19-21). Cores 10 cm in diameter and 30-50 cm in length were then taken by pushing core tubes into the top of the sediment column with gentle vacuum to minimize compression of the sediment. The cores were extruded using a Teflon plunger and sliced into 1 cm thick samples. As sediment emerged from the tube into a clear plastic ring (made of the same material as the core tube), slices were cut off with a stainless steel slicer. The samples were placed in Whirlpak bags and refrigerated until transferred to the Freshwater Institute after the ship reached Selkirk. Samples were then stored in a cold room at 4° C until taken for subsampling and freeze drying. Subsamples were supplied to a number of other investigators, notably W. Last, W. Buhay, H. Kling and S. Burbidge.

Two cores are being analysed for isotopes to determine sedimentation rates. Dating estimates are derived from counting each slice for radioactivity produced by lead-210 (a natural decay product from radon gas) and cesium-137 (a marker derived from nuclear explosions). Lead-210 and cesium-137 profiles may indicate that sediments are mixed extensively so that histories cannot be readily interpreted. Consequently, further analyses of the short cores have been delayed until after the radiochemical profiles are established. If the sedimentation histories are interpretable, then the cores will be submitted for additional geochemical analyses.

LONG CORES

Subsamples taken at 10 cm intervals from long cores 103 and 122a were also analysed for mercury (Table 2; Fig. 1). These cores suggest that mercury in sediment from the South Basin has exceeded that from the North Basin for a long period, and that both basins have increased levels near the tops of the cores. The increase near the top of the core is much more striking in the South Basin than in the North Basin. The mercury peak at 735 to 745 cm in core 103 is unexplained. The occurrence of aberrant values in two adjacent samples suggests that these points are not the result of analytical errors; however, additional analyses will be undertaken to try to confirm these values.

Piston coring normally fails to sample a small but unknown thickness of sediment at the top of each core (Todd, this volume). However, we detected excess lead-210 in the two top slices of core 122a and in the top slice of core 103. Because the limit for excess lead-210 is about 150 years before the present, this observation suggests that the tops of these cores reached within 150 years of the present, or that core top sediment had been mixed with material of that age.

Table 1. Analysis of Lake Winnipeg bottom sediment samples, August, 1994

Site	Latitude	Longitude	Al	Cd	Cu	Fe	Hg	Mn	Ni	Pb	Ti	V	Zn
	N	W	mg/g	ug/g	ug/g	mg/g	ug/g	ug/g	ug/g	ug/g	mg/g	ug/g	ug/g
1	53.222	98.849	81.83	0.384	39.26	32.48	0.049	830	51.67	25.34	3.69	144.8	113.4
2	53.428	98.820	84.71	0.221	37.68	35.74	0.044	610	53.38	16.90	3.67	137.3	109.7
3	53.638	98.788	67.60	0.147	24.77	18.88	0.039	513	33.80	15.78	3.02	84.5	67.7
4	53.737	98.465	73.73	0.241	29.96	29.44	0.053	482	39.84	15.26	3.44	108.5	83.3
5	53.609	98.184	82.78	0.372	41.40	30.29	0.059	650	50.71	19.58	3.72	134.7	114.5
6	53.521	98.501	89.00	0.390	42.80	32.35	0.056	765	52.17	19.20	4.05	154.1	118.0
7	53.316	98.534	80.66	0.338	43.25	31.64	0.068	686	50.51	18.52	3.31	146.2	114.5
8	53.400	98.218	83.73	0.385	24.60	30.64	0.070	618	50.58	21.66	3.59	155.2	116.3
10	53.279	97.935	81.87	0.257	44.59	29.03	0.028	531	52.02	11.70	3.43	140.2	105.8
25	52.302	97.210	81.48	0.250	38.12	27.57	0.086	407	38.60	18.53	3.23	112.7	82.5
28	52.112	97.130	84.96	0.205	35.39	30.42	0.049	439	45.69	18.12	3.76	140.2	95.0
29	51.956	97.020	82.81	0.337	42.89	30.63	0.059	574	53.16	23.77	4.02	168.8	108.5
30	51.804	96.908	75.84	0.390	40.18	27.14	0.100	887	45.55	23.61	3.56	140.9	92.7
31	51.654	96.743	74.16	0.288	30.23	22.45	0.039	601	32.00	14.76	2.94	124.4	74.5
32	51.483	96.679	76.20	0.273	25.16	20.05	0.077	685	28.50	25.95	2.88	99.3	64.4
33	51.319	96.588	20.98	0.107	13.02	9.06	0.028	309	11.33	15.76	1.23	43.7	27.2
34	51.201	96.580	66.24	0.225	28.56	28.74	0.034	3231	39.81	16.92	3.06	129.6	87.8
35	51.111	96.498	80.73	0.564	40.87	25.59	0.117	1050	45.66	18.16	3.55	154.6	98.0
36	51.022	96.590	90.85	0.561	40.57	39.47	0.123	1037	51.69	16.92	4.03	194.1	128.2
37	50.932	96.508	91.16	0.545	41.75	33.65	0.135	1025	48.68	21.06	4.25	203.7	133.1
39	50.750	96.433	72.28	0.504	32.26	38.79	0.075	3647	53.53	19.04	3.04	130.9	102.5
40	50.661	96.410	33.64	0.205	15.07	7.25	0.034	183	6.33	10.39	1.22	41.3	21.8
41	50.843	96.600	91.02	0.515	37.97	31.63	0.161	756	47.10	26.43	4.01	206.1	132.7
42	50.949	96.680	88.23	0.508	40.52	30.28	0.125	907	49.85	30.34	3.98	206.5	132.8
43	50.939	96.853	75.89	0.449	37.58	30.60	0.102	662	44.67	22.36	3.21	168.4	112.9
44	50.846	96.769	79.11	0.420	36.12	29.78	0.116	822	45.03	24.92	3.53	201.0	127.0
45	50.755	96.690	81.69	0.534	39.01	31.66	0.157	708	49.31	27.04	3.94	213.7	132.0
46	50.758	96.859	86.30	0.690	37.72	35.27	0.125	924	47.55	26.93	4.26	220.0	135.2
47	50.666	96.781	83.09	0.978	38.75	33.26	0.137	922	46.40	22.34	4.11	217.2	136.1
49	50.579	96.867	79.82	0.718	37.38	32.29	0.129	996	44.24	19.62	3.95	220.7	137.0
50	50.488	96.789	79.99	0.806	33.35	33.24	0.139	622	42.14	29.04	3.68	198.7	135.8

Table 2. Mercury concentrations in sediment from long cores.

Core 103:				Core 122a:			
Depth cm	Mercury ug/g dry wt	Depth cm	Mercury ug/g dry wt	Depth cm	Mercury ug/g dry wt	Depth cm	Mercury ug/g dry wt
5	0.037	415	0.028	5	0.116	245	0.046
15	0.059	425	0.020	15	0.105	255	0.047
25	0.038	435	0.023	25	0.081	265	0.056
35	0.031	445	0.022	35	0.049	275	0.048
45	0.035	455	0.025	45	0.061	285	0.044
55	0.034	465	0.019	55	0.051	295	0.049
65	0.032	475	0.022	65	0.051	305	0.046
75	0.028	485	0.021	75	0.053	315	0.052
85	0.030	495	0.023	85	0.053	325	0.048
95	0.031	505	0.021	95	0.051	335	0.045
105	0.029	515	0.018	105	0.049	345	0.042
115	0.025	525	0.022	115	0.044	355	0.048
125	0.027	535	0.020	125	0.046	365	0.043
135	0.030	545	0.025	135	0.054	375	0.040
145	0.025	555	0.021	145	0.050	385	0.042
155	0.026	565	0.023	155	0.046	395	0.047
165	0.027	575	0.021	165	0.050	405	0.032
175	0.027	585	0.022	175	0.051	415	0.035
185	0.025	595	0.021	185	0.047	425	0.035
195	0.023	605	0.026	195	0.055	435	0.034
205	0.027	615	0.021	205	0.049	445	0.028
215	0.025	625	0.019	215	0.049	455	0.029
225	0.027	635	0.020	225	0.049	465	0.034
235	0.024	645	0.024	235	0.051	475	0.033
245	0.028	655	0.020				
255	0.026	665	0.020				
265	0.027	675	0.022				
275	0.026	685	0.022				
285	0.024	695	0.022				
295	0.027	705	0.025				
305	0.028	715	0.023				
315	0.025	725	0.026				
325	0.026	735	0.041				
335	0.026	745	0.045				
345	0.021	755	0.022				
355	0.024	765	0.027				
365	0.028	775	0.028				
375	0.028	785	0.027				
385	0.023	795	0.027				
395	0.024	805	0.025				
405	0.025	815	0.028				

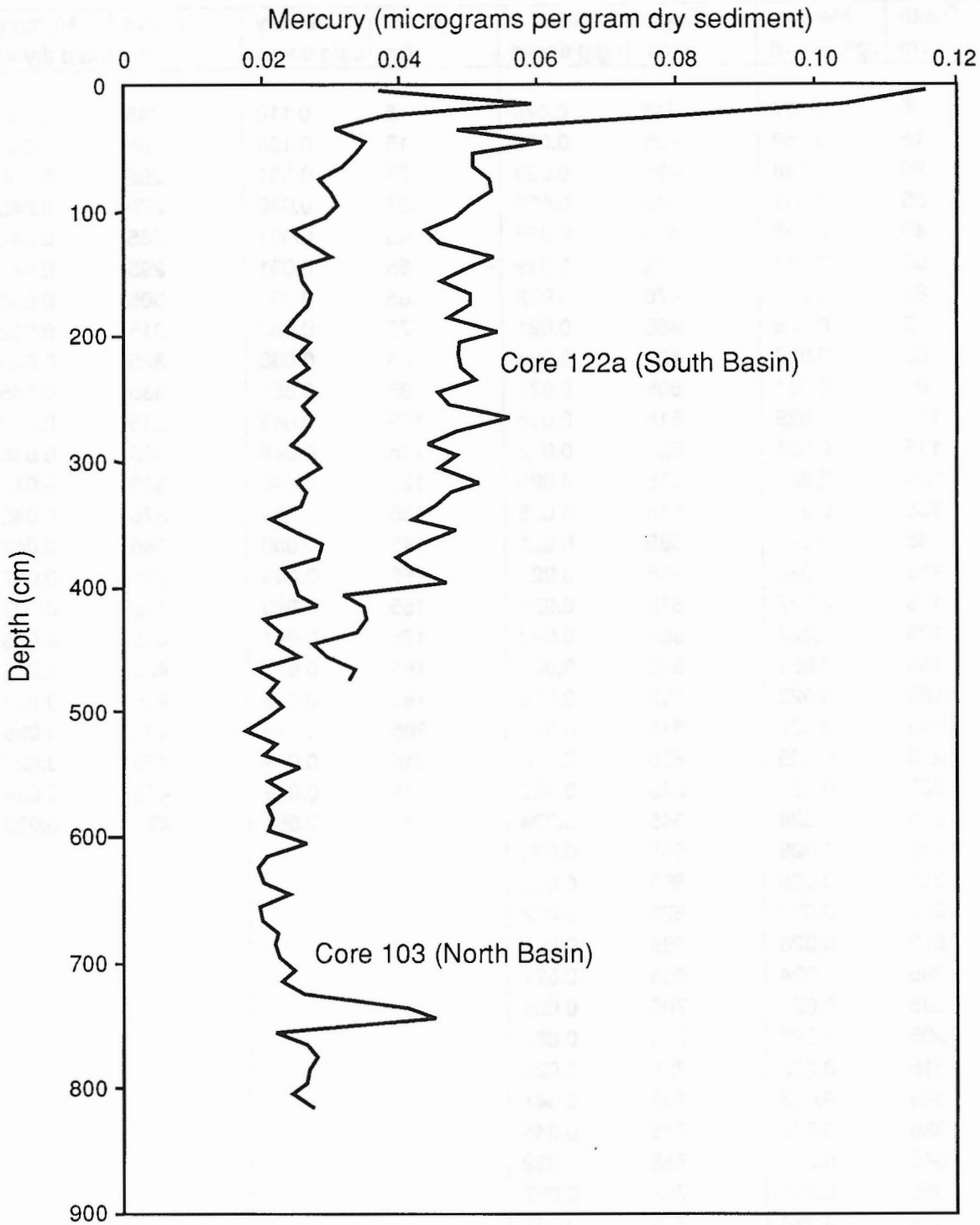

Figure 1. Mercury concentration in sediments from cores 103 and 122a.

4.7 Pore-water chemistry of Lake Winnipeg sediments

R.N. Betcher

Manitoba Water Resources Branch
1577 Dublin Avenue, Winnipeg, Manitoba R3E 3J5

W.M. Buhay

The Godwin Institute for Quaternary Research
University of Cambridge, Free School Lane,
Cambridge, United Kingdom CB2 3RS

ABSTRACT

The isotopic and geochemical composition of interstitial waters contained in Quaternary tills and lacustrine sediments underlying Lake Winnipeg initially reflected the composition of the overlying glacial or lake (Agassiz and Winnipeg) waters during deposition. Subsequently, the composition of the pore waters in these sediments may have been modified by a variety of processes including expulsion during compaction, diffusion under concentration gradients, replacement by upward advection of underlying groundwaters, and aqueous and water-sediment geochemical reactions. Depending on the degree of modification which has occurred, we may, by studying the composition of these pore waters, gain an understanding of the Late Pleistocene and Holocene geographic and climatic history of the lake and surrounding area.

In this study, pore waters collected at 20 cm intervals from cores 103 and 107 in the North Basin and 115 in the South Basin were analyzed for stable isotopes (oxygen-18 and deuterium) and a suite of dissolved components. Pore waters have retained an evaporative isotopic signature indicating they are original surface waters and have not been displaced by groundwaters from underlying bedrock aquifers. The degree of modification of the original pore water composition which has occurred is, however, not well understood and will be the subject of further study.

INTRODUCTION

The collection of undisturbed cores of Quaternary sediments underlying Lake Winnipeg during the 1994 Lake Winnipeg Project provided the opportunity to collect and analyze pore waters from discrete core segments in both the North and South Basins of the lake. The composition of these pore waters may hold clues to the climatic and geographic history of the lake and provide information on the role of the lake as a receiving body for groundwater flow systems originating to the east and west. This paper will discuss factors affecting the composition of pore waters in subaqueous sediments, the hydrogeological setting and history of Lake Winnipeg, and present some preliminary interpretations of pore water isotopic and major dissolved ion profiles obtained on pore water samples from three cores.

During sedimentation under aqueous conditions, the pore waters initially trapped in the interstitial spaces of a sediment will reflect the composition of the overlying surface waters. Over long periods of deposition, and barring processes which modify the composition of these waters, a profile of pore water quality will be developed in the sediments that will reflect the time varying composition of the overlying surface waters. At first glance then, the potential exists for examining past climatic conditions in southern and central Manitoba and changes in inflow/outflow conditions to Lake Winnipeg by studying the composition of pore waters in the sediments underlying the lake.

Unfortunately, several physical and chemical processes may alter the initial composition of the pore waters deposited in these sediments. As the sediment column grows, the weight of overlying sediments will compact underlying deposits, decreasing their porosity and expelling a portion of the pore waters. Expelled waters will move upward and discharge into the overlying lake but may also move downward in areas where permeable bedrock exists and acts as a "drain" to carry away downward moving pore waters. This process tends to homogenize the composition of pore waters in thick subaqueous sediment columns (Desaulniers and Cherry, 1989; Quigley et al., 1983).

Displacement of pore waters may also occur by upward or downward advection of water into or out of a lake, passing through the underlying sediments in the process. Most lakes in non-arid environments act as groundwater discharge areas. The influx of groundwaters at the base of the sediment column will force the original pore waters upward and replace them with groundwaters typically having a distinctly different composition. Upward moving pore waters will also, of course, displace overlying fluids. The rate of upward advection of the pore water column will depend on the magnitude of the gradient driving groundwaters into the overlying sediments and the porosity and permeability of these sediments. In some circumstances this process may reverse. If lake levels are subject to relatively rapid rises for instance, lake water elevation may exceed, for some period of time, groundwater elevations in the underlying bedrock. Under these conditions lake water may migrate downward into the underlying sediments.

The geochemistry of pore waters can also be altered by diffusion taking place under concentration gradients. Where advective fluid velocities are very low, diffusion may be the dominant process causing alteration in pore water composition

(Desaulniers and Cherry, 1989; Remenda, 1993). Concentration gradients will normally exist between deep pore waters and both overlying and underlying waters, either groundwaters or surface waters. Smaller scale concentration differences may also exist within the sediments due to variations in the composition of waters trapped in the pore spaces during deposition or spatial differences in subsequent geochemical development of the pore waters. Diffusion processes will operate to homogenize these differences and, over periods of thousands of years, may result in substantial alteration of the original pore water composition.

Sediment-water interactions may also result in significant changes to the original pore water composition. These processes tend to be rather complex and will not be discussed in detail here. Some parameters will act in a conservative manner - they will not change concentration as a result of aqueous or sediment-water interactions - while other parameters will act in a distinctly nonconservative manner. Conservative parameters include the stable isotopes of oxygen and hydrogen (assuming low temperature environments) and chloride. Typical nonconservative parameters include calcium, magnesium, sodium, bicarbonate and trace metals.

HYDROGEOLOGICAL AND HYDROGEOCHEMICAL SETTTING

Given the complexity of the physical setting of the lake and the processes affecting pore water chemistry, a brief overview of the hydrogeology and hydrogeochemistry of bedrock aquifers bordering and underlying Lake Winnipeg will be given prior to considering the pore water results. Through this discussion, we will attempt to provide the physical and chemical "boundary conditions" which could affect the lake sediment pore water composition.

Quaternary sediments underlying Lake Winnipeg overlie a bedrock of Precambrian crystalline rocks on the east and Paleozoic sandstones and shales (Winnipeg Formation) and carbonates on the west (Bezys, this volume). The Winnipeg Formation forms a significant but little utilized aquifer in Manitoba while the carbonates form the most extensive and heavily utilized aquifer in the province. The topographic low in which Lake Winnipeg lies is thought to form the regional discharge area for eastward and northward moving groundwaters in these aquifers (Figs. 1 and 2). Sandstones of the Winnipeg Formation aquifer are hydraulically separated from the overlying carbonates by shales forming the upper part of the formation. These shales are also thought to restrict to the outcrop area any active inflow and outflow from the formation. Westward moving regional groundwater flow systems in the Precambrian likely discharge into the lake as well; however little is known of the movement of groundwaters on a large scale in these rocks.

Groundwater quality in the Paleozoic aquifers is well understood. Figure 3 shows the distribution of total dissolved solids in the carbonate rock aquifer and Table 1 presents the average geochemical composition of 36 samples collected during 1994 from private wells completed in this aquifer in the southeastern Interlake. These groundwaters are "modern" with oxygen-18 values near the mean for precipitation in southern Manitoba (Fritz et al., 1974) and tritium detected in about half of the samples. It appears that "old" groundwaters (prior to the withdrawal of Lake Agassiz from the region) have been flushed from the fresh water portion of this very permeable aquifer. It is assumed in subsequent discussions that groundwaters in this aquifer where it underlies Lake Winnipeg have a similar major ion and isotopic content to that presented in Table 1. This assumption is open to discussion however since the sub-lake groundwater system may be much less active than the Interlake system if the tills and clays overlying the aquifer beneath the lake restrict upward movement of groundwater.

The geochemistry of groundwaters in the Winnipeg Formation west and south of the lake is more complex. Figure 4 shows the distribution of total dissolved solids in the aquifer. Saline groundwaters underlie the southwestern portion of the South Basin of Lake Winnipeg while fresh groundwaters are thought to underlie the rest of the lake. Table 1 presents the typical composition of fresh groundwaters in the Winnipeg Formation aquifer in the southeastern Interlake. Note particularly the elevated chloride and depleted oxygen-18 content of these groundwaters relative to groundwaters in the overlying carbonate rock aquifer. Betcher (1986) speculated that these groundwaters were recharged into the aquifer along the outcrop area during a cold climatic period (sub-glacially or influx of Lake Agassiz groundwaters?).

Much less is known of the groundwater quality in Precambrian rocks near Lake Winnipeg. Studies by Atomic Energy of Canada Limited in the Lac du Bonnet and Pinawa areas have shown a transition from fresh to saline groundwaters at a depth of about 150 m (Gascoyne et al., 1989). Groundwaters discharging from regional groundwater flow systems from these rocks may be quite saline.

Bedrock aquifers underlying Lake Winnipeg are overlain by a sequence of tills, Lake Agassiz lacustrine clays and silty clays and Lake Winnipeg silty clays (Last, this volume). Groundwater flow gradients have likely been upward through these sediments since the withdrawal of Lake Agassiz from the region although the expected low permeabilities of the sediments will have severely restricted the rate of upward groundwater discharge from the underlying aquifers. Studies of the isotopic and geochemical composition of pore waters in Lake Agassiz clays in southern Manitoba and North Dakota by Remenda (1993) and Remenda et al. (1994) indicate that the original pore water composition of these sediments had chloride concentrations of a few tens of milligrams per liter and oxygen-18 compositions near -25‰. It will be assumed that the pore waters laid down with glacial tills and Lake Agassiz clays underlying Lake Winnipeg had a similar composition although

it is possible that the pore waters contained in sediments laid down in the late (shallower) phases of Lake Agassiz were considerably more enriched. Pore waters deposited with Lake Winnipeg sediments are expected to have a roughly similar composition to modern lake waters, being much heavier isotopically than Lake Agassiz waters.

Given the physical and geochemical setting discussed above and the modifications which can occur to pore waters, the question which we wished to examine was whether the analysis of pore waters extracted from sediment cores beneath Lake Winnipeg could be used to elucidate the Late Pleistocene and Holocene climatic and inflow/outflow histories of the lake or to better understand fluid movement occurring in the sediments beneath the lake.

SAMPLE COLLECTION AND ANALYSIS

In this study, pore waters were extracted from samples collected at 20 cm intervals from cores 103 (8.16 m long) and 107 (6.96 m long, samples collected below 1.50 m) in the North Basin and 115 in the South Basin (for locations, see Lewis and Todd, this volume). These cores provided long sections of Lake Winnipeg and Lake Agassiz sediments. The cores were originally thought to overlie the carbonate rock aquifer near the erosional edge of the Paleozoic sediments but interpretation of the seismic data now indicates that the coring sites in fact overlie Precambrian rocks (Todd, this volume). The seismic reflection profile at site 103 indicates about 9 m of Lake Winnipeg sediments overlying about 12 to 20 m of Lake Agassiz sediments which in turn overlie glacial till or bedrock. The profile at site 107 indicates about 3 m of Lake Winnipeg sediments overlying a very thick Lake Agassiz sequence extending to perhaps 40 m. At site 115 about 4 m of Lake Winnipeg sediments overlie more than 40 m of Lake Agassiz sediments (Todd, this volume).

Pore waters were collected by squeezing the sediments in a confined piston. Typically about 10-20 ml of water was collected from each sediment sample but in some cases as little as 5 or 6 ml was all that could be recovered. Samples were sent to the University of Waterloo for analysis. All water samples were analyzed for the stable isotopes oxygen-18 and deuterium and for chloride. Additional analyses were carried out on water samples from 150 to 270 cm from core 107 and for all samples collected from core 103. Analyses included calcium, magnesium, silicon, bicarbonate and sulfate. Samples from core 103 below 290 cm were also analyzed for sodium.

RESULTS AND DISCUSSION

Oxygen-18, deuterium and chloride profiles for pore waters extracted from cores 103, 107 and 115 are shown in Figures 5 to 7. Portions of core 103 had been inadvertently frozen during storage. This may have affected the composition of pore waters in a few samples; the anomalous results at -490 cm are particularly suspect.

Buhay (this volume) has shown that the stable isotope content of the pore waters is displaced to the right of the Global Meteoric Water Line indicating that these waters have been subject to evaporation and are likely original lake waters. Shallow pore water samples from Lake Winnipeg sediments of cores 103 and 115 are isotopically very similar to grab samples of shallow lake water collected from the North and South Basins in 1985 (Betcher, unpublished). The oxygen-18 content of South Basin waters is about 2 ‰ heavier than North Basin waters. This is close to the difference that would be expected from the decline in mean annual air temperature between southern and central Manitoba. This temperature effect would appear as an isotopic difference in both the surface water and precipitation influx components to the basins.

The isotopic content of pore waters from Lake Winnipeg sediments in cores 103 and 115 become progressively lighter with depth, with the two profiles showing very similar slopes over the upper 2.5 m of sediments. This lightening of the isotopic signature continues to about 1 m above the Lake Winnipeg/Lake Agassiz sediment contact in core 103. This may indicate a gradual cooling of the climate over this period, with the signature of shorter term climatic changes perhaps having been lost through diffusive and compaction/expulsion mixing, particularly in the deeper parts of core 103. The issue of signal loss through mixing processes is a complex one and needs to be addressed through modeling studies.

The oxygen-18 content of pore waters from Lake Agassiz sediments in core 107 declines more or less linearly from -11‰ at the Lake Winnipeg/Lake Agassiz sediment contact to about -13‰ five meters below the contact. Pore waters in these sediments were expected to have an oxygen-18 content in the order of -25‰ at the time of deposition so it is surprising that a more depleted signature has not been observed. The Lake Agassiz sediments encountered in this core are interpreted as upper (late) sediments however, so it is possible that Lake Agassiz waters had a lessening glacial component at this time and were becoming progressively enriched and representative of "modern" lake waters. Arguing against this interpretation are the -12‰ oxygen-18 values found in older Lake Agassiz sediments encountered in core 103.

Chloride concentrations in pore water samples ranged from about 15-25 mg/L. There is no evidence in these profiles of an influx of high salinity groundwaters into the lake sediments. However, as discussed above, groundwater influxes from the carbonate rock aquifer are not expected to have chloride concentrations exceeding 20 mg/L and influx from Precambrian rocks may or may not have high salinity. It is interesting that individual chloride profiles show considerable vertical spatial fluctuations which are quite independent of the trends found in the isotopic profiles and do not exhibit the smoothed profiles characteristic of long-term diffusive mixing. This leads one to speculate that these profiles may not have

been seriously compromised by mixing processes.

CONCLUSIONS

Pore waters contained in Lake Agassiz and Lake Winnipeg sediments underlying Lake Winnipeg have an evaporative isotopic signature and thus appear to have originated as lake waters trapped in the sediments during deposition. There is no evidence in the core segments examined in this study of displacement of these original surface waters with groundwaters from underlying bedrock aquifers. The degree to which the composition of the waters has been affected by a variety of physical and geochemical processes is not currently well understood and will have to be examined through modeling studies and by comparison of these geochemical results with information gathered through other, more direct, approaches such as the work on the organic fraction by Buhay (this volume).

ACKNOWLEDGMENTS

We would like to thank Mike Lewis, Brian Todd, Harvey Thorleifson and Erik Nielsen for the tremendous organizational job they undertook to get the Lake Winnipeg project underway and the latter two individuals particularly for their encouragement in getting lake neophytes such as ourselves involved. We would also like to thank the Halifax group for collecting the core samples for us, V. Remenda for providing many constructive comments on this paper and M. Stainton for the chloride values on lake waters.

REFERENCES

Betcher, R.N.
1986. Regional hydrogeology of the Winnipeg Formation in Manitoba; in eds. G. van der Kamp and M. Madunicky, Proceedings of the third Canadian hydrogeological conference, April 20-23, 1986, Saskatoon, Saskatchewan, p. 159-174.

Desaulniers, D.E. and Cherry, J.A.
1989. Origin and movement of groundwater and major ions in a thick deposit of Champlain Sea clay near Montreal; Canadian Geotechnical Journal, v. 26, p. 80-89.

Fritz, P., Drimmie, R.D. and Render, F.W.
1974. Stable isotope contents of a major prairie aquifer in central Manitoba; in Isotope techniques in groundwater hydrology 1974, International Atomic Energy Agency, Vienna, v. 1, p. 379-398.

Gascoyne, M., Ross, J.D., Purdy, A., Frape, S.K., Drimmie, R.J., Fritz, P. and Betcher, R.N.
1989. Evidence for penetration of sedimentary basin brines into an Archean granite of the Canadian Shield; in ed. D.L. Miles, Proceedings of the 6th international symposium on water-rock interaction, Malvern, United Kingdom, p. 243-245.

Quigley, R.M., Gwyn, Q.H.J, White, O.L., Rowe, R.K., Haynes, J.E. and Bohdanowicz, A.
1983. Leda clay from deep boreholes at Hawkesbury, Ontario. Part I: geology and geotechnique; Canadian Geotechnical Journal, v. 20, p. 288-298.

Remenda, V.H.
1993. Origin and migration of natural groundwater tracers in thick clay tills of Saskatchewan and the Lake Agassiz clay plain; Unpublished Ph.D. thesis, University of Waterloo, Waterloo, Ontario, 271 p.

Remenda, V.H., Cherry, J. and Edwards, T.L.D.
1994: Isotopic composition of old ground water from Lake Agassiz: Implications for Late Pleistocene climate; Science, v. 266, p. 1975-1978.

Table 1: Geochemistry of bedrock aquifers in the southeastern Interlake.

	Carbonate rock aquifer	Winnipeg Formation aquifer
conductivity (S/cm)	853	1760
pH	7.50	8.75
temperature (°C)	7.43	6.3
D.O. (mg/L)	1.18	
calcium (mg/L)	66.2	16.9
magnesium (mg/L)	64.0	7.6
hardness (mg/L $CaCO_3$)	429	73.8
sodium (mg/L)	28.9	330
potassium (mg/L)	4.9	15.7
bicarbonate (mg/L)	487	220
chloride (mg/L)	12.7	231
sulfate (mg/L)	92.7	298
fluoride (mg/L)	0.42	3.04
nitrate (mg/L)	1.32	0.06
ammonia (mg/L-N)	0.1	
phosphate(mg/L)	0.006	
silica (mg/L)	12.4	6.3
boron (mg/L)	0.15	
manganese (mg/L)	0.47	N.D.
iron (mg/L)	0.47	0.13
tritium (T.U.)	54% >6	
oxygen-18 (‰ SMOW)	-14.4	-21.6

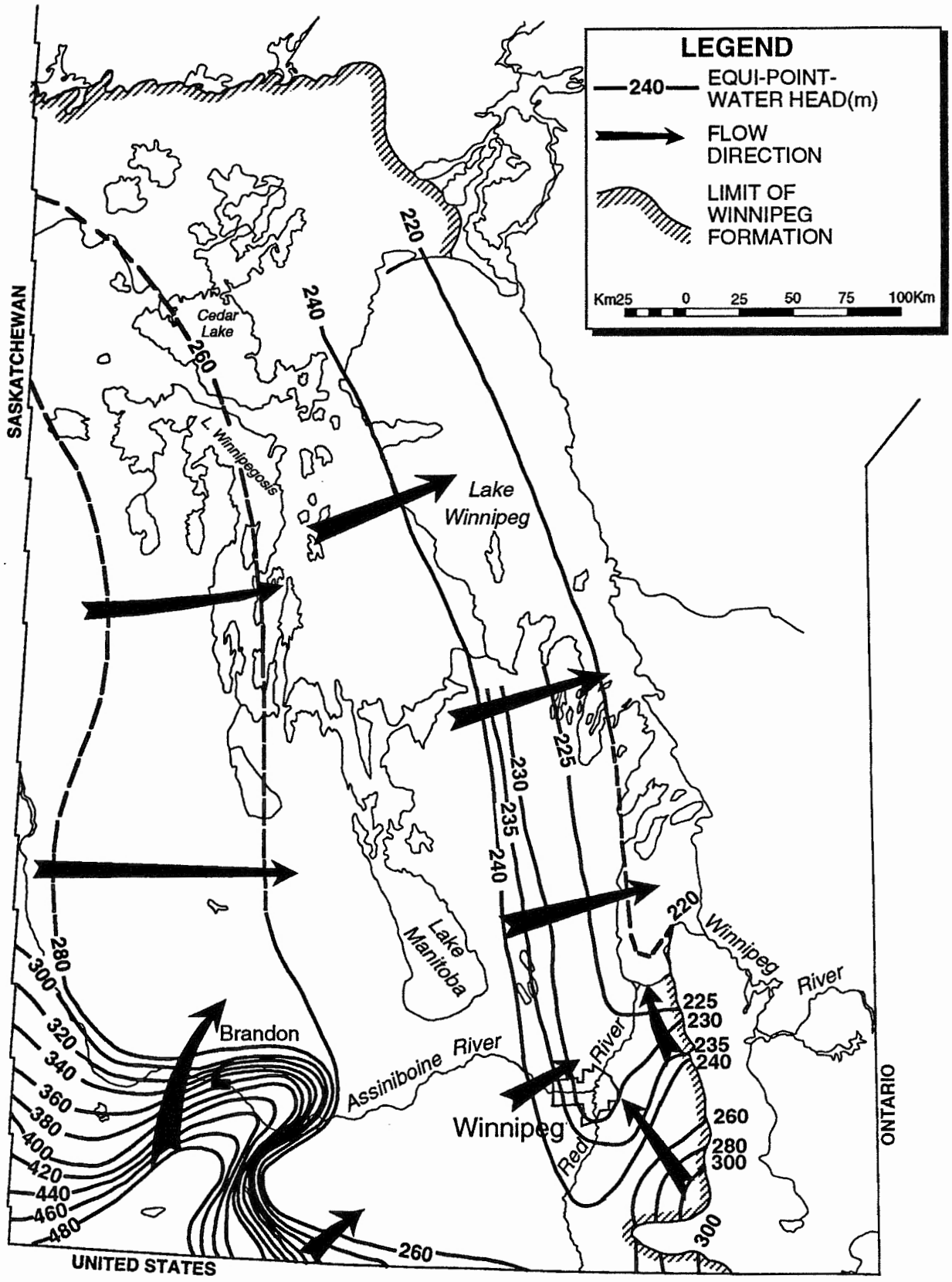

Figure 1. Regional groundwater flow in the Winnipeg Formation aquifer in Manitoba.

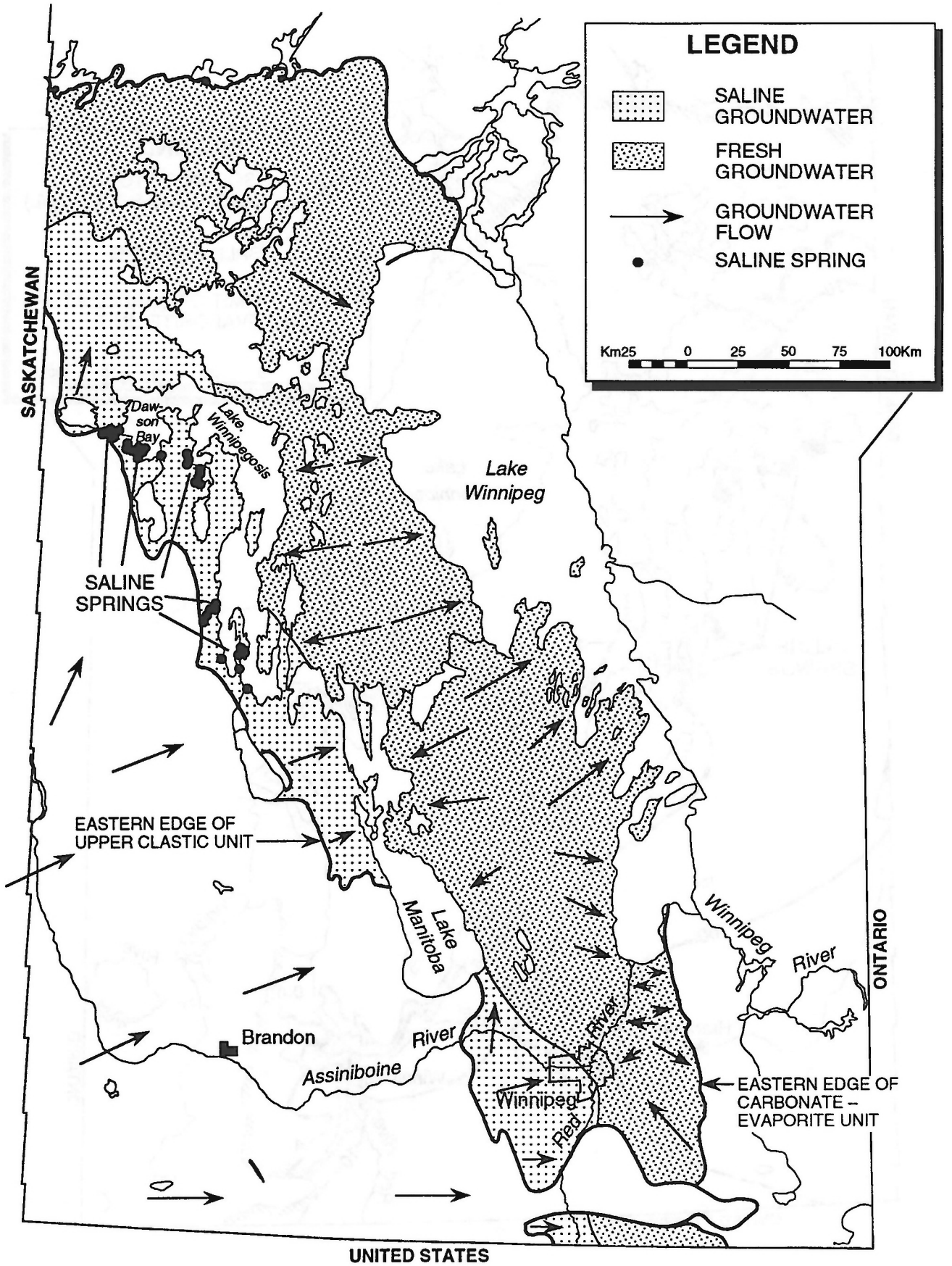

Figure 2. Regional groundwater flow in the carbonate rock aquifer in Manitoba.

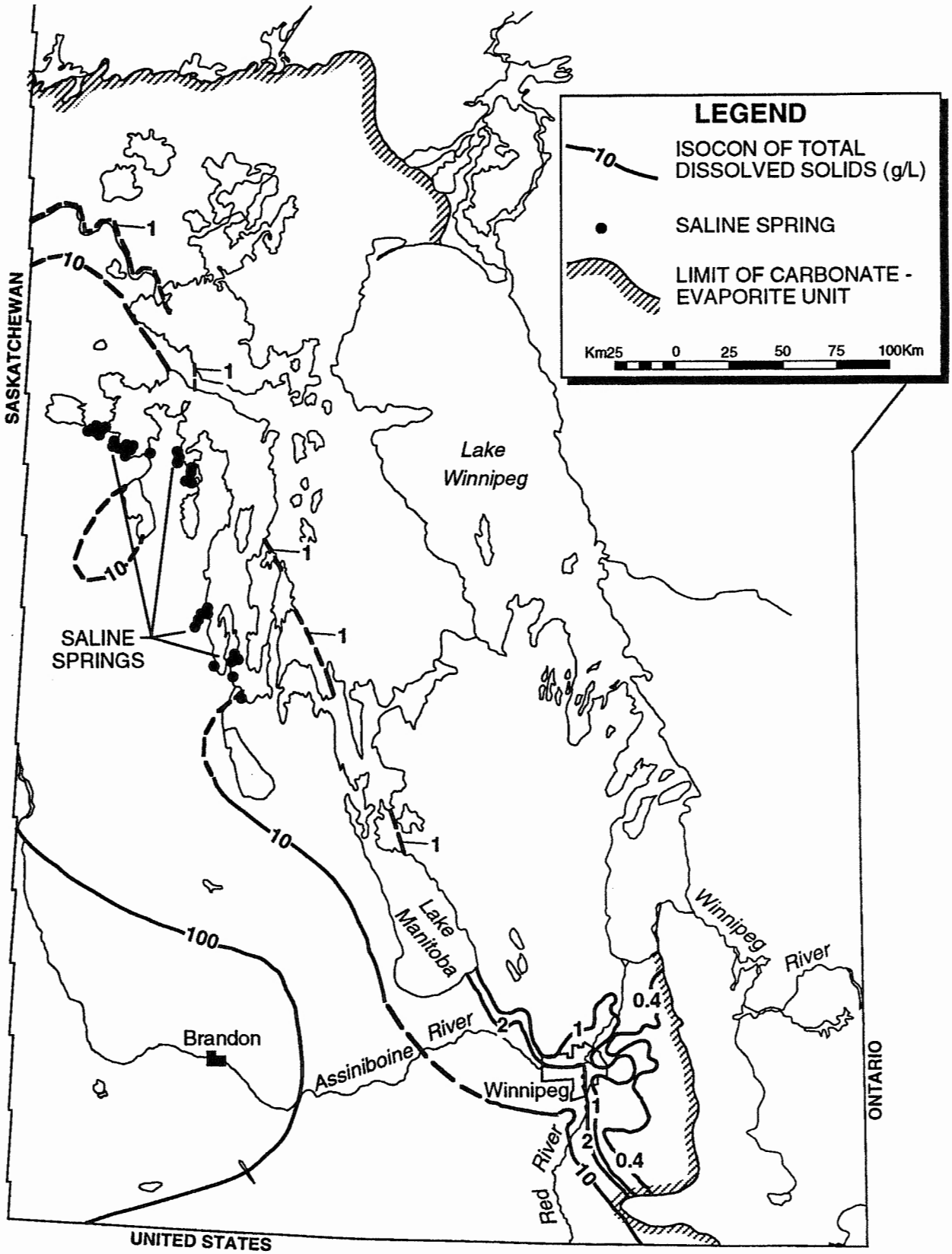

Figure 3. Groundwater quality in the carbonate rock aquifer.

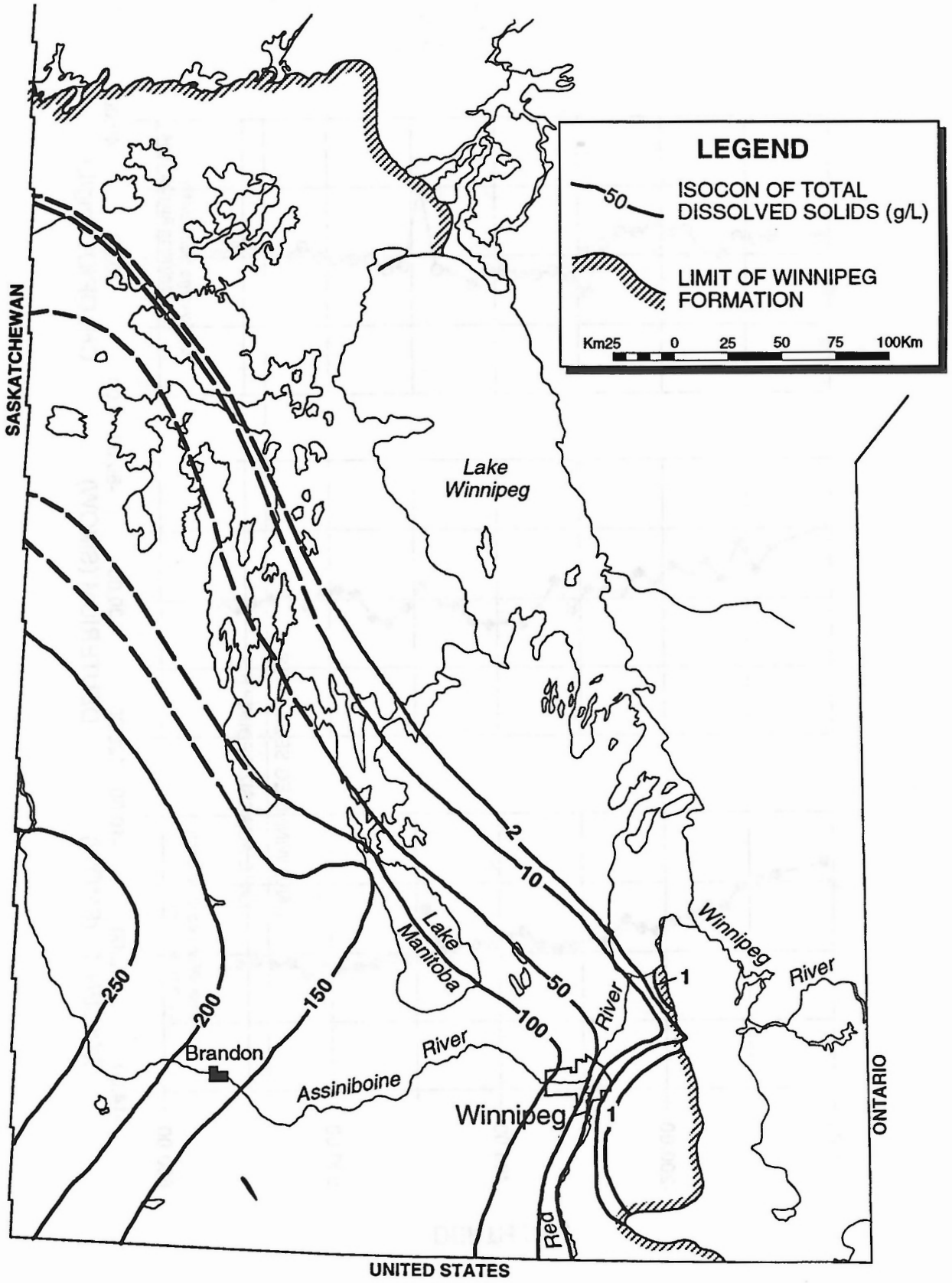

Figure 4. Groundwater quality in the Winnipeg Formation aquifer.

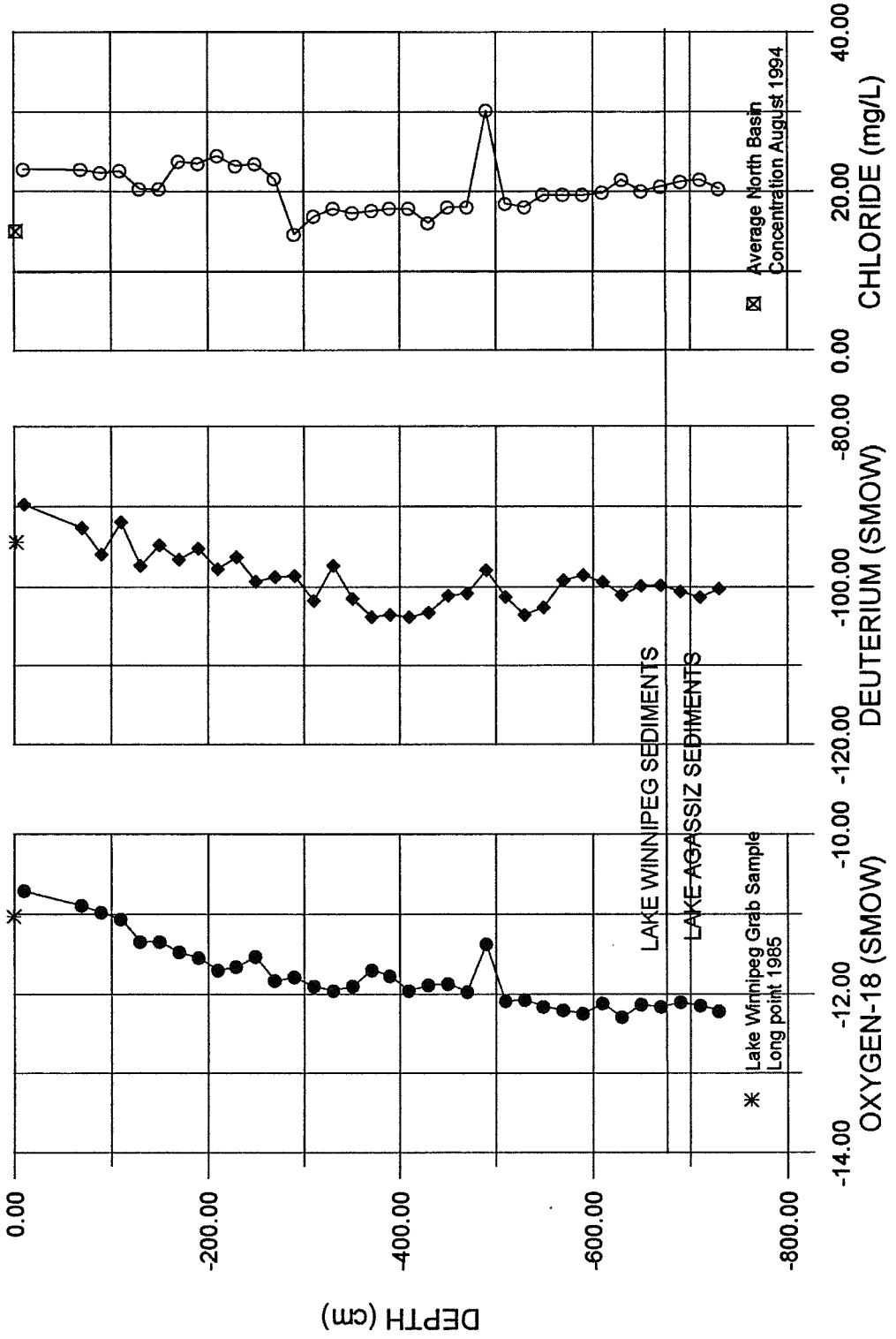

Figure 5. Stable isotope and chloride profiles for pore waters from core 103.

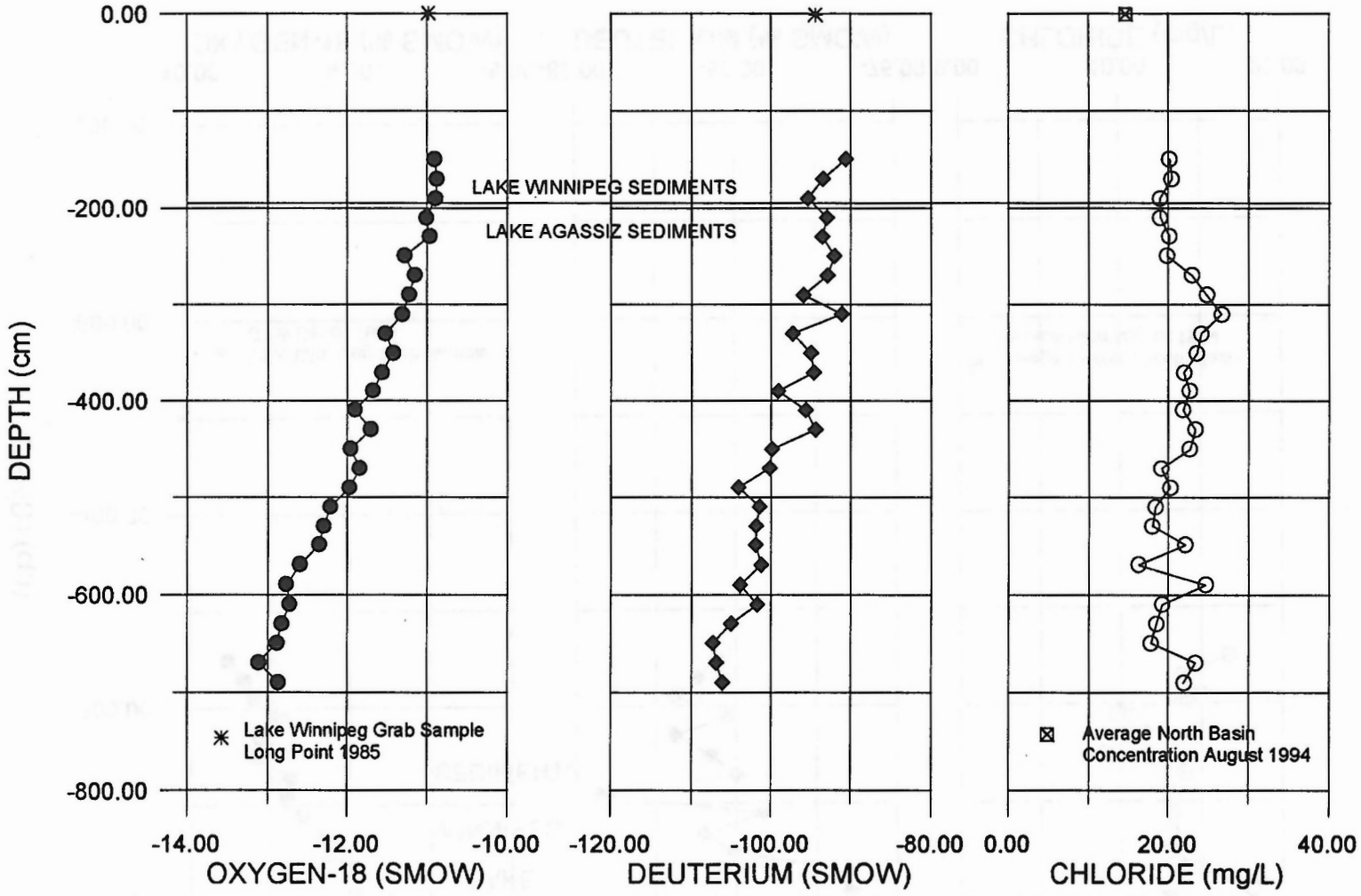

Figure 6. Stable isotope and chloride profiles for pore waters from core 107.

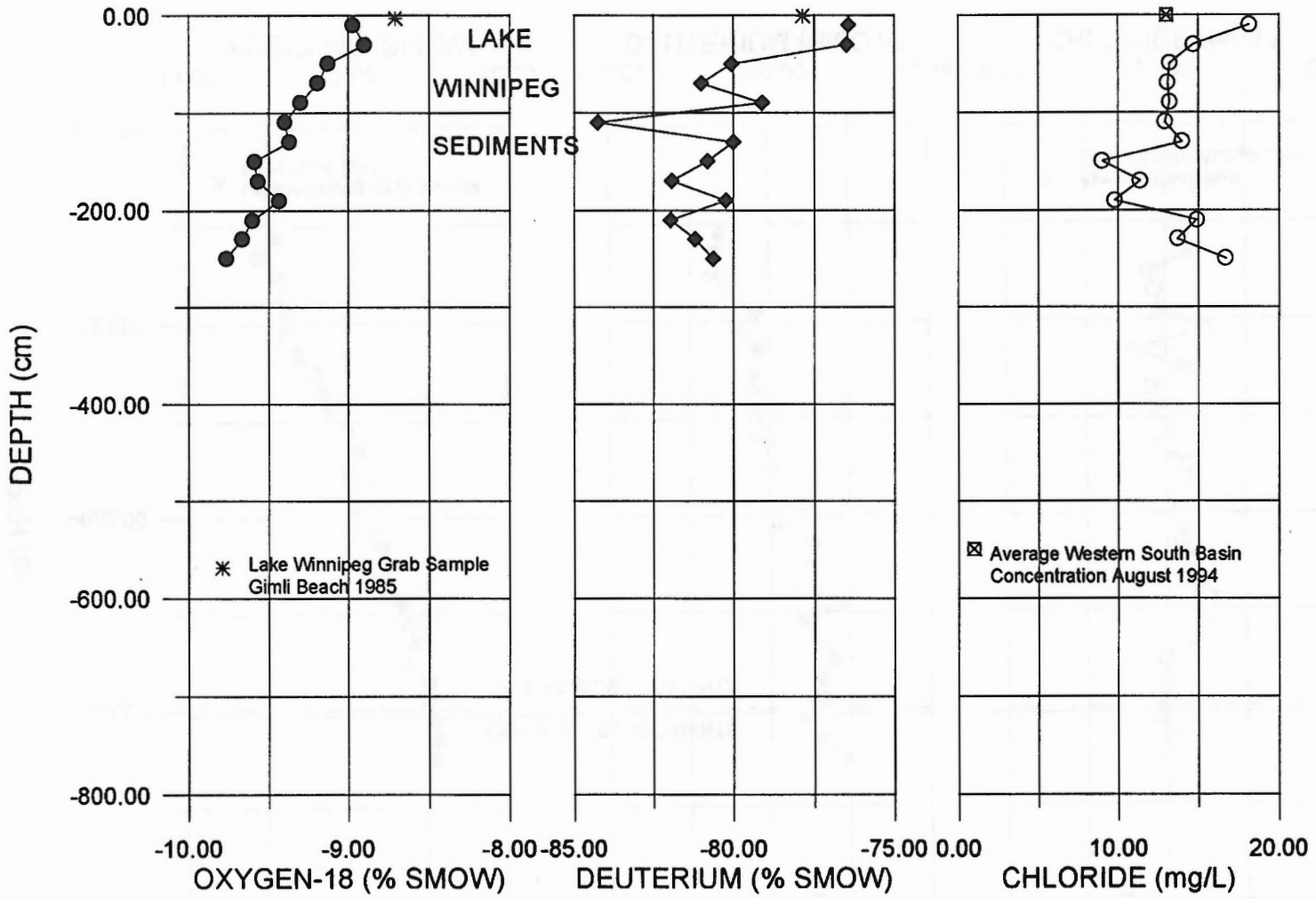

Figure 7. Stable isotope and chloride profiles for pore waters from core 115.

4.8 Stable isotopic composition of pore water and organic matter from Lake Winnipeg sediments

W.M. Buhay

The Godwin Institute for Quaternary Research
University of Cambridge, Free School Lane, Cambridge, United Kingdom CB2 3RS

INTRODUCTION

The oxygen and hydrogen isotopic composition of lake water is dependent on the varying isotopic effects of meteoric water supplying it, the hydrology of the lake basin and the effects of evaporation. Therefore, a record of the oxygen and hydrogen isotopic composition of lake water could be used to document past changes in the isotopic composition of the mean annual precipitation (related to changes in atmospheric circulation and mean annual temperature), basin hydrology and moisture regimes.

The primary objectives of this study were to investigate the properties of Lake Winnipeg sediment pore water and organic matter to obtain a better understanding of changes in former climatic and hydrologic conditions of central North America. At present the work is incomplete but the research is continuing. This report provides some preliminary results of the isotopic investigation of pore water and organic material from three Lake Winnipeg cores (103, 107 and 115, located in the central North Basin, the eastern North Basin and the South Basin, respectively).

SEDIMENT PORE WATER

The geochemistry of pore waters extracted from sediment cores 103, 107 and 115 (at 20 cm intervals using a confined piston extraction device) suggest that they are preserved lake water and that there has been no significant infiltration of groundwater into the lake from the Winnipeg Formation (Betcher and Buhay, this volume).

The oxygen and hydrogen isotopic composition of the pore waters extracted from the three cores are shown in Figure 1. The isotopic groupings are offset to the right of the Global Meteoric Water Line (GMWL; defined by the equation $\delta^2H = 8\delta^{18}O + 10$) (Dansgaard, 1964). This is a characteristic of lake waters that have been isotopically enriched in the heavy $^1H_2{}^{18}O$ and $^2H_2{}^{16}O$ molecules due to the preferential evaporation of lighter $^1H_2{}^{16}O$ molecules. Also in Figure 1, there is a distinct offset in these isotopic groupings along a line sub-parallel to the GMWL which probably reflects a differences in catchment drainage into the North and South Basins of the lake. For instance, drainage of northern catchments is probably responsible for the most depleted signals occurring in the core 103 and 107 pore waters. Water draining into the South Basin from southern catchments provides an enriched source for the 115 pore water.

The preservation of meteoric and evaporation isotopic signals in the pore waters of these three cores suggests that they may provide information on past regional climate and lake hydrology. However, some uncertainties are associated with the pore water isotopic measurements. For instance, it is not certain whether the time period represented by the sampling intervals (20 cm) was sufficient for pore water isolation due to sediment compaction. Therefore, it is not certain if the time interval represented by the pore water matches that of the sediment containing it. Also, isotopic diffusion of lighter isotopes and compaction-related movement of water may have homogenized the pore water vertically through the column and diluted the climate- and hydrology-related isotopic signals.

ORGANIC SEDIMENTS

In sediments, organic remnants of lacustrine organisms may also preserve a record of the oxygen and hydrogen isotopic composition of the lake water which they inhabited and, consequently, give clues to past regional climate and hydrology. Systematic biochemical fractionations between lake water and the cellulose and lipid fractions of aquatic material preserved in sediments make $\delta^{18}O$(cellulose) and δ^2H(lipid) measurements potentially useful for inferring past lake water $\delta^{18}O$(water) and δ^2H(water) values. Lipids are better suited to infer lake water hydrogen isotopic composition because, unlike cellulose, they contain few exchangeable OH^- groups.

Cellulose was prepared from sediment samples by solvent extraction, bleaching and alkaline hydrolysis (Edwards and Elgood, 1992). Oxygen isotope analysis was performed on CO_2 gas produced from sediment cellulose using a nickel pyrolysis technique (Edwards et al., 1994). Carbon isotope analysis was performed on CO_2 gas produced from sediment cellulose using a Carlo Erba™ Elemental Analyser. Lipids were extracted from the sediment using a non-polar solvent solution (Chloroform:methanol, 2:1). The solvent solution was evaporated away and the remaining lipids were freeze dried and stored at -4 ° C prior to isotopic analysis. Isotopic analysis of hydrogen was performed on H_2 gas obtained from zinc reduction of H_2O produced by combustion of dried lipids (DeNiro, 1981; Coleman et al., 1982). Oxygen ($^{18}O/^{16}O$) and hydrogen ($^2H/^1H$) isotope ratios (R) are expressed as parts per

thousand or 'per mil' (‰) in delta notation (δ) as; δ = (Rsample/RV-SMOW - 1)×10^3, where V-SMOW is Vienna - Standard Mean Ocean Water. Carbon isotopic measurements are expressed in delta notation with respect to PDB (Pee Dee Belemnite). The $\delta^{18}O$ (cellulose), $\delta^{13}C$ (cellulose) and $\delta^{2}H$ (lipid) values have analytical uncertainties of ± 0.2 ‰, ± 0.1 ‰ and ± 2.0 ‰, respectively.

Presently the organic extractions of cellulose and lipids and isotopic measurements of oxygen, carbon and hydrogen isotopic compositions of these organic materials are only partially completed for core 103.

In Figure 2, the $\delta^{18}O$ (pore water) measurements are directly compared to $\delta^{18}O$ (water) values inferred from the $\delta^{18}O$ (cellulose) measurements ($\delta^{18}O$(water) = $\delta^{18}O$(cellulose) - 28.8 ‰) (Edwards and McAndrews, 1989). There is a good correspondence between the minimum values of the inferred $\delta^{18}O$(water) compositions and their respective pore water isotopic compositions. This suggests that isotopic enrichments in the lake water during the past, preserved by the phytoplankton cellulose, have been effectively diluted from the pore water by isotopic diffusion and movement of lighter water upward through the sediment column. Alternatively, these processes may have been rather localized in the sediment column and the sediment pore water may represent preserved lake water. In this case the differences in the estimates of lake water isotopic compositions provided by the pore water and the cellulose may be explained in terms of differences in the isotopic composition of the lake water column. Pore water trapped in sediments of a lake such as Lake Winnipeg (in which the water column may, or may not, mix vertically) would represent the mean annual isotopic composition of the lake water. In contrast, the lake water isotopic composition inferred from phytoplankton cellulose would only represent the summer season isotopic composition of the lake. Warm dry summers, resulting in the isotopic enrichment of surface waters and consequently phytoplankton cellulose, do not necessarily result in a distinct enrichment of bottom lake water where sediment accumulation results in pore water entrapment. However, during times when surface water enrichment is minimal (cool and wet summers) estimates of lake water isotopic composition inferred from phytoplankton cellulose would be closer to that recorded by the sediment pore water.

Estimates of lake water hydrogen isotopic composition, inferred from $\delta^{2}H$ (lipid) measurements, were also attempted. Data for $\delta^{2}H$ (pore water) and $\delta^{2}H$ (lipid) measurements were compared (Figure 3). The biochemical factor accounting for isotopic fractionation of hydrogen between organic lipids and the water medium is not known at present. However, Figure 3 shows an encouraging correspondence between $\delta^{2}H$ (lipid) and their respective pore water values.

The excessive variation in the $\delta^{2}H$ (lipid) signal may indicate that the lipids were oxidized prior to isotopic analysis allowing exchangeable hydroxyl groups (OH^-) to form. Also, the presence of other organic molecules (pigments, sterols etc.), with potentially different biochemical fractionation factors, could account for some of the isotopic variability shown by the $\delta^{2}H$ (lipid) profile in Figure 3. In future steps will be taken to avoid contamination and enhance lipid purification.

Stable isotopic compositions of carbon from organic matter can reflect changes in the environmental conditions of deposition. The most important process controlling the carbon isotopic composition of the different carbon pools in lacustrine environments is the preferential removal of $^{12}CO_2$ from the carbon dioxide reservoir in the surface waters by photosynthetic fixation. Therefore, fluctuations in surface water productivity, resulting in a depleted surface water CO_2 reservoir, can produce significant changes in the $\delta^{13}C$ of the organic materials produced by photosynthesizing organisms.

Figure 4 shows a comparison between $\delta^{13}C$ (cellulose) and $\delta^{13}C$ (bulk organic) (incomplete at present) time-series profiles for core 103. The offset to more depleted values taken by the bulk organics at the -400 cm level may represent an increase in the productivity of photosynthesizing organisms that do not produce cellulose (algae). This can occur in accordance with elevated nutrient levels in the lake. Therefore, it is likely that at the time represented by the -400 cm sediment level there was a major change in the basin hydrology, possibly the diversion of the Saskatchewan River into the North Basin as discussed by McMartin (this volume).

A large river would also deliver terrestrial carbon enriched in ^{12}C which could explain the general depletion trend of the $\delta^{13}C$ (bulk organic) values in the upper section of the core. With an increase in algal productivity during the later half of the record the CO_2 reservoir, available to the phytoplankton, becomes depleted in ^{12}C which results in a slight enrichment of ^{13}C in their cellulose. The significant depletions in $\delta^{13}C$ that occur at core levels -90 and -670 cm probably reflects an increase in the preservation of depleted terrestrial organic material in these intervals.

CONCLUDING REMARKS

Based on the cellulose inferred $\delta^{18}O$ (water), $\delta^{13}C$ (cellulose) and $\delta^{13}C$ (bulk organic) profiles, the following preliminary inferences can be made about climate and hydrology in central North America during the late Holocene. In Figure 2, the enriched interval between -400 and -500 cm may correspond to a warm and dry interval in the past when Lake Winnipeg may have been a closed basin during mid-Holocene. After this interval the inferred depletion in $\delta^{18}O$ (water) may correspond to the diversion of the Saskatchewan River (originating in the central prairies) into Lake Winnipeg. This interpretation is supported by the separation of cellulose and bulk organic $\delta^{13}C$ profiles in Figure 4. The increased input of nutrients into Lake Winnipeg after 4,000 years BP is the most probable explanation for an elevation in productivity leading to a

depleted $\delta^{13}C$ profile for the algae and an enriched $\delta^{13}C$ profile for phytoplankton-produced cellulose.

Oscillations in the inferred $\delta^{18}O$ (water) isotopic composition above the -400 cm level (Fig. 2) suggest that climate was rather cyclic in central North America during the late Holocene. Further details about climate and hydrology in this region will become available in the future when the $\delta^{18}O$ (cellulose), $\delta^{2}H$ (lipid), $\delta^{13}C$(cellulose) and $\delta^{13}C$ (bulk organic) profiles are completed for cores 103 and 107. Core 107 will provide a record of climatic and hydrologic change in central North America during the Lake Agassiz period.

ACKNOWLEDGMENTS

I wish to acknowledge Mike Lewis, Brian Todd, Harvey Thorleifson and Erik Nielsen for allowing me to participate in the Lake Winnipeg Project. I would also like to thank Ray Hesslein, Lyle Lockhart and Hedy Kling at the Freshwater Institute for their support and advice during this research.

REFERENCES

Coleman, M.L., Shepherd, T.J., Durham, J.E., Rouse, J.E. and Moore, G.R.
1982. Reduction of water with zinc for hydrogen isotope analysis; Analytical Chemistry, v. 54, p. 993-995.

Dansgaard, W.
1964. Stable isotopes in precipitation; Tellus, v. 4, p. 436-468.

DeNiro, M.J.
1981. The effects of different methods of preparing cellulose nitrate on the determination of the D/H ratios of non-exchangeable hydrogen of cellulose; Earth and Planetary Science Letters, v. 54, p. 1845-1854.

Edwards, T.W.D., Buhay, W.M., Elgood, R.J. and Jiang, H.B.
1994. An improved nickel-tube pyrolysis method for oxygen isotope analysis of organic matter and water; Chemical Geology, v. 114, p. 179-183.

Edwards, T.W.D. and Elgood, R.J.
1992. Technical procedure 28.0; Environmental Isotope Laboratory, University of Waterloo.

Edwards, T.W.D. and McAndrews, J.H.
1989. Paleohydrology of a Canadian Shield lake inferred from ^{18}O in sediment cellulose; Canadian Journal of Earth Sciences, v. 26, p. 1850-1859.

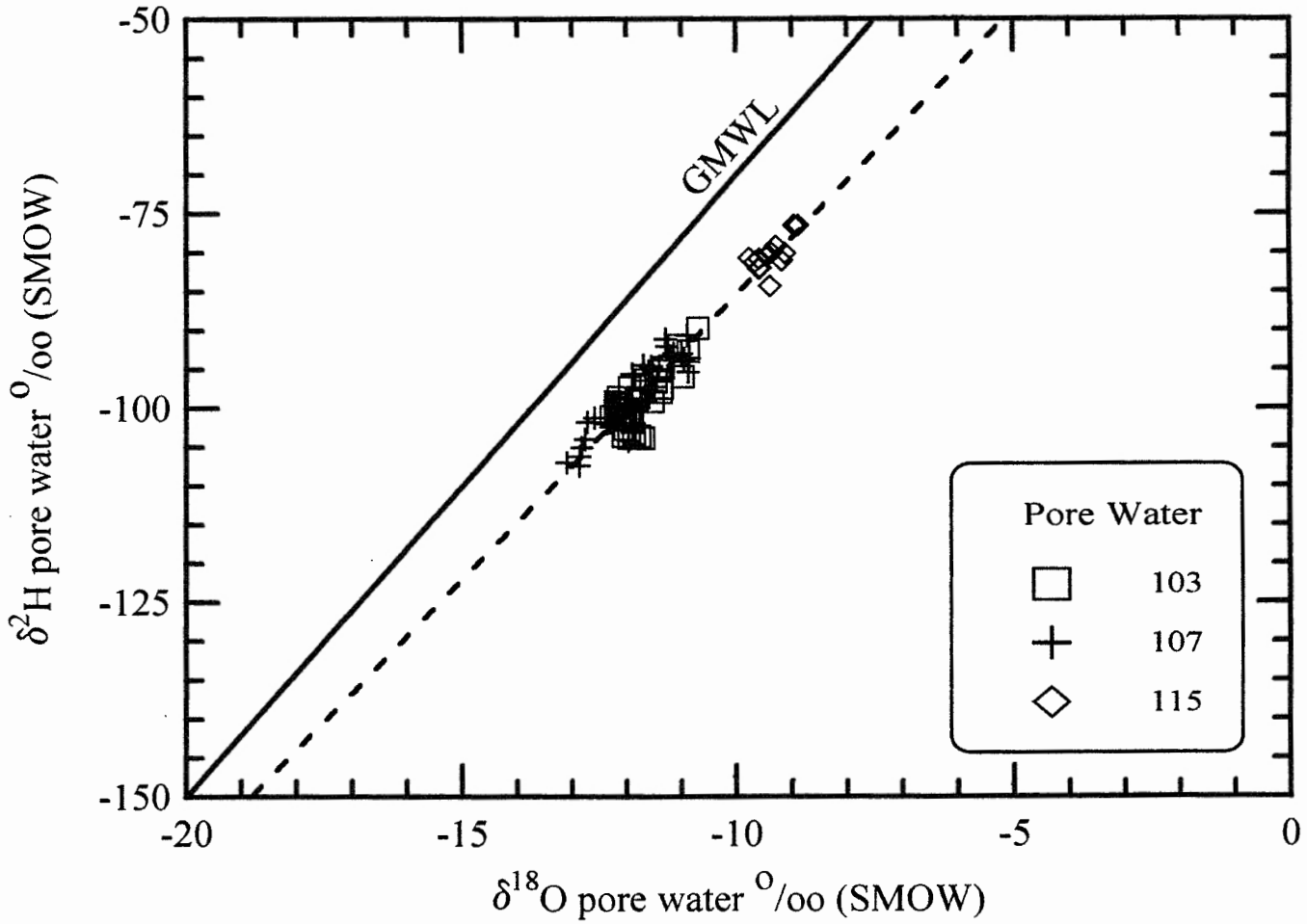

Figure 1. $\delta^{18}O$ vs. $\delta^{2}H$ for pore waters extracted from Lake Winnipeg cores 103, 107 and 115, compared to the Global Meteoric Water Line (GMWL).

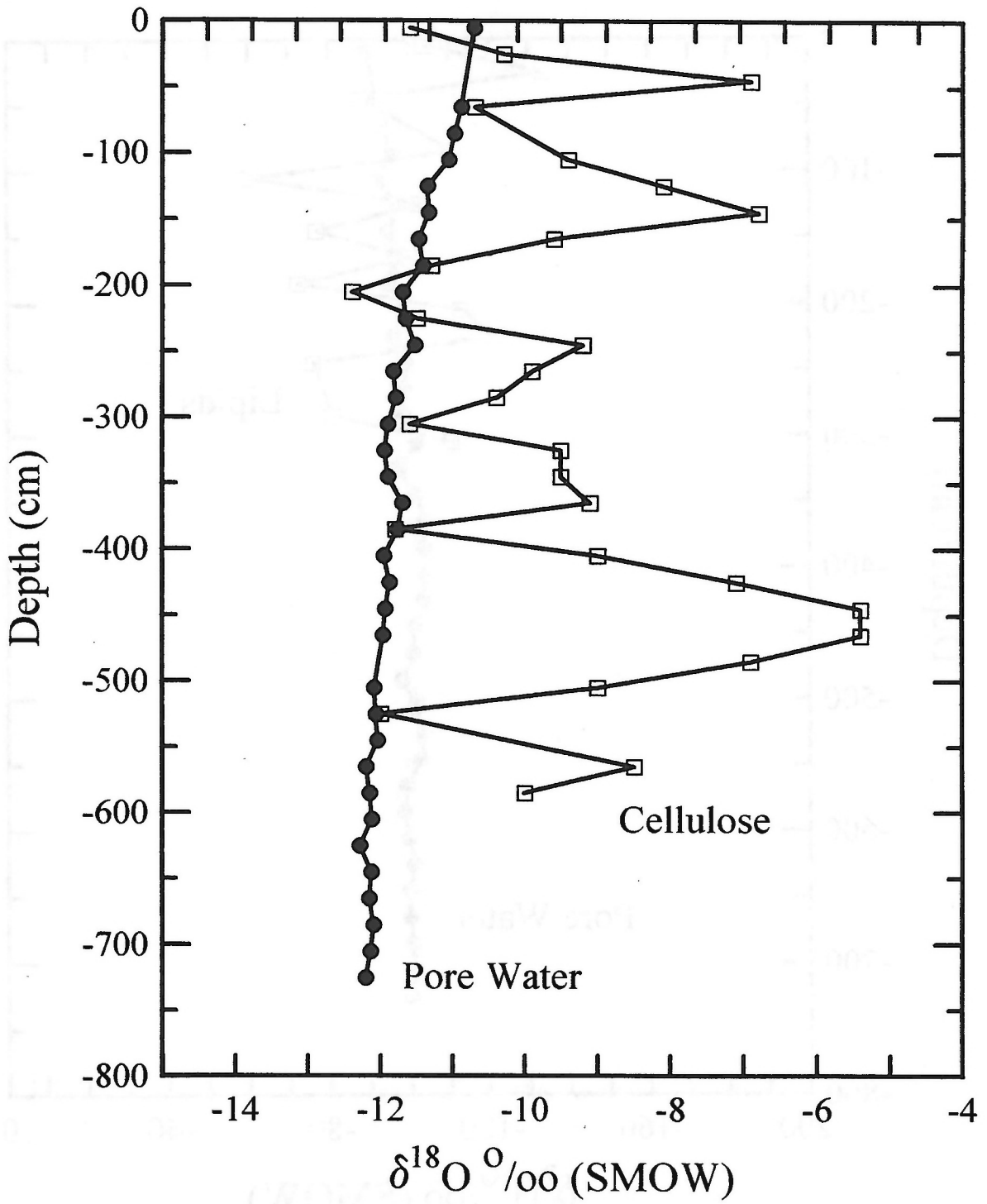

Figure 2. Core 103 time-series showing the comparison between $\delta^{18}O_{pore\ water}$ and the $\delta^{18}O_{water}$ values inferred from $\delta^{18}O_{cellulose}$ measurements.

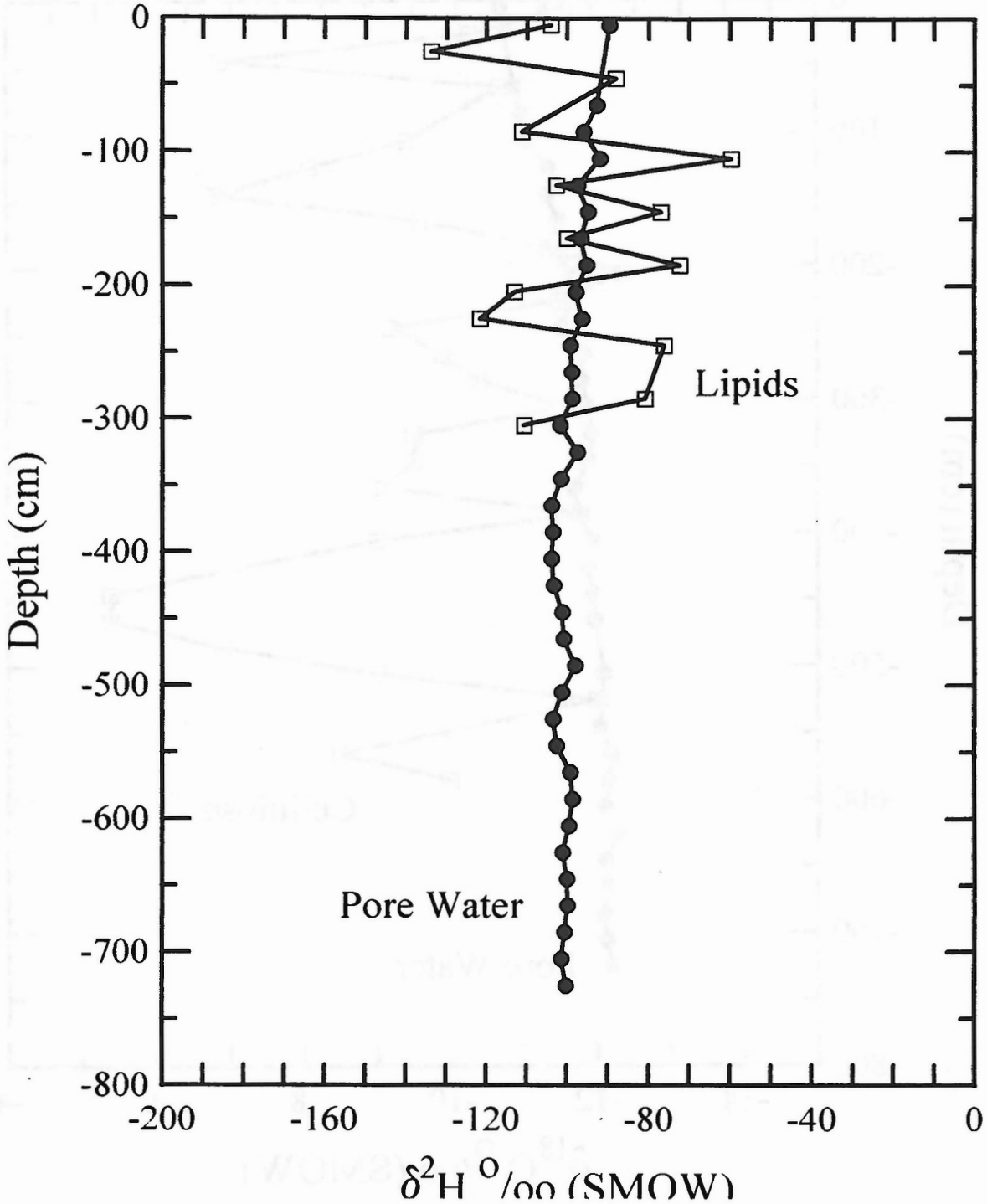

Figure 3. Core 103 time-series showing the comparison between $\delta^{18}H_{pore\ water}$ and the $\delta^{2}H_{lipid}$ measurements.

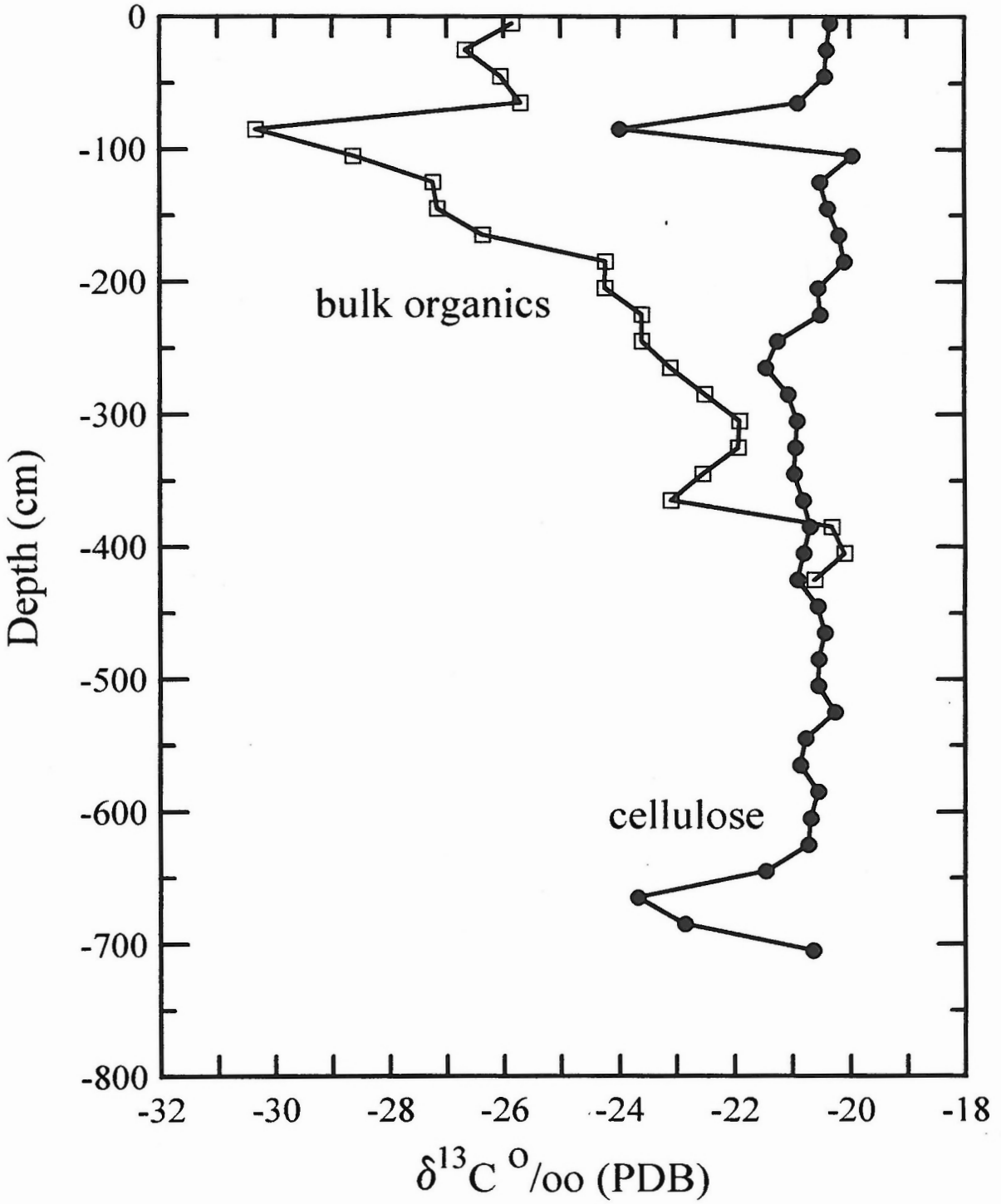

Figure 4. Core 103 time-series showing the comparison between $\delta^{13}C_{cellulose}$ and the $\delta^{13}C_{bulk\ organics}$.

4.9 Ostracode stratigraphy of Lake Winnipeg sediments

C.G. Rodrigues

Department of Earth Sciences
University of Windsor, Windsor, Ontario N9B 3P4

ABSTRACT

Three zones are recognized in cored sections from Lake Winnipeg. The oldest zone, C, is associated with Lake Agassiz sediments and the other two zones (A and B) are correlated with Lake Winnipeg sediments. Water depth was greater during the deposition of the Lake Agassiz sediments which are overlain unconformably by the shallower-water Lake Winnipeg sediments.

INTRODUCTION

Gravity and piston cores were collected during Cruise 94-900 of the CCGS *Namao*. Ten of these cores (Table 1 and Fig. 1) were selected for ostracode analysis. Samples ranging in volume from 5 to 12 cc were collected at intervals of 10 cm beginning at 0.5 m in each core. The samples were wet-sieved in a 63 μm sieve and the residues examined for ostracodes. A total of 444 samples were processed. A zonation of the cores based on the ostracodes in the residues is presented in this report.

ZONATION OF CORES

The cored sections are divided into three zones (Table 2). Ostracodes are absent or present in low numbers (*Candona* spp.) in the oldest zone (C). Zone B is subdivided into a lower B_2 interval and an upper B_1 interval. The lower interval (B_2) is characterized by congeners of *Candona* and *Limnocythere*. The number of ostracode valves are lower and *Limnocythere* is absent in the upper interval (B_1), where some of the valves are usually broken. Ostracodes are absent in zone A. The zonation of the cores is shown in Figures 2 and 3.

DISCUSSION

The cored sections have been subdivided into the older Lake Agassiz sediments and the younger Lake Winnipeg sediments on the basis of acoustic data. These data also indicate that the boundary between the Lake Agassiz and Lake Winnipeg sediments is unconformable. Zone C is associated with the Lake Agassiz sediments and the other zones (A and B) are associated with the Lake Winnipeg sediments (Figs. 2, 3).

Candona subtriangulata is the major ostracode species in zone C, indicating relatively deep-water conditions (up to 200 m) during the deposition of the Lake Agassiz sediments. The water depth was shallower during the deposition of the Lake Winnipeg sediments on the basis of the presence of *Limnocythere* spp. in zone B. The radiocarbon date of 4,040 ± 70 years BP for plant material from an organic-rich layer in core 122a (Vance, this volume; Fig. 3) provides a minimum age for the change from relatively deep to shallower water conditions in the Lake Winnipeg basin.

Table 1. Water depths for cores, length of cores and number of samples processed.

Basin	Core Number	Water Depth (m)	Length (m)	Number of Samples
North	103	15.9	8.16	80
	104a	16.2	3.65	38
	104b	-	-	8
	105	15.8	5.96	51
	106	16.9	7.89	70
	107	17.1	6.96	70
South	110a	11.3	2.26	23
	113a	9.8	2.14	21
	120	10.1	3.54	35
	122a	9.8	4.77	48

Table 2. Description of zones in the cored sections.

Sequence	Zone	Description
WINNIPEG	A	Diatoms present in upper part of interval. Thecamoebians present. Ostracodes absent.
	B_1	Thecamoebians present. Small gastropods and pelecypods (both rare) present. Ostracodes present, usually broken (*Candona*). Calcareous fossils etched and pitted.
	B_2	Thecamoebians present. Small gastropods and pelecypods (both rare) in lower part of zone. Ostracodes present; highest number of valves in lower part of zone (*Candona* and *Limnocythere*).
AGASSIZ	C	Ostracodes absent or present in low numbers (*Candona*).

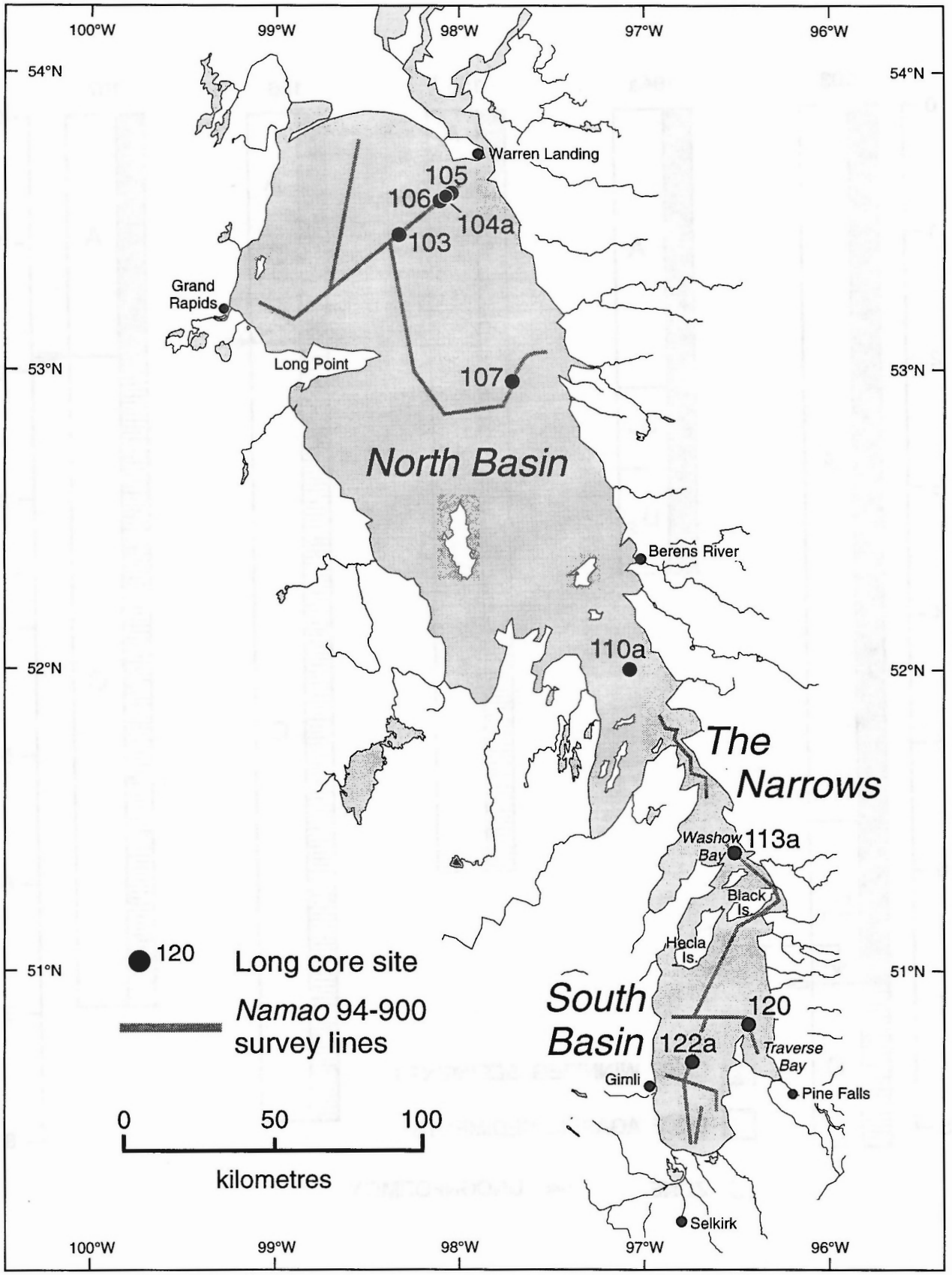

Figure 1. Location of core sites.

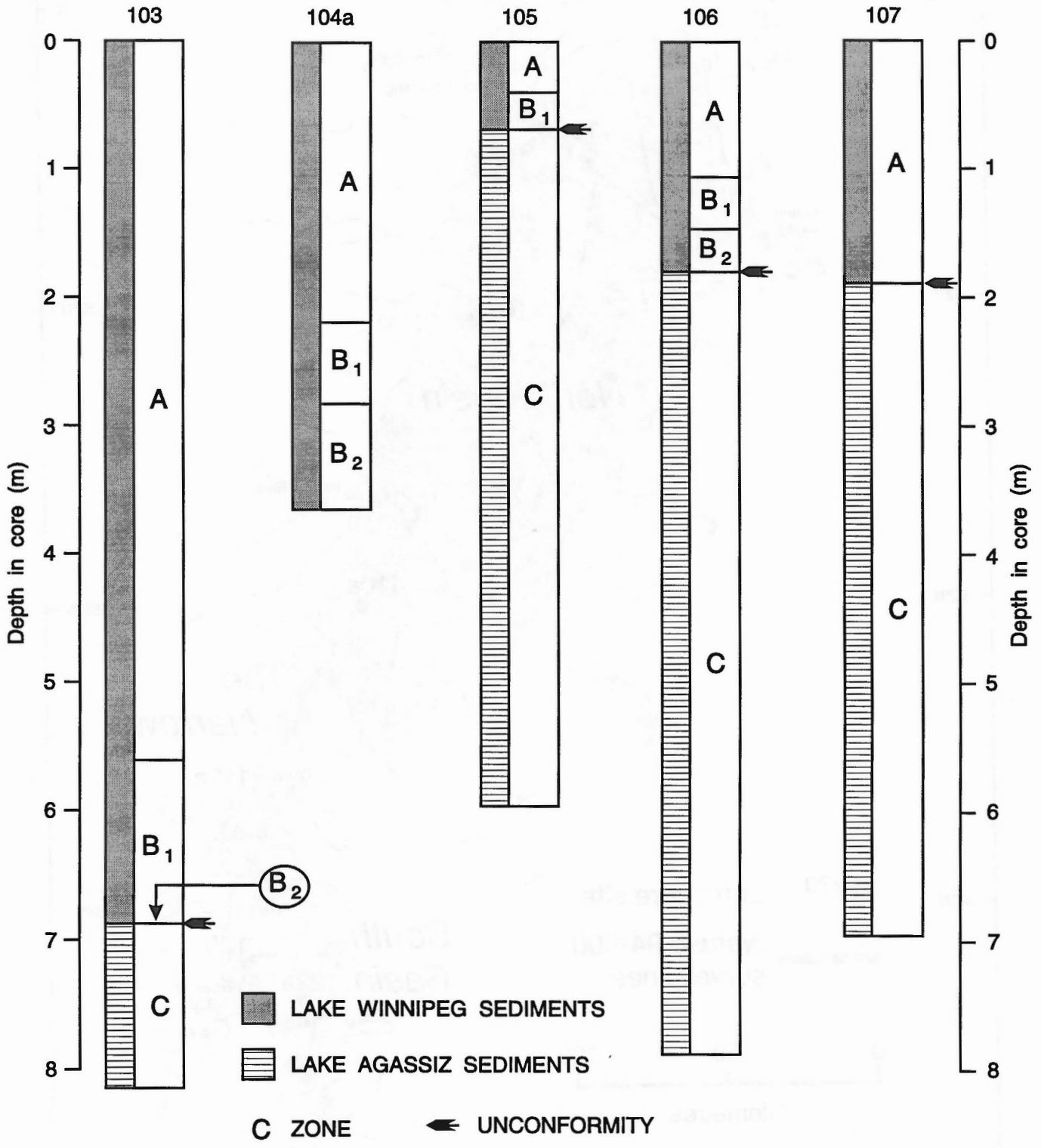

Figure 2. Zonation of cores from the North Basin of Lake Winnipeg on the basis of the ostracode fauna.

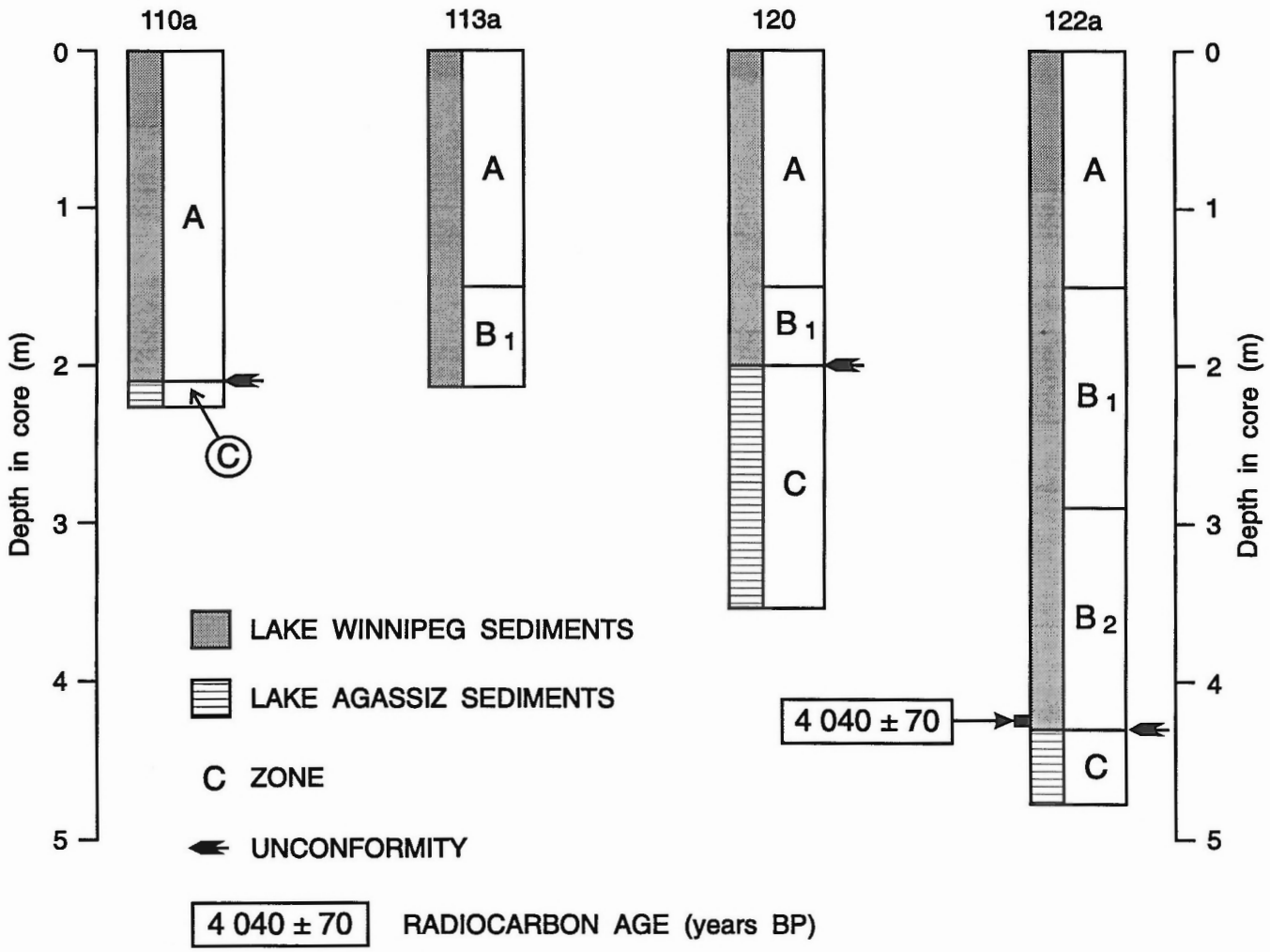

Figure 3. Zonation of cores from the South Basin of Lake Winnipeg on the basis of the ostracode fauna.

4.10 Thecamoebian stratigraphy of Lake Winnipeg sediments

S. M. Burbidge and C. J. Schröder-Adams

Department of Earth Sciences
Carleton University, Ottawa, Ontario K1S 5B6

ABSTRACT

Thecamoebians were studied from Core 103 of the North Basin and Core 122a from the South Basin of Lake Winnipeg. The Lake Agassiz sequence is barren of thecamoebians and tintinids whereas the overlying Lake Winnipeg sequence is characterized by an abundance of microfossils. In the South Basin three thecamoebian assemblages can be distinguished. Species compositions indicate an initial brackish phase followed by freshwater conditions. The final phase marks human settlement in the area causing eutrophication of the lake and resulting in a significant abundance increase. Thecamoebian distribution in the North Basin shows no indication of an initial brackish water phase which might suggest different recharge areas for the two basins. Eutrophication is also not evident in the North Basin. Thecamoebian abundance, however, varies significantly during lake history. Future comparisons with geochemical and sedimentological signals are needed to explain these fluctuations.

INTRODUCTION

Thecamoebians are an informal group of testate protozoans comprised mostly of taxa from the order Arcellinida but also including forms from the order Gromida (Loeblich and Tappan, 1964). Thecamoebians can be found in all types of freshwater bodies as well as a variety of moist environments such as mosses and soils. Although thecamoebians generally prefer freshwater, a few taxa are found in brackish water. Faunal preservation is more complete in lakes and bogs making this group an important paleolimnological tool (Medioli and Scott, 1988).

Studies have shown that thecamoebian assemblages may vary throughout lake history. However, ecological controls have only been established for a small number of species due to the lack of information about lake chemistry. The multidisciplinary nature of the Lake Winnipeg Project has the potential to significantly add to our understanding of the ecological requirements of thecamoebians.

Thecamoebians have a saclike test with a simple aperture for the extrusion of pseudopods (Fig. 1). The longest dimension of the test commonly ranges from 40 to 250 μm. Tests can be secreted by the organism (autogenous tests) or built by agglutinating foreign particles (xenogenous tests) in autogenous cement. Autogenous tests are of three basic types: proteinaceous (e.g. some species of *Arcella* and *Centropyxis*), siliceous or rarely, calcareous (Ogden and Hedley, 1980). Some siliceous tests are made of a mixture of idiosomes (secreted particles) and xenosomes (agglutinated particles) which increases their fossilization potential compared to tests composed completely of autogenous silica.

Almost all fossilized aquatic thecamoebians possess a xenogenous test characterized by particles cemented to an organic pellicule. The nature of the xenosomes varies from sand grains to diatom frustules and their nature appears to be controlled by the composition of the substrate (Medioli et al., 1987). Some genera (e.g. *Heleopera*) agglutinate idiosomes of thecamoebians on which they prey (Ogden and Hedley, 1980).

The general morphology of thecamoebian tests can be divided into two broad categories: (1) cap-shaped (e.g. *Arcella*, *Centropyxis*), with an invaginated aperture on the flattened ventral side; and (2) sack-shaped (e.g. *Difflugia*, *Pontigulasia*) with the aperture located at the tapered end of the structure.

The pseudopods are flowing extensions of the cytoplasm which protrude through the aperture of the shell and are used for amoeboid locomotion and food retrieval. Thecamoebians feed mainly upon bacteria, fungi, algae or other protozoans (Ogden and Hedley, 1980).

Thecamoebian reproduction occurs almost exclusively by replication of the parent during asexual binary fission (Loeblich and Tappan, 1964). While sexual reproduction has been documented it is extremely rare. The size of the test is probably controlled in a large degree by the volume of cytoplasm available in the parent test at the time of division which is, in turn, largely controlled by the availability of food in the period preceding reproduction.

Encystment occurs in a large number of thecamoebian species as a means of rest, dormancy or defense (Ogden and Hedley, 1980). Cysts are capable of withstanding extreme environmental conditions such as desiccation, freezing or lack of food. Encystment capability allows thecamoebians to be readily transported and distributed, while still alive, over long distances by a variety of agents.

Tintinids, which are also found in abundance in Lake Winnipeg are planktic, ciliated protozoans which possess a conical or bell-shaped shell called a lorica. The lorica, which is commonly 50-200 μm in length consists of agglutinated particles in a proteinaceous wall. While most species of tintinids are marine there are about 10 freshwater species.

METHODS

Core 103 in the North Basin and Core 122a in the South Basin were selected for preliminary qualitative and quantitative analyses of the thecamoebian fauna of Lake Winnipeg. Samples were analyzed at 40 cm intervals from each core beginning with the uppermost sample (5 cm) and proceeding downcore. A total of 32 samples, 12 from Core 122a and 20 from Core 103, were processed and examined.

In the laboratory, samples were weighed to determine approximate sample size. Since drying can cause disintegration of the thecamoebian tests, samples were not dried prior to weighing. Samples were soaked in water and soda ash for 30 minutes to aid breakdown of the consolidated mud. Each sample was then gently wet-sieved through a 325 mesh (0.044 mm) screen to remove the clays. The soaking and washing process was repeated if necessary to completely remove all the mud. The washed residues were then immersed in ethanol (95%) for storage and examination.

Analysis was performed using a combination of transmitted and reflected light under a binocular dissecting microscope. The whole sample was examined and all specimens were identified and tallied. Fractional abundance with associated uncertainty are presented in Tables 1 and 2. The uncertainty associated with the fractional abundance of each species was determined using a standard error equation described by Patterson and Fishbein (1989):

$$s_{x_i} = 1.96\sqrt{\frac{X_i[1-X_i]}{N}}$$

where (N) is the total number of counts, and (X_i) is the fractional abundance of species I. This provides abundance errors at the 95 percent confidence level.

An approximation of the number of Tintinids present in each sample was made by counting the number of individuals present in a fraction of the sample and multiplying this value by the appropriate factor to approximate the whole sample. Since this is only an approximation the whole sample product was rounded off to the nearest 50 (Tables 1 and 2).

RESULTS

Taxonomic Problems

Identification of thecamoebians at the species level can be somewhat arbitrary. This is because they are non-interbreeding organisms and consequently there is no objective way of determining the validity of a species (Medioli and Scott, 1983). The identification process is further complicated by the wide range of morphological variability exhibited by this group both within and between species.

For the purposes of this study specimens were sorted into morphologically similar groups (morphotypes) and identified as species according to current literature (Table 3). Although these distinctive morphotypes were assigned specific names, these are tentative and many of the so-called species may be synonymous (Medioli and Scott, 1983; Medioli et al., 1987). This is not to say that recognition of these morphotypes is not important, on the contrary, the abundance or dominance of a particular type may well be a response to distinctive environmental conditions (Asioli and Medioli, in press). Therefore, if thecamoebians are to be used as a tool in paleolimnological studies, the distinction between ecotypes within species is important. For this preliminary report, no distinction was made between ecotypes and species. Subsequent detailed work is required to determine which morphotypes are species and which are intraspecific variants.

Faunal Distribution

CORE 122a - South Basin

Two sequences are recognized in Core 122a (Fig. 2), the upper sequence from 0-435 cm and the lower sequence form 435-477 cm. The Lake Agassiz sediments of the lower sequence are barren of thecamoebians as well as other common microfauna such as tintinids. The Lake Winnipeg sediments of the upper sequence, on the other hand contain a rich assemblage of thecamoebians and tintinids. Species diversity increases gradually from 4 to about 15 species in the lower 150 cm of the Lake Winnipeg sediments and remains relatively constant above 150 cm. Abundance fluctuates significantly but shows a marked increase near the top of the core. Tintinids occur at relatively low numbers (50-550 specimens) except near the top of the core (45 cm) where 11300 specimens were counted.

In the South Basin three thecamoebian assemblages can be recognized within the Lake Winnipeg sequence. The lowest assemblage, occurring from about 425 - 325 cm, is dominated by *Arcella* spp. and *Centropyxis aculeata* (Fig. 2). The central portion of Core 122a (325 - 85 cm) is characterized by a mixed species association of the genus *Difflugia* commonly found in gyttja. This assemblage is dominated by small xenogenous species such as *Difflugia manicata, Difflugia ampullula, Difflugia curvicualis* and *Difflugia protaeiformis* while *Arcella* spp. and *Centropyxis aculeata* have disappeared. The top portion of Core 122a (above 85 cm) is characterized by an increase in the abundance of *Cucurbitella tricuspis*.

CORE 103 - North Basin

Core 103 (Fig. 3) contains the Lake Agassiz sequence (686 - 816 cm) overlain by the Lake Winnipeg sequence. As in Core 122a the Lake Agassiz sediments of Core 103 lack thecamoebians and tintinids while the Lake Winnipeg sequence contains abundant microfossils. The number of species represented in Core 103 varies between 8 and 12. The number of individuals varies more significantly and is higher than in the

South Basin, but also shows an increase near the top of the core. There is a marked decline in the thecamoebian population near the base of the Lake Winnipeg sequence (365 cm in Core 122a and 645 cm in Core 103). This decline appears to have been much more extreme in the North Basin. Another decrease in the thecamoebian population in Core 103 occurs in the interval between 165 and 85 cm. While the population does not drop to zero as in the previous case, the effect appears to have been prolonged. Between these two declines (at 325 cm) thecamoebian abundance peaks. Tintinids generally increase upwards in Core 103 and are much more abundant (600- 59000 specimens) in the North Basin than in the South Basin.

The Lake Winnipeg sequence of Core 103 is characterized by a mixed *Difflugia* assemblage which is dominated by *Difflugia manicata*. Core 103 lacks the early *Arcella* spp.-*Centropyxis aculeata* peak observed in the South Basin. In fact these usually common species (especially *Centropyxis aculeata*) are conspicuously absent. Far less pronounced in Core 103 is the increase in abundance of *Cucurbitella tricuspis* observed at the top of Core 122a.

DISCUSSION

Paleoenvironmental Changes

In Lake Winnipeg, thecamoebian abundance has increased through time with major fluctuations. Shortly after the establishment of a thecamoebian population at the base of the Lake Winnipeg sequence, an environmental change caused a significant decline of the assemblage (at 365 cm in Core 122a and 645 cm in Core 103). This decline appears to have been much more extreme in the North Basin with thecamoebians disappearing completely. This trend seems not to be the result of poor preservation in the lower core since no evidence of test destruction, such as fragmented or damaged tests has been observed.

A general upward increase of thecamoebian numbers is likely related to an increase in nutrient supply. Recent abundance increases have also been documented by Scott and Medioli (1983) for Lake Erie and Patterson et al. (1985) for Maritime lakes who suggest additional nutrient input due to human settlement around the lakes as its cause.

The three thecamoebian assemblages recognized in Core 122a represent different development stages of the South Basin. The earliest stage is characterized by the *Arcella-Centropyxis aculeata* assemblage. The genera of this assemblage are known to tolerate slightly brackish conditions while most other thecamoebians are extremely sensitive to even very low salinities. For example, *Centropyxis aculeata* can tolerate salinities of 1-2‰ (Scott and Medioli, 1980). *Centropyxis aculeata* is also found in sphagnum peatlands (Warner, 1988). The *Arcella-Centropyxis aculeata* species composition suggests that water in the South Basin was slightly brackish during the earliest stages of the Lake Winnipeg sequence. Plant macrofossils also indicate that the basin may have been a hyposaline environment (Vance, this volume). Similarly, Teller et al. (1995) document diatom evidence which suggests that Lake Manitoba may also have been brackish in the early Holocene (post-Lake Agassiz). Lack of the *Arcella-Centropyxis aculeata* assemblage in Core 103 suggests that the North Basin never experienced a brackish phase. This contrast may be related to differences in recharge of the two basins and restriction of the flow between them.

The mixed *Difflugia* assemblage characterizing the central portion of Core 122a and all of the Lake Winnipeg sequence of Core 103 is indicative of freshwater conditions (Medioli and Scott, 1988). During this phase of development the two basins contained similar faunas possibly suggesting increased north-south circulation.

The uppermost portion of Core 122a is characterized by an abundance of *Cucurbitella tricuspis*, an indicator of eutrophic conditions (Patterson et al., 1985; Medioli and Scott, 1988). Its population expands in response to blooms of green algae due to high nutrient input, especially fertilizer runoff resulting from human settlement. Its absence from the Core 103 is likely due to limited anthropogenic influences around the North Basin.

Future Work

This preliminary work has lead to some interesting results. Thecamoebian assemblages suggest that the North and South Basins have undergone different phases of development. The South Basin underwent a single brackish phase early in its development which was followed by the present freshwater conditions. The final phase was the relatively recent eutrophication of the South Basin as a result of anthropological influences. The North Basin, which lacks both the brackish phase and signs of eutrophication, has shown very little change through its history

Difflugia bidens is poorly represented in Lake Winnipeg. This species is of interest because it is often indicative of high terrigenous inputs as would be expected from increased shoreline erosion (Medioli and Scott, 1988). Conclusions about changes in recent shoreline erosion however should not be based on the lack of *Difflugia bidens* because the most recent sediments were probably lost during the coring process. Box core material will be examined in the future to look for increased abundance of *Difflugia bidens* as a proxy for increased terrigenous input in the most recent sediments. Also, a distributional study of sediment-water interface samples will also be completed in the coming year. This may help to determine the validity of *Difflugia bidens* as an indicator of increased sediment supply in Lake Winnipeg.

Work will also be continuing on the long cores. Examining the samples within the 40 cm intervals as well as the other cores will help distinguish real trends from anomalous occurrences.

Finally, as data on water chemistry, geochemistry, sedimentology, and the paleoecology of other floral and faunal assemblages becomes available, this information will be used to further refine the use of thecamoebian faunas as a paleolimnological tool. Much is still unknown about the ecological requirements of various species and their ecotypes. A comprehensive project such as this provides an invaluable source of information for the study of freshwater protozoa.

ACKNOWLEDGMENTS

We are grateful to Mike Lewis, Harvey Thorleifson and Brian Todd for giving us the opportunity to join this project. We would also like to thank the ship board scientists and crew for supplying the samples. Assistance on the SEM was provided by C. Huang and L. Ling. C. Langill is thanked for laboratory assistance. The research was funded by a Natural Sciences and Engineering Council of Canada Research Grant to C.J. Schröder-Adams and an Ontario Graduate Scholarship to S.M. Burbidge.

REFERENCES

Asioli, A., and Medioli, F.S.
in press. Thecamoebians as the tool for reconstruction of paleoenvironments in southern Alpine Lakes (Orta, Varese and Candia); Journal of Foraminiferal Research.

Loeblich, A.R., Jr. and Tappan, H.
1964. Sarcodina, chiefly "thecamoebians" and Foraminiferida; in ed. R.C. Moore, Treatise on invertebrate paleontology, Part C, Protista 2, v. 1 Geological Society of America and University of Kansas Press, Lawrence, Kansas, 510 p.

Medioli, F.S. and Scott, D.B.
1983. Holocene Arcellacea (Thecamoebians) from eastern Canada; Cushman Foundation for Foraminiferal Research, Special Publication v. 21, 63 p.

1988. Lacustrine Thecamoebians (mainly Arcellaceans) as potential tools for palaeolimnological interpretations; Palaeogeography, Palaeoclimatology, Palaeoecology, v. 62, p. 361-386.

Medioli, F.S., Scott, D.B. and Abbott, B.H.
1987. A case study of protozoan intraclonal variability: taxonomic implications; Journal of Foraminiferal Research, v. 17, p. 28-47.

Ogden, C.G. and Hedley, R.H.
1980. An atlas of freshwater testate amoebae; British Museum of Natural History, London and Oxford University Press, Oxford, 222 p.

Patterson, R.T. and Fishbein, E.
1989. Re-examination of the statistical methods used to determine the number of point counts needed for micropaleontological quantitative research; Journal of Paleontology, v. 63, p. 245-248.

Patterson, R.T., MacKinnon, K.D., Scott, D.B. and Medioli, F.S.
1985. Arcellaceans ("thecamoebians") in small lakes of New Brunswick and Nova Scotia: modern distribution and Holocene stratigraphic changes; Journal of Foraminiferal Research, v. 15, p. 114-137.

Scott, D.B. and Medioli, F.S.
1980. Quantitative studies of marsh foraminiferal distributions in Nova Scotia: implications for sea level studies; Cushman Foundation for Foraminiferal Research, Special Publication 17, 58 p.

1983. Testate rhizopods in Lake Erie: modern distribution and stratigraphic implications; Journal of Paleontology, v. 57, p. 809-820.

Teller, J.T., Last, W.M. and Risberg, J.
1995. The record and history of Lake Manitoba- an analog for Lake Winnipeg? Proceedings of the Lake Winnipeg Workshop, Winnipeg, March 1995.

Warner, B.G.
1988. Methods in Quaternary Ecology #5: Testate Amoebae (Protozoa); Geoscience Canada, v. 15, p. 251-260.

Table 1. Fractional abundances, core 122a, South Basin

Sample Interval (cm)	5	45	85	125	165	205	245	285	325	365	405	445
Total Count	1091	671	296	560	372	149	395	390	164	71	348	void
Number of Species	15	16	16	15	16	15	13	15	11	6	4	0
Arcella vugaris	0.0 ± 0.0	0.0 ± 0.0	0.0 ± 0.0	0.0 ± 0.0	0.0 ± 0.0	0.7 ± 1.3	0.0 ± 0.0	0.0 ± 0.0	0.0 ± 0.0	8.5 ± 6.5	27.3 ± 4.7	-
Arcella hemisphaerica	0.0 ± 0.0	0.0 ± 0.0	0.0 ± 0.0	0.0 ± 0.0	0.0 ± 0.0	0.0 ± 0.0	0.0 ± 0.0	0.0 ± 0.0	0.0 ± 0.0	0.0 ± 0.0	20.4 ± 4.2	-
Cucurbitella tricuspis	19.6 ± 2.4	37.0 ± 3.7	16.6 ± 4.2	2.1 ± 1.2	9.9 ± 3.0	1.3 ± 1.8	1.8 ± 1.3	2.3 ± 1.5	4.9 ± 3.3	0.0 ± 0.0	0.0 ± 0.0	-
Difflugia ampullula	18.3 ± 2.3	6.9 ± 1.9	5.1 ± 2.5	5.5 ± 1.9	8.9 ± 2.9	10.1 ± 4.8	1.5 ± 1.2	8.5 ± 2.8	8.5 ± 4.3	5.6 ± 5.4	0.0 ± 0.0	-
Difflugia bidens	0.0 ± 0.0	0.0 ± 0.0	0.0 ± 0.0	0.0 ± 0.0	0.0 ± 0.0	0.0 ± 0.0	0.3 ± 0.5	0.0 ± 0.0	0.0 ± 0.0	0.0 ± 0.0	0.3 ± 0.6	-
Difflugia corona	0.0 ± 0.0	0.7 ± 0.7	3.0 ± 2.0	2.0 ± 1.1	1.6 ± 1.3	0.0 ± 0.0	1.3 ± 1.1	0.5 ± 0.7	0.0 ± 0.0	0.0 ± 0.0	0.0 ± 0.0	-
Difflugia curvicaulis	11.1 ± 1.9	8.8 ± 2.1	12.8 ± 3.8	14.6 ± 2.9	7.5 ± 2.7	2.0 ± 2.3	17.5 ± 3.7	11.5 ± 3.2	10.4 ± 4.7	0.0 ± 0.0	0.0 ± 0.0	-
Difflugia fragosa	5.2 ± 1.3	3.7 ± 1.4	3.7 ± 2.2	4.5 ± 1.7	3.5 ± 1.9	4.7 ± 3.4	3.5 ± 1.8	3.3 ± 1.8	0.0 ± 0.0	0.0 ± 0.0	0.0 ± 0.0	-
Difflugia globulus	0.0 ± 0.0	0.0 ± 0.0	0.0 ± 0.0	0.0 ± 0.0	0.0 ± 0.0	0.0 ± 0.0	0.0 ± 0.0	0.0 ± 0.0	0.0 ± 0.0	0.0 ± 0.0	0.0 ± 0.0	-
Difflugia lacustris	0.1 ± 0.2	0.0 ± 0.0	0.0 ± 0.0	0.0 ± 0.0	0.0 ± 0.0	0.0 ± 0.0	0.0 ± 0.0	0.0 ± 0.0	0.6 ± 1.2	0.0 ± 0.0	0.0 ± 0.0	-
Difflugia lebes	0.8 ± 0.5	0.0 ± 0.0	7.1 ± 2.9	9.1 ± 2.4	11.0 ± 3.2	2.7 ± 2.6	9.9 ± 2.9	5.9 ± 2.3	2.4 ± 2.4	0.0 ± 0.0	0.0 ± 0.0	-
Difflugia manicata	18.1 ± 2.3	2.8 ± 1.3	10.8 ± 3.5	7.3 ± 2.2	9.1 ± 2.9	14.1 ± 5.6	9.4 ± 2.9	10.5 ± 3.0	11.6 ± 4.9	9.9 ± 6.9	0.0 ± 0.0	-
Difflugia minuta	0.0 ± 0.0	0.0 ± 0.0	0.0 ± 0.0	16.6 ± 3.1	18.8 ± 4.0	31.5 ± 7.5	37.0 ± 4.8	37.7 ± 4.8	38.4 ± 7.4	15.5 ± 8.4	4.0 ± 2.1	-
Difflugia oblonga	0.3 ± 0.3	1.5 ± 0.9	0.0 ± 0.0	0.0 ± 0.0	0.0 ± 0.0	0.0 ± 0.0	0.0 ± 0.0	0.0 ± 0.0	0.0 ± 0.0	0.0 ± 0.0	0.0 ± 0.0	-
Difflugia paulii	11.6 ± 1.9	7.0 ± 1.9	9.1 ± 3.3	7.1 ± 2.1	2.2 ± 1.5	1.3 ± 1.8	0.5 ± 0.7	0.5 ± 0.7	0.0 ± 0.0	0.0 ± 0.0	0.0 ± 0.0	-
Difflugia protaeiformis	0.5 ± 0.4	5.7 ± 1.7	1.0 ± 1.1	0.0 ± 0.0	0.8 ± 0.9	0.0 ± 0.0	0.5 ± 0.7	0.0 ± 0.0	0.0 ± 0.0	0.0 ± 0.0	0.0 ± 0.0	-
Difflugia urceolata	2.5 ± 0.9	0.4 ± 0.5	0.0 ± 0.0	0.2 ± 0.3	0.0 ± 0.0	0.7 ± 1.3	0.0 ± 0.0	0.0 ± 0.0	0.0 ± 0.0	0.0 ± 0.0	0.0 ± 0.0	-
Difflugia viscidula	2.8 ± 1.0	3.6 ± 1.4	3.7 ± 2.2	6.3 ± 2.0	6.7 ± 2.5	2.0 ± 2.3	3.8 ± 1.9	3.3 ± 1.8	2.4 ± 2.4	0.0 ± 0.0	0.0 ± 0.0	-
Difflugia sp a.	1.4 ± 0.7	6.3 ± 1.8	3.4 ± 2.1	3.0 ± 1.4	2.4 ± 1.6	6.7 ± 4.0	0.0 ± 0.0	1.8 ± 1.3	0.0 ± 0.0	0.0 ± 0.0	0.0 ± 0.0	-
Difflugia sp. b	0.0 ± 0.0	2.1 ± 1.1	3.0 ± 2.0	1.6 ± 1.0	0.5 ± 0.7	4.7 ± 3.4	0.3 ± 0.5	2.3 ± 1.5	4.9 ± 3.3	0.0 ± 0.0	0.0 ± 0.0	-
Difflugia sp. c	2.2 ± 0.9	10.4 ± 2.3	11.8 ± 3.7	7.0 ± 2.1	3.5 ± 1.9	3.4 ± 2.9	0.0 ± 0.0	0.0 ± 0.0	0.0 ± 0.0	0.0 ± 0.0	0.0 ± 0.0	-
Lagenodifflugia vas	2.3 ± 0.9	0.6 ± 0.6	0.0 ± 0.0	0.0 ± 0.0	0.3 ± 0.5	0.0 ± 0.0	0.3 ± 0.5	0.0 ± 0.0	0.0 ± 0.0	0.0 ± 0.0	0.0 ± 0.0	-
Pontigulasia compressa	1.2 ± 0.6	0.0 ± 0.0	0.0 ± 0.0	0.0 ± 0.0	0.0 ± 0.0	0.0 ± 0.0	0.0 ± 0.0	0.0 ± 0.0	0.0 ± 0.0	0.0 ± 0.0	0.0 ± 0.0	-
Heleopera sp. a	0.0 ± 0.0	0.4 ± 0.5	6.1 ± 2.7	8.6 ± 2.3	12.1 ± 3.3	14.1 ± 5.6	11.4 ± 3.1	10.0 ± 3.0	11.6 ± 4.9	11.3 ± 7.4	0.0 ± 0.0	-
Lesquereusia spiralis	1.3 ± 0.7	0.9 ± 0.7	0.7 ± 0.9	0.0 ± 0.0	0.0 ± 0.0	0.0 ± 0.0	0.0 ± 0.0	0.0 ± 0.0	0.0 ± 0.0	0.0 ± 0.0	0.0 ± 0.0	-
Centropyxis aculeata	0.0 ± 0.0	0.0 ± 0.0	0.0 ± 0.0	0.0 ± 0.0	0.0 ± 0.0	0.0 ± 0.0	0.0 ± 0.0	0.5 ± 0.7	0.0 ± 0.0	47.9 ± 11.6	46.8 ± 5.2	-
Centropyxis constricta	0.3 ± 0.3	0.6 ± 0.6	2.0 ± 1.6	2.0 ± 1.1	0.5 ± 0.7	0.0 ± 0.0	1.0 ± 1.0	1.0 ± 1.0	1.8 ± 2.1	0.0 ± 0.0	0.0 ± 0.0	-
Unidentified	0.4	0.6	0.0	2.5	0.5	0.0	0.3	0.3	2.4	1.4	1.1	-
Total Tintinids	250	11300	150	550	200	50	450	200	100	0	0	0

Table 2. Fractional abundances, core 103, North Basin

Sample Interval (cm)	5	45	85	125	165	205	245	285	325	365
Total Count	2000	1935	207	322	531	1669	2090	1237	3208	1336
Number of Species	13	8	12	10	12	10	10	8	11	11
Arcella vugaris	0.0 ± 0.0	0.0 ± 0.0	0.0 ± 0.0	0.0 ± 0.0	0.0 ± 0.0	0.0 ± 0.0	0.0 ± 0.0	0.0 ± 0.0	0.0 ± 0.0	0.0 ± 0.0
Arcella hemisphaerica	0.0 ± 0.0	0.0 ± 0.0	0.0 ± 0.0	0.0 ± 0.0	0.0 ± 0.0	0.0 ± 0.0	0.0 ± 0.0	0.0 ± 0.0	0.0 ± 0.0	0.0 ± 0.0
Cucurbitella tricuspis	0.1 ± 0.1	0.1 ± 0.1	0.5 ± 0.9	0.0 ± 0.0	0.0 ± 0.0	0.0 ± 0.0	0.0 ± 0.0	0.0 ± 0.0	0.2 ± 0.1	0.0 ± 0.0
Difflugia ampullula	8.5 ± 1.2	6.8 ± 1.1	15.5 ± 4.9	18.9 ± 4.3	19.6 ± 3.4	14.6 ± 1.7	11.5 ± 1.4	17.0 ± 2.1	14.1 ± 1.2	3.1 ± 0.9
Difflugia bidens	0.4 ± 0.3	0.0 ± 0.0	6.3 ± 3.3	8.1 ± 3.0	0.8 ± 0.7	0.5 ± 0.3	0.5 ± 0.3	0.0 ± 0.0	0.2 ± 0.2	0.0 ± 0.0
Difflugia corona	2.3 ± 0.7	0.0 ± 0.0	0.0 ± 0.0	5.3 ± 2.4	1.5 ± 1.0	0.6 ± 0.4	0.2 ± 0.2	0.3 ± 0.3	0.0 ± 0.0	0.7 ± 0.5
Difflugia curvicaulis	7.7 ± 1.2	13.9 ± 1.5	11.6 ± 4.4	9.9 ± 3.3	2.1 ± 1.2	3.9 ± 0.9	5.8 ± 1.0	3.8 ± 1.1	4.0 ± 0.7	37.7 ± 2.6
Difflugia fragosa	2.2 ± 0.6	5.5 ± 1.0	3.9 ± 2.6	3.7 ± 2.1	6.8 ± 2.1	9.0 ± 1.4	12.4 ± 1.4	9.8 ± 1.7	2.1 ± 0.5	1.6 ± 0.7
Difflugia globulus	0.1 ± 0.1	0.1 ± 0.1	0.0 ± 0.0	0.0 ± 0.0	0.0 ± 0.0	0.0 ± 0.0	0.0 ± 0.0	0.0 ± 0.0	0.0 ± 0.0	0.0 ± 0.0
Difflugia lacustris	3.8 ± 0.8	6.7 ± 1.1	2.9 ± 2.3	1.2 ± 1.2	1.9 ± 1.2	4.4 ± 1.0	1.4 ± 0.5	3.2 ± 1.0	4.5 ± 0.7	0.2 ± 0.3
Difflugia lebes	0.0 ± 0.0	0.0 ± 0.0	0.0 ± 0.0	0.0 ± 0.0	1.3 ± 1.0	3.2 ± 0.8	1.9 ± 0.6	3.2 ± 1.0	2.0 ± 0.5	4.3 ± 1.1
Difflugia manicata	47.7 ± 2.2	55.7 ± 2.2	20.3 ± 5.5	33.9 ± 5.2	58.0 ± 4.2	55.2 ± 2.4	48.0 ± 2.1	55.1 ± 2.8	59.2 ± 1.7	27.4 ± 2.4
Difflugia minuta	0.0 ± 0.0	0.0 ± 0.0	0.0 ± 0.0	0.0 ± 0.0	0.0 ± 0.0	0.0 ± 0.0	0.0 ± 0.0	0.0 ± 0.0	0.0 ± 0.0	0.0 ± 0.0
Difflugia oblonga	1.4 ± 0.5	0.2 ± 0.2	3.9 ± 2.6	4.7 ± 2.3	1.3 ± 1.0	3.9 ± 0.9	10.8 ± 1.3	4.2 ± 1.1	5.4 ± 0.8	9.1 ± 1.5
Difflugia paulii	6.8 ± 1.1	6.7 ± 1.1	20.3 ± 5.5	0.9 ± 1.0	0.6 ± 0.6	0.4 ± 0.3	4.9 ± 0.9	0.2 ± 0.3	0.9 ± 0.3	8.2 ± 1.5
Difflugia protaeiformis	2.2 ± 0.6	2.7 ± 0.7	4.3 ± 2.8	11.5 ± 3.5	2.8 ± 1.4	1.7 ± 0.6	1.3 ± 0.5	0.2 ± 0.3	2.8 ± 0.6	0.1 ± 0.1
Difflugia urceolata	3.2 ± 0.8	0.3 ± 0.2	0.0 ± 0.0	0.0 ± 0.0	0.0 ± 0.0	0.2 ± 0.2	0.0 ± 0.0	0.3 ± 0.3	0.0 ± 0.0	0.0 ± 0.0
Difflugia viscidula	8.4 ± 1.2	1.2 ± 0.5	0.5 ± 0.9	0.3 ± 0.6	3.4 ± 1.5	2.5 ± 0.7	1.2 ± 0.5	2.6 ± 0.9	3.8 ± 0.7	1.5 ± 0.7
Difflugia sp a.	2.5 ± 0.7	0.0 ± 0.0	0.0 ± 0.0	0.0 ± 0.0	0.0 ± 0.0	0.0 ± 0.0	0.0 ± 0.0	0.0 ± 0.0	0.0 ± 0.0	0.4 ± 0.3
Difflugia sp. b	0.0 ± 0.0	0.0 ± 0.0	0.0 ± 0.0	0.0 ± 0.0	0.0 ± 0.0	0.0 ± 0.0	0.0 ± 0.0	0.0 ± 0.0	0.0 ± 0.0	3.1 ± 0.9
Difflugia sp. c	0.0 ± 0.0	0.0 ± 0.0	0.0 ± 0.0	0.0 ± 0.0	0.0 ± 0.0	0.0 ± 0.0	0.0 ± 0.0	0.0 ± 0.0	0.0 ± 0.0	0.0 ± 0.0
Lagenodifflugia vas	0.5 ± 0.3	0.2 ± 0.2	1.0 ± 1.3	0.0 ± 0.0	0.0 ± 0.0	0.0 ± 0.0	0.0 ± 0.1	0.0 ± 0.0	0.8 ± 0.3	0.4 ± 0.3
Pontigulasia compressa	2.2 ± 0.6	0.1 ± 0.1	1.4 ± 1.6	0.3 ± 0.6	0.0 ± 0.0	0.0 ± 0.0	0.0 ± 0.0	0.0 ± 0.0	0.1 ± 0.1	0.2 ± 0.3
Heleopera sp. a	0.0 ± 0.0	0.0 ± 0.0	0.0 ± 0.0	0.0 ± 0.0	0.0 ± 0.0	0.0 ± 0.0	0.0 ± 0.0	0.1 ± 0.2	0.0 ± 0.0	0.0 ± 0.0
Lesquereusia spiralis	0.4 ± 0.3	0.1 ± 0.1	2.4 ± 2.1	0.0 ± 0.0	0.0 ± 0.0	0.0 ± 0.0	0.0 ± 0.0	0.0 ± 0.0	0.0 ± 0.0	0.0 ± 0.0
Centropyxis aculeata	0.0 ± 0.0	0.0 ± 0.0	0.0 ± 0.0	0.3 ± 0.6	0.0 ± 0.0	0.0 ± 0.0	0.0 ± 0.0	0.0 ± 0.0	0.0 ± 0.0	0.0 ± 0.0
Centropyxis constricta	0.0 ± 0.0	0.0 ± 0.0	0.0 ± 0.0	0.0 ± 0.0	0.0 ± 0.0	0.0 ± 0.0	0.0 ± 0.0	0.1 ± 0.2	0.0 ± 0.0	1.6 ± 0.7
Unidentified	0.3	0.1	5.3	0.9	0.0	0.0	0.0	0.0	0.0	0.3
Total Tintinids	39650	35500	5750	26350	8300	28000	59350	14850	32300	0

Table 2. Fractional abundances, core 103, North Basin (continued)

Sample Interval (cm)	405	445	485	525	565	605	645	685	725	765
Total Count	1228	577	1000	358	182	356	void	659	void	void
Number of Species	9	10	11	8	7	9	0	8	0	0
Arcella vugaris	0.0 ± 0.0	0.0 ± 0.0	0.0 ± 0.0	0.0 ± 0.0	0.0 ± 0.0	0.0 ± 0.0	-	0.0 ± 0.0	-	-
Arcella hemisphaerica	0.0 ± 0.0	0.0 ± 0.0	0.0 ± 0.0	0.0 ± 0.0	0.0 ± 0.0	0.0 ± 0.0	-	0.0 ± 0.0	-	-
Cucurbitella tricuspis	0.0 ± 0.0	0.0 ± 0.0	0.0 ± 0.0	0.3 ± 0.5	0.0 ± 0.0	0.0 ± 0.0	-	0.0 ± 0.0	-	-
Difflugia ampullula	11.2 ± 1.8	12.3 ± 2.7	7.9 ± 1.7	11.5 ± 3.3	3.8 ± 2.8	17.4 ± 3.9	-	13.4 ± 2.6	-	-
Difflugia bidens	0.0 ± 0.0	0.0 ± 0.0	0.0 ± 0.0	0.0 ± 0.0	0.0 ± 0.0	0.0 ± 0.0	-	0.0 ± 0.0	-	-
Difflugia corona	0.2 ± 0.2	0.0 ± 0.0	0.6 ± 0.5	0.0 ± 0.0	0.0 ± 0.0	0.0 ± 0.0	-	0.8 ± 0.7	-	-
Difflugia curvicaulis	13.2 ± 1.9	15.6 ± 3.0	21.3 ± 2.5	20.1 ± 4.2	15.9 ± 5.3	9.8 ± 3.1	-	6.7 ± 1.9	-	-
Difflugia fragosa	6.6 ± 1.4	3.6 ± 1.5	0.7 ± 0.5	3.6 ± 1.9	3.3 ± 2.6	1.7 ± 1.3	-	0.0 ± 0.0	-	-
Difflugia globulus	0.0 ± 0.0	0.0 ± 0.0	0.0 ± 0.0	0.0 ± 0.0	0.0 ± 0.0	0.0 ± 0.0	-	0.0 ± 0.0	-	-
Difflugia lacustris	0.6 ± 0.4	0.7 ± 0.7	0.0 ± 0.0	0.0 ± 0.0	2.2 ± 2.1	0.0 ± 0.0	-	0.0 ± 0.0	-	-
Difflugia lebes	4.5 ± 1.2	2.9 ± 1.4	4.2 ± 1.2	1.7 ± 1.3	3.8 ± 2.8	2.0 ± 1.4	-	0.9 ± 0.7	-	-
Difflugia manicata	45.7 ± 2.8	51.1 ± 4.1	53.5 ± 3.1	51.7 ± 5.2	67.0 ± 6.8	58.1 ± 5.1	-	57.8 ± 3.8	-	-
Difflugia minuta	0.0 ± 0.0	0.0 ± 0.0	1.4 ± 0.7	0.0 ± 0.0	0.0 ± 0.0	0.0 ± 0.0	-	0.0 ± 0.0	-	-
Difflugia oblonga	15.6 ± 2.0	8.0 ± 2.2	4.2 ± 1.2	3.4 ± 1.9	0.0 ± 0.0	4.5 ± 2.2	-	2.4 ± 1.2	-	-
Difflugia paulii	0.1 ± 0.2	0.0 ± 0.0	0.0 ± 0.0	0.0 ± 0.0	0.0 ± 0.0	0.0 ± 0.0	-	0.0 ± 0.0	-	-
Difflugia protaeiformis	0.7 ± 0.5	0.7 ± 0.7	0.5 ± 0.4	4.2 ± 2.1	0.0 ± 0.0	1.4 ± 1.2	-	1.1 ± 0.8	-	-
Difflugia urceolata	0.0 ± 0.0	0.0 ± 0.0	0.0 ± 0.0	0.0 ± 0.0	0.0 ± 0.0	0.0 ± 0.0	-	0.0 ± 0.0	-	-
Difflugia viscidula	1.6 ± 0.7	4.0 ± 1.6	2.2 ± 0.9	3.6 ± 1.9	3.8 ± 2.8	3.9 ± 2.0	-	17.0 ± 2.9	-	-
Difflugia sp a.	0.0 ± 0.0	0.5 ± 0.6	0.0 ± 0.0	0.0 ± 0.0	0.0 ± 0.0	0.0 ± 0.0	-	0.0 ± 0.0	-	-
Difflugia sp. b	0.0 ± 0.0	0.0 ± 0.0	0.0 ± 0.0	0.0 ± 0.0	0.0 ± 0.0	0.0 ± 0.0	-	0.0 ± 0.0	-	-
Difflugia sp. c	0.0 ± 0.0	0.0 ± 0.0	0.0 ± 0.0	0.0 ± 0.0	0.0 ± 0.0	0.0 ± 0.0	-	0.0 ± 0.0	-	-
Lagenodifflugia vas	0.0 ± 0.0	0.0 ± 0.0	0.0 ± 0.0	0.0 ± 0.0	0.0 ± 0.0	0.0 ± 0.0	-	0.0 ± 0.0	-	-
Pontigulasia compressa	0.2 ± 0.2	0.2 ± 0.3	2.3 ± 0.9	0.0 ± 0.0	0.0 ± 0.0	1.1 ± 1.1	-	0.0 ± 0.0	-	-
Heleopera sp. a	0.0 ± 0.0	0.0 ± 0.0	0.0 ± 0.0	0.0 ± 0.0	0.0 ± 0.0	0.0 ± 0.0	-	0.0 ± 0.0	-	-
Lesquereusia spiralis	0.0 ± 0.0	0.2 ± 0.3	0.0 ± 0.0	0.0 ± 0.0	0.0 ± 0.0	0.0 ± 0.0	-	0.0 ± 0.0	-	-
Centropyxis aculeata	0.0 ± 0.0	0.2 ± 0.3	0.0 ± 0.0	0.0 ± 0.0	0.0 ± 0.0	0.0 ± 0.0	-	0.0 ± 0.0	-	-
Centropyxis constricta	0.0 ± 0.0	0.0 ± 0.0	1.2 ± 0.7	0.0 ± 0.0	0.0 ± 0.0	0.0 ± 0.0	-	0.0 ± 0.0	-	-
Unidentified	0.0	0.0	0.0	0.0	0.0	0.0	-	0.0	-	-
Total Tintinids	13450	0	9950	1950	4650	6400	600	950	0	0

Table 3

FAUNAL LIST	
Order ARCELLINIDA Kent 1880	
Superfamily ARCELLACEA Ehrenberg 1830	
Family ARCELLIDAE Ehrenberg 1830	
Genus *Arcella* Ehrenberg 1830	
Arcella vulgaris Ehrenberg 1830	not illustrated
Arcella hemisphaerica Perty 1852	not illustrated
Family DIFFLUGIDAE Stein 1859	
Genus *Cucurbitella* Pénard 1902	
Cucurbitella tricuspis (Carter 1856)	Plate 2, figure 4
Genus *Difflugia* Leclerc in Lamarck 1816	
Difflugia ampullula Playfair 1918	Plate 1, figure 9
Difflugia bidens Pénard 1902	not illustrated
Difflugia corona Wallich 1864	Plate 1, figures 1,2
Difflugia curvicaulis Pénard 1899	Plate 1, figure 3
Difflugia fragosa Hempel 1898	Plate 2, figure 1
Difflugia globulus (Ehrenberg 1848)	not illustrated
Difflugia lacustris Cash and Hopkinson 1909	Plate 1, figure 6
Difflugia lebes Pénard 1893	Plate 2, figure 3
Difflugia manicata Pénard 1902	Plate 1, figure 10
Difflugia minuta Rampi 1950	not illustrated
Difflugia oblonga Ehrenberg 1832	Plate 1, figure 5
Difflugia paulii Oye 1953	Plate 1, figure 4
Difflugia protaeiformis Lamarck 1816	Plate 1, figure 7
Difflugia urceolata Carter 1864	Plate 2, figure 2
Difflugia viscidula Pénard 1902	Plate 1, figure 8
Difflugia sp.a	not illustrated
Difflugia sp.b	not illustrated
Difflugia sp.c	not illustrated
Genus *Lagenodifflugia* Medioli and Scott 1983	
Lagenodifflugia vas (Leidy 1874)	Plate 2, figure 5
Genus *Pontigulasia* Rhumbler 1895	
Pontigulasia compressa (Carter 1864)	Plate 2, figure 6
Family HYALOSPHENIIDAE Schulze 1877	
Genus *Heleopera* Leidy 1879	
Heleopera sp.a	not illustrated
Genus *Lesquereusia* Schlumberger 1845	
Lesquereusia spiralis (Ehrenberg 1840)	Plate 2, figure 7
Family CENTROPYXIDAE Deflandre 1953	
Genus *Centropyxis* Stein 1859	
Centropyxis aculeata (Ehrenberg 1832)	Plate 2, figure 9
Centropyxis constricta (Ehrenberg 1843)	Plate 2, figure 8

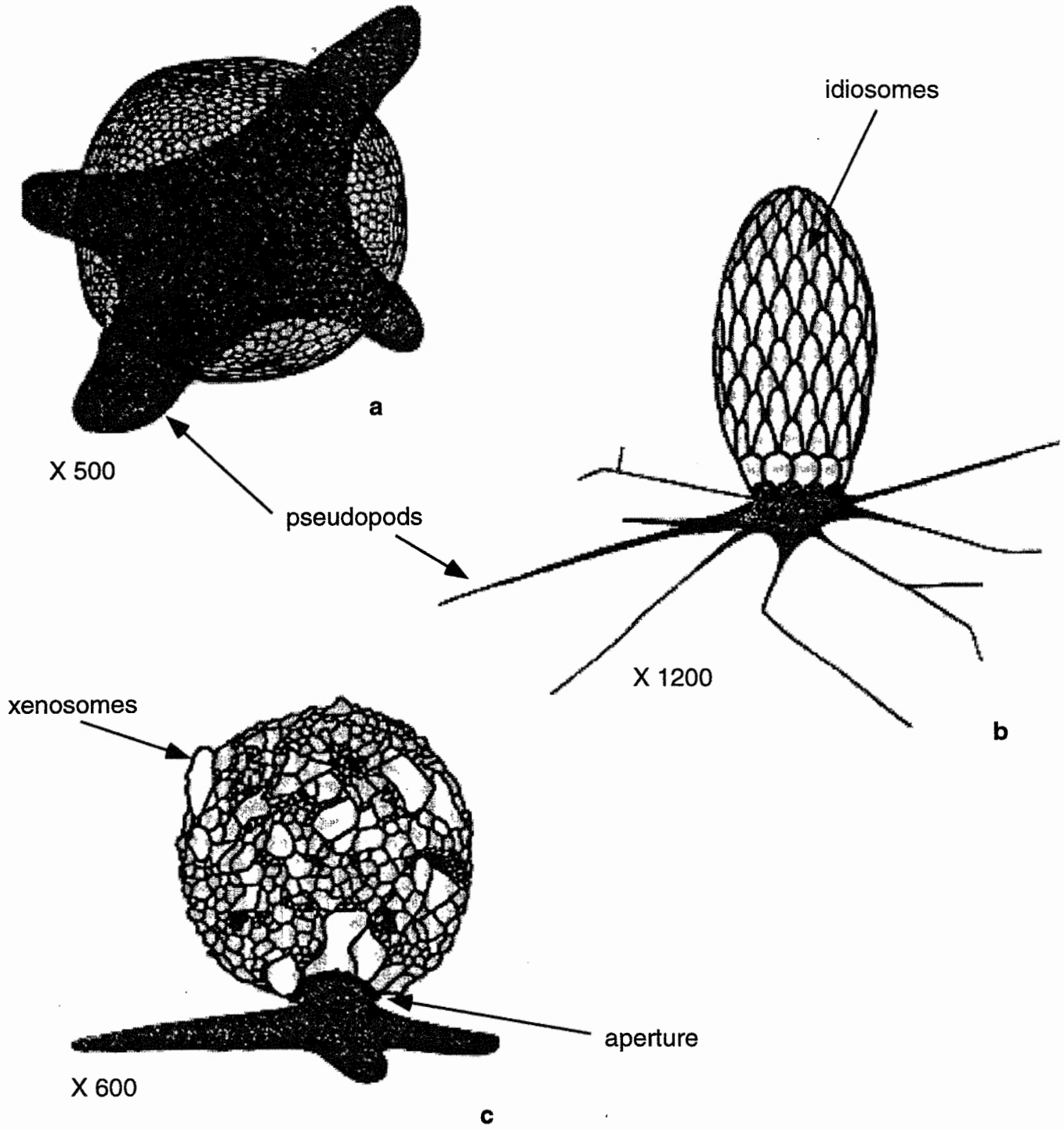

Figure 1. Schematic illustration of common test types showing variation in composition and form of pseudopodia. a) Plan view of *Arcella* sp. with a proteinaceous test; b) side view of *Euglypha* sp. with a test composed of siliceous idiosomes; c) side view of *Difflugia* sp. with a test composed of xenosomes. (After Ogden and Hedley, 1980).

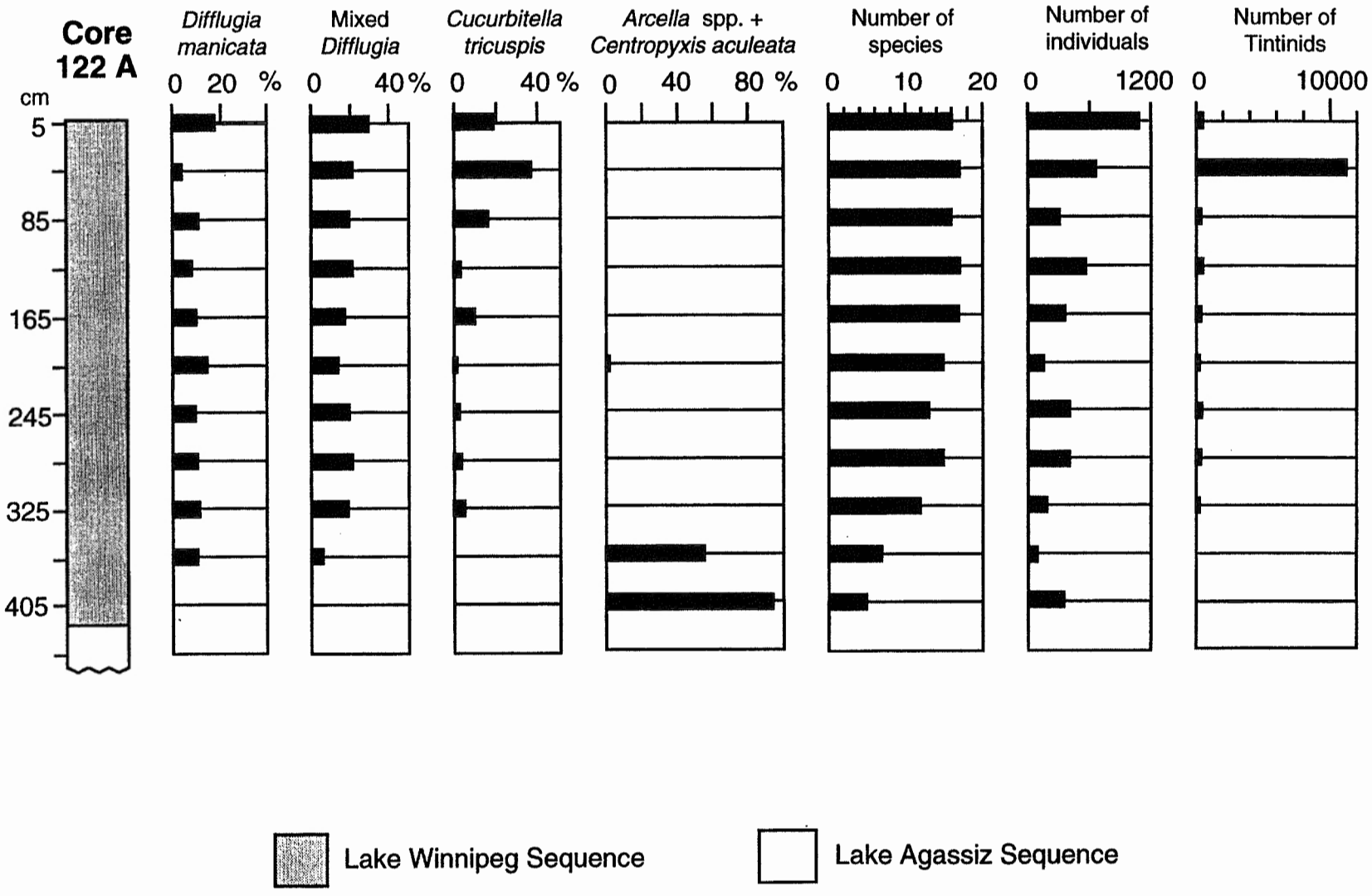

Figure 2. Lithologic column and distribution curves of the main thecamoebian species in core 122a. Horizontal lines represent sampled intervals. The Mixed *Difflugia* curve is the sum of the abundance of *Difflugia ampullula*, *Difflugia curvicaulis* and *Difflugia protaeiformis*. The number of species includes only those species which have an abundance greater than 0.5 %.

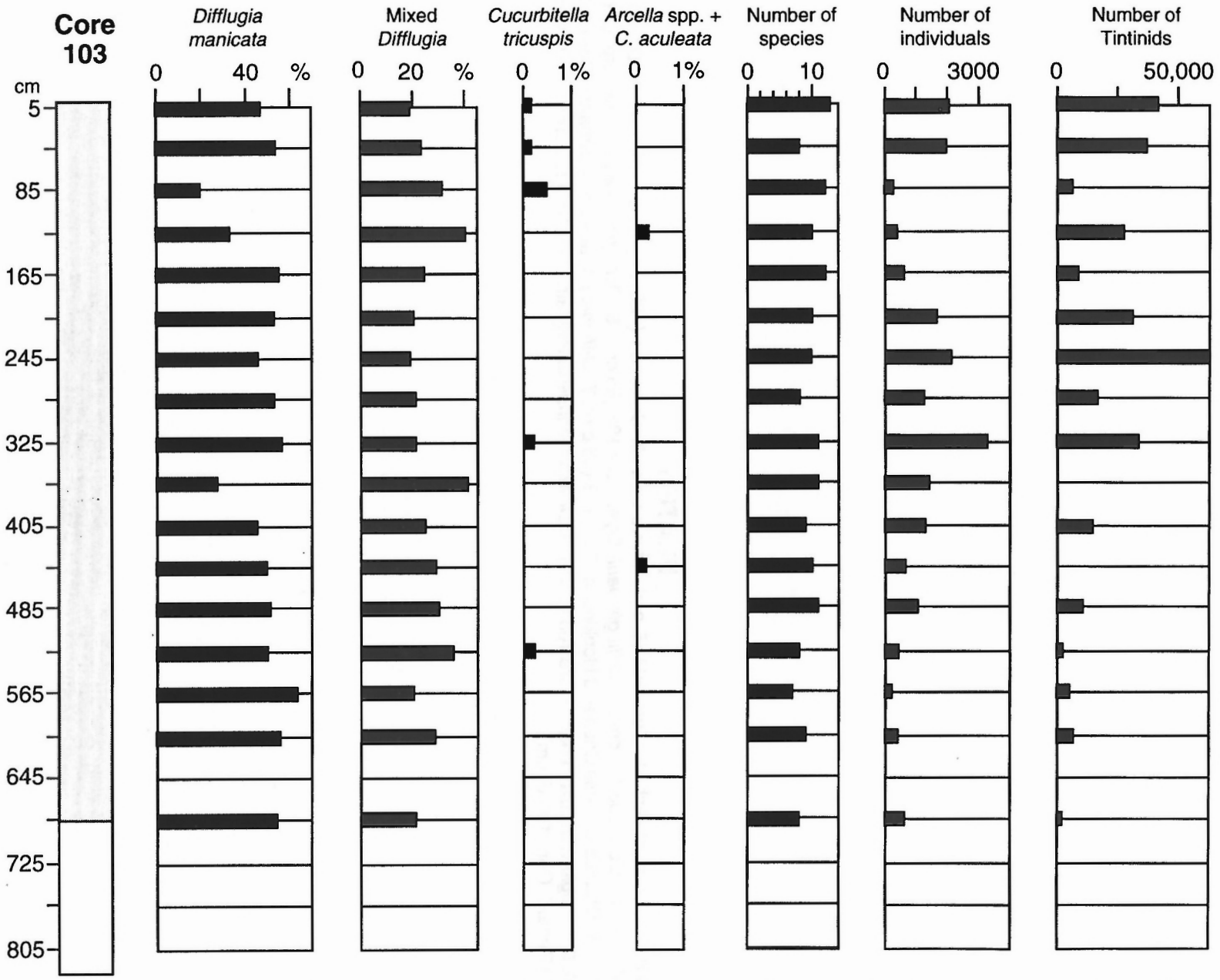

Figure 3. Lithologic column and distribution curves of the main thecamoebian species in core 103. Refer to Figure 2 for legend. Horizontal lines represent sampled intervals. The Mixed *Difflugia* curve is the sum of the abundance of *Difflugia ampullula*, *Difflugia curvicaulis* and *Difflugia protaeiformis*. The number of species includes only those species which have an abundance greater than 0.5 %.

PLATE 1

1,2. *Difflugia corona* Wallich. **1.** Core 103 (5 cm), lateral view. **2.** Core 103 (125 cm), apertural view. **3.** *Difflugia curvicaulis* Pénard. Core 103 (45 cm). **4.** *Difflugia paulii* Oye. Core 103 (85 cm). **5.** *Difflugia oblonga* Ehrenberg. Core 103 (5 cm). **6.** *Difflugia lacustris* Cash and Hopkinson. Core 103 (45 cm). **7.** *Difflugia protaeiformis* Lamarck. Core 103 (125 cm). **8.** *Difflugia viscidula* Pénard. Core 103 (5 cm). **9.** *Difflugia ampullula* Playfair. Core 103 (165 cm). 10. *Difflugia manicata* Pénard. Core 103 (5 cm).

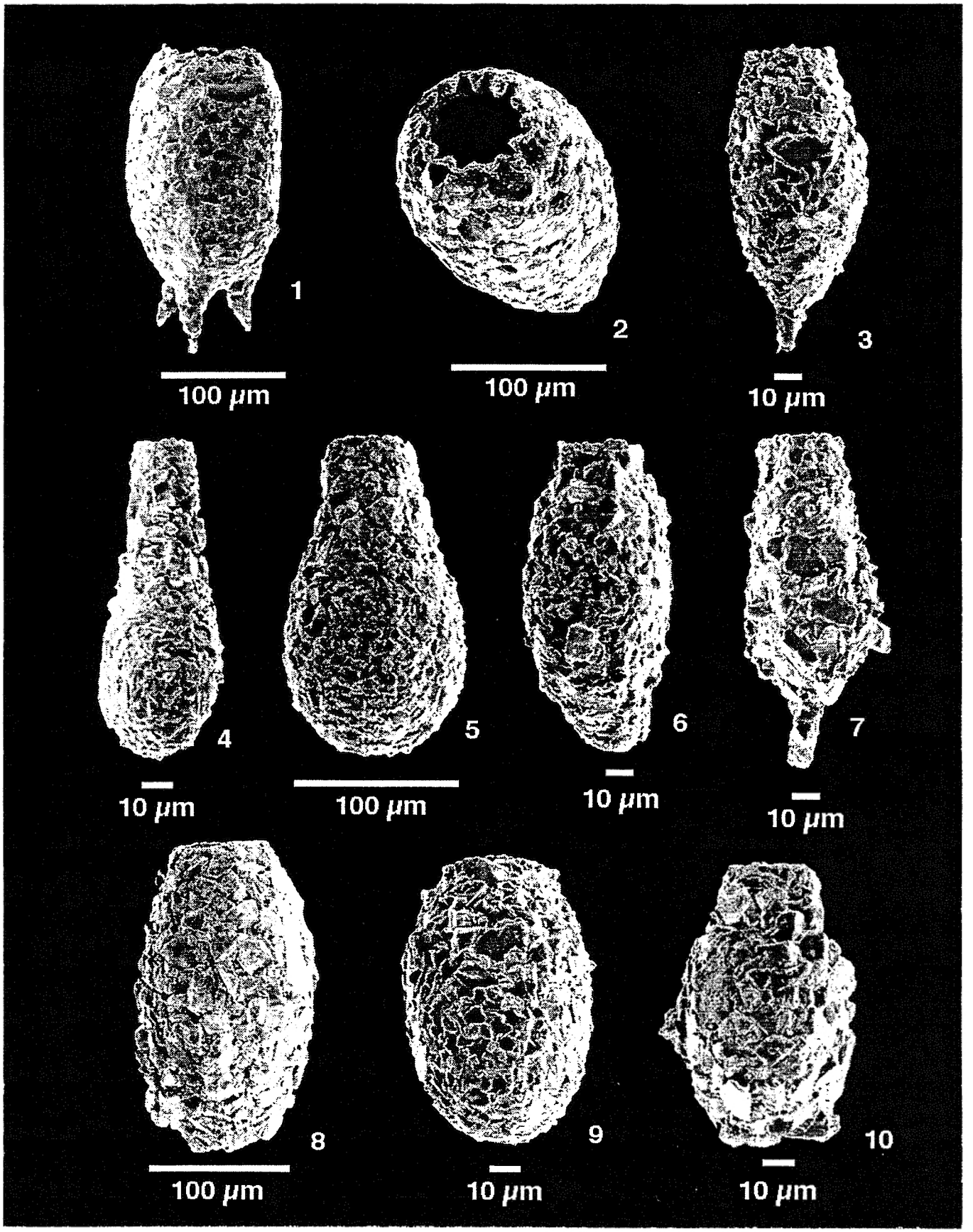
1
100 μm
2
100 μm
3
10 μm
4
10 μm
5
100 μm
6
10 μm
7
10 μm
8
100 μm
9
10 μm
10
10 μm

Plate 1.

PLATE 2

1. *Difflugia fragosa* Hempel. Core 103 (45 cm). **2.** *Difflugia urceolata* Carter . Core 103 (5 cm). **3.** *Difflugia lebes* Pénard. Core 103 (365 cm). **4.** *Cucurbitella tricuspis* (Carter). Core 122a (45 cm). **5.** *Lagenodifflugia vas* (Leidy) Core 103 (5 cm). **6.** *Pontigulasia compressa* (Carter) Core 103 (5 cm). **7.** *Lesquereusia spiralis* (Ehrenberg) Core 103 (85 cm). **8.** *Centropyxis constricta* (Ehrenberg) Core 103 (365 cm). **9.** *Centropyxis aculeata* (Ehrenberg) Core 122a (365 cm).

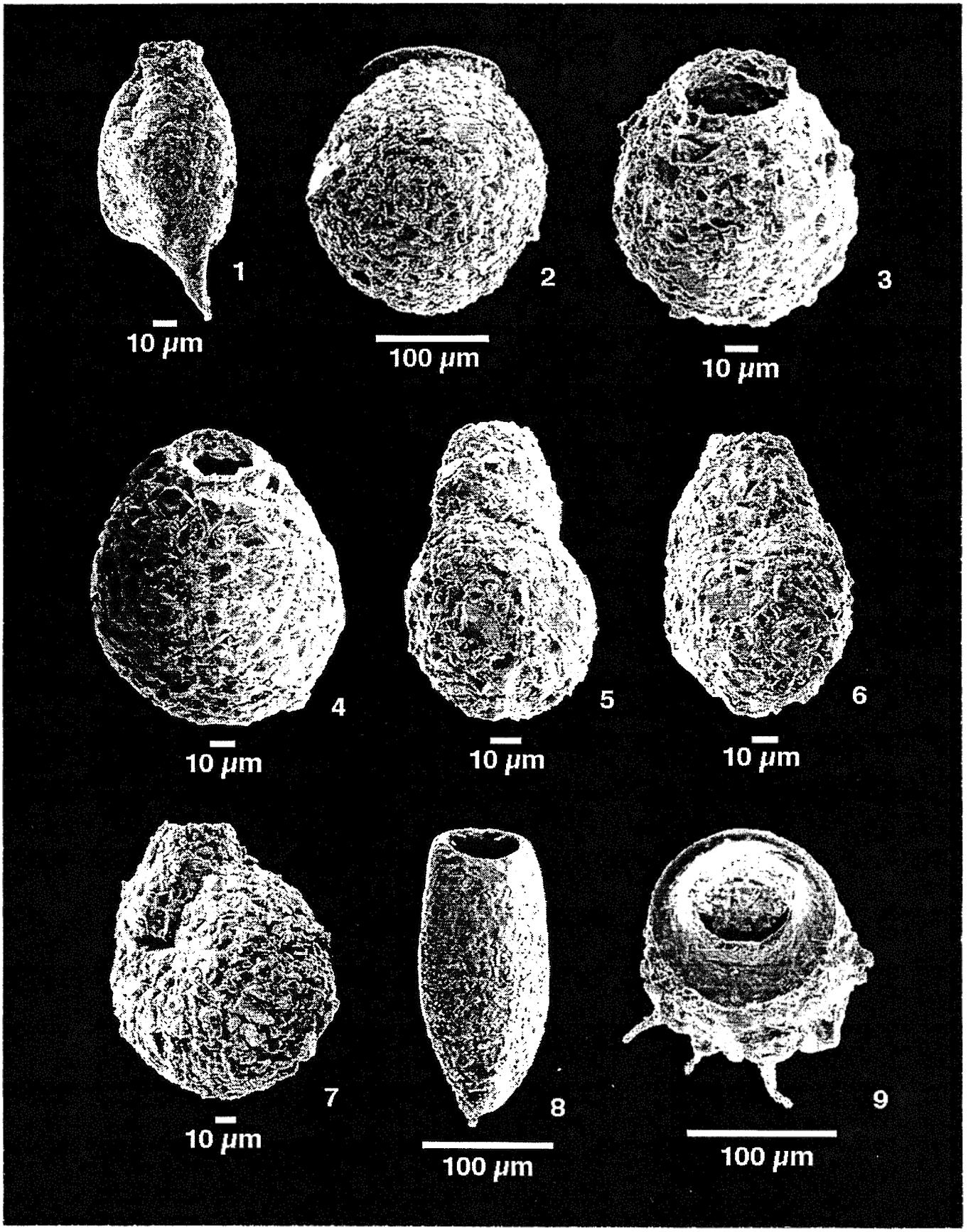

Plate 2.

4.11 Fossil and modern phytoplankton from Lake Winnipeg

H.J. Kling

Department of Fisheries and Oceans
Freshwater Institute, 501 University Crescent, Winnipeg, Manitoba R3T 2N6

ABSTRACT

Recent phytoplankton and protozoan assemblages are spatially and seasonally quite variable in Lake Winnipeg. However, main taxa are similar throughout lake history. Lake Winnipeg has always been a diatom-bluegreen algae lake with the Tintinnids and thecate amoebae significant components of the protozoan community. Changes in phytoplankton abundance and species composition between 1923, 1969, 1992 and 1994 reflect a general trend towards increased eutrophication of the lake (particularly the South Basin).

Microfossils found in sediment samples from cores can provide evidence about the stratigraphic relationships and environmental history of lacustrine deposits. Microfossils are reported from core 103 (8 m) taken from the North Basin of Lake Winnipeg in August 1994. Diatom assemblages are low in abundance throughout the core below 50 cm, except for a peak around 300-400 cm. Below 690-800 cm, in Lake Agassiz sediments, diatoms are virtually absent. *Stephanodiscus* and *Aulacoseira* are the two major pelagic diatom genera represented throughout the lake history. Species changes occur near the top, indicating increased anthropogenic eutrophication. Shallow water littoral taxa are not abundant at any level of this core. The presence of planktic cyanoprokaryote (cyanophyte, cyanobacteria, bluegreen algae) remains (akinetes) above 600 cm depth and the progressive increase in abundance from 400 cm to the top of the core indicates increasing phosphorus levels, warming summer temperatures and increasing summer lake nitrogen limitation. Nitrogen fixing bluegreens (*Anabaena* and *Aphanizomenon* akinetes) and the diatoms (*Aulacoseira ambigua*, *A. granulata*, *A. islandica*, *Stephanodiscus binderanus*, and *S. niagarae*) are abundant in the top sediments. These taxa, in addition to *S. agassizensis*, *Melosira varians* and *Cyclostephanos dubius*, are representative of present day plankton.

INTRODUCTION

This preliminary report presents a comparison of phytoplankton data from three surveys of Lake Winnipeg (1969, 1992 and 1994), depicts some of the dominant and more interesting taxa, and gives a preliminary glimpse into the historical plankton record using microfossil remains in the sediment of long core 103 from the North Basin (Lewis and Todd, this volume). A detailed description of phytoplankton species distribution and seasonality for Lake Winnipeg will be presented in a future publication of Canadian Journal of Fisheries and Aquatic Sciences Bulletin. A description of non-siliceous algal remains, diatoms and other microfossil remnants from core 103 and possibly some short cores will be prepared for presentation in 1996.

Lake Winnipeg is the 11th largest lake, by area (23650 km^2) in the world and the 7th largest in North America. It borders the Precambrian Shield on the north and east and Paleozoic limestones and dolomites on the west and southwestern shores. There is a great difference in the water quality of this system. The south and westerly portion receives waters with much higher alkalinity, mineral and nutrient content than the north and eastern areas of the lake which receives nutrient-limited, low pH and low alkalinity water from the Canadian Shield. The lake spans four degrees in latitude and water temperature may decrease between 1-5°C from south to north. Differences in water chemistry, light and temperature are the most important factors regulating the distribution of many forms of aquatic life.

PREVIOUS RESEARCH

The earliest records of phytoplankton in Lake Winnipeg are from 1923 (Lowe, 1924), 1928, and 1929 (Bajkov, 1930; 1934). Bluegreen blooms, typically appearing in mid-late August during hot, dry years were described; in wet years diatoms dominated (Fig. 1). Bajkov reported that, in the South Basin during late July of 1928, water temperatures were about 28° C and carpets of *Aphanizomenon flos-aquae* formed at the surface in some regions of the lake. The total plankton biomass maxima for 1928 and 1929 were 24,800 $\mu g \cdot L^{-1}$ and 20,200 $\mu g \cdot L^{-1}$ wet weight respectively (Bajkov 1930). Lowe (1924) reported that *Stephanodiscus niagarae* comprised up to 50% of the plankton in the South Basin in mid-summer of 1923. He also reported that *Rhizosolenia morsa* W. and G. S. West was abundant in the North Basin. This species had not been found in any other waters in central Canada despite being common in lakes of British Columbia. This taxon has not been found in Lake Winnipeg since Lowe's report.

Limited limnological studies were conducted in the North Basin (Rybicki, 1966) and South Basin (Crowe, 1973) in the 1960s. No phytoplankton records exist for these years.

A seasonal survey of Lake Winnipeg was undertaken in 1969 by a scientific research team from the Freshwater Institute led by G.J. Brunskill (Fig. 2). To date, this is the only comprehensive seasonal chemical, physical and biological

study of this lake (Brunskill, 1973; Brunskill and Graham, 1979; Brunskill et al., 1979a, 1979b; Brunskill et al., 1980).

A high degree of spatial and seasonal variability was observed in the 1969 phytoplankton in Lake Winnipeg (Fig. 2). This is largely related to climate (temperature and light) and drainage area (nutrient inputs and major ion composition). Diatoms dominated the spring plankton with both diatoms and bluegreens dominating the fall plankton. Bluegreen blooms were found in the South Basin in early July and in the western part of the North Basin in late July. These blooms usually begin nearshore in shallow quiet bays and later are blown offshore. Wet, cool years yield a plankton composition dominated by *Aulacoseira* (today) and *Stephanodiscus niagarae* (turn of the century) (Fig. 1). Warm dry years yield massive blooms of N-fixing bluegreens (*Anabaena* and *Aphanizomenon*). *Aphanizomenon flos-aquae* has a higher optimum temperature than many *Anabaena* species and therefore may be potentially a good indictor of increasing water temperatures as well as decreasing lake levels (Ernst, 1990).

In 1992, Manitoba Environment and the Canadian Coast Guard collected water chemistry and phytoplankton samples during monthly cruises on the lake. Attempts were made to sample open water stations comparable to the 1969 survey stations (D. Green, pers. comm.).

In 1994, a multidisciplinary study, funded by Natural Resources Canada, Manitoba Hydro, Manitoba Energy and Mines, and Fisheries and Oceans Canada, was conducted in cooperation with the Canadian Coast Guard. The study included a comprehensive geological, hydrological, chemical and biological survey of the entire lake between August 4 and 30.

A wide variety of biogenic remains can be recovered from lake sediments. The most common remains reported in stratigraphic records are pollen grains and siliceous microfossils (diatoms and chrysophyte cysts). Less frequently green algal (*Pediastrum* and *Staurastrum*) remains (Nipkow, 1927; Birks, 1976) are recorded.

Highly organic sediment (>50% organic component; i.e. 'sapropel') often contain remains of cyanophytes, chlorophytes, and dinoflagellates (Korde, 1960). A few studies have documented these non-siliceous remains from sediments (Bradley, 1966; Livingstone, 1984; Wolfe et al., 1994).

METHOD

Phyto- and proto-plankton were analysed after sedimentation of Lugol's-killed, formalin-preserved whole water samples. Aliquots of sample were enumerated in sedimentation chambers, using a Wild m40 inverted microscope and the methods of Utermohl (1958) and Nauwerk (1963). Single cells, colonies and filaments were measured and counted. Less numerous and large cells were counted at 200 x magnification and the small, more numerous cells were counted at 625 x. Samples excessively rich in plankton were diluted or fields were counted. Cell volumes were calculated based on measured dimensions of 15-20 cells of each taxon. Volume calculations were computed using the formula for the geometric shape or shapes most closely resembling each taxon (Rott, 1981). Wet weight biomass was obtained from cell volume by assuming a specific gravity of 1.

Untreated sediment samples were analysed using the same methods. One quarter cubic centimeter of sediment was diluted to 20 mL using distilled water. Subsamples of 0.25 mL of this sediment suspension were diluted 8-32 x and settled in a 2 mL Utermohl chamber. The degree of dilution depended on the concentration of algal remains and suspended sediment. The method is a modification of that described by Batterbee (1973) and Scherer (1994). The difference from methods used elsewhere is that the sediment sample is neither dried nor cleaned.

RESULTS AND DISCUSSION

Water samples

There was a dramatic difference in the phytoplankton composition between 1969 and 1992. Diatoms and cryptophytes (low temperature, low light taxa) dominate the 1992 data, a change relative to the dominance of bluegreens and diatoms in the 1969 plankton (Fig. 3). Cold and wet conditions prevailed in 1992. Phytoplankton in Lake Winnipeg presumably tended to experience less nutrient limitation and often the biomass was usually more light limited. Increased light limitation and less nutrient debt is a common phenomenon of larger lakes (Guildford et al., 1995). An examination of samples from August, 1994, further indicates, from the dominance of bluegreens, that there can be a high degree of year-to-year variability, as well as spatial and seasonal variation. The similar predominance of bluegreen nitrogen fixers in 1969 and 1994 during warm dry periods of both years suggests that limiting nitrogen must be accompanied by adequate phosphorus and light conditions to sustain the measured high algal standing crops. The maximum recorded biomass in 1994 was five times higher than in 1969 but mean basin values were only two times higher.

A comparison of dominant species of Lake Winnipeg between 1969 and 1994 shows that the principal species present in 1994 (Fig. 5) were also typical of the lake in 1969. Common taxa include *Aulacoseira islandica* (O. Muller) Simonsen (Fig. 6a), *Stephanodiscus binderanus* (Kutz.) Kreiger (Fig. 6b), *Aphanizomenon gracile* (Lemm.) Lemm. (Fig. 6c), *Planktothrix suspensa* (Pringsh.) Anagn. and Kom. formerly identified as *Oscillatoria aghardii* Gomont (Fig. 6d), *Aphanizomenon flos-aquae* Breb. ex Born. et Flah. (Fig. 6e) and *Anabaena mendotae* Trel.(Fig. 6f) In addition to the algae, several thecate protozoans *Strombidium* cf. viride (Fig. 6g), *Codonella cratera* (Fig. 6h) and *Tintinnidium* sp. (Fig. 6i) have

been common components of the plankton community since the turn of the century and even back to the early history of Lake Winnipeg immediately following the draining of Lake Agassiz.

Aulacoseira islandica (Figs. 6a and 7a) characteristically forms biomass maxima (2000-4000 $\mu g \cdot L^{-1}$ wet weight) under late winter, early spring ice with minimal snow cover. This phenomenon is not new to the lake and late winter diatom blooms were reported by Lowe and Bajkov as well as in the 1950s by fishermen. Under-ice *Aulacoseira* blooms typically occur in Lake Baikal, Russia (Kozhova, 1987) and probably are much more widespread in large lakes. *A. subarctica* (O. Mull.) Haworth (Fig. 7b) was very important in the North Basin in 1969. It is characteristic of many mid-size to large-size sub-arctic and arctic lakes. *Melosira varians* Ag. (Fig. 7c) was present primarily in the western region of the North Basin. It was never a dominant taxon. *Cyclotella meneghiniana* Kutz., *Stephanodiscus parvus* Stoermer and Håkansson, and *Cyclostephanos dubius* (Frike) Round (Fig. 7 d, e, and f resp.) have been increasing in the South Basin since 1969. They are typical of eutrophic prairie lakes. They have not yet been significant in the North Basin.

Several diatom taxa were rare or with limited lake-wide distribution in 1969 such as *Stephanodiscus agassizensis* Håkansson and Kling (Figs. 8a, d). SEM-confirmed identifications indicate that *S. agassizensis* occurs in the Red River, in Killarney Lake in southwestern Manitoba, in Lake Erie, and in several rivers in central USA. Analyses of core samples indicate that *S. agassizensis* is only a recent taxon in Killarney Lake. It begins to occur at 15 cm down core (unpublished data). However, this species is very widespread in temperate eutrophic, turbid European and Russian rivers, lakes and reservoirs. It has been found in increasing abundance in the turbid, eutrophic, light-limited southern part of Lake Winnipeg, and has limited distribution in the North Basin. *S. niagarae* Ehr. (Fig. 8a), dominant in 1923 (Fig. 1), is only present now and never dominates the plankton. *S. binderanus* (Kutz) Kreiger (Fig. 8b) was abundant in areas of higher chloride (western offshore regions). *A. ambigua* (O. Mull) Simonsen (Fig. 8e) dominates the diatom open-water plankton throughout the early spring and fall of most years competing with the bluegreens in midsummer. *A. granulata* (O. Mull.) Simonsen (Fig. 8f) is abundant in the South Basin and river mouths. It is typical of the summer fall plankton.

Several taxa are typical of the Lake Winnipeg plankton since 1969 but are generally rare or absent in most other Canadian lakes. *Acanthoceros magdeburgense* Honigmann (= *Attheya zacheriasi* J. Brun) (Fig. 9a), considered a rather primitive diatom taxon, was common in the 1969 and 1994 plankton but not recorded in the 1920s species lists. It is very distinctive and would not have been missed. Another rare species recorded as *Rhizosolenia morsa* by Lowe (1924) is now in the genus *Urosolenia* Round and Crawford. This taxon is presently absent or very rare in most Canadian lakes and has a very limited distribution, although it has been observed by the author in an ultra-oligotrophic lake in northwestern Ontario, and in a few mountain lakes in British Columbia and the Yukon. The other two freshwater *Urosolenia* are common in Canadian Shield lakes to the east. *Staurastrum leptocladum* Norst. var. *curvatum* Lowe (Fig. 9b), along with many desmids and other green algae, was more abundant in the early plankton than in present day plankton. *Entzii acuta* (Apst.) Lebour = (*Diplopsalis acuta* Entz) (Fig. 9c), rare in most Canadian lakes, is characteristic of Lake Winnipeg and of large inorganic lakes in northern Europe. Optimum values for this species are reported to be pH 7.5-7.8, calcium ≈50-80 $mg \cdot L^{-1}$, low phosphorus, and medium to low levels of chloride, sulphate, and carbonate (Huber-Pestalozzi, 1938). *E. acuta* was not reported by Lowe or Bajkov in the 1920s. Several species of *Microcysis*(Fig. 9d) may be found in the midsummer plankton of Lake Winnipeg but none have yet been recorded as forming unialgal blooms.

A few of the common taxa, other than diatoms, leave remains that are preserved in the sediments as microfossils. Figures 9e and 9f show the microfossil remains (akinetes or resting spores) of the nitrogen-fixing bluegreens such as *Aphanizomenon* and *Anabaena*. Other non-siliceous microfossils that provide information about the paleolimnology of the lake are zooplankton faecal pellets (Fig. 9g) and thecate amoeba lorica (Fig. 9h).

Core samples

Long core 103, taken from the central deep part of the Lake Winnipeg North Basin (Fig. 10), was analysed for microfossils. A variety of both non-siliceous and siliceous microfossils were found. These microfossils indicate that the lake has, through time, been an oligo-mesotrophic prairie lake with periodic blooms of bluegreens alternating with diatoms. The low abundance to absence of diatoms throughout several parts of the core may be due to diagenesis. Diatom blooms were most likely present during late winter/spring and fall as they are now. However, dissolution often occurs under high pH, high temperatures and low ambient silicon (Lawson et al., 1978; Hecky et al., 1986). The pH during a bluegreen bloom can increase to >9 and there is good evidence supporting valve dissolution as observed from SEM analysis.

Natural increases in phytoplankton production, increasing nitrogen limitation and a warming trend can be inferred from increasing bluegreen akinetes in the core (Fig. 11). The presence of bluegreen akinetes is apparent above 600 cm. However, there is a progressive increase from 400 cm towards the surface which corresponds to a general trend in eutrophication. *Anabaena* and *Aphanizomenon* form massive blooms in prairie lakes today under conditions of high phosphorus accompanied by hot dry weather. Nitrogen-fixing bluegreens can also be present under cooler conditions provided nitrogen is limiting. A rise in the recent particulate sediment phosphorus in sediment profiles also supports increased production (Buhay, pers. comm). Between 600 cm

and 400 cm, the diatom species *A. islandica* alternates with *S. niagarae* and bluegreen akinetes. These taxa indicate cold, dry springs with little snow cover and short, warm summers. This interpretation is supported by knowledge of the present day distribution. Massive under ice blooms of *A. islandica* occurred during springs with prolonged periods of little or no snow cover. *S. niagarae* is a summer species and reaches maximum biomass during mid- to late summer. In prairie lakes where it is presently found, it often co-occurs with nitrogen-fixing bluegreens, particularly *Aphanizomenon* and *Anabaena*. None of these taxa reach the high biomass levels of a unialgal bloom.

Other evidence from the fossil record pointing to increasing eutrophication are changes in diatom species composition from oligo-meso trophic taxa (*S. niagarae*, *Cyclotella bodanica*, and *A. islandica*) to more eutrophic taxa (*A. granulata*, *A. ambigua*, *S. parvus*, and *C. dubius*).

It is possible to infer a rise in microalgal food taxa such as small, green chrysophytes and cryptomonads corresponding to the observed increase in protozoan taxa, especially the tintinnids.

At 75 cm the fossil record indicates an influx of a variety of terrestrial remains (Fig. 12). The increase in terrestrial remains during the period of maximum increase in bluegreen algal remains provides supporting evidence for a warmer, drier, windy period. The distinct lack of benthic diatoms at any level in this core suggests that this site has always been a deep, pelagic offshore environment.

Micro-zooplankton remains and pyrite framboidals/ spherules (Fig. 13) indicate that there is a relatively recent increase in cladocerans in this offshore location that has been dominated historically by copepods, as indicated by the early record of high numbers of faecal pellets. Other carapace-forming zooplankton were rare and did not become significant until after increasing trophic status and increased warm, dry periods around 75 cm. Pyrite spherules and framboidals beginning around 600 cm down core indicate increasing periods of winter anoxia.

CONCLUSIONS

Several species recorded by Lowe (1924) and Bajkov (1930, 1934) were not recorded in the 1969 survey or in more recent surveys and appear to be no longer present in the lake. However, many more taxa typical of increases eutrophication not recorded in the 1920s have since developed significant populations in Lake Winnipeg. A few of these taxa (i.e. *S. agassizensis* and *C. dubius*) appear to be very recent additions to the plankton community of Lake Winnipeg.

Spatial variability of the phytoplankton in Lake Winnipeg can be explained by the geology of the basins, influxes from the drainage areas and variation in climate between the North and South Basins. Temporal variability over the lake seems to be a result of year-to-year variation in climatic conditions.

This preliminary study of core 103 shows the potential for using a variety of algal and non-algal (non-siliceous) microfossil remains, in conjunction with the traditionally used (siliceous) diatom/cyst remains, to obtain a more complete paleolimnolgical history of the lake.

Although the absence of an alga in the sediment does not indicate its absence in the plankton, the results from this core indicate that considerable information can be obtained by examination of sediments for non-siliceous algal remains, thus increasing the potential of paleoecological interpretation.

REFERENCES

Bajkov, A.
1930. Biological conditions of Manitoba lakes; Contributions to Canadian Biology and Fisheries, v. 5, p. 383-422.

1934. The plankton of Lake Winnipeg drainage system. Internationale Revue der Gesamten Hydrobiologie und Hydrographie, v. 31, p. 239-272.

Batterbee, R.W.
1973. A new method for the estimation of absolute microfossil numbers, with reference especially to diatoms; Limnology and Oceanography, v. 18, p. 647-653.

Birks, H.J.B.
1976. Late-Wisconsin vegetational history at Wolf Creek, central Minnesota; Ecological Monographs, v. 46, p. 385-429.

Bradley, W.H.
1966. Tropical lakes, copropel, and oil shale; Bulletin of the Geological Society of America, v. 77, p. 1333-1338.

Brunskill, G.J.
1973. Rates of supply of nitrogen and phosphorus to Lake Winnipeg, Manitoba, Canada; Internationale Vereinigung fuer Theoretische Angewandte Limnologie Verhandlungen, v. 18, p. 1755-1759.

Brunskill, G.J. and Graham, B.W.
1979. The offshore sediments of Lake Winnipeg; Canada Fisheries and Marine Service Manuscript Report 1540, 75 p.

Brunskill, G.J., Schindler, D.W., Elliott, S.E.M. and Campbell, P.
1979a. The attenuation of light in Lake Winnipeg waters; Canada Fisheries and Marine Service Manuscript Report 1522, 75 p.

Brunskill, G.J., Campbell, P. and Elliott, S.E.M.
1979b. Temperature, oxygen, conductance and dissolved major elements in Lake Winnipeg; Canada Fisheries and Marine Service Manuscript Report 1526, 127 p.

Brunskill, G.J., Elliott, S.E.M. and Campbell, P.
1980. Morphometry, hydrology, watershed data pertinent to the limnology of Lake Winnipeg; Canada Fisheries and Marine Service Manuscript Report, 37 p.

Crowe, J.M.E.
1973. Limnology of the South Basin of Lake Winnipeg, March 1965-March 1969; Manitoba Department of Mines and Environmental Management, Research Branch Manuscript Report No. 73-24, 37 p.

Ernst, A.
1990. Cyanobacteria in large lakes: A case study in Lake Constance; in ed. Max. M. Tilzer and C. Surruya, Large lakes: ecological structure and function, Springer Verlag, Berlin, p. 428-439.

Guildford. S.J, Hendzel, L.L., Kling, H.J., Fee, E.J., Robinson, G.G.C., Hecky, R.E. and Kasian, S.E.M.
1995. Effects of lake size on phytoplankton nutrient status; Canadian Journal of Fisheries and Aquatic Sciences, v. 51, p. 2769-2783.

Hecky, R.E., Kling, H.J. and Brunskill, G.J.
1986. Seasonality of phytoplankton in relation to silicon cycling and interstitial water circulation in large, shallow lakes of central Canada; Hydrobiologia, v. 138, p. 117-126.

Korde, N.V.
1966. Algal remains in lake sediments - a contribution to development history of lakes and the surrounding regions; Ergebnisse der Limnologie v. 3, p. 1-38 (English translation by Fisheries Research Board of Canada No. 1371).

Kozhova, O.M.
1987. Phytoplankton of Lake Baikal: Structural and functional characteristics; Archiv fur Hydrobiologie Beiheft: Ergebnisse der Limnologie, v. 25, p. 19-32.

Lawson, D.S., Hurd, D.C. and Pankratz, H.S.
1978. Silica dissolution rates of decomposing phytoplankton assemblages at various temperatures; American Journal of Science, v. 278, p. 1373-1393.

Livingstone, D.
1984. The preservation of algal remains in recent lake sediments; in eds. E.Y. Haworth and J.W.G. Lund, Lake sediments and environmental history, University of Minnesota Press, Minneapolis, Minnesota, p. 191-202.

Lowe, C.W.
1924. The freshwater algae of Canada; Transactions of the Royal Society of Canada, v. 18, Ottawa, p. 19-48.

Munawar, M., Munawar, I.F. and McCarthy, L.H.
1987. Phytoplankton ecology of large eutrophic and oligotrophic lakes of North America: Lake Ontario and Lake Superior; Archiv fur Hydrobiologie Beiheft: Ergebnisse der Limnologie, v. 25, p. 51-96.

Nauwerck, A.
1963. Die Beziehungen zwischen Zooplankton und Phytoplankton im See Erken; Symbolae Botanicae Upsalienses, v. 17, p. 1-163.

Nipkow, F.
1927. Uber das Verhalten der Skelette planktischer Kieselalgen im geschichteten Tiefenschlamm des Zurich and Baldeggersees; Schweizerische Zeitschrift Hydrologie, v. 4, p. 71-120.

Rott, E.
1981. Some results from phytoplankton counting intercalibrations; Schweizerische Zeitschrift Hydrologie, v. 43, p. 43-62.

Rybicki, R.W.
1966. Limnological study of the North Basin of Lake Winnipeg; 1963 and 1964; Manitoba Department of Mines and Natural Resources, Fisheries Branch, 12 p.

Scherer, R.P.
1994. A new method for determination of absolute abundance of diatoms and other silt-sized sedimentary particles; Journal of Paleolimnology, v. 12, p. 171-179.

Utermohl, H.
1958. Zur Vervollkommnung der quantitativen Phytoplanktonmethodik; Mitteilungen Internationale Vereinigung fur Theoretische und Angewandte Limnologie, v. 9, p. 1-38.

Wolfe, B., Kling, H.J., Brunskill, G.J. and Wilkinson, P.
1994. Multiple dating of a freeze core from Lake 227, an experimentally fertilized lake with varved sediments; Canadian Journal of Fisheries and Aquatic Sciences v. 51, p. 2274-2285.

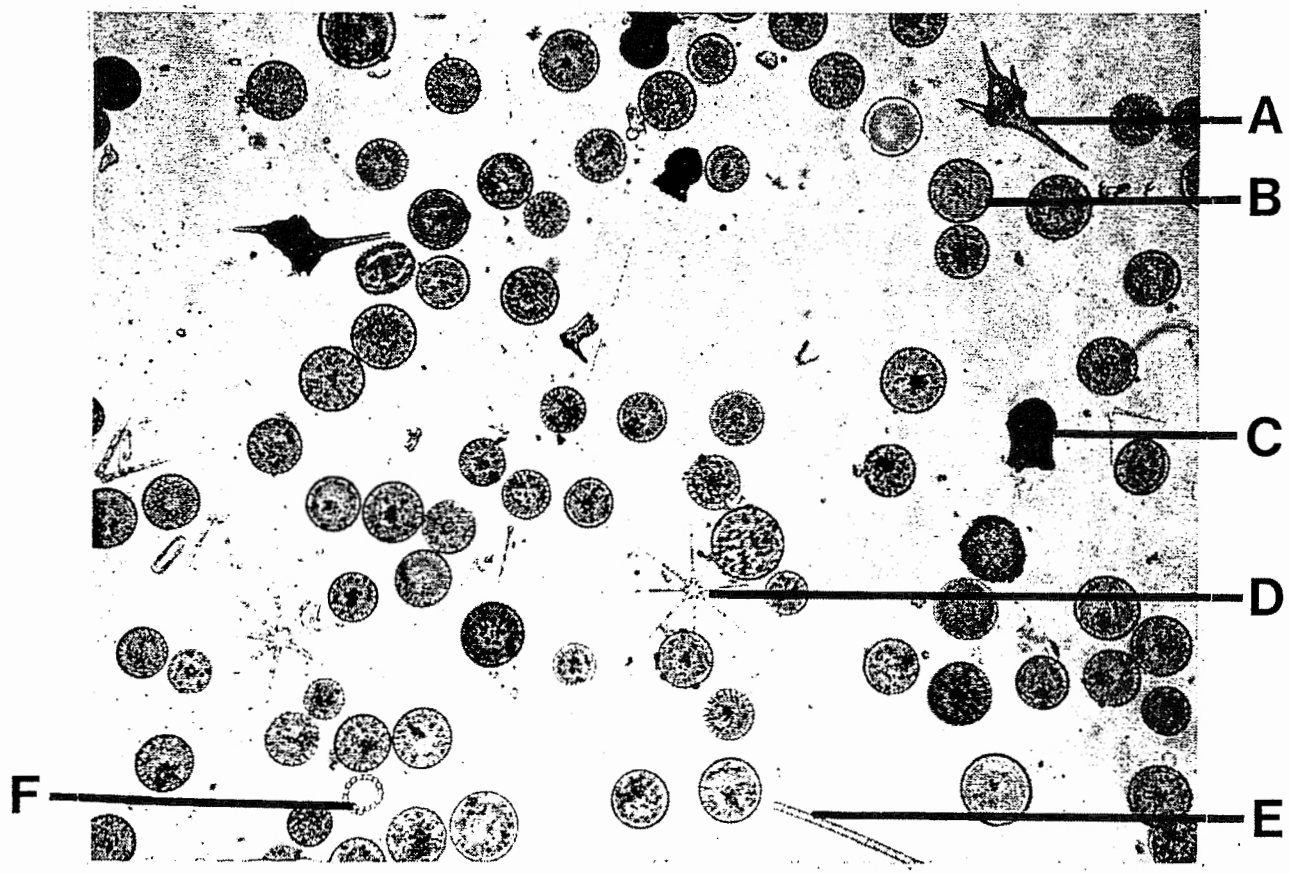

Figure 1. Midsummer 1923 phytoplankton (from Lowe, 1924). The plankton sample contained A) *Ceratium hirundinella,* B) *Stephanodiscus niagarae*, C) *Codonella cratera,* D) *Asterionella formosa*, E) *Aulacoseira* sp., F) *Anabaena* sp. The sample appears to be dominated by *S. niagarae*.

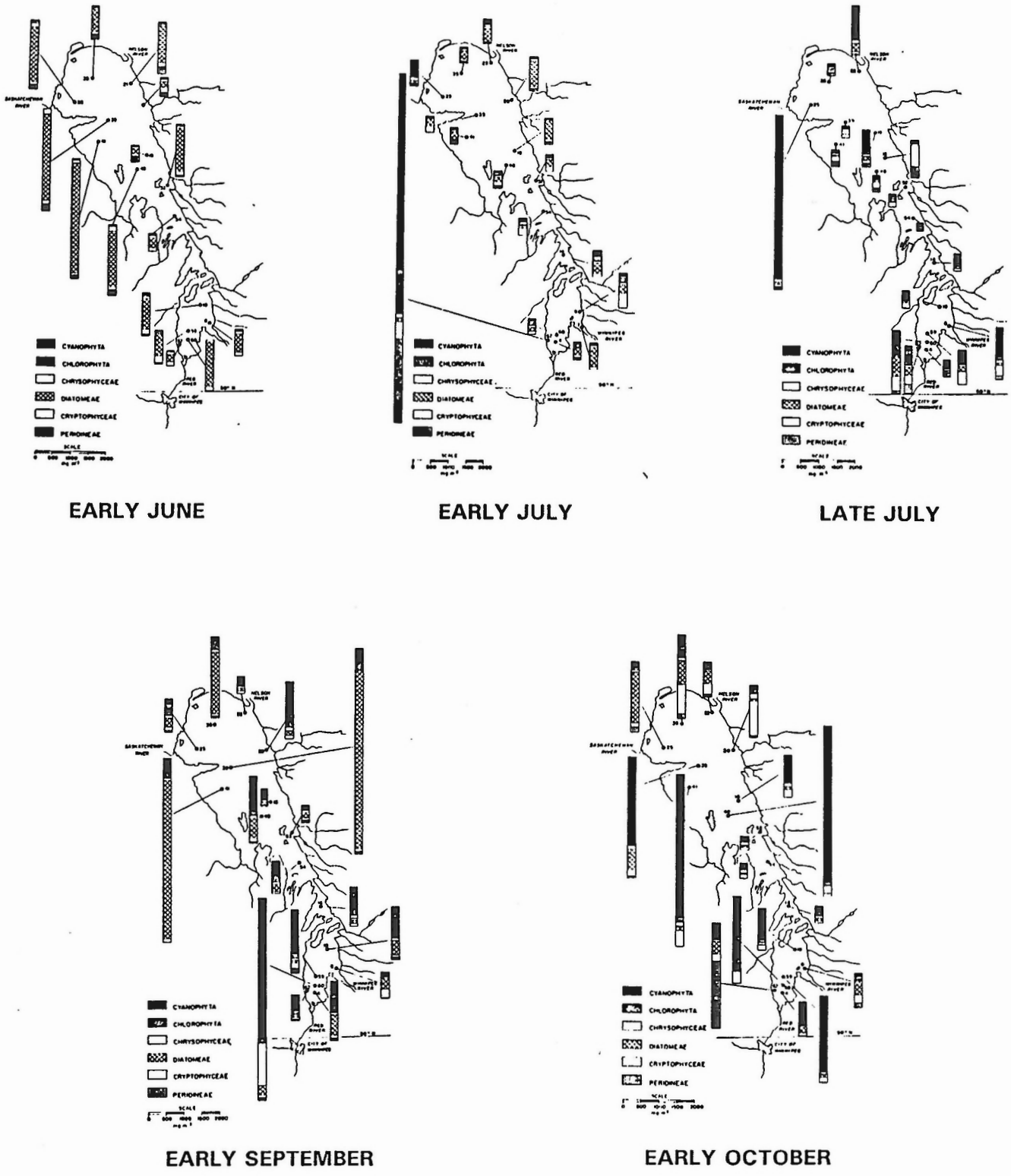

Figure 2. Phytoplankton surveys of Lake Winnipeg, summer of 1969.

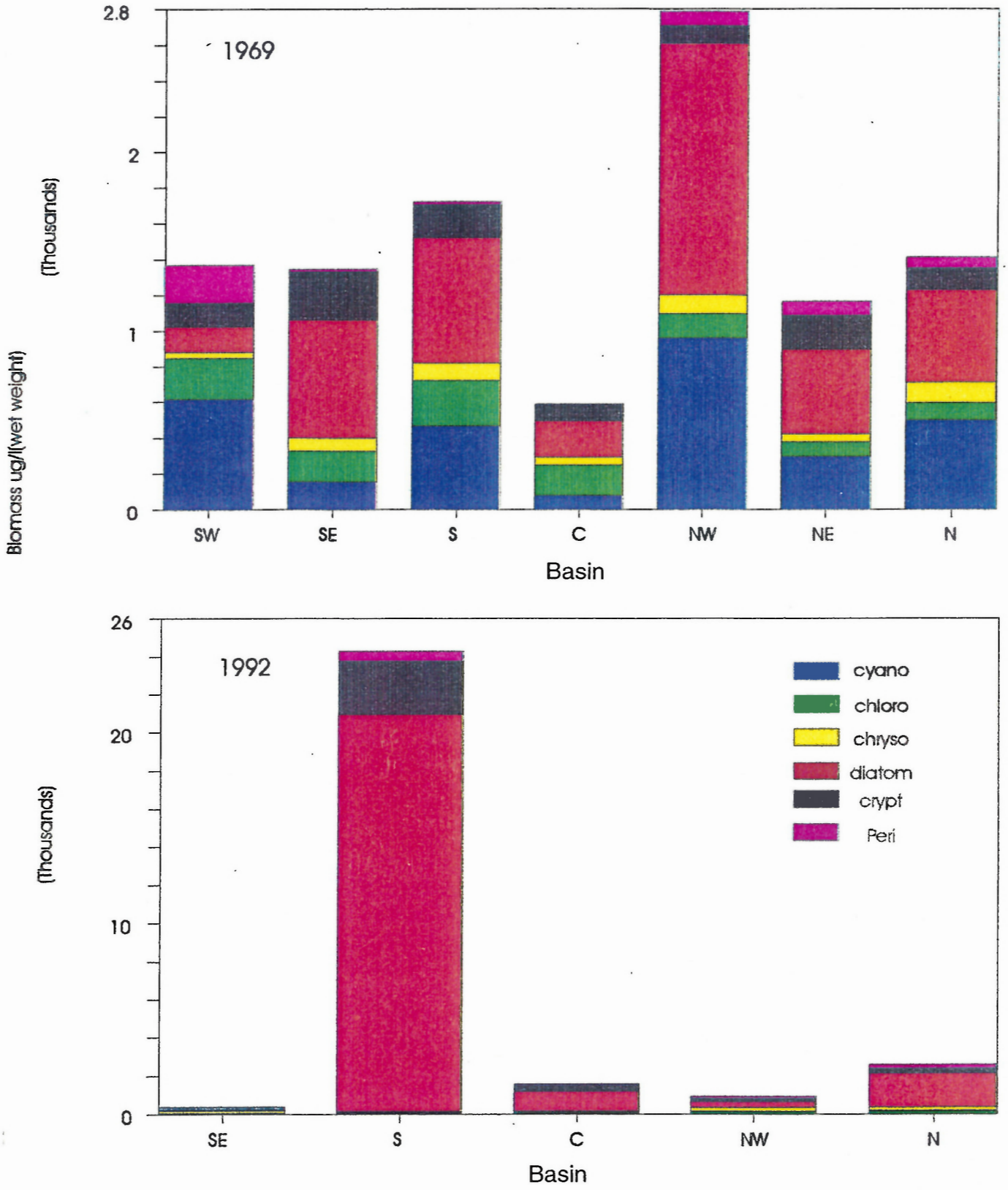

Figure 3. Basin mean phytoplankton biomass and composition for years 1969 and 1992 (open water season May-October).

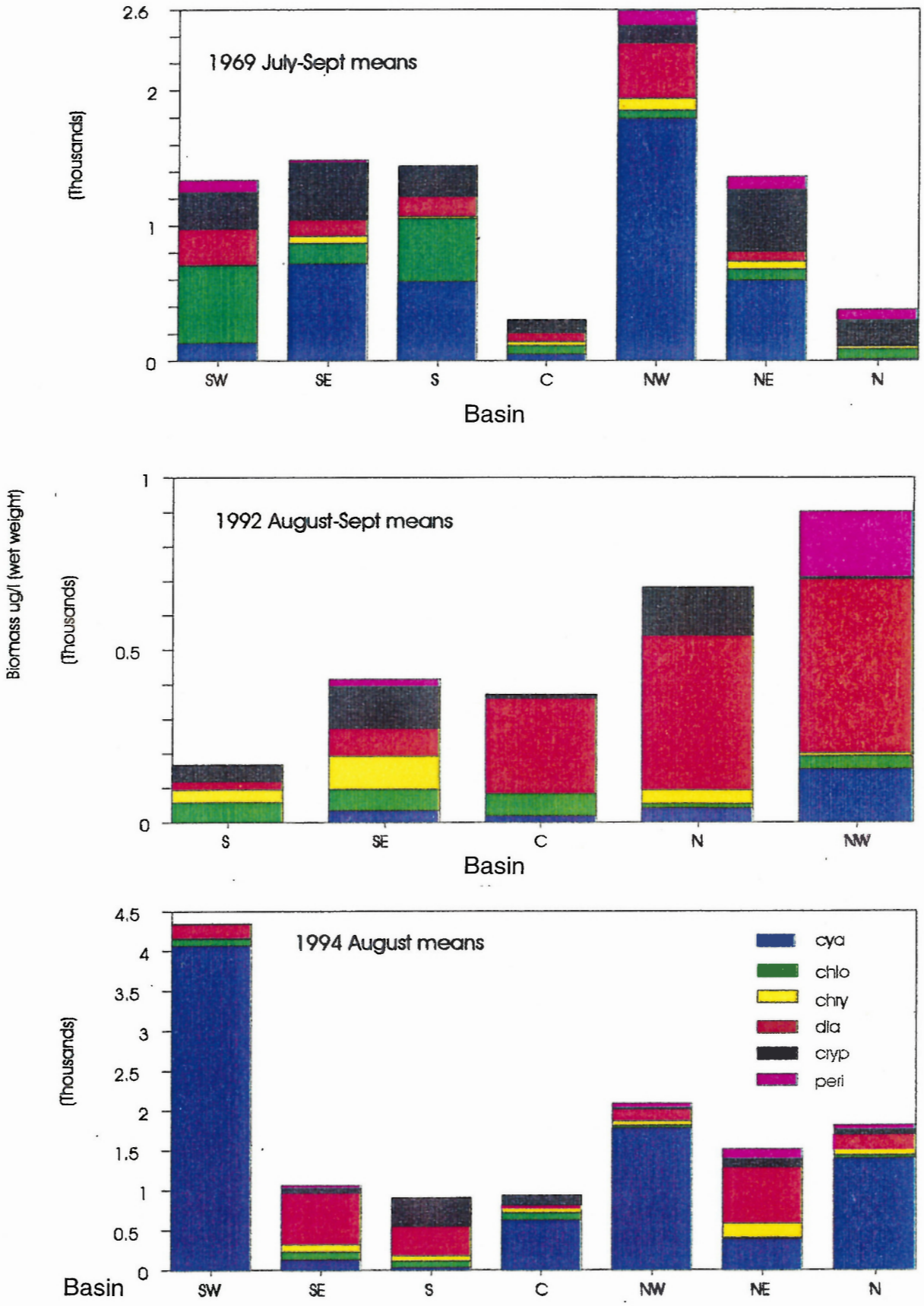

Figure 4. Basin mean phytoplankton biomass and composition for years 1969, 1992 and 1994 (late July-early September).

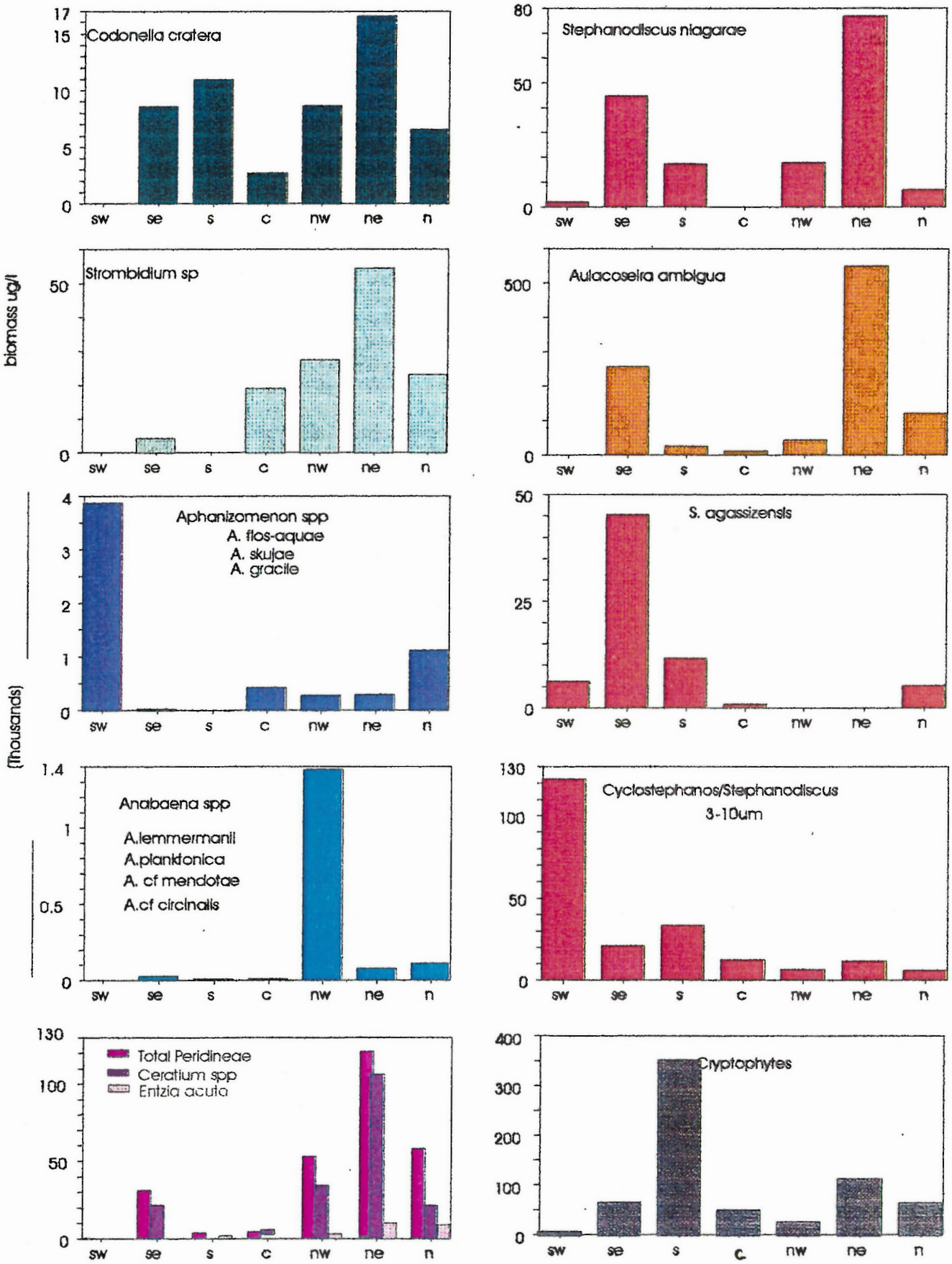

Figure 5. Distribution of major taxa dominating the phytoplankton and protozoan biomass in 1994.

Figure 6. Light Micrographs (LM): a) *Aulacoseira islandica* (O. Muller) Simonsen; b) *Stephanodiscus binderanus* (Kutz.) Kreiger; c) *Aphanizomenon gracile* (Lemm.) Lemm.; d) *Planktothrix suspensa* (Pringsh.) Anagn. and Kom. formerly identified as *Oscillatoria aghardii* Gomont; e) *A. flos-aquae* Breb. ex Born. et Flah.; f) *Anabaena mendotae* Trel.; Plates g-i are Thecate protozoans; g) *Strombidium*; h) *Codonella*; i) *Tintinnidium*.

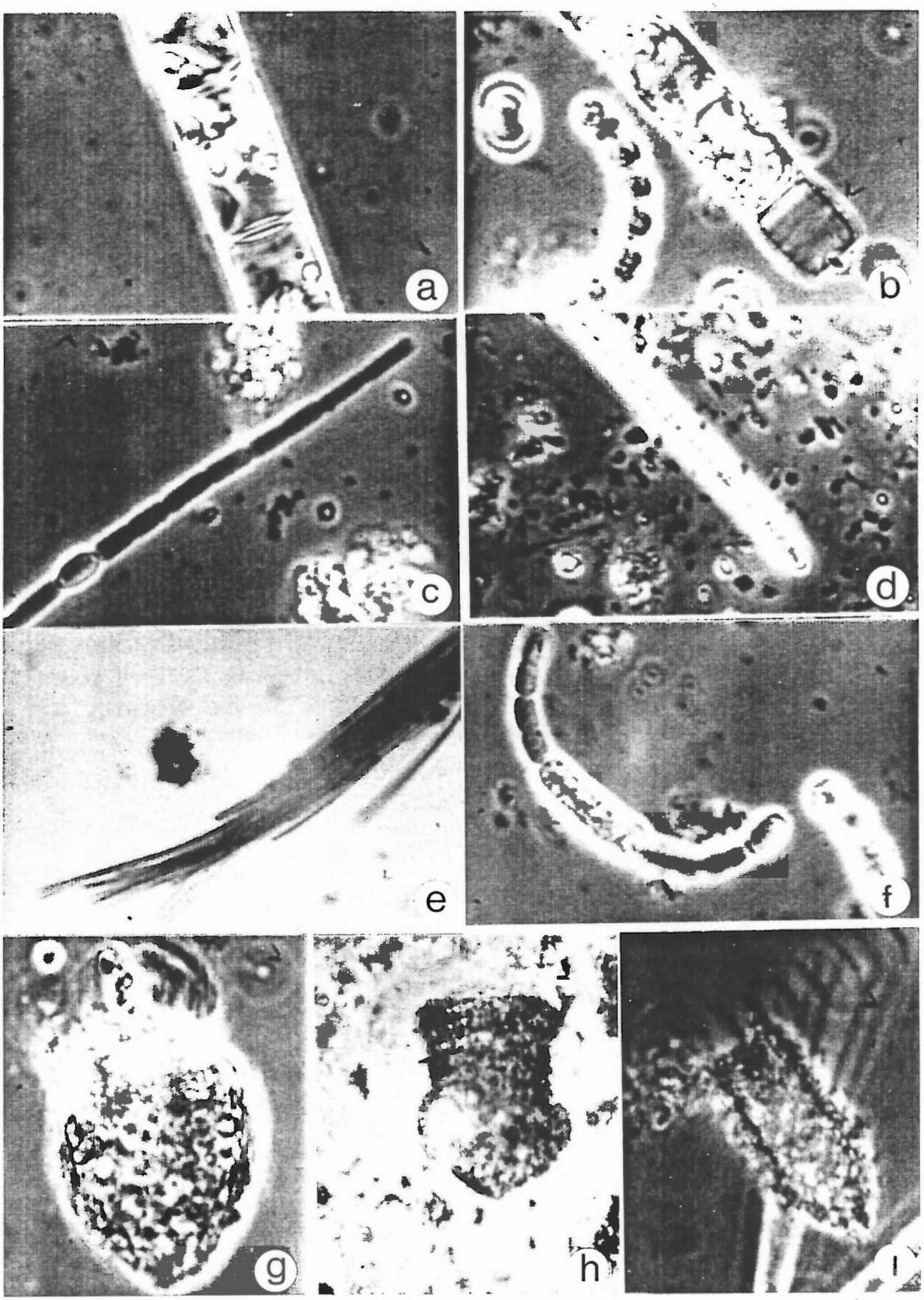
a
b
c
d
e
f
g
h
i

Figure 7. Scanning Electron Micrographs (SEM): a) *Aulacoseira islandica*; b) *A. subarctica* (O. Mull.) Haworth; c) *Melosira varians* Ag.; d) *Cyclotella meneghiniana* Kutz.; e) *Stephanodiscus parvus* Stoermer and Håkansson; f) *Cyclostephanos dubius* (Frike) Round.

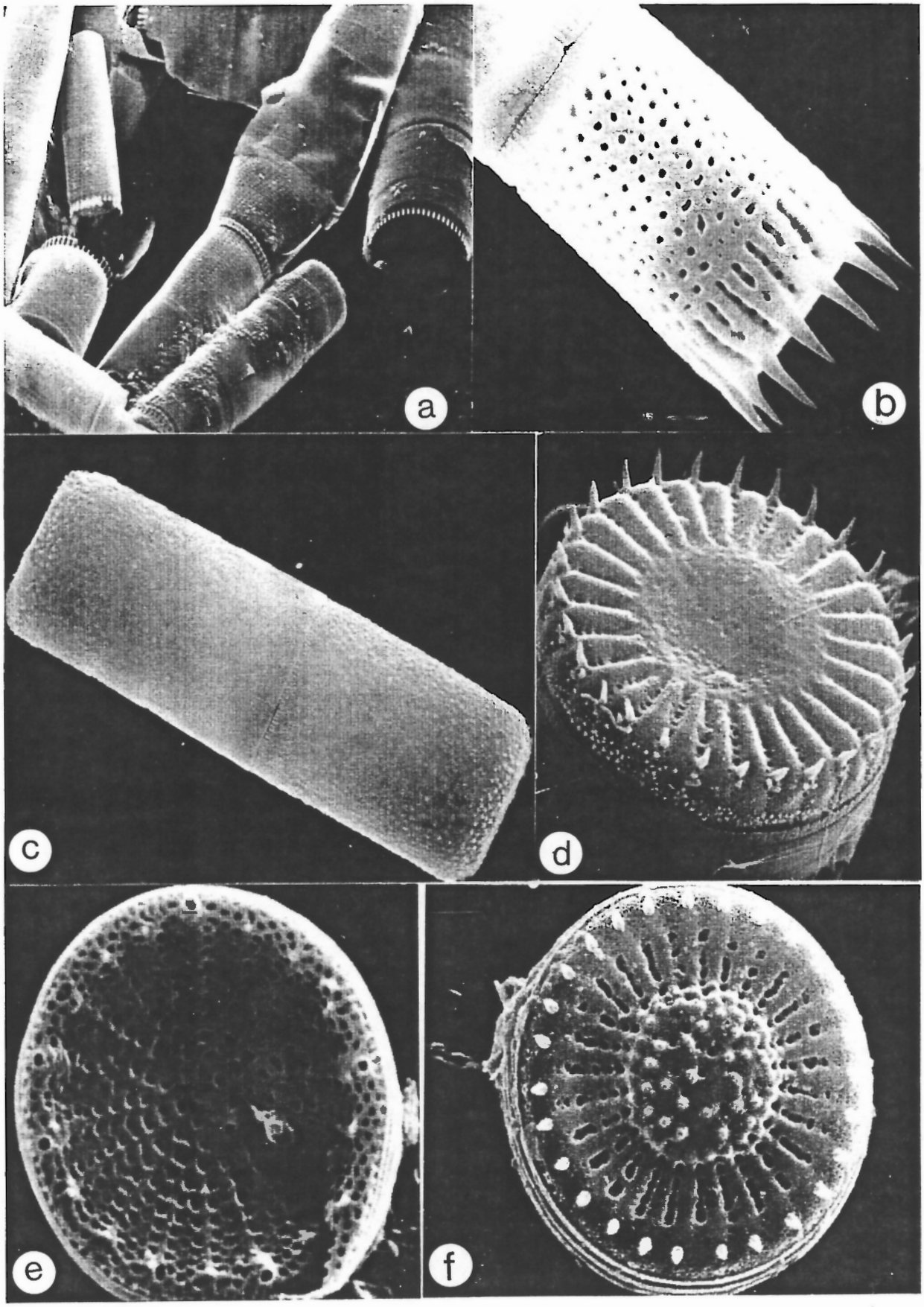
a
b
c
d
e
f

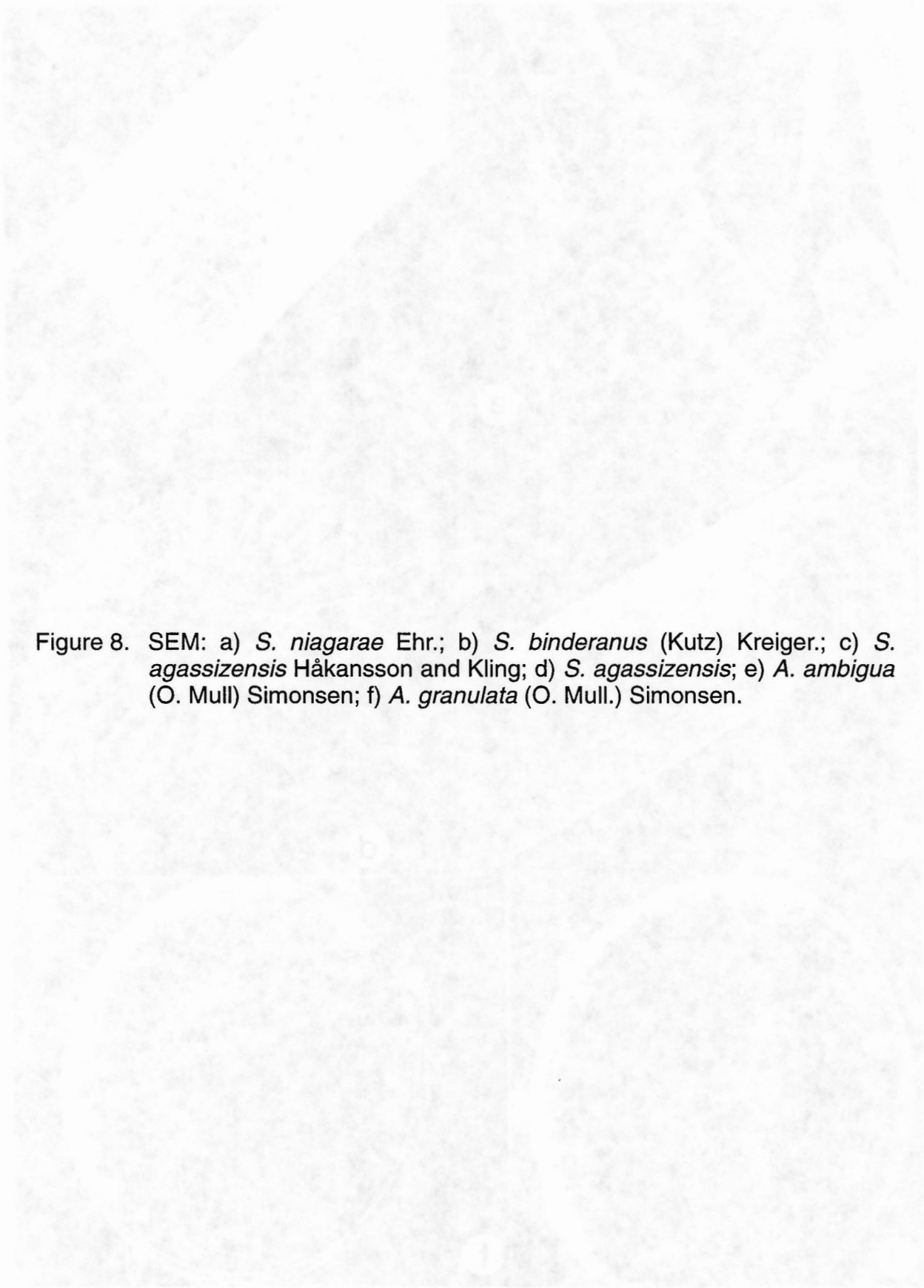

Figure 8. SEM: a) *S. niagarae* Ehr.; b) *S. binderanus* (Kutz) Kreiger.; c) *S. agassizensis* Håkansson and Kling; d) *S. agassizensis*; e) *A. ambigua* (O. Mull) Simonsen; f) *A. granulata* (O. Mull.) Simonsen.

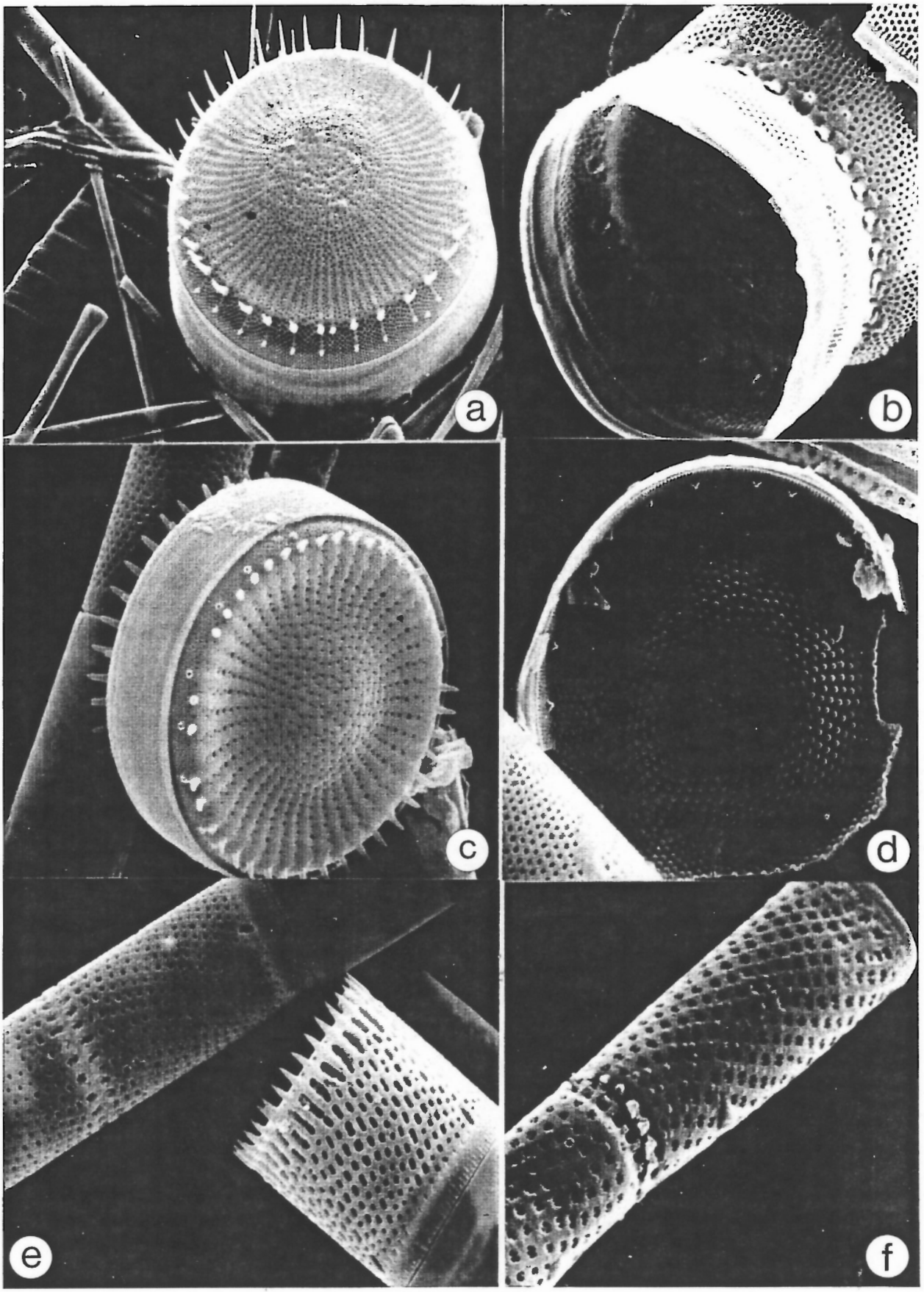
a
b
c
d
e
f

Figure 9. LM: a) *Acanthoceros magdeburgense* Honigmann (=*Attheya zacheriasi* J. Brun); b) *Staurastrum leptocladum* Norst. var. *curvatum* Lowe; c) *Entzii acuta* (Apst.) Lebour (=*Diplopsalis acuta* Entz); d) *Microcystis* sp.; Plates e-h are non-siliceous microfossil from the sediments. e) *Aphanizomenon* akinete (resting spore); f) *Anabaena* akinete; g) Zooplankton faecal pellet; h) Thecate amoeba lorica.

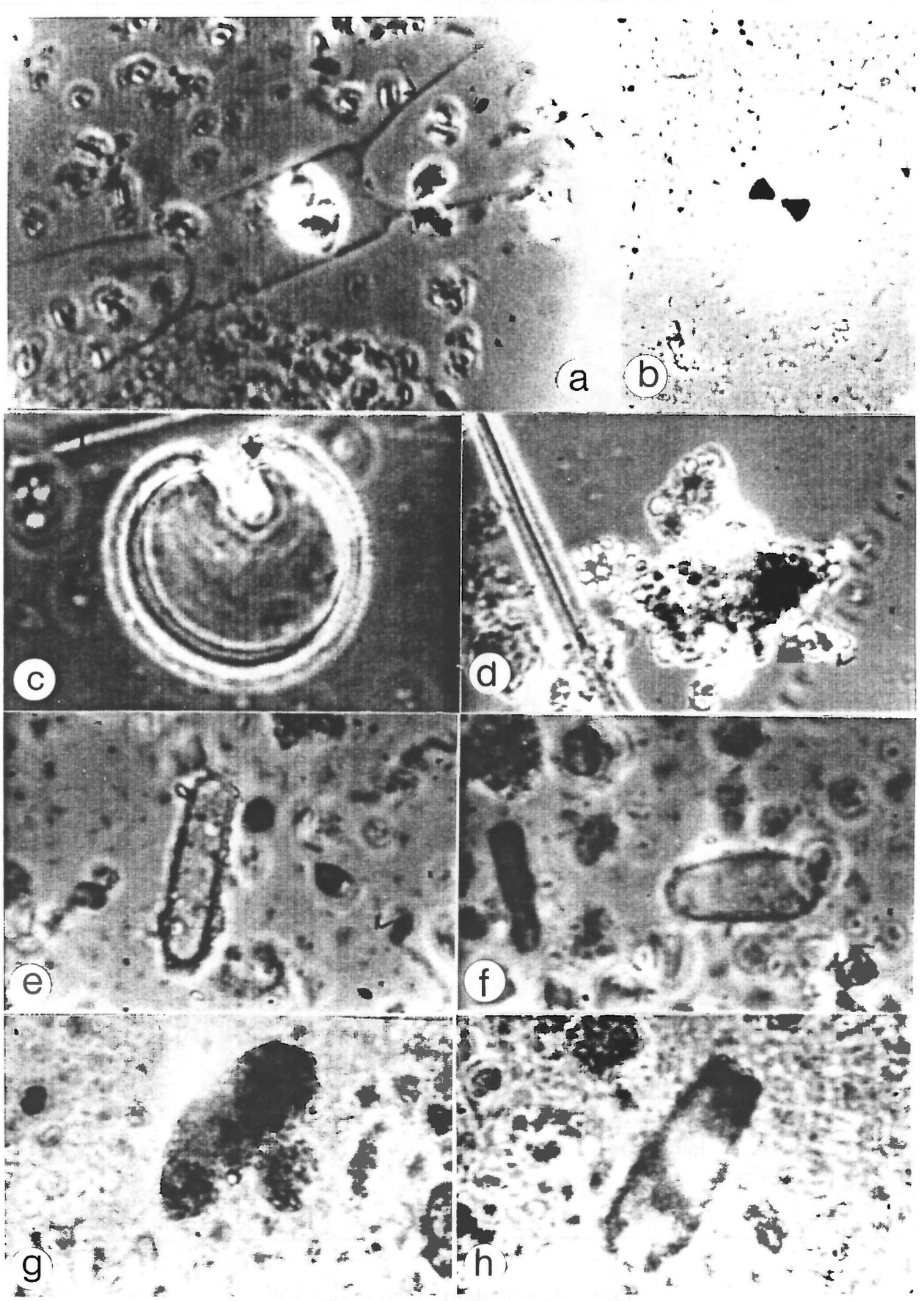
a
b
c
d
e
f
g
h

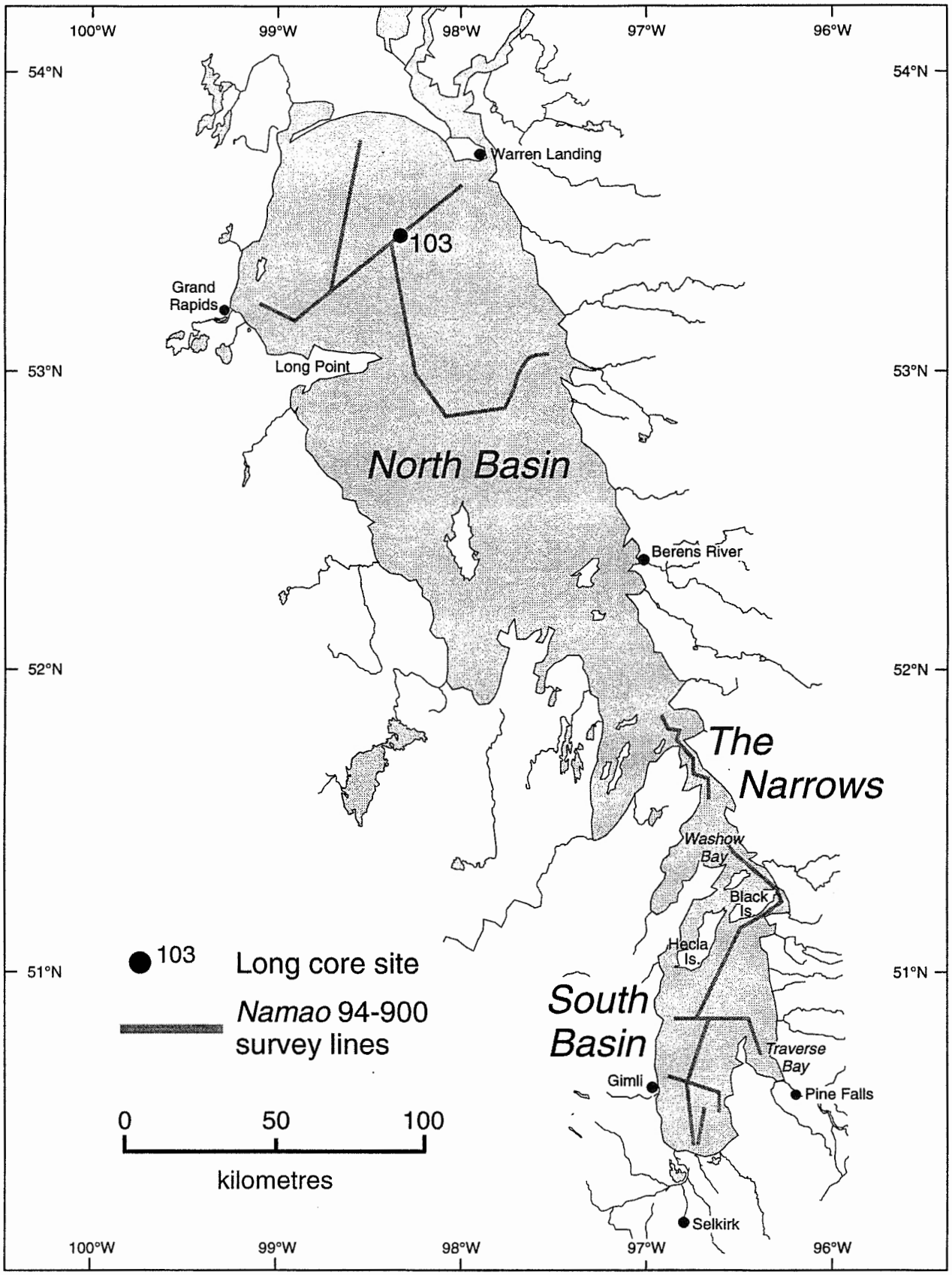

Figure 10. Location of long core 103.

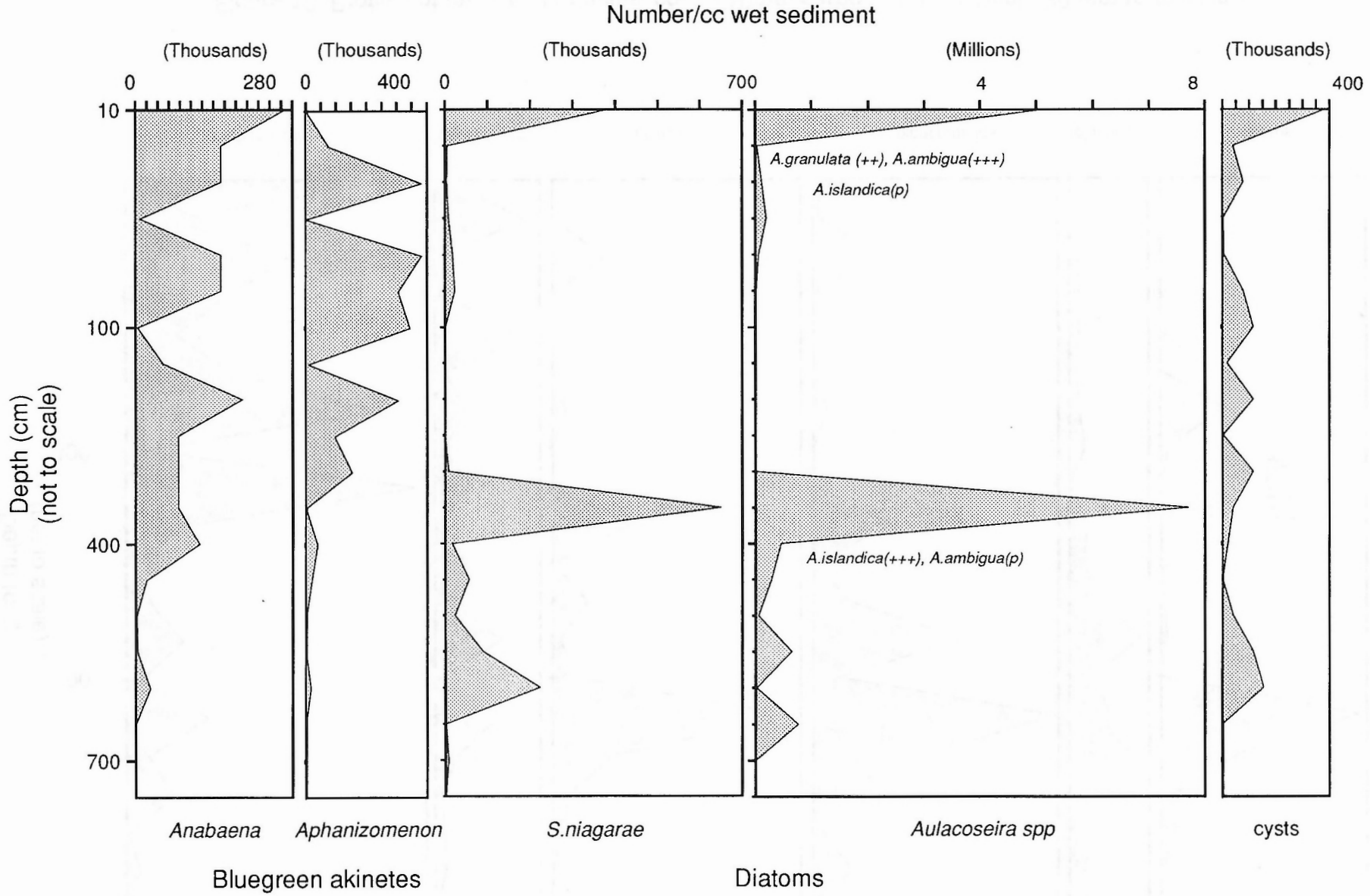

Figure 11. Algal fossil remains in core 103.

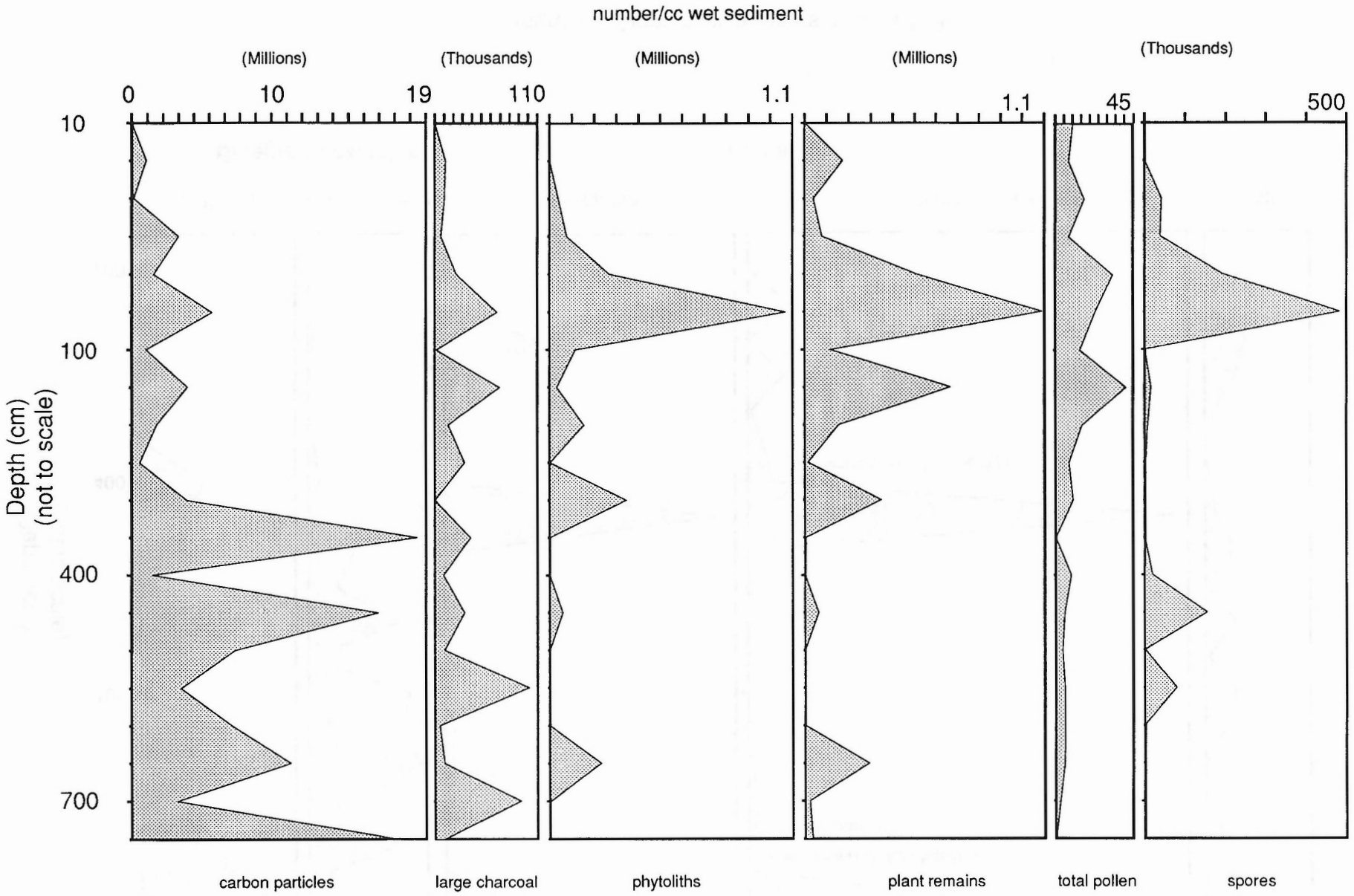

Figure 12. Profiles of terrestrial remains, coal, <10mm carbon and charcoal >20 mm from core 103.

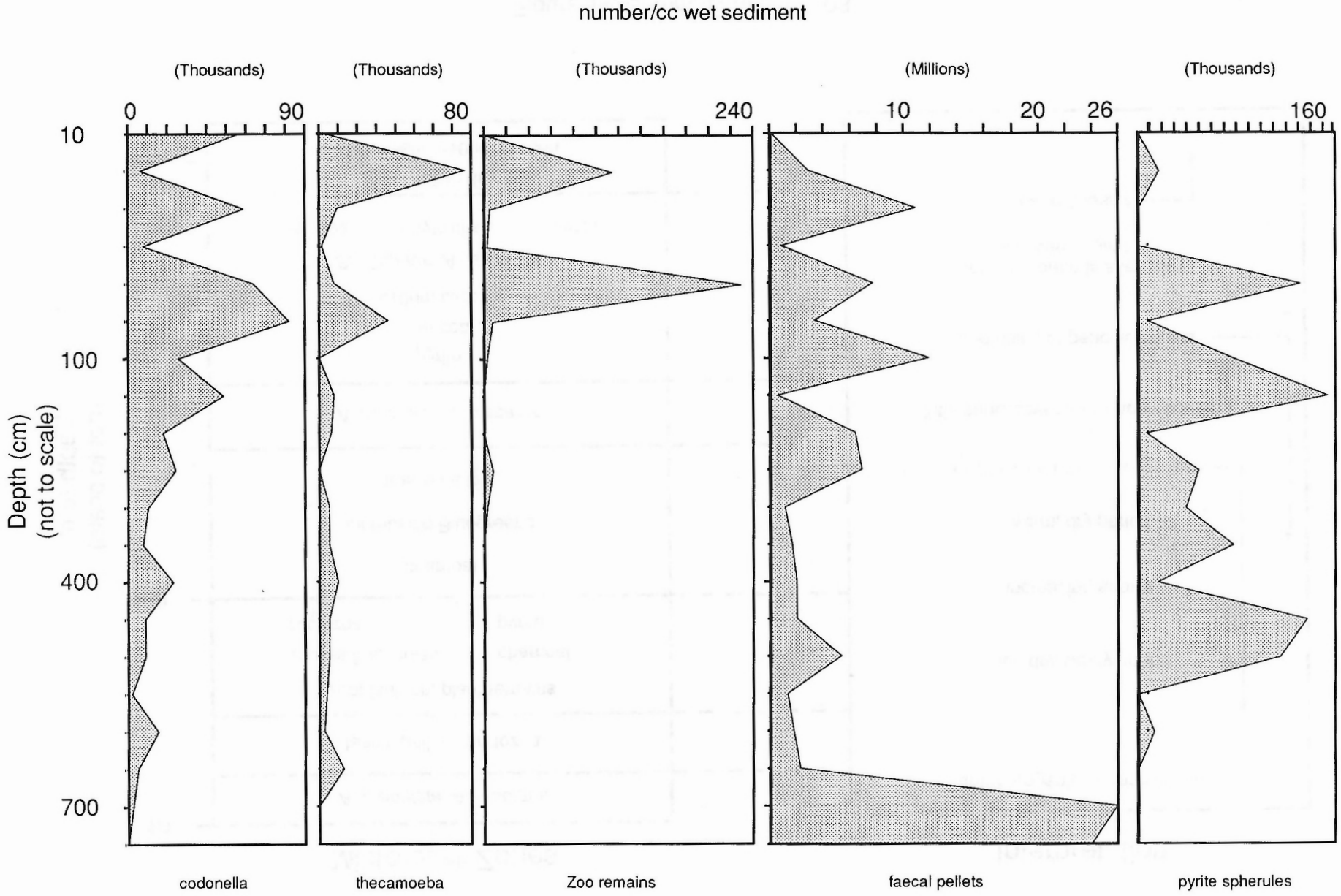

Figure 13. Micro-zooplankton remains and pyrite framboidals/spherules from core 103.

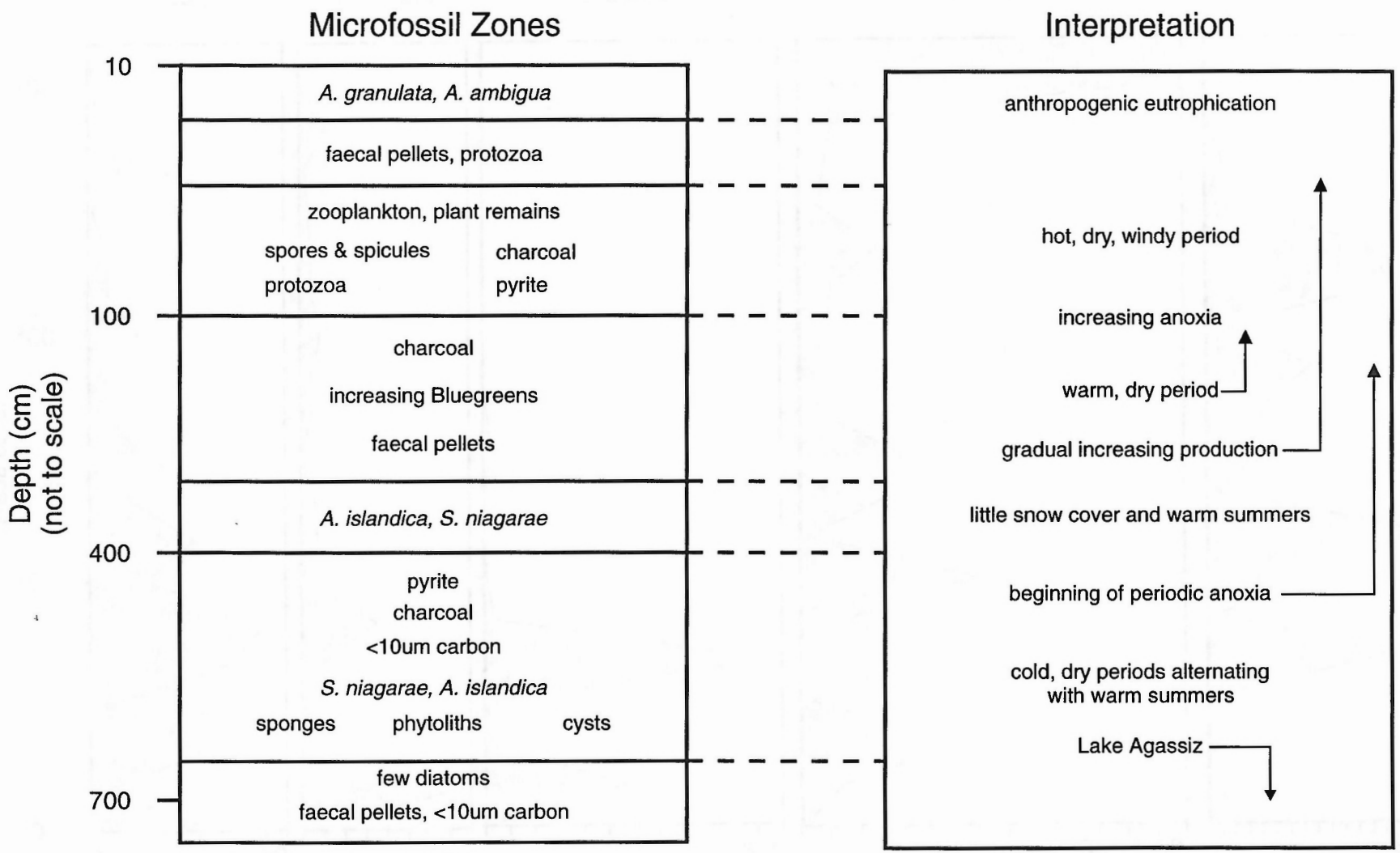

Figure 14. Summary of core 103.

4.12 Paleobotany of Lake Winnipeg sediments

R.E. Vance

Geological Survey of Canada
3303-33rd Street N.W., Calgary, Alberta T2L 2A7

The first step in development of pollen and plant macrofossil stratigraphies for select Lake Winnipeg sedimentary cores has been completed. Some 30 samples from core 103 (chosen at this early stage as the core with the most complete postglacial record) have been processed for pollen analysis (5 from Lake Agassiz sediment, the remainder from overlying Lake Winnipeg deposits). Preliminary scanning of the preparations indicates that pollen is well preserved and abundant in the Lake Winnipeg sediment. In underlying Lake Agassiz sediment, pollen is present but is much less abundant and not as well preserved as in the Lake Winnipeg section of the core. Detailed pollen analyses will be conducted once a reliable chronology is established for core 103 (or for any other Lake Winnipeg core that is shown to contain a complete postglacial sedimentary record). A pollen stratigraphy from Lake Winnipeg sediments would chronicle regional dynamics of postglacial vegetation development. Because of the extremely large size of the catchment area and the relative insensitivity of boreal forest pollen records to climate change (due to extremely high numbers of pine (*Pinus*) and spruce (*Picea*) pollen 'swamping out' more climatically-sensitive pollen taxa), significant events in the pollen record will likely be confined to the Late Wisconsin/early Holocene portion of the record.

One of the initial steps in isolating pollen in each of the 2 to 4 cm^3 samples involves washing the sediment through a 250 μm screen. To assess the number and diversity of plant macrofossil remains in core 103, the residue on the 250 μm screen from each pollen sample was systematically scanned under a stereomicroscope. This preliminary survey revealed that macrofossils are extremely rare in core 103; not one complete specimen was recovered. This is not an unexpected result considering the mid-lake location of the coring site and the size of Lake Winnipeg, since the majority of plant macrofossils are deposited in nearshore, shallow water settings.

In addition to pollen samples from core 103, other samples of Lake Winnipeg sediment that looked to the sampling team to contain atypically high organic matter content (three from core 107 and one from core 122a) were treated to isolate macrofossil remains. The most noteworthy result came from core 122a (425-433 cm below the sediment-water interface), since this sample contained an exceptionally rich and varied plant macrofossil assemblage that included rush (*Juncus*), sedge (*Carex*), bulrush (*Scirpus*), skunkweed (*Chara*), horned pondweed (*Zannichellia palustris*), cattail (*Typha*), pigweed (*Chenopodium*), and samphire (*Salicornia*). This assemblage compares favourably with modern macrofossil assemblages from shallow water/shoreline deposits in fresh to hyposaline carbonate-rich lakes and potholes on the Canadian prairies. Although some of the specimens bear some signs of redeposition, about half are in excellent condition. One exceptionally well preserved *Scirpus* achene (with bristles still attached) yielded an accelerator mass spectrometry (AMS) ^{14}C date of 4040 ± 70 yr BP (CAMS #17434), clearly indicating shoreline proximity to core site 122a at this time. In contrast to this abundant and informative assemblage, samples from core 107 contained little in the way of identifiable macrofossil remains (123 cm - several potentially identifiable wood fragments, the largest two approximately 1 x 2 cm in size; 392 cm - a few ostracodes; 418.5 cm - one cattail (*Typha*) seed, several unidentifiable organic fragments, a few ostracodes).

In summary, although AMS dating of well preserved upland and shoreline plant remains would be a reliable means of developing accurate chronologies for Lake Winnipeg core sections, macrofossil reconnaissance conducted to date indicates that suitable remains are extremely rare. This paucity of plant macrofossil remains also eliminates the possibility of developing plant macrofossil stratigraphies that could document postglacial changes in water depth, lake water chemistry, and shoreline position. However, pollen remains in the Lake Winnipeg cores are abundant and well preserved; well suited to outlining regional postglacial vegetation dynamics, provided accurate chronological control can be developed in any of the cores. The lack of suitable macrofossils for AMS dating combined with the 'hard water' effect in the basin make the development of reliable core chronologies the most pressing challenge facing the Lake Winnipeg research team.

5. Sampling survey results

5.1 Sampling polychlorinated biphenyls in Lake Winnipeg

G. Fisher-Smith and K. Friesen

Department of Chemistry
University of Winnipeg, 515 Portage Avenue, Winnipeg, Manitoba R3B 2E9

INTRODUCTION

Polychlorinated biphenyls (PCBs) are persistent, semi-volatile global contaminants which have a tendency to bioaccumulate. These compounds, which contain varying numbers of chlorine atoms on the biphenyl ring system, are frequently grouped into congener sets according to the degree of chlorination (Table 1; Figure 1; Alford-Stevens, 1986).

For lakes receiving little input from point sources, atmospheric deposition may be the dominant input mechanism. Although there have been a number of studies of PCBs in the Great Lakes (Hornbuckle et al., 1994; Jeremiason et al., 1994; Swackhamer et al., 1988), there is no comparable information for other "great lakes" such as Lake Winnipeg. The objectives of this investigation were, therefore, to determine the significance of atmospheric inputs of PCBs to Lake Winnipeg and to study the behaviour of PCBs at the air-water interface of the lake. Isomer-specific analysis will indicate the importance of deposition (air-to-water transfer) versus volatilization (water-to-air transfer) of specific PCB congeners under midsummer conditions.

A total of 12 water samples and 10 air samples were collected in the South and North basins of Lake Winnipeg in August 1994, for analyses of individual PCB congeners. Sampling procedures were designed to allow for differentiation of PCBs sorbed to particulate matter from PCBs in the nonsorbed states in both air and water samples. By comparing the concentrations of PCBs in corresponding gaseous and dissolved samples, the magnitude and the direction of the fluxes of these chemicals across the air-water interface of the lake may be calculated. Current literature for freshwater lakes such as the Great Lakes indicates that volatilization of PCBs (water-to-air transfer) will be a more important process than deposition into the lake during warm summer months (Mackay et al., 1986).

AIR SAMPLING

Air samples were collected using a General Metal Works High Volume Air Sampler mounted at the bow of the CCGS *Namao*. PCBs sorbed to particulate matter were collected on a glass fiber filter (GFF) (1 μm), whereas a polyurethane foam plug (PUF) (6.5 cm diameter x 7 cm) was used to trap gaseous PCBs (McConnell et al., 1993). Each transect air sample was collected over a period of 5-18 hours at a flow rate of 0.25 m^3/min while the CCGS *Namao* was steaming slowly. Air temperature, wind speed and direction, and ship direction were monitored regularly during sampling. GFFs were precleaned by baking overnight at 285° C and were transported to the field wrapped in aluminum foil. PUFs were precleaned by soxhlet extraction (12 hours) with hexane, and were stored and transported in glass jars.

WATER SAMPLING

Water samples (18 L) were collected from a depth of 1-2 m for the analysis of PCBs. A submersible water pump (March Mfg. Inc. model LC-2CP-MD) was used to pump water for 15-20 minutes prior to sample collection to rinse the collection vessels and to allow PCBs in the water to equilibrate with the tubing. Over a period of 15 minutes, 18 L of water were pumped into solvent-rinsed stainless steel containers. An additional 1 L water sample was collected in a Nalgene storage bottle for analysis of dissolved organic carbon (DOC), particulate carbon (PC) and total suspended matter (TSM) at each sampling site. The water temperature was recorded using a calibrated digital thermometer. Water samples were stored at 4° C until analysis.

ANALYTICAL PROCEDURES FOR AIR SAMPLES

Individual PUF and GFF samples were spiked with internal standards and soxhlet extracted overnight (Achman et al., 1993) using 300 mL of dichloromethane (DCM). Internal standards used were [U-^{13}C]-2,2',5,5'-tetrachlorobiphenyl (PCB 52), [U-^{13}C]-2,2',4,4',5,5'-hexachlorobiphenyl, (PCB 153), [U-^{13}C]-2,2',3,3',4,4',5,5'-octachlorobiphenyl (PCB 194), 2,4,6-trichlorobiphenyl (PCB 30), octachloronaphthalene, as well as two deuterated pesticide standards, 2-chloro-4-([d_5]-ethylamino)-6-(isopropylamino)-s-triazine (d_5-atrazine) and ([3,5,6,-d_3]- 2,4-dichlorophenoxy) acetic acid (d_3-2,4-D). The extracts were concentrated to 3-5 ml using a rotary evaporator and quantitatively transferred to graduated centrifuge tubes. The samples were methylated by reaction with diazomethane, concentrated to 500 μL, and fractionated on a Florisil column (Muir et al., 1993). The PCB fraction was collected and an internal standard 2,2',4,6,6'-pentachlorobiphenyl (PCB 104) was added before a final concentration by nitrogen blowdown to 100 μL.

ANALYTICAL PROCEDURES FOR WATER SAMPLES

Samples were removed from cold storage and allowed to reach thermal equilibrium in the laboratory. A set of internal standards was added (as described above) prior to stirring the samples for 30 minutes. After stirring, the tank was pressurized using prepurified nitrogen, and the water filtered through 1 μm GFFs into another tank. The pH of the filtrate was adjusted to 2 with the addition of 22 mL of concentrated sulfuric acid and extracted for 30 minutes with 1 L of DCM with stirring. After settling, the system was pressurized to collect the DCM in a 2 L separatory funnel for further separation of the organic and aqueous phases. The organic phase was drained through a 500 mL separatory funnel containing sodium sulfate, collected in a 500 mL round-bottom flask, and concentrated by rotary evaporation. A second extraction at pH 2 was performed in the same manner using 500 mL of DCM. All solvent extractions were combined for analysis. The water was then adjusted to a pH of 12 by adding 100 mL of 10 M sodium hydroxide, and extracted with 1 L of DCM as described above. This was followed by a fourth extraction, using 500 ml of DCM. The combined extracts were concentrated to 3-5 mL on a rotary evaporator and transferred to a graduated centrifuge tube. The sample was methylated, concentrated to 500 μL, and fractionated on a Florisil column. The PCB 104 internal standard was added to the PCB fraction which was then concentrated to 100 μL.

PCB ANALYSIS

GC-MS (gas chromatography coupled with mass spectroscopy) analyses are currently underway to determine the concentrations of sorbed and non-sorbed PCBs in all air and water samples collected. The analyses are being performed by high resolution gas chromatography on a 60 m DB-5 fused silica capillary column with a Hewlett Packard 5890 gas chromatograph. A Hewlett Packard 5970 mass selective detector (MSD) operated in the selected-ion-monitoring (SIM) mode is used for quantification of PCBs.

REFERENCES

Achman, D.R., Hornbuckle, K.C. and Eisenreich, S.J.
1993. Volatilization of polychlorinated biphenyls from Green Bay, Lake Michigan; Environmental Science and Technology, v. 27, p.75-87.

Alford-Stevens, A.L.
1986. Analyzing PCBs; Environmental Science and Technology, v. 20, p. 1194-1199.

Hornbuckle, K.C., Jeremiason, J.D., Sweet, C.W. and Eisenreich, S.J.
1994. Seasonal variations in air-water exchange of polychlorinated biphenyls in Lake Superior; Environmental Science and Technology, v. 28, p. 1491-1501.

Jeremiason, J.D., Hornbuckle, K.C. and Eisenreich, S.J.
1994. PCBs in Lake Superior, 1978 - 1992: Decreases in water concentrations reflect loss of volatilization; Environmental Science and Technology, v. 28, p. 903-914.

Mackay, D., Paterson, S. and Schroeder, W.H.
1986. Model describing the rates of transfer processes of organic chemicals between atmosphere and water; Environmental Science and Technology, v. 20, p. 810-816.

McConnell, L.L., Cotham, W.E. and Bidleman, T.F.
1993. Gas exchange of hexaclorocyclohexane in the Great Lakes; Environmental Science and Technology, v. 27, p. 1304-1311.

Muir, D.C.G., Segstro, M.D., Welbourn, P.M., Toom, D., Eisenreich, S.J., Macdonald, C.R. and Whelpdale, D.M.
1993. Patterns of accumulation of airborne organochlorine contaminants in lichens from the Upper Great Lakes region of Ontario; Environmental Science and Technology, v. 27, p. 1201-1210.

Swackhamer, D.L., McVeety, B.D. and Hites, R.A.
1988. Deposition and evaporation of polychlorobiphenyl congeners to and from Siskiwit Lake, Isle Royale, Lake Superior; Environmental Science and Technology, v. 22, p. 664-672.

Table 1.

Congener Group	Molecular Formula	No. of Compounds
Monochlorobiphenyls	$C_{12}H_9Cl$	3
Dichlorobiphenyls	$C_{12}H_8Cl_2$	12
Trichlorobiphenyls	$C_{12}H_7Cl_3$	24
Tetrachlorobiphenyls	$C_{12}H_6Cl_4$	42
Pentachlorobiphenyls	$C_{12}H_5Cl_5$	46
Hexachlorobiphenyls	$C_{12}H_4Cl_6$	42
Heptachlorobiphenyls	$C_{12}H_3Cl_7$	24
Octachlorobiphenyls	$C_{12}H_2Cl_8$	12
Nonachlorobiphenyls	$C_{12}HCl_9$	3
Decachlorobiphenyls	$C_{12}Cl_{10}$	1
Total Number of Congeners		**209**

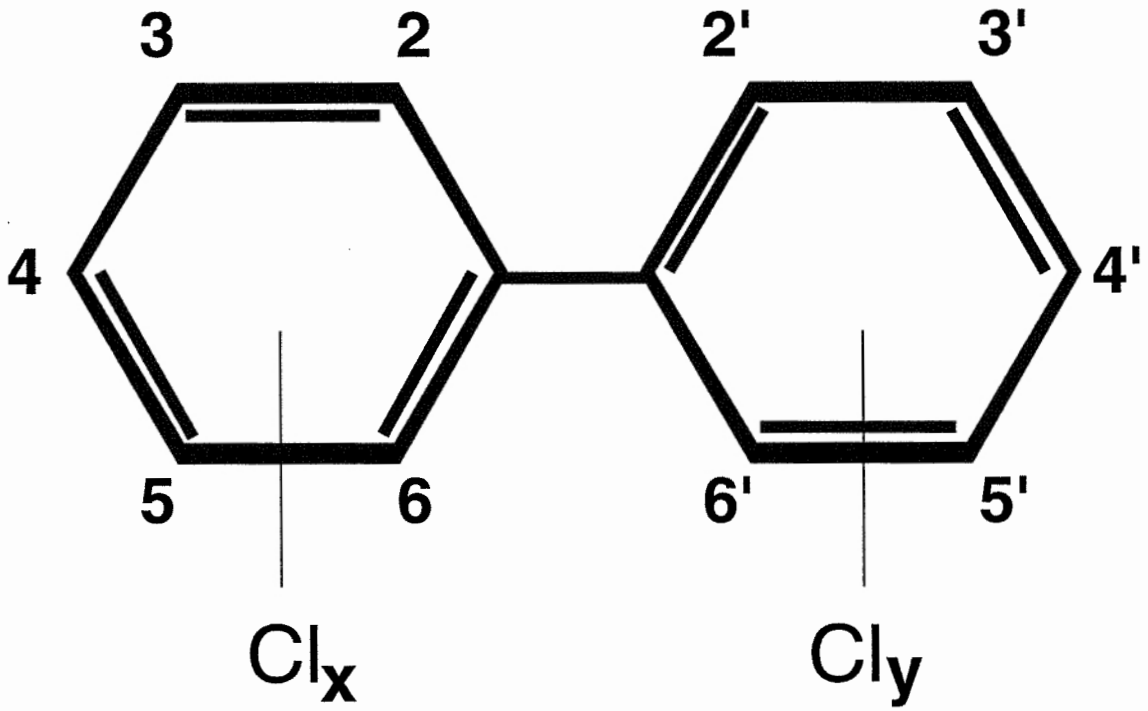

$$x + y = 1 - 10$$

Figure 1. Polychlorinated biphenyl structure.

5.2 The crustacean plankton community of Lake Winnipeg in 1929, 1969 and 1994

A. G. Salki

Department of Fisheries and Oceans
Freshwater Institute, 501 University Crescent, Winnipeg, Manitoba R3T 2N6

ABSTRACT

Bajkov's study of Lake Winnipeg in 1929 and two surveys by the Freshwater Institute in 1969 and 1994 enabled an evaluation of crustacean plankton community response to anthropogenic impacts during the 65 year period. In spite of substantially increased nutrient loadings to the South and North Basins since 1929, the zooplankton community exhibited little change in species composition during this period. Rivers draining different geological basins appear to have the most important impact on maintaining a diverse zooplankton community in Lake Winnipeg. Crustacean abundance in both basins was higher in 1969 than in 1929. In 1994, although zooplankton abundance in the turbid South Basin was similar to 1969 levels, a continuing increase in the more transparent North Basin seems attributable to continuing nutrient enrichment.

INTRODUCTION

The August 1994 Lake Winnipeg Project, co-sponsored by the Geological Survey of Canada, Manitoba Energy and Mines, Manitoba Hydro and the Freshwater Institute (FWI), was the second major survey conducted on the lake since 1929 when Bajkov (1934) initially characterized its limnology and biotic communities. Forty years after Bajkov's work, a FWI multidisciplinary study of Lake Winnipeg in 1969 documented the spatial complexity of this water body (Brunskill, 1973; Brunskill and Graham, 1979; Brunskill et al., 1979a; Brunskill et al., 1979b; Brunskill et al., 1980; Kenny, 1979; Patalas and Salki, 1992; Flannagan et al., 1994). To date, the 1969 survey is the major source of seasonal information on the Lake Winnipeg ecosystem. Although the 1994 survey was mainly intended to extend knowledge of the lake's postglacial history and geology, it also provided limited re-examination of biota to assess ecosystem changes during the past 65 years. This manuscript focuses on a comparison of crustacean plankton community composition and abundance in Lake Winnipeg during August of 1929, 1969 and 1994.

METHODS

From August 19 to 30, 1994, biological samples were obtained at 33 sites in Lake Winnipeg (Fig. 1a,b). For the purposes of this report, the lake was divided into two basins, North and South Basins, each with three main areas. South Basin sub-basins named Red River inflow (R), the main South Basin (SB), and the Winnipeg River inflow (W) were sampled in 1994 at 3, 14 and 2 stations, respectively. The North Basin was divided into The Narrows (N) region (4 stations), the northern North Basin (NBn) (9 stations), and the Saskatchewan River inflow area (S) (1 station). The 1969 June to October study included 51 locations. For comparative purposes, data for 27 stations from the 1969 network that corresponded to most of the 1994 locations were chosen. Data from two 1969 cruises, July 24 - August 1 and September 2 - 10, were averaged to provide comparison with the mid-August 1994 cruise.

Methods of sample collection and analysis were kept constant during both studies. A Wisconsin zooplankton net of 25 cm mouth diameter and 72μ mesh was hauled from just above the lake bottom to the surface. Each sample, preserved in a 5% formalin solution, was examined at 63X and at least 200 individuals per sample were identified at the species level. Complete methodological details are presented in Patalas and Salki (1992) and Salki and Patalas (1992). Bajkov (1934) employed similar methods to collect 500 samples from different parts of the lake during August 1928 and 1929. Samples were obtained with a 15 litre closing cylinder, filtered through number 20 silk bolting cloth (72μ mesh), settled in 5 mm diameter glass tubes for 24 hours to determine total net plankton volumes, and examined microscopically. Total settled net plankton volumes were also determined for 1969 samples with Bajkov's method (Bajkov, 1934).

RESULTS

Species composition

The 1969 FWI survey of Lake Winnipeg did not reveal any clear change in the species composition of the zooplankton community since 1929. As indicated by Patalas and Salki (1992), discrepancies in the species records of the two studies could be explained by differences in sampling intensity, location and taxonomy. Of the 34 species found lakewide in 1969, 23 were encountered in the set of 27 stations corresponding to the 1994 survey. A similar number of species, 25, was found in August 1994, indicating that no major change had occurred since 1969 (and hence Bajkov's study) (Tables 1, 2). The 12 "core species" (Patalas and Salki, 1992) which were abundant throughout the lake, *Diacyclops bicuspidatus thomasi*, *Acanthocyclops vernalis*, *Diaptomus ashlandi*, *Diaptomus oregonensis*, *Epischura lacustris*, *Epischura*

nevadensis, *Limnocalanus macrurus*, *Daphnia retrocurva*, *Daphnia galeata mendotae*, *Bosmina longirostris*, *Diaphanosoma leuchtenbergianum*, and *Leptodora kindtii* were present in both surveys. The variability between surveys of a few cladocerans such as *Daphnia pulex*, *Ceriodaphnia quadrangula*, and *Leydigia quadrangularis* can be attributed to the very low abundance of these taxa.

Zooplanktonic community structure in Lake Winnipeg appears to have remained relatively stable since 1969. Calanoids were the major group of species in the South Basin in both 1969 and 1994, representing 72.8 and 63.3% of total community abundance respectively (Fig. 2). In the North Basin, cyclopoids were numerically dominant at 66.0 and 57.4% in respective years.

Total abundance and settled net plankton volumes

All six regions of Lake Winnipeg exhibited higher total crustacean abundance in August 1994 than in 1969 (Fig. 3, Table 2). With the exception of region W where plankton abundance is reduced by high discharge of plankton-poor Winnipeg River water, total abundances in 1969 ranged from 41.8 to 89.9 individuals per litre and in 1994 from 81.9 to 135.0 individuals per litre. Ratios of total zooplankton abundances in 1994 versus 1969 in the South Basin were generally near 1.35 while in the North Basin ratios ranged higher, from 1.43 to 2.76. None of the three groups of planktonic crustaceans exhibited a consistent change throughout the lake. Cyclopoids displayed their highest ratio in The Narrows region, while calanoids and cladocerans appeared to gain most in the North Basin.

Comparison of Bajkov's 1929 estimates of lake mean plankton abundance (Bajkov, 1934) with 1969 volumes revealed respective seasonal mean settled net plankton volumes of 5.8 and 9.2 mm^3/L (Patalas and Salki, 1992).

Species distributions and abundance

Patalas and Salki (1992) demonstrated that the seasonal distributions and abundance of crustacean plankton species in Lake Winnipeg were complex and variable during 1969. Although seasonal information was not available from the limited 1994 survey, it nevertheless confirmed many of the species distributions detected in 1969. Several relatively common species, such as *Chydorus sphaericus*, *Daphnia longiremis*, and *Diaptomus minutus*, were found only in the North Basin in both years (Table 3, Fig 4). Many of the 12 species that were found exclusively in the South Basin during the 1969 study had occurred in relatively low numbers in shallower near-shore stations. Consequently, several of these species were not observed in the August 1994 survey when sites of shallower depth were not sampled. *Mesocyclops edax*, found in limited numbers only in the South Basin in 1969, appeared to expand into the North Basin in 1994 and occurred in relatively higher numbers. The 12 species distributed throughout the lake in 1969 exhibited similar patterns in 1994. *D. b. thomasi* once again was characterized by highest abundances in the North Basin and lower numbers in the South Basin. *C. vernalis* had highest abundances in the South Basin, as in 1969, but North Basin densities were reduced from those of the previous study. *D. ashlandi* was distributed as in 1969 with relatively uniform numbers in the South Basin extending into The Narrows region. Cladocerans *D. retrocurva* and *D. g. mendotae* were distributed throughout Lake Winnipeg as in 1969. At the same time, *E. lacustris*, *D. retrocurva* and *L. kindtii* were three species whose centres of distribution appeared to shift from the South to North Basins between 1969 and 1994 (Table 4). The occurrence of *Diaptomus siciloides*, not a core species, was restricted to the Red River inflow and Nelson River outflow areas much like the pattern observed in 1969.

DISCUSSION

During the 65 years since Bajkov's initial 1929 study of Lake Winnipeg (Bajkov, 1934), two surveys have not uncovered clear evidence of significant changes in the species composition and structure of the crustacean plankton community. In addition, the lakewide distribution of most species has remained unaltered between the 1969 and 1994 surveys. The underlying reasons for this stability are undoubtedly linked in part to the size and complexity of the Lake Winnipeg ecosystem.

Spanning almost 4° of latitude, the lake straddles a large climatic gradient, resulting in different conditions within each basin. At the north end of the lake, mean daily air temperatures are 2° C cooler during April - July and frosts are earlier. Also, there are 200 fewer degree days above 5.5° C and 10 cm less rainfall in the north than in the south end (Wier and Matthews, 1971). Basin geology and hydrology are also complex. Several rivers, including the Saskatchewan, Dauphin, and Red Rivers, carry nutrients into the lake from drainage basins to the south and west. The Winnipeg, Manigotagan, Berens and Poplar Rivers, among others, transport materials from the Precambrian Shield situated on the east side of the lake. Thus, it is unlikely that one single anthropogenic event would simultaneously affect zooplankton in all areas of the lake and hence the crustacean plankton community achieves a degree of resilience. The structural complexity of Lake Winnipeg supports 34 species. Other large lakes, such as Superior and Ontario, have only 18 and 23 species, respectively (Patalas, 1972).

The constancy of zooplankton community composition, particularly the 12 core species, is remarkable in view of the anthropogenic eutrophication of the lake. Patalas and Salki (1992) observed an increase in total settled net plankton volume compared to Bajkov (1934,) which they attributed to cultural eutrophication of Lake Winnipeg. Kling (this volume) also reported changes in phytoplankton abundance and species composition between 1923 and 1994, reflecting a trend of increasing eutrophication in the South Basin. The 12 core

species currently in Lake Winnipeg are among the most widely distributed zooplankton in Canada. Most of these species are found from the Maritimes to the Mackenzie Delta in a wide range of lakes of different size, morphometry, and limnology (Patalas et al., 1994). Consequently, a capacity to adapt to a wide range of environmental conditions likely has enabled these species to survive anthropogenic impacts in Lake Winnipeg. In addition to their comparatively wide physiological tolerance, these species are able to escape the effects of transient environmental perturbations by entering diapause or producing resting eggs.

The two previously unrecorded species, *Heterocope septentrionales* and *Eubosmina longispina*, found in Lake Winnipeg in 1994 likely represent the most recent "unsuccessful invaders" (Patalas and Salki, 1992). *H. septentrionales*, a large calanoid usually associated with the deeper, colder profundal zones of lakes, was found in station 2 of the North Basin, adjacent to the Saskatchewan River inflow (its likely entry point to the lake). Essentially a sub-arctic species, *H. septentrionales* occurs in Churchill River drainage lakes in northern Saskatchewan and Manitoba but has not been previously reported south of 55° N latitude (Patalas et al., 1994). The second species, *E. longispina*, observed in low abundance in Traverse Bay (Winnipeg River inflow) and the Nelson River outflow (station 9), is a cladoceran which until recently was not found in Manitoba (Patalas et al., 1994). Not detected in the Experimental Lakes Area (ELA) of Northwestern Ontario prior to 1968 (Patalas, 1971), it has recently invaded several lakes within the ELA region (Salki, 1992, 1995) and appears to be spreading westward.

Undoubtedly, *Eubosmina* entered Lake Winnipeg from the Winnipeg River system which drains Precambrian Shield regions similar to the ELA. Whether or not it penetrates the North Basin via the Saskatchewan River or any of the rivers draining the eastern shores of the lake is uncertain. Future tracking of these species in Lake Winnipeg could illuminate "core zooplankton community" resistance to invading species or to environmental modification.

Although samples were lacking from much of the North Basin during the 1994 survey, the 33 stations sampled were sufficient to compare the distribution of most species. Confirmation of many of the 1969 patterns by the 1994 survey supported the conclusion of Patalas and Salki (1992) that physical parameters such as basin morphometry and riverine discharge strongly influence the spatial distribution of zooplankton in Lake Winnipeg. Influence of the Saskatchewan River discharge was clearly discernable in the distribution of *B. longirostris*, *D. minutus*, *D. ashlandi*, and *E. lacustris*. Each of these species displayed lower abundances in the Saskatchewan River plume which spreads across the northern end of the lake to the Nelson River outflow. Similarly, the characteristic low abundance of plankton in the Winnipeg River inflow area was visible in the 1994 survey. Most core species displayed distributions which corresponded relatively closely with those observed in 1969, implying that environmental conditions have not varied beyond their natural range. Only *E. lacustris*, *D. retrocurva*, and *L. kindtii* had different distributions in 1994. These species were centred in the North Basin in 1994 rather than in the South Basin as in 1969. The cause of this reversal is uncertain but may be related to annual differences in weather, food and predation patterns.

Evaluation of zooplankton abundances in the August 1994 survey was complicated by the lack of full seasonal information. Further, comparison of zooplankton abundances in the 1969 and 1994 studies was constrained by asynchronous sampling. The increase in total crustacean abundance observed in the South and North Basins from August 1969 to August 1994, 1.35 and 1.4 - 2.8 x respectively, may be partially attributed to the fact that different periods were sampled in each year. During mid-August 1969, when air temperatures reached a maximum (Patalas and Salki, 1992), zooplankton abundances may have peaked in Lake Winnipeg. However, the lake was not sampled during this period. Differences observed in the regional distribution of highest total abundance, however, could not be explained by sampling variation. In 1969, with South Basin water temperatures warmer than those in the North Basin, South Basin zooplankton abundance was higher during spring and summer (and particularly in early August), but only slightly lower than North Basin levels during fall. On the other hand, in the August 1994 cruise, when water temperatures were similar to those in 1969 and the South Basin was correspondingly warmer than the North, highest abundances of zooplankton (135.0 ind/L) were found in the northern region of the North Basin (NBn). This suggests that zooplankton in the North Basin have continued to increase since 1929 but in the South Basin, where primary production is limited by light (Brunskill, 1973), they may have achieved a plateau. Excess domestic nutrients from the South Basin as well as increased levels of agricultural fertilizers in local runoff may be stimulating primary production in the North Basin. Stainton (personal communication, 1995) observed increased chlorophyll-a levels and a smaller phosphorous deficit in the North Basin in 1994 relative to 1969.

The 1969 Lake Winnipeg study revealed an increase in water transparency in the North Basin from 1.6 m in 1929 to 2.2 m in 1969, very likely as a result of the Grand Rapids Dam-Cedar Lake storage facility completed in 1964. Measurements in August 1994 suggested a further deepening of Secchi transparency in the North Basin. Comparison of 8 stations in region NBn during the August period of both studies revealed mean Secchi depths of 2.0 m (range 1.1 - 3.0 m) and 2.8 m (range 1.7 - 4.0 m) in 1969 and 1994, respectively. In contrast, Secchi depths (z= 0.3 - 1.3 m) at 19 South Basin stations during August 1994 were consistent with those observed during August-September 1969 (Brunskill et al., 1979). Although intensive grazing by zooplankton can clarify a water column (Daborn et al., 1978), the most likely cause for the increase in water transparency in the North Basin may be a shift in phytoplankton taxa from diatom to colonial bluegreen species

(Kling, this volume). This change in algal composition would also explain the increase in chlorophyll-a levels in the North Basin observed by Stainton (personal communication, 1995).

Has water level regulation affected the zooplankton community of Lake Winnipeg? Lake water level readings at Berens River from to 1914 to 1985 (Department of Environment hydrometric data) indicate that implementation of the Jenpeg control structure on the Nelson River in 1976 did not alter the range of natural mean annual lake levels, from 216.4 to 218.2 m above sea level. Even though such water level fluctuations may noticeably affect shoreline exposure, it is unlikely that they would adversely affect the zooplankton community in Lake Winnipeg. However, alteration of the natural periodicity of seasonal water levels by summer storage and winter drawdown may affect ecosystem dynamics in some manner. While these effects may be difficult to measure, they should not be hastily discounted and warrant further consideration.

The August 1994 survey of Lake Winnipeg reinforced the observations by Patalas and Salki (1992) that zooplankton community composition appears to have remained relatively stable since Bajkov's study in 1929 (Bajkov, 1934). Confirmation of the species distribution patterns found in 1969 reaffirmed the important influence of basin morphometry, riverine input and climate on zooplankton dynamics in Lake Winnipeg. The increased abundance of zooplankton in the North Basin provided evidence for progressive cultural enrichment of Lake Winnipeg since 1929.

REFERENCES

Bajkov, A.
1934. The plankton of Lake Winnipeg drainage system; Internationale revue der gesamten hydrobiologie, hydrographisches supplement, v. 31, p. 239-272.

Brunskill, G.J.
1973. Rates of supply of nitrogen and phosphorous to Lake Winnipeg, Manitoba, Canada; Verhandlungen der internationalen vereinligung fur theoretische und angewandte limnologie, v. 18, p. 1755-1759.

Brunskill, G.J., Campbell, P. and Elliot, S.E.M.
1979a. Temperature, oxygen, conductance and dissolved major elements in Lake Winnipeg; Canadian Fisheries and Marine Service Manuscript Report No. 1526, 127 p.

Brunskill, G.J., Schindler, D.W., Elliot, S.E.M. and P. Campbell.
1979b. The attenuation of light in Lake Winnipeg waters; Canadian Fisheries and Marine Service Manuscript Report No. 1522, 79 p.

Brunskill, G.J., Elliot, S.E.M. and Campbell, P.
1980. Morphometry, hydrology, and watershed data pertinent to the limnology of Lake Winnipeg; Canadian Manuscript Report of Fisheries and Aquatic Sciences No.1556, 23 p.

Brunskill, G.J. and Graham, B.W.
1979. The offshore sediments of Lake Winnipeg; Canadian Fisheries and Marine Service Manuscript Report No. 1540, 75 p.

Daborn, G.R., Hayward, J.A. and Quinney, T.E.
1978. Studies on *Daphnia pulex* Leydig in sewage oxidation pond; Canadian Journal of Zoology, v. 56, p. 1392-1401.

Flannagan, J.F., Cobb, D.G. and Flannagan, P.M.
1994. A review of the research on the benthos of Lake Winnipeg; Canadian Manuscript Report of Fisheries and Aquatic Sciences No. 2261, 17 p.

Kenny, B.C.
1979. Lake surface fluctuations and the mass flow through the Narrows of Lake Winnipeg; Journal of Geophysical Research, v. 84, p. 1225-1235.

Patalas, K.
1971. Crustacean plankton communities in forty-five lakes in the Experimental Lakes Area, northwestern Ontario; Journal of the Fisheries Research Board of Canada, v. 28, p. 231-244.

1972. Crustacean plankton and eutrophication of St. Lawrence Great Lakes; Journal of the Fisheries Research Board of Canada, v. 29, p. 1451-1462.

Patalas, K., Patalas, J. and Salki, A.G.
1994. Planktonic crustaceans in lakes of Canada (distribution of species, bibliography); Canadian Technical Report of Fisheries and Aquatic Sciences No. 1954, 218 p.

Patalas, K. and Salki, A.G.
1992. Crustacean plankton in Lake Winnipeg: variation in space and time as a function of lake morphology, geology and climate; Canadian Journal of Fisheries and Aquatic Sciences, v. 49, p. 1035-1059.

Salki, A.G.
1992. Lake variation and climate change study: VII. Crustacean plankton of a lake flushing rate series in the Experimental Lakes Area, Northwestern Ontario, 1987 - 1990; Canadian Data Report of Fisheries and Aquatic Sciences No. 880, 74 p.

1995. Lake variation and climate change study: Crustacean plankton of a lake flushing rate series in the Experimental Lakes Area, Northwestern Ontario, Part 2. 1990 - 1993; Canadian Data Report of Fisheries and Aquatic Sciences (in press).

Salki, A. and Patalas, K.
1992. The crustacean plankton of Lake Winnipeg, June to October, 1969: Canadian Data Report of Fisheries and Aquatic Sciences No. 868, 16 p.

Wier, T.R. and Matthews, G.
1971. Atlas of the prairie provinces; Oxford University Press, 31 p.

	Site:	1	2	3	4	5	6	7	8	9	10	25	28	29	30	31	32	33
a.	*C. sphaericus*	2.0	0.3	3.5	0.0	0.9	0.9	0.3	0.6	1.9	0.3	0	0	0	0	0	0	0
b.	*D. longiremis*	0.7	3.6	0.2	10.3	3.1	5.0	7.3	4.5	4.6	3.1	0	0	0	0	0	0	0
c.	*D. minutus*	4.2	1.0	3.4	2.3	0.7	0.8	0.9	0.8	0.3	2.5	0	0	0	0	0	0	0
d.	*M. edax*	0.7	0.1	0.4	0.6	0.4	0.004	0.4	0.6	0.3	0.001	0.5	0	0	0	0.002	0	0
e.	*B. b. thomasi*	11.1	29.1	25.1	31.6	21.3	18.7	19.6	14.8	24.4	22.9	1.0	0.6	0.4	0.7	0	0.3	0.4
f.	*A. vernalis*	8.0	5.0	5.8	6.4	1.9	7.2	5.5	3.9	4.7	10.9	25.4	15.6	10.6	5.4	3.2	2.1	0.4
g.	*D. ashlandi*	3.5	1.5	5.5	4.5	0.5	2.3	4.0	0.9	2.6	7.3	7.4	8.1	12.3	39.2	30.7	21.7	16.1
h.	*D. retrocurva*	3.3	2.3	0.7	4.5	2.0	0.7	1.8	0.9	3.8	6.2	2.6	1.1	2.6	5.6	1.6	0.3	0.4
i.	*D. g. mendotae*	0	2.6	2.9	0.7	1.4	1.1	2.4	1.2	1.2	2.8	7.7	10.6	3.9	1.3	1.7	0.9	1.8
j.	*E. lacustris*	0.20	0.02	0.05	1.6	0.3	0.06	1.9	0.03	0.05	0.6	0.3	0.2	0.1	0.5	0.3	0.06	0.2
k.	*E. nevadensis*	0.05	0.3	0.7	0.2	0	0.03	0.4	0.01	0.003	0.04	0.18	0.07	0.13	0.06	0.04	0.16	0.29
l.	*L. kindtii*	0	0	0	0.84	0.03	0	0	0.003	0.0	0.004	0	0	0.004	0	0.003	0.003	0
m.	*D. siciloides*	0	0	0	0.34	0.31	0	0	0	0	0	0	0	0	0	0	0	0
n.	*B. longirostris*	13.9	2.9	13.8	4.1	2.8	0.9	9.5	20.3	30.6	45.9	2.0	5.8	3.0	2.2	1.3	0.5	0.4

	Site:	34	35	36	37	38	39	40	41	42	43	44	45	46	47	49	50
a.	*C. sphaericus*	0	0	0	0	0	0	0	0	0	0	0	0	0	0	0	0
b.	*D. longiremis*	0	0	0	0	0	0	0	0	0	0	0	0	0	0	0	0
c.	*D. minutus*	0	0	0	0	0	0	0	0	0	0	0	0	0	0	0	0
d.	*M. edax*	0	0	0.23	0	0.01	0	0	0	0	0	0	0	0	0	0	0
e.	*B. b. thomasi*	0.4	0.1	0	0.1	0	0	0	0.4	0.1	0	3.9	0	0.4	0	0	0
f.	*A. vernalis*	1.2	0.5	1.9	0.9	3.8	0.1	0.7	1.8	7.2	4.8	9.2	0.9	3.4	9.7	24.9	23.8
g.	*D. ashlandi*	18.3	17.3	18.5	18.4	13.0	0.03	0	29.1	25.0	21.6	11.8	25.0	6.4	16.1	27.7	22.7
h.	*D. retrocurva*	3.2	0.9	4.2	0.9	7.8	0.2	0.7	1.3	2.4	0.6	0.5	0.7	0.8	2.8	0.6	1.5
i.	*D. g. mendotae*	2.8	3.3	6.9	4.9	0.6	0.003	0.0	10.4	17.3	6.2	7.1	1.2	5.2	6.4	30.4	5.6
j.	*E. lacustris*	1.0	0.4	0.3	0.6	0.2	0.009	0.04	0.3	0.1	0.1	0.01	0.005	0.07	0.05	0.08	0.003
k.	*E. nevadensis*	0.12	0.47	0.36	0.27	0.09	0.003	0.005	0.4	0.15	0.13	0.03	0.009	0.07	0.02	0.32	0.02
l.	*L. kindtii*	0.002	0.001	0	0	0.003	0.009	0	0	0	0.003	0	0.002	0.002	0	0	0
m.	*D. siciloides*	0	0	0	0	0	0	0	0	0	0	0	0	0	0	0	0.31
n.	*B. longirostris*	1.9	1.7	1.4	2.2	3.0	0.7	0.5	3.0	3.9	3.4	6.2	4.4	1.2	1.2	1.7	0.7

Table 1. Crustacean plankton abundance at each site (individuals per litre).

LAKE REGION	SOUTH BASIN									NORTH BASIN								
AUGUST 1994/1969	R	R		SB	SB		W	W		N	N		NBn	NBn		S	S	
SPECIES	MEAN IND/L	MEAN IND/L	RATIO 94/69	MEAN IND/L	MEAN IND/L	RATIO 94/69	MEAN IND/L	MEAN IND/L	RATIO 94/69	MEAN IND/L	MEAN IND/L	RATIO 94/69	MEAN IND/L	MEAN IND/L	RATIO 94/69	MEAN IND/L	MEAN IND/L	RATIO 94/69
H. septentrionales													0.02					
L. macrurus	0.01	0.00		0.01	0.07	0.19	0.00	0.00		0.06	0.04	1.53	0.02	0.04	0.51	0.00	0.00	
E. lacustris	0.15	0.69	0.22	1.02	1.85	0.55	0.25	0.42	0.61	0.98	1.18	0.83	0.87	0.12	7.44	0.73	0.02	48.65
E. nevadensis	0.42	3.55	0.12	0.73	2.69	0.27	0.05	0.69	0.07	0.42	0.87	0.48	0.19	0.02	8.60	0.18	0.03	6.08
D. ashlandi	22.10	27.88	0.79	19.49	15.11	1.29	0.01	0.44	0.03	16.77	11.11	1.51	3.25	5.01	0.65	3.45	1.74	1.98
D. oregonensis	1.01	1.60	0.63	2.31	1.10	2.11	0.82	0.44	1.88	0.22	0.18	1.23	0.43	0.94	0.46	1.09	1.32	0.83
D. siciloides	0.10	2.20	0.05	0.00	0.34	0.00	0.00	0.00		0.00	0.00		0.07	0.17	0.44	0.00	0.77	0.00
D. sicilis	0.37	0.00		0.00	0.00		0.00	0.00		0.00	0.00		0.24	0.07	3.59	0.66	0.00	
D. minutus		0.00			0.00			0.00			0.00		1.42	0.62	2.27	4.16	0.56	7.50
Calanoida nauplii	49.25	31.91	1.54	32.73	19.81	1.65	6.05	5.11	1.18	23.07	11.17	2.07	14.17	8.19	1.73	23.11	2.54	9.10
D. c. bicuspidatus	0.00	0.41	0.00	0.43	1.17	0.36	0.00	0.00	0.00	0.69	1.27	0.54	23.05	23.53	0.98	11.07	29.11	0.38
A. vernalis	19.48	5.68	3.43	2.96	3.87	0.76	0.38	0.03	11.64	14.25	2.17	6.57	5.71	4.72	1.21	8.03	4.92	1.63
M. edax	0.00	0.00		0.02	0.00	32.64	0.00	0.00		0.13	0.00		0.30	0.00		0.67	0.00	
E. agilis	0.00	0.00		0.00	0.00		0.00	0.00	0.00	0.00	0.00		0.00	0.00		0.00	0.00	
Cyclopidae nauplii	9.92	8.99	1.10	11.52	9.07	1.27	2.63	0.60	4.37	45.56	10.10	4.51	60.32	27.03	2.23	38.96	28.98	1.34
D. retrocurva	1.62	2.82	0.57	1.82	2.19	0.83	0.45	0.38	1.19	2.95	1.61	1.83	2.53	0.99	2.56	3.30	1.97	1.68
D. g. mendotae	14.12	1.99	7.10	5.01	1.24	4.04	0.00	0.01	0.15	5.89	0.37	15.88	1.82	0.86	2.10	0.00	1.26	0.00
D. longiremis	0.00	0.00		0.00	0.00		0.00	0.00		0.00	0.00		4.61	0.78	5.94	0.66	0.80	0.83
C. quadrangula	0.00	0.00		0.00	0.00		0.00	0.00	0.00	0.00	0.00		0.03	0.00		0.00	0.00	
B. longirostris	1.17	0.48	2.43	2.46	1.15	2.13	0.64	0.19	3.33	3.27	0.86	3.79	14.55	4.36	3.34	13.87	1.87	7.42
C. sphaericus	0.00	0.00		0.00	0.00		0.00	0.00		0.00	0.00		0.98	0.56	1.76	1.98	2.85	0.70
H. gibberum	0.00	0.00		0.00	0.00		0.00	0.00	0.00	0.00	0.00		0.01	0.00		0.00	0.00	
D. leuchtenbergianum	3.07	1.57	1.96	1.40	1.17	1.19	0.02	0.05	0.40	1.08	0.87	1.24	0.21	0.51	0.40	1.32	0.57	2.34
L. kindtii	0.00	0.07	0.00	0.00	0.04	0.03	0.00	0.02	0.30	0.00	0.04	0.03	0.13	0.03	4.53	0.05	0.01	5.04
L. setifera	0.00	0.00		0.00	0.00		0.00	0.00		0.00	0.00		0.00	0.00		0.00	0.00	
D. pulex		0.08	0.00		0.00			0.00			0.00			0.00			0.00	
L. quadrangularis		0.00			0.00			0.02	0.00		0.00			0.00			0.00	
E. longispina	0.00			0.00			0.15			0.00			0.03			0.00		
C. quadrangula	0.00			0.03			0.00			0.00			0.00			0.00		
TOTAL CYCLOPOIDA	29.39	15.09	1.95	14.93	14.11	1.06	3.01	0.64	4.70	60.62	13.54	4.48	89.37	55.28	1.62	58.73	63.01	0.93
TOTAL CALANOIDA	73.42	67.83	1.08	56.29	40.97	1.37	7.19	7.10	1.01	41.52	24.55	1.69	20.69	15.19	1.36	33.40	6.97	4.80
TOTAL CLADOCERA	19.98	7.00	2.85	10.72	5.79	1.85	1.27	0.67	1.89	13.19	3.75	3.52	24.90	8.09	3.08	21.18	9.32	2.27
TOTAL CRUSTACEA	122.79	89.91	1.37	81.94	60.80	1.35	11.47	8.41	1.36	115.34	41.83	2.76	135.00	78.56	1.72	113.31	79.30	1.43

Table 2. Crustacean plankton composition and mean abundance (individuals per litre) in six regions of Lake Winnipeg in August 1994 and 1969 and the 1994/1969 ratio.

SPECIES	AUG 1969 MEAN S	MEAN N	SPECIES	AUG 1994 MEAN S	MEAN N
D. sicilis	0.00	0.02	*D. sicilis*	0.12	0.30
D. minutus	0.00	0.39	*D. minutus*		2.79
D. longiremis	0.00	0.53	*D. longiremis*	0.00	1.76
C. sphaericus	0.00	1.13	*C. sphaericus*	0.00	0.99
L. macrurus	0.02	0.03	*L. macrurus*	0.01	0.03
E. lacustris	0.99	0.44	*E. lacustris*	0.47	0.86
E. nevadensis	2.31	0.31	*E. nevadensis*	0.40	0.26
D. ashlandi	14.48	5.95	*D. ashlandi*	13.87	7.82
D. oregonensis	1.04	0.81	*D. oregonensis*	1.38	0.58
D. siciloides	0.84	0.31	*D. siciloides*	0.03	0.02
Calanoida nauplii	18.95	7.30	Calanoida nauplii	29.34	20.12
D. c. bicuspidatus	0.53	17.97	*D. c. bicuspidatus*	0.14	11.60
A. vernalis	3.19	3.94	*A. vernalis*	7.60	9.33
Cyclopidae nauplii	6.22	22.04	Cyclopidae nauplii	8.02	48.28
D. retrocurva	1.80	1.52	*D. retrocurva*	1.30	2.93
D. g. mendotae	1.08	0.83	*D. g. mendotae*	6.38	2.57
B. longirostris	0.61	2.36	*B. longirostris*	1.42	10.56
D. leuchtenbergianum	0.93	0.65	*D. leuchtenbergianum*	1.50	0.87
L. kindtii	0.04	0.02	*L. kindtii*	0.0019	0.06
M. edax	0.0002	0.00	*M. edax*	0.01	0.36
E. agilis	0.0008	0.00	*E. agilis*	0.00	0.0004
C. quadrangula	0.0008	0.00	*C. quadrangula*	0.0001	0.01
H. gibberum	0.0008	0.00	*H. gibberum*	0.0000	0.0040
L. setifera	0.00	0.00	*L. setifera*	0.0001	0.00
D. pulex	0.03	0.00			
L. quadrangularis	0.01	0.00			
			H. septentrionales		0.02
			E. longispina	0.05	0.01
			C. lacustris	0.01	0.00

Table 3. Mean abundance of cyclopoid, calanoid, and cladoceran zooplankton in the six regions of Lake Winnipeg in 1969 and 1994. Letters R, S, W, N, NB, and S refer to regions of the lake as shown in Figure 1.

AUGUST SPECIES	1969 N/S	1994 N/S
H. septentrionales		
L. macrurus	1.10	4.42
E. lacustris	0.44	1.81
E. nevadensis	0.13	0.66
D. ashlandi	0.41	0.56
D. oregonensis	0.78	0.42
D. siciloides	0.37	0.69
D. sicilis		2.45
D. minutus		
Calanoida nauplii	0.39	0.69
D. c. bicuspidatus	33.99	81.84
A. vernalis	1.23	1.23
M. edax		46.94
E. agilis		
Cyclopidae nauplii	3.54	6.02
D. retrocurva	0.85	2.26
D. g. mendotae	0.77	0.40
D. longiremis		
C. quadrangula		87.16
B. longirostris	3.88	7.43
C. sphaericus		
H. gibberum		
D. leuchtenbergianum	0.70	0.58
L. kindtii	0.61	31.16
L. setifera		
E. longispina		0.23
C. quadrangula		
TOTAL CYCLOPOIDA	4.42	4.41
TOTAL CALANOIDA	0.40	0.70
TOTAL CLADOCERA	1.57	1.85
TOTAL CRUSTACEA	1.25	1.68

Table 4. Ratio of mean abundance in North and South Basins, August 1969 and 1994.

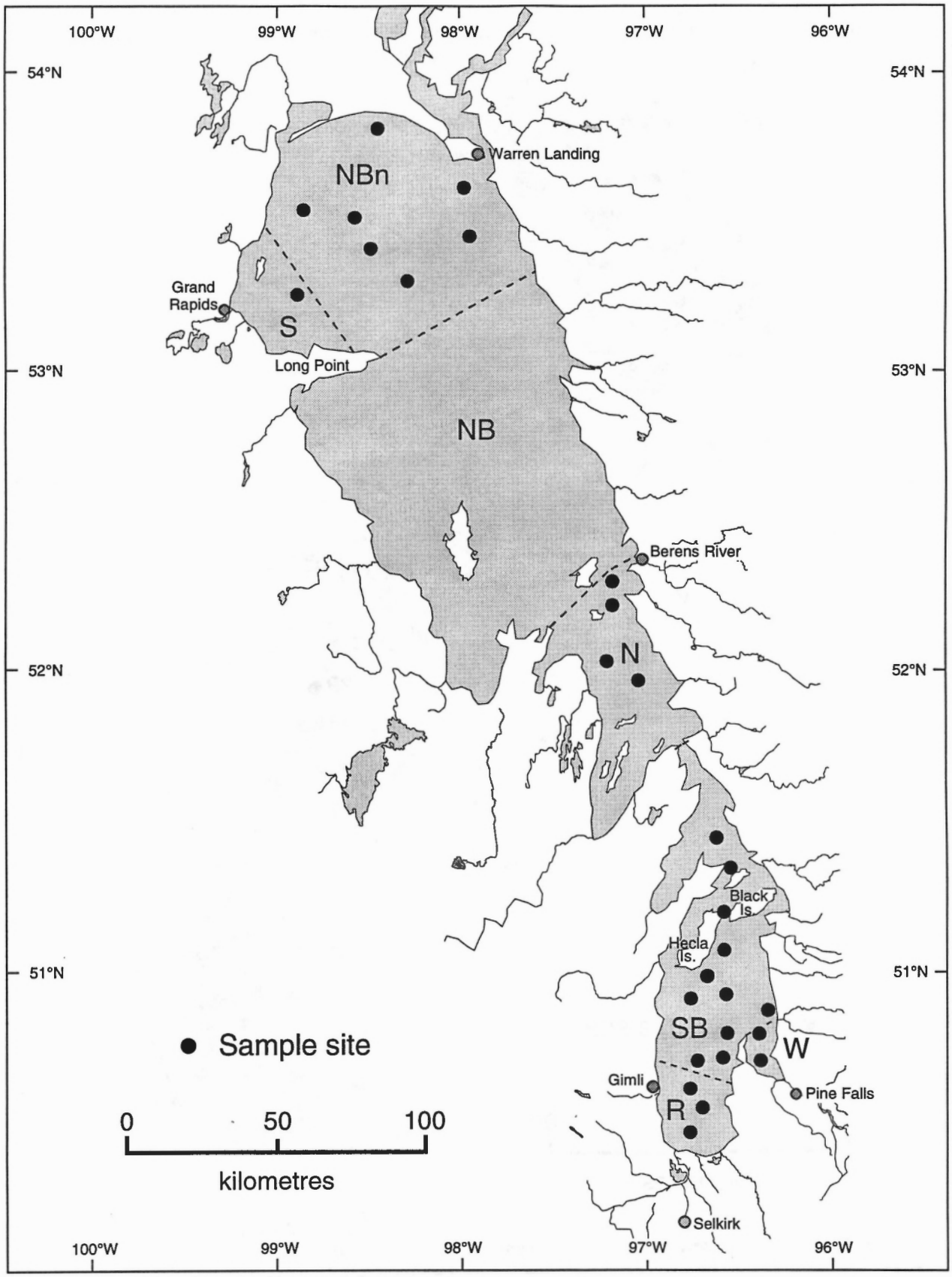

Figure 1a. Location of 1969 sampling stations used for comparison to the 1994 survey. Regions of Lake Winnipeg defined as R, Red River inflow; W, Winnipeg River inflow; SB, main part of South Basin; N, The Narrows; NBn, northern part of North Basin; S, Saskatchewan River inflow.

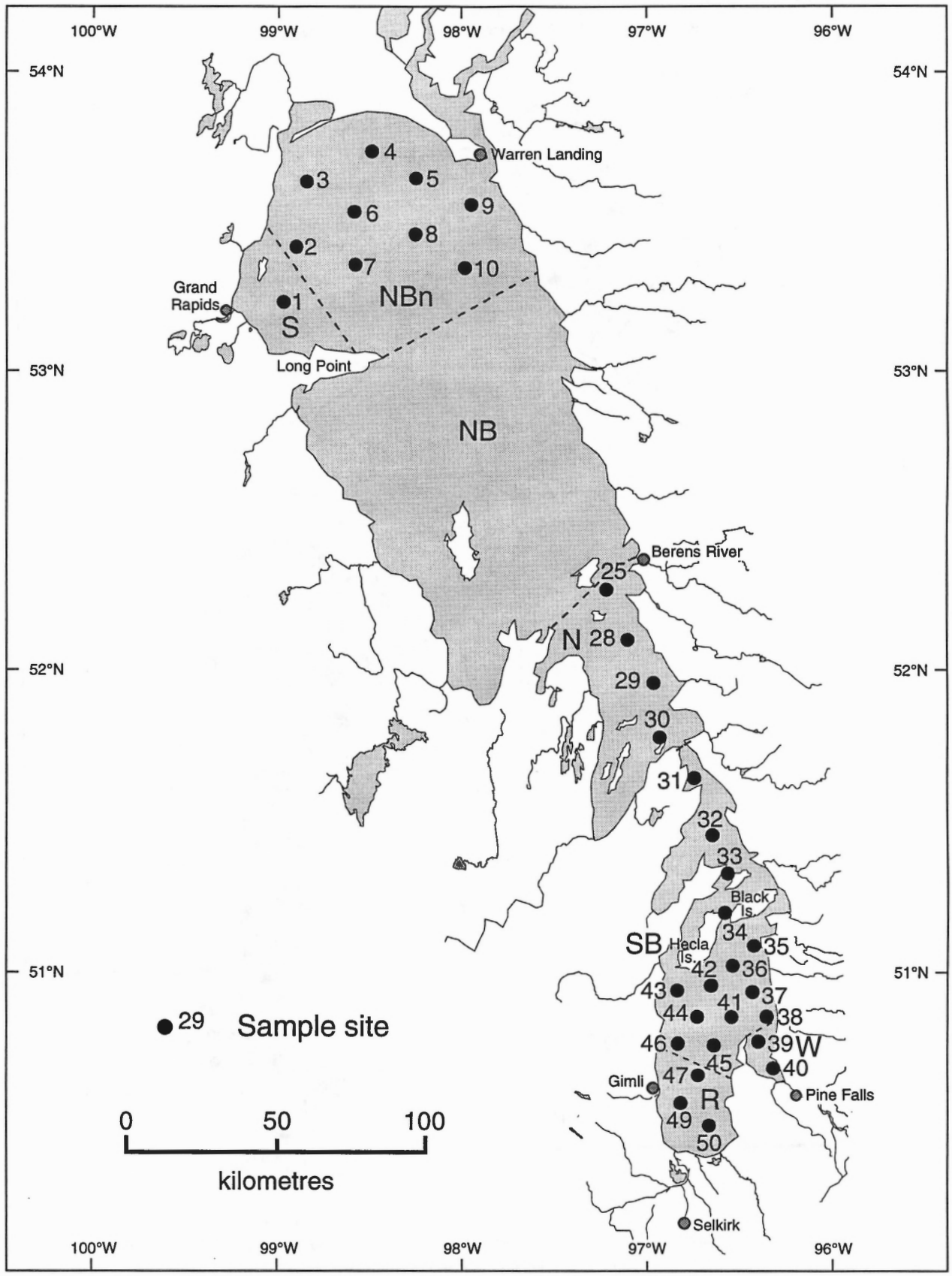

Figure 1b. Location of 1994 sampling stations. Regions defined as in Figure 1a.

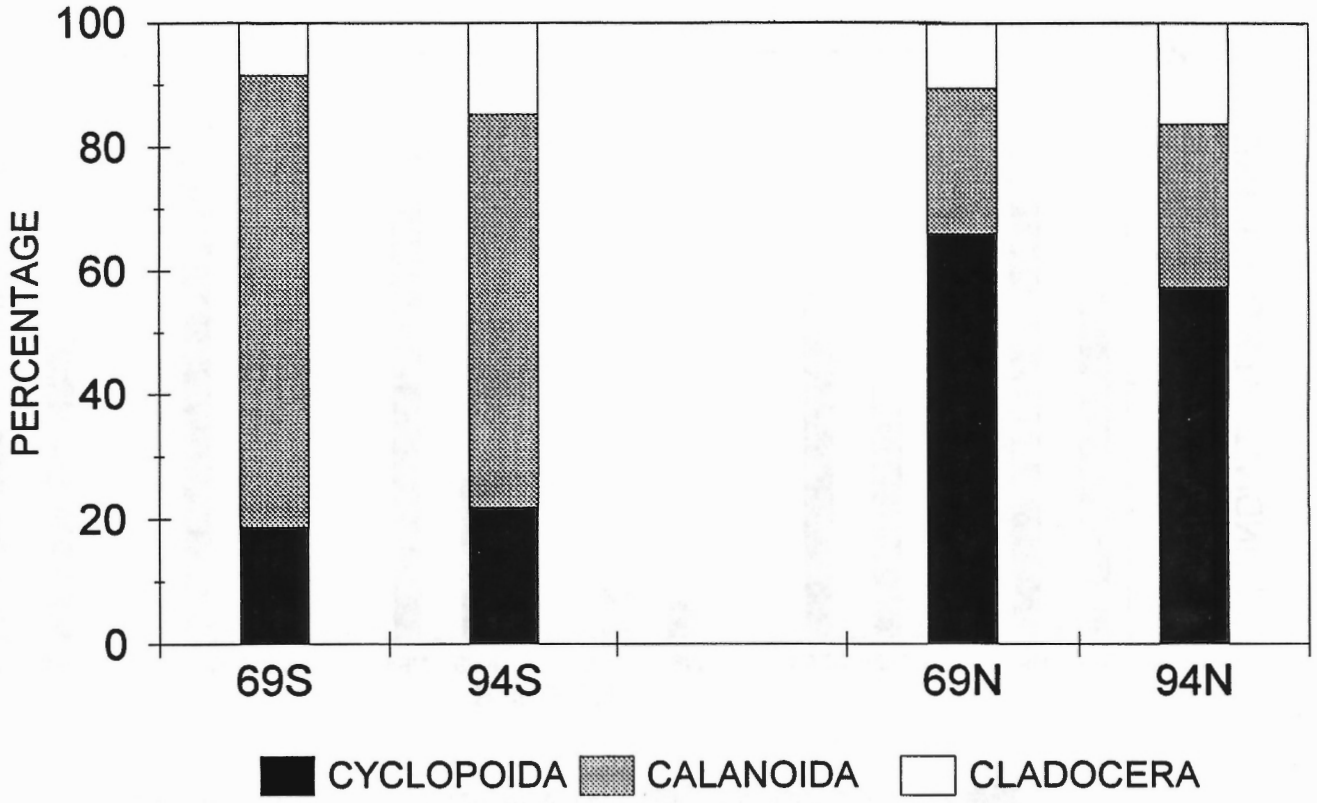

Figure 2. Mean percentage of cyclopoid, calanoid, and cladoceran abundance in the zooplankton community from the South and North Basins of Lake Winnipeg during 1969 and 1994.

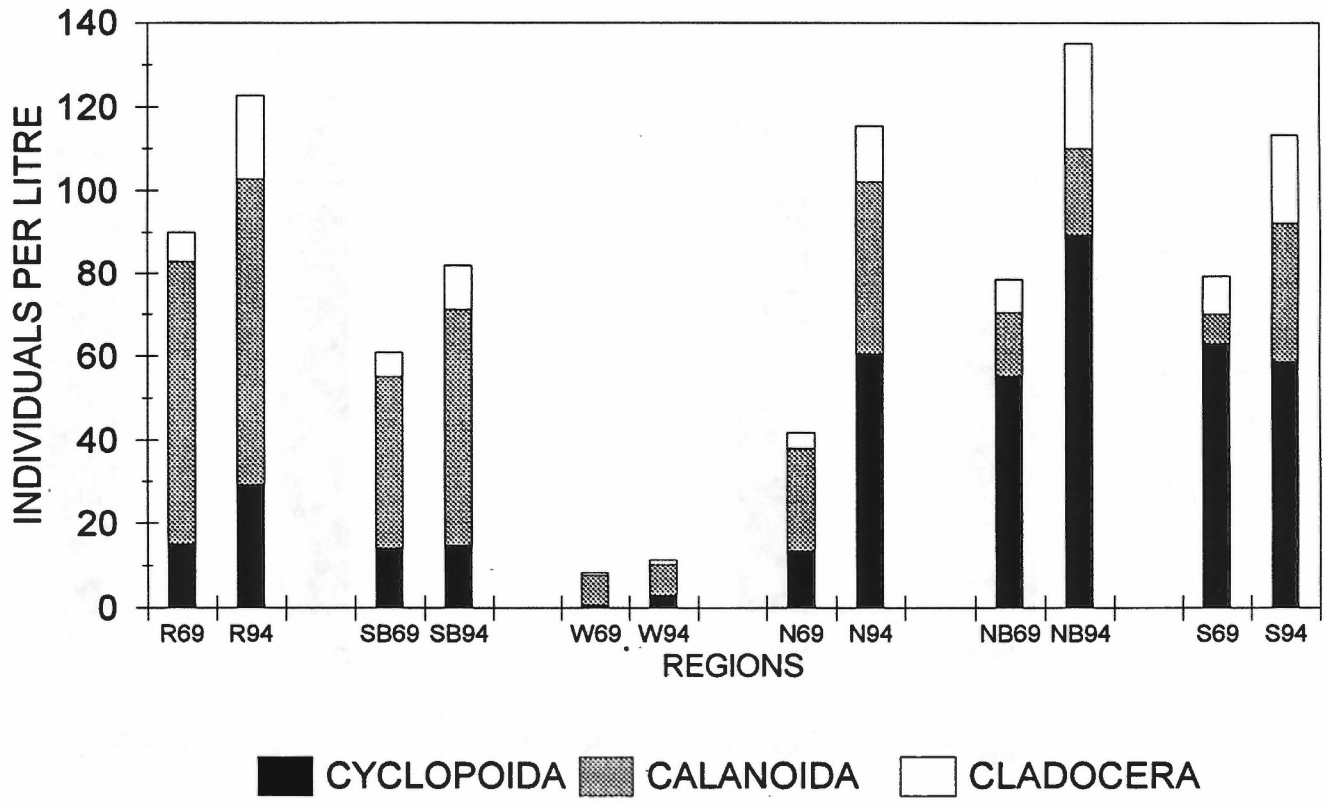

Figure 3. Mean abundance of cyclopoid, calanoid, and cladoceran zooplankton in the six regions of Lake Winnipeg in 1969 and 1994. Letters R, S, W, N, NB, and S refer to regions of the lake as shown in Figure 1.

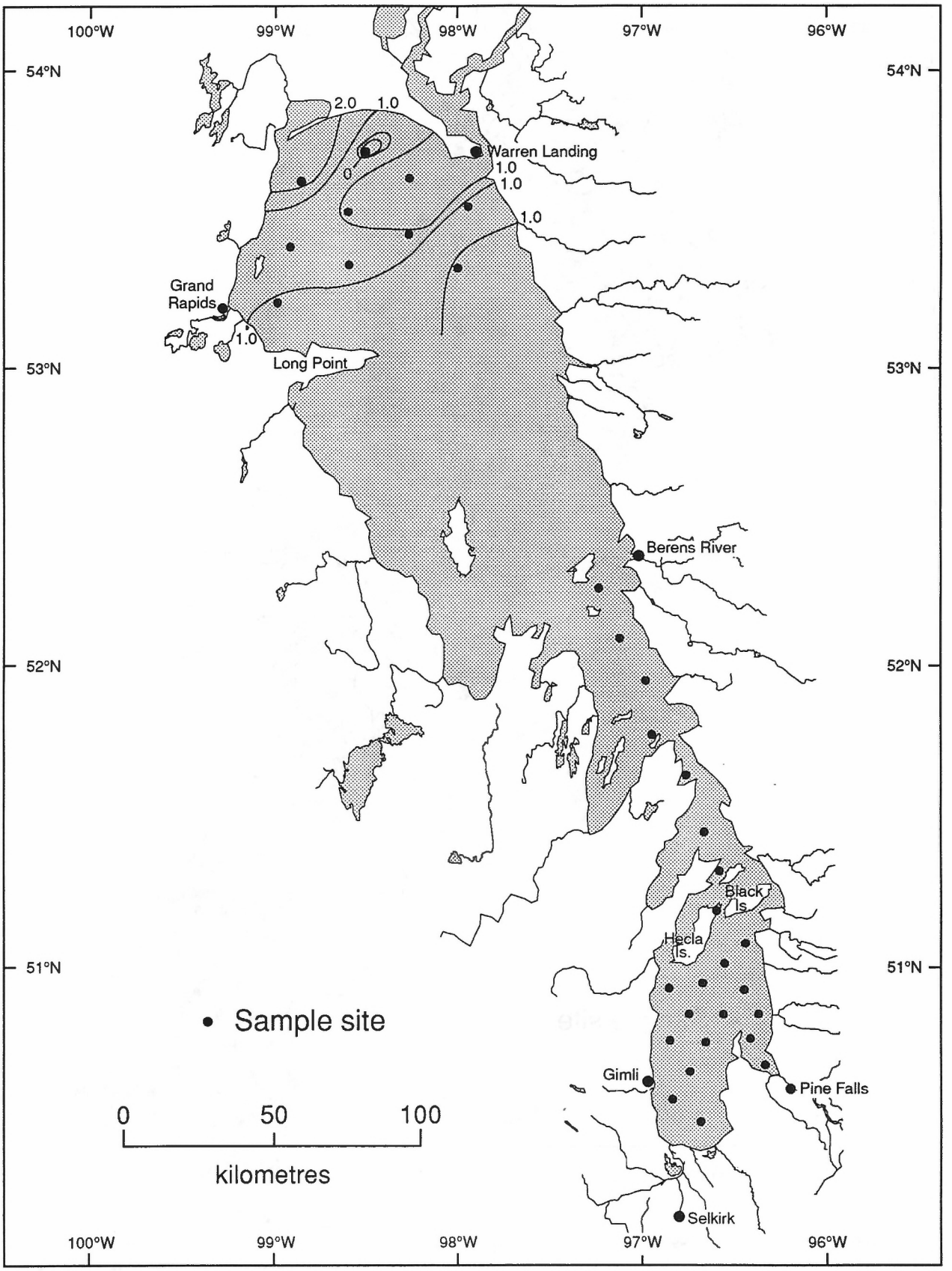

Figure 4a. Spatial distribution of total numbers (individuals per litre) of *Chydorus sphaericus* in Lake Winnipeg, August, 1994.

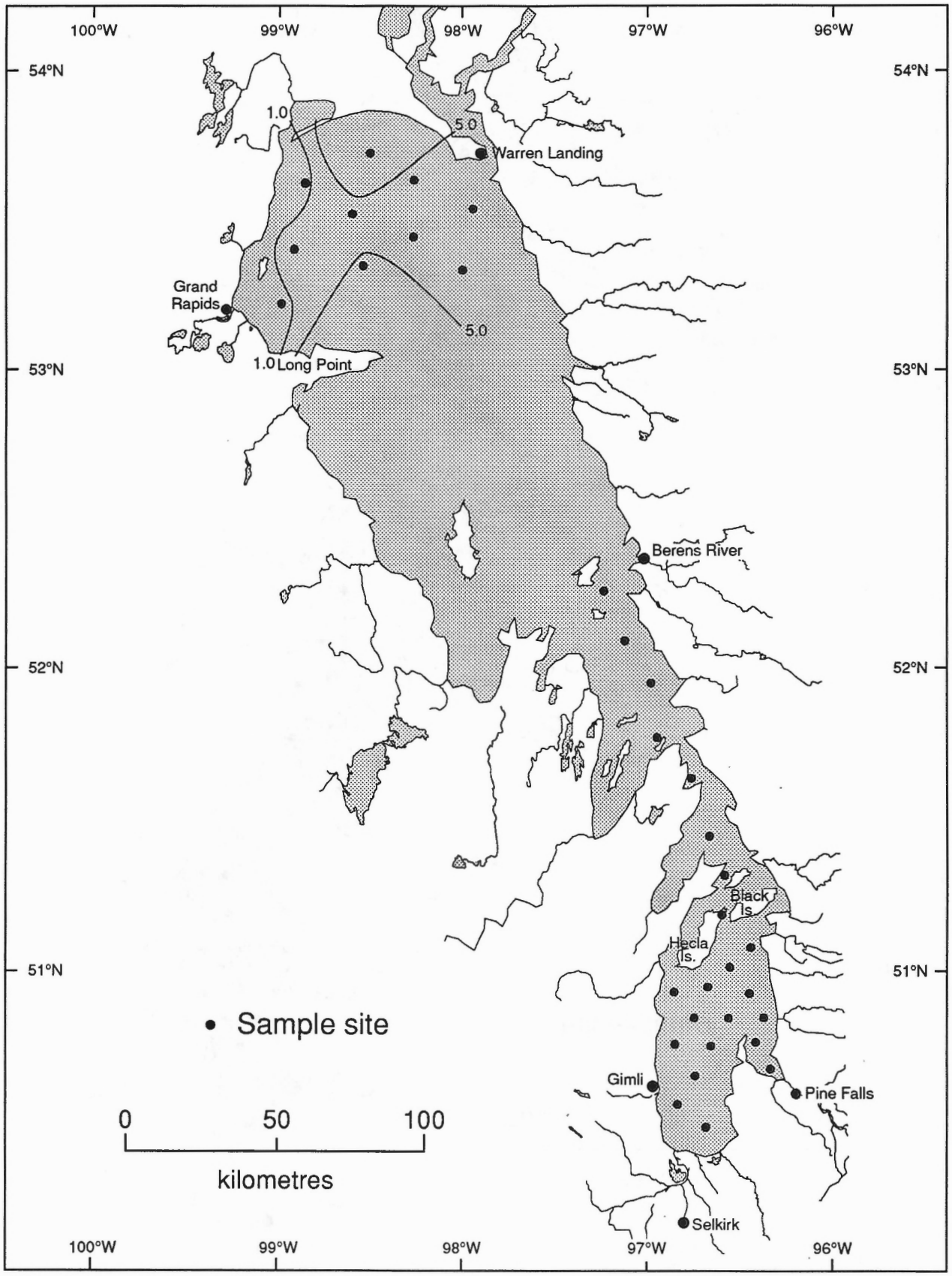

Figure 4b. Spatial distribution of total numbers (individuals per litre) of *Daphnia longiremis* in Lake Winnipeg, August, 1994.

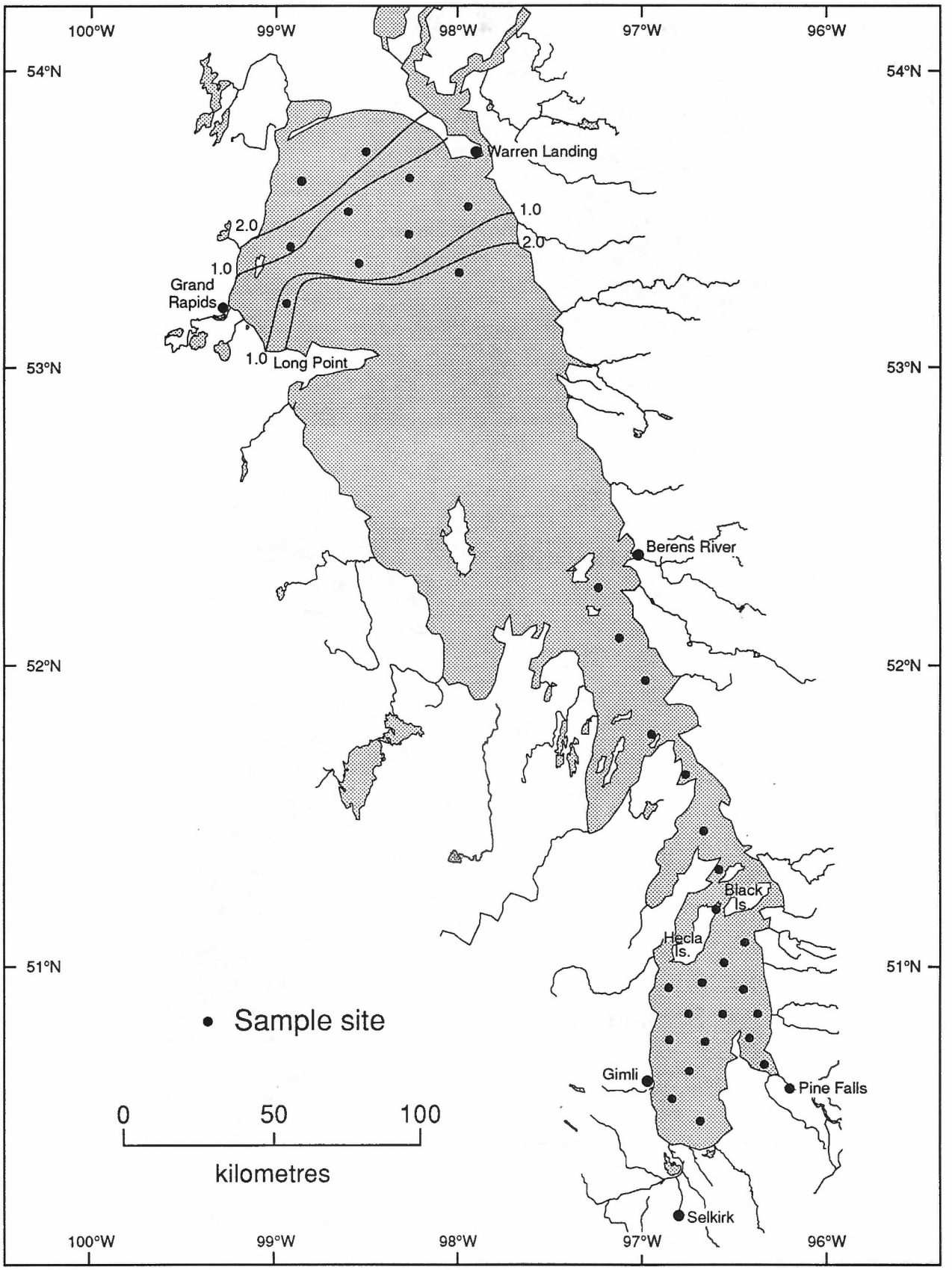

Figure 4c. Spatial distribution of total numbers (individuals per litre) of *Diaptomus minutus* in Lake Winnipeg, August, 1994.

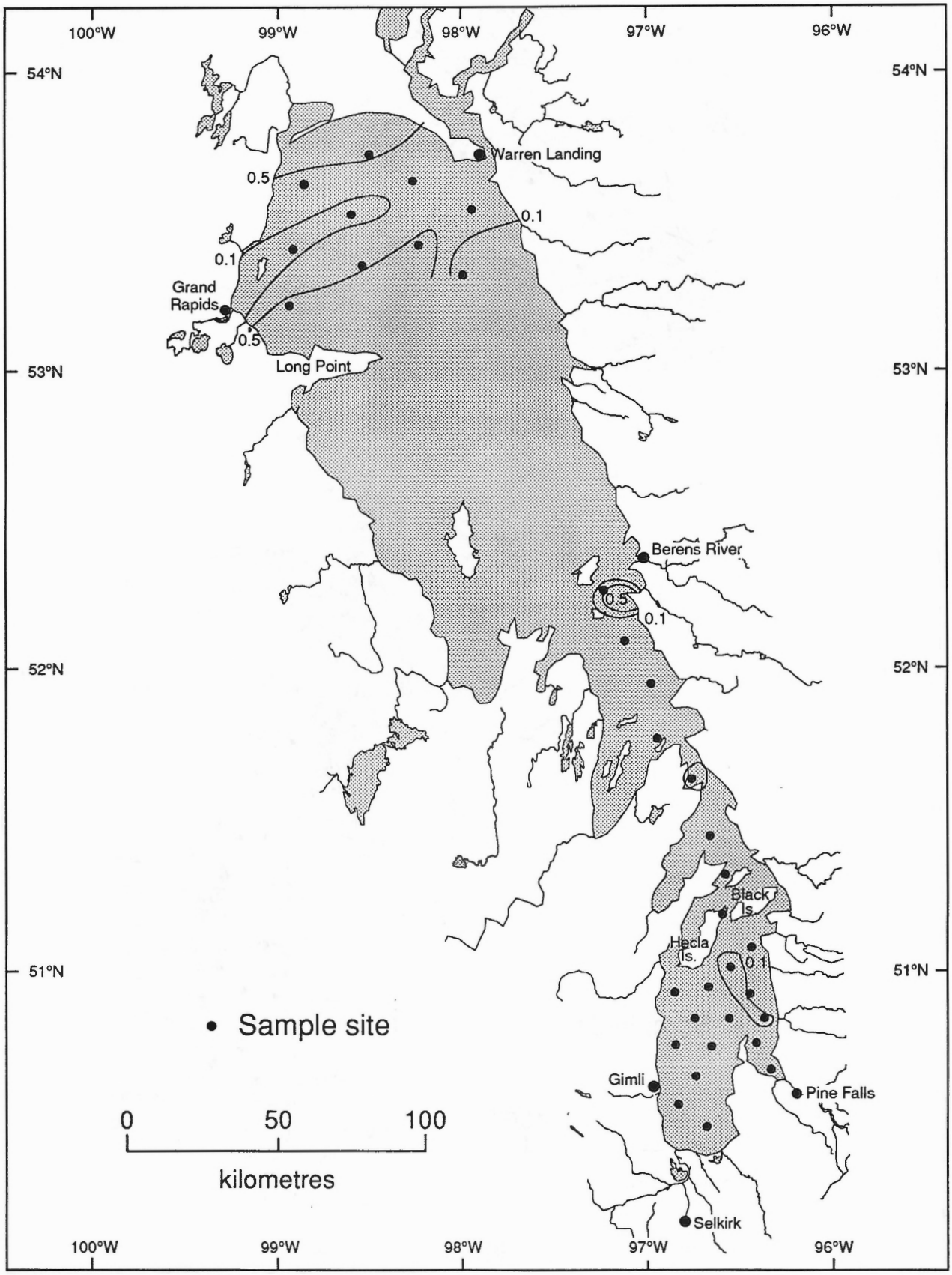

Figure 4d. Spatial distribution of total numbers (individuals per litre) of *Mesocyclops edax* in Lake Winnipeg, August, 1994.

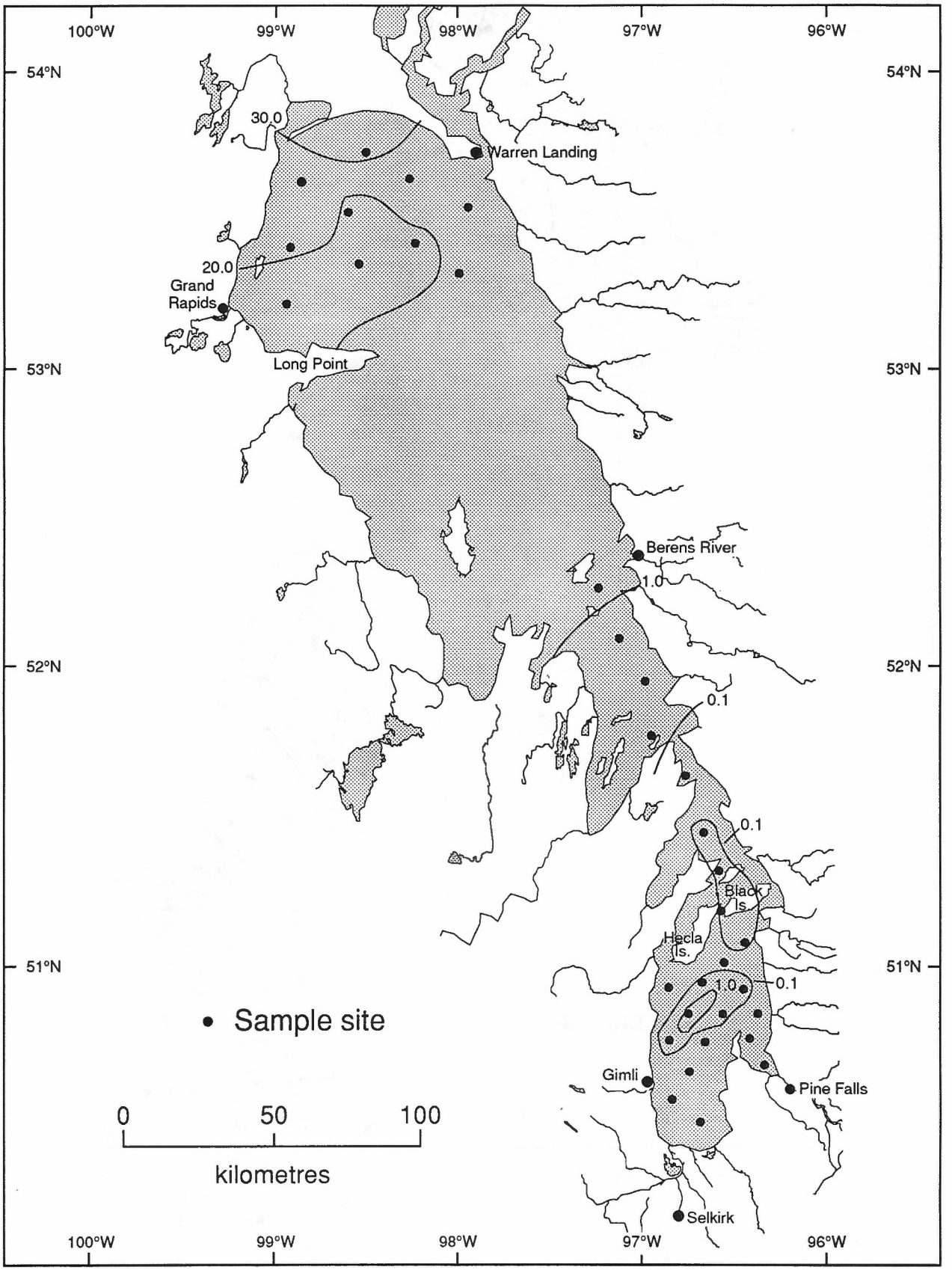

Figure 4e. Spatial distribution of total numbers (individuals per litre) of *Diacyclops bicuspidatus thomasi* in Lake Winnipeg, August, 1994.

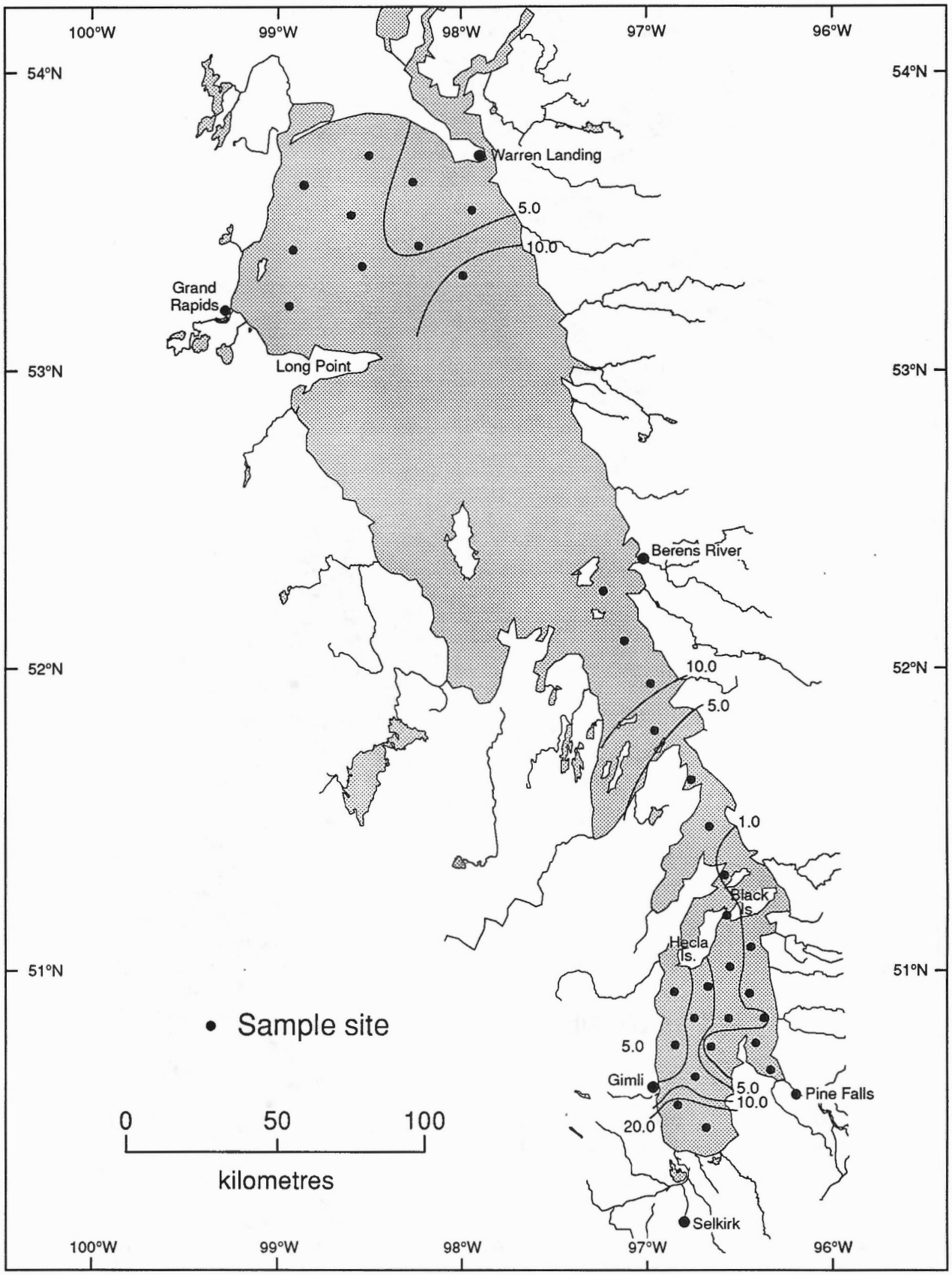

Figure 4f. Spatial distribution of total numbers (individuals per litre) of *Acanthocyclops vernalis* in Lake Winnipeg, August, 1994.

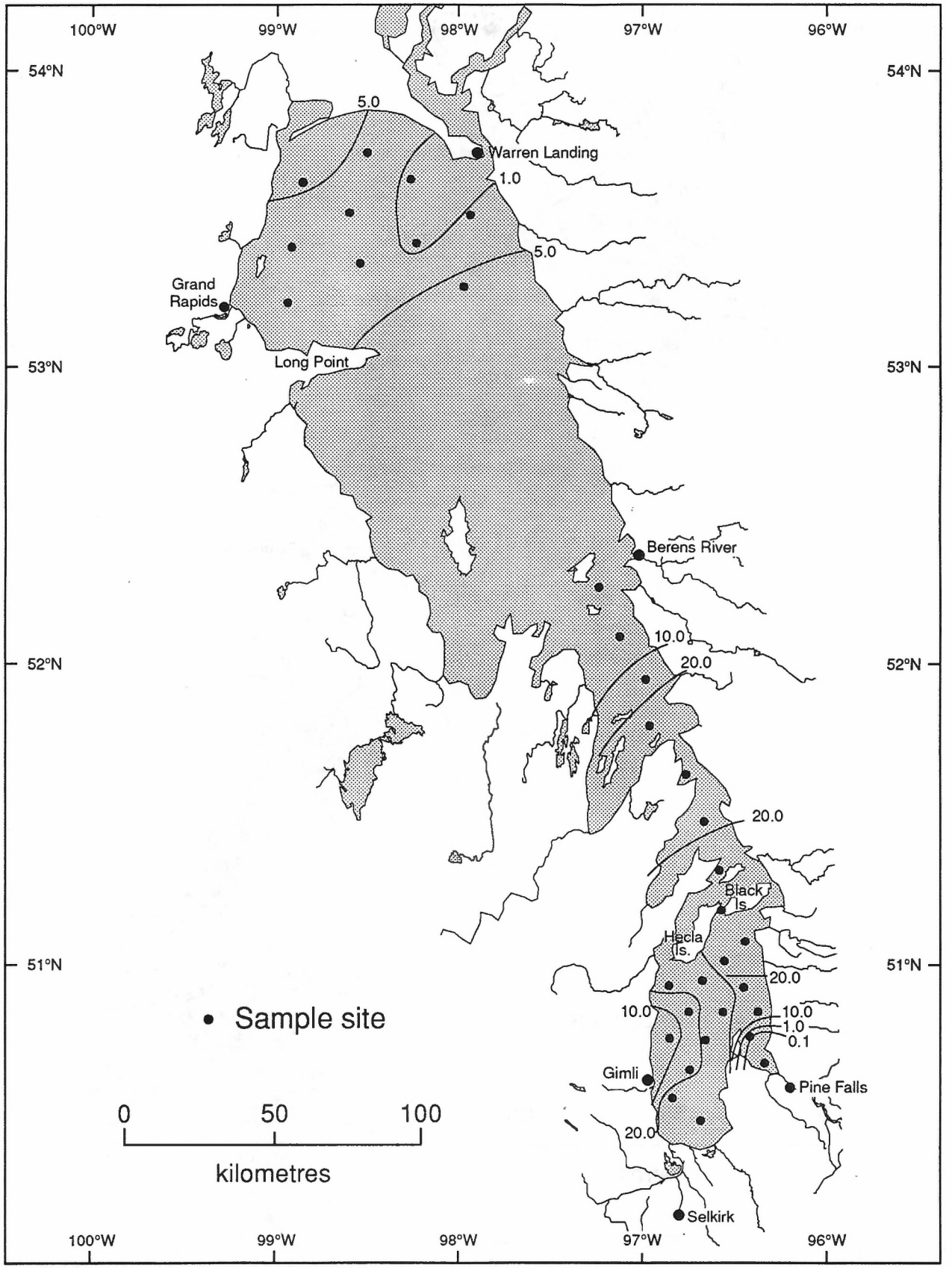

Figure 4g. Spatial distribution of total numbers (individuals per litre) of *Diaptomus ashlandi* in Lake Winnipeg, August, 1994.

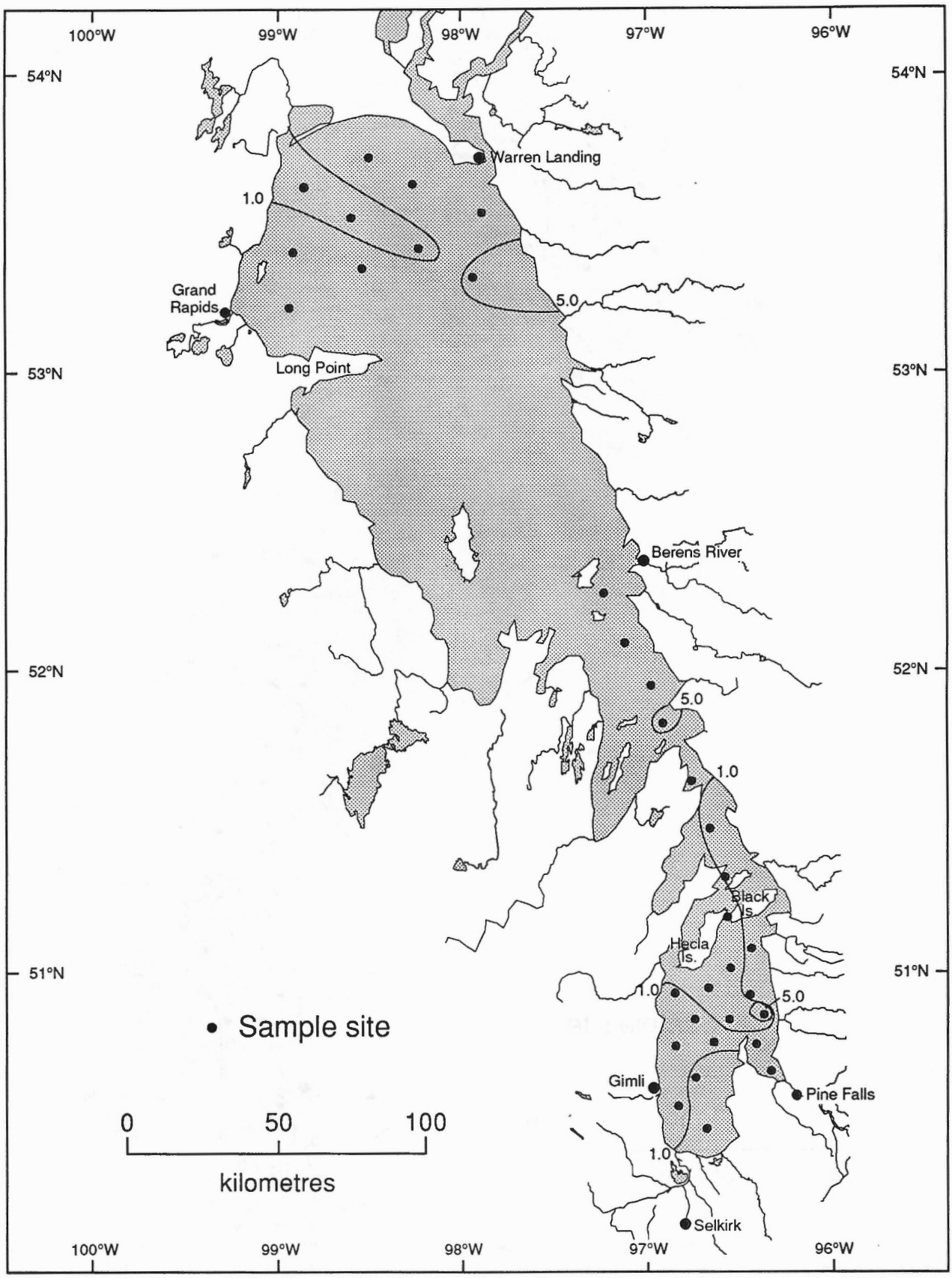

Figure 4h. Spatial distribution of total numbers (individuals per litre) of *Daphnia retrocurva* in Lake Winnipeg, August, 1994.

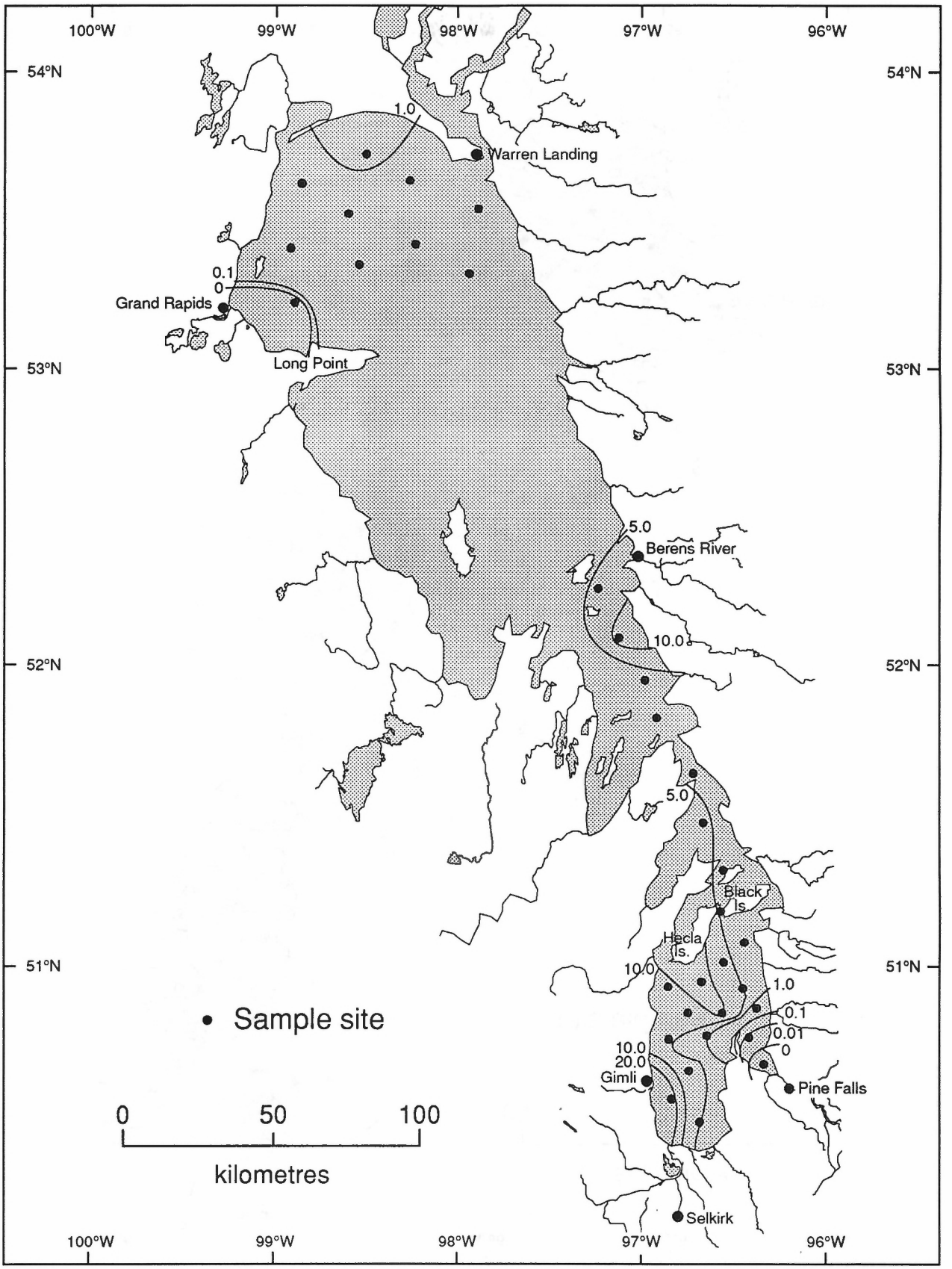

Figure 4i. Spatial distribution of total numbers (individuals per litre) of *Daphnia galeata mendotae* in Lake Winnipeg, August, 1994.

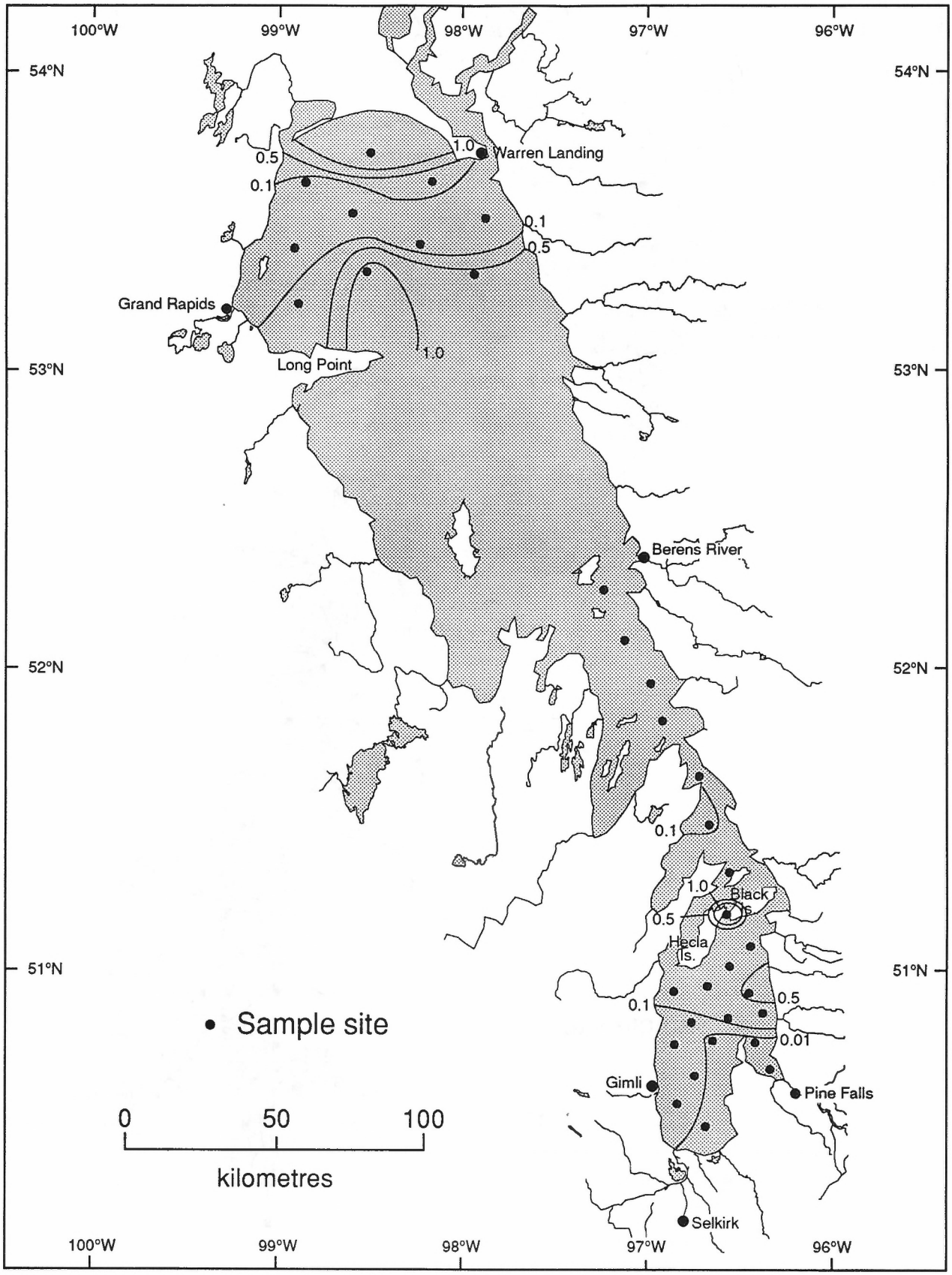

Figure 4j. Spatial distribution of total numbers (individuals per litre) of *Epischura lacustris* in Lake Winnipeg, August, 1994.

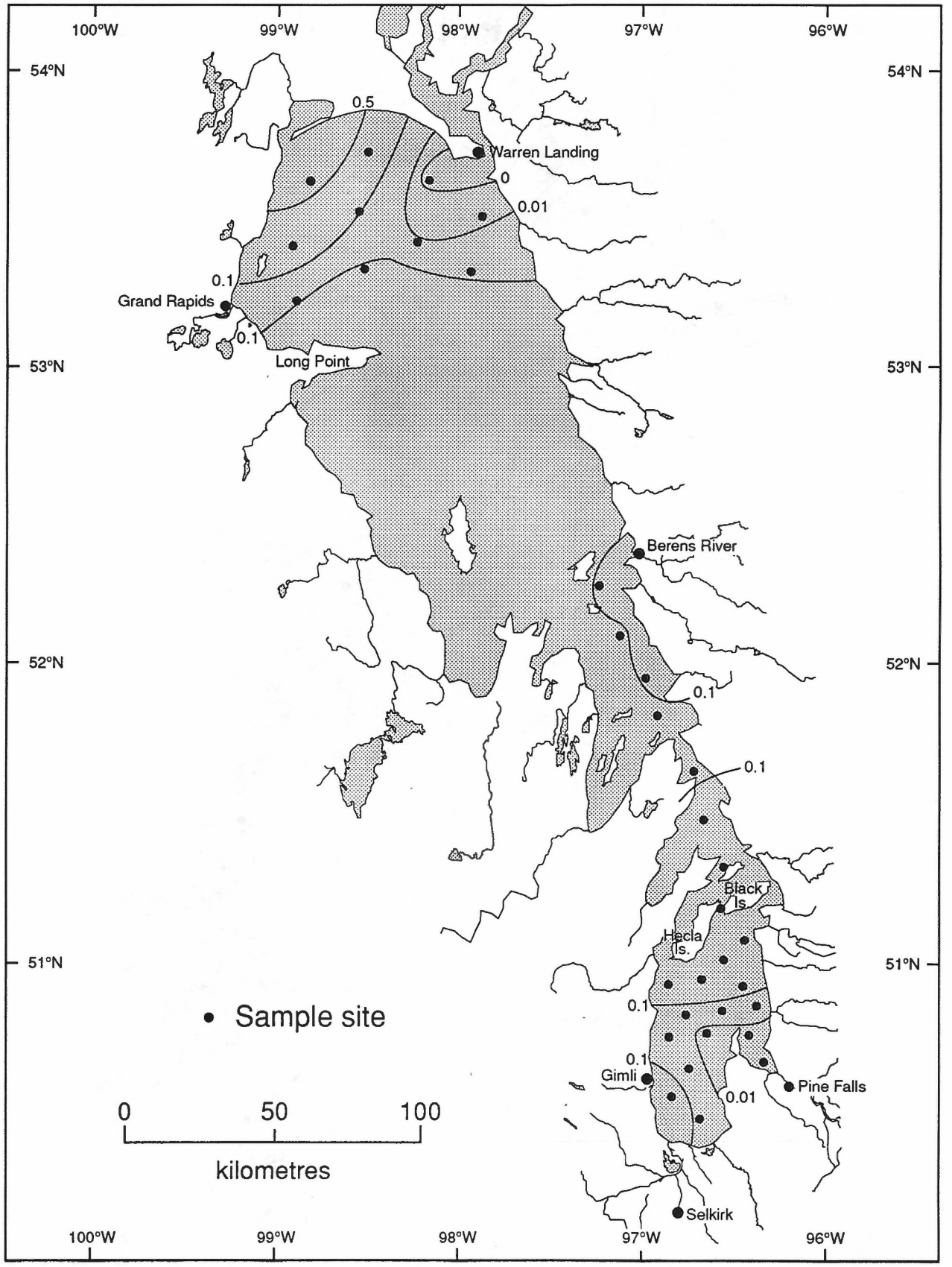

Figure 4k. Spatial distribution of total numbers (individuals per litre) of *Epischura nevadensis* in Lake Winnipeg, August, 1994.

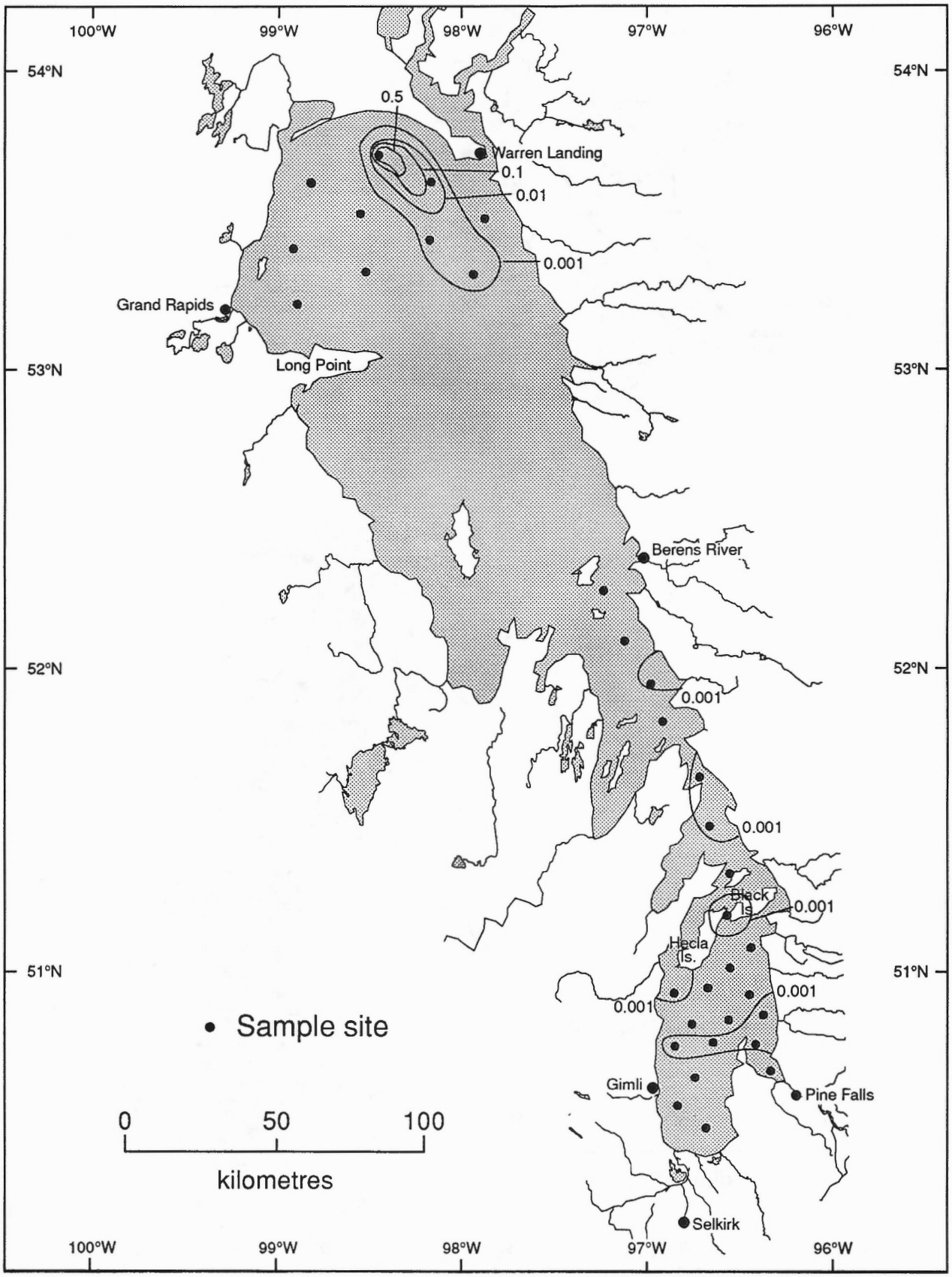

Figure 4l. Spatial distribution of total numbers (individuals per litre) of *Leptodora kindtii* in Lake Winnipeg, August, 1994.

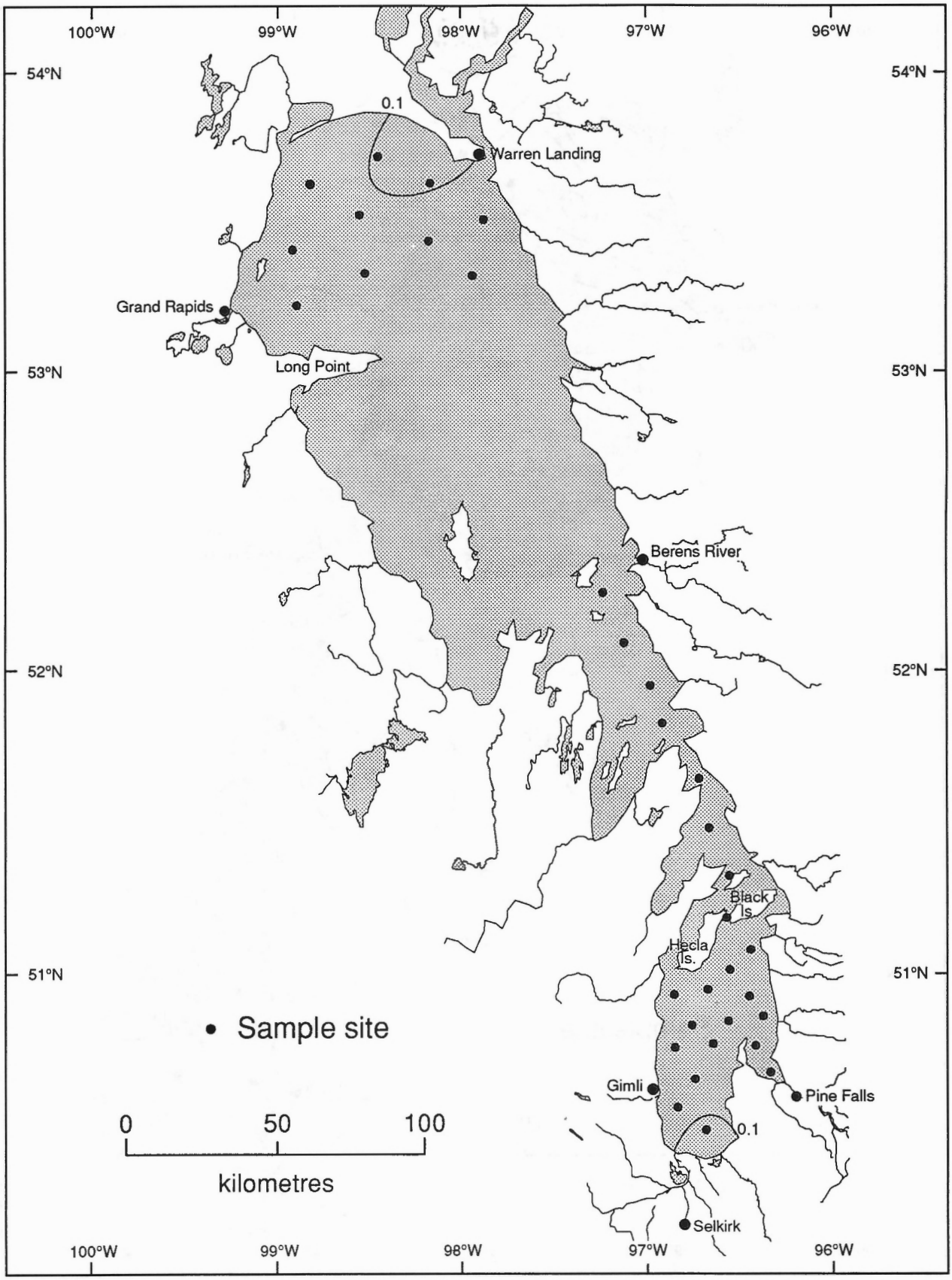

Figure 4m. Spatial distribution of total numbers (individuals per litre) of *Diaptomus siciloides* in Lake Winnipeg, August, 1994.

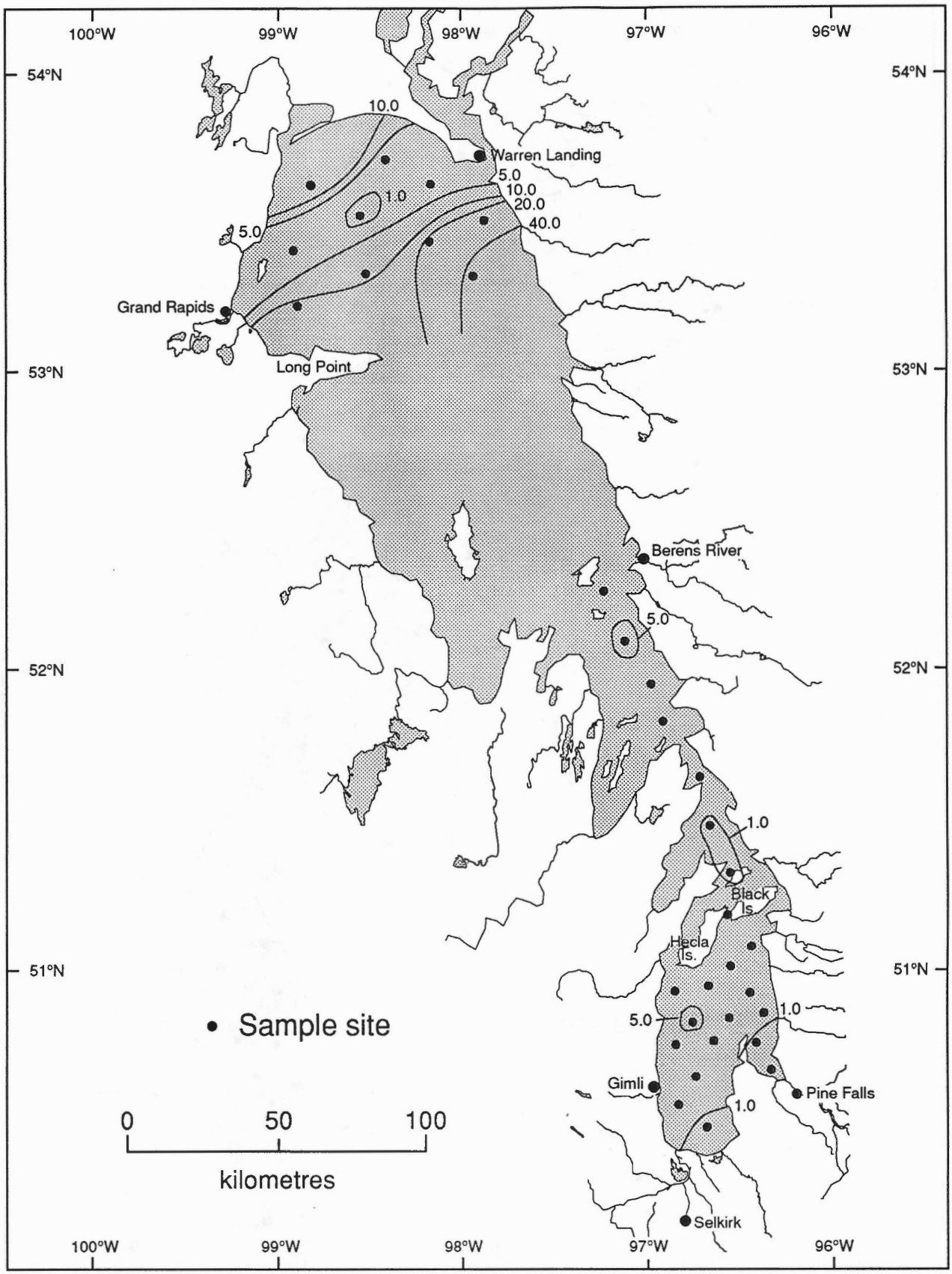

Figure 4n. Spatial distribution of total numbers (individuals per litre) of *Bosmina longirostris* in Lake Winnipeg, August, 1994.

5.3 Benthic Invertebrates of Lake Winnipeg

D.G. Cobb

Department of Fisheries and Oceans
Freshwater Institute, 501 University Crescent, Winnipeg, Manitoba R3T 2N6

INTRODUCTION

Benthic invertebrates are an integral component of lake ecosystems. They are a direct or indirect food source for most species of fish, and act as a link between primary producers and higher levels of the food chain. Moreover, they are widely used as indicators of change in water quality and physical habitat. Thus an understanding of the invertebrate community is a critical component of a whole lake ecosystem study.

The benthos of Lake Winnipeg was first studied in the late 1920s by Bajkov (1930) and Neave (1932, 1933, 1934). Apart from a few provincial government studies, the most recent intensive survey of the lake was in 1969, by scientists from the Freshwater Institute (FWI). Numerous reports have been published on the benthos of the lake from that study (e.g. Flannagan, 1979; Flannagan and Cobb, 1981, 1984, 1991, 1994). Flannagan et al. (1994) reviewed the research on the benthos of the lake. Several faunal changes occurred over the 40 year period, including the disappearance of several species from the South Basin, and the dominance of a new species of caddisfly (*Oecetis inconspicua*, Table 1). Since 1969, apart from a few surveys of parts of the lake by provincial government workers, research on the benthos of the lake has been virtually ignored.

Several changes, with potential implications to the ecosystem of the lake, have occurred since the 1960s. The lake-level has been regulated since 1975 for the production of hydroelectric power, and the Saskatchewan River has been dammed, reducing the input of sediment to the North Basin. Throughout the surrounding watershed, anthropogenic activities have increased inputs of nutrients and contaminants to the lake. Other potential impacts include the threat of introductions of exotic species (e.g. Mississippi fauna, zebra mussels) and climate change.

The Lake Winnipeg Project cruise of 1994 offered a chance to collect invertebrates lake-wide, thus allowing a comparison of the present community structure with earlier studies. In addition, retrieval of sediment cores presented the opportunity to examine changes in the benthos from an historical perspective. This progress report provides a synopsis of the invertebrate study, preliminary findings, and future plans.

MATERIAL AND METHODS

Thirty-three stations were sampled between August 19-30, using Ekman and Ponar grabs (Todd, this volume). One sample was collected at each station, a sediment sub-sample was removed prior to preservation in 4-10% formalin. In the lab, samples were washed through a 200 μm sieve, and transferred after sorting to 70% ethanol.

Seasonal densities and distributions, and annual production require sampling throughout the open-water period, and so were not evaluated. Not all taxa have been examined, due to the time required for taxonomy (e.g. Oligochaeta, Chironomidae). Samples processed to date include stations 1, 3, 32, 37, 40, 44, and 50.

PRELIMINARY RESULTS AND DISCUSSION

Seven samples were examined, representing regions of the lake where samples had been taken in 1969 (Table 2). As in 1969, the Amphipod *Diporeia brevicornis* (Serg.) was absent from the 4 South Basin stations, and was abundant in The Narrows and North Basin samples. Similarly, the caddisfly *Oecetis inconspicua* was still abundant in the South Basin, while *Molanna flavicorinis* was absent in the samples from the South Basin, but was abundant in the North Basin. *Hexagenia spp.* were present in the South Basin, abundant in The Narrows, and absent from the North Basin samples. In 1969, these insects were rare in many of the off-shore stations in the North Basin, being restricted to the near-shore stations, which were not visited in 1994.

Interpreting changes from a single sampling time must be done with caution, because life histories can determine their presence or absence (emergence, egg diapause, etc.). Species with multi-year life cycles, such as *Diporeia brevicornis* and *Hexagenia spp.*, should be present at all times. Only these species are useful as indicators of change in this limited type of study.

SUMMARY AND FUTURE PLANS

Preliminary examination of the samples indicate that the changes in the benthic invertebrate fauna, which had occurred between 1929 and 1969, have persisted. This does not mean that there haven't been changes in the relative abundance or production; a more detailed seasonal study would be required

to determine this.

Future plans include completion of sorting and identification of the benthic samples. The processing of samples will require additional funds and assistance. Once short core dating has been confirmed by Dr. W.L. Lockhart and others, one core from the South Basin will be processed to assess the trend of faunal change.

REFERENCES

Bajkov, A.

1930. Biological conditions in Manitoba lakes; Contributions to Canadian Biology and Fisheries, v. 5, p. 383-442.

Flannagan, J.F.

1979. The burrowing mayflies of Lake Winnipeg, Manitoba; in eds. K. Pasternak and R. Sowa, Proceedings of 2nd International Conference on Ephemeroptera, Krakow, Poland, p. 103-114.

Flannagan, J.F. and Cobb, D.G.

1981. Changes in the profundal Trichoptera of Lake Winnipeg 1928-32 to 1969; in ed. G.P. Moretti, Proceedings of 3rd International Symposium on Trichoptera, W. Junk, The Hague, p. 67-74.

1984. Production of *Hexagenia limbata* and *H. rigida* in Lake Winnipeg, Manitoba; in eds. V. Landa, T. Soldan and M. Tonner, Proceedings of the 4th International Conference on Ephemeroptera, Czechoslovakia Academy of Sciences, Českě, Budějovice, p. 307-315.

1991. The molluscs from the 1969 Lake Winnipeg baseline survey; Canadian Manuscript Report of Fisheries and Aquatic Sciences, v. 2127, 35 p.

1994. The benthic crustaceans from the 1969 Lake Winnipeg baseline survey; Canadian Data Report of Fisheries and Aquatic Sciences, v. 928, 11 p.

Flannagan, J.F., Cobb, D.G. and Flannagan, P.M..

1994. A review of the research on the benthos of Lake Winnipeg; Canadian Manuscript Report of Fisheries and Aquatic Sciences, v. 2261, 17 p.

Neave, F.

1932. A study of the mayflies (*Hexagenia*) of Lake Winnipeg; Contributions to Canadian Biology and Fisheries, v. 7, p. 177-201.

1933. Ecology of two species of Trichoptera in Lake Winnipeg; International Revue der gesamten Hydrobiologie und Hydrgraphie, v. 31, p. 17-28.

1934. A contribution to the aquatic fauna of Lake Winnipeg; International Revue der gesamten Hydrobiologie und Hydrographie, v. 31, p. 157-170.

Table 1. Summary of major benthic invertebrates of Lake Winnipeg and notes on major off-shore fauna (adapted from Flannagan et al., 1994).

Taxa (number species)	Important species	change between 1929 and 1969; comments
Ephemeroptera (18)	*Hexagenia spp.* (87,000 tonnes annual production, major fish food	20% reduction in south basin
Crustacea (6)	*Diporeia brevicornis* (67,000 tonnes annual production, major fish food	eliminated from South Basin
Trichoptera (87)		*Molanna flavicornis* and *Phryganea cinerea* eliminated from South Basin, replaced by *Oecetis inconspicua.*
Chironomidae (>200)	2 species dominate in South Basin	trend from moderate eutrophy South Basin to moderate oligotrophy in North Basin
Mollusca (50)	3 species dominate South Basin.	
Oligochaetae (29)		
Hirudinea (8)		

Table 2. Preliminary summary of major invertebrate fauna collected in 1994 Lake Winnipeg cruise. (present = 1-5 per sample, abundant = > 5 per sample).

	Basin (stations examined)		
Taxa	South (37,40,44,50)	Narrows (32)	North (1,3)
Diporeia brevicornis	absent	abundant	abundant
Hexagenia spp.	present	abundant	absent
Oecetis inconspicua	abundant	absent	absent
Molanna flavicornis	absent	absent	abundant

5.4 The fish and fisheries of Lake Winnipeg

W.G. Franzin

Department of Fisheries and Oceans
Freshwater Institute, 501 University Crescent,
Winnipeg, Manitoba R3T 2N6

K.W. Stewart, L. Heuring and G. Hanke

Department of Zoology
University of Manitoba, Winnipeg, Manitoba R3T 2N2

This is a short summary of a chapter on the fishes and fisheries of Lake Winnipeg that will appear in a volume on the limnology and fisheries of Lake Winnipeg to be published in 1995, probably as a special issue of the Canadian Bulletin of Fisheries and Aquatic Sciences. A complete species list is provided here (Table 1) along with a brief history, in graphical form (Fig. 1), of the catches of the three main commercial species of fish.

Fish colonization patterns in the post-glacial period, historical use of the fish community and present day introductions and invasions are fundamental to the understanding of the current fish fauna. All of these factors will be discussed in the chapter. An effort will be made to develop a community model of the Lake Winnipeg fish fauna. Local and literature knowledge will be used to present habitat requirements or preferences and predator-prey relationships of the fish community.

Climate change may alter the ecosystem of Lake Winnipeg and may affect the fish community. We will examine the utility of fish species temperature preference and tolerance ranges to predict potential changes in the fish community that may result from global warming. Potential effects of climate change on the fisheries of Lake Winnipeg also will be considered.

THE EFFORT OF SUMMER 1994

The relative abundance of pelagic and inshore fish species in Lake Winnipeg is poorly documented. Generally pelagic species abundances are assessed only through the commercial fishery using commercial gillnets. These gear provide data on larger species only and sample only poorly at best many of the smaller species and small size classes of commercial species. Also, commercial fishermen target certain high value species, biasing their effort to maximize catches of those species. Inshore species were sampled at many sites around the margin of the lake during 1990-1993 by University of Manitoba researchers. The Lake Winnipeg Project cruise of summer 1994 offered the opportunity to obtain some semi-quantitative collections of small fish in the pelagic zone of Lake Winnipeg. Unfortunately problems with gear resulted in no fish being collected.

Table 1: Fishes of Lake Winnipeg

Scientific Name	Common Name
***Acipenseridae*: Sturgeons**	
Acipenser fulvescens	Lake Sturgeon
***Salmonidae*: Trouts**	
Salvelinus namaycush	Lake Trout
Coregonus artedii	Lake Cisco
C. clupeaformis	Lake Whitefish
***Hiodontidae*: Mooneyes**	
Hiodon alosoides	Goldeye
H. tergisus	Mooneye
***Esocidae*: Pikes**	
Esox lucius	Northern Pike
***Percidae*: Perches**	
Perca flavescens	Yellow Perch
Stizostedion vitreum	Walleye
S. canadense	Sauger
Etheostoma nigrum	Johnny Darter
E. exile	Iowa Darter
Percina caprodes	Logperch
P. maculata	Blackside Darter
P. shumardi	River Darter
***Gadidae*: Cods**	
Lota lota	Burbot
***Ictaluridae*: Bullhead Catfishes**	
Ameiurus melas	Black Bullhead
Ameiurus nebulosus	Brown Bullhead
Ictarus punctatus	Channel Catfish
Noturus gyrinus	Tadpole Madtom
***Catostomidae*: Suckers**	
Catostomus catostomus	Longnose Sucker
C. commersoni	White Sucker
Moxostoma anisurum	Silver Redhorse
M. erythrurum	Golden Redhorse
M. macrolepidotum	Shorthead Redhorse
Carpiodes cyprinus	Quillback
***Cyprinidae*: Minnows**	
Cyprinus carpio	Carp
Notropis atherinoides	Emerald Shiner
N. volucellus	Mimic Shiner
N. heterolepis	Blacknose Shiner
N. hudsonius	Spottail Shiner
N. texanus	Weed Shiner
N. heterodon	Blackchin Shiner
Pimephalas promelas	Fathead Minnow
Rhinichthys cataractae	Blacknose Dace
Macrhybopsis storeriana	Silver Chub
Couesius plumbeus	Lake Chub
Platygobio gracilis	Flathead Chub
***Percopsidae*: Trout-perches**	
Percopsis omiscomaycus	Trout-perch
***Gasterosteidae*: Sticklebacks**	
Culaea inconstans	Brook Stickleback
Pungitius pungitius	Ninespine Stickleback
***Cottidae*: Sculpins**	
Cottus bairdi	Mottled Sculpin
C. cognatus	Slimy Sculpin
Cottus ricei	Spoonhead Sculpin
***Centrarchidae*: Sunfishes**	
Ambloplites rupestris	Rock Bass
Micropterus dolomieui	Smallmouth Bass
Pomoxis nigromaculatus	Black Crappy
***Petromyzontidae*: Lampreys**	
Ichthyomyzon castanaeus	Chestnut Lamprey
I. unicuspis	Silver Lamprey
***Sciaenidae*: Drums**	
Aplodinotus grunniens	Freshwater Drum
***Umbridae*: Mudminnows**	
Umbra limi	Central Mudminnow
***Osmeridae*: Smelts**	
Osmerus mordax	Rainbow Smelt
***Percichthyidae*: Temperate Basses**	
Morone chrysops	White Bass

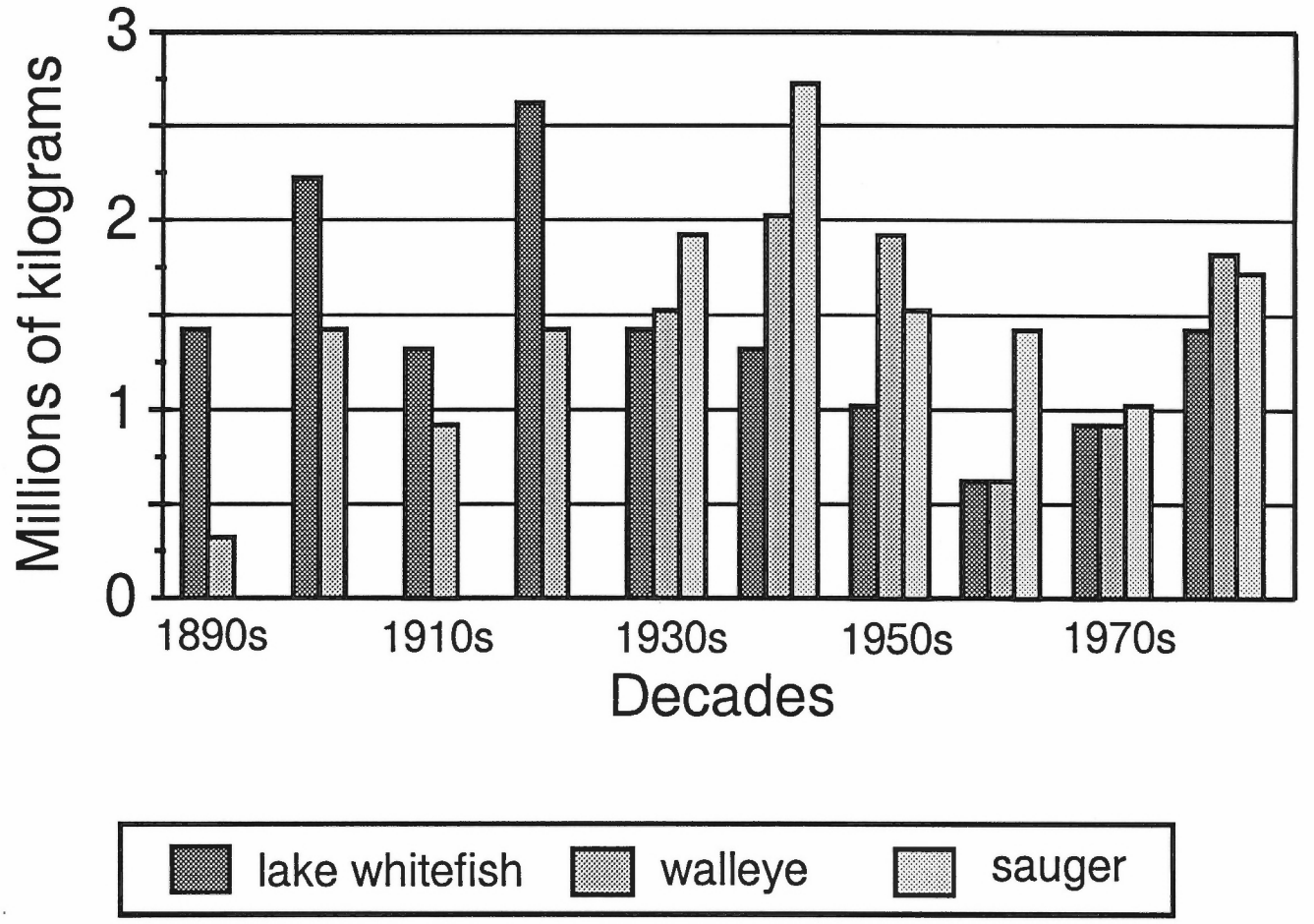

Figure 1. Catches of major fish species from Lake Winnipeg by decade.

6. Shoreline survey results

6.1 Shore-zone morphology and processes of Lake Winnipeg

D.L. Forbes and D. Frobel

Geological Survey of Canada (Atlantic)
P.O. Box 1006, Dartmouth, Nova Scotia B2Y 4A2

ABSTRACT

Reconnaissance surveys of the Lake Winnipeg shoreline were conducted in September 1994, to improve understanding of lake basin and shoreline evolution, past lake levels, and shore erosion processes. The surveys included approximately 12 hours of low-level aerial oblique video imagery, covering most of the mainland shore and central islands, supplemented by a voice commentary and oblique photography. Ground surveys were carried out at seven locations along the southern shore of the lake, previously surveyed in 1990, and at five other sites (Grand Beach, Grand Marais, western shore north of Gimli, Passage Point north of Fisher Bay, and Limestone Point on the north shore).

Physical shore-zone features (geomorphology and sediment type) were mapped from the video imagery. Fifteen shore types have been defined and combined into seven shore-type associations for mapping purposes. These include (A) low-energy marsh and deltaic shores (with or without a transgressive beach veneer); (B) low relief rock outcrop (often forming complex archipelagos, with marsh in protected embayments, restricted to the Precambrian shield rocks along the east shore); © sand-dominated beaches (sandy spits, barriers, fringing barriers, and beaches); (D) a heterogeneous group often incorporating repetitive sequences of sandy or gravelly beaches, low erosional scarps, and low-relief headlands of rock outcrop or boulder-lag shoals; (E) gravel beaches and barriers sourced from rock cliffs (restricted to the Ordovician sedimentary formations along the west side of the lake); (F) unlithified cliffs with or without basal beaches of sand or gravel, and steep slopes with discontinuous failures feeding a basal gravel beach; and (G) artificially modified shores (mapped in combination with the natural shore type).

The shores of the South Basin are predominantly erosional, as demonstrated in a 1974 study by Manitoba Natural Resources. Localised progradation occurs on the delta shoreline at the south end of the lake, but in general the southern shore is transgressive, with a thin barrier veneer migrating landward over delta plain and marsh deposits. Much of the western shore of the South Basin is cut into Lake Agassiz clays, with a thin wedge of sand or gravel at the base. Shore protection structures of various kinds (walls and groynes) have been installed with varying success. In some cases these have exacerbated shore erosion. The Willow Point barrier south of Gimli is a transgressive feature, moving onshore over the backbarrier marsh but partially stabilised by the boulder-lag platform holding the point. The eastern shore south of Elk Island is generally higher and cut into coarser glacial and proglacial deposits with a high proportion of cobbles and boulders. Coastal dunes have developed on sandy barriers at Beaconia Lake and Grand Beach. The gravel spit and barrier island at Grand Marais appear to be transgressive and the partial tombolo at Elk Island may have been initiated by breaching of a barrier comparable to Hillside Beach.

The most extensive sandy barrier, fringing barrier, and coastal dune tract on Lake Winnipeg occurs along the eastern shore of the North Basin, overlying Precambrian basement rocks at shallow depth. These beaches are assumed to have been sourced from the lakefloor. Other parts of the eastern shore have extensive sections of bare rock outcrop forming an irregular shoreline or archipelago, locally with thin marsh development. The western shore of the North Basin and central lake is a varied mix of rock cliff and gravel beaches, partly colonised sand and gravel beaches, extensive low sandy barriers, beaches and spits, often with extensive nearshore bar development, and sections of marsh and bog. The Long Point peninsula has a long stretch of gravel beach backed by locally active slope failures in Quaternary glacial deposits along its southern shore. The north shore of the North Basin has extensive high bluffs feeding sediment westward onto the 20 km Limestone Point spit, now anchored behind a rock reef at its distal end. Submerged ridges behind the spit and other evidence of transgressive shore processes in the northern lake raise questions about long-term lake-level fluctuations of climatic or other origin that may be superimposed on the southward isostatic tilting of the basin.

INTRODUCTION

A reconnaissance survey of the Lake Winnipeg shoreline was carried out over 10 days in mid-September 1994. This formed part of a larger field program to gather preliminary data on the geology of Lake Winnipeg in order to augment scientific understanding of lake processes and basin evolution and to help address public concerns on shore erosion and lake-level variation. The shore survey followed a month-long scientific cruise on the lake in August 1994 using the Coast Guard vessel CCGS *Namao* (Todd, this volume). The objectives of the shore survey were to collect oblique aerial video imagery of as much of the lake shore as possible, as a basis for preliminary mapping of physical shore-zone characteristics, for which no data were available north of Elk Island on the east side of the lake and Riverton (Icelandic River) on the west. To corroborate

the interpretation of shore-zone types from the air and later from the video imagery, we examined the shore on the ground at as many sites as possible during the 10-day field program. Secondary objectives of the survey were to collate existing information (primarily restricted to the South Basin), to establish an initial network of monitoring sites or to relocate previous survey sites from the 1970s (Penner and Swedlo, 1974), to evaluate shoreline stability and the geomorphological evolution of the lake shore, and to develop recommendations for a more comprehensive study of lake-shore processes. One of the outstanding questions to be resolved for an understanding of shoreline evolution in different parts of the North and South Basins of Lake Winnipeg is the relative importance of southward isostatic tilting, as revealed in part by studies of tilted beaches of glacial Lake Agassiz and successor lakes (Johnston, 1946; Thorleifson, 1983; Nielsen et al., 1987; Tackman and Currey, this volume), and basin-wide lake-level fluctuations that may be related to regional climate variability over the entire area, which drains to the lake via the Saskatchewan River, Winnipeg River, Red River, and other rivers (Fig. 1).

Previous work on the shores of Lake Winnipeg includes a comprehensive report on the South Basin by Penner and Swedlo (1974), a property owner's handbook prepared under the direction of Frank Penner by M. Young (Manitoba Water Resources Division, 1977), a number of academic theses completed at the University of Manitoba (Cheng, 1972; Solohub, 1967; Veldman, 1969), and a detailed study of the south shore by Nielsen and Conley (1994). Previous work on the lake bottom includes sampling programs by Kushnir (1971) and Brunskill and Graham (1979). Information on the physical limnology is provided by Einarsson and Lowe (1968). Other relevant work underway concurrently with this project includes new photography and mapping of the South Basin lake shore by Manitoba Hydro and a general analysis of lake-shore erosion problems in the South Basin by a team at the University of Manitoba (Hans and Doering, 1995).

With a surface area of 2.37×10^4 km^2, Lake Winnipeg is the 12th largest freshwater lake in the world (Nielsen and Conley, 1994). Larger than Lake Ontario, it is nevertheless very shallow, with a maximum water depth of about 18 m in the North Basin and somewhat less in the south, although depths greater than 65 m occur at the south end of The Narrows (Fig. 1). The name "Winnipeg" denotes muddy water in Cree, a description that may arise from the erosion of Lake Agassiz clays in the South Basin or of muddy sediment exposed along the north shore (Franklin, 1823). The major source of river-borne sediment is the Red River, entering at the south end of the lake. Natural lake storage and artificial impoundment in the Winnipeg River and Saskatchewan River basins (Fig. 1) restrict the input of sediment from these sources (Mackenzie, 1801; Upham, 1890; Brunskill and Graham, 1979). The regional geology is dominated by Precambrian rocks of the Superior Province exposed along the east shore of the lake and by Ordovician limestones, dolostones, and sandstones on the west (Manitoba Mineral Resources Division, 1979; Teller and Bluemle, 1983). The prominent Long Point peninsula in the North Basin is associated with a major Quaternary glacial moraine complex, The Pas Moraine (Manitoba Mineral Resources Division, 1981). Clays of glacial Lake Agassiz form a broad plain bordering the southwest end of the lake (Teller et al., 1983). Boulder-rich tills and outwash deposits are exposed along the eastern shore of the South Basin. An extensive body of unconsolidated muddy sands or sandy muds associated with the Hargrave Moraine complex (Klassen, 1983) occurs along the north shore of the North Basin, where it forms prominent bluffs. The Red River enters the lake through a wide deltaic marsh complex, Netley Marsh (Fig. 2), which is being slowly inundated by the lake as isostatic tilting causes the water level at the south end of the lake to rise (Penner and Swedlo, 1974; Nielsen and Conley, 1994).

METHODS

The field survey was conducted from 6 to 16 September 1994. Aerial video and photography were obtained for almost all of the mainland shore and some of the islands (primarily Hecla, Black, and Elk Islands), using a Cessna 185 high-wing monoplane on floats, chartered from Northway Aviation and flying from the Icelandic River at Riverton. The circuit of the North Basin required two days of flying with an overnight stop at Norway House. The starboard door of the aircraft was removed for the video survey. The cameraman sat in the rear seat, with the camera on his knee, shooting through the open door. The imagery was recorded using a Sony 3/4-inch U-matic system on 20 minute field tapes. A voice-over commentary was provided by the other member of the team, who also took photographic stills using a 35 mm camera. Positioning was by visual reference and non-differential GPS. A Navstar-5000 handheld GPS unit was used to collect the satellite data. It was placed on the aircraft dashboard and recorded fixes at 30-second intervals on an internal buffer. The data were downloaded to a notebook computer at the end of the day using an RS-232 link. Start and end times of each field tape and times noted on the voice commentary provide the correlation between the GPS fixes and the imagery. GPS fixes for part of the survey were lost due to a setup error that resulted in data overflow in the buffer. The missing GPS data were replaced by approximate fixes derived by plotting the estimated aircraft position from visual landmarks.

Ground surveys were obtained along the south shore of the lake at seven sites which had been previously surveyed in 1990 by Nielsen and Conley (1994; Fig. 2). Surveys were also completed at five other locations (Fig. 1): along the north shore of North Basin east of the head of Limestone Bay (site 8200), at Passage Point (site 8201), along the western shore of South Basin north of Gimli (site 8031), and at Grand Marais (site 8128) and Grand Beach (site 8136) on the east shore of South Basin. Surveys were carried out using a pair of graduated staffs with tape and a hand level or unobstructed lake horizon (the so-called Emery method) at all sites except Grand Marais, Grand Beach, and north of Gimli, where a Geodimeter model 140H infrared total station (electronic theodolite) was used. Vertical

control was based on the lake level at the time of the surveys, derived from water level records at several points around the lake, provided courtesy of the Water Survey of Canada.

The original data on which this report is based, consisting of oblique aerial video imagery, oblique photography, sediment samples, and shore survey data are archived at the Geological Survey of Canada (Atlantic), Bedford Institute of Oceanography, Dartmouth, Nova Scotia. These data will be reported more fully in a separate open-file survey report and the video imagery will be released on open file when editing has been completed. In the meantime, the source data can be accessed by contacting the authors.

SHORE TYPES OF LAKE WINNIPEG

Shore type (Fig. 3) is a complex function of geological inheritance, sediment supply, lake-level history, fetch length and exposure, wave climate and other shore-zone processes acting at a given location along the present lake shore. In settled areas it can also be modified by artificial structures or other human activities. On Lake Winnipeg, the underlying geology exerts a strong influence on the distribution of shore types. Five principal units are distinguished, as follows:

- shores on Precambrian shield (east side of the lake),
- shores on Ordovician limestone/dolostone/sandstone lithologies (west side of lake),
- shores on Late Quaternary glacial tills, outwash, and related deposits (various locations),
- shores on Late Quaternary proglacial Lake Agassiz clays (primarily toward the south end), and
- marsh deposits (primarily the south shore).

Obviously there is some overlap between the pre-Quaternary and Quaternary units, such that parts of the eastern shore of the lake are characterised by Precambrian exposures virtually devoid of modern sediments (e.g. the Kasakeemeemisekak Islands archipelago and other parts of the east-central lake shore), whereas other parts of the east coast have access to sediment sources enabling the development of extensive fringing sandy barriers with large coastal dune complexes (east shore north of Berens River and northeast shore south of Nelson River outlet).

In general terms, the eastern shore of the lake lies across an ancient low-relief erosion surface developed in resistant shield rocks of the Precambrian Superior Province, whereas the western shore extends onto overlying clastic and carbonate sedimentary rocks of Ordovician age, dipping gently toward the southwest (Manitoba Mineral Resources Division, 1970). In many areas, Quaternary glacial, proglacial, and postglacial deposits effectively mask the underlying bedrock (Manitoba Mineral Resources Division, 1981) and control the topography and sediment supply. Ice-contact and proglacial deposits with significant proportions of cobbles and boulders (tills, outwash gravels and sands, and glacio-lacustrine silts and sands) cover much of the eastern lakeshore of the South Basin and crop out elsewhere, either extensively (as along the south shore of Long Point in the North Basin) or locally (e.g. isolated headlands such as Willow Point south of Gimli). Distal lacustrine clays of proglacial Lake Agassiz form much of the plain along the western side of the South Basin, imparting a distinctive character to that shore (Penner and Swedlo, 1974).

The shore types and distribution of shore-zone characteristics presented here are derived from detailed thematic mapping at 1:50,000 and 1:250,000 map scales, using the oblique aerial video imagery collected in September 1994 as the primary data source. This was supplemented by direct observations (recorded on the video voice track) and 35 mm still photography obtained at the same time as the video imagery, by ground observations at 15 locations around the lake, and by published data on the South Basin (notably Penner and Swedlo, 1974; Nielsen and Conley, 1994).

Shore type classification

The following individual or composite shore types are observed around the lake:

0 - marsh
1 - delta and/or marsh with sandy beach and barrier veneer
2 - low-relief rock outcrop with discontinuous marsh
3 - low-relief rock-controlled coast with scattered pocket beaches and marsh
4 - sandy spits and barriers (locally with inlets, lagoons, coastal dunes, and minor gravel or boulders)
5 - low-relief shores with sand beaches and nearshore bars (locally forming fringing barriers with some washover)
6 - extensive dissipative to intermediate sand and gravel beaches (in places forming fringing barriers)
7 - rock-controlled coast with discontinuous sandy and mixed sand-gravel beaches and low erosional scarps
8 - repetitive sequences of mixed sand-gravel beach and boulder lag shoal (locally with colonising vegetation)
9 - gravel beaches, spits, and barriers (locally with small lagoons and occasional inlets)
10-rock cliff (commonly associated with gravel beaches and barriers)
11-steep slope with discontinuous failures and mixed sand-gravel beach
12-unlithified cliff with mixed sand-gravel and/or boulder beach at base
13-unlithified cliff with discontinuous sandy beach at base
14-artificial shore structures (walls, revetments, breakwaters, groynes).

Shore-type associations

For summary mapping and discussion purposes (Fig. 3), the shore types defined above have been grouped into six shore-type associations (groups) of natural origin and a seventh

representing artificial shore structures. The latter are superimposed on a number of the natural shore types.

A - The first group (types 0 and 1) represents predominantly low-energy marsh and deltaic shorelines (Fig. 4), with or without a transgressive beach veneer. Although present in some exposed settings (Fig. 4a), this shore-type association is most common in bayhead and bay-margin settings (Fig. 3), as in Gull Bay, Sturgeon Bay and Paterson Bay (just north of Berens River) in North Basin, at the head of Washow Bay in the central lake, and on the west side of Hecla Island, extending through Grassy Narrows into Riverton Harbour in South Basin. Type-0 shores are also found in apparently flooded river-mouth situations, as in the lower Pigeon River (Fig. 1). Small parts of some areas mapped as type 0 also include sections of eroding organic shore, characterised by a low cliff (<2 m) and toppling trees overhanging the water, with little or no beach. Type-1 shoreline dominates the south end of the South Basin across the Red River delta, where a thin, discontinuous, transgressive sandy barrier rests over peats of Netley Marsh (Figs. 2 and 4b-d). In this setting, the wave energy levels can be substantial under northerly winds with high lake levels and/or storm-surge setup, leading to localised washover (Nielsen and Conley, 1994).

B - The second shore-type association (types 2 and 3) consists of sediment-starved outcrop shores forming extensive archipelagos in some areas. This group is found exclusively along the east side of the lake (Fig. 3) on Precambrian outcrop. The many small islands and low headlands are characteristically devoid of sediment cover, except for a few scattered boulders and patches of thin soil supporting scrubby vegetation (Fig. 5a). Thin marsh often occurs in shallow embayments landward of the outer fringe of protecting outcrop islands and shoals (Fig. 5b). In some areas of type-3 shore, limited beach sand is also present, but the overall shore-zone character is still largely rock-controlled.

C- The third group (types 4, 5, 6) encompasses the major sandy beach and barrier segments of the Lake Winnipeg shore. In addition to extensive, low-relief, dissipative to intermediate, sandy (locally gravelly) beaches and fringing barriers (Fig. 6a) of the western North Basin, locally with one or more (in places up to eleven) nearshore bars (Fig. 6b), this group also includes type-4 sandy spits and barriers (many with large dune complexes) along the eastern shore of North Basin (Fig. 6b), locally along the western shore, and in major embayments of the southeast South Basin (Fig. 6d).

D- This association (types 7 and 8) combines a somewhat mixed group of sand and gravel beaches in areas where bedrock outcrop or boulder lag shoals exert a strong control on the shoreline morphology and cell boundaries (defining the limits of individual shore segments within which readjustment by longshore transport may occur). This group is widespread (Fig. 3) along the west side of the central narrows (Fig. 7a), locally on the west side of South Basin (Fig. 7b), along the entire east shore of South Basin north of the Winnipeg River (Fig. 7c), and in parts of North Basin, most extensively in the southwest (Fig. 7d). In many areas, repetitive successions of arcuate beaches grading from coarse to fine are interrupted and controlled by rock or boulder-lag shoal headlands (e.g. along the western shores of Sturgeon Bay and Fisher Bay). Vegetation extending down across the upper beach in some places implies a period of reduced runup. Colonising vegetation also commonly extends into the water on gravel shoal platforms and headlands (Fig. 7b). Short sections of low erosional cuts in organic or other backshore deposits, as described above for group A, are more commonly associated with updrift segments of rock- or shoal-controlled type-7 shores.

E- This fifth group (types 9 and 10) represents coarse gravel beaches and barriers and the rock cliffs from which most are sourced. This type of shore is best developed north of Grand Rapids (Fig. 3), where a succession of headland cliffs in Ordovician carbonates feeds a large number of small gravel spits and barriers. These are generally narrow, display well-developed alongshore cell structures and, in some cases, enclose small lagoons that drain by seepage (Fig. 8a). Because gravel beaches often preserve a record of extreme events, further investigation of these sites may be profitable. Some sites, as at the north end of Selkirk Island (Fig. 8b), display stacked berms with lichen growth on the upper beach, implying a period of reduced wave runup since formation of the higher berms.

F- The sixth shore-type association (types 11, 12, 13) combines erosional shorelines in unlithified deposits (excluding limited occurrences of low cuts in organic or other backshore deposits described for groups A and E above). These erosional shores are concentrated in three major areas (Fig. 3). Type 11 represents the southern shore of Long Point, where intermittent failures on a steep, wooded, backshore slope (difficult to discern from the air) are associated with a continuous mixed sand-gravel beach at the shoreline. Type 12 refers to the erosional shores of South Basin, which comprise a mixture of relatively low cliffs in Lake Agassiz clays along the western shore and higher, more stable, boulder-rich cliffs in glacigenic diamicts and gravels along the eastern shore (cf. Penner and Swedlo, 1974; see section on ground surveys below). Type 13 is the erosional north shore of North Basin from west of the Nelson River outlet to a point east of the head of Limestone Bay. This erosional section consists of cliffs cut into unlithified Quaternary silts and sands. At the time of our observations, the beach was narrow and discontinuous, but this may have been partly a result of wind setup and the high surf that prevented us landing to verify the cliff height and composition. Some sections of cliff are partly stabilised by vegetation but active slumping is common along the entire length.

G- Type 14 represents artificial modification of the shoreline by construction of harbour facilities (Fig. 10a) or shore-protection works such as walls, slope armouring, groynes (Fig. 10b) or other structures. Except for wharves, harbour and other navigation facilities at several locations around the lake,

structural modification is largely restricted to the South Basin between Hnausa (south of Riverton) and Sans Souci (west side of Netley Marsh) on the western shore and between Beaconia and Elk Island on the east (Figs. 1 and 2). These structures are superimposed on a variety of natural shore-type associations, including C, D, E and F (Fig. 3).

SHORE REACHES AND LITTORAL FEATURES: OVERVIEW AND DISCUSSION

This section contains a description and preliminary interpretation of selected reaches and littoral features of the Lake Winnipeg shore, including results of ground surveys and site inspections. The emphasis is on areas likely to contain important evidence of long-term shore evolution, changes in lake level, wave climate, sediment supply or other factors, and on data providing evidence of short-term changes in the heavily settled South Basin region. Special attention is drawn to the wide variety of spit, barrier and barrier island structures around the lake (Figs. 6a-d, 7a-b, 8a, 11a-d, 12) and associated back-barrier basins, which contain important geomorphological and geological records of shore-zone evolution and lake history. This section necessarily includes reference to many place names, too numerous to be shown on Figure 1. All place names mentioned in the text can be found on the 1:250,000 scale topographic maps of the National Topographic Series (maps 62I, 62O, 62P, 63A, 63B, 63G, 63H).

North shore of North Basin (including Limestone Point and Limestone Bay)

The north end of the lake contains a number of distinctive shore features without parallel elsewhere on Lake Winnipeg.

Apart from a small spit complex built north along the west side of the outlet passage at Warren Landing, enclosing a small marsh, the remainder of the shore extending about half way across the north end of the lake consists of high eroding bluffs of shore type 13 (Fig. 9a) cut into unconsolidated Quaternary silty sands or sandy silts. Our intention to land along this shore to examine the material in the cliffs was thwarted by strong southerly winds and associated surf. Further west, a change in shore type from group F to group A (Fig. 3) reflects a gradual reduction in backshore elevation. The cliffs give way to a fringing sandy beach and foredune ridge (shore type 4). The planform arc of the coast extends unbroken past the head of Limestone Bay along a 20 km spit to Limestone Point (Fig. 11a-b). Recurved beach and dune ridges (Fig. 12a) demonstrate the progressive westward growth of the spit toward its present distal terminus just 3 km from the western shore of the lake. The present dynamics of Limestone Point are somewhat unclear because of the influence of McIntosh Reef, a rock shoal off the distal end of the spit. In the lee of this outcrop, the beach has prograded lakeward to form a wide dissipative platform backed by marsh (Fig. 11b). It appears that sediment arriving alongshore from the east is contributing to this progradation rather than to spit extension or losses to Limestone Bay.

In the lee of Limestone Point, an extensive beach-ridge plain has accumulated by longshore transport of sand and gravel toward the head of Limestone Bay (Fig. 12c). A landing was made here to look at the inner bay shore, the proximal spit, and the bayhead beach-ridge complex on the ground, to core peat overlying the relict beach ridges, and to establish a beach profile site on the outer (Lake Winnipeg) shore. The inner bayhead beach consists of sandy fine gravel, with well-rounded coarse pebbles in the nearshore, about 2 m from the water line at the time of our visit (strong south wind at the time had raised the water level at the north end of the lake to about 217.8 m). A well-wooded dune ridge separates the inner shore from the exposed Lake Winnipeg beach at the proximal end of the spit and obscures any evidence of truncated beach ridges further east. Exploration along the inner margin of the dune ridge revealed no exposed beach sediments, but numerous auger probes encountered silty sand beneath a thin peat cover. At site 8200 (53°49.87'N, 98°42.54'W), a short distance east of the head of Limestone Bay (Fig. 12c), a Hiller core was obtained at the landward end of the surveyed beach and dune profile.

The core site was near the outer (southern) margin of the relict beach-ridge complex, just beyond the landward limit of dune transgression in the vicinity. The lithostratigraphy in the core was as follows:

0.00-0.38 m (downcore): muddy peat
0.38-0.81 m (downcore): compact peaty mud
0.81-0.94 m (downcore): poorly sorted silty medium sand

Fig. 13 shows grain-size distributions for sample 001 from the base of the core and for two samples from the active outer beach. Sample 005 is from a lower beachface swash concentrate and sample 006 represents the predominant beachface sediment. The latter is a medium sand (modal size d_M= 0.27 mm [1.9 ϕ]), much finer than the coarse sand concentrated at the water line (d_M= 1.1 mm [-0.1 ϕ]). The beachface sand (sample 006) is slightly finer and much better sorted than the sand at the base of the core (sample 001). The latter material, interpreted as a relict beach deposit, is a silty medium sand (d_M= 0.35 mm [1.5 ϕ]) with 10% coarser than 0.6 mm and 13% finer than 0.06 mm (Fig. 13). The poorer sorting and large fine fraction in the relict bayhead beach sand is consistent with lower wave energy in Limestone Bay and also with probable post-depositional addition and infiltration of silt as the surface became progressively covered by marsh. The core site appears to be slightly below mean lake level (Fig. 14), with the top of the sand at 216.4 m elevation, implying a lower lake level at the time of beach-ridge formation. We should note that the survey method used at this site, due to the limited payload of the Cessna 185 aircraft, is potentially subject to cumulative error, especially in a difficult survey through thick vegetation, and the site should therefore be resurveyed using conventional survey technology to confirm these results.

The fringing barrier and dune ridge at site 8200 is about 70 m wide (Fig. 14). The foredune ridge reaches an elevation of

222 m, about 4.5 m above mean lake level (based on an estimated setup-enhanced water level of 217.8 m at the time of the survey). The dunes have a characteristically steep landward slope, well vegetated with juniper, giving way to tall grass at the base (Fig. 14). This indicates a long-term trend of slow landward migration with very limited rates of sand transport except in active blowouts. The sandy beach extends about 25 m lakeward from the limit of vegetation on the outer dune face. A pronounced berm is present at 219 m elevation, about 1.5 m above mean lake level. The mean beachface slope below the berm is about 5° (tan β = 0.09), diminishing lakeward (Fig. 14).

Further investigation of this and several sites along Limestone Point would provide the first data on the chronology of this large coastal sediment complex and the history of lake levels at the north end of Lake Winnipeg. A curious feature of Limestone Bay, first noted on air photographs and then observed directly from the air and the water surface, is a linear growth pattern of subaqueous vegetation interpreted as indicating a set of submerged ridges, roughly parallel to the present spit (Fig. 12b). The nature and origin of these ridges is unclear. Whether they represent former shore features (beach ridges, an earlier spit, possibly even ice-pushed ridges) developed at a lower lake level is an important question in the context of stratigraphic evidence for possible lower lake levels (Lewis and Todd, this volume) and the potential for step increments in lake level caused by factors such as the possible diversion of the Saskatchewan River (McMartin, this volume). Alternatively, the presumed ridges may be older relict features.

Northwest shore of North Basin and north side of Long Point

Immediately opposite the end of Limestone Point, the shore consists of a type-1 (group A), transitional to type-5 (group C), sandy beach or fringing barrier with backshore bog, locally with small dunes, and small sand spits built northward into the entrance of Limestone Bay (the type-5 features here are too small to be mapped separately in Fig. 3). Shallow marshes are present behind these spits. A short distance to the south, the shore character changes to wide subaqueous flats with extensive, fringing, type-0 marsh of group A (Figs. 3 and 4a). South of Hungry Point, the shore type changes again with the appearance of gravel beaches and barriers sourced from carbonate bedrock cliffs up to 4 or 5 m high or higher (group E, Figs. 3 and 8a). The cliffs are near-vertical, without a basal beach in many places. Gravel beaches, gravel barriers, and rock cliffs alternate in a repetitive pattern southward toward Grand Rapids. Opposing gravel spits with inlets and small flood delta platforms supporting marsh are present north of Sturgeon Gill Point and south of Fiddler Point. Other gravel beaches, barriers and spits are well developed near Howell Point in the north and on Selkirk (Horse) Island offshore (Fig. 8b). Surveys of these gravel barriers would be valuable in establishing wave runup limits and other evidence of lake-level and wave climate variation along this shore. Further south, in the lee of the island and southward, the rock cliffs disappear and parts of the shore are apparently sediment-starved. Trailing gravel spits and shore-normal lag shoals at Eating Point north of Grand Rapids and Nistwawnayapiskaw Point to the east are similar to features observed on transgressive coasts in Nova Scotia and in areas of more stable relative sea level on the southeast and northwest coasts of Ireland (Taylor et al., 1986). They attest to coastal erosion and landward reworking of gravels, probably (though not necessarily) related to a rise in water level in this part of the lake. A small gravel spit extending southward across a small embayment at Baldys Bluffs, east of Grand Rapids, shows evidence of washover at its proximal (north) end.

The north shore of Long Point peninsula from this point east (group D) is characterised by numerous boulder platform headlands with sand and gravel beaches and barriers in the intervening embayments. The western part has two large embayments (group C) with sandy barriers at Saskachayweow Bar and Hole in the Wall. Both have nearshore bars, an inlet and lagoon, dunes, and the former shows some evidence of progradation.

Western shore of North Basin from Long Point to Sturgeon Bay

The southern shore of Long Point peninsula (type 11) is nearly straight and featureless. The beach, composed of sand and gravel with boulders, is continuous and shows little variation alongshore. Discontinuous slope failures estimated up to 10 m high, difficult to see from the air, are developed in unlithified (presumably glacigenic) material of unknown composition. The slope is extensively stabilised and hidden by vegetation, but gaps in the tree cover reveal the scars of recent rotational slumping. Net transport appears to be westward along this shore, at least at its west end, where it feeds into the 5 km spit at North Bar (Gull Bay). The inner shore of the bay is marsh (Fig. 3). Across the bay at South Bar, the situation is quite different. Here a complex set of old beach ridges has been truncated by landward migration of the outer shore. The barrier extending north into Gull Bay is extensively breached or awash along much of its length. The sediment in this system is being actively reworked into the bay and southward into an adjoining shallow embayment.

South of Gull Bay (Fig. 1), the shoreline exhibits a repetition of coastal cells with sandy barriers fronting narrow lagoons or bog. Each cell is defined by a resistant headland of rock or boulder platform (type 8). Some streams and inlets suggest transport to the south and others to the north and west (Fig. 15). The inlet at Ebb and Flow Lake west of Ashmall Point was sealed at the time of our observations. Some of the few indications of ice rideup observed during the 1994 survey (Fig. 15) were seen along this shore on the north side of Driftwood Point and about 2 km west of Shiel Point, both in the large embayment due west of Reindeer Island (Fig. 1). Nearshore bars become more common and prominent southward, with five bars present on the south side of Sandy Bar. Some barriers at headlands have multiple beach or dune ridges. The sandy fringing barrier at Morass Point (Fig. 6a) extends southward around the point, with evidence of

transgression and ridge truncation on the east side.

Clarks Point, at the mouth of Sturgeon Bay, is a rock-controlled headland with cliffs no more than 10 m high at its north end and a gravel beach with boulders along the outer (east) shore. This is an anomaly in the area: most of the shore is a complex mix of sand and gravel beaches with sections of boulder platform (sometimes forming headlands), localised shore erosion in embayments, discontinuous marsh, and occasional multiple bar complexes. In places, there appears to be an older high-level gravel beach behind the active beach (or vegetation has colonised the upper, recently inactive, part of the modern beach). This is a feature observed along many gravel shores from Sturgeon Bay to The Narrows (Fig. 1) and locally farther south. North of Dauphin River, on the west side of Sturgeon Bay, the Hay Point marsh is fringed by a discontinuous sandy barrier and locally by boulder platform.

The southwest and south shore of Sturgeon Bay has a sandy beach with scattered boulders and at least two sinuous nearshore bars giving way eastward to partly vegetated boulder platform and pocket beaches and then to a sandy barrier with dunes anchored on the prominent gravel platform headland of Willow Point. This barrier, fronted by at least two bars and backed by a narrow lagoon and wide marsh, has a prominent washover fan at its west end. Much more extensive washover and localised breaching is evident along the western end of Reedy Point spit at the head of the bay (Fig. 6b), where there also appears to have been progressive inundation of a large marsh. Up to 11 nearshore bars are present off Reedy Point and at least six off the Poplar Point beach on the east side of the inlet. A small sand spit is growing south into the inlet on the east side at Poplar Point.

From this point north along the east side of Sturgeon Bay, the shore becomes more gravelly, but three nearshore bars are present in a number of the more southerly embayments. Numerous ice scours are prominent on shallow subaqueous gravel flats fronting the shore directly opposite Willow Point.

South end of North Basin from Lynx Bay to Fisher Bay

Rock cliffs and associated gravel beaches, barriers, and spits occur in the vicinity of Lynx Point and Cat Head. A large sandy barrier, lagoon, and inlet system appears to be present at the head of Lynx Bay (this was seen only from a distance as we crossed the mouth of the bay to conserve flying time). A variety of spits and forelands are associated with headward sediment transport toward the south along both sides of Kinwow Bay (the long narrow bay east of Sturgeon Bay). The western shore of the lake southward from Wicked Point into Fisher Bay consists of a succession of rock outcrop or boulder lag headlands trapping small beaches and barriers on their north sides. This provides clear evidence of net southward sediment transport along this reach (Fig. 15). Very thin veneers of sand and gravel pushing back over low-relief woodland and marsh along the drift-aligned northerly (updrift) sections of many cells give way downdrift to wider, swash-aligned, sandy beach and barrier ridges at the south end against the confining headlands.

The north side of Passage Point (Fig. 1), south of Jackhead Harbour, provides a good example of this pattern. An updrift, east-facing, boulder beach (including both local carbonates and Precambrian shield lithologies from across the lake) sweeps around to a small downdrift, north-facing, sandy barrier at the point (Fig. 7d). Ground surveys here (site 8201) show that the distal barrier ridge (line 1 in Fig. 16) is about 65 m wide with a pond and marsh behind. The foredune crest elevation is 220.7 m (about 3.4 m above lake level at the time of the survey), with a vegetation cover of rose, dogwood, and poplar. At this time, there was a driftwood line at 218.6 m (lakeward limit of vegetation), small berms were present at 218.3 and 217.8 m, a pebbly step had developed at the water line (217.3 m), and a wide, shallow, nearshore bar lay beyond the shallow trough. The bar crest was about 25 m lakeward of the water line in a depth of 0.2 m (Fig. 16). The sandy beachface had a mean slope of about 4° ($\tan \beta = 0.07$) from the upper driftwood to the base of the step. A broad, inactive washover platform extends landward beneath the foredune at an elevation of about 219.4 m, terminating in the marsh behind (Fig. 16). The central bay (line 2 in Fig. 16) is quite different, with a very thin, narrow, sandy beach veneer partly colonised by marsh grasses (Fig. 7d). The upper beach is a transgressive gravel sheet migrating landward into the wooded bog behind. The sand beach consists of a thin swash bar resting on an erosional surface of marsh peat with rooted tree stumps projecting through the sand (Fig. 16). A small sandy berm is present at 217.7 m elevation. The beachface slope increases from 1.8° ($\tan \beta = 0.03$) in the nearshore to 7° ($\tan \beta = 0.12$) on the upper beach and >10° ($\tan \beta > 0.18$) on the uppermost gravel storm ridge. Fresh driftwood is piled at 218.6 m at the top of the storm ridge and older driftwood is present further landward at 218.7 m. Prominent red-stained seepage flows from the sandy berm, ponding behind the swash bar, where cross-ripples reflect swash overflow and longshore drainage. A Hiller core taken on top of the berm (51°51.30'N, 97°15.38'W) contained the following lithostratigraphy (Fig. 16):

0.00-0.10 m (downcore): beach sand
0.10-1.04 m (downcore): poorly sorted sandy peat
1.04-1.43 m (downcore): humified peat with gradational upper contact to
1.43-1.44 m (downcore): stiff blue clay
1.44-1.48 m (downcore): sand
1.48-1.58 m (downcore): stiff blue clay (in auger bit)

A second core taken nearby penetrated deeper, with the following lithostratigraphy:

1.00-1.67 m (downcore): [empty]
1.67-1.90 m (downcore): stiff blue clay
1.90-1.95 m (downcore): peaty sand [displaced?]
1.95-2.05 m (downcore): stiff blue clay (in auger bit)

The general situation is transgressive, with an erosional

unconformity developing across woody peat underlain by lacustrine blue clay. This changes eastward toward the confining headland, where the barrier is relatively stable. In contrast to sites further north (e.g. north of Sturgeon Bay on the west coast and north of Berens River on the east), there is no evidence of beach-ridge progradation, perhaps reflecting more limited sediment supply or more probably because the rate of long-term lake-level rise is greater at this latitude.

Thin, discontinuous, transgressive sandy barriers over marsh are present at the head of Fisher Bay.

East shore of North Basin from The Narrows north

The east side of The Narrows and the eastern shore of North Basin north through Bloodvein Bay, past Patricia Harbour to Split Rock Point is dominated by type 2 (Fig. 3). Extensive tracts of low-relief outcrop in resistant Precambrian shield rocks (Fig. 5a) form a very irregular shoreline, often associated with a broad archipelago of small islets, with thin marsh in embayments along the landward margin (Fig. 5b). This shore type reappears in the Berens River area, from Pigeon Point to Paterson Bay (inside Sandy Bar), and in the vicinity of Poplar River, continuing some distance to the north (Figs. 1 and 3). Type-3 rock-controlled, low-relief, sandy shores with scattered pocket beaches and marsh (mapped together with type 2 in group B) are found south of Pigeon Point and locally south and north of Poplar River (Fig. 3). Type-7 rock-controlled shoreline with discontinuous sandy beaches, locally with dunes, scattered marsh, and low erosional scarps in some places extends north from Big Black River (group D shoreline in Fig. 3). Scattered outcrops, rocky islets and shoals, and occasional rocky headlands occur throughout the area, including sections mapped as group C (Fig. 3).

As the extensive sections of group C shore imply, some parts of the eastern shore have relatively abundant sand supply, which has formed large spit and barrier structures with well developed coastal dunes. The most extensive sections of sandy beach, fringing sandy barrier, sandy barrier and lagoon complexes with inlets and coastal dunes to be found on Lake Winnipeg occur along the eastern shore, in a region of very limited onshore sediment supply. Extensive sandy beaches, locally prograded, some with well-developed dunes, are present south of Berens River in the Whoopee Harbour, Flour Point, and Catfish Point areas. One of Lake Winnipeg's major spits occurs just north of Berens River at Sandy Bar (Figs. 1 and 11c). This structure has built southward in front of Paterson Bay. It has a complex structure and contains a number of dune and pond deposits that may contain useful records of lake level, sediment supply, and long-term evolutionary trends in this south-central part of North Basin. From Sandy Bar north, a succession of shallow embayments and sandy headlands is best mapped as shore type 4 (group C), although elements of other types appear in the form of low erosional banks toward the north (updrift) end of many embayments, of occasional low outcrop, and scattered boulders or boulder platform in the nearshore. This section of the lakeshore is dominated by extensive sandy beaches, showing evidence of significant progradation at many headlands, such as the McKay Point foreland, where older beach or dune ridges lie landward of the present shore, primarily on the north sides of the headlands. This pattern also occurs further north (Figs. 1 and 3), as at Bélanger Point (south of Spider Islands). Some of the beaches and barriers in the areas mapped as group C (Fig. 3) contain very large dunes, as at Spider Islands (Fig. 6c). At this site, the lagoon inlet is deflected north behind a part of the barrier anchored on the rocky island headland. The absence of obvious sediment sources for these extensive coastal sand deposits implies an offshore source on the lakefloor of eastern North Basin, an hypothesis that clearly requires further investigation.

Before leaving this section of the lake, we also note that transgressive structures are less readily observed here, in part because of the resistant shield bedrock. Nevertheless, the low erosional banks north of Berens River, noted above, and the flooded lower reaches of Pigeon River (Fig. 1) provide evidence of rising lake levels in this area. The rocky outcrop and extensive marshes of the widespread group B shores along this side of the lake (Figs. 1 and 3) are also consistent with a long-term rise in relative lake levels. Coring of representative marshes in these areas may be worthwhile.

Western shore of central lake between The Narrows and Hecla Island

This part of the lake is dominated by shore-type associations D and E (Fig. 3). It is a relatively protected area with low wave energy. Coastal cells are small and there are frequent reversals of net longshore transport direction. Narrow gravel beaches and small spits (Fig. 7a) are associated locally with low rock cliffs. Elsewhere, the shore consists of a boulder veneer or frequently varying mixtures of sand and gravel in beaches of varying width. Low sandy barriers backed by small lagoons are rare, the best example being in Jackpine Bay, north of Bushy Point on the south side of Pine Dock (12 km south of The Narrows). Extensive areas of marshy shoreline of types 0 and 1 (group A) are found at the head of Washow Bay and on the west side of Hecla Island, extending through Grassy Narrows into the northern South Basin (Fig. 3). A long narrow spit, Sandy Point, extending west from the south end of Hecla Island, appears to be undergoing transgressive overwash along much of its length and the narrowest central section is covered at high water.

Western shore of South Basin

This shore, described in detail by Penner and Swedlo (1974), consists of low sand and mixed sand-gravel beaches in the north, giving way southward to extensive low cliffs in Lake Agassiz clays, fronted by narrow sand and gravel beaches. A small, northward-growing spit and barrier structure is present just south of Riverton. However, most of this shore is characterised by net southward longshore transport, as demonstrated by north-side sand accumulation and south-side shoreline offsets at harbour structures such as Hnausa (Fig.

10a) and Gimli and at groynes north of Gimli (Figs. 9c and 10b).

Ground surveys at site 8031 (line 31 of Penner and Swedlo, 1974) show a cliff 3 to 4 m high (top elevation at 221.5 m) with a narrow gravel beach at its base, giving way below lake level to a 60 m wide veneer of sand over an erosional nearshore profile (Fig. 17). At the base of the cliff (top of beach) is an erosional clay terrace at 218.5 m elevation. The beach from this point to the water line at 217.5 m is 7.7 m wide. A band of coarse cobbles and boulders 8.4 m wide lies between the pebbly swash bar (active berm) and the nearshore sand veneer on the lakeward side. The sand gives way to soft mud and then to mud over gravel 69 m from the water line. The site survey at this location (Fig. 18) shows a scalloped cliff morphology, reflecting enhanced erosion in embayments between the boulder groynes. Overlaying this survey on a map presented as Figure 10 by Penner and Swedlo (1974), we find 100 m of cliff-top recession at the south end of the site since 1971, but only about 2 m north of the most updrift groyne at the northern property line. Enhanced erosion on the downdrift side of the groynes is clearly evident in the survey data. The recession observed since 1971 (<0.1 to 4.3 m a^{-1}) can be compared to long-term recession (1876-1971) of about 2.3 m a^{-1} and a short-term rate of 3.6 to 4.6 m a^{-1} for the five years 1961-1966 (Fig. 10 of Penner and Swedlo, 1974).

The most prominent littoral structure along the west side of South Basin is the Willow Point foreland south of Gimli (Fig. 1). The point itself consists of a boulder shoal, presumably developed by winnowing of shallow till or other coarse glacial sediments, comparable to the deposits forming Grand Marais point on the east side of the South Basin, but extending only slightly above present lake level. Anchored on this quasi-resistant headland is a transgressive barrier on the north side and a relatively protected, sediment-starved, thin marsh- and lagoon-fringing barrier on the south, the latter possibly incorporating older relict structures. The north-facing barrier, on which residential development continues to occur, has probably suffered from an enhanced sediment deficit since construction of the Gimli breakwater. Efforts to prevent proximal breaching at the northwest end, using boulder rubble, emphasise the fragility of this barrier under long-term rising lake levels at the south end of the lake. The sediment deficit in this area is strongly implied by erosion rates of 1.5 to 3 m a^{-1} observed at the northwest end of the barrier (Fig. 11 of Penner and Swedlo, 1974).

The shore south of Willow Point, including the waterfronts of Sandy Hook, Beachside, Boundary Park, Winnipeg Beach, Dunnottar, and Matlock, is heavily developed and extensively modified by shore protection structures of varying type and effectiveness. Overall, this shore is undergoing slow recession relative to the rates north and south of Gimli, except at the south end between Matlock and Sans Souci (at the western edge of Netley Marsh), where Penner and Swedlo (1974) reported erosion rates of 5 to 6 m a^{-1}.

South shore of South Basin (Netley Marsh)

A thin veneer of beach sediments forms a fringing barrier shoreline (Figs. 19, 20, 21) along the northern (Lake Winnipeg) shore of Netley Marsh (Fig. 2; Nielsen and Conley, 1994). This barrier is migrating southward over the marsh deposits by intermittent washover, which has formed large sandy washover fans and splays in a number of places. The shoreline migration is also advanced by breaching of delta lakes, the most notable present example being the wide opening into Pruden Bay. This area is interpreted as the present leading edge of southward transgression associated with glacio-isostatic uplift of the outlet region at the north end of the lake. Deltaic sedimentation accompanied by progressively rising relative lake levels and gradual inundation of the lower Red River valley has produced the extensive complex of shallow lakes, ponds, and marshes collectively known as Netley Marsh.

The shoreface slope off the delta front is relatively gentle. Measured to the 4 m isobath, it ranges from 0.003-0.006 on the west side to 0.002-0.003 on the east, and as low as 0.001 over the prodelta lobe off Main and West Channels and Pruden Bay (Fig. 2). The outer barrier east of Pruden Bay is typically thin and very low, with crest elevations in the range of 218.5 to 219.2 m (Fig. 19). It is higher (up to about 221 m) in an area of prograded dune ridges west of Main Channel, in the vicinity of site 8208 (Figs. 2 and 20), and where an eroding foredune ridge is present west of Salamonia Channel at site 8210 (Figs. 2 and 21). Many sites along this shore show a very low-angle beachface or foreshore terrace, or both (Figs. 19, 20, 21). However, sites 8210 and 8217 in the west are notably different. The beach at site 8217 is gravelly and represents a sink for eastward longshore transport of gravel. Site 8210, a short distance to the east, is an erosional shore with coarse sand and granules and a correspondingly steep beachface. However, it flattens to a shallow terrace and very subtle nearshore bar before dropping away into deeper water (Fig. 21). Low-relief nearshore bars at sites 8207, 8208, 8209, and 8212 (Figs. 19, 20, 21) were evidenced by a wide surf zone and outer breaker line along much of the central delta shore during our overflight and video survey on 7 September 1994.

East of Parisian Lake (Fig. 2), the beach is largely replaced by foreshore marsh. This is consistent with near-complete blockage by Stoney Point of sediment moving south along the eastern shore, restricting sediment supply to the eastern delta front. The principal barrier sediment sources are the Red River, entering west of Pruden Bay, and longshore transport along the southwest shore onto the western part of the Netley Marsh lakefront (Fig. 2). This is believed to account for the more extensive beaches, coarser grain size, foredune development, and associated higher barrier crest in the west (Fig. 21). The prograded dune ridges west of Main Channel (Fig. 20) may have been fed in part by landward reworking of Red River sands, although much of the river load is fine-grained sediment deposited to sinks in deeper water (Brunskill and Graham, 1979).

Southeast and east shores of South Basin

From the east side of the Red River Delta (Stoney Point) north to Elk Island and east into Traverse Bay (Winnipeg River), there is a much greater variety of shore morphology, lithology, and sedimentary processes than along the opposite shore (Fig. 3). Beaches, barrier islands, spits, and barrier-inlet complexes with dunes are present along this shore. Major embayments with sandy barriers are present at Beaconia (Patricia Beach), Grand Marais, Grand Beach, Hillside Beach, and on the south side of Elk Island (Figs. 1 and 2). These are defined by resistant points or headlands at Stoney Point, Grand Marais Point, Ironwood Point, Victoria Beach (Fig. 9b), and Elk Island, associated at least in part with outcrops of Ordovician sandstone and carbonates (Nielsen and Conley, 1994; Penner and Swedlo, 1974). Much of this coast has cliffs cut into glacial till and other ice-contact or proglacial heterogeneous deposits with a large proportion of cobbles and boulders, including some very large blocks, which armour the shore in places (Penner and Swedlo, 1974), as on the south side of Grand Marais Point (Figs. 9d and 22). Shore protection structures of limited utility (primarily porous boulder groynes) have been constructed at a number of locations, particularly in the vicinity of Balsam Bay, Grand Marais, Hillside Beach, and Victoria Beach. Erosion rates are generally less along this shore than along the west side of the South Basin (Fig. 11 of Penner and Swedlo, 1974), although rates as high as 2 m a^{-1} were recorded south of Grand Marais and rates >0.5 m a^{-1} were recorded at the north end of Grand Marais spit (up to 1 m a^{-1} there), locally to the north of Grand Beach, at Hillside Beach and Victoria Beach, along the southwest side of Elk Island, and along the south shore of Traverse Bay.

The barrier at Beaconia Lake (shore type 4) has a sandy beach with minor gravel, dunes, and a back-barrier lagoon and marsh with amalgamated flood-delta and washover deposits along the backside of the barrier. There is a large central inlet with flood delta and flanking spits (best developed on the southwest side), and a minor inlet at the northeast end of the barrier. There is also a relict recurved spit structure developed between 1946 and 1971 (Fig. 49 of Nielsen and Conley, 1994) on the northeast side of a former inlet initiated by washover breaching in 1945 or 1946, a few hundred metres northeast of the present main inlet. Nielsen and Conley (1994) have documented the evolution of the inlets by washover breaching of the formerly unbreached barrier since 1932. They also illustrate exposures of tree stumps on the lower foreshore, evidence for landward migration of the barrier.

The spit and barrier island on the south side of Grand Marais are low, narrow, mixed sand-gravel structures associated with southward sediment transport from sources on the Grand Marais Point headland. We interpret the Grand Marais spit and barrier as a largely transgressive, sediment-starved, breached fringing barrier structure originally developed along the lakeward flank of the marshy lowland lying behind it on the south side of Grand Marais. While some southward sediment transport occurs along the shore here, forming recurve structures at the south end of the spit and barrier island, the supply is limited, leading to proximal erosion and longshore cell development. Much of the transport is landward across the barrier, primarily through the inlet at the south end of the spit and around the south end of the island.

Cliff recession at the Grand Marais headland is relatively slow but locally up to about 0.5 m a^{-1} (Penner and Swedlo, 1974). The cliffs here are cut into boulder-rich glacial deposits and the shore is armoured with cobbles, boulders, and some very large blocks (Fig. 9d). The nearshore slope is steep (0.03 or 1.6°) out to depths of at least 5 m and very rough across the inner 85 m of the profile (Penner and Swedlo, 1974). Our survey at site 8128 (approximate location of line 128 of Penner and Swedlo, 1974) shows an 11 m high cliff with a wedge of coarse gravel and boulders at its base (Fig. 22). The cliff profile is concave, indicating some downslope reworking, but the erosion rate is believed to be quite slow. The basal beach is almost linear (between boulder blocks) with a slope of about 6.5° ($\tan \beta = 0.11$).

Some of the largest coastal dunes on Lake Winnipeg are found on the barrier at Grand Beach (Figs. 6d and 23). This system has developed by accumulation of southward-moving sediment against the natural groyne of Grand Marais Point. There is very little sediment movement around this point and all material produced by shore erosion south of Ironwood Point moves either offshore to deep water or alongshore to accumulate at Grand Beach. This barrier has a large central inlet, a flood delta, and a low-angle dissipative nearshore profile with low-water terrace, subtle ebb shoal, and low-relief bars (Fig. 23). The shoreface becomes steeper lakeward across a convex profile interpreted as the subaqueous base of the barrier extending approximately 200 m out to a roughly horizontal lakefloor at about 214 m elevation (typically about 3 m water depth). Although Penner and Swedlo (1974) recorded local progradation in the central part of Grand Beach with minor erosion at the southwest and northeast ends, the very low-angle nearshore slope makes any photogrammetric interpretation suspect. There is clear evidence for shoreline erosion at the northeast end of the beach and dune blowouts are associated with parabolic dune migration landward over the barrier, backbarrier flats (including the parking lot in one section), and into the lagoon (Fig. 6d). Based on ground surveys at site 8136 (west of the inlet), the dunes are typically about 65 m wide in this area and attain crest elevations of at least 227.7 m (10.0 m above the estimated water level at the time of our survey). The beach is 36 to 38 m wide with a lower foreshore slope between 1.3° and 1.5° ($0.02 \leq \tan \beta \leq 0.03$). The inner bar crest lies 90 m lakeward of the water line (Fig. 23). Although generally transgressive, this barrier complex may be building primarily upward with rising lake levels. Some lakeward progradation may also occur. The effects of a former pier have not been evaluated, but valuable documentary and photographic evidence may be available for this site because of its resort history.

The barrier at Hillside Beach has a wide inlet near its north

end and some dune development on the crest. Penner and Swedlo (1974) recorded erosion along its entire length, with the highest rates at the southwest end and alongshore to the north (east side of Victoria Beach). However, like Grand Beach, this barrier has a wide nearshore and a convex-upward shoreface profile, distinct from the steep and concave profiles characteristic of the erosional shore south of Ironwood Point. The Hillside Beach barrier is interpreted as a slowly transgressive system, with sediment being transferred landward through the inlet and by wind across the barrier. The breached tombolo structure south of Elk Island may have developed in a similar fashion. Whereas a neck of land remains between Hillside Beach and Traverse Bay, the connection is gone south of Elk Island (Fig. 1). The west-facing outer barrier has transgressed over the neck, breached, and lost sediment to Traverse Bay. Despite relatively high sediment supply from erosion of sand and/or sandstone cliffs along the southwest shore of Elk Island, most of this sediment now passes through the gap in the barrier rather than helping to rebuild it. A secondary spit has grown westward along the south side of the island behind the barrier, fed by sediment derived from cliff erosion along the east side of Elk Island and moving south along that shore.

Erosion and eastward net transport along the south shore of Traverse Bay have fed the growth of a recurved spit complex at Jackfish Point. Detailed ground study of this structure and other prograded features like it, which have grown (despite rising lake levels) because of excess sediment supply, would help to establish age relations, sediment supply rates, and lake-level trends at different locations around the basin. A general pattern of submergence along this shore is supported by the estuarine morphology of the Winnipeg River mouth at the head of Traverse Bay, attesting to limited sediment discharge from this river, as from most others draining the shield terrain along the east side of the lake. The coast north of the Winnipeg River is relatively low and characterised by a succession of shallow embayments between rock or boulder-lag headlands. Mixed sand and gravel beaches fringe the embayment shores and shallow gravelly washover veneers are present at some headland locations.

Shore protection structures

A wide variety of structures has been constructed over the years to protect residential, recreational and institutional property and facilities along much of the South Basin shoreline south of Hnausa on the west and Elk Island on the east (Figs. 1 and 3). These represent a considerable cumulative investment with widely varying success. Harbour structures such as the breakwaters at Hnausa (Fig. 10a) can function as groynes, trapping longshore sediment transport on the updrift side and creating a sediment deficiency along the adjacent shore opposite. Some new or well maintained groynes (Fig. 10b) appear to be functioning well in trapping longshore sediment transport, although poor placement may reduce or negate their effectiveness as shore protection structures. Other structures show evidence of enhancing shore erosion (Figs. 9c and 18). In general, groynes will be ineffective where insufficient sediment is available to accumulate against them, where enhanced sediment deficiency induces erosion on the net downdrift side, where net shore-normal transport is a major factor, or where erosion rates, shoreface profile changes or other factors threaten their structural integrity. Rough boulder groynes at a number of sites, many with large voids or gaps, represent leaky structures with very limited trapping efficiency, although this failing may in fact limit the damage these structures might otherwise do. Walls and revetments can also have mixed results, as demonstrated by a number of partially collapsed structures and examples of enhanced erosion along adjacent shores. As noted by Hans and Doering (1995), individual structures along a shore segment "protected" by a mixture of structure types may be competing for limited sediment and be ultimately counter-productive. The University of Manitoba project reported by Hans and Doering has compiled a data base of shore types and structures around the South Basin.

CONCLUSIONS

The shoreline of Lake Winnipeg has been classified into fifteen types on the basis of physical shore-zone characteristics. Each type represents a distinctive combination of geomorphological features and some types are composite, including repetitive sequences of shore-zone morphology and materials alongshore. The fifteen individual or composite types have been combined for discussion and mapping purposes into seven shore-type associations or groups as follows (Fig. 3):

- A predominantly low-energy marsh and deltaic shores, with or without a transgressive beach veneer (these may be subject to high-energy events under some conditions in certain areas, notably along the south end of the lake);
- B low relief Precambrian outcrop, often forming complex archipelago shorelines, with marsh development in protected embayments (restricted to the east side of the lake);
- C sand-dominated beaches, sandy spits, barriers, and fringing barriers, locally with high dune development, back-barrier lagoons, inlets, and inlet-related structures analogous to ebb- and flood-tide deltas in tidal systems;
- D a mixed group including repetitive sequences of sandy or gravelly beaches, low erosional scarps, and low-relief headlands or rock outcrop or boulder-lag shoals, locally colonised across the foreshore;
- E gravel beaches and barriers sourced predominantly from rock cliffs;
- F erosional shores in unconsolidated deposits of glacial, glacio-fluvial, or glacio-lacustrine origin, with or without basal beaches of sand or gravel;
- G shores artificially modified by construction of various protective structures.

Predominantly erosional shores are found in three main areas: at the north end of the lake west of the Nelson River outlet; along the south side of Long Point; and along the western and southeastern shores of South Basin. Significant

erosion occurs locally in sedimentary rocks along the northwest and southwest shores of North Basin and along the west side of the central lake. Transgressive processes on low-relief shores, involving sandy washover, proximal spit erosion and truncation, barrier island migration, landward dune movement, marsh transgression, valley inundation, and breaching of small back-barrier lake basins is a widespread phenomenon observed at many places virtually throughout the lake. It is not restricted to South Basin, although the most prominent transgressive shore is at the south end of the lake across Netley Marsh. Other evidence of increasing relative lake levels in South Basin includes an apparently ergodic set of headland and barrier structures at progressively more advanced stages of evolution from south to north along the southeast shore - from Beaconia (Patricia Beach) in the south (where development from an unbreached narrow barrier to a complex barrier-inlet system has been documented over the past 60 years of the airphoto and map record) to Grand Marais, Grand Beach, Hillside Beach, and Elk Island. Local progradation and accretion continues at some sites, despite rising water levels, if sediment supply is sufficient (e.g. the prograded dune-ridge sequence at site 8208 near Main Channel of Red River - Fig. 20). Extensive sets of prograded beach- and dune-ridge deposits are found along the east and southwest shores of North Basin, but are rare further south. This may represent a mixture of factors including sediment supply and a north-to-south increase in the rate of lake-level rise. Estuarine-style flooding of the lower Winnipeg River in South Basin and Pigeon River in North Basin is suggestive of rising water levels in both parts of the lake. The large prograded beach-ridge complex in Limestone Bay (apparently at quite a low level) and the enigmatic submerged ridges behind Limestone Point spit in the bay are strongly suggestive of a basin-wide increase in mean lake level over recent centuries, but the details, mechanism, and chronology of this change are unknown.

A number of key questions can be posed concerning the history of Lake Winnipeg as it relates to shoreline evolution and stability and several promising lines of investigation may provide answers to these questions, including evidence bearing on wider climatic and tectonic issues. Geological records preserved in beach-ridge, spit, barrier, and back-barrier deposits and in various marsh complexes scattered about the lake should be examined on a priority basis. The basin-wide distribution of erosion rates, transgression rates, and runup should be examined in relation to lithology, exposure, lake levels, and storm events.

Among major outstanding research issues, we note the following:

- the history of large deposits in the North Basin (Limestone Point spit and Limestone Bay beach ridges, Sandy Bar near Berens River, gravel barriers along the western shore) and their implications for lake levels and sediment supply processes over time;
- the sources of sand forming extensive sandy beach and dune deposits along the eastern shore of the North Basin;
- the rate of colonisation of gravel platform and beach deposits and implications for lake-level and runup variability at sites along the west side of the lake;
- the origin of transgressive barriers at Willow Point, Grand Marais, and the Elk Island tombolo in relation to basin tilting and lake-level fluctuations;
- evidence for relict beach and nearshore features on the lakefloor and their implications for shoreline change and migration under southward basin tilting;
- sand transport rates alongshore and offshore and the extent and volume of nearshore sand in South Basin, in relation to the shore erosion problem and shoreface profile evolution;
- the role of shore structures in exacerbating erosion problems at some sites;
- nearshore sediment transport dynamics in relation to the maintenance of barrier and dune structures at sites in South and North Basins;
- rates of landward migration along the south shore of the lake and of erosion and sediment production at the north end;
- relation of shoreline recession to nearshore profile development and rates and extent of downcutting on the shoreface;
- the importance of frazil, slush, and anchor-ice sediment transport during freeze-up, of ice piling and lake-bottom scour during winter and spring, and the time variability of these processes.
- wind-driven water level fluctuations and their role in cross-shore transport;
- long-term variability in storminess, water level fluctuations, and wave energy in relation to shoreline evolution ;
- basin-wide variation in lake-level history and the shoreline response as a function of shore type and exposure.

ACKNOWLEDGEMENTS

We wish to thank Northway Aviation (Riverton), and pilot Chris Bridge in particular, for providing safe access to remote parts of the Lake Winnipeg shore and a reasonably stable platform for the aerial video and photography. We are grateful to Arnold Swedlo (Manitoba Natural Resources) for providing background information and turning up some of the original 1970s survey data. Thanks are due also to Ole Larsen of the Water Survey of Canada in Winnipeg for his assistance in providing data from water level recording stations on the lake. Erik Nielsen (Manitoba Energy and Mines) provided valuable local assistance in the field and collaborated in the resurvey of his 1990 beach profiles along the south end of the lake. We are pleased to acknowledge the efforts of Harvey Thorleifson, Mike Lewis, and Brian Todd (Geological Survey of Canada), together with Erik Nielsen (Manitoba Energy and Mines), in initiating this project and bringing it to fruition. We appreciate the support and encouragement of Randy Raban and Halina Zbigniewicz (Manitoba Hydro) and Jay Doering (University of Manitoba). Manuscript reviews by Brian Todd and Mike Lewis were helpful and constructive. This project was financially

supported by the Geological Survey of Canada, the Province of Manitoba, and Manitoba Hydro.

REFERENCES

Brunskill, G.J. and Graham, B.W.
1979. The offshore sediments of Lake Winnipeg; Canadian Fisheries and Marine Service, Manuscript Report 1540, 75 p.

Cheng, W.K.
1972. Longshore transport in the South Basin of Lake Winnipeg; Unpublished M.Sc. thesis, University of Manitoba, Winnipeg, 295 p.

Einarsson, E. and Lowe, A.B.
1968. Seiches and setup on Lake Winnipeg; Limnology and Oceanography, v. 13, p. 257-271.

Franklin, J.
1823. Narrative of a journey to the shores of the Polar Sea in the years 1819, 1820, 1821, and 1822; John Murray, London (reprinted by M.G. Hurtig, Edmonton, 1969), 768 p.

Hans, P. and Doering, J.C.
1995. An overview of the shoreline of the South Basin of Lake Winnipeg [abstract]; in Lake Winnipeg Workshop, Winnipeg, March 1995; Manitoba Energy and Mines, Winnipeg, n.p.

Johnston, W.A.
1946. Glacial Lake Agassiz, with special reference to the mode of deformation of the beaches; Geological Survey of Canada, Ottawa, Bulletin 7, 20 p.

Klassen, R.W.
1983. Lake Agassiz and the late glacial history of northern Manitoba; in eds. J.T. Teller and L. Clayton, Glacial Lake Agassiz, Geological Association of Canada, Special Paper, v. 26, p. 97-115.

Kushnir, D.W.
1971. Sediments in the South Basin of Lake Winnipeg; Unpublished M.Sc. thesis, University of Manitoba, Winnipeg, 92 p.

Mackenzie, A.
1801. Voyages from Montreal on the River St. Lawrence, through the continent of North America, to the frozen and Pacific Oceans...; T. Cadell and W. Davies, London (reprinted by Macmillan of Canada, Toronto, 1970), 412 p.

Manitoba Mineral Resources Division.
1979. Geological map of Manitoba; Map 79-2, scale 1:1,000,000.

1981. Surficial geological map of Manitoba; Map 81-1, scale 1:1,000,000.

Manitoba Water Resources Division.
1977. The Lake Winnipeg shoreline handbook: a property owner's guide to shoreline processes and erosion protection structures on the Southern Pool of Lake Winnipeg; Manitoba Department of Mines, Resources and Environmental Management, Winnipeg, 46 p.

Nielsen, E. and Conley, G.
1994. Sedimentology and geomorphic evolution of the south shore of Lake Winnipeg; Manitoba Department of Energy and Mines, Winnipeg, Geological Report GR94-1, 58 p.

Nielsen, E., McNeil, D.H. and McKillop, W.B.
1987. Origin and paleoecology of post-Lake Agassiz raised beaches in Manitoba; Canadian Journal of Earth Sciences v. 24, p. 1478-1485.

Penner, F. and Swedlo, A.
1974. Lake Winnipeg shoreline erosion, sand movement, and ice effects study; Water Resources Branch, Manitoba Department of Mines, Resources and Environmental Management; Lake Winnipeg, Churchill and Nelson Rivers Study Board, Winnipeg, 110 p.

Solohub, J.T.
1967. Grand Beach: a test of grain-size distribution statistics as indicators of depositional environments; Unpublished M.Sc. thesis, University of Manitoba, Winnipeg, 118 p.

Taylor, R.B., Carter, R.W.G., Forbes, D.L. and Orford, J.D.
1986. Beach sedimentation in Ireland: contrasts and similarities with Atlantic Canada; Geological Survey of Canada, Paper 86-1A, p. 55-64.

Teller, J.T. and Bluemle, J.P.
1983. Geological setting of the Lake Agassiz region; in eds. J.T. Teller and L. Clayton, Glacial Lake Agassiz; Geological Association of Canada, Special Paper 26, p. 7-20.

Teller, J.T., Thorleifson, L.H., Dredge, L.A., Hobbs, H.C. and Schreiner, B.T.
1983. Maximum extent and major features of Lake Agassiz; in eds. J.T. Teller and L. Clayton, Glacial Lake Agassiz; Geological Association of Canada, Special Paper 26, p. 43-45 and map, scale 1:3,000,000.

Thorleifson, L.H.
1983. The eastern outlets of Lake Agassiz. Unpublished M.Sc. thesis, University of Manitoba, Winnipeg, 87 p.

Upham, W.
1890. Report on the exploration of the glacial Lake Agassiz in Manitoba; Annual Reports, Geological and Natural History Survey of Canada (New Series), 4E, p. 1-121.

Veldman, W.M.
1969. Shoreline processes on Lake Winnipeg; Unpublished M.Sc. thesis, University of Manitoba, Winnipeg, 215 p.

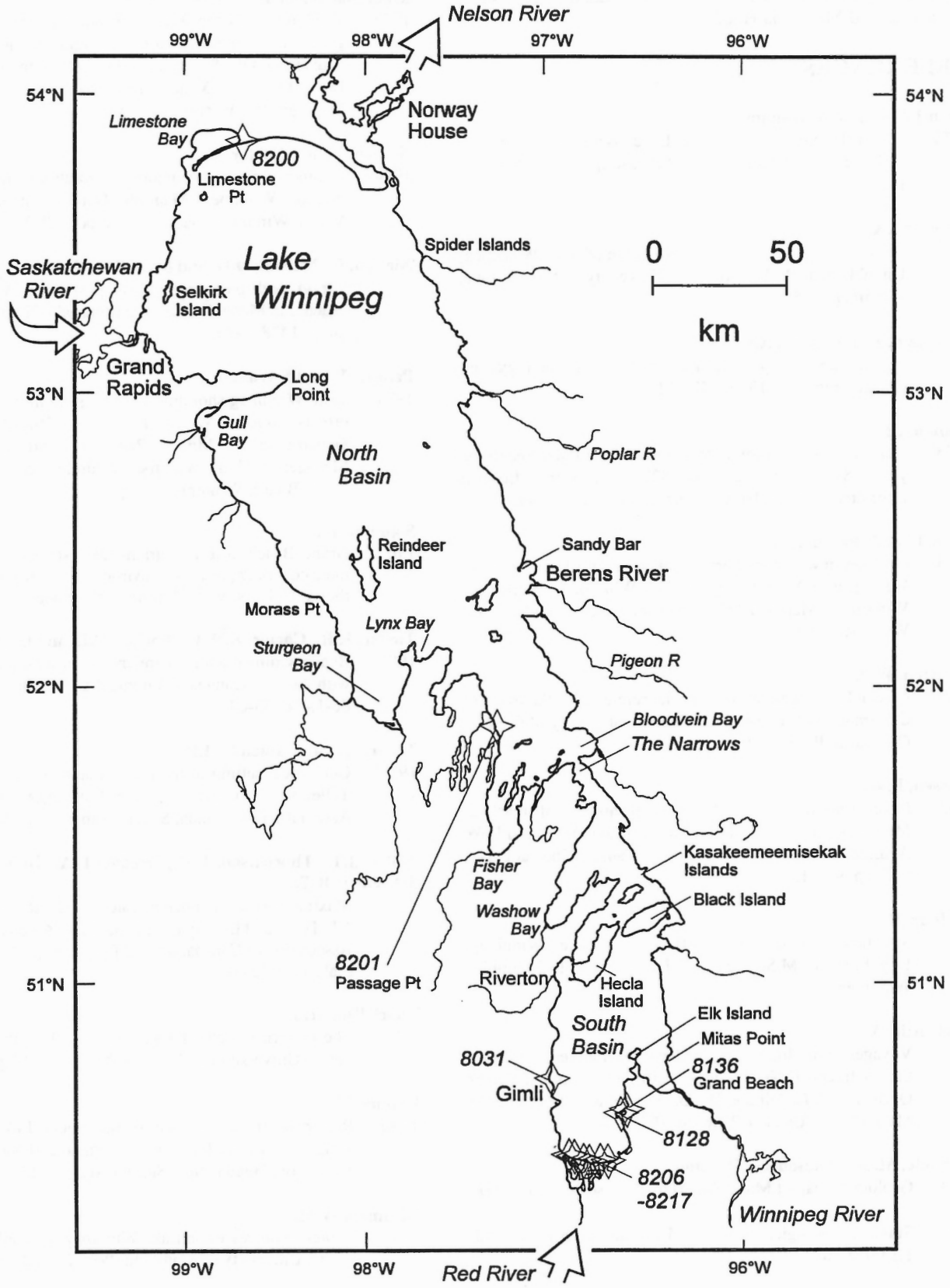

Figure 1. Lake Winnipeg shoreline, showing major rivers, key place names and locations of 1994 ground surveys (with site numbers).

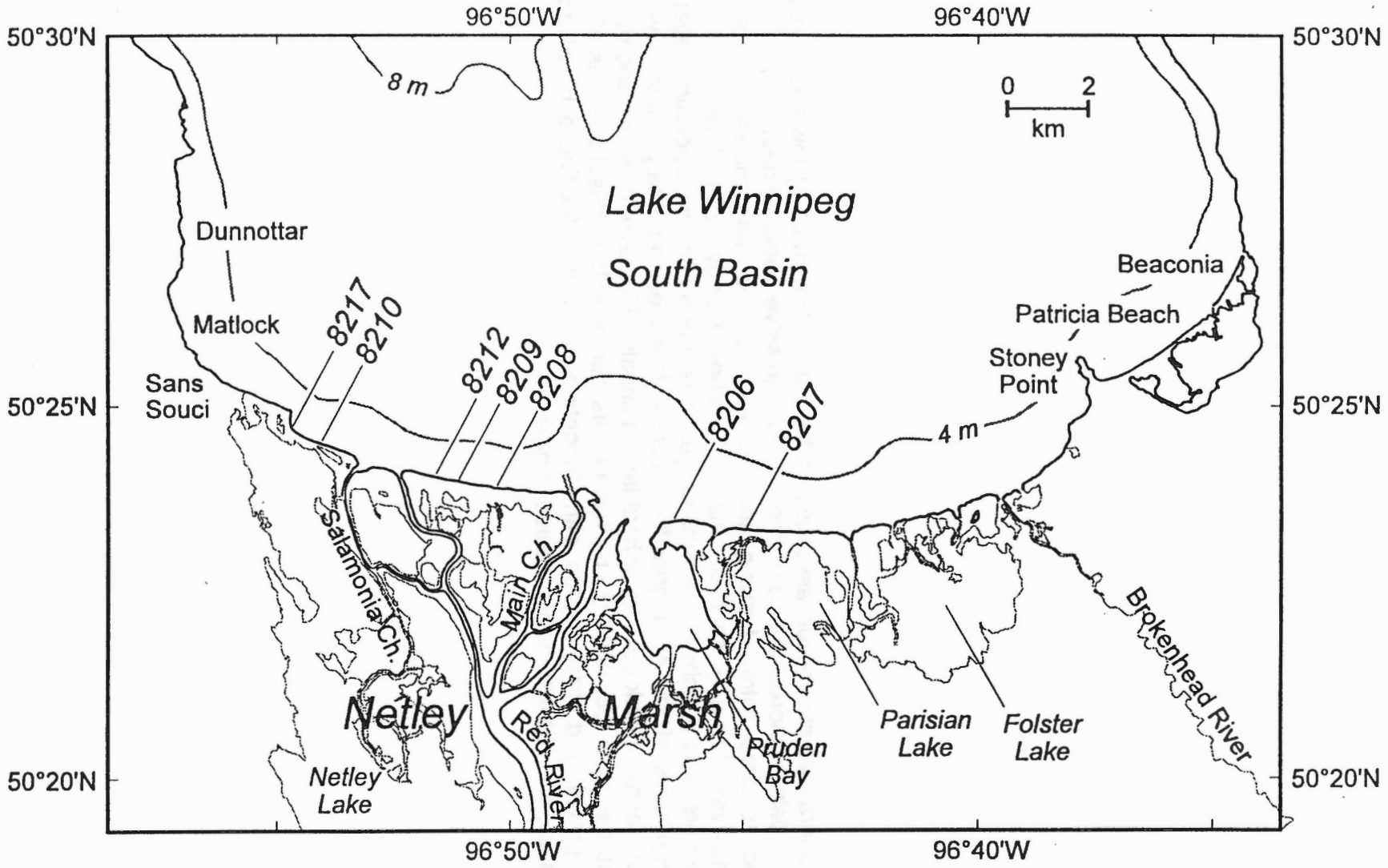

Figure 2. Netley Marsh shore and Red River delta at south end of South Basin, Lake Winnipeg, showing 1990 ground survey sites of Nielsen and Conley (1994) and sites resurveyed as part of this project in September 1994. Generalised bathymetry adapted from Brunskill and Graham (1979).

Figure 3. Generalised shore-type associations for Lake Winnipeg: (A) low-energy marsh and deltaic shores (with or without a transgressive beach veneer); (B) low-relief rock outcrop (often forming complex archipelagos, with marsh in protected embayments); (C) sand-dominated beaches (sandy spits, barriers, fringing barriers, and beaches); (D) a heterogeneous group often incorporating repetitive sequences of sandy or gravelly beaches, low erosional scarps, and low-relief headlands of rock outcrop or boulder-lag shoals; (E) gravel beaches and barriers sourced from rock cliffs; (F) unlithified cliffs with or without basal beaches of sand or gravel, and steep slopes with discontinuous failures feeding a basal gravel beach; and (G) artificially modified shores.

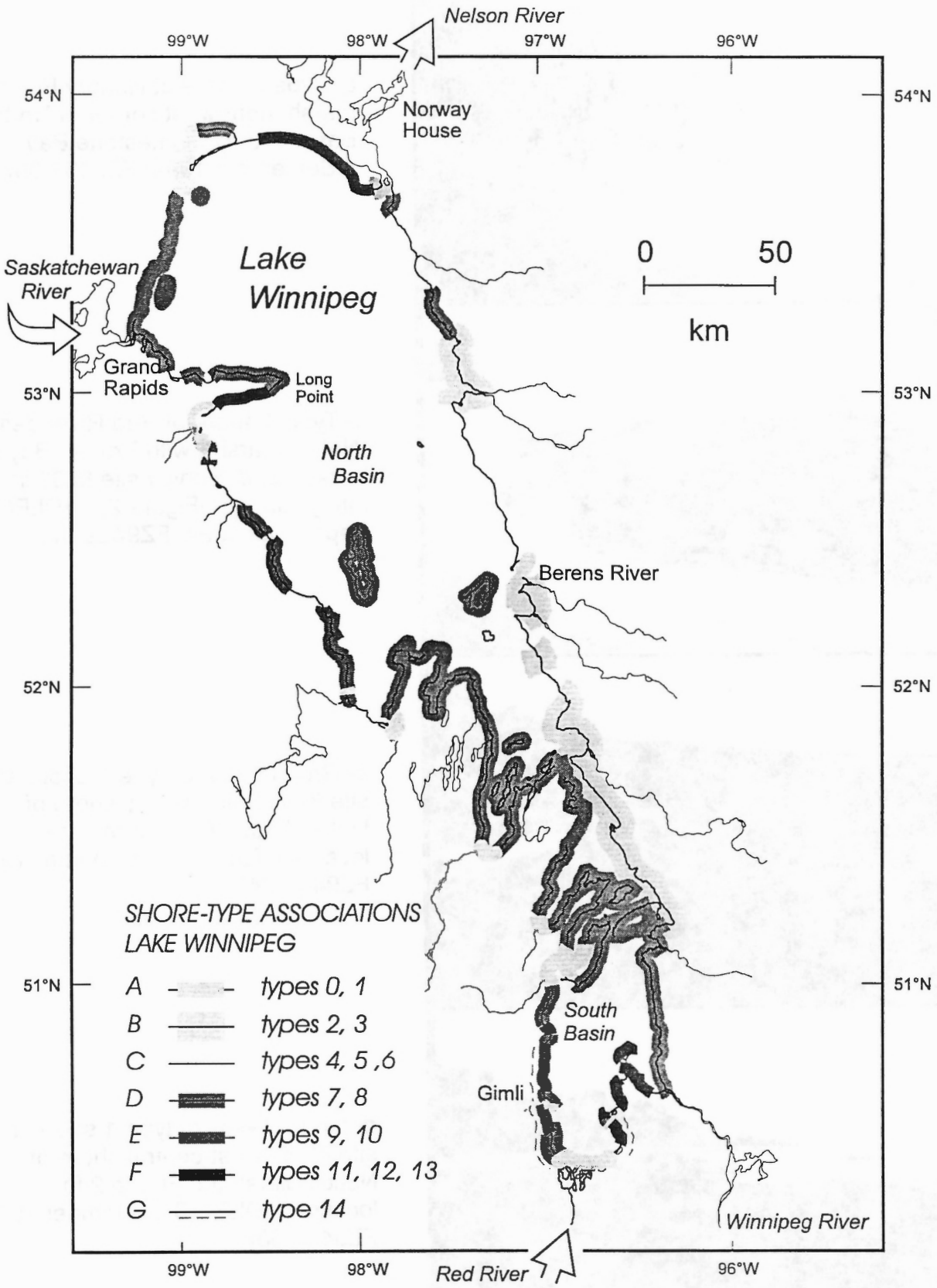
Nelson River
99°W
98°W
97°W
96°W
54°N
53°N
52°N
51°N
Norway House
Lake Winnipeg
Saskatchewan River
0
50
km
Grand Rapids
Long Point
North Basin
Berens River
South Basin
Gimli
Winnipeg River
Red River
SHORE-TYPE ASSOCIATIONS
LAKE WINNIPEG
A types 0, 1
B types 2, 3
C types 4, 5 ,6
D types 7, 8
E types 9, 10
F types 11, 12, 13
G type 14

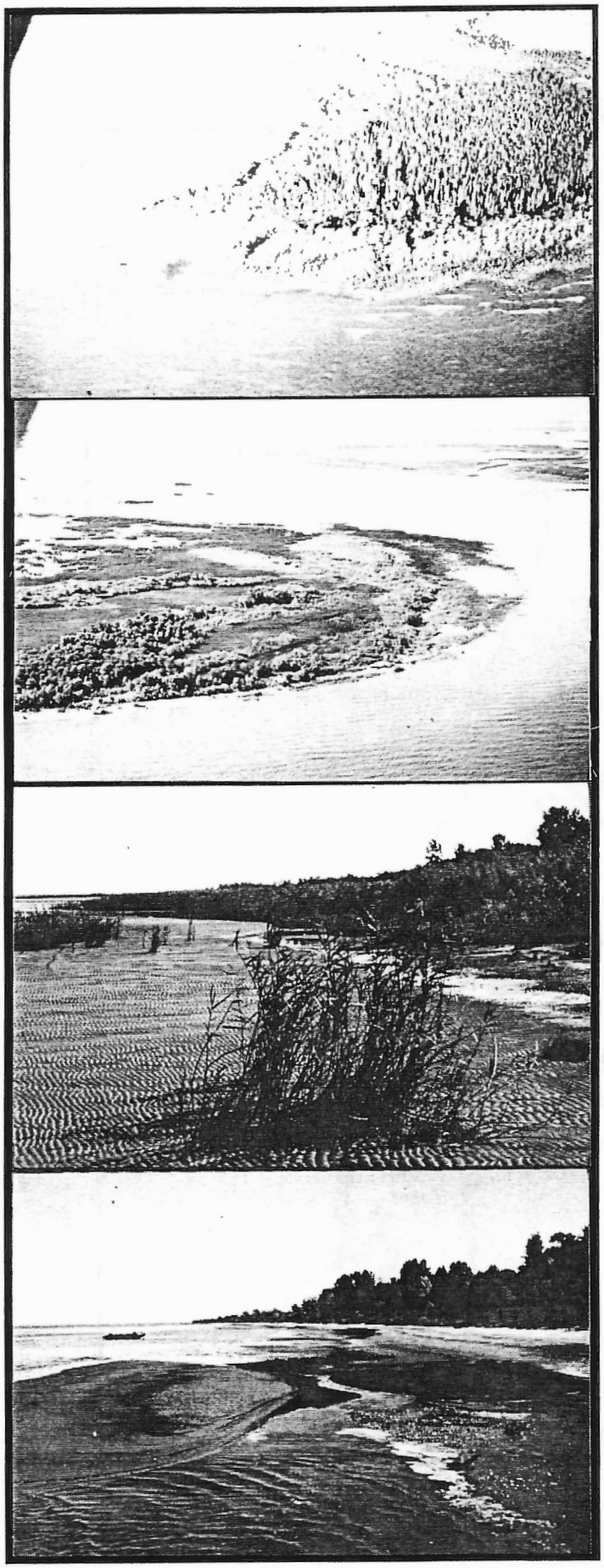

Figure 4. Shore-type association A.

a- Type-0 shore at Hungry Point marsh, northwest corner of North Basin south of Limestone Bay. [DLF/ 9 September 1994/ FZ9434-06]

b- Type-1 shore of Red River delta (Netley Marsh), with Pruden Bay in background. Survey site 8206 in left foreground (cf. Figure 2). [DLF/ 7 September 1994/ FZ9422-07]

c- Ground view of type-1 shore at site 8207, east-central shore of Netley Marsh (cf. Figure 2 for location). [DLF/ 13 September 1994/ FZ9441-24]

d- Ground view of type-1 shore at site 8208, west-central shore of Netley Marsh (cf. Figure 2 for location). [DLF/ 13 September 1994/ FZ9441-33]

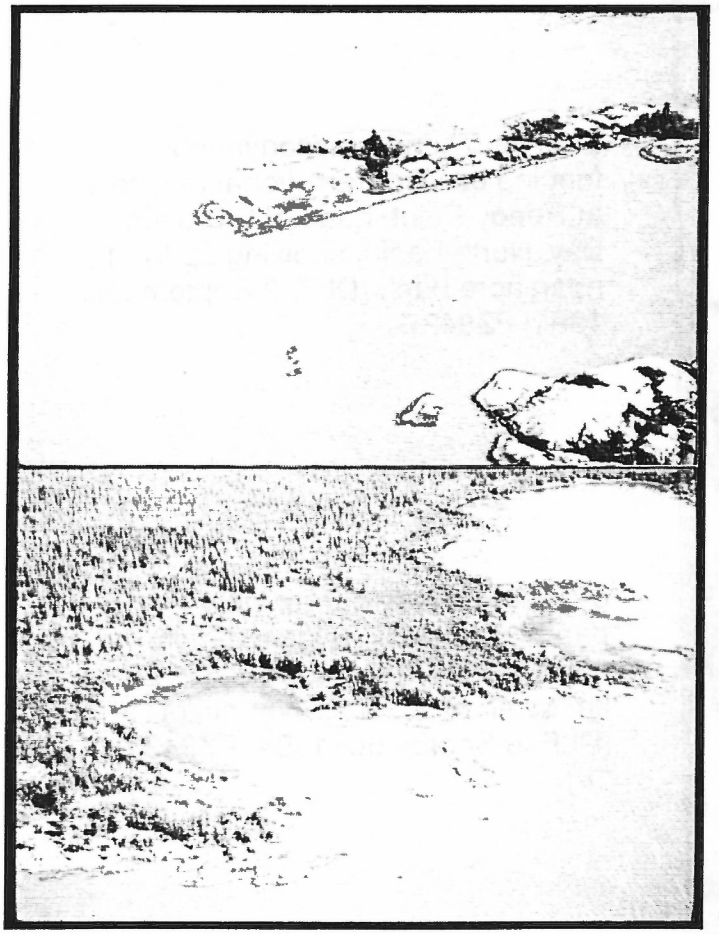

Figure 5. Shore-type association B.

a- Type-2 shore of bare Precambrian outcrop with a few scattered boulders, Kasakeemeemisekak Islands archipelago, east central Lake Winnipeg. [DLF/ 7 September 1994/ FZ9425-18]

b- Type-2 shore south of Pigeon Point, southeast North Basin, showing marsh developed in embayment behind outer fringe of bare outcrop headlands and islands.

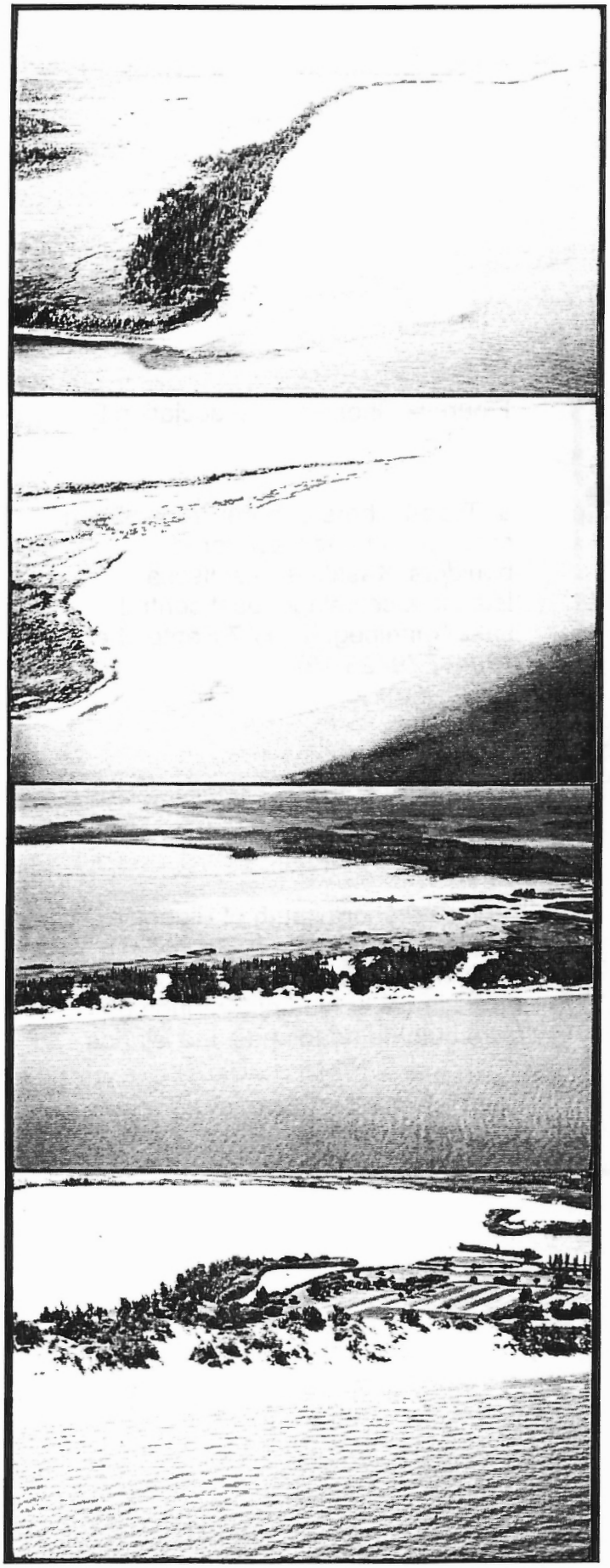

Figure 6. Shore-type association C.

a- Type-6 sandy barrier at Morass Point, west of Reindeer Island, North Basin, Lake Winnipeg. Note trees on relict beach ridges landward of the active beach and bog behind. This site is transitional to type 8, represented by the lag shoal in the foreground. [DLF/ 9 September 1994/ FZ9436-38]

b- Type-5 sandy, discontinuous, fringing barrier (transitional to type 1) at Reedy Point, head of Sturgeon Bay, North Basin, showing up to 11 nearshore bars. [DLF/ 9 September 1994/ FZ9437-31]

c- Type-4 sandy barrier with parabolic dunes, Spider Islands, northeast shore of North Basin 25 km south of Nelson River outlet. [DLF/ 8 September 1994/ FZ9430-14]

d- Type-4 sandy barrier with wide, dissipative, low-water flats and high dune ridge with parabolic blowouts, Grand Beach, east shore of South Basin. Dunes at right are migrating onto park lawn and carpark. Site 8136 survey profile (line 01) runs through blowout at far left (cf. Figure 23). [DLF/ 7 September 1994/ FZ9423-01]

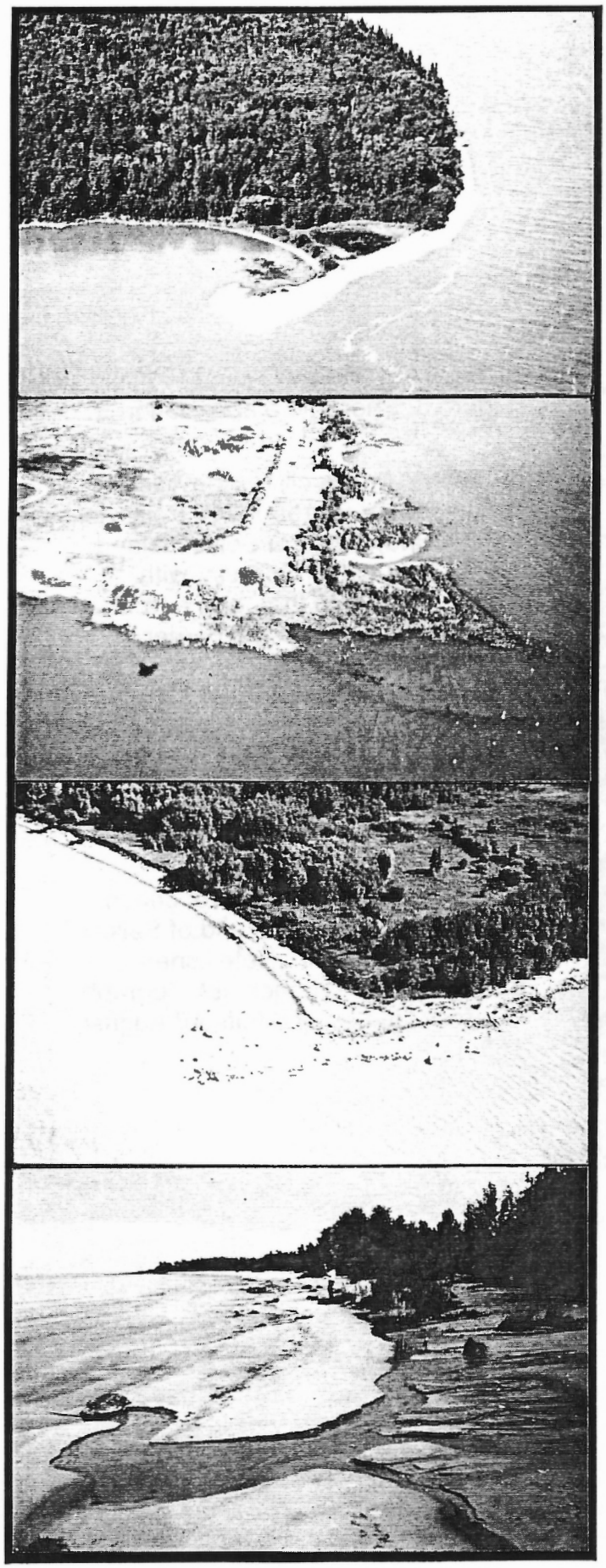

Figure 7. Shore-type association D.

a- Type-7 rock-controlled shore with small gravel spit, enclosed lagoon and protected boulder-lined shore behind spit, Bushy Point, west shore south of The Narrows. [DLF/ 7 September 1994/ FZ9426-19]

b- Type-8 boulder shoal anchoring the urbanised transgressive barrier at Willow Point south of Gimli. Note shoal extending along the face of the barrier to the west (top right) and vegetation extending into the water. [DLF/ 7 September 1994/ FZ9421-28]

c- Type-8 mixed sand-gravel foreland anchored on boulder lag shoal near Mitas Point, east shore of South Basin south of Black Island. [DLF/ 7 September 1994/ FZ9424-09]

d- Ground view looking east along type-7 beach at Passage Point (site 8201), showing thin sandy beach veneer with scattered boulders overlying peat and clay at line 2 (core site). Sandy barrier (vicinity of line 1) anchored on Passage Point headland in the distance. Beach grades to cobbles and boulders alongshore to the northwest (behind camera). Note colonising vegetation on the upper beach. [DLF/ 10 September 1994/ FZ9439-08]

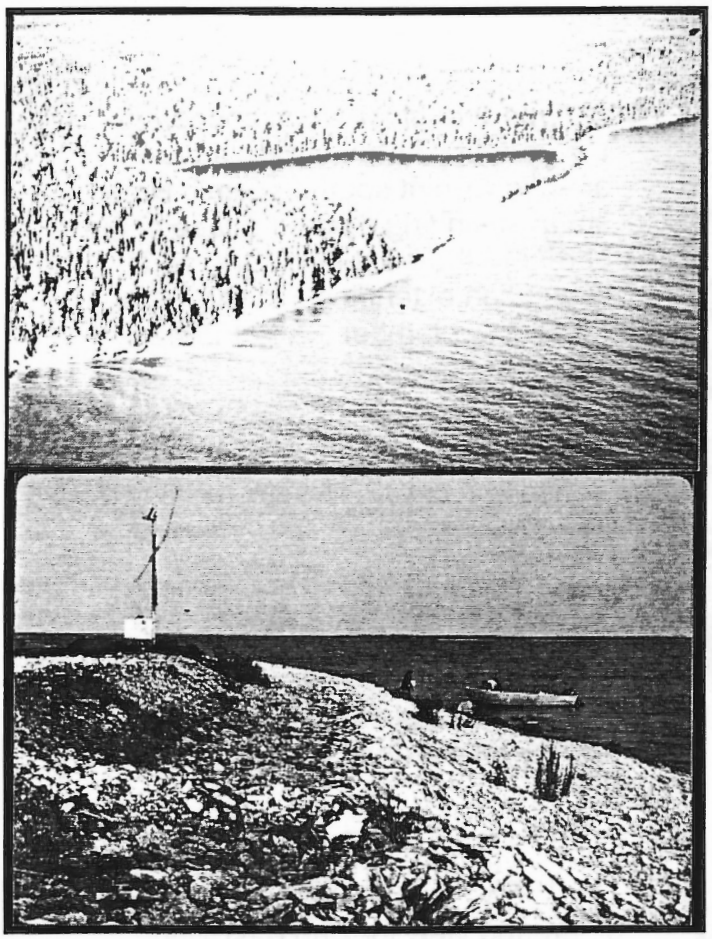

Figure 8. Shore-type association E.

a- Type -10 rock cliff (Ordovician limestone) at Sturgeon Gill Point (left foreground), north of Selkirk Island, west shore of North Basin, with longshore drift to the north and west feeding a narrow gravel barrier and beach in distance. [DLF/ 9 September 1994/ FZ9434-21]

b- Stacked berms on gravel beach (shore type 9) at north end of Selkirk Island, North Basin. Note lichen growth on upper beach. [photograph courtesy Harvey Thorleifson/ August 1994]

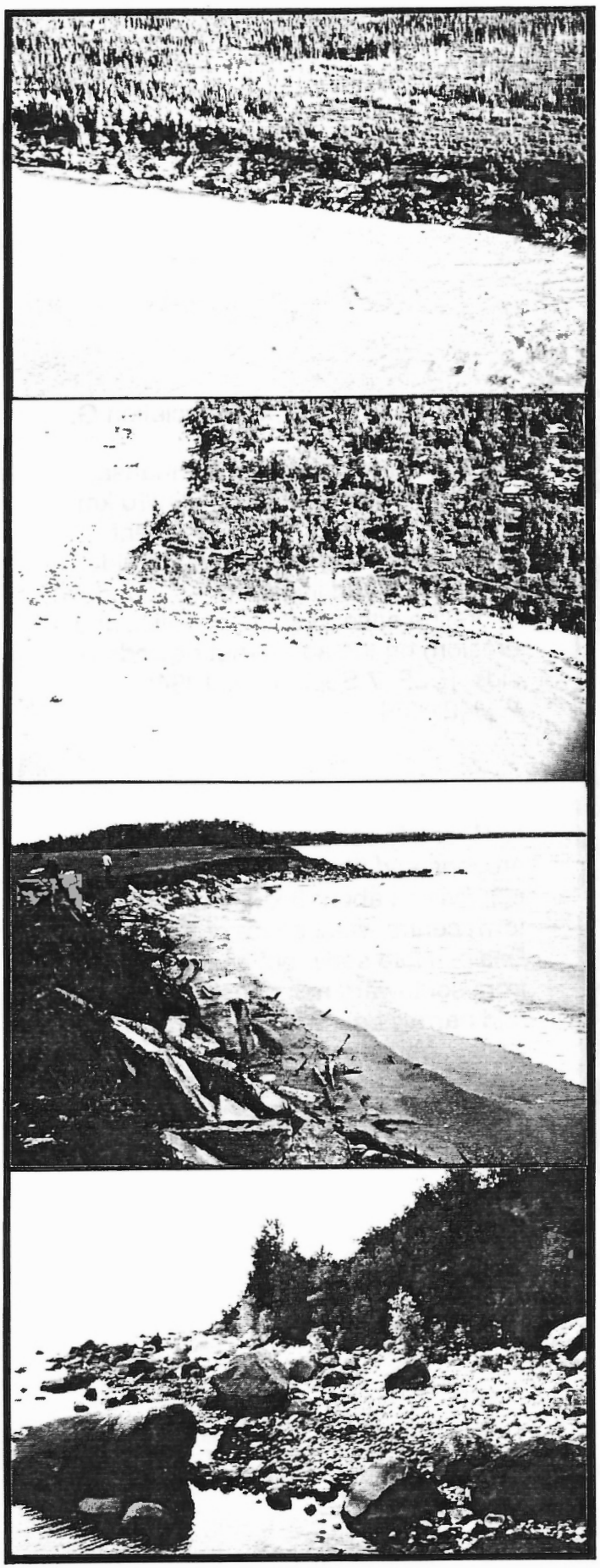

Figure 9. Shore-type association F.

a- Slumping bluffs of type 13 along northern shore of North Basin west of Nelson River outlet, Lake Winnipeg. [DLF/ 9 September 1994/ FZ9433-14]

b- Partially stabilised cliffs at Victoria Beach, east shore of South Basin north of Grand Beach. Note wide boulder lag shoal and wedge of colluvium covering the greater part of the cliff scarp. [DLF/ 7 September 1994/ FZ9423-13]

c- Severe erosion in lee of boulder groyne and concrete rubble armouring of type-12 cliff in Lake Agassiz clay, field 5 km north of Gimli (site 8031, line 31 of Penner and Swedlo, 1974). [DLF/ 11 September 1994/ FZ9441-03]

d- Coarse gravel beach with boulders at base of type-12 cliff, Grand Marais (site 8128, line 128 of Penner and Swedlo, 1974). [DLF/12 September 1994/ FZ9441-17]

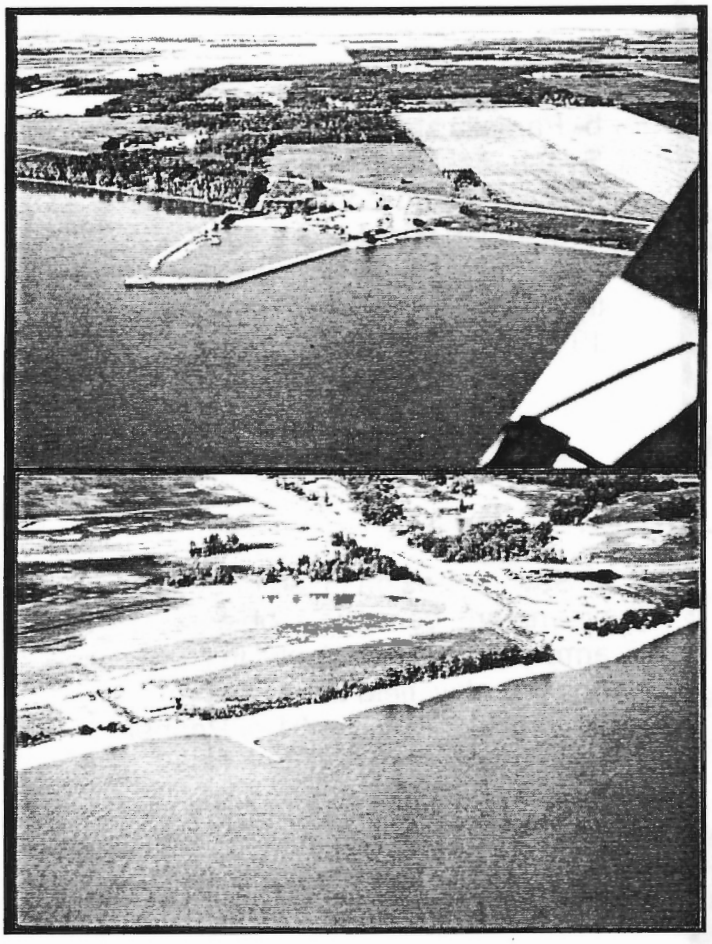

Figure 10. Shore-type association G.

a- Harbour breakwaters at Hnausa, western shore of South Basin 10 km south of Riverton. Note sediment accumulation against the north-side breakwater and inside harbour and shoreline offset (sediment deficit and erosion) on the south (net downdrift) side. [DLF/ 7 September 1994/ FZ9421-05]

b- Recently constructed boulder groynes and house in new subdivision about 3 km north of Gimli town centre, west shore of South Basin. Note sediment accumulation from southward net longshore drift and narrow beach immediately in front of house on the south side of the nearest groyne. [DLF/ 7 September 1994/ FZ9421-21]

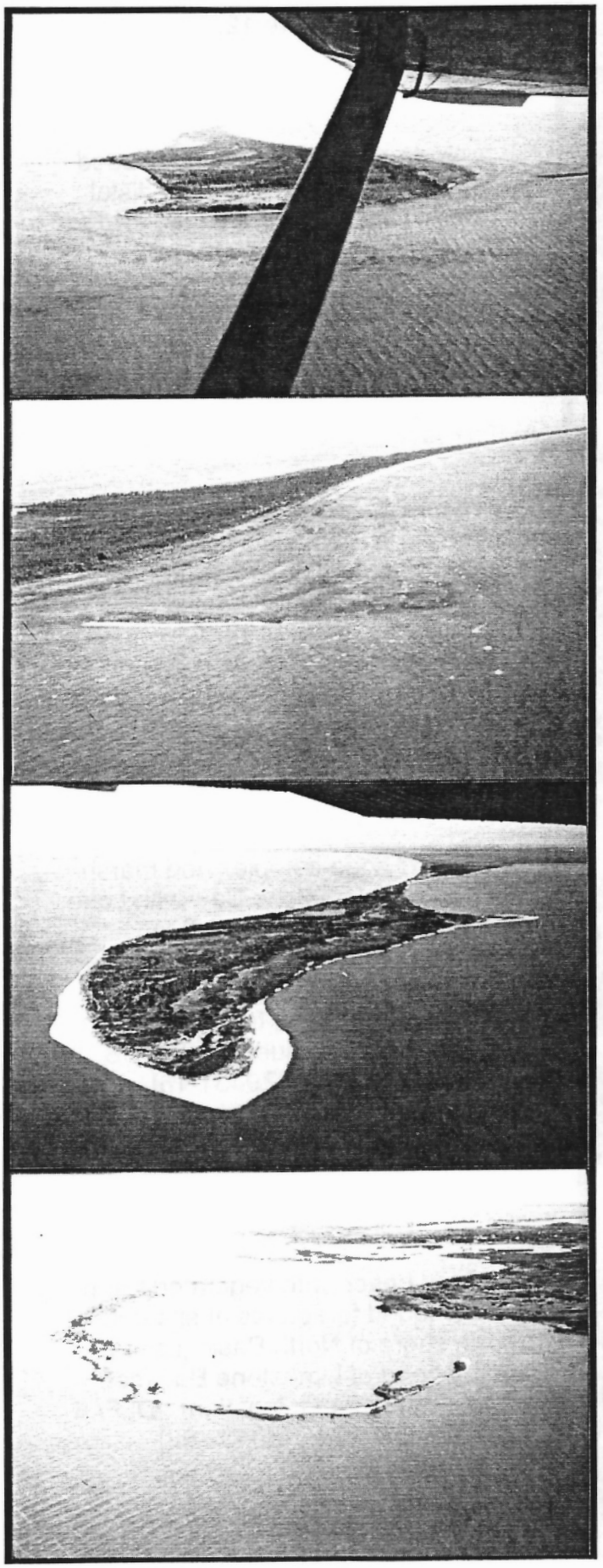

Figure 11.

a- Looking northeast along axis of Limestone Point spit with Limestone Bay at left, northwest corner of North Basin. Note recurve structures. [DLF/ 8 September 1994/ FZ9431-29]

b- Wide spit platform in lee of bedrock shoal at distal end of Limestone Point spit. [DLF/ 8 September 1994/ FZ9431-27]

c- Complex spit structure of Sandy Bar, north of Berens River, east shore of North Basin. [DLF/ 8 September 1994/ FZ9429-33]

d- Grand Marais barrier island with Grand Marais spit and cliffs (site 8128) in far distance, east shore of South Basin. [DLF/ 7 September 1994/ FZ9422-22]

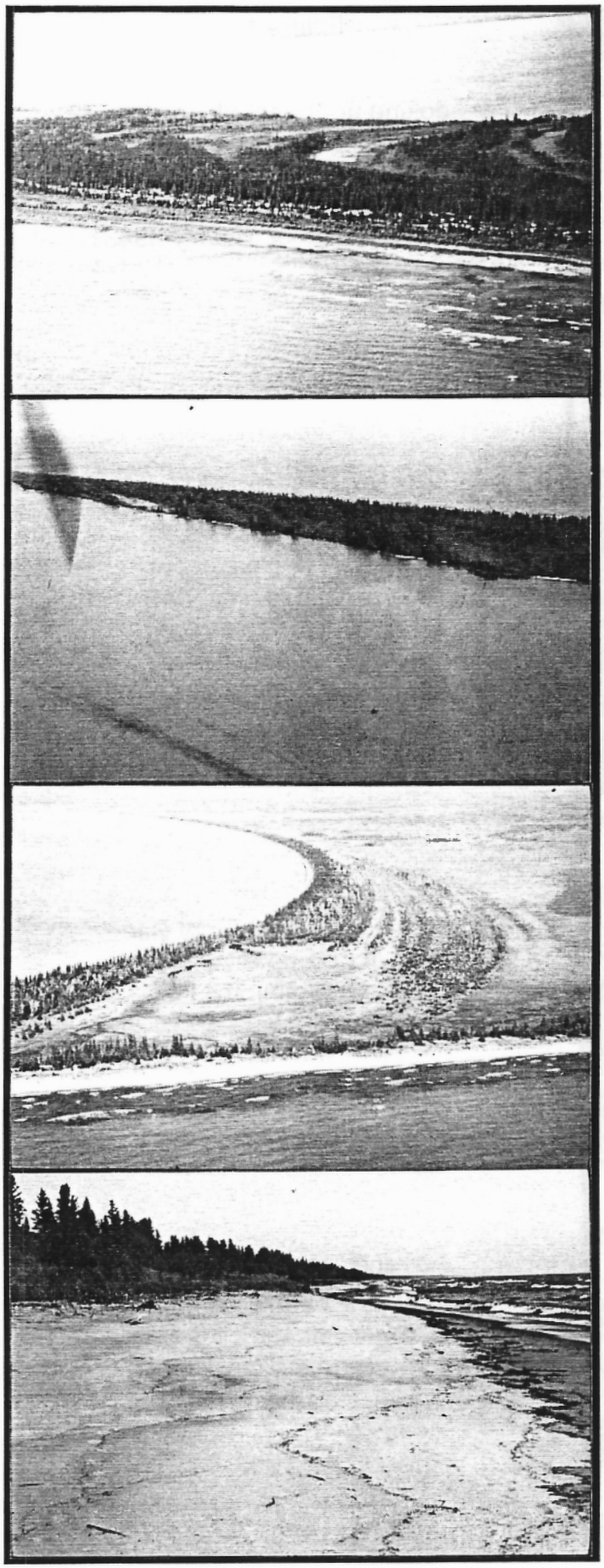

Figure 12.

a- Wide surf zone, beach, wooded dunes and recurved ridges, distal end of Limestone Point spit. [DLF/ 8 September 1994/ FZ9431-25]

b- Limestone Bay shore of Limestone Point spit, with line of aquatic vegetation in foreground, indicating suspected position of a submerged ridge. [DLF/ 8 September 1994/ FZ9431-34]

c- Beach-ridge complex and marsh at head of Limestone Bay, with Lake Winnipeg shore (site 8200) in foreground. The latter consists of a transgressive fringing sandy barrier and foredune ridge, truncating the bayhead ridge sequence. [DLF/ 8 September 1994/ FZ9431-16]

d- Sand beach with vegetated berm and wooded foredunes at site 8200, north shore of North Basin just east of the head of Limestone Bay (see Figs. 1 and 12c for location). [DLF/ 8 September 1994/ FZ9432-02]

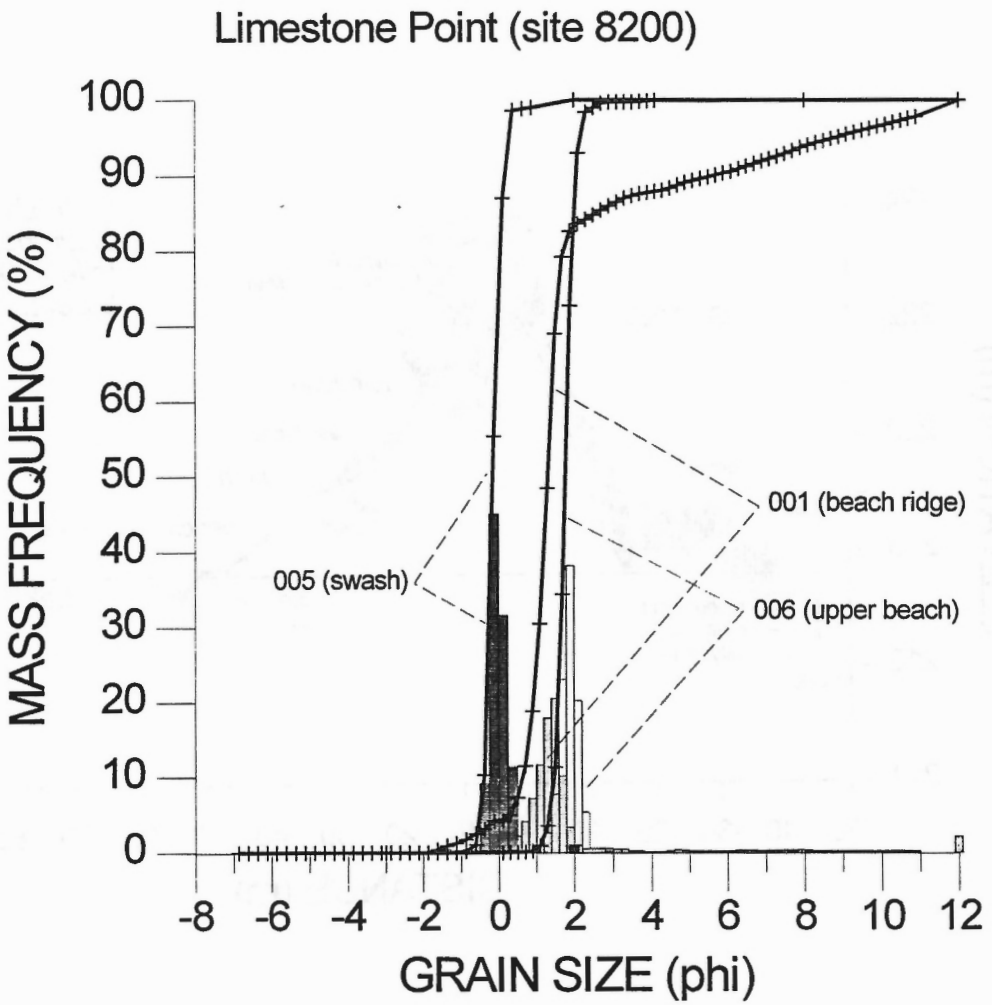

Figure 13. Mass-frequency histograms and cumulative grain-size distributions for three samples from north shore of North Basin near head of Limestone Bay (site 8200). See Figures 1 and 14 for locations. Sample 001 from base of core (interpreted as relict beach-ridge sand), sample 005 from swash concentrate on outer beach, and sample 006 from berm-face on outer beach.

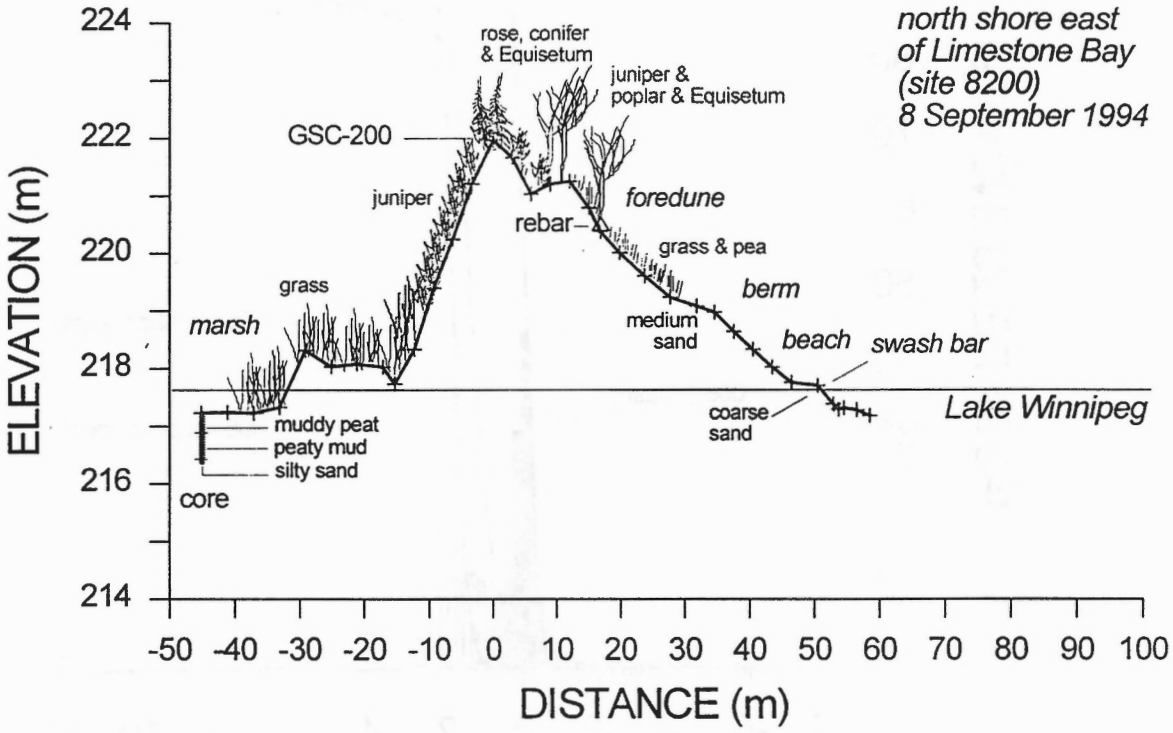

Figure 14. Surveyed shore profile at north shore east of Limestone Bay (site 8200). See Figure 1 for location. Vertical exaggeration ~8.9x (identical to Figs. 16, 19, 20, 21). Vegetation schematic, incomplete, and not to scale. Lake to right with approximate water level at time of survey. Horizontal origin at benchmark on dune crest (GSC-200); rebar represents a secondary benchmark. Also shows core location and approximate lithostratigraphy.

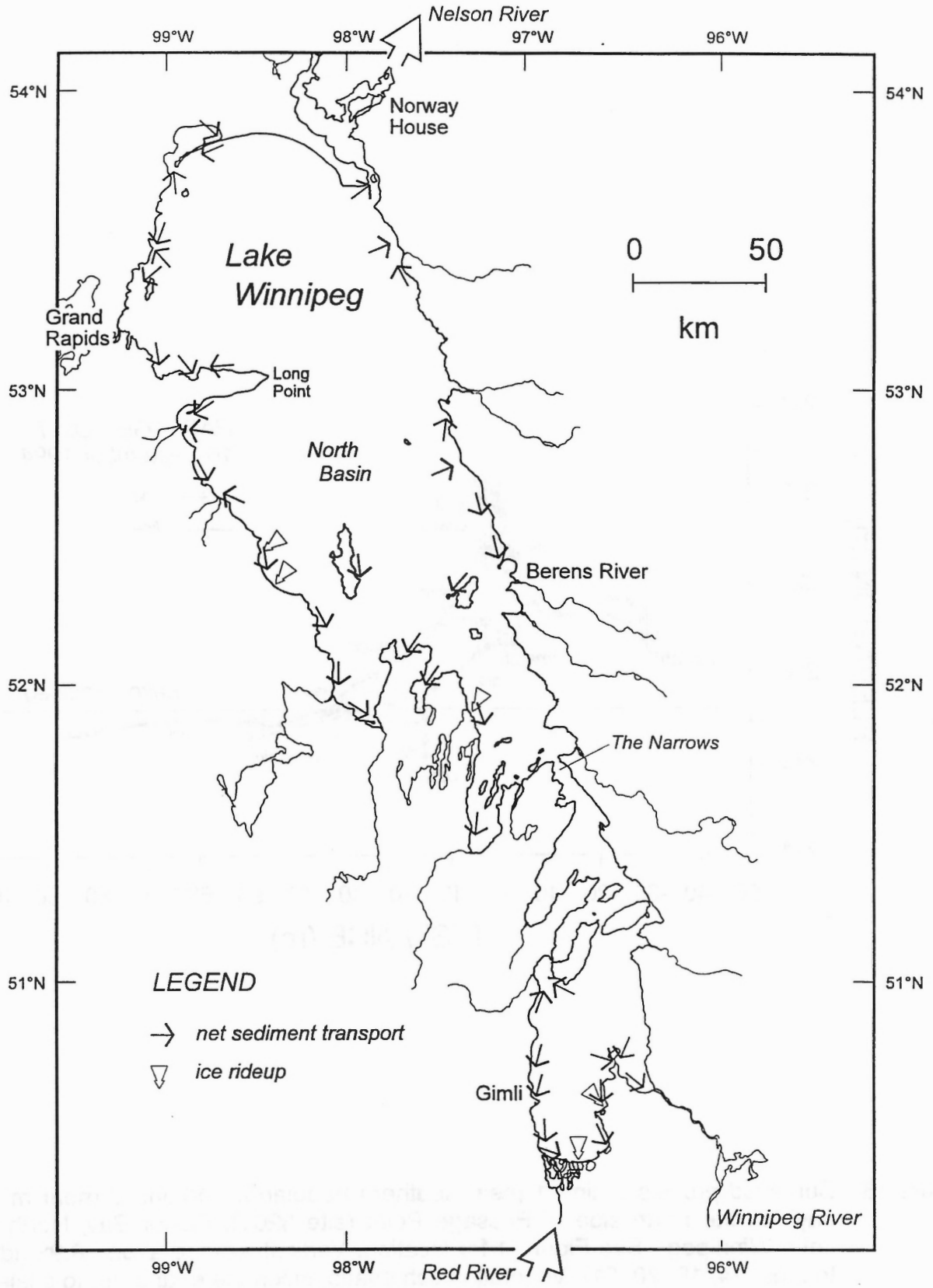

Figure 15. Geomorphic indicators of net longshore and cross-shore sediment transport and sites where evidence of ice rideup was observed in 1994.

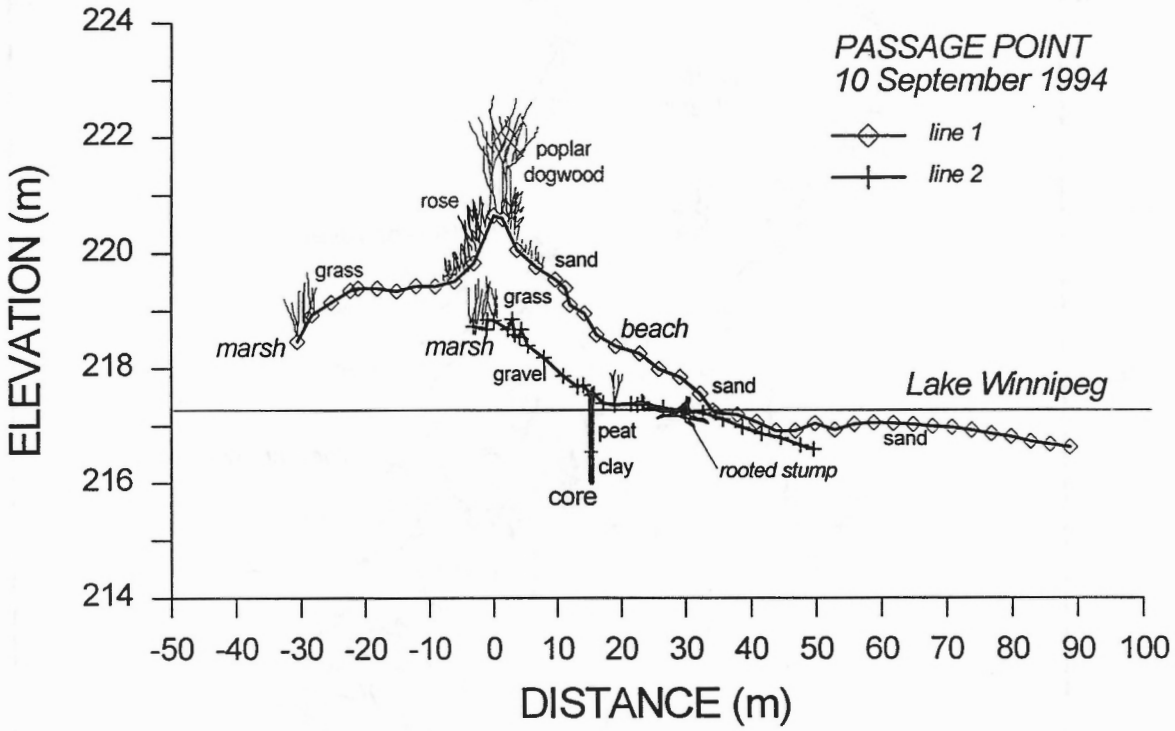

Figure 16. Surveyed profiles at line 1 (near southern headland) and line 2 (near middle of bay) on the north side of Passage Point (site 8201), Fisher Bay, North Basin, Lake Winnipeg. See Figure 1 for location. Vertical exaggeration ~8.9x (identical to Figs. 14, 19, 20, 21). Vegetation schematic, incomplete, and not to scale. Lake to right with approximate water level at time of survey. Horizontal origin at benchmarks on each line (GSC-201 on line 1, GSC-202 on line 2). Also shows core location on line 2 and approximate lithostratigraphy.

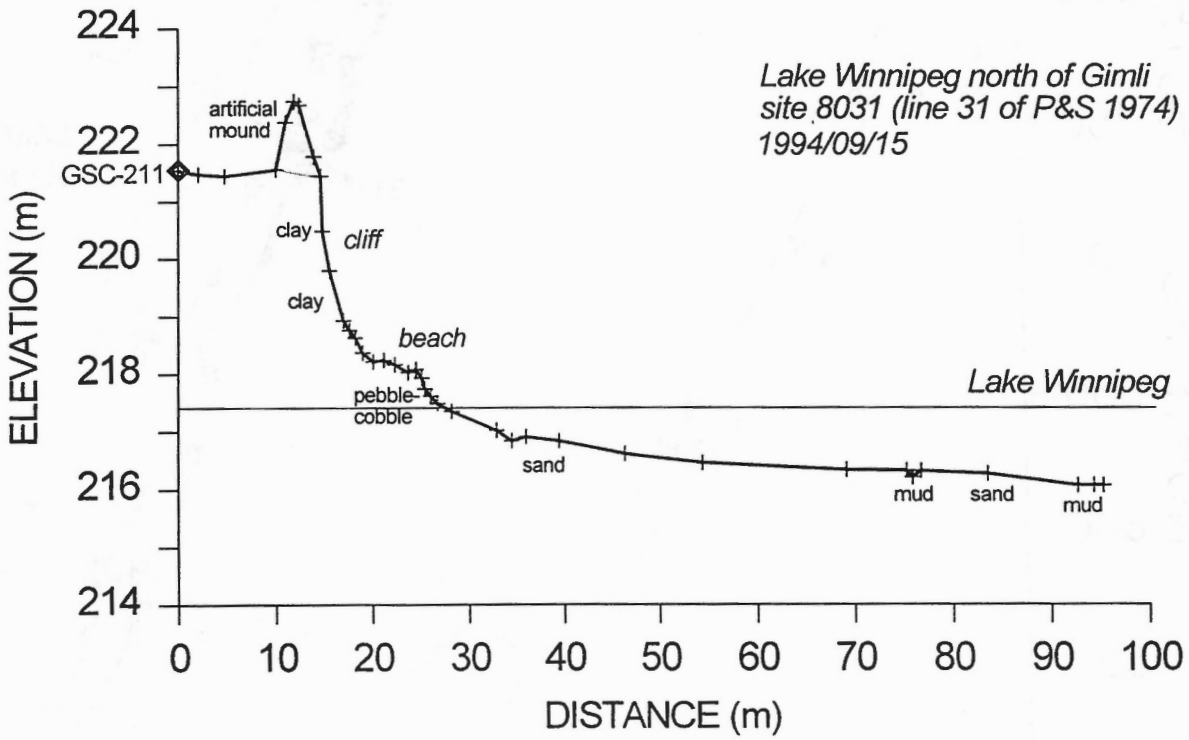

Figure 17. Surveyed cliff and shore profile at site 8031, line 31 of Penner and Swedlo (1974), north of Gimli (Figure 1). The detailed line setting is shown in Figure 18. Lake to right, with water level at time of survey. Horizontal origin at benchmark (GSC-211) in field behind cliff. Vertical exaggeration ~6x.

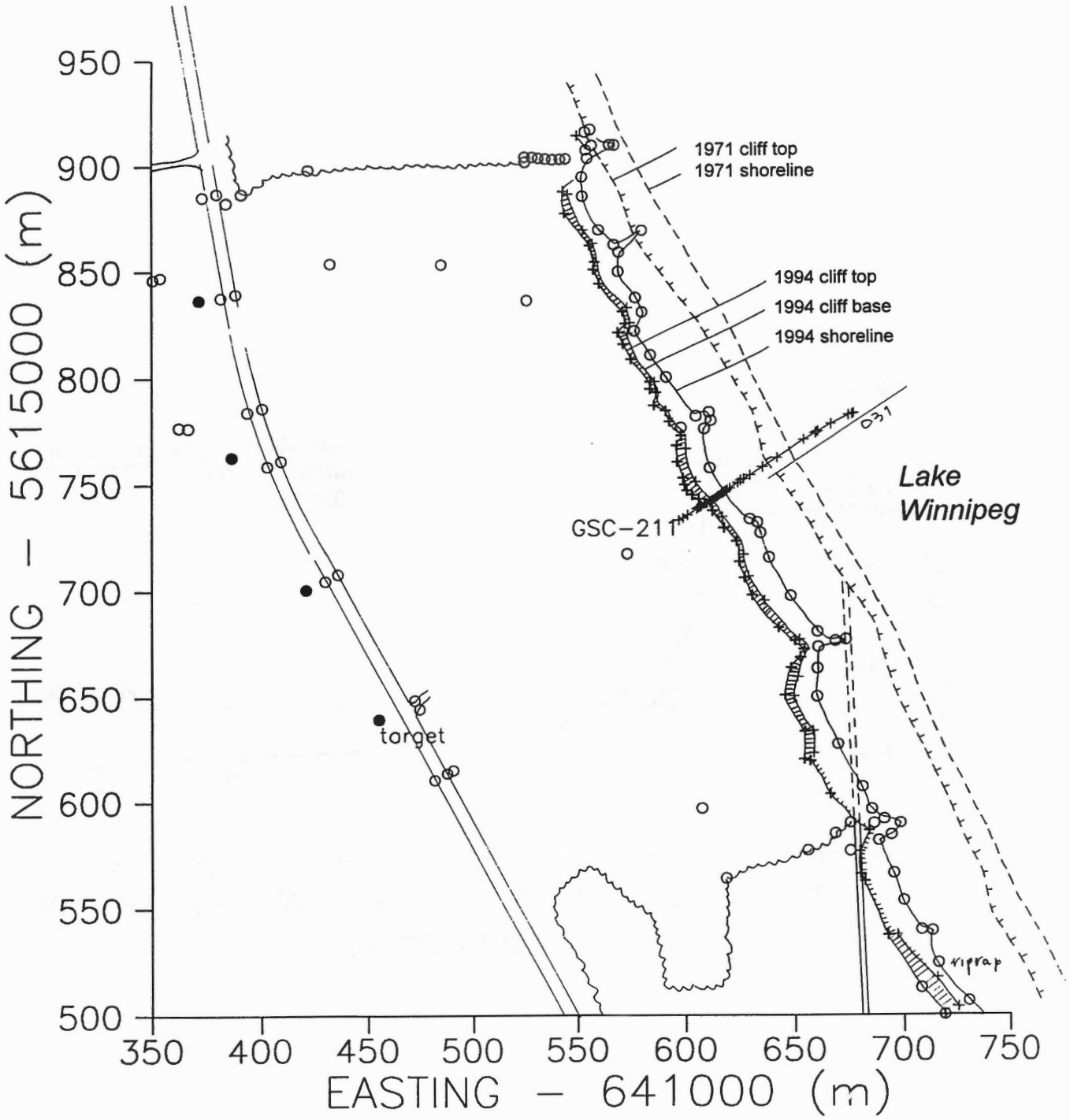

Figure 18. Cliff top, cliff base, and water line as surveyed 15 September 1994 at site 8031 (line 31 of Penner and Swedlo, 1974), north of Gimli (Figure 1). Note field boundaries at edge of woodland (scalloped line), road, and telephone poles (solid circles) also shown in the 1971 survey. Broken line with and without bar denote the 1971 shoreline and cliff top, respectively. Note that the north-running track (closely-spaced parallel lines) at the south end of the site has been truncated by approximately 200 m since 1971.

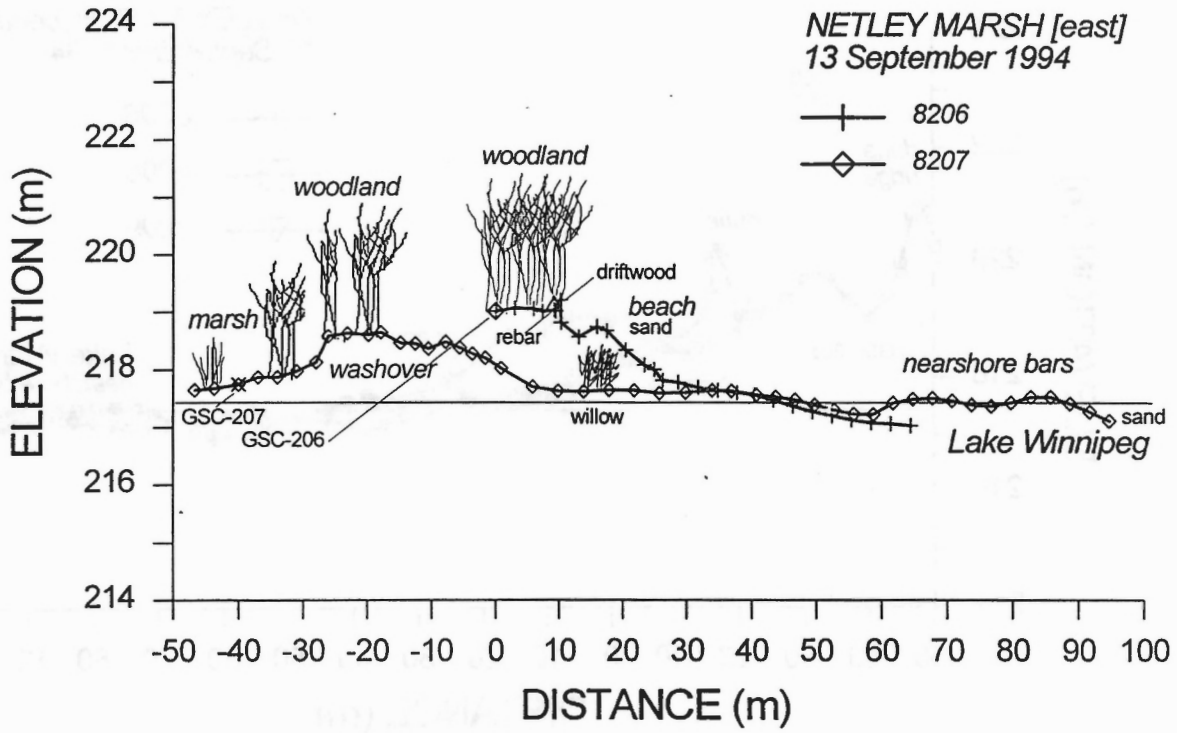

Figure 19. Surveyed shore profiles at sites 8206 and 8207 (benchmarks GSC-206 and GSC-207, respectively), east-central shore of Netley Marsh (Red River delta) east of Pruden Bay. See Figure 2 for locations. Vertical exaggeration ~8.9x (identical to Figs. 14, 16, 20, 21). Vegetation schematic, incomplete, and not to scale. Lake to right with approximate water level at time of survey. Rebar 9.2 m north of GSC-206 is secondary benchmark.

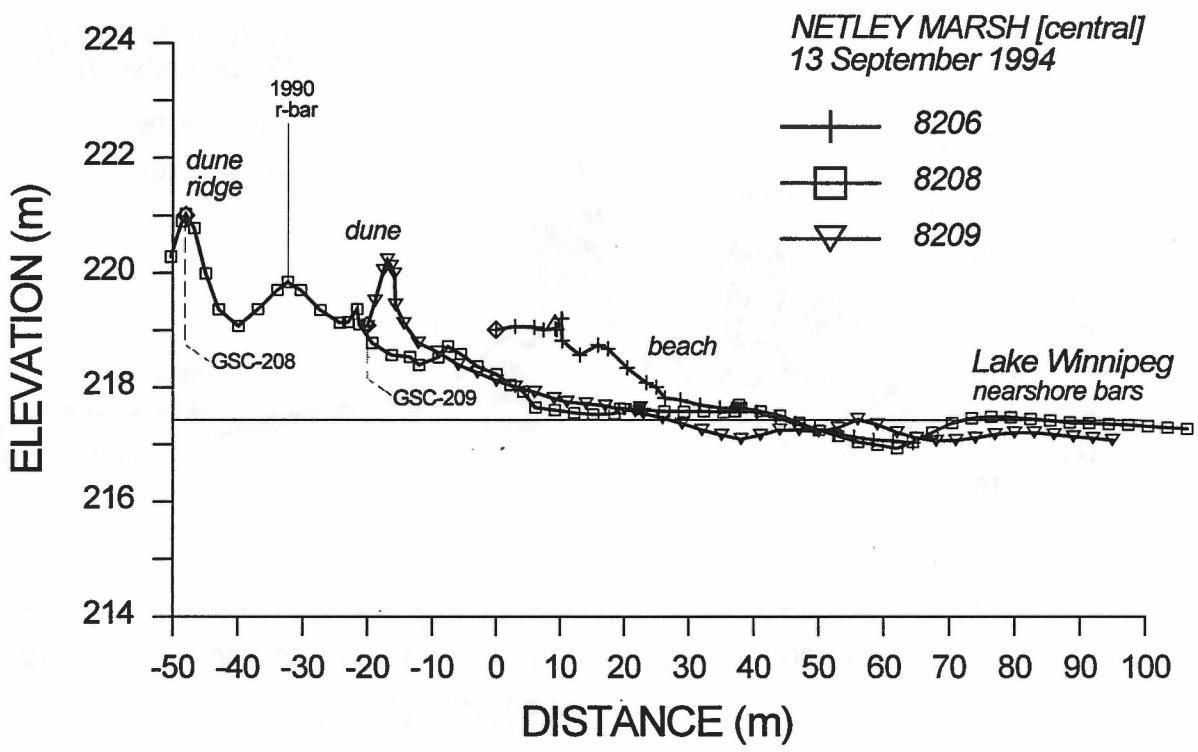

Figure 20. Surveyed shore profiles at sites 8208 and 8209 (with profile 8206 again for comparison), central shore of Netley Marsh (Red River delta) west of Main Channel. See Figure 2 for locations. Vertical exaggeration ~8.9x (identical to Figs. 14, 16, 19, 21). Lake to right with approximate water level at time of survey. Rebar is benchmark installed in 1990 (Nielsen and Conley, 1994).

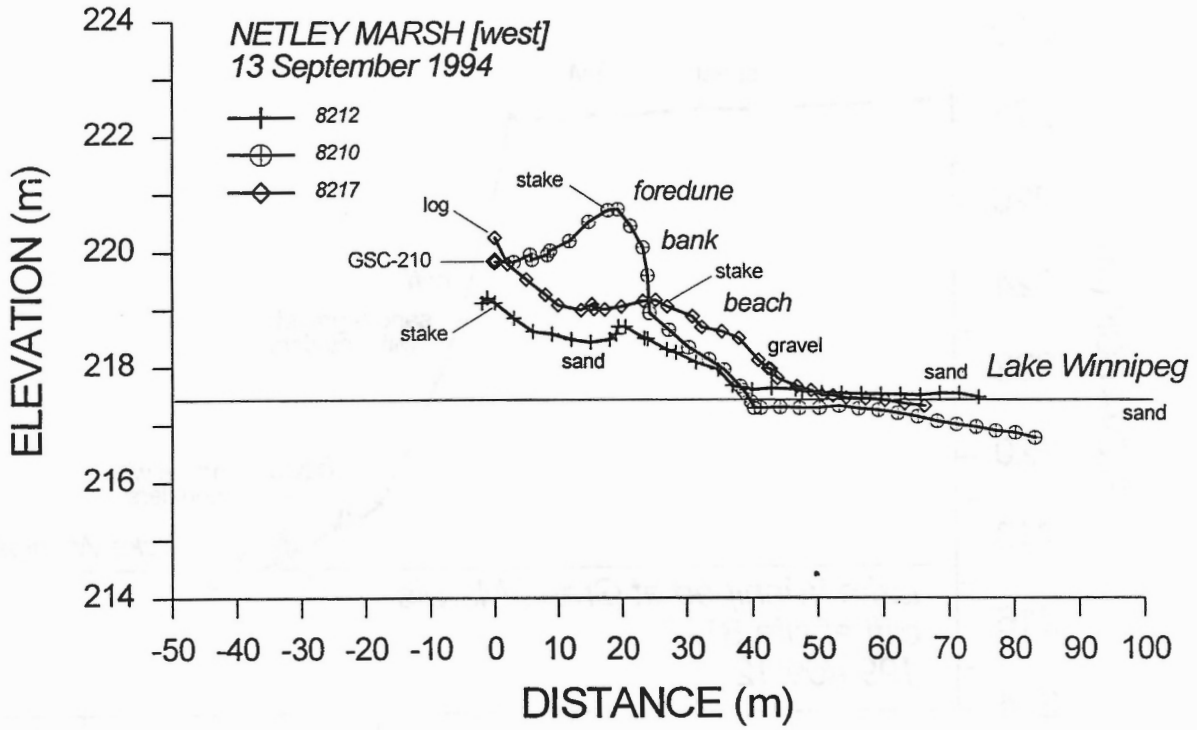

Figure 21. Surveyed shore profiles at sites 8217, 8210, and 8212 (in order from west to east), western Netley Marsh shoreline in the vicinity of Salamonia Channel. See Figure 2 for locations. Vertical exaggeration ~8.9x (identical to Figs. 14, 16, 19, 20). Lake to right with approximate water level at time of survey. Benchmark GSC-210 at horizontal origin of line 8210. Log at site 8217 represents control for 1990 survey (Nielsen and Conley, 1990). Stakes are temporary benchmarks installed in 1994.

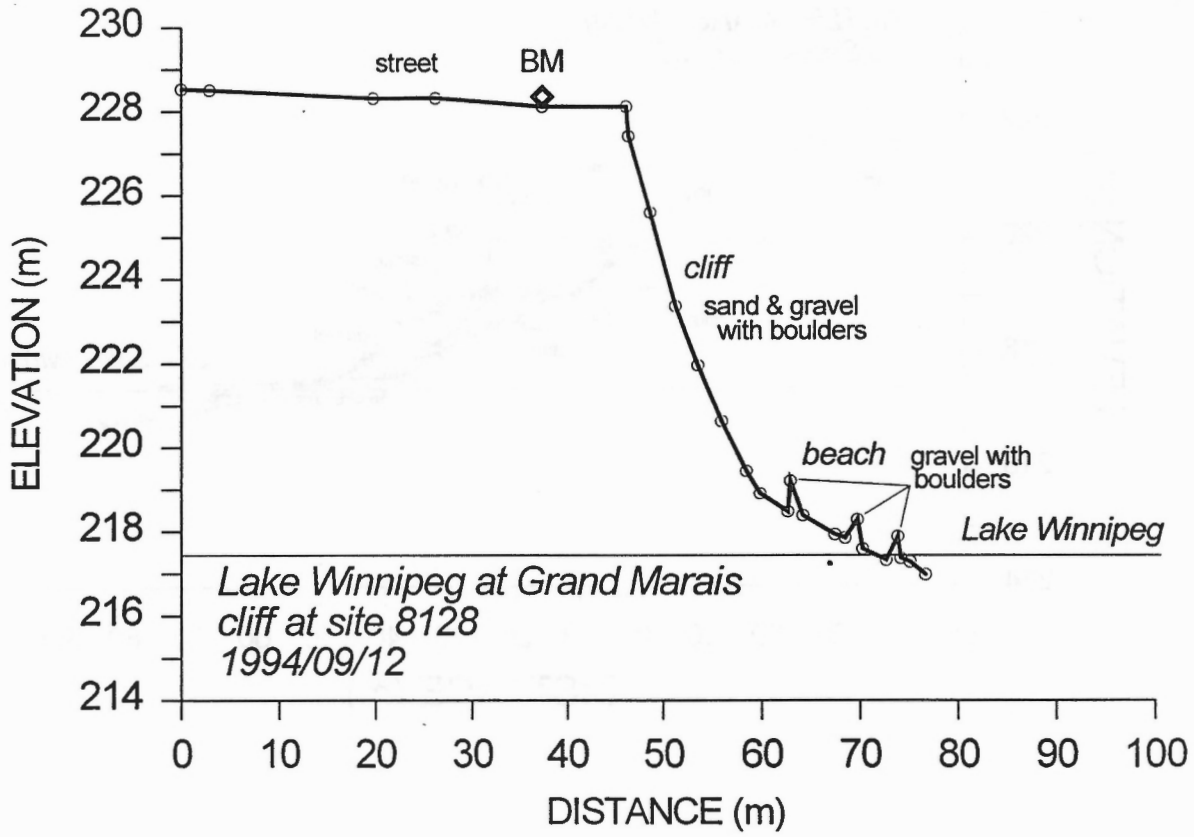

Figure 22. Surveyed shore and cliff profile at Grand Marais (site 8128). See Figure 1 for location. Vertical exaggeration ~4.4x. BM is GSC-205. Lake to right with approximate water level at time of survey. Large boulders on beach shown schematically.

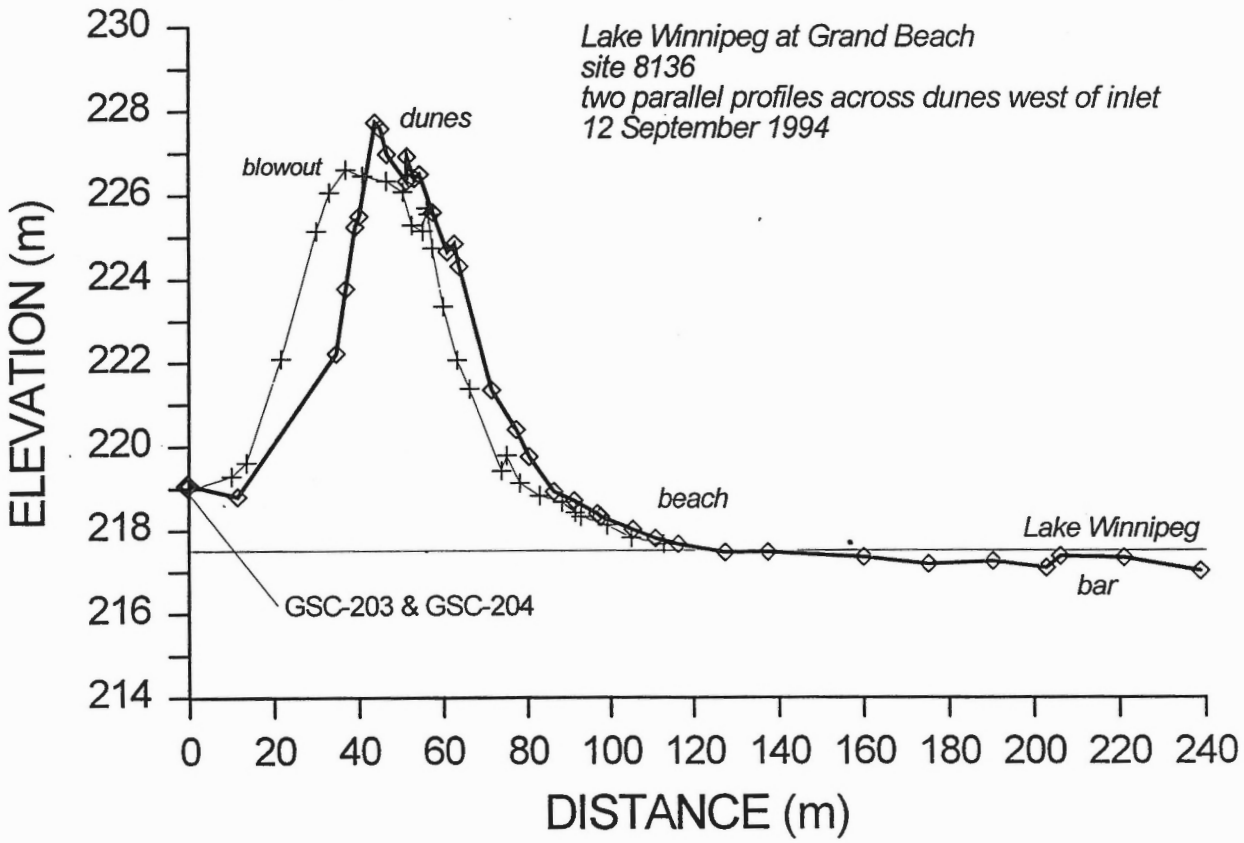

Figure 23. Surveyed nearshore and beach profile with two parallel profiles over dunes at Grand Beach west of inlet (site 8136). See Figures 1 & 6d for location. Vertical exaggeration ~9.8x.

6.2 Lake Winnipeg coastal submergence over the last three centuries

Erik Nielsen

Manitoba Energy and Mines
1395 Ellice Avenue, Winnipeg, Manitoba R3G 3P2

INTRODUCTION

In 1990, investigations along the barrier island system which forms the south shore of Lake Winnipeg between Matlock and Beaconia Beach (Fig. 1) revealed evidence of both historic and pre-historic coastal submergence (Nielsen and Conley, 1994). The results of this investigation form the basis of this report. The purpose of the study was, in part, to develop a relative water-level curve for the south end of the lake based on radiocarbon dating of inundated terrestrial organic materials. Wind set-down and set-up can cause daily water-level changes of up to 2 m depending on the wind direction, while seasonal water-level fluctuations may be as much as 1 m (Penner and Swedlo, 1974). Key outcrops examined for the study were exposed on the upper foreshore due to a combination of seasonally low Lake Winnipeg water levels and wind set-down.

METHODS

Six sites where organic marsh sediments and associated logs, tree stumps and tree roots were exposed on the upper foreshore of the lake were radiocarbon dated. Cross-sectional profiles, measured relative to the lake level and the position of organic samples, were surveyed at each site. The present day vegetation zonation was also noted. A curve showing relative lake-level rise at the southern shore was constructed by plotting calibrated radiocarbon dates from West Channel, Pruden Bay, Patricia Beach and Beaconia Beach against the water-level datum represented by the samples. The radiocarbon dates were calibrated to calendar years using the method outlined by Stuiver and Reimer (1993).

The water-level, using modern vegetation zonation as an analogue, is estimated to have been at least 0.5 m below each sample. This estimate is difficult to substantiate as the dated trees comprise only willow and poplar. Willow has a known affinity for water and while it may not grow on the foreshore to within half a metre of the water level, primarily a result of shore ice action, it is possible that it may occur closer to lake level on the lagoon side of the barrier island. Poplar does not have the same affinity for water as willow and may be a better indicator of low water levels. Unfortunately only one dated sample was identified as poplar.

RESULTS

Five of the six sites are on the southern shore. A sixth site, in the northern South Basin, was examined for comparison. At the five southern shore sites, nine radiocarbon dates were obtained. Seven of the nine were obtained from wood, which most effectively provides an upper constraint on lake level. A date on soil dates a subaerial landscape with no affiliation with the lake, while dated lagoon sediment marks inundation.

Sans Souci

Desiccation cracks, infilled with wind-blown topsoil, occur in Lake Agassiz sediments exposed on the foreshore at Sans Souci. Though not directly related to water level changes in the last few centuries, these features clearly indicate that the site was subaerially exposed. A radiocarbon date of 3885 years BP (calibrated) was obtained from the soil (Table 1). Organic muck, unconformably overlying the Lake Agassiz sediments and dated at 1080 years BP (calibrated), records marsh sediment accumulation in a lagoon environment (Fig. 2A). The stratigraphy and associated radiocarbon dates at Sans Souci indicate that a lagoon and barrier island were established at the site between 3900 and 1100 years before the present (1835 B.C. and 870 A.D.), in response to southward transgression of the lake.

West Channel

Approximately 0.8 km east of West Channel, a mud flat, in places more than 100 m wide, overlain by a thin discontinuous sheet of nearshore beach sand, is exposed at times of low lake level (Fig. 2B). Logs, in varying states of decay, may be found on the surface of the mud flat. Tree roots protrude from the underlying clay, but *in situ* tree stumps are absent, perhaps due to ice scouring to a level below the root collar of the stumps. Tree stumps, in growth position, were thus removed leaving only the roots. The radiocarbon dates from this site may therefore represent a datum slightly higher than that indicated by the elevation of the samples.

Calibrated radiocarbon ages of 320 and 290 years BP (1660 and 1630 A.D.) were obtained on two root samples from this site. The older dated sample was collected 17 m further offshore than the younger sample, so the relative position of the root samples and their radiocarbon ages are in agreement.

Pruden Bay

The foreshore to the east of the mouth of Pruden Bay is relatively narrow and steep compared to most other areas along the south shore. The eroding foreshore exposes rooted tree stumps and organic detritus in places interbedded with sand

and associated with numerous bison bones. Two rooted stumps, one willow and one unidentified from this site dated to 280 and 310 years BP (calibrated) (1670 and 1640 A.D.) (Table 1). The radiocarbon dates and the associated bison bones are in agreement as bison is known to have become extinct in the wild in Manitoba in the 1870s.

Patricia Beach

During periods of low water, the foreshore at Patricia Beach exposes numerous rooted tree stumps and fibrous organic material interbedded with clay (Fig. 3A). An *in situ* poplar stump, rooted in the foreshore at an elevation of 217.4 m dated to 275 years BP (calibrated) (1675 A.D.) (Table 1).

Beaconia Beach

The foreshore at the south end of Beaconia Beach exposes the most extensive drowned forest encountered along the entire barrier island system (Fig. 3B). A total of 24 willow stumps are rooted in marsh clay and peat at an elevation of 217.4 m asl. A single rooted stump was dated to 275 years BP (calibrated) (1675 A.D.)

At the north end of the beach, a prominent black fibrous organic muck layer, exposed on the lower foreshore at an elevation of 217.4 m asl, was dated to 295 years BP (calibrated) (1655 A.D.) (Table 1). The fibrous organic layer is, in places, overlain by pebbly gravel and sand of the present foreshore beach.

Observation Point

A single radiocarbon date of 265 years BP (calibrated) (1680 A.D.) (Table 1) was obtained from a rooted tree stump exposed on the foreshore at Observation Point near Manigotagan, located on the northeastern shore of the South Basin.

DISCUSSION

The six sites examined in this study expose *in situ* rooted tree stumps, logs, roots and organic sediments on the present-day foreshore and all record a similar sequence of events. Fine textured organic-rich sediments, of undetermined thickness, exposed at the base of the stratigraphic succession are interpreted to be marsh sediments similar to those currently deposited in the lagoons and marshes behind the barrier islands. The presence of marsh sediment on the foreshore clearly indicates that the barrier islands have moved landward in response to transgression of the lake. Rooted tree stumps, roots, fallen logs and fibrous organic sediment associated with the fine textured marsh sediments at the various sites represent trees and marsh plants that previously grew in and along the edges of the marsh or lagoon behind the barrier islands. As the lake level rose, the barrier islands transgressed landward, burying the trees and underlying marsh sediments (Fig. 4). With continued transgression, the tree stumps and marsh sediments became exposed on the foreshore and are now being eroded by waves and drifting lake ice.

The elevations and age of the 6 wood samples from West Channel, Pruden Bay, Patricia Beach and Beaconia Beach were used to construct a water-level curve for the southern shore (Fig. 5). Elevations of the samples were estimated to vary from 217.2 and 217.4 metres above sea level (asl) (Table 1) or a mean of 217.3 m asl. The 1918-1967 mean water level of the lake is 217.4 m (Penner and Swedlo, 1974), 0.1 m higher than the mean elevation of the dated samples. The seven calibrated dates cluster around 300 years BP (1650 A.D.). Hence, if it is accepted that the trees grew 0.5 m above lake level, a rise from 216.8 m asl at 1650 A.D. to 217.4 m asl at 1950 A.D., or 20 cm/century, is indicated. If the trees grew closer to the water level, a lesser rate would be implied.

Analysis of 1914 to 1971 water level records by Penner and Swedlo (1974) suggests tilting and southward transgression of the Lake Winnipeg basin. They concluded that Berens River is rising relative to Gimli at a rate of 6.7 cm/century. Prior to the present study, geological evidence for long term changes in the lake basin consisted of two radiocarbon dates from a single core taken in shallow water near Victoria Beach. Radiocarbon dates of 1660 ± 60 years BP (GSC-1977) and 1060 ± 210 years BP (GSC-1980), were obtained from the bottom and top of a 40 cm thick peat layer, approximately 3 m below the long term mean lake level (Teller, 1980), and suggest a water level rise of approximately 20 cm/century through the last millennium and a half. Land-based work on raised beaches at the north end of Lake Winnipegosis by Nielsen et al. (1987) further indicates the north end of that lake has been uplifted an estimated 6 m in the last 5000 years as a result of isostatic tilting. This suggests an average rate of tilting of 12 cm/century for Lake Winnipegosis. The new geological data and radiocarbon dates are thus in agreement with the available data and suggest the water level at the south end of Lake Winnipeg is rising at a rate of about 20 cm/century as the result of isostatic uplift of the outlet at the north end of the lake.

The discovery of similar inundated stumps farther north at Observation Point and at Washow Bay (Forbes, pers. com. 1994) may indicate that at least some of the recent water-level fluctuations may be basin-wide. A lake level rise of 20 cm/century at the southern shore, driven by differential uplift of the outlet, would correspond to only 15 cm/century at these more northerly sites. Alternatively, the water-level rise in Lake Winnipeg during the last three centuries may be, at least in part, due to climatic variations, a conclusion supported by the work of Fritz et al. (1994) on cores taken from Devils Lake, North Dakota. They concluded that the pre-1850 climate of the Little Ice Age was cold and dry, not unlike the 1930s, but colder.

CONCLUSIONS

Marsh sediments and associated rooted stumps, logs and tree roots on the foreshore of Lake Winnipeg indicate the level of the lake has risen over recent geological time. Radiocarbon dating of wood associated with the marsh sediments suggests that the rate of this rise has been 20 cm/century during the last three hundred years. This is comparable to similar rates determined previously by direct water level measurements and uplift rates for Lake Winnipegosis (Penner and Swedlo 1974; Nielsen et al. 1987). Isostatic uplift of the outlet at the north end of Lake Winnipeg may account for this change in the water level. However, the discovery of similar submerged shoreline features at Observation Point and Washow Bay may indicate the water level rise is basin-wide. Basin-wide water level increases can not be the result of differential isostatic uplift but may be due to climate change. Increased precipitation at the end of the Little Ice Age, ca. 1850, may be partially responsible for the observed increase in Lake Winnipeg water levels. Lake level reduction in Lake Winnipegosis over the last 5000 years can not, however, be attributed to climate fluctuations. The relative roles of isostatic uplift and changed inflow into the lake as a result of climate change remain to be resolved.

ACKNOWLEDGMENTS

I would like to thank Harvey Thorleifson, of the Geological Survey of Canada, for our many helpful discussions and his advice over the last few years on water-level fluctuations in Lake Winnipeg and Lake Winnipegosis. The critical reviews by Gaywood Matile (Manitoba Energy and Mines), Harvey Thorleifson, Dan Kerr (Geological Survey of Canada) and David McLeod (Manitoba Historic Resources) greatly improved the manuscript.

REFERENCES

Fritz, S., Engstrom, D.R. and Haskell, B.J.
1994. 'Little Ice Age' aridity in the North American Great Plains: a high-resolution reconstruction of salinity fluctuations from Devils Lake, North Dakota, USA; Holocene, v. 4, no. 1, p. 69-73.

Nielsen E. and Conley, G.
1994. Sedimentology and geomorphic evolution of the south shore of Lake Winnipeg; Manitoba Energy and Mines, Geological Report GR94-1, 58p.

Nielsen E., McNeil, D.H. and McKillop, W.B.
1987. Origin and paleoecology of post-Lake Agassiz raised beaches in Manitoba; Canadian Journal of Earth Sciences, v. 24, p. 1478-1485.

Penner, F. and Swedlo, A.
1974. Lake Winnipeg shoreline erosion, sand movement, and ice effects study; The hydrologic, hydraulic and geomorphic studies, technical report appendix 2, v. 1-B, Water Resources Branch, Department of Mines, Resources and Environmental Management.

Stuiver, M. and Reimer, P.J.
1993. Extended ^{14}C data base and revised CALIB rev 3.0.3 ^{14}C age calibration program; Radiocarbon, v. 35, p. 215-230.

Teller, J.T.
1980. Radiocarbon dates in Manitoba; Manitoba Department of Energy and Mines, Mineral Resource Division, Geological Report GR80-4, 61p.

Table 1. Radiocarbon dates from the south end of Lake Winnipeg

Site	Lab. No.	^{14}C Age Yrs. B.P.*	Calibrated Yrs. B.P.	Calendar Yrs. A.D.	Material	Elevation (m)
Sans Souci	BGS-1477 BGS-1478	3600 ± 80 1200 ± 70	3885 1080	(1835 B.C.) 870	soil organic muck	216.9 216.9
West Channel	BGS-1439 BGS-1448	335 ± 65 230 ± 70	320 290	1630 1660	*Salix* wood	217.2 217.2
Pruden Bay	BGS-1440 BGS-1450	290 ± 70 210 ± 70	310 280	1640 1670	*Salix* wood	217.3 217.3
Patricia Beach	BGS-1442	190 ± 65	275	1675	Populus	217.4
Beaconia Beach	BGS-1443 BGS-1444	260 ± 80 185 ± 65	295 275	1655 1675	organic muck *Salix*	217.4 217.4
Observation Point	BGS-1632	160 ± 70	265	1685	*Larix*	217.4

*Radiocarbon years are expressed as years before 1950

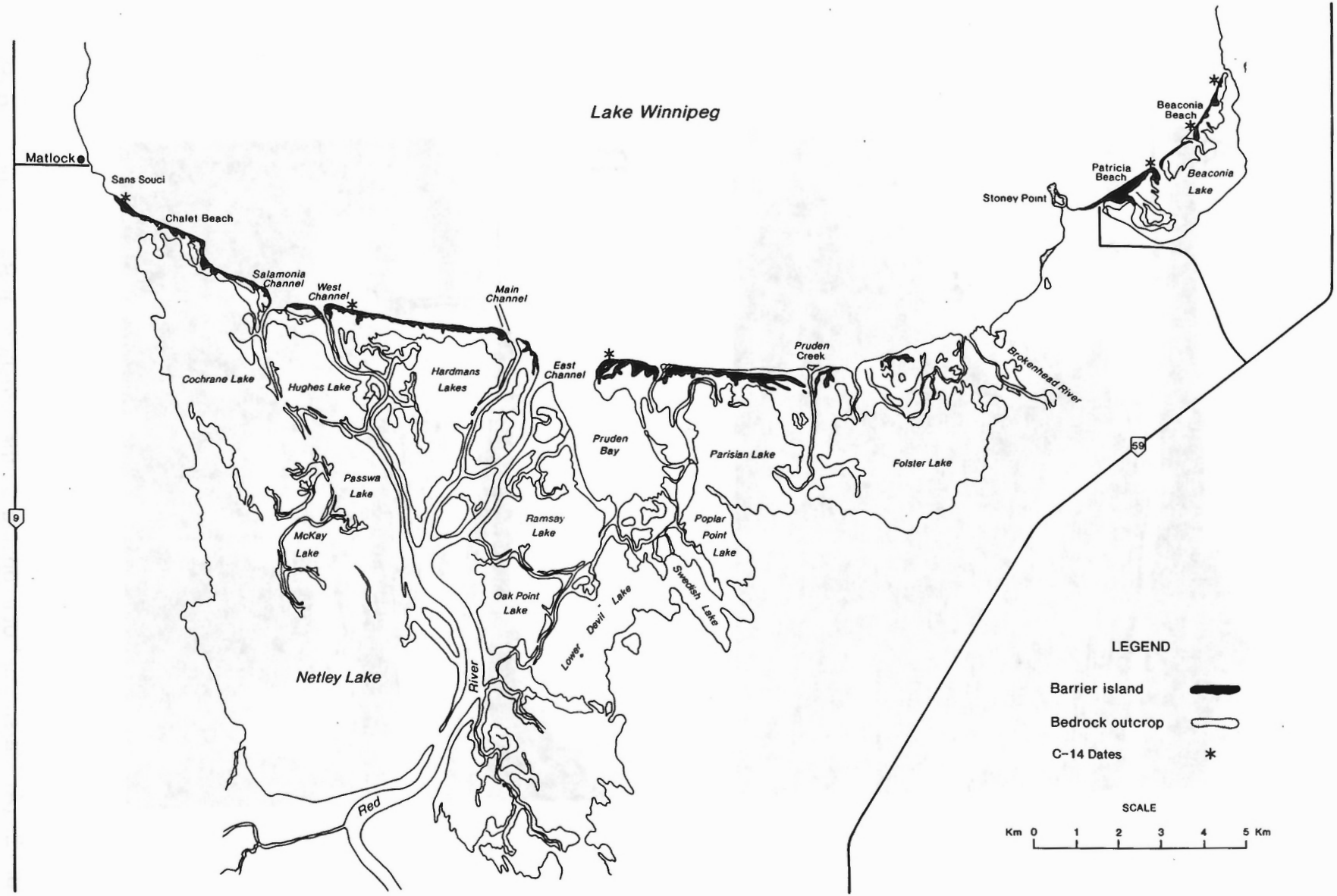

Figure 1. Location of barrier islands and radiocarbon dated sites at the south end of Lake Winnipeg.

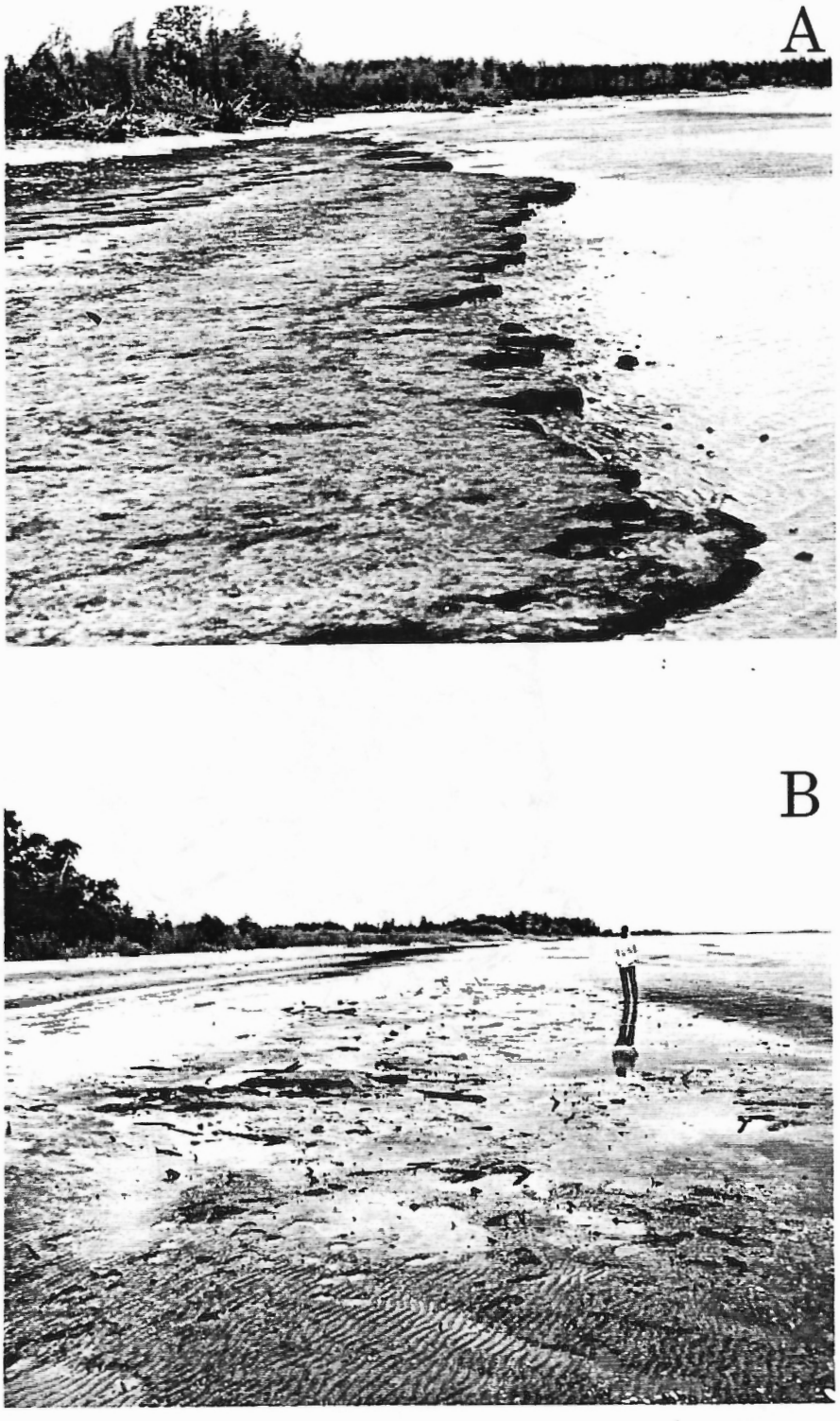

Figure 2. (A) Marsh peat outcropping on the foreshore at Sans Souci, and (B) tree roots on the foreshore near the mouth of West Channel.

A

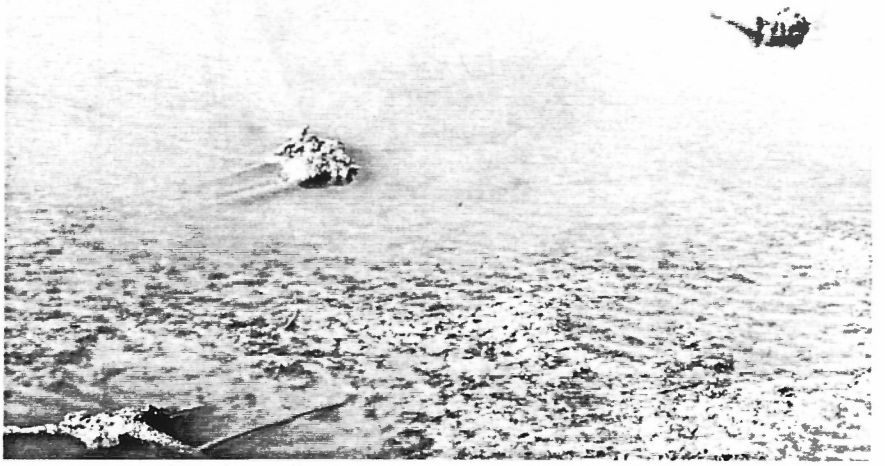

B

Figure 3. (A) Rooted tree stumps on the foreshore at Patricia Beach, and (B) drowned forest at Beaconia Beach.

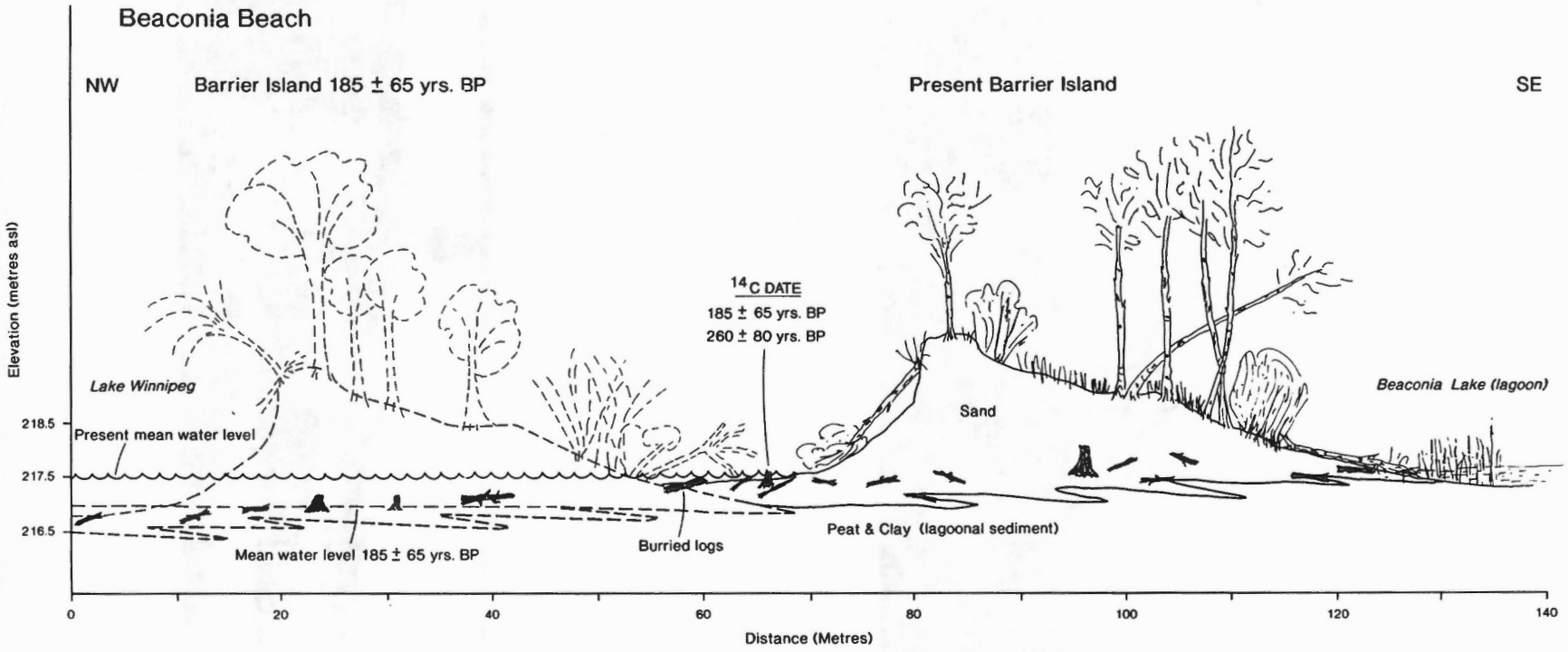

Figure 4. Cross section of the barrier island at Beaconia Beach, showing the burial of logs due to the proposed rising lake levels and the landward migration of the shore.

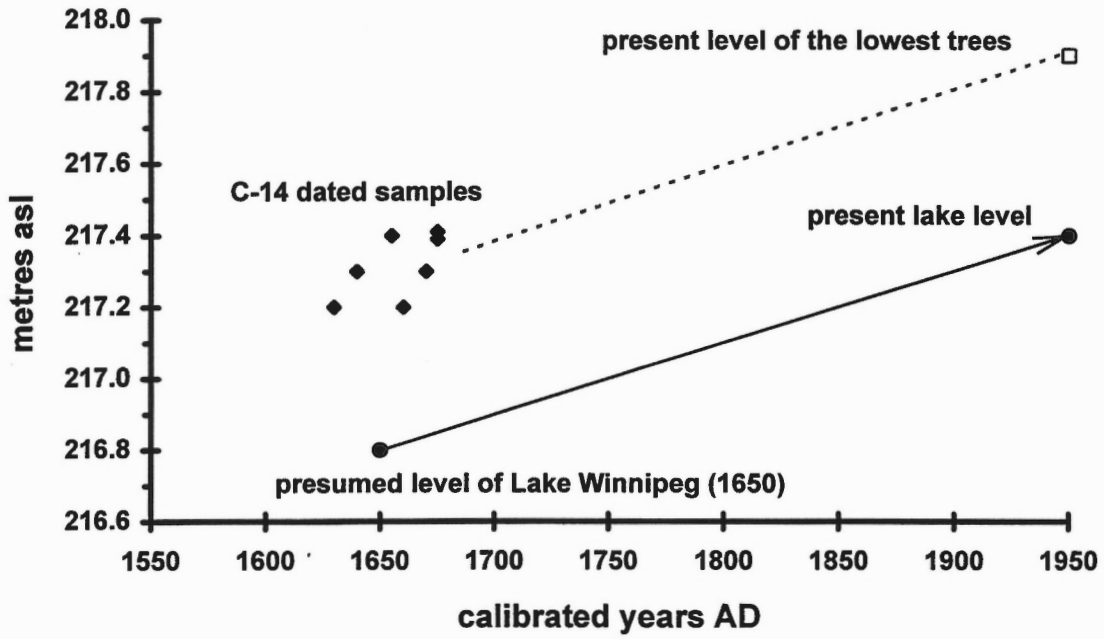

Figure 5. Plot of elevation of wood samples vs. age, in calendar years, from the southern shore of Lake Winnipeg. The inferred 20 cm/century lake level rise is indicated by the arrow.

6.3 Lake Agassiz beaches and reconstruction of lower lake levels in the Shield Margin area, northwest of Lake Winnipeg

Isabelle McMartin

Geological Survey of Canada
601 Booth Street, Ottawa, Ontario K1A 0E8

INTRODUCTION

Numerous glacial Lake Agassiz raised beaches have been identified in the NATMAP (National Geoscience Mapping Program) Shield Margin Project area (Fig. 1) since surficial mapping of the area at 1:100 000 scale was initiated by the Geological Survey of Canada in 1991. Surficial mapping and altitude measurements of major beach ridges were used to calculate isostatic tilts and reconstruct major paleo-lake levels. Since the study area is located immediately to the northwest of the Lake Winnipeg region, this study has implications for the understanding of the Lake Winnipeg tilt history in post-glacial time. The study also documents the post-Lake Agassiz diversion of the Saskatchewan River from the Minago River, by-passing Lake Winnipeg, to Cedar Lake and into Lake Winnipeg at Grand Rapids. The flow diversion may have had a significant effect on lake level as well as sedimentation in the Lake Winnipeg North Basin.

REGIONAL SETTING

The study area straddles the Paleozoic/Precambrian contact near the Manitoba-Saskatchewan border (Fig. 1). The Shield portion is underlain by parts of the Flin Flon greenstone belt and its metamorphic equivalent. The Precambrian rocks are overlain by a Phanerozoic platform composed of subhorizontal Paleozoic carbonate rocks.

On the Shield, relief is low to moderate, and drift cover is generally thin (<2 m) and discontinuous. South of the Shield margin, the drift cover is thick in places, up to 50 m thick on The Pas Moraine, which represents a dominant glacial landform extending from the Shield Margin area into Lake Winnipeg (Fig. 1). The predominant ice flow direction across the Shield portion and west of The Pas Moraine is to the south-southwest, indicating that glacier ice was flowing from the Keewatin Sector of the Laurentide Ice Sheet (McMartin, 1994a). East of the moraine, ice flow was toward the west-southwest, originating in the Hudson Bay area from a Labradorian Ice centre. Following ice retreat, the entire study area was inundated by glacial Lake Agassiz (Fig. 2).

Fine grained glaciolacustrine sediments form a discontinuous veneer on the irregular topography, with thickest accumulations in the low areas between bedrock highs on the Shield, or in low lying areas across the Paleozoic terrane. The eastern part of the area, referred to as the Grass River Basin (Elson, 1967), is mantled by fine grained laminated sediments up to 45 m thick. This north-south trending belt east of Hargrave Lake masks both Shield and Paleozoic terrane (Fig. 3). Lake Agassiz beach deposits occur mostly on the Paleozoic cover as scattered low ridges of gravel, sand, and bedrock rubble (Fig. 4). On the Shield, segments of weakly developed beaches or lag deposits occur on the sides of bedrock hills. Nearly continuous flights of shingle beaches occur along the carbonate bedrock bluffs east of Talbot Lake (Figs. 5, 6). Isolated or series of continuous beach ridges are found along Highway 6 (sandy facies) and along the crest and west facing slope of The Pas Moraine (pebbly facies).

The eastern part of the study area slopes gently towards the Nelson River and Hudson Bay. The southern part drains into the Saskatchewan River which flows to the southeast towards Lake Winnipeg. The northern areas are part of the Churchill River basin.

METHODS

Lake Agassiz nearshore and littoral deposits were compiled from surficial geology maps, including the Talbot Lake and Mitishto River maps for the Grass River Basin (McMartin, 1994b; 1994c), the North Moose Lake map (McMartin and Boucher, in press), parts of the Cormorant Lake (63K) map (Clarke, 1989), and parts of the Kississing Lake (63N) map (Kaszycki and Nee, 1990). Other non-published sources include preliminary surficial geology maps from the Nelson House area compiled by McMartin, and from the Cumberland Lake and Mirond Lake areas in Saskatchewan compiled by McMartin, Campbell and Boucher.

Major continuous shoreline features were identified and measured in the field with an altimeter (± 2m) in the Ponton area, along Highway 6 south of the junction with Highway 39 (Fig. 3), and in The Pas Moraine area. The altimeter measurements were calibrated through the day with known altitudes of several bench marks. Other measurements were taken from Road Survey Profiles (Manitoba Department of Transportation) or inferred from topographic maps at 1:50 000 scale (± 10m and ± 25 feet). Altitudes were plotted on a Lake Agassiz strandline diagram (Fig. 7) against distance perpendicular to lines of equal post-glacial uplift, isobases, synthesized by Teller and Thorleifson (Fig. 2). The higher levels, mostly located on the Shield, were not reconstructed for

this study. The compilation resulted in the identification of five major lake phases.

PHASE 1

Phase 1 represents the highest lake level compiled for this study (Fig. 8). This phase delineates the extent of Lake Agassiz during the Nipigon Phase at approximately 8500 years B.P. (Teller and Thorleifson, 1983), 10 m above the Upper Pas beaches (defined by Johnston, 1946). The lower beach level in front of The Pas Moraine formed during this phase, with measured altitudes of 291 m and 293 m, and a differential uplift of approximately 0.2 m/km. This level corresponds to one of the six unnamed beach levels recognized by Johnston (1946) between the Stonewall and the Upper Pas beaches. Nielsen and Groom (1987) reconstructed this lake level for the area around The Pas, although they did not consider the isostatic tilt on the water plane (cf. Phase B, Fig. 17). The Pas level was not compiled since the Upper Pas beaches are not present in front of The Pas Moraine within the study area, and are poorly developed east of the moraine.

During this phase, most of the Paleozoic cover was submerged under less than 35 m of water, with the exception of The Pas Moraine and other high plateaus which formed large islands near the Shield margin (Fig. 8). On the Shield, the Snow Lake area and the Kississing Lake basin were submerged in shallow waters generally less than 15 m deep. The Grass River Basin was certainly the deepest part of the Lake within the study area, with depths exceeding 60 m in its eastern extremity.

PHASE 2

Phase 2 represents the extent of Lake Agassiz immediately prior to the Grand Rapids Level (Fig. 9), at the end of the Nipigon Phase, shortly after 8500 years B.P. (Teller and Thorleifson, 1983). This level was certainly part of the series of Grand Rapids beaches described by Johnston (1946), although it was not thoroughly documented in the Grand Rapids area. The Lower Pas level and the Gimli level were not reconstructed mainly because of the scarcity of the beaches in the study area and the lack of precise measurements on these beaches. The highest flight of beaches composed of rock shingles across the faces of dolomitic escarpments in the Talbot Lake area formed during this phase (Fig. 6). The elevation of the ridges in that area is between 264 and 272 m, indicating a drop of some 35 m from the previous level. The approximate tilt is 0.16 m/km, increasing towards the northeast to 0.28 m/km, and was calculated from altitudes inferred on topographic maps where continuous ridges occur.

During this phase, most of the Shield and the area west of The Pas Moraine had emerged from the shallow Lake Agassiz waters. In the Grass River Basin, glaciolacustrine clay and silt continued to be transported to the southwest by glacial meltwater and were deposited in thicknesses in excess of 40 m in places, forming extensive and thick deposits of laminated sediments.

PHASE 3

Phase 3 (Fig. 10) illustrates the extent of Lake Agassiz at the beginning of the Ojibway Phase about 8400 years ago (Teller and Thorleifson, 1983). This level was first documented by Johnston (1946) for the Grand Rapids area and later by Klassen (1983). The elevation of the Grand Rapids beaches is 246 m near Grand Rapids (Johnston, 1946) and increases to 259 and 267 m east and northeast of Talbot Lake, indicating a water level drop of 5 to 6 m from the previous level. This level represents the lowest flight of beaches that is part of a series of shingle beaches in the Talbot Lake area. Along a few escarpments in that area, there are at least four other beach ridges that can be recognized above the Grand Rapids level and below the Phase 2 level (Fig. 6). The elevation differences between the ridges indicate a tilt between 0.16 and 0.28 m/km, increasing towards the northeast. Johnston (1946) incorrectly correlated the Ponton beaches for the Grand Rapids beaches around Ponton, and calculated a differential uplift of 0.07 m/km for the area north of Grand Rapids. Klassen (1983) had a substantially higher figure of 0.5 m/km, but he apparently mistook the upper flight of shingle beaches (Phase 2) for the Grand Rapids beaches. Moreover, to obtain this high figure, he must have inaccurately estimated the altitudes of "a complex of ridges across the face of an escarpment ... above the northwestern shore of Lake Winnipeg" (Klassen, 1983, p. 102) at 228 to 243 m (750' to 800'). Based on the 1:50 000 topographic map and the description of the locality where he estimated the elevations, these beaches are at an elevation between 850' and 900'.

During this phase, the Grass River Basin was still a fairly deep basin (up to 30 m deep) where glacial meltwater deposited the distal end of turbidity currents.

PHASES 4 AND 5

Phases 4 and 5 depict the extent of Lake Agassiz about 8000 to 8300 years ago (Phase 4, Klassen, 1983). The Ponton beaches, named by Bell (1978), but described earlier by Tyrrell (1917) and Johnston (1946), were formed during these phases when the water level fell about 20 m from the Grand Rapids level, and later by 5 to 6 m (Fig. 11). These beaches represent the lowest Lake Agassiz beaches in the study area, and probably in the whole lake basin, although Klassen (1983) identified a discontinuous beach ridge along the Northern Indian moraine, 80 m below the Ponton level, which he named the Fidler beach.

The Ponton beaches are sandy, flat topped, and commonly developed into spits overlain by eolian sands. The beach deposits are thought to be derived in part from the reworking of a possible moraine composed of subaqueous outwash sand. This deposit was named the Hargrave Moraine by Tarnocai (1970). The morainic material was described as a mixture of

till, clay till, sandy till, calcareous till, overridden material, and subaqueous outwash. Morphologic expression is subdued, perhaps due to the wave action of Lake Agassiz or burial under laminated sediments in the Grass River Basin. A low and broad plateau oriented NW-SE east of Hargrave lake could correspond to the morainic belt of Tarnocai, although the nature of the material remains unclear.

Two different but closely spaced beaches have been identified in the area, and this explains the various levels and calculated tilts obtained by the previous authors, who apparently incorrectly identified the lower Ponton Level as the upper Ponton level, or the upper Ponton level as the Grand Rapids level. In fact, the two beaches converge into one along several rock escarpments, namely immediately south of the Grass River, and southeast of the Minago River where the beaches follow a gentle step in the carbonate bedrock, possibly marking the contact between the Red River and Stony Mountain Formations. The beaches occur between 239 m and 270 m, increasing in elevation toward the northeast. A tilt of 0.28 m/km was calculated for both levels from measured altitudes of the most continuous ridges along Highway 6 and northeast of Snow Lake. This figure is within the range of uplift rates calculated by Klassen (1983, 0.2 to 0.3 m/km) and by Ringrose (1975) for the corresponding Minago beaches (0.2 m/km).

THE MINAGO RIVER CHANNEL

When the lake level dropped below the Grand Rapids Level, the Saskatchewan River flowed along the Minago River channel towards the Nelson River, bypassing Lake Winnipeg. Tyrrell (1902) first noticed that the Minago River had been excavated by a large river. Tarnocai (1970) suggested that the Saskatchewan River built a large delta in the Ponton area when it entered Lake Agassiz via the Minago River channel. No deltaic deposits have been recognized in this boggy terrain.

During both of the Ponton phases, the Saskatchewan River entered Lake Agassiz via the Minago River channel, which can be described as a series of lakes and a valley presently occupied by the Minago River, between South Moose Lake and the Nelson River. The abandoned channel is about 400 m wide, but may reach 1200 m in width, 100 km long, and was cut down up to 20 m in the glaciolacustrine plain (Figs. 12, 13). Bell (1978) suggested that the Ponton beaches were dissected by the river since they are absent within the channel. However, recent surficial mapping in the Minago River area indicates that the beaches are skewed towards the channel, suggesting that they are contemporaneous or postdate the higher reaches of the channel, as illustrated in Figure 11. Several smaller abandoned channels also join or parallel the main channel.

The Minago River spillway was probably abandoned sometime after the final drainage of Lake Agassiz, perhaps as a result of uplift to the north and breaching of a till barrier between Cedar Lake and Cross Lake, now Cross Bay, resulted in the capture of the Saskatchewan River and its entering into Lake Winnipeg. Grice (1970) identified two small abandoned channels at 254 m and 257 m elevation northeast of Cross Lake that could have been successively used by the Saskatchewan River after the abandonment of the Minago Channel. Before the reservoir was filled, the river flowed eastward through Cross Lake draining over rapids at 248 m elevation. He estimated that isostatic tilting caused the piracy of the Saskatchewan river, and that the recent lower course at 248 m was developed during the last 8 000 ± 250 years, based on the premise that isostatic tilting would have been negligible during the last 8 000 years. The measured tilt on the Ponton beaches indisputably refutes this suggestion.

Several radiocarbon ages have been obtained on samples collected in the NATMAP Shield Margin project area to document the post-glacial history of the study area (Table 1). Two of these samples were collected within the Minago River channel. A basal fen peat sample, collected at the highest rock bottom altitude of the channel (259 m) northeast of South Moose Lake, yielded a ^{14}C age of 2530 ± 70 B.P. (GSC-5880). This date would seem to be a reliable minimum age for channel abandonment.

Several basal fen peat samples located in the surrounding peatlands have been radiocarbon dated between 4600 and 5000 B.P. (Table 1), suggesting a delay between the final drainage of Lake Agassiz and the establishment of peat-forming fen vegetation, as discussed by Zoltai and Witt (1990). The basal peat age in the abandoned Minago River channel is anomalously young compared to dates from the same context in the region. This implies that the channel was abandoned in mid-Holocene time.

Freshwater shells in calcareous silt below a small fen located immediately east of Highway 6 and within the channel, were radiocarbon dated at 5860 ± 60 B.P. (TO-4910). This date likely is too old, due to the hard-water effect from the calcareous sediments and the hardness of the Saskatchewan River water. Nielsen et al. (1987) have applied a correction factor of 350 years to freshwater shells collected in post-Lake Agassiz beaches around Lake Winnipegosis, based on an age obtained from a modern shell sample. Although it is difficult to estimate the correction factor that should be applied on the ^{14}C age of the Minago shell samples, the date probably is a reliable indicator of the maximum age for channel abandonment. This supports again that the channel was abandoned in early to mid-Holocene time.

SUMMARY

Measured elevations on the most continuous and lowest Lake Agassiz beach ridges in the study area indicate that differential isostatic uplift has caused the beaches to tilt up towards the northeast in post-Lake Agassiz time. The tilts measured on the Ponton beaches, which are approximately dated at 8000 years B.P., is about 0.28 m/km, which is similar to the figures obtained on the higher beaches. This suggests that the whole

area around northern Lake Winnipeg experienced a sustained tilting in post-Lake Agassiz time.

The diversion of the Saskatchewan River from the Minago River channel to its present course through Cedar Lake, probably due to isostatic uplift to the northeast and breaching of a till barrier west of Grand Rapids, occurred in mid-Holocene time, between 2.5 and 5.9 ka B.P.

Additional field work in Saskatchewan hopefully will result in the reconstruction of higher lake levels. Follow-up work is also planned north of Grand Rapids to document the Ponton and Grand Rapids levels towards Lake Winnipeg and to obtain more radiocarbon dates in the Minago River channel.

REFERENCES

Bell, C.K.
1978. Geology, Wekusko Lake Map-Area, Manitoba; Geological Survey of Canada, Memoir 384, 84 p.

Clarke, M.D.
1989. Surficial geology, Cormorant Lake, Manitoba-Saskatchewan; Geological Survey of Canada, Map 1699A, scale 1:250 000.

Elson, J.A.
1967. Geology of Glacial Lake Agassiz; in ed. W.J. Mayer-Oakes, Life, Land and Water, University of Manitoba Press, Winnipeg, p. 36-95.

Grice, R.H.
1970. Quaternary geology of the Grand Rapids area, Manitoba, Canada; Canadian Journal of Earth Sciences, v. 7, p. 853-857.

Johnston, W.A.
1946. Glacial Lake Agassiz, with special reference to the mode of deformation of the beaches; Geological Survey of Canada Bulletin 7, 20 p.

Kaszycki, C. A. and Way Nee, V.J.
1990. Surficial geology, Kississing Lake, Manitoba; Geological Survey of Canada, Map 1757A, scale 1:250 000.

Klassen, R.W.
1983. Lake Agassiz and the late glacial history of northern Manitoba; in eds. J.T. Teller and L. Clayton, Glacial Lake Agassiz, Geological Association of Canada, Special Paper 26, p. 97-115.

Lowdon, J.A., Robertson, I.M. and Blake, W.
1977. Geological Survey of Canada radiocarbon dates, XVII; Geological Survey of Canada, Paper 77-7, Ottawa, Ontario, 25 p.

McMartin, I.
1994a. Ice flow events in the Cormorant Lake - Wekusko Lake area, Northern Manitoba; Current Research, Part C, Geological Survey of Canada, Paper 1994-C, p. 175-182.

1994b. Surficial Geology of the Talbot Lake area, Manitoba (NTS 63J3 to J6); Geological Survey of Canada, Open File 2744, 1 sheet, scale 1:100 000.

1994c. Surficial Geology of the Mitishto River area, Manitoba (NTS 63J11,12 and 14); Geological Survey of Canada, Open File 2835, 1 sheet, scale 1:100 000.

McMartin, I. and Boucher, R.
in press. Surficial geology of the North Moose Lake Area, Manitoba (NTS 63/K1,K2,K7,K8); Geological Survey of Canada, Open File 3060, 1 sheet, scale 1:100 000.

Nielsen, E. and Groom, H.D.
1987. Glacial and late glacial history of The Pas area; in ed. B.T. Schreiner, The Quaternary between Hudson Bay and the Rocky Mountains, XIIth INQUA Congress, Ottawa, Excursion Guide C-13, National Research Council of Canada, NRC 27533, 45 p.

Nielsen, E., McNeil, D.H. and McKillop, W.B.
1987. Origin and paleoecology of post-Lake Agassiz beaches in Manitoba; Canadian Journal of Earth Sciences, v. 24, p. 1478-1485.

Ringrose, S.
1975. A re-evaluation of Late Lake Agassiz shoreline data from North Central Manitoba; The Albertan Geographer, No. 11, p. 33-41.

Teller, J.T. and Thorleifson, L.H.
1983. The Lake Agassiz - Lake Superior Connection; in eds. J.T. Teller and L. Clayton, Glacial Lake Agassiz, Geological Association of Canada, Special Paper 26, p. 261-290.

Tarnocai, C.
1970. Glacial history, surface deposits, soils and vegetation of Wekusko and portions of Cross Lake, Norway House and Grand Rapids map areas; Proceedings of the Fourteenth Annual Manitoba Soil Science Meeting, p. 21-25.

Tyrrell, J.B.
1902. Report on explorations in the northeastern portion of the District of Saskatchewan and adjacent parts of the District of Keewatin; Geological Survey of Canada Annual Report, v. XIII, Pt. F, 218 p.

1917. Records of Lake Agassiz, in southeastern Manitoba and adjacent parts of Ontario, Canada; Geological Society of America Bulletin, v. 28, no.1, p. 146-148.

Zoltai, S.C.
1988. Wetlands of Canada; Ecological Land Classification Series, No. 24, Environment Canada, Ottawa, Ontario.

Zoltai, S.C. and Vitt, D.H.
1990. Holocene Climatic Change and Distribution of Peatlands in Western Interior Canada; Quaternary Research, No. 33, p. 231-240.

Table 1: Selected radiocarbon dates in the Minago River area

Location	Radiocarbon age (Years B.P.)	Lab No.	Reference	Comments
54°04'09"N, 99°34'54"W	2530±70	GSC-5880	This paper	Basal fen peat at bottom of channel
54°24'41"N, 99°36'42"W	4930±80	GSC-5931	This paper	Basal fen peat SE of Hargrave Lake
54°16'N, 99°09'W	4900±100	BGS-868	Zoltai et al., 1988	Basal fen peat north of channel, along Highway 6
54°36'N, 98°34'W	4500±120	GSC-1958	Lowdon et al., 1977	Basal peat on clay plain, north of Minago River
52°53'N, 99°08'W	4670±130	GSC-410	Lowdon et al., 1977	Basal peat, south of Grand Rapids
54°12'05"N, 99°10'04"W	5860±60	TO-4910	This paper	Freshwater shells below peat within channel

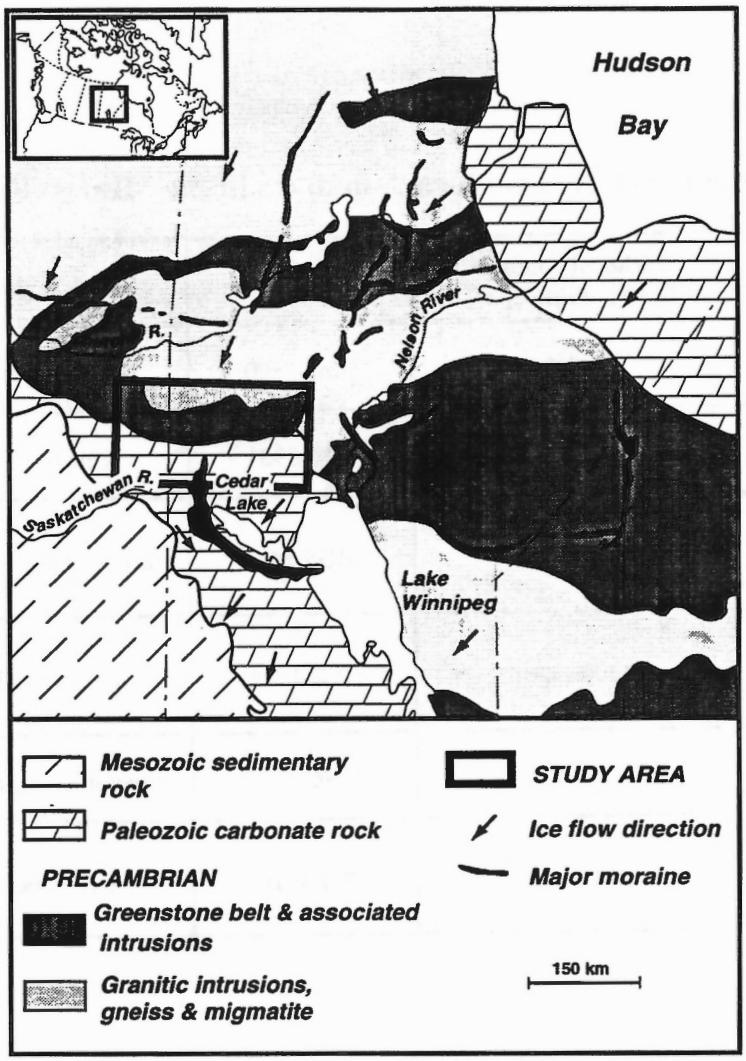

Figure 1. Location map of study area showing generalized bedrock geology, regional ice flow trends and location of major moraines. The Pas moraine is located southwest of Cedar Lake.

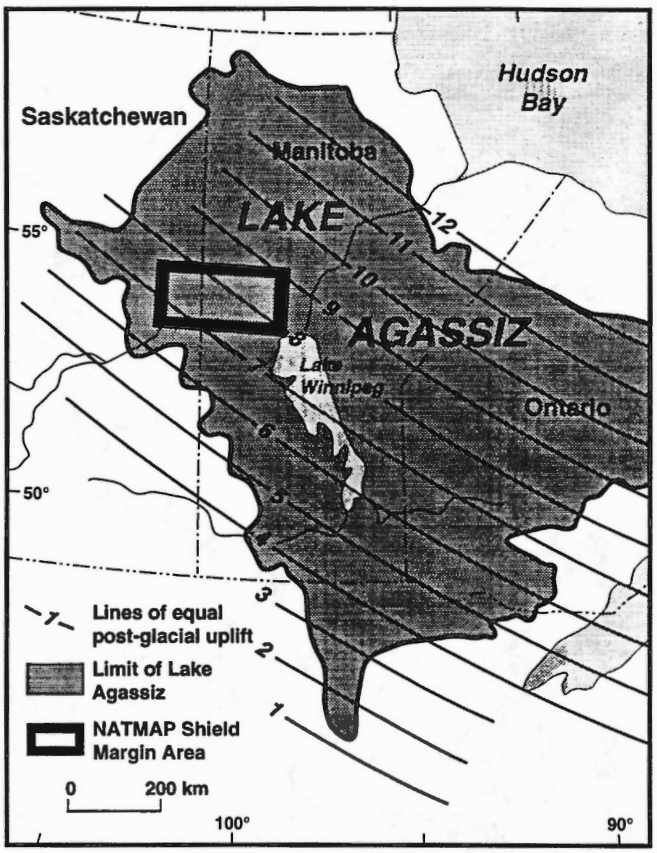

Figure 2. Location of study area within Lake Agassiz basin, with isobases showing lines of equal post-glacial uplift (taken, in part, from Teller and Thorleifson, 1983).

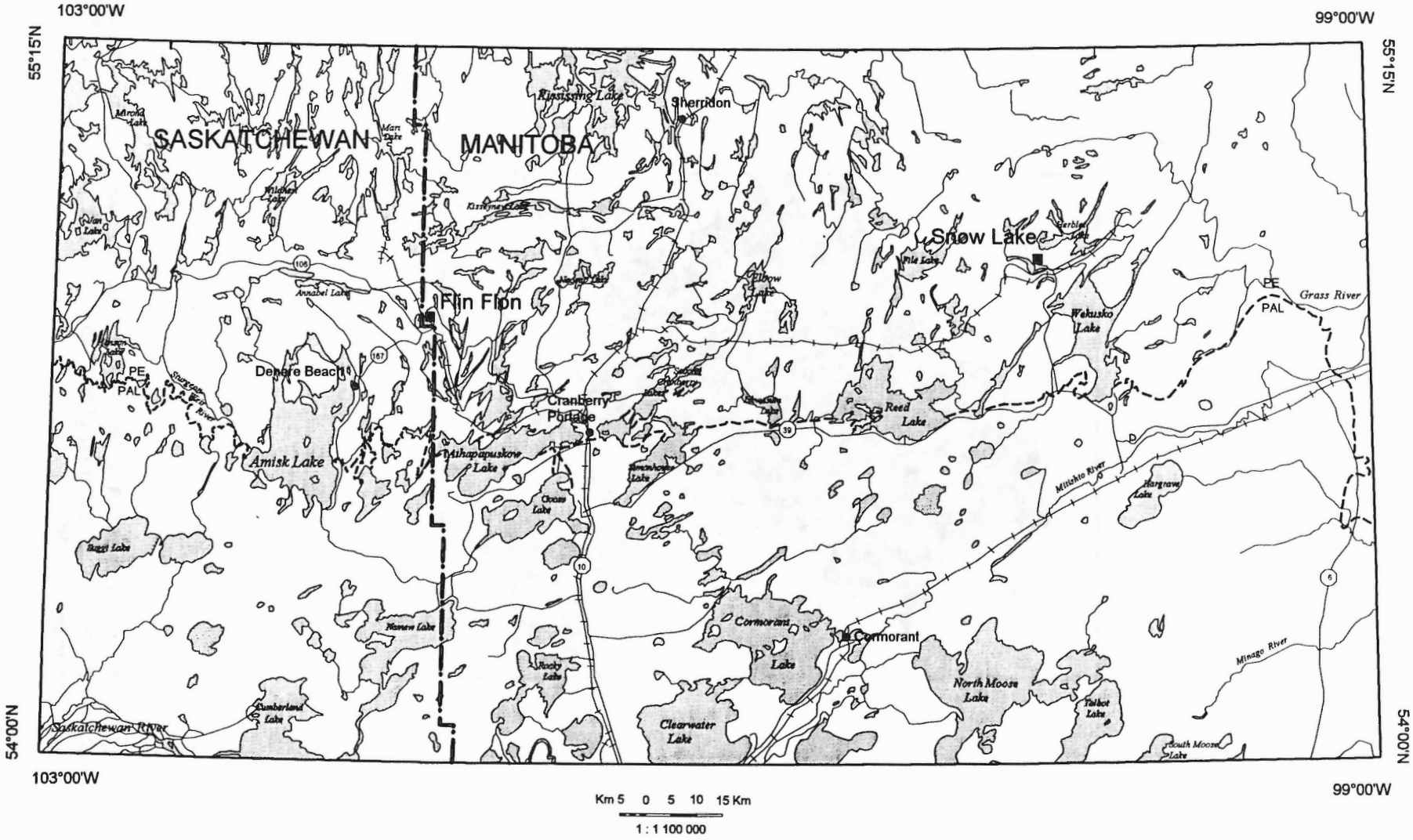

Figure 3. Detailed location map of the Shield Margin area. PE and PAL indicate Precambrian and Paleozoic bedrock, respectively.

Figure 4. Section in Lake Agassiz beach sediments, reworked from calcareous till. The sediments are moderately well sorted, horizontally bedded and coarsening upward.

Figure 5. Section in a shingle beach deposit along a small carbonate escarpment, exposing angular dolomitic pebbles and cobbles. Ridge is less than 2 m high.

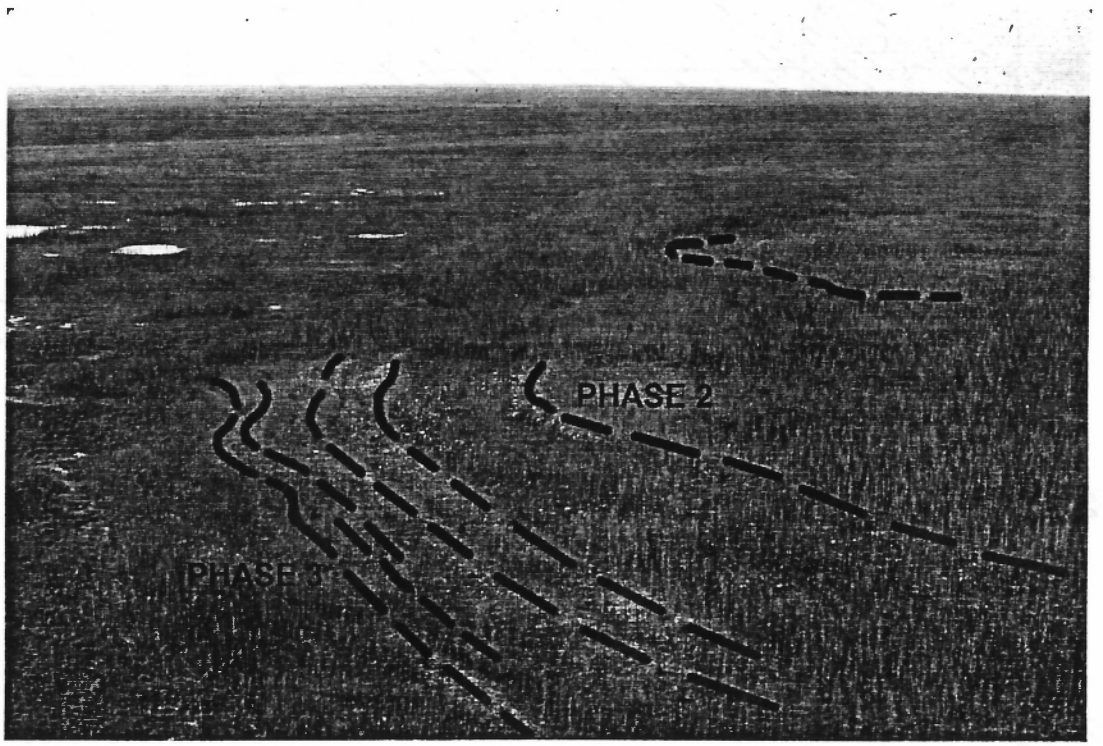

Figure 6. Flight of shingle beaches along bedrock escarpment east of Talbot Lake. The higher beaches are part of the Phase 2 level. The lower beaches are part of the Grand Rapids level.

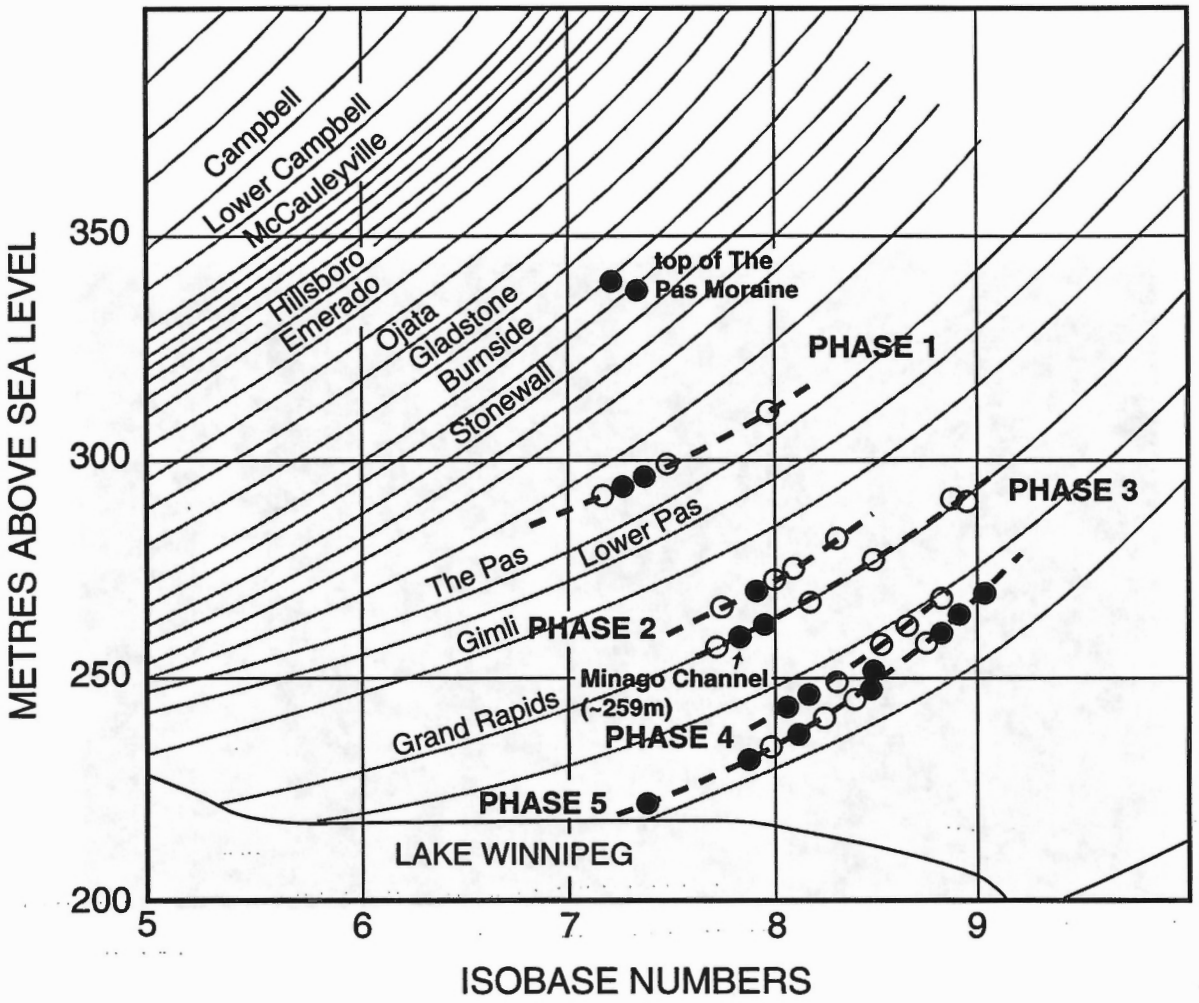

Figure 7. Lake Agassiz strandline diagram, showing former water planes, projected onto a vertical plan orthogonal to the isobases depicted on Figure 2 (taken, in part, from Teller and Thorleifson, 1983). Filled circles are altimeter measurements; open circles are inferred altitudes from 1:50 000 maps.

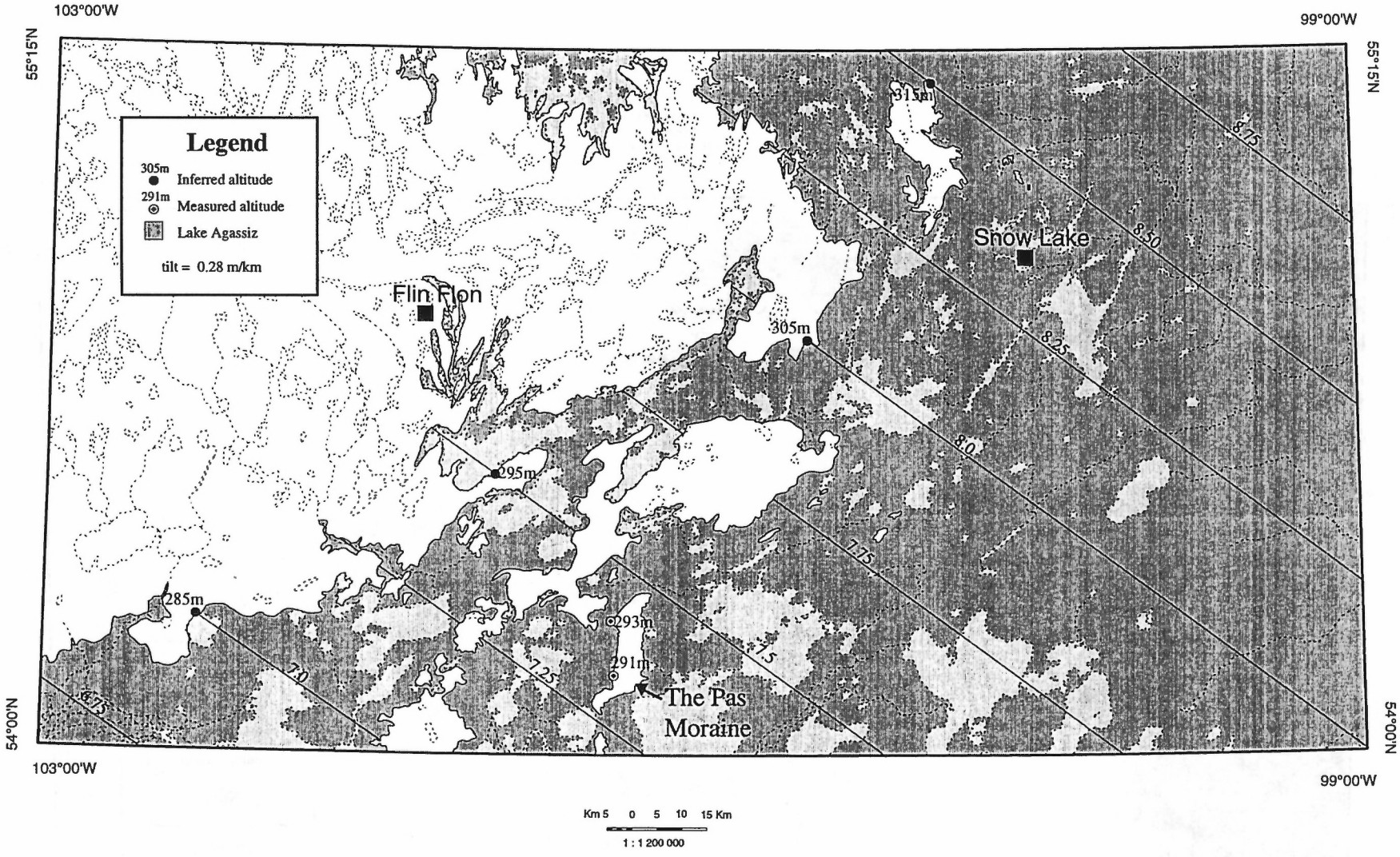

Figure 8. Extent of Lake Agassiz during Phase 1. Tilt value indicates present gradient of the former water plane.

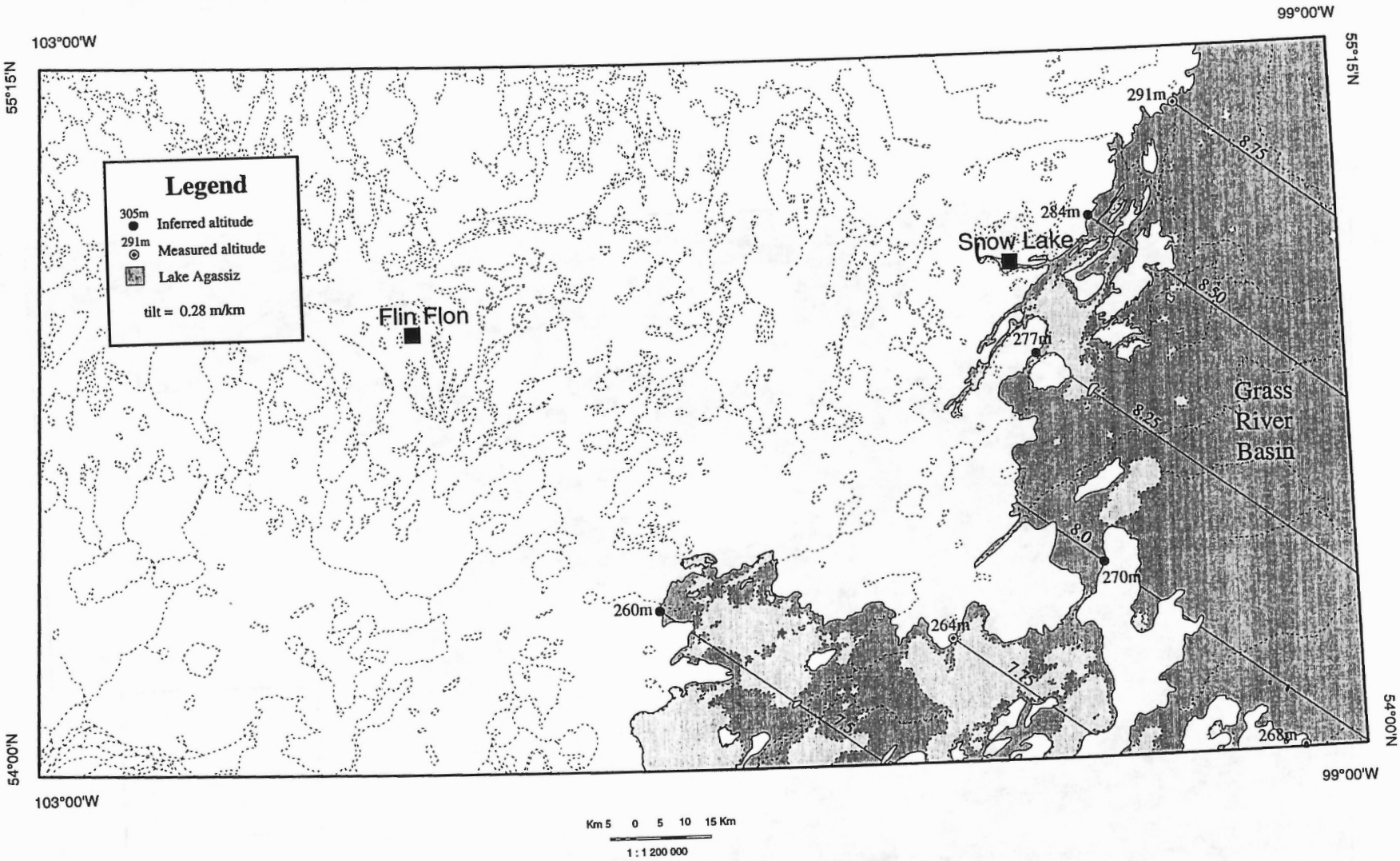

Figure 9. Extent of Lake Agassiz during Phase 2.

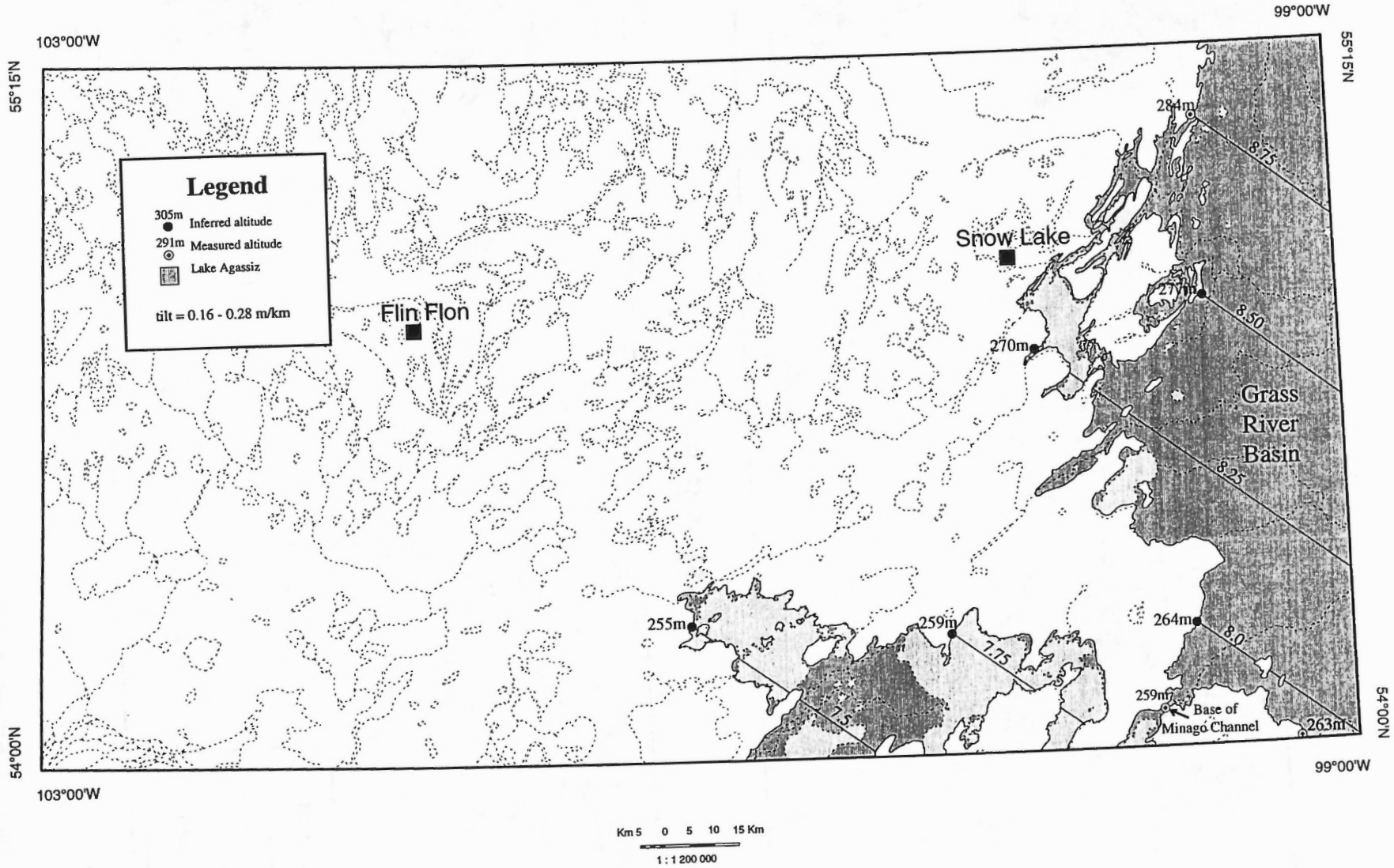

Figure 10. Extent of Lake Agassiz during Phase 3.

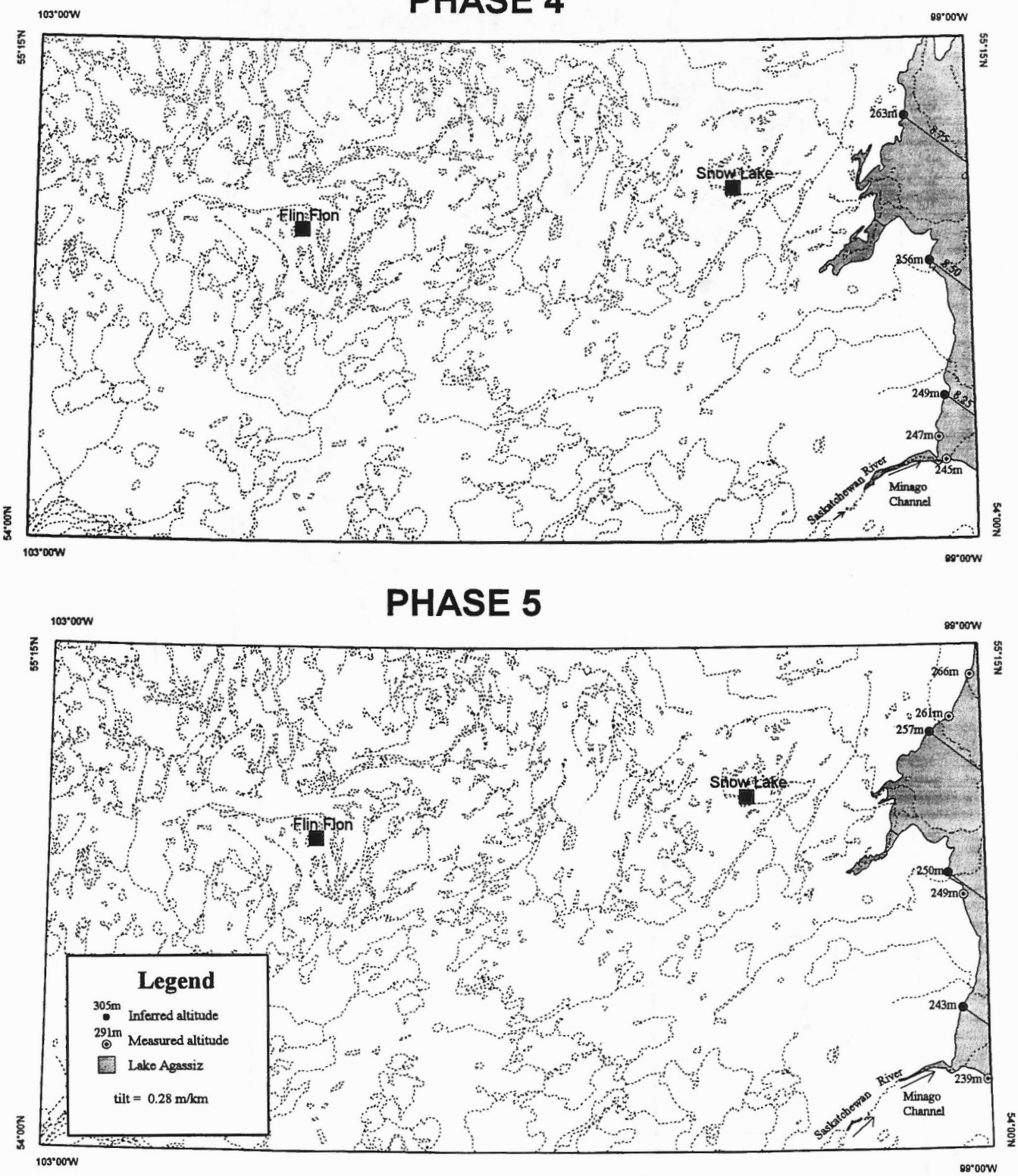

Figure 11. Extent of Lake Agassiz during Phase 4 and Phase 5.

Figure 12. Fen peat developed on alluvial sediments at the bottom of the Minago River channel, north of the Minago River along Highway 6. The south side of the channel appears on the left, where the former course of the Saskatchewan River cut down 6 m into fine-grained glaciolacustrine sediments.

Figure 13. Aerial view of the abandoned river channel where it splits temporarily into two arms around a bedrock plateau, west of Highway 6. The Minago River runs at the bottom of the channel. The abandoned channel is about 300 m wide in this area.

6.4 Paleoshoreline and lake gauge evidence for post-Lake Agassiz regional tilting in Manitoba

Gary Tackman and Donald Currey

Department of Geography
University of Utah, Salt Lake City, Utah 84112

INTRODUCTION

One of the more important objectives of geodynamic research is to model mantle rheology, lithosphere thickness, and glacial loading history from observations of vertical surface motions (glacio-isostatic rebound) induced by the glacial load. Within the Laurentide sector of North America, one of the more important and frequently used glacial models is ICE-3G of Tushingham and Peltier (1991, 1992). ICE-3G is based substantially on an extensive compilation of relative sea level histories (RSL) and a theoretical model of the glacial isostatic adjustment process, but is also constrained by geological evidence such as moraines. At each RSL location local ice thickness was adjusted to yield a reasonably accurate fit to the local RSL curve (Tushingham and Peltier, 1991). Thus, ICE-3G has been calibrated by an extensive data set of RSL curves along the marine coast. Few observational constraints from the glacial isostatic adjustment process come from continental interior locations. This creates the potential risk of misspecifying the load and/or its history at distal continental interior locations, a concept we refer to as a "marine bias." The objectives of our work center on providing glacio-isostatic rebound observations from the continental interior region of southern Manitoba that can serve as constraints for ICE-3G and other glacial models (e.g. ICE-4G of Peltier, 1994) and for geodynamic modeling of lithosphere thickness and mantle rheology.

Excellent opportunity to add observational constraints from the continental interior exists in southern Manitoba. Well preserved post-Lake Agassiz abandoned shorelines are present around Lake Winnipegosis and Dauphin Lake and a network of lake level gauges has been in operation for Lakes Winnipeg, Manitoba, and Winnipegosis that, in a few cases, extend back to 1914 (Fig. 1). The main objective of our research is to determine the amount, rate, and direction of the regional glacio-isostatic tilting that has occurred over southern Manitoba since the recession of Lake Agassiz from the area between about 9000 and 8000 years ago. The results can then be compared against predictions based on ICE-3G to assess its adequacy for this particular continental interior location.

After completing two, of three scheduled, month-long field seasons in Manitoba and two years of lab and office research, we have compiled interim results from 80 ^{14}C dates, over 200 surveyed shoreline elevation points, and the mapping of most of the recognizable post-Lake Agassiz abandoned shorelines around the basins of Lake Winnipegosis and Dauphin Lake from field work and a collection of over 2000 air photos. We have also performed numerical analysis on all the available lake level gauges from Lakes Winnipeg (8 stations), Manitoba (6 stations), and Winnipegosis (2 stations) (Fig. 1) and obtained contemporary rates of separation between surface topography and the geoid according to an ICE-3G loading history and 1066B earth structure for comparison. We caution that the results presented in this report are preliminary and subject to change as we obtain more information from our 1995 field season and acquire benchmark and site maintenance histories for the lake gauge stations. Our best estimate is that the revisions (if any) would be no greater than ± 25%.

BENEFITS AND SIGNIFICANCE OF WORK

An important goal of our work is to extend the glacio-isostatic rebound record known from the tilted shorelines of former Lake Agassiz. Combining the tilting histories of Lake Winnipegosis, Dauphin Lake, and the historic record of the lake gauges with what is known from Lake Agassiz would create an almost complete record of differential rebound history from the time of deglaciation to the present for a continental interior region. It is also noteworthy that the Winnipegosis and Dauphin records overlap in time with the marine shoreline record (RSL histories) of Hudson Bay. Thus, our Manitoba interior data will provide a history of differential rebound that can complement the Hudson Bay marine record and serve as a test against geodynamic model predictions for a continental interior region.

As an integral part of our work, we must reconstruct the post-Lake Agassiz lacustrine histories of these lakes from their shoreline records. These lake level histories will be an important contribution to the post-glacial natural history record of southern Manitoba and can serve as both a model and test for other chronologies of nearby lakes constructed from shorelines and/or other proxy data, such as the core stratigraphy obtained by the Lake Winnipeg Project. Better yet, we think the combined data from a lake's shoreline record and offshore core stratigraphy can be a powerful combination for reconstructing the total water level fluctuation (highs and lows) history.

Our work also has implications for regional Holocene climate change. Because fluctuating lake levels, associated with changes in surface area, are substantially controlled by regional

climate change, a lake's surface elevation history can serve as an indicator of changing regional paleoclimate. For example, we have constructed a hydrograph for Dauphin Lake (Fig. 2) from its shoreline record and find it resembles the water level record of the Lake Michigan basin according to Hansel et al. (1985) over the last 6000 years.

DAUPHIN LAKE

We have pieced together much of the post-Lake Agassiz history of Dauphin Lake from its shoreline record. The Dauphin Lake shorelines, dated thus far, range in age from 7800 to 460 B.P. The highest shoreline, tentatively named Id (see Appendix I for an explanation of our Dauphin Lake shoreline identification system), dates to 4600 B.P. (average of three ^{14}C dates from mollusc shells) and seems to correspond to the high shoreline of the Nipissing I phase of the Lake Michigan basin. South of Methley Beach Provincial Park, along the southeast margin of the lake, it has an elevation of 263.9 m (865.8 ft) ASL. The Id shoreline is part of a complex of four distinct shorelines we have tentatively named Ib through Ie. Ia is also a prominent complex of three shorelines we have tentatively named Ia1, Ia2, and Ia3. In contrast to the complex character of shoreline I, shorelines II, III, and IV are distinct single-crested beaches. Shoreline III does, however, display a double crest along the north margin of Dauphin Lake. Shoreline II is difficult to find anywhere except at its type locality south of Methley Beach.

Shoreline IV is the oldest and most landward beach. Morphologically, it is generally broad and well rounded, showing the signs of geomorphic decay associated with its "old" age. A mollusc sample collected from a south-shore locality near Methley Beach produced a radiocarbon age of 7730 ± 140 B.P., while another mollusc sample from a north-shore site produced an age of 7970 ± 60 B.P. In the Methley Beach area it is at an elevation of 262.5 m (861.3 ft) ASL.

Shoreline III dates to between 6540 and 6100 B.P. from four mollusc samples collected from two south-shore and two north-shore localities. South of Methley Beach it has an elevation of 262.4 m (861.0 ft) ASL. It cannot be determined from the shoreline record how low the lake fell between the stable period that formed shoreline IV and that which formed III. This is a situation where offshore core stratigraphy could possibly fill the information gap between shorelines.

The three shorelines we best understand (Ib, Id, and IV) have all been tilted up to the northeast. As expected, shoreline IV (figures 3 and 4) exhibits the greatest slope (18.5 ± 0.4) cm/km. This translates to a tilt rate of (2.4 ± 0.5) x 10^{-8} radians yr^{-1}, or equivalently, over a 100-km baseline, a differential uplift rate of (2.4 ± 0.5) mm yr^{-1}. The Ib-Id shorelines are similar in elevation and age (Ib = 4300 B.P. and Id = 4600 B.P.) and thus we have combined them into one tilt rate (figure 4). As expected, the measured slope (10.0 ± 0.2) cm/km, is significantly less than that of shoreline IV. This translates to a tilt rate of (2.3 ± 0.4) x 10^{-8} radians yr^{-1}, similar in magnitude to shoreline IV. Over a 100-km baseline the differential uplift rate is (2.3 ± 0.4) mm yr^{-1}. As a comparison, the southern portion of the Ponton beach of Lake Agassiz, which dates to ~ 8300 B.P., has an estimated slope of 20 cm/km (Klassen, 1983), which works out to a tilt rate of 2.2 x 10^{-8} radians yr^{-1}. Although the Ponton beach is farther north where differential rebound rates are higher, it appears that "average" tilt rates have remained reasonably stable over the region during the last 8000 years.

Although average tilt rates computed over the life of the shoreline are meaningful, the next step in resolution is to determine the rate of change in the tilt rate. The prediction is that tilt rates decrease with time as isostatic recovery approaches equilibrium. Changing tilt rates can be computed by differencing the slopes between two shorelines, computing the resulting angle and dividing by the time difference. For example, between the time shorelines IV and Id-Ib were formed (3450 years), shoreline IV experienced a tilt rate of 2.5 x 10^{-8} radians yr^{-1}. Since 4350 B.P. the tilt rate of shoreline IV has decreased to 2.3 x 10^{-8} radians yr^{-1}. Although the change in rate is small (and statistically insignificant with respect to the errors), when a sufficient number of tilt rate changes is known a trend can be determined from which relaxation time can be computed. This is an important parameter in geodynamics because it can be used to compute mantle viscosity. Thus, one of our major objectives during the 1995 field season is to map, survey, and understand as many of Dauphin Lake's shorelines as we possibly can in an effort to determine as many tilt rates as possible. For Dauphin Lake we may be limited to something like 6 or 7 shorelines. On Lake Winnipegosis, however, significantly more potential exists.

LAKE WINNIPEGOSIS

Although Lake Winnipegosis holds more potential in terms of abandoned shorelines, it involves covering a much greater area in more remote, relatively inaccessible, terrain. Therefore, to date we know much less about Lake Winnipegosis than Dauphin Lake. Because of its potential, however, Lake Winnipegosis will be the major focus of our 1995 field season.

One prominent shoreline, named the Dawson level by Nielsen et al. (1987), dates to 5200 B.P. and is tilted up to the northeast. We do not have a sufficient number or an appropriate spatial distribution of survey points to compute a trend surface. Thus, we have assumed a tilt direction of 45°, which is consistent with the elevation-location relationship of the points and the tilt directions of Lake Agassiz shorelines and our work from Dauphin Lake. Figure 5 shows the profile from which we compute a tilt rate of 2.1 x 10^{-8} radians yr^{-1}, which is consistent with the tilt rates of Dauphin Lake. Three other shorelines, tentatively named 0, 1, and 2 do not exhibit any tilt (increasing number in a landward direction). Shoreline 0 is very young, probably representing the high water levels of 1955. Shorelines 1 and 2 date to between 350 and 590 B.P.,

which probably represents the Little Ice Age period. The amount of tilting that has occurred since the formation of these shorelines has not been large enough to show elevation differences that significantly exceed the geomorphic noise inherent in the beach-forming process. Another beach, shoreline 3, is in a position that indicates a maximum limiting age of 3100 B.P. It has an apparent tilt but not enough points have been surveyed to confidently compute a tilt rate.

Other shorelines exist above and below the Dawson level that will be instrumental in unravelling the lacustrine and rebound history of Lake Winnipegosis. These are shown in the bottom plot of Figure 5. The plot suggests a tilt up to the northeast. At Denbeigh Point, in the northeast segment of the lake, the highest Winnipegosis shoreline was surveyed at 264.0 m (866.3 ft) ASL, 10 m below the lowest Lake Agassiz beach and 11 m above the present water level of the lake. Gastropod shells from the beach crest produced a ^{14}C age of 6590 B.P. Correlation of this shoreline at enough other locations is critical for obtaining an early post-Agassiz tilt rate of the Winnipegosis basin and for unravelling the transition from the final phase of Lake Agassiz in the Winnipegosis basin to earliest Lake Winnipegosis time. The dating of the Agassiz shorelines has proven difficult because of the lack of carbon-bearing material present in the coarse beach sediment. Nevertheless, if Lake Agassiz receded from the Denbeigh Point vicinity between 8700 and 8300 B.P. (Phase 3 to Phase 4 of Klassen, 1983), then roughly 2000 years of missing history is indicated.

LAKE GAUGES

We have analyzed the pair-wise station differences of the monthly averages for Lakes Winnipeg, Manitoba, and Winnipegosis according to the concepts discussed in Figure 7 of Appendix I. From these pair-wise rates we have computed tilt rates for Lakes Winnipeg and Manitoba according to the best-fitting planar representation of the data (see Appendix II for a computational summary). Lake Winnipegosis has only two gauges and thus could not be included in the trend surface analysis. The station-pair gives a strong tilt signal. The differential rebound rate between the Winnipegosis and Dawson Bay stations is 3.9 mm yr^{-1} (the land surface at Dawson Bay is rising relative to Winnipegosis) and is the highest and one of the strongest signals from all the station pairs.

For Lake Winnipeg we compute a tilt rate of $(2.1 \pm 0.3) \times 10^{-8}$ radians yr^{-1} ($r^2 = 0.96$) with a bearing in the upslope direction of $N(41.8 \pm 3.7)°E$ and for Lake Manitoba $(2.3 \pm 0.8) \times 10^{-8}$ radians yr^{-1} ($r^2 = 0.90$) and bearing of $N(50.5 \pm 9.9)°E$. The direction and tilt rates are consistent with the shoreline observations from Dauphin Lake and Lake Winnipegosis. Figure 6 shows the planar fits from the lake gauge data imposed on the predicted rebound pattern computed according to the ICE-3G model and 1066B earth structure (computation performed for us by Tom James of the Geological Survey of Canada).

The model results of Figure 6 represent relative rates of separation between surface topography and the geoid. Using these rates computed at each gauge station and performing the same planar trend surface fit gives a tilt rate of $(0.89 \pm 0.02) \times 10^{-8}$ radians yr^{-1} with an upslope bearing of $N(29.2 \pm 1.5)°E$ for Lake Winnipeg and $(1.10 \pm 0.04) \times 10^{-8}$ radians yr^{-1} with an upslope bearing of $N(38.0 \pm 2.6)°E$ for Lake Manitoba. The gauge observations are more than two times greater than the topography-geoid separation rates and considerably more easterly in uptilt direction. Although there is some agreement between the model and the lake gauge data, there is enough disagreement to raise concerns about errors in the ice/earth model and/or problems with the lake gauge data. With regard to the model one area of concern is a possible "marine bias" discussed earlier in this report. Although ICE-3G performs well for regions reasonably close to the marine coast where the calibration locations exist, it may not fit so well within this particular continental interior location, possibly due to a lack of interior control points.

However, before this can be more confidently stated we must be sure there are no problems with the lake gauge data. As of this writing there appears to be a potential problem with benchmark changes for some of the gauges. Several of the time series of the pair-wise differences exhibit significant unexplained periodicities which adversely affect our regression slopes. The periodicities may not be real, but instead might be an artifact of the station's benchmark history and other adjustments, some of which are based on the principle that a lake surface is a level surface. Although this is true over short periods of time during calm water conditions, in this region where glacio-isostatic tilting is occurring these latter types of adjustments could corrupt the tilt signal. As the lake basin tilts through time adjustments may have been made to "re-equalize" the elevation readings for the network of stations (i.e. the Lake Winnipeg datum adjustment). Presently, we do not have information that would allow us to assess the magnitude of these potential problems. However, Manitoba Hydro has graciously agreed to supply us with benchmark histories for all gauge stations and other information related to adjustments that have been made over the years. We expect this data will enable us to assess the magnitude of the problem and make appropriate corrections to better resolve the tilt signal, which we will report in the future.

It is also worth noting that both the separation figures and observations from the gauges indicate Lake Manitoba has a higher tilt rate than Lake Winnipeg (although it is recognized that, according to the gauge observations, there is no significant difference between the lakes within the errors). The tilt-rate ratio of Lake Manitoba to Lake Winnipeg for the gauges is 1.1, and for the topography-separation model is 1.2. The near equivalence between the two ratios suggests there may be something real. However, given that Lake Winnipeg is closer to the center of isostatic deflection located in northern Hudson

Bay, it is reasonable to expect that it should experience a greater tilt rate than Lake Manitoba. One explanation may relate to differences in local glacial loading history. If this is the case, then this is an example of where our continental observations could locally improve ICE-3G and other glacial models. Another explanation may relate to the greater water load of Lake Winnipeg, which could suppress rebound in the Winnipeg basin relative to the Lake Manitoba basin. At present, however, this apparent anomaly cannot be explained.

CONCLUDING REMARKS

We are encouraged by the consistency of the results between the different lakes and data sources. Preliminary tilt rates computed from the post-Agassiz shorelines of Dauphin Lake and Lake Winnipegosis and lake gauge data for lakes Winnipeg and Manitoba all consistently show regional tilting up to the northeast at rates that vary between (2.0 and 2.5) x 10^{-8} radians yr^{-1}. The rates are consistent with the 2.2 x 10^{-8} radians yr^{-1} measured on the Ponton beach of Lake Agassiz which dates to ~ 8300 B.P. The implication is that long-term average tilt rates have been relatively stable throughout the region over the last 8000 years.

The contemporary rates computed from the lake gauge data are more than two times greater than the topography-geoid separation rates and considerably more easterly in uptilt direction. The topography-geoid separation rates are based on an ICE-3G loading history and 1066B earth structure. One implication is that ICE-3G may have a marine bias because it is primarily based on relative sea level curves and thus may not be adequate for all continental interior locations. An additional problem may rest with the lake gauges themselves. Over the years numerous adjustments have been made to the station benchmarks based on the principle that a lake surface is a level surface. This type of adjustment could have corrupted the tilt signal. At present we do not have information to assess the magnitude of this potential problem.

Our work is still in progress and the results presented here could be revised as we collect more information during our 1995 field season and acquire benchmark and site maintenance histories for the lake gauge stations. Nevertheless, we are reasonably confident that any revisions in our tilt-rate figures would be no greater than ± 25%.

ACKNOWLEDGMENTS

This work is supported by a NASA grant (NAG-5-2055) to Don Currey and partial support from a Geological Society of America research grant (GSA 5718-95) to Gary Tackman. We are also indebted to Damon Roberts and Tammy Wambeam for field assistance. We thank Tom James for his computation of rebound rates according to ICE-3G and Tony Lambert for reviewing this paper. Carol Walker, Ole Larsen, and Jim Way of Water Survey of Canada supplied the lake gauge data and other information pertaining to the lake gauge analysis.

REFERENCES

Hansel, A.K., Mickelson, D.M., Schneider, A.F. and Larsen, C.E.
1985. Late Wisconsinan and Holocene history of the Lake Michigan basin; in eds. P.F. Karrow and P.E. Calkin, Quaternary evolution of the Great Lakes, Geological Association of Canada Special Paper 30, p. 39-54.

Klassen, R.W.
1983. Lake Agassiz and the late glacial history of northern Manitoba in eds. J.T. Teller and Lee Clayton, Glacial Lake Agassiz, Geological Association of Canada, Special Paper 26, p. 97-115.

Neter, J., Wasserman, W. and Kutner, M.H.
1990. Applied linear statistical models; Richard D. Irwin, Inc., Boston.

Nielsen, E., McNeil, D.H. and McKillop, W.B.
1987. Origin and paleoecology of post-Lake Agassiz raised beaches in Manitoba; Canadian Journal of Earth Sciences, v. 24, p. 1478-1485.

Peltier, W.R.
1986. Deglaciation-induced vertical motion of the North American continent and transient lower mantle rheology; Journal of Geophysical Research, v. 91, p. 9099-9123.

1994. Ice age paleotopography; Science, v. 265, p. 195-201.

Stuiver, M. and Pearson, G.W.
1986. High-precision calibration of the radiocarbon time scale; Radiocarbon, v. 25, p. 805-838.

Tushingham, A.M. and Peltier, W.R.
1991. ICE-3G: a new global model of late Pleistocene deglaciation based upon geophysical predictions of post-glacial relative sea level change; Journal of Geophysical Research, v. 96, p. 4497-4523.

1992. Validation of the ICE-3G model of Würm-Wisconsin deglaciation using a global data base of relative sea level histories; Journal of Geophysical Research, v. 97, p. 3285-3304.

APPENDIX I

CONVENTIONS FOLLOWED IN THIS REPORT

Ia. ^{14}C Ages

All B.P. ages associated with our work are ^{14}C ages corrected for fractionation based on their $^{13}C/^{12}C$ ratios. We have not corrected shell dates for a hard-water effect, nor have we calibrated any of our dates to calendrical time. We intend to correct our shell ages for the hard-water effect and then convert all dates to calendar time. Currently, we have only one sample pair that suggests the hard-water effect may be causing shell samples to be ~ 300 years too old. This is based on a collection of charred wood found in conjunction with small clam shells believed to be contemporaneous. The sample was collected from beach sediment near Camperville on Lake Winnipegosis. This is consistent with a 350-year hard-water-effect error estimated by Nielsen et al. (1987), also on Lake Winnipegosis. Our intention is to collect more of these pair-wise samples in order to better constrain the hard-water effect over a range of ages. It is necessary to remove the hard-water effect before converting to calendar age because the calibration curves assume the sample was in equilibrium with atmospheric CO_2 while alive (Stuiver and Pearson, 1986).

Ib. Dauphin Lake Shoreline Identification System

Our identification system for Dauphin Lake shorelines is an interim system. It is not based on age but on position landward from the current lake margin. First-level Roman numerals, second-level Latin letters, and third-level Arabic numerals all increase landward and, as it happened, with shoreline age. The system was developed out of expediency in the field as a short-term classification system before we knew the ages of shorelines. We intend to revise the system to conform with chronology upon completion of our project.

Ic. Tilt Rate Measure

Because our measurements from paleoshorelines and lake gauges do not allow the computation of rebound rates relative to the geoid, tilt rates are expressed in radians yr^{-1}. Rates of tilting expressed in angular measure are a unitless measure of vertical motion under a linear geometry assumption. The advantage is that differential uplift rates can be computed over any desired baseline length which, under the linear assumption, should generally not exceed 100 km. Over longer distances the linear assumption breaks down because differential rebound can cause the uplift profile to assume an exponential form. Differential uplift rates are usually computed along a baseline that is perpendicular to the isobases or isorates. Figure 7 graphically explains the geometry involved. The example is for two gauges on a lake controlled by an outlet that does not erode over the time period considered. The example is also directly applicable to tilting shorelines.

At time t_0 water surface elevation measurements for the two lake-level gauges begins. The difference between the two gauge readings at t_0 is $\Delta z_0 = 0$. After sufficient time has elapsed (t_0 to t_1) to allow for measurable differential rebound to occur, the two gauges are read again. The difference is $\Delta z_1 > 0$. Two more measurements are made at the same time interval (although the same time interval is not a requirement) which produce increasing Δz values ($\Delta z_3 > \Delta z_2 > \Delta z_1 > \Delta z_0$) with time. A plot of Δz on time shows the steady drift of Δz over time. Assuming a steady tilt rate, the slope of the regression line is the rate of vertical motion of gauge **b** relative to gauge **a**. The geometry at the base of the diagram for time t_3 shows that the elevation difference being measured is the relative difference between the gauges, not relative to the datum, which is represented by the heavier horizontal dashed line. In reality this datum would be a reference geoid (e.g. NAVD 1927 or NAVD 1988). If the lake basin is not too distant from the "pivot point," which is the boundary between subsidence and uplift, then the geometry can be easily worked out to give uplift rates relative to the geoid. However, this can be risky business if the location of the subsidence-uplift boundary is not well constrained.

APPENDIX II

SUMMARY OF COMPUTATIONAL PROCEDURES FOR FIRST-ORDER TREND SURFACE ANALYSIS

Fitting a plane to a field of co-temporal measured shoreline elevations or a network of lake gauge stations was accomplished through standard multiple regression techniques (e.g. Neter et al., 1990). The dependent variable is the elevation of the shoreline points and the independent variables are the UTM (Universal Transverse Mercator) Easting and Northing coordinates of each point. For the lake gauges the annual rates serve as the dependent variable. The best-fit equation of a plane to the points is computed by the ordinary least squares method (OLS). The equation for the planar surface is:

$$z = b_0 + b_1 x + b_2 y + e$$

where z is the observed elevation, x is UTM Easting, y is UTM Northing, b_0 is the elevation of the plane at (x=0, y=0; the intercept), b_1 is the easterly slope, b_2 is the northerly slope, and e is the residual or error term.

Among the advantages of using a plane to represent a tilted surface is the ease of computing a slope and upslope tilt direction. If θ is upslope tilt direction in UTM grid space then:

$$\theta = \arctan \frac{|b_1|}{|b_2|}$$

where the vertical bars indicate absolute value and θ is measured from either the north or south half of the north-south axis according to table 1.

The slope (S) is computed from:

$$S = \sqrt{b_1^2 + b_2^2}$$

and tilt rate

$$\left(\frac{\Delta \phi}{\Delta t} \right)$$

is readily computed from the slope by:

$$\frac{\Delta \phi}{\Delta t} = \frac{\arctan(S)}{t} \cong \frac{S}{t}$$

where ϕ is in radians and t is the age of the paleoshoreline. The last part of the above equation holds well for the small numbers ($< 10^{-7}$) encountered with the tilting rates in southern Manitoba because the tangent of an angle is very nearly equal to the value of the angle for very small numbers.

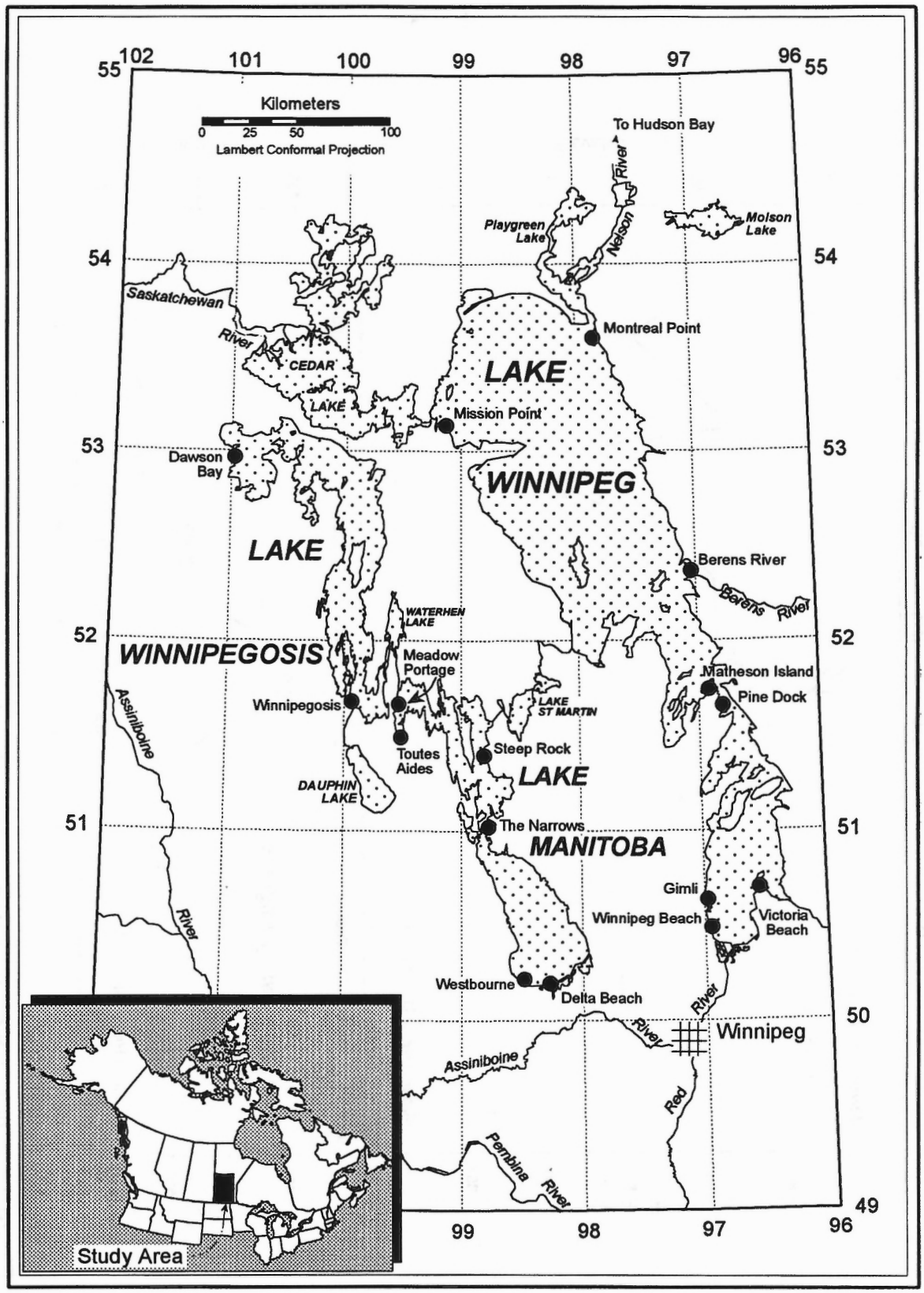

Figure 1. Location map of southern Manitoba. Lake gauge stations are indicated with a solid circle and labelled with their name.

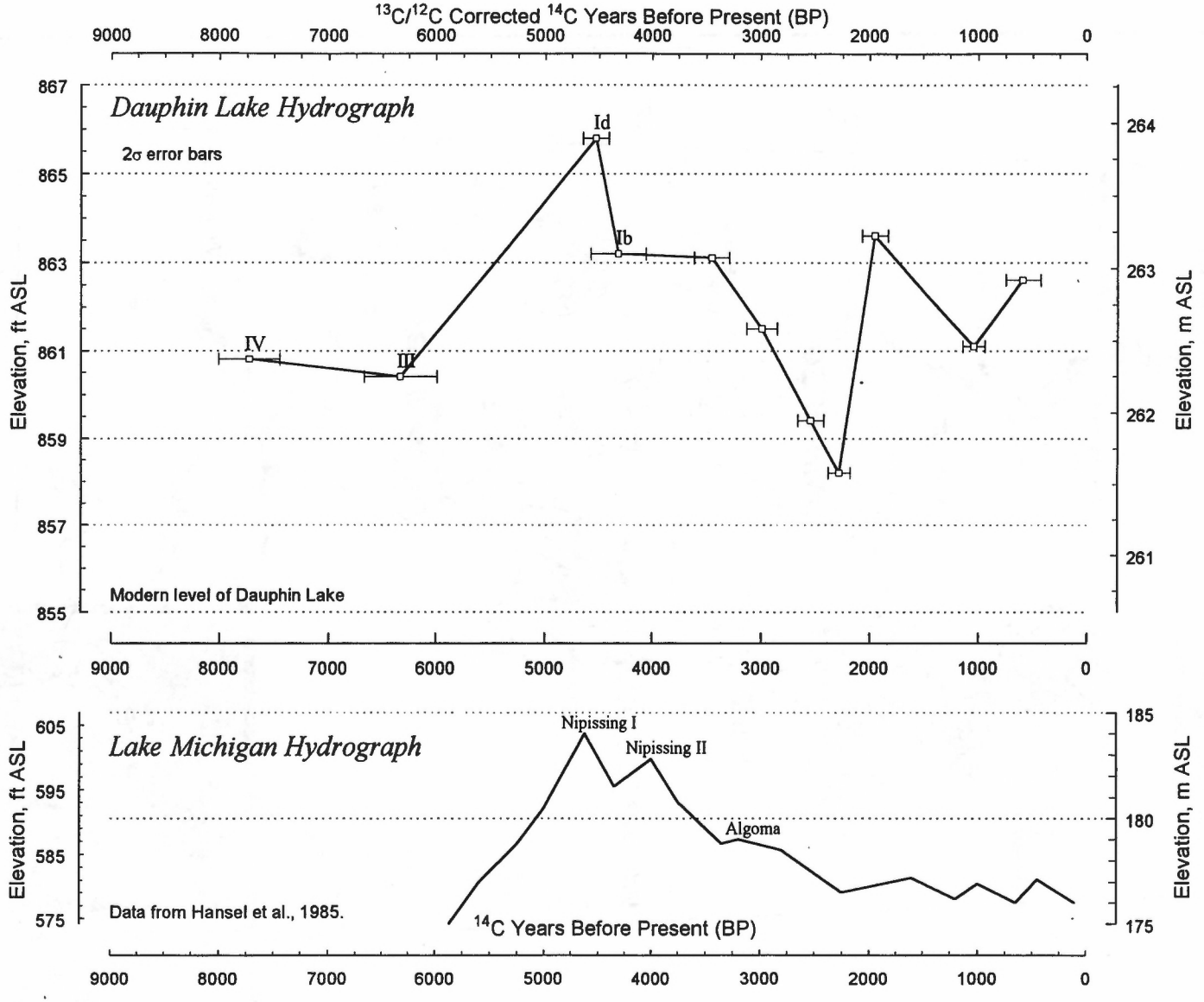

Figure 2. Dauphin Lake hydrograph constructed from its paleoshoreline record. The open squares represent the elevation-radiocarbon date pairs from which the graph was constructed. All Dauphin Lake radiocarbon ages are from mollusc shells. The Lake Michigan hydrograph was digitized from Hansel et al. (1985).

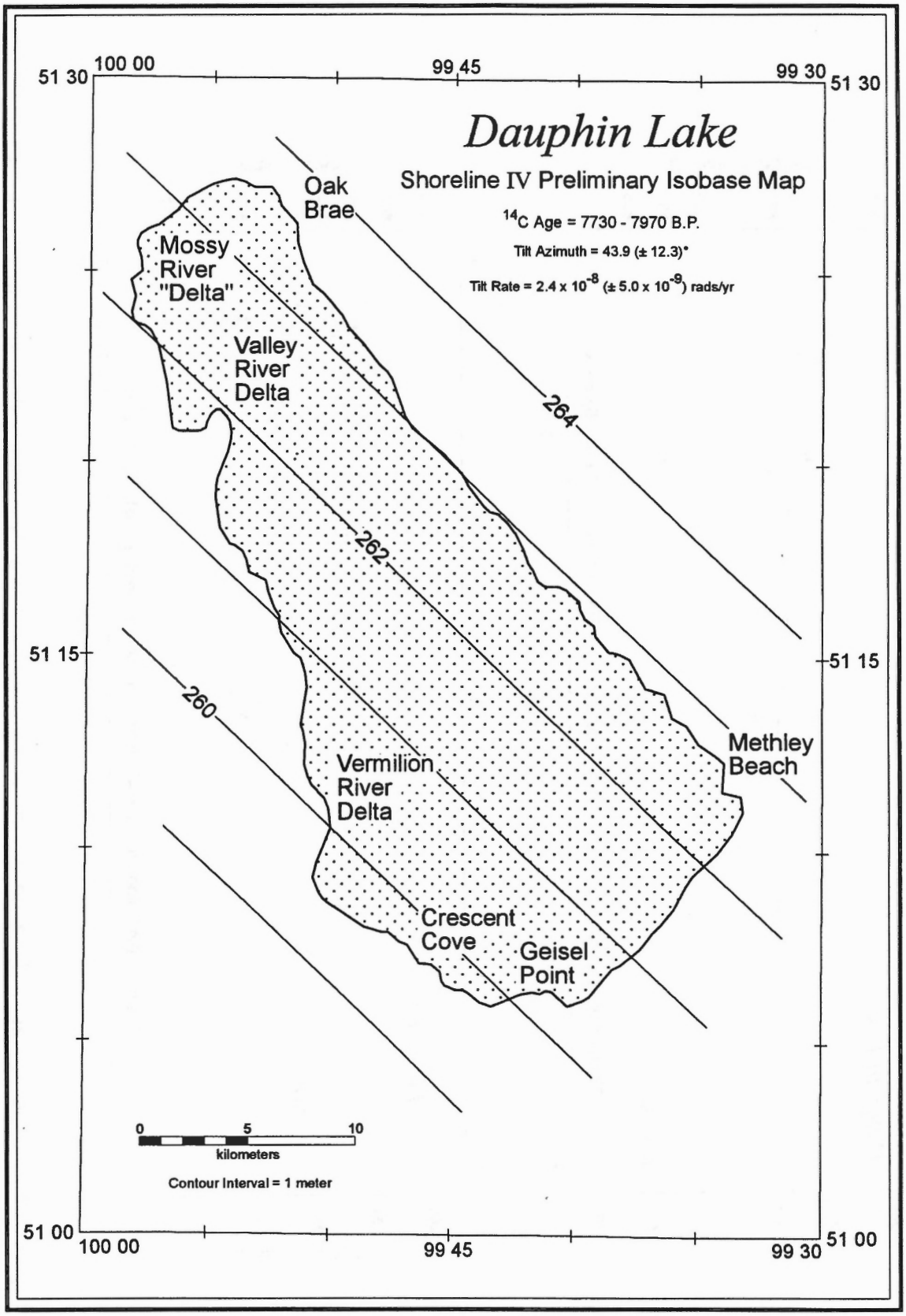

Figure 3. Isobase map of shoreline IV on Dauphin Lake.

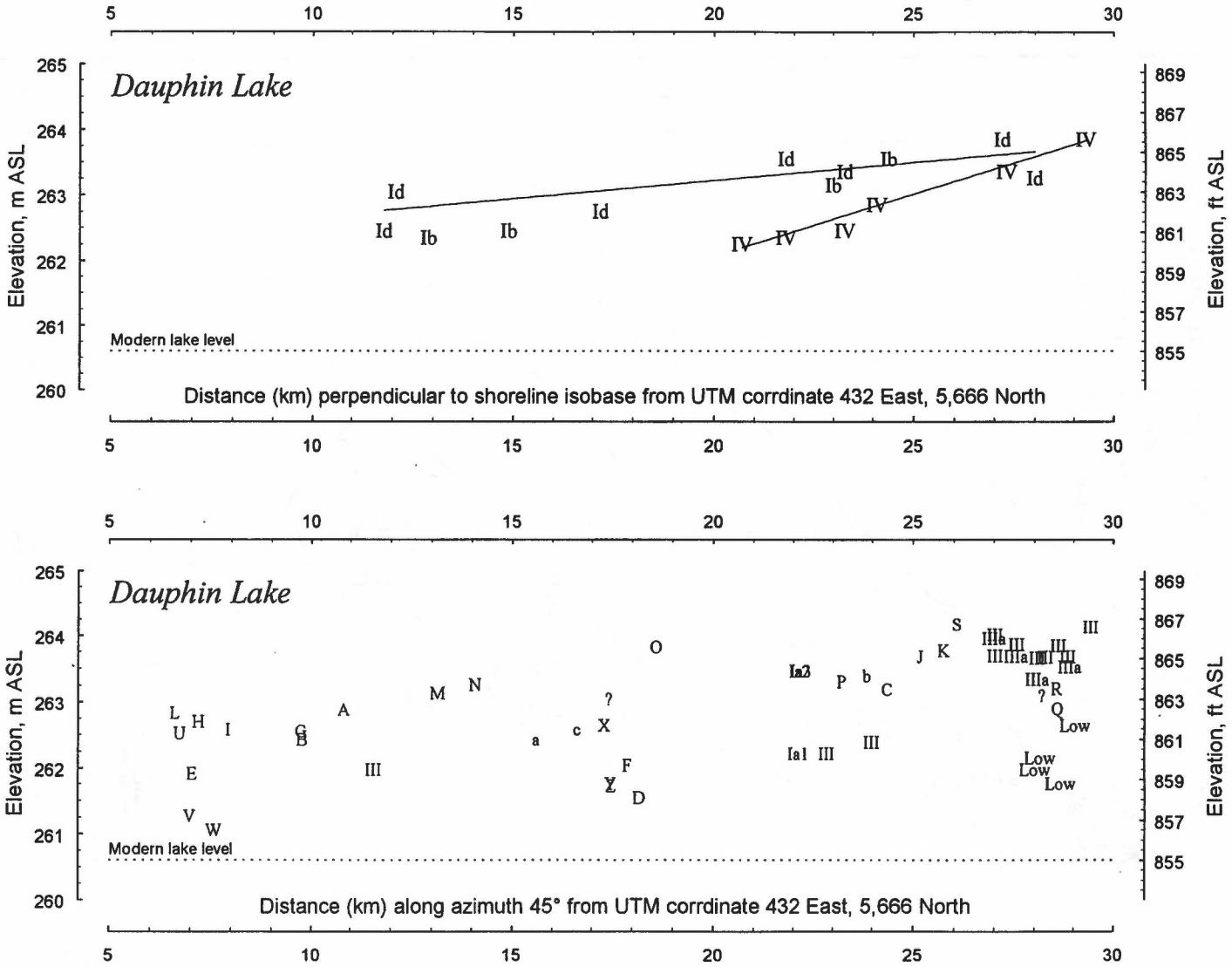

Figure 4. Shoreline elevation-distance diagrams for Dauphin Lake. Shorelines IV and Id-Ib are plotted perpendicular to their isobases — 43.9° and 47.5°, respectively. The bottom plot shows the remaining, mostly uncorrelated survey points. The numbers, letters, and symbols are keyed to a data base. They have been plotted along a 45° azimuth. Note the steady rise from left to right suggesting the shorelines have been tilted up to the northeast.

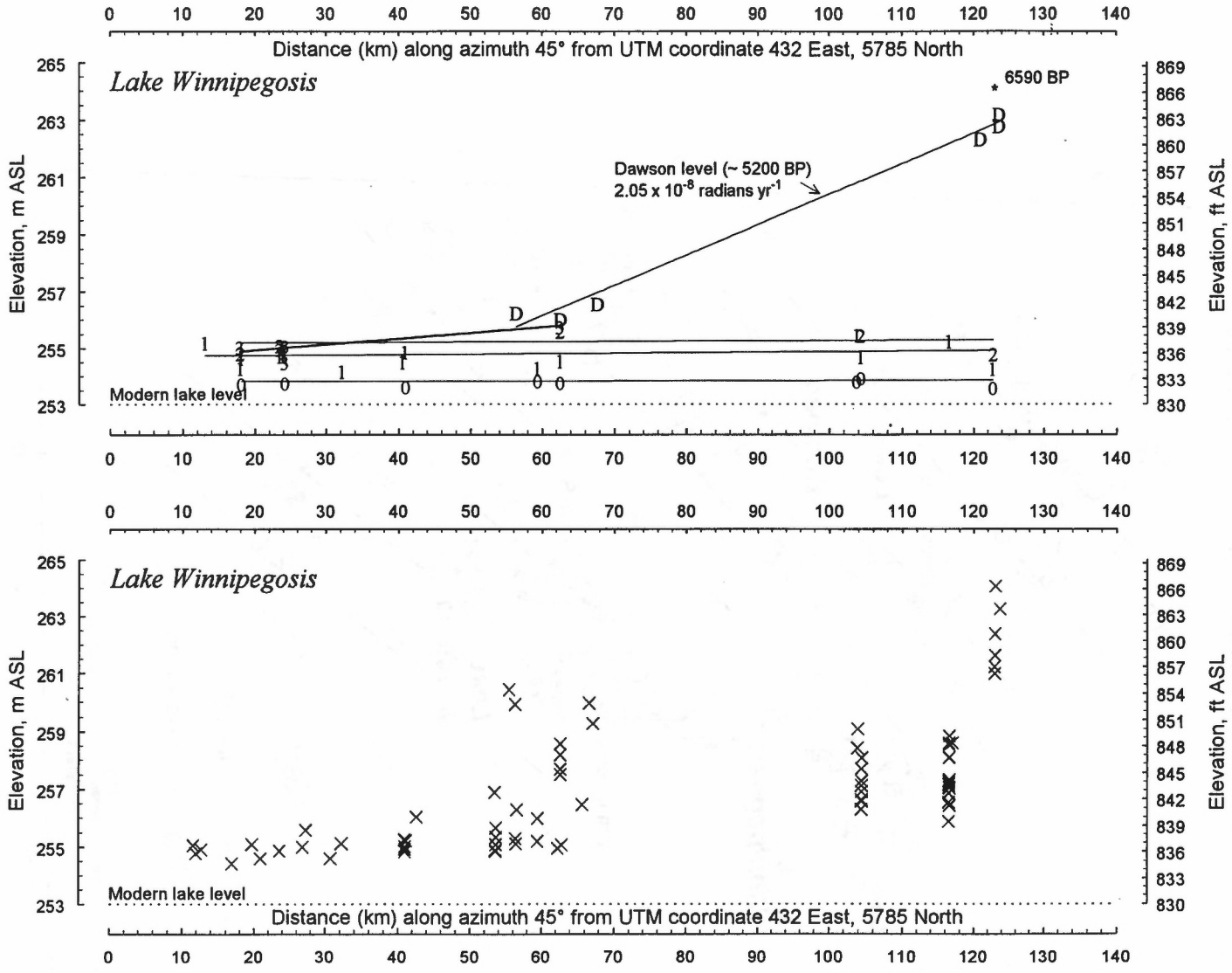

Figure 5. Shoreline elevation-distance diagrams for Lake Winnipegosis plotted along a 45° azimuth. The Dawson level has been correlated at several locations in the north basin and exhibits a tilt rate consistent with shorelines IV and Id-Ib of Dauphin Lake. The bottom plot shows the remaining, mostly uncorrelated survey points. Note the general rise from left to right, suggesting the shorelines have been tilted up to the northeast. *(Editors' note: The age of the Dawson level (upper diagram) is determined as 4550 BP (^{14}C years) by Nielsen et al. (1987)).*

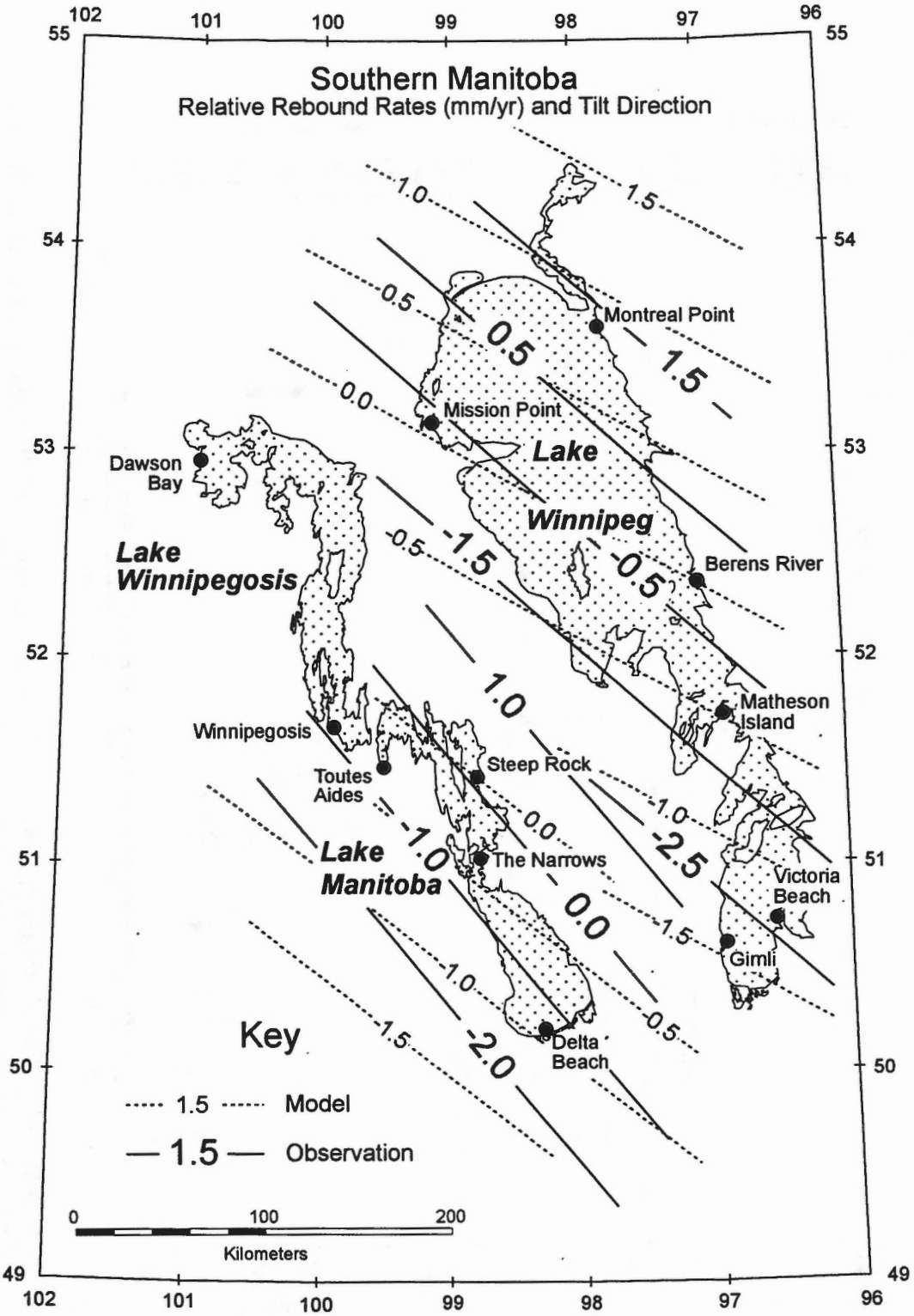

Figure 6. Relative rebound rates computed from the lake gauge data (solid lines) superimposed on predicted relative rates of separation between surface topography and the geoid (dashed lines) based on an ICE-3G loading history and 1066B earth structure. All rates for Lake Winnipeg are relative to the Berens River station, and for Lake Manitoba, relative to the Steep Rock station.

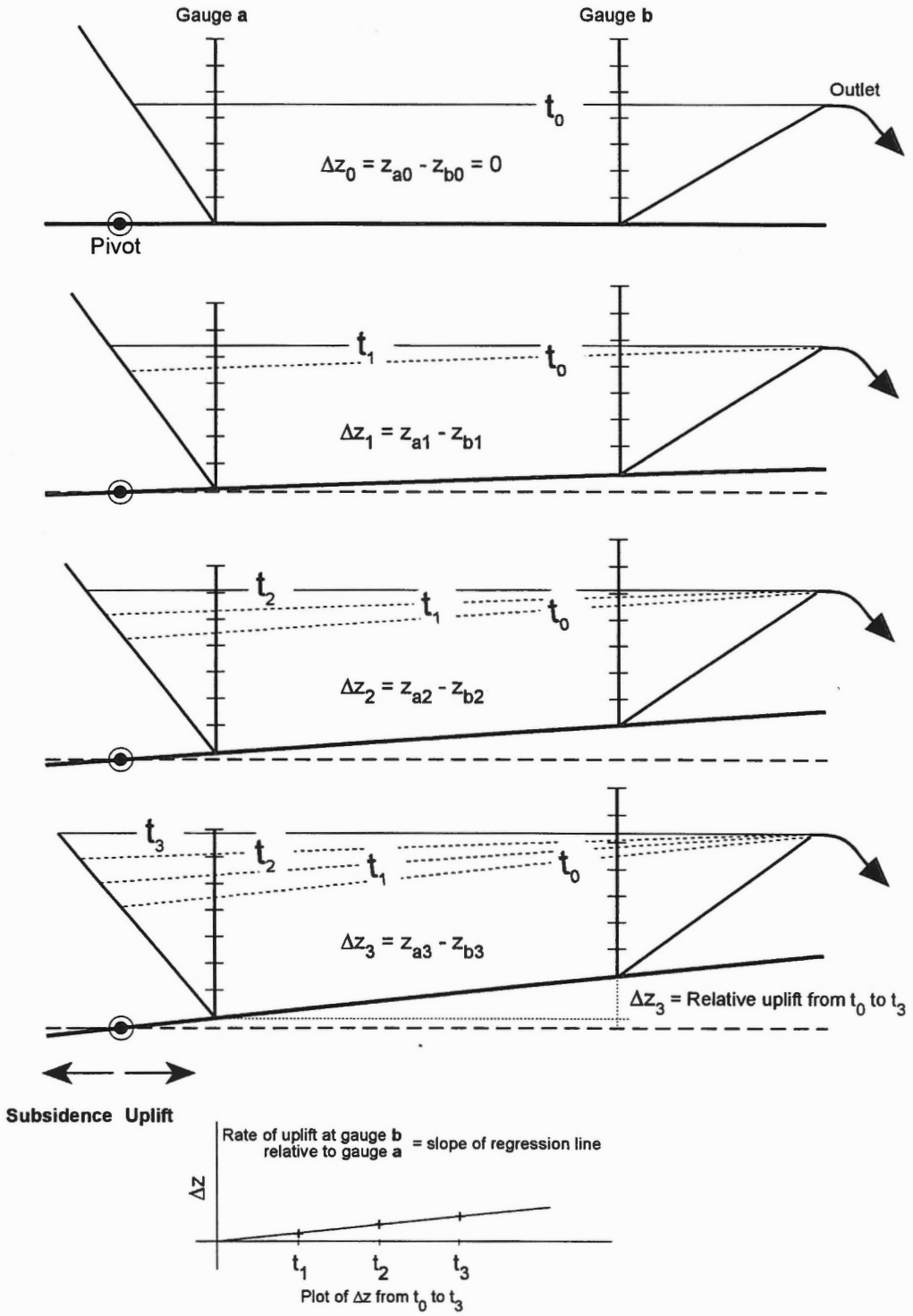

Figure 7. Profile view of a tilting lake basin controlled by an outlet that does not erode over the time period considered. Note that as the basin tilts with time, the elevation difference (△z) between the two gauges represents the relative difference. The total uplift is relative to the datum (reference geoid) indicated by the heavy dashed horizontal line. The slope of a regression line through △z plotted on time is the rate of differential vertical motion between the two gauges. The pivot point is the boundary between subsidence and uplift. See text for a more detailed discussion.

6.5 Estimating postglacial rebound tilt in Manitoba: present status and future prospects

A. Lambert

Geological Survey of Canada,
3 Observatory Crescent, Ottawa, Ontario K1A 0Y3

INTRODUCTION

The unloading of the earth's surface associated with the melting of the Laurentide Ice Sheet has resulted in present-day vertical movement rates of the order of 10 mm/yr in the Hudson Bay - James Bay region as well as horizontal movement rates of 2 mm/yr and tilting of 1-2 mm/100 km/yr in central and eastern Canada and the north eastern U.S. This pattern of vertical and horizontal movement is predicted by theoretical earth loading/unloading calculations (e.g., James and Lambert, 1993) based on the ICE-3G model of Laurentide deglaciation history developed by Tushingham and Peltier (1991). Such models are useful in a number of scientific studies. For example, the results of such models allows one to correct sea level trends for vertical land movement as a step in obtaining a more accurate estimate of the change in ocean volume. Postglacial rebound can also directly affect our local environment.

EFFECTS IN MANITOBA

Why are postglacial rebound models important in the Manitoba context? Because they specify the rate of regional tilt of the Earth's surface in Manitoba which affects the long-term trends in water levels and flow rates in lakes and rivers draining into Hudson Bay. Some of the consequences of regional postglacial rebound tilt in Manitoba can be illustrated by a simplified model (Fig. 1). If we assume that the outlet of the lake remains unobstructed and does not erode through time, the effect of regional tilting resulting from the flow of mass in the mantle toward Hudson Bay is to lengthen the lake toward the southwest. The Hudson Bay shoreline will move seaward because the sea level tends to remain constant. Another effect which is not shown here is that the mantle flow of mass also tilts the geoid in the same direction as the solid surface. This reduces the effect by about 10%.

CURRENT ACCURACY OF POSTGLACIAL TILT PREDICTIONS

The question is - how accurately can we predict postglacial rebound in Manitoba using an Earth loading theory? To understand the strengths and weaknesses of the theory a quick overview of what goes into the modelling is required. The two main components of the model are 1) the loading history, and 2) a visco-elastic model which predicts how the Earth will respond to a point load (or removal of a point load). These two components are combined to predict the movement at every point of a regular grid over the Earth's surface. The loading history is expressed in terms of time slices every 1000 years from 100,000 years BP to the present. The model which predicts the response of the Earth to a concentrated load is a spherically symmetric model that includes all the major features of the earth. However, these models do not yet distinguish between oceanic and continental lithosphere, for example.

The data which constrain these models at present are 1) data on the extent of the ice sheet (ice limits) at various times and data on ice flow directions, still being debated among geomorphologists, and 2) relative sea-level curves from a number of locations at former coastal sites.

To see how the evolution of data and theory can lead to changes in vertical movement rates in Manitoba, in particular, we compare two maps of vertical crustal movement rates, one based on ICE-3G (Tushingham and Peltier, 1991) and the other based on the most recently published ice model ICE-4G (Peltier, 1994) (Fig. 2). It can be seen that uplift rates at Churchill change from around 7 or 8 mm/yr in the ICE-3G model to around 10 mm/yr in the ICE-4G model. At the north end of Lake Winnipeg rates have decreased from 5 mm/yr to around 3 mm/yr. Clearly, this uncertainty of approximately 40% in the rate of uplift is not acceptable and needs to be reduced by introducing new observational constraints on the models, particularly at inland locations. Moreover, ICE-4G is still undergoing some final development and could be modified slightly (W. R. Peltier, pers. comm., 1995). In addition, the record of past tilting from the large amount of lake strandline data in and around Manitoba has not been fully exploited as a constraint on Laurentide ice sheet history.

An independent study of vertical crustal movements was carried out by Carrera, Vanicek and Craymer (1991) who combined all available sea level and lake level data and repeated geodetic levelling data to produce a map of vertical crustal movements for Canada. The resulting map shows vertical motion contour lines in Manitoba which differ significantly in orientation and sign (east-west tilt) from the contours in the postglacial rebound models (north-east/south-west tilt). The detailed map for Manitoba shows quite significant variations that have been smoothed out on the national map. However, it is not known how much of the vertical motion could be the result of factors such as

groundwater depletion, for example, in non-bedrock areas.

MODERN GEODETIC CONSTRAINTS

Fortunately, the new high-precision geodetic techniques of the Global Positioning System (GPS) and absolute gravimetry can be used to measure the present-day surface movement rates to calibrate the theoretical models. Continuous measurements of the position of one GPS receiver antenna with respect to another can be made by simultaneously ranging to a constellation of GPS satellites. By combining several baselines the position of a station can be determined with respect to a global network of stations and trends in height can be measured after a few years of daily observation. An example of the measurement of changes in GPS baseline length and orientation is the Cascadia Subduction Zone crustal deformation work in British Columbia which shows changes between receivers 300 km and 600 km apart (Fig. 3) (Dragert and Hyndman, 1995). Absolute gravity observations can also be used to constrain postglacial rebound models. Absolute gravimeters are now capable of measuring gravity at a precision of 1-2 parts per billion (10-20 nm/s^2) by measuring the acceleration of a mass falling freely in a vacuum. The observed change in gravity with time (Fig. 4) can be compared with the gravity changes predicted. The advantages of the combined GPS/absolute gravity technique are: 1) changes are measured independently of a local reference, 2) measurement sites are not restricted to ocean or lake shores, 3) measurements are more accurate and less expensive than long-distance, high-precision levelling, 4) observing the ratio of height change over gravity change confirms the dominant process, and 5) observing corresponding changes in gravity provides verification that high-precision GPS is bias-free.

PROPOSED MEASUREMENTS

A proposal is being developed for the establishment of two new continuously operating GPS stations at Flin Flon and Pinawa and two new stations in Quebec over a five year period to be combined with existing stations at Yellowknife, Churchill, North Liberty, Iowa and other existing stations in eastern Canada and the U.S. (Fig. 5). Absolute gravity measurements would be made twice a year at the continuous GPS stations by Natural Resources Canada (NRCan) and the National Oceanic and Atmospheric Administration (NOAA) from the United States. This would provide an independent verification that the changes observed by GPS are actually the result of postglacial rebound (There is a theoretically predicted ratio between them). Other intermediate stations will be observed using GPS and absolute-g on an opportunity basis in connection with other projects related to the maintenance of national reference networks by Geodetic Survey of Canada. Assistance with GPS instrumentation is being sought from NASA and NOAA under existing agreements. Funding is being sought for the completion of site preparations, the establishment of data communications facilities, the cost of data transmission and field operations. At the end of the five year period of the project a new postglacial rebound model would be computed taking into account the new geodetic constraints as well as all the available geomorphological information on the Laurentide ice sheet. The new model would be used to generate a realistic regional tilt history for Manitoba going back before 10,000 years BP.

ACKNOWLEDGMENTS

I thank T.S. James for the computation of vertical movement rates for ICE-3G and ICE-4G and N. Courtier for assistance with the figures.

REFERENCES

Carrera, G., Vanicek, P. and Craymer, M.R.
1991. The compilation of a map of recent vertical crustal movements in Canada; Department of Survey Engineering, University New Brunswick, Energy, Mines and Resources Contract Report 91-001 (three volumes).

Dragert, H.D. and Hyndman, R.D.
1995. Continuous GPS monitoring of elastic strain in the northern Cascadia subduction zone; Geophysical Research Letters, v. 22, p. 755-758.

James, T.S. and Lambert, A.
1993. A comparison of VLBI data with the ICE-3G glacial rebound model; Geophysical Research Letters, v. 20, p. 871-874.

Peltier, W.R.
1994. Ice-age paleotopography; Science, v. 265, p. 195-201.

Tushingham, A.M. and Peltier, W.R.
1991. Ice-3G: A new global model of late Pleistocene deglaciation based upon geophysical predictions of post-glacial relative sea level change; Journal of Geophysical Research, v. 96, p. 4497-4523.

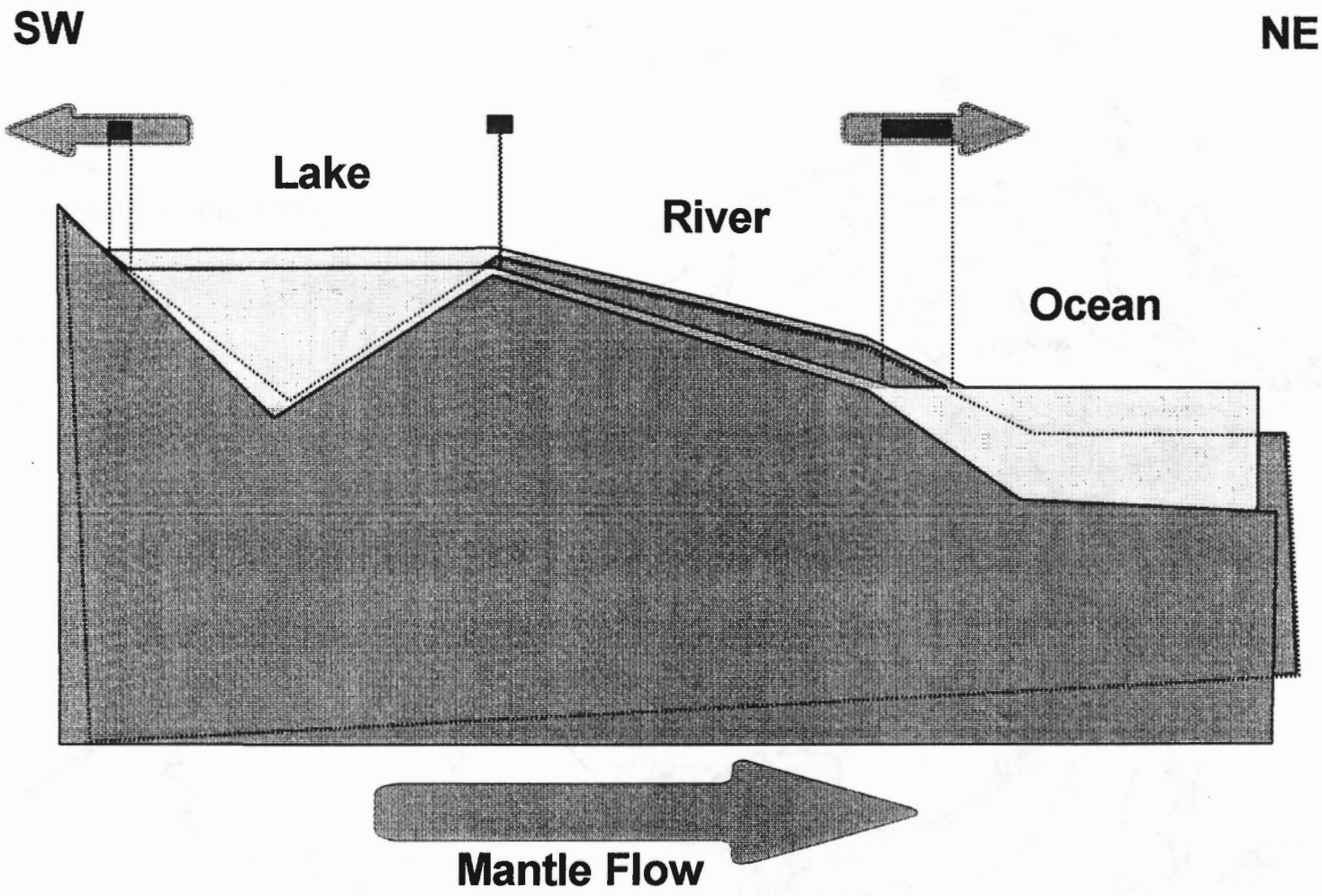

Figure 1. Cartoon showing the effect of postglacial land tilt on the water levels of a lake and the estuary of a river flowing into Hudson Bay. The original configuration of land and water is in the foreground. The configuration after postglacial tilting is in the background. Arrows above the diagram show the direction and magnitude of expected shoreline migration.

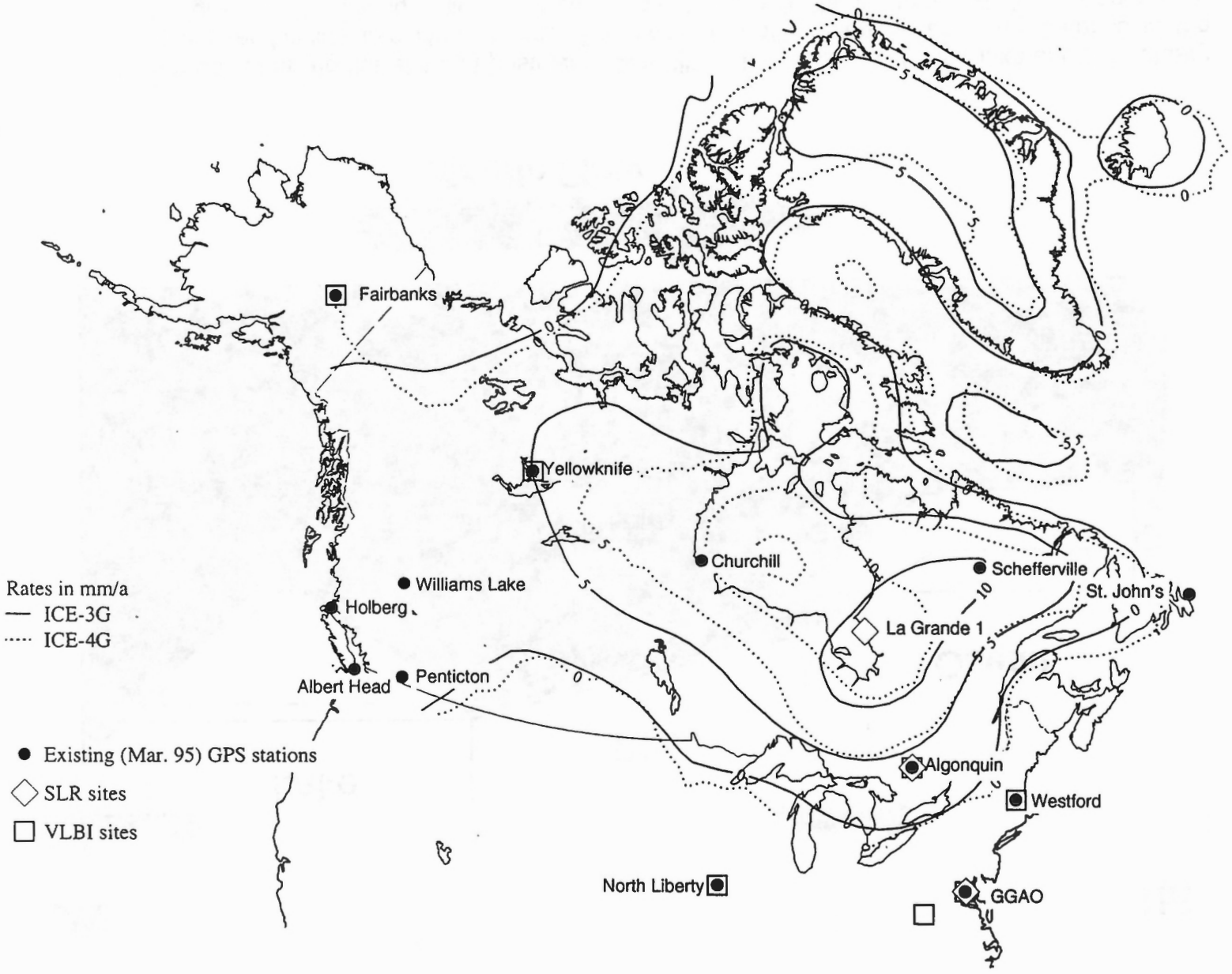

Figure 2. Comparison of ICE-3G and ICE-4G vertical velocities calculated by T.S. James from published information.

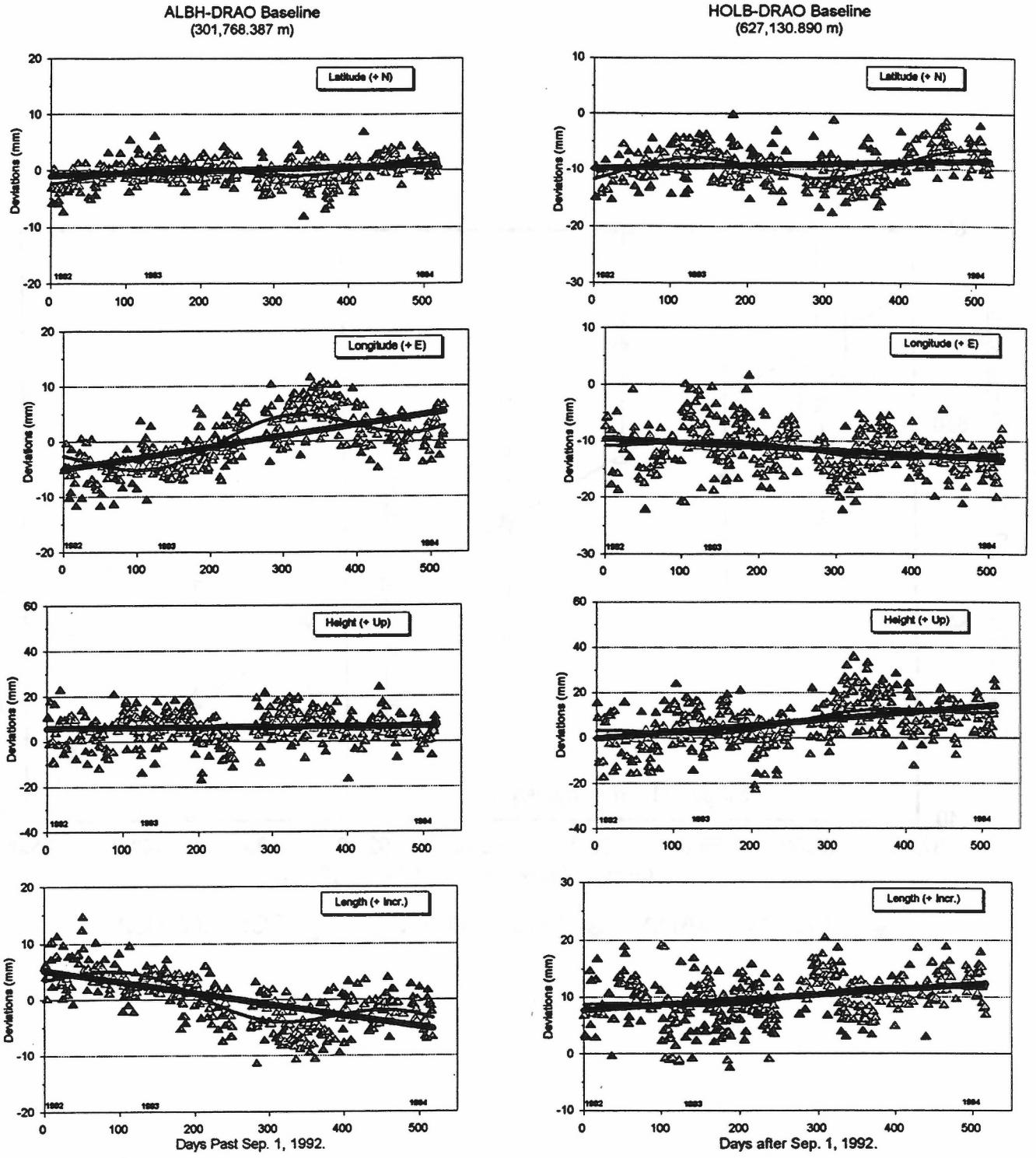

Figure 3. Results from a GPS network in British Columbia showing detection of crustal movement from 500 days of data (H. Dragert and R.D. Hyndman, pers. comm.).

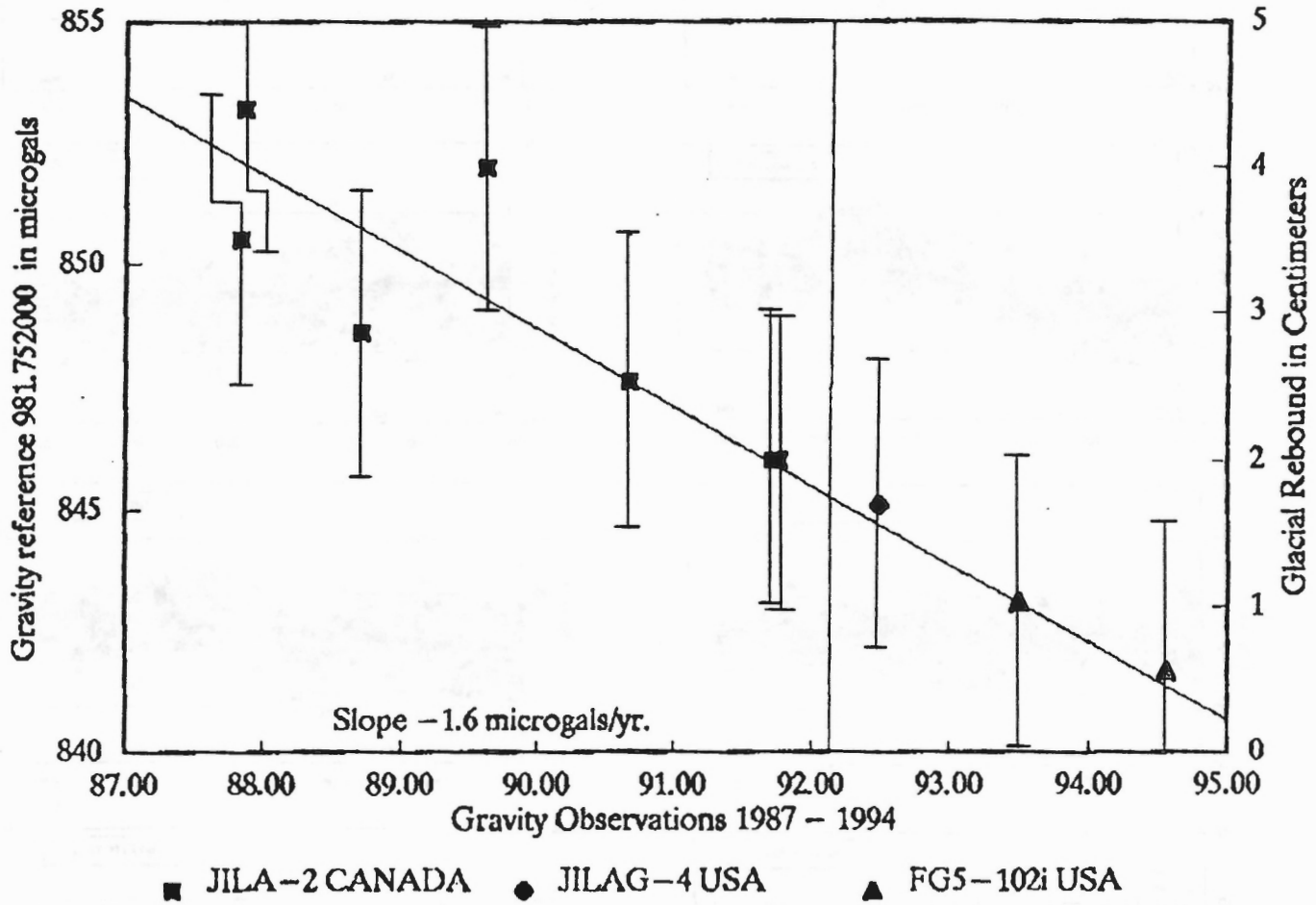

Figure 4. Absolute gravity values at Churchill, Manitoba measured by Natural Resources Canada and NOAA showing a temporal decrease in gravity (courtesy NOAA).

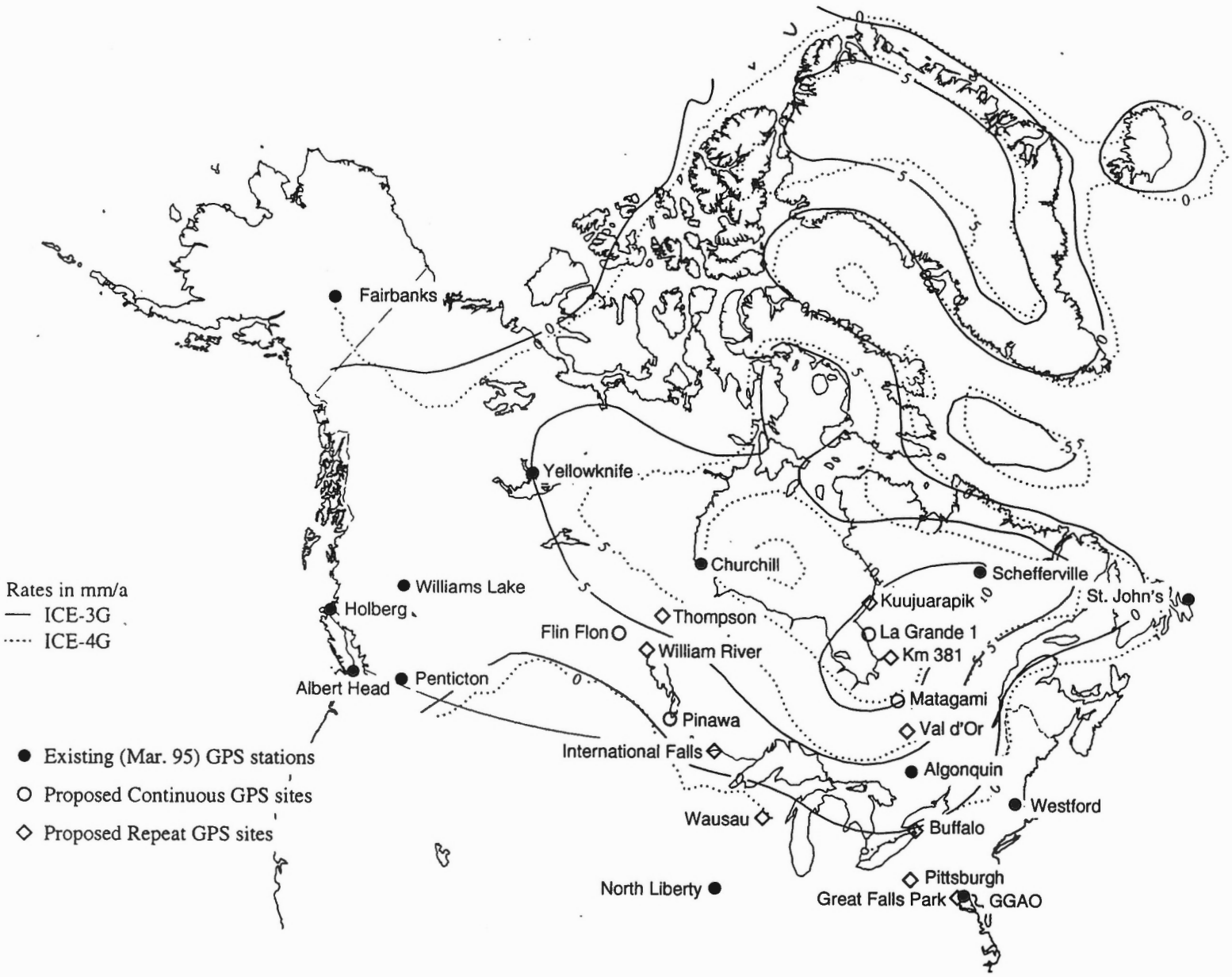

Figure 5. Location of existing and proposed GPS stations in Manitoba and Quebec for determination of postglacial rebound rates.

Appendix 7.1: Summary core logs and corresponding seismostratigraphic sequences

C.F.M. Lewis

Geological Survey of Canada (Atlantic)
P.O. Box 1006, Dartmouth, Nova Scotia B2Y 4A2

Brian J. Todd

Geological Survey of Canada
601 Booth Street, Ottawa, Ontario K1A 0E8

Legend for graphic core logs

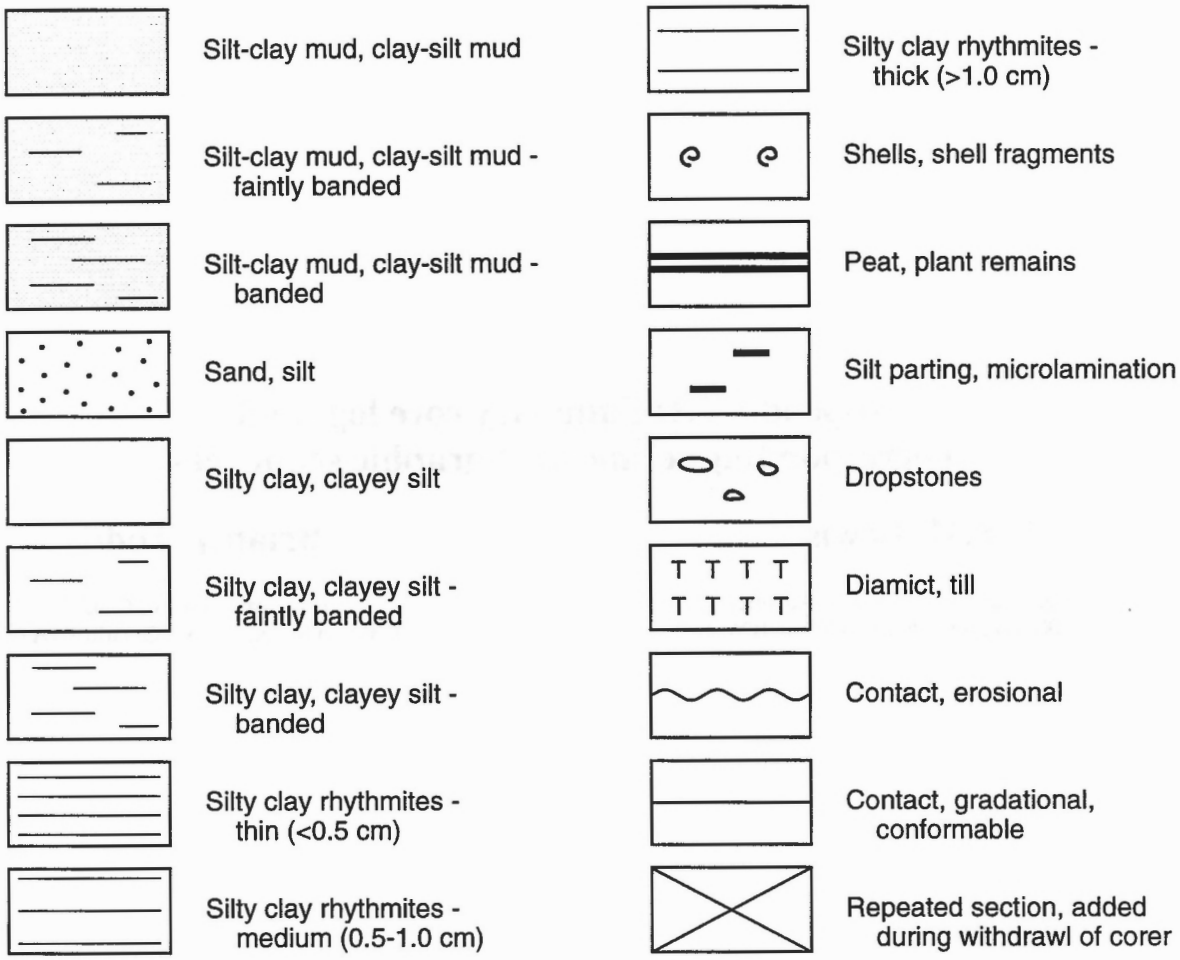

ACKNOWLEDGEMENTS

We thank the members of the sediment processing team for their contributions to the description, measurement, subsampling and documentation of the Lake Winnipeg cores October 17-26, 1994, at the Geological Survey of Canada (Atlantic) core processing facility in Dartmouth, Nova Scotia. We gratefully acknowledge the assistance of team members R. Archer, G. Cameron, K. Moran, C. Jarrett, E. Nielsen, H. Thorleifson, P. Henderson (October 17-18), C. Schröder-Adams (October 17) and S. Burbidge (October 17). K. Moran organised the core processing and led the measurement of sediment physical properties. The cores are held in cold storage for future reference and study under the care of I. Hardy, Curator, Geological Survey of Canada (Atlantic). Illustrations were prepared by the GSCA Publications and Drafting Unit.

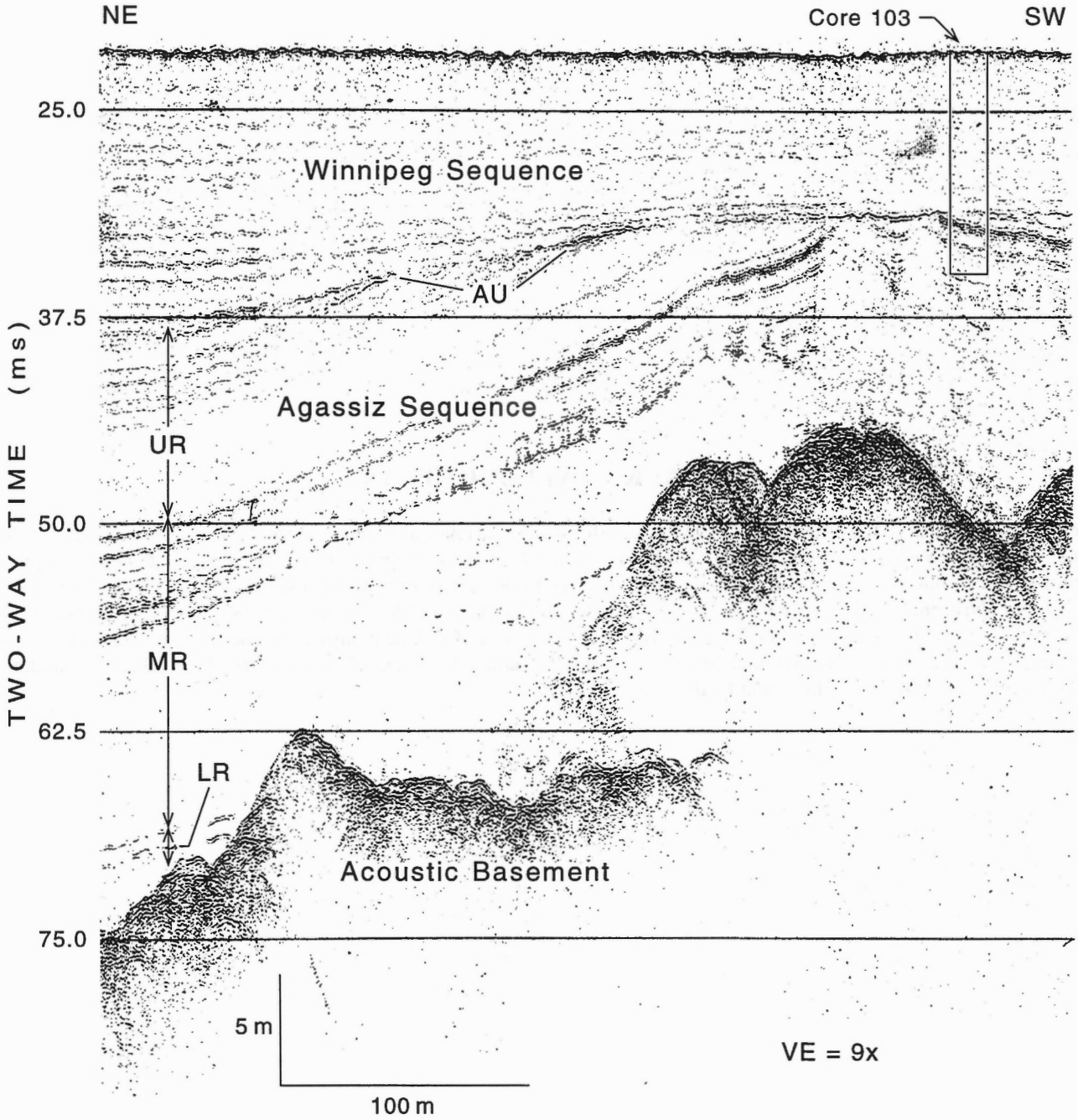

High resolution seismic reflection (Seistec) profile through the core 103 site in central northern Lake Winnipeg showing seismostratigraphic sequences. VE = Vertical Exaggeration, vertical scale bar assumes a sound velocity of 1500 m/s. AU = Agassiz Unconformity. Within the Agassiz Sequence, UR = Upper Reflective Interval, MR = Middle Reflective Interval, LR = Lower Reflective Interval. (Seistec record, line NB9, Day 229, 1555 UTC).

Station 103

Latitude	53° 27.29' N	10 cm wide piston core
Longitude	98° 21.95' W	8.16 m long
Water Depth	15.9 m	

Lithology:

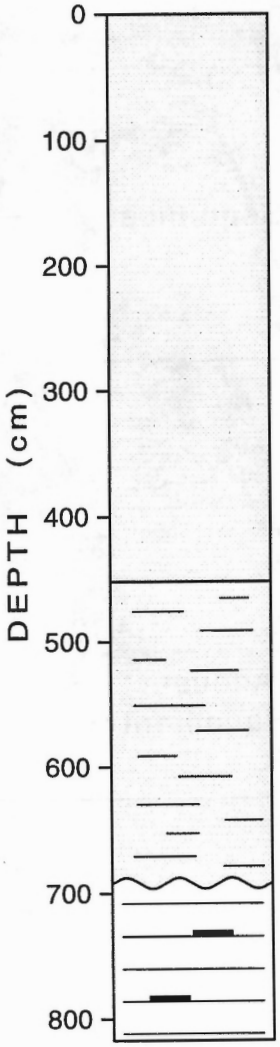

0-461 cm **Silt-clay mud;** soft, olive gray (2.3GY4.3/0.7) with black FeS streaks and discontinuous laminations above 84 cm, and scattered lighter gray (dark greenish gray 6.3GY4.4/0.6) mm-scale diffuse bands and blotches below 125 cm. Noncalcareous. Disturbed 90-160 cm and broken crumbly texture 265-330 cm (probably frozen slightly in storage or transit).

461-686 cm **Silt-clay mud;** banded, soft-firm olive gray. Mm-scale, lighter gray (dark greenish gray 5.3GY4.3/0.6) diffuse bands common throughout (2-4 bands per cm). Noncalcareous; weakly calcareous at base.

686 cm **Contact;** erosional.

686-816 cm **Silty clay rhythmites;** firm, comprising couplets of light brownish gray (3.7Y4.7/1) grading up into darker (olive gray 4.5Y4.4/0.8) layers. Couplet thickness about 0.5 cm increasing to >1 cm in places below 770 cm. Light layers are highly calcareous (effervescent in 10% HCl); dark layers are slightly calcareous. Broken and crumbly texture 720-770 cm (probably frozen slightly in transit).

Core intervals equivalent to seismostratigraphic sequences:

0-686 cm	Winnipeg Sequence (Lake Winnipeg sediments).
686-816 cm	Agassiz Sequence, Middle Reflective Interval (MR) (Lake Agassiz sediments, upper middle part).

Summary lithologic log for core 103 correlated to seismostratigraphic sequences, central northern Lake Winnipeg.

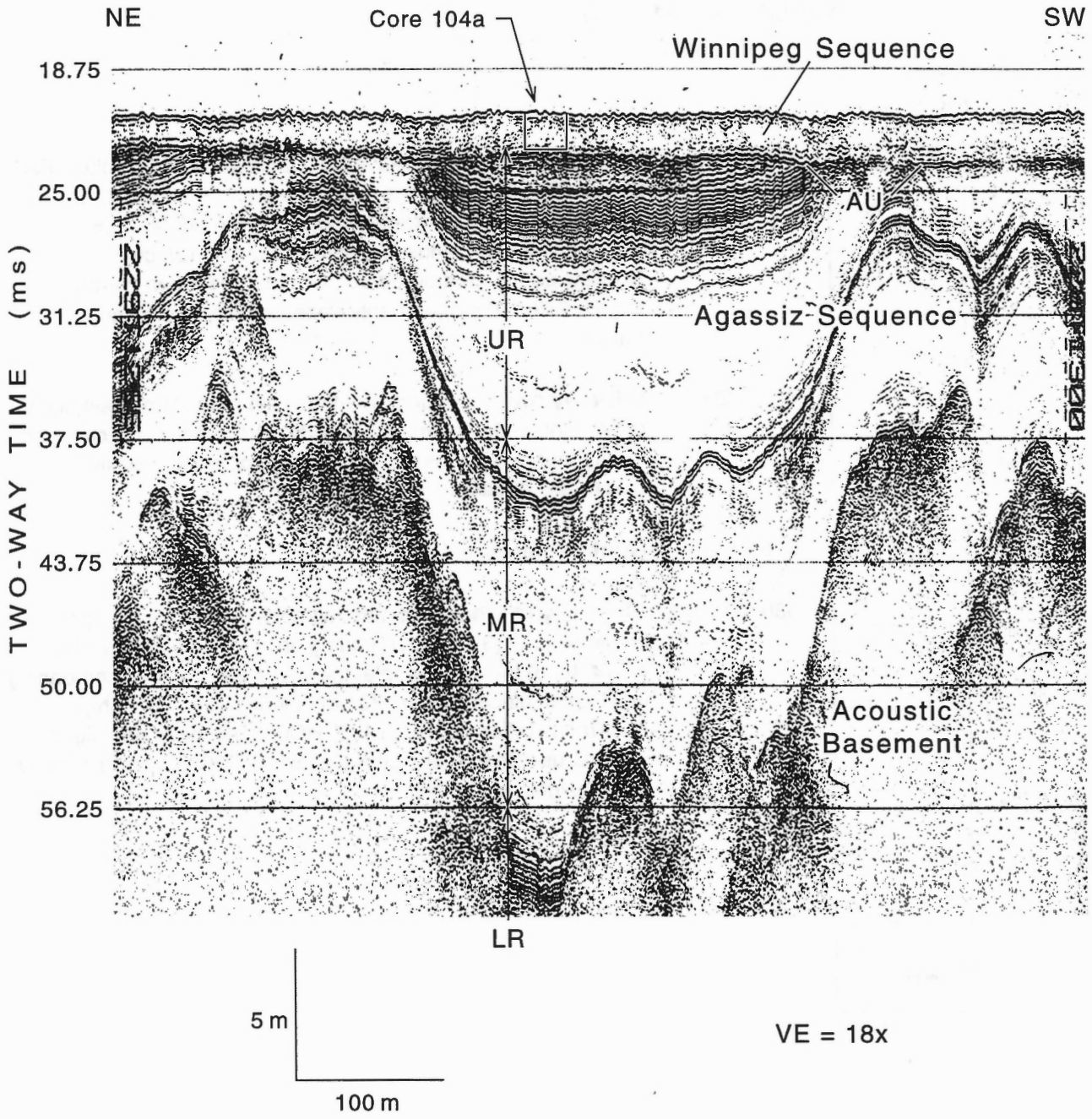

High resolution seismic reflection (Seistec) profile through the core 104a site in northeastern Lake Winnipeg showing seismostratigraphic sequences. VE = Vertical Exaggeration, vertical scale bar assumes a sound velocity of 1500 m/s. AU = Agassiz Unconformity. Within the Agassiz Sequence, UR = Upper Reflective Interval, MR = Middle Reflective Interval, LR = Lower Reflective Interval. (Seistec record, line NB9, Day 229, 1255 UTC).

Station 104a

Latitude	53° 35.05' N	10 cm wide gravity core
Longitude	98° 05.11' W	3.65 m long
Water Depth	16.2 m	

Lithology:

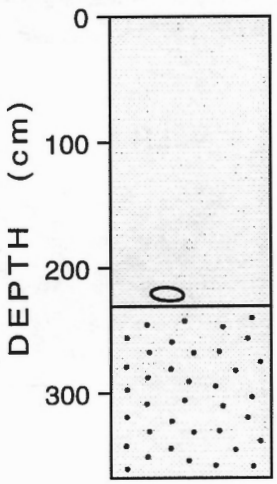

0-230 cm **Clay-silt mud;** soft, olive gray (1GY4.3/0.8) with trace of sand. Noncalcareous. A few black FeS specks and scattered lighter gray mm-scale diffuse bands as in core 103. Angular granite pebble at 221 cm.

230-365 cm **Clay-silt mud and silty fine sand;** alternating beds. Light olive gray (9.3Y4.6/0.8) and olive gray (8.9Y4.3/0.8). Calcareous (silty fine sand is more calcareous than clay-silt mud). Beds progressively more tilted downcore below 160 cm (corer probably tipped over during penetration).

Core intervals equivalent to seismostratigraphic sequences:

0-365 cm Winnipeg Sequence (Lake Winnipeg sediments).

Summary lithologic log for core 104a correlated to seismostratigraphic sequences, northeastern Lake Winnipeg.

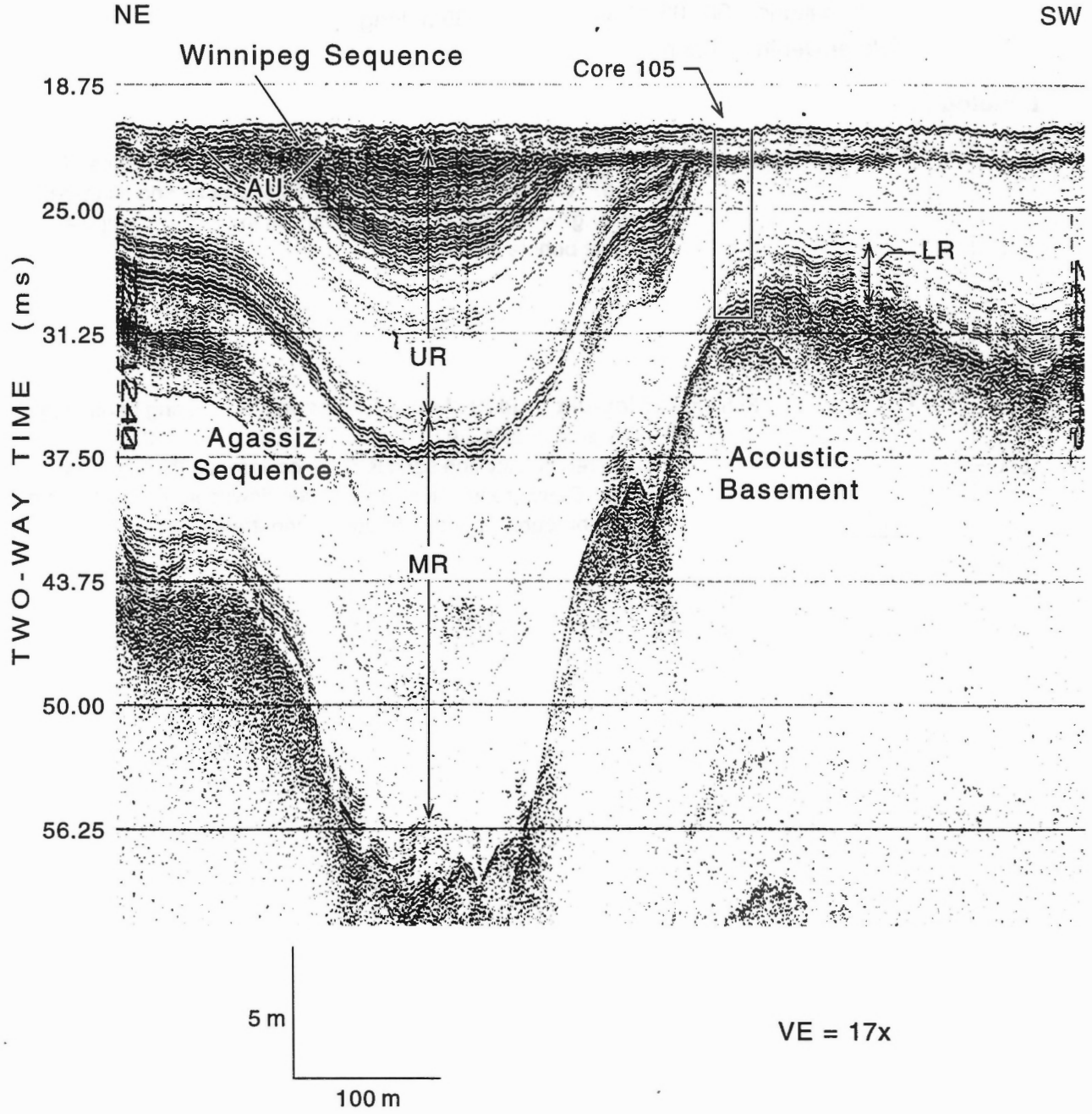

High resolution seismic reflection (Seistec) profile through the core 105 site in northeastern Lake Winnipeg showing seismostratigraphic sequences. VE = Vertical Exaggeration, vertical scale bar assumes a sound velocity of 1500 m/s. AU = Agassiz Unconformity. Within the Agassiz Sequence, UR = Upper Reflective Interval, MR = Middle Reflective Interval, LR = Lower Reflective Interval. (Seistec record, line NB9, Day 229, 1240 UTC).

Station 105

Latitude	53° 35.64' N	10 cm wide piston core
Longitude	98° 03.80' W	5.96 m long
Water Depth	15.8 m	

Lithology:

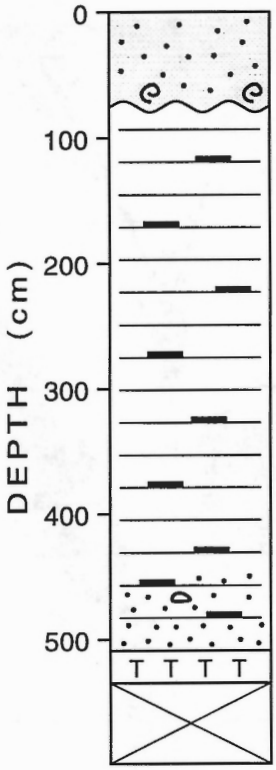

0-64.5 cm	**Clay-silt mud;** soft, olive gray (9.3Y4.4/0.8) with silt/sand grains. Noncalcareous. Small shells and shell fragments in basal calcareous zone (62-64.5 cm).
64.5 cm	**Contact;** erosional, sharp.
64.5-510 cm	**Silty clay rhythmites;** firm, olive gray (7.6Y4.4/0.7) to light olive gray (6.5Y4.6/0.9). Couplets (0.3-1 cm thick) of thinner and lighter bands grading up to thicker and darker bands; lighter bands more calcareous than darker bands. White silt partings (highly calcareous) are common below 350 cm, rare above. Rare reddish bands (about 1 cm) occur below 300 cm. Gritty below 440 cm. Granite dropstone at 463 cm.
510-539 cm	**Till;** stony, hard, light olive gray (5.8Y4.9/1.0) with calcareous sandy matrix.
539-596 cm	Recored section across soft-firm clay contact, as at 64.5 cm above.

Core intervals equivalent to seismostratigraphic sequences:

0-64.5 cm	Winnipeg Sequence (Lake Winnipeg sediments).
64.5-510 cm	Agassiz Sequence, Lower Reflective Interval (LR) (Lake Agassiz sediments, lower part).
510-539 cm	Acoustic Basement Sequence.

Summary lithologic log for core 105 correlated to seismostratigraphic sequences, northeastern Lake Winnipeg.

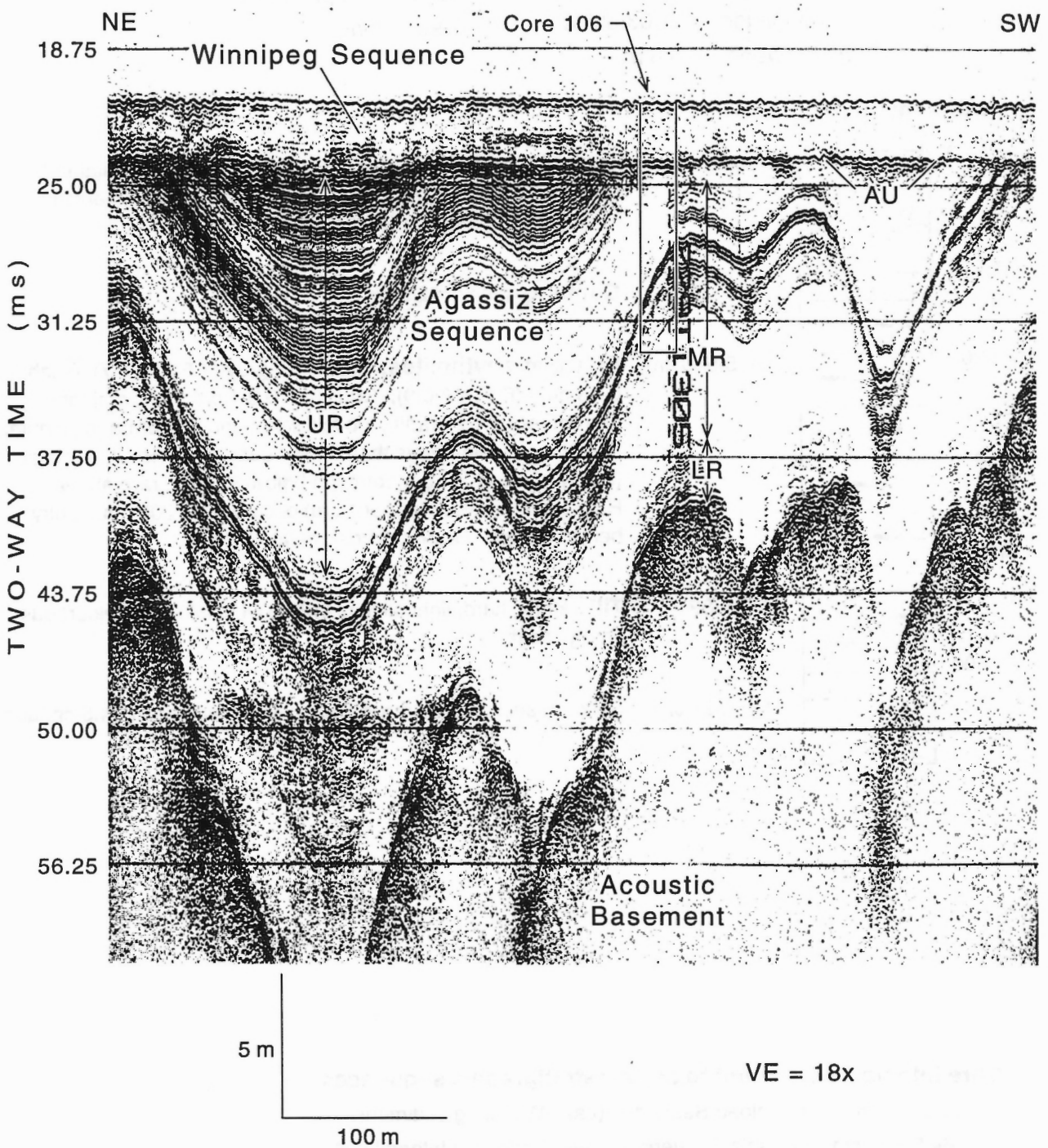

High resolution seismic reflection (Seistec) profile through the core 106 site in northeastern Lake Winnipeg showing seismostratigraphic sequences. VE = Vertical Exaggeration, vertical scale bar assumes a sound velocity of 1500 m/s. AU = Agassiz Unconformity. Within the Agassiz Sequence, UR = Upper Reflective Interval, MR = Middle Reflective Interval, LR = Lower Reflective Interval. (Seistec record, line NB9, Day 229, 1240 UTC).

Station 106

Latitude	53° 34.70' N	10 cm wide piston core
Longitude	98° 05.83' W	7.89 m long
Water Depth	16.8 m	

Lithology:

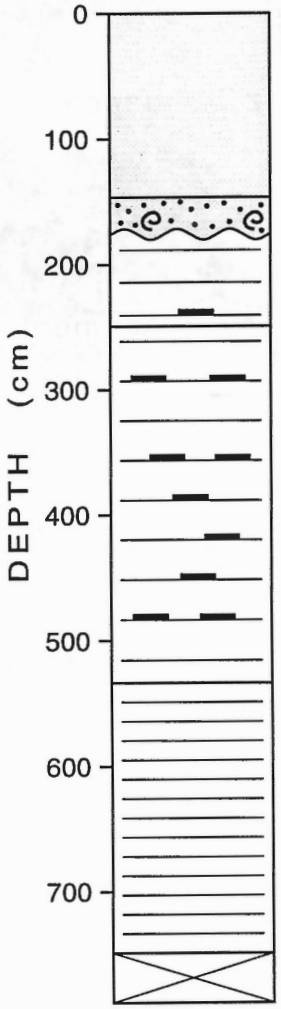

0-159 cm	**Clay-silt mud;** soft, olive gray (7.1Y4.4/0.8 – 2GY4.3/0.7) with trace of sand. A few black FeS lenses and specks, especially in upper 12 cm. Some very faint, incipient lighter gray clay lenses. Noncalcareous, becoming slightly calcareous below 120 cm.
159-182 cm	**Clay-silt mud;** soft, olive gray as above with layers of silt and fine sand, 1-1.5 cm thick. Small gastropods in silt/fine sand layers; silt/fine sand is moderately calcareous.
182 cm	**Contact;** erosional.
182-248 cm	**Silty clay rhythmites;** medium thickness (0.5-1 cm), very firm. Rhythmites very thin above 190 cm and thicken downwards, changing gradually into underlying unit. Rhythmites are couplets of thin, mm-scale, lighter (light olive gray 4.1Y4.6/1.1 to light brownish gray 3.8Y4.6/1.0) and thicker (about 0.5 cm), darker (olive gray 4.4Y4.4/0.9 to brownish gray 3.9Y4.3/0.9) layers. Scattered light gray silt microlaminations (<1 mm). Silt and lighter layers more calcareous than darker layers.
248-530 cm	**Silty clay rhythmites;** thick (1-5 cm). Thicker rhythmites comprise several bands of lighter (brownish gray 4Y4.5/1.0) silty clay grading up to a distinctive, thick (about 1 cm), darker (olive gray 4.5Y4.2/0.9) layer. Thin (<1 mm), highly calcareous white silt partings are common between the lighter bands which are moderately calcareous. Darker layers are weakly calcareous. Gradational 520-530 cm to underlying unit.
530-750 cm	**Silty clay rhythmites;** thin (2-4 mm) and rarely 1 cm, each comprising a couplet of a lighter layer grading up to a darker layer. Averaged colour is olive gray (4.6Y4.2/0.8). Lighter layers more calcareous than darker layers. White silt partings absent below 535 cm. Disturbed 700-750 cm.
750-789 cm	Recored section across soft-firm clay contact, as at 182 cm.

Core intervals equivalent to seismostratigraphic sequences:

0-182 cm	Winnipeg Sequence (Lake Winnipeg sediments).
182-750 cm	Agassiz Sequence, parts of Upper and Middle Reflective Intervals (UR and MR) (Lake Agassiz sediments, middle part).

Summary lithologic log for core 106 correlated to seismostratigraphic sequences.

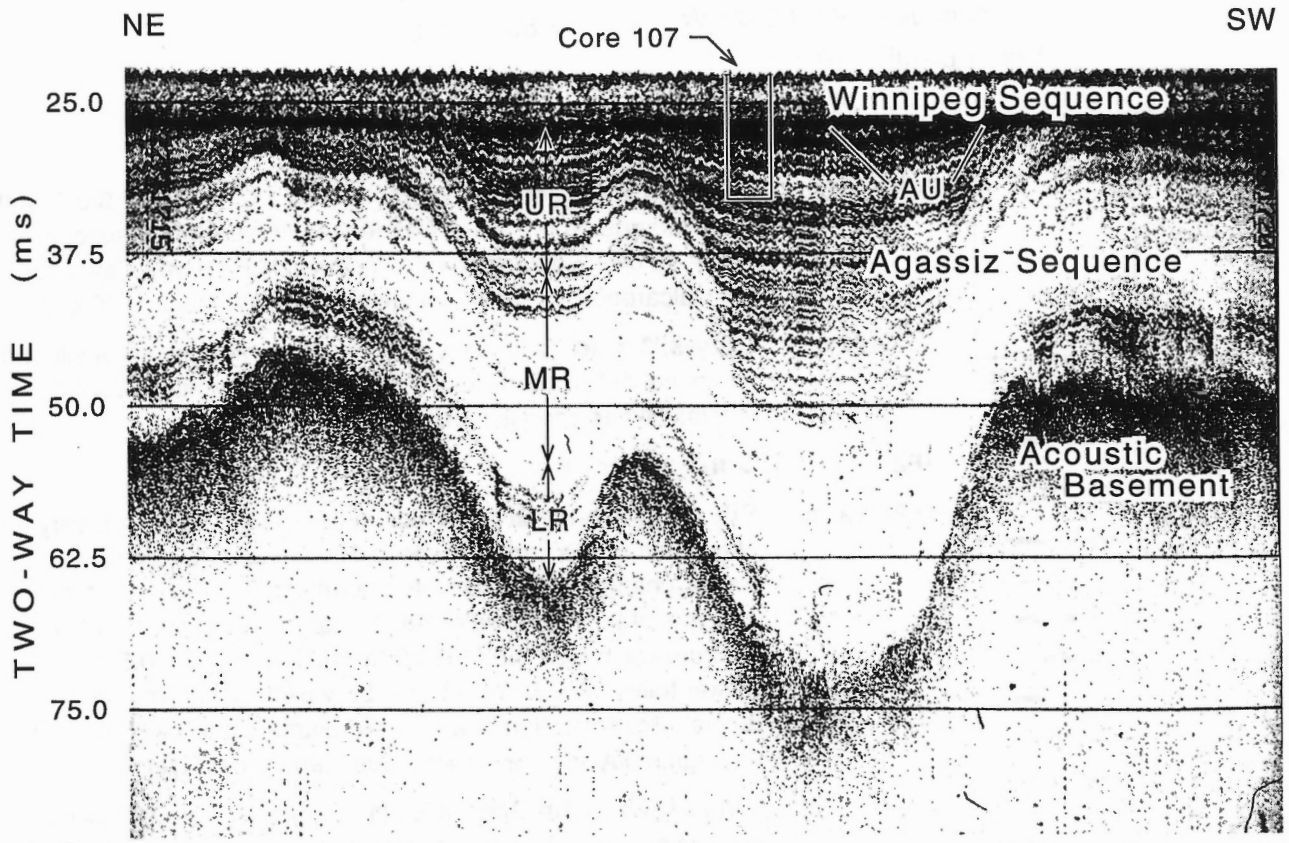

High resolution seismic reflection (Seistec) profile through the core 107 site in northern Lake Winnipeg showing seismostratigraphic sequences. VE = Vertical Exaggeration, vertical scale bar assumes a sound velocity of 1500 m/s. AU = Agassiz Unconformity. Within the Agassiz Sequence, UR = Upper Reflective Interval, MR = Middle Reflective Interval, LR = Lower Reflective Interval. (Seistec record, line NB8, Day 227, 1715 UTC).

Station 107

Latitude	52° 55.45' N	10 cm wide piston core
Longitude	97° 47.31' W	6.96 m long
Water Depth	17.1 m	

Lithology:

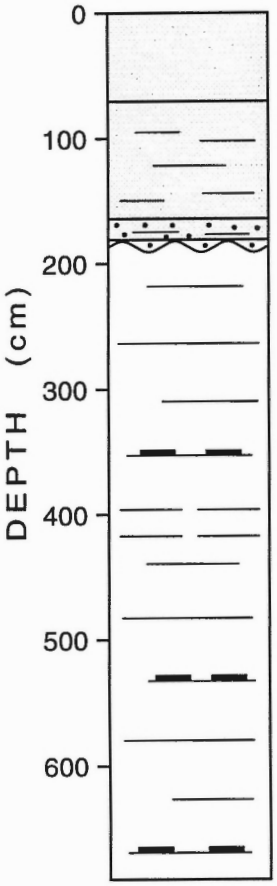

0-60 cm **Clay-silt mud;** soft, olive gray (9.7Y4.1/0.7 – 1.8GY4.2/0.7) with scattered blebs of lighter gray mud and rare black FeS specks. Noncalcareous to very weakly calcareous.

60-172 cm **Clay-silt mud;** soft, diffusely banded, light (1-4 mm) and dark gray (1-2 cm). Noncalcareous to very weakly calcareous. Gradational below 157 cm with increasing frequency of silty layers to unit below.

172-192.5 cm **Clay-silt mud;** soft, clearly banded, light and dark gray, layers 1-3 mm thick. Very weakly calcareous.

192.5-193.5 cm **Sand;** clean, poorly sorted.

193.5 cm **Contact;** slightly irregular, possibly eroded.

193.5-696 cm **Silty clay;** firm, banded, gray. Moderately calcareous. Diffuse layers 0.1-1 cm thick with a few thicker (3-7 cm) and darker layers. Thin calcareous white silt lenses and laminations sporadically present. Two thin dark brown beds at 391 and 418.5 cm. Crumbly texture and softened zones present, notably at 633-638 cm, probably a result of slight freezing during transit.

Core intervals equivalent to seismostratigraphic sequences:

0-194 cm Winnipeg Sequence (Lake Winnipeg sediments).

194-696 cm Agassiz Sequence, Upper Reflective Interval (UR) (Lake Agassiz sediments, upper part).

Summary lithologic log for core 107 correlated to seismostratigraphic sequences, northern Lake Winnipeg (north of George Island).

Station 110a

Latitude	52° 00.15' N	6 cm wide gravity core
Longitude	97° 01.45' W	2.26 m long
Water Depth	11.3 m	

Lithology:

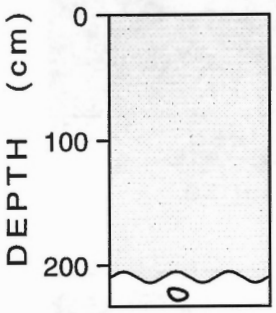

0-209 cm **Clay-silt mud;** soft, olive gray (5Y3.7/0.8 – 9Y4.1/0.7). Scattered black FeS specks throughout, and diffuse incipient lenses of lighter gray mud below 40 cm. Slightly lighter below 115 cm. All noncalcareous.

209-226 cm **Silty clay;** hard, olive gray (2.3GY4.2/0.6), noncalcareous with faint, diffuse lighter-toned bands and blebs. Limestone pebble at 216 cm.

Core intervals equivalent to seismostratigraphic sequences:

No seismic profile available.

Summary lithologic log for core 110a, central Lake Winnipeg.

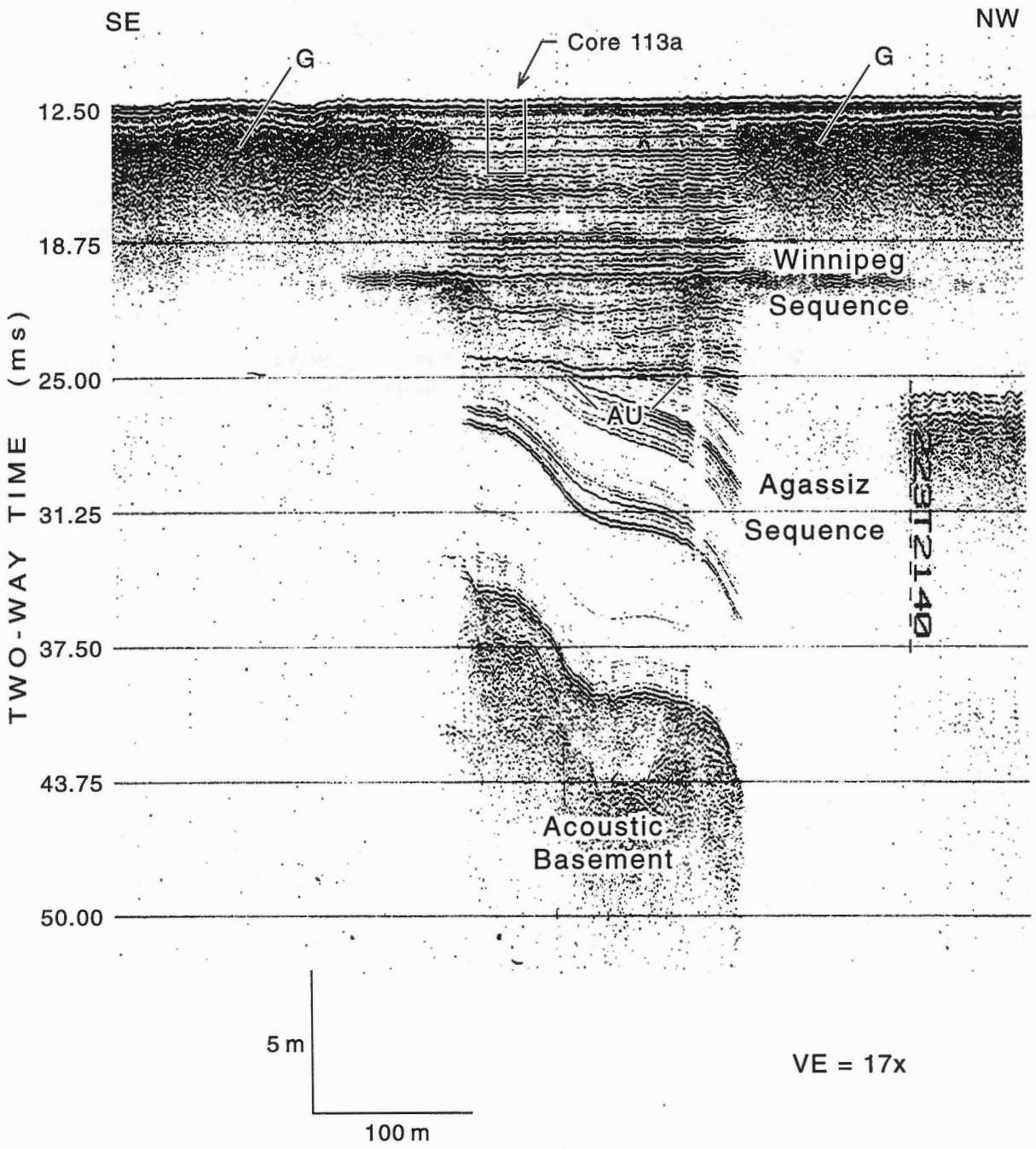

High resolution seismic reflection (Seistec) profile through the core 113a site in central northern Lake Winnipeg showing seismostratigraphic sequences. VE = Vertical Exaggeration, vertical scale bar assumes a sound velocity of 1500 m/s. AU = Agassiz Unconformity. G = Gas masking. (Seistec record, line SB6, Day 223, 2137 UTC).

Station 113a

Latitude	51° 24.09' N	6 cm wide gravity core
Longitude	96° 37.53' W	2.14 m long
Water Depth	9.8 m	

Lithology:

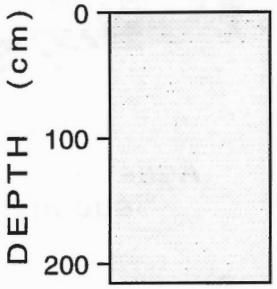

0-214 cm **Clay-silt mud;** soft, olive gray (4.2Y3.5/0.8 – 4.6Y4.2/0.6). Black FeS specks and laminations, scarcer below 15 cm. Slightly lighter below 115 cm. Noncalcareous except near base.

Core intervals equivalent to seismostratigraphic sequences:

0-214 cm Winnipeg Sequence (Lake Winnipeg sediments).

Summary lithologic log for core 113a correlated to seismostratigraphic sequences, central Lake Winnipeg (Washow Bay area).

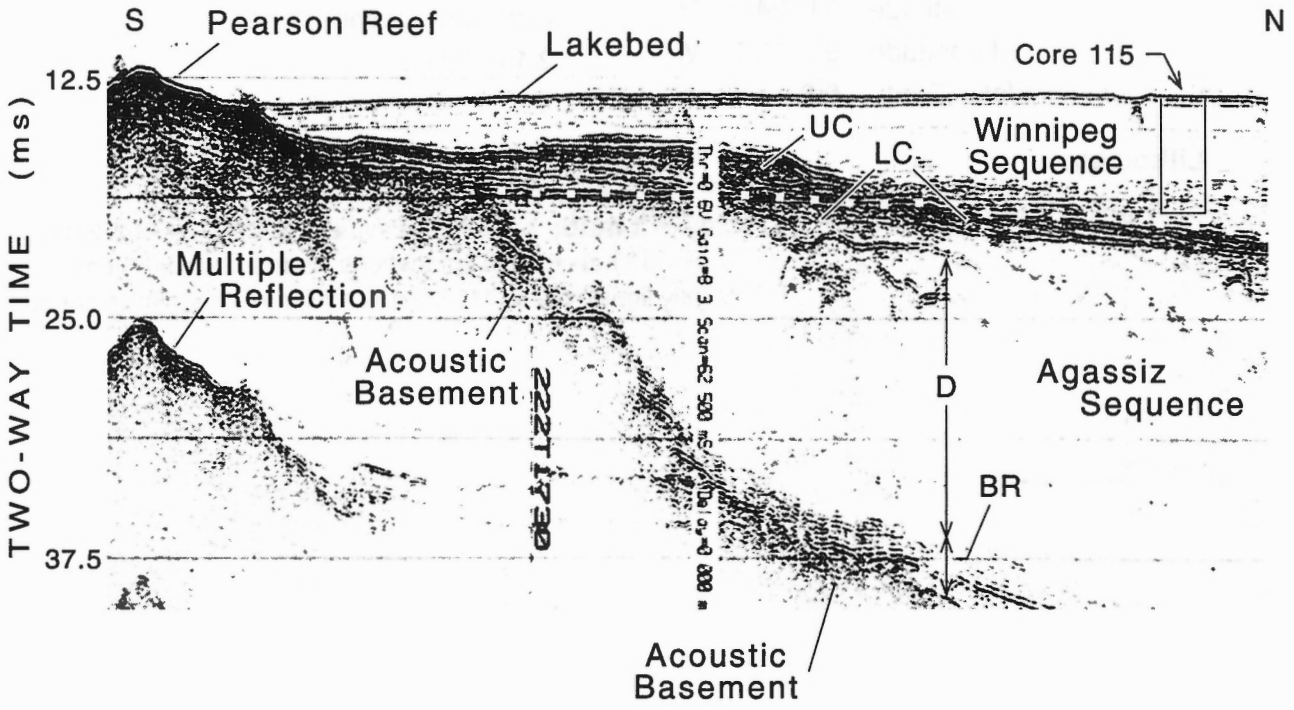

High resolution seismic reflection (Seistec) profile through the core 115 site in southern Lake Winnipeg showing seismostratigraphic sequences. VE = Vertical Exaggeration, vertical scale bar assumes a sound velocity of 1500 m/s. UC = Upper Clinoform Interval, and LC = Lower Clinoform Interval. AU = Agassiz Unconformity, marked with white dots. Within the Agassiz Sequence, D = Disturbed Interval, BR = Basal Reflective Interval. (Seistec record, line SB5, Day 222, 1730 UTC).

Station 115

Latitude	50° 56.76' N	6 cm wide gravity core
Longitude	96° 40.90' W	2.76 m long
Water Depth	10.7 m	

Lithology:

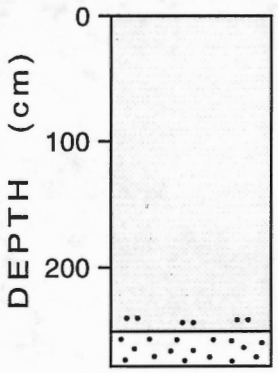

0-268 cm **Silt-clay mud;** soft, olive gray (8.8Y3.8/0.7 – 2.2GY3.6/0.5) with black FeS specks and lenses throughout. Noncalcareous. Lenses of fine sand (bioturbated?) in lower 20 cm.

268-276 cm **Sand;** fine and medium, sorted. Diffusely banded with lighter and darker brownish gray (3.1Y3.9/1.0) layers. Lighter gray sand is highly rounded and sorted.

Core intervals equivalent to seismostratigraphic sequences:

0-276 cm Winnipeg Sequence (Lake Winnipeg sediments).

Summary lithologic log for core 115 correlated to seismostratigraphic sequences, southern Lake Winnipeg (Pearson Reef area).

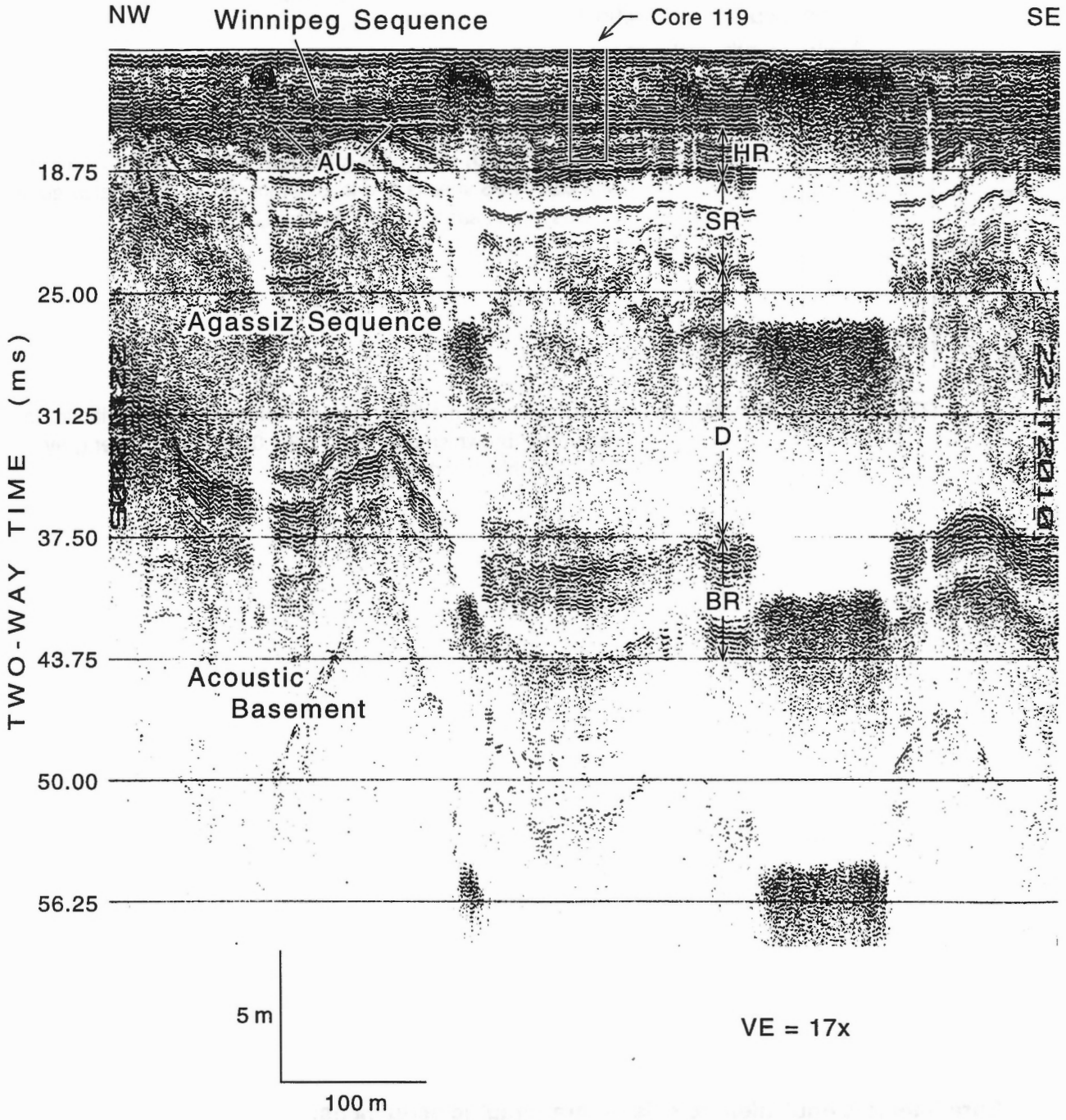

High resolution seismic reflection (Seistec) profile through the core 119 site in southern Lake Winnipeg (Traverse Bay area) showing seismostratigraphic sequences. VE = Vertical Exaggeration, vertical scale bar assumes a sound velocity of 1500 m/s. AU = Agassiz Unconformity. Within the Agassiz Sequence, HR = Higher Reflective Interval, SR = Segmented Reflector Interval, D = Disturbed Interval, BR = Basal Reflective Interval. (Seistec record, line SB4, Day 221, 2005 UTC).

Station 119

Latitude	50° 48.19' N	6 cm wide gravity core
Longitude	96° 31.80' W	3.21 m long
Water Depth	9.8 m	

Lithology:

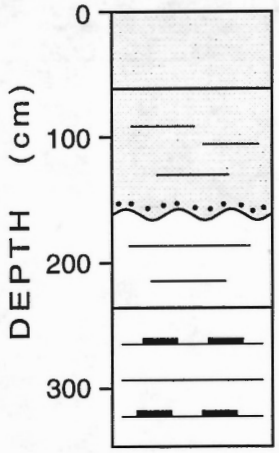

0-60 cm	**Clay-silt mud;** soft, olive gray (5.9Y3.8/1.0 – 9.9Y3.9/0.6) with black FeS specks, streaks, and laminations.
60-171 cm	**Clay-silt mud;** faintly and irregularly banded, soft, olive gray (4.5Y3.8/1.2 – 6.8Y3.9/0.8). Sandy and weakly calcareous at base.
171 cm	**Contact;** sharp, erosional.
171-220 cm	**Banded silty clay;** stiff to hard, olive gray (5Y4.4/1.0). Alternating lighter and darker diffuse bands 0.25-0.5 cm thick, some with an orange-brown cast. Thin (<1 mm) calcareous white silt laminations throughout at 2-20 cm intervals, commonly resting on eroded silty clay surfaces. Clay is weakly calcareous. Grades to underlying unit.
220-321 cm	**Silty clay rhythmites;** stiff (couplets), commonly of medium thickness (0.5-1 cm) and brownish gray (3.9Y4.2/0.9) to moderate olive brown (1.9Y4.3/1.5) colour. Couplets consist of lighter and darker layers. Weakly calcareous. Calcareous white silt laminations as in unit above.

Core intervals equivalent to seismostratigraphic sequences:

0-171 cm	Winnipeg Sequence (Lake Winnipeg sediments).
171-321 cm	Agassiz Sequence, Higher Reflective Interval (HR) (Lake Agassiz sediments, upper part).

Summary lithologic log for core 119 correlated to seismostratigraphic sequences, southern Lake Winnipeg (Traverse Bay area).

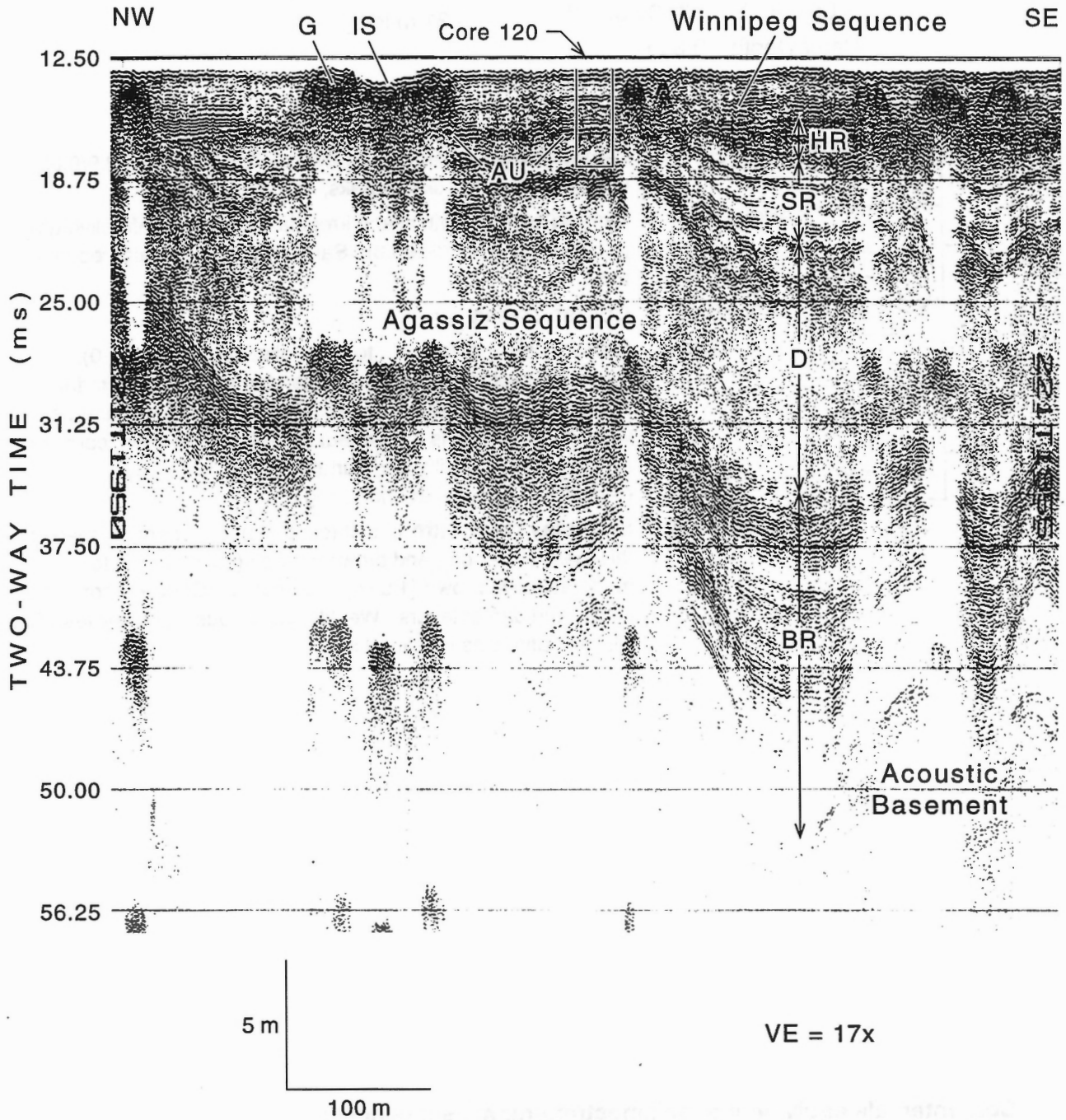

High resolution seismic reflection (Seistec) profile through the core 120 site in southern Lake Winnipeg (Traverse Bay area) showing seismostratigraphic sequences. VE = Vertical Exaggeration, vertical scale bar assumes a sound velocity of 1500 m/s. G = Gas masking. IS = Ice Scour. AU = Agassiz Unconformity. Within the Agassiz Sequence, HR = Higher Reflective Interval, SR = Segmented Reflector Interval, D = Disturbed Interval, BR = Basal Reflective Interval. (Seistec record, line SB4, Day 221, 1950 UTC).

Station 120

Latitude	50° 48.91' N	6 cm wide piston core
Longitude	96° 32.70' W	3.54 m long
Water Depth	10.1 m	

Lithology:

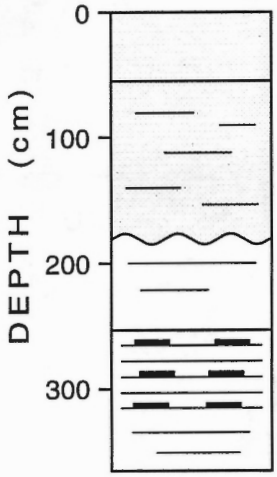

0-60 cm	**Clay-silt mud;** soft, olive gray (8.1Y3.7/0.7) with black FeS streaks and laminations. Noncalcareous.
60-196 cm	**Clay-silt mud;** faintly banded, soft, olive gray (8.1Y3.8/0.8). Noncalcareous. Firmer at base.
196 cm	**Contact;** sharp undulating, erosional.
196-245 cm	**Silty clay;** stiff-hard, olive gray (6.8Y4.1/0.6), banded below 201 cm. Crumbly dry texture. Very weakly calcareous to non calcareous. Grades downward to underlying unit.
245-318 cm	**Silty clay rhythmites;** complex, brownish gray (3Y3.9/0.8 – 3Y4.2/1.2) 1-5 mm layers of lighter and darker brownish gray with browner bands up to 1 cm thick. Noncalcareous except for scattered thin white silt lenses and laminations. Granite dropstones at 262 and 311 cm. Grades downward.
318-354 cm	**Silty clay;** moderate olive brown (1.2Y3.8/2.0), diffusely banded and calcareous with gray-coloured cracks. Grades downward to thinly laminated silty clay below 349 cm.

Core intervals equivalent to seismostratigraphic sequences:

0-196 cm	Winnipeg Sequence (Lake Winnipeg sediments).
196-354 cm	Agassiz Sequence, Segmented Reflector Interval (SR) (Lake Agassiz sediments, upper middle part).

Summary lithologic log for core 120 correlated to seismostratigraphic sequences, southern Lake Winnipeg (Traverse Bay area).

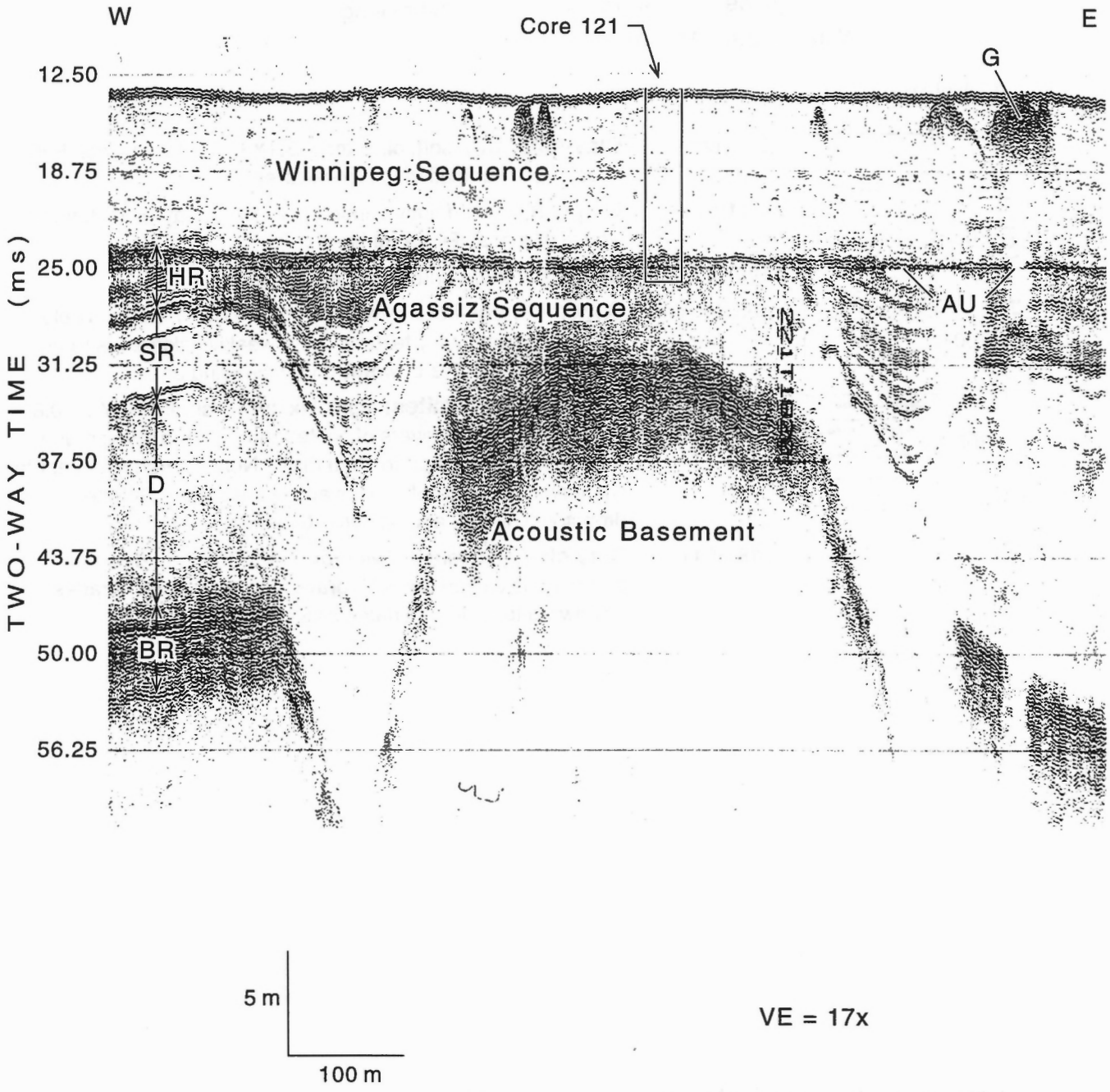

High resolution seismic reflection (Seistec) profile through the core 121 site in southern Lake Winnipeg showing seismostratigraphic sequences. VE = Vertical Exaggeration, vertical scale bar assumes a sound velocity of 1500 m/s. G = Gas masking. AU = Agassiz Unconformity. Within the Agassiz Sequence, HR = Higher Reflective Interval, SR = Segmented Reflector Interval, D = Disturbed Interval, BR = Basal Reflective Interval. (Seistec record, line SB4, Day 221, 1616 UTC).

Station 121

Latitude	50° 50.01' N	6 cm wide gravity core
Longitude	96° 49.20' W	5.47 m long
Water Depth	10.4 m	

Lithology:

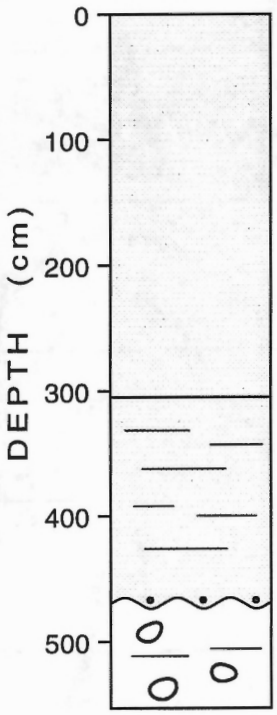

0-300 cm	**Clay-silt mud;** soft, dark gray (2.6Y4.1/0.4) to olive gray (1.8GY3.8/0.7). Black FeS specks and incipient laminations common. Noncalcareous.
300-475 cm	**Clay-silt mud;** soft to semi-firm, olive gray (2.1GY3.7/0.6), faintly banded. Noncalcareous. Some black FeS specks and incipient laminations. Laminated and weakly calcareous below 468 cm.
475 cm	**Contact;** sharp, erosional, with a few sand grains.
475-547 cm	**Silty clay;** stiff, olive gray (4.8Y3.9/0.8) faintly and thinly banded. Weak to moderately calcareous. Light gray buff clasts and layers of calcareous silt throughout, especially common 480-495 cm. Fractured and polished dolomite dropstone at 495 cm.

Core intervals equivalent to seismostratigraphic sequences:

0-475 cm	Winnipeg Sequence (Lake Winnipeg sediments).
475-547 cm	Agassiz Sequence, Disturbed Interval (D) (Lake Agassiz sediments, lower part).

Summary lithologic log for core 121 correlated to seismostratigraphic sequences, central southern Lake Winnipeg.

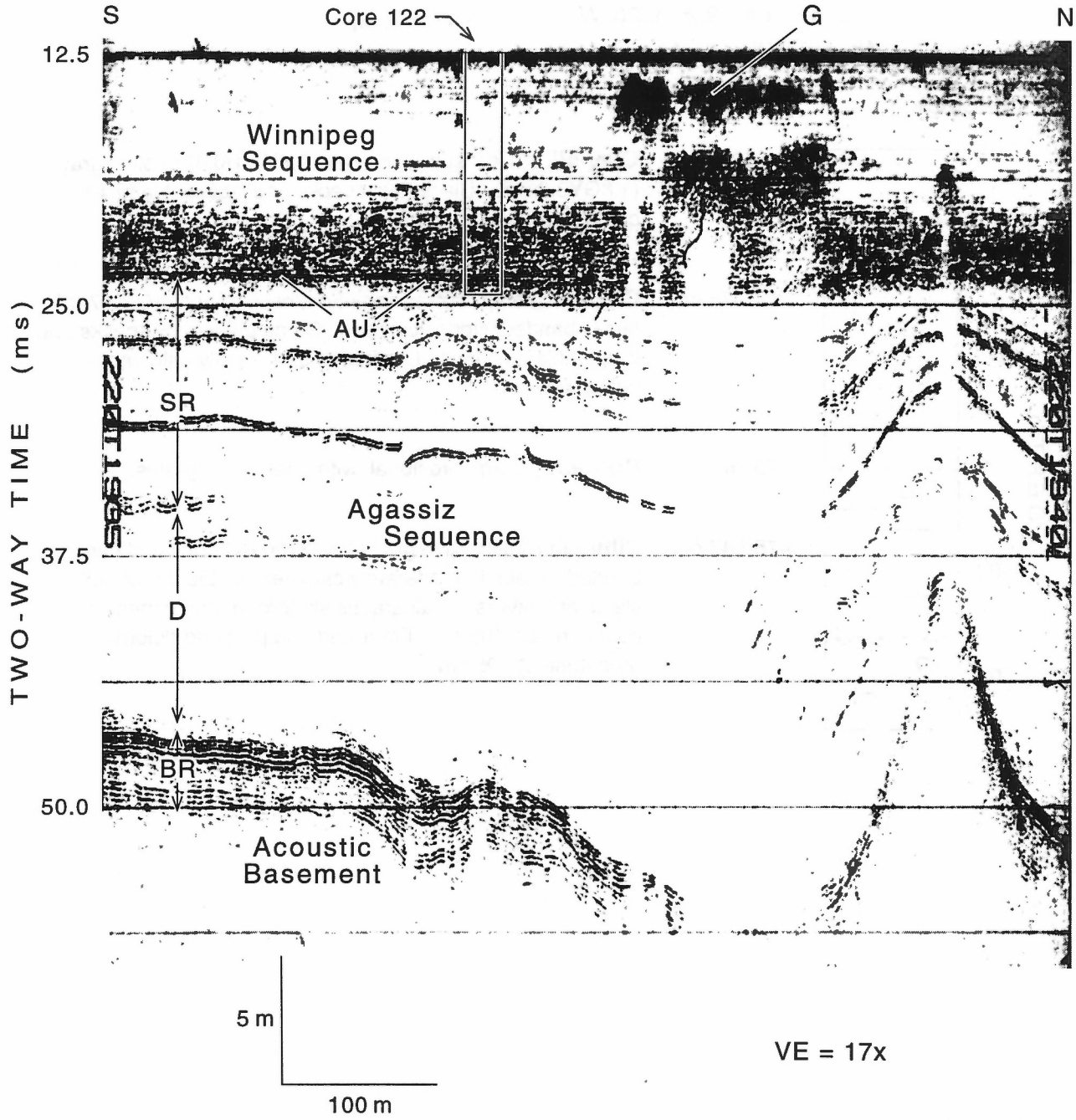

High resolution seismic reflection (Seistec) profile through the core 122 site in southern Lake Winnipeg showing seismostratigraphic sequences. VE = Vertical Exaggeration, vertical scale bar assumes a sound velocity of 1500 m/s. G = Gas Masking. AU = Agassiz Unconformity. Within the Agassiz Sequence, HR = Higher Reflective Interval, SR = Segmented Reflector Interval, D = Disturbed Interval, BR = Basal Reflective Interval. (Seistec record, line SB3, Day 220, 1935 UTC).

Station 122

Latitude	50° 39.39' N	6 cm wide gravity core
Longitude	96° 48.29' W	4.77 m long
Water Depth	9.8 m	

Lithology:

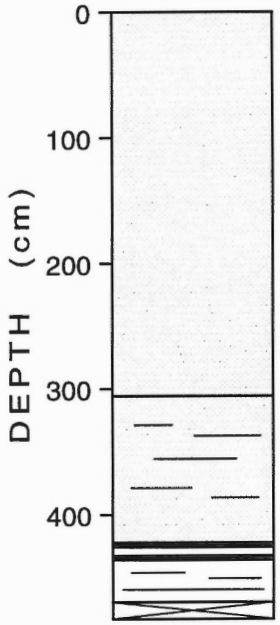

0-300 cm	**Clay-silt mud;** soft, olive gray (9.2Y3.9/0.7 – 5GY3.6/0.5). Becomes firm at base. Black FeS specks and incipient laminations common. Noncalcareous. Grades downward to next unit.
300-426.5 cm	**Clay-silt mud;** faintly banded. Soft-firm, olive gray (9.8Y4.1/0.7). Weakly calcareous below 320 cm. Silt laminations below 390 cm, shell fragments at base.
426.5 cm	**Contact;** conformable.
426.5-435 cm	**Peat;** two beds of clayey silt and peat particles grading up to fine-grained peat, a darker shade of olive gray (4.7Y2.7/0.6). Grades downward to next unit.
435-472 cm	**Clayey silt;** stiff, olive gray (9.1Y4.3/0.6 – 6.4Y4.0/0.8) with light buff specks and incipient banding.
472-477 cm	Recored sediment; disturbed. From organic section just above stiff clay as at 435 cm.

Core intervals equivalent to seismostratigraphic sequences:

0-435 cm	Winnipeg Sequence (Lake Winnipeg sediments).
435-472 cm	Agassiz Sequence, Segmented Reflector Interval (SR) (Lake Agassiz sediments, upper middle part).

Summary lithologic log for core 122 correlated to seismostratigraphic sequences, central southern Lake Winnipeg.

Appendix 7.2: Downcore plots of Lake Winnipeg sediment physical properties

K. Moran

Geological Survey of Canada (Atlantic)
P.O. Box 1006, Dartmouth, Nova Scotia B2Y 4A2

C.A. Jarrett

K&K Geoservices
17 Hawthorne Street, Dartmouth, Nova Scotia B2Y 2Y4

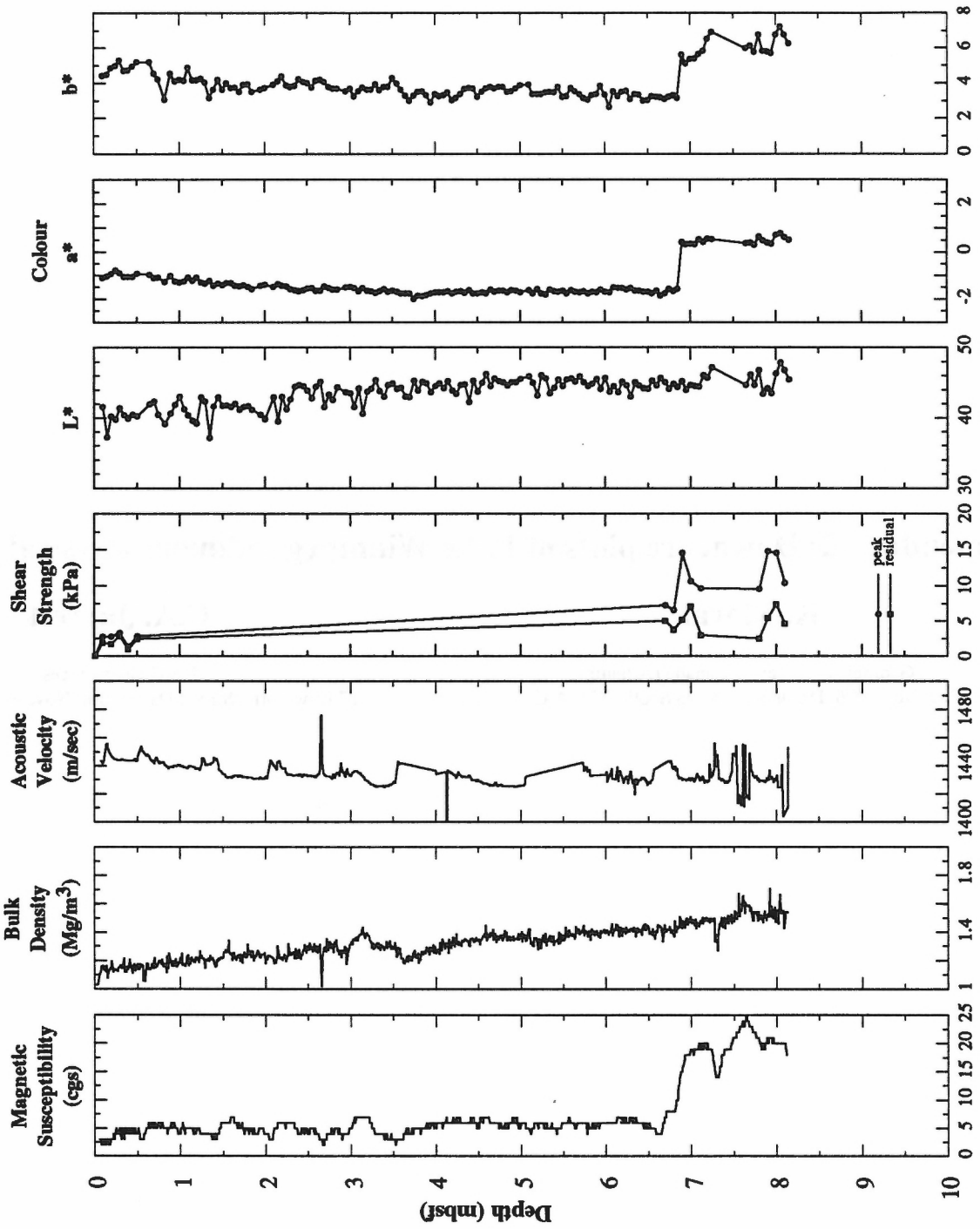
94900 PC103
Depth (mbsf)
Magnetic Susceptibility (cgs)
Bulk Density (Mg/m3)
Acoustic Velocity (m/sec)
Shear Strength (kPa)
peak
residual
L*
Colour
a*
b*

94900 GC104a

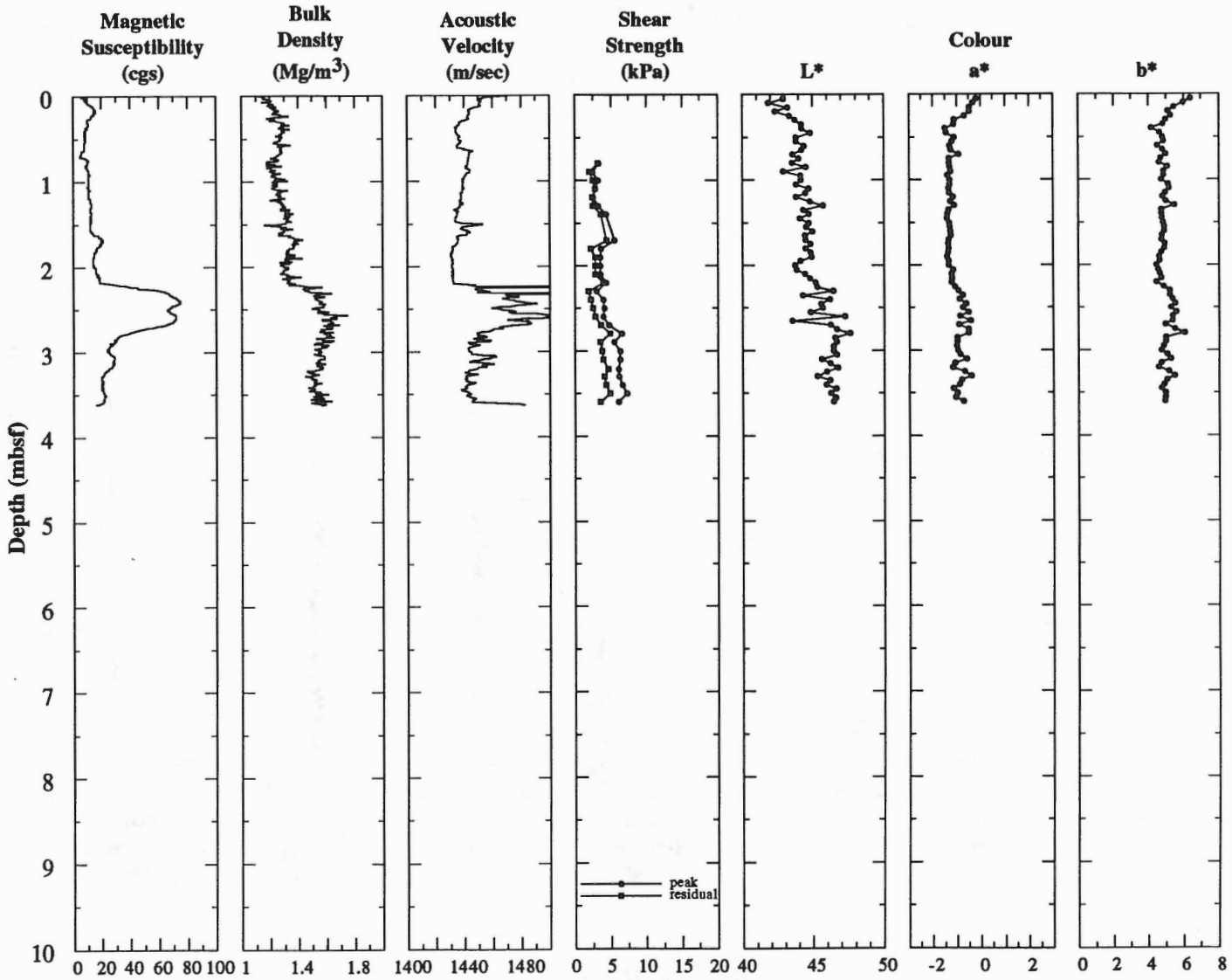

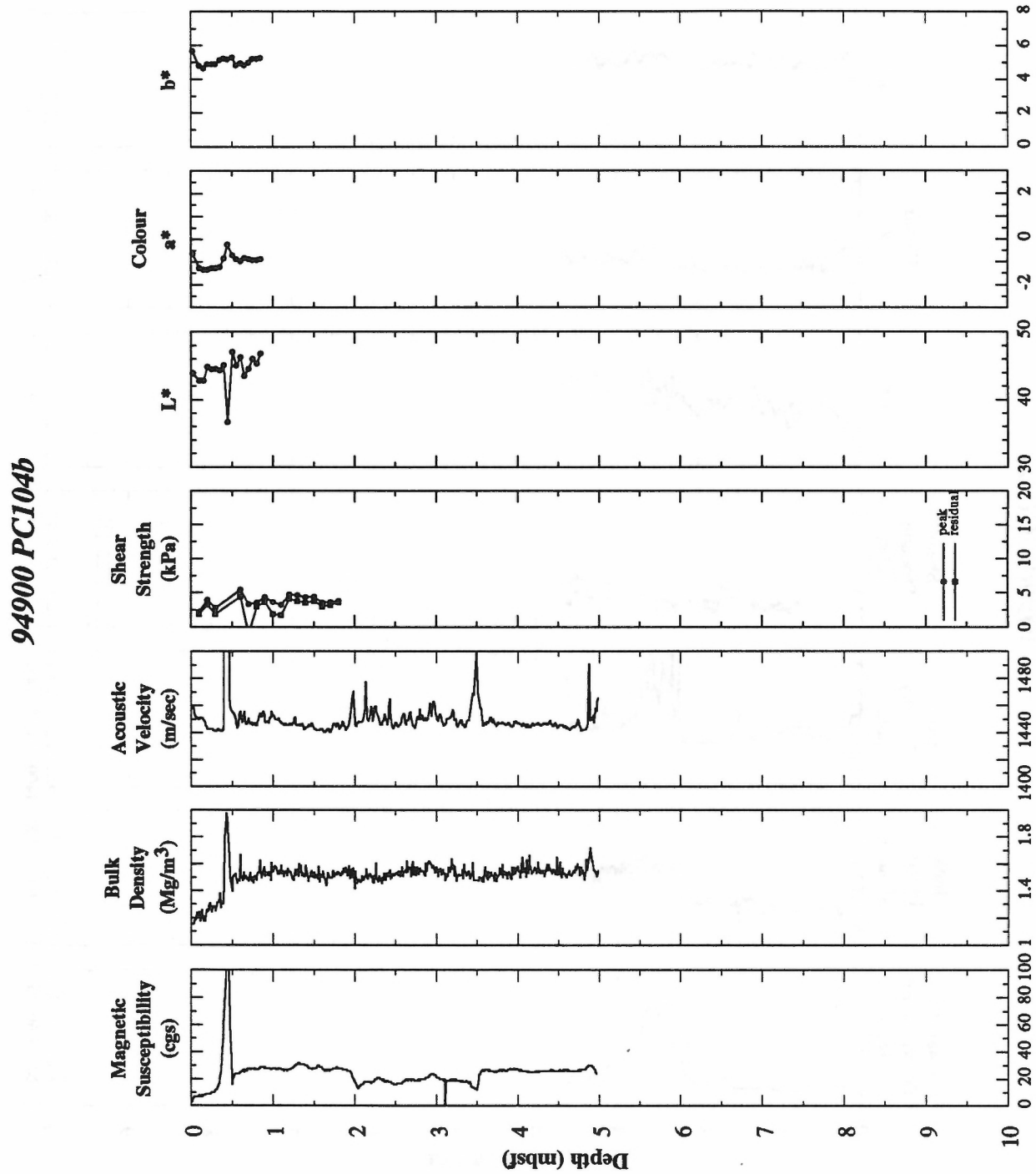
94900 PC104b
Depth (mbsf)
0
1
2
3
4
5
6
7
8
9
10
Magnetic Susceptibility (cgs)
0 20 40 60 80 100
Bulk Density (Mg/m3)
1 1.4 1.8
Acoustic Velocity (m/sec)
1400 1440 1480
Shear Strength (kPa)
0 5 10 15 20
peak
residual
L*
30 40 50
Colour
a*
-2 0 2
b*
0 2 4 6 8

94900 PC105

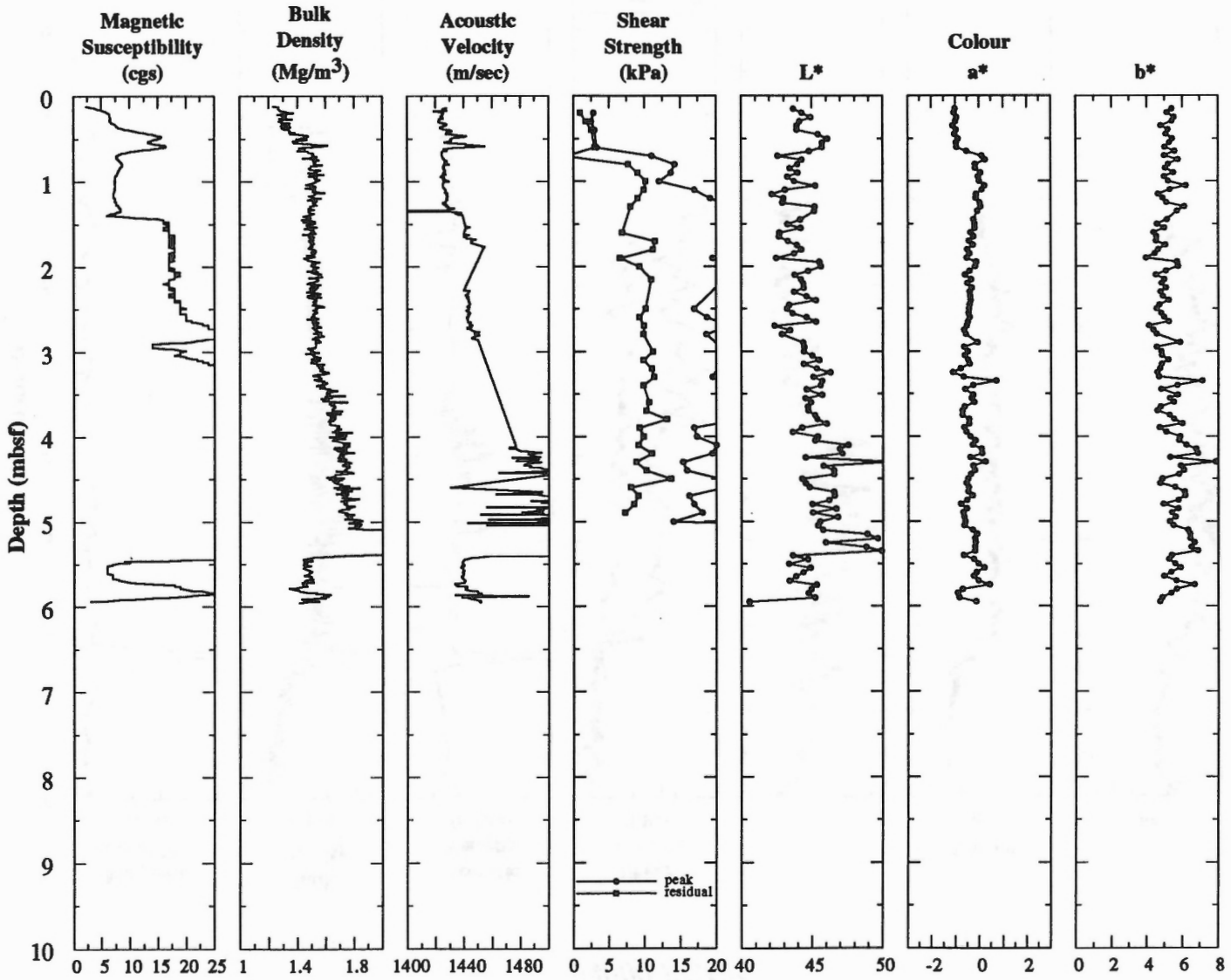
Magnetic Susceptibility (cgs)
Bulk Density (Mg/m3)
Acoustic Velocity (m/sec)
Shear Strength (kPa)
L*
Colour a*
b*
Depth (mbsf)
0
1
2
3
4
5
6
7
8
9
10
0 5 10 15 20 25
1 1.4 1.8
1400 1440 1480
0 5 10 15 20
peak
residual
40 45 50
-2 0 2
0 2 4 6 8

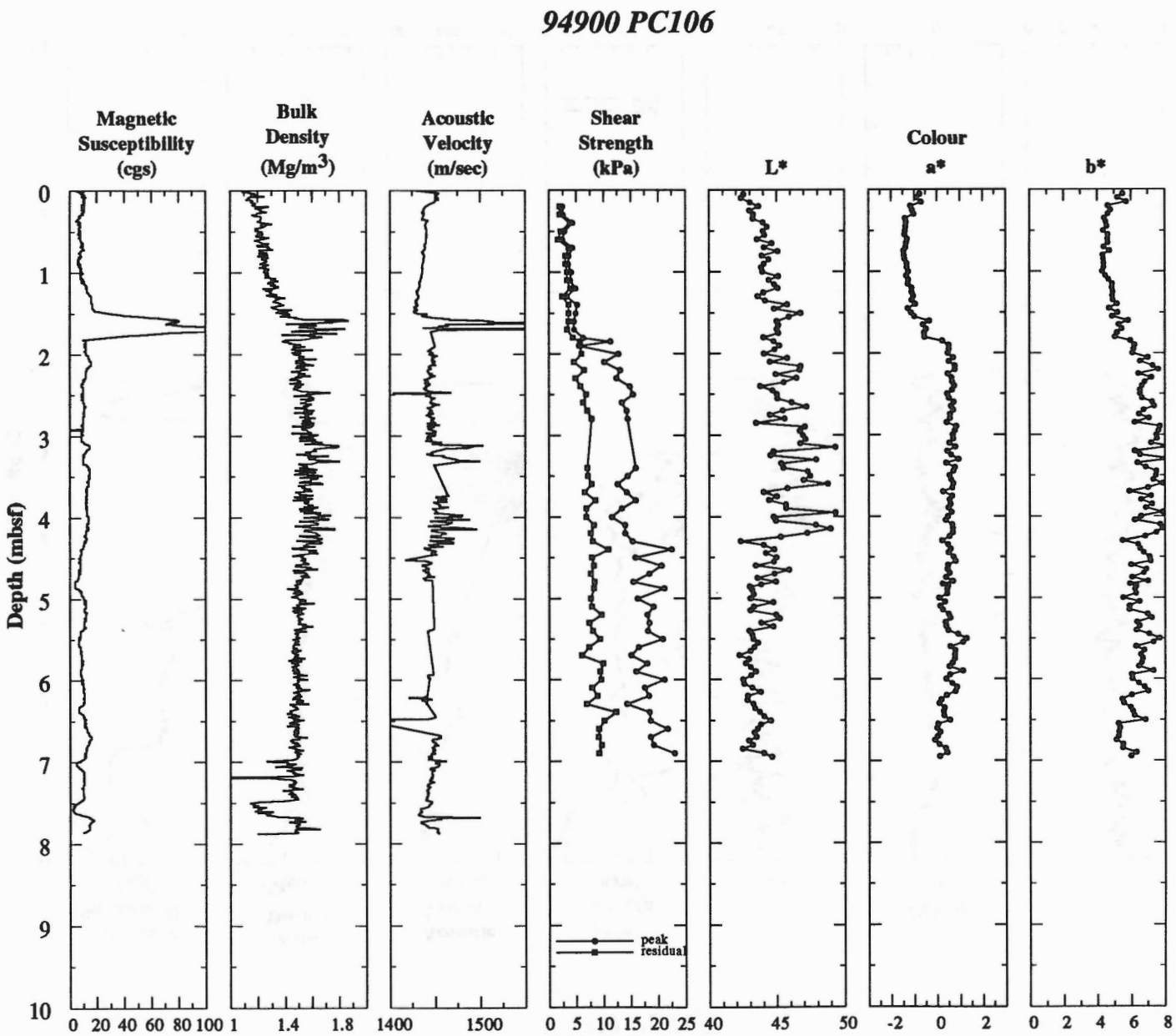
94900 PC106
Magnetic Susceptibility (cgs)
Bulk Density (Mg/m3)
Acoustic Velocity (m/sec)
Shear Strength (kPa)
L*
Colour a*
b*
Depth (mbsf)
0
1
2
3
4
5
6
7
8
9
10
0 20 40 60 80 100
1 1.4 1.8
1400 1500
0 5 10 15 20 25
peak
residual
40 45 50
-2 0 2
0 2 4 6 8

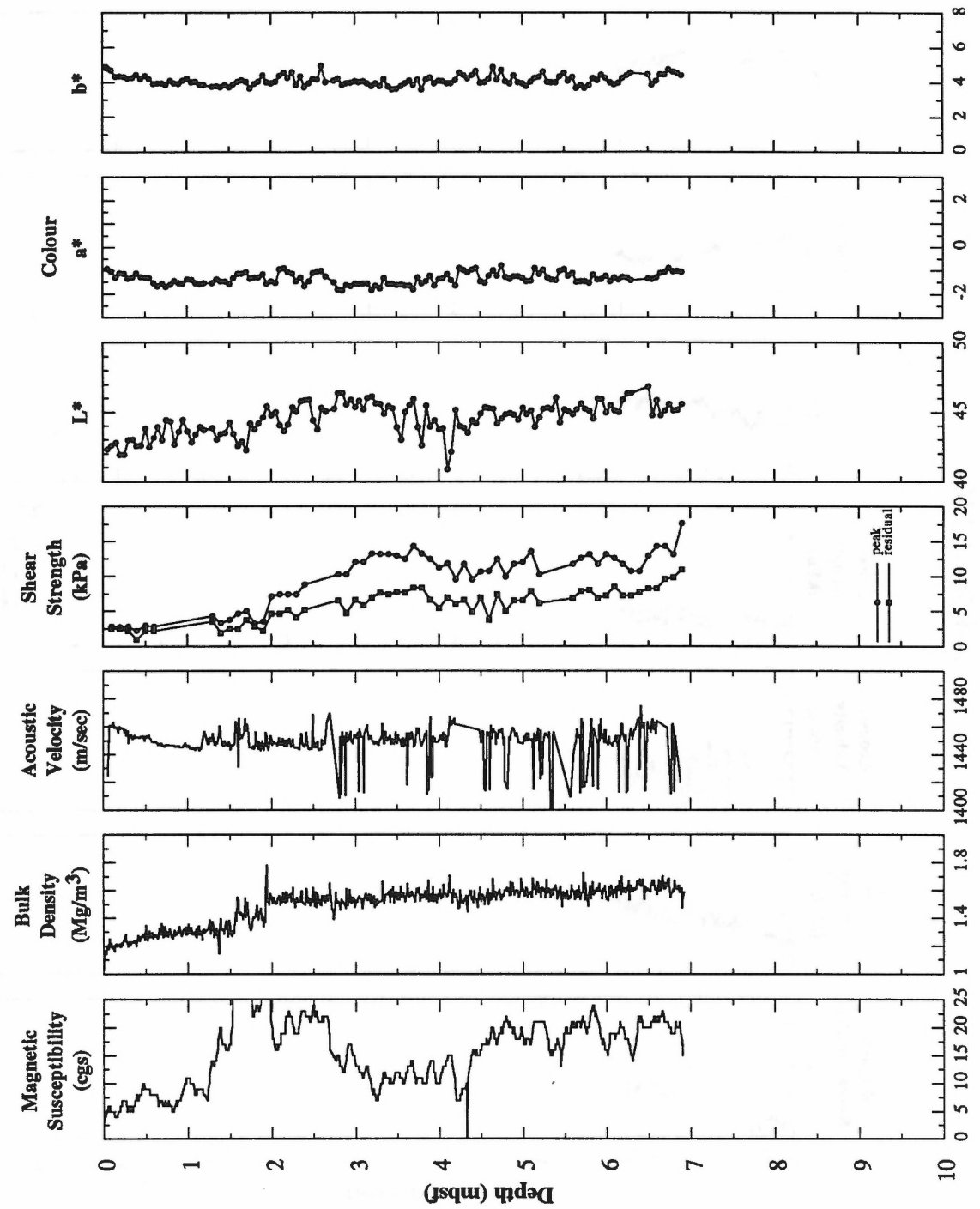
94900 PC107a
Depth (mbsf)
Magnetic Susceptibility (cgs)
Bulk Density (Mg/m3)
Acoustic Velocity (m/sec)
Shear Strength (kPa)
peak
residual
L*
Colour
a*
b*

94900 GC110a

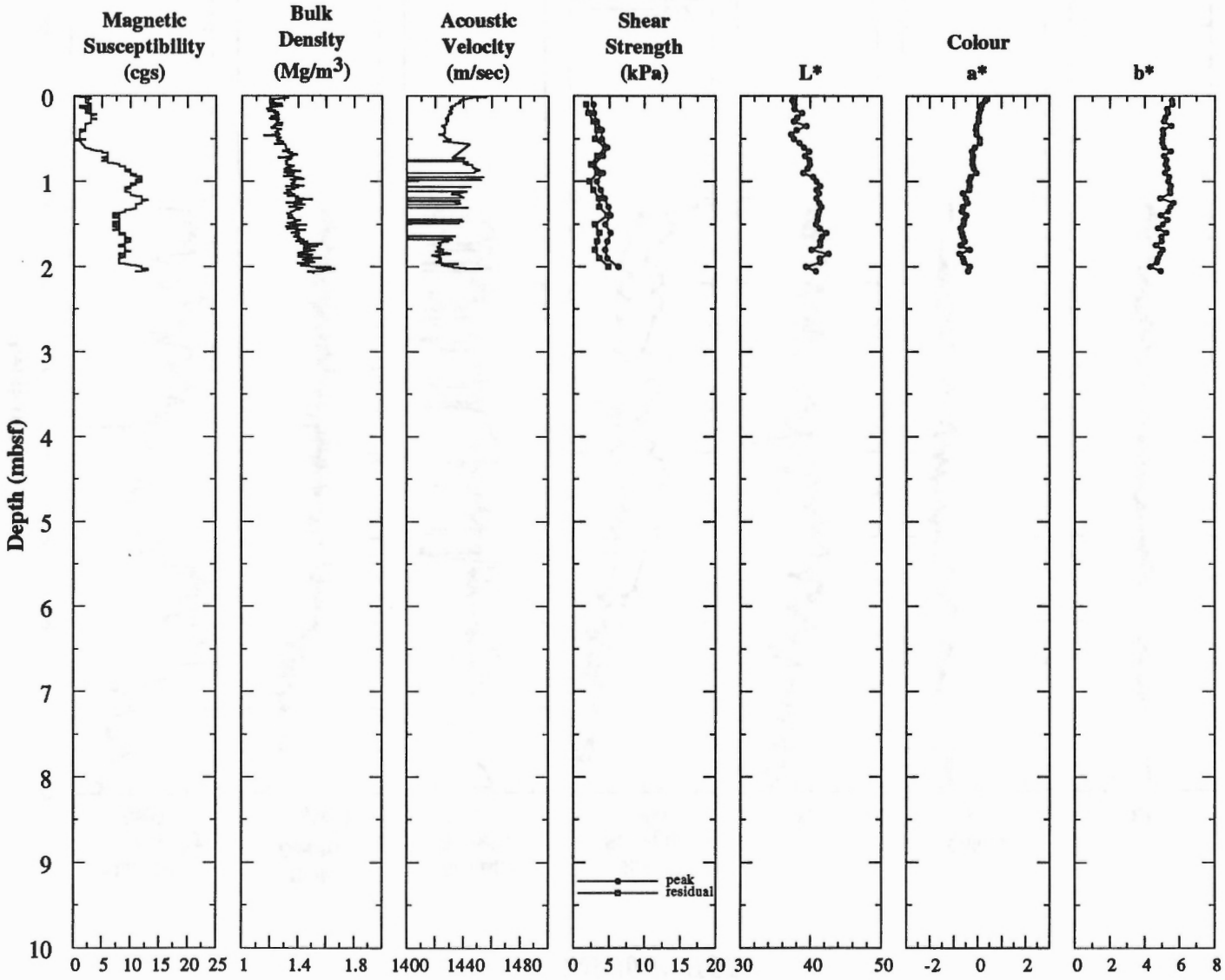

94900 GC113a

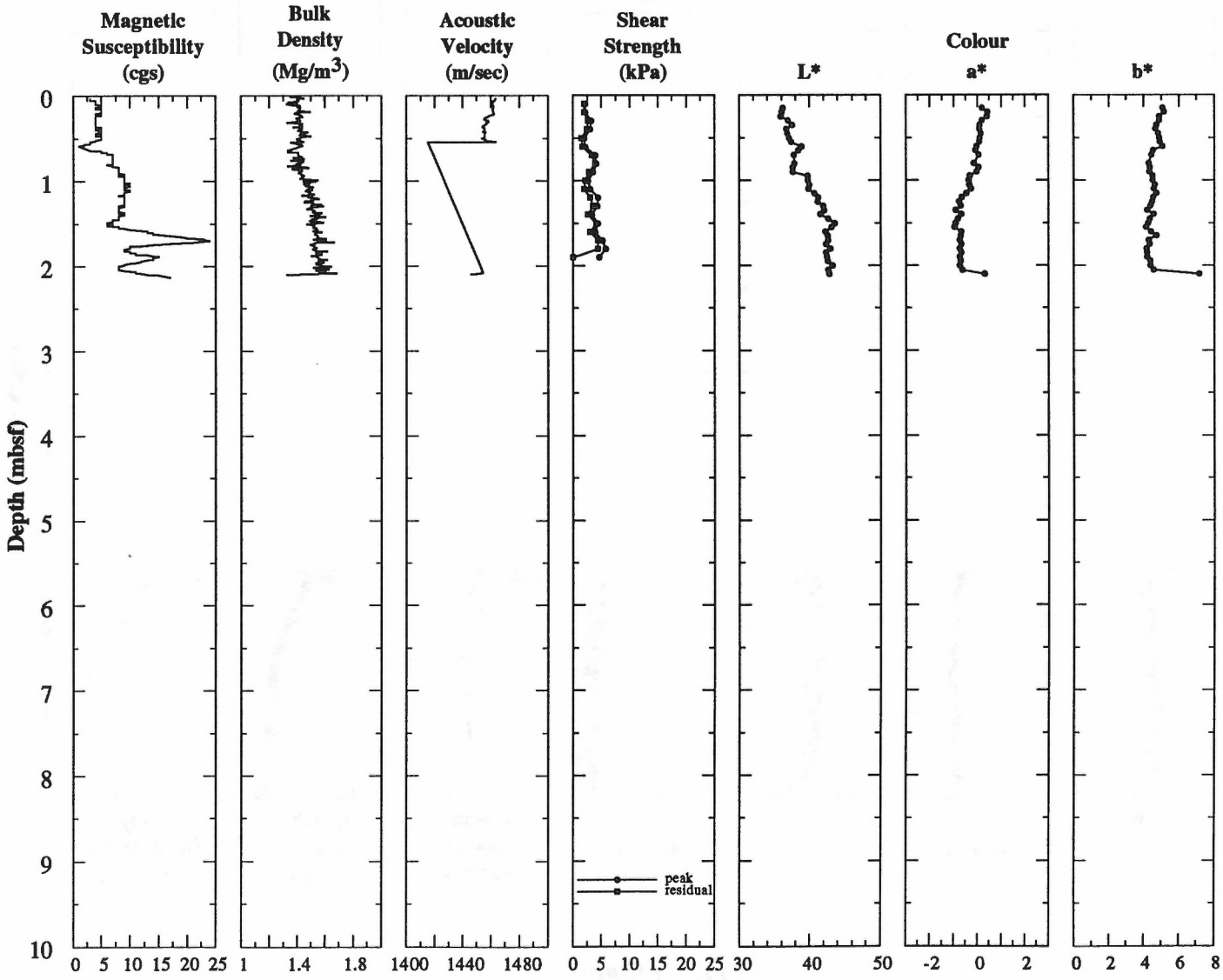

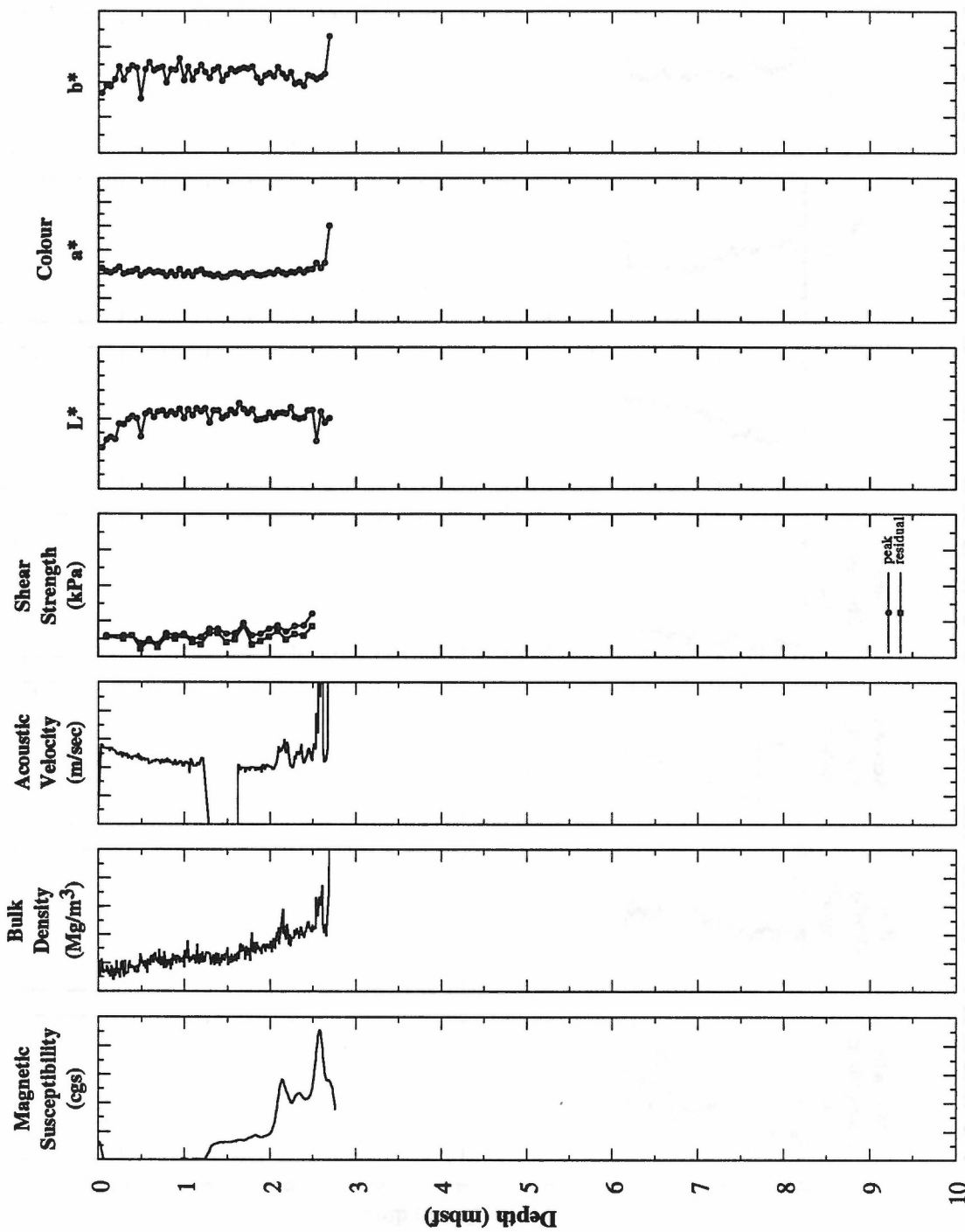
94900 GC115
Depth (mbsf)
Magnetic Susceptibility (cgs)
Bulk Density (Mg/m3)
Acoustic Velocity (m/sec)
Shear Strength (kPa)
peak
residual
L*
Colour
a*
b*

94900 GC119

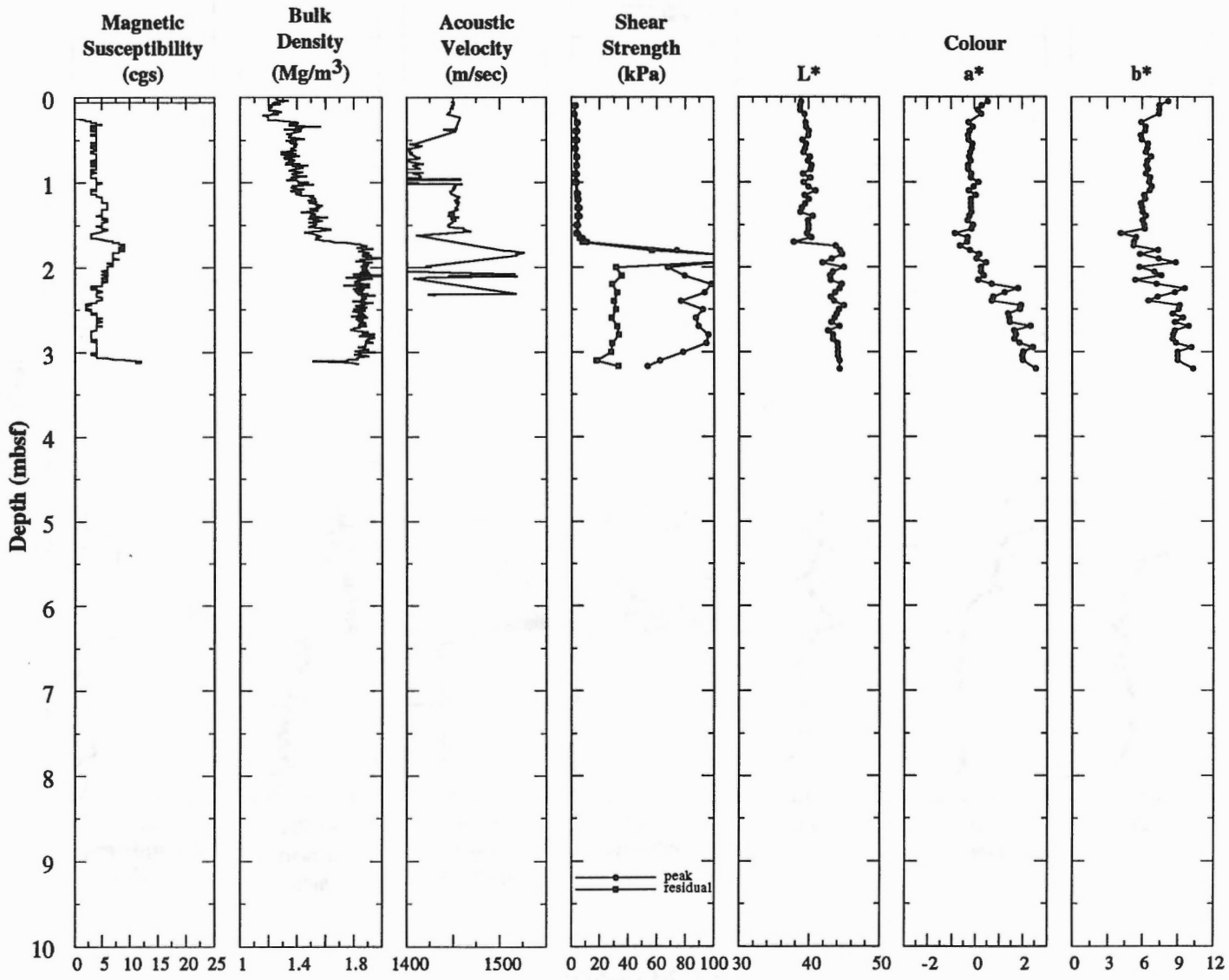
Magnetic Susceptibility (cgs)
Bulk Density (Mg/m3)
Acoustic Velocity (m/sec)
Shear Strength (kPa)
Colour
L*
a*
b*
Depth (mbsf)
0
1
2
3
4
5
6
7
8
9
10
0 5 10 15 20 25
1 1.4 1.8
1400 1500
0 20 40 60 80 100
peak
residual
30 40 50
-2 0 2
0 3 6 9 12

94900 PC120

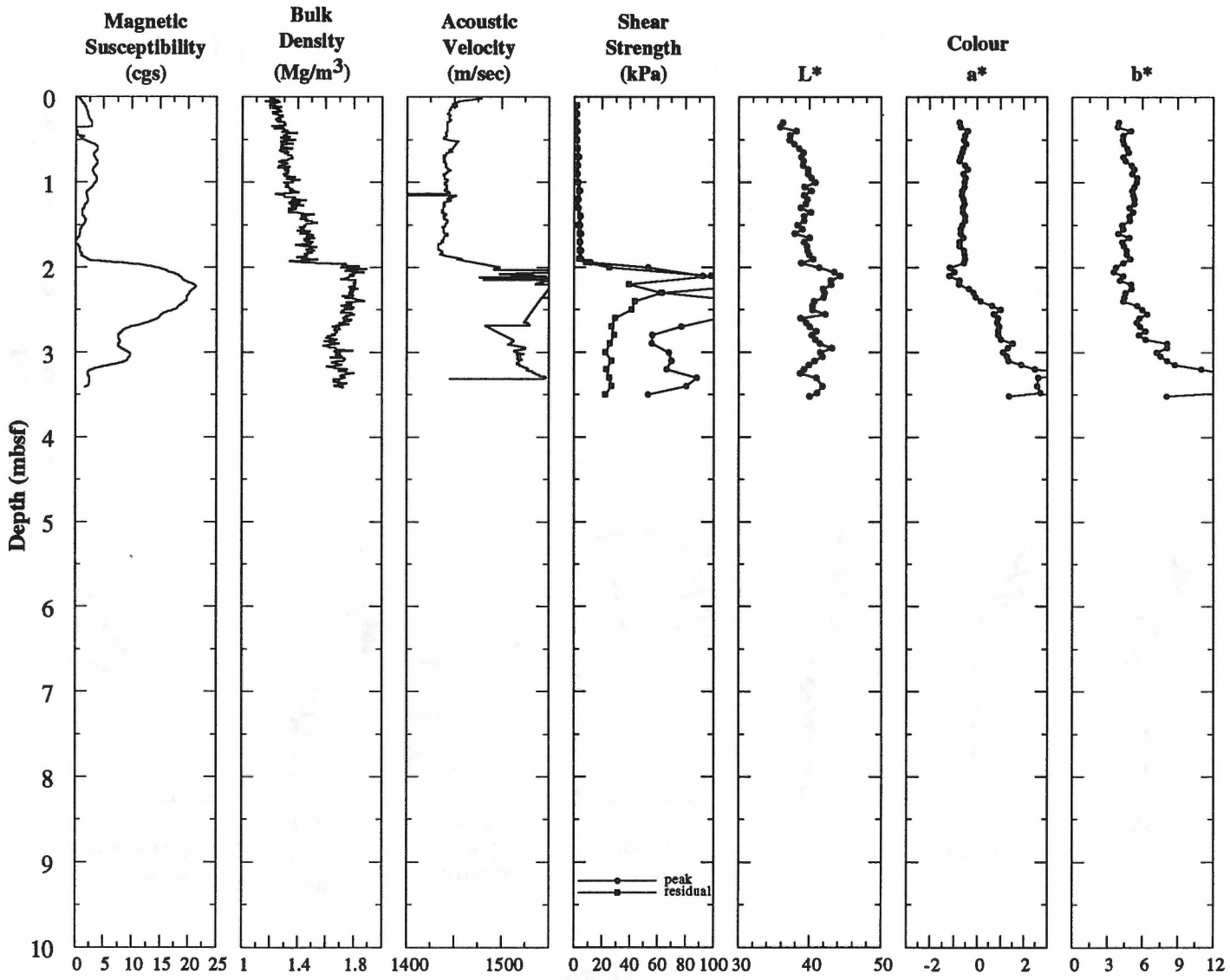
Magnetic Susceptibility (cgs)
Bulk Density (Mg/m3)
Acoustic Velocity (m/sec)
Shear Strength (kPa)
L*
Colour a*
b*
Depth (mbsf)
0
1
2
3
4
5
6
7
8
9
10
0 5 10 15 20 25
1 1.4 1.8
1400 1500
0 20 40 60 80 100
peak
residual
30 40 50
-2 0 2
0 3 6 9 12

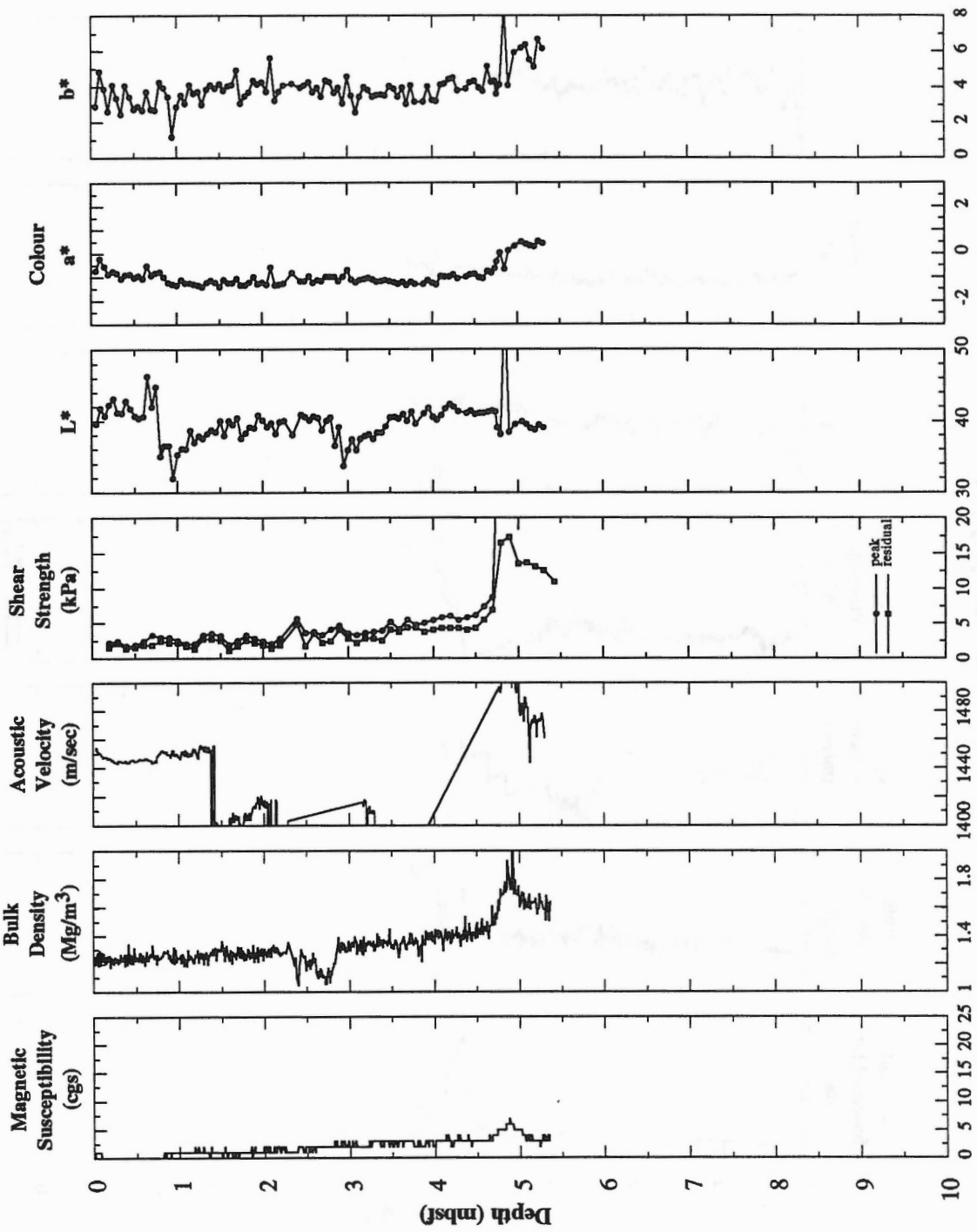
94900 GC121
Depth (mbsf)
Magnetic Susceptibility (cgs)
Bulk Density (Mg/m3)
Acoustic Velocity (m/sec)
Shear Strength (kPa)
peak
residual
L*
Colour
a*
b*

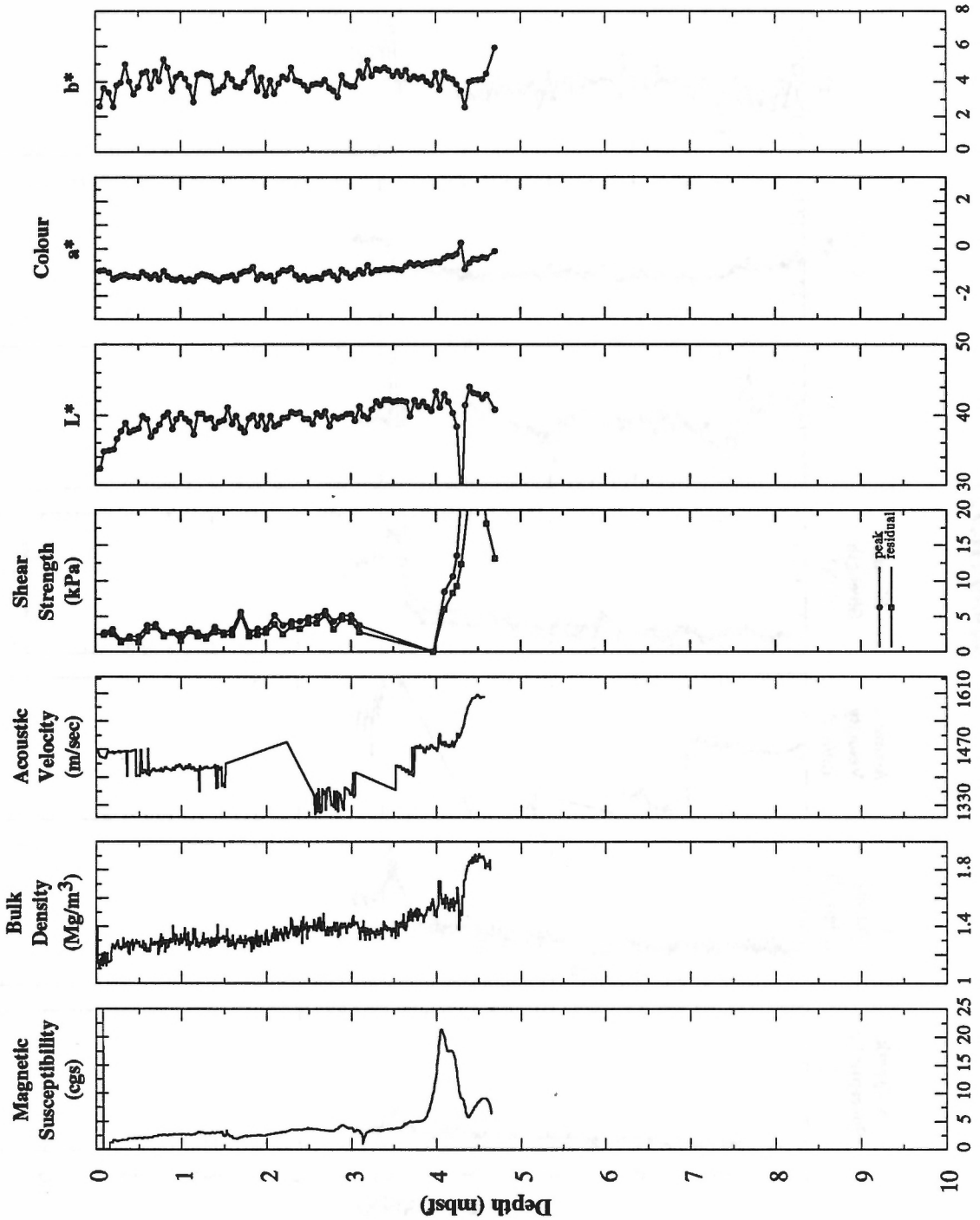
94900 GC122a
Depth (mbsf)
Magnetic Susceptibility (cgs)
Bulk Density (Mg/m3)
Acoustic Velocity (m/sec)
Shear Strength (kPa)
peak
residual
L*
Colour
a*
b*

Appendix 7.3: Bulk composition, texture, and mineralogy of Lake Winnipeg sediments

W.M. Last

Department of Geological Sciences
University of Manitoba, Winnipeg, Manitoba R3T 2N2

SAMPLE			BULK COMPOSITION			TEXTURE					
Seq	Site	Depth	Moisture	Organic	Carbonate	Clay	Silt	Sand	Mean	St Dev	Median
no	ID	cm	%	%	%	%	%	%	um	um	um
1	103	5	75.6	7.4	3.2	31.9	60.4	7.7	4.6	8.4	5.8
2	103	15	80.6	8.8	3.8	31.4	68.6	0.0	4.5	7.2	6.9
3	103	25	74.2	6.7	3.5	46.7	53.3	0.0	3.2	5.0	4.3
4	103	35	76.1	7.4	3.5	19.3	80.7	0.0	6.6	9.7	17.0
5	103	45	76.0	7.7	3.0	18.4	76.0	5.6	6.7	10.4	14.7
6	103	55	73.2	7.4	3.4	11.3	84.6	4.1	9.3	13.5	26.1
7	103	65	73.1	7.2	2.9	28.8	68.6	2.6	4.9	7.1	6.2
8	103	75	72.8	6.9	3.1	23.7	67.9	8.4	5.7	10.6	12.1
9	103	85	72.6	6.7	3.2	16.8	75.8	7.4	7.3	13.0	21.4
10	103	95	70.8	5.2	5.2	13.3	79.6	7.1	8.7	13.4	29.3
11	103	105	70.7	6.7	3.1	16.0	74.2	9.8	7.8	13.3	26.1
12	103	115	71.8	6.7	3.0	39.0	61.0	0.0	3.8	6.1	5.4
13	103	125	71.3	6.8	3.0	34.2	63.5	2.3	4.2	5.8	5.2
14	103	135	71.2	6.8	3.1	25.1	74.9	0.0	5.6	9.4	12.5
15	103	145	69.2	6.1	3.8	20.3	73.9	5.8	6.4	10.4	13.8
16	103	155	63.8	5.7	3.7	20.1	73.0	6.9	6.7	10.8	16.6
17	103	165	64.6	6.3	3.1	42.8	57.2	0.0	3.6	4.5	4.5
18	103	175	69.1	5.8	3.7	52.2	47.8	0.0	2.9	5.1	3.8
19	103	185	68.0	6.1	3.1	33.9	64.8	1.3	4.3	6.3	5.5
20	103	195	67.4	6.1	3.1	38.9	57.0	4.1	3.9	7.0	5.8
21	103	205	66.1	4.6	4.7	19.6	73.6	6.8	6.8	12.4	30.1
22	103	215	66.6	4.9	3.9	45.3	43.0	11.7	3.5	8.2	4.5
23	103	225	66.0	4.4	4.3	41.7	58.4	0.0	3.7	4.7	4.6
24	103	235	66.3	4.1	4.8	39.2	57.7	3.1	3.8	5.6	4.8
25	103	245	66.0	4.9	4.0	54.3	45.7	0.0	2.8	3.1	3.7
26	103	255	65.4	5.3	3.2	63.6	36.4	0.0	2.5	2.1	3.2
27	103	265	66.7	6.1	3.1	26.6	73.4	0.0	5.6	10.0	21.1
28	103	275	65.1	6.0	2.6	33.8	66.2	0.0	4.3	6.7	5.9
29	103	285	65.7	5.9	2.7	37.9	62.1	0.0	3.9	4.5	4.9
30	103	295	65.6	5.6	3.3	35.6	64.4	0.0	4.3	6.5	5.4
31	103	305	56.5	5.8	2.9	51.8	48.2	0.0	3.1	2.0	3.9
32	103	315	54.1	5.5	3.2	38.4	61.6	0.0	3.9	4.9	4.9
33	103	325	59.7	4.1	4.7	38.2	56.0	5.8	4.0	7.1	4.9
34	103	335	62.8	5.7	3.1	20.4	74.2	5.4	6.7	11.5	18.7
35	103	345	63.3	5.6	2.9	55.1	36.7	8.3	2.8	5.9	3.6
36	103	355	63.2	5.3	3.0	33.5	56.4	10.0	4.5	9.1	5.7
37	103	365	62.0	4.6	3.8	51.9	45.0	3.1	3.1	3.8	3.9
38	103	375	61.6	5.8	2.7	72.0	28.0	0.0	2.4	1.8	3.0
39	103	385	61.6	5.3	3.2	62.3	37.7	0.0	2.6	1.9	3.4
40	103	395	61.3	6.0	2.8	41.3	58.7	0.0	3.8	6.8	4.8
41	103	405	60.9	5.6	3.3	53.1	41.5	5.3	3.0	5.1	3.8
42	103	415	60.2	5.5	3.1	56.7	43.3	0.0	2.8	2.4	3.7
43	103	425	60.7	5.9	2.8	51.4	48.6	0.0	2.8	2.7	3.9
44	103	435	58.5	4.8	3.4	40.6	47.9	11.5	3.9	8.1	4.8
45	103	445	59.3	4.3	5.0	40.6	54.7	4.7	3.8	6.1	4.8
46	103	455	58.3	5.5	3.5	39.4	51.1	9.5	4.0	8.8	5.5
47	103	465	57.6	3.5	5.0	29.0	52.5	18.4	5.1	11.5	8.7
48	103	475	57.6	3.7	4.8	39.6	60.4	0.0	3.9	5.4	5.2
49	103	485	56.4	5.2	3.3	46.3	53.7	0.0	3.4	5.0	4.3
50	103	495	56.9	5.6	2.8	31.4	66.7	1.9	4.6	6.8	6.1

SAMPLE			BULK COMPOSITION			TEXTURE					
Seq	Site	Depth	Moisture	Organic	Carbonate	Clay	Silt	Sand	Mean	St Dev	Median
no	ID	cm	%	%	%	%	%	%	um	um	um
51	103	505	57.3	5.4	3.4	50.1	43.9	6.0	3.3	6.3	4.0
52	103	515	54.6	4.8	4.0	44.3	55.7	0.0	3.5	3.6	4.4
53	103	525	55.4	5.0	4.0	34.8	54.6	10.6	4.3	8.6	5.7
54	103	535	56.9	5.0	3.8	46.9	53.1	0.0	3.3	3.2	4.2
55	103	545	56.0	5.0	3.7	45.2	48.9	6.0	3.5	6.5	4.3
56	103	555	55.9	5.4	3.8	34.2	63.9	1.9	4.4	6.8	5.8
57	103	565	55.2	5.0	4.0	69.1	30.9	0.0	2.3	2.0	3.0
58	103	575	55.8	5.1	3.6	50.1	44.9	5.0	3.3	6.2	4.0
59	103	585	56.3	5.5	3.4	60.1	39.9	0.0	2.7	2.6	3.4
60	103	595	55.4	4.7	4.5	42.1	57.9	0.0	3.6	3.7	4.5
61	103	605	54.8	4.7	4.4	29.0	66.8	4.3	5.0	7.8	7.3
62	103	615	54.0	4.7	4.7	43.4	53.1	3.5	3.6	6.3	4.5
63	103	625	54.0	4.7	4.1	50.5	49.5	0.0	3.2	4.1	4.0
64	103	635	53.4	5.1	4.8	47.2	52.9	0.0	3.2	2.3	4.2
65	103	645	53.2	5.2	4.1	49.8	50.2	0.0	3.1	2.3	4.0
66	103	655	54.1	5.3	4.1	47.3	50.0	2.8	3.3	4.3	4.2
67	103	665	51.5	4.3	4.9	44.8	55.2	0.0	3.5	4.6	4.3
68	103	675	50.9	3.8	5.9	33.8	66.2	0.0	4.2	5.1	5.3
69	103	685	52.1	4.8	4.5	40.6	59.4	0.0	3.7	4.2	4.6
70	103	695	48.6	2.8	7.4	51.5	26.6	21.9	3.2	9.3	3.9
71	103	705	48.6	3.5	7.1	50.8	30.2	19.0	3.2	8.9	4.0
72	103	715	48.1	3.2	8.0	63.4	36.6	0.0	2.6	3.6	3.1
73	103	725	48.4	6.0	4.9	64.4	35.6	0.0	2.6	3.3	3.1
74	103	735	51.5	5.4	4.7	65.1	34.9	0.0	2.5	2.5	3.2
75	103	745	49.6	5.7	4.3	62.0	38.0	0.0	2.6	3.1	3.3
76	103	755	45.0	6.2	4.7	69.4	30.6	0.0	2.3	1.6	2.9
77	103	765	42.4	5.3	5.8	82.0	18.0	0.0	1.8	1.5	1.9
78	103	775	45.9	3.8	8.8	74.3	21.2	4.6	2.1	3.1	2.5
79	103	785	46.4	4.9	8.3	65.8	34.2	0.0	2.6	2.7	3.2
80	103	795	47.6	5.8	5.6	46.1	44.5	9.4	3.4	6.7	4.3
81	103	805	37.7	4.0	13.5	66.9	29.7	3.5	2.5	4.3	2.9
82	103	815	43.3	5.6	6.8	83.2	16.8	0.0	1.9	1.3	2.3
83	104A	5	69.8	6.0	4.4	30.1	61.5	8.4	3.4	6.2	4.1
84	104A	15	67.6	6.0	3.9	24.3	56.9	18.9	4.1	10.2	5.0
85	104A	25	67.1	5.8	5.1	32.0	65.5	2.5	3.3	5.0	4.0
86	104A	35	61.1	4.9	5.4	33.9	61.5	4.6	3.2	5.2	4.0
87	104A	45	63.5	5.6	4.8	28.4	68.6	3.0	3.7	5.7	4.5
88	104A	55	66.0	5.7	5.0	34.0	63.7	2.4	3.2	5.0	3.9
89	104A	65	65.2	5.8	4.9	32.5	67.5	0.0	3.3	4.4	4.0
90	104A	75	69.3	6.0	4.0	33.4	66.6	0.0	3.2	3.4	4.0
91	104A	85	65.3	5.4	5.2	41.7	49.4	8.9	2.9	6.5	3.6
92	104A	95	65.9	5.2	4.8	29.6	56.5	14.0	3.6	8.3	4.3
93	104A	105	67.5	5.2	4.7	33.9	66.1	0.0	3.2	5.1	4.3
94	104A	115	64.3	5.2	4.9	38.8	61.2	0.0	2.9	4.0	3.8
95	104A	125	60.5	4.8	5.4	29.6	64.9	5.6	3.7	4.6	5.4
96	104A	135	61.0	5.1	5.6	42.8	57.2	0.0	2.8	3.9	3.4
97	104A	145	60.1	4.7	5.9	43.1	56.9	0.0	2.7	3.8	3.4
98	104A	155	57.8	4.6	6.3	36.1	60.2	3.7	3.1	4.4	3.7
99	104A	165	52.0	4.6	8.3	25.3	74.7	0.0	3.7	5.0	4.5
100	104A	175	57.5	4.7	6.5	34.3	65.7	0.0	3.1	3.7	3.9

SAMPLE			BULK COMPOSITION			TEXTURE					
Seq	Site	Depth	Moisture	Organic	Carbonate	Clay	Silt	Sand	Mean	St Dev	Median
no	ID	cm	%	%	%	%	%	%	um	um	um
101	104A	185	60.1	4.8	5.7	37.1	62.9	0.0	2.9	2.5	3.7
102	104A	195	59.9	5.1	5.9	49.6	50.4	0.0	2.4	1.9	3.0
103	104A	205	59.4	5.3	5.7	61.7	38.3	0.0	2.1	1.9	2.5
104	104A	215	56.0	4.5	6.0	37.0	58.3	4.7	3.1	5.8	3.8
105	104A	225	52.2	3.4	7.1	37.7	57.7	4.6	3.0	5.9	4.4
106	104A	235	48.0	3.2	9.7	36.4	52.4	11.3	3.1	7.1	4.0
107	104A	245	36.6	2.0	7.4	34.5	65.5	0.0	3.1	4.3	4.1
108	104A	255	33.8	1.7	8.1	34.6	65.4	0.0	3.1	3.9	4.2
109	104A	265	43.4	2.4	9.1	42.6	57.4	0.0	2.8	2.3	3.4
110	104A	275	42.1	2.8	10.3	37.1	60.2	2.7	3.0	4.6	3.9
111	104A	285	42.8	2.9	9.8	42.1	57.9	0.0	2.8	3.2	3.5
112	104A	295	42.2	3.1	10.3	35.1	64.9	0.0	2.9	2.7	3.9
113	104A	305	46.2	2.7	10.0	31.4	57.1	11.6	3.4	7.0	4.3
114	104A	315	44.7	3.1	10.0	51.0	49.0	0.0	2.4	2.1	3.0
115	104A	325	46.5	2.6	9.5	40.1	57.1	2.8	2.9	4.9	3.6
116	104A	335	44.3	2.3	10.6	17.1	82.9	0.0	4.9	6.9	7.5
117	104A	345	44.7	2.1	10.5	29.6	46.1	24.4	3.9	11.6	5.5
118	104A	355	45.0	2.2	10.6	35.5	64.6	0.0	3.1	3.8	3.8
119	104A	365	34.7	2.1	11.3	33.1	57.7	9.2	3.3	6.6	4.1
120	104B	5	67.0	5.1	5.2	40.6	53.5	5.9	2.8	5.2	3.6
121	104B	15	68.4	5.2	5.9	23.2	74.0	2.8	3.9	5.4	4.8
122	104B	25	61.2	4.7	5.9	49.7	50.4	0.0	2.4	2.7	3.0
123	104B	35	61.0	5.2	5.6	42.6	54.9	2.5	2.8	4.2	3.5
124	104B	45	33.6	2.1	9.5	38.7	56.9	4.4	2.9	4.7	3.6
125	104B	55	47.1	3.6	9.4	32.9	58.6	8.5	3.3	5.7	4.0
126	104B	65	44.6	3.2	10.0	32.8	60.5	6.7	3.3	6.7	4.1
127	104B	75	46.0	3.6	9.4	41.4	58.6	0.0	2.7	2.3	3.5
128	105	5	64.5	5.9	5.8	41.5	56.8	1.8	3.7	4.8	4.6
129	105	15	61.6	4.9	6.4	44.7	49.5	5.8	3.6	6.3	4.4
130	105	25	58.4	4.5	7.9	60.3	31.7	8.0	2.7	5.3	3.4
131	105	35	58.0	4.7	5.5	58.0	39.1	2.9	2.7	4.0	3.5
132	105	45	55.6	4.1	6.4	65.0	35.0	0.0	2.6	1.9	3.2
133	105	55	53.9	3.7	7.9	49.7	39.6	10.7	2.8	7.4	4.0
134	105	65	56.2	4.4	7.5	54.1	43.3	2.6	3.0	4.8	3.8
135	105	75	45.3	5.0	6.3	56.5	43.5	0.0	2.7	2.3	3.5
136	105	85	45.5	4.1	6.5	48.4	41.2	10.4	3.3	7.0	4.1
137	105	95	46.8	4.7	5.6	56.0	36.4	7.6	2.8	6.4	3.6
138	105	105	45.7	3.9	7.4	58.5	41.5	0.0	2.7	2.8	3.5
139	105	115	43.6	3.6	8.0	63.0	37.0	0.0	2.6	2.4	3.3
140	105	125	45.9	3.6	6.9	67.8	32.2	0.0	2.4	2.8	3.0
141	105	135	44.9	3.9	6.6	69.9	30.1	0.0	2.3	2.2	2.9
142	105	145	44.2	3.4	8.4	36.3	54.8	8.9	4.1	8.1	5.9
143	105	155	43.0	3.7	8.5	47.0	50.7	2.4	3.3	4.4	4.2
144	105	165	43.8	3.9	7.6	66.8	33.2	0.0	2.5	1.9	3.2
145	105	175	43.1	3.8	8.1	60.8	29.5	9.8	2.6	5.4	3.3
146	105	185	42.7	4.7	6.4	53.6	46.4	0.0	3.0	3.4	3.8
147	105	195	43.3	4.3	6.2	59.5	40.5	0.0	2.6	2.1	3.4
148	105	205	43.6	3.8	7.2	56.2	43.8	0.0	2.9	4.6	3.6
149	105	215	44.7	4.8	6.7	43.5	42.4	14.2	3.6	9.5	4.9
150	105	225	43.6	4.5	6.9	66.9	33.1	0.0	2.3	2.6	2.8

SAMPLE			BULK COMPOSITION			TEXTURE					
Seq	Site	Depth	Moisture	Organic	Carbonate	Clay	Silt	Sand	Mean	St Dev	Median
no	ID	cm	%	%	%	%	%	%	um	um	um
151	105	235	43.0	4.9	5.3	33.0	64.0	3.0	4.2	6.3	6.6
152	105	245	42.6	5.0	5.4	48.2	41.1	10.7	3.4	7.9	4.2
153	105	255	42.9	4.6	6.4	61.6	24.6	13.8	2.2	6.0	2.5
154	105	265	42.7	4.5	6.6	70.4	29.6	0.0	2.4	2.1	3.0
155	105	275	41.9	4.3	7.0	70.3	29.7	0.0	2.4	2.0	2.9
156	105	285	39.7	4.2	7.2	55.1	44.9	0.0	3.0	3.2	3.7
157	105	295	41.1	4.1	6.5	46.4	53.6	0.0	3.3	5.7	4.3
158	105	305	40.0	3.6	7.8	50.7	47.0	2.3	3.3	5.4	4.0
159	105	315	38.8	3.8	7.5	23.8	57.8	18.4	5.8	11.9	11.3
160	105	325	39.1	3.8	7.8	57.8	42.2	0.0	2.9	3.2	3.6
161	105	335	38.6	3.8	10.2	46.3	39.1	14.7	3.6	9.2	4.4
162	105	345	36.0	3.2	8.2	60.7	32.6	6.6	2.6	5.3	3.3
163	105	355	39.9	4.1	9.1	54.6	42.7	2.7	3.0	4.1	3.7
164	105	365	37.5	2.9	8.0	70.0	30.0	0.0	2.3	2.3	2.9
165	105	375	34.4	2.2	7.5	45.9	45.2	9.0	3.4	7.2	4.5
166	105	385	36.9	2.8	7.5	56.7	43.3	0.0	2.8	2.3	3.6
167	105	395	31.5	2.2	6.5	40.5	59.5	0.0	3.7	5.2	5.1
168	105	405	33.0	2.8	9.4	52.3	47.7	0.0	3.1	2.3	3.9
169	105	415	33.2	2.5	10.2	60.4	39.6	0.0	2.6	2.8	3.4
170	105	425	32.2	1.8	10.1	57.6	42.4	0.0	3.0	3.5	3.6
171	105	435	29.6	1.8	9.7	66.0	34.0	0.0	2.7	2.0	3.2
172	105	445	26.9	1.8	10.7	42.7	46.5	10.8	3.8	7.6	4.5
173	105	455	32.3	2.4	11.0	58.1	37.6	4.3	3.0	4.4	3.6
174	105	465	27.9	1.9	10.2	64.5	28.0	7.5	2.8	5.3	3.3
175	105	475	28.4	1.7	11.4	44.6	50.7	4.7	3.6	5.9	4.3
176	105	485	30.6	2.1	12.1	51.7	48.3	0.0	3.2	2.2	3.9
177	105	495	24.4	2.3	11.6	59.1	40.9	0.0	2.6	3.5	3.3
178	105	505	27.1	1.9	7.7	46.3	37.9	15.8	3.6	8.0	4.2
179	106	5	72.0	6.3	4.9	33.1	62.2	4.7	4.4	7.4	5.8
180	106	15	66.5	6.1	4.2	59.0	41.0	0.0	2.7	2.1	3.4
181	106	25	64.8	5.9	4.9	32.1	67.9	0.0	4.6	6.8	6.7
182	106	35	65.0	6.5	4.0	40.6	59.4	0.0	3.6	4.4	4.8
183	106	45	65.1	6.5	3.9	44.5	53.4	2.1	3.5	5.2	4.4
184	106	55	65.7	6.1	4.3	49.2	50.8	0.0	3.1	3.4	4.1
185	106	65	63.4	5.7	4.9	49.5	50.5	0.0	2.8	4.2	4.1
186	106	75	62.9	5.4	5.1	51.3	48.7	0.0	3.0	2.9	3.9
187	106	85	64.4	6.0	4.3	48.6	51.4	0.0	3.2	4.3	4.1
188	106	95	63.6	5.8	5.0	46.5	53.5	0.0	3.3	4.7	4.2
189	106	105	62.6	5.9	4.8	56.1	43.9	0.0	2.9	2.5	3.7
190	106	115	60.7	5.5	5.3	48.9	51.1	0.0	3.2	2.8	4.1
191	106	125	58.4	5.0	6.7	43.6	56.4	0.0	3.4	4.0	4.4
192	106	135	57.1	4.7	6.8	38.8	52.1	9.1	3.9	7.4	4.8
193	106	145	57.9	4.8	6.9	44.9	55.1	0.0	3.4	3.9	4.3
194	106	155	52.2	3.7	7.4	45.7	54.3	0.0	3.4	3.1	4.3
195	106	165	42.5	2.4	8.9	35.3	64.8	0.0	4.0	4.5	5.2
196	106	175	39.9	2.2	8.0	40.6	59.4	0.0	3.6	3.6	4.7
197	106	185	46.0	3.6	7.9	41.8	48.8	9.4	3.8	8.9	5.4
198	106	195	45.9	3.8	8.9	60.7	32.1	7.3	2.7	6.5	3.2
199	106	205	43.3	3.9	10.0	61.4	38.6	0.0	2.4	3.4	3.0
200	106	215	38.7	2.1	13.6	56.6	43.4	0.0	2.9	2.6	3.7

SAMPLE			BULK COMPOSITION			TEXTURE					
Seq	Site	Depth	Moisture	Organic	Carbonate	Clay	Silt	Sand	Mean	St Dev	Median
no	ID	cm	%	%	%	%	%	%	um	um	um
201	106	225	44.0	3.0	10.5	46.4	53.6	0.0	3.2	2.9	4.2
202	106	235	46.6	3.7	8.5	45.8	54.2	0.0	3.3	3.7	4.3
203	106	245	44.6	4.2	9.4	43.0	57.0	0.0	3.3	2.8	4.4
204	106	255	40.3	3.7	12.1	50.4	49.6	0.0	3.3	2.6	4.0
205	106	265	39.4	3.7	12.9	50.1	46.8	3.1	3.3	4.5	4.0
206	106	275	42.5	4.1	11.0	54.3	45.7	0.0	3.0	2.1	3.8
207	106	285	38.5	3.3	14.6	54.2	43.1	2.7	3.1	3.6	3.8
208	106	295	40.1	3.5	12.3	56.9	43.1	0.0	2.9	1.9	3.7
209	106	305	40.3	3.4	12.0	78.5	21.5	0.0	2.1	2.5	2.3
210	106	315	32.1	2.6	15.9	49.1	47.2	3.7	3.6	5.8	4.1
211	106	325	41.6	4.4	11.3	63.6	36.4	0.0	2.6	1.7	3.3
212	106	335	38.8	3.9	11.3	52.4	47.7	0.0	3.1	2.9	3.9
213	106	345	36.4	3.6	13.9	51.9	29.5	18.6	3.2	9.1	3.8
214	106	355	35.1	3.5	13.8	50.0	48.2	1.9	3.5	5.2	4.0
215	106	365	37.3	3.7	14.2	79.6	20.4	0.0	1.9	1.6	2.0
216	106	375	37.2	3.5	12.5	62.7	37.3	0.0	2.6	3.3	3.2
217	106	385	39.7	3.9	12.3	59.3	40.7	0.0	2.8	3.0	3.5
218	106	395	36.2	3.3	12.0	43.0	48.8	8.2	3.7	6.9	4.4
219	106	405	39.0	3.6	11.3	67.4	28.0	4.5	2.4	3.7	2.9
220	106	415	29.2	2.2	14.2	41.7	58.3	0.0	3.7	2.8	4.4
221	106	425	42.7	4.2	10.2	48.7	33.5	17.8	3.4	9.1	4.1
222	106	435	44.8	4.7	9.5	64.4	32.3	3.3	2.4	4.5	2.9
223	106	445	42.4	3.8	10.5	60.5	39.5	0.0	2.8	3.6	3.4
224	106	455	42.5	4.1	11.8	51.6	37.0	11.4	3.2	7.4	3.9
225	106	465	41.8	3.6	11.0	77.4	22.6	0.0	2.1	1.8	2.6
226	106	475	44.6	4.9	8.5	41.5	50.1	8.4	3.3	7.6	6.0
227	106	485	42.7	4.8	8.1	71.8	28.2	0.0	2.2	2.2	2.7
228	106	495	44.2	4.5	8.2	58.4	41.7	0.0	2.6	2.7	3.5
229	106	505	41.1	4.1	9.4	46.1	45.1	8.8	3.0	7.9	5.2
230	106	515	43.8	4.7	7.5	60.8	39.2	0.0	2.6	4.2	3.2
231	106	525	42.0	4.4	8.8	61.5	38.5	0.0	2.6	3.1	3.3
232	106	535	39.7	3.8	9.5	70.0	30.0	0.0	2.2	1.8	2.7
233	106	545	46.3	5.6	7.1	62.1	37.9	0.0	2.3	2.7	2.9
234	106	555	46.1	5.6	7.1	80.1	19.9	0.0	1.7	2.2	1.8
235	106	565	46.2	4.8	7.1	72.1	27.9	0.0	2.1	2.3	2.4
236	106	575	45.6	5.1	6.6	88.7	11.3	0.0	1.7	1.2	1.9
237	106	585	46.3	5.2	5.5	71.9	28.1	0.0	2.1	3.4	2.4
238	106	595	44.7	5.1	8.4	82.1	18.0	0.0	1.9	1.7	2.1
239	106	605	45.2	5.5	6.2	35.1	64.9	0.0	4.0	6.2	6.0
240	106	615	45.0	5.1	6.4	64.2	30.6	5.2	2.4	4.7	2.9
241	106	625	43.9	4.8	6.8	71.7	28.3	0.0	2.4	1.7	3.0
242	106	635	43.3	4.6	7.4	64.6	35.4	0.0	2.4	3.3	3.0
243	106	645	43.4	4.8	7.0	66.7	33.3	0.0	2.4	4.0	2.8
244	106	655	43.4	4.5	6.8	69.1	30.9	0.0	2.3	3.3	2.7
245	106	665	43.5	4.4	7.7	54.1	38.2	7.7	2.9	6.3	3.7
246	106	675	44.1	3.9	6.9	65.3	34.7	0.0	2.5	2.9	3.1
247	106	685	43.1	3.6	9.0	69.5	30.5	0.0	2.3	1.9	2.9
248	106	695	44.3	3.9	7.4	69.5	30.5	0.0	2.3	3.2	2.8
249	107	5	70.1	7.6	2.5	43.5	56.5	0.0	3.5	4.1	4.4
250	107	15	71.0	7.6	2.5	43.1	56.9	0.0	3.5	3.6	4.4

SAMPLE			BULK COMPOSITION			TEXTURE					
Seq	Site	Depth	Moisture	Organic	Carbonate	Clay	Silt	Sand	Mean	St Dev	Median
no	ID	cm	%	%	%	%	%	%	um	um	um
251	107	25	68.2	7.2	2.5	41.2	58.8	0.0	3.7	3.7	4.6
252	107	35	68.4	7.0	2.3	40.5	59.5	0.0	3.7	4.5	4.6
253	107	45	67.3	6.2	2.6	35.2	64.8	0.0	4.2	6.7	5.2
254	107	55	66.7	5.9	3.1	42.9	51.9	5.2	3.6	4.4	4.4
255	107	65	66.6	6.2	2.8	39.9	56.7	3.4	3.8	4.4	4.8
256	107	75	66.8	7.0	2.5	34.9	65.1	0.0	4.1	5.4	5.2
257	107	85	67.5	5.6	3.0	23.5	71.5	5.0	5.7	7.9	9.3
258	107	95	65.3	5.7	2.9	51.9	48.1	0.0	3.2	3.8	3.9
259	107	105	63.1	5.7	3.4	37.8	60.5	1.7	3.8	3.4	4.8
260	107	115	64.3	6.3	3.1	44.3	55.7	0.0	3.4	2.8	4.3
261	107	125	61.9	6.0	3.4	42.2	57.8	0.0	3.6	2.9	4.4
262	107	135	63.9	5.6	2.6	36.0	64.0	0.0	4.0	4.2	5.0
263	107	145	62.2	5.7	3.4	53.0	47.0	0.0	3.1	2.3	3.9
264	107	155	58.8	4.7	3.2	43.1	56.9	0.0	3.5	3.3	4.4
265	107	165	53.1	4.2	3.4	37.1	62.9	0.0	3.9	3.7	4.9
266	107	175	58.3	4.5	4.5	39.2	60.8	0.0	3.9	4.9	4.6
267	107	185	54.1	3.7	4.9	31.2	65.8	3.0	4.4	5.7	5.3
268	107	195	47.3	3.3	5.9	37.7	59.6	2.7	4.2	10.2	5.0
269	107	205	45.5	3.3	6.4	48.8	29.6	21.6	3.3	2.8	4.1
270	107	215	44.8	3.2	6.8	43.9	56.1	0.0	3.5	5.2	4.3
271	107	225	43.7	3.3	6.3	39.9	55.3	4.8	3.8	4.7	4.6
272	107	235	43.0	3.9	6.1	38.9	59.2	1.9	3.8	5.5	4.7
273	107	245	46.3	4.3	6.0	49.7	44.4	6.0	3.2	4.9	4.0
274	107	255	44.2	4.0	5.7	42.6	52.1	5.3	3.7	6.7	4.5
275	107	265	43.5	4.9	5.4	56.3	36.7	7.0	2.9	1.9	3.7
276	107	275	42.0	4.2	6.1	54.4	45.6	0.0	3.1	3.8	3.8
277	107	285	45.2	4.4	5.2	45.7	54.3	0.0	3.6	7.1	4.3
278	107	295	43.3	5.1	5.1	52.6	38.6	8.8	3.2	5.6	3.9
279	107	305	44.2	5.2	5.0	58.3	36.6	5.2	2.8	2.1	3.6
280	107	315	43.5	5.0	5.4	47.0	53.0	0.0	3.4	5.7	4.2
281	107	325	45.8	5.7	4.6	47.0	47.7	5.2	3.5	4.9	4.2
282	107	335	44.8	4.7	4.5	42.6	55.4	2.0	3.8	8.4	4.5
283	107	345	44.8	4.8	4.4	51.5	35.7	12.8	3.2	5.2	3.9
284	107	355	43.3	5.1	5.3	49.5	46.0	4.5	3.1	2.1	4.0
285	107	365	43.0	4.8	5.2	46.6	53.4	0.0	3.3	2.7	4.2
286	107	375	42.5	4.5	5.2	42.2	57.8	0.0	3.6	3.5	4.4
287	107	385	43.7	6.0	5.0	49.0	51.0	0.0	3.3	3.9	4.1
288	107	395	44.9	5.7	3.9	53.8	46.2	0.0	3.1	3.2	3.8
289	107	405	42.4	5.6	4.9	45.9	54.1	0.0	3.4	2.7	4.3
290	107	415	43.3	4.9	5.5	51.9	48.1	0.0	3.2	5.9	3.9
291	107	425	41.4	4.9	7.2	44.8	49.5	5.7	3.4	4.7	4.3
292	107	435	44.5	4.3	5.3	49.8	46.4	3.8	3.2	2.6	4.0
293	107	445	40.6	3.4	6.9	53.1	46.9	0.0	3.0	2.3	3.8
294	107	455	42.3	3.7	6.8	57.5	42.5	0.0	2.9	2.6	3.6
295	107	465	42.4	4.3	6.0	42.7	57.4	0.0	3.6	4.0	4.4
296	107	475	42.0	3.1	6.9	36.2	63.9	0.0	4.0	4.0	4.9
297	107	485	40.8	4.3	6.2	45.3	54.7	0.0	3.4	2.9	4.3
298	107	495	40.7	3.4	7.3	41.8	58.2	0.0	3.6	3.7	4.5
299	107	505	41.5	3.0	7.4	48.4	51.7	0.0	3.3	4.4	4.1
300	107	515	39.7	3.4	7.6	41.2	57.0	1.9	3.6	2.6	4.6

SAMPLE			BULK COMPOSITION			TEXTURE					
Seq	Site	Depth	Moisture	Organic	Carbonate	Clay	Silt	Sand	Mean	St Dev	Median
no	ID	cm	%	%	%	%	%	%	um	um	um
301	107	525	39.8	3.8	7.3	36.8	63.2	0.0	3.9	3.2	4.9
302	107	535	42.9	3.5	6.9	38.5	61.5	0.0	3.9	8.0	4.8
303	107	545	39.6	3.5	7.4	44.0	45.1	10.9	3.4	2.6	4.4
304	107	555	40.2	3.6	7.4	37.9	62.1	0.0	3.9	5.8	4.8
305	107	565	42.1	4.3	6.7	45.0	48.7	6.3	3.5	4.4	4.3
306	107	575	41.0	3.8	6.8	51.3	46.4	2.3	3.0	2.2	3.9
307	107	585	38.5	3.2	7.6	45.7	54.3	0.0	3.5	5.3	4.3
308	107	595	39.1	3.6	7.2	44.5	53.5	2.1	3.5	5.1	4.4
309	107	605	42.5	4.5	6.6	39.7	58.4	1.9	3.6	2.9	4.6
310	107	615	39.4	3.2	7.6	47.3	52.7	0.0	3.3	2.6	4.2
311	107	625	41.5	2.9	7.3	41.7	58.3	0.0	3.7	5.7	4.5
312	107	635	40.8	3.6	7.5	49.7	47.0	3.3	3.2	2.6	4.0
313	107	645	39.7	3.6	7.5	44.5	55.6	0.0	3.7	9.0	4.4
314	107	655	38.8	3.1	7.3	52.1	31.9	16.0	3.0	2.1	3.9
315	107	665	39.7	3.5	7.9	50.7	49.3	0.0	3.1	3.2	4.0
316	107	675	39.1	2.9	8.3	45.8	54.2	0.0	3.2	2.2	4.2
317	107	685	38.5	2.9	8.2	57.9	42.2	0.0	2.8	2.0	3.6
318	107	695	39.1	2.3	8.2	52.9	47.1	0.0	3.1	3.6	3.9
319	110A	5	70.5	11.2	2.5	26.0	63.6	10.4	5.2	9.0	6.9
320	110A	15	69.7	10.1	2.4	26.6	65.4	8.1	5.2	8.4	6.9
321	110A	25	67.3	9.9	2.1	41.0	59.0	0.0	3.8	3.4	4.7
322	110A	35	67.6	9.6	2.6	37.4	62.6	0.0	3.8	3.1	4.8
323	110A	45	65.1	9.4	2.0	45.8	48.5	5.7	3.5	5.4	4.3
324	110A	55	61.2	8.9	2.8	39.8	58.2	2.0	3.8	5.1	4.7
325	110A	65	60.4	8.3	2.3	44.6	55.4	0.0	3.5	2.9	4.3
326	110A	75	59.6	7.4	2.6	51.4	48.6	0.0	2.9	2.8	3.9
327	110A	85	54.7	6.9	1.6	39.8	56.4	3.8	4.0	6.7	4.8
328	110A	95	53.6	6.6	1.6	27.3	67.7	5.1	5.1	7.5	6.8
329	110A	105	54.5	5.9	2.2	37.5	51.4	11.1	4.1	8.5	5.0
330	110A	115	57.9	5.8	3.2	47.7	52.3	0.0	3.3	4.1	4.1
331	110A	125	53.7	5.1	3.0	54.8	45.2	0.0	3.0	2.1	3.8
332	110A	135	56.5	6.4	2.8	41.7	50.0	8.3	3.8	7.1	4.5
333	110A	145	56.3	6.0	3.3	43.3	56.7	0.0	3.6	3.6	4.4
334	110A	155	55.2	6.3	3.0	49.0	51.0	0.0	3.4	4.0	4.1
335	110A	165	52.8	6.4	2.3	41.0	59.0	0.0	3.7	3.2	4.5
336	110A	175	40.2	6.3	2.7	39.5	60.5	0.0	3.9	4.0	4.7
337	110A	185	47.8	6.3	2.8	33.7	66.3	0.0	4.3	5.8	5.3
338	110A	195	48.8	6.1	3.5	40.7	59.3	0.0	3.8	4.6	4.5
339	110A	205	39.9	5.1	4.2	47.6	47.5	4.9	3.4	5.0	4.1
340	110A	215	30.6	5.4	3.7	63.5	36.5	0.0	2.4	2.1	3.1
341	110A	225	32.0	5.0	4.4	73.8	26.3	0.0	2.0	1.6	2.5
342	113A	5	70.8	10.5	2.1	17.5	82.5	0.0	6.6	7.9	11.0
343	113A	15	66.5	9.8	2.0	22.5	77.5	0.0	5.7	7.8	9.4
344	113A	25	64.3	9.7	2.1	24.4	65.9	9.7	5.7	10.2	10.3
345	113A	35	64.8	9.5	2.2	36.1	40.6	23.3	4.2	11.4	6.6
346	113A	45	63.0	9.4	2.0	23.3	66.9	9.7	5.9	10.5	12.3
347	113A	55	63.5	9.6	2.0	29.7	67.0	3.3	4.8	8.2	7.2
348	113A	65	55.9	8.6	2.1	29.1	67.8	3.1	4.7	7.2	6.0
349	113A	75	56.5	8.5	2.1	22.3	70.4	7.3	5.8	9.1	8.4
350	113A	85	58.5	8.5	2.2	28.0	65.5	6.5	5.0	8.6	6.6

SAMPLE			BULK COMPOSITION			TEXTURE					
Seq	Site	Depth	Moisture	Organic	Carbonate	Clay	Silt	Sand	Mean	St Dev	Median
no	ID	cm	%	%	%	%	%	%	um	um	um
351	113A	95	56.5	7.3	2.3	56.2	43.8	0.0	3.0	2.0	3.7
352	113A	105	55.8	6.8	2.5	27.8	69.0	3.2	5.0	8.0	7.6
353	113A	115	54.4	5.8	2.6	45.4	44.7	9.9	3.6	7.4	4.3
354	113A	125	54.5	5.7	2.9	44.6	55.4	0.0	3.5	4.4	4.3
355	113A	135	54.4	5.3	4.1	33.2	61.8	5.0	4.3	6.2	5.2
356	113A	145	52.5	4.9	6.2	34.1	51.1	14.8	4.4	9.7	5.1
357	113A	155	52.1	5.6	5.1	32.7	57.5	9.8	4.4	7.9	5.3
358	113A	165	50.2	6.1	5.3	40.8	56.2	3.1	3.7	4.4	4.5
359	113A	175	51.8	5.3	5.7	36.9	49.8	13.4	4.2	8.8	4.8
360	113A	185	51.1	5.6	4.9	39.9	60.2	0.0	3.7	2.7	4.5
361	113A	195	51.4	6.0	5.2	30.5	69.5	0.0	4.3	3.8	5.2
362	113A	205	49.7	5.2	6.5	39.2	53.3	7.5	4.0	7.9	4.7
363	115	5	77.1	10.3	3.0	37.8	38.1	24.1	4.2	11.2	5.3
364	115	15	74.8	9.5	3.5	43.3	56.7	0.0	3.5	4.9	4.5
365	115	25	72.9	9.0	3.2	46.8	53.2	0.0	3.4	3.4	4.2
366	115	35	71.6	9.1	2.8	47.5	52.5	0.0	3.2	3.9	4.2
367	115	45	71.1	8.9	3.2	63.8	36.2	0.0	2.6	1.8	3.3
368	115	55	70.0	8.2	3.6	53.5	46.5	0.0	3.1	2.6	3.8
369	115	65	68.5	8.1	3.6	61.9	38.1	0.0	2.8	2.6	3.4
370	115	75	69.5	8.7	3.4	52.3	40.3	7.4	3.2	6.1	3.9
371	115	85	68.0	8.1	3.4	55.1	44.9	0.0	2.9	2.2	3.8
372	115	95	67.1	8.8	2.9	58.3	41.7	0.0	2.8	3.5	3.6
373	115	105	66.4	8.2	3.6	37.1	62.9	0.0	4.1	5.7	5.1
374	115	115	66.2	8.2	3.4	47.5	49.9	2.6	3.3	4.3	4.2
375	115	125	64.4	8.4	3.0	43.8	48.2	8.0	3.7	7.1	4.5
376	115	135	62.4	8.0	3.5	56.1	43.9	0.0	2.8	2.4	3.6
377	115	145	62.4	7.8	4.0	62.1	37.9	0.0	2.7	3.0	3.4
378	115	155	62.2	7.5	3.8	47.3	42.1	10.6	3.5	7.6	4.2
379	115	165	62.0	7.0	3.9	45.0	55.0	0.0	3.6	4.6	4.3
380	115	175	61.2	6.8	4.4	56.4	43.6	0.0	2.9	3.1	3.6
381	115	185	59.7	7.1	4.2	66.2	33.8	0.0	2.6	2.1	3.2
382	115	195	58.6	6.1	4.4	48.5	45.4	6.1	3.4	6.0	4.1
383	115	205	57.1	5.7	4.9	66.2	33.8	0.0	2.6	1.7	3.2
384	115	215	46.7	3.9	4.1	53.7	46.3	0.0	3.1	2.8	3.8
385	115	225	54.7	5.5	5.1	73.9	26.1	0.0	2.2	2.1	2.7
386	115	235	48.0	4.7	5.2	58.0	42.0	0.0	2.8	2.5	3.6
387	115	245	69.2	5.0	4.6	57.0	43.0	0.0	2.8	3.2	3.5
388	115	255	39.7	4.4	3.7	57.0	43.0	0.0	2.8	3.2	3.5
389	115	265	48.2	5.8	4.7	34.7	59.9	5.4	4.1	5.7	4.9
390	120	5	75.5	9.9	3.8	28.6	71.4	0.0	4.6	4.5	5.8
391	120	15	70.6	9.2	4.0	33.1	66.9	0.0	4.2	4.6	5.2
392	120	25	70.2	8.6	3.6	36.3	61.9	1.8	4.1	5.5	5.2
393	120	35	69.0	7.6	3.4	28.3	66.5	5.3	4.7	7.1	5.8
394	120	45	64.2	8.0	3.5	20.5	77.3	2.2	5.9	7.5	7.8
395	120	55	57.2	6.0	4.5	37.3	62.7	0.0	3.8	4.2	5.0
396	120	65	59.3	7.2	4.7	13.7	83.6	2.8	8.0	11.4	18.8
397	120	75	61.5	7.7	3.8	17.9	82.1	0.0	6.1	6.7	8.9
398	120	85	59.4	5.3	5.5	31.3	61.7	7.1	4.5	7.4	5.4
399	120	95	57.6	6.7	5.0	31.9	65.7	2.5	4.4	5.7	5.3
400	120	105	59.5	6.3	4.9	46.1	53.9	0.0	3.2	2.6	4.2

SAMPLE			BULK COMPOSITION			TEXTURE					
Seq	Site	Depth	Moisture	Organic	Carbonate	Clay	Silt	Sand	Mean	St Dev	Median
no	ID	cm	%	%	%	%	%	%	um	um	um
401	120	115	59.5	7.8	4.3	34.6	59.9	5.5	4.1	6.1	5.0
402	120	125	57.3	7.1	5.2	23.5	76.5	0.0	5.1	5.0	6.4
403	120	135	54.8	5.5	5.8	32.1	64.1	3.8	4.3	5.9	5.4
404	120	145	49.0	5.3	7.7	28.9	71.1	0.0	4.7	7.1	6.4
405	120	155	53.6	7.4	5.5	27.9	71.0	1.1	4.7	5.3	6.0
406	120	165	48.8	4.8	7.8	32.7	58.6	8.8	4.4	8.4	6.3
407	120	175	51.7	6.2	7.2	34.1	65.9	0.0	4.0	4.0	5.0
408	120	185	49.6	5.4	7.9	32.8	67.2	0.0	4.3	5.8	5.9
409	120	195	32.5	3.0	3.0	56.2	41.3	2.6	2.9	4.0	3.6
410	120	205	30.2	3.8	2.8	54.7	45.3	0.0	2.9	4.2	3.7
411	120	215	29.1	3.2	3.2	70.1	29.9	0.0	2.3	1.9	2.8
412	120	225	27.9	3.4	3.1	59.1	40.9	0.0	2.5	3.3	3.2
413	120	235	28.6	3.9	2.6	47.9	46.5	5.6	3.4	6.2	4.1
414	120	245	28.3	4.8	2.1	47.8	52.2	0.0	3.2	3.7	4.1
415	120	255	29.3	4.9	2.8	55.5	39.0	5.5	2.8	4.4	3.6
416	120	265	29.2	5.4	2.5	53.7	46.4	0.0	3.0	2.5	3.8
417	120	275	32.5	5.5	3.8	60.5	35.0	4.5	2.4	4.4	3.1
418	120	285	34.0	5.8	4.1	53.3	43.5	3.2	2.8	4.0	3.8
419	120	295	33.4	4.9	3.9	56.2	43.8	0.0	2.7	3.2	3.6
420	120	305	32.9	5.2	4.2	39.9	41.1	19.0	3.8	9.3	4.8
421	120	315	34.6	8.7	2.8	55.9	44.1	0.0	2.6	2.3	3.5
422	120	325	32.3	6.5	5.5	50.9	40.3	8.9	3.4	7.6	4.0
423	120	335	30.1	7.9	4.6	56.2	43.8	0.0	3.0	2.3	3.7
424	120	345	27.5	7.1	4.8	43.4	47.7	8.9	3.8	7.4	4.4
425	121	5	75.3	8.9	2.9	41.4	58.6	0.0	3.8	3.6	4.5
426	121	15	74.1	10.4	2.6	39.2	59.3	1.5	3.9	4.6	4.7
427	121	25	75.5	9.7	2.7	30.9	60.8	8.3	4.9	9.1	6.7
428	121	35	74.3	7.9	2.8	50.9	49.1	0.0	3.2	4.7	4.0
429	121	45	75.6	9.4	3.1	64.8	35.2	0.0	2.6	2.1	3.2
430	121	55	75.4	9.7	3.1	67.4	26.1	6.5	2.5	4.7	3.0
431	121	65	74.7	8.9	2.9	51.0	46.4	2.7	3.2	5.2	4.0
432	121	75	72.5	8.6	3.3	44.1	55.9	0.0	3.5	2.7	4.3
433	121	85	72.1	7.9	2.5	46.9	43.5	9.6	3.6	7.4	4.2
434	121	95	72.1	7.9	2.6	43.9	42.5	13.6	3.7	8.0	4.4
435	121	105	71.9	9.1	2.7	52.4	42.9	4.7	3.2	5.4	3.9
436	121	115	70.5	9.0	2.5	51.3	48.7	0.0	3.2	2.4	3.9
437	121	125	69.7	8.8	2.6	52.5	47.6	0.0	3.1	4.1	3.8
438	121	135	69.6	9.1	2.4	65.1	34.9	0.0	2.6	2.1	3.2
439	121	145	69.3	7.3	2.7	53.4	38.1	8.5	3.1	6.0	3.8
440	121	155	68.8	8.5	2.6	42.6	57.5	0.0	3.8	4.6	4.4
441	121	165	69.6	7.4	2.7	48.6	51.4	0.0	3.3	3.5	4.1
442	121	175	69.2	8.9	2.6	50.7	49.3	0.0	3.2	2.5	4.0
443	121	185	68.2	6.2	3.4	37.2	54.6	8.2	4.2	7.4	4.9
444	121	195	67.5	7.5	3.6	48.9	40.2	11.0	3.4	7.5	4.1
445	121	205	66.0	5.7	4.2	45.6	49.5	5.0	3.6	5.7	4.3
446	121	215	66.5	8.3	3.1	52.5	41.3	6.2	3.2	6.1	3.9
447	121	225	63.6	6.6	3.1	46.0	54.0	0.0	3.5	3.0	4.2
448	121	235	60.1	5.3	4.2	39.4	58.2	2.4	4.0	5.5	4.7
449	121	245	61.0	7.7	3.3	50.6	49.5	0.0	3.2	2.3	4.0
450	121	255	62.4	7.6	3.3	46.7	44.9	8.3	3.6	7.7	4.3

SAMPLE			BULK COMPOSITION			TEXTURE					
Seq	Site	Depth	Moisture	Organic	Carbonate	Clay	Silt	Sand	Mean	St Dev	Median
no	ID	cm	%	%	%	%	%	%	um	um	um
451	121	265	61.8	6.0	3.2	62.0	38.0	0.0	2.8	2.1	3.4
452	121	275	60.9	8.0	2.7	47.9	48.1	4.0	3.4	4.8	4.1
453	121	285	60.1	7.9	3.1	34.9	58.4	6.8	4.3	7.1	5.0
454	121	295	60.0	6.2	3.2	47.4	52.6	0.0	3.5	4.4	4.2
455	121	305	60.5	6.4	3.2	45.4	48.2	6.4	3.6	6.2	4.3
456	121	315	62.4	7.9	3.1	54.9	45.2	0.0	3.1	2.5	3.8
457	121	325	59.8	7.9	2.9	52.6	47.4	0.0	3.2	2.6	3.9
458	121	335	57.4	6.4	3.9	38.6	54.4	7.0	3.9	6.0	4.6
459	121	345	56.6	6.2	4.1	63.2	36.8	0.0	2.7	1.9	3.4
460	121	355	57.2	7.5	3.9	43.3	56.7	0.0	3.6	3.3	4.4
461	121	365	57.0	7.5	3.9	45.8	45.6	8.7	3.6	6.8	4.2
462	121	375	56.2	6.3	4.4	58.1	41.9	0.0	2.9	3.4	3.6
463	121	385	52.1	5.9	4.9	55.1	44.9	0.0	2.9	3.2	3.7
464	121	395	54.5	7.4	4.4	45.8	54.2	0.0	3.5	2.9	4.2
465	121	405	53.0	5.7	5.5	31.4	68.6	0.0	4.5	5.4	5.3
466	121	415	53.9	6.2	4.8	37.8	55.7	6.5	4.1	7.1	4.8
467	121	425	53.1	6.1	5.5	44.4	52.6	3.0	3.6	5.2	4.3
468	121	435	50.4	5.2	6.5	40.3	59.7	0.0	3.8	5.3	4.6
469	121	445	50.9	4.1	6.8	39.6	51.6	8.8	3.9	7.7	4.8
470	121	455	49.8	4.3	7.3	43.9	48.7	7.5	3.7	6.3	4.4
471	121	465	48.6	4.4	7.1	31.9	62.5	5.6	4.5	7.5	5.4
472	121	475	37.1	6.3	6.2	41.2	47.7	11.1	3.8	8.8	5.8
473	121	485	31.5	5.1	8.9	49.1	50.9	0.0	3.2	4.3	4.1
474	121	495	35.6	7.4	6.4	42.1	54.7	3.2	3.8	5.8	4.5
475	121	505	38.1	7.4	5.4	57.5	42.5	0.0	2.9	2.3	3.7
476	121	515	40.2	7.6	5.5	36.9	57.8	5.3	4.2	7.4	5.3
477	121	525	37.8	6.5	5.8	42.2	47.3	10.6	3.8	7.4	4.4
478	121	535	38.5	6.3	6.8	33.1	56.6	10.3	4.5	8.4	5.3
479	121	545	38.4	5.9	7.7	46.4	53.6	0.0	3.4	2.7	4.2
480	122A	5	75.0	9.1	4.9	37.9	60.1	2.0	4.1	6.2	4.9
481	122A	15	71.7	8.4	4.2	30.9	63.1	6.1	4.6	7.6	5.6
482	122A	25	70.9	8.3	4.4	40.2	53.3	6.5	3.8	6.0	4.6
483	122A	35	72.1	6.5	5.1	42.0	54.8	3.1	3.7	5.4	4.4
484	122A	45	70.1	7.5	4.6	38.4	52.3	9.3	4.2	8.3	5.1
485	122A	55	70.1	7.9	3.3	48.9	46.7	4.4	3.3	4.9	4.1
486	122A	65	69.6	8.0	3.6	54.4	45.6	0.0	3.0	2.3	3.8
487	122A	75	68.9	8.7	3.2	38.3	61.8	0.0	3.9	3.8	4.7
488	122A	85	68.7	8.9	3.5	42.4	55.5	2.1	3.7	4.9	4.4
489	122A	95	66.8	7.5	3.7	35.8	56.6	7.6	4.3	7.7	5.0
490	122A	105	67.1	8.4	3.5	51.7	48.3	0.0	3.2	2.1	3.9
491	122A	115	65.6	10.4	2.9	44.0	48.6	7.4	3.6	5.9	4.4
492	122A	125	66.6	9.4	2.8	47.8	47.0	5.3	3.4	5.5	4.1
493	122A	135	65.2	9.1	3.5	46.3	53.8	0.0	3.5	2.7	4.2
494	122A	145	65.6	6.9	3.2	42.5	53.2	4.4	3.6	4.9	4.4
495	122A	155	65.1	8.1	3.1	47.3	51.4	1.4	3.4	3.9	4.1
496	122A	165	59.1	7.4	3.1	42.4	57.6	0.0	3.6	2.9	4.4
497	122A	175	60.6	7.2	3.9	63.2	36.8	0.0	2.3	4.0	2.9
498	122A	185	59.7	7.2	3.5	68.3	31.7	0.0	2.5	2.0	3.2
499	122A	195	61.1	7.6	3.6	53.8	46.2	0.0	3.2	2.9	3.8
500	122A	205	60.8	7.1	4.1	39.8	56.3	3.9	3.9	5.5	4.6

SAMPLE			BULK COMPOSITION			TEXTURE					
Seq	Site	Depth	Moisture	Organic	Carbonate	Clay	Silt	Sand	Mean	St Dev	Median
no	ID	cm	%	%	%	%	%	%	um	um	um
501	122A	215	58.8	6.7	4.1	44.2	52.3	3.5	3.6	6.5	4.5
502	122A	225	58.4	6.5	4.1	48.1	51.9	0.0	3.3	2.1	4.1
503	122A	235	59.7	6.8	3.9	49.1	50.9	0.0	3.2	2.3	4.0
504	122A	245	57.0	6.8	4.2	57.3	38.3	4.5	3.0	5.0	3.6
505	122A	255	56.7	6.4	3.6	38.1	54.2	7.7	4.0	6.9	4.8
506	122A	265	57.3	7.0	3.1	32.7	58.0	9.3	4.5	8.5	5.3
507	122A	275	55.9	7.0	4.1	51.6	45.9	2.5	3.2	4.8	3.9
508	122A	285	43.3	7.2	4.2	37.2	62.8	0.0	3.8	2.5	4.6
509	122A	295	55.1	6.2	4.5	49.5	41.3	9.2	3.2	5.9	4.0
510	122A	305	54.9	5.9	4.7	35.0	65.0	0.0	4.0	3.8	4.9
511	122A	315	51.1	7.5	6.1	40.0	60.0	0.0	3.7	3.7	4.7
512	122A	325	51.2	7.3	5.7	46.6	53.4	0.0	3.3	2.3	4.2
513	122A	335	52.8	6.3	4.9	55.9	44.1	0.0	2.9	2.5	3.7
514	122A	345	51.0	6.0	6.1	57.6	42.4	0.0	2.8	2.4	3.6
515	122A	355	51.0	7.2	6.3	35.9	64.1	0.0	3.9	2.9	4.9
516	122A	365	46.0	6.2	9.0	38.5	61.5	0.0	2.9	3.8	4.1
517	122A	375	45.6	6.1	9.4	37.7	62.3	0.0	3.8	2.7	4.6
518	122A	385	45.2	6.3	9.2	30.4	69.6	0.0	4.5	4.5	5.5
519	122A	395	39.0	4.7	11.2	36.4	63.6	0.0	3.7	2.6	4.8
520	122A	405	34.9	5.0	12.2	28.8	65.6	5.7	4.7	6.9	5.8
521	122A	415	39.0	3.8	11.8	33.7	56.3	10.0	4.3	8.1	5.1
522	122A	425	35.7	4.8	12.3	29.0	63.2	7.9	4.6	7.7	5.7
523	122A	435	31.6	7.1	6.5	42.0	58.0	0.0	3.7	4.4	4.5
524	122A	445	24.8	4.7	11.2	38.2	61.8	0.0	3.9	4.5	4.9
525	122A	455	24.3	3.5	12.3	33.2	64.7	2.2	4.3	6.0	5.4
526	122A	465	25.0	3.8	11.8	43.5	56.5	0.0	3.5	3.7	4.4
527	122A	475	30.2	5.7	6.4	40.8	52.1	7.1	3.6	6.4	4.6
528	1A	1	82.4	10.1	na	16.7	77.5	5.7	19.5	23.5	10.7
529	1A	2	78.5	7.7	na	14.6	83.0	2.4	20.1	19.2	14.7
530	1A	3	75.7	4.8	na	13.2	83.6	3.2	26.4	25.2	18.7
531	1A	4	73.3	7.7	na	12.2	80.4	7.4	23.6	28.1	15.0
532	1A	5	71.5	5.9	na	17.5	80.2	2.3	22.6	20.2	17.6
533	1A	6	69.2	6.1	na	25.1	74.9	0.0	13.0	13.1	7.0
534	1A	7	69.8	5.6	na	17.6	82.4	0.0	16.3	14.9	10.5
535	1A	8	69.2	5.3	na	15.3	79.2	5.5	20.4	24.8	12.0
536	1A	9	69.0	6.0	na	16.2	76.0	7.8	22.8	30.0	12.1
537	1A	10	67.9	6.4	na	21.9	70.4	7.7	17.3	26.2	7.5
538	1A	11	67.2	6.6	na	15.2	84.8	0.0	21.2	18.1	14.8
539	1A	12	65.5	6.3	na	26.5	65.3	8.2	20.2	32.6	6.4
540	1A	13	66.2	7.1	na	18.0	82.0	0.0	17.5	16.1	11.2
541	1A	14	67.6	6.8	na	14.3	85.8	0.0	21.0	16.2	16.5
542	1A	15	67.8	7.9	na	18.1	71.9	10.0	27.2	29.5	14.9
543	1A	16	68.7	7.8	na	27.5	72.5	0.0	13.8	14.7	6.5
544	1A	17	68.4	7.3	na	20.0	68.3	11.7	23.6	28.8	10.6
545	1A	18	68.2	7.6	na	21.1	78.9	0.0	15.3	13.3	10.0
546	1A	19	69.3	8.0	na	31.2	64.8	3.9	13.6	19.9	5.6
547	1A	20	70.1	7.1	na	35.9	55.9	8.3	17.9	26.9	5.5
548	1A	21	68.6	7.5	na	28.6	65.9	5.5	19.4	26.9	6.4
549	1A	22	69.0	7.0	na	28.0	61.9	10.1	20.2	31.9	6.4
550	1A	23	69.3	8.0	na	33.6	64.4	2.0	12.7	16.9	5.4

SAMPLE			BULK COMPOSITION			TEXTURE					
Seq	Site	Depth	Moisture	Organic	Carbonate	Clay	Silt	Sand	Mean	St Dev	Median
no	ID	cm	%	%	%	%	%	%	um	um	um
551	1A	24	69.2	7.8	na	24.1	70.3	5.6	21.2	25.5	8.6
552	1A	25	67.5	8.0	na	31.4	66.7	2.0	11.5	15.3	5.8
553	1A	26	68.1	7.9	na	31.8	68.2	0.0	10.9	13.6	5.5
554	1A	27	69.2	7.8	na	36.9	63.1	0.0	6.7	5.2	4.8
555	1A	28	69.0	8.3	na	43.1	56.9	0.0	6.5	7.3	4.4
556	1A	29	69.7	7.6	na	39.2	56.8	4.1	14.8	28.7	4.8
557	1A	30	68.7	7.5	na	50.1	49.9	0.0	4.4	2.5	4.0
558	1A	31	69.0	7.4	na	38.6	61.4	0.0	7.3	7.0	4.8
559	1A	32	68.5	6.7	na	29.7	68.9	1.4	12.3	14.8	6.0
560	1A	33	68.0	6.4	na	29.1	69.0	1.9	13.6	16.9	6.2
561	1A	34	68.5	6.1	na	35.0	65.0	0.0	9.4	11.7	5.0
562	1A	35	67.5	7.2	na	39.8	60.3	0.0	6.7	5.6	4.7
563	1A	36	70.0	7.2	na	30.2	57.5	12.3	24.8	38.2	6.3
564	1A	37	70.5	7.7	na	31.6	68.4	0.0	9.6	11.1	5.5
565	1A	38	70.0	8.1	na	38.2	61.8	0.0	7.5	7.1	4.8
566	1A	39	68.6	7.3	na	30.9	59.9	9.2	20.8	33.7	5.9
567	1A	40	68.7	7.8	na	31.5	68.5	0.0	10.0	10.0	5.7
568	1A	41	67.3	7.0	na	45.9	54.1	0.0	5.5	4.5	4.2
569	1A	42	65.8	7.4	na	44.8	55.2	0.0	6.2	6.1	4.3
570	2A	1	86.1	10.6	na	49.7	50.3	0.0	6.9	8.0	4.0
571	2A	2	82.3	8.5	na	61.6	38.4	0.0	3.9	2.5	3.4
572	2A	3	83.0	9.6	na	17.0	83.0	0.0	23.9	19.0	19.9
573	2A	4	82.9	9.9	na	16.5	83.5	0.0	22.3	17.8	18.1
574	2A	5	82.5	8.9	na	25.3	69.7	5.0	16.9	24.8	6.9
575	2A	6	83.0	10.1	na	24.4	66.7	9.0	21.1	30.6	7.8
576	2A	7	83.4	10.0	na	26.0	74.0	0.0	12.7	11.3	7.6
577	2A	8	82.5	9.7	na	32.7	67.3	0.0	10.7	11.3	5.6
578	2A	9	81.0	9.1	na	42.1	54.6	3.4	13.6	18.5	4.8
579	2A	10	81.5	9.3	na	30.3	66.1	3.5	11.4	15.5	5.7
580	2A	11	79.3	8.8	na	32.1	60.0	7.9	16.8	29.6	5.7
581	2A	12	78.4	8.3	na	48.0	48.8	3.2	10.3	16.7	4.1
582	2A	13	77.7	8.0	na	49.2	50.9	0.0	5.8	8.0	4.1
583	2A	14	76.1	6.8	na	33.6	38.9	27.5	44.8	54.6	16.6
584	2A	15	74.1	7.5	na	38.0	44.7	17.4	31.1	37.6	11.2
585	2A	16	74.8	7.9	na	46.4	51.8	1.8	10.8	17.4	4.2
586	2A	17	74.3	6.8	na	52.3	47.7	0.0	4.7	3.3	3.9
587	2A	18	72.6	6.9	na	46.0	54.0	0.0	5.4	4.4	4.2
588	2A	19	74.0	7.8	na	53.5	46.5	0.0	4.5	3.0	3.8
589	2A	20	73.4	7.4	na	37.0	60.0	3.0	12.2	20.9	5.0
590	2A	21	73.8	7.3	na	34.4	54.3	11.4	22.0	32.1	5.3
591	2A	22	73.2	7.7	na	42.0	58.0	0.0	8.1	11.2	4.5
592	2A	23	73.0	8.0	na	39.9	60.1	0.0	9.3	12.1	4.7
593	2A	24	73.5	7.7	na	47.5	52.5	0.0	5.6	4.8	4.1
594	2A	25	73.5	7.7	na	44.5	55.6	0.0	6.8	8.0	4.3
595	2A	26	74.0	8.2	na	52.7	47.3	0.0	6.7	9.0	3.8
596	2A	27	74.3	8.0	na	51.6	48.4	0.0	5.1	4.9	3.9
597	2A	28	74.8	7.5	na	27.8	69.5	2.7	13.9	18.5	6.5
598	2A	29	74.9	8.6	na	46.0	54.0	0.0	4.7	2.7	4.2
599	2A	30	74.5	8.1	na	50.1	49.9	0.0	6.1	7.0	4.0
600	2A	31	72.4	8.2	na	61.7	38.3	0.0	5.6	7.0	3.3

SAMPLE			BULK COMPOSITION			TEXTURE					
Seq	Site	Depth	Moisture	Organic	Carbonate	Clay	Silt	Sand	Mean	St Dev	Median
no	ID	cm	%	%	%	%	%	%	um	um	um
601	2A	32	73.1	7.8	na	54.6	45.4	0.0	4.6	3.6	3.7
602	2A	33	72.4	7.9	na	40.2	59.8	0.0	7.0	6.3	4.6
603	2A	34	73.4	7.4	na	36.2	58.4	5.4	16.8	24.7	5.2
604	2A	35	72.2	8.2	na	51.1	48.9	0.0	5.4	4.5	3.9
605	2A	36	72.9	8.3	na	69.5	30.5	0.0	4.8	5.6	2.9
606	2A	38	74.1	8.7	na	57.2	42.8	0.0	7.2	8.8	3.5
607	2A	39	72.2	8.5	na	68.3	31.7	0.0	4.2	3.9	2.9
608	2A	40	72.8	7.7	na	69.2	30.8	0.0	4.4	4.6	2.8
609	2A	41	71.9	7.2	na	62.3	37.7	0.0	4.5	3.7	3.3
610	2A	42	69.3	7.2	na	43.0	57.0	0.0	8.6	13.2	4.5
611	3A	1	88.9	11.4	na	12.3	83.8	3.9	22.8	19.9	17.0
612	3A	2	86.4	11.0	na	15.1	84.9	0.0	18.3	13.3	17.0
613	3A	3	81.8	9.9	na	17.7	82.3	0.0	16.6	13.1	14.4
614	3A	4	83.4	8.6	na	15.5	84.5	0.0	24.6	18.7	21.9
615	3A	5	77.9	8.6	na	19.6	80.4	0.0	15.1	13.1	10.6
616	3A	6	76.8	7.5	na	12.6	80.5	6.9	27.3	21.0	23.5
617	3A	7	76.2	7.3	na	8.7	87.4	3.9	28.9	19.4	27.0
618	3A	8	75.8	7.8	na	11.9	85.3	2.9	29.5	21.6	26.0
619	3A	9	74.7	7.8	na	8.8	83.4	7.7	35.6	21.1	34.5
620	3A	10	75.8	8.0	na	31.5	68.6	0.0	11.7	12.3	6.5
621	3A	11	75.1	7.8	na	26.5	73.5	0.0	16.9	17.4	7.9
622	3A	12	74.7	7.7	na	24.8	64.3	10.9	28.4	36.4	10.3
623	3A	13	76.0	7.8	na	8.7	84.0	7.3	33.5	22.4	31.3
624	3A	14	75.2	8.0	na	50.4	49.6	0.0	4.8	3.6	4.0
625	3A	15	74.6	8.5	na	54.4	39.1	6.5	13.5	27.2	3.8
626	3A	16	74.0	7.9	na	16.2	83.8	0.0	19.3	15.3	15.7
627	3A	17	75.1	8.0	na	25.1	74.9	0.0	12.9	12.0	7.3
628	3A	18	76.1	7.8	na	28.2	71.8	0.0	9.9	8.2	6.4
629	3A	19	74.2	7.3	na	32.7	67.3	0.0	9.1	8.9	5.4
630	3A	20	73.1	8.5	na	38.2	61.8	0.0	11.6	14.4	4.9
631	3A	21	73.7	8.1	na	37.8	62.2	0.0	10.6	10.4	5.5
632	3A	22	70.7	8.3	na	35.5	64.5	0.0	14.1	15.5	6.4
633	3A	23	73.5	6.8	na	28.4	69.6	2.0	13.9	15.5	7.2
634	3A	24	75.5	6.1	na	28.7	71.3	0.0	10.7	9.6	6.3
635	3A	25	75.3	8.5	na	31.4	68.6	0.0	9.8	9.1	5.8
636	3A	26	74.1	7.9	na	32.6	67.4	0.0	13.7	15.1	6.6
637	3A	27	74.6	7.2	na	42.0	58.0	0.0	6.9	6.9	4.5
638	3A	28	74.5	8.2	na	20.8	79.2	0.0	15.2	14.7	10.0
639	3A	29	74.5	8.0	na	33.0	63.3	3.7	14.6	28.2	5.5
640	3A	30	75.1	8.7	na	31.8	66.2	2.1	12.2	15.4	5.7
641	3A	31	74.9	7.2	na	31.6	63.3	5.2	14.5	22.7	5.6
642	3A	32	74.9	8.4	na	34.7	63.2	2.0	10.1	13.6	5.2
643	3A	33	75.5	7.7	na	42.7	57.3	0.0	8.1	9.7	4.5
644	3A	34	74.1	7.3	na	47.8	52.2	0.0	6.2	6.2	4.1
645	3A	35	73.6	7.6	na	52.2	47.8	0.0	4.5	3.0	3.9
646	3A	36	73.3	7.5	na	56.2	43.9	0.0	4.8	3.9	3.7
647	3A	37	72.1	7.2	na	34.5	65.5	0.0	9.7	10.4	5.2
648	3A	38	72.8	7.3	na	36.8	63.2	0.0	8.2	7.5	5.0
649	3A	39	74.9	6.9	na	36.5	63.5	0.0	7.6	6.9	5.0
650	3A	40	72.3	7.8	na	38.1	61.9	0.0	9.3	10.2	4.9

SAMPLE			BULK COMPOSITION			TEXTURE					
Seq	Site	Depth	Moisture	Organic	Carbonate	Clay	Silt	Sand	Mean	St Dev	Median
no	ID	cm	%	%	%	%	%	%	um	um	um
651	3A	41	73.4	7.5	na	30.7	69.4	0.0	13.3	14.2	6.2
652	3A	42	71.6	7.9	na	31.6	66.1	2.3	13.9	17.1	5.9
653	3A	43	71.8	7.0	na	36.9	60.2	3.0	11.4	20.3	5.0
654	3A	44	73.1	7.6	na	46.1	48.5	5.4	12.6	24.2	4.3
655	3A	45	72.6	7.3	na	31.3	68.7	0.0	11.1	11.4	5.9
656	4A	1	73.7	10.1	na	15.5	79.7	4.8	19.9	21.4	11.5
657	4A	2	65.9	9.8	na	15.6	77.7	6.8	23.9	31.3	11.8
658	4A	3	63.3	9.8	na	12.7	75.5	11.9	29.1	29.6	17.5
659	4A	4	70.9	11.2	na	24.3	71.6	4.1	15.9	19.2	7.2
660	4A	5	69.3	10.9	na	17.2	73.7	9.2	27.7	31.6	17.1
661	4A	6	71.6	11.5	na	17.7	79.8	2.5	21.5	19.7	14.3
662	4A	7	70.0	11.8	na	16.7	74.3	9.1	27.8	26.4	20.2
663	4A	8	70.4	11.1	na	20.1	76.1	3.8	19.6	20.2	11.5
664	4A	9	69.9	11.2	na	24.4	67.0	8.6	23.4	26.2	10.9
665	4A	10	69.3	11.4	na	20.5	62.6	16.9	34.0	40.8	16.6
666	4A	11	66.7	10.9	na	29.3	58.8	11.9	27.8	38.1	7.5
667	4A	12	68.8	11.4	na	21.0	74.6	4.5	21.9	21.0	12.8
668	4A	13	67.7	10.0	na	24.1	75.9	0.0	19.9	19.9	10.3
669	4A	14	67.7	9.2	na	26.4	73.6	0.0	13.9	14.1	7.2
670	4A	15	69.0	9.2	na	31.4	67.6	1.0	12.9	14.6	6.0
671	4A	16	67.7	8.9	na	31.7	68.3	0.0	13.4	15.7	5.9
672	4A	17	66.8	10.2	na	27.2	72.8	0.0	14.1	14.2	6.8
673	4A	18	67.9	10.4	na	35.2	64.8	0.0	9.4	10.2	5.0
674	4A	19	69.0	9.9	na	53.9	46.1	0.0	5.2	4.5	3.8
675	4A	20	68.5	9.4	na	23.2	47.4	29.4	44.3	51.1	12.7
676	4A	21	66.7	8.1	na	24.2	71.1	4.7	18.0	23.9	7.1
677	4A	22	68.4	9.2	na	33.3	61.0	5.7	14.0	20.3	5.4
678	4A	23	67.7	9.2	na	36.1	58.3	5.6	18.0	25.5	5.4
679	4A	24	67.7	9.2	na	48.9	51.1	0.0	6.8	10.3	4.1
680	4A	25	66.7	8.4	na	48.9	51.1	0.0	5.2	4.0	4.1
681	4A	26	65.9	8.7	na	41.7	58.3	0.0	10.9	12.6	4.8
682	4A	27	66.6	9.5	na	32.6	62.6	4.9	20.1	31.7	5.7
683	4A	28	65.9	9.5	na	32.3	55.6	12.1	25.3	36.0	6.6
684	4A	29	66.2	9.8	na	43.2	56.8	0.0	6.1	5.0	4.3
685	4A	30	66.5	8.8	na	52.8	47.2	0.0	4.7	3.4	3.9
686	4A	31	65.7	9.1	na	27.8	65.2	7.0	18.3	25.4	6.4
687	4A	32	66.6	9.9	na	52.3	47.7	0.0	4.3	2.5	3.9
688	4A	33	66.7	8.4	na	47.5	52.5	0.0	5.3	3.9	4.2
689	4A	34	65.5	8.6	na	37.1	61.3	1.6	13.4	18.5	5.0
690	4A	35	63.8	7.0	na	33.9	66.1	0.0	9.6	10.5	5.4
691	4A	36	66.5	8.2	na	43.1	56.9	0.0	8.5	12.0	4.4
692	4A	37	65.2	8.2	na	45.9	54.2	0.0	4.8	3.0	4.2
693	4A	38	66.7	9.1	na	34.5	58.4	7.2	14.9	26.1	5.2
694	4A	39	59.6	7.0	na	36.1	61.8	2.1	14.2	20.0	5.0
695	4A	40	63.1	8.0	na	40.5	59.5	0.0	8.8	10.3	4.6
696	4A	41	65.0	8.3	na	38.6	61.4	0.0	8.7	10.3	4.7
697	4A	42	63.9	8.4	na	54.5	40.6	4.9	10.9	19.2	3.7
698	4A	43	63.6	7.6	na	46.0	54.0	0.0	7.5	9.8	4.2
699	5A	1	86.8	11.9	na	24.7	64.2	11.2	24.3	38.6	6.9
700	5A	2	73.9	10.2	na	16.3	76.6	7.1	23.5	30.0	12.1

SAMPLE			BULK COMPOSITION			TEXTURE					
Seq	Site	Depth	Moisture	Organic	Carbonate	Clay	Silt	Sand	Mean	St Dev	Median
no	ID	cm	%	%	%	%	%	%	um	um	um
701	5A	3	75.7	9.5	na	23.9	70.2	6.0	19.8	27.5	7.4
702	5A	4	64.5	9.7	na	29.1	67.9	3.0	13.3	18.2	5.8
703	5A	5	64.9	8.9	na	29.9	68.6	1.5	15.1	17.2	6.2
704	5A	6	66.3	9.0	na	25.9	55.8	18.3	36.7	46.4	12.2
705	5A	7	66.1	9.2	na	28.8	67.5	3.8	14.3	20.4	6.0
706	5A	8	67.0	10.5	na	21.6	78.4	0.0	14.1	13.4	8.2
707	5A	9	66.6	10.2	na	26.9	65.4	7.7	21.6	25.8	8.6
708	5A	10	65.9	10.0	na	19.7	74.3	6.1	25.3	22.4	19.9
709	5A	11	66.1	10.4	na	18.3	81.7	0.0	15.4	14.2	9.9
710	5A	12	67.0	10.2	na	17.7	82.3	0.0	19.3	17.2	13.6
711	5A	13	64.3	10.3	na	29.2	68.1	2.7	14.2	22.7	6.1
712	5A	14	64.1	10.1	na	44.4	50.4	5.3	13.1	24.9	4.4
713	5A	15	63.1	9.2	na	17.2	78.1	4.7	26.4	22.0	20.7
714	5A	16	63.2	8.6	na	19.0	73.4	7.6	22.2	31.7	9.7
715	5A	17	61.1	9.5	na	15.4	84.7	0.0	17.6	14.6	13.0
716	5A	18	60.3	9.0	na	17.5	72.3	10.2	25.8	27.7	14.3
717	5A	19	59.0	9.8	na	12.8	83.6	3.5	23.5	21.1	15.5
718	5A	20	61.5	10.4	na	20.1	71.0	8.9	20.9	28.0	9.2
719	5A	21	64.1	9.3	na	32.7	67.4	0.0	6.9	5.0	5.0
720	5A	22	65.0	9.9	na	18.0	73.2	8.8	24.3	25.5	12.3
721	5A	23	61.8	9.3	na	15.4	79.4	5.3	22.3	21.8	13.6
722	5A	24	63.0	9.3	na	15.2	82.7	2.1	19.8	17.1	15.3
723	5A	25	64.4	10.0	na	20.5	69.7	9.8	23.6	26.7	11.0
724	5A	26	67.0	10.6	na	25.2	72.8	2.0	16.1	18.4	6.7
725	5A	27	65.1	9.9	na	24.6	69.7	5.7	16.3	20.4	6.8
726	5A	28	63.3	10.7	na	24.6	68.7	6.7	22.0	31.2	7.8
727	5A	29	63.5	10.6	na	21.9	73.4	4.6	20.1	26.9	8.7
728	5A	30	66.3	10.0	na	28.3	65.4	6.3	15.8	21.8	6.2
729	5A	31	65.4	9.5	na	22.6	74.7	2.7	16.7	21.8	7.7
730	5A	32	65.0	10.6	na	24.1	73.6	2.3	16.5	20.0	7.1
731	5A	33	65.6	10.0	na	19.9	72.5	7.6	21.9	27.2	10.6
732	5A	34	64.4	9.2	na	21.1	63.8	15.1	33.8	42.9	12.5
733	5A	35	64.8	9.0	na	27.8	72.2	0.0	12.4	13.7	6.0
734	5A	36	64.5	9.0	na	38.4	61.6	0.0	5.7	4.0	4.7
735	5A	37	65.4	9.1	na	39.1	60.9	0.0	6.0	4.4	4.7
736	5A	38	65.3	9.7	na	27.1	67.1	5.8	18.0	24.1	6.7
737	5A	39	65.0	9.3	na	24.7	71.6	3.7	17.4	19.5	7.4
738	5A	40	63.0	9.5	na	28.9	62.9	8.2	21.7	33.6	6.3
739	6A	1	84.7	11.7	na	41.8	58.2	0.0	6.6	6.4	4.5
740	6A	2	81.7	11.2	na	40.6	59.4	0.0	6.7	7.5	4.6
741	6A	3	79.5	10.8	na	38.5	61.5	0.0	8.4	8.3	4.8
742	6A	4	79.8	10.8	na	36.8	61.0	2.3	11.4	17.0	5.0
743	6A	5	78.5	9.6	na	30.7	69.3	0.0	14.9	16.2	6.2
744	6A	6	77.7	9.9	na	39.6	56.4	4.0	11.8	24.8	4.7
745	6A	7	76.6	10.1	na	41.2	53.0	5.9	13.0	23.8	4.6
746	6A	8	77.4	10.0	na	38.3	61.7	0.0	9.9	12.1	4.9
747	6A	9	75.9	11.0	na	45.9	51.9	2.2	9.0	14.5	4.3
748	6A	10	76.9	10.9	na	40.2	59.8	0.0	7.9	7.7	4.7
749	6A	11	76.5	10.4	na	36.2	62.3	1.5	10.3	14.7	4.9
750	6A	12	75.6	9.9	na	46.0	54.0	0.0	5.7	4.7	4.3

SAMPLE			BULK COMPOSITION			TEXTURE					
Seq	Site	Depth	Moisture	Organic	Carbonate	Clay	Silt	Sand	Mean	St Dev	Median
no	ID	cm	%	%	%	%	%	%	um	um	um
751	6A	13	76.1	11.1	na	35.1	56.9	7.9	18.0	25.4	5.3
752	6A	14	75.3	10.6	na	37.2	54.8	8.0	18.0	32.7	4.9
753	6A	15	73.9	10.3	na	39.7	54.3	6.0	13.6	20.5	4.8
754	6A	16	75.0	10.0	na	48.3	51.7	0.0	5.1	4.2	4.1
755	6A	17	75.8	10.1	na	43.5	50.9	5.6	13.7	25.3	4.5
756	6A	18	72.6	10.8	na	37.4	60.9	1.6	10.3	14.4	4.9
757	6A	19	72.3	9.8	na	41.8	56.1	2.1	10.5	16.7	4.5
758	6A	20	72.9	10.7	na	50.0	50.1	0.0	4.6	3.1	4.0
759	6A	21	73.5	8.0	na	38.1	55.8	6.1	14.5	22.6	4.9
760	6A	22	75.6	9.6	na	27.0	65.0	7.9	19.2	26.2	7.4
761	6A	23	74.6	9.8	na	28.2	63.1	8.7	23.8	36.2	6.6
762	6A	24	73.0	9.8	na	39.4	60.6	0.0	7.4	7.1	4.7
763	6A	25	72.8	10.0	na	24.0	76.0	0.0	20.7	19.8	10.6
764	6A	26	74.6	9.8	na	35.3	64.7	0.0	7.2	5.9	5.0
765	6A	27	73.0	8.6	na	42.8	52.2	5.0	12.6	25.2	4.4
766	6A	28	72.4	9.3	na	39.6	54.0	6.4	15.5	28.9	4.7
767	6A	29	73.4	9.2	na	51.5	48.5	0.0	6.8	7.5	3.9
768	6A	30	72.8	9.2	na	43.6	56.4	0.0	6.5	6.9	4.3
769	6A	31	72.6	9.9	na	46.6	53.4	0.0	4.7	2.8	4.2
770	6A	32	70.5	9.3	na	54.9	45.1	0.0	5.4	6.0	3.8
771	6A	33	72.6	9.1	na	38.4	59.5	2.1	10.9	16.1	4.7
772	6A	34	70.7	9.6	na	62.8	37.2	0.0	4.2	3.4	3.5
773	6A	35	72.2	9.9	na	59.5	40.5	0.0	4.9	4.5	3.4
774	6A	36	71.1	7.5	na	38.2	61.8	0.0	6.9	5.9	4.7
775	6A	37	71.1	8.9	na	35.0	58.0	7.0	17.1	34.1	5.1
776	6A	38	69.8	8.0	na	48.0	52.0	0.0	5.4	4.5	4.1
777	6A	39	71.3	9.5	na	49.0	51.0	0.0	7.7	10.4	4.1
778	6A	40	70.8	8.8	na	35.6	64.4	0.0	9.2	9.4	5.0
779	6A	41	69.6	7.3	na	59.0	41.0	0.0	4.6	3.9	3.5
780	7A	1	82.2	9.3	5.3	20.5	61.3	18.2	6.4	12.6	11.3
781	7A	2	80.5	9.5	4.5	32.2	67.9	0.0	4.4	4.8	5.4
782	7A	3	79.3	9.8	4.3	29.2	70.8	0.0	4.7	5.4	5.8
783	7A	4	78.8	16.7	8.8	39.2	56.5	4.3	3.9	6.1	4.8
784	7A	5	78.2	8.6	5.5	47.1	52.9	0.0	3.3	2.4	4.2
785	7A	6	76.5	10.5	3.8	35.2	61.4	3.4	4.1	5.2	4.9
786	7A	7	75.4	8.5	5.5	38.7	55.5	5.8	3.9	6.1	4.7
787	7A	8	73.9	9.2	4.8	33.7	62.6	3.8	4.4	6.9	5.3
788	7A	9	74.9	9.8	4.4	36.8	63.2	0.0	4.1	5.2	4.9
789	7A	10	73.7	9.8	4.3	31.8	62.4	5.9	4.6	7.4	5.6
790	7A	11	75.7	10.3	3.7	38.8	54.6	6.6	3.9	6.5	4.7
791	7A	12	72.8	10.2	3.8	44.4	55.6	0.0	3.6	3.0	4.4
792	7A	13	74.9	9.8	4.0	39.0	61.0	0.0	3.7	3.0	4.5
793	7A	14	73.2	9.7	4.2	35.2	62.3	2.5	4.2	5.7	5.0
794	7A	15	71.6	10.3	3.5	36.5	63.5	0.0	3.9	3.3	4.9
795	7A	16	72.0	9.9	3.6	34.3	65.7	0.0	4.3	5.1	5.4
796	7A	17	71.4	9.5	4.1	34.4	60.1	5.6	4.3	6.9	5.2
797	7A	18	73.7	9.6	3.9	33.8	48.1	18.1	4.5	10.7	5.5
798	7A	19	73.7	9.9	3.8	53.4	46.6	0.0	3.1	2.6	3.8
799	7A	20	74.4	9.2	4.2	30.8	58.6	10.6	4.8	9.1	6.0
800	7A	21	74.4	8.7	4.6	33.7	61.5	4.9	4.3	7.0	5.2

SAMPLE			BULK COMPOSITION			TEXTURE					
Seq	Site	Depth	Moisture	Organic	Carbonate	Clay	Silt	Sand	Mean	St Dev	Median
no	ID	cm	%	%	%	%	%	%	um	um	um
801	7A	22	72.9	8.6	4.4	36.5	59.6	3.9	4.1	5.8	4.9
802	7A	23	73.2	9.1	4.0	40.7	49.7	9.7	3.9	7.5	4.6
803	7A	24	71.7	8.7	4.3	42.2	57.8	0.0	3.6	2.7	4.5
804	7A	25	72.2	9.0	4.3	31.2	63.1	5.7	4.6	7.1	5.5
805	7A	26	71.7	8.6	4.4	37.6	62.4	0.0	4.0	3.7	4.8
806	7A	27	73.7	8.9	3.9	35.1	62.1	2.8	4.2	5.1	5.0
807	7A	28	73.0	9.3	3.6	39.1	60.9	0.0	3.9	3.0	4.6
808	7A	29	72.3	9.1	3.9	31.6	62.6	5.8	4.5	6.6	5.4
809	7A	30	73.0	9.0	4.0	35.9	57.4	6.8	4.1	6.6	4.9
810	7A	31	71.7	9.2	3.6	42.8	57.2	0.0	3.6	2.6	4.4
811	7A	32	71.4	9.2	3.5	41.1	50.5	8.4	3.8	7.0	4.5
812	7A	33	70.4	9.0	3.8	40.3	59.7	0.0	3.7	3.1	4.5
813	7A	34	71.4	9.0	3.9	47.3	52.7	0.0	3.4	3.3	4.1
814	7A	35	71.2	9.1	3.7	40.3	58.0	1.6	3.8	4.8	4.5
815	7A	36	72.3	9.4	3.6	46.3	53.7	0.0	3.4	2.5	4.2
816	7A	37	71.4	8.6	4.0	53.5	43.1	3.4	3.2	4.6	3.8
817	7A	38	70.2	10.0	4.9	54.0	46.0	0.0	3.1	2.3	3.8
818	8A	1	na	10.7	4.6	42.4	57.6	0.0	3.6	3.9	4.5
819	8A	2	na	10.8	4.0	46.1	53.9	0.0	3.4	2.3	4.2
820	8A	3	na	8.8	5.7	41.8	54.5	3.7	3.8	5.6	4.5
821	8A	4	na	8.8	5.4	34.1	61.6	4.3	4.4	6.8	5.3
822	8A	5	na	9.1	5.0	37.2	55.7	7.2	4.2	7.7	5.0
823	8A	6	na	9.3	4.7	34.7	65.4	0.0	4.3	6.3	5.3
824	8A	7	na	9.3	4.7	36.3	63.7	0.0	4.1	4.8	5.1
825	8A	8	na	10.6	3.5	33.7	63.7	2.6	4.5	6.8	5.6
826	8A	9	na	10.5	3.8	40.5	59.5	0.0	3.8	3.9	4.6
827	8A	10	na	10.4	3.7	38.0	62.0	0.0	4.0	4.9	4.8
828	8A	11	na	10.6	3.4	43.9	56.1	0.0	3.5	3.4	4.4
829	8A	12	na	10.6	3.3	30.0	70.0	0.0	4.7	7.4	6.5
830	8A	13	na	10.5	3.4	36.8	59.1	4.2	4.1	5.9	5.0
831	8A	14	na	10.1	3.5	29.9	65.7	4.3	4.8	7.3	6.2
832	8A	15	na	11.0	2.8	37.8	62.2	0.0	4.0	4.8	4.9
833	8A	16	na	10.6	3.1	51.7	40.6	7.7	3.2	5.3	3.9
834	8A	17	na	10.1	3.3	52.6	47.4	0.0	3.1	4.5	3.9
835	8A	18	na	9.8	3.3	60.2	39.8	0.0	2.9	2.7	3.5
836	8A	19	na	9.7	3.0	29.1	56.0	15.0	5.1	9.7	6.3
837	8A	20	na	10.0	3.0	45.0	48.1	6.9	3.6	6.2	4.3
838	8A	21	na	9.6	3.4	41.2	48.8	10.0	3.8	7.1	4.6
839	8A	22	na	9.4	3.6	44.1	45.2	10.7	3.7	7.5	4.4
840	8A	23	na	9.5	3.3	42.9	57.1	0.0	3.5	2.6	4.4
841	8A	24	na	9.6	3.3	32.1	60.6	7.3	4.8	8.4	5.7
842	8A	25	na	7.4	5.1	36.2	62.1	1.7	4.3	6.2	5.0
843	8A	26	na	7.9	4.7	22.2	65.4	12.4	6.3	12.2	15.0
844	8A	27	na	8.8	4.0	38.8	59.7	1.5	4.0	4.7	4.7
845	8A	28	na	8.6	4.1	34.7	63.6	1.7	4.4	6.8	5.5
846	8A	29	na	9.3	3.9	31.1	66.5	2.5	5.0	8.6	7.3
847	8A	30	na	10.2	2.5	43.5	56.5	0.0	3.7	5.6	4.4
848	8A	31	na	10.1	2.6	45.7	54.3	0.0	3.5	3.9	4.2
849	8A	32	na	9.9	2.8	36.2	61.0	2.8	4.1	5.8	4.9
850	8A	33	na	10.2	2.4	32.0	68.0	0.0	4.6	6.7	5.6

SAMPLE			BULK COMPOSITION			TEXTURE					
Seq	Site	Depth	Moisture	Organic	Carbonate	Clay	Silt	Sand	Mean	St Dev	Median
no	ID	cm	%	%	%	%	%	%	um	um	um
851	8A	34	na	10.3	2.5	27.8	66.7	5.5	4.9	7.3	5.9
852	8A	35	na	10.4	2.4	46.1	53.9	0.0	3.4	3.4	4.2
853	8A	36	na	8.7	4.1	55.1	44.9	0.0	3.0	3.1	3.7
854	8A	37	na	9.9	2.6	48.7	51.4	0.0	3.2	2.1	4.1
855	8A	38	na	9.7	2.8	52.7	47.3	0.0	3.1	2.2	3.9
856	8A	39	na	8.5	4.2	53.0	47.0	0.0	3.2	2.1	3.9
857	8A	40	na	9.5	3.1	39.2	56.3	4.5	4.0	5.6	4.6
858	Grab-1	3	79.2	8.8	4.2	35.4	64.6	0.0	4.1	6.1	5.2
859	Grab-2	3	78.8	8.1	4.4	28.8	71.3	0.0	4.6	5.0	6.2
860	Grab-3	3	69.1	5.0	10.5	22.2	74.3	3.5	5.5	7.0	7.3
861	Grab-4	3	73.2	6.2	7.5	20.6	75.7	3.7	5.8	8.0	9.0
862	Grab-5	3	79.3	8.6	3.6	28.8	69.1	2.1	4.8	6.7	6.7
863	Grab-6	3	81.0	9.5	2.8	32.2	59.8	8.0	4.4	8.1	5.8
864	Grab-7	3	84.5	10.4	3.5	50.2	47.1	2.7	3.1	4.4	4.0
865	Grab-8	3	80.4	9.1	2.9	41.8	56.2	2.0	3.6	4.2	4.5
866	Grab-10	3	65.5	6.4	2.2	53.3	39.5	7.3	3.1	5.3	3.8
867	Grab-25	3	62.4	9.0	1.7	6.6	78.7	14.7	13.7	19.9	35.8
868	Grab-28	3	66.3	9.4	2.4	14.8	77.4	7.7	8.1	13.0	26.0
869	Grab-29	3	71.6	12.9	2.5	22.2	72.9	4.9	5.7	8.2	9.7
870	Grab-30	3	67.3	11.7	2.0	14.7	73.3	12.0	7.5	11.4	15.3
871	Grab-31	3	41.9	4.6	4.1	32.5	63.9	3.6	4.4	6.0	5.2
872	Grab-32	3	59.2	7.2	2.3	28.3	71.7	0.0	4.8	6.8	6.3
873	Grab-33	3	33.9	2.9	1.5	37.0	56.9	6.1	4.1	7.0	4.9
874	Grab-34	3	32.8	5.0	3.0	51.0	49.0	0.0	3.1	3.4	4.0
875	Grab-35	3	67.5	9.3	2.5	41.8	55.9	2.3	3.6	3.9	4.5
876	Grab-36	3	73.6	9.0	4.1	30.6	69.4	0.0	4.6	6.4	6.4
877	Grab-37	3	76.4	8.2	4.8	34.4	61.8	3.8	4.2	6.3	5.2
878	Grab-39	3	67.2	8.3	7.7	34.9	61.9	3.2	4.1	6.2	5.3
879	Grab-40	3	34.0	2.3	3.8	13.1	75.7	11.2	8.0	12.1	15.6
880	Grab-41	3	74.7	8.2	4.8	51.9	48.1	0.0	3.1	3.4	3.9
881	Grab-42	3	78.9	9.1	4.3	50.2	49.8	0.0	3.2	4.0	4.0
882	Grab-43	3	71.8	9.4	6.8	37.8	55.5	6.7	3.4	6.7	5.5
883	Grab-44	3	78.5	10.4	3.2	18.2	77.7	4.2	6.6	11.0	18.9
884	Grab-45	3	76.0	10.4	2.8	47.6	52.4	0.0	3.2	2.4	4.1
885	Grab-46	3	74.0	9.9	3.1	40.0	52.5	7.6	3.9	7.2	4.8
886	Grab-47	3	74.6	9.7	3.5	38.8	58.9	2.3	3.9	5.6	4.8
887	Grab-49	3	73.2	9.7	4.2	43.4	56.7	0.0	3.6	3.7	4.4
888	Grab-50	3	72.2	9.2	5.2	46.0	54.0	0.0	3.4	2.6	4.3

SAMPLE			MINERALOGY														
			Silicates					Carbonates							Evaporites		Sulfides
Seq	Site	Depth	Quartz	Kspar	Plag	Amph	ClayMin	Calcite	HiMgCal	Protodol	Dolomite	Mhydcal	Aragon	Magne	Thenar	Gypsum	Pyrite
no	ID	cm	%	%	%	%	%	%	%	%	%	%	%	%	%	%	%
1	103	5	6.3	12.4	7.5	0.0	71.0	0.0	0.0	0.0	2.9	0.0	0.0	0.0	0.0	0.0	0.0
2	103	15	6.3	10.5	8.9	0.0	62.3	0.0	2.0	3.3	3.8	0.0	0.0	0.0	3.0	0.0	0.0
3	103	25	6.5	9.9	8.8	0.0	58.9	0.0	0.0	2.9	0.0	0.0	0.0	0.0	0.0	13.1	0.0
4	103	35	6.3	11.9	7.8	2.1	69.7	2.2	0.0	0.0	0.0	0.0	0.0	0.0	0.0	0.0	0.0
5	103	45	6.6	5.6	8.9	1.9	74.5	0.0	0.0	2.6	0.0	0.0	0.0	0.0	0.0	0.0	0.0
6	103	55	8.6	0.0	11.2	0.0	73.5	0.0	3.0	3.7	0.0	0.0	0.0	0.0	0.0	0.0	0.0
7	103	65	5.8	10.8	7.2	1.7	71.5	0.0	0.0	3.0	0.0	0.0	0.0	0.0	0.0	0.0	0.0
8	103	75	5.9	6.3	9.2	2.1	59.6	0.0	0.0	0.0	0.0	0.0	0.0	0.0	0.0	16.9	0.0
9	103	85	5.5	9.5	7.2	0.0	60.5	0.0	0.0	2.9	0.0	0.0	0.0	0.0	0.0	14.4	0.0
10	103	95	7.3	6.1	8.0	2.1	69.0	0.0	0.0	3.8	3.7	0.0	0.0	0.0	0.0	0.0	0.0
11	103	105	5.3	5.6	6.8	0.0	61.1	0.0	2.5	2.8	0.0	0.0	0.0	0.0	0.0	16.0	0.0
12	103	115	5.7	11.7	6.9	1.8	73.9	0.0	0.0	0.0	0.0	0.0	0.0	0.0	0.0	0.0	0.0
13	103	125	6.9	6.4	9.6	0.0	70.8	0.0	2.6	3.8	0.0	0.0	0.0	0.0	0.0	0.0	0.0
14	103	135	6.2	7.2	7.8	2.2	67.5	0.0	2.3	3.1	3.7	0.0	0.0	0.0	0.0	0.0	0.0
15	103	145	5.5	8.6	6.2	0.0	58.0	0.0	2.4	2.5	2.8	0.0	0.0	0.0	0.0	14.2	0.0
16	103	155	5.8	6.4	10.0	3.0	69.7	0.0	0.0	0.0	3.0	0.0	0.0	0.0	0.0	2.2	0.0
17	103	165	6.8	8.6	10.4	2.6	68.9	0.0	2.7	0.0	0.0	0.0	0.0	0.0	0.0	0.0	0.0
18	103	175	5.1	6.2	6.3	0.0	63.2	0.0	0.0	3.3	0.0	0.0	0.0	0.0	0.0	16.0	0.0
19	103	185	5.8	10.9	7.7	0.0	59.7	0.0	2.3	0.0	0.0	0.0	0.0	0.0	0.0	13.6	0.0
20	103	195	6.6	0.0	7.2	0.0	78.1	2.1	2.6	3.5	0.0	0.0	0.0	0.0	0.0	0.0	0.0
21	103	205	5.5	7.9	9.5	4.4	68.7	0.0	0.0	0.0	3.9	0.0	0.0	0.0	0.0	0.0	0.0
22	103	215	5.5	10.4	13.0	0.0	50.4	0.0	2.3	2.9	2.7	0.0	0.0	0.0	0.0	12.8	0.0
23	103	225	6.6	6.4	7.9	1.8	58.4	0.0	0.0	3.6	0.0	0.0	0.0	0.0	0.0	15.4	0.0
24	103	235	6.3	6.2	10.3	2.4	71.6	0.0	0.0	3.3	0.0	0.0	0.0	0.0	0.0	0.0	0.0
25	103	245	5.8	5.9	7.7	0.0	62.7	0.0	2.0	0.0	0.0	0.0	0.0	0.0	0.0	15.9	0.0
26	103	255	5.5	10.1	8.5	0.0	55.6	1.6	0.0	2.6	0.0	0.0	0.0	0.0	0.0	16.1	0.0
27	103	265	5.7	11.1	7.0	0.0	68.0	0.0	2.0	3.1	3.0	0.0	0.0	0.0	0.0	0.0	0.0
28	103	275	5.5	12.6	9.2	0.0	66.6	0.0	2.3	0.0	3.8	0.0	0.0	0.0	0.0	0.0	0.0
29	103	285	6.2	12.1	8.1	0.0	62.6	1.8	2.5	3.6	3.2	0.0	0.0	0.0	0.0	0.0	0.0
30	103	295	4.8	8.9	7.1	0.0	57.2	0.0	2.0	2.5	3.6	0.0	0.0	0.0	0.0	13.9	0.0
31	103	305	6.1	11.5	8.0	2.0	70.0	0.0	2.5	0.0	0.0	0.0	0.0	0.0	0.0	0.0	0.0
32	103	315	6.0	13.3	14.3	0.0	59.2	0.0	0.0	3.5	3.7	0.0	0.0	0.0	0.0	0.0	0.0
33	103	325	5.1	10.4	8.1	0.0	68.3	0.0	2.1	3.1	3.0	0.0	0.0	0.0	0.0	0.0	0.0
34	103	335	5.7	6.5	8.4	1.7	71.3	0.0	0.0	3.2	3.3	0.0	0.0	0.0	0.0	0.0	0.0
35	103	345	6.4	12.4	8.7	0.0	67.1	0.0	2.3	0.0	3.2	0.0	0.0	0.0	0.0	0.0	0.0

SAMPLE			MINERALOGY														
			Silicates					Carbonates							Evaporites		Sulfides
Seq	Site	Depth	Quartz	Kspar	Plag	Amph	ClayMin	Calcite	HiMgCal	Protodol	Dolomite	Mhydcal	Aragon	Magne	Thenar	Gypsum	Pyrite
no	ID	cm	%	%	%	%	%	%	%	%	%	%	%	%	%	%	%
36	103	355	6.9	8.8	11.0	0.0	71.0	2.3	0.0	0.0	0.0	0.0	0.0	0.0	0.0	0.0	0.0
37	103	365	4.2	11.5	7.4	0.0	57.2	0.0	0.0	0.0	2.8	0.0	0.0	0.0	0.0	16.9	0.0
38	103	375	5.5	12.2	10.1	0.0	69.9	0.0	2.3	0.0	0.0	0.0	0.0	0.0	0.0	0.0	0.0
39	103	385	5.0	10.6	6.1	0.0	59.1	0.0	2.2	0.0	3.2	0.0	0.0	0.0	0.0	13.9	0.0
40	103	395	5.8	13.3	8.7	0.0	59.8	2.2	2.6	3.4	4.1	0.0	0.0	0.0	0.0	0.0	0.0
41	103	405	4.5	12.9	7.6	0.0	53.3	0.0	0.0	3.2	0.0	0.0	0.0	0.0	0.0	18.5	0.0
42	103	415	6.1	7.5	9.8	2.1	66.1	0.0	0.0	4.2	4.1	0.0	0.0	0.0	0.0	0.0	0.0
43	103	425	5.3	11.4	7.1	1.6	67.0	0.0	0.0	3.3	4.5	0.0	0.0	0.0	0.0	0.0	0.0
44	103	435	5.4	13.5	9.1	0.0	65.2	0.0	2.6	0.0	4.2	0.0	0.0	0.0	0.0	0.0	0.0
45	103	445	6.0	5.8	9.7	0.0	67.4	0.0	2.0	3.5	5.6	0.0	0.0	0.0	0.0	0.0	0.0
46	103	455	5.4	6.0	7.4	1.8	56.4	1.7	0.0	3.1	4.0	0.0	0.0	0.0	0.0	14.2	0.0
47	103	465	5.1	6.1	7.9	0.0	55.3	0.0	2.0	3.0	3.8	0.0	0.0	0.0	0.0	16.9	0.0
48	103	475	7.2	14.8	10.9	1.9	61.1	0.0	0.0	0.0	4.1	0.0	0.0	0.0	0.0	0.0	0.0
49	103	485	6.5	8.0	9.4	0.0	68.8	2.6	0.0	4.8	0.0	0.0	0.0	0.0	0.0	0.0	0.0
50	103	495	6.9	6.7	9.7	0.0	68.0	0.0	0.0	3.9	4.8	0.0	0.0	0.0	0.0	0.0	0.0
51	103	505	6.3	7.4	8.6	2.3	66.7	0.0	0.0	3.8	4.9	0.0	0.0	0.0	0.0	0.0	0.0
52	103	515	4.0	10.7	7.1	1.8	53.4	0.0	2.1	0.0	4.8	0.0	0.0	0.0	0.0	16.3	0.0
53	103	525	5.3	11.1	6.4	1.7	53.1	0.0	2.0	3.0	4.6	0.0	0.0	0.0	0.0	12.9	0.0
54	103	535	7.0	7.4	10.1	0.0	66.8	0.0	0.0	3.5	5.3	0.0	0.0	0.0	0.0	0.0	0.0
55	103	545	5.2	7.6	6.9	0.0	59.2	0.0	0.0	3.6	0.0	0.0	0.0	0.0	0.0	17.7	0.0
56	103	555	5.3	5.8	8.2	0.0	51.1	0.0	2.3	3.2	3.9	0.0	0.0	0.0	2.9	17.4	0.0
57	103	565	5.2	5.1	9.6	0.0	53.1	0.0	2.0	3.6	4.4	0.0	0.0	0.0	0.0	17.1	0.0
58	103	575	6.4	7.8	10.9	0.0	67.2	0.0	2.7	0.0	5.0	0.0	0.0	0.0	0.0	0.0	0.0
59	103	585	6.2	6.7	8.6	0.0	52.6	0.0	2.8	0.0	4.5	0.0	0.0	0.0	0.0	18.7	0.0
60	103	595	4.6	12.4	7.5	0.0	53.6	0.0	0.0	3.4	4.8	0.0	0.0	0.0	0.0	13.8	0.0
61	103	605	4.6	11.5	6.5	1.8	64.2	2.1	2.4	0.0	3.5	0.0	0.0	3.4	0.0	0.0	0.0
62	103	615	6.4	7.5	9.5	2.0	65.3	0.0	2.3	0.0	7.1	0.0	0.0	0.0	0.0	0.0	0.0
63	103	625	6.8	8.9	0.0	0.0	77.1	0.0	0.0	0.0	7.3	0.0	0.0	0.0	0.0	0.0	0.0
64	103	635	6.6	7.7	8.6	0.0	65.8	0.0	0.0	4.1	7.2	0.0	0.0	0.0	0.0	0.0	0.0
65	103	645	6.7	6.7	11.6	0.0	68.5	0.0	0.0	0.0	6.6	0.0	0.0	0.0	0.0	0.0	0.0
66	103	655	4.2	11.3	6.9	0.0	51.8	0.0	1.9	3.3	4.8	0.0	0.0	0.0	0.0	15.8	0.0
67	103	665	5.2	8.3	7.8	0.0	72.7	0.0	0.0	0.0	6.1	0.0	0.0	0.0	0.0	0.0	0.0
68	103	675	4.2	10.9	6.5	1.4	50.4	3.1	2.5	0.0	5.5	0.0	0.0	0.0	0.0	15.5	0.0
69	103	685	5.0	10.0	9.2	1.7	53.2	0.0	0.0	0.0	4.4	0.0	0.0	0.0	0.0	16.5	0.0
70	103	695	3.4	8.0	9.1	2.3	55.6	4.6	0.0	4.9	7.2	0.0	0.0	0.0	4.9	0.0	0.0

SAMPLE			MINERALOGY														
			Silicates					Carbonates							Evaporites		Sulfides
Seq	Site	Depth	Quartz	Kspar	Plag	Amph	ClayMin	Calcite	HiMgCal	Protodol	Dolomite	Mhydcal	Aragon	Magne	Thenar	Gypsum	Pyrite
no	ID	cm	%	%	%	%	%	%	%	%	%	%	%	%	%	%	%
71	103	705	3.6	8.8	7.9	2.7	61.6	5.7	0.0	4.6	5.2	0.0	0.0	0.0	0.0	0.0	0.0
72	103	715	4.3	7.5	7.2	2.4	62.7	5.4	0.0	4.2	6.3	0.0	0.0	0.0	0.0	0.0	0.0
73	103	725	2.8	5.6	5.3	0.0	57.3	4.0	0.0	3.3	4.1	0.0	0.0	0.0	0.0	17.6	0.0
74	103	735	5.1	14.6	9.5	0.0	59.8	4.4	0.0	0.0	6.6	0.0	0.0	0.0	0.0	0.0	0.0
75	103	745	3.7	6.6	7.1	0.0	48.0	4.0	2.9	0.0	5.7	0.0	0.0	0.0	0.0	22.1	0.0
76	103	755	4.5	7.2	7.9	0.0	47.0	5.0	0.0	0.0	6.4	0.0	0.0	0.0	0.0	22.0	0.0
77	103	765	4.1	15.0	9.1	0.0	52.0	5.4	0.0	0.0	7.4	0.0	0.0	0.0	0.0	7.1	0.0
78	103	775	4.8	7.7	9.0	0.0	62.9	7.3	0.0	0.0	8.3	0.0	0.0	0.0	0.0	0.0	0.0
79	103	785	5.6	7.4	10.4	0.0	60.3	8.3	0.0	0.0	8.1	0.0	0.0	0.0	0.0	0.0	0.0
80	103	795	5.6	13.6	7.7	0.0	59.3	5.0	2.6	0.0	6.4	0.0	0.0	0.0	0.0	0.0	0.0
81	103	805	5.5	6.2	7.6	0.0	58.8	11.6	0.0	0.0	10.4	0.0	0.0	0.0	0.0	0.0	0.0
82	103	815	6.2	12.7	10.0	0.0	49.1	8.4	0.0	3.9	9.7	0.0	0.0	0.0	0.0	0.0	0.0
83	104A	5	11.6	7.3	11.7	0.0	63.0	0.0	0.0	0.0	6.4	0.0	0.0	0.0	0.0	0.0	0.0
84	104A	15	9.1	14.3	9.6	2.7	57.6	0.0	0.0	0.0	6.8	0.0	0.0	0.0	0.0	0.0	0.0
85	104A	25	6.0	7.9	9.1	0.0	68.2	0.0	2.5	0.0	6.3	0.0	0.0	0.0	0.0	0.0	0.0
86	104A	35	3.0	3.6	3.9	0.9	85.2	0.0	0.0	0.0	3.5	0.0	0.0	0.0	0.0	0.0	0.0
87	104A	45	5.6	5.8	8.1	0.0	55.6	0.0	2.1	2.6	5.4	0.0	0.0	0.0	0.0	15.0	0.0
88	104A	55	7.1	7.4	13.8	2.0	62.2	0.0	0.0	0.0	7.6	0.0	0.0	0.0	0.0	0.0	0.0
89	104A	65	6.8	9.8	9.7	0.0	48.1	1.6	1.8	2.9	5.9	0.0	0.0	0.0	0.0	13.4	0.0
90	104A	75	6.2	5.5	8.6	0.0	53.1	2.2	2.7	0.0	4.5	0.0	0.0	0.0	0.0	17.2	0.0
91	104A	85	6.0	13.6	7.2	1.7	58.5	0.0	2.8	3.8	6.4	0.0	0.0	0.0	0.0	0.0	0.0
92	104A	95	5.0	7.3	12.6	0.0	66.2	0.0	2.4	0.0	6.6	0.0	0.0	0.0	0.0	0.0	0.0
93	104A	105	8.0	8.2	9.6	0.0	67.8	0.0	0.0	0.0	6.4	0.0	0.0	0.0	0.0	0.0	0.0
94	104A	115	6.8	7.9	10.4	0.0	62.6	0.0	0.0	3.8	8.5	0.0	0.0	0.0	0.0	0.0	0.0
95	104A	125	8.7	13.8	10.7	1.7	52.7	0.0	0.0	4.1	8.2	0.0	0.0	0.0	0.0	0.0	0.0
96	104A	135	7.1	8.6	10.8	3.1	58.2	0.0	0.0	3.7	8.5	0.0	0.0	0.0	0.0	0.0	0.0
97	104A	145	6.1	9.8	6.6	0.0	52.0	0.0	1.9	3.4	5.9	0.0	0.0	0.0	0.0	14.5	0.0
98	104A	155	5.8	8.0	29.3	1.5	45.8	0.0	0.0	2.9	6.8	0.0	0.0	0.0	0.0	0.0	0.0
99	104A	165	6.4	5.3	11.3	2.8	61.2	0.0	0.0	4.6	8.5	0.0	0.0	0.0	0.0	0.0	0.0
100	104A	175	6.6	8.3	8.4	2.2	58.3	2.2	0.0	3.8	10.3	0.0	0.0	0.0	0.0	0.0	0.0
101	104A	185	5.1	7.5	9.9	1.8	48.9	0.0	5.0	0.0	7.7	0.0	0.0	0.0	0.0	14.2	0.0
102	104A	195	6.0	6.3	9.2	0.0	50.4	2.6	0.0	0.0	8.6	0.0	0.0	0.0	0.0	16.8	0.0
103	104A	205	9.1	0.0	11.4	0.0	67.4	2.5	0.0	0.0	9.5	0.0	0.0	0.0	0.0	0.0	0.0
104	104A	215	7.9	15.3	11.4	2.3	53.1	0.0	2.4	0.0	7.5	0.0	0.0	0.0	0.0	0.0	0.0
105	104A	225	13.6	8.5	10.2	1.8	45.3	3.1	2.5	4.0	11.0	0.0	0.0	0.0	0.0	0.0	0.0

SAMPLE			MINERALOGY														
			Silicates					Carbonates							Evaporites		Sulfides
Seq	Site	Depth	Quartz	Kspar	Plag	Amph	ClayMin	Calcite	HiMgCal	Protodol	Dolomite	Mhydcal	Aragon	Magne	Thenar	Gypsum	Pyrite
no	ID	cm	%	%	%	%	%	%	%	%	%	%	%	%	%	%	%
106	104A	235	8.3	13.0	9.9	1.6	35.2	5.1	0.0	2.5	13.1	0.0	0.0	0.0	0.0	11.4	0.0
107	104A	245	21.4	10.0	15.2	0.0	28.1	5.4	2.5	4.3	13.3	0.0	0.0	0.0	0.0	0.0	0.0
108	104A	255	14.3	9.0	23.1	1.6	27.2	6.8	2.2	3.4	12.5	0.0	0.0	0.0	0.0	0.0	0.0
109	104A	265	9.3	6.4	17.6	0.0	32.6	6.9	2.2	3.2	10.1	0.0	0.0	0.0	0.0	11.7	0.0
110	104A	275	9.2	6.9	14.4	3.0	47.5	7.1	0.0	0.0	11.8	0.0	0.0	0.0	0.0	0.0	0.0
111	104A	285	8.1	7.8	20.5	0.0	32.0	6.5	0.0	2.9	10.8	0.0	0.0	0.0	0.0	11.4	0.0
112	104A	295	8.5	8.0	18.2	1.6	41.2	7.5	0.0	3.2	11.7	0.0	0.0	0.0	0.0	0.0	0.0
113	104A	305	3.8	5.9	4.7	0.0	69.2	3.4	0.0	0.0	5.4	0.0	0.0	0.0	0.0	7.6	0.0
114	104A	315	10.2	14.6	10.5	0.0	41.6	7.1	0.0	3.5	12.4	0.0	0.0	0.0	0.0	0.0	0.0
115	104A	325	8.4	6.6	10.4	2.3	46.9	6.0	2.8	5.8	10.7	0.0	0.0	0.0	0.0	0.0	0.0
116	104A	335	9.6	5.3	8.9	2.8	41.9	6.1	2.1	0.0	10.5	0.0	0.0	0.0	0.0	12.8	0.0
117	104A	345	10.0	6.9	10.7	1.6	35.2	5.7	0.0	4.8	10.3	0.0	0.0	0.0	0.0	14.9	0.0
118	104A	355	6.3	13.2	11.1	4.3	31.8	5.5	2.1	2.3	23.4	0.0	0.0	0.0	0.0	0.0	0.0
119	104A	365	8.7	10.7	8.4	1.7	32.4	6.6	1.6	0.0	13.5	0.0	0.0	0.0	0.0	16.4	0.0
120	104B	5	7.5	8.6	7.2	0.0	55.0	0.0	0.0	2.7	6.2	0.0	0.0	0.0	0.0	12.8	0.0
121	104B	15	9.4	8.7	10.4	1.8	56.7	2.4	2.4	0.0	8.2	0.0	0.0	0.0	0.0	0.0	0.0
122	104B	25	8.0	6.1	11.5	1.6	59.2	2.4	0.0	3.4	7.7	0.0	0.0	0.0	0.0	0.0	0.0
123	104B	35	5.7	10.9	9.7	0.0	47.1	0.0	0.0	2.9	8.9	0.0	0.0	0.0	0.0	14.8	0.0
124	104B	45	14.3	7.0	22.6	0.0	28.0	7.7	0.0	5.6	14.8	0.0	0.0	0.0	0.0	0.0	0.0
125	104B	55	8.8	12.4	16.6	0.0	42.8	7.3	0.0	0.0	12.1	0.0	0.0	0.0	0.0	0.0	0.0
126	104B	65	9.2	11.4	9.5	1.7	31.5	6.6	0.0	3.0	11.9	0.0	0.0	0.0	0.0	15.2	0.0
127	104B	75	9.2	6.3	10.1	0.0	51.4	6.2	0.0	0.0	16.8	0.0	0.0	0.0	0.0	0.0	0.0
128	105	5	10.7	8.3	14.4	2.5	53.3	0.0	0.0	0.0	10.8	0.0	0.0	0.0	0.0	0.0	0.0
129	105	15	12.2	5.7	10.7	1.4	43.0	0.0	2.0	2.8	8.5	0.0	0.0	0.0	0.0	13.8	0.0
130	105	25	10.6	6.9	11.3	0.0	50.8	4.1	0.0	0.0	16.3	0.0	0.0	0.0	0.0	0.0	0.0
131	105	35	8.4	8.1	16.7	2.0	54.3	0.0	2.9	0.0	7.7	0.0	0.0	0.0	0.0	0.0	0.0
132	105	45	8.0	4.9	9.6	2.0	45.6	2.7	2.2	0.0	8.0	0.0	0.0	0.0	0.0	16.9	0.0
133	105	55	8.6	8.7	9.0	2.2	37.9	3.9	0.0	3.2	12.0	0.0	0.0	0.0	0.0	14.5	0.0
134	105	65	6.8	10.0	8.0	1.6	46.5	3.4	2.3	0.0	7.5	0.0	0.0	0.0	0.0	13.8	0.0
135	105	75	5.1	6.8	10.0	2.2	63.6	3.7	0.0	3.2	5.5	0.0	0.0	0.0	0.0	0.0	0.0
136	105	85	7.0	9.0	13.1	0.0	57.1	5.8	0.0	0.0	8.0	0.0	0.0	0.0	0.0	0.0	0.0
137	105	95	4.3	13.8	8.3	1.9	63.2	3.8	0.0	0.0	4.6	0.0	0.0	0.0	0.0	0.0	0.0
138	105	105	6.7	6.3	10.7	0.0	59.1	6.5	0.0	3.7	7.1	0.0	0.0	0.0	0.0	0.0	0.0
139	105	115	4.4	7.1	6.7	1.7	50.3	5.2	0.0	3.2	5.7	0.0	0.0	0.0	0.0	15.7	0.0
140	105	125	4.6	6.4	6.9	1.9	54.5	4.0	0.0	0.0	5.5	0.0	0.0	0.0	0.0	16.2	0.0

SAMPLE			MINERALOGY														
			Silicates					Carbonates							Evaporites		Sulfides
Seq	Site	Depth	Quartz	Kspar	Plag	Amph	ClayMin	Calcite	HiMgCal	Protodol	Dolomite	Mhydcal	Aragon	Magne	Thenar	Gypsum	Pyrite
no	ID	cm	%	%	%	%	%	%	%	%	%	%	%	%	%	%	%
141	105	135	6.3	12.1	0.0	0.0	66.7	3.7	0.0	4.5	6.7	0.0	0.0	0.0	0.0	0.0	0.0
142	105	145	5.4	15.0	10.7	0.0	55.2	4.7	0.0	3.1	6.0	0.0	0.0	0.0	0.0	0.0	0.0
143	105	155	5.1	6.9	9.8	0.0	40.6	7.5	0.0	4.0	6.5	0.0	0.0	0.0	0.0	19.6	0.0
144	105	165	5.1	8.9	7.9	1.3	48.2	4.8	1.9	2.7	5.2	0.0	0.0	0.0	0.0	14.1	0.0
145	105	175	6.3	5.6	10.8	0.0	61.1	6.5	0.0	3.5	6.2	0.0	0.0	0.0	0.0	0.0	0.0
146	105	185	6.5	7.2	11.6	0.0	57.1	5.4	2.2	3.5	6.5	0.0	0.0	0.0	0.0	0.0	0.0
147	105	195	7.3	7.2	8.7	2.0	59.6	5.0	0.0	0.0	6.6	0.0	0.0	0.0	0.0	0.0	3.6
148	105	205	7.0	6.6	9.6	0.0	56.9	6.4	0.0	3.4	7.3	0.0	0.0	0.0	2.8	0.0	0.0
149	105	215	5.5	10.9	6.7	0.0	63.0	6.0	0.0	2.9	5.0	0.0	0.0	0.0	0.0	0.0	0.0
150	105	225	6.7	12.4	13.5	0.0	50.1	8.2	2.8	0.0	6.3	0.0	0.0	0.0	0.0	0.0	0.0
151	105	235	5.9	7.8	10.1	2.2	56.9	4.1	3.1	3.9	6.1	0.0	0.0	0.0	0.0	0.0	0.0
152	105	245	7.1	13.2	9.8	0.0	56.0	4.8	0.0	3.6	5.5	0.0	0.0	0.0	0.0	0.0	0.0
153	105	255	5.9	12.1	8.3	0.0	56.9	5.2	2.6	2.9	6.2	0.0	0.0	0.0	0.0	0.0	0.0
154	105	265	5.1	16.3	9.5	0.0	55.7	4.6	2.9	0.0	6.1	0.0	0.0	0.0	0.0	0.0	0.0
155	105	275	5.6	7.2	8.1	0.0	52.8	6.0	0.0	0.0	5.9	0.0	0.0	0.0	0.0	14.5	0.0
156	105	285	5.5	11.3	11.7	0.0	39.7	5.3	2.1	2.9	5.6	0.0	0.0	0.0	0.0	15.9	0.0
157	105	295	5.9	10.8	8.6	2.0	43.2	5.1	2.1	0.0	5.3	0.0	0.0	0.0	0.0	17.0	0.0
158	105	305	6.2	10.2	11.8	0.0	41.5	7.0	0.0	3.3	7.2	0.0	0.0	0.0	0.0	12.9	0.0
159	105	315	6.5	12.1	8.1	0.0	42.4	6.1	1.9	3.1	6.2	0.0	0.0	0.0	0.0	13.5	0.0
160	105	325	6.4	10.8	12.0	0.0	42.8	7.5	0.0	0.0	7.1	0.0	0.0	0.0	0.0	13.4	0.0
161	105	335	7.2	11.8	10.8	1.9	37.5	9.2	0.0	3.1	6.6	0.0	0.0	0.0	0.0	11.8	0.0
162	105	345	9.0	15.8	13.3	0.0	45.0	8.0	0.0	0.0	8.9	0.0	0.0	0.0	0.0	0.0	0.0
163	105	355	5.8	12.6	9.5	0.0	51.9	9.5	0.0	4.1	6.7	0.0	0.0	0.0	0.0	0.0	0.0
164	105	365	10.8	12.5	13.1	0.0	49.2	7.5	0.0	0.0	6.9	0.0	0.0	0.0	0.0	0.0	0.0
165	105	375	11.6	7.7	15.7	1.9	34.2	4.6	0.0	3.3	5.9	0.0	0.0	0.0	0.0	15.0	0.0
166	105	385	8.7	10.8	17.9	2.6	41.8	6.3	2.3	3.2	6.5	0.0	0.0	0.0	0.0	0.0	0.0
167	105	395	13.4	8.9	22.5	0.0	36.8	5.3	0.0	4.0	9.0	0.0	0.0	0.0	0.0	0.0	0.0
168	105	405	11.3	7.3	13.4	0.0	43.3	10.6	0.0	4.1	10.0	0.0	0.0	0.0	0.0	0.0	0.0
169	105	415	7.0	10.3	10.5	2.5	39.6	10.4	0.0	0.0	7.5	0.0	0.0	0.0	0.0	12.2	0.0
170	105	425	12.5	8.8	16.5	0.0	36.2	10.4	2.2	3.4	10.0	0.0	0.0	0.0	0.0	0.0	0.0
171	105	435	10.9	13.0	16.9	0.0	31.3	7.7	0.0	3.4	6.1	0.0	0.0	0.0	0.0	10.8	0.0
172	105	445	10.4	14.0	12.5	1.8	29.5	8.7	0.0	3.3	8.6	0.0	0.0	0.0	0.0	11.3	0.0
173	105	455	7.6	11.2	11.7	1.7	26.2	9.8	2.6	3.6	8.5	0.0	0.0	2.5	0.0	14.7	0.0
174	105	465	12.0	10.0	11.8	2.0	30.5	9.0	0.0	3.0	8.5	0.0	0.0	0.0	0.0	13.3	0.0
175	105	475	9.9	10.9	11.1	1.8	28.8	11.0	0.0	2.9	10.7	0.0	0.0	0.0	0.0	13.1	0.0

SAMPLE			MINERALOGY														
			Silicates					Carbonates							Evaporites		Sulfides
Seq	Site	Depth	Quartz	Kspar	Plag	Amph	ClayMin	Calcite	HiMgCal	Protodol	Dolomite	Mhydcal	Aragon	Magne	Thenar	Gypsum	Pyrite
no	ID	cm	%	%	%	%	%	%	%	%	%	%	%	%	%	%	%
176	105	485	10.5	5.3	14.6	2.0	41.0	14.3	0.0	0.0	12.3	0.0	0.0	0.0	0.0	0.0	0.0
177	105	495	10.8	6.4	13.0	0.0	30.9	11.6	0.0	3.0	11.3	0.0	0.0	0.0	0.0	12.9	0.0
178	105	505	15.0	11.0	16.9	2.7	23.9	4.7	0.0	3.1	7.5	0.0	0.0	0.0	0.0	15.2	0.0
179	106	5	8.2	10.8	8.7	0.0	60.5	1.6	2.5	0.0	7.7	0.0	0.0	0.0	0.0	0.0	0.0
180	106	15	9.3	8.4	12.5	0.0	58.6	0.0	0.0	4.7	6.4	0.0	0.0	0.0	0.0	0.0	0.0
181	106	25	8.1	10.0	8.5	1.8	50.3	2.0	0.0	0.0	6.3	0.0	0.0	0.0	0.0	13.2	0.0
182	106	35	6.4	15.5	7.8	0.0	50.3	0.0	0.0	2.8	3.8	0.0	0.0	0.0	0.0	13.5	0.0
183	106	45	11.0	7.7	10.1	0.0	62.2	0.0	0.0	3.2	5.9	0.0	0.0	0.0	0.0	0.0	0.0
184	106	55	8.5	6.6	10.4	2.0	61.5	0.0	2.1	3.0	5.9	0.0	0.0	0.0	0.0	0.0	0.0
185	106	65	10.3	7.8	8.2	0.0	61.4	0.0	2.0	2.9	7.3	0.0	0.0	0.0	0.0	0.0	0.0
186	106	75	8.8	7.1	10.7	2.0	60.3	0.0	2.2	0.0	8.9	0.0	0.0	0.0	0.0	0.0	0.0
187	106	85	9.0	6.8	11.3	2.2	61.3	0.0	0.0	3.5	6.1	0.0	0.0	0.0	0.0	0.0	0.0
188	106	95	6.6	6.6	8.6	0.0	54.6	0.0	0.0	0.0	7.5	0.0	0.0	0.0	0.0	16.1	0.0
189	106	105	7.5	0.0	8.8	0.0	71.5	0.0	2.4	4.1	5.7	0.0	0.0	0.0	0.0	0.0	0.0
190	106	115	5.9	11.9	8.1	0.0	62.4	1.8	0.0	3.1	6.8	0.0	0.0	0.0	0.0	0.0	0.0
191	106	125	7.1	6.2	8.9	0.0	52.9	2.4	1.7	0.0	8.5	0.0	0.0	0.0	0.0	12.4	0.0
192	106	135	12.6	6.5	12.5	2.0	49.2	3.1	0.0	3.8	10.3	0.0	0.0	0.0	0.0	0.0	0.0
193	106	145	6.1	0.0	8.4	0.0	70.3	2.8	0.0	3.5	8.9	0.0	0.0	0.0	0.0	0.0	0.0
194	106	155	16.7	0.0	9.9	0.0	56.8	3.8	0.0	3.3	9.5	0.0	0.0	0.0	0.0	0.0	0.0
195	106	165	18.7	8.7	17.4	3.1	30.0	8.0	0.0	4.1	10.1	0.0	0.0	0.0	0.0	0.0	0.0
196	106	175	15.2	26.4	14.9	1.6	24.2	5.9	2.1	2.8	6.9	0.0	0.0	0.0	0.0	0.0	0.0
197	106	185	7.0	11.3	9.3	0.0	56.7	5.5	0.0	3.5	6.7	0.0	0.0	0.0	0.0	0.0	0.0
198	106	195	5.4	8.1	9.1	0.0	46.4	7.2	0.0	0.0	7.3	0.0	0.0	0.0	0.0	16.6	0.0
199	106	205	5.6	11.7	8.4	0.0	53.0	8.5	2.2	0.0	10.7	0.0	0.0	0.0	0.0	0.0	0.0
200	106	215	6.7	5.0	6.8	0.0	58.0	10.3	1.8	0.0	11.3	0.0	0.0	0.0	0.0	0.0	0.0
201	106	225	7.2	16.0	9.2	0.0	36.3	9.2	3.3	4.8	14.1	0.0	0.0	0.0	0.0	0.0	0.0
202	106	235	6.1	6.0	8.0	0.0	63.1	7.6	0.0	0.0	9.3	0.0	0.0	0.0	0.0	0.0	0.0
203	106	245	6.6	12.7	10.0	0.0	51.9	10.9	0.0	0.0	8.0	0.0	0.0	0.0	0.0	0.0	0.0
204	106	255	7.0	11.8	10.5	0.0	45.3	15.2	0.0	0.0	10.2	0.0	0.0	0.0	0.0	0.0	0.0
205	106	265	5.7	10.2	8.2	0.0	41.1	11.8	0.0	0.0	8.7	0.0	0.0	0.0	0.0	14.2	0.0
206	106	275	5.9	6.0	28.4	0.0	40.8	11.0	0.0	0.0	7.9	0.0	0.0	0.0	0.0	0.0	0.0
207	106	285	6.9	9.4	8.1	0.0	45.1	17.4	0.0	3.4	9.9	0.0	0.0	0.0	0.0	0.0	0.0
208	106	295	6.2	11.2	7.3	1.9	37.9	12.5	0.0	0.0	9.5	0.0	0.0	0.0	0.0	13.4	0.0
209	106	305	5.6	4.2	8.5	0.0	44.6	13.7	0.0	0.0	8.4	0.0	0.0	0.0	0.0	15.0	0.0
210	106	315	8.2	11.7	9.0	0.0	40.7	17.1	0.0	0.0	13.3	0.0	0.0	0.0	0.0	0.0	0.0

SAMPLE			MINERALOGY														
			Silicates					Carbonates							Evaporites		Sulfides
Seq	Site	Depth	Quartz	Kspar	Plag	Amph	ClayMin	Calcite	HiMgCal	Protodol	Dolomite	Mhydcal	Aragon	Magne	Thenar	Gypsum	Pyrite
no	ID	cm	%	%	%	%	%	%	%	%	%	%	%	%	%	%	%
211	106	325	6.5	5.3	6.2	1.8	55.7	12.7	2.6	0.0	9.3	0.0	0.0	0.0	0.0	0.0	0.0
212	106	335	8.1	5.9	10.3	0.0	52.9	12.3	0.0	0.0	10.6	0.0	0.0	0.0	0.0	0.0	0.0
213	106	345	7.6	11.6	6.2	0.0	42.0	17.2	0.0	3.8	11.4	0.0	0.0	0.0	0.0	0.0	0.0
214	106	355	7.2	9.7	8.8	1.7	35.4	14.1	0.0	0.0	11.2	0.0	0.0	0.0	0.0	12.0	0.0
215	106	365	5.8	8.7	5.7	1.9	40.2	15.0	0.0	2.6	8.0	0.0	0.0	0.0	0.0	12.0	0.0
216	106	375	8.0	12.2	6.8	1.8	41.8	15.0	0.0	4.2	10.1	0.0	0.0	0.0	0.0	0.0	0.0
217	106	385	8.1	12.5	9.0	2.5	37.9	16.2	0.0	3.8	9.9	0.0	0.0	0.0	0.0	0.0	0.0
218	106	395	9.6	7.6	12.2	0.0	51.6	0.0	2.9	3.7	12.4	0.0	0.0	0.0	0.0	0.0	0.0
219	106	405	7.1	12.0	7.7	1.7	45.9	11.4	0.0	3.6	10.7	0.0	0.0	0.0	0.0	0.0	0.0
220	106	415	11.6	12.4	10.7	0.0	32.1	17.5	2.4	0.0	13.2	0.0	0.0	0.0	0.0	0.0	0.0
221	106	425	5.1	10.2	7.2	0.0	50.4	8.8	0.0	0.0	6.4	0.0	0.0	0.0	0.0	11.9	0.0
222	106	435	4.8	11.3	7.4	0.0	57.6	10.3	0.0	2.9	5.7	0.0	0.0	0.0	0.0	0.0	0.0
223	106	445	6.8	10.9	10.0	0.0	54.3	12.1	0.0	0.0	5.9	0.0	0.0	0.0	0.0	0.0	0.0
224	106	455	5.2	5.3	7.2	0.0	58.9	13.0	0.0	3.5	6.9	0.0	0.0	0.0	0.0	0.0	0.0
225	106	465	7.0	7.9	11.1	0.0	51.5	12.3	2.7	7.5	0.0	0.0	0.0	0.0	0.0	0.0	0.0
226	106	475	5.3	11.8	8.5	0.0	55.8	9.0	0.0	3.4	6.2	0.0	0.0	0.0	0.0	0.0	0.0
227	106	485	6.1	13.9	9.0	0.0	55.6	8.6	0.0	0.0	6.9	0.0	0.0	0.0	0.0	0.0	0.0
228	106	495	6.2	8.5	7.6	2.5	60.5	7.5	2.6	0.0	4.6	0.0	0.0	0.0	0.0	0.0	0.0
229	106	505	5.3	10.7	9.7	0.0	41.6	9.3	0.0	3.2	5.5	0.0	0.0	0.0	0.0	14.6	0.0
230	106	515	5.7	14.5	9.8	2.1	54.9	7.9	0.0	0.0	5.1	0.0	0.0	0.0	0.0	0.0	0.0
231	106	525	5.2	12.2	8.5	0.0	58.0	9.6	0.0	0.0	6.4	0.0	0.0	0.0	0.0	0.0	0.0
232	106	535	7.4	5.7	11.8	1.6	53.6	10.6	0.0	0.0	9.2	0.0	0.0	0.0	0.0	0.0	0.0
233	106	545	3.5	6.0	7.9	0.0	56.5	6.2	0.0	0.0	4.3	0.0	0.0	0.0	0.0	15.7	0.0
234	106	555	4.9	13.3	7.2	0.0	62.8	7.0	0.0	0.0	4.9	0.0	0.0	0.0	0.0	0.0	0.0
235	106	565	4.2	6.5	6.8	0.0	57.1	6.4	0.0	0.0	4.1	0.0	0.0	0.0	0.0	14.8	0.0
236	106	575	4.6	6.3	8.4	0.0	54.6	4.7	2.5	3.9	0.0	0.0	0.0	0.0	0.0	15.1	0.0
237	106	585	5.1	6.7	9.2	0.0	52.4	3.7	0.0	4.0	0.0	0.0	0.0	0.0	0.0	18.9	0.0
238	106	595	4.6	6.9	7.5	2.3	63.3	8.1	0.0	0.0	4.8	0.0	0.0	2.6	0.0	0.0	0.0
239	106	605	3.2	41.3	5.6	0.0	28.8	3.4	1.4	2.2	3.3	0.0	0.0	0.0	0.0	10.8	0.0
240	106	615	4.1	10.6	6.5	0.0	53.5	4.2	0.0	3.4	4.1	0.0	0.0	0.0	0.0	13.6	0.0
241	106	625	5.5	6.6	8.9	0.0	51.2	4.5	0.0	0.0	5.6	0.0	0.0	0.0	0.0	17.8	0.0
242	106	635	4.7	12.1	7.1	0.0	50.7	5.2	0.0	2.5	4.2	0.0	0.0	0.0	0.0	13.5	0.0
243	106	645	6.0	11.4	7.8	1.9	54.9	6.0	2.2	3.0	6.7	0.0	0.0	0.0	0.0	0.0	0.0
244	106	655	5.7	6.8	8.4	0.0	50.0	4.9	0.0	3.2	5.7	0.0	0.0	0.0	0.0	15.4	0.0
245	106	665	5.9	7.3	9.2	2.5	58.6	6.5	0.0	3.9	6.2	0.0	0.0	0.0	0.0	0.0	0.0

SAMPLE			MINERALOGY														
			Silicates					Carbonates							Evaporites		Sulfides
Seq	Site	Depth	Quartz	Kspar	Plag	Amph	ClayMin	Calcite	HiMgCal	Protodol	Dolomite	Mhydcal	Aragon	Magne	Thenar	Gypsum	Pyrite
no	ID	cm	%	%	%	%	%	%	%	%	%	%	%	%	%	%	%
246	106	675	5.9	14.6	9.7	0.0	56.3	4.8	2.1	0.0	6.6	0.0	0.0	0.0	0.0	0.0	0.0
247	106	685	5.9	12.3	9.2	0.0	55.5	8.1	2.4	0.0	6.7	0.0	0.0	0.0	0.0	0.0	0.0
248	106	695	5.2	5.4	8.8	0.0	49.2	5.1	2.3	3.0	5.8	0.0	0.0	0.0	0.0	15.3	0.0
249	107	5	7.5	12.0	10.8	0.0	64.4	0.0	2.0	3.2	0.0	0.0	0.0	0.0	0.0	0.0	0.0
250	107	15	5.8	11.1	8.5	0.0	71.6	0.0	0.0	3.0	0.0	0.0	0.0	0.0	0.0	0.0	0.0
251	107	25	9.0	0.0	16.7	0.0	74.3	0.0	0.0	0.0	0.0	0.0	0.0	0.0	0.0	0.0	0.0
252	107	35	6.5	11.0	20.9	1.6	55.2	1.7	0.0	0.0	3.0	0.0	0.0	0.0	0.0	0.0	0.0
253	107	45	7.9	7.4	8.3	0.0	72.6	0.0	0.0	3.8	0.0	0.0	0.0	0.0	0.0	0.0	0.0
254	107	55	6.8	10.6	9.9	0.0	53.8	0.0	2.0	3.2	0.0	0.0	0.0	0.0	0.0	13.8	0.0
255	107	65	7.3	6.5	7.7	2.0	73.5	0.0	0.0	3.0	0.0	0.0	0.0	0.0	0.0	0.0	0.0
256	107	75	5.0	6.1	8.1	1.8	58.3	1.6	0.0	2.8	0.0	0.0	0.0	2.9	0.0	13.5	0.0
257	107	85	6.6	6.2	7.4	0.0	59.5	0.0	0.0	3.3	2.8	0.0	0.0	0.0	0.0	14.1	0.0
258	107	95	6.4	5.8	8.9	2.1	56.6	0.0	1.9	2.7	2.9	0.0	0.0	0.0	0.0	12.8	0.0
259	107	105	6.6	10.7	8.8	0.0	54.5	0.0	0.0	2.6	4.9	0.0	0.0	0.0	0.0	12.0	0.0
260	107	115	8.8	10.8	8.2	0.0	63.0	0.0	0.0	3.9	5.3	0.0	0.0	0.0	0.0	0.0	0.0
261	107	125	5.9	10.0	11.4	0.0	52.3	0.0	0.0	2.9	4.8	0.0	0.0	0.0	0.0	12.7	0.0
262	107	135	7.2	9.1	14.9	0.0	62.5	0.0	2.6	0.0	3.7	0.0	0.0	0.0	0.0	0.0	0.0
263	107	145	8.7	7.6	11.4	1.7	61.6	0.0	0.0	3.8	5.3	0.0	0.0	0.0	0.0	0.0	0.0
264	107	155	6.8	12.0	11.7	1.4	59.0	0.0	2.0	2.7	4.4	0.0	0.0	0.0	0.0	0.0	0.0
265	107	165	9.9	8.0	13.0	0.0	50.4	0.0	0.0	0.0	4.9	0.0	0.0	0.0	0.0	13.7	0.0
266	107	175	6.1	0.0	8.2	0.0	59.3	0.0	2.4	3.6	4.4	0.0	0.0	0.0	0.0	15.9	0.0
267	107	185	9.2	12.1	11.4	2.8	55.0	1.8	0.0	0.0	7.8	0.0	0.0	0.0	0.0	0.0	0.0
268	107	195	5.8	16.0	10.6	0.0	55.6	2.7	0.0	3.6	5.7	0.0	0.0	0.0	0.0	0.0	0.0
269	107	205	5.4	10.6	7.1	0.0	48.6	2.3	1.9	3.7	6.0	0.0	0.0	0.0	0.0	14.5	0.0
270	107	215	6.1	12.0	10.5	0.0	59.8	3.1	0.0	0.0	8.6	0.0	0.0	0.0	0.0	0.0	0.0
271	107	225	8.0	7.8	12.0	0.0	39.7	2.8	0.0	3.8	6.5	0.0	0.0	0.0	2.7	16.7	0.0
272	107	235	10.7	7.8	13.1	2.2	32.6	3.9	0.0	0.0	11.1	0.0	0.0	0.0	0.0	18.7	0.0
273	107	245	7.1	8.1	9.6	0.0	49.9	3.1	0.0	0.0	8.2	0.0	0.0	0.0	0.0	14.1	0.0
274	107	255	7.2	13.5	8.9	0.0	45.2	3.3	0.0	3.2	7.4	0.0	0.0	0.0	0.0	11.3	0.0
275	107	265	8.4	7.6	12.7	2.4	58.9	3.2	0.0	0.0	6.8	0.0	0.0	0.0	0.0	0.0	0.0
276	107	275	8.3	8.4	12.4	0.0	52.9	4.1	0.0	3.9	10.1	0.0	0.0	0.0	0.0	0.0	0.0
277	107	285	6.1	11.7	8.8	2.0	57.1	3.6	0.0	4.0	6.8	0.0	0.0	0.0	0.0	0.0	0.0
278	107	295	8.5	6.3	10.8	1.9	57.5	4.1	0.0	4.0	7.0	0.0	0.0	0.0	0.0	0.0	0.0
279	107	305	5.3	5.4	9.1	1.8	53.0	2.7	0.0	3.2	5.7	0.0	0.0	0.0	0.0	13.8	0.0
280	107	315	6.1	12.7	8.7	0.0	46.3	3.4	0.0	0.0	7.5	0.0	0.0	0.0	0.0	15.4	0.0

SAMPLE			MINERALOGY														
			Silicates					Carbonates							Evaporites		Sulfides
Seq	Site	Depth	Quartz	Kspar	Plag	Amph	ClayMin	Calcite	HiMgCal	Protodol	Dolomite	Mhydcal	Aragon	Magne	Thenar	Gypsum	Pyrite
no	ID	cm	%	%	%	%	%	%	%	%	%	%	%	%	%	%	%
281	107	325	6.0	8.3	11.3	0.0	58.6	4.4	0.0	4.2	7.2	0.0	0.0	0.0	0.0	0.0	0.0
282	107	335	5.9	13.0	10.3	0.0	53.8	3.9	0.0	4.2	5.6	0.0	0.0	0.0	3.4	0.0	0.0
283	107	345	6.9	9.1	11.6	0.0	55.4	5.1	3.7	0.0	8.2	0.0	0.0	0.0	0.0	0.0	0.0
284	107	355	5.2	7.4	9.4	2.2	52.1	3.5	0.0	0.0	6.3	0.0	0.0	0.0	0.0	14.0	0.0
285	107	365	7.0	7.5	10.8	0.0	61.1	3.1	2.8	0.0	7.7	0.0	0.0	0.0	0.0	0.0	0.0
286	107	375	7.2	12.3	9.8	0.0	58.0	3.8	2.2	0.0	6.8	0.0	0.0	0.0	0.0	0.0	0.0
287	107	385	6.5	15.3	11.3	0.0	53.0	5.0	0.0	0.0	9.0	0.0	0.0	0.0	0.0	0.0	0.0
288	107	395	5.2	13.4	9.1	0.0	61.3	3.1	2.8	0.0	5.3	0.0	0.0	0.0	0.0	0.0	0.0
289	107	405	6.4	11.7	7.5	0.0	57.3	3.6	2.2	3.3	8.1	0.0	0.0	0.0	0.0	0.0	0.0
290	107	415	5.0	7.5	17.7	0.0	56.2	3.3	0.0	3.9	6.5	0.0	0.0	0.0	0.0	0.0	0.0
291	107	425	10.4	7.9	11.8	0.0	52.0	6.7	0.0	0.0	11.3	0.0	0.0	0.0	0.0	0.0	0.0
292	107	435	6.1	7.4	11.9	0.0	58.7	3.5	0.0	4.6	7.9	0.0	0.0	0.0	0.0	0.0	0.0
293	107	445	8.4	6.1	30.7	0.0	40.4	2.5	2.2	2.8	6.9	0.0	0.0	0.0	0.0	0.0	0.0
294	107	455	7.7	13.0	12.1	0.0	49.1	3.2	2.3	4.1	8.6	0.0	0.0	0.0	0.0	0.0	0.0
295	107	465	9.5	13.1	9.5	0.0	54.5	3.5	0.0	0.0	9.8	0.0	0.0	0.0	0.0	0.0	0.0
296	107	475	5.7	11.7	9.7	0.0	38.9	3.2	2.3	0.0	7.0	0.0	0.0	3.0	0.0	18.5	0.0
297	107	485	6.0	15.0	11.0	2.0	50.9	3.6	0.0	3.4	8.2	0.0	0.0	0.0	0.0	0.0	0.0
298	107	495	8.1	18.6	13.3	0.0	40.0	5.3	0.0	4.5	10.2	0.0	0.0	0.0	0.0	0.0	0.0
299	107	505	7.7	12.7	7.7	0.0	55.9	3.8	0.0	4.1	8.2	0.0	0.0	0.0	0.0	0.0	0.0
300	107	515	7.1	10.4	10.2	0.0	44.5	3.1	0.0	0.0	9.3	0.0	0.0	0.0	0.0	15.4	0.0
301	107	525	7.1	15.2	11.8	2.2	46.3	4.7	0.0	3.9	8.7	0.0	0.0	0.0	0.0	0.0	0.0
302	107	535	7.5	13.2	9.3	1.8	56.0	3.8	0.0	0.0	8.4	0.0	0.0	0.0	0.0	0.0	0.0
303	107	545	6.5	10.6	10.7	0.0	46.2	3.1	0.0	3.1	7.0	0.0	0.0	0.0	0.0	12.8	0.0
304	107	555	8.1	8.1	14.1	0.0	55.5	4.4	0.0	0.0	9.8	0.0	0.0	0.0	0.0	0.0	0.0
305	107	565	6.5	7.4	8.4	3.0	62.2	5.4	0.0	0.0	7.2	0.0	0.0	0.0	0.0	0.0	0.0
306	107	575	6.2	43.3	4.6	0.0	34.2	2.3	1.6	2.4	5.3	0.0	0.0	0.0	0.0	0.0	0.0
307	107	585	11.3	16.8	15.3	0.0	0.0	6.8	0.0	7.1	13.6	0.0	0.0	0.0	0.0	29.1	0.0
308	107	595	5.6	46.6	6.4	0.0	32.0	2.6	0.0	0.0	6.8	0.0	0.0	0.0	0.0	0.0	0.0
309	107	605	3.5	38.8	4.6	0.0	35.2	2.8	0.0	0.0	4.2	0.0	0.0	0.0	0.0	10.9	0.0
310	107	615	10.3	7.5	11.3	2.4	51.1	4.2	3.2	0.0	10.0	0.0	0.0	0.0	0.0	0.0	0.0
311	107	625	3.9	40.6	6.2	1.4	35.8	3.1	1.5	2.2	5.2	0.0	0.0	0.0	0.0	0.0	0.0
312	107	635	6.7	9.3	10.5	0.0	61.1	5.2	0.0	0.0	7.3	0.0	0.0	0.0	0.0	0.0	0.0
313	107	645	3.9	44.6	6.8	0.0	33.0	3.2	1.6	2.4	4.5	0.0	0.0	0.0	0.0	0.0	0.0
314	107	655	4.8	6.6	9.6	0.0	45.6	3.9	2.6	3.5	6.7	0.0	0.0	0.0	0.0	16.8	0.0
315	107	665	3.7	43.3	7.4	0.0	34.2	2.9	0.0	2.4	4.2	0.0	0.0	0.0	1.9	0.0	0.0

SAMPLE			MINERALOGY														
			Silicates					Carbonates							Evaporites		Sulfides
Seq	Site	Depth	Quartz	Kspar	Plag	Amph	ClayMin	Calcite	HiMgCal	Protodol	Dolomite	Mhydcal	Aragon	Magne	Thenar	Gypsum	Pyrite
no	ID	cm	%	%	%	%	%	%	%	%	%	%	%	%	%	%	%
316	107	675	3.5	47.5	6.6	0.0	31.8	3.0	0.0	0.0	4.8	0.0	0.0	2.8	0.0	0.0	0.0
317	107	685	4.2	40.9	5.5	1.1	30.7	2.8	0.0	0.0	4.2	0.0	0.0	0.0	0.0	10.7	0.0
318	107	695	4.7	6.7	8.7	2.2	45.0	4.5	0.0	2.8	6.0	0.0	0.0	3.0	0.0	16.4	0.0
319	110A	5	7.0	10.4	11.1	1.7	47.2	1.6	1.9	3.2	0.0	0.0	2.1	0.0	0.0	14.0	0.0
320	110A	15	11.8	12.7	11.8	0.0	56.1	2.0	2.3	3.3	0.0	0.0	0.0	0.0	0.0	0.0	0.0
321	110A	25	10.3	6.8	14.1	0.0	48.7	0.0	1.6	3.1	0.0	0.0	0.0	0.0	0.0	15.4	0.0
322	110A	35	9.3	8.9	8.4	1.7	57.5	0.0	0.0	2.7	0.0	0.0	0.0	0.0	0.0	11.5	0.0
323	110A	45	9.0	11.3	11.3	0.0	62.2	1.5	1.9	2.9	0.0	0.0	0.0	0.0	0.0	0.0	0.0
324	110A	55	10.1	11.8	9.0	1.8	51.1	0.0	0.0	2.6	0.0	0.0	0.0	0.0	0.0	13.6	0.0
325	110A	65	8.3	6.5	11.1	1.6	55.8	0.0	1.6	2.6	0.0	0.0	0.0	0.0	0.0	12.5	0.0
326	110A	75	9.1	9.0	12.9	0.0	49.7	0.0	1.6	2.6	0.0	0.0	0.0	0.0	0.0	15.1	0.0
327	110A	85	14.7	8.9	13.8	0.0	46.3	0.0	1.7	3.0	0.0	0.0	0.0	0.0	0.0	11.7	0.0
328	110A	95	11.8	11.1	18.4	1.6	36.9	1.4	1.4	2.6	0.0	0.0	0.0	0.0	0.0	14.9	0.0
329	110A	105	15.7	13.5	14.5	2.6	47.1	0.0	2.1	4.5	0.0	0.0	0.0	0.0	0.0	0.0	0.0
330	110A	115	8.1	9.9	13.2	1.2	51.2	0.0	0.0	2.9	0.0	0.0	0.0	0.0	0.0	13.5	0.0
331	110A	125	11.5	12.6	17.7	0.0	41.7	0.0	1.4	2.4	0.0	0.0	0.0	0.0	0.0	12.7	0.0
332	110A	135	9.1	7.9	0.0	0.0	58.2	1.9	2.1	3.4	0.0	0.0	0.0	0.0	0.0	17.4	0.0
333	110A	145	8.3	6.8	10.7	0.0	58.1	0.0	1.7	1.9	0.0	0.0	0.0	0.0	0.0	12.5	0.0
334	110A	155	7.8	8.2	8.6	0.0	55.6	1.3	1.9	2.6	0.0	0.0	0.0	0.0	0.0	14.0	0.0
335	110A	165	10.6	8.0	9.9	0.0	63.6	1.5	2.5	3.9	0.0	0.0	0.0	0.0	0.0	0.0	0.0
336	110A	175	11.0	5.9	13.6	0.0	48.3	0.0	1.9	2.9	2.8	0.0	0.0	0.0	0.0	13.5	0.0
337	110A	185	11.6	16.9	20.6	0.0	38.9	0.0	2.7	3.6	5.6	0.0	0.0	0.0	0.0	0.0	0.0
338	110A	195	7.5	11.5	9.2	1.7	46.2	0.0	1.7	2.6	5.0	0.0	0.0	0.0	0.0	14.6	0.0
339	110A	205	13.4	8.2	11.8	0.0	40.4	1.1	1.8	2.8	6.0	0.0	0.0	0.0	0.0	14.5	0.0
340	110A	215	4.7	11.2	9.2	0.0	52.4	2.2	0.0	4.1	0.0	0.0	0.0	0.0	0.0	16.2	0.0
341	110A	225	5.1	7.0	9.7	0.0	67.3	2.8	0.0	4.2	3.9	0.0	0.0	0.0	0.0	0.0	0.0
342	113A	5	11.4	6.0	11.9	0.0	51.8	0.0	0.0	3.0	2.1	0.0	1.6	0.0	0.0	12.2	0.0
343	113A	15	12.8	13.4	16.6	0.0	53.1	0.0	0.0	4.2	0.0	0.0	0.0	0.0	0.0	0.0	0.0
344	113A	25	15.2	6.1	9.9	2.6	60.2	0.0	2.2	3.8	0.0	0.0	0.0	0.0	0.0	0.0	0.0
345	113A	35	9.9	7.2	11.8	1.7	47.6	0.0	1.7	2.9	0.0	0.0	0.0	0.0	0.0	17.3	0.0
346	113A	45	10.1	8.9	11.5	0.0	44.3	1.2	1.4	3.4	0.0	0.0	0.0	0.0	0.0	19.2	0.0
347	113A	55	10.4	7.6	11.2	0.0	65.7	0.0	1.8	3.3	0.0	0.0	0.0	0.0	0.0	0.0	0.0
348	113A	65	8.0	9.8	10.6	0.0	53.8	1.3	1.7	13.1	0.0	0.0	1.8	0.0	0.0	0.0	0.0
349	113A	75	9.6	5.2	16.4	0.0	48.7	0.0	2.0	2.6	1.8	0.0	0.0	0.0	0.0	13.7	0.0
350	113A	85	9.9	12.1	12.8	1.9	58.5	0.0	1.8	3.0	0.0	0.0	0.0	0.0	0.0	0.0	0.0

SAMPLE			MINERALOGY														
			Silicates					Carbonates							Evaporites		Sulfides
Seq	Site	Depth	Quartz	Kspar	Plag	Amph	ClayMin	Calcite	HiMgCal	Protodol	Dolomite	Mhydcal	Aragon	Magne	Thenar	Gypsum	Pyrite
no	ID	cm	%	%	%	%	%	%	%	%	%	%	%	%	%	%	%
351	113A	95	11.8	6.8	11.4	0.0	52.2	0.0	2.0	2.9	0.0	0.0	0.0	0.0	0.0	12.9	0.0
352	113A	105	9.7	8.5	8.6	1.5	50.8	0.0	1.6	2.6	0.0	0.0	0.0	0.0	0.0	16.6	0.0
353	113A	115	11.8	6.4	17.3	0.0	62.9	1.7	0.0	0.0	0.0	0.0	0.0	0.0	0.0	0.0	0.0
354	113A	125	8.7	7.8	19.5	0.0	58.1	0.0	2.0	3.8	0.0	0.0	0.0	0.0	0.0	0.0	0.0
355	113A	135	9.6	7.7	13.2	2.1	51.7	0.0	2.0	0.0	4.2	0.0	0.0	0.0	0.0	9.6	0.0
356	113A	145	8.0	6.6	6.7	0.0	55.3	0.0	1.4	2.1	7.6	0.0	0.0	0.0	0.0	12.3	0.0
357	113A	155	10.3	6.9	8.1	0.0	59.1	0.0	2.7	4.2	8.7	0.0	0.0	0.0	0.0	0.0	0.0
358	113A	165	9.2	10.2	8.5	0.0	48.4	0.0	0.0	2.5	8.1	0.0	0.0	0.0	0.0	13.2	0.0
359	113A	175	8.6	12.0	9.1	1.7	58.7	0.0	0.0	2.7	7.2	0.0	0.0	0.0	0.0	0.0	0.0
360	113A	185	10.0	6.0	7.4	0.0	65.9	0.0	1.9	0.0	8.8	0.0	0.0	0.0	0.0	0.0	0.0
361	113A	195	10.3	10.8	9.8	0.0	60.6	0.0	0.0	0.0	8.6	0.0	0.0	0.0	0.0	0.0	0.0
362	113A	205	9.6	6.6	10.0	0.0	58.4	0.0	0.0	3.7	11.6	0.0	0.0	0.0	0.0	0.0	0.0
363	115	5	5.6	8.9	6.1	0.0	77.3	0.0	0.0	0.0	2.2	0.0	0.0	0.0	0.0	0.0	0.0
364	115	15	6.3	9.1	4.7	0.0	77.4	0.0	0.0	2.4	0.0	0.0	0.0	0.0	0.0	0.0	0.0
365	115	25	6.6	0.0	5.6	0.0	71.0	0.0	0.0	0.0	0.0	0.0	0.0	2.4	0.0	14.5	0.0
366	115	35	8.1	5.8	9.1	0.0	70.7	0.0	2.5	0.0	0.0	0.0	0.0	3.8	0.0	0.0	0.0
367	115	45	6.7	5.4	6.5	1.8	77.2	0.0	2.2	0.0	0.0	0.0	0.0	0.0	0.0	0.0	0.0
368	115	55	7.6	6.9	6.8	0.0	78.8	0.0	0.0	0.0	0.0	0.0	0.0	0.0	0.0	0.0	0.0
369	115	65	9.4	6.6	6.7	0.0	71.6	0.0	2.4	3.2	0.0	0.0	0.0	0.0	0.0	0.0	0.0
370	115	75	6.3	0.0	5.6	0.0	85.3	0.0	0.0	0.0	2.8	0.0	0.0	0.0	0.0	0.0	0.0
371	115	85	8.1	6.8	7.6	0.0	71.3	0.0	2.7	0.0	3.6	0.0	0.0	0.0	0.0	0.0	0.0
372	115	95	7.2	5.8	6.2	0.0	75.7	0.0	1.9	0.0	3.2	0.0	0.0	0.0	0.0	0.0	0.0
373	115	105	7.0	0.0	7.3	1.9	77.2	0.0	0.0	3.1	3.5	0.0	0.0	0.0	0.0	0.0	0.0
374	115	115	7.7	5.7	8.3	0.0	68.0	2.4	0.0	0.0	3.8	0.0	4.1	0.0	0.0	0.0	0.0
375	115	125	8.8	0.0	8.4	0.0	80.2	0.0	2.6	0.0	0.0	0.0	0.0	0.0	0.0	0.0	0.0
376	115	135	5.8	4.1	5.5	0.0	65.0	0.0	0.0	2.8	3.0	0.0	0.0	0.0	0.0	13.8	0.0
377	115	145	6.9	5.0	5.4	0.0	66.4	0.0	0.0	0.0	3.4	0.0	0.0	0.0	0.0	13.0	0.0
378	115	155	9.4	6.8	13.6	0.0	66.2	0.0	0.0	0.0	4.0	0.0	0.0	0.0	0.0	0.0	0.0
379	115	165	8.1	9.7	6.2	0.0	69.6	0.0	0.0	2.6	3.8	0.0	0.0	0.0	0.0	0.0	0.0
380	115	175	7.9	6.4	6.0	0.0	70.1	0.0	2.4	3.0	4.2	0.0	0.0	0.0	0.0	0.0	0.0
381	115	185	10.1	6.1	6.1	0.0	73.2	0.0	0.0	0.0	4.6	0.0	0.0	0.0	0.0	0.0	0.0
382	115	195	7.3	8.9	5.4	0.0	62.8	0.0	0.0	0.0	3.1	0.0	0.0	0.0	0.0	12.6	0.0
383	115	205	11.0	7.3	2.9	0.0	61.1	0.0	0.0	0.0	4.1	0.0	0.0	0.0	0.0	13.5	0.0
384	115	215	26.0	7.1	15.3	0.0	44.8	0.0	2.2	0.0	4.6	0.0	0.0	0.0	0.0	0.0	0.0
385	115	225	12.9	5.0	8.0	0.0	63.1	0.0	1.6	3.0	6.4	0.0	0.0	0.0	0.0	0.0	0.0

SAMPLE			MINERALOGY														
			Silicates					Carbonates							Evaporites		Sulfides
Seq	Site	Depth	Quartz	Kspar	Plag	Amph	ClayMin	Calcite	HiMgCal	Protodol	Dolomite	Mhydcal	Aragon	Magne	Thenar	Gypsum	Pyrite
no	ID	cm	%	%	%	%	%	%	%	%	%	%	%	%	%	%	%
386	115	235	19.5	7.5	9.0	2.1	51.8	0.0	2.3	0.0	7.8	0.0	0.0	0.0	0.0	0.0	0.0
387	115	245	19.1	5.3	10.7	0.0	54.4	0.0	0.0	3.0	7.5	0.0	0.0	0.0	0.0	0.0	0.0
388	115	255	21.5	8.4	21.3	1.9	36.6	0.0	0.0	4.2	6.1	0.0	0.0	0.0	0.0	0.0	0.0
389	115	265	14.4	5.9	5.9	0.0	50.8	0.0	1.9	2.2	7.9	0.0	0.0	0.0	0.0	11.1	0.0
390	120	5	7.0	9.5	6.6	0.0	71.9	0.0	0.0	0.0	5.1	0.0	0.0	0.0	0.0	0.0	0.0
391	120	15	7.3	0.0	8.9	0.0	76.5	0.0	2.1	0.0	5.3	0.0	0.0	0.0	0.0	0.0	0.0
392	120	25	9.7	5.5	7.1	0.0	73.4	0.0	0.0	0.0	4.4	0.0	0.0	0.0	0.0	0.0	0.0
393	120	35	9.4	9.7	6.4	0.0	64.8	0.0	2.0	4.7	3.0	0.0	0.0	0.0	0.0	0.0	0.0
394	120	45	8.9	7.3	6.7	0.0	58.4	0.0	1.4	2.4	4.4	0.0	10.6	0.0	0.0	0.0	0.0
395	120	55	10.9	5.5	6.1	0.0	59.3	0.0	0.0	0.0	6.7	0.0	11.5	0.0	0.0	0.0	0.0
396	120	65	10.4	5.3	7.1	0.0	53.4	0.0	0.0	2.7	6.3	0.0	13.4	0.0	0.0	1.5	0.0
397	120	75	8.6	4.8	6.1	0.0	60.2	0.0	0.0	0.0	4.7	0.0	13.9	0.0	0.0	1.7	0.0
398	120	85	10.1	4.9	6.6	0.0	57.1	0.0	1.7	0.0	8.1	0.0	11.6	0.0	0.0	0.0	0.0
399	120	95	10.6	10.6	9.6	0.0	57.3	0.0	1.9	2.7	7.2	0.0	0.0	0.0	0.0	0.0	0.0
400	120	105	9.0	4.8	6.0	0.0	57.9	0.0	0.0	2.7	5.4	0.0	12.4	0.0	0.0	1.8	0.0
401	120	115	8.8	5.6	6.5	0.0	53.6	1.4	0.0	2.2	7.6	0.0	14.3	0.0	0.0	0.0	0.0
402	120	125	9.5	10.2	8.2	0.0	51.5	0.0	0.0	0.0	8.2	0.0	12.4	0.0	0.0	0.0	0.0
403	120	135	10.1	4.4	6.1	0.0	52.9	0.0	1.9	2.5	9.0	0.0	13.1	0.0	0.0	0.0	0.0
404	120	145	10.3	9.0	7.2	0.0	46.5	0.0	0.0	2.7	13.7	0.0	10.6	0.0	0.0	0.0	0.0
405	120	155	10.4	0.0	6.7	0.0	64.9	0.0	2.0	3.0	11.5	0.0	0.0	0.0	0.0	1.5	0.0
406	120	165	11.1	5.7	9.1	0.0	56.1	0.0	0.0	3.6	14.5	0.0	0.0	0.0	0.0	0.0	0.0
407	120	175	10.2	5.2	8.2	0.0	58.2	0.0	2.4	0.0	15.8	0.0	0.0	0.0	0.0	0.0	0.0
408	120	185	10.2	11.8	5.5	0.0	51.8	1.6	0.0	2.6	14.7	0.0	0.0	0.0	0.0	1.9	0.0
409	120	195	6.8	8.8	10.6	0.0	61.6	0.0	2.9	5.3	0.0	0.0	0.0	4.0	0.0	0.0	0.0
410	120	205	5.9	13.5	11.1	0.0	46.8	0.0	2.4	3.1	0.0	0.0	14.6	0.0	0.0	2.6	0.0
411	120	215	4.8	10.1	35.1	0.0	31.2	0.0	1.5	2.6	1.9	0.0	12.8	0.0	0.0	0.0	0.0
412	120	225	8.6	15.3	12.7	0.0	54.1	0.0	2.0	4.5	0.0	0.0	0.0	0.0	0.0	2.8	0.0
413	120	235	5.9	12.7	10.8	0.0	46.1	0.0	2.5	4.2	0.0	0.0	17.8	0.0	0.0	0.0	0.0
414	120	245	8.7	16.5	11.5	0.0	59.0	0.0	0.0	4.2	0.0	0.0	0.0	0.0	0.0	0.0	0.0
415	120	255	8.4	8.3	0.0	0.0	55.0	0.0	2.9	4.5	0.0	0.0	20.8	0.0	0.0	0.0	0.0
416	120	265	6.2	8.0	11.1	0.0	48.2	0.0	0.0	4.0	0.0	0.0	20.2	0.0	0.0	2.5	0.0
417	120	275	6.4	8.4	8.5	0.0	68.9	0.0	3.1	4.8	0.0	0.0	0.0	0.0	0.0	0.0	0.0
418	120	285	7.3	13.7	8.2	0.0	66.7	0.0	0.0	4.2	0.0	0.0	0.0	0.0	0.0	0.0	0.0
419	120	295	7.2	6.3	10.2	0.0	72.2	0.0	0.0	4.2	0.0	0.0	0.0	0.0	0.0	0.0	0.0
420	120	305	8.0	8.6	10.3	0.0	66.8	2.3	0.0	0.0	4.0	0.0	0.0	0.0	0.0	0.0	0.0

SAMPLE			MINERALOGY														
			Silicates					Carbonates							Evaporites		Sulfides
Seq	Site	Depth	Quartz	Kspar	Plag	Amph	ClayMin	Calcite	HiMgCal	Protodol	Dolomite	Mhydcal	Aragon	Magne	Thenar	Gypsum	Pyrite
no	ID	cm	%	%	%	%	%	%	%	%	%	%	%	%	%	%	%
421	120	315	7.4	7.1	7.9	0.0	68.3	0.0	3.0	3.1	3.2	0.0	0.0	0.0	0.0	0.0	0.0
422	120	325	7.5	0.0	0.0	0.0	81.8	4.0	2.3	0.0	4.4	0.0	0.0	0.0	0.0	0.0	0.0
423	120	335	9.4	0.0	5.8	0.0	73.6	3.0	0.0	0.0	5.3	0.0	0.0	2.9	0.0	0.0	0.0
424	120	345	9.5	5.4	5.7	0.0	67.7	3.5	2.3	0.0	6.0	0.0	0.0	0.0	0.0	0.0	0.0
425	121	5	5.7	10.7	6.0	0.0	70.8	0.0	0.0	3.9	0.0	0.0	0.0	2.9	0.0	0.0	0.0
426	121	15	5.4	5.7	6.0	0.0	76.2	2.9	0.0	3.9	0.0	0.0	0.0	0.0	0.0	0.0	0.0
427	121	25	5.3	0.0	6.2	0.0	81.9	0.0	0.0	3.9	2.8	0.0	0.0	0.0	0.0	0.0	0.0
428	121	35	6.9	0.0	6.7	0.0	83.9	0.0	2.6	0.0	0.0	0.0	0.0	0.0	0.0	0.0	0.0
429	121	45	5.7	5.3	7.4	0.0	69.6	0.0	0.0	0.0	0.0	0.0	0.0	0.0	0.0	12.0	0.0
430	121	55	5.9	6.1	6.9	0.0	81.2	0.0	0.0	0.0	0.0	0.0	0.0	0.0	0.0	0.0	0.0
431	121	65	7.2	0.0	7.3	0.0	85.5	0.0	0.0	0.0	0.0	0.0	0.0	0.0	0.0	0.0	0.0
432	121	75	6.2	4.7	5.7	0.0	78.5	0.0	2.3	2.6	0.0	0.0	0.0	0.0	0.0	0.0	0.0
433	121	85	6.5	10.1	5.6	0.0	75.7	0.0	2.1	0.0	0.0	0.0	0.0	0.0	0.0	0.0	0.0
434	121	95	4.4	0.0	5.4	0.0	72.9	0.0	0.0	2.5	0.0	0.0	0.0	0.0	0.0	14.8	0.0
435	121	105	7.3	6.4	6.4	0.0	80.0	0.0	0.0	0.0	0.0	0.0	0.0	0.0	0.0	0.0	0.0
436	121	115	6.1	4.8	5.5	0.0	74.4	1.7	4.7	2.8	0.0	0.0	0.0	0.0	0.0	0.0	0.0
437	121	125	7.0	5.2	6.2	0.0	79.3	0.0	2.4	0.0	0.0	0.0	0.0	0.0	0.0	0.0	0.0
438	121	135	5.8	8.2	5.0	0.0	76.7	0.0	1.8	2.6	0.0	0.0	0.0	0.0	0.0	0.0	0.0
439	121	145	5.9	5.3	6.2	0.0	79.3	0.0	0.0	3.3	0.0	0.0	0.0	0.0	0.0	0.0	0.0
440	121	155	6.3	0.0	5.9	0.0	76.6	0.0	11.2	0.0	0.0	0.0	0.0	0.0	0.0	0.0	0.0
441	121	165	6.5	0.0	5.9	0.0	84.9	0.0	0.0	0.0	0.0	0.0	0.0	2.8	0.0	0.0	0.0
442	121	175	5.9	8.5	5.8	0.0	77.6	0.0	2.2	0.0	0.0	0.0	0.0	0.0	0.0	0.0	0.0
443	121	185	5.6	4.8	6.0	0.0	79.5	0.0	2.2	1.9	0.0	0.0	0.0	0.0	0.0	0.0	0.0
444	121	195	5.9	9.6	5.0	0.0	64.8	0.0	0.0	0.0	0.0	0.0	0.0	0.0	0.0	14.7	0.0
445	121	205	7.5	5.2	5.7	0.0	76.5	0.0	2.3	2.9	0.0	0.0	0.0	0.0	0.0	0.0	0.0
446	121	215	5.7	9.0	5.2	0.0	62.3	0.0	0.0	0.0	2.6	0.0	0.0	0.0	0.0	15.3	0.0
447	121	225	6.2	4.7	7.8	1.6	64.8	0.0	0.0	2.4	0.0	0.0	0.0	0.0	0.0	12.5	0.0
448	121	235	7.9	5.7	6.2	0.0	74.3	0.0	2.7	0.0	3.2	0.0	0.0	0.0	0.0	0.0	0.0
449	121	245	6.1	5.5	5.4	0.0	67.3	0.0	0.0	2.8	0.0	0.0	0.0	0.0	0.0	13.0	0.0
450	121	255	7.2	5.0	6.3	0.0	76.1	0.0	2.4	0.0	2.9	0.0	0.0	0.0	0.0	0.0	0.0
451	121	265	7.8	5.3	7.4	0.0	73.4	0.0	0.0	3.3	2.8	0.0	0.0	0.0	0.0	0.0	0.0
452	121	275	7.5	5.9	7.2	0.0	73.9	0.0	2.3	0.0	3.3	0.0	0.0	0.0	0.0	0.0	0.0
453	121	285	7.0	9.8	6.6	0.0	66.3	1.8	2.0	3.4	3.2	0.0	0.0	0.0	0.0	0.0	0.0
454	121	295	5.5	5.1	5.6	0.0	74.3	0.0	2.4	2.9	4.2	0.0	0.0	0.0	0.0	0.0	0.0
455	121	305	6.9	5.7	6.0	0.0	73.5	0.0	0.0	3.1	5.0	0.0	0.0	0.0	0.0	0.0	0.0

SAMPLE			MINERALOGY														
			Silicates					Carbonates							Evaporites		Sulfides
Seq	Site	Depth	Quartz	Kspar	Plag	Amph	ClayMin	Calcite	HiMgCal	Protodol	Dolomite	Mhydcal	Aragon	Magne	Thenar	Gypsum	Pyrite
no	ID	cm	%	%	%	%	%	%	%	%	%	%	%	%	%	%	%
456	121	315	8.8	6.5	7.4	0.0	71.8	0.0	0.0	0.0	5.6	0.0	0.0	0.0	0.0	0.0	0.0
457	121	325	7.1	11.7	6.9	0.0	66.9	0.0	0.0	3.5	3.9	0.0	0.0	0.0	0.0	0.0	0.0
458	121	335	8.4	5.3	5.9	0.0	59.3	0.0	2.2	0.0	6.0	0.0	0.0	0.0	0.0	13.0	0.0
459	121	345	9.5	6.5	7.9	0.0	69.6	0.0	0.0	0.0	6.6	0.0	0.0	0.0	0.0	0.0	0.0
460	121	355	8.6	0.0	5.7	0.0	75.4	0.0	2.9	0.0	7.4	0.0	0.0	0.0	0.0	0.0	0.0
461	121	365	6.8	9.8	7.0	0.0	71.1	0.0	0.0	0.0	5.4	0.0	0.0	0.0	0.0	0.0	0.0
462	121	375	7.4	6.4	6.9	2.1	68.7	0.0	1.6	0.0	7.0	0.0	0.0	0.0	0.0	0.0	0.0
463	121	385	7.0	0.0	6.4	2.0	73.1	0.0	0.0	0.0	7.9	0.0	0.0	0.0	3.7	0.0	0.0
464	121	395	7.1	5.8	7.5	0.0	65.7	0.0	0.0	3.4	7.3	0.0	0.0	0.0	3.1	0.0	0.0
465	121	405	7.4	5.5	7.4	0.0	70.7	0.0	2.0	0.0	7.0	0.0	0.0	0.0	0.0	0.0	0.0
466	121	415	7.4	10.9	8.5	0.0	65.1	0.0	0.0	0.0	8.2	0.0	0.0	0.0	0.0	0.0	0.0
467	121	425	7.9	5.5	7.8	0.0	68.7	0.0	0.0	3.1	7.1	0.0	0.0	0.0	0.0	0.0	0.0
468	121	435	8.5	9.8	5.8	0.0	61.4	0.0	2.2	2.9	9.5	0.0	0.0	0.0	0.0	0.0	0.0
469	121	445	7.4	0.0	6.8	1.6	73.5	0.0	2.2	0.0	8.6	0.0	0.0	0.0	0.0	0.0	0.0
470	121	455	7.9	5.0	6.4	0.0	71.0	0.0	0.0	0.0	9.7	0.0	0.0	0.0	0.0	0.0	0.0
471	121	465	8.0	4.6	6.2	0.0	69.7	0.0	0.0	0.0	11.5	0.0	0.0	0.0	0.0	0.0	0.0
472	121	475	5.3	4.5	5.3	0.0	74.4	2.6	2.3	0.0	5.7	0.0	0.0	0.0	0.0	0.0	0.0
473	121	485	4.6	0.0	7.0	0.0	57.9	4.0	0.0	2.8	9.6	0.0	0.0	2.6	0.0	11.7	0.0
474	121	495	6.1	4.6	4.5	0.0	58.3	4.4	0.0	0.0	9.6	0.0	0.0	0.0	0.0	12.5	0.0
475	121	505	6.8	0.0	6.9	0.0	74.8	5.7	0.0	0.0	5.7	0.0	0.0	0.0	0.0	0.0	0.0
476	121	515	6.0	5.3	5.4	0.0	71.2	4.2	0.0	3.1	4.8	0.0	0.0	0.0	0.0	0.0	0.0
477	121	525	7.0	0.0	4.7	0.0	64.3	3.6	2.4	0.0	4.4	0.0	0.0	0.0	0.0	13.6	0.0
478	121	535	7.6	0.0	5.3	0.0	75.8	3.8	2.1	0.0	5.5	0.0	0.0	0.0	0.0	0.0	0.0
479	121	545	6.5	0.0	5.6	0.0	76.2	5.1	0.0	0.0	6.6	0.0	0.0	0.0	0.0	0.0	0.0
480	122A	5	7.1	9.7	5.9	0.0	74.9	0.0	0.0	0.0	2.4	0.0	0.0	0.0	0.0	0.0	0.0
481	122A	15	5.8	4.0	4.7	0.0	71.8	0.0	1.5	2.0	0.0	0.0	0.0	0.0	0.0	10.3	0.0
482	122A	25	8.1	5.2	6.0	0.0	78.5	0.0	2.2	0.0	0.0	0.0	0.0	0.0	0.0	0.0	0.0
483	122A	35	8.4	0.0	5.7	0.0	85.9	0.0	0.0	0.0	0.0	0.0	0.0	0.0	0.0	0.0	0.0
484	122A	45	7.6	0.0	5.6	0.0	84.5	0.0	2.3	0.0	0.0	0.0	0.0	0.0	0.0	0.0	0.0
485	122A	55	7.2	0.0	4.8	0.0	69.8	0.0	1.7	2.2	2.3	0.0	0.0	0.0	0.0	12.1	0.0
486	122A	65	8.4	0.0	4.9	0.0	82.4	0.0	2.0	2.3	0.0	0.0	0.0	0.0	0.0	0.0	0.0
487	122A	75	7.5	4.6	5.9	0.0	78.1	0.0	1.9	0.0	2.1	0.0	0.0	0.0	0.0	0.0	0.0
488	122A	85	6.4	7.8	5.4	0.0	76.7	0.0	1.7	0.0	2.0	0.0	0.0	0.0	0.0	0.0	0.0
489	122A	95	6.9	4.7	4.9	0.0	79.0	0.0	2.0	0.0	2.6	0.0	0.0	0.0	0.0	0.0	0.0
490	122A	105	6.8	3.6	5.6	0.0	80.3	0.0	1.5	0.0	2.2	0.0	0.0	0.0	0.0	0.0	0.0

SAMPLE			MINERALOGY														
			Silicates					Carbonates							Evaporites		Sulfides
Seq	Site	Depth	Quartz	Kspar	Plag	Amph	ClayMin	Calcite	HiMgCal	Protodol	Dolomite	Mhydcal	Aragon	Magne	Thenar	Gypsum	Pyrite
no	ID	cm	%	%	%	%	%	%	%	%	%	%	%	%	%	%	%
491	122A	115	6.0	3.8	4.7	0.0	85.5	0.0	0.0	0.0	0.0	0.0	0.0	0.0	0.0	0.0	0.0
492	122A	125	7.6	4.8	5.7	0.0	80.5	1.4	0.0	0.0	0.0	0.0	0.0	0.0	0.0	0.0	0.0
493	122A	135	7.4	0.0	6.0	0.0	80.8	0.0	1.9	3.9	0.0	0.0	0.0	0.0	0.0	0.0	0.0
494	122A	145	7.0	4.0	4.8	0.0	82.3	0.0	0.0	1.9	0.0	0.0	0.0	0.0	0.0	0.0	0.0
495	122A	155	8.2	4.9	6.4	0.0	74.6	0.0	2.6	0.0	3.3	0.0	0.0	0.0	0.0	0.0	0.0
496	122A	165	8.8	5.9	7.1	0.0	74.3	0.0	0.0	0.0	3.9	0.0	0.0	0.0	0.0	0.0	0.0
497	122A	175	7.3	0.0	4.9	0.0	81.9	0.0	0.0	2.6	3.3	0.0	0.0	0.0	0.0	0.0	0.0
498	122A	185	7.4	5.2	6.0	0.0	76.4	0.0	1.8	0.0	3.2	0.0	0.0	0.0	0.0	0.0	0.0
499	122A	195	7.4	0.0	5.0	0.0	82.3	0.0	2.2	0.0	3.1	0.0	0.0	0.0	0.0	0.0	0.0
500	122A	205	6.5	4.1	4.4	0.0	81.2	0.0	0.0	0.0	3.7	0.0	0.0	0.0	0.0	0.0	0.0
501	122A	215	9.2	7.5	6.9	0.0	66.8	0.0	3.0	0.0	6.5	0.0	0.0	0.0	0.0	0.0	0.0
502	122A	225	8.5	0.0	5.8	0.0	80.7	0.0	0.0	2.5	2.5	0.0	0.0	0.0	0.0	0.0	0.0
503	122A	235	6.9	5.3	5.7	0.0	76.5	0.0	2.0	0.0	3.6	0.0	0.0	0.0	0.0	0.0	0.0
504	122A	245	8.1	4.7	6.6	0.0	75.1	0.0	0.0	0.0	5.5	0.0	0.0	0.0	0.0	0.0	0.0
505	122A	255	8.6	9.9	6.8	0.0	56.6	0.0	1.9	0.0	4.0	0.0	0.0	0.0	0.0	12.3	0.0
506	122A	265	7.4	5.4	5.6	0.0	74.5	0.0	0.0	2.5	4.6	0.0	0.0	0.0	0.0	0.0	0.0
507	122A	275	9.1	11.3	6.8	0.0	65.4	0.0	2.3	0.0	5.1	0.0	0.0	0.0	0.0	0.0	0.0
508	122A	285	8.6	5.8	6.8	0.0	69.6	1.5	2.2	0.0	5.6	0.0	0.0	0.0	0.0	0.0	0.0
509	122A	295	9.8	5.3	7.4	0.0	66.2	0.0	2.2	0.0	9.1	0.0	0.0	0.0	0.0	0.0	0.0
510	122A	305	9.1	0.0	6.4	0.0	72.9	0.0	2.0	0.0	6.4	0.0	3.3	0.0	0.0	0.0	0.0
511	122A	315	9.7	4.7	5.8	0.0	71.4	0.0	0.0	0.0	8.4	0.0	0.0	0.0	0.0	0.0	0.0
512	122A	325	9.6	0.0	7.7	0.0	72.8	0.0	0.0	0.0	10.0	0.0	0.0	0.0	0.0	0.0	0.0
513	122A	335	6.5	6.8	5.4	0.0	63.8	0.0	1.5	0.0	6.4	0.0	0.0	0.0	0.0	9.5	0.0
514	122A	345	8.0	0.0	6.0	0.0	71.3	1.5	1.7	2.3	9.2	0.0	0.0	0.0	0.0	0.0	0.0
515	122A	355	10.1	5.8	6.9	0.0	64.0	0.0	0.0	0.0	11.3	0.0	0.0	2.0	0.0	0.0	0.0
516	122A	365	7.7	4.7	5.8	0.0	57.3	2.1	1.9	2.7	18.0	0.0	0.0	0.0	0.0	0.0	0.0
517	122A	375	10.7	6.5	7.1	0.0	53.4	2.6	0.0	0.0	19.6	0.0	0.0	0.0	0.0	0.0	0.0
518	122A	385	8.6	5.2	8.1	0.0	50.4	2.9	1.9	2.7	20.2	0.0	0.0	0.0	0.0	0.0	0.0
519	122A	395	8.1	0.0	8.8	0.0	56.9	3.7	0.0	0.0	22.5	0.0	0.0	0.0	0.0	0.0	0.0
520	122A	405	7.1	5.6	12.5	0.0	45.6	2.9	0.0	3.0	23.5	0.0	0.0	0.0	0.0	0.0	0.0
521	122A	415	8.0	4.6	7.3	0.0	57.2	3.0	0.0	0.0	19.8	0.0	0.0	0.0	0.0	0.0	0.0
522	122A	425	7.9	11.0	6.9	0.0	39.9	1.9	0.0	0.0	22.3	0.0	0.0	0.0	0.0	10.1	0.0
523	122A	435	7.6	4.5	5.7	0.0	74.7	0.0	2.2	0.0	5.4	0.0	0.0	0.0	0.0	0.0	0.0
524	122A	445	7.0	6.1	8.8	0.0	58.9	0.0	4.5	0.0	14.8	0.0	0.0	0.0	0.0	0.0	0.0
525	122A	455	8.0	0.0	8.4	0.0	59.2	5.0	0.0	2.8	16.7	0.0	0.0	0.0	0.0	0.0	0.0

SAMPLE			MINERALOGY														
			Silicates					Carbonates							Evaporites		Sulfides
Seq	Site	Depth	Quartz	Kspar	Plag	Amph	ClayMin	Calcite	HiMgCal	Protodol	Dolomite	Mhydcal	Aragon	Magne	Thenar	Gypsum	Pyrite
no	ID	cm	%	%	%	%	%	%	%	%	%	%	%	%	%	%	%
526	122A	465	6.5	5.1	7.7	0.0	45.7	4.3	0.0	0.0	15.6	0.0	0.0	0.0	0.0	15.2	0.0
527	122A	475	10.0	4.1	7.8	0.0	64.7	0.0	2.1	3.1	8.2	0.0	0.0	0.0	0.0	0.0	0.0
528	1A	1	7.9	9.0	10.9	0.0	49.8	0.0	0.0	3.1	19.3	0.0	0.0	0.0	0.0	0.0	0.0
529	1A	2	8.0	6.1	7.9	0.0	55.4	0.0	2.2	0.0	20.4	0.0	0.0	0.0	0.0	0.0	0.0
530	1A	3	9.5	8.5	8.9	0.0	44.0	0.0	0.0	0.0	16.9	0.0	0.0	0.0	0.0	12.3	0.0
531	1A	4	10.1	10.2	9.7	0.0	45.7	1.1	2.0	0.0	21.2	0.0	0.0	0.0	0.0	0.0	0.0
532	1A	5	7.0	8.9	5.1	0.0	51.4	0.0	1.6	2.6	14.3	0.0	0.0	0.0	0.0	9.1	0.0
533	1A	6	10.3	5.2	11.5	0.0	52.0	0.0	0.0	2.7	18.4	0.0	0.0	0.0	0.0	0.0	0.0
534	1A	7	9.4	10.2	10.8	0.0	47.9	0.0	1.6	0.0	17.8	0.0	0.0	2.3	0.0	0.0	0.0
535	1A	8	10.6	6.1	7.3	0.0	56.1	0.0	0.0	0.0	20.0	0.0	0.0	0.0	0.0	0.0	0.0
536	1A	9	9.0	5.1	6.4	1.7	44.8	0.0	1.3	2.4	17.3	0.0	0.0	0.0	0.0	11.9	0.0
537	1A	10	9.0	6.5	6.9	1.8	49.1	0.0	1.7	3.2	20.1	0.0	0.0	0.0	1.8	0.0	0.0
538	1A	11	8.9	10.3	7.1	0.0	49.9	0.0	1.7	3.4	18.6	0.0	0.0	0.0	0.0	0.0	0.0
539	1A	12	8.5	9.7	8.8	0.0	54.0	0.0	2.4	0.0	16.7	0.0	0.0	0.0	0.0	0.0	0.0
540	1A	13	9.6	9.7	7.6	0.0	59.2	0.0	0.0	0.0	14.0	0.0	0.0	0.0	0.0	0.0	0.0
541	1A	14	9.6	4.5	6.4	0.0	46.9	0.0	1.5	0.0	16.2	0.0	0.0	0.0	0.0	10.9	3.9
542	1A	15	7.9	10.8	7.0	0.0	45.3	0.0	0.0	3.8	13.9	0.0	0.0	0.0	0.0	11.4	0.0
543	1A	16	7.8	4.3	5.8	0.0	57.4	1.6	0.0	0.0	11.3	0.0	0.0	0.0	0.0	11.9	0.0
544	1A	17	7.2	8.3	5.9	1.5	55.0	0.0	0.0	0.0	11.1	0.0	0.0	0.0	0.0	10.9	0.0
545	1A	18	6.9	4.6	5.6	0.0	57.6	0.0	0.0	0.0	12.8	0.0	0.0	0.0	0.0	12.6	0.0
546	1A	19	7.4	5.3	7.5	0.0	66.9	0.0	0.0	0.0	13.0	0.0	0.0	0.0	0.0	0.0	0.0
547	1A	20	6.4	5.3	9.6	1.9	65.2	0.0	0.0	0.0	11.5	0.0	0.0	0.0	0.0	0.0	0.0
548	1A	21	5.8	4.3	5.9	0.0	61.5	0.0	0.0	0.0	9.0	0.0	0.0	0.0	0.0	13.4	0.0
549	1A	22	7.2	8.8	8.5	0.0	61.9	0.0	1.9	0.0	11.7	0.0	0.0	0.0	0.0	0.0	0.0
550	1A	23	6.4	8.7	6.5	0.0	63.5	0.0	0.0	0.0	9.9	0.0	0.0	0.0	0.0	5.0	0.0
551	1A	24	6.5	5.6	5.6	0.0	54.1	0.0	1.6	2.4	12.5	0.0	0.0	0.0	0.0	11.7	0.0
552	1A	25	7.2	6.1	7.4	0.0	63.4	1.8	0.0	3.0	11.1	0.0	0.0	0.0	0.0	0.0	0.0
553	1A	26	7.7	4.9	4.9	0.0	70.8	0.0	0.0	0.0	11.7	0.0	0.0	0.0	0.0	0.0	0.0
554	1A	27	6.5	4.5	6.2	0.0	57.4	0.0	0.0	0.0	13.3	0.0	0.0	0.0	0.0	12.1	0.0
555	1A	28	7.5	9.2	6.1	1.6	61.2	0.0	0.0	0.0	14.4	0.0	0.0	0.0	0.0	0.0	0.0
556	1A	29	6.2	7.6	5.9	0.0	56.8	0.0	1.7	2.2	10.0	0.0	0.0	0.0	0.0	9.8	0.0
557	1A	30	7.9	4.3	4.2	0.0	59.4	0.0	1.8	0.0	11.5	0.0	0.0	0.0	0.0	10.9	0.0
558	1A	31	8.2	4.4	5.6	0.0	60.8	0.0	0.0	0.0	11.0	0.0	0.0	0.0	0.0	10.1	0.0
559	1A	32	7.1	4.3	16.6	1.0	58.5	0.0	0.0	0.0	12.4	0.0	0.0	0.0	0.0	0.0	0.0
560	1A	33	6.1	4.4	5.8	0.0	69.3	0.0	2.0	2.7	9.8	0.0	0.0	0.0	0.0	0.0	0.0

SAMPLE			MINERALOGY														
			Silicates					Carbonates							Evaporites		Sulfides
Seq	Site	Depth	Quartz	Kspar	Plag	Amph	ClayMin	Calcite	HiMgCal	Protodol	Dolomite	Mhydcal	Aragon	Magne	Thenar	Gypsum	Pyrite
no	ID	cm	%	%	%	%	%	%	%	%	%	%	%	%	%	%	%
561	1A	34	7.0	6.3	7.9	0.0	62.5	2.4	0.0	0.0	14.0	0.0	0.0	0.0	0.0	0.0	0.0
562	1A	35	8.2	5.5	8.4	1.8	63.7	0.0	0.0	0.0	12.5	0.0	0.0	0.0	0.0	0.0	0.0
563	1A	36	6.8	5.6	6.7	0.0	67.3	1.6	0.0	2.7	9.4	0.0	0.0	0.0	0.0	0.0	0.0
564	1A	37	8.9	6.1	9.5	0.0	61.5	0.0	0.0	0.0	14.1	0.0	0.0	0.0	0.0	0.0	0.0
565	1A	38	7.8	8.4	6.7	0.0	63.1	0.0	2.1	2.6	9.4	0.0	0.0	0.0	0.0	0.0	0.0
566	1A	39	9.4	12.3	8.3	0.0	55.8	0.0	2.3	0.0	11.9	0.0	0.0	0.0	0.0	0.0	0.0
567	1A	40	7.5	9.8	7.2	0.0	63.8	0.0	2.0	0.0	9.9	0.0	0.0	0.0	0.0	0.0	0.0
568	1A	41	9.1	6.9	7.1	0.0	61.9	0.0	0.0	0.0	15.0	0.0	0.0	0.0	0.0	0.0	0.0
569	1A	42	7.1	7.5	5.5	0.0	56.7	0.0	1.9	0.0	9.6	0.0	0.0	0.0	0.0	11.6	0.0
570	2A	1	5.1	11.4	6.9	0.0	70.9	0.0	2.5	3.2	0.0	0.0	0.0	0.0	0.0	0.0	0.0
571	2A	2	5.7	10.8	6.4	0.0	58.9	0.0	1.7	0.0	2.5	0.0	0.0	0.0	0.0	14.0	0.0
572	2A	3	6.4	12.1	8.2	0.0	69.9	0.0	0.0	0.0	3.5	0.0	0.0	0.0	0.0	0.0	0.0
573	2A	4	6.5	6.1	8.0	0.0	60.3	0.0	2.1	0.0	2.5	0.0	0.0	0.0	0.0	14.5	0.0
574	2A	5	7.3	12.7	9.7	1.9	64.7	0.0	0.0	3.7	0.0	0.0	0.0	0.0	0.0	0.0	0.0
575	2A	6	5.9	9.7	7.3	0.0	56.9	0.0	1.5	2.8	0.0	0.0	0.0	0.0	0.0	16.0	0.0
576	2A	7	5.4	9.7	7.7	0.0	58.7	0.0	1.9	2.8	0.0	0.0	0.0	0.0	0.0	13.9	0.0
577	2A	8	7.4	7.7	9.0	0.0	72.8	0.0	0.0	0.0	3.1	0.0	0.0	0.0	0.0	0.0	0.0
578	2A	9	6.8	10.7	6.4	1.9	53.9	0.0	1.8	2.8	0.0	0.0	0.0	0.0	0.0	15.7	0.0
579	2A	10	7.3	10.1	7.0	0.0	59.5	0.0	0.0	0.0	0.0	0.0	0.0	0.0	0.0	16.1	0.0
580	2A	11	7.2	11.5	7.8	0.0	64.6	0.0	2.5	3.5	2.9	0.0	0.0	0.0	0.0	0.0	0.0
581	2A	12	6.4	11.3	7.1	0.0	68.2	0.0	0.0	3.1	0.0	0.0	0.0	0.0	0.0	0.0	4.0
582	2A	13	6.9	6.0	7.8	0.0	58.1	0.0	0.0	3.5	0.0	0.0	0.0	3.0	0.0	14.7	0.0
583	2A	14	7.7	6.7	8.4	0.0	73.4	0.0	0.0	3.7	0.0	0.0	0.0	0.0	0.0	0.0	0.0
584	2A	15	6.8	6.9	6.7	2.5	70.0	0.0	2.8	4.2	0.0	0.0	0.0	0.0	0.0	0.0	0.0
585	2A	16	6.3	5.2	7.4	1.3	62.7	0.0	2.0	0.0	0.0	0.0	0.0	0.0	0.0	15.1	0.0
586	2A	17	6.2	6.5	8.9	0.0	75.1	0.0	0.0	3.3	0.0	0.0	0.0	0.0	0.0	0.0	0.0
587	2A	18	6.4	5.4	7.2	0.0	62.8	0.0	1.7	2.7	0.0	0.0	0.0	0.0	0.0	13.7	0.0
588	2A	19	8.0	7.4	8.5	0.0	76.1	0.0	0.0	0.0	0.0	0.0	0.0	0.0	0.0	0.0	0.0
589	2A	20	8.2	6.4	8.5	1.8	69.8	0.0	2.0	3.2	0.0	0.0	0.0	0.0	0.0	0.0	0.0
590	2A	21	5.8	6.4	8.4	2.3	77.2	0.0	0.0	0.0	0.0	0.0	0.0	0.0	0.0	0.0	0.0
591	2A	22	8.1	14.0	10.6	0.0	60.1	0.0	0.0	3.8	0.0	0.0	0.0	3.4	0.0	0.0	0.0
592	2A	23	5.0	5.2	6.1	0.0	65.5	0.0	0.0	2.6	0.0	0.0	0.0	0.0	0.0	15.7	0.0
593	2A	24	7.1	11.8	9.9	0.0	65.4	0.0	2.8	3.0	0.0	0.0	0.0	0.0	0.0	0.0	0.0
594	2A	25	6.9	6.2	8.8	1.8	74.1	0.0	2.3	0.0	0.0	0.0	0.0	0.0	0.0	0.0	0.0
595	2A	26	4.5	10.1	6.4	0.0	59.0	0.0	1.6	3.1	0.0	0.0	0.0	0.0	0.0	15.2	0.0

SAMPLE			MINERALOGY														
			Silicates					Carbonates							Evaporites		Sulfides
Seq	Site	Depth	Quartz	Kspar	Plag	Amph	ClayMin	Calcite	HiMgCal	Protodol	Dolomite	Mhydcal	Aragon	Magne	Thenar	Gypsum	Pyrite
no	ID	cm	%	%	%	%	%	%	%	%	%	%	%	%	%	%	%
596	2A	27	5.9	9.8	8.5	0.0	57.2	0.0	0.0	0.0	2.8	0.0	0.0	0.0	0.0	15.9	0.0
597	2A	28	6.9	11.1	6.4	0.0	73.1	0.0	2.5	0.0	0.0	0.0	0.0	0.0	0.0	0.0	0.0
598	2A	29	7.0	6.4	8.4	0.0	68.8	0.0	0.0	0.0	6.6	0.0	0.0	2.8	0.0	0.0	0.0
599	2A	30	7.2	7.2	6.8	0.0	75.4	0.0	0.0	3.5	0.0	0.0	0.0	0.0	0.0	0.0	0.0
600	2A	31	5.9	9.6	8.6	0.0	59.1	0.0	0.0	3.1	0.0	0.0	0.0	0.0	0.0	13.7	0.0
601	2A	32	8.1	7.3	8.5	2.1	74.0	0.0	0.0	0.0	0.0	0.0	0.0	0.0	0.0	0.0	0.0
602	2A	33	5.8	10.7	6.0	0.0	61.6	0.0	0.0	0.0	0.0	0.0	0.0	0.0	2.3	13.6	0.0
603	2A	34	7.1	6.9	7.5	0.0	72.8	0.0	2.5	3.3	0.0	0.0	0.0	0.0	0.0	0.0	0.0
604	2A	35	6.3	11.7	6.5	1.7	69.2	0.0	1.8	2.8	0.0	0.0	0.0	0.0	0.0	0.0	0.0
605	2A	36	7.4	10.9	6.7	0.0	54.5	0.0	2.4	2.7	0.0	0.0	0.0	0.0	0.0	15.4	0.0
606	2A	38	7.5	12.6	9.4	2.2	68.4	0.0	0.0	0.0	0.0	0.0	0.0	0.0	0.0	0.0	0.0
607	2A	39	5.9	13.8	7.6	1.8	64.3	0.0	2.6	4.0	0.0	0.0	0.0	0.0	0.0	0.0	0.0
608	2A	40	6.1	6.1	6.4	0.0	64.5	0.0	2.2	0.0	0.0	0.0	0.0	0.0	0.0	14.7	0.0
609	2A	41	7.7	5.6	9.0	0.0	59.5	0.0	0.0	2.4	0.0	0.0	0.0	0.0	0.0	15.7	0.0
610	2A	42	6.8	10.3	8.3	0.0	59.1	0.0	0.0	0.0	0.0	0.0	0.0	0.0	0.0	15.5	0.0
611	3A	1	5.2	6.1	8.3	0.0	59.3	0.0	0.0	0.0	4.1	0.0	0.0	0.0	0.0	17.0	0.0
612	3A	2	4.7	10.4	8.9	0.0	52.8	0.0	2.5	3.4	2.8	0.0	0.0	0.0	0.0	14.5	0.0
613	3A	3	5.8	6.6	8.8	0.0	56.5	0.0	0.0	3.3	2.9	0.0	0.0	0.0	0.0	16.2	0.0
614	3A	4	6.8	7.0	6.8	0.0	67.9	0.0	0.0	3.2	3.6	0.0	0.0	0.0	0.0	0.0	4.7
615	3A	5	6.5	13.6	10.2	0.0	69.7	0.0	0.0	0.0	0.0	0.0	0.0	0.0	0.0	0.0	0.0
616	3A	6	7.0	12.8	8.8	0.0	65.8	0.0	2.1	0.0	3.5	0.0	0.0	0.0	0.0	0.0	0.0
617	3A	7	6.6	6.6	6.9	0.0	76.3	0.0	0.0	3.6	0.0	0.0	0.0	0.0	0.0	0.0	0.0
618	3A	8	6.1	11.3	9.0	0.0	58.7	0.0	0.0	3.1	0.0	0.0	0.0	0.0	0.0	11.8	0.0
619	3A	9	5.1	5.5	7.9	0.0	60.3	0.0	1.8	0.0	2.5	0.0	0.0	0.0	0.0	16.9	0.0
620	3A	10	5.1	12.4	7.7	0.0	71.1	0.0	0.0	0.0	3.7	0.0	0.0	0.0	0.0	0.0	0.0
621	3A	11	5.3	10.3	7.5	0.0	57.9	0.0	1.9	2.5	0.0	0.0	0.0	0.0	0.0	14.8	0.0
622	3A	12	6.0	6.2	5.8	1.7	62.4	0.0	2.1	2.6	0.0	0.0	0.0	0.0	0.0	13.3	0.0
623	3A	13	6.8	6.6	10.9	0.0	75.7	0.0	0.0	0.0	0.0	0.0	0.0	0.0	0.0	0.0	0.0
624	3A	14	9.4	0.0	12.4	0.0	74.9	0.0	0.0	0.0	0.0	0.0	0.0	3.3	0.0	0.0	0.0
625	3A	15	5.1	5.3	6.5	0.0	66.3	0.0	2.0	0.0	0.0	0.0	0.0	0.0	0.0	14.7	0.0
626	3A	16	6.9	7.3	7.4	2.0	72.0	0.0	0.0	4.3	0.0	0.0	0.0	0.0	0.0	0.0	0.0
627	3A	17	5.1	6.6	7.5	0.0	72.4	2.4	2.6	3.4	0.0	0.0	0.0	0.0	0.0	0.0	0.0
628	3A	18	6.6	7.6	6.8	0.0	75.0	0.0	0.0	4.0	0.0	0.0	0.0	0.0	0.0	0.0	0.0
629	3A	19	7.0	7.3	10.3	0.0	71.3	0.0	0.0	0.0	4.2	0.0	0.0	0.0	0.0	0.0	0.0
630	3A	20	7.6	7.2	9.1	2.5	73.6	0.0	0.0	0.0	0.0	0.0	0.0	0.0	0.0	0.0	0.0

SAMPLE			MINERALOGY														
			Silicates					Carbonates							Evaporites		Sulfides
Seq	Site	Depth	Quartz	Kspar	Plag	Amph	ClayMin	Calcite	HiMgCal	Protodol	Dolomite	Mhydcal	Aragon	Magne	Thenar	Gypsum	Pyrite
no	ID	cm	%	%	%	%	%	%	%	%	%	%	%	%	%	%	%
631	3A	21	5.3	5.1	7.2	0.0	63.4	0.0	1.6	0.0	3.0	0.0	0.0	0.0	0.0	14.5	0.0
632	3A	22	4.7	11.4	7.7	0.0	53.9	0.0	2.1	3.1	0.0	0.0	0.0	0.0	2.6	14.5	0.0
633	3A	23	5.8	8.1	7.5	0.0	74.5	0.0	0.0	0.0	4.1	0.0	0.0	0.0	0.0	0.0	0.0
634	3A	24	5.9	7.3	8.6	0.0	68.6	2.3	0.0	3.9	3.4	0.0	0.0	0.0	0.0	0.0	0.0
635	3A	25	5.7	12.2	7.5	0.0	71.1	0.0	0.0	0.0	3.5	0.0	0.0	0.0	0.0	0.0	0.0
636	3A	26	6.7	7.3	9.7	0.0	71.7	0.0	0.0	0.0	4.7	0.0	0.0	0.0	0.0	0.0	0.0
637	3A	27	5.3	10.8	6.5	0.0	58.0	0.0	0.0	3.1	0.0	0.0	0.0	0.0	0.0	16.4	0.0
638	3A	28	7.1	11.8	7.4	0.0	65.7	0.0	0.0	3.6	4.4	0.0	0.0	0.0	0.0	0.0	0.0
639	3A	29	5.3	7.7	9.6	0.0	51.3	0.0	0.0	4.0	0.0	0.0	0.0	0.0	0.0	22.1	0.0
640	3A	30	6.0	12.0	8.6	0.0	62.5	2.2	0.0	4.2	4.5	0.0	0.0	0.0	0.0	0.0	0.0
641	3A	31	5.2	0.0	9.5	2.4	78.0	0.0	0.0	4.9	0.0	0.0	0.0	0.0	0.0	0.0	0.0
642	3A	32	4.8	7.5	7.6	0.0	66.0	0.0	2.9	3.4	4.2	0.0	0.0	0.0	3.7	0.0	0.0
643	3A	33	5.9	6.5	9.0	2.3	72.8	0.0	0.0	3.6	0.0	0.0	0.0	0.0	0.0	0.0	0.0
644	3A	34	4.8	11.2	7.1	0.0	54.7	0.0	0.0	0.0	3.1	0.0	3.5	0.0	0.0	15.5	0.0
645	3A	35	4.8	11.0	8.0	0.0	55.3	0.0	2.4	0.0	0.0	0.0	0.0	0.0	2.8	15.7	0.0
646	3A	36	6.5	7.8	7.2	0.0	69.9	0.0	2.2	3.1	3.2	0.0	0.0	0.0	0.0	0.0	0.0
647	3A	37	7.6	7.4	10.6	0.0	70.9	0.0	0.0	0.0	3.6	0.0	0.0	0.0	0.0	0.0	0.0
648	3A	38	6.8	10.7	7.5	0.0	70.0	0.0	2.2	0.0	2.9	0.0	0.0	0.0	0.0	0.0	0.0
649	3A	39	6.7	7.3	7.4	0.0	75.6	0.0	0.0	0.0	3.1	0.0	0.0	0.0	0.0	0.0	0.0
650	3A	40	6.1	6.5	9.5	0.0	70.3	0.0	0.0	3.8	3.7	0.0	0.0	0.0	0.0	0.0	0.0
651	3A	41	6.6	10.5	7.4	0.0	57.0	0.0	1.6	0.0	3.2	0.0	0.0	0.0	0.0	13.7	0.0
652	3A	42	7.5	10.1	8.5	0.0	70.2	0.0	0.0	0.0	3.7	0.0	0.0	0.0	0.0	0.0	0.0
653	3A	43	7.4	7.4	8.4	0.0	67.9	0.0	2.1	3.5	3.2	0.0	0.0	0.0	0.0	0.0	0.0
654	3A	44	5.9	10.4	6.6	0.0	57.7	0.0	1.9	0.0	2.9	0.0	0.0	0.0	0.0	14.7	0.0
655	3A	45	8.6	12.1	8.1	0.0	71.1	0.0	0.0	0.0	0.0	0.0	0.0	0.0	0.0	0.0	0.0
656	4A	1	14.7	7.1	13.4	0.0	60.9	0.0	0.0	3.9	0.0	0.0	0.0	0.0	0.0	0.0	0.0
657	4A	2	12.8	13.2	19.0	0.0	35.8	0.0	0.0	2.7	0.0	0.0	0.0	2.8	0.0	13.7	0.0
658	4A	3	9.7	11.2	18.4	0.0	40.4	0.0	1.7	3.5	0.0	0.0	0.0	0.0	0.0	15.0	0.0
659	4A	4	9.8	9.4	13.5	2.3	57.7	1.6	2.3	3.6	0.0	0.0	0.0	0.0	0.0	0.0	0.0
660	4A	5	8.1	6.5	9.2	0.0	57.6	0.0	0.0	2.8	0.0	0.0	0.0	0.0	0.0	15.9	0.0
661	4A	6	7.1	10.4	9.8	1.8	56.4	0.0	0.0	0.0	0.0	0.0	0.0	0.0	0.0	14.6	0.0
662	4A	7	10.2	7.0	11.8	0.0	67.5	0.0	3.6	0.0	0.0	0.0	0.0	0.0	0.0	0.0	0.0
663	4A	8	8.2	7.0	9.8	0.0	54.8	0.0	0.0	3.4	0.0	0.0	0.0	0.0	0.0	16.9	0.0
664	4A	9	7.9	6.7	12.9	0.0	55.2	0.0	1.8	3.1	0.0	0.0	0.0	0.0	0.0	12.5	0.0
665	4A	10	6.1	5.3	15.0	1.6	55.9	0.0	0.0	2.4	0.0	0.0	0.0	0.0	0.0	13.8	0.0

SAMPLE			MINERALOGY														
			Silicates					Carbonates							Evaporites		Sulfides
Seq	Site	Depth	Quartz	Kspar	Plag	Amph	ClayMin	Calcite	HiMgCal	Protodol	Dolomite	Mhydcal	Aragon	Magne	Thenar	Gypsum	Pyrite
no	ID	cm	%	%	%	%	%	%	%	%	%	%	%	%	%	%	%
666	4A	11	7.6	5.1	12.4	0.0	54.7	0.0	2.2	3.3	0.0	0.0	0.0	0.0	0.0	14.8	0.0
667	4A	12	7.4	12.9	12.2	0.0	61.5	0.0	2.1	3.8	0.0	0.0	0.0	0.0	0.0	0.0	0.0
668	4A	13	9.7	8.7	13.1	2.1	62.3	0.0	0.0	4.0	0.0	0.0	0.0	0.0	0.0	0.0	0.0
669	4A	14	8.6	6.0	7.8	2.0	55.7	0.0	0.0	0.0	0.0	0.0	0.0	0.0	0.0	19.9	0.0
670	4A	15	10.9	10.8	10.1	0.0	52.1	1.4	0.0	2.8	0.0	0.0	0.0	0.0	0.0	11.8	0.0
671	4A	16	8.1	9.2	7.7	1.9	54.9	0.0	0.0	3.0	0.0	0.0	0.0	0.0	0.0	15.2	0.0
672	4A	17	7.4	9.2	11.6	0.0	53.0	0.0	0.0	2.8	0.0	0.0	0.0	0.0	0.0	16.1	0.0
673	4A	18	8.3	15.1	8.4	2.8	62.0	0.0	0.0	3.4	0.0	0.0	0.0	0.0	0.0	0.0	0.0
674	4A	19	7.4	7.5	9.2	2.3	69.3	0.0	0.0	4.3	0.0	0.0	0.0	0.0	0.0	0.0	0.0
675	4A	20	8.7	6.8	15.1	2.3	62.9	0.0	0.0	4.3	0.0	0.0	0.0	0.0	0.0	0.0	0.0
676	4A	21	7.2	8.8	11.3	2.0	67.6	0.0	0.0	3.1	0.0	0.0	0.0	0.0	0.0	0.0	0.0
677	4A	22	8.1	13.5	9.1	2.2	61.5	0.0	2.4	3.2	0.0	0.0	0.0	0.0	0.0	0.0	0.0
678	4A	23	8.5	6.6	11.3	0.0	52.0	0.0	3.0	3.4	0.0	0.0	0.0	0.0	0.0	15.2	0.0
679	4A	24	8.3	0.0	11.1	0.0	67.1	0.0	0.0	0.0	0.0	0.0	0.0	0.0	0.0	13.4	0.0
680	4A	25	8.0	10.1	9.7	1.5	50.2	1.8	1.7	2.8	0.0	0.0	0.0	0.0	0.0	14.1	0.0
681	4A	26	9.6	6.2	9.4	2.1	53.7	1.9	2.0	3.2	0.0	0.0	0.0	0.0	0.0	12.0	0.0
682	4A	27	10.5	11.7	13.5	1.5	48.7	0.0	0.0	0.0	0.0	0.0	0.0	0.0	0.0	14.1	0.0
683	4A	28	5.9	6.0	17.4	0.0	49.7	0.0	0.0	3.1	0.0	0.0	0.0	0.0	0.0	18.0	0.0
684	4A	29	6.8	11.4	11.6	1.8	50.9	0.0	0.0	2.8	0.0	0.0	0.0	0.0	2.6	12.2	0.0
685	4A	30	8.4	10.0	7.0	1.8	57.3	0.0	0.0	2.7	0.0	0.0	0.0	0.0	0.0	12.8	0.0
686	4A	31	6.1	10.0	10.6	2.0	51.8	1.8	0.0	2.4	0.0	0.0	0.0	0.0	0.0	15.4	0.0
687	4A	32	8.9	7.9	15.3	1.9	49.2	0.0	2.1	0.0	0.0	0.0	0.0	0.0	0.0	14.7	0.0
688	4A	33	8.0	6.2	10.5	1.9	55.3	0.0	0.0	0.0	0.0	0.0	0.0	0.0	0.0	18.2	0.0
689	4A	34	8.2	10.8	14.2	0.0	50.4	0.0	1.8	2.6	0.0	0.0	0.0	0.0	0.0	12.2	0.0
690	4A	35	7.6	9.6	16.2	1.5	49.3	0.0	0.0	3.6	0.0	0.0	0.0	0.0	0.0	12.2	0.0
691	4A	36	8.1	7.6	11.0	2.4	67.4	0.0	0.0	3.5	0.0	0.0	0.0	0.0	0.0	0.0	0.0
692	4A	37	8.0	13.2	20.0	0.0	56.7	0.0	2.1	0.0	0.0	0.0	0.0	0.0	0.0	0.0	0.0
693	4A	38	7.6	10.0	10.9	0.0	67.3	2.2	2.0	0.0	0.0	0.0	0.0	0.0	0.0	0.0	0.0
694	4A	39	7.8	11.7	23.6	1.7	35.7	0.0	1.9	3.1	0.0	0.0	0.0	0.0	0.0	14.5	0.0
695	4A	40	7.3	11.0	12.3	2.6	64.4	0.0	2.4	0.0	0.0	0.0	0.0	0.0	0.0	0.0	0.0
696	4A	41	8.3	9.9	13.8	0.0	48.1	0.0	0.0	2.9	0.0	0.0	0.0	0.0	0.0	17.1	0.0
697	4A	42	10.4	5.0	13.4	0.0	62.3	0.0	2.4	3.6	0.0	0.0	0.0	0.0	2.9	0.0	0.0
698	4A	43	8.4	7.0	10.2	0.0	66.3	2.3	2.2	3.7	0.0	0.0	0.0	0.0	0.0	0.0	0.0
699	5A	1	9.0	8.0	9.3	0.0	67.8	0.0	2.4	3.6	0.0	0.0	0.0	0.0	0.0	0.0	0.0
700	5A	2	9.3	15.5	20.4	0.0	47.9	0.0	2.4	4.5	0.0	0.0	0.0	0.0	0.0	0.0	0.0

SAMPLE			MINERALOGY														
			Silicates					Carbonates							Evaporites		Sulfides
Seq	Site	Depth	Quartz	Kspar	Plag	Amph	ClayMin	Calcite	HiMgCal	Protodol	Dolomite	Mhydcal	Aragon	Magne	Thenar	Gypsum	Pyrite
no	ID	cm	%	%	%	%	%	%	%	%	%	%	%	%	%	%	%
701	5A	3	10.0	6.0	20.7	2.0	52.8	1.6	2.7	4.2	0.0	0.0	0.0	0.0	0.0	0.0	0.0
702	5A	4	8.0	10.4	17.2	0.0	44.5	0.0	0.0	2.8	0.0	0.0	0.0	0.0	0.0	17.2	0.0
703	5A	5	10.5	7.4	15.2	1.8	45.4	0.0	0.0	4.4	0.0	0.0	0.0	0.0	0.0	15.3	0.0
704	5A	6	7.7	6.3	20.3	0.0	48.3	0.0	0.0	3.2	0.0	0.0	0.0	0.0	0.0	14.1	0.0
705	5A	7	6.8	9.0	9.1	2.0	52.6	0.0	0.0	2.9	0.0	0.0	0.0	0.0	0.0	17.7	0.0
706	5A	8	8.2	11.0	13.3	1.6	48.6	0.0	0.0	2.6	0.0	0.0	0.0	0.0	0.0	14.7	0.0
707	5A	9	7.9	9.9	10.8	0.0	50.2	0.0	0.0	2.3	0.0	0.0	0.0	0.0	0.0	18.8	0.0
708	5A	10	7.6	7.4	9.1	0.0	54.0	0.0	0.0	4.3	0.0	0.0	0.0	0.0	0.0	17.6	0.0
709	5A	11	16.5	7.4	14.7	0.0	58.6	0.0	0.0	2.9	0.0	0.0	0.0	0.0	0.0	0.0	0.0
710	5A	12	11.2	11.4	14.5	0.0	46.8	0.0	0.0	3.0	0.0	0.0	0.0	0.0	0.0	13.2	0.0
711	5A	13	9.2	7.6	15.2	1.6	52.4	0.0	0.0	0.0	0.0	0.0	0.0	0.0	0.0	14.0	0.0
712	5A	14	9.2	8.5	25.0	0.0	54.1	0.0	0.0	3.2	0.0	0.0	0.0	0.0	0.0	0.0	0.0
713	5A	15	11.4	7.8	11.8	2.4	45.4	1.6	0.0	3.2	0.0	0.0	0.0	0.0	0.0	16.6	0.0
714	5A	16	12.4	14.6	11.5	1.8	56.2	0.0	0.0	3.5	0.0	0.0	0.0	0.0	0.0	0.0	0.0
715	5A	17	8.5	13.2	12.2	2.4	44.9	2.7	0.0	3.4	0.0	0.0	0.0	0.0	0.0	12.8	0.0
716	5A	18	12.0	19.4	16.0	1.4	47.6	0.0	0.0	3.6	0.0	0.0	0.0	0.0	0.0	0.0	0.0
717	5A	19	10.0	14.9	12.2	0.0	46.2	0.0	0.0	3.5	0.0	0.0	0.0	0.0	0.0	13.2	0.0
718	5A	20	13.2	7.1	11.0	2.1	59.9	0.0	2.5	4.3	0.0	0.0	0.0	0.0	0.0	0.0	0.0
719	5A	21	9.2	9.1	14.6	0.0	60.7	2.6	0.0	3.9	0.0	0.0	0.0	0.0	0.0	0.0	0.0
720	5A	22	10.5	6.7	19.6	0.0	58.0	0.0	2.0	0.0	0.0	0.0	0.0	0.0	3.1	0.0	0.0
721	5A	23	9.3	11.8	16.0	0.0	53.6	2.0	2.9	4.4	0.0	0.0	0.0	0.0	0.0	0.0	0.0
722	5A	24	10.2	8.5	14.0	0.0	43.9	0.0	2.3	4.2	0.0	0.0	0.0	0.0	0.0	17.0	0.0
723	5A	25	14.4	7.2	14.6	2.9	42.2	0.0	0.0	4.2	0.0	0.0	0.0	0.0	0.0	14.5	0.0
724	5A	26	10.8	10.7	7.4	1.7	53.0	0.0	1.8	2.8	0.0	0.0	0.0	0.0	0.0	11.7	0.0
725	5A	27	8.0	8.9	7.7	1.6	45.6	1.6	1.6	2.7	0.0	0.0	0.0	8.6	0.0	13.7	0.0
726	5A	28	13.3	12.1	12.5	0.0	55.4	0.0	2.4	4.3	0.0	0.0	0.0	0.0	0.0	0.0	0.0
727	5A	29	12.4	12.7	11.1	2.0	46.7	0.0	0.0	0.0	0.0	0.0	0.0	0.0	0.0	15.1	0.0
728	5A	30	9.2	6.4	9.5	0.0	53.0	0.0	0.0	3.4	0.0	0.0	0.0	0.0	0.0	18.5	0.0
729	5A	31	7.9	10.0	20.6	2.8	40.5	0.0	1.8	2.5	0.0	0.0	0.0	0.0	1.8	12.1	0.0
730	5A	32	6.3	11.8	9.5	1.7	61.3	2.4	0.0	3.7	0.0	0.0	0.0	0.0	3.5	0.0	0.0
731	5A	33	8.9	5.3	11.7	1.8	48.6	0.0	1.9	3.5	0.0	0.0	0.0	0.0	0.0	18.3	0.0
732	5A	34	9.2	6.3	9.7	0.0	49.9	0.0	2.6	3.9	0.0	0.0	0.0	0.0	0.0	18.4	0.0
733	5A	35	7.6	8.9	10.3	2.0	50.3	0.0	2.4	3.3	0.0	0.0	0.0	0.0	0.0	15.3	0.0
734	5A	36	7.8	13.4	15.3	1.8	58.5	0.0	0.0	3.3	0.0	0.0	0.0	0.0	0.0	0.0	0.0
735	5A	37	7.2	7.7	25.1	0.0	54.2	2.6	0.0	3.3	0.0	0.0	0.0	0.0	0.0	0.0	0.0

SAMPLE			MINERALOGY														
			Silicates					Carbonates							Evaporites		Sulfides
Seq	Site	Depth	Quartz	Kspar	Plag	Amph	ClayMin	Calcite	HiMgCal	Protodol	Dolomite	Mhydcal	Aragon	Magne	Thenar	Gypsum	Pyrite
no	ID	cm	%	%	%	%	%	%	%	%	%	%	%	%	%	%	%
736	5A	38	8.2	12.1	7.4	2.0	50.6	0.0	0.0	3.9	0.0	0.0	0.0	0.0	0.0	15.9	0.0
737	5A	39	10.3	17.6	12.8	0.0	54.9	0.0	1.7	2.9	0.0	0.0	0.0	0.0	0.0	0.0	0.0
738	5A	40	7.9	11.2	10.3	1.5	51.5	0.0	0.0	2.4	1.7	0.0	0.0	0.0	0.0	13.6	0.0
739	6A	1	9.7	0.0	6.3	0.0	78.7	0.0	2.4	3.0	0.0	0.0	0.0	0.0	0.0	0.0	0.0
740	6A	2	6.1	4.8	6.0	0.0	78.5	0.0	2.2	2.4	0.0	0.0	0.0	0.0	0.0	0.0	0.0
741	6A	3	5.8	6.0	7.2	0.0	77.8	0.0	0.0	3.3	0.0	0.0	0.0	0.0	0.0	0.0	0.0
742	6A	4	5.5	6.1	5.6	0.0	72.3	0.0	3.1	3.4	4.1	0.0	0.0	0.0	0.0	0.0	0.0
743	6A	5	6.2	5.3	5.6	0.0	77.2	0.0	0.0	2.9	2.8	0.0	0.0	0.0	0.0	0.0	0.0
744	6A	6	5.2	4.6	5.5	0.0	68.9	0.0	0.0	0.0	0.0	0.0	0.0	0.0	0.0	15.8	0.0
745	6A	7	4.6	5.7	4.9	0.0	60.9	0.0	0.0	0.0	0.0	0.0	0.0	0.0	0.0	24.0	0.0
746	6A	8	5.3	9.6	5.4	0.0	62.6	0.0	0.0	0.0	0.0	0.0	0.0	0.0	0.0	17.1	0.0
747	6A	9	4.8	0.0	6.4	0.0	72.0	2.1	0.0	0.0	0.0	0.0	0.0	0.0	0.0	14.7	0.0
748	6A	10	7.8	0.0	7.2	0.0	81.1	0.0	0.0	0.0	3.8	0.0	0.0	0.0	0.0	0.0	0.0
749	6A	11	5.6	5.8	6.8	0.0	66.7	0.0	0.0	0.0	0.0	0.0	0.0	0.0	0.0	15.2	0.0
750	6A	12	5.7	11.3	7.0	0.0	76.1	0.0	0.0	0.0	0.0	0.0	0.0	0.0	0.0	0.0	0.0
751	6A	13	6.6	5.5	6.2	0.0	79.5	0.0	0.0	2.3	0.0	0.0	0.0	0.0	0.0	0.0	0.0
752	6A	14	7.4	0.0	7.5	0.0	79.5	0.0	2.7	3.1	0.0	0.0	0.0	0.0	0.0	0.0	0.0
753	6A	15	5.5	6.1	7.2	0.0	78.4	0.0	2.8	0.0	0.0	0.0	0.0	0.0	0.0	0.0	0.0
754	6A	16	6.1	5.7	6.0	0.0	82.2	0.0	0.0	0.0	0.0	0.0	0.0	0.0	0.0	0.0	0.0
755	6A	17	7.4	6.3	6.8	0.0	74.5	0.0	2.3	0.0	0.0	0.0	0.0	2.9	0.0	0.0	0.0
756	6A	18	7.4	7.8	8.1	2.2	74.6	0.0	0.0	0.0	0.0	0.0	0.0	0.0	0.0	0.0	0.0
757	6A	19	6.6	5.5	7.1	0.0	61.7	0.0	2.5	0.0	0.0	0.0	0.0	0.0	0.0	16.7	0.0
758	6A	20	6.2	0.0	7.5	0.0	82.0	0.0	0.0	4.3	0.0	0.0	0.0	0.0	0.0	0.0	0.0
759	6A	21	5.6	6.8	7.2	0.0	77.9	0.0	2.6	0.0	0.0	0.0	0.0	0.0	0.0	0.0	0.0
760	6A	22	6.0	7.1	6.5	0.0	73.5	0.0	2.9	4.0	0.0	0.0	0.0	0.0	0.0	0.0	0.0
761	6A	23	6.3	6.8	6.6	0.0	80.4	0.0	0.0	0.0	0.0	0.0	0.0	0.0	0.0	0.0	0.0
762	6A	24	4.9	11.0	5.8	0.0	75.0	0.0	0.0	3.3	0.0	0.0	0.0	0.0	0.0	0.0	0.0
763	6A	25	5.9	0.0	8.2	0.0	82.2	0.0	0.0	3.7	0.0	0.0	0.0	0.0	0.0	0.0	0.0
764	6A	26	6.0	0.0	7.3	0.0	83.5	0.0	0.0	3.2	0.0	0.0	0.0	0.0	0.0	0.0	0.0
765	6A	27	6.0	5.0	5.2	0.0	67.1	0.0	2.6	0.0	0.0	0.0	0.0	0.0	0.0	14.2	0.0
766	6A	28	5.3	0.0	7.3	0.0	70.6	0.0	0.0	0.0	0.0	0.0	0.0	0.0	0.0	16.8	0.0
767	6A	29	5.7	7.2	6.9	0.0	77.4	2.7	0.0	0.0	0.0	0.0	0.0	0.0	0.0	0.0	0.0
768	6A	30	6.7	12.8	7.6	0.0	69.0	0.0	0.0	0.0	0.0	0.0	3.9	0.0	0.0	0.0	0.0
769	6A	31	6.0	6.2	6.8	0.0	75.1	0.0	2.6	3.4	0.0	0.0	0.0	0.0	0.0	0.0	0.0
770	6A	32	5.9	0.0	7.2	0.0	86.9	0.0	0.0	0.0	0.0	0.0	0.0	0.0	0.0	0.0	0.0

SAMPLE			MINERALOGY														
			Silicates					Carbonates							Evaporites		Sulfides
Seq	Site	Depth	Quartz	Kspar	Plag	Amph	ClayMin	Calcite	HiMgCal	Protodol	Dolomite	Mhydcal	Aragon	Magne	Thenar	Gypsum	Pyrite
no	ID	cm	%	%	%	%	%	%	%	%	%	%	%	%	%	%	%
771	6A	33	6.8	6.1	7.2	0.0	72.8	0.0	3.1	4.1	0.0	0.0	0.0	0.0	0.0	0.0	0.0
772	6A	34	6.0	5.5	6.2	0.0	76.4	0.0	2.2	3.7	0.0	0.0	0.0	0.0	0.0	0.0	0.0
773	6A	35	6.4	5.4	6.2	0.0	77.3	0.0	2.1	2.7	0.0	0.0	0.0	0.0	0.0	0.0	0.0
774	6A	36	7.6	5.9	6.6	2.0	75.0	0.0	2.9	0.0	0.0	0.0	0.0	0.0	0.0	0.0	0.0
775	6A	37	6.4	12.6	7.1	0.0	67.5	0.0	0.0	3.1	0.0	0.0	0.0	3.3	0.0	0.0	0.0
776	6A	38	6.5	6.1	6.6	0.0	77.2	0.0	0.0	3.7	0.0	0.0	0.0	0.0	0.0	0.0	0.0
777	6A	39	4.4	6.1	7.3	0.0	76.4	2.3	0.0	3.6	0.0	0.0	0.0	0.0	0.0	0.0	0.0
778	6A	40	7.0	0.0	8.6	0.0	80.8	0.0	0.0	3.6	0.0	0.0	0.0	0.0	0.0	0.0	0.0
779	6A	41	6.4	10.3	5.8	0.0	74.6	0.0	0.0	0.0	2.9	0.0	0.0	0.0	0.0	0.0	0.0
780	7A	1	7.3	0.0	5.9	0.0	86.8	0.0	0.0	0.0	0.0	0.0	0.0	0.0	0.0	0.0	0.0
781	7A	2	6.1	5.4	5.8	0.0	82.7	0.0	0.0	0.0	0.0	0.0	0.0	0.0	0.0	0.0	0.0
782	7A	3	6.7	5.4	6.5	0.0	75.8	0.0	0.0	2.6	3.0	0.0	0.0	0.0	0.0	0.0	0.0
783	7A	4	8.6	5.3	6.8	0.0	79.3	0.0	0.0	0.0	0.0	0.0	0.0	0.0	0.0	0.0	0.0
784	7A	5	7.2	6.6	5.6	0.0	80.6	0.0	0.0	0.0	0.0	0.0	0.0	0.0	0.0	0.0	0.0
785	7A	6	5.7	4.9	5.0	0.0	70.2	1.4	0.0	0.0	0.0	0.0	0.0	0.0	0.0	12.7	0.0
786	7A	7	5.2	4.2	4.3	0.0	70.1	0.0	0.0	0.0	0.0	0.0	2.4	0.0	2.1	11.8	0.0
787	7A	8	5.9	0.0	5.2	0.0	88.9	0.0	0.0	0.0	0.0	0.0	0.0	0.0	0.0	0.0	0.0
788	7A	9	6.3	9.7	5.7	0.0	75.9	0.0	2.4	0.0	0.0	0.0	0.0	0.0	0.0	0.0	0.0
789	7A	10	6.0	10.0	4.7	0.0	79.3	0.0	0.0	0.0	0.0	0.0	0.0	0.0	0.0	0.0	0.0
790	7A	11	6.8	5.2	5.4	0.0	78.7	0.0	1.7	0.0	0.0	0.0	0.0	2.3	0.0	0.0	0.0
791	7A	12	6.5	4.6	4.8	0.0	77.9	0.0	1.9	2.2	2.2	0.0	0.0	0.0	0.0	0.0	0.0
792	7A	13	7.5	0.0	5.9	0.0	84.4	0.0	2.2	0.0	0.0	0.0	0.0	0.0	0.0	0.0	0.0
793	7A	14	5.4	5.0	4.1	0.0	74.7	0.0	0.0	0.0	0.0	0.0	0.0	0.0	0.0	10.8	0.0
794	7A	15	7.6	8.4	5.8	0.0	76.2	0.0	2.1	0.0	0.0	0.0	0.0	0.0	0.0	0.0	0.0
795	7A	16	5.4	4.7	4.8	0.0	75.1	0.0	0.0	0.0	0.0	0.0	0.0	0.0	0.0	10.1	0.0
796	7A	17	7.2	3.5	5.2	0.0	77.9	0.0	1.9	2.4	2.0	0.0	0.0	0.0	0.0	0.0	0.0
797	7A	18	6.3	4.3	5.6	0.0	79.3	2.1	0.0	2.4	0.0	0.0	0.0	0.0	0.0	0.0	0.0
798	7A	19	7.7	0.0	5.9	0.0	83.9	0.0	0.0	2.5	0.0	0.0	0.0	0.0	0.0	0.0	0.0
799	7A	20	6.6	5.4	4.8	0.0	83.3	0.0	0.0	0.0	0.0	0.0	0.0	0.0	0.0	0.0	0.0
800	7A	21	6.1	8.5	4.9	0.0	78.8	0.0	1.7	0.0	0.0	0.0	0.0	0.0	0.0	0.0	0.0
801	7A	22	6.9	0.0	5.1	0.0	83.9	0.0	1.8	0.0	2.4	0.0	0.0	0.0	0.0	0.0	0.0
802	7A	23	6.9	0.0	6.3	0.0	82.3	0.0	2.1	2.5	0.0	0.0	0.0	0.0	0.0	0.0	0.0
803	7A	24	6.3	4.8	6.0	0.0	80.5	0.0	0.0	2.3	0.0	0.0	0.0	0.0	0.0	0.0	0.0
804	7A	25	6.2	4.6	5.2	0.0	79.9	0.0	1.9	0.0	2.2	0.0	0.0	0.0	0.0	0.0	0.0
805	7A	26	8.0	5.0	6.5	0.0	75.9	0.0	2.2	2.4	0.0	0.0	0.0	0.0	0.0	0.0	0.0

SAMPLE			MINERALOGY														
			Silicates					Carbonates							Evaporites		Sulfides
Seq	Site	Depth	Quartz	Kspar	Plag	Amph	ClayMin	Calcite	HiMgCal	Protodol	Dolomite	Mhydcal	Aragon	Magne	Thenar	Gypsum	Pyrite
no	ID	cm	%	%	%	%	%	%	%	%	%	%	%	%	%	%	%
806	7A	27	6.1	5.2	4.3	0.0	71.7	0.0	0.0	0.0	0.0	0.0	0.0	0.0	0.0	12.7	0.0
807	7A	28	7.5	4.2	5.7	0.0	80.7	0.0	0.0	1.9	0.0	0.0	0.0	0.0	0.0	0.0	0.0
808	7A	29	8.2	4.9	5.6	0.0	77.3	0.0	1.5	2.5	0.0	0.0	0.0	0.0	0.0	0.0	0.0
809	7A	30	6.9	0.0	5.3	0.0	82.8	0.0	1.9	0.0	0.0	0.0	0.0	0.0	3.1	0.0	0.0
810	7A	31	7.1	5.1	5.2	0.0	79.8	0.0	0.0	2.8	0.0	0.0	0.0	0.0	0.0	0.0	0.0
811	7A	32	7.3	4.7	5.6	0.0	82.4	0.0	0.0	0.0	0.0	0.0	0.0	0.0	0.0	0.0	0.0
812	7A	33	6.8	4.2	5.2	0.0	81.1	0.0	0.0	2.7	0.0	0.0	0.0	0.0	0.0	0.0	0.0
813	7A	34	8.3	0.0	5.3	0.0	86.5	0.0	0.0	0.0	0.0	0.0	0.0	0.0	0.0	0.0	0.0
814	7A	35	6.7	0.0	5.7	0.0	85.9	0.0	1.7	0.0	0.0	0.0	0.0	0.0	0.0	0.0	0.0
815	7A	36	6.6	0.0	4.9	0.0	86.0	0.0	0.0	2.5	0.0	0.0	0.0	0.0	0.0	0.0	0.0
816	7A	37	6.2	4.4	5.8	0.0	81.9	1.7	0.0	0.0	0.0	0.0	0.0	0.0	0.0	0.0	0.0
817	7A	38	7.2	4.3	6.0	0.0	68.6	0.0	0.0	0.0	0.0	0.0	0.0	0.0	0.0	13.9	0.0
818	8A	1	6.0	4.6	4.8	0.0	82.3	0.0	0.0	2.4	0.0	0.0	0.0	0.0	0.0	0.0	0.0
819	8A	2	6.5	9.6	6.2	0.0	75.7	0.0	0.0	0.0	2.0	0.0	0.0	0.0	0.0	0.0	0.0
820	8A	3	8.1	0.0	6.4	0.0	82.9	0.0	0.0	2.6	0.0	0.0	0.0	0.0	0.0	0.0	0.0
821	8A	4	6.0	4.5	5.9	0.0	80.5	0.0	0.0	0.0	3.1	0.0	0.0	0.0	0.0	0.0	0.0
822	8A	5	6.0	4.9	6.4	0.0	80.8	0.0	2.0	0.0	0.0	0.0	0.0	0.0	0.0	0.0	0.0
823	8A	6	6.5	4.9	4.9	0.0	81.1	0.0	0.0	0.0	2.7	0.0	0.0	0.0	0.0	0.0	0.0
824	8A	7	6.9	0.0	7.7	0.0	78.3	0.0	0.0	3.7	3.5	0.0	0.0	0.0	0.0	0.0	0.0
825	8A	8	5.2	4.3	5.2	0.0	78.3	0.0	1.7	2.7	2.6	0.0	0.0	0.0	0.0	0.0	0.0
826	8A	9	5.6	10.0	5.0	0.0	76.6	0.0	0.0	0.0	2.9	0.0	0.0	0.0	0.0	0.0	0.0
827	8A	10	5.8	5.0	5.9	0.0	81.2	0.0	2.1	0.0	0.0	0.0	0.0	0.0	0.0	0.0	0.0
828	8A	11	4.8	4.8	5.0	0.0	69.9	0.0	0.0	2.4	0.0	0.0	0.0	0.0	0.0	13.1	0.0
829	8A	12	6.8	5.3	6.0	0.0	79.2	0.0	0.0	2.7	0.0	0.0	0.0	0.0	0.0	0.0	0.0
830	8A	13	4.8	3.9	5.1	0.0	73.7	0.0	0.0	2.3	0.0	0.0	0.0	0.0	0.0	10.2	0.0
831	8A	14	6.9	5.6	6.2	0.0	81.3	0.0	0.0	0.0	0.0	0.0	0.0	0.0	0.0	0.0	0.0
832	8A	15	5.3	5.9	5.4	0.0	83.4	0.0	0.0	0.0	0.0	0.0	0.0	0.0	0.0	0.0	0.0
833	8A	16	6.4	5.5	6.0	0.0	82.1	0.0	0.0	0.0	0.0	0.0	0.0	0.0	0.0	0.0	0.0
834	8A	17	7.0	5.9	6.6	0.0	78.1	0.0	0.0	2.4	0.0	0.0	0.0	0.0	0.0	0.0	0.0
835	8A	18	5.9	0.0	7.9	0.0	80.7	2.1	0.0	3.4	0.0	0.0	0.0	0.0	0.0	0.0	0.0
836	8A	19	6.7	5.1	6.2	0.0	82.0	0.0	0.0	0.0	0.0	0.0	0.0	0.0	0.0	0.0	0.0
837	8A	20	6.4	9.8	6.5	0.0	74.5	0.0	0.0	2.8	0.0	0.0	0.0	0.0	0.0	0.0	0.0
838	8A	21	5.4	9.0	5.7	0.0	66.4	0.0	0.0	0.0	0.0	0.0	0.0	0.0	0.0	13.6	0.0
839	8A	22	7.0	4.9	5.2	0.0	80.5	0.0	2.4	0.0	0.0	0.0	0.0	0.0	0.0	0.0	0.0
840	8A	23	5.4	4.3	4.8	0.0	72.9	0.0	0.0	0.0	0.0	0.0	0.0	0.0	0.0	12.5	0.0

SAMPLE			MINERALOGY														
			Silicates					Carbonates							Evaporites		Sulfides
Seq	Site	Depth	Quartz	Kspar	Plag	Amph	ClayMin	Calcite	HiMgCal	Protodol	Dolomite	Mhydcal	Aragon	Magne	Thenar	Gypsum	Pyrite
no	ID	cm	%	%	%	%	%	%	%	%	%	%	%	%	%	%	%
841	8A	24	5.5	10.6	6.8	0.0	77.2	0.0	0.0	0.0	0.0	0.0	0.0	0.0	0.0	0.0	0.0
842	8A	25	5.6	4.7	5.0	1.4	66.9	0.0	0.0	2.6	0.0	0.0	0.0	0.0	0.0	14.0	0.0
843	8A	26	6.7	11.1	6.4	0.0	73.4	0.0	2.5	0.0	0.0	0.0	0.0	0.0	0.0	0.0	0.0
844	8A	27	6.6	5.0	5.8	0.0	82.7	0.0	0.0	0.0	0.0	0.0	0.0	0.0	0.0	0.0	0.0
845	8A	28	6.5	0.0	6.0	0.0	81.6	0.0	0.0	3.2	2.7	0.0	0.0	0.0	0.0	0.0	0.0
846	8A	29	5.9	4.8	6.0	0.0	79.0	0.0	1.9	2.4	0.0	0.0	0.0	0.0	0.0	0.0	0.0
847	8A	30	5.7	5.2	5.7	0.0	80.6	0.0	0.0	2.8	0.0	0.0	0.0	0.0	0.0	0.0	0.0
848	8A	31	7.4	5.5	5.9	0.0	81.2	0.0	0.0	0.0	0.0	0.0	0.0	0.0	0.0	0.0	0.0
849	8A	32	7.3	4.1	6.8	0.0	81.9	0.0	0.0	0.0	0.0	0.0	0.0	0.0	0.0	0.0	0.0
850	8A	33	5.6	4.8	4.8	0.0	71.0	0.0	0.0	0.0	0.0	0.0	0.0	0.0	0.0	13.8	0.0
851	8A	34	6.3	0.0	5.2	0.0	70.1	0.0	2.0	1.9	0.0	0.0	0.0	0.0	0.0	14.5	0.0
852	8A	35	6.4	5.8	6.0	2.1	76.6	0.0	0.0	3.1	0.0	0.0	0.0	0.0	0.0	0.0	0.0
853	8A	36	5.7	4.5	5.5	1.3	83.1	0.0	0.0	0.0	0.0	0.0	0.0	0.0	0.0	0.0	0.0
854	8A	37	6.6	6.0	6.3	0.0	75.7	0.0	2.4	3.1	0.0	0.0	0.0	0.0	0.0	0.0	0.0
855	8A	38	7.1	5.9	6.2	0.0	80.8	0.0	0.0	0.0	0.0	0.0	0.0	0.0	0.0	0.0	0.0
856	8A	39	5.0	10.9	5.4	1.8	77.0	0.0	0.0	0.0	0.0	0.0	0.0	0.0	0.0	0.0	0.0
857	8A	40	6.3	0.0	6.0	2.1	82.1	0.0	0.0	3.6	0.0	0.0	0.0	0.0	0.0	0.0	0.0
858	Grab-1	3	6.3	6.8	7.9	0.0	68.0	0.0	0.0	4.3	6.6	0.0	0.0	0.0	0.0	0.0	0.0
859	Grab-2	3	6.4	7.6	7.4	0.0	55.6	0.0	0.0	2.9	4.9	0.0	0.0	0.0	0.0	15.3	0.0
860	Grab-3	3	14.8	8.1	12.1	0.0	41.5	2.0	1.9	0.0	19.6	0.0	0.0	0.0	0.0	0.0	0.0
861	Grab-4	3	14.4	7.6	8.5	0.0	51.3	0.0	2.2	0.0	16.0	0.0	0.0	0.0	0.0	0.0	0.0
862	Grab-5	3	7.6	11.5	10.6	2.3	61.1	0.0	2.4	0.0	4.5	0.0	0.0	0.0	0.0	0.0	0.0
863	Grab-6	3	5.8	6.1	9.0	0.0	66.8	2.4	2.2	3.2	4.6	0.0	0.0	0.0	0.0	0.0	0.0
864	Grab-7	3	5.2	5.7	7.0	0.0	62.9	0.0	0.0	0.0	3.5	0.0	0.0	0.0	0.0	15.8	0.0
865	Grab-8	3	7.4	8.2	9.5	0.0	74.9	0.0	0.0	0.0	0.0	0.0	0.0	0.0	0.0	0.0	0.0
866	Grab-10	3	6.8	8.4	25.0	1.7	41.8	0.0	0.0	2.2	2.9	0.0	0.0	0.0	0.0	11.1	0.0
867	Grab-25	3	12.5	6.3	10.1	0.0	45.1	0.0	0.0	2.8	2.5	0.0	0.0	0.0	0.0	20.8	0.0
868	Grab-28	3	8.7	6.3	11.6	1.6	52.5	1.6	0.0	2.9	1.8	0.0	0.0	0.0	0.0	13.0	0.0
869	Grab-29	3	10.6	13.5	8.5	2.4	65.0	0.0	0.0	0.0	0.0	0.0	0.0	0.0	0.0	0.0	0.0
870	Grab-30	3	9.3	10.6	9.0	0.0	53.7	0.0	0.0	2.7	0.0	0.0	0.0	0.0	0.0	14.8	0.0
871	Grab-31	3	13.4	10.3	15.7	0.0	36.8	0.0	0.0	4.6	5.4	0.0	0.0	0.0	0.0	13.9	0.0
872	Grab-32	3	12.4	9.2	16.7	2.5	38.6	1.3	1.7	2.8	0.0	0.0	0.0	0.0	0.0	14.9	0.0
873	Grab-33	3	63.1	4.1	5.1	0.0	0.0	0.0	1.2	2.3	2.2	0.0	0.0	0.0	0.0	21.9	0.0
874	Grab-34	3	18.0	8.1	9.2	0.0	42.8	0.0	0.0	2.3	3.6	0.0	0.0	0.0	0.0	16.1	0.0
875	Grab-35	3	8.9	13.1	13.7	0.0	59.1	1.8	0.0	3.5	0.0	0.0	0.0	0.0	0.0	0.0	0.0

SAMPLE			MINERALOGY														
			Silicates					Carbonates							Evaporites		Sulfides
Seq	Site	Depth	Quartz	Kspar	Plag	Amph	ClayMin	Calcite	HiMgCal	Protodol	Dolomite	Mhydcal	Aragon	Magne	Thenar	Gypsum	Pyrite
no	ID	cm	%	%	%	%	%	%	%	%	%	%	%	%	%	%	%
876	Grab-36	3	7.5	0.0	7.2	0.0	82.0	0.0	0.0	3.3	0.0	0.0	0.0	0.0	0.0	0.0	0.0
877	Grab-37	3	6.8	5.8	6.0	1.5	79.9	0.0	0.0	0.0	0.0	0.0	0.0	0.0	0.0	0.0	0.0
878	Grab-39	3	5.9	8.7	6.0	0.0	56.7	0.0	1.4	2.1	6.2	0.0	0.0	2.3	0.0	10.7	0.0
879	Grab-40	3	49.5	6.2	19.6	1.3	0.0	0.0	2.0	0.0	9.9	0.0	0.0	0.0	0.0	11.5	0.0
880	Grab-41	3	4.9	5.0	5.5	0.0	66.9	0.0	0.0	0.0	2.9	0.0	0.0	0.0	0.0	14.9	0.0
881	Grab-42	3	6.6	5.6	6.4	0.0	81.4	0.0	0.0	0.0	0.0	0.0	0.0	0.0	0.0	0.0	0.0
882	Grab-43	3	6.1	4.9	6.2	0.0	69.4	2.2	0.0	0.0	11.2	0.0	0.0	0.0	0.0	0.0	0.0
883	Grab-44	3	5.8	5.7	5.8	0.0	82.7	0.0	0.0	0.0	0.0	0.0	0.0	0.0	0.0	0.0	0.0
884	Grab-45	3	5.2	0.0	7.4	0.0	85.7	0.0	1.8	0.0	0.0	0.0	0.0	0.0	0.0	0.0	0.0
885	Grab-46	3	5.6	4.9	4.9	0.0	77.6	0.0	1.8	2.7	2.5	0.0	0.0	0.0	0.0	0.0	0.0
886	Grab-47	3	7.1	0.0	6.5	0.0	84.1	0.0	0.0	0.0	2.3	0.0	0.0	0.0	0.0	0.0	0.0
887	Grab-49	3	6.4	5.2	5.5	0.0	78.5	0.0	0.0	0.0	4.4	0.0	0.0	0.0	0.0	0.0	0.0
888	Grab-50	3	4.8	0.0	3.7	0.0	58.5	0.0	27.3	1.9	3.9	0.0	0.0	0.0	0.0	0.0	0.0

SAMPLE			XRD				ORGANIC GEOCHEM PYROLYSIS YIELDS			CLAY MINERALOGY		
Seq	Site	Depth	Mg in Cal	Mg in HMC	Ca in Pd	Ca in Dol	S1	S2	S3	Expand	Illite	Kao+Chlo
no	ID	cm	%	%	%	%	mg/cc	mg/cc	mg/cc	%	%	%
1	103	5				49.09	na	na	na	na	na	na
2	103	15		14.73	62.16	47.82	na	na	na	na	na	na
3	103	25			60.85		na	na	na	na	na	na
4	103	35	0.24				na	na	na	na	na	na
5	103	45			65.18		19.80	34.10	9.50	na	na	na
6	103	55		10.34	71.84		na	na	na	na	na	na
7	103	65			63.93		na	na	na	na	na	na
8	103	75					na	na	na	na	na	na
9	103	85			69.53		na	na	na	na	na	na
10	103	95			66.88	49.42	na	na	na	na	na	na
11	103	105		12.93	65.22		na	na	na	na	na	na
12	103	115					na	na	na	na	na	na
13	103	125		14.18	67.92		12.01	23.16	5.76	na	na	na
14	103	135		14.34	67.19	50.78	na	na	na	na	na	na
15	103	145		16.53	66.66	50.03	na	na	na	na	na	na
16	103	155			50.30	0.17	0.40	1.37	na	na	na	na
17	103	165		13.39			0.27	0.76	1.81	na	na	na
18	103	175			52.06		na	na	na	na	na	na
19	103	185		14.57			na	na	na	na	na	na
20	103	195	0.58	14.14	65.97		na	na	na	na	na	na
21	103	205			50.69		na	na	na	na	na	na
22	103	215		14.67	65.78	49.51	na	na	na	na	na	na
23	103	225			65.47		na	na	na	na	na	na
24	103	235			71.46		na	na	na	na	na	na
25	103	245		14.83			na	na	na	na	na	na
26	103	255	1.22		75.06		na	na	na	na	na	na
27	103	265		15.78	65.94	49.94	na	na	na	na	na	na
28	103	275		15.81		47.76	na	na	na	na	na	na
29	103	285	3.40	15.42	64.46	48.36	18.20	26.30	9.70	na	na	na
30	103	295		19.83	63.65	48.79	15.30	27.10	7.20	na	na	na
31	103	305		14.99			0.04	0.11	1.10	na	na	na
32	103	315			70.41	49.97	0.10	0.26	1.34	na	na	na
33	103	325		15.42	64.06	47.16	na	na	na	na	na	na
34	103	335			65.50	48.51	na	na	na	na	na	na
35	103	345		13.55		49.00	6.10	10.20	5.30	na	na	na
36	103	355	1.56				na	na	na	na	na	na
37	103	365				49.72	na	na	na	na	na	na
38	103	375		17.50			na	na	na	na	na	na
39	103	385		14.50		49.60	18.20	29.60	9.80	na	na	na
40	103	395	3.40	16.17	70.66	48.00	na	na	na	na	na	na
41	103	405			65.25		na	na	na	na	na	na
42	103	415			66.47	50.00	na	na	na	na	na	na
43	103	425			66.09	50.75	na	na	na	na	na	na
44	103	435		14.37		50.82	na	na	na	na	na	na
45	103	445		15.42	64.68	50.39	na	na	na	na	na	na
46	103	455	1.42		66.34	50.60	na	na	na	na	na	na
47	103	465		18.05	69.62	49.33	na	na	na	na	na	na
48	103	475				50.30	na	na	na	na	na	na
49	103	485	2.16		66.50		na	na	na	na	na	na
50	103	495			65.56	48.42	na	na	na	na	na	na

SAMPLE			XRD				ORGANIC GEOCHEM PYROLYSIS YIELDS			CLAY MINERALOGY		
Seq	Site	Depth	Mg in Cal	Mg in HMC	Ca in Pd	Ca in Dol	S1	S2	S3	Expand	Illite	Kao+Chlo
no	ID	cm	%	%	%	%	mg/cc	mg/cc	mg/cc	%	%	%
51	103	505			65.87	50.66	na	na	na	na	na	na
52	103	515		14.73		50.72	na	na	na	na	na	na
53	103	525		13.59	67.85	50.45	na	na	na	na	na	na
54	103	535			64.50	51.06	na	na	na	na	na	na
55	103	545			53.68		na	na	na	na	na	na
56	103	555		15.74	67.73	49.81	na	na	na	na	na	na
57	103	565		15.19	66.28	49.94	na	na	na	na	na	na
58	103	575		11.95		50.27	na	na	na	na	na	na
59	103	585		13.29		50.21	na	na	na	na	na	na
60	103	595			64.84	50.75	na	na	na	na	na	na
61	103	605	1.05	13.03		51.21	na	na	na	na	na	na
62	103	615		15.09		50.78	8.50	14.40	6.80	na	na	na
63	103	625				49.63	na	na	na	na	na	na
64	103	635			63.37	47.97	na	na	na	na	na	na
65	103	645				48.60	na	na	na	na	na	na
66	103	655		16.72	74.35	50.45	27.60	40.00	10.30	na	na	na
67	103	665				50.48	na	na	na	na	na	na
68	103	675	2.16	13.98		49.36	na	na	na	na	na	na
69	103	685				48.72	na	na	na	na	na	na
70	103	695	2.16		64.68	50.33	na	na	na	na	na	na
71	103	705	0.98		64.28	50.57	0.17	0.74	1.18	na	na	na
72	103	715	0.78		65.72	50.60	na	na	na	na	na	na
73	103	725	1.22		66.22	51.57	0.10	0.40	1.40	na	na	na
74	103	735	0.45			49.69	na	na	na	na	na	na
75	103	745	1.02	14.50		49.54	na	na	na	na	na	na
76	103	755	1.29			50.66	na	na	na	na	na	na
77	103	765	0.11			51.27	0.09	0.28	1.83	na	na	na
78	103	775	1.02			50.42	0.10	0.34	1.30	na	na	na
79	103	785	1.08			50.60	na	na	na	na	na	na
80	103	795	1.25	15.55		50.63	0.53	1.30	2.60	na	na	na
81	103	805	0.88			51.54	na	na	na	na	na	na
82	103	815	2.13		65.75	49.72	0.24	0.90	2.04	na	na	na
83	104A	5				50.91	na	na	na	na	na	na
84	104A	15				50.42	na	na	na	48	24	26
85	104A	25		12.64		51.48	na	na	na	na	na	na
86	104A	35				50.42	na	na	na	na	na	na
87	104A	45		5.27	66.25	49.54	na	na	na	na	na	na
88	104A	55				50.03	na	na	na	na	na	na
89	104A	65	3.36	14.01	64.59	49.66	na	na	na	5	43	51
90	104A	75	0.68	13.29		49.91	na	na	na	na	na	na
91	104A	85		3.66	68.74	48.94	na	na	na	na	na	na
92	104A	95		18.02		45.41	na	na	na	na	na	na
93	104A	105				47.07	na	na	na	na	na	na
94	104A	115			60.76	45.62	na	na	na	37	31	31
95	104A	125			66.85	50.57	na	na	na	na	na	na
96	104A	135			66.12	50.48	na	na	na	na	na	na
97	104A	145		13.03	67.73	49.27	na	na	na	na	na	na
98	104A	155			65.34	49.69	na	na	na	na	na	na
99	104A	165			66.69	50.72	na	na	na	55	24	20
100	104A	175	2.19		62.41	50.48	na	na	na	na	na	na

SAMPLE			XRD				ORGANIC GEOCHEM PYROLYSIS YIELDS			CLAY MINERALOGY		
Seq	Site	Depth	Mg in Cal	Mg in HMC	Ca in Pd	Ca in Dol	S1	S2	S3	Expand	Illite	Kao+Chlo
no	ID	cm	%	%	%	%	mg/cc	mg/cc	mg/cc	%	%	%
101	104A	185		16.79		50.66	na	na	na	na	na	na
102	104A	195	1.08			50.24	na	na	na	na	na	na
103	104A	205	0.88			50.42	na	na	na	na	na	na
104	104A	215		12.87		51.42	na	na	na	na	na	na
105	104A	225	0.61	14.70	66.50	50.57	na	na	na	na	na	na
106	104A	235	0.92		65.06	50.69	na	na	na	na	na	na
107	104A	245	0.98	11.75	65.81	50.45	na	na	na	na	na	na
108	104A	255	0.78	12.93	66.09	50.97	na	na	na	47	27	25
109	104A	265	-0.43	14.24	67.89	51.85	na	na	na	na	na	na
110	104A	275	0.51			50.88	na	na	na	na	na	na
111	104A	285	0.55		66.56	50.66	na	na	na	na	na	na
112	104A	295	0.55		66.53	51.70	na	na	na	na	na	na
113	104A	305	0.95			51.09	na	na	na	31	36	32
114	104A	315	0.88		71.17	50.85	na	na	na	na	na	na
115	104A	325	0.82	14.11	66.19	51.09	na	na	na	na	na	na
116	104A	335	-0.02	13.69		51.54	na	na	na	na	na	na
117	104A	345	0.72		67.19	51.27	na	na	na	33	32	33
118	104A	355	1.05	14.05	75.66	50.51	na	na	na	na	na	na
119	104A	365	0.51	14.11		51.51	na	na	na	na	na	na
120	104B	5			66.66	49.57	na	na	na	na	na	na
121	104B	15	2.39	14.47		49.57	na	na	na	na	na	na
122	104B	25	2.53		65.22	49.69	na	na	na	na	na	na
123	104B	35			66.25	49.87	na	na	na	na	na	na
124	104B	45	1.72		66.22	49.78	na	na	na	na	na	na
125	104B	55	0.88			50.60	na	na	na	na	na	na
126	104B	65	1.32		74.51	50.60	na	na	na	na	na	na
127	104B	75	1.72			50.42	na	na	na	na	na	na
128	105	5				49.42	na	na	na	na	na	na
129	105	15		13.23	67.85	50.54	na	na	na	na	na	na
130	105	25	2.39			50.15	na	na	na	na	na	na
131	105	35		14.54		50.72	na	na	na	na	na	na
132	105	45	0.88	15.55		51.48	na	na	na	na	na	na
133	105	55	1.32		65.72	49.81	na	na	na	na	na	na
134	105	65	1.22	12.74		50.66	na	na	na	na	na	na
135	105	75	1.42		67.10	50.15	na	na	na	na	na	na
136	105	85	1.45			49.84	na	na	na	na	na	na
137	105	95	1.45			50.33	na	na	na	na	na	na
138	105	105	1.99		63.18	51.09	na	na	na	na	na	na
139	105	115	1.12		64.50	49.54	na	na	na	na	na	na
140	105	125	1.89			49.84	na	na	na	na	na	na
141	105	135	0.92		72.57	50.63	na	na	na	na	na	na
142	105	145	6.53		79.33	45.86	na	na	na	na	na	na
143	105	155	1.42		65.47	50.63	na	na	na	na	na	na
144	105	165	1.99	17.11	66.09	49.94	na	na	na	na	na	na
145	105	175	1.66		66.56	50.66	na	na	na	na	na	na
146	105	185	2.69	17.34	64.87	49.94	na	na	na	na	na	na
147	105	195	2.39			50.24	na	na	na	na	na	na
148	105	205	2.83		63.37	49.45	na	na	na	na	na	na
149	105	215	1.32		66.53	50.18	na	na	na	na	na	na
150	105	225	0.88	15.12		51.06	na	na	na	na	na	na

SAMPLE			XRD				ORGANIC GEOCHEM PYROLYSIS YIELDS			CLAY MINERALOGY		
Seq	Site	Depth	Mg in Cal	Mg in HMC	Ca in Pd	Ca in Dol	S1	S2	S3	Expand	Illite	Kao+Chlo
no	ID	cm	%	%	%	%	mg/cc	mg/cc	mg/cc	%	%	%
151	105	235	2.76	13.75	64.37	49.24	na	na	na	na	na	na
152	105	245	2.59		65.44	49.66	na	na	na	na	na	na
153	105	255	1.69	15.97	66.47	50.33	na	na	na	na	na	na
154	105	265	1.32	15.48		50.42	na	na	na	na	na	na
155	105	275	2.39			49.60	na	na	na	na	na	na
156	105	285	1.56	15.65	66.44	50.15	na	na	na	na	na	na
157	105	295	2.06	13.85		50.36	na	na	na	na	na	na
158	105	305	2.66		64.62	49.30	na	na	na	na	na	na
159	105	315	2.29	16.69	64.56	49.87	na	na	na	na	na	na
160	105	325	1.08			50.60	na	na	na	na	na	na
161	105	335	2.16		64.65	50.18	na	na	na	na	na	na
162	105	345	2.86			49.42	na	na	na	na	na	na
163	105	355	2.76		64.09	49.63	na	na	na	na	na	na
164	105	365	3.93			48.88	na	na	na	na	na	na
165	105	375	0.85		66.66	51.48	na	na	na	na	na	na
166	105	385	1.52	14.47	66.69	50.36	na	na	na	na	na	na
167	105	395	3.87		62.59	48.12	na	na	na	na	na	na
168	105	405	3.16		64.46	49.24	na	na	na	na	na	na
169	105	415	1.56			50.45	na	na	na	na	na	na
170	105	425	2.36	15.42	72.66	49.60	na	na	na	na	na	na
171	105	435	1.99		66.78	50.06	na	na	na	na	na	na
172	105	445	0.82		66.88	51.33	na	na	na	na	na	na
173	105	455	1.02	14.14	65.53	51.03	na	na	na	na	na	na
174	105	465	1.05		67.26	50.60	na	na	na	na	na	na
175	105	475	1.08		67.19	50.72	na	na	na	na	na	na
176	105	485	1.15			50.60	na	na	na	na	na	na
177	105	495	1.08		66.16	50.30	na	na	na	na	na	na
178	105	505	1.66		65.34	49.81	na	na	na	na	na	na
179	106	5	0.14	15.94		49.24	na	na	na	na	na	na
180	106	15			63.06	45.38	na	na	na	na	na	na
181	106	25	3.23			49.84	na	na	na	na	na	na
182	106	35			65.59	50.15	na	na	na	na	na	na
183	106	45			65.03	49.84	na	na	na	na	na	na
184	106	55		15.74	68.39	50.21	na	na	na	na	na	na
185	106	65		17.53	62.94	48.33	na	na	na	na	na	na
186	106	75		15.32		50.42	na	na	na	na	na	na
187	106	85			66.47	49.63	na	na	na	na	na	na
188	106	95				49.60	na	na	na	na	na	na
189	106	105		15.09	68.17	48.03	na	na	na	na	na	na
190	106	115	3.13		66.41	49.18	na	na	na	na	na	na
191	106	125	3.66	17.24		47.46	na	na	na	na	na	na
192	106	135	1.76		70.25	50.21	na	na	na	na	na	na
193	106	145	3.77		62.87	48.00	na	na	na	na	na	na
194	106	155	3.66		63.15	48.09	na	na	na	na	na	na
195	106	165	0.95		65.47	50.36	na	na	na	na	na	na
196	106	175	0.78	12.87	65.40	51.18	na	na	na	na	na	na
197	106	185	1.05		65.75	50.72	na	na	na	na	na	na
198	106	195	0.85			50.72	na	na	na	na	na	na
199	106	205	0.95	13.91		50.45	na	na	na	na	na	na
200	106	215	1.76	14.93		50.21	na	na	na	na	na	na

SAMPLE			XRD				ORGANIC GEOCHEM PYROLYSIS YIELDS			CLAY MINERALOGY		
Seq	Site	Depth	Mg in Cal	Mg in HMC	Ca in Pd	Ca in Dol	S1	S2	S3	Expand	Illite	Kao+Chlo
no	ID	cm	%	%	%	%	mg/cc	mg/cc	mg/cc	%	%	%
201	106	225	0.75	14.37	66.47	50.85	na	na	na	na	na	na
202	106	235	1.42			50.54	na	na	na	na	na	na
203	106	245	1.22			50.69	na	na	na	na	na	na
204	106	255	1.05			50.85	na	na	na	na	na	na
205	106	265	0.92			50.88	na	na	na	na	na	na
206	106	275	1.08			50.82	na	na	na	na	na	na
207	106	285	2.16		65.37	49.69	na	na	na	na	na	na
208	106	295	1.42			50.60	na	na	na	na	na	na
209	106	305	2.02			49.84	na	na	na	na	na	na
210	106	315	0.45			51.39	na	na	na	na	na	na
211	106	325	1.22	13.75		50.54	na	na	na	na	na	na
212	106	335	1.92			49.84	na	na	na	na	na	na
213	106	345	1.89		66.34	50.18	na	na	na	na	na	na
214	106	355	1.05			50.78	na	na	na	na	na	na
215	106	365	0.98		67.16	51.27	na	na	na	na	na	na
216	106	375	1.42		64.37	50.45	na	na	na	na	na	na
217	106	385	0.75		67.48	51.18	na	na	na	na	na	na
218	106	395		15.58	64.43	49.36	na	na	na	na	na	na
219	106	405	1.59		65.03	50.51	na	na	na	na	na	na
220	106	415	1.56	16.72		50.06	na	na	na	na	na	na
221	106	425	1.22			50.48	na	na	na	na	na	na
222	106	435	1.79		66.75	50.12	na	na	na	na	na	na
223	106	445	1.22			51.85	na	na	na	na	na	na
224	106	455	2.36		63.72	49.87	na	na	na	na	na	na
225	106	465	2.26	16.62	52.49		na	na	na	na	na	na
226	106	475	1.99		66.34	50.39	na	na	na	na	na	na
227	106	485	2.09			50.21	na	na	na	na	na	na
228	106	495	1.42	16.36		51.24	na	na	na	na	na	na
229	106	505	1.89		66.28	50.45	na	na	na	na	na	na
230	106	515	0.98			50.06	na	na	na	na	na	na
231	106	525	1.49			50.97	na	na	na	na	na	na
232	106	535	1.19			50.91	na	na	na	na	na	na
233	106	545	2.86			49.69	na	na	na	na	na	na
234	106	555	1.05			51.54	na	na	na	na	na	na
235	106	565	1.05			51.39	na	na	na	na	na	na
236	106	575	0.35	12.90	52.40		na	na	na	na	na	na
237	106	585	2.39		53.16		na	na	na	na	na	na
238	106	595	0.38			51.85	na	na	na	na	na	na
239	106	605	1.62	16.04	65.56	50.63	na	na	na	na	na	na
240	106	615	0.88		65.15	51.73	na	na	na	na	na	na
241	106	625	0.88			49.94	na	na	na	na	na	na
242	106	635	1.39		67.13	50.21	na	na	na	na	na	na
243	106	645	1.79	16.88	65.97	50.66	na	na	na	na	na	na
244	106	655	1.02		65.56	50.78	na	na	na	na	na	na
245	106	665	0.72		66.44	51.15	na	na	na	na	na	na
246	106	675	1.19	15.61		51.64	na	na	na	na	na	na
247	106	685	1.92	13.62		50.36	na	na	na	na	na	na
248	106	695	2.66	14.31	64.03	50.24	na	na	na	na	na	na
249	107	5		14.93	66.97		na	na	na	na	na	na
250	107	15			64.15		na	na	na	na	na	na

SAMPLE			XRD				ORGANIC GEOCHEM PYROLYSIS YIELDS			CLAY MINERALOGY		
Seq	Site	Depth	Mg in Cal	Mg in HMC	Ca in Pd	Ca in Dol	S1	S2	S3	Expand	Illite	Kao+Chlo
no	ID	cm	%	%	%	%	mg/cc	mg/cc	mg/cc	%	%	%
251	107	25					na	na	na	na	na	na
252	107	35	0.41			50.82	na	na	na	67	15	17
253	107	45			68.70		na	na	na	na	na	na
254	107	55		13.85	65.18		na	na	na	43	24	32
255	107	65			63.72		na	na	na	na	na	na
256	107	75	1.15		66.60		na	na	na	36	31	31
257	107	85			64.68	51.94	na	na	na	na	na	na
258	107	95		14.86	66.63	50.82	na	na	na	21	36	41
259	107	105			68.33	50.30	na	na	na	na	na	na
260	107	115			75.47	50.03	na	na	na	37	38	25
261	107	125			65.15	49.75	na	na	na	na	na	na
262	107	135		4.53		50.45	na	na	na	48	25	26
263	107	145			66.19	50.24	na	na	na	na	na	na
264	107	155		13.19	65.78	50.51	na	na	na	na	na	na
265	107	165				50.42	na	na	na	44	27	27
266	107	175		14.24	63.93	49.39	na	na	na	na	na	na
267	107	185	2.46			49.24	na	na	na	na	na	na
268	107	195	1.96		64.03	49.66	na	na	na	23	33	42
269	107	205	1.96	12.57	65.62	49.60	na	na	na	na	na	na
270	107	215	3.53			47.97	na	na	na	na	na	na
271	107	225	1.62		64.78	49.51	na	na	na	55	20	24
272	107	235	1.66			49.78	na	na	na	na	na	na
273	107	245	1.79			49.33	na	na	na	na	na	na
274	107	255	1.45		64.31	49.97	na	na	na	34	31	34
275	107	265	2.16			49.91	na	na	na	na	na	na
276	107	275	2.63		67.48	49.24	na	na	na	na	na	na
277	107	285	1.32		65.09	49.75	na	na	na	54	24	21
278	107	295	1.99		65.59	50.18	na	na	na	na	na	na
279	107	305	3.03		63.15	49.18	na	na	na	na	na	na
280	107	315	1.56			49.45	na	na	na	10	40	50
281	107	325	1.19		67.63	50.33	na	na	na	na	na	na
282	107	335	0.78		65.31	50.00	na	na	na	na	na	na
283	107	345	5.40	17.24		46.64	na	na	na	0	62	37
284	107	355	-0.02			51.36	na	na	na	na	na	na
285	107	365	1.02	14.27		50.57	na	na	na	na	na	na
286	107	375	2.46	15.32		49.33	na	na	na	na	na	na
287	107	385	1.99			49.54	na	na	na	6	46	46
288	107	395	1.22	14.54		50.03	na	na	na	na	na	na
289	107	405	1.35	14.31	67.13	50.57	na	na	na	na	na	na
290	107	415	1.15		66.66	50.69	na	na	na	na	na	na
291	107	425	2.33			50.06	na	na	na	66	16	16
292	107	435	1.29		65.37	49.36	na	na	na	na	na	na
293	107	445	5.27	19.80	60.88	45.77	na	na	na	na	na	na
294	107	455	2.02	16.20	64.28	49.27	na	na	na	21	36	41
295	107	465	1.56			49.60	na	na	na	na	na	na
296	107	475	2.26	12.80		50.30	na	na	na	0	64	35
297	107	485	3.36		64.75	48.33	na	na	na	na	na	na
298	107	495	6.80		62.41	45.86	na	na	na	na	na	na
299	107	505	2.43		64.56	49.60	na	na	na	34	32	33
300	107	515	1.35			49.81	na	na	na	na	na	na

SAMPLE			XRD				ORGANIC GEOCHEM PYROLYSIS YIELDS			CLAY MINERALOGY		
Seq	Site	Depth	Mg in Cal	Mg in HMC	Ca in Pd	Ca in Dol	S1	S2	S3	Expand	Illite	Kao+Chlo
no	ID	cm	%	%	%	%	mg/cc	mg/cc	mg/cc	%	%	%
301	107	525	1.89		66.22	49.60	na	na	na	na	na	na
302	107	535	2.06			49.72	na	na	na	20	40	40
303	107	545	3.60		62.69	48.03	na	na	na	na	na	na
304	107	555	2.63			50.09	na	na	na	38	30	30
305	107	565	1.05			50.42	na	na	na	na	na	na
306	107	575	1.29	13.88	66.53	49.54	na	na	na	na	na	na
307	107	585	1.59		64.87	50.54	na	na	na	20	40	40
308	107	595	2.13			49.57	na	na	na	na	na	na
309	107	605	3.20			50.33	na	na	na	na	na	na
310	107	615	1.66	14.47		50.30	na	na	na	na	na	na
311	107	625	1.39	13.36	71.62	50.21	na	na	na	20	80	na
312	107	635	0.65			50.63	na	na	na	na	na	na
313	107	645	0.85	14.31	65.37	50.60	na	na	na	na	na	na
314	107	655	0.82	12.90	73.65	50.85	na	na	na	na	na	na
315	107	665	4.83		65.47	47.82	na	na	na	25	60	15
316	107	675	1.76			49.97	na	na	na	na	na	na
317	107	685	0.88			50.78	na	na	na	na	na	na
318	107	695	1.96		77.97	50.78	na	na	na	na	na	na
319	110A	5	1.69	14.96	66.38		na	na	na	na	na	na
320	110A	15	0.88	15.61	67.54		na	na	na	na	na	na
321	110A	25		14.90	66.72		na	na	na	na	na	na
322	110A	35			66.34		na	na	na	na	na	na
323	110A	45	1.19	14.47	65.47		na	na	na	na	na	na
324	110A	55			65.75		na	na	na	na	na	na
325	110A	65		13.33	65.56		na	na	na	na	na	na
326	110A	75		17.60	65.56		na	na	na	na	na	na
327	110A	85		14.50	64.75		na	na	na	na	na	na
328	110A	95	-0.13	14.93	66.22		na	na	na	na	na	na
329	110A	105		14.70	67.04		na	na	na	na	na	na
330	110A	115			65.59		na	na	na	na	na	na
331	110A	125		19.25	68.11		na	na	na	na	na	na
332	110A	135	3.77	15.09	64.65		na	na	na	na	na	na
333	110A	145		14.47	55.94		na	na	na	na	na	na
334	110A	155	1.52	15.87	67.19		na	na	na	na	na	na
335	110A	165	0.78	11.59	65.12		na	na	na	na	na	na
336	110A	175		14.96	67.32	50.54	na	na	na	na	na	na
337	110A	185		17.86	66.25	49.97	na	na	na	na	na	na
338	110A	195		14.47	70.92	49.78	na	na	na	na	na	na
339	110A	205	0.01	13.59	67.73	49.87	na	na	na	na	na	na
340	110A	215	0.78		52.06		na	na	na	na	na	na
341	110A	225	1.79		66.69	49.84	na	na	na	na	na	na
342	113A	5			65.53	51.82	na	na	na	na	na	na
343	113A	15			64.81		na	na	na	na	na	na
344	113A	25		14.80	65.84		na	na	na	na	na	na
345	113A	35		13.33	64.25		na	na	na	na	na	na
346	113A	45	-0.02	12.67	64.31		na	na	na	na	na	na
347	113A	55		15.68	64.34		na	na	na	na	na	na
348	113A	65	3.50	15.16	54.17		na	na	na	na	na	na
349	113A	75		13.39	65.81	50.30	na	na	na	na	na	na
350	113A	85		15.09	67.85		na	na	na	na	na	na

SAMPLE			XRD				ORGANIC GEOCHEM PYROLYSIS YIELDS			CLAY MINERALOGY		
Seq	Site	Depth	Mg in Cal	Mg in HMC	Ca in Pd	Ca in Dol	S1	S2	S3	Expand	Illite	Kao+Chlo
no	ID	cm	%	%	%	%	mg/cc	mg/cc	mg/cc	%	%	%
351	113A	95		15.22	65.25		na	na	na	na	na	na
352	113A	105		15.71	66.63		na	na	na	na	na	na
353	113A	115	2.83				na	na	na	na	na	na
354	113A	125		15.48	66.63		na	na	na	na	na	na
355	113A	135		14.18		50.27	na	na	na	na	na	na
356	113A	145		14.96	64.75	49.39	na	na	na	na	na	na
357	113A	155		14.50	65.44	49.63	na	na	na	na	na	na
358	113A	165			64.78	48.57	na	na	na	na	na	na
359	113A	175			66.19	49.87	na	na	na	na	na	na
360	113A	185		14.01		49.81	na	na	na	na	na	na
361	113A	195				50.39	na	na	na	na	na	na
362	113A	205			65.47	50.12	na	na	na	na	na	na
363	115	5				49.97	na	na	na	na	na	na
364	115	15			55.27		na	na	na	na	na	na
365	115	25					na	na	na	na	na	na
366	115	35		14.80			na	na	na	na	na	na
367	115	45		14.73			na	na	na	na	na	na
368	115	55					na	na	na	na	na	na
369	115	65		14.11	68.96		na	na	na	na	na	na
370	115	75				48.63	na	na	na	na	na	na
371	115	85		16.20		50.66	na	na	na	na	na	na
372	115	95		13.69		50.48	na	na	na	na	na	na
373	115	105			67.92	51.36	na	na	na	na	na	na
374	115	115	-1.47			50.30	na	na	na	na	na	na
375	115	125		14.21			na	na	na	na	na	na
376	115	135			66.53	51.39	na	na	na	na	na	na
377	115	145				50.57	na	na	na	na	na	na
378	115	155				50.09	na	na	na	na	na	na
379	115	165			66.16	51.48	na	na	na	na	na	na
380	115	175		14.37	67.19	50.15	na	na	na	na	na	na
381	115	185				50.18	na	na	na	na	na	na
382	115	195				49.63	na	na	na	na	na	na
383	115	205				50.48	na	na	na	na	na	na
384	115	215		14.21		50.15	na	na	na	na	na	na
385	115	225		14.24	58.69	50.36	na	na	na	na	na	na
386	115	235		12.93		50.42	na	na	na	na	na	na
387	115	245			66.78	50.54	na	na	na	na	na	na
388	115	255			67.44	49.91	na	na	na	na	na	na
389	115	265		13.26	66.16	50.39	na	na	na	na	na	na
390	120	5				49.45	na	na	na	na	na	na
391	120	15		15.19		49.33	na	na	na	na	na	na
392	120	25				48.79	na	na	na	na	na	na
393	120	35		18.38	56.41	49.69	na	na	na	na	na	na
394	120	45		15.29	67.16	50.00	na	na	na	na	na	na
395	120	55				49.33	na	na	na	na	na	na
396	120	65			64.68	50.03	na	na	na	na	na	na
397	120	75				50.09	na	na	na	na	na	na
398	120	85		14.08		50.27	na	na	na	na	na	na
399	120	95		15.48	68.55	50.27	na	na	na	na	na	na
400	120	105			68.64	49.97	na	na	na	na	na	na

SAMPLE			XRD				ORGANIC GEOCHEM PYROLYSIS YIELDS			CLAY MINERALOGY		
Seq	Site	Depth	Mg in Cal	Mg in HMC	Ca in Pd	Ca in Dol	S1	S2	S3	Expand	Illite	Kao+Chlo
no	ID	cm	%	%	%	%	mg/cc	mg/cc	mg/cc	%	%	%
401	120	115	3.00		64.34	50.66	na	na	na	na	na	na
402	120	125				50.33	na	na	na	na	na	na
403	120	135		10.99	68.17	50.39	na	na	na	na	na	na
404	120	145			66.31	49.30	na	na	na	na	na	na
405	120	155		16.10	64.75	50.15	na	na	na	na	na	na
406	120	165			72.98	50.09	na	na	na	na	na	na
407	120	175		15.78		50.06	na	na	na	na	na	na
408	120	185	1.08		65.50	49.21	na	na	na	na	na	na
409	120	195		14.57	66.44		na	na	na	na	na	na
410	120	205		14.34	68.93		na	na	na	na	na	na
411	120	215		12.08	69.08	51.27	na	na	na	na	na	na
412	120	225		13.36	66.41		na	na	na	na	na	na
413	120	235		15.48	64.56		na	na	na	na	na	na
414	120	245			64.90		na	na	na	na	na	na
415	120	255		16.23	66.34		na	na	na	na	na	na
416	120	265			65.50		na	na	na	na	na	na
417	120	275		19.93	61.97		na	na	na	na	na	na
418	120	285			64.28		na	na	na	na	na	na
419	120	295			62.81		na	na	na	na	na	na
420	120	305	2.80			51.76	na	na	na	na	na	na
421	120	315		20.74	69.11	47.88	na	na	na	na	na	na
422	120	325	2.36	17.86		49.09	na	na	na	na	na	na
423	120	335	3.00			49.48	na	na	na	na	na	na
424	120	345	1.92	14.67		49.36	na	na	na	na	na	na
425	121	5			67.19		na	na	na	na	na	na
426	121	15	2.59		52.92		na	na	na	36	30	33
427	121	25			66.31	51.73	na	na	na	na	na	na
428	121	35		13.85			na	na	na	na	na	na
429	121	45					na	na	na	36	27	36
430	121	55					na	na	na	na	na	na
431	121	65					na	na	na	na	na	na
432	121	75		15.48	76.95		na	na	na	31	47	21
433	121	85		8.98			na	na	na	na	na	na
434	121	95			66.06		na	na	na	48	21	30
435	121	105					na	na	na	na	na	na
436	121	115	0.00	9.11	70.13		na	na	na	na	na	na
437	121	125		15.06			na	na	na	30	27	42
438	121	135		6.80	65.40		na	na	na	42	28	29
439	121	145			64.87		na	na	na	na	na	na
440	121	155		6.36			na	na	na	na	na	na
441	121	165					na	na	na	na	na	na
442	121	175		15.19			na	na	na	45	25	30
443	121	185		15.65	76.63		na	na	na	na	na	na
444	121	195					na	na	na	36	30	33
445	121	205		14.21	75.86		na	na	na	na	na	na
446	121	215				51.45	na	na	na	49	25	25
447	121	225			66.19		na	na	na	na	na	na
448	121	235		14.14		49.42	na	na	na	26	28	45
449	121	245			66.72		na	na	na	na	na	na
450	121	255		14.34		50.27	na	na	na	na	na	na

SAMPLE			XRD				ORGANIC GEOCHEM PYROLYSIS YIELDS			CLAY MINERALOGY		
Seq	Site	Depth	Mg in Cal	Mg in HMC	Ca in Pd	Ca in Dol	S1	S2	S3	Expand	Illite	Kao+Chlo
no	ID	cm	%	%	%	%	mg/cc	mg/cc	mg/cc	%	%	%
451	121	265			65.47	51.48	na	na	na	na	na	na
452	121	275		14.37		49.33	na	na	na	na	na	na
453	121	285	-0.29	11.95	65.44	50.27	na	na	na	42	27	30
454	121	295		14.14	64.34	50.85	na	na	na	na	na	na
455	121	305			67.54	50.33	na	na	na	na	na	na
456	121	315				50.69	na	na	na	na	na	na
457	121	325			66.00	51.39	na	na	na	27	35	36
458	121	335		16.88		50.09	na	na	na	na	na	na
459	121	345				50.15	na	na	na	na	na	na
460	121	355		13.10		50.39	na	na	na	na	na	na
461	121	365				49.66	na	na	na	na	na	na
462	121	375		11.26		49.51	na	na	na	30	27	41
463	121	385				50.45	na	na	na	na	na	na
464	121	395			65.53	50.33	na	na	na	36	29	28
465	121	405		19.28		49.33	na	na	na	na	na	na
466	121	415				49.09	na	na	na	na	na	na
467	121	425			66.78	49.60	na	na	na	48	22	29
468	121	435		15.19	65.56	49.75	na	na	na	na	na	na
469	121	445		17.18		49.24	na	na	na	na	na	na
470	121	455				49.78	na	na	na	na	na	na
471	121	465				49.09	na	na	na	45	29	24
472	121	475	2.06	17.53		49.15	na	na	na	na	na	na
473	121	485	1.69		77.78	49.91	na	na	na	na	na	na
474	121	495	0.98			49.81	na	na	na	na	na	na
475	121	505	0.75			51.06	na	na	na	60	15	24
476	121	515	1.35		72.60	49.72	na	na	na	na	na	na
477	121	525	2.39	16.46		48.51	na	na	na	na	na	na
478	121	535	1.86	15.09		49.63	na	na	na	na	na	na
479	121	545	0.78			50.60	na	na	na	12	50	37
480	122A	5				49.94	6.90	27.70	6.90	na	na	na
481	122A	15		17.40	66.16		8.60	22.90	6.96	na	na	na
482	122A	25		15.87			na	na	na	na	na	na
483	122A	35					8.30	17.70	7.10	na	na	na
484	122A	45		14.47			na	na	na	na	na	na
485	122A	55		12.44	64.15	49.12	1.50	4.40	2.80	na	na	na
486	122A	65		16.75	64.03		na	na	na	na	na	na
487	122A	75		14.31		48.06	0.35	1.60	1.50	na	na	na
488	122A	85		16.88		48.63	na	na	na	na	na	na
489	122A	95		14.14		50.54	4.05	19.43	4.14	na	na	na
490	122A	105		16.46		50.39	na	na	na	na	na	na
491	122A	115					0.86	3.71	4.06	na	na	na
492	122A	125	2.83				na	na	na	na	na	na
493	122A	135		13.16	57.61		1.51	6.21	4.33	na	na	na
494	122A	145			63.84		na	na	na	na	na	na
495	122A	155		14.05		49.45	1.11	5.33	3.28	na	na	na
496	122A	165				49.42	na	na	na	na	na	na
497	122A	175			66.00	49.27	1.84	5.98	3.61	na	na	na
498	122A	185		14.90		49.45	na	na	na	na	na	na
499	122A	195		14.24		49.81	2.15	8.07	3.41	na	na	na
500	122A	205				48.88	na	na	na	na	na	na

SAMPLE			XRD				ORGANIC GEOCHEM PYROLYSIS YIELDS			CLAY MINERALOGY		
Seq	Site	Depth	Mg in Cal	Mg in HMC	Ca in Pd	Ca in Dol	S1	S2	S3	Expand	Illite	Kao+Chlo
no	ID	cm	%	%	%	%	mg/cc	mg/cc	mg/cc	%	%	%
501	122A	215		15.48		49.21	1.97	7.18	3.50	na	na	na
502	122A	225			66.66	49.66	na	na	na	na	na	na
503	122A	235		18.12		49.36	0.59	2.32	2.65	na	na	na
504	122A	245				49.18	na	na	na	na	na	na
505	122A	255		13.65		49.21	1.16	3.81	3.60	na	na	na
506	122A	265			67.26	50.03	na	na	na	na	na	na
507	122A	275		11.52		49.87	1.41	4.22	3.80	na	na	na
508	122A	285	3.03	14.93		48.97	na	na	na	na	na	na
509	122A	295		16.36		49.00	1.91	5.36	4.30	na	na	na
510	122A	305		15.84		49.15	na	na	na	na	na	na
511	122A	315				49.15	5.56	24.77	4.80	na	na	na
512	122A	325				49.21	na	na	na	na	na	na
513	122A	335		15.61		49.27	0.75	7.01	2.00	na	na	na
514	122A	345	2.73	12.18	63.15	49.15	na	na	na	na	na	na
515	122A	355				47.73	0.39	3.35	1.32	na	na	na
516	122A	365	2.19	15.25	65.69	49.42	na	na	na	na	na	na
517	122A	375	1.86			49.39	0.11	0.76	0.74	na	na	na
518	122A	385	1.39	14.08	68.48	49.21	na	na	na	na	na	na
519	122A	395	0.58			50.36	0.02	0.42	0.50	na	na	na
520	122A	405	1.89		66.85	49.63	na	na	na	na	na	na
521	122A	415	0.98			50.09	0.02	0.24	0.50	na	na	na
522	122A	425	1.72			49.60	na	na	na	na	na	na
523	122A	435		14.83		49.72	0.03	0.25	0.39	na	na	na
524	122A	445		4.80		49.78	na	na	na	na	na	na
525	122A	455	2.29		66.60	50.12	0.01	0.14	0.33	na	na	na
526	122A	465	2.53			50.15	na	na	na	na	na	na
527	122A	475		4.87	67.04	50.03	0.02	0.23	0.38	na	na	na
528	1A	1			70.00	48.12	na	na	na	na	na	na
529	1A	2		13.82		49.51	na	na	na	na	na	na
530	1A	3				49.69	na	na	na	na	na	na
531	1A	4	-0.29	15.68		49.57	na	na	na	na	na	na
532	1A	5		15.38	64.59	49.72	na	na	na	na	na	na
533	1A	6			65.09	49.66	na	na	na	na	na	na
534	1A	7		14.76		49.78	na	na	na	na	na	na
535	1A	8				49.54	na	na	na	na	na	na
536	1A	9		15.16	65.15	49.78	na	na	na	na	na	na
537	1A	10		12.21	72.57	49.27	na	na	na	na	na	na
538	1A	11		14.27	64.71	50.18	na	na	na	na	na	na
539	1A	12		10.83		50.33	na	na	na	na	na	na
540	1A	13				49.57	na	na	na	na	na	na
541	1A	14		15.52		50.45	na	na	na	na	na	na
542	1A	15			72.44	49.72	na	na	na	na	na	na
543	1A	16	0.51			50.33	na	na	na	na	na	na
544	1A	17				50.00	na	na	na	na	na	na
545	1A	18				49.48	na	na	na	na	na	na
546	1A	19				50.45	na	na	na	na	na	na
547	1A	20				50.42	na	na	na	na	na	na
548	1A	21				50.39	na	na	na	na	na	na
549	1A	22		14.37		49.42	na	na	na	na	na	na
550	1A	23				50.21	na	na	na	na	na	na

SAMPLE			XRD				ORGANIC GEOCHEM PYROLYSIS YIELDS			CLAY MINERALOGY		
Seq	Site	Depth	Mg in Cal	Mg in HMC	Ca in Pd	Ca in Dol	S1	S2	S3	Expand	Illite	Kao+Chlo
no	ID	cm	%	%	%	%	mg/cc	mg/cc	mg/cc	%	%	%
551	1A	24		14.63	69.97	49.94	na	na	na	na	na	na
552	1A	25	2.23		71.08	50.00	na	na	na	na	na	na
553	1A	26				49.78	na	na	na	na	na	na
554	1A	27				50.36	na	na	na	na	na	na
555	1A	28				50.60	na	na	na	na	na	na
556	1A	29		14.60	69.02	50.51	na	na	na	na	na	na
557	1A	30		16.26		50.24	na	na	na	na	na	na
558	1A	31				50.48	na	na	na	na	na	na
559	1A	32				50.39	na	na	na	na	na	na
560	1A	33		11.78	65.22	50.51	na	na	na	na	na	na
561	1A	34	1.32			50.72	na	na	na	na	na	na
562	1A	35				50.45	na	na	na	na	na	na
563	1A	36	1.66		65.50	50.24	na	na	na	na	na	na
564	1A	37				50.48	na	na	na	na	na	na
565	1A	38		14.86	65.47	49.81	na	na	na	na	na	na
566	1A	39		14.60		49.33	na	na	na	na	na	na
567	1A	40		10.70		50.48	na	na	na	na	na	na
568	1A	41				49.69	na	na	na	na	na	na
569	1A	42		14.34		50.54	na	na	na	na	na	na
570	2A	1		12.31	65.44		na	na	na	na	na	na
571	2A	2		12.44		51.15	na	na	na	na	na	na
572	2A	3				51.76	na	na	na	na	na	na
573	2A	4		14.47		50.85	na	na	na	na	na	na
574	2A	5			65.22		na	na	na	na	na	na
575	2A	6		13.42	66.78		na	na	na	na	na	na
576	2A	7		12.80	68.52		na	na	na	na	na	na
577	2A	8				48.00	na	na	na	na	na	na
578	2A	9		14.80	67.10		na	na	na	na	na	na
579	2A	10					na	na	na	na	na	na
580	2A	11		14.37	65.22	49.30	na	na	na	na	na	na
581	2A	12			66.12		na	na	na	na	na	na
582	2A	13			65.44		na	na	na	na	na	na
583	2A	14			70.44		na	na	na	na	na	na
584	2A	15		14.44	68.93		na	na	na	na	na	na
585	2A	16		14.99			na	na	na	na	na	na
586	2A	17			66.97		na	na	na	na	na	na
587	2A	18		12.57	64.97		na	na	na	na	na	na
588	2A	19					na	na	na	na	na	na
589	2A	20		15.22	64.00		na	na	na	na	na	na
590	2A	21					na	na	na	na	na	na
591	2A	22			66.88		na	na	na	na	na	na
592	2A	23			66.19		na	na	na	na	na	na
593	2A	24		12.80	65.40		na	na	na	na	na	na
594	2A	25		15.09			na	na	na	na	na	na
595	2A	26		14.47	67.60		na	na	na	na	na	na
596	2A	27				50.82	na	na	na	na	na	na
597	2A	28		16.53			na	na	na	na	na	na
598	2A	29				51.33	na	na	na	na	na	na
599	2A	30			69.05		na	na	na	na	na	na
600	2A	31			67.44		na	na	na	na	na	na

SAMPLE			XRD				ORGANIC GEOCHEM PYROLYSIS YIELDS			CLAY MINERALOGY		
Seq	Site	Depth	Mg in Cal	Mg in HMC	Ca in Pd	Ca in Dol	S1	S2	S3	Expand	Illite	Kao+Chlo
no	ID	cm	%	%	%	%	mg/cc	mg/cc	mg/cc	%	%	%
601	2A	32					na	na	na	na	na	na
602	2A	33					na	na	na	na	na	na
603	2A	34		15.32	66.85		na	na	na	na	na	na
604	2A	35		13.00	67.57		na	na	na	na	na	na
605	2A	36		13.26	53.13		na	na	na	na	na	na
606	2A	38					na	na	na	na	na	na
607	2A	39		11.22	66.56		na	na	na	na	na	na
608	2A	40		13.91			na	na	na	na	na	na
609	2A	41			53.07		na	na	na	na	na	na
610	2A	42					na	na	na	na	na	na
611	3A	1				50.54	na	na	na	na	na	na
612	3A	2		15.78	65.12	50.54	na	na	na	na	na	na
613	3A	3			65.62	51.88	na	na	na	na	na	na
614	3A	4			65.12	49.45	na	na	na	na	na	na
615	3A	5					na	na	na	na	na	na
616	3A	6		17.73		49.97	na	na	na	na	na	na
617	3A	7			65.37		na	na	na	na	na	na
618	3A	8			67.66		na	na	na	na	na	na
619	3A	9		12.08		50.00	na	na	na	na	na	na
620	3A	10				51.30	na	na	na	na	na	na
621	3A	11		15.12	68.61		na	na	na	na	na	na
622	3A	12		14.24	68.55		na	na	na	na	na	na
623	3A	13					na	na	na	na	na	na
624	3A	14					na	na	na	na	na	na
625	3A	15		13.55			na	na	na	na	na	na
626	3A	16			65.40		na	na	na	na	na	na
627	3A	17	2.13	13.39	64.12		na	na	na	na	na	na
628	3A	18			65.91		na	na	na	na	na	na
629	3A	19				50.45	na	na	na	na	na	na
630	3A	20					na	na	na	na	na	na
631	3A	21		14.41		50.18	na	na	na	na	na	na
632	3A	22		12.67	66.25		na	na	na	na	na	na
633	3A	23				50.39	na	na	na	na	na	na
634	3A	24	-0.23		64.65	50.63	na	na	na	na	na	na
635	3A	25				50.54	na	na	na	na	na	na
636	3A	26				50.60	na	na	na	na	na	na
637	3A	27			65.65		na	na	na	na	na	na
638	3A	28			66.85	50.60	na	na	na	na	na	na
639	3A	29			66.82		na	na	na	na	na	na
640	3A	30	1.32		67.85	50.48	na	na	na	na	na	na
641	3A	31			67.22		na	na	na	na	na	na
642	3A	32		16.33	63.56	50.88	na	na	na	na	na	na
643	3A	33			72.63		na	na	na	na	na	na
644	3A	34				49.91	na	na	na	na	na	na
645	3A	35		15.29			na	na	na	na	na	na
646	3A	36		13.75	68.29	49.60	na	na	na	na	na	na
647	3A	37				46.43	na	na	na	na	na	na
648	3A	38		16.72		48.21	na	na	na	na	na	na
649	3A	39				50.69	na	na	na	na	na	na
650	3A	40			65.18	50.33	na	na	na	na	na	na

SAMPLE			XRD				ORGANIC GEOCHEM PYROLYSIS YIELDS			CLAY MINERALOGY		
Seq	Site	Depth	Mg in Cal	Mg in HMC	Ca in Pd	Ca in Dol	S1	S2	S3	Expand	Illite	Kao+Chlo
no	ID	cm	%	%	%	%	mg/cc	mg/cc	mg/cc	%	%	%
651	3A	41		12.14		49.72	na	na	na	na	na	na
652	3A	42				49.48	na	na	na	na	na	na
653	3A	43		12.21	65.44	48.94	na	na	na	na	na	na
654	3A	44		15.42		50.78	na	na	na	na	na	na
655	3A	45					na	na	na	na	na	na
656	4A	1			66.19		na	na	na	na	na	na
657	4A	2			65.72		na	na	na	na	na	na
658	4A	3		12.77	66.56		na	na	na	na	na	na
659	4A	4		15.35	66.78		na	na	na	na	na	na
660	4A	5			67.22		na	na	na	na	na	na
661	4A	6					na	na	na	na	na	na
662	4A	7		13.00			na	na	na	na	na	na
663	4A	8			66.38		na	na	na	na	na	na
664	4A	9		13.03	67.00		na	na	na	na	na	na
665	4A	10			55.64		na	na	na	na	na	na
666	4A	11		12.97	66.88		na	na	na	na	na	na
667	4A	12		13.55	66.56		na	na	na	na	na	na
668	4A	13			67.07		na	na	na	na	na	na
669	4A	14					na	na	na	na	na	na
670	4A	15			67.51		na	na	na	na	na	na
671	4A	16			67.32		na	na	na	na	na	na
672	4A	17			64.71		na	na	na	na	na	na
673	4A	18			67.00		na	na	na	na	na	na
674	4A	19			65.59		na	na	na	na	na	na
675	4A	20			65.40		na	na	na	na	na	na
676	4A	21			65.84		na	na	na	na	na	na
677	4A	22		14.60	65.62		na	na	na	na	na	na
678	4A	23		13.03	66.75		na	na	na	na	na	na
679	4A	24					na	na	na	na	na	na
680	4A	25		13.49	65.78		na	na	na	na	na	na
681	4A	26		14.27	65.94		na	na	na	na	na	na
682	4A	27					na	na	na	na	na	na
683	4A	28			65.59		na	na	na	na	na	na
684	4A	29			67.32		na	na	na	na	na	na
685	4A	30			65.87		na	na	na	na	na	na
686	4A	31			57.39		na	na	na	na	na	na
687	4A	32		12.51			na	na	na	na	na	na
688	4A	33					na	na	na	na	na	na
689	4A	34		11.59	65.87		na	na	na	na	na	na
690	4A	35			67.73		na	na	na	na	na	na
691	4A	36			65.28		na	na	na	na	na	na
692	4A	37		13.26			na	na	na	na	na	na
693	4A	38		15.06			na	na	na	na	na	na
694	4A	39		16.26	65.22		na	na	na	na	na	na
695	4A	40		10.70			na	na	na	na	na	na
696	4A	41			67.73		na	na	na	na	na	na
697	4A	42		19.02	61.85		na	na	na	na	na	na
698	4A	43		17.01	76.95		na	na	na	na	na	na
699	5A	1		16.53	65.50		na	na	na	na	na	na
700	5A	2		16.43	66.82		na	na	na	na	na	na

SAMPLE			XRD				ORGANIC GEOCHEM PYROLYSIS YIELDS			CLAY MINERALOGY		
Seq	Site	Depth	Mg in Cal	Mg in HMC	Ca in Pd	Ca in Dol	S1	S2	S3	Expand	Illite	Kao+Chlo
no	ID	cm	%	%	%	%	mg/cc	mg/cc	mg/cc	%	%	%
701	5A	3		13.26	64.56		na	na	na	na	na	na
702	5A	4			67.60		na	na	na	na	na	na
703	5A	5			64.03		na	na	na	na	na	na
704	5A	6			66.00		na	na	na	na	na	na
705	5A	7			68.04		na	na	na	na	na	na
706	5A	8			51.94		na	na	na	na	na	na
707	5A	9			52.79		na	na	na	na	na	na
708	5A	10			65.97		na	na	na	na	na	na
709	5A	11			78.23		na	na	na	na	na	na
710	5A	12			65.75		na	na	na	na	na	na
711	5A	13					na	na	na	na	na	na
712	5A	14			54.17		na	na	na	na	na	na
713	5A	15			65.81		na	na	na	na	na	na
714	5A	16			68.04		na	na	na	na	na	na
715	5A	17			65.56		na	na	na	na	na	na
716	5A	18			65.06		na	na	na	na	na	na
717	5A	19			64.37		na	na	na	na	na	na
718	5A	20		13.16	67.41		na	na	na	na	na	na
719	5A	21			53.37		na	na	na	na	na	na
720	5A	22		16.95			na	na	na	na	na	na
721	5A	23		19.54	61.38		na	na	na	na	na	na
722	5A	24		11.29	65.09		na	na	na	na	na	na
723	5A	25			67.22		na	na	na	na	na	na
724	5A	26		15.55	66.50		na	na	na	na	na	na
725	5A	27		15.22	69.11		na	na	na	na	na	na
726	5A	28		14.67	67.79		na	na	na	na	na	na
727	5A	29					na	na	na	na	na	na
728	5A	30			66.97		na	na	na	na	na	na
729	5A	31		13.42	66.75		na	na	na	na	na	na
730	5A	32			68.55		na	na	na	na	na	na
731	5A	33		13.65	68.45		na	na	na	na	na	na
732	5A	34		13.13	66.50		na	na	na	na	na	na
733	5A	35		15.32	67.73		na	na	na	na	na	na
734	5A	36			65.18		na	na	na	na	na	na
735	5A	37			66.82		na	na	na	na	na	na
736	5A	38			67.00		na	na	na	na	na	na
737	5A	39		3.23	68.36		na	na	na	na	na	na
738	5A	40			66.63		na	na	na	na	na	na
739	6A	1		11.78	55.42		na	na	na	na	na	na
740	6A	2		14.70	66.31		na	na	na	na	na	na
741	6A	3			62.90		na	na	na	na	na	na
742	6A	4		15.19	67.98		na	na	na	na	na	na
743	6A	5			69.34		na	na	na	na	na	na
744	6A	6					na	na	na	na	na	na
745	6A	7					na	na	na	na	na	na
746	6A	8					na	na	na	na	na	na
747	6A	9					na	na	na	na	na	na
748	6A	10					na	na	na	na	na	na
749	6A	11					na	na	na	na	na	na
750	6A	12					na	na	na	na	na	na

SAMPLE			XRD				ORGANIC GEOCHEM PYROLYSIS YIELDS			CLAY MINERALOGY		
Seq	Site	Depth	Mg in Cal	Mg in HMC	Ca in Pd	Ca in Dol	S1	S2	S3	Expand	Illite	Kao+Chlo
no	ID	cm	%	%	%	%	mg/cc	mg/cc	mg/cc	%	%	%
751	6A	13			55.88		na	na	na	na	na	na
752	6A	14		16.23	61.07		na	na	na	na	na	na
753	6A	15		16.79			na	na	na	na	na	na
754	6A	16					na	na	na	na	na	na
755	6A	17		14.93			na	na	na	na	na	na
756	6A	18					na	na	na	na	na	na
757	6A	19		14.31			na	na	na	na	na	na
758	6A	20			66.34		na	na	na	na	na	na
759	6A	21		10.80			na	na	na	na	na	na
760	6A	22		13.69	71.77		na	na	na	na	na	na
761	6A	23					na	na	na	na	na	na
762	6A	24			65.47		na	na	na	na	na	na
763	6A	25			70.13		na	na	na	na	na	na
764	6A	26			77.75		na	na	na	na	na	na
765	6A	27		13.00			na	na	na	na	na	na
766	6A	28					na	na	na	na	na	na
767	6A	29					na	na	na	na	na	na
768	6A	30					na	na	na	na	na	na
769	6A	31		13.72	54.41		na	na	na	na	na	na
770	6A	32					na	na	na	na	na	na
771	6A	33		13.23	53.13		na	na	na	na	na	na
772	6A	34		12.93	66.56		na	na	na	na	na	na
773	6A	35		10.90	53.37		na	na	na	na	na	na
774	6A	36		12.93			na	na	na	na	na	na
775	6A	37			64.65		na	na	na	na	na	na
776	6A	38			52.92		na	na	na	na	na	na
777	6A	39			69.46		na	na	na	na	na	na
778	6A	40			65.75		na	na	na	na	na	na
779	6A	41					na	na	na	na	na	na
780	7A	1					na	na	na	na	na	na
781	7A	2					na	na	na	na	na	na
782	7A	3					na	na	na	na	na	na
783	7A	4					na	na	na	na	na	na
784	7A	5					na	na	na	na	na	na
785	7A	6					na	na	na	na	na	na
786	7A	7					na	na	na	na	na	na
787	7A	8					na	na	na	na	na	na
788	7A	9					na	na	na	na	na	na
789	7A	10					na	na	na	na	na	na
790	7A	11					na	na	na	na	na	na
791	7A	12					na	na	na	na	na	na
792	7A	13					na	na	na	na	na	na
793	7A	14					na	na	na	na	na	na
794	7A	15					na	na	na	na	na	na
795	7A	16					na	na	na	na	na	na
796	7A	17					na	na	na	na	na	na
797	7A	18					na	na	na	na	na	na
798	7A	19					na	na	na	na	na	na
799	7A	20					na	na	na	na	na	na
800	7A	21					na	na	na	na	na	na

SAMPLE			XRD				ORGANIC GEOCHEM PYROLYSIS YIELDS			CLAY MINERALOGY		
Seq	Site	Depth	Mg in Cal	Mg in HMC	Ca in Pd	Ca in Dol	S1	S2	S3	Expand	Illite	Kao+Chlo
no	ID	cm	%	%	%	%	mg/cc	mg/cc	mg/cc	%	%	%
801	7A	22					na	na	na	na	na	na
802	7A	23					na	na	na	na	na	na
803	7A	24					na	na	na	na	na	na
804	7A	25					na	na	na	na	na	na
805	7A	26					na	na	na	na	na	na
806	7A	27					na	na	na	na	na	na
807	7A	28					na	na	na	na	na	na
808	7A	29					na	na	na	na	na	na
809	7A	30					na	na	na	na	na	na
810	7A	31					na	na	na	na	na	na
811	7A	32					na	na	na	na	na	na
812	7A	33					na	na	na	na	na	na
813	7A	34					na	na	na	na	na	na
814	7A	35					na	na	na	na	na	na
815	7A	36					na	na	na	na	na	na
816	7A	37					na	na	na	na	na	na
817	7A	38					na	na	na	na	na	na
818	8A	1					na	na	na	na	na	na
819	8A	2					na	na	na	na	na	na
820	8A	3					na	na	na	na	na	na
821	8A	4					na	na	na	na	na	na
822	8A	5					na	na	na	na	na	na
823	8A	6					na	na	na	na	na	na
824	8A	7					na	na	na	na	na	na
825	8A	8					na	na	na	na	na	na
826	8A	9					na	na	na	na	na	na
827	8A	10					na	na	na	na	na	na
828	8A	11					na	na	na	na	na	na
829	8A	12					na	na	na	na	na	na
830	8A	13					na	na	na	na	na	na
831	8A	14					na	na	na	na	na	na
832	8A	15					na	na	na	na	na	na
833	8A	16					na	na	na	na	na	na
834	8A	17					na	na	na	na	na	na
835	8A	18					na	na	na	na	na	na
836	8A	19					na	na	na	na	na	na
837	8A	20					na	na	na	na	na	na
838	8A	21					na	na	na	na	na	na
839	8A	22					na	na	na	na	na	na
840	8A	23					na	na	na	na	na	na
841	8A	24					na	na	na	na	na	na
842	8A	25					na	na	na	na	na	na
843	8A	26					na	na	na	na	na	na
844	8A	27					na	na	na	na	na	na
845	8A	28					na	na	na	na	na	na
846	8A	29					na	na	na	na	na	na
847	8A	30					na	na	na	na	na	na
848	8A	31					na	na	na	na	na	na
849	8A	32					na	na	na	na	na	na
850	8A	33					na	na	na	na	na	na

SAMPLE			XRD				ORGANIC GEOCHEM			CLAY MINERALOGY		
							PYROLYSIS YIELDS					
Seq	Site	Depth	Mg in Cal	Mg in HMC	Ca in Pd	Ca in Dol	S1	S2	S3	Expand	Illite	Kao+Chlo
no	ID	cm	%	%	%	%	mg/cc	mg/cc	mg/cc	%	%	%
851	8A	34					na	na	na	na	na	na
852	8A	35					na	na	na	na	na	na
853	8A	36					na	na	na	na	na	na
854	8A	37					na	na	na	na	na	na
855	8A	38					na	na	na	na	na	na
856	8A	39					na	na	na	na	na	na
857	8A	40					na	na	na	na	na	na
858	Grab-1	3					na	na	na	na	na	na
859	Grab-2	3					na	na	na	na	na	na
860	Grab-3	3					na	na	na	na	na	na
861	Grab-4	3					na	na	na	na	na	na
862	Grab-5	3					na	na	na	na	na	na
863	Grab-6	3					na	na	na	na	na	na
864	Grab-7	3					na	na	na	na	na	na
865	Grab-8	3					na	na	na	na	na	na
866	Grab-10	3					na	na	na	na	na	na
867	Grab-25	3					na	na	na	na	na	na
868	Grab-28	3					na	na	na	na	na	na
869	Grab-29	3					na	na	na	na	na	na
870	Grab-30	3					na	na	na	na	na	na
871	Grab-31	3					na	na	na	na	na	na
872	Grab-32	3					na	na	na	na	na	na
873	Grab-33	3					na	na	na	na	na	na
874	Grab-34	3					na	na	na	na	na	na
875	Grab-35	3					na	na	na	na	na	na
876	Grab-36	3					na	na	na	na	na	na
877	Grab-37	3					na	na	na	na	na	na
878	Grab-39	3					na	na	na	na	na	na
879	Grab-40	3					na	na	na	na	na	na
880	Grab-41	3					na	na	na	na	na	na
881	Grab-42	3					na	na	na	na	na	na
882	Grab-43	3					na	na	na	na	na	na
883	Grab-44	3					na	na	na	na	na	na
884	Grab-45	3					na	na	na	na	na	na
885	Grab-46	3					na	na	na	na	na	na
886	Grab-47	3					na	na	na	na	na	na
887	Grab-49	3					na	na	na	na	na	na
888	Grab-50	3					na	na	na	na	na	na

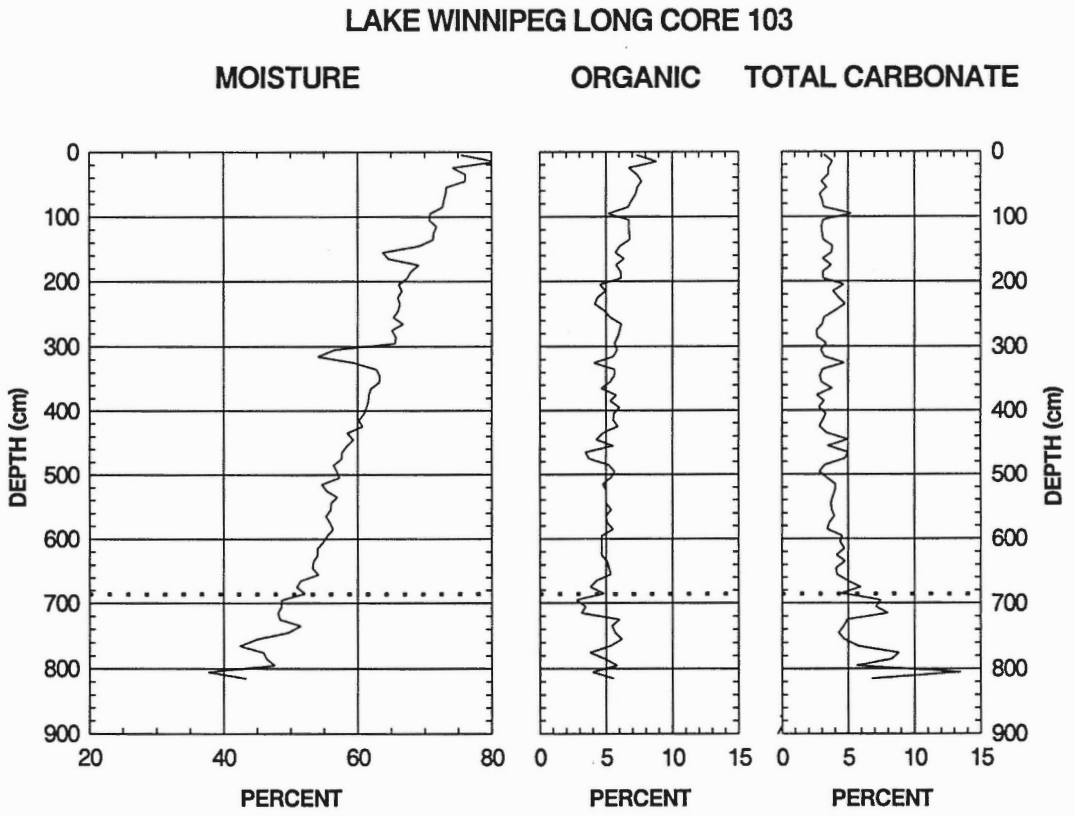
LAKE WINNIPEG LONG CORE 103
MOISTURE
ORGANIC
TOTAL CARBONATE
DEPTH (cm)
0
100
200
300
400
500
600
700
800
900
20
40
60
80
0
5
10
15
PERCENT

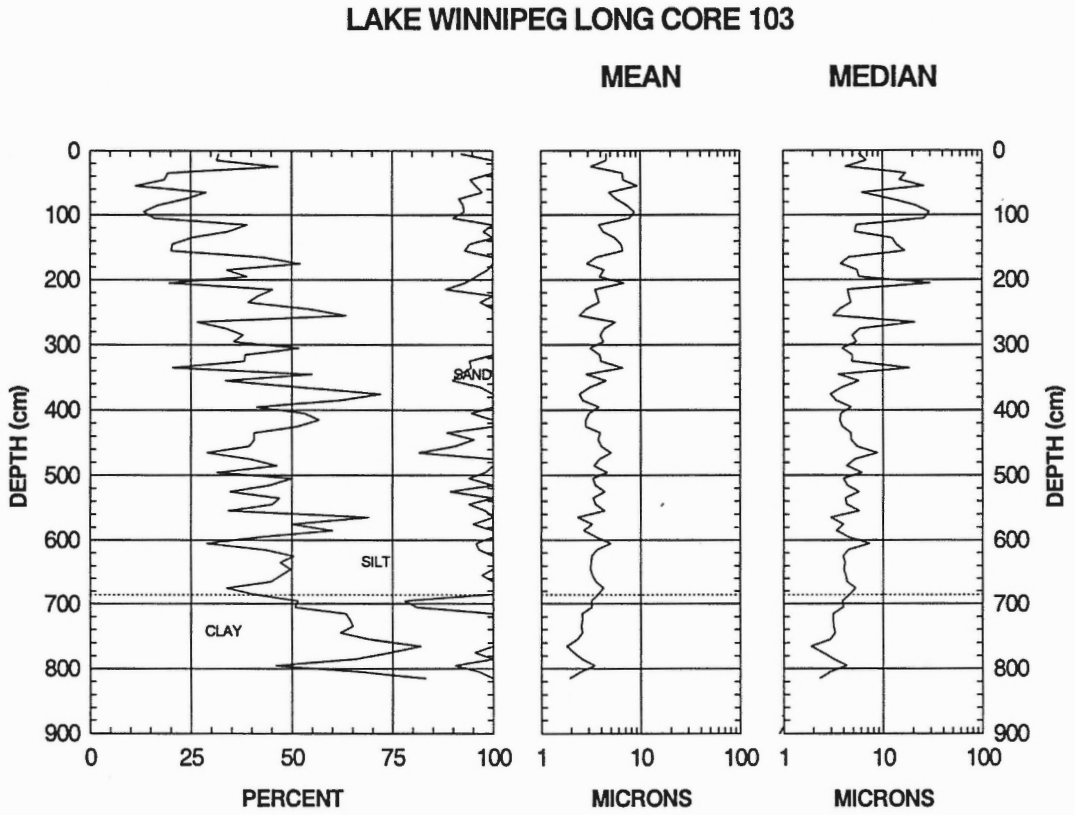
LAKE WINNIPEG LONG CORE 103
MEAN
MEDIAN
DEPTH (cm)
SAND
SILT
CLAY
0
25
50
75
100
1
10
100
PERCENT
MICRONS

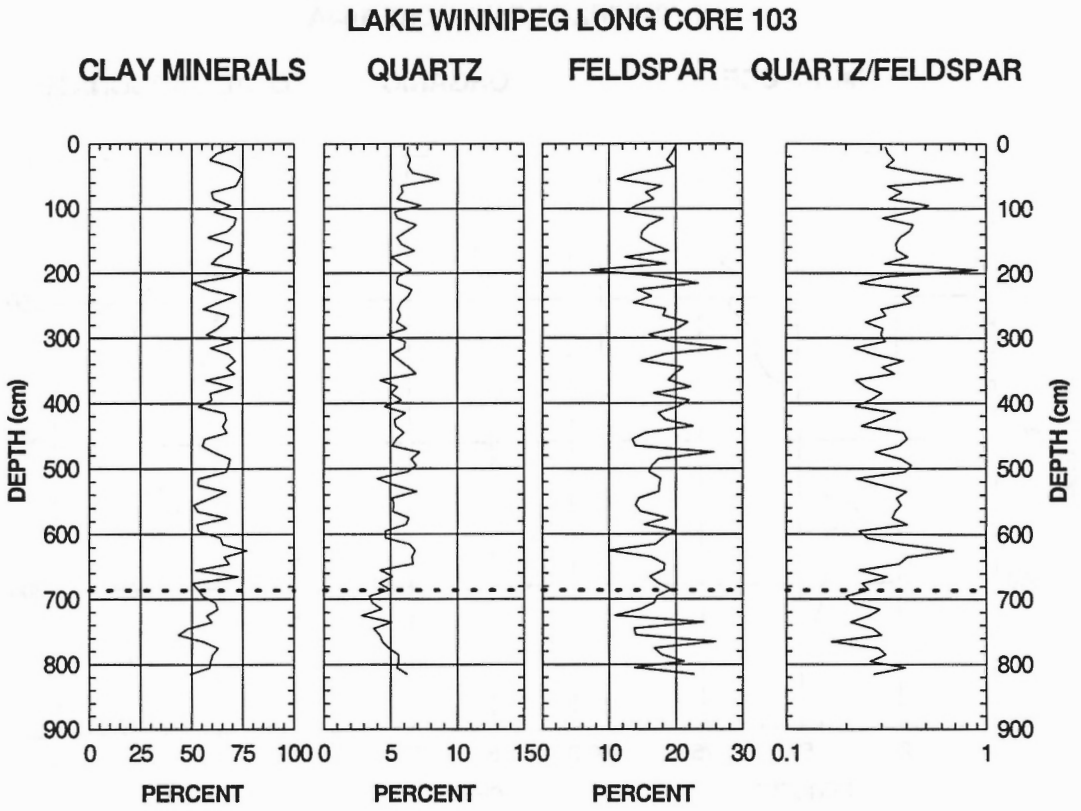
LAKE WINNIPEG LONG CORE 103
CLAY MINERALS
QUARTZ
FELDSPAR
QUARTZ/FELDSPAR
DEPTH (cm)
0
100
200
300
400
500
600
700
800
900
0 25 50 75 100
0 5 10 150
10 20 30
0.1 1
PERCENT
PERCENT
PERCENT

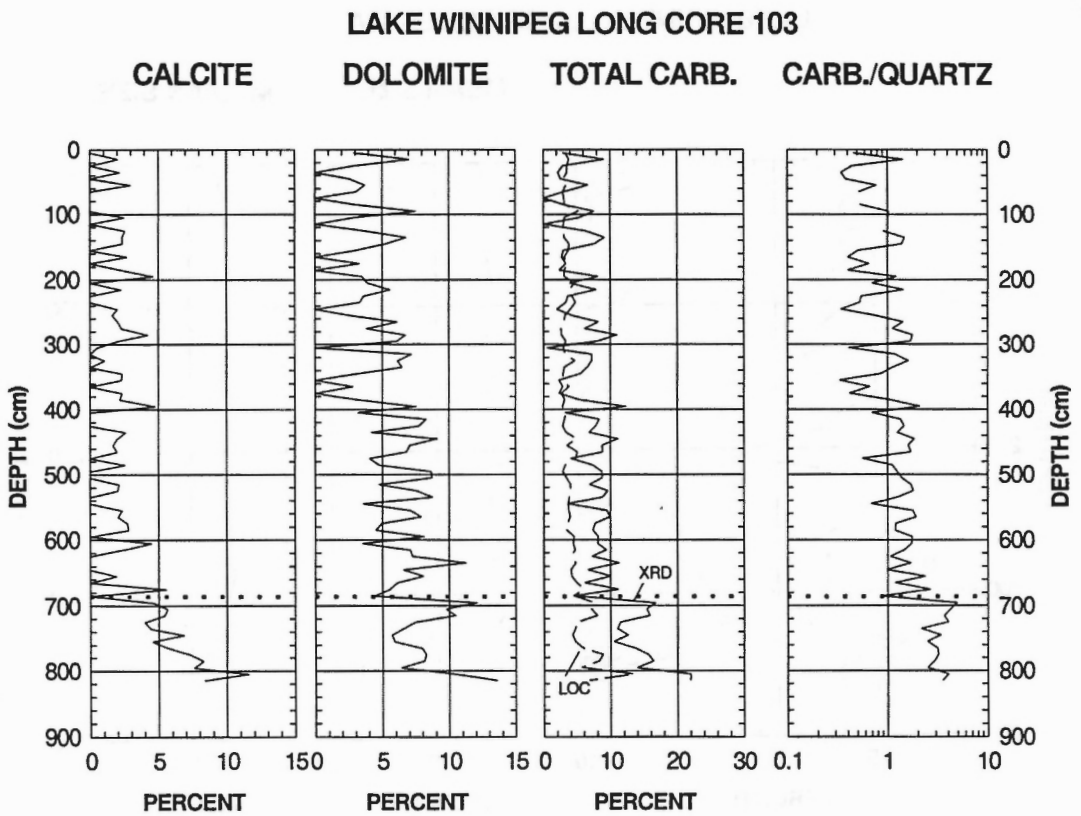
LAKE WINNIPEG LONG CORE 103
CALCITE
DOLOMITE
TOTAL CARB.
CARB./QUARTZ
DEPTH (cm)
0
100
200
300
400
500
600
700
800
900
XRD
LOC
0 5 10 150
5 10 15
0 10 20 30
0.1 1 10
PERCENT
PERCENT
PERCENT

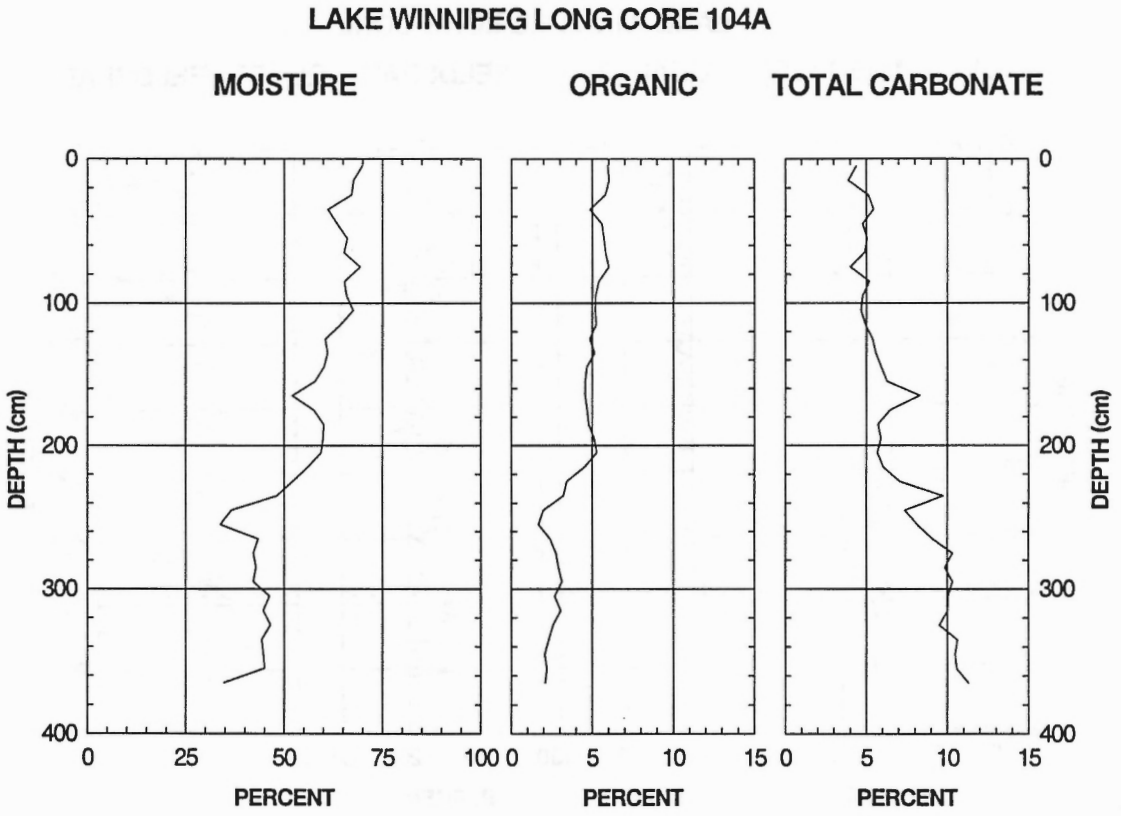
LAKE WINNIPEG LONG CORE 104A
MOISTURE
ORGANIC
TOTAL CARBONATE
DEPTH (cm)
0
100
200
300
400
0
25
50
75
100
PERCENT
0
5
10
15
PERCENT
PERCENT

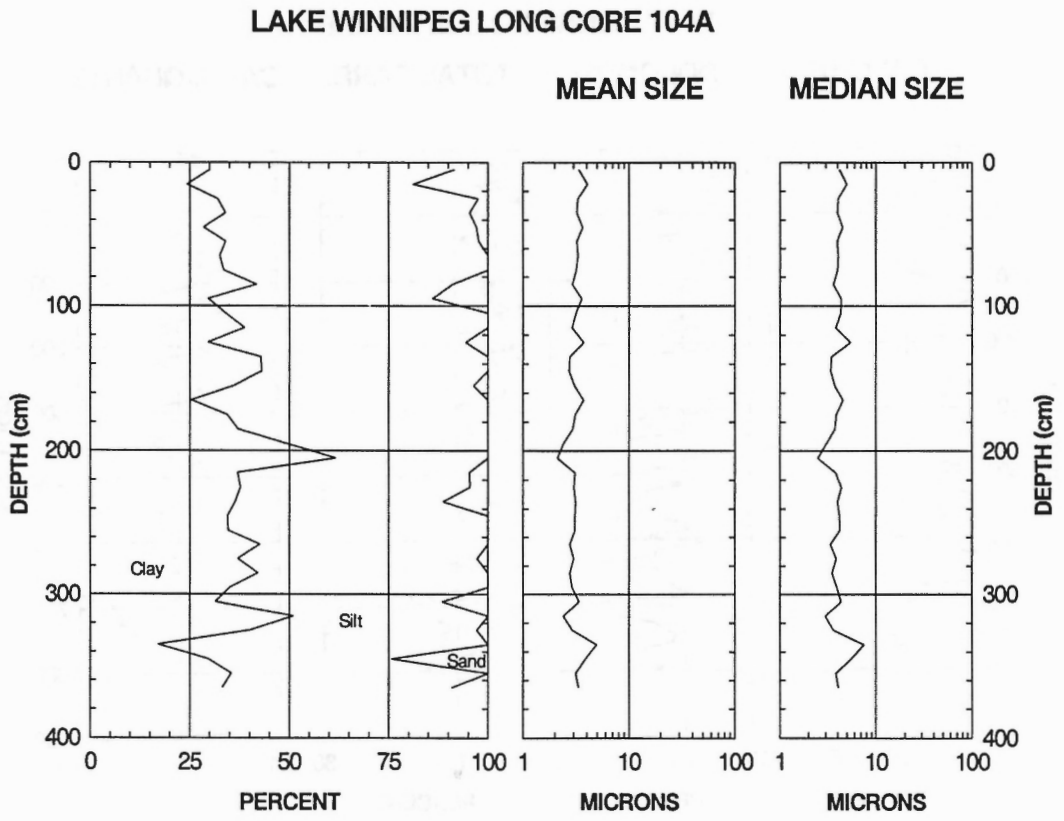
LAKE WINNIPEG LONG CORE 104A
MEAN SIZE
MEDIAN SIZE
DEPTH (cm)
Clay
Silt
Sand
PERCENT
1
10
100
MICRONS
MICRONS

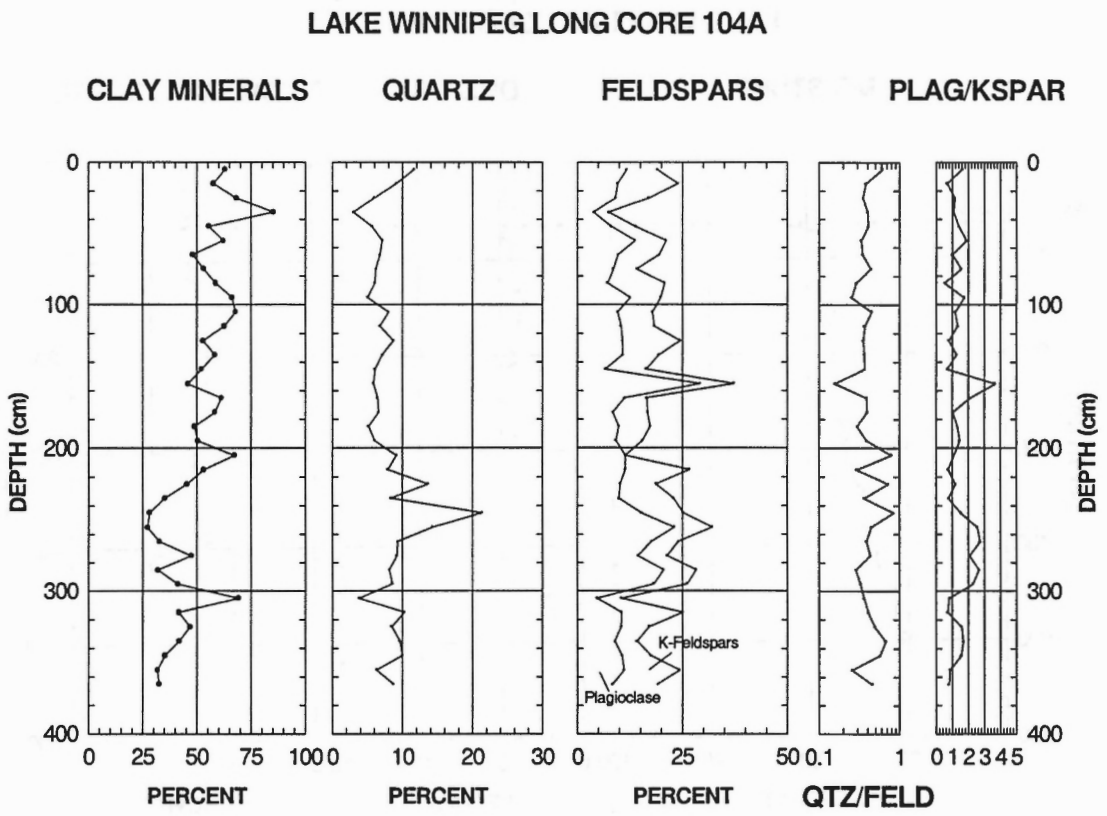
LAKE WINNIPEG LONG CORE 104A
CLAY MINERALS
QUARTZ
FELDSPARS
PLAG/KSPAR
DEPTH (cm)
0
100
200
300
400
0 25 50 75 100
PERCENT
0 10 20 30
PERCENT
K-Feldspars
Plagioclase
0 25 50
PERCENT
0.1 1
QTZ/FELD
0 1 2 3 4 5

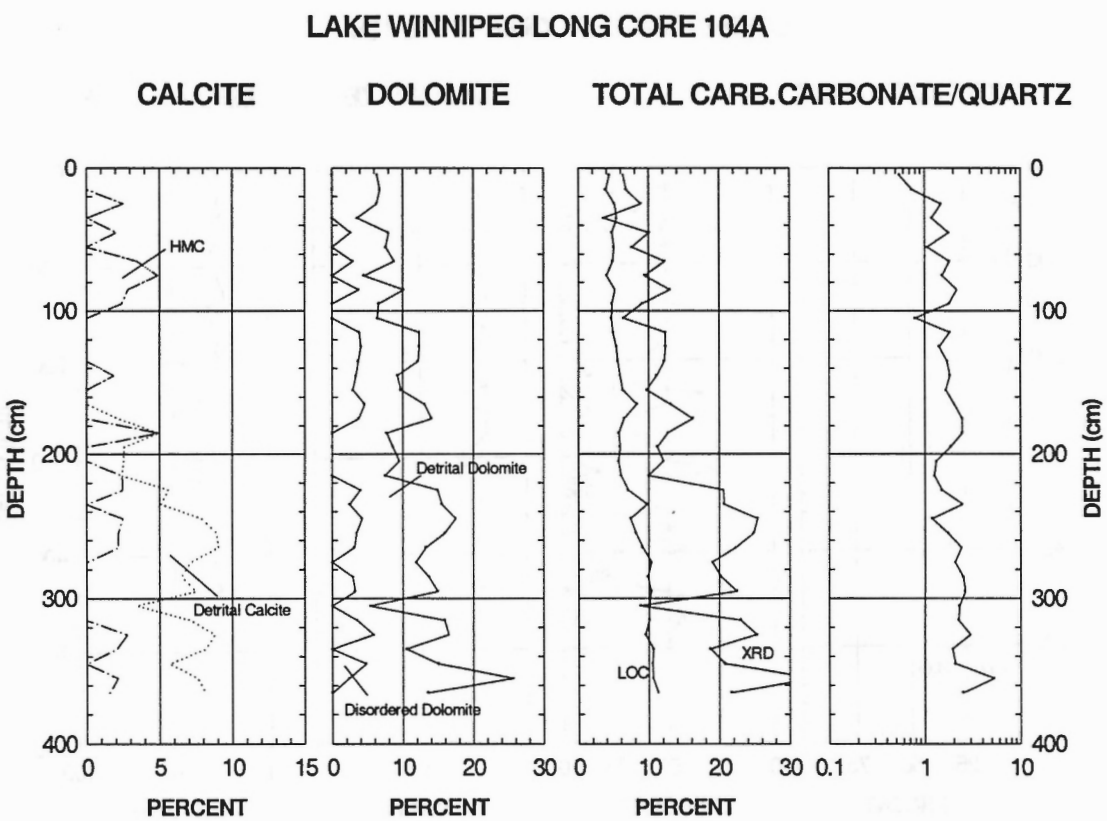
LAKE WINNIPEG LONG CORE 104A
CALCITE
DOLOMITE
TOTAL CARB.CARBONATE/QUARTZ
DEPTH (cm)
0
100
200
300
400
HMC
Detrital Calcite
0 5 10 15
PERCENT
Detrital Dolomite
Disordered Dolomite
0 10 20 30
PERCENT
LOC
XRD
0 10 20 30
PERCENT
0.1 1 10

LAKE WINNIPEG LONG CORE 105

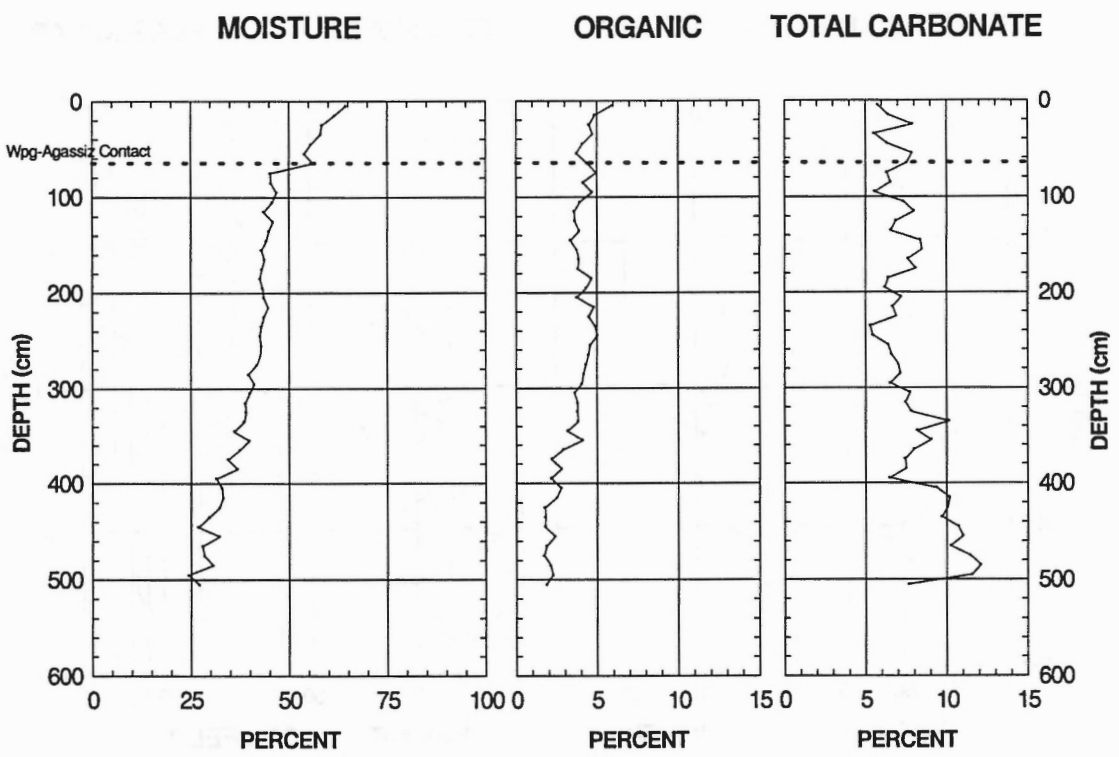

LAKE WINNIPEG LONG CORE 105

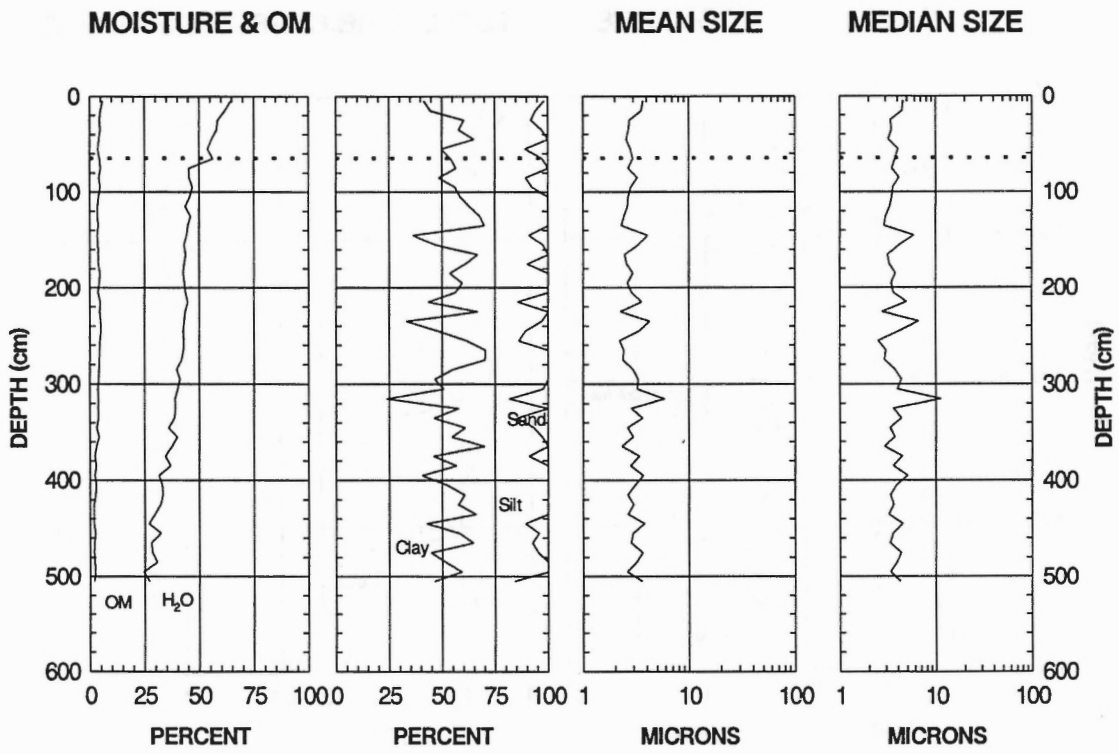

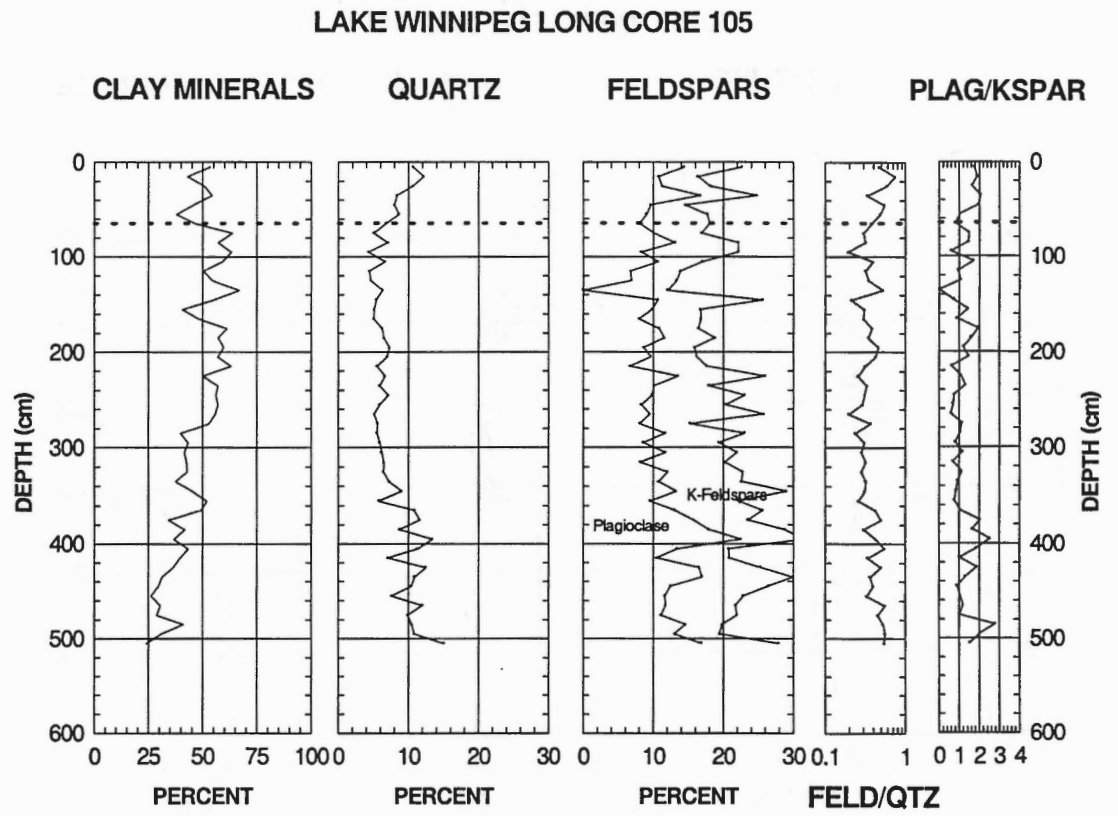
LAKE WINNIPEG LONG CORE 105
CLAY MINERALS
QUARTZ
FELDSPARS
PLAG/KSPAR
DEPTH (cm)
0
100
200
300
400
500
600
0 25 50 75 100
PERCENT
0 10 20 30
PERCENT
K-Feldspars
Plagioclase
0 10 20 30
PERCENT
0.1 1
FELD/QTZ
0 1 2 3 4

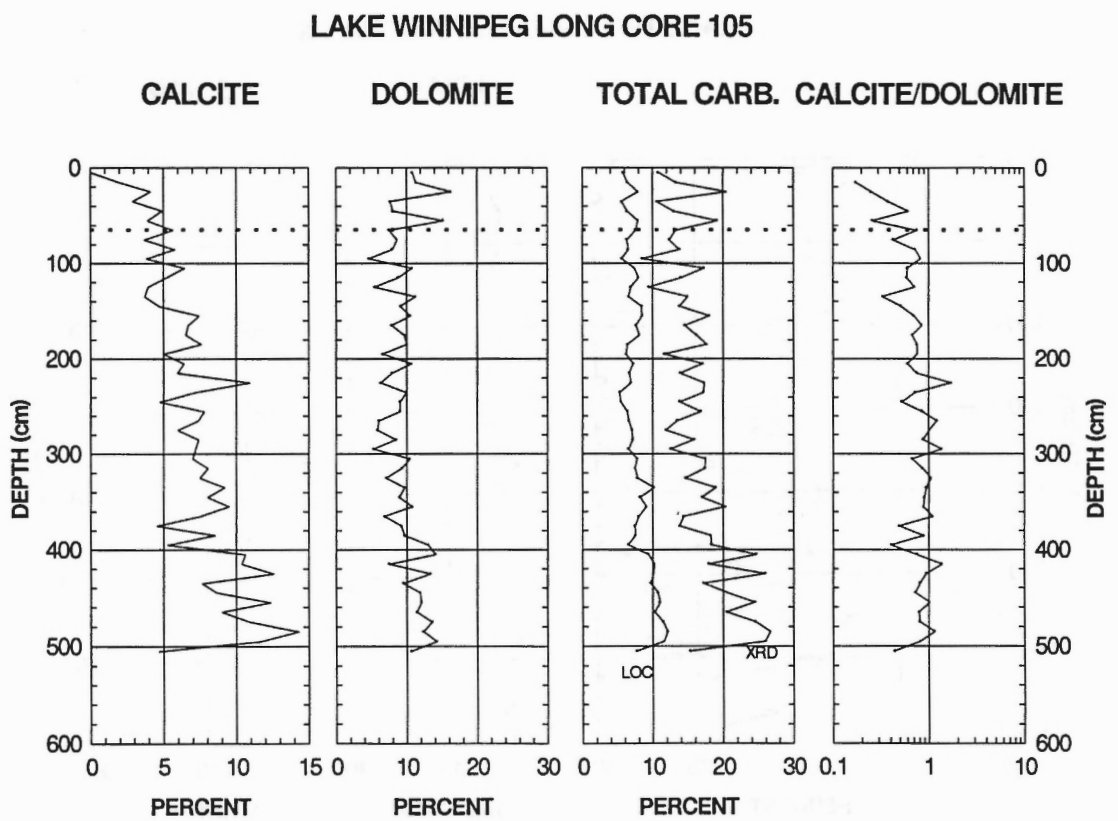
LAKE WINNIPEG LONG CORE 105
CALCITE
DOLOMITE
TOTAL CARB.
CALCITE/DOLOMITE
DEPTH (cm)
0
100
200
300
400
500
600
0 5 10 15
PERCENT
0 10 20 30
PERCENT
LOC
XRD
0 10 20 30
PERCENT
0.1 1 10

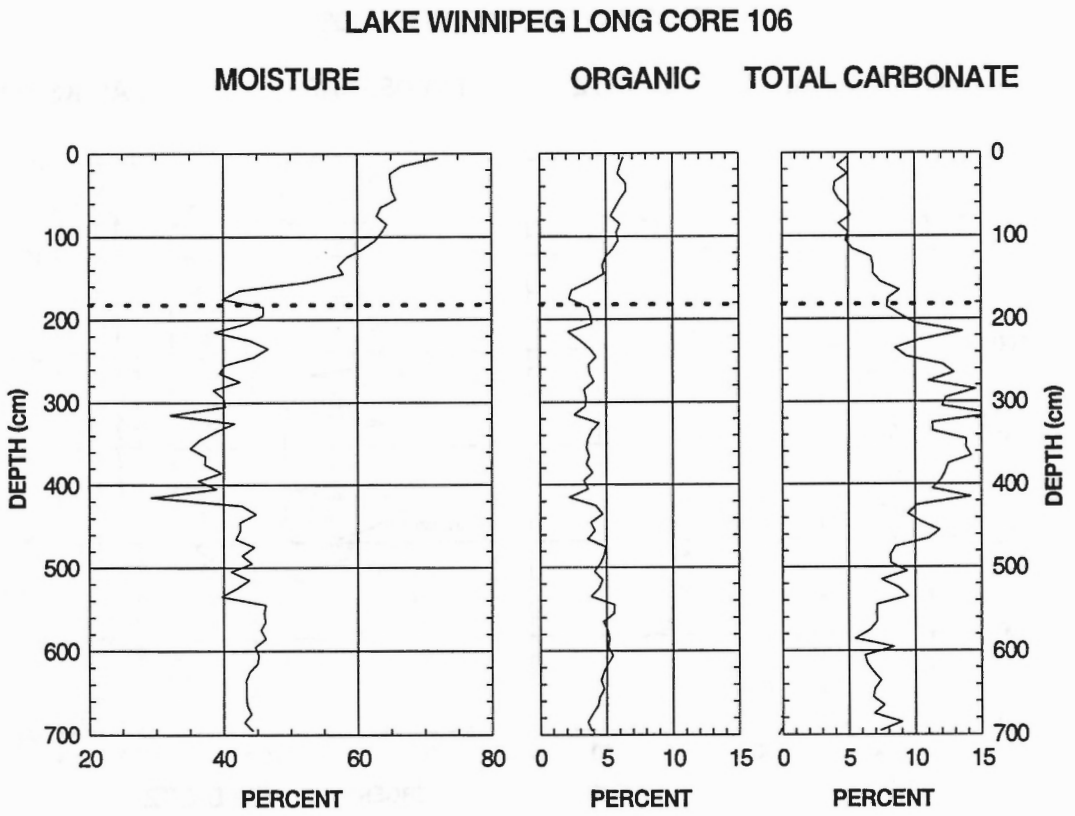
LAKE WINNIPEG LONG CORE 106
MOISTURE
ORGANIC
TOTAL CARBONATE
DEPTH (cm)
0
100
200
300
400
500
600
700
20
40
60
80
0
5
10
15
PERCENT

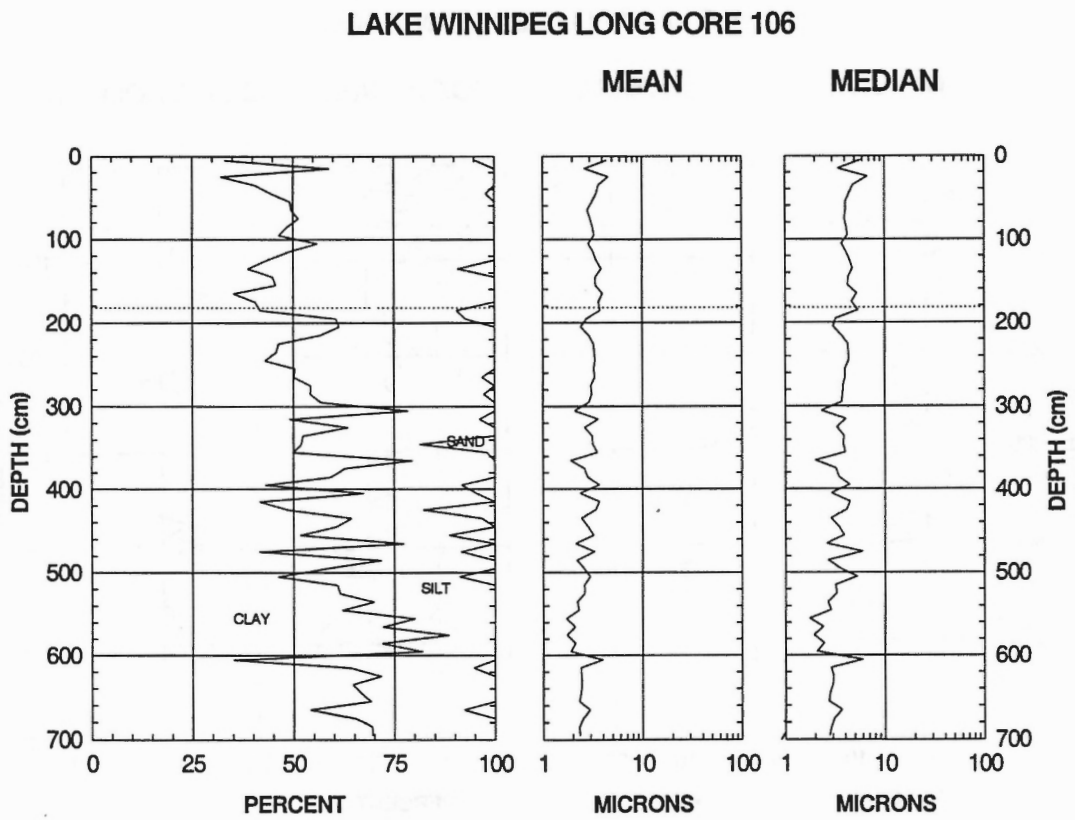
LAKE WINNIPEG LONG CORE 106
MEAN
MEDIAN
DEPTH (cm)
SAND
SILT
CLAY
0
25
50
75
100
1
10
100
PERCENT
MICRONS

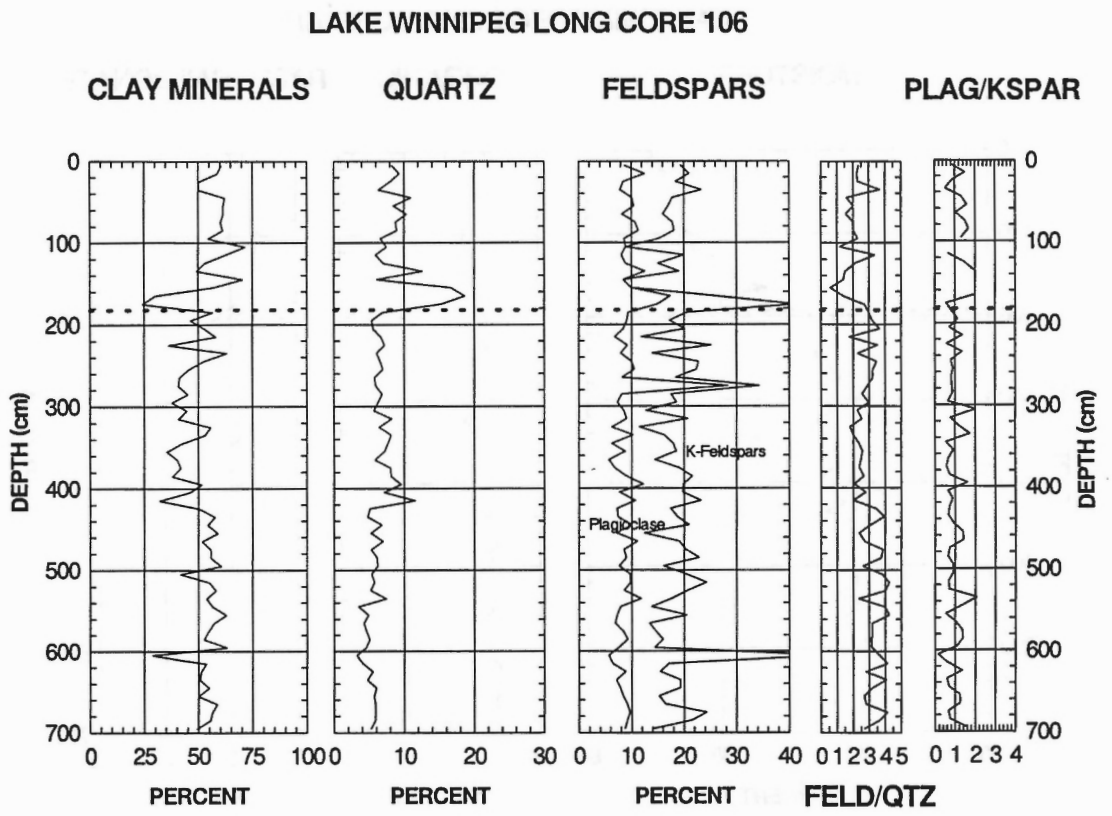
LAKE WINNIPEG LONG CORE 106
CLAY MINERALS
QUARTZ
FELDSPARS
PLAG/KSPAR
DEPTH (cm)
0
100
200
300
400
500
600
700
0 25 50 75 100
0 10 20 30
0 10 20 30 40
0 1 2 3 4 5
0 1 2 3 4
PERCENT
PERCENT
PERCENT
FELD/QTZ
K-Feldspars
Plagioclase

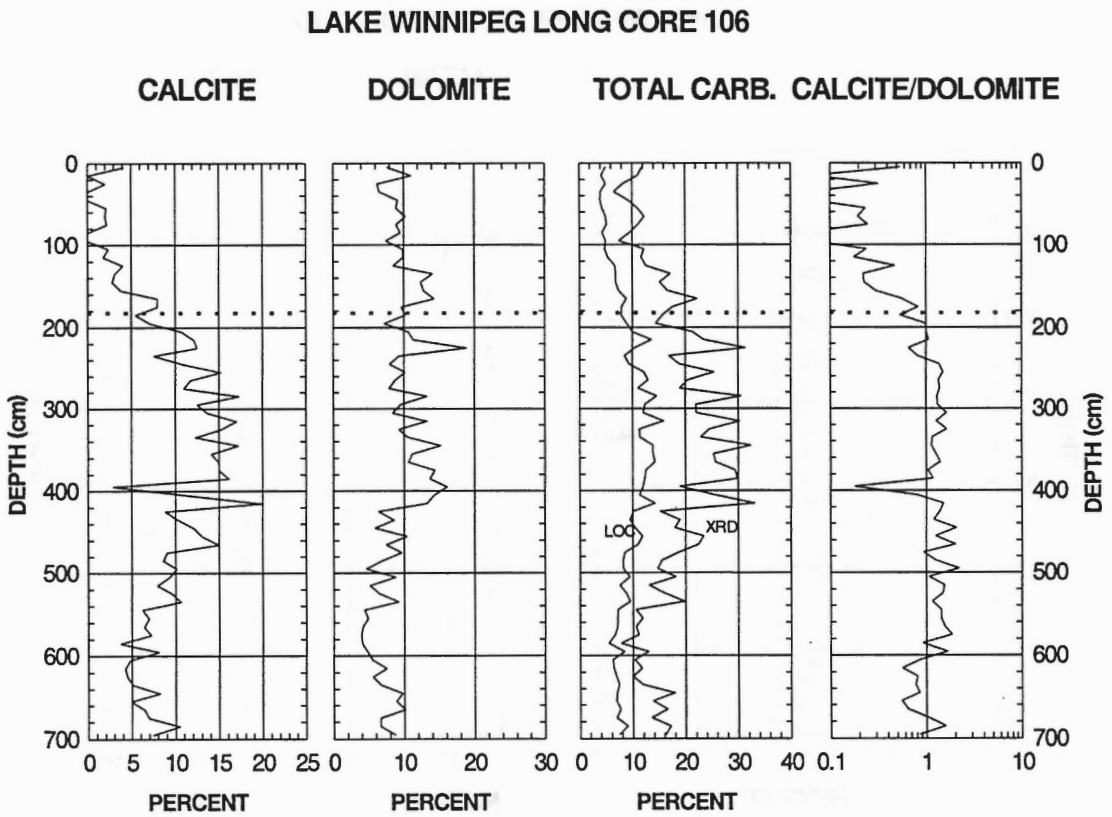
LAKE WINNIPEG LONG CORE 106
CALCITE
DOLOMITE
TOTAL CARB.
CALCITE/DOLOMITE
DEPTH (cm)
0
100
200
300
400
500
600
700
0 5 10 15 20 25
0 10 20 30
0 10 20 30 40
0.1 1 10
PERCENT
PERCENT
PERCENT
LOC
XRD

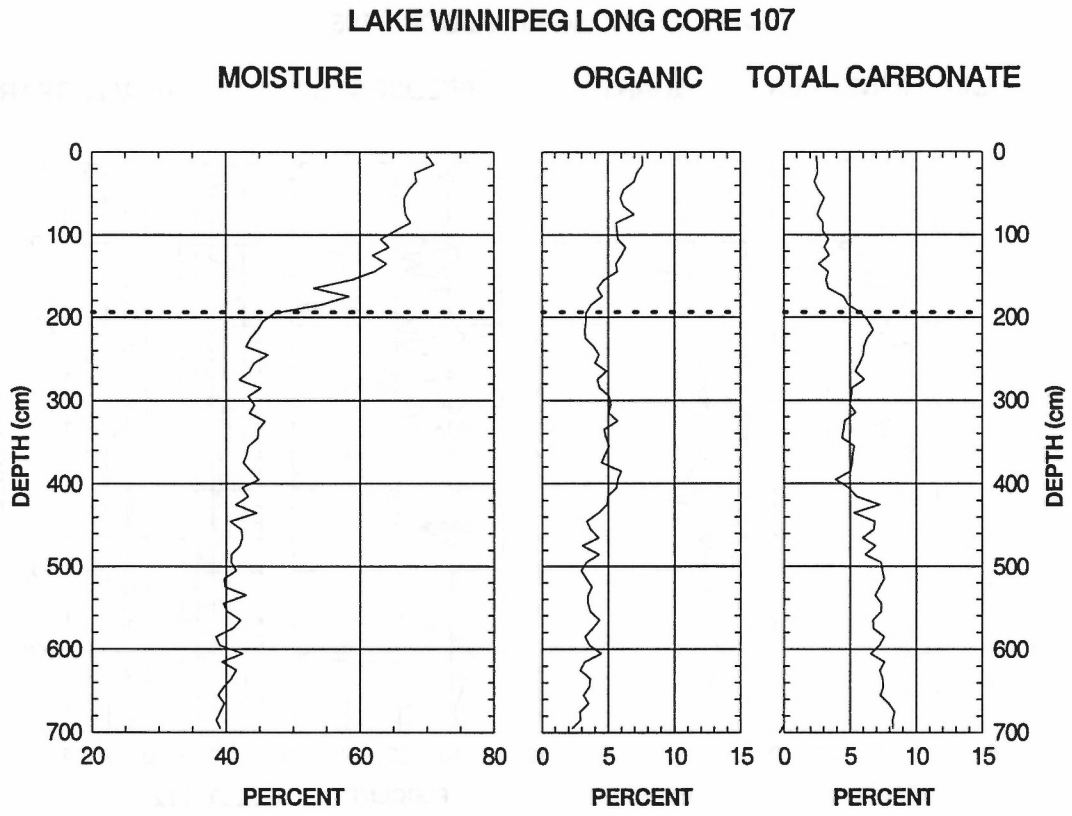
LAKE WINNIPEG LONG CORE 107
MOISTURE
ORGANIC
TOTAL CARBONATE
DEPTH (cm)
0
100
200
300
400
500
600
700
20
40
60
80
0
5
10
15
PERCENT

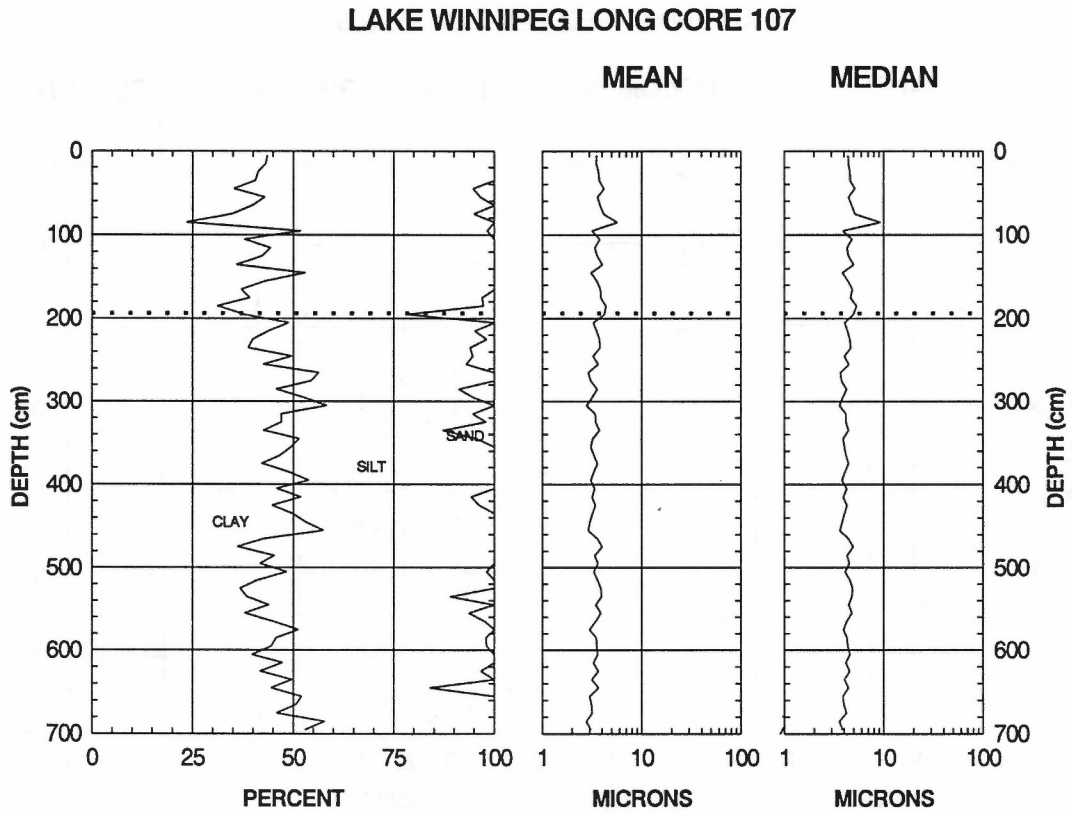
LAKE WINNIPEG LONG CORE 107
MEAN
MEDIAN
DEPTH (cm)
CLAY
SILT
SAND
0
25
50
75
100
1
10
100
PERCENT
MICRONS

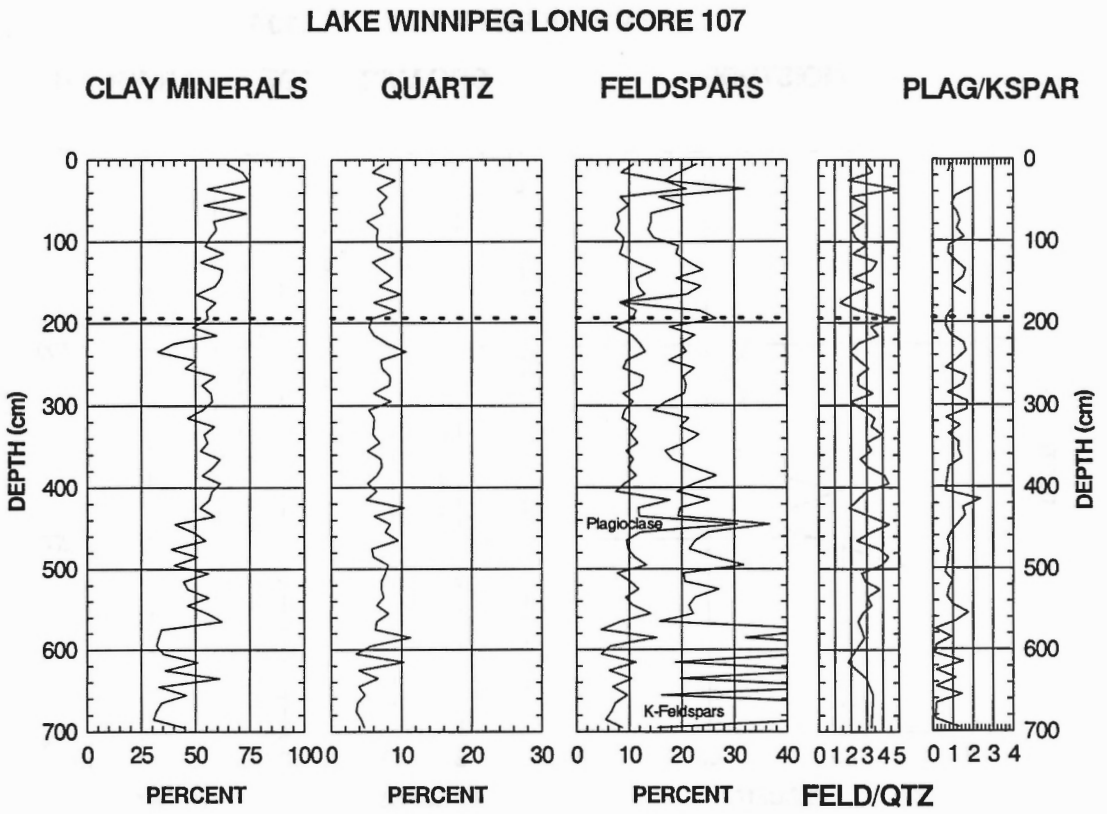
LAKE WINNIPEG LONG CORE 107
CLAY MINERALS
QUARTZ
FELDSPARS
PLAG/KSPAR
DEPTH (cm)
0
100
200
300
400
500
600
700
Plagioclase
K-Feldspars
0 25 50 75 100
0 10 20 30
0 10 20 30 40
0 1 2 3 4 5
0 1 2 3 4
PERCENT
PERCENT
PERCENT
FELD/QTZ

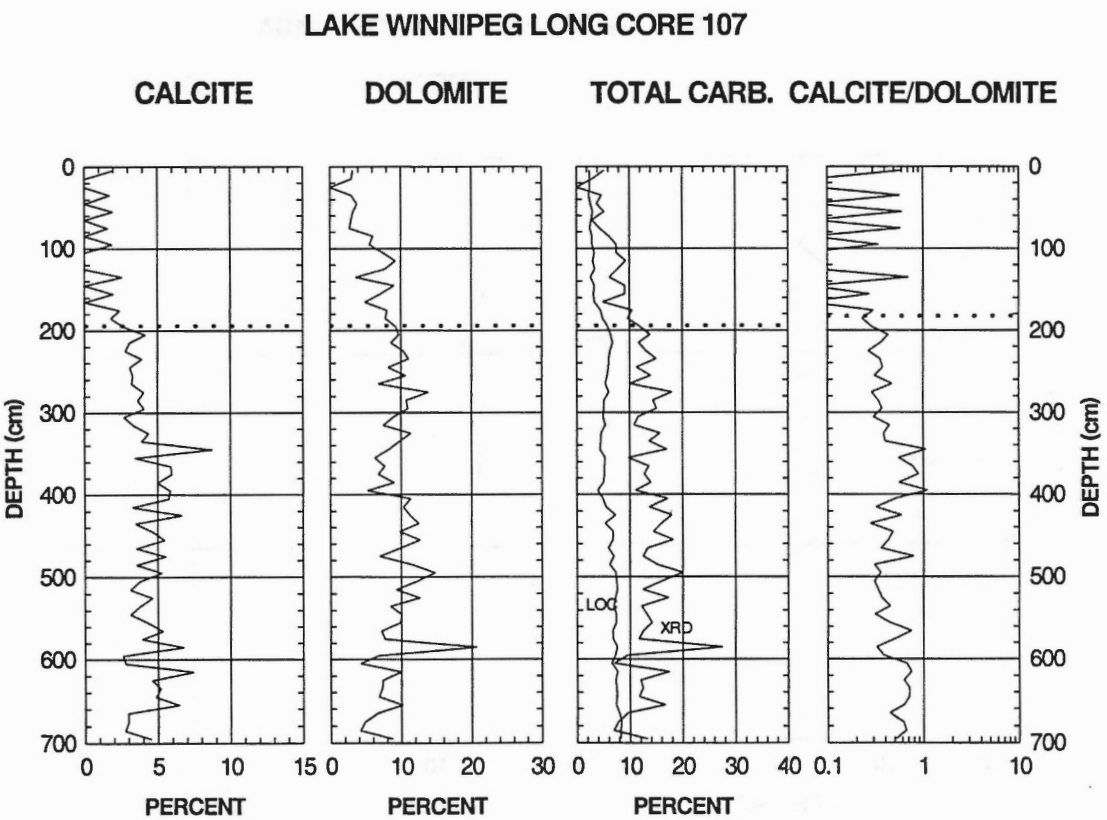
LAKE WINNIPEG LONG CORE 107
CALCITE
DOLOMITE
TOTAL CARB.
CALCITE/DOLOMITE
DEPTH (cm)
0
100
200
300
400
500
600
700
LOC
XRD
0 5 10 15
0 10 20 30
0 10 20 30 40
0.1 1 10
PERCENT
PERCENT
PERCENT

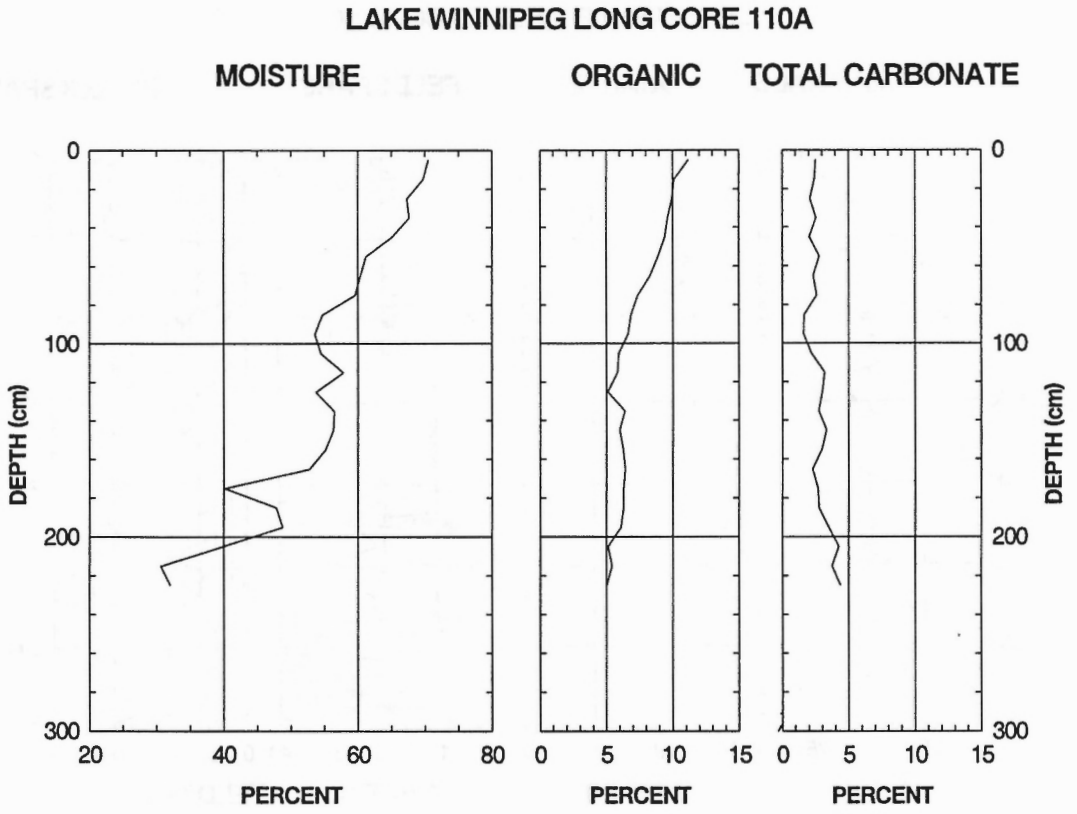
LAKE WINNIPEG LONG CORE 110A
MOISTURE
ORGANIC
TOTAL CARBONATE
DEPTH (cm)
0
100
200
300
20
40
60
80
0
5
10
15
PERCENT

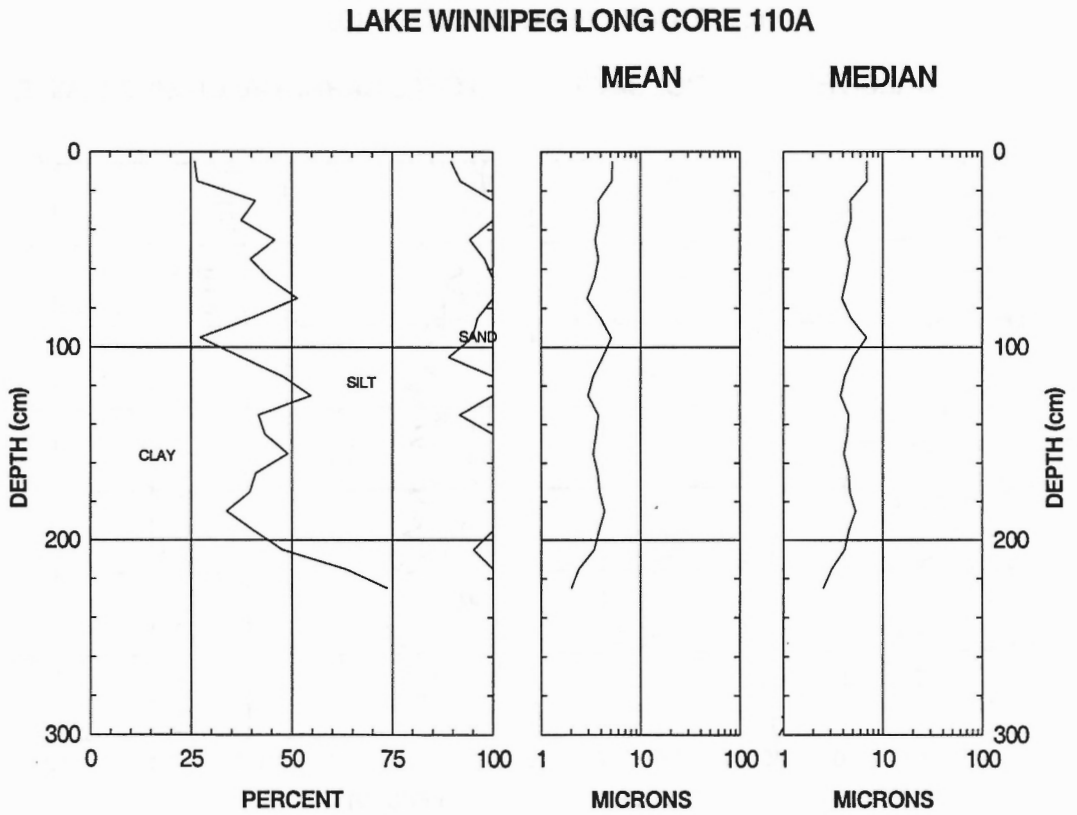
LAKE WINNIPEG LONG CORE 110A
MEAN
MEDIAN
DEPTH (cm)
CLAY
SILT
SAND
0
25
50
75
100
1
10
100
PERCENT
MICRONS

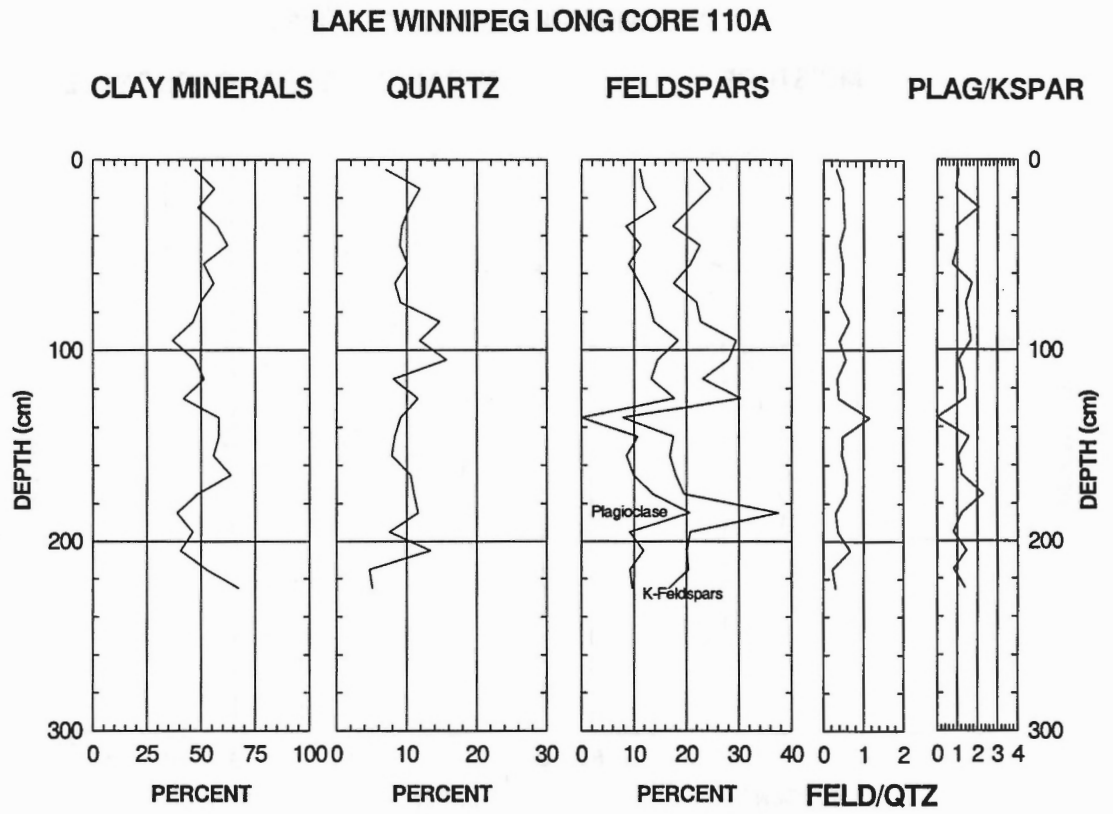
LAKE WINNIPEG LONG CORE 110A
CLAY MINERALS
QUARTZ
FELDSPARS
PLAG/KSPAR
DEPTH (cm)
0
100
200
300
0 25 50 75 100
PERCENT
0 10 20 30
PERCENT
Plagioclase
K-Feldspars
0 10 20 30 40
PERCENT
0 1 2
0 1 2 3 4
FELD/QTZ

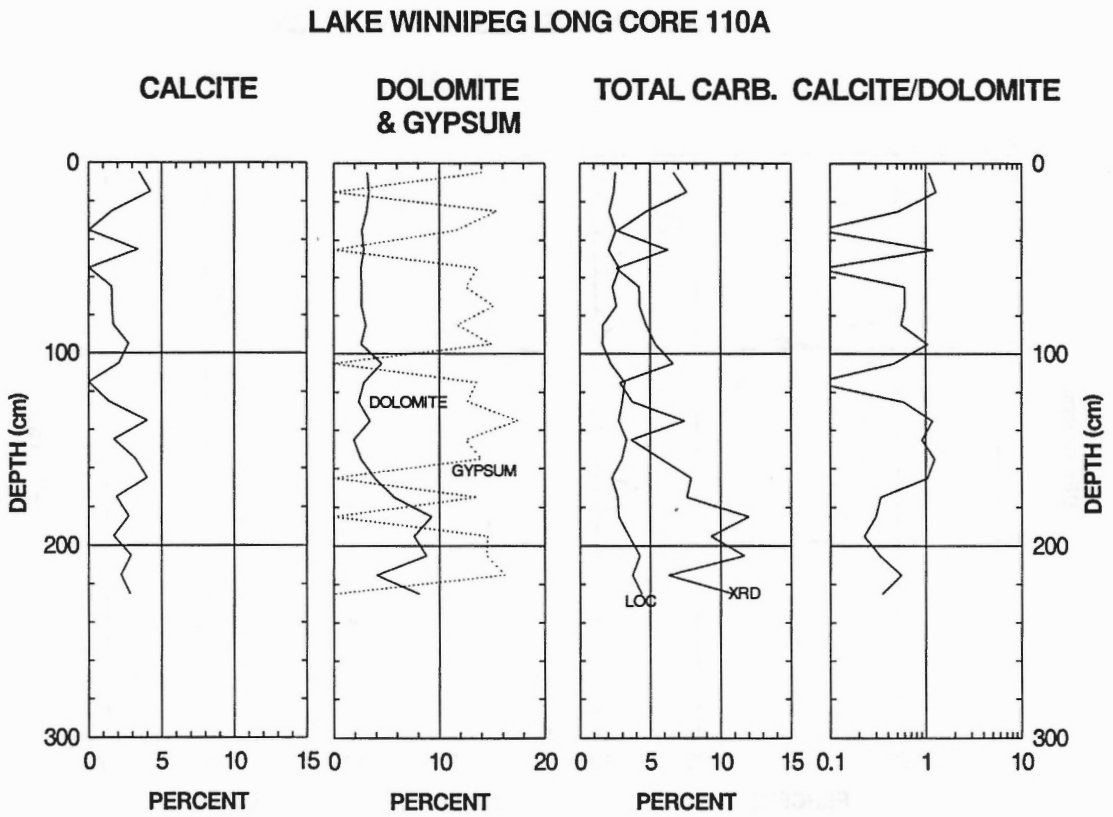
LAKE WINNIPEG LONG CORE 110A
CALCITE
DOLOMITE & GYPSUM
TOTAL CARB.
CALCITE/DOLOMITE
DEPTH (cm)
0
100
200
300
0 5 10 15
PERCENT
DOLOMITE
GYPSUM
0 10 20
PERCENT
LOC
XRD
0 5 10 15
PERCENT
0.1 1 10

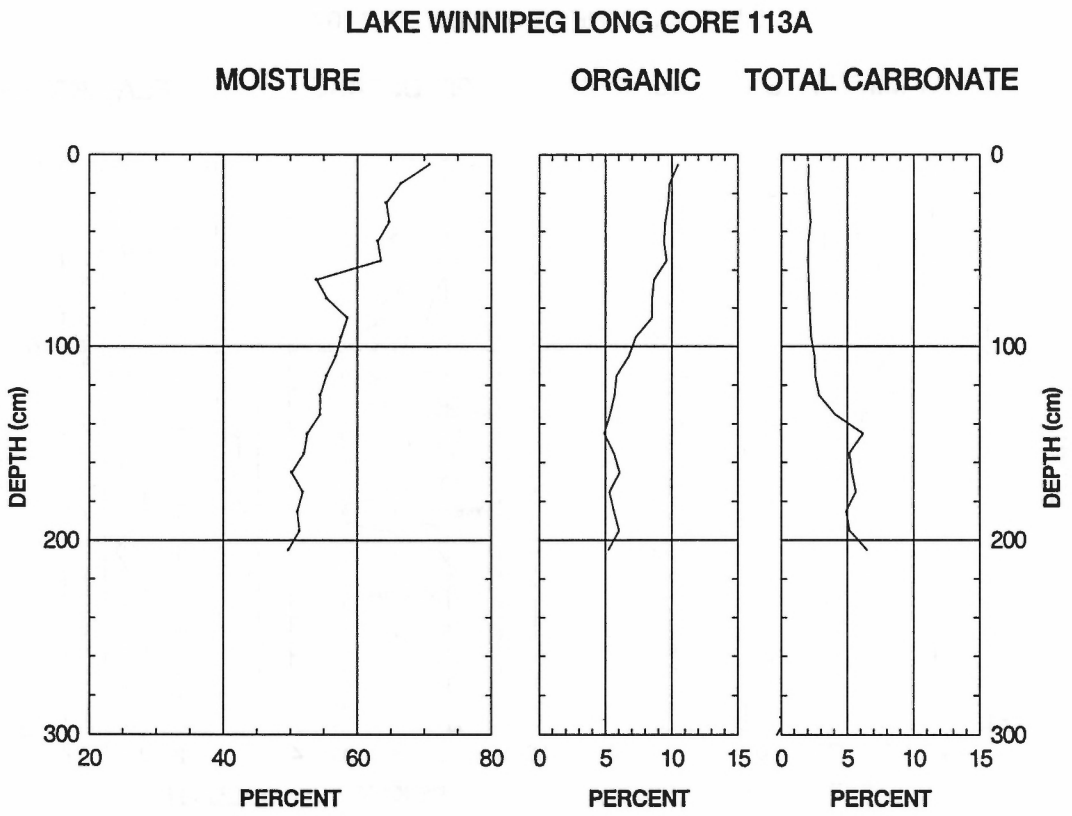
LAKE WINNIPEG LONG CORE 113A
MOISTURE
ORGANIC
TOTAL CARBONATE
DEPTH (cm)
0
100
200
300
20
40
60
80
0
5
10
15
PERCENT

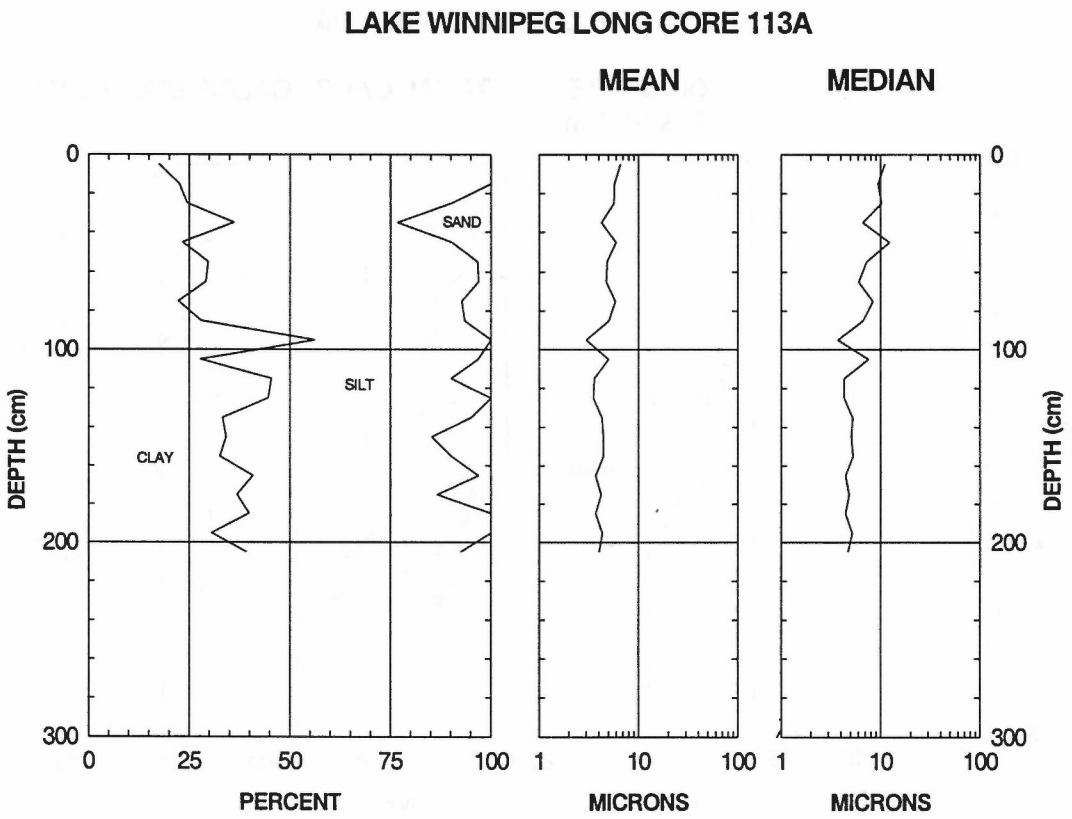
LAKE WINNIPEG LONG CORE 113A
MEAN
MEDIAN
DEPTH (cm)
SAND
SILT
CLAY
0
25
50
75
100
1
10
100
PERCENT
MICRONS

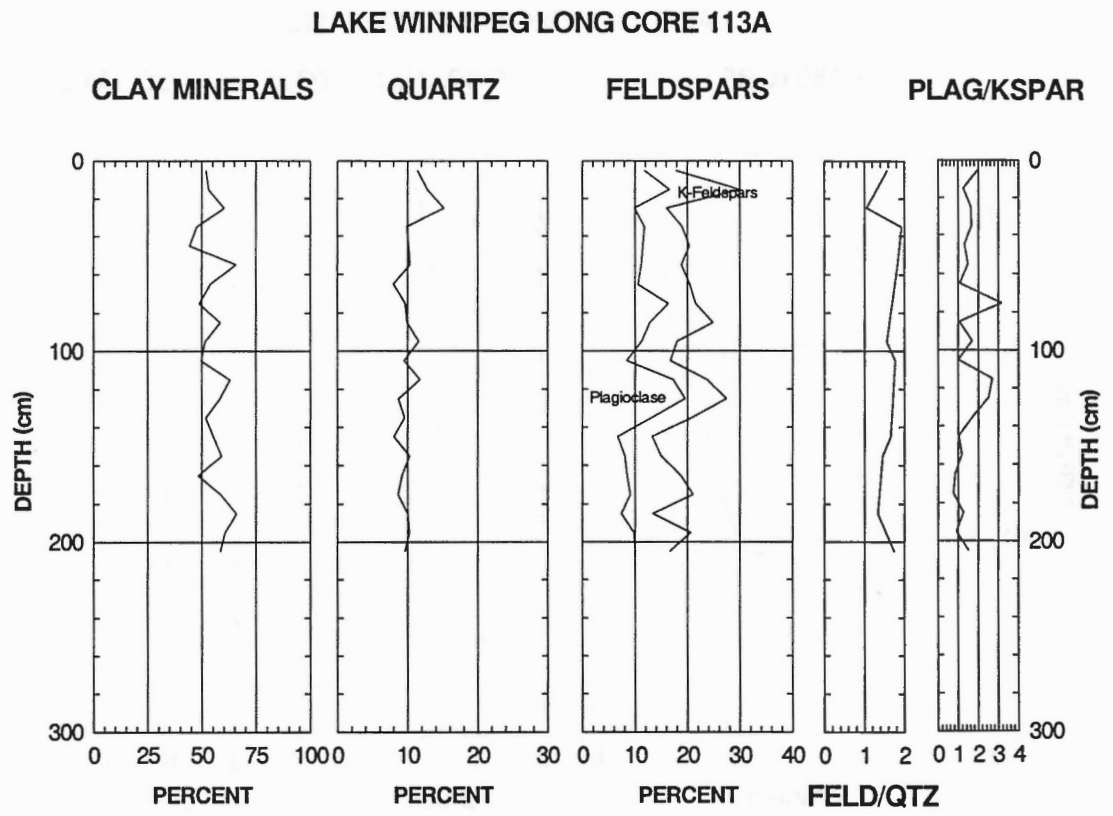
LAKE WINNIPEG LONG CORE 113A
CLAY MINERALS
QUARTZ
FELDSPARS
PLAG/KSPAR
K-Feldspars
Plagioclase
DEPTH (cm)
0
100
200
300
0 25 50 75 100
0 10 20 30
0 10 20 30 40
0 1 2
0 1 2 3 4
PERCENT
PERCENT
PERCENT
FELD/QTZ

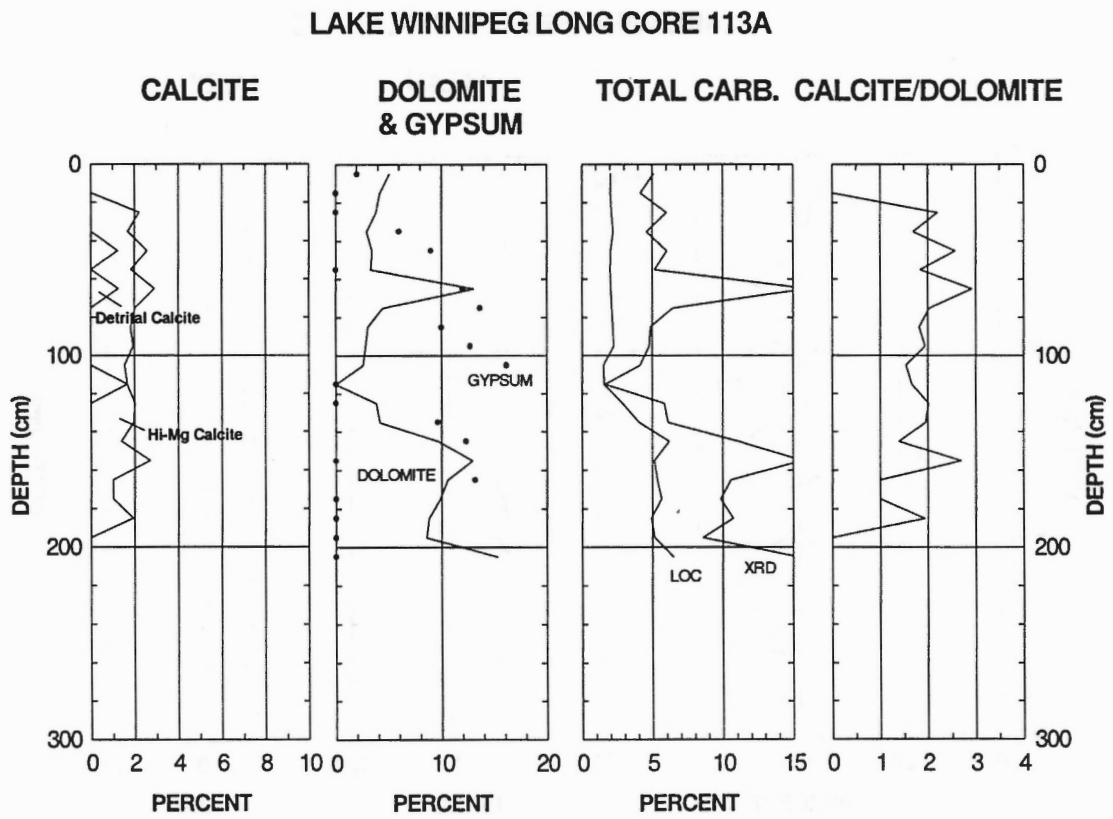
LAKE WINNIPEG LONG CORE 113A
CALCITE
DOLOMITE & GYPSUM
TOTAL CARB.
CALCITE/DOLOMITE
Detrital Calcite
Hi-Mg Calcite
GYPSUM
DOLOMITE
LOC
XRD
DEPTH (cm)
0
100
200
300
0 2 4 6 8 10
0 10 20
0 5 10 15
0 1 2 3 4
PERCENT
PERCENT
PERCENT

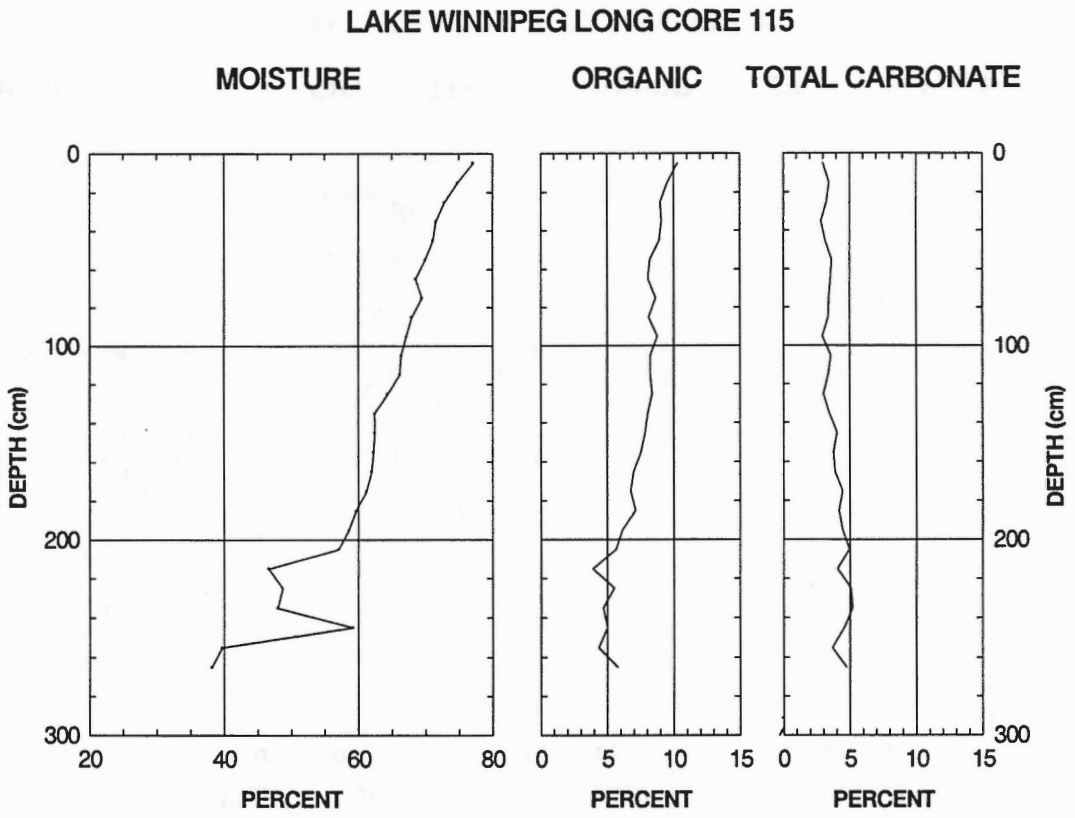
LAKE WINNIPEG LONG CORE 115
MOISTURE
ORGANIC
TOTAL CARBONATE
DEPTH (cm)
0
100
200
300
20
40
60
80
0
5
10
15
PERCENT

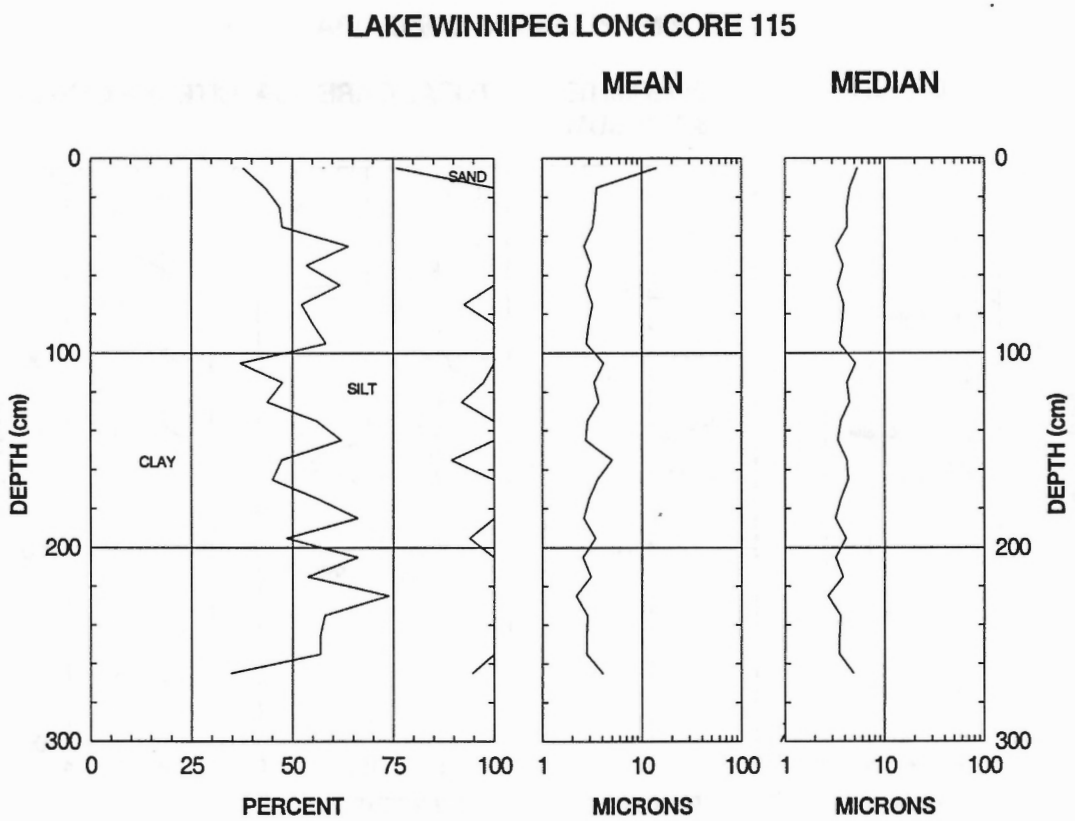
LAKE WINNIPEG LONG CORE 115
MEAN
MEDIAN
DEPTH (cm)
SAND
SILT
CLAY
0
25
50
75
100
1
10
100
PERCENT
MICRONS

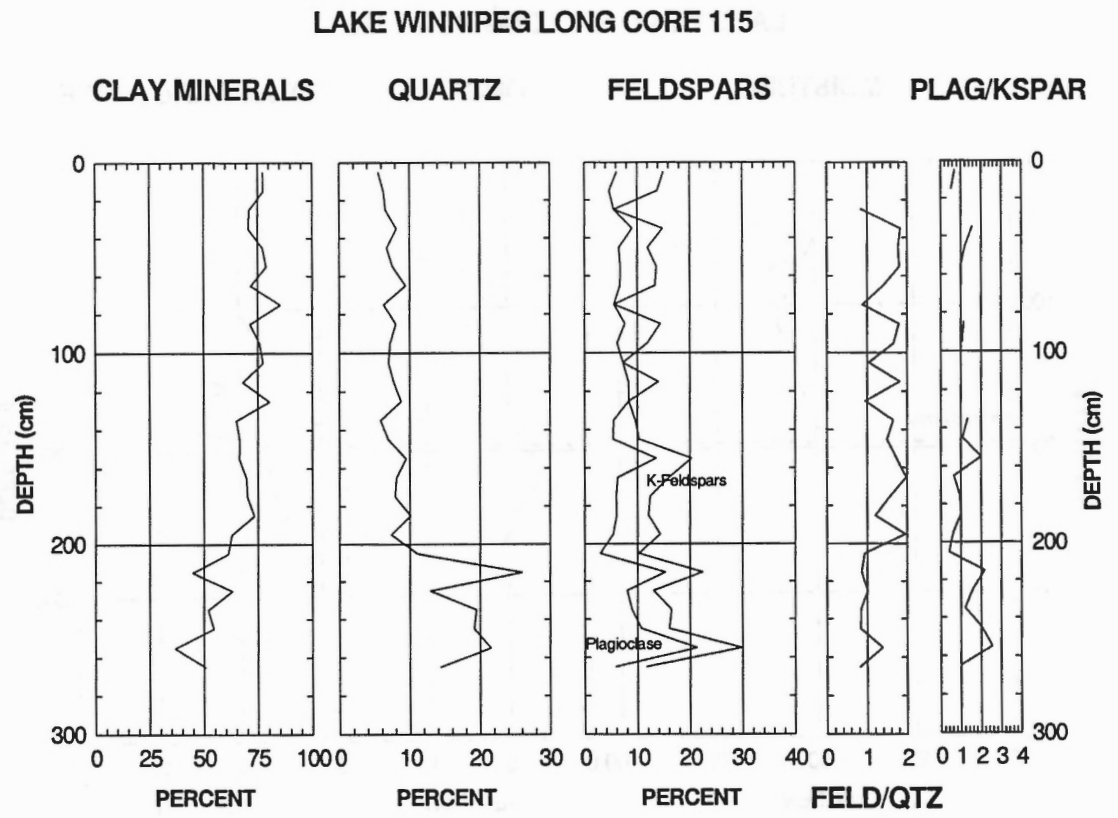
LAKE WINNIPEG LONG CORE 115
CLAY MINERALS
QUARTZ
FELDSPARS
PLAG/KSPAR
DEPTH (cm)
0
100
200
300
K-Feldspars
Plagioclase
0 25 50 75 100
0 10 20 30
0 10 20 30 40
0 1 2
0 1 2 3 4
PERCENT
PERCENT
PERCENT
FELD/QTZ

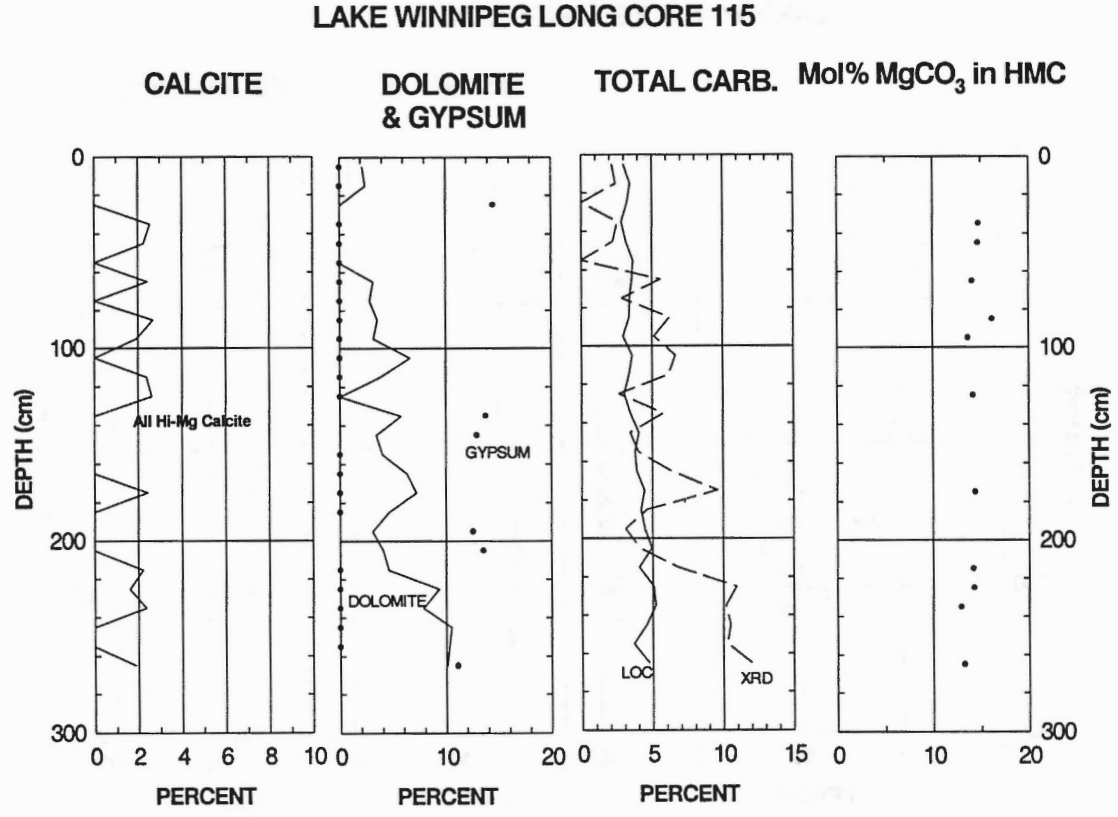
LAKE WINNIPEG LONG CORE 115
CALCITE
DOLOMITE & GYPSUM
TOTAL CARB.
Mol% MgCO3 in HMC
DEPTH (cm)
0
100
200
300
All Hi-Mg Calcite
GYPSUM
DOLOMITE
LOC
XRD
0 2 4 6 8 10
0 10 20
0 5 10 15
0 10 20
PERCENT
PERCENT
PERCENT

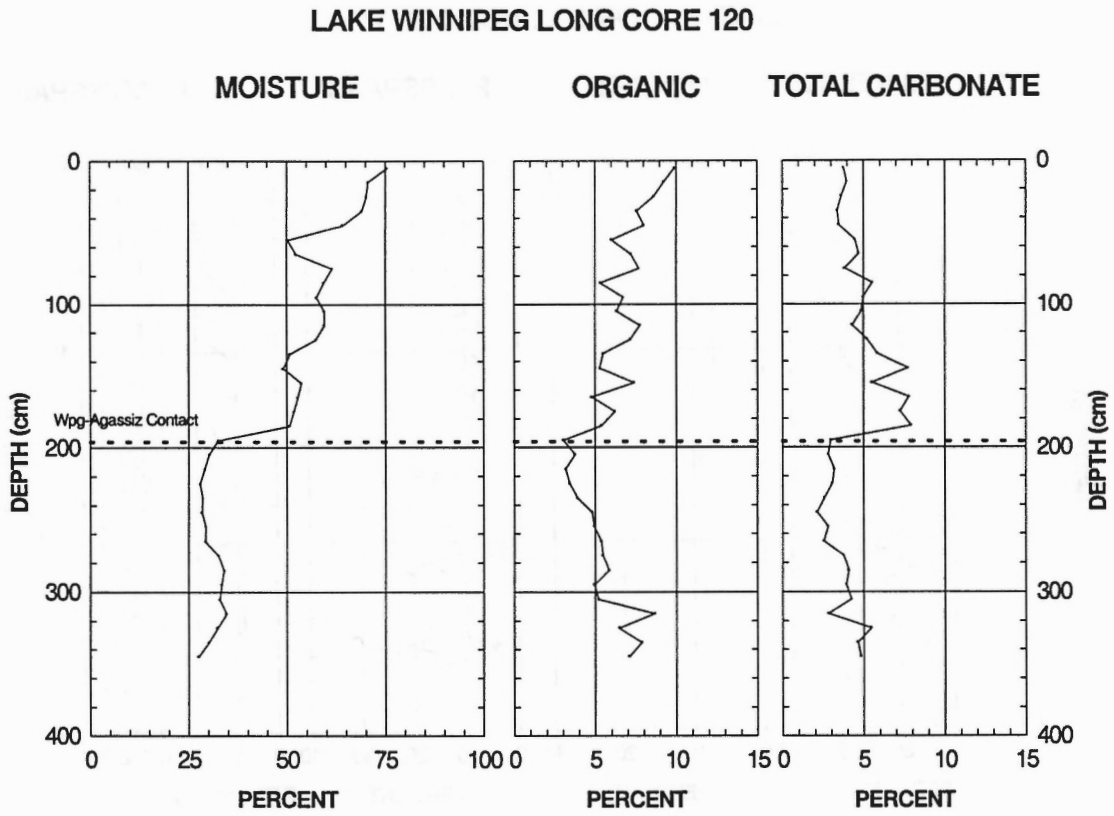
LAKE WINNIPEG LONG CORE 120
MOISTURE
ORGANIC
TOTAL CARBONATE
DEPTH (cm)
Wpg-Agassiz Contact
0
100
200
300
400
0
25
50
75
100
0
5
10
15
PERCENT

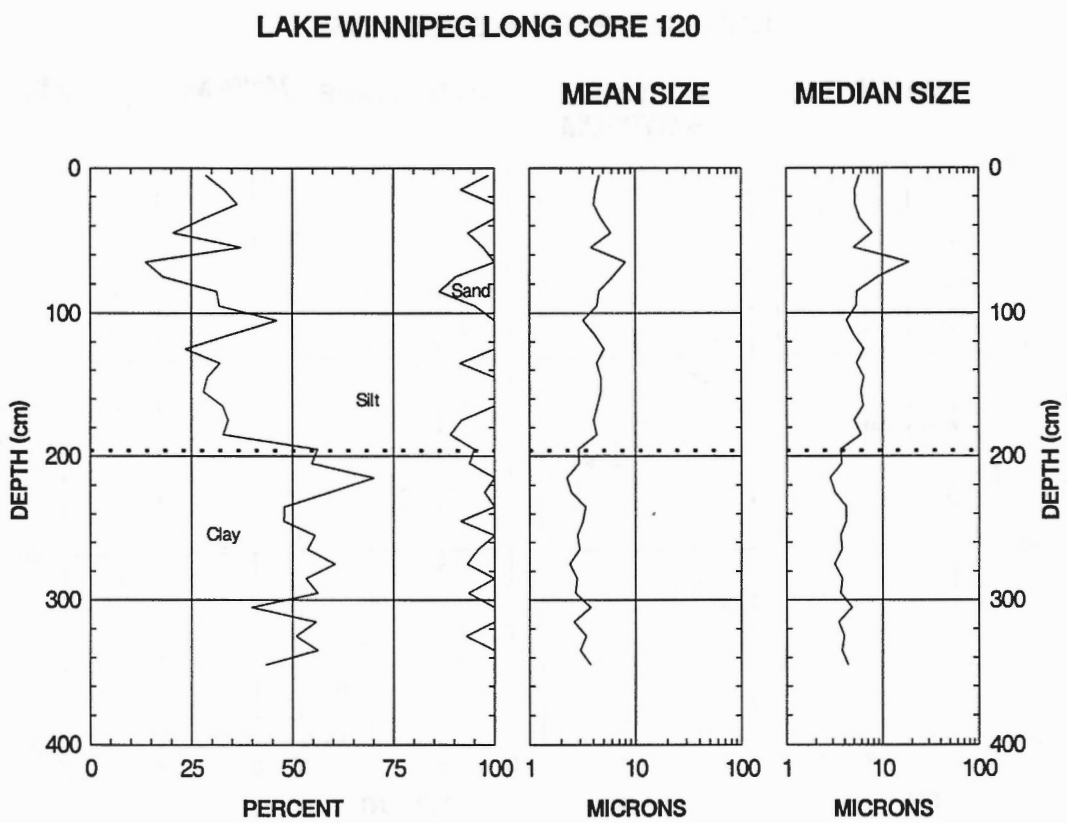
LAKE WINNIPEG LONG CORE 120
MEAN SIZE
MEDIAN SIZE
DEPTH (cm)
Sand
Silt
Clay
0
100
200
300
400
0
25
50
75
100
1
10
100
PERCENT
MICRONS

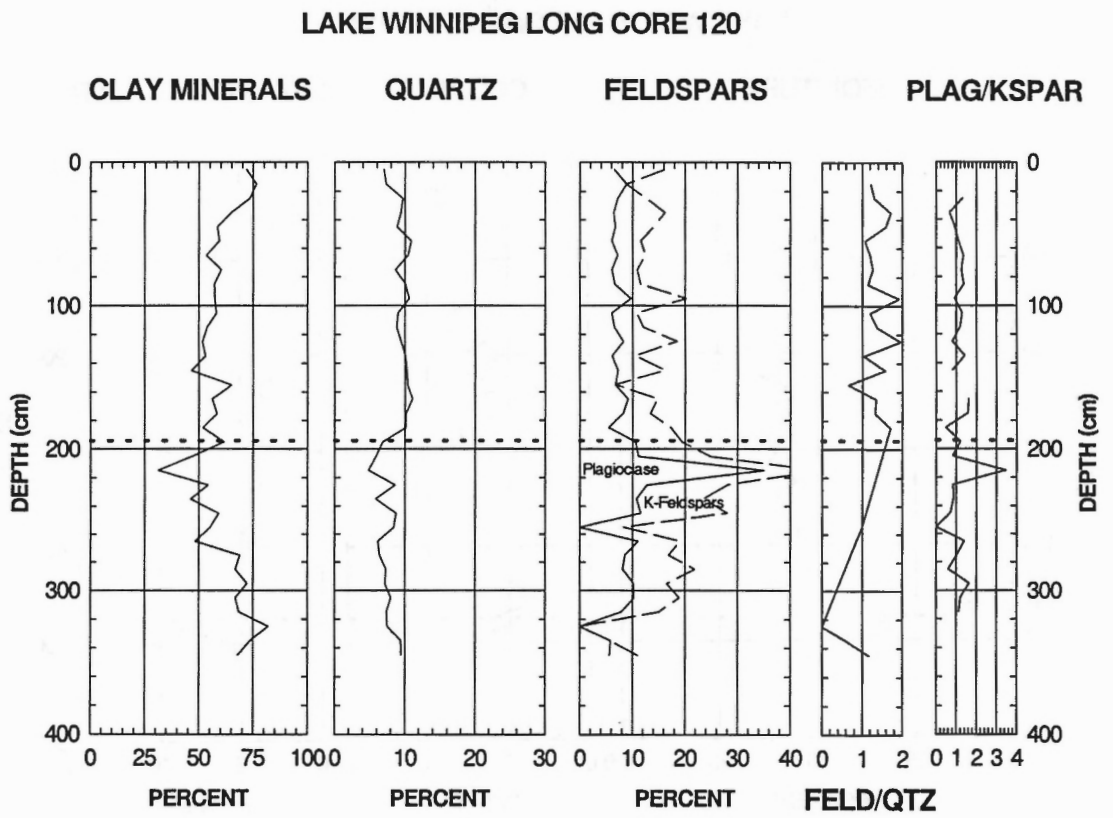
LAKE WINNIPEG LONG CORE 120
CLAY MINERALS
QUARTZ
FELDSPARS
PLAG/KSPAR
DEPTH (cm)
0
100
200
300
400
0 25 50 75 100
PERCENT
0 10 20 30
PERCENT
Plagiocase
K-Feldspars
0 10 20 30 40
PERCENT
0 1 2
FELD/QTZ
0 1 2 3 4

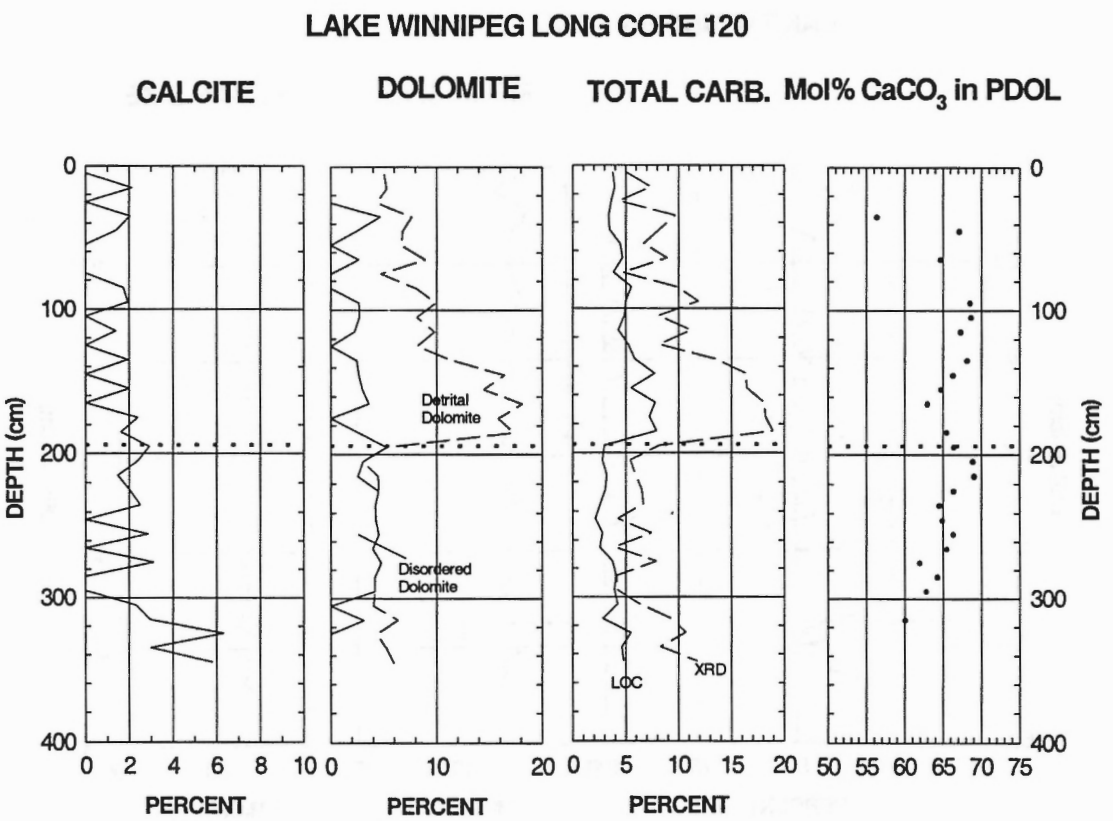
LAKE WINNIPEG LONG CORE 120
CALCITE
DOLOMITE
TOTAL CARB. Mol% CaCO3 in PDOL
DEPTH (cm)
0
100
200
300
400
0 2 4 6 8 10
PERCENT
Detrital Dolomite
Disordered Dolomite
0 10 20
PERCENT
LOC
XRD
0 5 10 15 20
PERCENT
50 55 60 65 70 75

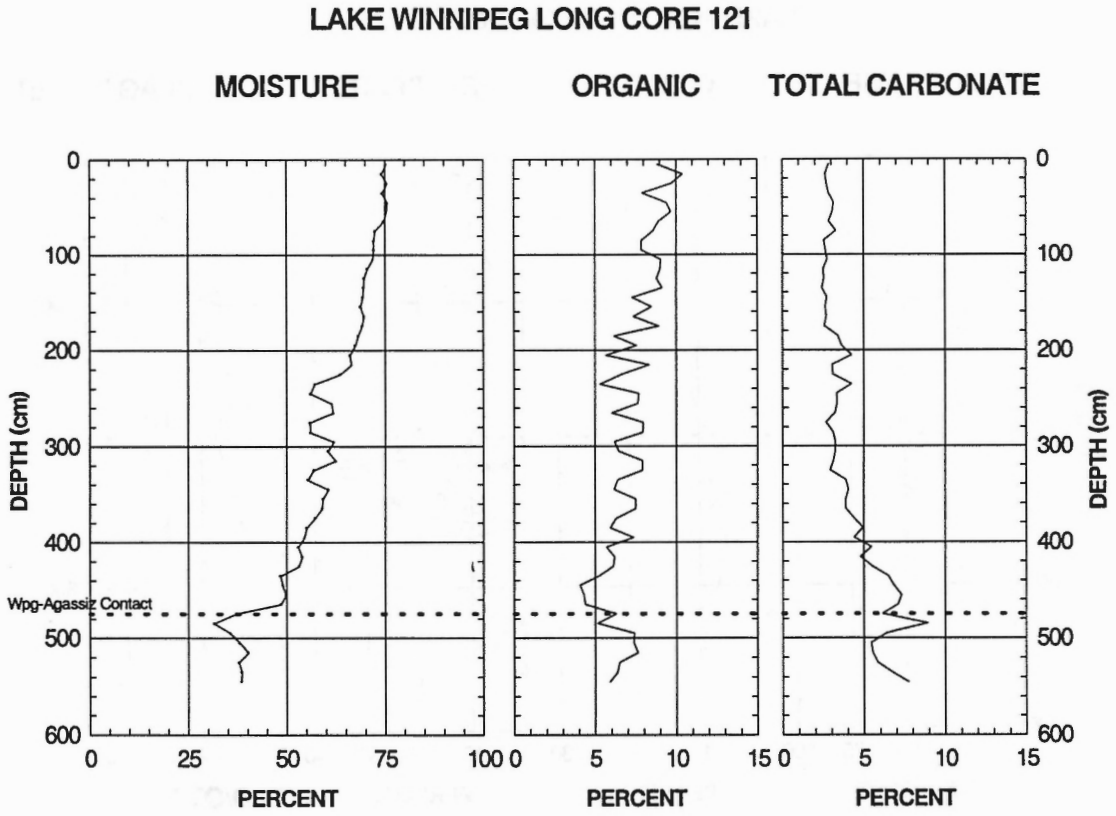
LAKE WINNIPEG LONG CORE 121
MOISTURE
ORGANIC
TOTAL CARBONATE
DEPTH (cm)
0
100
200
300
400
500
600
Wpg-Agassiz Contact
0
25
50
75
100
PERCENT
0
5
10
15
PERCENT
PERCENT

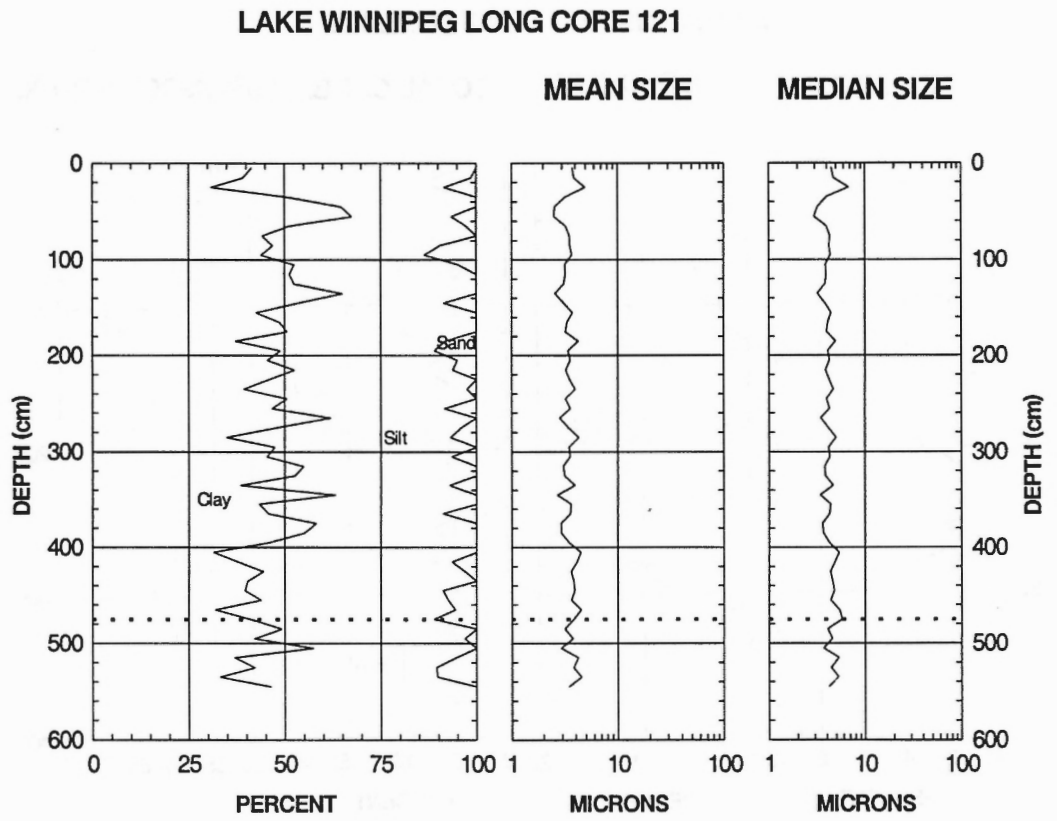
LAKE WINNIPEG LONG CORE 121
MEAN SIZE
MEDIAN SIZE
DEPTH (cm)
0
100
200
300
400
500
600
Clay
Silt
Sand
0
25
50
75
100
PERCENT
1
10
100
MICRONS
MICRONS

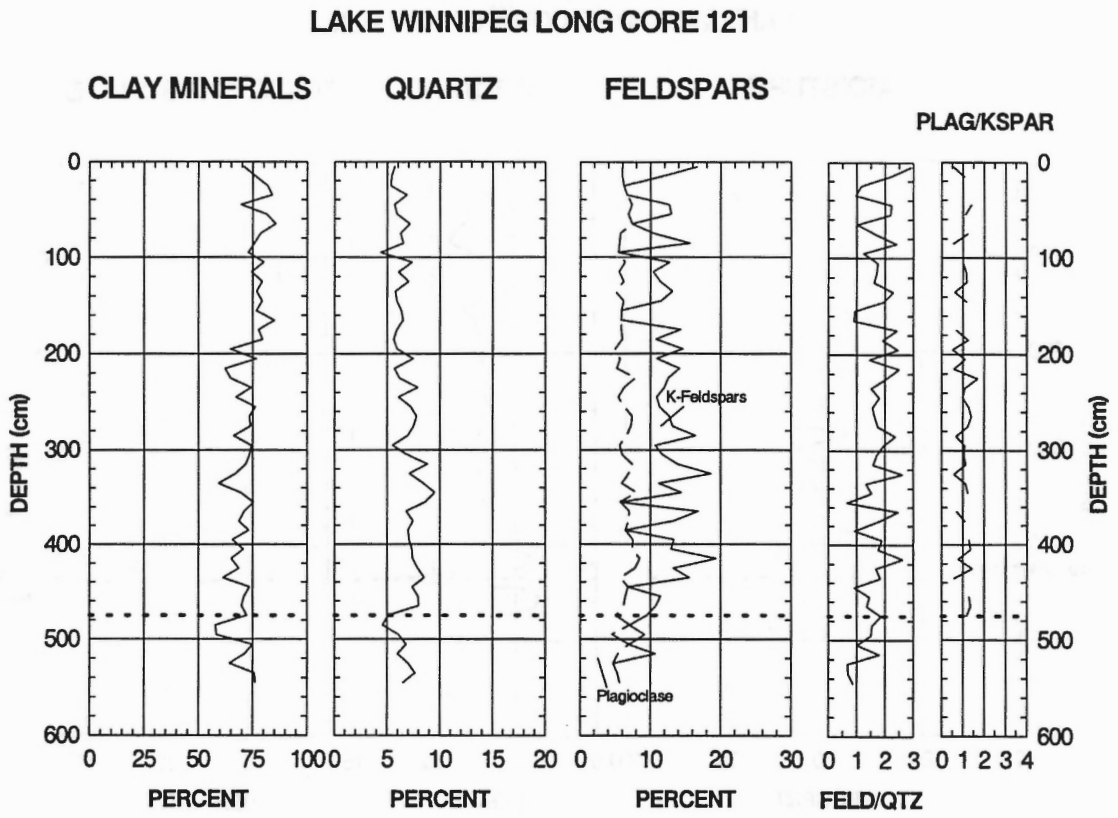
LAKE WINNIPEG LONG CORE 121
CLAY MINERALS
QUARTZ
FELDSPARS
PLAG/KSPAR
DEPTH (cm)
0
100
200
300
400
500
600
K-Feldspars
Plagioclase
0 25 50 75 100
0 5 10 15 20
0 10 20 30
0 1 2 3
0 1 2 3 4
PERCENT
PERCENT
PERCENT
FELD/QTZ

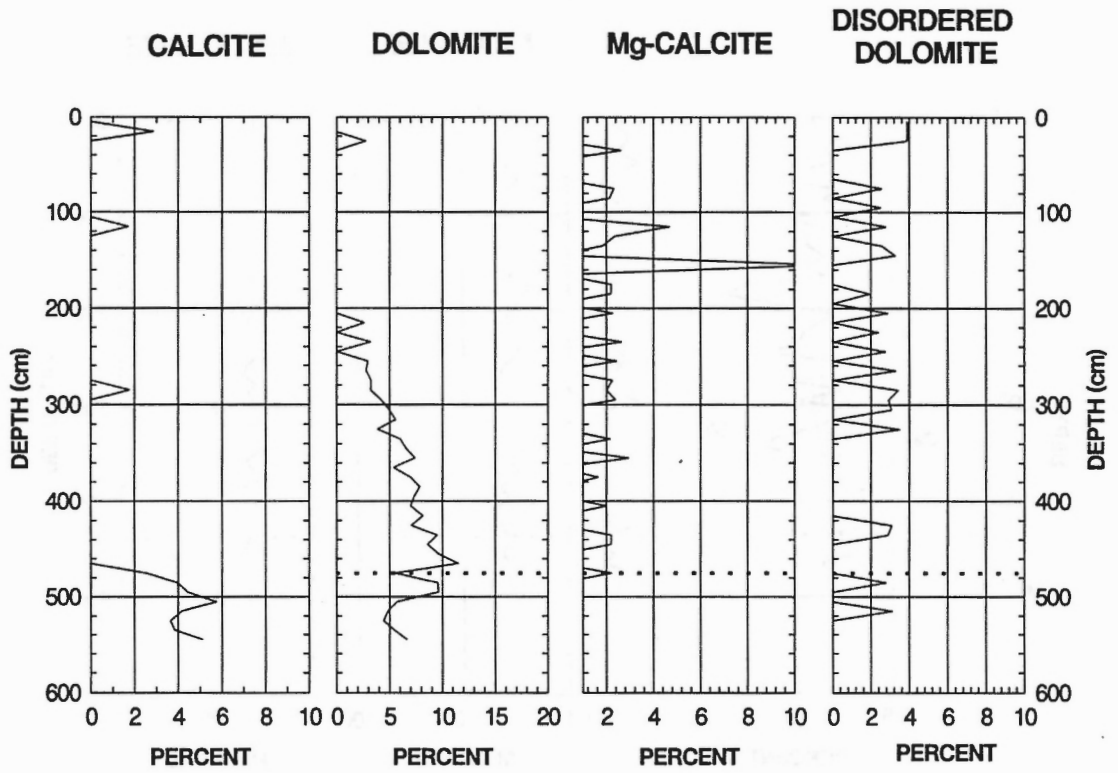
LAKE WINNIPEG LONG CORE 121
CALCITE
DOLOMITE
Mg-CALCITE
DISORDERED DOLOMITE
DEPTH (cm)
0
100
200
300
400
500
600
0 2 4 6 8 10
0 5 10 15 20
2 4 6 8 10
0 2 4 6 8 10
PERCENT
PERCENT
PERCENT
PERCENT

LAKE WINNIPEG LONG CORE 122A

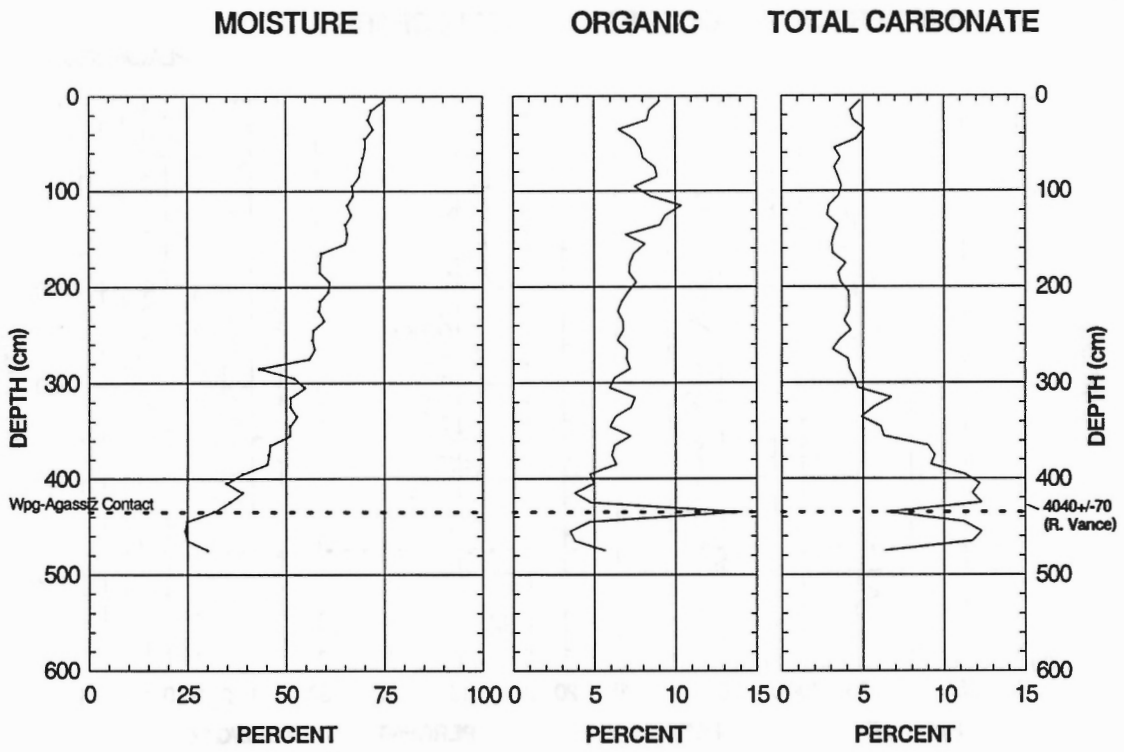

LAKE WINNIPEG LONG CORE 122A

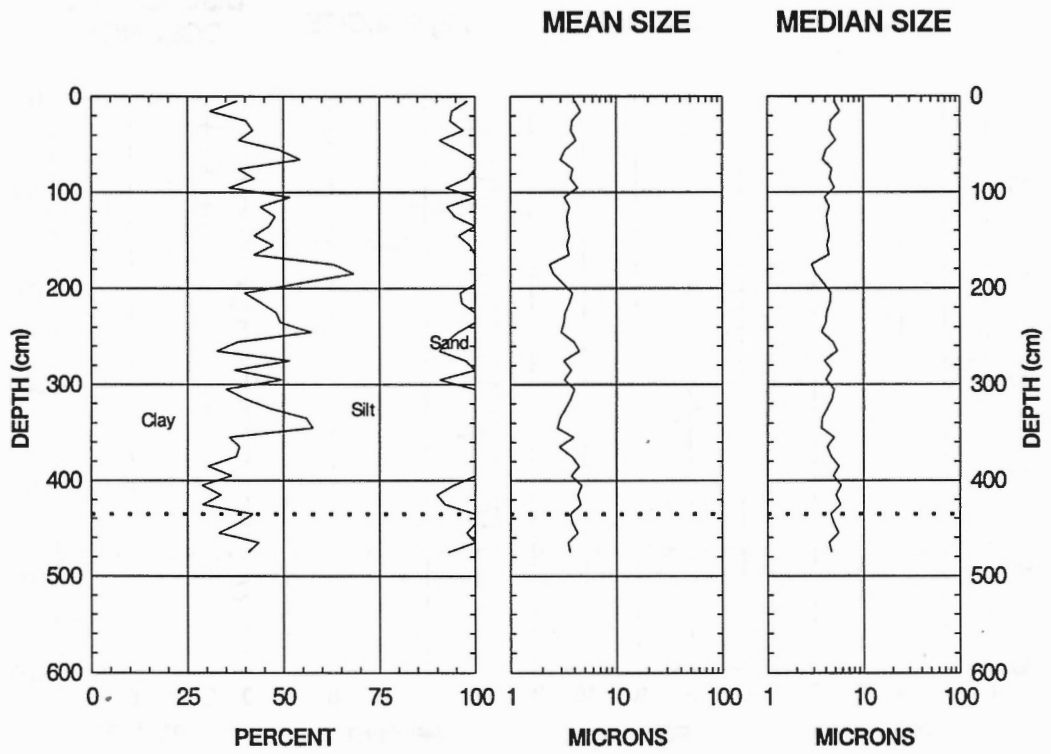

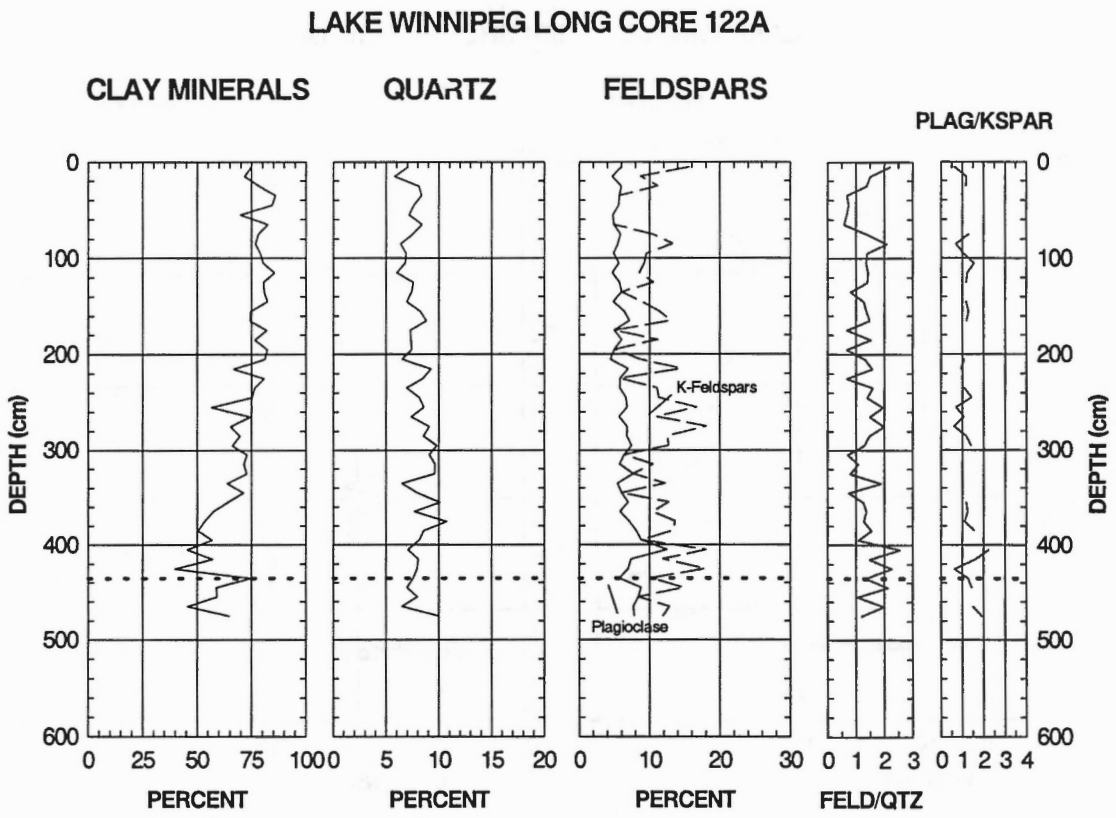
LAKE WINNIPEG LONG CORE 122A
CLAY MINERALS
QUARTZ
FELDSPARS
PLAG/KSPAR
DEPTH (cm)
0
100
200
300
400
500
600
0 25 50 75 100
PERCENT
0 5 10 15 20
PERCENT
K-Feldspars
Plagioclase
0 10 20 30
PERCENT
0 1 2 3
0 1 2 3 4
FELD/QTZ

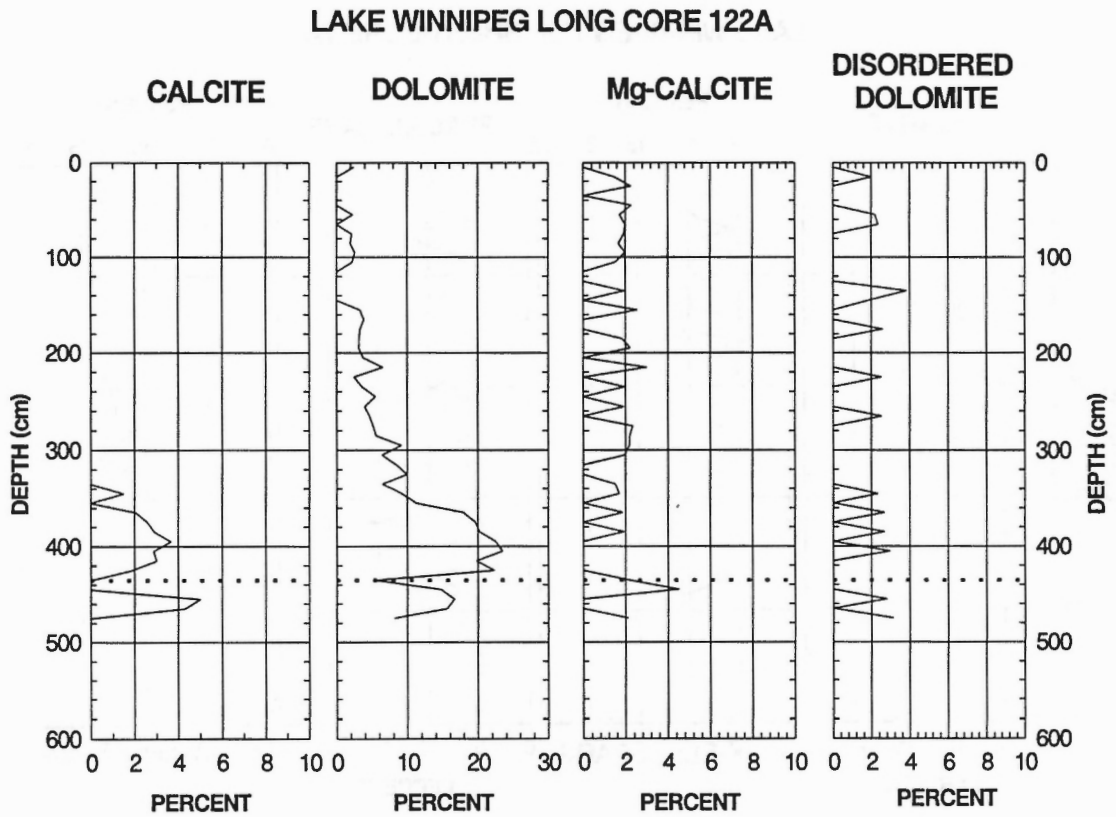
LAKE WINNIPEG LONG CORE 122A
CALCITE
DOLOMITE
Mg-CALCITE
DISORDERED DOLOMITE
DEPTH (cm)
0
100
200
300
400
500
600
0 2 4 6 8 10
PERCENT
0 10 20 30
PERCENT
0 2 4 6 8 10
PERCENT
0 2 4 6 8 10
PERCENT

LAKE WINNIPEG 1994 SHORT CORE 1A

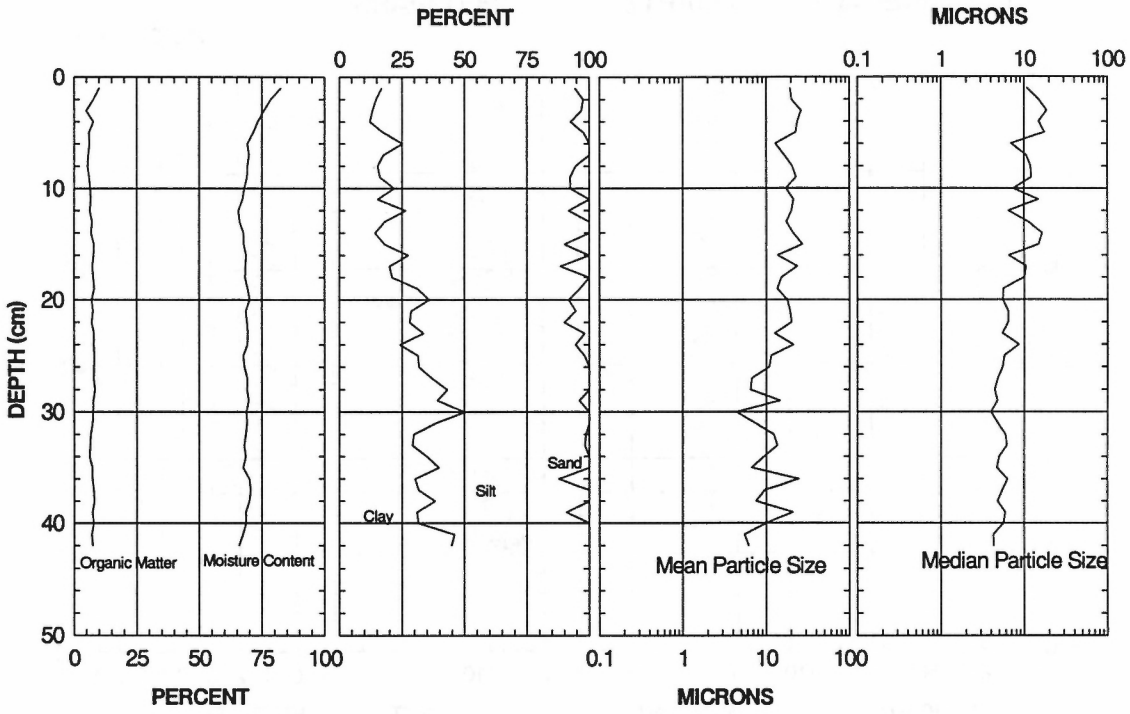

LAKE WINNIPEG 1994 SHORT CORE 1A

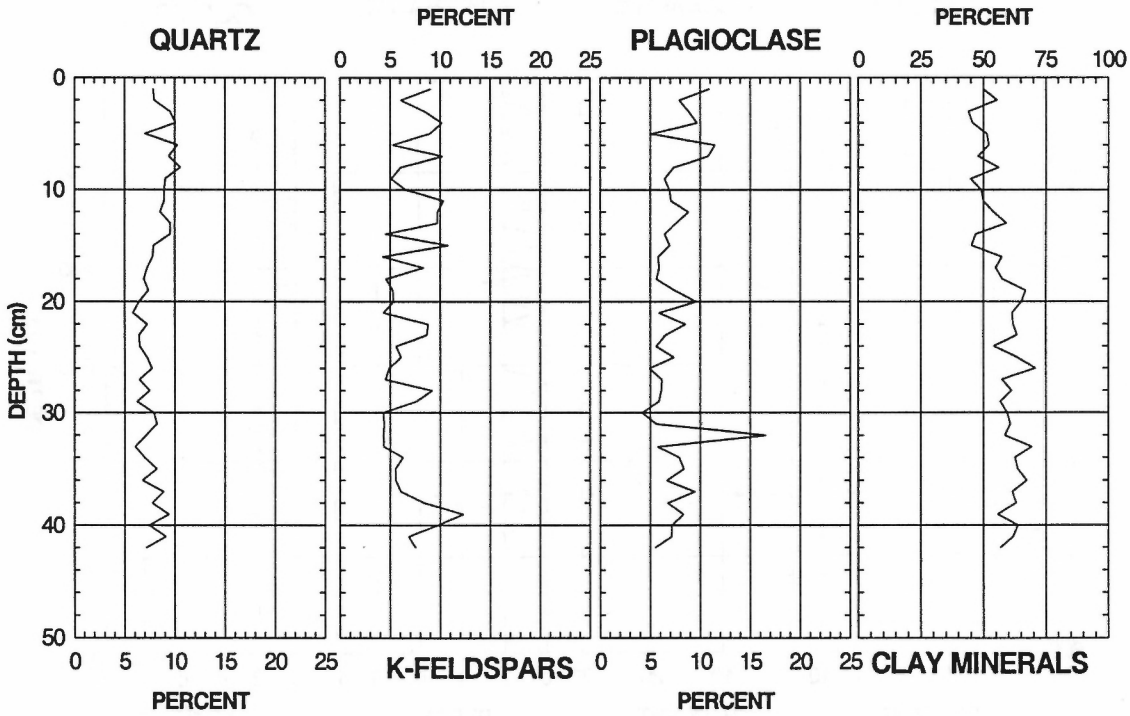

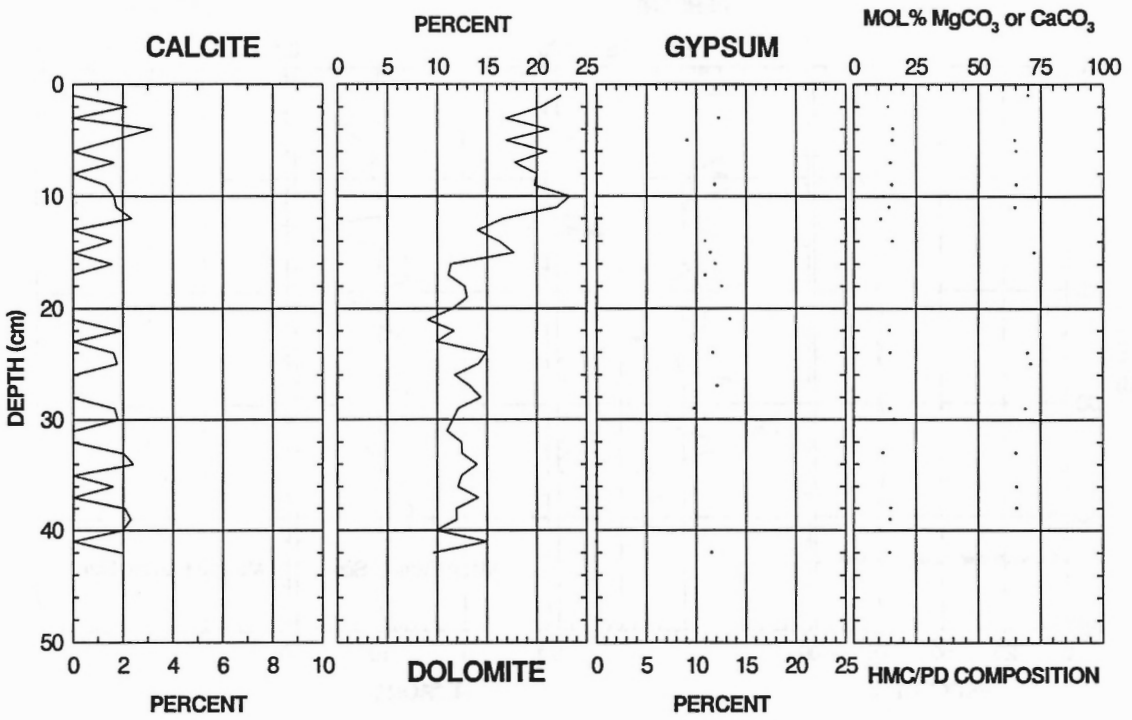
LAKE WINNIPEG 1994 SHORT CORE 1A
CALCITE
PERCENT
GYPSUM
MOL% MgCO3 or CaCO3
DEPTH (cm)
0
10
20
30
40
50
0 2 4 6 8 10
PERCENT
0 5 10 15 20 25
DOLOMITE
0 5 10 15 20 25
PERCENT
0 25 50 75 100
HMC/PD COMPOSITION

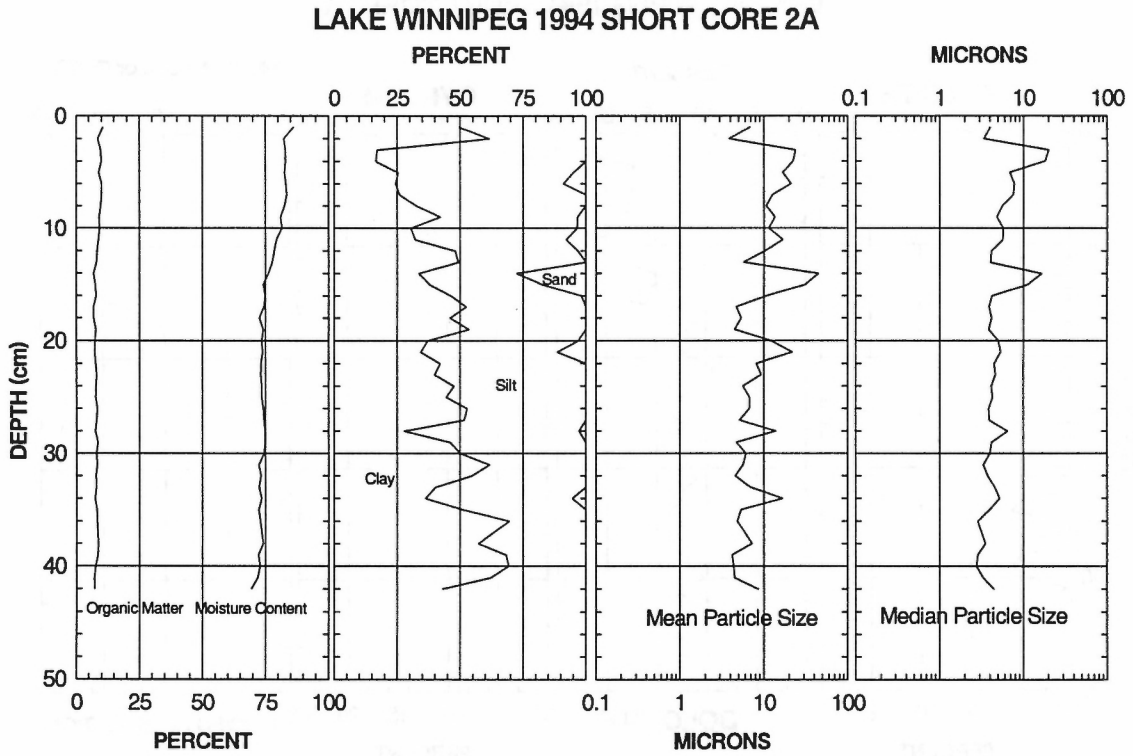
LAKE WINNIPEG 1994 SHORT CORE 2A
PERCENT
MICRONS
DEPTH (cm)
Organic Matter
Moisture Content
Sand
Silt
Clay
Mean Particle Size
Median Particle Size
PERCENT
MICRONS

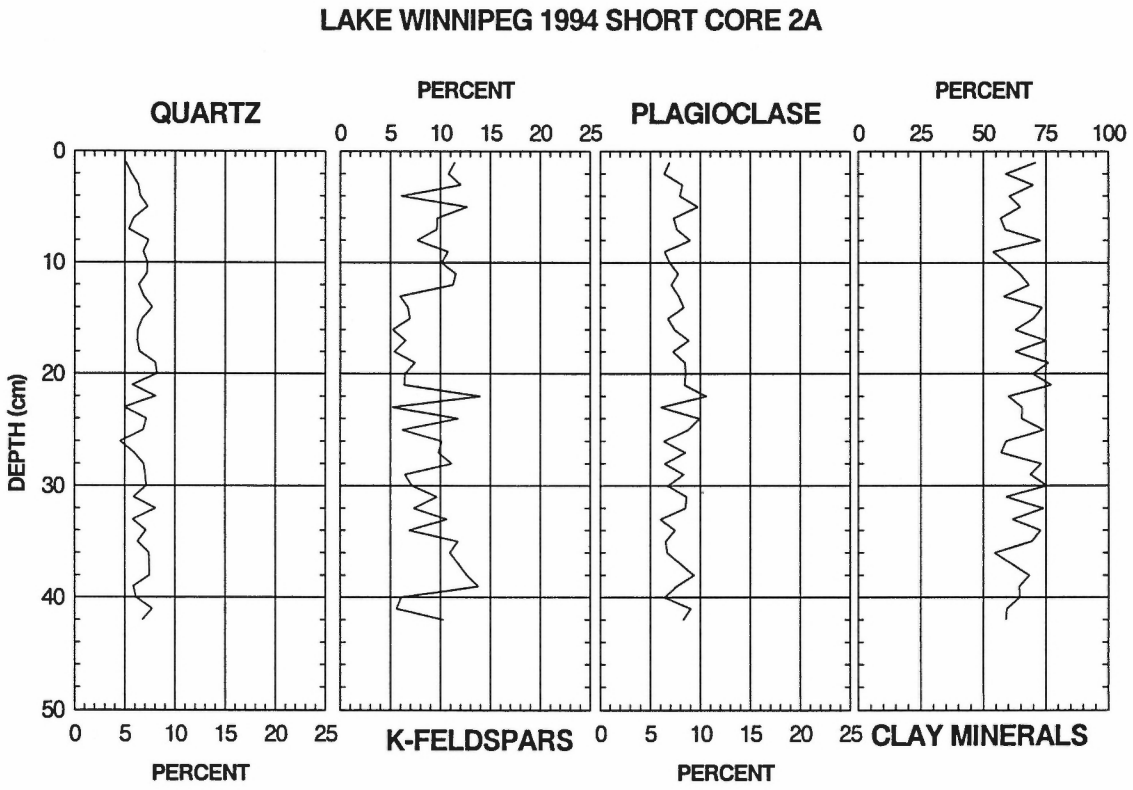
LAKE WINNIPEG 1994 SHORT CORE 2A
QUARTZ
PERCENT
PLAGIOCLASE
PERCENT
DEPTH (cm)
K-FELDSPARS
CLAY MINERALS
PERCENT
PERCENT

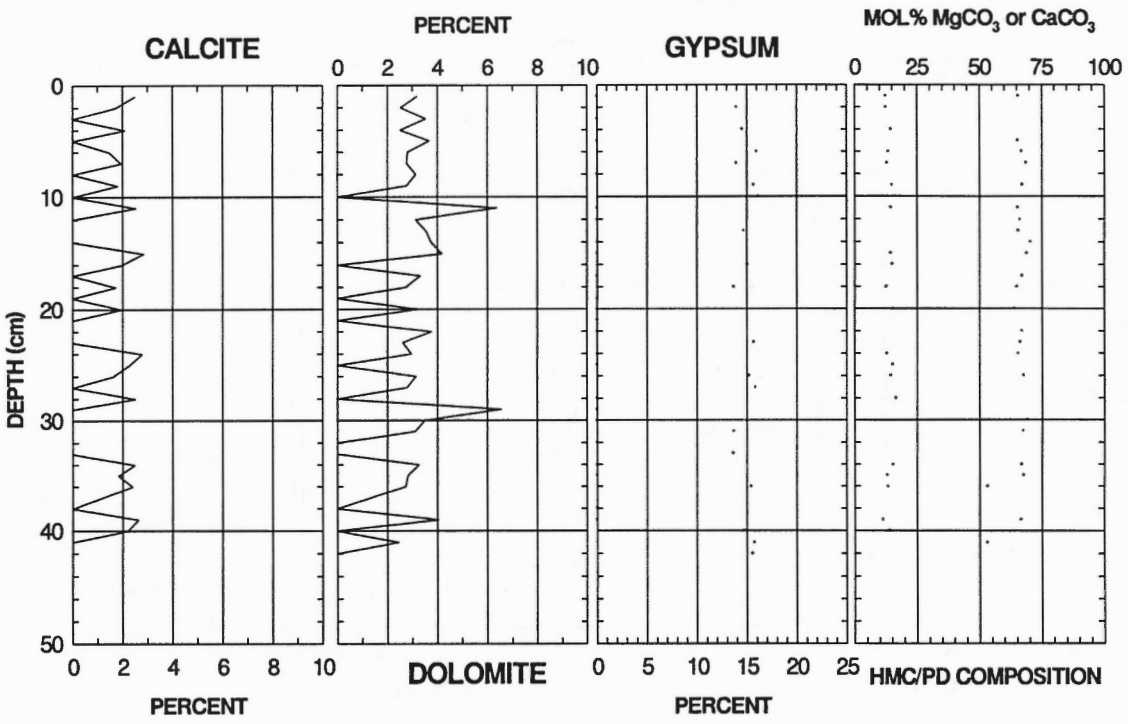
LAKE WINNIPEG 1994 SHORT CORE 2A
CALCITE
PERCENT
DOLOMITE
GYPSUM
MOL% MgCO3 or CaCO3
HMC/PD COMPOSITION
DEPTH (cm)
0
10
20
30
40
50
0 2 4 6 8 10
0 5 10 15 20 25
0 25 50 75 100

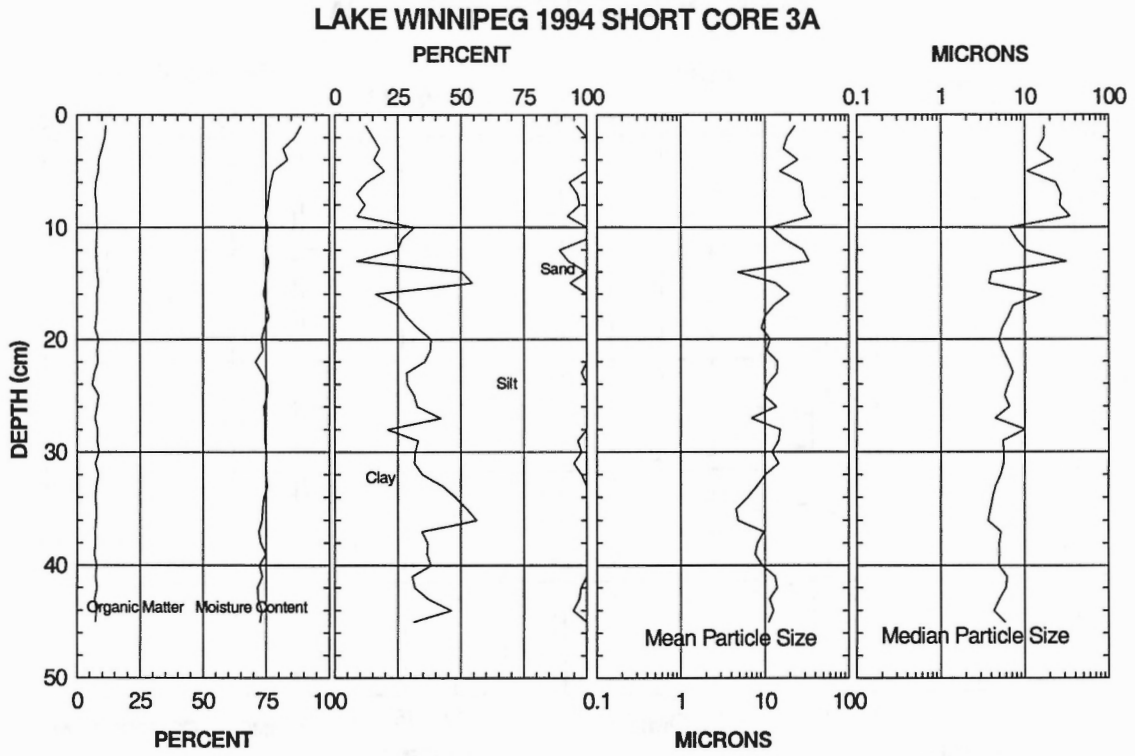
LAKE WINNIPEG 1994 SHORT CORE 3A
PERCENT
MICRONS
DEPTH (cm)
Organic Matter
Moisture Content
Sand
Silt
Clay
Mean Particle Size
Median Particle Size
PERCENT
MICRONS

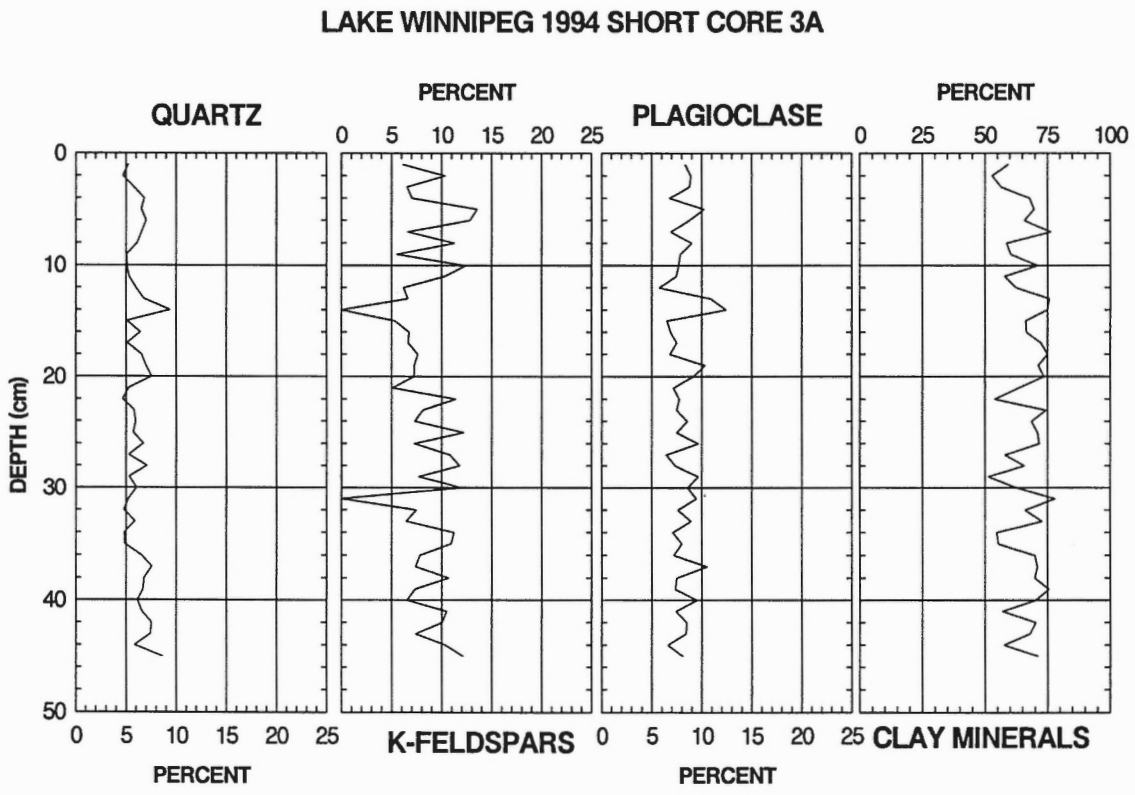
LAKE WINNIPEG 1994 SHORT CORE 3A
QUARTZ
PERCENT
PLAGIOCLASE
PERCENT
DEPTH (cm)
K-FELDSPARS
CLAY MINERALS
PERCENT
PERCENT

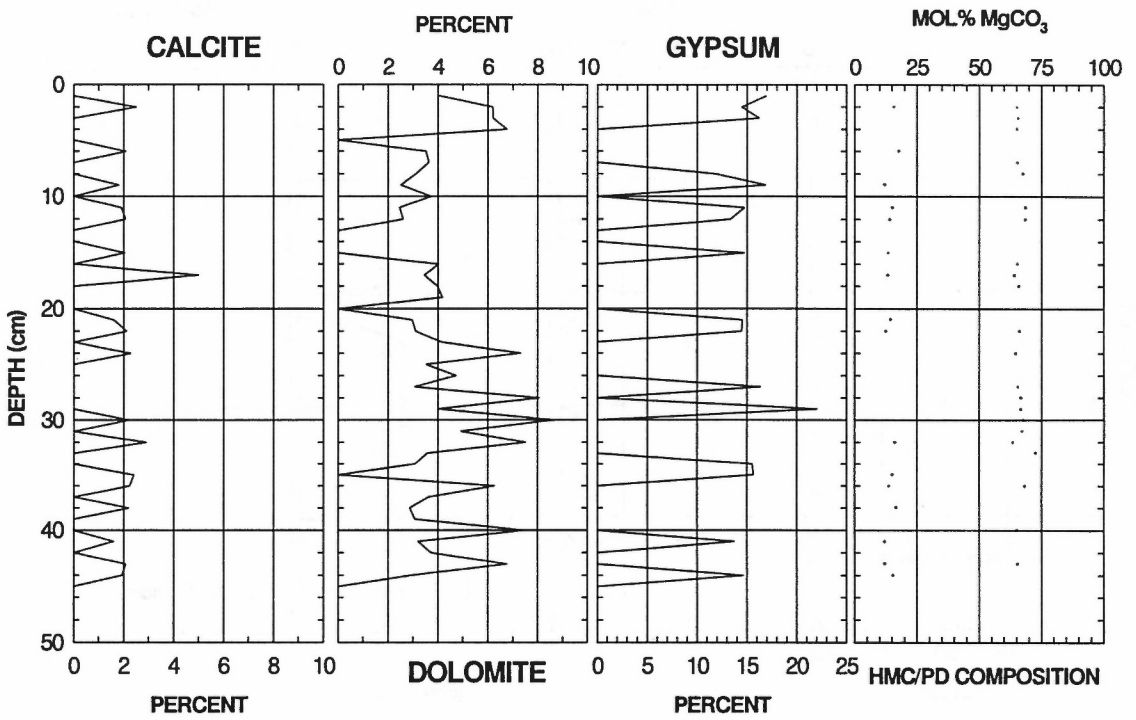
LAKE WINNIPEG 1994 SHORT CORE 3A
CALCITE
PERCENT
GYPSUM
MOL% MgCO3
DEPTH (cm)
0
10
20
30
40
50
0 2 4 6 8 10
0 2 4 6 8 10
0 25 50 75 100
0 5 10 15 20 25
PERCENT
DOLOMITE
PERCENT
HMC/PD COMPOSITION

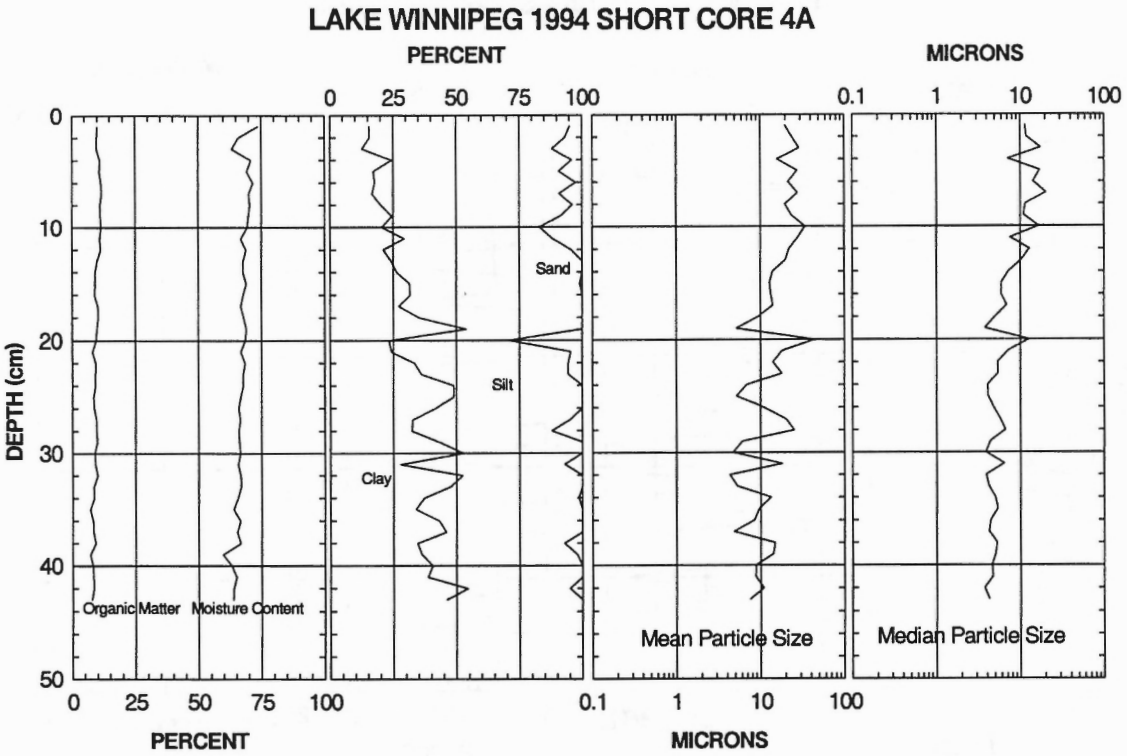
LAKE WINNIPEG 1994 SHORT CORE 4A
PERCENT
MICRONS
DEPTH (cm)
Sand
Silt
Clay
Organic Matter
Moisture Content
Mean Particle Size
Median Particle Size
PERCENT
MICRONS

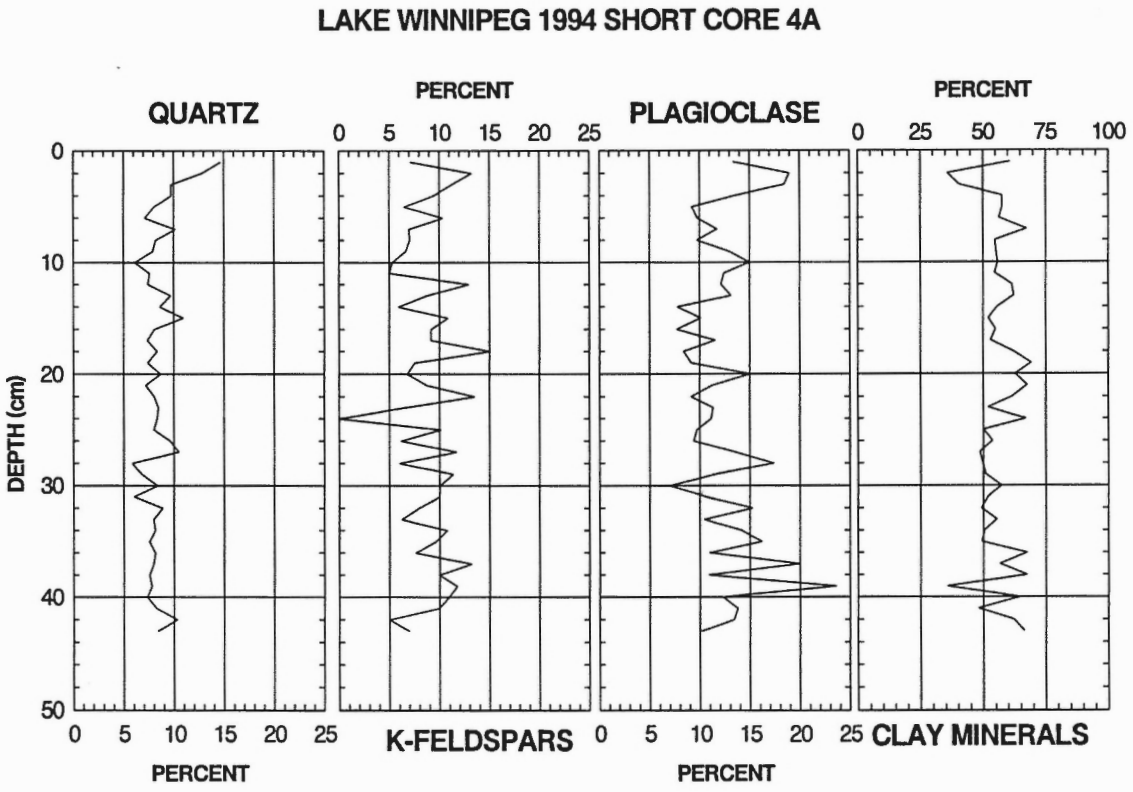
LAKE WINNIPEG 1994 SHORT CORE 4A
QUARTZ
PERCENT
PLAGIOCLASE
PERCENT
DEPTH (cm)
K-FELDSPARS
CLAY MINERALS
PERCENT
PERCENT

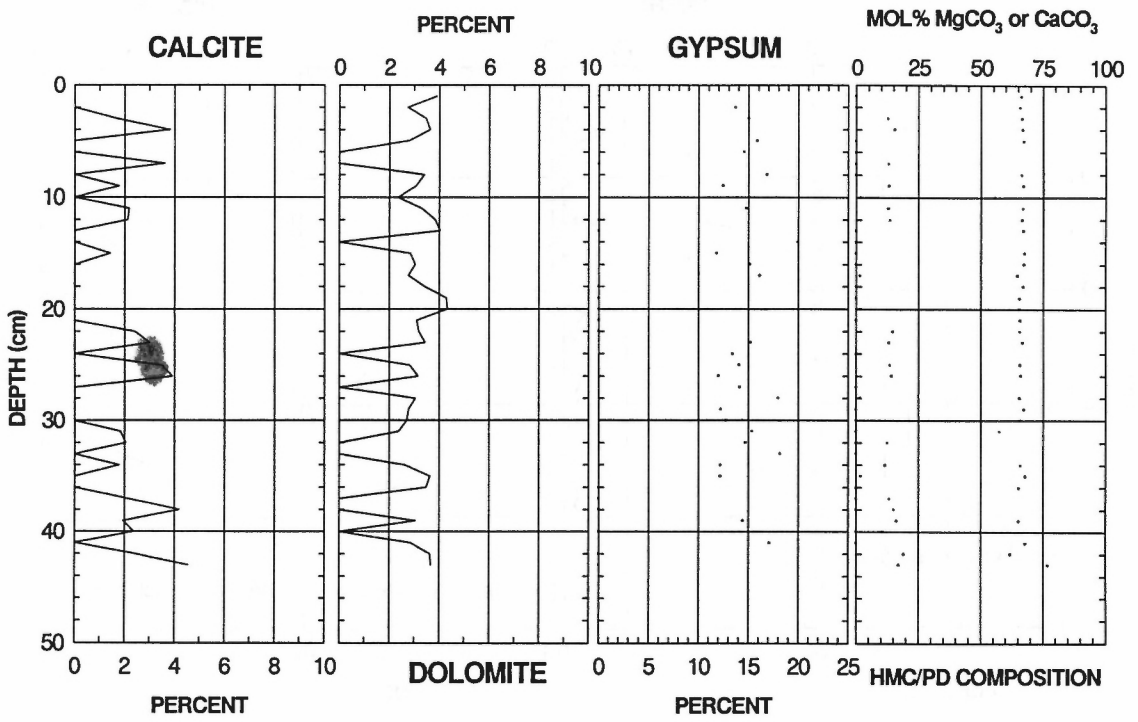
LAKE WINNIPEG 1994 SHORT CORE 4A
CALCITE
PERCENT
GYPSUM
MOL% MgCO3 or CaCO3
DEPTH (cm)
0
10
20
30
40
50
0 2 4 6 8 10
0 2 4 6 8 10
0 25 50 75 100
0 2 4 6 8 10
PERCENT
DOLOMITE
0 5 10 15 20 25
PERCENT
HMC/PD COMPOSITION

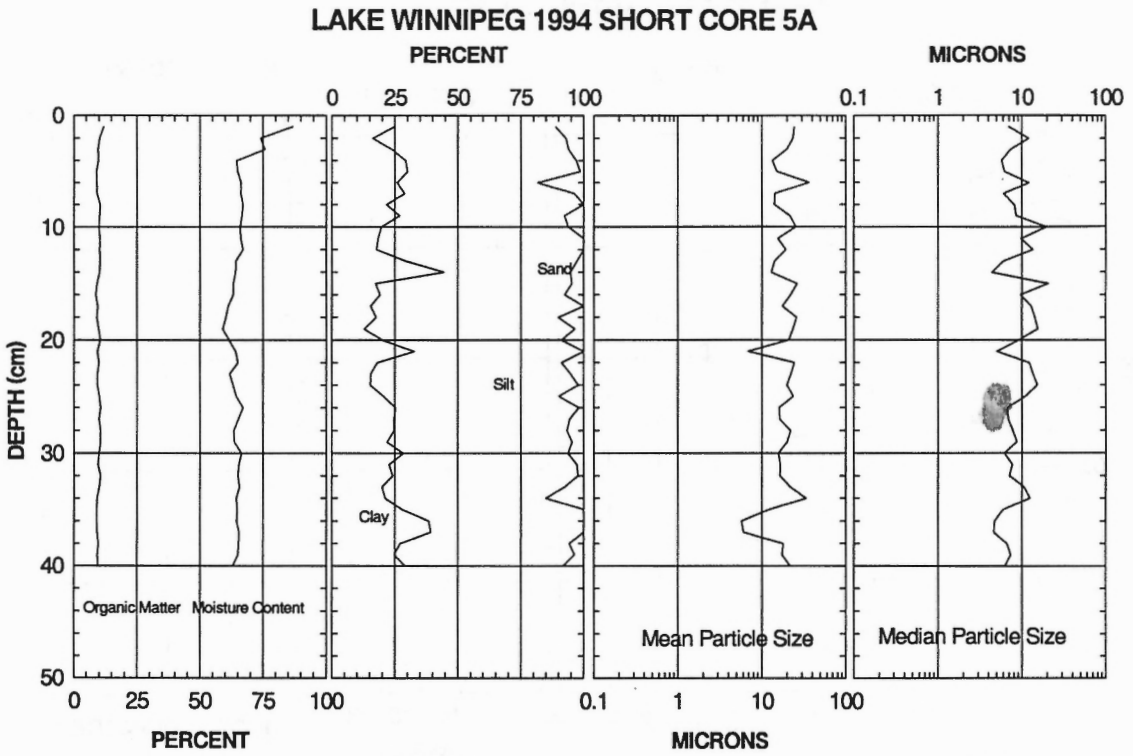
LAKE WINNIPEG 1994 SHORT CORE 5A
PERCENT
MICRONS
DEPTH (cm)
Sand
Silt
Clay
Organic Matter
Moisture Content
Mean Particle Size
Median Particle Size
PERCENT
MICRONS

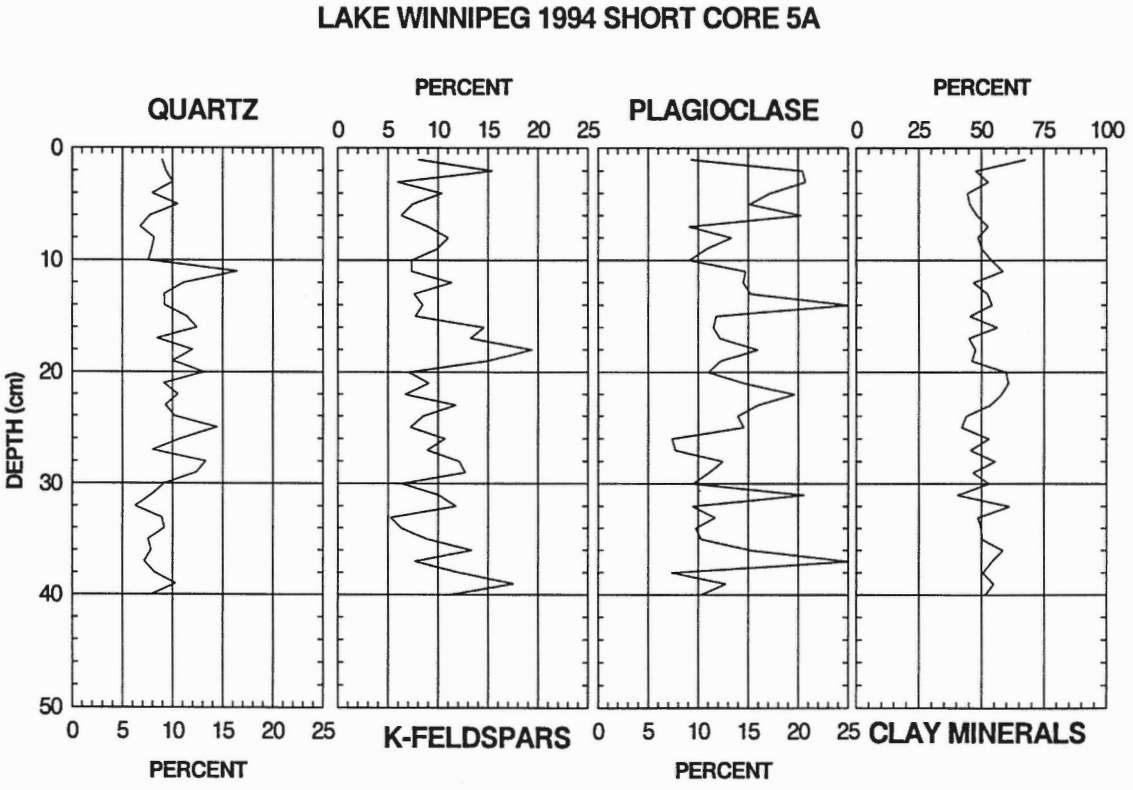
LAKE WINNIPEG 1994 SHORT CORE 5A
QUARTZ
PERCENT
PLAGIOCLASE
PERCENT
DEPTH (cm)
K-FELDSPARS
CLAY MINERALS
PERCENT
PERCENT

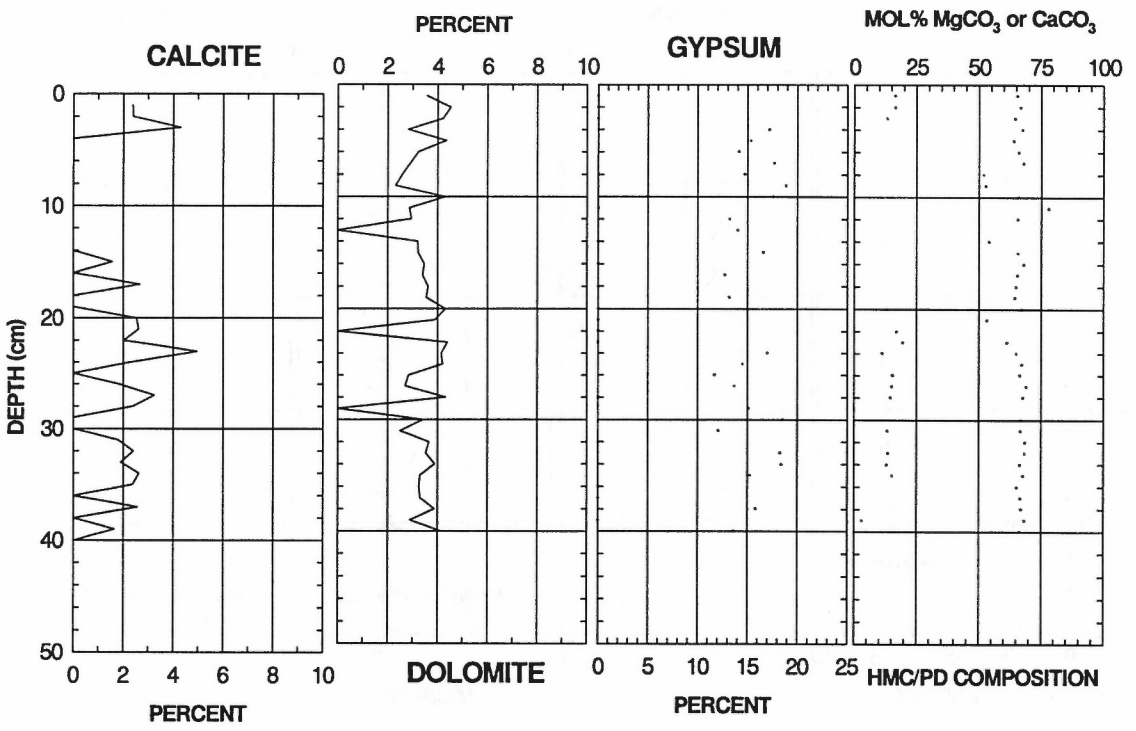
LAKE WINNIPEG 1994 SHORT CORE 5A
CALCITE
PERCENT
DOLOMITE
GYPSUM
MOL% MgCO3 or CaCO3
HMC/PD COMPOSITION
DEPTH (cm)
0
10
20
30
40
50
0 2 4 6 8 10
0 5 10 15 20 25
0 25 50 75 100

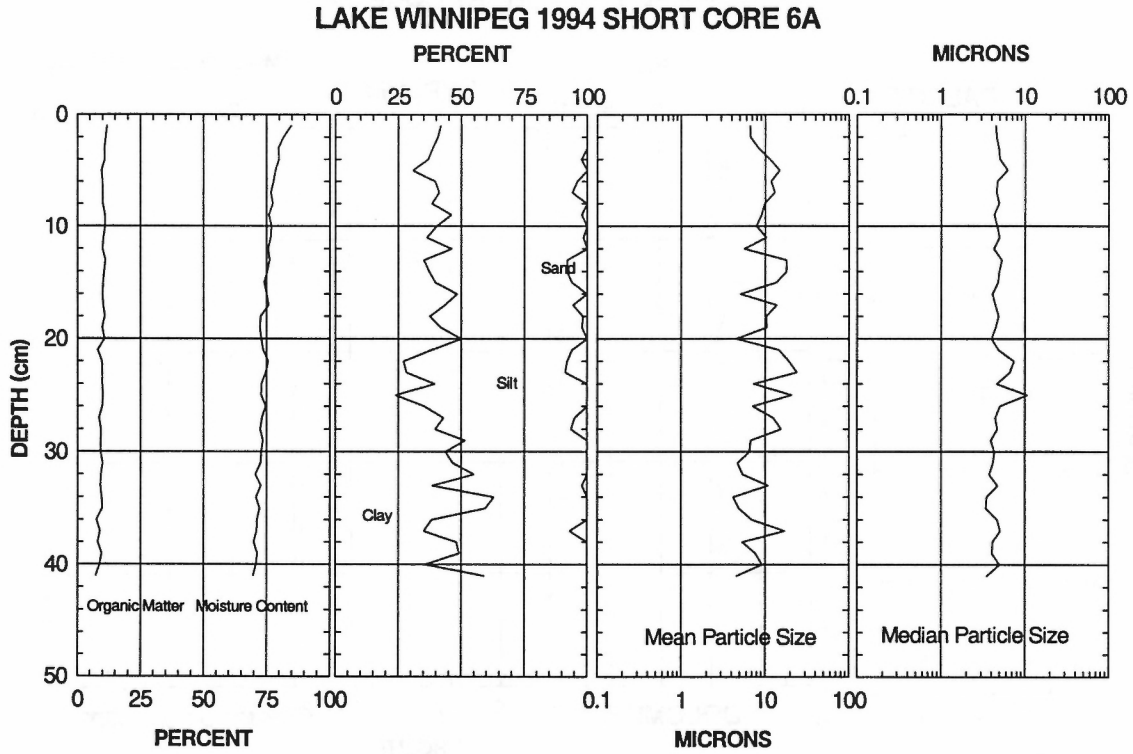
LAKE WINNIPEG 1994 SHORT CORE 6A
PERCENT
MICRONS
DEPTH (cm)
Organic Matter
Moisture Content
Clay
Silt
Sand
Mean Particle Size
Median Particle Size
PERCENT
MICRONS

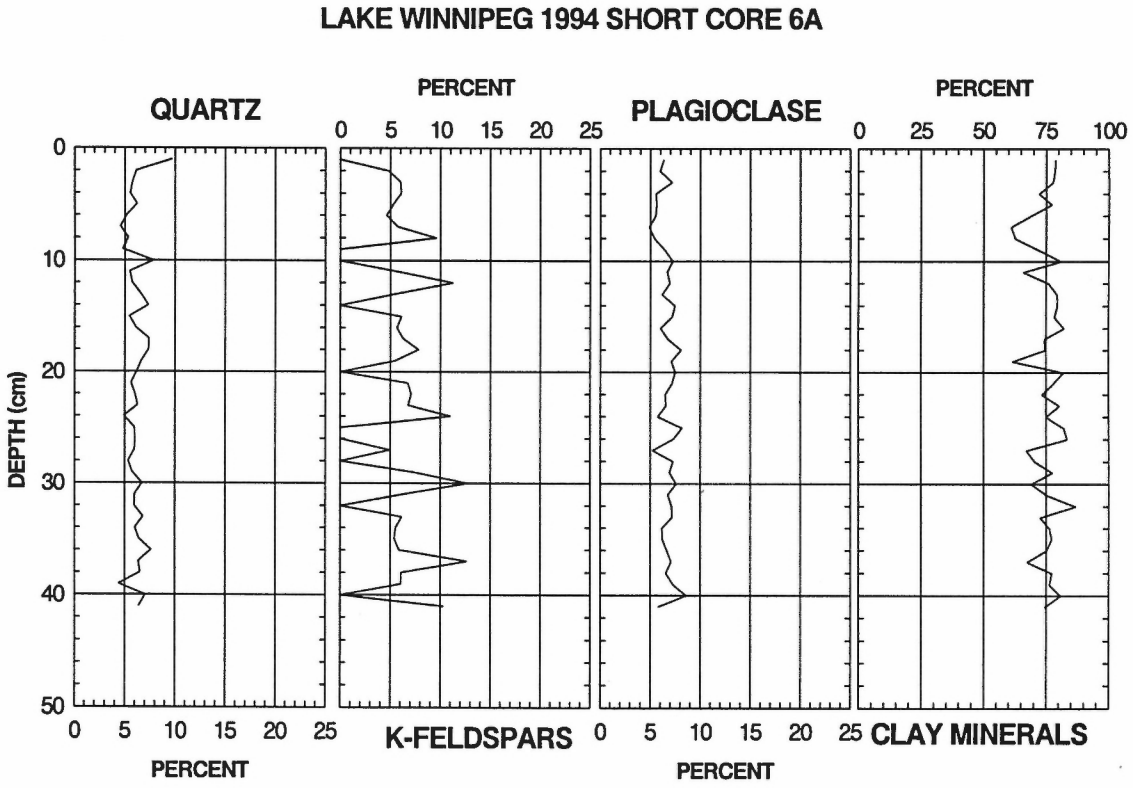
LAKE WINNIPEG 1994 SHORT CORE 6A
QUARTZ
PERCENT
PLAGIOCLASE
PERCENT
DEPTH (cm)
K-FELDSPARS
CLAY MINERALS
PERCENT
PERCENT

LAKE WINNIPEG 1994 SHORT CORE 6A

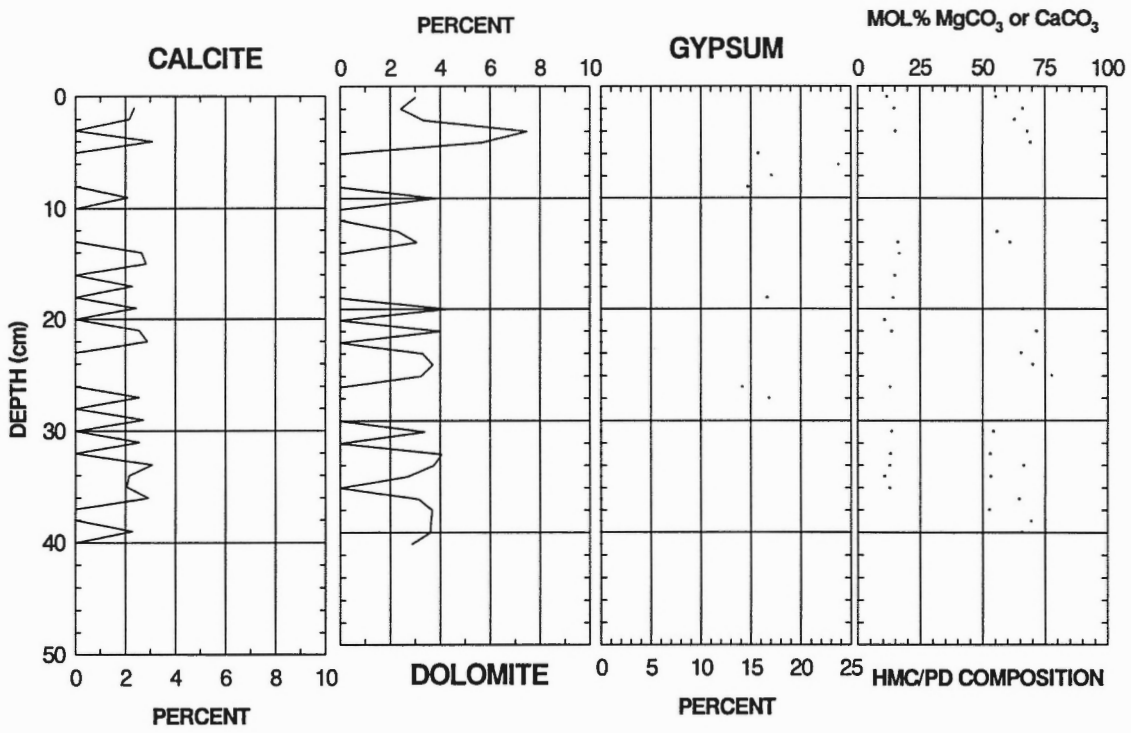

Appendix 7.4: Geochemistry of Lake Winnipeg sediments

P.J. Henderson

Geological Survey of Canada
601 Booth Street, Ottawa, Ontario K1A 0E8

Appendix 1

Bulk Sediment Geochemistry - Lake Winnipeg Long Cores

Analytical preparation: Hydrofluoric acid total leach

	Element	Analytical Method	Detection Limit	Upper Limit
Ag	ppm	AAS	0.2	200
Al	%	ICP-AES	0.01	25.00
Ba	ppm	ICP-AES	10	10000
Be	ppm	ICP-AES	0.5	1000
Bi	ppm	ICP-AES	2	10000
Ca	%	ICP-AES	0.01	25.00
Cd	ppm	ICP-AES	0.5	500
Co	ppm	ICP-AES	1	10000
Cr	ppm	ICP-AES	1	10000
Cu	ppm	ICP-AES	1	10000
Fe	%	ICP-AES	0.01	25.00
K	%	ICP-AES	0.01	10.00
Mg	%	ICP-AES	0.01	15.00
Mn	ppm	ICP-AES	5	10000
Mo	ppm	ICP-AES	1	10000
Na	%	ICP-AES	0.01	10.00
Ni	ppm	ICP-AES	1	10000
P	ppm	ICP-AES	10	10000
Pb	ppm	AAS	2	10000
Sr	ppm	ICP-AES	1	10000
Ti	%	ICP-AES	0.01	10.00
V	ppm	ICP-AES	1	10000
W	ppm	ICP-AES	10	10000
Zn	ppm	ICP-AES	2	10000

Analytical preparation: Nitric aqua-regia leach

	Element	Analytical Method	Detection Limit	Upper Limit
As	ppm	AAS-HYDRIDE/EDL	1	10000

% H_2O	Moisture Content (from Last, this volume)
% OM	Total Organic Content (from Last, this volume)
% CO_3	Total Carbonate Content (from Last, this volume)
% Clay	(from Last, this volume)
%Sand	(from Last, this volume)
% Silt	(from Last, this volume)

Core 103 (82 samples)

Depth (cm)	Ag ppm	Al %	Ba ppm	Be ppm	Bi ppm	Ca %	Cd ppm	Co ppm	Cr ppm	Cu ppm	Fe %	K %	Mg %	Mn ppm	Mo ppm	Na %	Ni ppm	P ppm	Pb ppm	Sr ppm	Ti %	V ppm	W ppm	Zn ppm	As ppm
5	<0.2	8.31	710	0.5	2	1.17	<0.5	19	114	44	4.70	2.28	1.71	885	<1	1.00	63	840	18	177	0.40	147	<10	122	<1
15	<0.2	7.62	640	0.5	<2	1.25	<0.5	16	101	40	3.93	2.17	1.61	680	<1	1.04	50	900	24	173	0.34	127	<10	116	<1
25	<0.2	8.63	760	0.5	4	1.19	<0.5	19	121	46	4.83	2.34	1.76	910	2	1.00	63	830	18	179	0.42	155	<10	130	
35	<0.2	8.47	730	0.5	<2	1.18	<0.5	19	117	45	4.72	2.30	1.71	880	1	1.00	62	820	20	180	0.41	147	<10	124	<1
45	<0.2	8.56	730	0.5	<2	1.19	<0.5	20	134	45	4.88	2.32	1.77	945	<1	0.99	70	830	20	179	0.42	152	<10	128	
55	<0.2	8.61	730	0.5	<2	1.23	<0.5	20	123	47	4.96	2.33	1.80	1010	<1	0.96	67	900	18	178	0.42	153	<10	130	<1
65	<0.2	8.34	700	0.5	<2	1.16	<0.5	17	115	44	4.72	2.25	1.71	840	<1	0.96	55	800	16	175	0.40	146	<10	122	<1
75	<0.2	8.49	710	0.5	<2	1.17	<0.5	20	115	44	4.76	2.30	1.74	825	1	0.97	64	810	18	176	0.40	150	<10	130	<1
85	<0.2	8.84	740	0.5	<2	1.17	<0.5	20	121	43	4.83	2.43	1.78	825	1	1.03	62	800	18	185	0.41	153	<10	136	<1
95	<0.2	8.74	720	0.5	2	1.21	<0.5	18	120	44	4.83	2.34	1.79	800	<1	0.96	61	790	18	178	0.41	157	<10	130	<1
105	<0.2	8.49	710	0.5	<2	1.12	<0.5	18	119	45	4.78	2.32	1.74	750	1	0.96	57	800	18	173	0.40	154	<10	128	<1
115	<0.2	8.68	720	0.5	4	1.14	<0.5	19	119	44	4.85	2.35	1.78	720	<1	0.95	61	790	18	176	0.42	158	<10	130	<1
125	<0.2	8.44	700	0.5	<2	1.20	<0.5	18	118	44	4.70	2.30	1.76	800	1	0.98	58	830	20	177	0.40	149	<10	126	<1
135	<0.2	8.49	710	0.5	<2	1.20	<0.5	18	117	44	4.68	2.33	1.78	720	<1	0.99	57	780	18	179	0.41	150	<10	128	<1
145	<0.2	8.83	740	<0.5	<2	1.23	<0.5	16	121	43	4.74	2.40	1.80	760	<1	1.05	55	710	18	176	0.42	152	<10	128	<1
155	<0.2	8.78	720	0.5	2	1.51	<0.5	20	123	45	4.92	2.43	2.00	885	<1	1.05	64	830	20	187	0.43	152	<10	130	<1
165	<0.2	7.60	620	0.5	<2	1.10	<0.5	22	103	37	4.28	2.06	1.61	635	1	0.89	59	650	18	160	0.37	132	<10	112	<1
175	<0.2	8.81	720	0.5	6	1.32	<0.5	19	122	45	4.89	2.39	1.90	735	1	1.04	59	800	20	186	0.43	154	<10	130	<1
185	<0.2	8.79	710	0.5	<2	1.27	<0.5	19	121	43	4.94	2.44	1.89	760	<1	1.05	60	800	16	185	0.42	154	<10	130	<1
195	<0.2	8.99	730	0.5	<2	1.28	<0.5	20	123	42	5.00	2.52	1.93	770	1	1.09	61	810	16	190	0.42	152	<10	132	<1
205	<0.2	8.74	720	0.5	<2	1.33	<0.5	20	118	43	5.00	2.46	1.93	705	<1	1.08	64	790	20	187	0.41	145	<10	126	<1
215	<0.2	8.46	710	0.5	<2	1.24	<0.5	19	117	41	4.85	2.43	1.85	735	<1	1.10	59	780	16	184	0.40	143	<10	130	<1
225	<0.2	8.14	710	0.5	2	1.24	<0.5	18	119	42	4.83	2.45	1.83	730	1	1.14	60	770	16	187	0.42	144	<10	126	
235	<0.2	8.62	710	0.5	<2	1.21	<0.5	19	118	43	4.93	2.44	1.86	730	1	1.06	60	770	18	184	0.41	147	<10	128	<1
245	<0.2	8.54	700	0.5	2	1.37	<0.5	19	120	43	4.89	2.45	1.96	755	1	1.08	59	730	16	184	0.40	143	<10	128	
255	<0.2	8.68	710	0.5	<2	1.27	<0.5	18	118	41	4.87	2.45	1.88	700	<1	1.13	56	740	16	188	0.39	143	<10	126	<1
265	<0.2	8.52	700	0.5	<2	1.35	<0.5	19	116	41	4.72	2.49	1.91	685	1	1.14	59	730	16	188	0.38	140	<10	122	<1
275	<0.2	8.61	710	0.5	<2	1.35	<0.5	18	115	41	4.71	2.48	1.91	710	1	1.15	57	720	16	191	0.39	140	<10	122	<1
285	<0.2	8.72	710	0.5	<2	1.29	<0.5	19	120	42	4.87	2.49	1.91	730	<1	1.10	59	760	16	188	0.41	149	<10	128	<1
295	<0.2	8.49	680	0.5	<2	1.35	<0.5	20	120	42	4.78	2.39	1.92	745	<1	1.05	63	740	18	181	0.41	146	<10	124	<1
305	<0.2	8.44	680	0.5	<2	1.42	<0.5	19	119	43	4.83	2.39	1.96	740	1	1.04	57	760	18	180	0.41	145	<10	124	<1
315	<0.2	8.67	700	0.5	2	1.34	<0.5	19	118	42	4.89	2.47	1.94	750	1	1.11	63	760	18	185	0.39	147	<10	126	<1
325	<0.2	8.62	700	0.5	<2	1.42	<0.5	18	118	44	4.81	2.46	1.99	740	2	1.11	57	740	18	187	0.41	142	<10	124	
335	<0.2	8.03	650	0.5	<2	1.31	<0.5	16	109	38	4.49	2.31	1.85	655	1	1.05	53	690	16	175	0.37	132	<10	116	<1
345	<0.2	8.06	670	0.5	<2	1.35	<0.5	17	114	38	4.53	2.39	1.87	690	1	1.10	54	730	16	180	0.37	132	<10	118	<1
355	<0.2	8.73	720	0.5	<2	1.38	<0.5	21	117	40	4.80	2.57	1.97	700	<1	1.21	62	750	16	195	0.38	141	<10	124	<1
365	<0.2	8.70	710	0.5	<2	1.21	<0.5	18	119	38	4.74	2.53	1.87	665	<1	1.19	56	730	14	190	0.37	139	<10	122	<1

Depth (cm)	Ag ppm	Al %	Ba ppm	Be ppm	Bi ppm	Ca %	Cd ppm	Co ppm	Cr ppm	Cu ppm	Fe %	K %	Mg %	Mn ppm	Mo ppm	Na %	Ni ppm	P ppm	Pb ppm	Sr ppm	Ti %	V ppm	W ppm	Zn ppm	As ppm
375	<0.2	8.44	680	0.5	<2	1.26	<0.5	17	115	39	4.64	2.46	1.88	650	<1	1.12	52	720	14	182	0.37	135	<10	120	<1
385	<0.2	8.33	680	0.5	<2	1.27	<0.5	17	111	38	4.38	2.44	1.84	620	<1	1.16	51	680	14	184	0.35	132	<10	116	<1
395	<0.2	8.37	670	0.5	<2	1.37	<0.5	17	116	41	4.61	2.42	1.95	665	<1	1.07	52	700	16	179	0.38	136	<10	120	<1
405	<0.2	8.19	700	0.5	4	1.40	<0.5	18	116	39	4.67	2.52	1.91	690	<1	1.22	55	730	16	192	0.39	139	<10	122	1
415	<0.2	8.44	680	0.5	4	1.43	<0.5	17	118	39	4.60	2.49	1.96	700	1	1.18	55	710	16	187	0.37	134	<10	122	1
425	<0.2	8.25	660	0.5	6	1.43	<0.5	18	119	41	4.59	2.41	1.97	670	<1	1.10	54	720	50	178	0.38	134	<10	120	1
435	<0.2	8.28	700	0.5	4	1.40	<0.5	17	117	38	4.58	2.53	1.92	655	1	1.23	53	720	20	192	0.37	131	<10	118	2
445	<0.2	7.84	630	0.5	<2	1.66	<0.5	17	112	38	4.30	2.32	2.06	715	<1	1.08	51	640	18	171	0.37	123	<10	112	1
455	<0.2	8.58	680	0.5	6	1.48	<0.5	18	123	47	4.88	2.54	2.07	690	<1	1.14	55	750	20	186	0.41	140	<10	126	1
465	<0.2	8.66	710	0.5	4	1.62	<0.5	18	122	40	4.69	2.65	2.13	725	1	1.25	57	730	16	194	0.38	133	<10	124	1
475	<0.2	8.55	700	0.5	4	1.58	<0.5	17	116	37	4.56	2.59	2.05	680	<1	1.27	52	720	16	196	0.38	130	<10	118	2
485	<0.2	8.24	680	0.5	2	1.51	<0.5	17	113	35	4.38	2.53	1.95	645	<1	1.25	52	670	16	192	0.36	124	<10	114	1
495	<0.2	8.34	680	0.5	6	1.50	<0.5	18	115	38	4.49	2.54	1.96	655	<1	1.23	55	730	18	193	0.38	131	<10	116	1
505	<0.2	8.32	660	0.5	4	1.52	<0.5	17	116	38	4.49	2.49	1.97	660	1	1.21	54	710	16	188	0.37	131	<10	116	1
515	<0.2	8.47	670	0.5	<2	1.76	<0.5	17	112	37	4.46	2.56	2.12	675	<1	1.24	55	730	18	190	0.36	130	<10	116	1
525	<0.2	7.96	630	0.5	4	1.72	<0.5	16	106	35	4.21	2.41	2.00	660	<1	1.17	49	700	16	180	0.35	126	<10	110	2
535	<0.2	8.35	640	0.5	4	1.69	<0.5	17	111	37	4.38	2.47	2.05	645	<1	1.17	51	740	16	184	0.37	134	<10	116	2
545	<0.2	8.15	630	0.5	4	1.44	<0.5	17	104	35	4.20	2.42	1.84	600	<1	1.20	50	680	18	183	0.34	130	<10	110	1
555	<0.2	8.59	660	0.5	4	1.64	<0.5	17	117	38	4.56	2.55	2.07	645	<1	1.20	54	740	16	186	0.37	137	<10	120	1
565	<0.2	8.41	650	0.5	4	1.78	<0.5	16	111	36	4.24	2.53	2.03	650	<1	1.24	52	700	18	189	0.34	133	<10	112	
575	<0.2	8.23	630	0.5	6	1.54	<0.5	18	110	35	4.32	2.44	1.94	630	1	1.14	50	710	16	178	0.35	135	<10	114	1
585	<0.2	8.41	640	0.5	4	1.56	<0.5	17	112	38	4.44	2.48	1.99	610	3	1.17	52	700	16	180	0.35	137	<10	116	2
595	<0.2	8.41	630	0.5	4	1.81	<0.5	17	114	38	4.42	2.50	2.11	665	1	1.17	52	730	16	182	0.36	136	<10	118	1
605	<0.2	8.15	610	0.5	4	1.75	<0.5	16	111	37	4.27	2.40	2.02	625	<1	1.11	50	720	16	176	0.35	136	<10	114	1
615	<0.2	8.01	600	0.5	6	1.94	<0.5	16	109	38	4.11	2.35	2.09	635	<1	1.12	49	710	16	175	0.35	134	<10	110	1
625	<0.2	8.31	630	0.5	4	1.65	<0.5	17	109	36	4.28	2.46	2.02	595	<1	1.17	54	690	14	180	0.36	135	<10	114	2
635	<0.2	8.37	640	0.5	6	2.13	<0.5	17	116	38	4.39	2.54	2.20	675	<1	1.24	51	730	14	188	0.35	133	<10	114	1
645	<0.2	8.29	630	0.5	8	1.80	<0.5	18	108	36	4.25	2.49	2.08	625	<1	1.24	56	710	16	185	0.34	130	<10	112	2
655	<0.2	8.32	620	0.5	4	1.62	<0.5	16	109	35	4.35	2.47	2.02	585	1	1.17	51	690	14	178	0.34	132	<10	114	1
665	<0.2	8.68	650	0.5	<2	1.85	<0.5	18	118	43	4.51	2.60	2.17	620	<1	1.23	60	750	20	188	0.36	136	<10	122	1
675	<0.2	8.39	640	0.5	4	2.62	<0.5	17	115	40	4.32	2.56	2.30	660	1	1.25	56	720	18	191	0.36	126	<10	116	1
685	<0.2	8.45	640	0.5	4	1.98	<0.5	19	113	40	4.32	2.54	2.20	615	2	1.22	58	750	18	186	0.37	134	<10	116	1
695	<0.2	8.60	680	0.5	6	2.73	<0.5	19	119	48	4.87	2.83	2.58	835	<1	1.30	57	740	22	189	0.38	115	<10	118	1
705	<0.2	8.32	660	0.5	2	3.05	<0.5	18	119	48	4.78	2.75	2.47	815	<1	1.25	59	710	24	182	0.37	111	<10	116	2
715	<0.2	8.28	660	0.5	4	3.17	<0.5	19	128	55	4.80	2.74	2.49	790	<1	1.23	60	750	68	182	0.36	110	<10	122	1
725	<0.2	7.94	640	0.5	6	3.79	<0.5	18	111	44	4.47	2.67	2.49	780	<1	1.22	51	680	24	181	0.36	103	<10	110	2
735	<0.2	8.56	680	0.5	6	2.95	<0.5	19	120	49	4.82	2.78	2.49	730	1	1.27	58	730	26	186	0.38	117	<10	118	2
745	<0.2	8.54	680	0.5	6	2.85	<0.5	19	121	46	4.85	2.79	2.52	715	<1	1.27	56	730	22	184	0.38	114	<10	120	1
755	<0.2	8.12	660	0.5	4	2.91	<0.5	18	116	46	4.69	2.71	2.41	685	<1	1.19	55	690	20	176	0.36	107	<10	114	1

Depth (cm)	Ag ppm	Al %	Ba ppm	Be ppm	Bi ppm	Ca %	Cd ppm	Co ppm	Cr ppm	Cu ppm	Fe %	K %	Mg %	Mn ppm	Mo ppm	Na %	Ni ppm	P ppm	Pb ppm	Sr ppm	Ti %	V ppm	W ppm	Zn ppm	As ppm
765	<0.2	7.83	630	0.5	4	4.01	<0.5	18	115	43	4.37	2.62	2.49	670	<1	1.20	52	660	20	180	0.35	104	<10	108	1
775	<0.2	7.98	660	0.5	2	5.03	<0.5	18	114	45	4.37	2.69	2.70	690	<1	1.28	55	680	20	194	0.36	104	<10	108	1
785	<0.2	7.84	640	0.5	2	4.57	<0.5	17	115	45	4.41	2.63	2.55	665	<1	1.21	54	630	22	183	0.35	103	<10	108	1
795	<0.2	7.69	630	0.5	6	5.46	<0.5	18	110	42	4.18	2.61	2.73	625	<1	1.26	51	630	20	191	0.35	101	<10	104	1
805	<0.2	6.59	550	0.5	<2	8.50	<0.5	14	94	36	3.39	2.34	2.78	685	<1	1.19	40	560	18	198	0.31	84	<10	84	1
815	<0.2	7.46	600	0.5	<2	5.34	<0.5	17	113	50	4.08	2.68	2.63	605	1	1.30	49	600	18	185	0.34	99	<10	100	1

Core 103
Depth (cm)
Al (%)
Ca (%)
Fe (%)
K (%)
Mg (%)
Na (%)
Ti (%)
Co (ppm)
Cr (ppm)
Cu (ppm)
Ni (ppm)
Pb (ppm)
Zn (ppm)
As (ppm)

Core 103
Depth (cm)
Ba (ppm)
Mn (ppm)
P (ppm)
P (ppm)
V (ppm)
% Moisture
% Organic Matter
% Carbonate
% Clay
% Silt
% Sand

Core 104A (37 samples)

Interval	Ag ppm	Al %	Ba ppm	Be ppm	Bi ppm	Ca %	Cd ppm	Co ppm	Cr ppm	Cu ppm	Fe %	K %	Mg %	Mn ppm	Mo ppm	Na %	Ni ppm	P ppm	Pb ppm	Sr ppm	Tl %	V ppm	W ppm	Zn ppm	As ppm
5	<0.2	7.57	670	1.5	<2	1.98	0.5	18	94	39	3.65	2.16	1.86	705	<1	1.20	61	690	24	187	0.35	120	<10	98	1
15	<0.2	7.83	670	1.5	<2	2.01	<0.5	20	102	42	4.05	2.18	1.95	800	<1	1.16	63	690	22	190	0.37	128	<10	104	1
25	<0.2	7.80	670	1.5	<2	2.28	<0.5	18	103	42	4.29	2.22	2.16	800	<1	1.13	59	650	24	186	0.37	126	<10	104	1
35	<0.2	8.06	670	1.5	<2	2.56	<0.5	18	108	40	4.15	2.35	2.39	745	<1	1.18	53	650	20	192	0.38	125	<10	106	2
45	<0.2	8.40	690	1.5	<2	2.03	<0.5	18	111	43	4.48	2.42	2.23	700	<1	1.13	57	680	22	188	0.39	135	<10	116	1
55	<0.2	8.00	650	1.5	<2	2.13	<0.5	18	105	40	4.19	2.26	2.15	610	<1	1.09	55	660	22	183	0.39	131	<10	108	2
65	<0.2	7.51	610	1	<2	1.95	3	17	102	37	3.87	2.10	2.02	555	<1	1.02	49	580	16	165	0.35	115	<10	100	1
75	<0.2	5.18	470	0.5	2	1.30	1.5	11	69	26	2.75	1.45	1.40	390	<1	0.71	34	400	24	115	0.25	80	<10	74	1
85	<0.2	7.93	700	1.5	<2	2.31	<0.5	17	105	40	4.21	2.28	2.25	650	1	1.14	54	630	26	187	0.37	124	<10	104	1
95	<0.2	8.29	700	1.5	<2	2.00	<0.5	20	114	42	4.50	2.38	2.18	665	<1	1.10	59	660	24	184	0.40	135	<10	114	1
105	<0.2	8.24	720	1.5	<2	2.03	<0.5	17	111	43	4.36	2.34	2.15	635	<1	1.14	55	670	26	192	0.39	134	<10	110	1
115	<0.2	7.84	670	1.5	<2	2.28	<0.5	17	108	40	4.08	2.26	2.21	585	<1	1.15	54	620	24	188	0.38	123	<10	102	1
125	<0.2	7.68	630	1.5	<2	2.55	<0.5	17	101	38	3.90	2.23	2.29	570	1	1.18	51	620	20	191	0.36	120	<10	98	2
135	<0.2	7.94	640	1.5	<2	2.63	<0.5	17	106	38	4.23	2.35	2.39	585	<1	1.18	54	640	20	190	0.37	122	<10	104	1
145	<0.2	7.79	630	1.5	<2	2.72	<0.5	17	104	36	4.00	2.31	2.37	590	<1	1.17	50	610	22	187	0.36	119	<10	106	2
155	<0.2	7.47	610	1.5	<2	2.73	<0.5	17	101	36	4.04	2.22	2.37	565	<1	1.18	51	600	20	187	0.35	111	<10	94	2
165	<0.2	7.75	630	1.5	<2	2.63	<0.5	16	102	37	4.04	2.28	2.33	580	<1	1.17	50	600	22	188	0.36	117	<10	100	1
175	<0.2	7.77	680	1.5	<2	2.81	<0.5	16	104	36	3.95	2.29	2.41	590	<1	1.17	51	600	20	187	0.36	118	<10	100	1
185	<0.2	7.98	640	1.5	<2	2.73	<0.5	17	108	38	4.09	2.39	2.41	615	1	1.18	51	610	22	189	0.37	121	<10	104	1
195	<0.2	8.00	640	1.5	<2	2.82	<0.5	18	108	38	4.07	2.40	2.42	605	1	1.20	54	600	20	191	0.37	120	<10	104	1
205	<0.2	7.91	640	1.5	<2	2.63	<0.5	17	109	38	4.03	2.34	2.34	580	1	1.22	51	630	22	191	0.37	123	<10	102	2
215	<0.2	7.75	630	1.5	<2	2.85	<0.5	17	107	38	4.05	2.34	2.42	605	<1	1.22	51	650	20	192	0.38	119	<10	100	1
225	<0.2	7.08	590	1.5	<2	3.92	0.5	15	92	32	3.47	2.18	2.37	540	<1	1.29	45	600	20	200	0.33	101	<10	84	1
235	<0.2	6.53	550	1.5	<2	5.59	<0.5	14	83	29	3.05	2.09	2.64	570	<1	1.24	42	560	18	196	0.31	91	<10	74	2
245	<0.2	5.93	540	1	<2	4.76	<0.5	10	62	19	2.22	1.88	1.87	390	<1	1.57	28	530	16	229	0.24	66	<10	50	1
255	<0.2	5.74	520	1	<2	5.55	<0.5	11	59	20	2.16	1.86	2.00	420	<1	1.51	28	490	16	226	0.23	64	<10	48	1
265	<0.2	6.52	550	1	<2	5.85	<0.5	13	79	27	2.92	2.07	2.34	510	<1	1.35	36	580	18	212	0.29	86	<10	70	1
275	<0.2	6.69	570	1.5	2	6.14	0.5	15	84	31	3.23	2.25	2.70	555	<1	1.32	41	600	16	204	0.30	89	<10	76	1
285	<0.2	7.11	600	1.5	<2	5.71	<0.5	15	95	33	3.46	2.34	2.70	575	<1	1.32	40	620	16	203	0.32	95	<10	84	2
295	<0.2	6.93	580	1.5	<2	5.74	<0.5	15	91	32	3.36	2.30	2.68	565	<1	1.29	42	590	16	198	0.32	92	<10	82	1
305	<0.2	7.07	590	1.5	<2	5.91	<0.5	15	91	33	3.44	2.35	2.72	575	<1	1.31	42	620	18	202	0.32	94	<10	84	1
315	<0.2	6.79	570	1.5	<2	5.87	<0.5	14	87	31	3.29	2.25	2.67	545	<1	1.30	39	590	16	202	0.31	89	<10	78	1
325	<0.2	7.44	610	1.5	<2	4.65	<0.5	16	100	35	3.73	2.41	2.48	585	<1	1.29	47	620	20	195	0.33	102	<10	92	2
335	<0.2	7.01	590	1.5	<2	5.71	<0.5	15	87	31	3.40	2.31	2.65	560	<1	1.32	43	600	16	202	0.32	92	<10	82	2
345	<0.2	7.08	590	1.5	<2	5.71	<0.5	15	91	32	3.46	2.34	2.65	570	<1	1.30	41	620	18	200	0.33	95	<10	84	1
355	<0.2	7.06	590	1.5	<2	5.67	<0.5	15	93	33	3.48	2.31	2.63	565	<1	1.30	45	600	18	200	0.32	95	<10	84	1
365	<0.2	6.28	550	1	<2	6.80	<0.5	15	74	27	2.87	2.15	2.75	500	<1	1.36	38	560	14	210	0.28	78	<10	66	1

Core 104A
Depth (cm)
Al (%)
Ca (%)
Fe (%)
K (%)
Mg (%)
Na (%)
Ti (%)
Au (ppm)
Zn (ppm)
Pb (ppm)
Ni (ppm)
Cu (ppm)
Cr (ppm)
Co (ppm)
V (ppm)
Sr (ppm)
P (ppm)
Mn (ppm)
Ba (ppm)
% Sand
% Silt
% Clay
% Carbonate
% Organic Matter
% Moisture

Core 104B (8 Samples)

Interval	Ag ppm	Al %	Ba ppm	Be ppm	Bi ppm	Ca %	Cd ppm	Co ppm	Cr ppm	Cu ppm	Fe %	K %	Mg %	Mn ppm	Mo ppm	Na %	Ni ppm	P ppm	Pb ppm	Sr ppm	Ti %	V ppm	W ppm	Zn ppm	As ppm
5	<0.2	8.58	700	0.5	2	2.28	<0.5	19	162	92	4.59	2.45	2.32	690	2	1.21	78	730	48	194	0.40	135	<10	144	1
15	<0.2	7.83	640	0.5	2	2.50	<0.5	17	103	42	4.16	2.28	2.28	620	1	1.19	57	690	24	187	0.37	120	<10	130	2
25	<0.2	7.65	610	0.5	4	2.75	<0.5	18	103	38	4.17	2.30	2.39	595	1	1.21	55	670	22	184	0.35	111	<10	102	1
35	<0.2	7.70	610	0.5	<2	2.76	<0.5	16	105	38	4.07	2.30	2.41	595	1	1.21	55	650	20	184	0.35	113	<10	104	1
45	<0.2	5.53	480	0.5	2	5.27	<0.5	8	58	21	1.93	1.72	1.64	340	1	1.73	23	550	12	231	0.21	51	<10	42	1
55	<0.2	7.26	590	0.5	2	5.96	<0.5	14	89	35	3.48	2.38	2.77	595	<1	1.35	44	630	18	201	0.32	92	<10	88	2
65	<0.2	6.75	550	0.5	<2	5.91	<0.5	14	84	33	3.20	2.23	2.74	540	<1	1.30	41	590	16	193	0.30	85	<10	80	2
75	<0.2	6.95	570	0.5	2	5.56	<0.5	14	86	33	3.31	2.29	2.70	540	<1	1.33	41	630	16	195	0.31	88	<10	84	1

Core 104B
Depth (cm)
Al (%)
Ca (%)
Fe (%)
K (%)
Mg (%)
Na (%)
Ti (%)
Co (ppm)
Cr (ppm)
Cu (ppm)
Ni (ppm)
Pb (ppm)
Zn (ppm)
As (ppm)
Ba (ppm)
Mn (ppm)
P (ppm)
Sr (ppm)
V (ppm)
% Carbonate
% Clay
% Silt
% Sand
% Moisture
% Organic Matter

Core 105 (50 samples)

Interval	Ag ppm	Al %	Ba ppm	Be ppm	Bi ppm	Ca %	Cd ppm	Co ppm	Cr ppm	Cu ppm	Fe %	K %	Mg %	Mn ppm	Mo ppm	Na %	Ni ppm	P ppm	Pb ppm	Sr ppm	Ti %	V ppm	W ppm	Zn ppm	As ppm
Interval	Ag	Al	Ba	Be	Bi	Ca	Cd	Co	Cr	Cu	Fe	K	Mg	Mn	Mo	Na	Ni	P	Pb	Sr	Ti	V	W	Zn	As
5	<0.2	7.71	640	0.5	2	2.84	<0.5	16	101	39	4.04	2.25	2.48	730	1	1.20	52	660	22	184	0.35	115	<10	102	1
15	<0.2	7.60	610	0.5	<2	2.90	<0.5	16	101	39	3.79	2.26	2.47	655	1	1.23	51	640	20	189	0.35	111	<10	96	1
25	<0.2	7.06	570	0.5	<2	3.72	<0.5	14	90	34	3.43	2.13	2.58	555	<1	1.25	45	610	18	188	0.33	99	<10	90	1
35	<0.2	7.51	600	0.5	<2	2.88	<0.5	14	99	37	3.64	2.25	2.32	545	1	1.35	50	630	20	199	0.34	105	<10	94	1
45	<0.2	7.25	590	0.5	<2	3.30	<0.5	14	94	35	3.44	2.20	2.34	515	<1	1.33	45	630	16	199	0.33	99	<10	88	1
55	<0.2	6.91	560	0.5	<2	4.14	<0.5	14	95	32	3.36	2.15	2.44	510	<1	1.25	44	580	18	188	0.32	94	<10	84	2
65	<0.2	7.83	620	0.5	<2	4.41	<0.5	16	111	42	3.85	2.42	2.57	585	1	1.32	51	640	20	201	0.35	113	<10	102	1
75	<0.2	8.50	630	0.5	<2	3.61	<0.5	18	123	47	4.59	2.57	2.37	725	<1	1.22	57	660	20	187	0.37	122	<10	116	1
85	<0.2	8.57	650	0.5	2	3.25	<0.5	20	125	46	4.80	2.62	2.37	725	<1	1.26	60	690	20	190	0.37	122	<10	118	1
95	<0.2	8.33	630	0.5	<2	2.71	<0.5	19	121	46	4.65	2.59	2.24	675	<1	1.22	57	680	20	183	0.36	114	<10	116	1
105	<0.2	8.41	630	0.5	<2	3.84	<0.5	19	127	47	4.70	2.61	2.40	760	1	1.25	57	670	20	189	0.36	116	<10	116	1
115	<0.2	8.16	610	0.5	<2	3.87	<0.5	18	119	44	4.38	2.49	2.38	740	2	1.27	54	650	20	193	0.36	114	<10	112	1
125	<0.2	8.76	650	0.5	4	3.42	<0.5	20	130	47	4.83	2.67	2.43	745	<1	1.30	59	730	20	197	0.37	123	<10	120	2
135	<0.2	8.32	630	0.5	4	3.45	<0.5	19	118	43	4.31	2.52	2.40	690	<1	1.32	53	680	18	198	0.37	117	<10	112	1
145	<0.2	8.16	610	0.5	2	3.64	<0.5	19	119	41	4.73	2.50	2.29	700	1	1.23	57	660	18	184	0.35	112	<10	112	1
155	<0.2	8.50	630	0.5	4	3.86	<0.5	20	124	45	4.66	2.62	2.40	735	<1	1.29	58	690	20	193	0.36	117	<10	118	1
165	<0.2	8.31	620	0.5	<2	3.76	<0.5	18	116	45	4.50	2.49	2.36	690	<1	1.27	55	650	20	192	0.37	117	<10	114	2
175	<0.2	8.49	640	0.5	4	4.58	<0.5	20	125	46	4.77	2.60	2.49	815	<1	1.34	60	680	20	200	0.37	118	<10	116	1
185	<0.2	8.10	620	0.5	<2	3.51	<0.5	18	114	43	4.33	2.47	2.37	700	<1	1.35	57	670	20	197	0.36	112	<10	110	1
195	<0.2	8.38	630	0.5	2	3.73	<0.5	18	121	45	4.39	2.52	2.42	690	<1	1.36	54	680	20	203	0.37	119	<10	110	1
205	2.8	8.32	650	0.5	<2	4.03	<0.5	20	123	47	4.56	2.58	2.49	770	<1	1.40	57	670	20	203	0.37	116	<10	114	1
215	<0.2	8.43	640	0.5	<2	4.91	<0.5	20	129	48	4.77	2.58	2.50	835	<1	1.33	62	650	20	198	0.37	120	<10	116	2
225	<0.2	8.31	630	0.5	2	3.85	<0.5	19	124	47	4.67	2.55	2.37	745	<1	1.32	59	630	18	193	0.37	118	<10	114	2
235	<0.2	8.39	660	0.5	<2	3.16	<0.5	19	127	46	4.57	2.58	2.36	690	<1	1.37	56	670	18	200	0.36	115	<10	114	1
245	<0.2	8.41	650	0.5	2	3.27	<0.5	19	122	46	4.54	2.55	2.35	685	<1	1.36	59	660	20	201	0.37	119	<10	114	1
255	<0.2	8.28	640	0.5	2	3.87	<0.5	19	122	46	4.60	2.54	2.40	725	1	1.39	59	660	18	202	0.36	115	<10	112	1
265	<0.2	8.28	640	0.5	2	3.85	<0.5	19	118	46	4.48	2.54	2.39	720	1	1.39	59	680	18	201	0.36	115	<10	112	1
275	<0.2	8.44	660	0.5	<2	4.53	<0.5	20	125	47	4.56	2.61	2.51	760	1	1.47	59	690	20	211	0.37	116	<10	114	1
285	<0.2	7.96	630	0.5	<2	3.92	<0.5	20	122	45	4.38	2.45	2.36	700	2	1.38	59	650	18	199	0.35	110	<10	108	2
295	<0.2	8.29	660	0.5	2	3.79	<0.5	19	122	45	4.56	2.56	2.41	695	<1	1.43	57	670	18	204	0.36	114	<10	112	2
305	<0.2	7.78	620	0.5	<2	4.64	<0.5	18	116	42	4.16	2.42	2.38	690	<1	1.44	54	630	18	206	0.34	104	<10	102	1
315	<0.2	7.90	630	0.5	<2	4.25	<0.5	17	116	42	4.17	2.43	2.33	665	<1	1.49	54	650	18	211	0.34	105	<10	104	1
325	<0.2	7.87	650	0.5	<2	4.57	<0.5	18	116	41	4.09	2.43	2.34	660	<1	1.50	53	640	18	214	0.34	105	<10	102	2
335	<0.2	7.62	600	0.5	<2	5.83	<0.5	16	110	39	3.83	2.38	2.33	675	<1	1.49	51	650	16	220	0.33	98	<10	92	1
345	<0.2	7.51	610	0.5	<2	4.87	<0.5	15	98	36	3.50	2.30	2.19	595	<1	1.63	44	630	16	233	0.32	93	<10	86	1
355	<0.2	7.68	600	0.5	<2	5.62	<0.5	18	115	42	4.18	2.41	2.37	680	<1	1.37	53	640	16	200	0.34	103	<10	100	1

Interval	Ag ppm	Al %	Ba ppm	Be ppm	Bi ppm	Ca %	Cd ppm	Co ppm	Cr ppm	Cu ppm	Fe %	K %	Mg %	Mn ppm	Mo ppm	Na %	Ni ppm	P ppm	Pb ppm	Sr ppm	Ti %	V ppm	W ppm	Zn ppm	As ppm
365	<0.2	7.77	630	0.5	<2	5.15	<0.5	16	106	38	3.80	2.41	2.36	615	<1	1.61	49	650	16	229	0.33	99	<10	94	1
375	<0.2	7.72	640	0.5	<2	4.83	<0.5	15	105	38	3.57	2.37	2.28	585	<1	1.74	49	670	16	248	0.32	95	<10	88	2
385	<0.2	7.62	610	0.5	<2	5.04	<0.5	16	111	39	3.80	2.36	2.33	615	<1	1.59	50	630	18	227	0.33	97	<10	92	1
395	<0.2	7.26	610	0.5	<2	3.98	<0.5	13	86	33	3.05	2.19	1.98	475	<1	1.82	39	630	16	259	0.29	83	<10	72	1
405	<0.2	6.97	560	0.5	<2	5.71	<0.5	14	91	33	3.25	2.17	2.19	530	<1	1.48	41	600	16	218	0.30	88	<10	78	2
415	<0.2	7.38	610	0.5	<2	6.85	<0.5	15	99	34	3.34	2.36	2.39	565	<1	1.67	42	650	14	243	0.32	90	<10	80	1
425	<0.2	6.98	580	0.5	<2	5.71	<0.5	12	89	30	2.98	2.19	2.10	500	<1	1.69	36	600	14	243	0.29	81	<10	72	1
435	<0.2	7.22	600	0.5	<2	6.25	<0.5	13	90	31	3.06	2.27	2.31	520	<1	1.74	42	640	14	251	0.31	85	<10	76	2
445	<0.2	6.15	550	<0.5	<2	6.40	<0.5	10	77	26	2.80	1.96	2.06	500	<1	1.47	32	500	12	217	0.29	71	<10	64	1
455	<0.2	6.60	550	0.5	<2	6.07	<0.5	13	91	31	2.97	2.10	2.22	515	<1	1.52	37	550	14	220	0.28	79	<10	72	1
465	<0.2	6.27	540	0.5	<2	7.95	<0.5	11	82	26	2.60	2.08	2.40	510	<1	1.60	34	560	12	238	0.28	70	<10	62	1
475	<0.2	6.22	530	0.5	<2	8.23	<0.5	11	81	26	2.53	2.05	2.47	500	<1	1.55	34	550	14	234	0.27	73	<10	62	1
485	<0.2	7.54	640	0.5	<2	8.50	<0.5	15	98	35	3.31	2.49	2.71	630	<1	1.86	44	660	16	271	0.33	87	<10	80	1
495	<0.2	7.00	620	0.5	<2	6.52	<0.5	12	84	30	2.77	2.27	2.39	500	<1	1.83	38	600	14	256	0.28	75	<10	70	2
505	<0.2	6.46	590	1	<2	5.11	<0.5	9	70	25	2.43	2.06	2.02	390	<1	1.70	30	500	14	233	0.25	65	<10	58	1

Core 105
Depth (cm)
Al (%)
Ca (%)
Fe (%)
K (%)
Mg (%)
Na (%)
Ti (%)
Ba (ppm)
Co (ppm)
Cr (ppm)
Cu (ppm)
Ni (ppm)
Pb (ppm)
Zn (ppm)
As (ppm)
Mn (ppm)
P (ppm)
Sr (ppm)
V (ppm)
% Moisture
% Organic Matter
% Carbonate
% Clay
% Sand
% Silt

Core 106 (70 samples)

Interval	Ag ppm	Al %	Ba ppm	Be ppm	Bi ppm	Ca %	Cd ppm	Co ppm	Cr ppm	Cu ppm	Fe %	K %	Mg %	Mn ppm	Mo ppm	Na %	Ni ppm	P ppm	Pb ppm	Sr ppm	Ti %	V ppm	W ppm	Zn ppm	As ppm
5	<0.2	7.19	600	1	<2	2.37	<0.5	17	95	49	3.69	2.15	2.02	820	1	1.16	52	720	20	176	0.34	111	<10	98	1
15	<0.2	7.79	640	1.5	<2	1.95	<0.5	18	111	40	4.23	2.29	2.00	730	<1	1.21	55	730	18	182	0.36	123	<10	110	1
25	<0.2	7.84	630	1.5	<2	2.29	<0.5	18	113	44	4.31	2.32	2.25	760	<1	1.20	54	700	20	179	0.37	122	<10	112	1
35	<0.2	8.10	640	1.5	<2	1.94	<0.5	19	114	40	4.49	2.35	2.11	730	<1	1.18	59	740	16	180	0.38	129	<10	118	1
45	<0.2	8.24	660	1.5	<2	1.98	<0.5	20	109	40	4.55	2.45	2.18	720	1	1.23	58	740	20	185	0.37	130	<10	118	2
55	<0.2	8.13	640	1.5	<2	1.84	<0.5	19	110	39	4.43	2.34	2.05	690	<1	1.18	56	720	20	184	0.38	129	<10	118	2
65	<0.2	7.72	610	1.5	<2	2.23	<0.5	18	102	37	4.12	2.26	2.16	660	<1	1.21	52	700	16	184	0.37	118	<10	108	1
75	<0.2	7.85	620	1.5	<2	2.35	<0.5	19	107	37	4.38	2.35	2.30	670	<1	1.21	52	680	18	181	0.36	119	<10	112	2
85	<0.2	8.17	640	1.5	<2	1.95	<0.5	19	113	39	4.52	2.39	2.17	650	1	1.19	58	720	16	182	0.38	128	<10	118	1
95	<0.2	8.17	640	1.5	<2	2.24	<0.5	19	114	39	4.46	2.41	2.31	650	1	1.19	57	710	16	182	0.38	128	<10	118	1
105	<0.2	3.93	300	0.5	<2	1.08	<0.5	10	49	18	2.19	1.14	1.14	310	<1	0.56	30	370	6	87	0.19	62	<10	60	2
115	<0.2	7.96	620	1.5	<2	2.38	<0.5	20	110	38	4.36	2.41	2.41	630	1	1.21	53	720	16	181	0.36	122	<10	114	1
125	<0.2	7.81	610	1.5	<2	3.29	<0.5	19	106	36	4.20	2.42	2.67	635	<1	1.25	58	710	14	185	0.36	115	10	108	1
135	<0.2	7.57	590	1.5	<2	3.46	<0.5	18	105	35	3.99	2.33	2.58	585	<1	1.25	52	710	16	186	0.36	115	<10	104	1
145	<0.2	7.78	590	1.5	<2	3.15	<0.5	19	108	37	4.14	2.34	2.56	605	<1	1.18	51	710	16	178	0.37	123	<10	110	1
155	<0.2	7.38	580	1.5	<2	4.11	<0.5	16	95	31	3.56	2.31	2.41	560	1	1.36	44	680	14	197	0.32	104	<10	94	1
165	<0.2	6.71	550	1	<2	5.22	<0.5	15	85	28	3.08	2.17	2.36	515	<1	1.41	40	610	12	207	0.29	84	<10	78	1
175	<0.2	5.85	510	1	<2	5.05	<0.5	11	66	20	2.40	1.89	1.92	405	<1	1.47	30	550	8	211	0.24	65	<10	58	2
185	<0.2	8.12	640	1.5	<2	3.68	<0.5	21	113	40	4.66	2.71	2.63	640	<1	1.26	53	700	14	180	0.36	108	10	116	1
195	<0.2	8.11	630	1.5	<2	4.40	<0.5	22	113	41	4.59	2.72	2.66	680	<1	1.28	58	730	16	183	0.36	108	<10	116	2
205	<0.2	7.46	590	1.5	<2	6.62	<0.5	18	101	36	3.97	2.58	2.95	650	<1	1.29	49	690	12	193	0.33	96	<10	102	2
215	<0.2	7.69	610	1.5	<2	5.42	<0.5	19	103	38	4.22	2.68	2.74	635	<1	1.29	48	690	14	185	0.34	101	10	106	2
225	<0.2	7.84	610	1.5	<2	5.37	<0.5	19	110	39	4.28	2.69	2.73	615	<1	1.31	50	710	18	188	0.34	104	10	106	2
235	<0.2	7.94	620	1.5	<2	4.06	<0.5	19	111	40	4.45	2.65	2.50	585	2	1.24	54	710	16	177	0.35	108	10	112	1
245	<0.2	7.58	600	1.5	<2	5.79	<0.5	18	102	38	4.16	2.62	2.53	610	<1	1.28	50	700	12	189	0.34	97	10	104	2
255	<0.2	6.99	560	1.5	<2	7.67	<0.5	17	98	34	3.73	2.45	2.59	625	<1	1.27	43	690	12	194	0.32	93	10	94	1
265	<0.2	6.96	550	1.5	<2	7.62	<0.5	17	96	34	3.65	2.38	2.59	600	<1	1.21	44	680	12	188	0.31	94	<10	94	1
275	<0.2	6.94	560	1	<2	7.42	<0.5	17	97	33	3.59	2.40	2.59	585	2	1.30	39	670	14	197	0.31	91	10	92	2
285	<0.2	6.29	510	1	<2	10.15	<0.5	16	89	31	3.28	2.23	2.59	660	<1	1.18	41	670	16	198	0.30	84	<10	82	1
295	<0.2	6.98	550	1.5	<2	7.78	<0.5	17	96	34	3.59	2.41	2.62	565	1	1.27	44	670	16	196	0.31	92	10	92	1
305	<0.2	6.53	510	1	<2	9.66	<0.5	16	92	32	3.49	2.29	2.56	660	<1	1.13	40	660	12	191	0.30	87	<10	88	1
315	<0.2	5.61	470	1	<2	11.05	<0.5	13	71	23	2.47	2.06	2.85	520	1	1.23	28	600	8	209	0.27	67	<10	62	1
325	<0.2	6.25	500	1	<2	9.86	<0.5	15	87	29	3.10	2.20	2.68	590	1	1.20	36	620	14	198	0.29	81	10	78	1
335	<0.2	6.99	550	1	<2	7.11	<0.5	16	95	33	3.52	2.38	2.64	520	<1	1.28	43	660	16	194	0.31	93	10	90	2
345	<0.2	6.19	500	1	<2	9.47	<0.5	15	88	29	3.16	2.18	2.57	595	1	1.19	40	630	14	196	0.30	81	10	80	2
355	<0.2	6.11	500	1	<2	9.58	<0.5	15	86	28	3.03	2.19	2.61	590	<1	1.21	34	640	16	198	0.30	81	10	78	1
365	<0.2	6.26	500	1	<2	8.75	<0.5	14	87	32	3.39	2.17	2.43	645	<1	1.11	38	620	16	185	0.30	88	10	86	1

Interval	Ag ppm	Al %	Ba ppm	Be ppm	Bi ppm	Ca %	Cd ppm	Co ppm	Cr ppm	Cu ppm	Fe %	K %	Mg %	Mn ppm	Mo ppm	Na %	Ni ppm	P ppm	Pb ppm	Sr ppm	Ti %	V ppm	W ppm	Zn ppm	As ppm
375	<0.2	6.94	550	1.5	<2	7.59	<0.5	17	98	33	3.60	2.37	2.49	590	<1	1.26	43	670	16	194	0.33	95	10	92	1
385	<0.2	6.84	530	1	<2	8.09	<0.5	17	95	33	3.64	2.33	2.47	645	<1	1.20	46	640	16	191	0.32	93	10	92	1
395	<0.2	6.12	510	1	<2	8.21	<0.5	13	83	27	2.84	2.19	2.50	520	<1	1.32	35	630	14	198	0.29	79	10	74	1
405	<0.2	6.96	540	1	<2	7.31	<0.5	16	91	32	3.47	2.20	2.55	550	<1	1.27	42	620	14	195	0.32	93	10	90	1
415	<0.2	6.16	510	1	<2	9.42	<0.5	13	70	23	2.60	2.07	2.70	515	<1	1.41	33	590	12	216	0.29	74	<10	66	1
425	<0.2	7.78	570	1	<2	5.35	<0.5	20	112	40	4.37	2.34	2.36	605	<1	1.18	52	660	24	180	0.34	110	<10	110	2
435	<0.2	8.10	600	1	<2	4.19	<0.5	20	115	45	4.62	2.42	2.27	565	<1	1.18	56	660	38	176	0.34	114	10	116	1
445	<0.2	7.50	560	1	<2	5.87	<0.5	19	107	36	4.19	2.30	2.34	585	<1	1.14	51	640	16	179	0.34	108	10	108	2
455	<0.2	7.50	550	1	<2	6.65	<0.5	19	109	38	4.30	2.31	2.35	680	<1	1.08	53	640	14	177	0.33	105	10	108	1
465	<0.2	7.16	540	1	<2	5.74	<0.5	18	98	35	3.94	2.23	2.31	550	<1	1.12	48	630	12	176	0.32	102	10	102	1
475	<0.2	7.95	600	1.5	<2	5.15	<0.5	21	115	38	4.53	2.47	2.36	625	<1	1.18	57	650	14	179	0.34	109	10	116	1
485	<0.2	8.06	610	1.5	<2	4.14	<0.5	20	113	38	4.48	2.46	2.27	535	<1	1.24	53	670	16	181	0.34	112	<10	116	2
495	<0.2	8.04	610	1	<2	4.77	<0.5	20	112	39	4.53	2.49	2.31	600	<1	1.21	58	660	20	182	0.34	109	<10	114	2
505	<0.2	7.96	600	1	<2	5.80	<0.5	20	113	36	4.32	2.52	2.27	655	<1	1.24	54	640	16	190	0.32	106	10	110	2
515	<0.2	8.20	610	1.5	<2	4.43	<0.5	19	111	37	4.46	2.51	2.23	580	<1	1.26	53	650	12	186	0.34	111	10	114	2
525	<0.2	7.63	570	1	<2	5.05	<0.5	19	109	35	4.11	2.37	2.23	570	<1	1.20	53	630	14	180	0.32	105	10	106	2
535	<0.2	7.43	570	1	<2	5.62	<0.5	17	98	34	3.92	2.36	2.37	545	<1	1.26	45	640	12	189	0.31	100	<10	102	1
545	<0.2	8.26	580	1.5	<2	3.97	<0.5	22	124	42	5.09	2.51	2.26	625	<1	1.10	61	740	14	172	0.36	122	<10	124	1
555	<0.2	8.33	580	1.5	<2	3.92	<0.5	20	121	42	4.96	2.48	2.26	630	<1	1.08	59	680	14	169	0.36	119	<10	122	1
565	<0.2	8.18	570	1.5	<2	3.63	<0.5	21	122	41	4.92	2.47	2.23	620	<1	1.09	60	720	16	166	0.35	119	<10	122	1
575	<0.2	8.63	610	1.5	<2	2.91	<0.5	22	123	43	5.01	2.57	2.29	590	1	1.18	59	730	14	176	0.37	126	10	126	1
585	<0.2	8.86	630	1.5	<2	2.61	<0.5	23	125	46	5.09	2.61	2.32	590	2	1.20	61	730	14	177	0.37	130	10	130	2
595	<0.2	8.36	580	1.5	<2	4.03	<0.5	22	122	45	4.82	2.55	2.36	695	<1	1.12	56	730	14	173	0.35	123	10	122	2
605	<0.2	8.28	580	1.5	<2	3.51	<0.5	21	115	43	4.79	2.46	2.28	640	<1	1.14	56	680	14	172	0.35	120	10	122	1
615	<0.2	8.27	590	1.5	<2	3.11	<0.5	22	120	45	4.81	2.49	2.28	635	<1	1.16	57	720	14	174	0.36	124	10	122	1
625	<0.2	8.14	590	1.5	<2	3.44	<0.5	20	115	44	4.59	2.43	2.31	630	1	1.18	52	670	14	177	0.37	122	<10	120	2
635	<0.2	8.38	610	1.5	<2	3.66	<0.5	21	118	44	4.73	2.53	2.37	665	<1	1.25	57	700	14	183	0.36	119	10	122	1
645	<0.2	8.09	580	1.5	<2	3.45	<0.5	20	113	45	4.64	2.41	2.29	645	1	1.18	59	660	14	175	0.35	116	<10	118	1
655	<0.2	8.12	590	1.5	<2	3.15	<0.5	19	112	43	4.55	2.38	2.24	615	<1	1.18	55	670	16	178	0.36	116	<10	116	1
665	<0.2	8.37	610	1.5	<2	3.84	<0.5	22	121	50	4.80	2.49	2.47	710	<1	1.25	57	690	30	184	0.37	124	10	124	1
675	<0.2	8.42	620	1	<2	3.21	<0.5	22	121	51	4.87	2.50	2.39	675	<1	1.28	61	720	32	184	0.36	123	<10	124	2
685	<0.2	8.29	610	1.5	<2	4.53	<0.5	21	122	45	4.75	2.51	2.46	745	<1	1.25	59	690	14	187	0.36	119	10	122	2
695	<0.2	8.14	610	1	<2	3.58	<0.5	19	118	44	4.60	2.41	2.37	675	<1	1.29	54	650	14	188	0.36	115	<10	118	1

Core 106
Depth (cm)
Al (%)
Ca (%)
Fe (%)
K (%)
Mg (%)
Na (%)
Ti (%)
As (ppm)
Zn (ppm)
Pb (ppm)
Ni (ppm)
Cu (ppm)
Cr (ppm)
Co (ppm)

Core 106
Depth (cm)
Ba (ppm)
Mn (ppm)
P (ppm)
Sr (ppm)
V (ppm)
% Moisture
% Organic Matter
% Carbonate
% Clay
% Sand
% Silt

Core 107 (70 samples)

Interval	Ag ppm	Al %	Ba ppm	Be ppm	Bi ppm	Ca %	Cd ppm	Co ppm	Cr ppm	Cu ppm	Fe %	K %	Mg %	Mn ppm	Mo ppm	Na %	Ni ppm	P ppm	Pb ppm	Sr ppm	Ti %	V ppm	W ppm	Zn ppm	As ppm
5	<0.2	8.85	720	1.5	4	1.33	<0.5	21	115	43	4.57	2.40	1.71	605	<1	1.21	64	750	22	210	0.40	152	<10	120	1
15	<0.2	8.13	650	1.5	<2	1.16	<0.5	18	110	38	4.25	2.17	1.60	555	1	1.02	54	640	24	178	0.37	142	<10	112	2
25	<0.2	8.19	660	1.5	2	1.29	<0.5	18	106	40	4.12	2.17	1.53	540	<1	1.20	57	660	22	210	0.38	139	<10	108	1
35	<0.2	8.66	680	2	2	1.30	<0.5	19	115	41	4.44	2.32	1.65	565	<1	1.21	56	690	22	206	0.40	154	<10	118	2
45	<0.2	8.38	670	1.5	4	1.35	<0.5	19	107	40	4.27	2.26	1.61	545	<1	1.23	57	700	24	208	0.39	141	<10	112	1
55	<0.2	8.16	650	1.5	2	1.54	<0.5	18	105	41	4.11	2.21	1.66	520	<1	1.25	53	700	24	210	0.38	139	<10	108	1
65	<0.2	8.70	690	2	4	1.42	<0.5	25	117	41	4.79	2.37	1.82	575	<1	1.19	68	690	22	200	0.41	148	<10	118	1
75	<0.2	8.14	650	1.5	<2	1.38	<0.5	19	111	43	4.34	2.22	1.73	565	<1	1.10	56	650	24	188	0.40	141	<10	112	1
85	<0.2	8.50	670	2	<2	1.40	<0.5	20	115	45	4.59	2.31	1.80	595	<1	1.14	63	700	24	191	0.42	149	<10	120	1
95	<0.2	8.61	680	2	2	1.44	<0.5	20	115	40	4.53	2.40	1.83	560	<1	1.19	58	700	22	197	0.40	148	<10	120	2
105	<0.2	8.52	680	1.5	2	1.77	0.5	22	110	43	4.40	2.37	1.93	550	<1	1.28	69	720	26	210	0.41	145	<10	114	1
115	<0.2	8.31	660	1.5	2	1.72	<0.5	18	112	41	4.31	2.29	1.91	545	1	1.21	57	660	22	198	0.39	141	<10	112	2
125	<0.2	8.24	660	1.5	2	1.84	<0.5	19	108	40	4.25	2.27	1.94	525	<1	1.23	54	690	20	205	0.39	138	<10	108	2
135	<0.2	8.29	670	1.5	2	1.75	<0.5	19	107	40	4.31	2.30	1.88	540	<1	1.28	56	690	18	212	0.39	136	<10	110	1
145	<0.2	8.49	680	1.5	<2	1.76	0.5	19	114	40	4.47	2.37	1.96	565	<1	1.22	56	710	24	205	0.40	141	<10	114	1
155	<0.2	7.60	620	1.5	<2	2.03	<0.5	15	95	35	3.61	2.09	1.78	465	<1	1.40	44	620	22	231	0.35	115	<10	90	1
165	<0.2	7.71	650	1.5	2	1.99	<0.5	16	93	33	3.56	2.18	1.67	465	<1	1.53	46	660	20	249	0.35	113	<10	88	1
175	<0.2	8.27	640	1.5	2	1.85	<0.5	19	110	40	4.21	2.29	1.97	605	<1	1.07	56	680	20	181	0.39	160	<10	114	1
185	<0.2	7.65	630	1.5	<2	2.56	<0.5	16	100	39	3.55	2.18	2.07	630	<1	1.33	50	670	22	217	0.36	123	<10	94	1
195	<0.2	8.20	700	1.5	<2	2.39	<0.5	19	100	38	4.08	2.43	2.05	680	1	1.54	52	630	18	228	0.35	116	<10	102	1
205	<0.2	8.05	660	1.5	<2	2.91	<0.5	19	113	42	4.26	2.46	2.33	745	<1	1.34	53	670	18	201	0.36	118	<10	106	1
215	<0.2	8.17	670	1.5	2	3.17	<0.5	19	111	41	4.28	2.49	2.41	735	<1	1.37	53	700	18	208	0.37	120	<10	106	2
225	<0.2	7.56	620	1.5	<2	2.95	<0.5	17	101	40	3.82	2.28	2.17	695	<1	1.33	51	640	20	200	0.36	113	<10	106	1
235	<0.2	7.83	650	1.5	6	3.74	<0.5	19	99	40	3.86	2.37	2.41	780	<1	1.50	49	710	18	227	0.35	112	<10	96	2
245	<0.2	8.25	670	1.5	4	3.24	<0.5	20	111	46	4.30	2.52	2.38	790	<1	1.35	56	710	20	205	0.37	124	<10	108	1
255	<0.2	7.81	640	1.5	<2	3.26	<0.5	18	105	40	3.99	2.35	2.33	735	<1	1.36	51	670	20	207	0.35	115	<10	100	2
265	<0.2	7.95	650	1.5	4	3.25	<0.5	18	106	39	4.05	2.40	2.34	750	1	1.37	51	670	18	209	0.36	117	<10	100	1
275	<0.2	7.95	650	1.5	<2	3.75	<0.5	16	93	35	3.53	2.29	2.44	690	1	1.48	47	650	18	224	0.33	108	<10	92	1
285	<0.2	8.27	650	1.5	4	3.12	<0.5	19	101	37	4.03	2.41	2.32	725	<1	1.30	48	660	16	197	0.35	120	<10	106	1
295	<0.2	8.33	660	1.5	<2	3.29	<0.5	17	102	38	3.93	2.40	2.35	695	<1	1.37	50	680	18	206	0.36	120	<10	104	1
305	<0.2	8.48	660	1.5	6	3.03	<0.5	19	104	39	4.16	2.45	2.34	680	<1	1.31	52	670	18	195	0.36	125	<10	110	1
315	<0.2	8.35	670	1.5	2	3.23	<0.5	17	101	37	3.94	2.40	2.31	670	1	1.38	48	680	18	204	0.35	120	<10	106	1
325	<0.2	8.76	680	2	2	2.73	<0.5	20	112	43	4.43	2.49	2.29	715	<1	1.28	57	670	20	193	0.38	133	<10	118	2
335	<0.2	8.74	700	1.5	<2	2.78	<0.5	19	112	39	4.30	2.50	2.27	680	1	1.34	53	680	20	201	0.37	131	<10	114	1
345	<0.2	8.80	700	1.5	2	2.74	<0.5	19	108	39	4.34	2.55	2.25	675	1	1.38	54	700	20	203	0.37	129	<10	114	1
355	<0.2	8.71	660	1.5	4	1.25	0.5	19	101	33	4.11	2.12	1.59	1090	<1	0.87	51	680	20	152	0.40	171	<10	118	1
365	<0.2	8.29	660	1.5	2	3.37	0.5	18	103	37	3.90	2.40	2.40	660	<1	1.39	48	670	18	206	0.35	118	<10	104	2

Interval	Ag ppm	Al %	Ba ppm	Be ppm	Bi ppm	Ca %	Cd ppm	Co ppm	Cr ppm	Cu ppm	Fe %	K %	Mg %	Mn ppm	Mo ppm	Na %	Ni ppm	P ppm	Pb ppm	Sr ppm	Ti %	V ppm	W ppm	Zn ppm	As ppm
375	<0.2	8.42	670	1.5	<2	3.29	<0.5	18	105	39	3.95	2.43	2.35	665	<1	1.43	49	690	18	214	0.36	120	<10	106	1
385	<0.2	8.44	670	1.5	2	3.20	<0.5	19	110	40	4.17	2.49	2.30	705	1	1.34	50	660	18	196	0.36	121	<10	110	2
395	<0.2	8.73	680	1.5	2	2.48	<0.5	19	111	39	4.33	2.53	2.20	650	<1	1.35	52	660	20	197	0.37	127	<10	116	1
405	<0.2	8.54	670	1.5	4	2.95	<0.5	19	107	41	4.16	2.45	2.34	690	<1	1.37	52	680	20	202	0.38	126	<10	114	1
415	<0.2	8.01	640	1.5	<2	3.40	<0.5	17	100	36	3.79	2.36	2.32	680	<1	1.41	45	640	18	206	0.34	109	<10	100	1
425	<0.2	8.31	650	1.5	2	3.81	<0.5	18	108	40	4.15	2.48	2.41	670	<1	1.30	52	660	20	193	0.37	118	<10	110	1
435	<0.2	8.50	660	1.5	<2	2.73	0.5	18	108	39	4.12	2.50	2.31	615	1	1.33	50	670	20	192	0.36	118	10	112	1
445	<0.2	7.70	610	1	2	3.10	3.5	16	99	35	3.82	2.23	2.31	605	<1	1.30	44	590	20	193	0.34	105	10	96	2
455	<0.2	7.72	620	1	2	3.36	2.5	16	100	36	3.89	2.31	2.38	685	<1	1.33	46	590	18	196	0.34	101	<10	96	2
465	<0.2	8.26	650	1.5	2	3.47	0.5	18	103	40	3.89	2.40	2.49	730	1	1.41	46	680	20	207	0.37	119	10	102	1
475	<0.2	8.12	640	1.5	<2	3.61	<0.5	17	100	37	3.80	2.39	2.45	720	2	1.40	46	650	20	203	0.36	113	10	100	2
485	<0.2	8.49	670	1.5	4	3.42	<0.5	18	107	38	3.95	2.52	2.44	735	<1	1.49	52	690	20	215	0.36	116	10	104	2
495	<0.2	8.41	670	1.5	2	3.67	<0.5	18	107	39	3.94	2.51	2.48	730	<1	1.45	48	660	20	210	0.36	114	10	104	1
505	<0.2	8.20	640	1.5	2	3.68	0.5	17	103	39	3.77	2.44	2.49	700	<1	1.46	46	670	20	209	0.35	111	<10	100	1
515	<0.2	8.38	660	1.5	2	3.80	0.5	18	107	38	3.90	2.49	2.59	710	<1	1.46	48	680	18	211	0.36	116	<10	104	1
525	<0.2	8.14	640	1.5	2	3.39	0.5	18	107	37	3.79	2.39	2.45	685	<1	1.41	49	650	20	204	0.35	115	10	102	1
535	<0.2	7.22	570	1	<2	3.22	3	16	93	34	3.66	2.14	2.22	605	<1	1.17	43	540	20	174	0.32	98	<10	92	2
545	<0.2	8.24	660	1.5	<2	3.72	<0.5	18	105	39	3.83	2.47	2.50	700	1	1.50	51	660	20	212	0.37	112	10	110	1
555	<0.2	8.03	630	1.5	2	3.84	<0.5	16	99	36	3.64	2.38	2.46	650	<1	1.45	43	640	18	212	0.35	110	<10	98	1
565	<0.2	8.48	660	1.5	2	3.58	0.5	18	110	40	4.08	2.55	2.47	705	<1	1.42	51	670	20	203	0.36	119	10	108	1
575	<0.2	8.20	650	1.5	2	3.58	<0.5	17	103	37	3.85	2.45	2.42	660	<1	1.40	48	660	18	202	0.35	114	10	104	1
585	<0.2	8.01	640	1.5	<2	3.91	<0.5	16	100	35	3.60	2.37	2.47	660	<1	1.47	45	630	18	214	0.34	107	10	96	1
595	<0.2	8.15	650	1.5	4	3.64	0.5	16	104	37	3.76	2.44	2.38	630	<1	1.45	47	640	18	208	0.35	111	10	100	1
605	<0.2	8.50	660	1.5	2	3.26	0.5	19	112	41	4.13	2.49	2.42	665	<1	1.30	49	660	18	193	0.38	126	<10	112	1
615	<0.2	8.55	670	1.5	<2	3.65	0.5	19	112	40	4.04	2.56	2.45	670	<1	1.43	51	670	22	208	0.36	119	10	108	2
625	<0.2	8.39	660	1.5	<2	3.47	0.5	17	112	39	3.96	2.48	2.39	625	<1	1.37	50	640	22	199	0.36	118	10	108	1
635	<0.2	8.73	670	1.5	<2	3.53	0.5	19	116	42	4.22	2.57	2.46	660	<1	1.34	52	650	20	196	0.38	127	10	112	1
645	<0.2	8.42	670	1.5	2	3.92	<0.5	18	110	39	3.95	2.55	2.44	645	<1	1.45	48	650	20	207	0.35	113	10	104	2
655	<0.2	8.35	660	1.5	<2	3.40	<0.5	17	108	39	3.94	2.46	2.39	625	2	1.40	50	650	18	206	0.37	119	10	104	2
665	<0.2	8.44	660	1.5	2	3.72	0.5	18	113	41	4.08	2.53	2.49	680	<1	1.38	49	640	20	199	0.37	118	10	108	1
675	<0.2	8.13	650	1.5	<2	3.97	0.5	17	106	38	3.83	2.44	2.43	635	<1	1.39	47	620	18	202	0.36	112	10	102	1
685	<0.2	8.47	670	1.5	<2	3.80	<0.5	17	113	40	4.03	2.55	2.45	655	<1	1.46	49	640	20	212	0.36	114	10	106	2
695	<0.2	8.46	670	1.5	<2	3.43	<0.5	18	115	41	4.09	2.55	2.36	625	1	1.38	53	650	20	198	0.36	116	10	110	1

Core 107
Depth (cm)
Al (%)
Ca (%)
Fe (%)
K (%)
Mg (%)
Na (%)
Ti (%)
Co (ppm)
Cr (ppm)
Cu (ppm)
Ni (ppm)
Pb (ppm)
Zn (ppm)

Core 107
Depth (cm)
Ba (ppm)
Mn (ppm)
P (ppm)
Sr (ppm)
V (ppm)
% Moisture
% Organic Matter
% Carbonate
% Clay
% Silt
% Sand

Core 110A (23 samples)

Interval	Ag ppm	Al %	Ba ppm	Be ppm	Bi ppm	Ca %	Cd ppm	Co ppm	Cr ppm	Cu ppm	Fe %	K %	Mg %	Mn ppm	Mo ppm	Na %	Ni ppm	P ppm	Pb ppm	Sr ppm	Ti %	V ppm	W ppm	Zn ppm	As ppm
5	<0.2	7.68	580	1	<2	1.29	<0.5	19	96	41	3.85	1.94	1.38	580	1	1.17	52	680	20	188	0.35	133	<10	130	1
15	<0.2	7.72	600	1	<2	1.28	<0.5	16	97	40	3.72	1.97	1.35	570	<1	1.25	49	680	14	197	0.35	131	<10	108	1
25	<0.2	7.94	610	1	4	1.29	<0.5	17	93	40	3.79	2.04	1.38	545	2	1.29	51	710	16	203	0.36	136	<10	112	1
35	<0.2	8.04	600	1	<2	1.20	<0.5	18	99	40	3.84	2.03	1.42	535	<1	1.17	53	660	18	186	0.37	143	<10	116	1
45	<0.2	7.99	610	1	<2	1.24	<0.5	17	96	37	3.69	2.03	1.39	520	<1	1.22	49	660	16	196	0.37	136	<10	110	1
55	<0.2	7.87	610	1	2	1.25	<0.5	17	98	37	3.60	2.03	1.34	510	<1	1.30	50	690	16	203	0.36	133	<10	106	1
65	<0.2	7.94	610	1	<2	1.24	<0.5	16	91	35	3.59	2.02	1.32	495	<1	1.30	46	670	18	206	0.36	134	<10	108	2
75	<0.2	7.97	630	1	4	1.30	<0.5	17	90	35	3.52	2.06	1.31	500	<1	1.41	47	690	16	219	0.36	132	<10	106	1
85	<0.2	7.64	610	1	<2	1.32	<0.5	17	83	30	3.17	1.95	1.15	450	<1	1.50	48	650	18	234	0.34	116	<10	94	1
95	<0.2	7.06	570	1	<2	1.21	<0.5	13	73	32	2.93	1.80	1.05	420	1	1.40	51	590	14	220	0.31	105	<10	90	2
105	<0.2	7.35	600	1	<2	1.21	<0.5	12	79	27	3.11	1.90	1.12	435	<1	1.38	37	650	30	219	0.33	114	<10	92	1
115	<0.2	8.09	640	1	<2	1.16	<0.5	15	97	61	3.90	2.09	1.39	540	<1	1.23	48	710	16	197	0.36	137	<10	112	1
125	<0.2	7.96	630	1	<2	1.21	<0.5	15	89	29	3.64	2.01	1.29	520	1	1.31	45	720	16	212	0.36	132	<10	104	1
135	<0.2	8.26	640	1	<2	1.16	<0.5	16	98	37	4.05	2.10	1.44	560	<1	1.20	48	720	18	195	0.38	142	<10	114	2
145	<0.2	8.31	630	1	<2	1.13	<0.5	17	100	33	4.12	2.09	1.46	565	<1	1.14	50	710	18	187	0.40	148	<10	116	2
155	<0.2	8.14	620	1	<2	1.16	<0.5	18	100	32	4.03	2.09	1.45	550	<1	1.16	50	730	20	189	0.38	144	<10	112	1
165	<0.2	7.97	610	1	<2	1.20	<0.5	18	96	32	3.82	2.06	1.41	530	<1	1.20	48	720	18	195	0.37	139	<10	110	2
175	<0.2	7.91	630	1	<2	1.39	<0.5	18	98	92	3.87	2.11	1.55	565	<1	1.24	47	720	20	198	0.38	131	<10	138	2
185	<0.2	7.93	620	1	<2	1.60	<0.5	16	93	33	3.69	2.09	1.61	545	<1	1.31	44	720	20	210	0.36	128	<10	104	2
195	<0.2	7.96	610	1	<2	1.61	<0.5	16	97	32	3.82	2.10	1.72	560	<1	1.21	45	730	20	195	0.37	132	<10	108	2
205	<0.2	7.12	590	1	<2	2.22	<0.5	15	78	27	2.90	1.97	1.76	530	<1	1.47	38	660	20	224	0.31	103	<10	86	2
215	<0.2	8.67	700	1	<2	3.03	<0.5	22	125	55	5.13	2.56	2.31	1460	<1	1.41	63	770	16	195	0.37	125	<10	136	1
225	<0.2	8.39	670	1	<2	1.80	<0.5	22	122	77	5.19	2.49	2.16	1085	<1	1.29	59	740	24	182	0.36	118	10	126	1

Core 110a
Depth (cm)
Al (%)
Ca (%)
Fe (%)
K (%)
Mg (%)
Na (%)
Ti (%)
Co (ppm)
Cr (ppm)
Cu (ppm)
Ni (ppm)
Pb (ppm)
Zn (ppm)
As (ppm)

Core 110a
Depth (cm)
Ba (ppm)
Mn (ppm)
P (ppm)
Sr (ppm)
V (ppm)
% Moisture
% Organic Matter
% Total Carbonate
% Clay
% Sand
% Silt

Core 113A (21 samples)

Interval	Ag ppm	Al %	Ba ppm	Be ppm	Bi ppm	Ca %	Cd ppm	Co ppm	Cr ppm	Cu ppm	Fe %	K %	Mg %	Mn ppm	Mo ppm	Na %	Ni ppm	P ppm	Pb ppm	Sr ppm	Ti %	V ppm	W ppm	Zn ppm	As ppm
5	<0.2	7.70	630	1.5	<2	1.37	<0.5	15	84	36	3.18	1.98	1.19	1175	<1	1.37	45	730	30	215	0.32	122	<10	94	1
15	<0.2	7.72	640	1.5	4	1.39	0.5	16	80	36	3.05	1.97	1.14	920	<1	1.44	47	700	28	228	0.31	118	<10	90	1
25	<0.2	7.67	640	1.5	<2	1.40	0.5	15	76	35	2.84	1.97	1.07	795	<1	1.51	43	690	24	239	0.32	115	<10	80	1
35	<0.2	7.49	630	1.5	<2	1.35	0.5	15	80	37	3.19	1.96	1.14	765	<1	1.41	43	670	22	225	0.34	124	<10	86	1
45	<0.2	7.56	640	1.5	2	1.34	<0.5	16	83	37	3.23	2.01	1.13	755	<1	1.44	45	670	20	228	0.34	124	<10	86	1
55	<0.2	7.73	660	1.5	4	1.31	0.5	16	88	39	3.35	2.05	1.19	785	<1	1.40	46	700	24	221	0.36	133	<10	92	2
65	<0.2	7.66	660	1.5	<2	1.34	0.5	15	82	37	3.18	2.03	1.14	745	<1	1.46	42	700	22	231	0.34	127	<10	86	1
75	<0.2	7.72	660	1.5	<2	1.32	0.5	16	82	39	3.27	2.03	1.18	750	<1	1.42	46	700	24	225	0.35	132	<10	90	1
85	<0.2	7.90	670	1.5	2	1.30	1	17	87	39	3.42	2.07	1.21	750	<1	1.38	49	690	24	223	0.36	135	<10	94	1
95	<0.2	7.99	680	1.5	2	1.29	0.5	18	88	36	3.39	2.13	1.22	715	<1	1.41	47	730	22	224	0.37	137	<10	94	1
105	<0.2	7.91	680	1.5	<2	1.34	<0.5	17	86	36	3.32	2.10	1.21	700	1	1.45	45	700	24	231	0.36	132	<10	90	1
115	<0.2	7.94	680	1.5	<2	1.33	<0.5	17	87	34	3.41	2.11	1.27	675	<1	1.39	44	710	20	221	0.36	136	<10	94	2
125	<0.2	8.21	700	1.5	<2	1.30	0.5	17	92	35	3.59	2.19	1.32	700	<1	1.39	49	730	24	220	0.38	141	<10	98	2
135	<0.2	8.04	670	1.5	<2	1.61	0.5	16	92	33	3.54	2.16	1.58	750	<1	1.27	44	710	22	204	0.37	140	<10	98	1
145	<0.2	7.87	640	1.5	<2	2.51	0.5	16	91	34	3.57	2.14	2.23	800	<1	1.15	46	700	20	181	0.36	142	<10	100	2
155	<0.2	8.15	670	1.5	<2	2.24	<0.5	17	97	35	3.72	2.21	2.12	785	1	1.17	46	710	20	187	0.38	145	<10	102	1
165	<0.2	7.84	650	1.5	2	2.44	0.5	17	94	34	3.81	2.16	2.18	785	1	1.18	45	680	20	186	0.36	137	<10	96	2
175	<0.2	8.33	660	1.5	2	2.23	0.5	19	102	38	3.94	2.23	2.15	840	<1	1.15	51	710	24	183	0.39	151	<10	106	1
185	<0.2	8.37	660	1.5	<2	2.16	0.5	18	114	39	3.87	2.24	2.11	825	1	1.14	56	730	24	184	0.39	155	<10	106	1
195	<0.2	8.22	630	1.5	<2	2.31	<0.5	17	98	37	3.81	2.21	2.23	845	<1	1.07	46	690	22	172	0.37	155	<10	108	1
205	<0.2	8.05	630	1.5	2	2.56	0.5	17	98	36	3.78	2.18	2.33	840	<1	1.11	47	690	20	176	0.36	146	<10	102	1

Core 113a
Depth (cm)
Al (%)
Ca (%)
Fe (%)
K (%)
Na (%)
Tl (%)
Co (ppm)
Cr (ppm)
Cu (ppm)
Ni (ppm)
Pb (ppm)
Zn (ppm)

Core 113a
Depth (cm)
5
25
45
65
85
105
125
145
165
185
205
Ba (ppm)
625
650
675
700
725
Mn (ppm)
600
700
800
900
1000
1100
1200
P (ppm)
650
675
700
725
750
Sr (ppm)
160
180
200
220
240
V (ppm)
110
120
130
140
150
160
As (ppm)
0
1
2
3
% Moisture
45
50
55
60
65
70
75
% Organic Matter
4
6
8
10
12
% Total Carbonate
0
2
4
6
8
% Clay
10
20
30
40
50
60
70
% Silt
30
40
50
60
70
80
90
% Sand
0
5
10
15
20
25

Core 115 (27samples)

Interval	Ag ppm	Al %	Ba ppm	Be ppm	Bi ppm	Ca %	Cd ppm	Co ppm	Cr ppm	Cu ppm	Fe %	K %	Mg %	Mn ppm	Mo ppm	Na %	Ni ppm	P ppm	Pb ppm	Sr ppm	Ti %	V ppm	W ppm	Zn ppm	As ppm
5	<0.2	8.43	620	1.5	4	1.09	0.5	17	102	37	4.19	2.07	1.49	1100	<1	0.74	48	730	24	135	0.36	177	<10	130	1
15	<0.2	8.62	640	2	4	0.99	0.5	18	106	36	4.32	2.12	1.47	1220	<1	0.74	51	730	20	137	0.38	184	<10	128	1
25	<0.2	8.43	630	1.5	<2	1.01	<0.5	17	101	35	4.24	2.08	1.46	1200	2	0.74	48	690	22	134	0.37	180	<10	118	1
35	<0.2	8.27	620	1.5	<2	1.04	0.5	16	98	36	4.03	2.08	1.43	1185	<1	0.78	44	680	24	138	0.36	176	<10	116	2
45	<0.2	7.36	530	1	<2	0.93	3	15	90	29	3.68	1.74	1.29	1005	<1	0.61	41	510	20	113	0.32	151	<10	106	2
55	<0.2	8.59	640	1.5	<2	1.00	<0.5	18	104	36	4.31	2.11	1.47	1180	1	0.75	51	660	24	136	0.38	186	<10	122	1
65	<0.2	8.63	660	1.5	<2	1.06	0.5	19	106	39	4.22	2.15	1.50	1155	1	0.81	54	680	24	144	0.38	184	<10	120	2
75	<0.2	8.53	630	1.5	2	1.05	0.5	17	106	37	4.22	2.10	1.52	1165	1	0.73	50	660	24	133	0.37	185	<10	120	1
85	<0.2	8.49	650	2	6	1.02	<0.5	17	100	38	4.17	2.12	1.49	1120	1	0.81	50	670	20	142	0.38	177	<10	118	1
95	<0.2	7.96	590	1	4	1.00	3	17	96	32	4.02	1.88	1.41	1030	<1	0.69	48	560	18	125	0.35	157	<10	112	1
105	<0.2	8.20	600	1	<2	1.07	3.5	16	101	34	4.06	1.95	1.48	1045	<1	0.70	45	570	20	128	0.37	163	<10	114	1
115	<0.2	8.38	610	1.5	<2	1.03	3.5	17	105	33	4.12	2.01	1.48	1075	<1	0.69	48	580	20	130	0.38	172	<10	120	2
125	<0.2	8.73	650	1.5	2	1.08	<0.5	20	105	37	4.35	2.18	1.51	1165	1	0.82	57	750	18	143	0.39	189	10	126	2
135	<0.2	8.31	610	1.5	<2	1.18	<0.5	17	104	34	4.17	2.04	1.55	1155	1	0.77	51	710	18	134	0.37	177	<10	118	1
145	<0.2	8.32	620	1.5	4	1.28	<0.5	20	104	37	4.19	2.05	1.59	1185	<1	0.80	56	700	20	139	0.38	177	<10	120	1
155	<0.2	8.27	620	1.5	<2	1.16	<0.5	18	101	36	4.09	2.06	1.53	1120	<1	0.79	48	700	20	140	0.38	173	<10	118	2
165																									
175	<0.2	8.26	640	1.5	<2	1.43	0.5	18	103	36	4.02	2.14	1.65	1125	<1	0.91	53	700	16	152	0.38	164	<10	114	1
185	<0.2	8.37	640	1.5	4	1.59	0.5	19	102	60	4.22	2.17	1.70	1070	<1	0.95	88	710	18	156	0.40	170	10	140	1
195	<0.2	7.88	620	1.5	2	1.36	<0.5	18	94	34	3.82	2.05	1.55	1030	<1	0.89	47	690	16	150	0.37	161	<10	110	1
205	<0.2	7.73	600	1.5	4	1.47	0.5	18	90	32	3.74	2.03	1.60	1025	<1	0.87	47	670	14	148	0.36	158	<10	106	1
215	<0.2	6.17	490	1	2	1.26	0.5	14	73	27	2.90	1.67	1.28	785	<1	0.81	40	570	12	138	0.29	118	<10	82	1
225	<0.2	7.47	580	1.5	<2	1.71	<0.5	16	93	33	3.63	1.98	1.73	1000	<1	0.87	48	660	12	148	0.34	146	10	102	1
235	<0.2	6.40	510	1	4	2.03	0.5	15	79	29	3.01	1.80	1.75	895	<1	0.87	39	620	12	147	0.29	119	<10	84	1
245	<0.2	6.30	500	1	<2	1.90	<0.5	15	76	29	3.02	1.80	1.66	865	<1	0.88	39	630	12	147	0.29	115	<10	82	1
255	<0.2	5.75	460	1	<2	1.85	<0.5	13	69	25	2.70	1.71	1.51	745	<1	0.91	37	650	10	154	0.26	98	<10	70	2
265	<0.2	7.34	570	1.5	2	2.06	<0.5	16	87	34	3.65	2.02	1.91	1080	<1	0.88	42	670	14	149	0.34	141	<10	98	1

Core 115
Depth (cm)
Al (%)
Ca (%)
Fe (%)
K (%)
Mg (%)
Na (%)
Ti (%)
Co (ppm)
Cr (ppm)
Cu (ppm)
Ni (ppm)
Pb (ppm)
Zn (ppm)
As (ppm)

Core 115
Depth (cm)
Ba (ppm)
Mn (ppm)
P (ppm)
Sr (ppm)
V (ppm)
% Moisture
% Organic Matter
% Carbonate
% Clay

Core 119 (30 samples)

Depth (cm)	Ag ppm	Al %	Ba ppm	Be ppm	Bi ppm	Ca %	Cd ppm	Co ppm	Cr ppm	Cu ppm	Fe %	K %	Mg %	Mn ppm	Mo ppm	Na %	Ni ppm	P ppm	Pb ppm	Sr ppm	Ti %	V ppm	W ppm	Zn ppm	As ppm
15	<0.2	8.04	590	1.5	8	1.94	<0.5	18	96	31	3.82	2.11	1.88	690	<1	1.02	43	670	18	149	0.35	153	<10	122	1
25	<0.2	7.06	570	1	8	2.71	<0.5	14	78	25	2.86	1.91	2.02	600	<1	1.27	32	620	12	183	0.30	118	<10	76	2
35	<0.2	7.55	590	1	8	2.74	<0.5	15	81	28	3.18	1.97	2.20	620	<1	1.18	34	620	14	170	0.32	134	<10	86	1
45	<0.2	7.24	570	1	4	2.82	<0.5	13	81	28	3.06	1.88	2.22	715	<1	1.14	36	580	12	166	0.31	129	<10	82	2
55	<0.2	6.87	560	1	4	3.24	<0.5	14	74	29	2.82	1.82	2.40	680	<1	1.18	33	590	12	172	0.30	115	<10	74	1
65	<0.2	7.10	580	1	4	3.14	<0.5	14	79	27	3.00	2.06	2.38	930	<1	1.29	34	700	12	172	0.31	124	<10	78	1
75	<0.2	6.79	540	1	6	2.78	<0.5	12	77	28	2.91	1.84	2.15	810	<1	1.14	33	660	12	160	0.29	118	<10	76	1
85	<0.2	7.40	600	1	4	2.85	<0.5	14	84	35	3.25	1.98	2.26	940	<1	1.18	35	760	14	169	0.33	130	<10	88	1
95	0.2	7.28	620	1	4	3.11	<0.5	14	84	37	3.17	1.94	2.41	875	<1	1.21	34	660	16	170	0.32	126	<10	82	2
105	<0.2	7.34	600	1	6	2.85	<0.5	15	85	34	3.17	1.99	2.27	820	<1	1.16	39	680	12	167	0.32	130	<10	84	2
115	0.2	6.75	540	1	6	3.48	<0.5	14	73	27	2.79	1.87	2.57	615	<1	1.19	36	590	10	165	0.28	115	<10	74	1
125	<0.2	6.37	520	1	4	3.98	<0.5	13	68	24	2.50	1.86	2.78	530	<1	1.29	30	550	12	174	0.27	103	<10	66	1
135	<0.2	7.28	560	1	6	3.25	0.5	13	83	29	3.12	1.91	2.52	650	<1	1.11	35	620	12	163	0.32	131	<10	86	2
145	<0.2	6.53	520	1	2	3.81	<0.5	14	72	26	2.65	1.84	2.71	505	<1	1.26	33	550	10	172	0.27	107	<10	70	1
155	<0.2	6.79	530	1	4	3.70	<0.5	14	78	27	2.83	1.83	2.73	505	<1	1.17	35	560	8	165	0.29	116	<10	76	1
165	<0.2	6.91	540	1	2	3.35	<0.5	14	77	30	2.91	1.85	2.54	475	<1	1.17	34	570	10	167	0.29	117	<10	78	1
175	<0.2	7.91	600	1	6	3.40	<0.5	16	94	40	3.88	2.19	2.85	1000	<1	1.18	44	650	12	167	0.34	137	<10	96	1
185	<0.2	7.98	620	1.5	8	3.31	<0.5	17	100	40	3.83	2.34	2.80	1010	<1	1.21	53	660	14	168	0.35	133	10	102	2
195	<0.2	7.55	570	1	4	3.72	<0.5	14	94	34	4.03	2.18	2.96	745	<1	1.16	39	700	12	158	0.34	130	10	90	1
205	<0.2	7.74	610	1	4	3.51	1	15	96	48	4.15	2.34	2.96	685	<1	1.24	45	640	12	166	0.35	123	10	98	2
215	<0.2	7.54	590	1	8	4.08	<0.5	19	95	39	3.50	2.28	3.13	615	<1	1.29	46	580	16	172	0.33	122	<10	94	1
225	<0.2	7.87	600	1.5	8	3.88	<0.5	17	104	35	3.93	2.42	3.30	540	<1	1.27	49	620	16	170	0.35	119	10	102	1
235	<0.2	7.50	580	1	6	4.20	<0.5	15	95	35	3.57	2.18	3.24	565	<1	1.21	44	600	16	167	0.33	118	<10	100	2
245	<0.2	7.91	590	1.5	10	3.82	0.5	17	104	34	3.73	2.42	3.21	520	<1	1.28	49	590	14	168	0.35	120	<10	104	2
255	<0.2	7.78	610	1.5	10	4.20	<0.5	18	100	38	4.06	2.53	3.49	550	<1	1.36	48	660	14	167	0.35	119	10	100	1
265	<0.2	7.23	550	1	6	4.76	<0.5	16	93	41	3.45	2.20	3.40	525	<1	1.21	42	580	14	158	0.32	121	<10	90	4
275	<0.2	7.59	600	1	6	4.21	<0.5	15	94	32	3.53	2.13	3.24	500	<1	1.12	43	580	12	159	0.34	126	10	92	1
285	<0.2	7.00	550	1	6	5.34	<0.5	15	90	35	3.31	2.13	3.99	565	<1	1.17	41	610	12	161	0.32	112	10	86	1
295	<0.2	7.43	550	1	8	4.62	<0.5	17	90	35	3.74	2.18	3.63	565	<1	1.16	43	660	14	164	0.35	121	<10	92	2
305	<0.2	7.46	670	1.5	10	4.23	<0.5	17	94	43	3.86	2.19	3.45	575	<1	1.17	42	660	14	170	0.34	121	<10	96	1

Core 119
Depth (cm)
Al (%)
Ca (%)
Fe(%)
K (%)
Mg (%)
Na (%)
Ti (%)
Co (ppm)
Cr (ppm)
Cu (ppm)
Ni (ppm)
Pb (ppm)
Zn (ppm)
As (ppm)

Core 119
Depth (cm)
Ba (ppm)
Mn (ppm)
P (ppm)
Sr (ppm)
V (ppm)

Core 120 (35 samples)

Interval	Ag ppm	Al %	Ba ppm	Be ppm	Bi ppm	Ca %	Cd ppm	Co ppm	Cr ppm	Cu ppm	Fe %	K %	Mg %	Mn ppm	Mo ppm	Na %	Ni ppm	P ppm	Pb ppm	Sr ppm	Ti %	V ppm	W ppm	Zn ppm	As ppm
5	<0.2	7.83	560	1	<2	1.49	<0.5	17	98	32	3.86	1.88	1.60	1055	<1	0.80	42	730	26	140	0.35	150	<10	124	2
15	<0.2	8.13	580	1.5	<2	1.37	<0.5	17	98	37	4.02	1.97	1.62	865	<1	0.79	45	680	28	136	0.36	162	<10	130	1
25	<0.2	7.82	580	1	<2	1.26	<0.5	19	95	35	3.90	1.90	1.46	795	<1	0.84	46	690	26	144	0.35	149	<10	116	2
35	<0.2	7.86	600	1	<2	1.27	<0.5	17	100	30	3.79	1.94	1.44	800	<1	0.90	44	680	24	153	0.36	150	<10	116	2
45	<0.2	7.39	580	1	<2	1.69	<0.5	18	87	26	3.39	1.86	1.56	730	<1	0.99	42	640	20	164	0.33	131	<10	96	2
55	<0.2	6.95	560	1	<2	1.99	<0.5	16	81	27	3.25	1.79	1.69	665	1	1.02	40	610	24	164	0.31	121	<10	92	4
65	<0.2	6.93	540	1	<2	2.07	<0.5	15	83	24	3.06	1.75	1.73	655	<1	0.97	38	640	22	162	0.32	122	<10	88	1
75	<0.2	7.78	590	1	<2	1.79	<0.5	16	93	29	3.65	1.90	1.72	705	<1	0.95	42	640	24	160	0.36	144	<10	104	1
85	<0.2	7.12	550	1	<2	1.94	<0.5	14	85	28	3.16	1.77	1.73	645	<1	0.93	36	600	28	152	0.33	129	<10	100	4
95	<0.2	7.29	570	1	<2	2.11	<0.5	13	82	24	3.19	1.82	1.83	655	<1	0.99	35	630	24	163	0.33	129	<10	94	2
105	<0.2	7.36	570	1	<2	1.93	<0.5	14	89	26	3.32	1.82	1.77	680	<1	0.94	40	620	22	155	0.33	135	<10	98	2
115	<0.2	7.47	580	1	<2	1.92	<0.5	15	90	27	3.44	1.87	1.79	720	<1	0.96	38	660	22	158	0.34	136	<10	100	1
125	<0.2	7.34	580	1	<2	2.37	<0.5	15	88	24	3.31	1.86	2.02	675	<1	0.98	39	650	18	162	0.33	131	<10	96	1
135	<0.2	6.82	550	1	<2	2.43	<0.5	13	76	22	2.93	1.74	1.95	645	<1	1.01	35	630	20	165	0.31	117	<10	90	1
145	<0.2	6.91	550	1	<2	3.38	<0.5	14	80	23	2.95	1.78	2.56	615	<1	1.04	36	610	18	168	0.31	119	<10	84	2
155	<0.2	7.29	560	1	<2	2.69	<0.5	16	88	27	3.30	1.85	2.28	635	<1	0.97	38	610	18	158	0.31	131	<10	94	2
165	<0.2	6.73	530	1	<2	3.29	<0.5	13	75	22	2.83	1.73	2.51	585	<1	1.05	35	600	18	166	0.30	113	<10	82	1
175	<0.2	7.03	540	1	<2	3.02	<0.5	13	83	27	3.08	1.77	2.41	610	<1	0.98	35	600	20	157	0.32	125	<10	90	1
185	<0.2	7.01	540	1	<2	3.11	<0.5	14	82	25	3.01	1.77	2.46	585	<1	0.99	36	610	16	162	0.31	123	<10	86	1
195	<0.2	8.46	730	1	<2	1.39	<0.5	21	108	43	4.51	2.39	1.82	775	<1	1.64	55	770	20	242	0.37	121	<10	120	1
205	<0.2	8.79	760	1	<2	1.47	<0.5	21	111	44	4.52	2.48	1.91	835	<1	1.72	57	800	20	254	0.38	124	<10	124	1
215	<0.2	8.83	790	1	<2	1.60	<0.5	21	112	45	4.44	2.55	1.94	975	<1	1.85	57	810	22	279	0.38	117	10	122	1
225	<0.2	8.94	770	1	<2	1.55	<0.5	21	115	44	4.42	2.52	1.90	915	1	1.76	60	810	18	273	0.38	125	10	120	1
235	<0.2	8.65	740	1	<2	1.48	<0.5	20	112	47	4.23	2.45	1.82	730	<1	1.68	59	780	20	264	0.37	123	<10	114	2
245	<0.2	8.94	730	1	<2	1.50	<0.5	21	118	44	4.46	2.52	1.85	745	<1	1.67	61	810	20	265	0.38	130	<10	120	1
255	<0.2	9.08	720	1.5	<2	1.50	<0.5	20	118	44	4.40	2.43	1.83	750	2	1.57	63	800	20	259	0.38	143	10	122	1
265	<0.2	9.18	730	1.5	<2	1.45	<0.5	20	116	43	4.30	2.43	1.82	670	<1	1.43	63	810	20	246	0.38	152	10	120	1
275	<0.2	9.14	660	1.5	<2	1.27	<0.5	21	114	40	4.31	2.30	1.73	615	<1	1.15	60	760	18	215	0.37	166	10	120	1
285	<0.2	9.17	580	1.5	<2	1.15	<0.5	19	117	37	4.19	2.15	1.60	540	<1	0.94	57	740	20	190	0.37	179	<10	114	2
295	<0.2	9.29	630	1.5	<2	1.16	<0.5	23	117	59	4.36	2.23	1.64	600	<1	0.99	58	740	22	199	0.38	181	10	122	1
305	<0.2	9.39	680	1.5	<2	1.26	<0.5	20	123	46	4.54	2.29	1.73	510	<1	1.06	61	730	20	209	0.39	176	10	124	1
315	<0.2	9.13	550	1.5	<2	1.18	<0.5	17	111	48	4.42	2.04	1.58	460	1	0.78	54	700	26	170	0.38	181	10	124	1
325	<0.2	8.41	630	1	<2	1.82	<0.5	24	94	36	4.55	1.68	1.49	1070	1	0.43	44	590	22	123	0.33	175	10	114	10
335	<0.2	8.27	670	1	<2	1.98	<0.5	13	91	38	4.02	1.75	1.54	490	<1	0.53	37	620	18	133	0.34	167	<10	112	4
345	<0.2	7.69	670	1	<2	2.21	<0.5	12	90	30	3.68	1.74	1.56	465	1	0.60	35	640	16	141	0.32	154	10	106	1

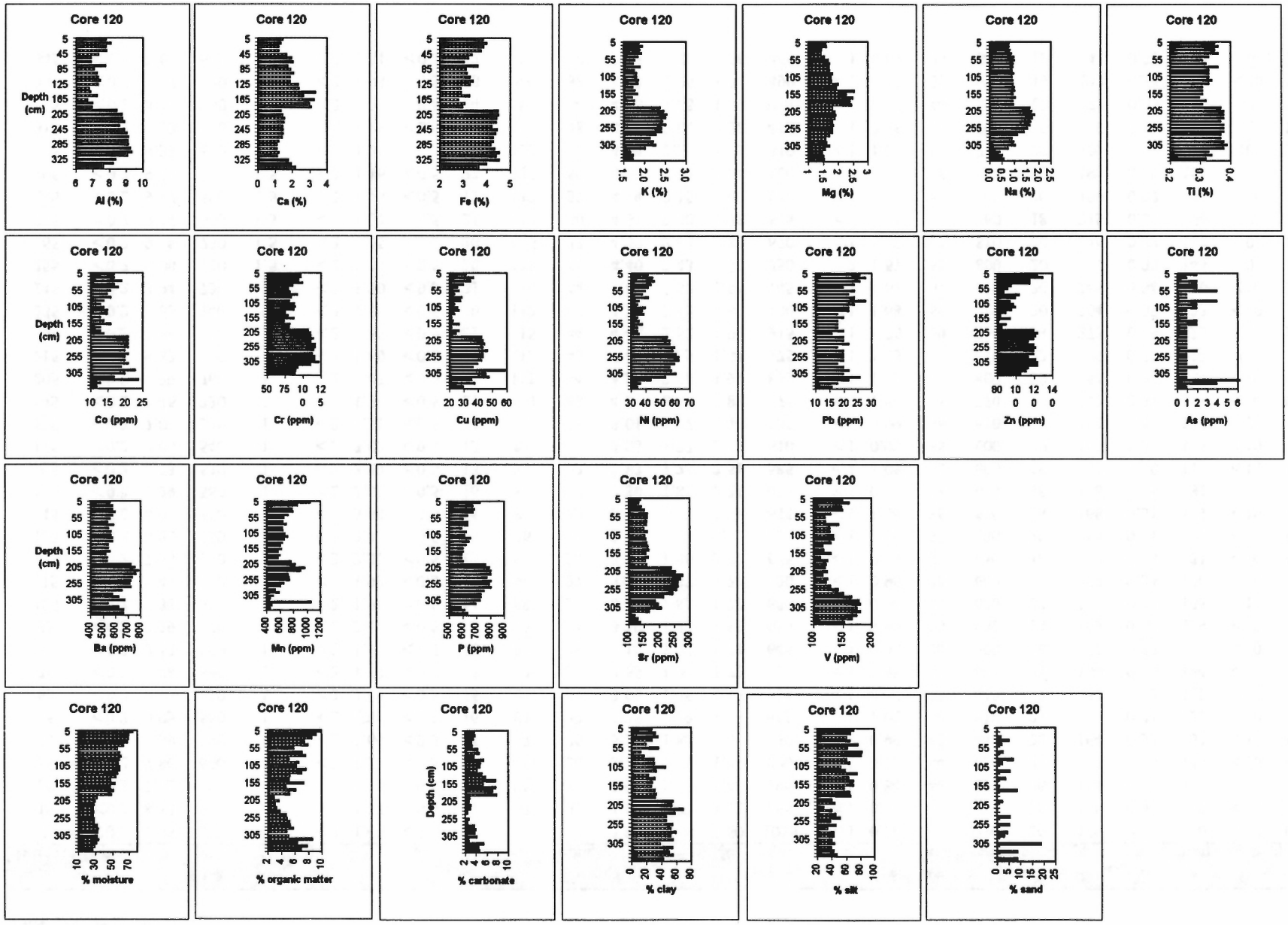
Core 120
Depth (cm)
Al (%)
Ca (%)
Fe (%)
K (%)
Mg (%)
Na (%)
Ti (%)
Co (ppm)
Cr (ppm)
Cu (ppm)
Ni (ppm)
Pb (ppm)
Zn (ppm)
As (ppm)
Ba (ppm)
Mn (ppm)
P (ppm)
Sr (ppm)
V (ppm)
% moisture
% organic matter
% carbonate
% clay
% silt
% sand

Core 121 (55 samples)

Interval	Ag ppm	Al %	Ba ppm	Be ppm	Bi ppm	Ca %	Cd ppm	Co ppm	Cr ppm	Cu ppm	Fe %	K %	Mg %	Mn ppm	Mo ppm	Na %	Ni ppm	P ppm	Pb ppm	Sr ppm	Ti %	V ppm	W ppm	Zn ppm	As ppm
5	<0.2	8.19	570	1.5	2	1.02	<0.5	16	106	32	4.11	1.92	1.42	955	<1	0.62	45	690	30	121	0.34	177	<10	136	2
15	<0.2	8.32	580	1.5	2	0.98	<0.5	17	107	32	4.37	1.95	1.43	995	<1	0.63	51	690	28	122	0.35	180	<10	136	1
25	<0.2	8.38	580	1.5	<2	0.89	<0.5	18	104	29	4.46	1.96	1.41	1070	<1	0.61	49	660	24	119	0.35	181	<10	130	2
35	<0.2	8.45	590	1.5	2	0.91	<0.5	17	108	29	4.53	1.98	1.43	1065	<1	0.62	51	680	26	121	0.35	182	<10	132	1
45	<0.2	8.75	610	1.5	4	0.97	<0.5	18	108	31	4.56	2.06	1.49	1160	<1	0.65	51	690	26	126	0.37	188	10	136	1
55	<0.2	8.66	600	1.5	<2	0.99	<0.5	19	114	32	4.66	2.03	1.49	1065	<1	0.63	51	720	30	126	0.37	188	10	140	1
65	<0.2	8.50	600	1.5	<2	0.92	<0.5	17	113	29	4.43	2.00	1.44	1115	<1	0.63	50	670	28	123	0.37	182	10	134	1
75	<0.2	8.58	610	1.5	<2	0.94	<0.5	18	110	29	4.50	2.03	1.46	1175	<1	0.64	49	680	26	125	0.36	186	10	134	1
85	<0.2	8.57	590	1.5	2	0.93	<0.5	17	105	30	4.40	2.00	1.45	1220	<1	0.61	48	690	26	122	0.37	189	10	134	2
95	<0.2	8.66	600	1.5	2	0.95	<0.5	18	109	31	4.55	2.01	1.48	1235	<1	0.61	53	700	26	123	0.36	193	10	138	1
105	<0.2	8.41	590	1.5	2	0.90	<0.5	17	103	30	4.32	1.96	1.42	1175	1	0.61	49	650	24	122	0.37	186	10	132	2
115	<0.2	8.88	640	1.5	2	0.97	<0.5	19	118	32	4.74	2.09	1.48	1300	<1	0.69	52	740	26	135	0.40	196	10	140	1
125	<0.2	8.29	610	1.5	<2	0.91	<0.5	17	103	29	4.32	1.98	1.39	1195	1	0.65	47	690	26	126	0.37	181	10	132	1
135	<0.2	8.52	620	1.5	<2	0.90	<0.5	17	104	30	4.42	2.02	1.44	1190	<1	0.65	48	680	26	128	0.37	186	<10	130	1
145	<0.2	8.52	610	1.5	<2	0.91	<0.5	19	107	32	4.44	2.00	1.45	1200	<1	0.63	49	690	24	123	0.37	187	<10	136	2
155	<0.2	8.63	630	1.5	6	0.92	<0.5	17	107	33	4.41	2.04	1.46	1175	<1	0.67	50	670	26	128	0.39	188	<10	134	2
165	<0.2	8.70	630	1.5	2	0.90	<0.5	18	106	34	4.49	2.04	1.45	1195	1	0.65	48	690	22	127	0.37	189	10	134	1
175	<0.2	8.46	610	1.5	<2	0.89	<0.5	20	102	30	4.40	1.99	1.42	1150	<1	0.64	53	680	24	124	0.36	184	<10	132	1
185	<0.2	8.59	630	1.5	2	0.90	<0.5	20	104	33	4.41	2.06	1.44	1120	<1	0.68	52	700	24	129	0.38	184	10	134	1
195	<0.2	8.63	620	1.5	<2	1.02	<0.5	18	109	31	4.46	2.05	1.52	1170	<1	0.68	54	690	22	130	0.38	185	10	132	1
205	<0.2	8.58	630	1.5	<2	1.09	<0.5	17	104	31	4.47	2.08	1.54	1135	<1	0.71	49	700	24	133	0.37	181	10	130	1
215	<0.2	8.87	640	1.5	2	1.05	<0.5	19	108	31	4.68	2.10	1.57	1205	1	0.69	51	710	22	132	0.37	191	10	136	2
225	<0.2	8.17	590	1.5	<2	0.98	<0.5	17	100	28	4.21	1.96	1.44	1075	<1	0.66	49	680	24	125	0.35	178	<10	126	1
235	<0.2	7.99	580	1.5	2	1.04	<0.5	19	99	28	4.08	1.92	1.46	1035	<1	0.65	52	660	22	123	0.36	173	<10	122	2
245	<0.2	8.48	620	1.5	<2	1.02	<0.5	17	108	31	4.40	2.04	1.51	1135	<1	0.70	49	730	24	133	0.38	181	<10	130	1
255	<0.2	8.66	630	1.5	2	1.05	<0.5	18	107	31	4.39	2.10	1.54	1085	<1	0.73	53	730	22	136	0.39	183	<10	132	1
265	<0.2	8.41	620	1.5	<2	1.13	<0.5	16	105	31	4.34	2.07	1.55	1075	<1	0.75	47	730	24	139	0.38	176	10	130	1
275	<0.2	8.49	640	1.5	<2	1.19	<0.5	18	106	31	4.31	2.12	1.60	1030	<1	0.82	50	720	24	146	0.38	169	10	126	1
285	<0.2	8.51	650	1.5	<2	1.25	<0.5	18	107	31	4.34	2.12	1.64	1070	<1	0.81	51	710	28	145	0.39	171	10	126	2
295	<0.2	8.38	620	1.5	<2	1.23	<0.5	17	107	29	4.24	2.06	1.61	1045	<1	0.75	52	720	24	137	0.37	175	<10	126	2
305	<0.2	8.50	620	1.5	<2	1.26	<0.5	18	105	29	4.30	2.08	1.64	1070	<1	0.74	51	710	24	135	0.37	183	<10	130	2
315	<0.2	8.15	600	1.5	<2	1.28	<0.5	19	104	27	4.12	2.01	1.61	1040	<1	0.71	50	680	22	131	0.35	176	10	126	1
325	<0.2	8.17	600	1.5	<2	1.23	<0.5	16	102	28	4.08	2.00	1.58	1000	<1	0.71	47	690	24	130	0.35	173	10	124	1
335	<0.2	8.10	610	1	<2	1.59	<0.5	17	97	29	4.05	2.04	1.78	1010	<1	0.80	48	700	24	140	0.37	163	10	120	2
345	<0.2	8.19	620	1.5	<2	1.68	<0.5	18	101	29	4.05	2.06	1.86	985	<1	0.80	50	680	24	141	0.37	167	10	122	1
355	<0.2	8.28	610	1.5	<2	1.70	<0.5	16	101	28	4.12	2.07	1.89	1015	<1	0.77	48	710	20	137	0.36	172	10	124	2
365	<0.2	8.02	590	1.5	<2	1.61	<0.5	16	99	27	3.99	2.02	1.80	955	<1	0.76	47	690	22	135	0.35	165	<10	120	1

Interval	Ag ppm	Al %	Ba ppm	Be ppm	Bi ppm	Ca %	Cd ppm	Co ppm	Cr ppm	Cu ppm	Fe %	K %	Mg %	Mn ppm	Mo ppm	Na %	Ni ppm	P ppm	Pb ppm	Sr ppm	Ti %	V ppm	W ppm	Zn ppm	As ppm
375	<0.2	8.25	600	1.5	<2	1.76	<0.5	16	100	28	4.06	2.07	1.93	1015	<1	0.79	46	700	24	140	0.35	169	10	124	1
385	<0.2	7.87	580	1	<2	1.89	<0.5	16	96	26	3.96	2.01	1.98	955	<1	0.77	45	670	18	135	0.33	157	10	116	1
395	<0.2	8.31	600	1.5	<2	1.92	<0.5	17	105	31	4.11	2.12	2.05	970	<1	0.82	48	710	24	144	0.36	165	<10	122	1
405	<0.2	8.43	620	1.5	<2	2.02	<0.5	17	107	30	4.25	2.17	2.14	980	<1	0.83	49	730	22	143	0.36	174	10	128	1
415	<0.2	8.05	590	1	<2	1.91	<0.5	18	100	30	4.06	2.08	2.04	900	<1	0.82	48	680	24	140	0.34	159	<10	120	1
425	<0.2	8.07	590	1.5	<2	1.90	<0.5	16	101	34	4.01	2.07	2.03	875	<1	0.80	46	680	26	140	0.33	159	10	122	2
435	<0.2	7.87	590	1	<2	2.24	<0.5	16	94	27	3.82	2.06	2.16	815	<1	0.84	40	690	22	144	0.32	151	10	112	1
445	<0.2	8.14	570	1.5	<2	1.97	<0.5	16	100	29	3.91	2.05	2.03	830	<1	0.76	46	670	24	138	0.34	165	10	118	2
455	<0.2	7.99	570	1	<2	2.38	<0.5	15	99	29	3.85	2.05	2.25	780	<1	0.79	46	670	24	143	0.33	160	10	118	2
465	<0.2	7.73	560	1	<2	2.43	<0.5	16	95	27	3.68	1.98	2.25	740	<1	0.77	45	690	24	141	0.32	156	10	112	1
475	<0.2	9.09	550	1.5	<2	2.52	<0.5	17	108	36	4.20	1.98	1.92	740	<1	0.58	47	640	10	135	0.34	196	10	118	1
485	<0.2	7.82	510	1	<2	4.70	<0.5	18	93	30	3.44	1.87	2.56	850	1	0.74	44	560	24	150	0.28	155	10	100	4
495	<0.2	8.62	550	1.5	<2	3.24	<0.5	14	100	34	3.99	1.88	2.01	710	<1	0.55	45	580	24	129	0.30	176	10	106	1
505	<0.2	8.45	530	1.5	<2	2.62	<0.5	15	97	33	3.97	1.83	1.69	500	<1	0.51	43	580	20	128	0.32	173	10	108	2
515	<0.2	8.68	490	1.5	<2	2.35	<0.5	15	101	35	4.07	1.85	1.64	465	1	0.51	46	580	22	130	0.33	180	10	112	1
525	<0.2	8.49	490	1	<2	2.55	<0.5	15	91	33	3.96	1.84	1.62	465	1	0.59	41	550	22	133	0.32	169	10	106	4
535	<0.2	8.29	710	1	<2	3.31	<0.5	14	89	32	3.83	1.82	1.86	485	<1	0.59	38	560	24	145	0.31	165	10	104	2
545	<0.2	8.13	460	1	<2	3.11	<0.5	15	85	34	3.79	1.78	1.88	465	<1	0.57	38	550	18	132	0.30	161	10	104	1

Core 121
Depth (cm)
Al (%)
Ca (%)
Fe (%)
K (%)
Mg (%)
Na (%)
Ti (%)
Co (ppm)
Cr (ppm)
Cu (ppm)
Ni (ppm)
Pb (ppm)
Zn (ppm)
As (ppm)

Core 121
Depth (cm)
Ba (ppm)
Mn (ppm)
P (ppm)
Sr (ppm)
V (ppm)
% Moisture
% Organic Matter
% Carbonate
% Clay
% Silt
% Sand

Core 122A (48 samples)

Interval	Ag ppm	Al %	Ba ppm	Be ppm	Bi ppm	Ca %	Cd ppm	Co ppm	Cr ppm	Cu ppm	Fe %	K %	Mg %	Mn ppm	Mo ppm	Na %	Ni ppm	P ppm	Pb ppm	Sr ppm	Ti %	V ppm	W ppm	Zn ppm	As ppm
5	<0.2	7.63	510	1	<2	0.99	<0.5	17	245	35	5.99	1.78	1.36	1145	2	0.57	55	690	38	109	0.30	168	10	142	2
15																									1
25																									1
35	<0.2	8.18	580	1.5	<2	0.94	<0.5	17	97	27	4.22	1.95	1.40	1020	<1	0.62	46	670	22	119	0.34	177	<10	128	1
45	<0.2	8.10	560	1.5	<2	0.95	<0.5	17	97	26	4.14	1.90	1.38	1100	<1	0.62	50	630	34	119	0.34	178	<10	126	2
55	<0.2	8.07	560	1	<2	0.93	<0.5	17	97	26	4.07	1.90	1.37	1115	<1	0.61	45	630	32	117	0.34	180	<10	126	1
65																									2
75	<0.2	8.25	600	1.5	<2	1.00	<0.5	18	98	32	4.21	1.98	1.43	1095	<1	0.69	49	670	28	128	0.37	178	<10	128	2
85	<0.2	8.53	610	1.5	4	0.95	<0.5	18	98	28	4.33	2.02	1.45	1095	<1	0.65	49	690	28	124	0.37	188	<10	132	1
95	<0.2	8.44	610	1.5	2	1.04	<0.5	20	99	31	4.32	1.99	1.48	1110	<1	0.68	50	680	28	125	0.36	190	<10	132	1
105	<0.2	8.46	620	1.5	<2	0.97	<0.5	18	98	28	4.37	2.00	1.45	1140	<1	0.66	47	690	26	124	0.35	185	<10	130	1
115	<0.2	8.48	610	1.5	<2	1.04	<0.5	17	102	29	4.40	2.00	1.51	1175	<1	0.65	49	660	46	121	0.36	187	10	132	4
125	<0.2	8.37	600	1.5	<2	0.91	<0.5	16	100	27	4.28	1.99	1.42	1075	<1	0.64	45	670	18	120	0.35	186	<10	130	1
135	<0.2	8.27	590	1.5	<2	1.03	<0.5	16	99	27	4.23	1.95	1.48	1090	<1	0.62	43	670	20	117	0.34	186	<10	130	1
145	<0.2	8.43	620	1.5	<2	0.94	<0.5	17	99	29	4.28	2.01	1.44	1060	<1	0.66	47	660	26	125	0.38	183	<10	130	2
155	<0.2	8.31	600	1.5	2	1.06	<0.5	20	99	27	4.35	1.98	1.51	1090	<1	0.67	50	690	22	122	0.35	181	10	128	2
165	<0.2	8.50	630	1.5	<2	1.06	<0.5	17	104	29	4.34	2.04	1.51	1045	<1	0.71	48	680	20	130	0.38	178	10	128	1
175	<0.2	8.41	610	1.5	2	1.15	<0.5	17	100	28	4.26	2.00	1.56	1080	<1	0.68	48	690	18	124	0.36	184	<10	128	1
185	<0.2	8.23	590	1	<2	1.05	<0.5	16	100	28	4.12	1.94	1.49	1015	<1	0.65	46	670	20	122	0.37	180	<10	126	1
195	<0.2	8.13	580	1.5	2	1.17	<0.5	16	97	27	4.02	1.92	1.55	1030	<1	0.66	48	630	20	119	0.34	182	10	126	1
205	<0.2	8.42	610	1.5	<2	1.29	<0.5	18	103	29	4.27	2.03	1.66	1065	<1	0.70	50	680	20	127	0.35	185	10	130	2
215	<0.2	8.30	610	1	<2	1.22	<0.5	20	101	28	4.15	2.02	1.59	945	<1	0.71	50	700	18	130	0.35	178	10	126	1
225	<0.2	8.18	610	1.5	<2	1.18	<0.5	16	98	29	4.05	2.01	1.55	905	<1	0.75	48	680	20	133	0.37	172	<10	124	2
235	<0.2	8.46	630	1.5	<2	1.23	<0.5	18	101	28	4.22	2.08	1.63	945	<1	0.79	50	650	20	139	0.37	168	10	124	2
245	<0.2	7.88	590	1	<2	1.43	<0.5	17	96	26	3.89	1.94	1.67	980	<1	0.74	46	620	18	130	0.35	160	<10	116	1
255	<0.2	8.23	630	1	2	1.29	<0.5	18	99	28	4.11	2.05	1.61	870	<1	0.82	48	710	20	141	0.37	166	<10	122	1
265	<0.2	7.94	590	1	<2	1.23	<0.5	16	97	26	3.96	1.94	1.57	860	<1	0.70	48	650	20	127	0.34	169	10	122	2
275	<0.2	8.03	600	1	<2	1.56	<0.5	19	96	28	3.89	1.98	1.76	915	<1	0.72	50	690	20	130	0.36	173	<10	124	1
285	<0.2	8.13	610	1	<2	1.51	<0.5	18	98	27	3.99	2.01	1.76	890	<1	0.75	44	690	18	133	0.36	168	10	122	2
295	<0.2	7.73	570	1	<2	1.62	<0.5	15	91	24	3.70	1.90	1.79	855	<1	0.70	41	630	18	122	0.33	164	<10	116	1
305	<0.2	7.97	610	1	<2	1.72	<0.5	18	95	31	3.85	2.02	1.87	835	<1	0.79	45	660	20	136	0.33	163	<10	118	1
315	<0.2	7.60	570	1	<2	2.01	<0.5	15	87	25	3.68	1.92	2.02	895	<1	0.75	42	640	18	130	0.31	156	<10	112	1
325	<0.2	7.80	590	1	<2	2.19	<0.5	16	94	27	3.79	1.97	2.16	920	<1	0.80	45	650	18	136	0.35	157	10	112	1
335	<0.2	7.74	570	1	<2	1.90	<0.5	18	93	27	3.78	1.94	1.98	795	<1	0.73	48	670	18	130	0.33	161	10	116	2
345	<0.2	7.54	550	1	<2	2.32	<0.5	15	90	26	3.68	1.93	2.26	895	<1	0.78	44	650	18	131	0.31	152	10	110	1
355	<0.2	7.76	570	1	<2	2.55	<0.5	15	92	26	3.70	1.97	2.36	915	<1	0.76	44	650	16	132	0.32	158	10	114	2
365	<0.2	7.32	570	1	<2	3.35	<0.5	18	85	27	3.53	1.93	2.87	810	<1	0.85	45	660	16	137	0.32	140	10	104	2

Interval	Ag ppm	Al %	Ba ppm	Be ppm	Bi ppm	Ca %	Cd ppm	Co ppm	Cr ppm	Cu ppm	Fe %	K %	Mg %	Mn ppm	Mo ppm	Na %	Ni ppm	P ppm	Pb ppm	Sr ppm	Ti %	V ppm	W ppm	Zn ppm	As ppm
375	<0.2	7.20	530	1	<2	3.99	<0.5	14	88	26	3.34	1.90	3.14	745	<1	0.86	39	650	14	137	0.31	137	10	102	1
385	<0.2	6.94	510	1	<2	4.64	<0.5	15	79	27	3.13	1.85	3.25	715	<1	0.87	37	640	16	141	0.28	133	<10	96	1
395	<0.2	6.88	530	1	<2	5.42	<0.5	16	86	29	3.12	1.90	3.64	725	<1	0.98	39	680	14	155	0.28	129	10	94	2
405	<0.2	6.15	510	1	<2	6.28	<0.5	14	72	27	3.10	1.75	4.04	695	<1	0.96	35	590	36	152	0.24	107	10	84	4
415	<0.2	6.93	500	1	<2	4.87	<0.5	15	84	29	3.15	1.90	3.31	775	<1	0.93	40	640	14	152	0.28	134	10	98	1
425	<0.2	6.42	490	1	<2	5.37	<0.5	15	76	31	3.08	1.79	3.62	720	<1	1.00	39	630	16	159	0.26	112	<10	86	2
435	<0.2	7.48	510	1	<2	2.15	<0.5	14	85	34	4.09	1.94	2.16	540	<1	0.73	44	640	14	135	0.30	161	10	110	1
445	<0.2	7.49	560	1	<2	5.75	<0.5	16	92	32	3.51	1.96	3.18	675	<1	1.01	40	660	14	179	0.31	139	10	98	1
455	<0.2	7.35	540	1	<2	5.56	<0.5	14	91	31	3.45	1.91	3.20	620	<1	1.02	40	610	14	182	0.30	129	10	96	1
465	<0.2	7.68	540	1	<2	5.19	<0.5	15	93	35	3.58	1.97	3.28	560	<1	1.04	43	610	14	182	0.30	132	10	100	2
475	<0.2	7.63	540	1	<2	2.19	<0.5	15	94	36	4.12	1.98	2.13	775	1	0.76	42	630	14	146	0.30	155	10	110	2

Core 122
Depth (cm)
Al (%)
Ca (%)
Fe (%)
K (%)
Mg (%)
Na (%)
Ti (%)
Co (ppm)
Cr (ppm)
Cu (ppm)
Ni (ppm)
Pb (ppm)
Zn (ppm)
As (ppm)

Core 122
Depth (cm)
Ba (ppm)
Mn (ppm)
P (ppm)
Sr (ppm)
V (ppm)
% moisture
% organic matter
% carbonate
% clay
% silt

Appendix 2

MULTI-PARAMETER CORRELATIONS

LAKE WINNIPEG LONG CORES

PARAMETERS:

Bulk Geochemistry (see Appendix 1)

% H_2O	Moisture Content (from Last, this volume)
% OM	Total Organic Content (from Last, this volume)
% CO_3	Total Carbonate Content (from Last, this volume)
% Clay	(from Last, this volume)
%Sand	(from Last, this volume)
% Silt	(from Last, this volume)

Core 103																							
Lale Winnipeg Sequence (0-685cm)																							
	Al	Ba	Ca	Co	Cr	Cu	Fe	K	Mg	Mn	Na	Ni	Pb	P	Sr	Ti	V	Zn	% H_2O	% OM	% CO_3	%Clay	% Silt	%Sand
Al	1.00																							
Ba	0.70	1.00																						
Ca	-0.19	-0.66	1.00																					
Co	0.40	0.54	-0.44	1.00																				
Cr	0.76	0.76	-0.30	0.47	1.00																			
Cu	0.55	0.74	-0.49	0.55	0.72	1.00																		
Fe	0.76	0.87	-0.58	0.63	0.84	0.78	1.00																	
K	0.42	-0.03	0.53	-0.20	0.20	-0.30	0.03	1.00																
Mg	0.08	-0.48	0.89	-0.33	-0.05	-0.40	-0.31	0.77	1.00															
Mn	0.40	0.74	-0.51	0.53	0.64	0.79	0.66	-0.40	-0.50	1.00														
Na	-0.05	-0.41	0.69	-0.45	-0.24	-0.66	-0.43	0.86	0.77	-0.65	1.00													
Ni	0.56	0.72	-0.45	0.84	0.68	0.75	0.76	-0.18	-0.36	0.76	-0.51	1.00												
Pb	-0.07	0.03	-0.08	0.11	0.13	0.23	0.04	-0.18	-0.09	0.11	-0.17	0.10	1.00											
P	0.38	0.60	-0.42	0.44	0.47	0.75	0.52	-0.34	-0.47	0.77	-0.55	0.65	0.17	1.00										
Sr	0.48	0.25	0.30	-0.01	0.30	-0.13	0.21	0.88	0.51	-0.16	0.74	0.03	-0.16	-0.09	1.00									
Ti	0.61	0.84	-0.59	0.63	0.78	0.87	0.90	-0.23	-0.43	0.76	-0.62	0.76	0.12	0.62	-0.01	1.00								
V	0.67	0.77	-0.61	0.58	0.68	0.83	0.81	-0.30	-0.50	0.73	-0.70	0.75	0.04	0.70	-0.15	0.86	1.00							
Zn	0.74	0.88	-0.60	0.61	0.80	0.85	0.91	-0.10	-0.41	0.71	-0.54	0.77	0.09	0.69	0.08	0.90	0.89	1.00						
% H_2O	0.19	0.69	-0.79	0.44	0.37	0.69	0.52	-0.65	-0.85	0.75	-0.79	0.58	0.14	0.73	-0.36	0.66	0.69	0.67	1.00					
% OM	-0.03	0.35	-0.59	0.28	0.12	0.47	0.19	-0.67	-0.74	0.56	-0.68	0.36	0.20	0.63	-0.48	0.34	0.47	0.35	0.76	1.00				
% CO_3	-0.04	-0.31	0.63	-0.26	-0.13	-0.17	-0.28	0.29	0.56	-0.21	0.34	-0.16	-0.10	-0.15	0.14	-0.24	-0.27	-0.24	-0.40	-0.66	1.00			
%Clay	-0.20	-0.38	0.24	-0.30	-0.29	-0.49	-0.31	0.31	0.30	-0.55	0.47	-0.49	-0.08	-0.51	0.20	-0.46	-0.44	-0.41	-0.48	-0.35	-0.06	1.00		
% Silt	0.20	0.34	-0.21	0.30	0.26	0.50	0.27	-0.35	-0.30	0.53	-0.49	0.49	0.10	0.51	-0.23	0.45	0.45	0.38	0.48	0.41	0.03	-0.95	1.00	
%Sand	0.06	0.21	-0.15	0.09	0.17	0.10	0.18	0.04	-0.08	0.20	-0.04	0.11	-0.04	0.11	0.04	0.13	0.07	0.18	0.11	-0.10	0.09	-0.38	0.09	1.00

Core 103																								
Lale Agassiz Sequence (695-815cm)																								
	Al	Ba	Ca	Co	Cr	Cu	Fe	K	Mg	Mn	Na	Ni	Pb	P	Sr	Ti	V	Zn	% H_2O	% OM	% CO_3	%Clay	% Silt	%Sand
Al	1.00																							
Ba	0.98	1.00																						
Ca	-0.95	-0.92	1.00																					
Co	0.94	0.93	-0.91	1.00																				
Cr	0.89	0.85	-0.89	0.89	1.00																			
Cu	0.67	0.61	-0.70	0.70	0.88	1.00																		
Fe	0.99	0.96	-0.98	0.92	0.92	0.72	1.00																	
K	0.95	0.92	-0.92	0.92	0.89	0.78	0.94	1.00																
Mg	-0.67	-0.62	0.85	-0.60	-0.69	-0.55	-0.77	-0.62	1.00															
Mn	0.58	0.52	-0.55	0.42	0.44	0.38	0.59	0.48	-0.44	1.00														
Na	0.42	0.38	-0.24	0.45	0.35	0.44	0.31	0.58	0.22	0.10	1.00													
Ni	0.93	0.93	-0.90	0.89	0.95	0.79	0.95	0.89	-0.66	0.54	0.33	1.00												
Pb	0.29	0.25	-0.30	0.36	0.58	0.66	0.36	0.25	-0.30	0.42	-0.08	0.47	1.00											
P	0.94	0.92	-0.90	0.89	0.86	0.68	0.94	0.87	-0.66	0.72	0.30	0.90	0.50	1.00										
Sr	-0.48	-0.43	0.71	-0.49	-0.59	-0.48	-0.60	-0.49	0.92	-0.16	0.29	-0.51	-0.23	-0.42	1.00									
Ti	0.99	0.97	-0.92	0.92	0.81	0.59	0.95	0.94	-0.61	0.56	0.48	0.88	0.17	0.91	-0.41	1.00								
V	0.99	0.96	-0.94	0.93	0.89	0.70	0.97	0.95	-0.67	0.54	0.44	0.93	0.28	0.92	-0.48	0.98	1.00							
Zn	0.97	0.95	-0.96	0.94	0.94	0.75	0.99	0.92	-0.75	0.58	0.29	0.96	0.47	0.96	-0.59	0.93	0.96	1.00						
% H_2O	0.89	0.88	-0.79	0.86	0.75	0.60	0.85	0.84	-0.49	0.50	0.48	0.82	0.28	0.80	-0.33	0.91	0.88	0.85	1.00					
% OM	-0.11	-0.09	-0.01	0.01	-0.16	-0.24	-0.10	-0.09	-0.19	-0.60	-0.22	-0.24	-0.41	-0.27	-0.38	-0.06	-0.10	-0.11	0.01	1.00				
% CO_3	-0.68	-0.66	0.76	-0.77	-0.59	-0.39	-0.68	-0.69	0.66	-0.03	-0.21	-0.54	0.04	-0.53	0.69	-0.70	-0.68	-0.66	-0.67	-0.61	1.00			
%Clay	-0.33	-0.32	0.21	-0.25	-0.12	0.00	-0.30	-0.22	-0.05	-0.49	-0.18	-0.29	-0.12	-0.33	-0.16	-0.36	-0.30	-0.29	-0.51	0.28	0.06	1.00		
% Silt	0.21	0.24	-0.15	0.21	0.12	-0.02	0.22	0.06	-0.06	0.17	-0.14	0.18	0.29	0.24	-0.02	0.22	0.19	0.26	0.50	0.19	-0.23	-0.73	1.00	
%Sand	0.25	0.21	-0.15	0.14	0.05	0.02	0.20	0.25	0.15	0.53	0.41	0.23	-0.14	0.23	0.26	0.28	0.24	0.14	0.21	-0.61	0.15	-0.68	-0.01	1.00

Core 104A																								
Lake Winnipeg Sequence (0-365cm)																								
	Al	Ba	Ca	Co	Cr	Cu	Fe	K	Mg	Mn	Na	Ni	P	Pb	Sr	Ti	V	Zn	% H_2O	% OM	% CO_3	%Clay	%Sand	% Silt
Al	1.00																							
Ba	0.94	1.00																						
Ca	-0.60	-0.63	1.00																					
Co	0.91	0.86	-0.59	1.00																				
Cr	0.97	0.88	-0.63	0.90	1.00																			
Cu	0.94	0.91	-0.69	0.94	0.95	1.00																		
Fe	0.96	0.90	-0.69	0.91	0.98	0.97	1.00																	
K	0.79	0.68	0.00	0.67	0.75	0.64	0.69	1.00																
Mg	0.08	-0.05	0.68	0.03	0.09	-0.05	0.02	0.64	1.00															
Mn	0.78	0.81	-0.45	0.86	0.73	0.85	0.77	0.59	0.03	1.00														
Na	-0.30	-0.29	0.75	-0.41	-0.45	-0.54	-0.52	0.16	0.49	-0.28	1.00													
Ni	0.90	0.90	-0.73	0.95	0.88	0.96	0.92	0.56	-0.15	0.87	-0.50	1.00												
P	0.86	0.85	-0.30	0.84	0.77	0.81	0.77	0.80	0.22	0.84	-0.01	0.80	1.00											
Pb	0.57	0.66	-0.82	0.53	0.59	0.69	0.65	0.10	-0.53	0.51	-0.64	0.70	0.38	1.00										
Sr	-0.11	-0.09	0.66	-0.23	-0.29	-0.36	-0.35	0.30	0.51	-0.11	0.97	-0.33	0.17	-0.53	1.00									
Ti	0.97	0.91	-0.66	0.92	0.98	0.97	0.98	0.72	0.04	0.78	-0.45	0.92	0.82	0.63	-0.26	1.00								
V	0.95	0.92	-0.79	0.91	0.95	0.97	0.97	0.58	-0.16	0.79	-0.55	0.95	0.77	0.74	-0.36	0.97	1.00							
Zn	0.94	0.88	-0.75	0.91	0.97	0.97	0.98	0.62	-0.09	0.76	-0.60	0.93	0.73	0.70	-0.44	0.97	0.98	1.00						
% H_2O	0.64	0.67	-0.94	0.69	0.69	0.79	0.75	0.09	-0.56	0.59	-0.82	0.82	0.42	0.85	-0.71	0.73	0.84	0.82	1.00					
% OM	0.62	0.64	-0.94	0.68	0.67	0.76	0.72	0.06	-0.57	0.56	-0.81	0.79	0.37	0.77	-0.70	0.70	0.82	0.79	0.97	1.00				
% CO_3	-0.51	-0.58	0.96	-0.52	-0.52	-0.60	-0.57	0.10	0.76	-0.42	0.65	-0.66	-0.27	-0.77	0.56	-0.56	-0.71	-0.64	-0.90	-0.91	1.00			
%Clay	0.04	-0.05	0.05	-0.07	0.11	-0.04	0.01	0.12	0.16	-0.18	0.08	-0.10	-0.08	0.00	0.07	0.01	-0.01	0.00	-0.04	0.01	0.00	1.00		
%Sand	0.07	0.12	0.07	0.27	0.04	0.13	0.07	0.11	0.09	0.33	0.02	0.19	0.29	0.07	0.05	0.11	0.08	0.06	0.05	-0.03	0.05	-0.35	1.00	
% Silt	-0.09	-0.04	-0.10	-0.12	-0.13	-0.06	-0.06	-0.19	-0.23	-0.07	-0.09	-0.04	-0.14	-0.06	-0.10	-0.10	-0.05	-0.05	0.01	0.01	-0.03	-0.73	-0.39	1.00

Core 105																								
Lake Winnipeg Sequence (0-64.5 cm)																								
	Al	Ba	Ca	Co	Cr	Cu	Fe	K	Mg	Mn	Na	Ni	P	Pb	Sr	Tl	V	Zn	% H_2	% OM	% CO	% Cla	% San	% Silt
Al	1.00																							
Ba	0.96	1.00																						
Ca	-0.97	-0.89	1.00																					
Co	0.77	0.81	-0.62	1.00																				
Cr	0.85	0.80	-0.75	0.76	1.00																			
Cu	0.99	0.93	-0.95	0.82	0.82	1.00																		
Fe	0.93	0.96	-0.81	0.88	0.83	0.92	1.00																	
K	0.94	0.85	-0.93	0.67	0.92	0.91	0.80	1.00																
Mg	-0.18	-0.10	0.31	0.29	-0.30	-0.07	0.09	-0.44	1.00															
Mn	0.80	0.87	-0.65	0.94	0.69	0.83	0.95	0.62	0.36	1.00														
Na	-0.15	-0.29	-0.07	-0.70	-0.22	-0.23	-0.47	0.03	-0.79	-0.70	1.00													
Ni	0.96	0.91	-0.90	0.80	0.89	0.96	0.94	0.90	-0.07	0.84	-0.27	1.00												
P	0.94	0.95	-0.93	0.71	0.65	0.93	0.87	0.81	-0.10	0.78	-0.14	0.83	1.00											
Pb	0.76	0.76	-0.62	0.74	0.78	0.74	0.89	0.65	0.19	0.84	-0.50	0.89	0.59	1.00										
Sr	-0.03	-0.18	-0.18	-0.57	-0.12	-0.10	-0.39	0.16	-0.83	-0.62	0.98	-0.19	-0.02	-0.50	1.00									
Tl	0.97	0.92	-0.92	0.85	0.80	0.99	0.93	0.86	0.05	0.87	-0.32	0.96	0.90	0.79	-0.20	1.00								
V	0.96	0.96	-0.88	0.89	0.81	0.97	0.98	0.84	0.09	0.93	-0.41	0.96	0.91	0.85	-0.31	0.98	1.00							
Zn	0.93	0.95	-0.86	0.81	0.73	0.93	0.97	0.76	0.13	0.92	-0.39	0.94	0.90	0.87	-0.32	0.95	0.98	1.00						
% H_2O	0.85	0.88	-0.74	0.87	0.63	0.88	0.94	0.64	0.36	0.97	-0.58	0.87	0.84	0.84	-0.50	0.92	0.95	0.97	1.00					
% OM	0.85	0.91	-0.76	0.77	0.63	0.85	0.95	0.64	0.24	0.93	-0.47	0.87	0.86	0.86	-0.42	0.88	0.93	0.98	0.97	1.00				
% CO_3	-0.88	-0.83	0.92	-0.42	-0.76	-0.80	-0.70	-0.92	0.60	-0.47	-0.28	-0.79	-0.83	-0.52	-0.37	-0.74	-0.72	-0.71	-0.53	-0.62	1.00			
% Clay	-0.49	-0.56	0.27	-0.84	-0.73	-0.52	-0.73	-0.45	-0.33	-0.79	0.80	-0.64	-0.32	-0.80	0.75	-0.57	-0.65	-0.59	-0.65	-0.59	0.18	1.00		
% Sand	-0.65	-0.68	0.75	-0.21	-0.35	-0.58	-0.46	-0.62	0.55	-0.28	-0.38	-0.44	-0.79	-0.11	-0.48	-0.50	-0.49	-0.50	-0.35	-0.46	0.83	-0.19	1.00	
% Silt	0.77	0.84	-0.59	0.92	0.87	0.76	0.92	0.71	0.09	0.91	-0.63	0.82	0.65	0.84	-0.54	0.78	0.86	0.80	0.80	0.78	-0.53	-0.91	-0.24	1.00

Core 105																								
Lake Agassiz Sequence (64.5-596 cm)																								
	Al	Ba	Ca	Co	Cr	Cu	Fe	K	Mg	Mn	Na	Ni	P	Pb	Sr	Ti	V	Zn	% H_2	% OM	% CO	% Cla	% San	% Silt
Al	1.00																							
Ba	0.87	1.00																						
Ca	-0.79	-0.66	1.00																					
Co	0.95	0.79	-0.73	1.00																				
Cr	0.96	0.78	-0.74	0.98	1.00																			
Cu	0.97	0.81	-0.79	0.97	0.98	1.00																		
Fe	0.96	0.76	-0.79	0.98	0.98	0.98	1.00																	
K	0.98	0.88	-0.69	0.95	0.95	0.95	0.94	1.00																
Mg	0.46	0.43	0.07	0.51	0.52	0.48	0.43	0.58	1.00															
Mn	0.90	0.70	-0.60	0.95	0.95	0.93	0.95	0.91	0.58	1.00														
Na	-0.67	-0.30	0.69	-0.73	-0.76	-0.75	-0.80	-0.63	-0.26	-0.73	1.00													
Ni	0.96	0.80	-0.75	0.98	0.98	0.98	0.98	0.94	0.50	0.95	-0.73	1.00												
P	0.91	0.82	-0.61	0.86	0.84	0.83	0.82	0.91	0.52	0.77	-0.44	0.84	1.00											
Pb	0.91	0.73	-0.79	0.88	0.89	0.92	0.90	0.88	0.45	0.84	-0.74	0.89	0.77	1.00										
Sr	-0.69	-0.36	0.75	-0.76	-0.77	-0.77	-0.83	-0.64	-0.20	-0.74	0.98	-0.76	-0.43	-0.75	1.00									
Ti	0.96	0.78	-0.72	0.95	0.96	0.97	0.96	0.94	0.54	0.93	-0.75	0.96	0.85	0.90	-0.75	1.00								
V	0.97	0.77	-0.80	0.96	0.97	0.98	0.98	0.94	0.48	0.92	-0.80	0.97	0.84	0.93	-0.81	0.98	1.00							
Zn	0.97	0.78	-0.81	0.97	0.98	0.98	0.99	0.95	0.46	0.93	-0.81	0.98	0.83	0.92	-0.83	0.97	0.99	1.00						
% H_2O	0.86	0.62	-0.77	0.85	0.88	0.89	0.88	0.82	0.43	0.79	-0.83	0.86	0.72	0.89	-0.83	0.88	0.93	0.91	1.00					
% OM	0.84	0.67	-0.76	0.86	0.88	0.91	0.88	0.81	0.39	0.82	-0.78	0.89	0.66	0.84	-0.82	0.87	0.90	0.90	0.86	1.00				
% CO_3	-0.74	-0.68	0.90	-0.68	-0.69	-0.75	-0.73	-0.65	-0.01	-0.56	0.57	-0.71	-0.57	-0.74	0.63	-0.69	-0.75	-0.74	-0.71	-0.76	1.00			
% Clay	0.14	0.06	0.02	0.12	0.09	0.12	0.07	0.15	0.24	0.13	-0.05	0.08	0.18	0.07	-0.03	0.18	0.14	0.11	0.11	0.04	0.01	1.00		
% Sand	-0.13	-0.11	0.02	-0.12	-0.08	-0.10	-0.04	-0.14	-0.20	-0.03	-0.04	-0.04	-0.24	-0.11	-0.06	-0.14	-0.11	-0.08	-0.07	0.02	-0.03	-0.54	1.00	
% Silt	-0.08	-0.01	-0.03	-0.07	-0.05	-0.08	-0.06	-0.09	-0.15	-0.14	0.08	-0.07	-0.06	-0.01	0.07	-0.12	-0.09	-0.08	-0.09	-0.06	0.00	-0.85	0.02	1.00

Core 106																								
Lake Winnipeg Sequence (0-182 cm)																								
	Al	Ba	Ca	Co	Cr	Cu	Fe	K	Mg	Mn	Na	Ni	P	Pb	Sr	Ti	V	Zn	% H_2O	% OM	% CO	Cla	San	% Silt
Al	1.00																							
Ba	0.98	1.00																						
Ca	-0.14	-0.06	1.00																					
Co	0.95	0.89	-0.32	1.00																				
Cr	0.98	0.93	-0.27	0.96	1.00																			
Cu	0.80	0.81	-0.41	0.83	0.84	1.00																		
Fe	0.95	0.89	-0.43	0.98	0.98	0.83	1.00																	
K	0.97	0.96	0.08	0.89	0.92	0.72	0.86	1.00																
Mg	0.72	0.68	0.43	0.67	0.67	0.42	0.57	0.84	1.00															
Mn	0.82	0.85	-0.37	0.81	0.83	0.98	0.82	0.74	0.40	1.00														
Na	0.51	0.61	0.72	0.28	0.36	0.18	0.22	0.66	0.69	0.26	1.00													
Ni	0.91	0.86	-0.45	0.95	0.95	0.87	0.97	0.82	0.53	0.86	0.17	1.00												
P	0.97	0.97	-0.10	0.92	0.94	0.86	0.90	0.95	0.72	0.87	0.54	0.89	1.00											
Pb	0.83	0.84	-0.38	0.84	0.84	0.94	0.85	0.75	0.42	0.94	0.24	0.84	0.85	1.00										
Sr	0.60	0.69	0.64	0.37	0.45	0.27	0.32	0.73	0.70	0.35	0.99	0.27	0.62	0.33	1.00									
Ti	0.97	0.93	-0.29	0.97	0.99	0.86	0.97	0.91	0.65	0.85	0.34	0.95	0.95	0.86	0.44	1.00								
V	0.94	0.88	-0.45	0.97	0.97	0.87	0.99	0.84	0.53	0.85	0.19	0.97	0.91	0.87	0.29	0.98	1.00							
Zn	0.93	0.86	-0.48	0.97	0.97	0.84	1.00	0.83	0.53	0.82	0.15	0.97	0.88	0.85	0.25	0.97	0.99	1.00						
% H_2O	0.38	0.33	-0.91	0.53	0.49	0.72	0.60	0.18	-0.17	0.68	-0.50	0.66	0.40	0.66	-0.41	0.52	0.65	0.65	1.00					
% OM	0.36	0.30	-0.95	0.53	0.48	0.65	0.61	0.16	-0.22	0.61	-0.54	0.66	0.36	0.59	-0.46	0.51	0.65	0.66	0.97	1.00				
% CO_3	-0.31	-0.28	0.94	-0.42	-0.40	-0.54	-0.54	-0.10	0.37	-0.54	0.49	-0.56	-0.28	-0.52	0.40	-0.42	-0.56	-0.57	-0.90	-0.95	1.00			
% Clay	-0.11	-0.18	-0.48	-0.01	-0.06	-0.24	0.05	-0.21	-0.36	-0.23	-0.44	-0.01	-0.19	-0.16	-0.42	-0.07	0.04	0.07	0.24	0.30	-0.40	1.00		
% Sand	0.03	0.05	0.08	0.07	0.04	0.20	0.01	0.07	0.19	0.14	0.04	0.10	0.17	0.21	0.04	0.09	0.06	0.02	0.11	0.05	0.09	-0.38	1.00	
% Silt	0.18	0.23	0.30	0.13	0.17	0.38	0.07	0.24	0.32	0.34	0.31	0.11	0.26	0.34	0.31	0.18	0.10	0.07	-0.05	-0.11	0.23	-0.92	0.43	1.00

Core 106																								
LakeAgassiz Sequence (182-789 cm)																								
	Al	Ba	Ca	Co	Cr	Cu	Fe	K	Mg	Mn	Na	Ni	P	Pb	Sr	Tl	V	Zn	% H_2O	% OM	% CO	Cla	San	% Silt
Al	1.00																							
Ba	0.91	1.00																						
Ca	-0.97	-0.88	1.00																					
Co	0.96	0.85	-0.90	1.00																				
Cr	0.97	0.84	-0.93	0.97	1.00																			
Cu	0.92	0.82	-0.91	0.91	0.93	1.00																		
Fe	0.98	0.86	-0.95	0.97	0.99	0.94	1.00																	
K	0.79	0.90	-0.72	0.77	0.74	0.69	0.76	1.00																
Mg	-0.60	-0.35	0.64	-0.55	-0.64	-0.54	-0.63	-0.12	1.00															
Mn	0.44	0.38	-0.33	0.53	0.53	0.59	0.51	0.43	-0.11	1.00														
Na	-0.19	0.13	0.17	-0.29	-0.33	-0.25	-0.34	0.11	0.56	-0.25	1.00													
Ni	0.96	0.84	-0.92	0.95	0.97	0.91	0.98	0.73	-0.65	0.50	-0.32	1.00												
P	0.69	0.68	-0.64	0.75	0.72	0.71	0.72	0.82	-0.14	0.46	-0.11	0.67	1.00											
Pb	0.29	0.29	-0.28	0.32	0.32	0.46	0.30	0.13	-0.22	0.16	0.00	0.33	0.16	1.00										
Sr	-0.79	-0.59	0.81	-0.80	-0.84	-0.77	-0.87	-0.53	0.73	-0.35	0.67	-0.84	-0.56	-0.21	1.00									
Tl	0.94	0.87	-0.93	0.92	0.93	0.93	0.95	0.75	-0.52	0.51	-0.19	0.91	0.73	0.28	-0.77	1.00								
V	0.97	0.81	-0.95	0.95	0.97	0.95	0.98	0.67	-0.69	0.47	-0.34	0.95	0.68	0.32	-0.85	0.94	1.00							
Zn	0.98	0.87	-0.96	0.97	0.98	0.94	1.00	0.75	-0.65	0.50	-0.31	0.97	0.70	0.30	-0.86	0.95	0.98	1.00						
% H_2O	0.86	0.79	-0.83	0.86	0.89	0.83	0.90	0.76	-0.51	0.45	-0.35	0.87	0.71	0.24	-0.83	0.83	0.84	0.89	1.00					
% OM	0.66	0.41	-0.64	0.66	0.71	0.61	0.70	0.33	-0.72	0.21	-0.57	0.68	0.43	0.14	-0.74	0.59	0.72	0.70	0.72	1.00				
% CO_3	-0.91	-0.79	0.93	-0.85	-0.89	-0.84	-0.89	-0.63	0.66	-0.30	0.21	-0.88	-0.59	-0.20	0.75	-0.86	-0.91	-0.90	-0.85	-0.79	1.00			
% Clay	0.28	0.08	-0.29	0.25	0.32	0.32	0.32	0.02	-0.39	0.16	-0.43	0.28	0.19	0.00	-0.39	0.29	0.38	0.33	0.26	0.34	-0.30	1.00		
% Sand	-0.12	-0.10	0.14	-0.02	-0.06	-0.09	-0.10	-0.14	0.05	0.07	-0.06	-0.06	-0.17	0.17	0.05	-0.10	-0.12	-0.10	-0.10	-0.09	0.17	-0.40	1.00	
% Silt	-0.20	-0.01	0.23	-0.15	-0.21	-0.22	-0.23	0.08	0.36	-0.03	0.37	-0.20	-0.08	0.02	0.31	-0.22	-0.30	-0.24	-0.15	-0.26	0.24	-0.93	0.43	1.00

Core 107																								
Lake Winnipeg Sequence (0-194 cm)																								
	Al	Ba	Ca	Co	Cr	Cu	Fe	K	Mg	Mn	Na	Ni	P	Pb	Sr	Tl	V	Zn	% H_2	% OM	% CO	% Cla	% Sand	% Silt
Al	1.00																							
Ba	0.90	1.00																						
Ca	-0.65	-0.54	1.00																					
Co	0.83	0.76	-0.47	1.00																				
Cr	0.71	0.54	-0.44	0.64	1.00																			
Cu	0.91	0.71	-0.62	0.78	0.79	1.00																		
Fe	0.94	0.79	-0.70	0.86	0.76	0.96	1.00																	
K	0.89	0.85	-0.29	0.79	0.60	0.80	0.82	1.00																
Mg	-0.05	-0.12	0.71	0.09	0.12	0.07	-0.02	0.31	1.00															
Mn	0.46	0.33	-0.08	0.42	0.66	0.62	0.45	0.49	0.36	1.00														
Na	-0.50	-0.20	0.61	-0.42	-0.61	-0.74	-0.65	-0.28	0.07	-0.59	1.00													
Ni	0.84	0.76	-0.48	0.93	0.79	0.79	0.84	0.78	0.09	0.53	-0.46	1.00												
P	0.76	0.81	-0.20	0.62	0.59	0.55	0.59	0.82	0.16	0.44	-0.09	0.67	1.00											
Pb	0.20	0.12	-0.33	0.21	0.41	0.27	0.24	0.08	-0.19	0.15	-0.28	0.36	0.15	1.00										
Sr	-0.47	-0.14	0.50	-0.42	-0.61	-0.74	-0.64	-0.32	-0.08	-0.61	0.98	-0.46	-0.07	-0.27	1.00									
Tl	0.88	0.71	-0.52	0.83	0.88	0.90	0.93	0.83	0.14	0.52	-0.56	0.87	0.66	0.31	-0.58	1.00								
V	0.85	0.58	-0.61	0.69	0.75	0.89	0.84	0.70	0.00	0.64	-0.79	0.73	0.55	0.19	-0.77	0.81	1.00							
Zn	0.93	0.73	-0.71	0.77	0.81	0.97	0.96	0.79	-0.04	0.57	-0.75	0.81	0.61	0.28	-0.74	0.91	0.94	1.00						
% H_2O	0.68	0.56	-0.92	0.49	0.61	0.69	0.73	0.32	-0.56	0.23	-0.66	0.55	0.28	0.39	-0.56	0.57	0.63	0.75	1.00					
% OM	0.58	0.55	-0.87	0.39	0.47	0.60	0.61	0.23	-0.58	0.13	-0.59	0.44	0.18	0.31	-0.47	0.43	0.52	0.62	0.92	1.00				
% CO_3	-0.47	-0.51	0.85	-0.30	-0.23	-0.37	-0.50	-0.15	0.74	0.25	0.22	-0.28	-0.08	-0.17	0.11	-0.32	-0.23	-0.43	-0.81	-0.81	1.00			
% Clay	0.22	0.21	-0.13	0.02	-0.24	0.18	0.16	0.24	0.00	-0.23	-0.05	-0.09	0.08	-0.02	-0.02	-0.06	0.09	0.14	0.11	0.24	-0.14	1.00		
% Sand	-0.18	-0.14	0.14	0.01	0.21	-0.16	-0.13	-0.20	0.03	0.18	0.11	0.13	-0.07	-0.04	0.08	0.07	-0.12	-0.14	-0.11	-0.21	0.10	-0.96	1.00	
% Silt	-0.16	-0.29	-0.01	-0.12	0.14	-0.08	-0.12	-0.17	-0.08	0.19	-0.21	-0.14	-0.04	0.23	-0.22	-0.02	0.08	-0.01	-0.01	-0.10	0.16	-0.21	-0.06	1.00

Core 107																								
Lake Agassiz Sediments (194-696 cm)																								
	Al	Ba	Ca	Co	Cr	Cu	Fe	K	Mg	Mn	Na	Ni	P	Pb	Sr	Tl	V	Zn	% H_2	% OM	% CO	% Cla	% Sand	% Silt
Al	1.00																							
Ba	0.84	1.00																						
Ca	-0.26	-0.25	1.00																					
Co	0.60	0.66	-0.45	1.00																				
Cr	0.38	0.48	0.07	0.65	1.00																			
Cu	0.67	0.61	0.00	0.57	0.75	1.00																		
Fe	0.66	0.67	-0.52	0.84	0.67	0.73	1.00																	
K	0.68	0.71	0.30	0.46	0.69	0.81	0.54	1.00																
Mg	-0.07	-0.07	0.90	-0.23	0.28	0.20	-0.27	0.50	1.00															
Mn	0.14	0.13	-0.51	0.40	-0.03	-0.09	0.21	-0.32	-0.55	1.00														
Na	-0.06	0.21	0.68	-0.19	0.18	0.02	-0.31	0.48	0.72	-0.51	1.00													
Ni	0.57	0.69	-0.43	0.79	0.71	0.65	0.84	0.51	-0.23	0.27	-0.13	1.00												
P	0.56	0.67	-0.15	0.64	0.50	0.36	0.48	0.45	0.04	0.44	0.13	0.59	1.00											
Pb	0.24	0.07	-0.06	0.13	0.26	0.39	0.20	0.20	-0.03	0.00	-0.12	0.26	-0.02	1.00										
Sr	-0.12	0.25	0.55	-0.11	0.17	-0.08	-0.28	0.35	0.58	-0.32	0.94	-0.06	0.26	-0.24	1.00									
Tl	0.72	0.58	-0.42	0.66	0.52	0.62	0.70	0.38	-0.26	0.46	-0.37	0.65	0.55	0.28	-0.34	1.00								
V	0.69	0.54	-0.71	0.64	0.17	0.35	0.62	0.07	-0.63	0.68	-0.62	0.57	0.53	0.16	-0.52	0.82	1.00							
Zn	0.83	0.67	-0.52	0.72	0.49	0.69	0.82	0.49	-0.33	0.23	-0.38	0.74	0.48	0.33	-0.42	0.84	0.78	1.00						
% H_2O	0.04	0.24	-0.67	0.54	0.23	-0.07	0.53	-0.12	-0.50	0.31	-0.30	0.45	0.31	-0.17	-0.14	0.13	0.33	0.27	1.00					
% OM	0.37	0.28	-0.46	0.42	0.06	-0.01	0.43	-0.03	-0.34	0.26	-0.33	0.31	0.38	-0.15	-0.25	0.30	0.49	0.45	0.54	1.00				
% CO_3	-0.25	-0.32	0.67	-0.44	-0.02	0.13	-0.44	0.12	0.49	-0.26	0.29	-0.36	-0.41	0.18	0.14	-0.19	-0.45	-0.37	-0.79	-0.84	1.00			
% Clay	0.19	0.12	-0.12	-0.04	0.03	0.15	0.24	0.11	-0.08	-0.02	-0.16	0.17	-0.01	-0.10	-0.16	0.04	0.11	0.14	0.00	0.22	-0.16	1.00		
% Sand	-0.07	-0.21	0.22	-0.04	0.03	0.01	-0.26	-0.05	0.27	0.07	0.08	-0.17	0.10	0.17	0.02	0.17	-0.03	-0.03	-0.29	-0.20	0.27	-0.69	1.00	
% Silt	-0.15	0.12	-0.14	0.10	-0.08	-0.20	0.04	-0.07	-0.25	-0.07	0.10	0.01	-0.12	-0.09	0.17	-0.27	-0.09	-0.15	0.38	-0.03	-0.15	-0.36	-0.42	1.00

Core 110a																								
Lake Winnipeg Sequence (0-209 cm)																								
	Al	Ba	Ca	Co	Cr	Cu	Fe	K	Mg	Mn	Na	Ni	P	Pb	Sr	Tl	V	Zn	% H_2O	% OM	% CO_3	% Clay	% Sand	% Silt
Al	1.00																							
Ba	0.78	1.00																						
Ca	-0.48	-0.26	1.00																					
Co	0.56	0.17	-0.12	1.00																				
Cr	0.87	0.53	-0.35	0.71	1.00																			
Cu	0.22	0.33	-0.11	0.29	0.37	1.00																		
Fe	0.91	0.59	-0.45	0.63	0.95	0.35	1.00																	
K	0.85	0.81	-0.03	0.52	0.79	0.36	0.78	1.00																
Mg	0.27	0.23	0.66	0.34	0.42	0.18	0.35	0.64	1.00															
Mn	0.60	0.35	0.11	0.62	0.80	0.36	0.79	0.69	0.73	1.00														
Na	-0.70	-0.27	0.44	-0.51	-0.85	-0.27	-0.89	-0.54	-0.31	-0.72	1.00													
Ni	0.42	-0.03	-0.58	0.61	0.51	0.21	0.52	0.10	-0.21	0.27	-0.52	1.00												
P	0.75	0.73	-0.04	0.44	0.72	0.25	0.77	0.88	0.58	0.74	-0.54	0.02	1.00											
Pb	-0.20	-0.07	0.18	-0.26	-0.20	-0.08	-0.17	-0.06	0.09	-0.15	0.06	-0.64	0.04	1.00										
Sr	-0.66	-0.20	0.38	-0.55	-0.86	-0.30	-0.87	-0.53	-0.36	-0.75	0.99	-0.55	-0.50	0.10	1.00									
Tl	0.95	0.70	-0.45	0.61	0.89	0.31	0.92	0.84	0.31	0.63	-0.77	0.42	0.74	-0.11	-0.73	1.00								
V	0.95	0.59	-0.56	0.63	0.92	0.21	0.95	0.74	0.21	0.65	-0.84	0.56	0.67	-0.21	-0.83	0.93	1.00							
Zn	0.62	0.34	-0.35	0.71	0.78	0.70	0.80	0.55	0.27	0.71	-0.75	0.52	0.53	-0.08	-0.76	0.72	0.70	1.00						
% H_2O	0.24	-0.19	-0.57	0.28	0.33	-0.16	0.29	-0.16	-0.42	0.11	-0.33	0.62	-0.17	-0.34	-0.38	0.14	0.42	0.23	1.00					
% OM	0.06	-0.40	-0.25	0.46	0.31	0.06	0.19	-0.18	-0.18	0.21	-0.26	0.59	-0.22	-0.30	-0.35	0.05	0.26	0.36	0.85	1.00				
% CO_3	0.16	0.29	0.57	0.03	0.23	0.02	0.20	0.47	0.79	0.54	-0.18	-0.38	0.49	0.14	-0.21	0.16	0.10	0.04	-0.44	-0.43	1.00			
% Clay	0.40	0.64	0.05	0.02	0.10	-0.06	0.12	0.49	0.20	0.02	0.07	-0.27	0.40	-0.03	0.10	0.30	0.24	-0.10	-0.28	-0.49	0.42	1.00		
% Sand	-0.49	-0.47	0.01	-0.32	-0.33	-0.20	-0.34	-0.60	-0.31	-0.18	0.15	-0.20	-0.47	0.33	0.14	-0.46	-0.39	-0.18	0.25	0.27	-0.24	-0.52	1.00	
% Silt	-0.18	-0.48	-0.06	0.16	0.08	0.19	0.05	-0.23	-0.05	0.08	-0.17	0.43	-0.19	-0.15	-0.20	-0.08	-0.05	0.22	0.18	0.42	-0.35	-0.87	0.02	1.00

Core 113a																							
Lake Winnipeg Sequence (0-214 cm)																							
	Al	Ba	Ca	Co	Cr	Cu	Fe	K	Mg	Mn	Na	Ni	Pb	P	Sr	Tl	V	Zn	% H_2O	% OM	% CO_3	%Clay	% Silt	%Sand
Al	1.00																						
Ba	0.40	1.00																					
Ca	0.54	-0.34	1.00																				
Co	0.82	0.44	0.41	1.00																			
Cr	0.87	0.14	0.71	0.74	1.00																		
Cu	-0.02	-0.09	-0.19	0.15	0.12	1.00																	
Fe	0.83	0.15	0.78	0.76	0.92	0.00	1.00																
K	0.93	0.36	0.69	0.80	0.90	-0.13	0.94	1.00															
Mg	0.67	-0.21	0.98	0.53	0.81	-0.16	0.87	0.80	1.00														
Mn	-0.09	-0.61	0.17	-0.24	0.03	0.08	-0.07	-0.22	0.11	1.00													
Na	-0.69	0.23	-0.94	-0.52	-0.84	0.09	-0.89	-0.80	-0.98	-0.18	1.00												
Ni	0.71	0.22	0.32	0.72	0.76	0.46	0.58	0.57	0.41	0.09	-0.45	1.00											
Pb	-0.12	-0.09	-0.43	-0.20	-0.23	0.32	-0.39	-0.41	-0.43	0.65	0.36	0.20	1.00										
P	0.55	0.53	-0.08	0.36	0.37	-0.06	0.20	0.38	0.03	0.20	-0.07	0.47	0.40	1.00									
Sr	-0.67	0.25	-0.95	-0.50	-0.82	0.11	-0.88	-0.79	-0.98	-0.21	1.00	-0.42	0.35	-0.07	1.00								
Tl	0.84	0.54	0.46	0.79	0.82	0.07	0.85	0.91	0.60	-0.42	-0.62	0.58	-0.43	0.36	-0.59	1.00							
V	0.89	0.22	0.69	0.76	0.92	0.08	0.94	0.95	0.81	-0.16	-0.85	0.61	-0.38	0.31	-0.83	0.90	1.00						
Zn	0.88	0.08	0.74	0.70	0.90	0.00	0.92	0.89	0.84	0.15	-0.90	0.63	-0.16	0.39	-0.89	0.76	0.93	1.00					
% H_2O	-0.73	-0.33	-0.68	-0.66	-0.72	0.17	-0.83	-0.88	-0.76	0.46	0.70	-0.35	0.64	-0.11	0.69	-0.80	-0.84	-0.69	1.00				
% OM	-0.80	-0.35	-0.69	-0.67	-0.75	0.38	-0.84	-0.92	-0.78	0.34	0.74	-0.37	0.55	-0.26	0.73	-0.81	-0.85	-0.77	0.92	1.00			
% CO_3	0.64	-0.19	0.97	0.49	0.77	-0.25	0.84	0.79	0.99	0.07	-0.95	0.36	-0.46	0.01	-0.95	0.58	0.77	0.80	-0.76	-0.81	1.00		
%Clay	0.50	0.47	0.23	0.61	0.44	-0.26	0.50	0.59	0.31	-0.49	-0.29	0.27	-0.50	0.32	-0.28	0.63	0.51	0.38	-0.57	-0.61	0.33	1.00	
% Silt	-0.25	-0.24	-0.26	-0.41	-0.26	0.25	-0.38	-0.39	-0.29	0.53	0.25	-0.08	0.64	0.02	0.25	-0.51	-0.37	-0.22	0.46	0.52	-0.35	-0.84	1.00
%Sand	-0.29	-0.27	0.12	-0.18	-0.19	-0.06	-0.07	-0.18	0.06	-0.22	-0.02	-0.27	-0.41	-0.53	-0.02	-0.04	-0.11	-0.19	0.04	-0.02	0.13	0.00	-0.55	1.00

Core 115																							
Lake Winnipeg Sediments (0-276 cm)																							
	Al	Ba	Ca	Co	Cr	Cu	Fe	K	Mg	Mn	Na	Ni	P	Pb	Sr	Ti	V	Zn	As	% H_2	% OM	% CO	%Cla
Al	1.00																						
Ba	0.97	1.00																					
Ca	-0.70	-0.58	1.00																				
Co	0.81	0.86	-0.38	1.00																			
Cr	0.98	0.94	-0.67	0.80	1.00																		
Cu	0.61	0.66	-0.15	0.65	0.60	1.00																	
Fe	0.99	0.95	-0.70	0.81	0.98	0.62	1.00																
K	0.89	0.95	-0.36	0.84	0.86	0.71	0.87	1.00															
Mg	-0.13	-0.01	0.79	0.12	-0.10	0.23	-0.13	0.22	1.00														
Mn	0.94	0.91	-0.59	0.76	0.93	0.52	0.94	0.87	-0.02	1.00													
Na	-0.36	-0.15	0.77	0.03	-0.38	0.22	-0.39	0.08	0.68	-0.33	1.00												
Ni	0.56	0.61	-0.15	0.70	0.57	0.95	0.58	0.64	0.18	0.45	0.24	1.00											
P	0.46	0.57	0.04	0.60	0.43	0.49	0.44	0.74	0.37	0.53	0.45	0.45	1.00										
Pb	0.82	0.73	-0.80	0.50	0.80	0.42	0.82	0.61	-0.42	0.79	-0.62	0.30	0.20	1.00									
Sr	-0.26	-0.05	0.71	0.10	-0.28	0.25	-0.30	0.19	0.68	-0.23	0.98	0.25	0.55	-0.52	1.00								
Ti	0.96	0.97	-0.58	0.88	0.95	0.70	0.95	0.91	-0.01	0.88	-0.18	0.67	0.49	0.69	-0.09	1.00							
V	0.99	0.95	-0.74	0.80	0.97	0.57	0.98	0.87	-0.20	0.95	-0.40	0.52	0.47	0.85	-0.30	0.93	1.00						
Zn	0.95	0.92	-0.64	0.81	0.94	0.76	0.96	0.85	-0.12	0.86	-0.31	0.72	0.47	0.78	-0.23	0.94	0.94	1.00					
As	0.02	-0.05	-0.23	-0.04	0.02	-0.12	0.00	-0.06	-0.34	-0.01	-0.20	-0.12	-0.10	0.18	-0.16	-0.04	0.05	-0.02	1.00				
% H_2O	0.71	0.61	-0.74	0.42	0.69	0.29	0.72	0.48	-0.41	0.69	-0.63	0.20	0.13	0.82	-0.56	0.57	0.73	0.69	0.03	1.00			
% OM	0.82	0.69	-0.81	0.48	0.81	0.36	0.84	0.56	-0.42	0.79	-0.70	0.28	0.20	0.90	-0.62	0.67	0.83	0.81	0.15	0.87	1.00		
% CO_3	-0.48	-0.34	0.81	-0.13	-0.46	-0.10	-0.51	-0.19	0.73	-0.41	0.70	-0.07	0.01	-0.71	0.64	-0.31	-0.52	-0.47	-0.43	-0.63	-0.79	1.00	
%Clay	-0.23	-0.18	0.21	0.01	-0.19	0.07	-0.23	-0.19	0.07	-0.26	0.27	0.23	-0.17	-0.31	0.19	-0.17	-0.22	-0.18	-0.04	-0.23	-0.35	0.38	1.00

Core 119																			
Lake Winnipeg Sequence (0-171 cm)																			
	Al	Ba	Ca	Co	Cr	Cu	Fe	K	Mg	Mn	Na	Ni	P	Pb	Sr	Ti	V	Zn	As
Al	1.00																		
Ba	0.81	1.00																	
Ca	-0.87	-0.68	1.00																
Co	0.69	0.43	-0.55	1.00															
Cr	0.95	0.75	-0.83	0.67	1.00														
Cu	0.57	0.77	-0.40	0.29	0.63	1.00													
Fe	0.97	0.74	-0.86	0.71	0.98	0.61	1.00												
K	0.80	0.72	-0.68	0.69	0.77	0.39	0.80	1.00											
Mg	-0.76	-0.63	0.97	-0.44	-0.70	-0.28	-0.72	-0.59	1.00										
Mn	0.44	0.73	-0.47	0.00	0.45	0.62	0.46	0.56	-0.46	1.00									
Na	-0.65	-0.25	0.61	-0.43	-0.71	-0.39	-0.73	-0.25	0.46	-0.07	1.00								
Ni	0.75	0.45	-0.64	0.76	0.83	0.45	0.83	0.63	-0.49	0.23	-0.77	1.00							
P	0.62	0.76	-0.62	0.25	0.62	0.64	0.64	0.72	-0.59	0.89	-0.19	0.37	1.00						
Pb	0.76	0.74	-0.73	0.55	0.72	0.54	0.78	0.71	-0.67	0.51	-0.39	0.44	0.58	1.00					
Sr	-0.47	-0.07	0.43	-0.41	-0.59	-0.28	-0.63	-0.31	0.26	-0.10	0.87	-0.76	-0.18	-0.33	1.00				
Ti	0.97	0.86	-0.82	0.60	0.94	0.65	0.95	0.80	-0.71	0.58	-0.61	0.69	0.72	0.78	-0.43	1.00			
V	0.98	0.73	-0.86	0.67	0.96	0.52	0.98	0.79	-0.73	0.43	-0.73	0.81	0.59	0.73	-0.61	0.95	1.00		
Zn	0.90	0.56	-0.81	0.79	0.93	0.45	0.96	0.76	-0.67	0.27	-0.77	0.85	0.48	0.75	-0.71	0.86	0.94	1.00	
As	0.27	0.44	-0.22	-0.14	0.30	0.30	0.17	0.08	-0.24	0.22	-0.07	0.11	0.10	0.16	0.20	0.30	0.23	0.05	1.00

Core 119																			
Lake Agassiz Sequence (171-305 cm)																			
	Al	**Ba**	**Ca**	**Co**	**Cr**	**Cu**	**Fe**	**K**	**Mg**	**Mn**	**Na**	**Ni**	**P**	**Pb**	**Sr**	**Ti**	**V**	**Zn**	**As**
Al	1.00																		
Ba	0.51	1.00																	
Ca	-0.89	-0.52	1.00																
Co	0.29	0.29	-0.06	1.00															
Cr	0.77	0.39	-0.55	0.38	1.00														
Cu	0.11	0.45	-0.29	0.14	-0.05	1.00													
Fe	0.66	0.49	-0.70	0.02	0.43	0.38	1.00												
K	0.65	0.31	-0.40	0.56	0.85	0.17	0.54	1.00											
Mg	-0.73	-0.35	0.93	0.06	-0.36	-0.29	-0.49	-0.18	1.00										
Mn	0.48	0.22	-0.66	-0.07	0.02	0.33	0.35	-0.03	-0.69	1.00									
Na	0.40	0.15	-0.19	0.65	0.67	0.19	0.30	0.90	-0.04	-0.16	1.00								
Ni	0.74	0.35	-0.50	0.58	0.81	0.09	0.25	0.77	-0.35	0.26	0.61	1.00							
P	0.24	0.26	-0.36	-0.13	-0.06	0.19	0.73	0.09	-0.21	0.51	-0.12	-0.08	1.00						
Pb	0.12	0.07	0.03	0.62	0.40	-0.10	-0.15	0.35	0.06	-0.29	0.51	0.44	-0.32	1.00					
Sr	0.52	0.59	-0.40	0.72	0.51	0.30	0.26	0.53	-0.21	0.15	0.56	0.63	0.00	0.62	1.00				
Ti	0.79	0.45	-0.64	0.25	0.59	0.06	0.78	0.62	-0.38	0.21	0.28	0.57	0.48	0.00	0.39	1.00			
V	0.57	0.25	-0.75	-0.11	0.04	0.17	0.39	-0.10	-0.82	0.84	-0.28	0.13	0.41	-0.35	-0.03	0.31	1.00		
Zn	0.83	0.53	-0.65	0.40	0.87	0.13	0.49	0.75	-0.45	0.15	0.59	0.83	0.03	0.48	0.70	0.67	0.12	1.00	
As	-0.19	-0.38	0.16	-0.08	-0.07	0.26	-0.24	-0.04	-0.01	-0.11	0.00	0.03	-0.31	0.13	-0.31	-0.24	-0.08	-0.01	1.00

Core 120																									
Lake Winnipeg Sequence (0-195cm)																									
	Al	Ba	Ca	Co	Cr	Cu	Fe	K	Mg	Mn	Na	Ni	P	Pb	Sr	Tl	V	Zn	As	% H_2O	%OM	%CO_3	%Clay	%Sand	% Silt
Al	1.00																								
Ba	0.79	1.00																							
Ca	-0.78	-0.56	1.00																						
Co	0.82	0.76	-0.72	1.00																					
Cr	0.97	0.78	-0.77	0.83	1.00																				
Cu	0.90	0.77	-0.69	0.84	0.89	1.00																			
Fe	0.98	0.82	-0.80	0.88	0.97	0.95	1.00																		
K	0.86	0.97	-0.56	0.81	0.85	0.87	0.89	1.00																	
Mg	-0.59	-0.36	0.96	-0.57	-0.58	-0.48	-0.61	-0.34	1.00																
Mn	0.74	0.35	-0.74	0.62	0.74	0.64	0.76	0.46	-0.66	1.00															
Na	0.19	0.72	0.07	0.32	0.20	0.32	0.25	0.65	0.22	-0.23	1.00														
Ni	0.89	0.87	-0.74	0.94	0.89	0.90	0.94	0.91	-0.55	0.61	0.43	1.00													
P	0.86	0.77	-0.71	0.80	0.86	0.81	0.90	0.83	-0.54	0.80	0.32	0.86	1.00												
Pb	0.45	0.07	-0.74	0.27	0.41	0.46	0.46	0.12	-0.77	0.60	-0.42	0.29	0.31	1.00											
Sr	0.22	0.74	0.03	0.35	0.22	0.32	0.28	0.67	0.17	-0.19	1.00	0.45	0.36	-0.41	1.00										
Tl	0.95	0.72	-0.84	0.71	0.92	0.81	0.91	0.76	-0.69	0.72	0.09	0.81	0.81	0.58	0.13	1.00									
V	0.71	0.16	-0.70	0.44	0.68	0.53	0.64	0.26	-0.64	0.76	-0.56	0.44	0.47	0.68	-0.53	0.74	1.00								
Zn	0.92	0.57	-0.83	0.73	0.90	0.87	0.92	0.68	-0.68	0.88	-0.07	0.78	0.83	0.66	-0.05	0.89	0.82	1.00							
As	-0.16	-0.15	-0.18	0.03	-0.10	-0.03	-0.08	-0.19	-0.29	0.01	-0.17	-0.08	-0.24	0.44	-0.19	-0.14	-0.01	-0.01	1.00						
% H_2O	0.22	-0.33	-0.54	0.12	0.21	0.05	0.19	-0.26	-0.64	0.62	-0.86	0.02	0.13	0.67	-0.83	0.33	0.79	0.47	0.21	1.00					
%OM	0.32	-0.24	-0.48	0.22	0.30	0.12	0.27	-0.14	-0.53	0.64	-0.78	0.08	0.22	0.50	-0.74	0.36	0.81	0.48	-0.03	0.91	1.00				
%CO_3	-0.77	-0.63	0.96	-0.77	-0.76	-0.64	-0.80	-0.61	0.92	-0.70	-0.04	-0.75	-0.72	-0.59	-0.09	-0.80	-0.61	-0.75	-0.13	-0.44	-0.46	1.00			
%Clay	0.32	0.53	-0.13	0.24	0.31	0.50	0.38	0.53	0.04	0.07	0.54	0.42	0.33	0.01	0.50	0.19	-0.11	0.26	0.09	-0.44	-0.49	-0.06	1.00		
%Sand	-0.19	-0.04	0.01	-0.16	-0.18	-0.15	-0.18	-0.09	-0.03	-0.19	0.11	-0.16	-0.09	0.07	0.10	-0.10	-0.24	-0.13	0.08	-0.10	-0.29	0.07	0.02	1.00	
% Silt	-0.25	-0.50	0.12	-0.18	-0.25	-0.44	-0.31	-0.48	-0.03	-0.01	-0.55	-0.35	-0.29	-0.03	-0.50	-0.15	0.17	-0.21	-0.11	0.45	0.55	0.04	-0.96	-0.30	1.00

Core 120																									
Lake Agassiz sequence, middle part (196-354cm)																									
	Al	Ba	Ca	Co	Cr	Cu	Fe	K	Mg	Mn	Na	Ni	P	Pb	Sr	Ti	V	Zn	As	% H_2O	%OM	%CO_3	%Clay	%Sand	% silt
Al	1.00																								
Ba	-0.12	1.00																							
Ca	-0.88	0.25	1.00																						
Co	0.55	0.22	-0.54	1.00																					
Cr	0.90	0.16	-0.84	0.55	1.00																				
Cu	0.66	0.07	-0.66	0.50	0.63	1.00																			
Fe	0.60	0.20	-0.58	0.83	0.56	0.52	1.00																		
K	0.56	0.66	-0.53	0.51	0.80	0.52	0.51	1.00																	
Mg	0.31	0.86	-0.24	0.41	0.58	0.34	0.44	0.94	1.00																
Mn	-0.07	0.57	0.13	0.68	0.01	0.03	0.56	0.33	0.47	1.00															
Na	0.30	0.81	-0.30	0.44	0.60	0.38	0.44	0.95	0.98	0.47	1.00														
Ni	0.85	0.30	-0.79	0.66	0.96	0.61	0.64	0.87	0.69	0.20	0.72	1.00													
P	0.55	0.62	-0.51	0.44	0.79	0.47	0.41	0.98	0.92	0.26	0.93	0.86	1.00												
Pb	0.45	-0.37	-0.52	0.38	0.27	0.55	0.57	0.06	-0.09	0.12	-0.03	0.27	0.02	1.00											
Sr	0.43	0.76	-0.38	0.46	0.70	0.44	0.45	0.98	0.97	0.41	0.99	0.80	0.97	-0.01	1.00										
Tl	0.86	0.26	-0.81	0.50	0.94	0.73	0.64	0.85	0.68	0.05	0.68	0.92	0.82	0.38	0.75	1.00									
V	0.24	-0.90	-0.20	-0.16	-0.10	-0.02	-0.17	-0.66	-0.83	-0.57	-0.85	-0.26	-0.63	0.24	-0.76	-0.22	1.00								
Zn	0.78	0.19	-0.72	0.58	0.75	0.72	0.81	0.66	0.55	0.19	0.52	0.76	0.61	0.55	0.56	0.88	-0.12	1.00							
As	-0.35	-0.28	0.39	0.17	-0.57	-0.37	0.10	-0.64	-0.56	0.40	-0.55	-0.49	-0.69	0.13	-0.59	-0.62	0.31	-0.40	1.00						
% H_2O	0.44	-0.76	-0.64	0.23	0.19	0.26	0.34	-0.26	-0.48	-0.30	-0.44	0.09	-0.28	0.56	-0.40	0.17	0.69	0.31	0.16	1.00					
%OM	-0.19	-0.79	0.24	-0.61	-0.48	-0.33	-0.46	-0.81	-0.85	-0.61	-0.87	-0.58	-0.75	0.16	-0.84	-0.50	0.76	-0.37	0.32	0.32	1.00				
%CO_3	-0.41	-0.48	0.43	-0.24	-0.62	-0.47	-0.36	-0.84	-0.78	-0.13	-0.83	-0.71	-0.86	-0.22	-0.84	-0.73	0.62	-0.56	0.64	0.28	0.48	1.00			
%Clay	0.17	0.22	-0.16	0.24	0.07	0.22	0.23	0.30	0.33	0.40	0.34	0.18	0.32	0.24	0.31	0.24	-0.27	0.33	-0.11	0.03	-0.28	-0.22	1.00		
%Sand	-0.05	-0.16	0.09	-0.04	-0.01	-0.25	-0.02	-0.27	-0.27	-0.17	-0.32	-0.10	-0.35	-0.19	-0.28	-0.18	0.31	-0.16	0.21	0.14	0.11	0.49	-0.68	1.00	
% silt	-0.18	-0.15	0.12	-0.29	-0.09	-0.04	-0.29	-0.14	-0.18	-0.37	-0.13	-0.14	-0.09	-0.13	-0.14	-0.14	0.05	-0.29	-0.07	-0.19	0.26	-0.19	-0.68	-0.08	1.00

Core 121																								
Lake Winnipeg sequence (0-475cm)																								
	Al	Ba	Ca	Co	Cr	Cu	Fe	K	Mg	Mn	Na	Ni	P	Pb	Sr	Ti	V	Zn	As	$\%H_2$	%OM	%CO	Cla	San	%Silt
Al	1.00																							
Ba	0.49	1.00																						
Ca	-0.49	-0.48	1.00																					
Co	0.51	0.46	-0.53	1.00																				
Cr	0.82	0.43	-0.55	0.45	1.00																			
Cu	0.69	0.23	-0.20	0.29	0.56	1.00																		
Fe	0.86	0.57	-0.79	0.61	0.84	0.50	1.00																	
K	0.22	0.63	0.26	0.05	0.15	0.14	0.08	1.00																
Mg	-0.54	-0.37	0.97	-0.52	-0.56	-0.27	-0.77	0.39	1.00															
Mn	0.61	0.66	-0.88	0.55	0.59	0.20	0.84	0.01	-0.81	1.00														
Na	-0.52	0.17	0.65	-0.34	-0.49	-0.33	-0.61	0.69	0.76	-0.51	1.00													
Ni	0.58	0.50	-0.62	0.73	0.61	0.28	0.69	0.09	-0.59	0.61	-0.36	1.00												
P	0.23	0.64	-0.15	0.13	0.35	0.09	0.29	0.64	-0.03	0.27	0.37	0.24	1.00											
Pb	-0.04	0.21	-0.50	0.08	0.30	0.01	0.29	-0.07	-0.38	0.36	-0.12	0.18	0.25	1.00										
Sr	-0.30	0.17	0.73	-0.33	-0.34	-0.12	-0.53	0.74	0.79	-0.55	0.93	-0.34	0.38	-0.29	1.00									
Ti	0.67	0.82	-0.66	0.52	0.64	0.37	0.72	0.34	-0.62	0.77	-0.19	0.68	0.50	0.24	-0.12	1.00								
V	0.89	0.33	-0.70	0.54	0.78	0.54	0.87	-0.17	-0.77	0.74	-0.80	0.62	0.06	0.07	-0.65	0.61	1.00							
Zn	0.72	0.46	-0.85	0.53	0.81	0.47	0.91	-0.07	-0.82	0.83	-0.66	0.63	0.29	0.50	-0.65	0.65	0.84	1.00						
As	-0.10	-0.08	-0.01	-0.10	-0.14	0.04	-0.12	-0.09	0.01	-0.03	0.00	-0.04	-0.18	0.11	-0.05	0.01	-0.05	-0.03	1.00					
$\%H_2O$	0.43	0.31	-0.91	0.44	0.57	0.17	0.76	-0.31	-0.86	0.79	-0.68	0.50	0.08	0.66	-0.79	0.48	0.64	0.88	-0.01	1.00				
%OM	0.49	0.25	-0.71	0.37	0.61	0.25	0.69	-0.25	-0.72	0.62	-0.59	0.42	0.05	0.43	-0.61	0.43	0.61	0.74	-0.10	0.78	1.00			
$\%CO_3$	-0.50	-0.52	0.92	-0.49	-0.56	-0.19	-0.75	0.18	0.90	-0.85	0.54	-0.58	-0.22	-0.43	0.61	-0.68	-0.66	-0.80	0.04	-0.82	-0.81	1.00		
%Clay	0.24	0.24	-0.32	0.11	0.26	-0.01	0.32	0.01	-0.31	0.38	-0.19	0.12	0.12	0.14	-0.16	0.28	0.28	0.32	-0.31	0.30	0.32	-0.37	1.00	
%Sand	0.21	-0.16	0.10	0.16	0.05	0.23	0.06	0.00	0.05	-0.08	-0.14	0.20	-0.13	-0.17	-0.02	0.02	0.15	0.00	0.24	-0.09	-0.15	0.17	-0.32	1.00
%Silt	-0.35	-0.18	0.29	-0.19	-0.29	-0.10	-0.37	-0.01	0.29	-0.36	0.27	-0.22	-0.06	-0.06	0.18	-0.30	-0.36	-0.33	0.20	-0.27	-0.26	0.31	-0.89	-0.15	1.00

Core 121																									
Lake Agassiz sequence (485-547cm)																									
	Al	Ba	Ca	Co	Cr	Cu	Fe	K	Mg	Mn	Na	Ni	P	Pb	Sr	Ti	V	Zn	As	$\%H_2$	%OM	%CO	Cla	San	%Silt
Al	1																								
Ba	0.01	1.00																							
Ca	-0.84	0.15	1.00																						
Co	-0.74	-0.40	0.70	1.00																					
Cr	0.62	-0.10	-0.25	-0.08	1.00																				
Cu	0.80	-0.31	-0.82	-0.68	0.33	1.00																			
Fe	0.97	-0.02	-0.93	-0.80	0.47	0.86	1.00																		
K	0.19	0.03	0.29	0.27	0.75	-0.21	-0.04	1.00																	
Mg	-0.78	0.03	0.98	0.73	-0.11	-0.74	-0.89	0.39	1.00																
Mn	-0.50	-0.03	0.85	0.64	0.24	-0.62	-0.67	0.70	0.92	1.00															
Na	-0.85	0.03	0.91	0.79	-0.37	-0.88	-0.93	0.26	0.86	0.72	1.00														
Ni	0.37	-0.34	-0.01	0.26	0.93	0.16	0.19	0.82	0.15	0.45	-0.09	1.00													
P	0.58	0.08	-0.26	-0.23	0.91	0.37	0.48	0.52	-0.15	0.13	-0.52	0.75	1.00												
Pb	0.01	0.56	0.44	0.11	0.37	-0.44	-0.20	0.78	0.43	0.58	0.43	0.36	0.21	1.00											
Sr	-0.78	0.43	0.82	0.58	-0.40	-0.87	-0.84	0.12	0.72	0.51	0.87	-0.25	-0.44	0.53	1.00										
Ti	0.81	-0.01	-0.94	-0.58	0.33	0.67	0.87	-0.18	-0.94	-0.82	-0.81	0.10	0.33	-0.26	-0.63	1.00									
V	0.97	-0.04	-0.78	-0.63	0.76	0.78	0.93	0.28	-0.69	-0.40	-0.84	0.53	0.74	0.02	-0.77	0.78	1.00								
Zn	0.88	-0.18	-0.88	-0.52	0.62	0.82	0.89	0.02	-0.80	-0.60	-0.87	0.42	0.61	-0.23	-0.76	0.90	0.92	1.00							
As	-0.48	-0.05	0.42	0.63	-0.25	-0.76	-0.54	0.27	0.36	0.34	0.71	-0.04	-0.49	0.32	0.57	-0.29	-0.53	-0.52	1.00						
$\%H_2O$	0.66	0.07	-0.90	-0.73	0.00	0.77	0.79	-0.55	-0.93	-0.95	-0.85	-0.26	0.12	-0.47	-0.60	0.87	0.60	0.76	-0.55	1.00					
%OM	0.95	0.03	-0.78	-0.67	0.74	0.76	0.92	0.21	-0.70	-0.41	-0.89	0.47	0.78	-0.04	-0.79	0.76	0.98	0.90	-0.58	0.61	1.00				
$\%CO_3$	-0.92	-0.05	0.91	0.68	-0.51	-0.67	-0.94	-0.03	0.89	0.65	0.86	-0.24	-0.51	0.13	0.74	-0.92	-0.89	-0.88	0.31	-0.73	-0.90	1.00			
%Clay	-0.30	-0.47	0.15	0.43	0.04	-0.23	-0.24	-0.03	0.20	0.25	0.07	0.16	0.13	-0.46	-0.20	-0.23	-0.20	-0.16	0.20	-0.36	-0.11	0.11	1.00		
%Sand	0.39	0.49	-0.36	-0.46	-0.11	0.08	0.36	0.02	-0.46	-0.43	-0.12	-0.27	-0.26	0.41	0.11	0.47	0.23	0.19	0.22	0.41	0.15	-0.40	-0.76	1.00	
%Silt	0.10	0.28	0.09	-0.24	0.03	0.27	0.04	0.03	0.11	0.01	-0.01	-0.01	0.03	0.33	0.20	-0.07	0.10	0.08	-0.49	0.18	0.02	0.19	-0.83	0.25	1.00

Core 122																								
Lake Winnipeg sequence (0-435cm)																								
	Al	Ba	Ca	Co	Cr	Cu	Fe	K	Mg	Mn	Na	Ni	P	Pb	Sr	Ti	V	Zn	As	$\%H_2O$	% OM	% CO	%Cla	San	%Silt
Al	1.00																							
Ba	0.99	1.00																						
Ca	0.08	0.15	1.00																					
Co	0.97	0.97	0.14	1.00																				
Cr	0.74	0.70	0.00	0.73	1.00																			
Cu	0.93	0.93	0.31	0.94	0.80	1.00																		
Fe	0.95	0.92	-0.02	0.92	0.90	0.92	1.00																	
K	0.98	0.99	0.25	0.96	0.71	0.95	0.91	1.00																
Mg	0.35	0.41	0.96	0.40	0.20	0.54	0.23	0.50	1.00															
Mn	0.95	0.92	-0.08	0.90	0.78	0.87	0.96	0.90	0.18	1.00														
Na	0.75	0.80	0.70	0.77	0.49	0.85	0.63	0.85	0.86	0.58	1.00													
Ni	0.98	0.97	0.06	0.97	0.81	0.94	0.97	0.96	0.33	0.94	0.72	1.00												
P	0.98	0.98	0.27	0.97	0.75	0.97	0.92	0.99	0.52	0.89	0.85	0.96	1.00											
Pb	0.66	0.63	0.01	0.65	0.68	0.68	0.75	0.62	0.17	0.76	0.40	0.69	0.62	1.00										
Sr	0.86	0.90	0.56	0.87	0.59	0.92	0.76	0.94	0.76	0.72	0.98	0.84	0.93	0.51	1.00									
Ti	0.99	0.99	0.03	0.95	0.70	0.91	0.93	0.97	0.30	0.93	0.72	0.97	0.96	0.63	0.84	1.00								
V	0.98	0.96	-0.08	0.94	0.74	0.88	0.95	0.93	0.19	0.97	0.61	0.96	0.93	0.68	0.76	0.98	1.00							
Zn	0.98	0.96	-0.04	0.95	0.81	0.91	0.98	0.94	0.23	0.97	0.64	0.98	0.94	0.71	0.78	0.97	0.99	1.00						
As	0.00	0.03	0.27	0.04	0.07	0.11	0.05	0.04	0.24	0.02	0.15	0.05	0.03	0.46	0.12	-0.02	-0.04	0.00	1.00					
$\%H_2O$	-0.12	-0.20	-0.88	-0.16	0.08	-0.27	0.05	-0.28	-0.87	0.12	-0.70	-0.08	-0.28	0.17	-0.56	-0.09	0.05	0.03	-0.18	1.00				
% OM	-0.04	-0.11	-0.74	-0.11	0.12	-0.19	0.11	-0.18	-0.70	0.19	-0.57	-0.03	-0.18	0.26	-0.45	-0.02	0.11	0.08	0.03	0.78	1.00			
% CO_3	0.00	0.02	0.13	-0.03	-0.03	-0.01	-0.03	0.03	0.13	-0.03	0.10	-0.02	0.03	-0.06	0.08	-0.03	-0.03	-0.02	-0.08	-0.19	-0.04	1.00		
%Clay	0.17	0.14	-0.44	0.10	0.07	-0.02	0.16	0.09	-0.36	0.22	-0.17	0.15	0.07	-0.04	-0.09	0.21	0.24	0.20	-0.27	0.30	0.22	-0.11	1.00	
%Sand	-0.13	-0.15	0.03	-0.12	-0.12	-0.11	-0.12	-0.13	-0.04	-0.10	-0.08	-0.11	-0.14	0.15	-0.08	-0.15	-0.12	-0.12	0.13	0.06	-0.09	-0.12	-0.37	1.00
%Silt	-0.13	-0.09	0.47	-0.06	-0.02	0.06	-0.12	-0.04	0.40	-0.20	0.21	-0.12	-0.02	-0.02	0.13	-0.17	-0.21	-0.17	0.24	-0.34	-0.20	0.17	-0.93	0.00	1.00

Core 122																								
Lake Agassiz sequence (435-477cm)																								
	Al	Ba	Ca	Co	Cr	Cu	Fe	K	Mg	Mn	Na	Ni	P	Sr	Ti	V	Zn	As	$\%H_2$	% O	CO	%Cla	San	%Silt
Al	1.00																							
Ba	0.07	1.00																						
Ca	-0.27	0.70	1.00																					
Co	0.42	0.80	0.36	1.00																				
Cr	0.46	0.79	0.38	0.59	1.00																			
Cu	0.88	-0.30	-0.67	0.09	0.20	1.00																		
Fe	0.34	-0.64	-0.99	-0.26	-0.33	0.72	1.00																	
K	0.92	0.26	-0.29	0.67	0.51	0.80	0.38	1.00																
Mg	-0.16	0.63	0.98	0.31	0.38	-0.58	-0.98	-0.25	1.00															
Mn	0.17	0.54	-0.17	0.47	0.66	0.21	0.22	0.44	-0.27	1.00														
Na	-0.13	0.68	0.98	0.34	0.46	-0.55	-0.98	-0.21	1.00	-0.19	1.00													
NI	0.52	-0.80	-0.68	-0.37	-0.47	0.71	0.68	0.31	-0.56	-0.47	-0.59	1.00												
P	-0.10	0.20	-0.13	0.56	-0.23	-0.11	0.20	0.25	-0.25	0.25	-0.28	-0.13	1.00											
Sr	-0.12	0.73	0.97	0.36	0.54	-0.54	-0.97	-0.19	0.98	-0.09	0.99	-0.65	-0.29	1.00										
Ti	-0.15	0.69	0.48	0.80	0.16	-0.43	-0.41	0.16	0.37	0.24	0.36	-0.56	0.79	0.35	1.00									
V	0.18	-0.61	-0.94	-0.16	-0.49	0.54	0.95	0.30	-0.96	0.16	-0.97	0.60	0.47	-0.98	-0.17	1.00								
Zn	0.38	-0.65	-0.99	-0.23	-0.34	0.75	1.00	0.42	-0.97	0.17	-0.96	0.72	0.21	-0.96	-0.40	0.95	1.00							
As	0.90	0.10	-0.24	0.22	0.65	0.84	0.28	0.76	-0.13	0.32	-0.07	0.36	-0.43	-0.03	-0.41	0.02	0.30	1.00						
$\%H_2O$	0.20	-0.73	-0.98	-0.34	-0.50	0.60	0.98	0.24	-0.98	0.09	-0.99	0.70	0.26	-1.00	-0.38	0.97	0.98	0.10	1.00					
% OM	0.08	-0.66	-0.86	-0.19	-0.64	0.42	0.87	0.20	-0.89	-0.01	-0.92	0.62	0.54	-0.95	-0.09	0.98	0.88	-0.14	0.94	1.00				
% CO_3	-0.25	0.60	0.98	0.21	0.36	-0.64	-0.99	-0.35	0.99	-0.26	0.99	-0.61	-0.32	0.98	0.30	-0.98	-0.98	-0.17	-0.98	-0.91	1.00			
%Clay	0.84	-0.34	-0.48	0.19	-0.08	0.84	0.54	0.74	-0.37	-0.20	-0.38	0.84	0.10	-0.43	-0.18	0.48	0.60	0.59	0.49	0.47	-0.47	1.00		
%Sand	0.22	0.08	-0.49	-0.03	0.49	0.45	0.49	0.31	-0.52	0.83	-0.45	-0.11	-0.17	-0.35	-0.34	0.30	0.44	0.50	0.35	0.10	-0.47	-0.10	1.00	
%Silt	-0.85	0.24	0.71	-0.14	-0.25	-0.99	-0.76	-0.82	0.64	-0.36	0.60	-0.63	0.02	0.58	0.36	-0.60	-0.78	-0.81	-0.64	-0.46	0.70	-0.78	-0.55	1.00

Appendix 3

Bulk Sediment Geochemistry - Bottom Sediment Samples

Analytical preparation: Hydrofluoric acid total leach

	Element	Analytical Method	Detection Limit	Upper Limit
Ag	ppm	AAS	0.2	200
Al	%	ICP-AES	0.01	25.00
Ba	ppm	ICP-AES	10	10000
Be	ppm	ICP-AES	0.5	1000
Bi	ppm	ICP-AES	2	10000
Ca	%	ICP-AES	0.01	25.00
Cd	ppm	ICP-AES	0.5	500
Co	ppm	ICP-AES	1	10000
Cr	ppm	ICP-AES	1	10000
Cu	ppm	ICP-AES	1	10000
Fe	%	ICP-AES	0.01	25.00
K	%	ICP-AES	0.01	10.00
Mg	%	ICP-AES	0.01	15.00
Mn	ppm	ICP-AES	5	10000
Mo	ppm	ICP-AES	1	10000
Na	%	ICP-AES	0.01	10.00
Ni	ppm	ICP-AES	1	10000
P	ppm	ICP-AES	10	10000
Pb	ppm	AAS	2	10000
Sr	ppm	ICP-AES	1	10000
Ti	%	ICP-AES	0.01	10.00
V	ppm	ICP-AES	1	10000
W	ppm	ICP-AES	10	10000
Zn	ppm	ICP-AES	2	10000

Analytical preparation: Nitric-aqua regia partial leach

	Element	Analytical Method	Detection Limit	Upper Limit
As	ppm	AAS-HYDRIDE/EDL	1	10000

Geochemistry of Lake Winnipeg Bottom Sediment Samples (Ponar)

Sample No	Ag	Al	As	Ba	Be	Bi	Ca	Cd	Co	Cr	Cu	Fe	K	Mg	Mn	Mo	Na	Ni	P	Pb	Sr	Ti	V	W	Zn
	ppm	%	ppm	ppm	ppm	ppm	%	ppm	ppm	ppm	ppm	%	%	%	ppm	ppm	%	ppm	ppm	ppm	ppm	%	ppm	ppm	ppm
1	<0.2	7.35	1	600	1.5	<2	1.83	0.5	20	96	43	4.17	2.08	1.94	755	<1	0.97	65	810	24	161	0.33	128	<10	130
2	<0.2	7.43	<1	610	1.0	<2	1.96	<0.5	20	96	42	3.95	2.13	2.00	695	<1	1.03	67	810	24	168	0.34	125	<10	114
3	<0.2	6.02	1	530	1.0	<2	5.09	0.5	13	74	27	2.66	1.96	3.30	545	<1	1.27	42	710	20	185	0.28	83	<10	68
4	<0.2	6.50	2	550	1.0	<2	3.49	0.5	15	80	33	2.97	2.02	2.68	505	<1	1.22	49	760	28	180	0.30	97	<10	86
5	<0.2	7.30	1	590	1.0	<2	1.66	0.5	19	93	39	3.84	2.08	1.74	720	<1	1.14	61	890	30	179	0.34	119	<10	106
6	<0.2	7.46	1	600	1.0	<2	1.26	1.0	18	98	42	3.98	2.06	1.58	600	<1	1.05	56	800	30	172	0.34	129	<10	112
7	<0.2	7.52	1	610	1.5	<2	1.40	<0.5	21	95	45	4.09	2.04	1.72	640	<1	0.96	61	940	28	166	0.34	132	<10	118
8	<0.2	7.85	<1	640	1.5	<2	1.23	0.5	23	102	47	4.34	2.12	1.60	695	<1	1.02	87	870	28	176	0.36	140	<10	124
10	<0.2	7.65	1	560	1.0	<2	1.49	<0.5	21	90	36	3.97	1.94	1.47	600	<1	1.34	53	690	22	203	0.34	123	<10	106
25	<0.2	6.72	1	570	1.0	<2	1.44	<0.5	14	67	30	2.80	1.84	0.99	520	<1	1.54	37	780	22	244	0.27	92	<10	76
28	<0.2	7.38	2	570	1.5	<2	1.29	<0.5	14	81	36	3.32	1.92	1.26	430	<1	1.20	41	650	20	199	0.33	123	<10	96
29	<0.2	7.34	1	540	1.5	<2	1.27	0.5	18	84	41	3.67	1.86	1.33	575	<1	1.01	53	700	24	174	0.35	134	<10	106
30	<0.2	7.05	<1	550	1.0	<2	1.29	<0.5	17	78	39	3.43	1.83	1.24	715	<1	1.12	50	760	24	186	0.32	121	<10	106
31	<0.2	6.51	<1	520	1.0	<2	2.25	<0.5	12	55	24	2.43	1.39	1.58	410	<1	1.39	36	540	16	213	0.24	90	<10	72
32	<0.2	6.83	1	570	1.0	<2	1.46	<0.5	14	61	27	2.68	1.82	0.97	705	<1	1.52	37	740	22	244	0.27	95	<10	74
33	<0.2	2.96	<1	240	0.5	<2	0.68	<0.5	6	27	14	1.39	0.83	0.62	440	<1	0.42	19	320	14	82	0.13	49	<10	42
34	<0.2	6.75	1	740	1.0	<2	1.14	0.5	25	110	29	4.22	1.72	1.80	3320	<1	0.92	66	690	14	150	0.31	130	<10	88
35	<0.2	7.09	1	550	1.0	<2	1.15	0.5	14	75	33	3.38	1.75	1.14	1315	<1	1.04	45	730	24	178	0.31	125	<10	96
36	<0.2	7.64	1	560	1.5	<2	1.09	<0.5	17	87	35	3.91	1.84	1.38	1140	<1	0.75	49	690	26	138	0.35	154	<10	120
37	<0.2	7.72	1	550	1.5	<2	0.98	<0.5	16	91	33	3.97	1.82	1.34	1100	<1	0.69	46	790	24	129	0.35	159	<10	122
39	<0.2	6.63	10	550	1.0	<2	2.81	0.5	20	83	34	3.74	1.74	2.21	1160	<1	0.95	46	1020	18	152	0.29	115	<10	92
40	<0.2	3.04	2	260	0.5	<2	2.17	<0.5	6	21	8	0.84	0.85	1.23	160	<1	0.83	12	320	10	135	0.10	33	<10	24
41	<0.2	7.90	1	530	1.5	<2	1.03	0.5	19	101	34	4.09	1.83	1.40	795	<1	0.62	50	740	28	121	0.35	173	<10	134
42	<0.2	7.89	1	550	1.5	<2	1.06	0.5	18	99	35	4.15	1.83	1.42	1120	<1	0.63	52	850	32	124	0.35	171	<10	130
43	<0.2	7.14	2	490	1.5	<2	2.50	0.5	17	95	34	3.52	1.71	2.19	880	<1	0.66	46	760	28	121	0.31	149	<10	110
44	<0.2	7.73	<1	530	1.5	<2	1.01	<0.5	18	101	34	3.97	1.78	1.39	660	<1	0.59	51	750	34	115	0.33	170	<10	128
45	<0.2	8.13	1	550	1.5	<2	1.05	<0.5	19	103	37	4.14	1.88	1.43	720	<1	0.64	57	740	48	124	0.36	180	10	134
46	<0.2	7.88	2	540	1.5	<2	0.92	0.5	19	101	34	4.18	1.81	1.35	1040	<1	0.56	49	730	46	113	0.36	180	<10	128
47	<0.2	8.10	4	540	1.5	<2	0.99	0.5	18	107	36	4.24	1.84	1.41	965	<1	0.57	50	780	62	115	0.35	183	<10	136
49	<0.2	7.60	4	510	1.5	<2	1.28	0.5	16	102	32	3.84	1.72	1.53	820	<1	0.51	48	730	50	104	0.33	178	<10	130
50	<0.2	7.42	2	500	1.5	<2	1.69	0.5	17	101	33	3.65	1.70	1.70	650	<1	0.49	43	760	44	102	0.33	179	<10	138

Correlation Matrix
Lake Winnipeg Bottom sediment (ponar)

	Al	*As*	*Ba*	*Be*	*Ca*	*Co*	*Cr*	*Cu*	*Fe*	*K*	*Mg*	*Mn*	*Na*	*Ni*	*P*	*Pb*	*Sr*	*Ti*	*V*	*Zn*
Al	1.00																			
As	0.01	1.00																		
Ba	**0.76**	-0.04	1.00																	
Be	**0.80**	0.04	0.43	1.00																
Ca	-0.26	0.23	-0.04	-0.29	1.00															
Co	**0.77**	0.09	**0.84**	0.54	-0.19	1.00														
Cr	**0.89**	0.09	0.74	**0.75**	-0.21	**0.88**	1.00													
Cu	**0.82**	-0.04	**0.75**	0.63	-0.17	**0.80**	**0.78**	1.00												
Fe	**0.91**	0.08	**0.77**	0.74	-0.32	**0.91**	**0.96**	**0.85**	1.00											
K	**0.82**	-0.04	**0.85**	0.52	0.09	**0.75**	**0.75**	**0.89**	**0.78**	1.00										
Mg	0.10	0.24	0.29	0.05	**0.86**	0.26	0.27	0.20	0.15	0.40	1.00									
Mn	0.22	0.12	0.52	0.09	-0.21	0.52	0.43	0.08	0.42	0.11	0.06	1.00								
Na	-0.04	-0.15	0.35	-0.39	0.39	-0.03	-0.28	0.08	-0.22	0.30	0.17	-0.17	1.00							
Ni	0.71	-0.13	**0.81**	0.50	-0.13	**0.90**	**0.80**	**0.87**	**0.84**	**0.80**	0.29	0.35	0.04	1.00						
P	**0.75**	0.33	0.74	0.50	0.06	**0.75**	0.73	**0.81**	**0.77**	**0.83**	0.37	0.21	0.11	0.71	1.00					
Pb	0.58	0.18	0.14	0.61	-0.27	0.30	0.62	0.37	0.53	0.31	-0.02	-0.03	-0.51	0.27	0.34	1.00				
Sr	0.05	-0.18	0.40	-0.30	0.28	0.01	-0.23	0.15	-0.15	0.35	0.06	-0.16	**0.99**	0.08	0.16	-0.45	1.00			
Ti	**0.97**	0.00	**0.77**	**0.78**	-0.23	**0.81**	**0.92**	**0.88**	**0.95**	**0.86**	0.18	0.26	-0.09	**0.78**	**0.76**	0.55	-0.01	1.00		
V	**0.85**	0.10	0.44	**0.87**	-0.42	0.63	**0.87**	0.59	**0.85**	0.49	-0.02	0.29	-0.54	0.52	0.53	**0.78**	-0.46	**0.83**	1.00	
Zn	**0.89**	0.03	0.53	**0.86**	-0.38	0.72	**0.90**	**0.77**	**0.91**	0.65	0.05	0.17	-0.42	0.67	0.65	0.72	-0.34	**0.90**	**0.95**	1.00

Bottom Sediment Samples
Lake Winnipeg

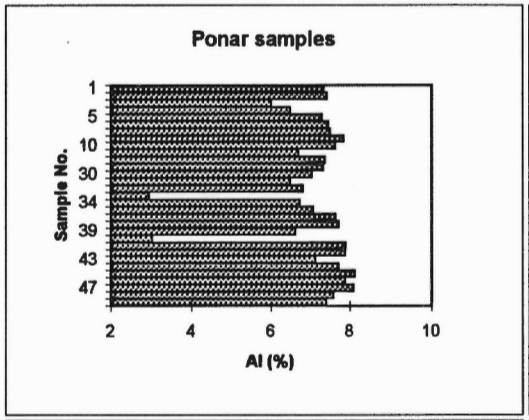

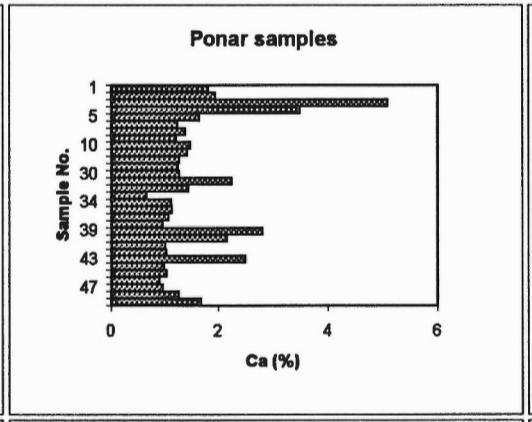

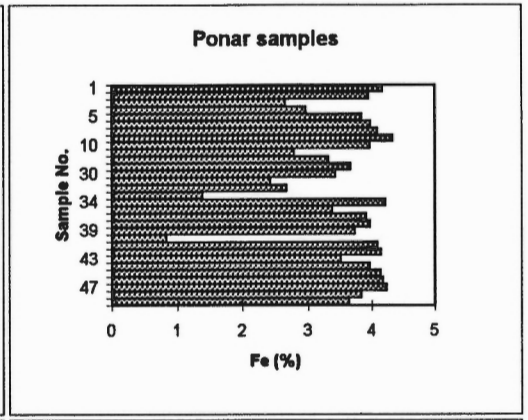

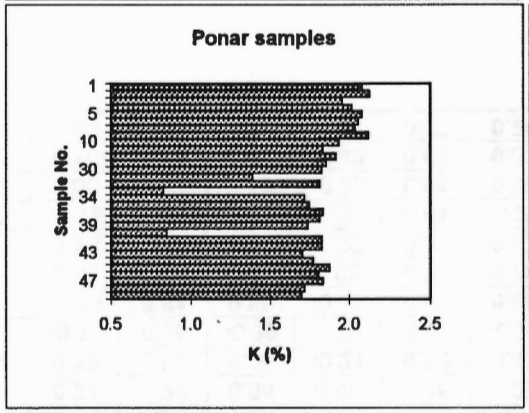

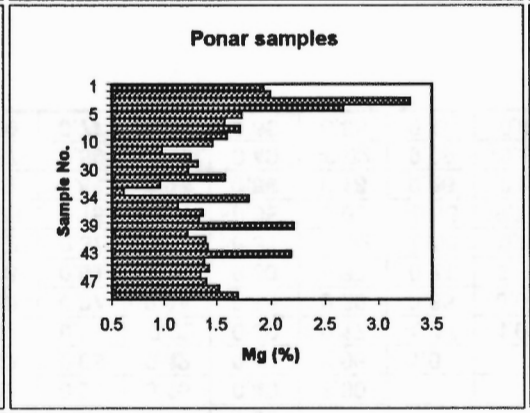

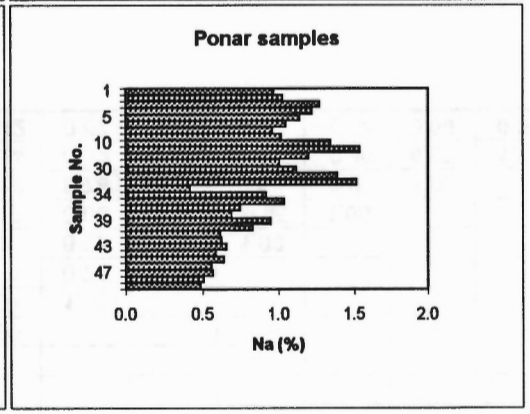

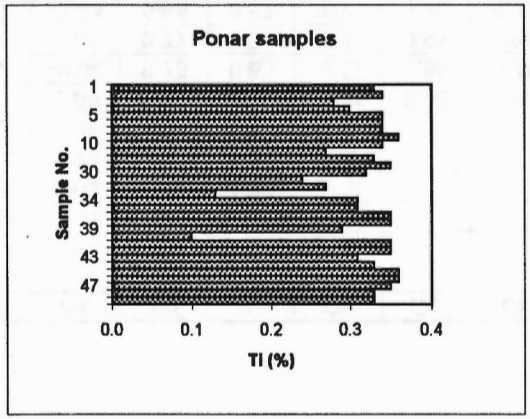

Bottom Sediment Samples
Lake Winnipeg

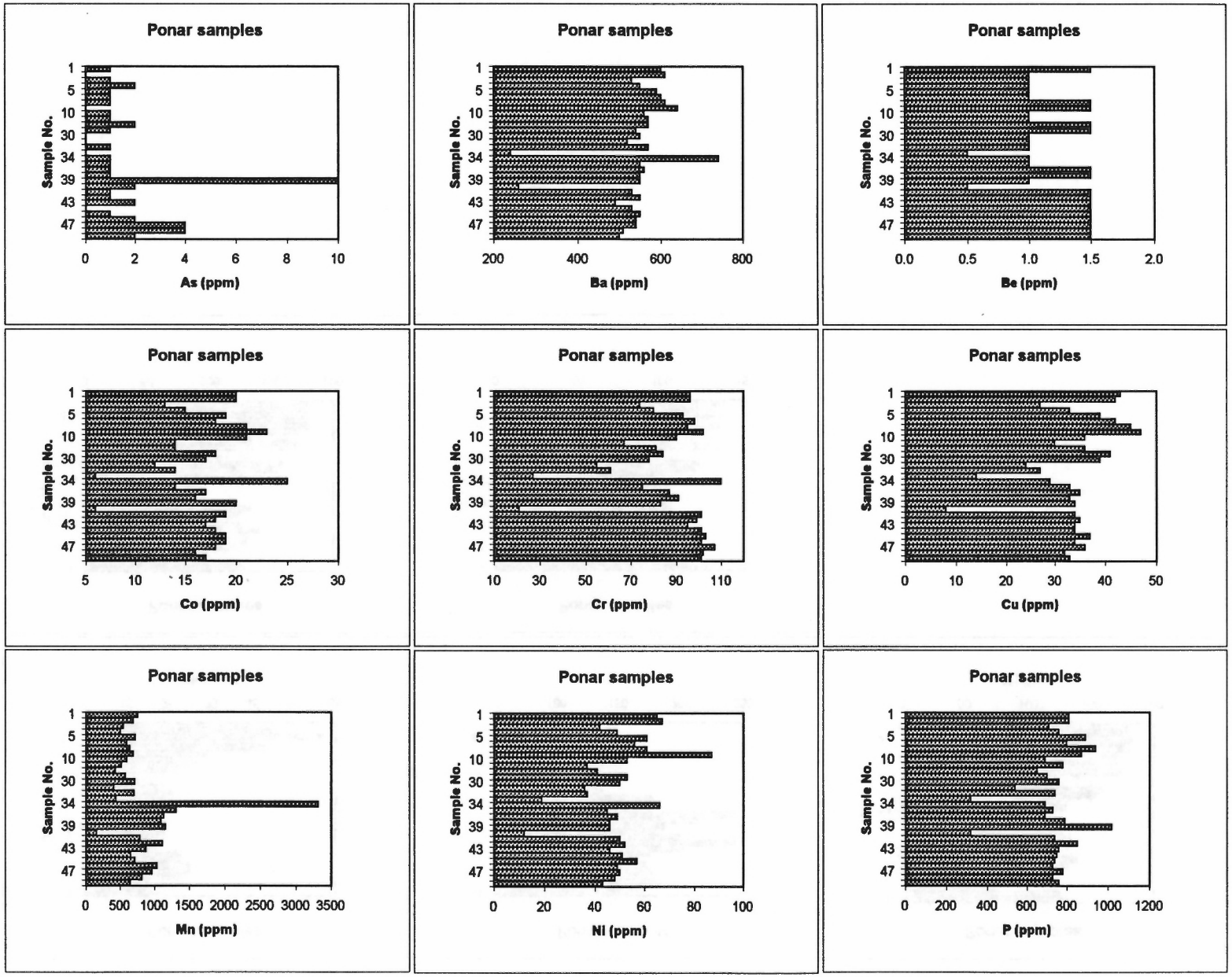
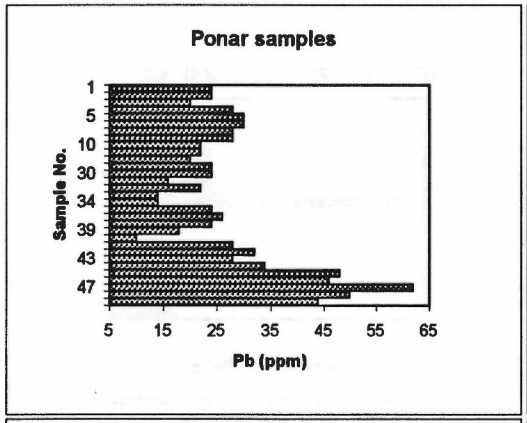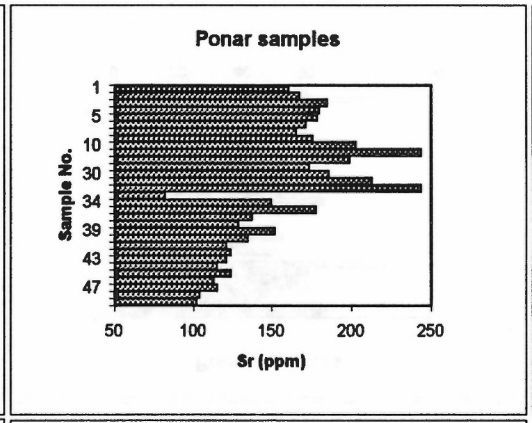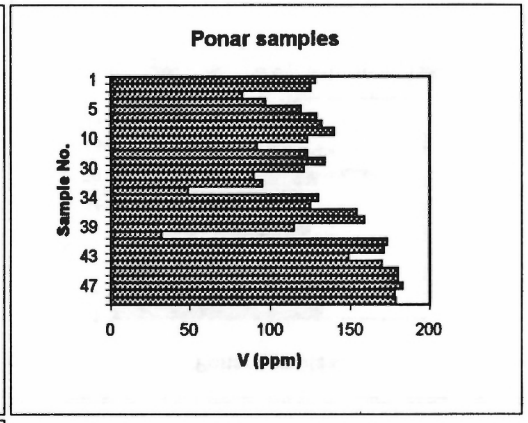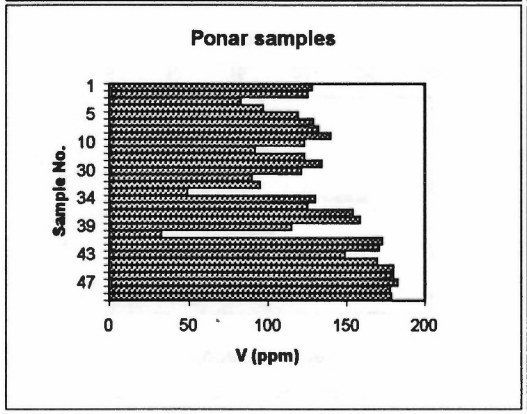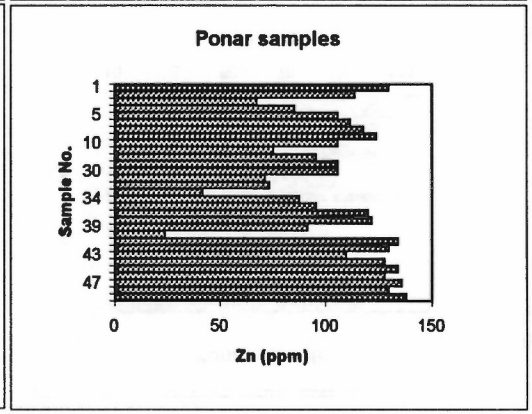
Bottom Sediment Samples
Lake Winnipeg